FACULTY OF MECHANICAL ENGINEERING KRALJEVO
UNIVERSITY OF KRAGUJEVAC
KRALJEVO – SERBIA

THE SIXTH INTERNATIONAL TRIENNIAL CONFERENCE

HEAVY MACHINERY
HM 2008

PROCEEDINGS

KRALJEVO, 24. – 29. JUNE 2008.

FACULTY OF MECHANICAL ENGINEERING KRALJEVO
UNIVERSITY OF KRAGUJEVAC
KRALJEVO – SERBIA

THE SIXTH INTERNATIONAL TRIENNIAL CONFERENCE

HEAVY MACHINERY
HM 2008

PROCEEDINGS

ORGANIZATION SUPPORTED BY:

Ministry of Science, Republic of Serbia

KRALJEVO, 24. – 29. JUNE 2008.

FACULTY OF MECHANICAL ENGINEERING KRALJEVO
UNIVERSITY OF KRAGUJEVAC
KRALJEVO – SERBIA

PUBLISHER:
Faculty of Mechanical Engineering, Kraljevo

EDITORS:
Prof. dr Novak Nedić, mech. eng.

PRINTOUT:
Riža d.o.o., Kraljevo

TECHNICAL COMMITTEE

M.Sc. Nebojša Bogojević
M.Sc. Ljubiša Dubonjić
M.Sc. Slobodan Ivanović
M.Sc. Rade Karamarković
M.Sc. Miljan Marašević
M.Sc. Goran Marković
M.Sc. Goran Miodragović
M.Sc. Aleksandra Petrović
Bojan Beloica
Mišo Bjelić
Zoran Bogićević
Slobodan Bukarica
Miljan Veljović
Milorad Stambolić
Nebojša Zdravković

No. of copies: 200

REVIEWS:
All papers have been reviewed by members of scientific committee

FACULTY OF MECHANICAL ENGINEERING KRALJEVO
UNIVERSITY OF KRAGUJEVAC
KRALJEVO – SERBIA

CONFERENCE CHAIRMAN

Prof. dr Novak Nedić, FME Kraljevo

CHAIRMAN OF PROGRAM COMMITTEE

Prof. Dr Milomir Gašić, FME Kraljevo

MEMBERS

1. Prof. Dr M. Alamoreanu, TU, Bucharest, Romania
2. Prof. Dr S. Arsovski, FME Kragujevac, Serbia
3. Prof. Dr D. Atmadzhova, VTU "Todor Kableshkov" Sofia, Bulgaria
4. Prof. Dr A. Babić, FME Kraljevo, Serbia
5. Prof. Dr H. Bogdevicius, Technical University, Vilnus, Lithuania
6. Prof. Dr A. Bruja, TU, Bucharest, Romania
7. Prof. Dr Z. Bučevac, FME Belgrade, Serbia
8. Prof. Dr A. Bukvić, FME East Sarajevo, Bosnia and Herzegovina
9. Prof. Dr V. Čović, FME Belgrade, Serbia
10. Prof. Dr M. Dedić, FME Kraljevo, Serbia
11. Prof. Dr R. Durković, FME Podgorica, Montenegro
12. Prof. Dr Lj. Djordjević, FME Kraljevo, Serbia
13. Prof. Dr K. Ehmann, Northwestern University, Chicago, USA
14. Prof. Dr A. Emeljanova, HGTUSA Harkov, Ukraine
15. Prof. Dr I. Filonov, MGTU Minsk, Belorus
16. Prof. Dr C. Fragassa, University of Bologna, Italy
17. Prof. Dr V. Jovišević, FME Banja Luka, Bosnia and Herzegovina
18. Prof. Dr Z. Jugović, Technical Faculty Cacak, Serbia
19. Prof. Dr V. Karamarković, FME Kraljevo, Serbia
20. Prof. Dr M. Karasahin, Demirel University, Istanbul, Turkey
21. Prof. Dr I. Kiričenko, HNADU Kiev, Ukraine
22. Prof. Dr M. Kostic, Northern Illinois University, DeKalb, USA
23. Prof. Dr E. Kudrjavcev, MGSU, Moscow, Russia
24. Prof. Dr Lj. Lukić, FME Kraljevo, Serbia
25. Prof. Dr Z. Marinković, FME Nis, Serbia
26. Prof. Dr N. Mešćerin, MGSU, Moscow, Russia
27. Prof. Dr N. Nenov, VTU "Todor Kableshkov" Sofia, Bulgaria
28. Prof. Dr V. Nikolić, FME Nis, Serbia
29. Prof. Dr E. Nikolov, Technical University, Sofia, Bulgaria
30. Prof. Dr I. Nikulin, VGASU, Voronez, Russia
31. Prof. Dr M. Ognjanović, FME Belgrade, Serbia
32. Prof. Dr M. Pavličić, FME Kraljevo, Serbia
33. Prof. Dr Z. Petković, FME Belgrade, Serbia
34. Prof. Dr D. Petrović, FME Kraljevo, Serbia
35. Prof. Dr R. Petrović, FME Kraljevo, Serbia
36. Prof. Dr J. Polajnar, BC University, Prince George, Canada
37. Prof. Dr S. Radović, FME Kraljevo, Serbia
38. Prof. Dr V. Raičević, FME Kosovska Mitrovica, Serbia
39. Prof. Dr M. Rajović, FME Kraljevo, Serbia
40. Prof. Dr R. Rakanović, FME Kraljevo, Serbia
41. Prof. Dr M. Stefanović, FME Kragujevac, Serbia
42. Prof. Dr Lj. Tanović, FME Belgrade, Serbia
43. Prof. Dr S. Trifunović, FME Kraljevo, Serbia
44. Prof. Dr M. Vesković, FME Kraljevo, Serbia
45. Prof. Dr J. Vladić, Faculty of Technical Sciences, Novi Sad, Serbia
46. Prof. Dr M. Vukićević, FME Kraljevo, Serbia
47. Prof. Dr K. Weinert, University of Dortmund, Germany

FACULTY OF MECHANICAL ENGINEERING KRALJEVO
UNIVERSITY OF KRAGUJEVAC
KRALJEVO – SERBIA

ORGANIZING COMMITTEE

Charman: Prof. Dr Ljubomir Lukić, FME Kraljevo

Members:
Prof. Dr Arandjel Babić, FME Kraljevo
Doc. Dr Radovan Bulatović, FME Kraljevo
Doc. Dr Mirko Djapić, FME Kraljevo
Doc. Dr Zoran Petrović, FME Kraljevo
Doc. Dr Dragan Pršić, FME Kraljevo
Doc. Dr Mile Savković, FME Kraljevo
Doc. Dr Tomislav Simović, FME Kraljevo
Doc. Dr Zlatan Šoškić, FME Kraljevo
M.Sc. Nebojša Bogojević, FME Kraljevo
M.Sc. Snežana Ćirić-Kostić, FME Kraljevo
M.Sc. Ljubiša Dubonjić, FME Kraljevo
M.Sc. Zoran Glavčić, FME Kraljevo
M.Sc. Slobodan Ivanović, FME Kraljevo
M.Sc. Rade Karamarković, FME Kraljevo
M.Sc. Ljubica Lalović, FME Kraljevo
M.Sc. Miljan Marašević, FME Kraljevo
M.Sc. Goran Marković, FME Kraljevo
M.Sc. Goran Miodragović, FME Kraljevo
M.Sc. Jovan Nešović, FME Kraljevo
M.Sc. Radovan Nikolić, FME Kraljevo
M.A. Nataša Pavlović, FME Kraljevo
M.Sc. Slaviša Šalinić, FME Kraljevo
Mišo Bjelić, FME Kraljevo
Zoran Bogićević, FME Kraljevo
Aleksandra Petrović, FME Kraljevo
Branko Radičević, FME Kraljevo
Miljan Veljović, FME Kraljevo
Nebojša Zdravković, FME Kraljevo

PREFACE

The Faculty of Mechanical Engineering Kraljevo has been traditionally organizing the international scientific conference devoted to heavy machinery every three years. The VI International Scientific Conference HM 2008 is considering modern methods and new technologies in the fields of design in machinery, production technologies, urban engineering and QMS through thematic sessions for the purpose of sustainable competitiveness of economic systems. Modern technologies are exposed to fast changes at the global world level so that their timely application both in large industrial systems and in medium and small enterprises is of considerable importance for the entire development and technological progress of economy as a whole.

The VI International Scientific Conference Heavy Machinery HM 2008 is a place for exchange of experiences and results accomplished in domestic and foreign science and practice, with the goal to indicate directions of further development of our industry on its way toward integration in European economic trends. Exchange of experiences between our and foreign scientific workers should contribute to extension of international scientific-technical collaboration, initiation of new international scientific-research projects and broader international collaboration among universities.

The papers which will be presented at this Conference have been classified into three thematic fields. In the first thematic field: Machine Building Design, the scientific-research issues refer to:

A. Automatic Control and Fluid Technique
B. Earth-Moving and Transportation Mechanisation
C. Railway Engineering
D. Termotechnique, Environment Protection and Urban Engineering
E. Mechanical Design and Mechanics
F. Production Technologies, Material Application and Enterpreneurial Engineering and Management
G. Computer-Integrated Processes and Designing of Machining Processes

Within this Conference, a round table with the topic “Energy Efficiency in Heavy Machinery” will be held. The aim is to open a scientific discussion on this actual problem in industry.

The sponsorship by the Ministry of Science of the Republic of Serbia is the proper way to promote science and technology in the area of mechanical engineering in Serbia.

On behalf of the organizer, I would like to express our thanks to all organizations and institutions that have supported this Conference. I would also like to extend our thanks to all authors and participants from abroad and from our country for their contribution to the Conference. And last but not the least, dear guests and participants in the Conference, I wish you a good time in Kraljevo – Mataruška Banja and see you again at the Seventh Conference, in three years.

Kraljevo, 19 June 2008

Conference Chairman,

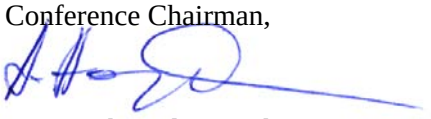

Prof. Dr Novak Nedić, mech eng.

FACULTY OF MECHANICAL ENGINEERING KRALJEVO
UNIVERSITY OF KRAGUJEVAC
KRALJEVO – SERBIA

CONTENTS

PLENARY SESSION

SESSION A: AUTOMATIC CONTROL AND FLUID TECHNIQUE

SESSION B: EARTH MOVING AND MINIG MACHINES AND TRANSPORTATION SYSTEMS

SESSION C: RAILWAY ENGINEERING

SESSION D: TERMOTECHNIQUE, ENVIRONMENT PROTECTION AND URBAN ENGINEERING

E SESSION: MECHANICAL DESIGN AND MECHANICS

F SESSION: PRODUCTION TECHNOLOGIES, MATERIAL APPLICATION AND ENTERPRENEURIAL ENGINEERING AND MANAGMENT

FACULTY OF MECHANICAL ENGINEERING KRALJEVO
UNIVERSITY OF KRAGUJEVAC
KRALJEVO – SERBIA

G SESSION: COMPUTER-INTEGRATED PROCESSES AND DESIGN OF MACHINING PROCESSES

ANNEX

SESSION B

SESSION D

PLENARY SESSION

DESIGN METHODOLOGY FOR TECHNOLOGICAL PLATFORMS

V. Milačić, M. Milačić

Abstract: *In last quarter of 20th century we had dramatic changes in America and Euro-Asia technological map through generating knowledge as new ingredient of the nation's wealth. Presently, knowledge and technology are driving force in economy and industry.*

Key words: *design, methodology, development, supply managment, technological platforms, AUTOSAR, MFC*

1. INTRODUCTION

Today, technological development is more and more based on established technological platforms as conglomerate of economic-cultural-technological-management modules generating complex functional enterprises which consist of one or more establishments. The establishment, in general, is physical location where business or industrial operations are conducted or where services are provided, like factory, mill, store, hotel, theater, mine, farm, airport, office, to mention few. Our technological platforms are infrastructures which emerge with new products or services in certain environments.

In this paper we cover following topics:

I. Strategy on the edge of chaos
II. Multi-business technological platforms as synergy of human, technological and financial resources
III. Flexible structure of technological platforms
IV. Technological platform supply managements
V. Technological platform and value innovation
VI. Sustainability along the lifecycle of technological platform
VII. Some examples of developed technological platforms [1]

2. STRATEGY ON EDGE OF CHAOS

Competing on the edge is one among five models of strategy. Along a historical development of models of strategy we start with strategy based on five forces, as stable industry structure, defensive position, industry structure, pick an industry, and profit. The next developments bring us to strategy based on core competence and game theory. Nowadays, more and more world is approaching a strategy which recognizes competition on the edge. It means gaining the edge of time pace and shape semi coherent strategic direction. In the new model of strategy it is assumed that industry is in rapid and unpredictable change which has to gain continuous flow of advantage through performance driver which provides ability to change in order to continually reinvent itself.

Competing on the edge means that enterprise has to understand where it wants to go. In addition, the enterprise has to have plan how to get there and be capable to change through self-reinventing process.

Five building blocks construct the strategy for competing on the edge. In the base is edge of chaos supporting level of edge of time and time pacing, shown in Figure 1 [2].

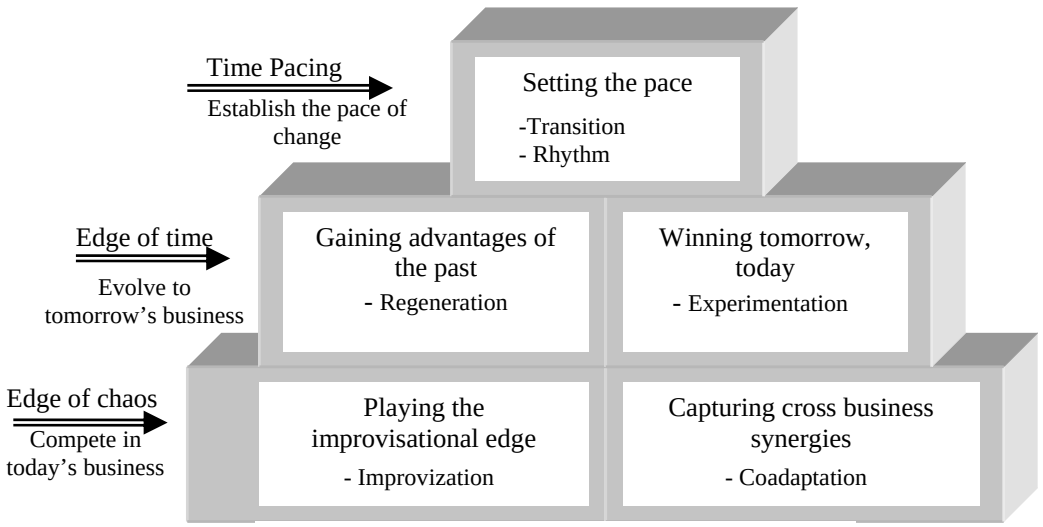

Figure 1: Competing on the edge [2]

Vladimir Milačić , Professor emeritus, University of Belgrade, Belgrade, Serbia
Miloš Milačić , Ford Motor Company, Dearborn, Michigan, USA

3. MULTI-BUSINESS TECHNOLOGICAL PLATFORM

Key aspects of the economic structure, understanding of that structure and functions of the economy could be analyzed using economical information which are categorized and presented. In the NAICS[1)] [3] structure offer "business establishments producing the same or similar products by similar production methods as placed in the same industry. Related industries are grouped together in the higher levels of classification building up to 20 major economical sectors."

Two more features for understanding economical structure are vertical integration and joint production of goods and services. "Vertical integration involves consecutive stages of fabrication of production processes in which the output of the one step is input to the next step. In general, establishments will be classified based on the final process on vertically integrated production environment, unless specifically identified as classified in another industry." The second type of combined activities is joint production of goods and services. A good example is relationship between automotive OEMs and their suppliers.

Different technological platforms are built using content of any combination of 20 industries. One of the results of industrial achievements in building is a nuclear aircraft carrier. It is "the most dangerous four and one half acres in the word" which is filled with up to eighty jet aircraft armed with most sophisticated weapons systems. Six thousand people are crammed into this floating city which is 360 meters long and displaces 95 thousand tons of water. To assure highest level of performance the utmost importance is placed on achieving synergy among people, technology and financial resources. Personnel on the carrier add value (to its country) by achieving the military objectives. In the factory the basic task is to move products or services out the front door and bring raw materials in the back.

4. FLEXIBLE STRUCTURE OF TECHNOLOGICAL PLATFORMS

Flexibility of the technological platform is its ability to foresight a new horizon in life cycle by performance enhancement or incarnation.

For example, Boeing Company made their first global plane model 747 model with more than 400 seats. However, the most successful model commercially is small 737, which presently is in its eight cycle (737-800).

New technological platform was 777 model based on digital design and digital production approach. Project lead, Phil Condit insisted on cultural base of the platform. His explanation was that "in our culture we gain quantities like respect to competitor and offer better product that competitor. Simply listen carefully and meet customer's needs."

Presently Boeing is working on "Dreamliner" – Boeing 787 introducing lean production technology and outsourcing concept, similar to automotive OEMs.

Given example can offer new way of thinking about flexibility which is ingrained in every step of a lifecycle of the particular product or service.

5. TECHNOLOGICAL PLATFORM SUPPLY MANAGEMENTS

Previously mentioned technological platforms of Boeing company face very strong competition in EADS' Airbus. The ferocity of the fight for this market is summarized in Table 1.

	Dreamliner (Boeing 787)	Airbus 350
Passenger capacity	210-250	270
Range (nautical miles)	8200	8300
Fuel consumption	20% less than 767-300	25% less than 767-300
List price (M$)	157-167	199.3
Orders & (total value B$)	525 (82.4)	109 (21.7)
Materials	50% composites 20% aluminum 10% steel 5% other	52% composites 20% aluminum 14% titanium 7% steel 7% other

Table 1: Boeing 787 vs. Airbus 350

Performance and structure of both products is very similar. However, preliminary market hype is on Boeing side. Boeing is shifting the emphasis on production line speed using lean manufacturing concept. In the same time, Boeing has restructured its partner base by outsourcing 70% of the aircraft manufacturing. Global efforts involve 17 companies form 10 countries to build a dreamliner[5].

Dr. Deming in early fifties developed statistical methods for quality control in manufacturing, which later got launched by Motorola as 6 methodology. These methods have become true quality control platform used word wide.

Evident success in manufacturing environment was transferred to banking, insurance and other financial sectors. Further development in this area was focused on reducing sensitivity of the process rather than reducing variability of the outcome which became known as DFSS – Design For Six Sigma.

[1)] North American Industry classification system

6. TECHNOLOGICAL PLATFORM AND VALUE INNOVATION

Value innovation is more than simple innovation – it is strategy that embraces the entire system of company's activities. Value innovation is not the same as technological innovation. There are structural views or environmental determinism as existing strategies for the competition. It shall be emphasized that "value innovation is based in the view that market boundaries and industry structure are not given and can be constructed by the actions and beliefs of industry players"[6]. It means that we have two builders of technological platform in order to define domain of value innovation, as shown in Figure 3.

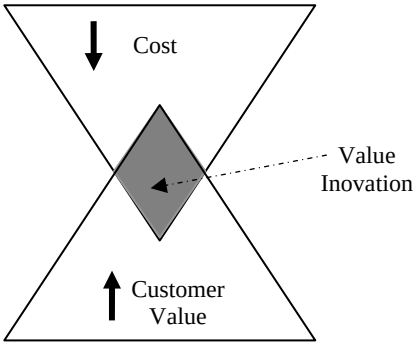

Figure 3: Value Innovation

Value innovation is achieved only when the whole system, comprising of company's utility, price and cost activities, is perfectly aligned. We shall mention again, an earlier mentioned example of Boeing 777 when the functional requirements were defined by "gang of eight."[2)]

Technological platform is multidimensional entity, and to demonstrate we will use transportation example – airlines and automobile transport. As dimensions in this analysis we will use:

1. Cost
2. Meals
3. Lounges
4. Seats in class of choice
5. Hub connectivity
6. Friendly service
7. Speed
8. Frequent departures

Plot of a diagram of levels of value innovation in each dimension, for 3 vastly different "carriers" - traditional airline, Southwest Airlines and car transportation – is shown in Figure 4.

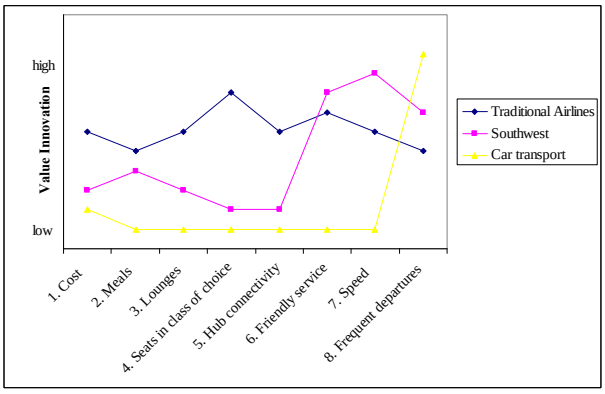

Figure 4: Multidimensional value innovation example in people transportation

Consumer utility levels are connected with six stages of their experience cycles – productivity, simplicity, convenience, risk, fun factor, and environmental friendliness.

7. SOME EXAMPLES OF DEVELOPED TECHNOLOGICAL PLATFORMS

Sustainable development is based on continuous creative cycle performed through basic concepts which:

- Generate system for value innovation
- Design technological platform in the scope of sustainable economical development

Space for creation and sustainable existence of technological platforms could be defined as Red Ocean or Blue Ocean [6], where it is necessary to apply "survival" strategies, as shown in Table 2.

Red Ocean Strategies	Blue Ocean Strategies
• Compete in existing market places • Beat the competition • Exploit existing demand • Make value-cost tradeoffs • Align the whole system of company's activities with its strategic choice of differentiation or low cost.	• Create uncontested market space • Make competition irrelevant • Create and capture new demand • Break value-cost tradeoffs • Align the whole system of enterprise's activities in pursuit of differentiation and low cost.

Table 2: Survivability strategies in Blue and Red Ocean

[2)] Leading eight airline companies at the time

Technological platforms design approach is based on concurrent principles. One principle, which is based on production driven by process, is applied by Toyota, General Motors and Ford motor Company. Other principle, which is applied by smaller volume manufacturer, is production based on product. Which of these two design principles is "better" it is impossible to say, since they span two different corners of the input domain. However, introducing flexibility, increasing value of products, sustainability it becomes more evident that process driven production does hold some advantages.

8. SOME EXAMPLES OF DEVELOPED TECHNOLOGICAL PLATFORMS [1]

Browsing through the history of Fortune 500 companies it is not difficult to follow the line of sustainable prosperity growth by introductions of new methodologies for technological platform design.

In this paper, we would like to mention several examples of developed technological platforms, such as:

1. AUTOSAR (automotive open system architecture) is an example that shows how automotive industry shifted foundation of the embedded code, such low level drivers and diagnostics to their supplier. Meanwhile, all "know how" of the embedded code is still responsibility of the automotive company which can focus on features and performance, rather than non-value added tasks.

2. Microsoft Foundation Classes (MFC) – Visual studio platform (basic and C++) has been allowing programmers to utilize this set of classes. Rather than programming opening and closing dialog box along with all parameters (color, location, etc) programmer can just call function "MessageBox(…)"

3. Global automotive platforms are used by all high volume automotive manufacturers. This concept was initially accepted by Japanese manufacturers, but today all leading automotive companies use this technological platform. Idea is that parts are not unique to the model, but almost (exterior and interior parts still must have differentiation) all parts are shared - Mazda 6, Ford Fusion (American model), Mercury Milan and Lincoln MkZ are all manufactured on the same platform, saving tremendously on the production cost.
4. Six Sigma platform is process that is developed primarily in manufacturing as defect reduction set of analytical tools. Later it has expanded into design for 6-σ (DFSS) and financial institutions as tool for data analysis.

Presently increased globalization and innovation moved the technological platforms from solely engineering design disciplines to everyday domains like fashion, sport and art.
Center for Advanced Technology, on last JUPITER conference, has proposed a joint project – "National technological Platform for Domestic Production Engineering".

REFERENCES

[1] V.R. Milačić., M.V. Milačić Design Methodology for Techological Platforms, JUPITER conference, Belgrade, 2008

[2] S. L. Brown, K. M. Eisenhardt. Competing the EDGE, Harvard Business School Press, Boston , 1998

[3] North American Industry Classification System, Executive offioce of the president, United States, 1997

[4] K. E. Weick, K. M. Sutcliffe, Managing the Unexpeted, Jossey Bass A Wiley Company, 2001

[5] C. Masters, How Boeing Got Going, Time, Sept.17 2007

[6] W.C. Kim, R. Mauborgne, Blue Ocean Strategy, Harward Business School Press, 2005

МОДЕЛИРОВАНИЕ, ПРОЕКТИРОВАНИЕ И РАСЧЕТ В СРЕДЕ КОМПАС-3D

Е.М. Кудрявцев

Аннотация: *В докладе описываются наиболее часто используемые системы (приложения) для моделирования, проектирования и расчета различных механических систем в среде КОМПАС-3D (КОМПлексная Автоматизированная Система) фирмы АСКОН (Автоматизированная Система КОНструирования, Россия):*
- ***Универсальный механизм Express*** *(UMExpress) для моделирования механических систем;*
- ***КОМПАС-SHAFT 2D*** *для проектирования двухмерных тел вращения;*
- ***КОМПАС-ShaftCalc*** *для расчета валов и подшипников, смоделированных в системе* ***КОМПАС-SHAFT 2D****;*
- ***КОМПАС-SHAFT 3D*** *для проектирования шлицевых, резьбовых и шпоночных участков на трехмерных моделях тел вращения.*
- ***КОМПАС-SPRING*** *для проектирования и расчета различных пружин растяжения и сжатия;*
- ***КОМПАС-GEARS 2D*** *для расчета механических передач.*

Ключевые слова: *моделирование, проектирование, систем, КОМПАС*

Система **Универсальный механизм Express** (UMExpress**)** предназначена для экспресс-анализа динамических, кинематических и статических систем спроектированных в КОМПАС-3D V8+ и выше. Система ориентирована на инженеров, занимающихся проблемами анализа динамического поведения машин и механизмов, и является стандартным приложением для системы КОМПАС-3D. Механизмы описываются как системы твердых тел, шарниров и силовых элементов.

В процессе анализа поддерживается непосредственная анимация движения трехмерной модели в процессе расчета. Для анализа доступны практически все необходимые величины: координаты, скорости, ускорения, силы реакций в шарнирах, усилия в пружинах и т.д.

В систему включены следующие возможности:

- работа с линейными силовыми элементами или изменяющимися по гармоническому закону, которые выбираются из фиксированной базы моделей;
- для решения задач кинематики можно задавать равномерное, равноускоренное/равнозамедленное движение, либо изменение по гармоническому закону;
- возможность решения контактных взаимодействий тел, задача решается с условием не пересечения тел при кинематическом или динамическом движении.

В системе **Универсальный механизм Express** доступны:
- параметризация силовых элементов и кинематических соотношений;
- создание анимационных файлов по результатам моделирования движения, анимации сохраняются в видеоролик движения в формате avi;
- построение графиков любой динамический или кинематической характеристики;
- расчет положений равновесия и собственных частот модели в зависимости от параметров.

Обеспечено полное чтение моделей КОМПАС 3D. Визуализация работы и результатов библиотеки создается в отдельном окне и пользователю предоставляется возможность получать визуальную информацию о движении объекта и о его динамических и кинематических характеристиках непосредственно в процессе моделирования.

Эта система позволяет создавать модели объектов, состоящих из неограниченного числа абсолютно твердых тел, на основе трехмерных моделей сборок построенных в системе КОМПАС-3D.

Широкий перечень шарниров позволяет создавать кинематические схемы механизмов практически любой сложности.

Доступны следующие типы шарниров (кинематических пар): поступательный; вращательный; карданов;
- сферический; 6 степеней свободы.

В системе **Универсальный механизм Express** предусмотрены следующие методы анализа динамических моделей.

1. Кинематический и динамический анализ механизмов путем интегрирования автоматически синтезируемых уравнений движения с расчетом всех основных кинематических и динамических характеристик:
- координат, скоростей и ускорений центров масс тел;

Евгений Михайлович Кудрявцев, проф., д.т.н., Московский Государственный Строительный Университет, Москва, Россия

- шарнирных координат, скоростей и ускорений - угловых скоростей и ускорений тел;
- сил реакций в шарнирах;
- сил в активных силовых элементах (пружинах, гасителях и пр.);
- сил и моментов сил инерции для всех тел.

2. Линейный анализ механизмов:
- расчет положений равновесия, значений координат и сил реакций в зависимости от параметров силовых элементов;
- расчет собственных частот и форм колебаний, корней характеристических уравнений и динамических форм;
- определение степени демпфированности системы по динамическим формам;
- определение устойчивости положений равновесия;
- расчет корневых годографов (корней характеристических уравнений в зависимости от параметров), расчет собственных частот в зависимости от параметров.

В системе реализованы два режима работы: **Режим корректировки** (**Режим конструктора**) и **Режим моделирования**.

Режим корректировки или **Режим конструктора** предназначен для создания и корректировки динамической модели.

Режим моделирования предназначен для исследования созданной модели с использованием алгоритмов аналитического анализа динамических систем (модуль **Линейного анализа**) и численного моделирования динамики ССТ.

В функциональные возможности режима входят также средства отображения полученных результатов и процесса моделирования.

Система **КОМПАС-SHAFT 2D** предназначена для параметрического проектирования:
- валов и втулок;
- цилиндрических и конических шестерен;
- червячных колес и червяков;
- шкивов ременных передач;
- звездочек цепных передач.

Система **КОМПАС-ShaftCalc** предназначена для расчета валов и подшипников, смоделированных в **КОМПАС-SHAFT 2D**. Эта система является составной частью интегрированной системы проектирования тел вращения КОМПАС-SHAFT 2D.

С помощью системы **КОМПАС-ShaftCalc** можно:
- выполнять полный спектр прочностных расчетов вала, модель которого построена в КОМПАС-SHAFT 2D, и получать результаты расчета в виде графиков распределения:

– радиальных сил в горизонтальной и вертикальной плоскостях;
– изгибающих моментов в горизонтальной и вертикальной плоскостях (если опора одна, то данная опора считается абсолютно жесткой, т.е. заделкой);
– крутящих моментов;
– нормальных напряжений (по IV теории прочности);
– касательных напряжений при кручении;
– относительного угла закручивания;
– прогиба вала относительно опор в горизонтальной и вертикальной плоскостях (при наличии двух опор);
– коэффициента запаса усталостной прочности.

- получать информацию о значении рассчитанной величины в указанной точке графика (осуществлять трассировку графика);
- формировать отчет о выполненных расчетах в формате FastReport или на листе (листах) чертежа КОМПАС-ГРАФИК;
- выполнять расчет подшипников на грузоподъемность и долговечность, на тепловыделение;
- получать результаты расчета подшипников в виде таблиц в формате FastReport;
- обращаться к модулю выбора материалов для назначения марки материала для рассчитываемого вала.

Система **КОМПАС-SHAFT 3D** предназначена для создания моделей валов, втулок и цилиндрических прямозубых шестерен внешнего и внутреннего зацепления в трехмерном виде. С помощью системы можно построить цилиндрические и конические ступени вала, а также ступени, поперечным сечением которых является многогранник или квадрат.

Система КОМПАС-SHAFT 3D обеспечивает построение шлицевых, резьбовых и шпоночных участков на ступенях моделей. С помощью библиотеки могут быть созданы и другие конструктивные элементы модели - канавки, проточки, пазы и т.д. Сложность моделей и количество ступеней не ограничиваются.

Система КОМПАС-SHAFT 3D позволяет в десятки раз увеличить скорость проектирования трехмерных тел вращения и выпуска документации на них.

Система **КОМПАС-SPRING** предназначена для выполнения проектного и проверочного расчетов цилиндрических винтовых пружин сжатия и растяжения, тарельчатых, конических и фасонных пружин, а также для построения их чертежей (с созданием вида, диаграммы, технических требований, заполнением основной надписи) в среде системы КОМПАС-3D V6 и выше. В основу системы положены **ГОСТ 13764-86**, **ГОСТ 13765-86**, **ГОСТ 3057-90** и методики, разработанные в расчетно-вычислительном центре ОАО «Специальное конструкторское бюро машиностроения» (г. Курган).

Система расчета механических передач **КОМПАС-GEARS 2D** предназначена для выполнения геометрически[и прочностных расчетов следующих типов передач:
- Цилиндрическая передача внешнего зацепления;
- Цилиндрическая передача внутреннего зацепления;
- Коническая передача с круговыми зубьями;
- Коническая передача с прямыми зубьями;
- Червячная цилиндрическая передача;
- Роликовая цепная передача;

- Клиноременная передача;
- Зубчатоременная передача.

Рассматриваемые в докладе системы входят в состав системы КОМПАС-3D V9 в качестве библиотек. Они быстро устанавливается и отличается высокой эффективностью и производительностью. Все рассматриваемые системы предъявляют минимальные требования к компьютеру.

Излагаемые системы это мощные, постоянно совершенствующие специализированные системы автоматизированного проектирования (САПР).

Рассматриваемые системы входят в состав системы КОМПАС-3D V9 и выше в качестве библиотек. Они быстро устанавливается и отличается высокой эффективностью и производительностью. Все рассматриваемые системы предъявляют минимальные требования к компьютеру.

ЛИТЕРАТУРА

[1] Кудрявцев Е.М. КОМПАС-3D V8. Наиболее полное руководство. М.: ДМК-Пресс, 2006 г. 75.4 п.л.

[2] Кудрявцев Е.М. КОМПАС-3D. Моделирование, проектирование и расчет механических систем. М.: ДМК-Пресс, 2008 г. 32.5 п.л

СПЕЦИАЛИЗИРОВАННЫЕ СИСТЕМЫ АВТОМАТИЗИРОВАННОГО ПРОЕКТИРОВАНИЯ В СРЕДЕ КОМПАС-3D

Е.М. Кудрявцев

Аннотация: *В докладе рассматриваются специализированные системы автоматизированного проектирования, облегчающие на порядок представление изображения самых разнообразных машиностроительных объектов в конструкторских документах.*
Описывается работа с наиболее используемыми системами (библиотеками): Библиотека материалов и сортаментов, Библиотека проектирования металлоконструкций, Конструкторская библиотека, Библиотека редукторов, Библиотека подбора электродвигателей, Библиотека условных обозначений Пневмо- и Гидросхем, Библиотека изображения сварных швов и их конструктивных элементов и др.
Библиотеки системы КОМПАС-3D это постоянно увеличивающийся набор библиотек, включающий свыше 50 библиотек. Он постоянно обновляется и совершенствуется.
Система КОМПАС-3D поддерживает одновременную работу с несколькими подключенными библиотеками. Режимы работы с библиотекой могут быть различными (окно, диалог, меню или панель). Как сама система КОМПАС-3D, так и ее библиотеки предъявляют минимальные требования к компьютеру. Библиотеки быстро устанавливается и отличается высокой эффективностью и производительностью.

Ключевые слова: *моделирование, проектирование, систем, КОМПАС*

При проведении проектно-конструкторских работ в различных сферах деятельности, технологической подготовке производства, подготовке конструкторской документации инженеру часто требуется информация о материалах, применяемых при изготовлении изделий. Это могут быть, например, обозначения черных и цветных металлов и их сплавов, неметаллических материалов, смазок и технических жидкостей, их физико-механические, технологические свойства, химический состав, назначение и области применения, возможные заменители и условия замены, используемые сортаменты.

Для этих и других целей в системе КОМПАС 3D имеется соответствующая библиотека - **Библиотека материалов и сортаментов** (далее Справочник). Он позволяет просматривать необходимую информацию и использовать содержащиеся сведения в документах системы КОМПАС для оформления чертежей, спецификаций, расчетов массо-центровочных характеристик моделей.

Справочник может быть использован в качестве самостоятельной программы либо совместно со следующими программами:
- программные продукты ЗАО АСКОН системы КОМПАС;
- КОМПАС-Автопроект и ЛОЦМАН:PLM;
- системы SolidWorks, Inventor, Unigraphics.

Большую часть главного окна системы занимают рабочие панели – это **Панель выбора** и **Информационная панель**.

Панель выбора - это панель, которая предназначена для выбора объектов Справочника из различных классификаторов. Она содержит четыре вкладки: **Материалы**; **Обработки**; **Формы**; **Документы**.

Каждая из вкладок соответствуют способам классификации объектов Справочника.

Информационная панель располагается в правой части главного окна библиотеки и включает, в свою очередь, три панели: **Панель свойств** (вверху), **Параметры объекта** (внизу) и по середине **Панели сортамента**.

Панели сортамента включают панель **Типоразмеры** (слева) и панель (справа) с двумя вкладками: **Сортамент** и **Размеры**.

В рабочих панелях производится выбор материалов, форм, видов обработки и прочих объектов, а также выводится справочная информация. Наименование текущего объекта и его положение в Справочнике отображается в поле **Выбранный объект**.

Библиотека проектирования металлоконструкций обеспечивает возможность:
- формирования геометрической схемы металлоконструкции;
- нанесения профилей на геометрическую схему конструкции;
- построения различных видов соединений простого, крестового, фасонного, паук);
- формирования рабочей документации;
- редактирования конструкции (замена профилей) , обозначений узлов;

Евгений Михайлович Кудрявцев, проф., д.т.н., Московский Государственный Строительный Университет, Москва, Россия

- контроля конструкции.

Формирование рабочей документации предусматривает подготовку следующих видов документов:

- создание рабочих чертежей элементов проектируемой конструкции - деталировка;
- формирование ведомости отправочных марок;
- формирование ведомости метизов;
- формирование выборки металлов;
- формирование сборочного чертежа.

Конструкторская библиотека включает большой набор стандартных конструктивных элементов: болты, винты, гайки, заклепки, конструктивные элементы, манжеты, оси, подшипники, профили, пружины, тела вращения, трубопроводы, шайбы, шпильки, шпонки, штифты, шурупы.

Библиотека редукторов предназначена для подбора и отрисовки редукторов различных типов:

- цилиндрических одноступенчатых;
- цилиндрических двухступенчатых;
- цилиндрических трехступенчатых;
- червячных одноступенчатых;
- червячных двухступенчатых.

Библиотека содержит следующие основные сведения о редукторах: типоразмер редуктора; межосевое расстояние; номинальное передаточное отношение; номинальный крутящий момент на выходном валу в непрерывном режиме работы; номинальные радиальные нагрузки на входном и выходном валах; значение КПД; значение массы редуктора; сведения о климатических исполнений; списание с указанием области применения редуктора; сведения о разработчиках и производителях.

Кроме того, указаны значения номинальных моментов и нагрузок при тяжелых, средних, легких условиях работы, а также приведены параметры конических входных и выходных валов, зубчатых полумуфт редукторов.

Библиотека позволяет выбирать варианта сборки редуктора и вид входного/выходного валов (конические, цилиндрические, полые, в виде части зубчатой муфты).

Библиотека электродвигателей предназначена для подбора и отрисовки электродвигателей различных типов:

- асинхронных трехфазных общего применения,
- асинхронных трехфазных взрывозащищенных,
- крановых и металлургических,
- асинхронных однофазных общего применения,
- двигателей постоянного тока с независимым возбуждением,
- шаговых,
- коллекторных двигателей, применяющихся в бытовой технике различного назначения.

Библиотека содержит следующие основные сведения о трехфазных и однофазных асинхронных электродвигателях: мощность, число оборотов вала, в том числе с учетом скольжения, момент инерции вала, масса, основные монтажные исполнения, климатические исполнения, описание с указанием области применения двигателя, сведения о разработчиках и производителях.

Кроме того, для электродвигателей постоянного тока указаны все возможные сочетания питающих токов и напряжений, для шаговых двигателей и коллекторных приведены некоторые дополнительные параметры.

Библиотека условных обозначений Пневмо- и Гидро схем предназначена для создания различных пневматических и гидравлических, используя условные обозначения данной библиотеки.

Библиотека сварных швов предназначена для автоматизации оформления строительных чертежей, содержащих изображения сварных соединений.

Библиотека автоматически формирует изображения сварных швов следующих типов: стыковой, угловой, тавровый, нахлесточный, точечный, а также катетов сварных швов.

Типы швов, параметры их изображений (длина штрихов, расстояние между ними, тип линий, и т.д.), а также расположение на чертеже и конфигурация определяются пользователем.

Библиотека шаблонов – это файл формата ***.tlm**, содержащий набор шаблонов определенного назначения, например, **Сварка. tlm**.

Шаблон – это элемент библиотеки, созданной с помощью системы **Менеджер шаблонов**.

Шаблон представляет собой совокупность трех составляющих:

- *изображение шаблона* - документ КОМПАС-3D (фрагмент или деталь) – файл формата ***.frw** (***.m3d**);
- *схема переменных параметров шаблона* (фрагмент, деталь или файл с рисунком), содержащая имена переменных параметров;
- *EXCEL- таблица переменных параметров шаблона* – файл формата ***.xls**.

Шаблоны могут быть двухмерными (фрагмент) и трехмерными (деталь). Двухмерный шаблон состоит из одного слоя.

Схема переменных параметров (фрагмент, деталь или файл с рисунком) - это схема, которая содержит изображение конструктивного элемента и имена переменных (размеров и базовых точек), которые нужно выбирать из EXCEL- таблицы переменных параметров.

С системой КОМПАС-3D поставляются различные библиотеки шаблонов: сварные швы, крепежные изделия, профили и т. д.

Используя систему **Менеджер шаблонов**, встроенную в систему,, вы сможете создать целый спектр тематических библиотек КОМПАС-3D и наполнить их необходимыми для работы объектами (шаблонами).

Готовый шаблон может быть вставлен в активный документ КОМПАС-3D. Перед тем, как вставлять шаблон, необходимо выбрать значения его параметров из ряда данных, которые содержатся в EXCEL-файле, ассоциированном с вставляемым фрагментом (деталью). Если шаблон

параметризирован, то после вставки в документ значения его параметров будут соответствовать выбранным значениям переменных.

Шаблон может быть вставлен в документ КОМПАС-3D:

- как набор объектов (отрезков, дуг, кривых и т.д.);
- как не редактируемый макроэлемент;
- как редактируемый макроэлемент.

Разработка нового шаблона сводится к выполнению следующих этапов*:*

- создание фрагмента (детали) КОМПАС-3D;
- формирование в Microsoft Excel таблицы параметров в соответствии с определенными правилами;
- установка связи между параметрами фрагмента (детали) КОМПАС-3D и значениями, заданными в таблице;
- создание схемы, содержащей имена параметров.

ЛИТЕРАТУРА

[1] Кудрявцев Е.М. КОМПАС-3D V8. Наиболее полное руководство. М.: ДМК-Пресс, 2006 г. 75.4 п.л.

[2] Кудрявцев Е.М. Практикум по КОМПАС-3D V8. Машиностроительные библиотеки. М.: ДМК-Пресс, 2007 г. 35.75 п.л

THE FACULTY OF MECHANICAL ENGINEERING KRALJEVO IN THE EUROPEAN STREAM OF INTEGRATION AND TRANSITION OF THE INDUSTRY

N. Nedić, Lj. Lukić, R. Bulatović, D. Petrović

Abstract: *The main task of the Faculty of Mechanical Engineering, Kraljevo throughout its thirty-year development has been to guide its educational and scientific research in accordance with the economic requirements, and together with the network of other engineering faculties contribute to the transformation process of the economy and domestic manufacturing. In the transitional processes, the key component is the knowledge to implement the new technologies, knowledge to implement new work models, knowledge of the technology used to create new knoledge, its distribution and practical application. It is necessary for industry and science to closer cooperate on the common task of creating the new Serbian economy based on the knowledge compatible with the economy of the European Union. In this paper we present the basic elements of the strategic development direction for the educational, the scientific and reasearch tasks of the Faculty of Mechanical Engineering, Kraljevo, as well as its role of the creator of the regional technical end technological advancements.*

Key words: *Faculty of Mechanical Engineering, Kraljevo, European integrations, economy*

1. INTRODUCTION

The main task of the Faculty of Mechanical Engineering, Kraljevo (Fig.1) throughout its thirty-year development has been to guide its educational and scientific research in accordance with the economic requirements, and together with the network of other engineering faculties contribute to the transformation process of the economy and domestic manufacturing. In the transitional processes, the key component is the knowledge to implement the new technologies, knowledge to implement new work models, knowledge of the technology used to create new knoledge, its distribution and practical application. It is necessary for industry and science to closer cooperate on the common task of creating the new Serbian economy based on the knowledge compatible with the economy of the European Union. In this paper we present the basic elements of the strategic development direction for the educational, the scientific and reasearch tasks of the Faculty of Mechanical Engineering, Kraljevo, as well as its role of the creator of the regional technical end technological advancements.

Programs Faculty of Mechanical Engineering, in field design in machinery:

- Railway engineering,
- Earth-moving and transportation systems (Fig.2),
- Termotechnique and environment protection,
- Automatic control and fluid technique,
- Mechanical design and mechanics,
- Computer-aided design,

Production technology:

- Computer-integrated processes,
- Design of machining processes and
- Enterpreneurial engineering and management.

The Faculty of Mechanical Engineering, Kraljevo, has achieved significant result in the Basic research, Innovation projects, and special projects that are of significance for technical, technological, and industrial development of Republic of Serbia.

Prof. Novak Nedić, PhD, dean Faculty of Mechanical Engineering Kraljevo, University of Kragujevac, nedic.n@mfkv.kg.ac.yu,
Prof. Ljubomir Lukić, PhD, vice-dean for science, research, & development, Faculty of Mechanical Engineering - Kraljevo, University of Kragujevac, lukic.lj@mfkv.kg.ac.yu,
Doc. Radovan Bulatović, PhD, vice-dean for education, Faculty of Mechanical Engineering - Kraljevo, University of Kragujevac, bulatovic.r@mfkv.kg.ac.yu,
Prof. Dragan Petrović, PhD, president of the board of governers, Faculty of Mechanical Engineering - Kraljevo, University of Kragujevac, petrovic.d@mfkv.kg.ac.yu.

Fig.1. The Faculty of Mechanical Engineering, Kraljevo - Education & Research institution of regional importance

Fig.2. Sistems for transport and building machinery

2. THE CURRENT ECONOMIC ENVIRONMENT OF SERBIA

Statistics data showing that there is a little bit over 7% university educated people in Serbia is worrisome. Even more worrisome is information that 32.000 of this people is unemployed, and 30% of them are more than 2 year without job, as well as that many of them as well as of the ones that are employed will get employment or are employed in the area of their expertise. In addition, the constant problem of brain drain is present, where high number of people with university degree has left the country. Some analytical data shows that 30 000 to 300 000 people with university degree have left country in the last 10 years. Many of them are very successful in the major foreign companies, looking for the opportunity to capitalize their knowledge received at our universities.

Unfortunately, the state of the mechanical and power engineering, and other related industry branches indicates that the same applies to the experts in mechanical engineering and other technical professions. Although the need for these experts and average salary for engineers are above average salaries, which results in almost full employment, the salary level and the job challenges do not give enough motivation for extra efforts in order to establish themselves within the domestic industry. On the other hand, the young scientists and their professors cannot resist the temptations coming from abroad, and there are not rare examples of them being very successful professors or researchers in other countries, while we struggle with the shortage of the university educated professionals.

The problem of unsatisfactory cooperation of the university and industry, brain drain, migration from the rural and central counties of the country, and insufficient effectiveness of the scientific and research processes had led Europe to the approaches that are summarized in the Bologna process for the post secondary education and Lisbon declaration of effective research and innovation processes that would lead to a balanced regional development.

The cumulative direct foreign investments in Serbia from 2000 to today are at the level of 14 million dollars. It is interesting to point that around 85% of these direct investments originate from European Union, while there are pointer that indicate that in the next 2-3 years the increased investments will come from Russia, mainly as a result of the South Stream contract, privatization of the electro-power industry, air traffic industry, and increased investments in infrastructures. At present, the Russian investments are at modest 400 million dollars. The construction of the gas pipe, the gas reservoir in Banatski Dvor, and reconstruction of the NIS, after the privatization, may increase the employment rate, investments, and technological level of metal processing industries, because there are expectations that these projects would, directly or indirectly employ at least 50 000 employees. In addition, there are preliminary talks on building the gas pipes from Constance to Trieste that will create potential investments of nearly 3 billion dollars. The announcement of reviving the auto industry in Kragujevac, trough the cooperation with Fiat and other potential strategic partners creates significant basis for the affirmation of the engineering profession in Serbia. Privatization of the major metal processing

industrial complexes and cooperation with the strategic partners from the developed countries will revive the manufacturing in factories, that will require the high quality design and technology knowledge in the area of manufacturing engineering in order to stay competitive on the world market.

3. FINANCING THE SCIENTIFIC RESEARCH PROGRAMMES

In the knowledge management field there is no competition. As a consequence, we have for decades the smallest government's allocation for science in Europe. For many years we have been emphasizing that is unthinkable to allocate only 0.3-0.4% from the budget for science, when is well known that the countries such as Finland, Sweden, and Ireland have 10 times grater allocation, and taking into consideration that their GDP is 10 times ours, we have them allocating a 100 times more for science than us. At the European level that average is somewhat smaller and it is thought that the goal of the Lisbon declaration is to be about 3% in average, where one third will come from the budget, and the rest from the private companies. This is very ambitious plan. If we compare ourselves with our neighbors, Montenegro is allocating only 0.1%, while Croatia and Slovenia are at the level of 1%, with Slovenia having 6 times bigger GDP than Serbia (around 25 000 dollars per capita).

The additional allocation source into development and transfer of the scientific knowledge is Seventh Framework Programme of the European Community-FP7, whose budget for the next five years is more than 50 billion euro, which is three times the FP6 budget. Our universities, research institutes, and companies can equally consider applying for these resources with the rest of European countries, in order to concur and implement new knowledge. Through FP7 there will be 13.5 million euro invested into scientific institutions and projects that looks insufficient, but is mach more than what we had from FP6, when there was three times less accepted project. In addition, there investments from the Tempus projects, which amounted to 7 million euro in 2007 and are allocated for the development of new educational programs and training of the university management. More 27 faculties are financed from these investments in Serbia, among them is one project at the Faculty of Mechanical Engineering in Kraljevo Fig.3). It is very important to emphasize that in the budget structure of FP7, the major item, over 40% (20 million euro) from the total budget, is dedicated for the projects related to development of new technologies and new materials, such as information and communication technologies, nanotechnologies, electric power, and transport.

In order to make a significant advancement in the science and education, most of the countries have established the link between the education and science, through joint government ministry that is responsible for both sectors. Recently, at the national level, there has been introduced the European institute for innovations and technologies as well as European scientific advisory board, that are responsible for fulfillment of the program 7 – FP7 goals. In addition, at the national level but open to international community, there have been created numerous scientific and technology parks, business incubators inside the universities, realization centers, industrial clusters, and other flexible forms, that have to enable highly secured financial, material, and human potentials.

Fig.3. Relway - Transport systems for integrated economy in European streams

4. THE STATE IN METAL PROCESSING INDUSTRY

There 4.5 thousand industrial societies in the metal processing end electro industries, with over 133 thousand employees. The structure of these industry braches changes with the time, where the number of the small and medium companies and their influence is growing employing more than 55% of the working force in the branch. This is good indicator because the small companies are agile and can develop faster, but without big industrial complexes (such as Zastava, Prva Petoletka, and others), that could integrate all the production steps for products and compete on the international market, we cannot expect significant results. It is very important for these industrial complexes to speed up their reconstruction process, to find strategic partners or investors, and to take those places in the Serbian and regional economy that they earlier had.

Until then, we should be concerned over the facts that the production in metal processing industry branch, last year, was around 8%, and its contribution to the total Serbian export is only 20.1%. On the other hand, the contribution of metal products and machines import in the total import is near 35%, which indicates our import dependence in this branch. In particular it is worrisome that 12.3% of total workforce is in the branch, with only 6.3% contribution to the GDP, which proves lack of modern machinery to the critical level. This indicates the

need for very serious investments in new machines and technologies (Fig.4 and Fig. 5).

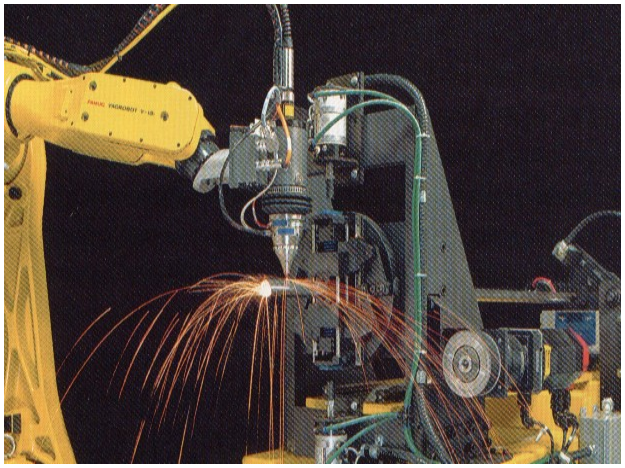

Fig.4. Production technology form metal working processes

Fig.5. Integrated design of product and technology for industrial applications

In 2007, the metal processing and electro industries have exchanged goods with international community valued to 8 billions dollars. Of this, 1.8 billion is exported, and 6.2 billions imported. In comparison to 2006, import and export of the metal processing and electro industries have 50% increased, with the increased deficit, but if the increase comes mostly from the import of the production equipment, the indicators are not that tragic.

5. INTEGRTION OF THE FACULTY OF THE MECHANICAL ENGINEERING, KRALJEVO EDUCATIONAL SYSTEM INTO EUROPEAN STREAM

Faculty of Mechanical Engineering, Kraljevo, has finished accreditation process with the Ministry for science of Republic Serbia, for performing scientific research. Education system for mechanical engineers is directed to creating engineer's profile that will be able to license on the European Union engineering market.

In addition, the teaching programs are designed so that students can take courses at any university that are licensed by the Bologna declaration.

Presently, accreditation of the Faculty of Mechanical Engineering by the standards of the independent Committee for accreditation of universities, collages, and academies of fin art of Serbia is in process, for all four educational levels:

- The basic academic studies,
- Academic studies with diploma – master of engineering, and
- Doctoral studies (PhD).

At the Academic studies with diploma there are four study groups:

- Design and construction of machining systems,
- Power machining and automatic control,
- Production technologies,
- Urban engineering multidisciplinary module.

Faculty of Mechanical Engineering, Kraljevo is capable of providing the high level of teaching, with constant improvement of the communication infrastructure, up to date laboratory equipment, and cooperation with other faculties of mechanical engineering in the country.

We have established fruitful cooperation with the Moscow State University in the area of civil engineering mechanization, and with the State University in Voronez, with which we have student exchange program and other types of university cooperations.

6. THE SCIENTIFIC PROJECTS

Faculty of Mechanical Engineering, Kraljevo has numerous scientific research projects in the area of technology development, that are partly financed by the Ministry of science, in the following areas:

- Integrated product and technology design,
- Design of fluid-controlled components and systems,
- Development of building machinery and transport systems,
- Energy efficiency,
- Development of train cars and the railway transportation system
- Application of modern information technologies in the control of industrial environment (Fig.6).

The Faculty of Mechanical Engineering, Kraljevo, has achieved significant result in the Basic research, Innovation projects, and special projects that are of significance for technical, technological, and industrial development of Republic of Serbia.

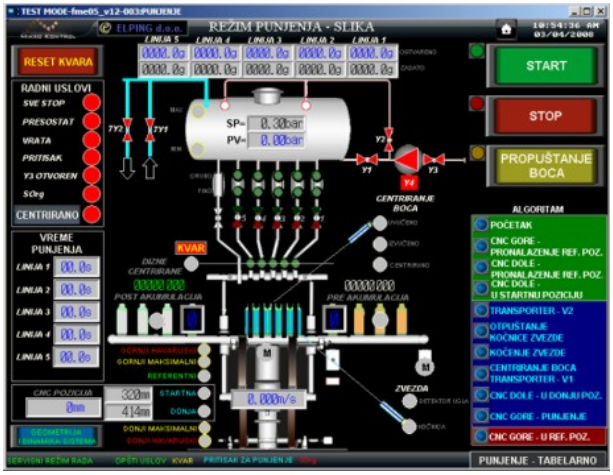

Fig.6. Sistems for automatic monitoring of industrial processes

7. CENTERS OF THE FACULTY OF MECHANICAL ENGENEERING, KRALJEVO

Faculty of Mechanical Engineering, Kraljevo owns a number of centers that are directed toward industrial partnership and cooperation with industrial enterprises, that backbone of the regional and international scientific and technical cooperation. In addition to a number of research centers there the following three regional Centers:

- Regional center for power efficiency established at Faculty of Mechanical Engineering, Kraljevo, and its main task is realizing program for efficient consumption of energy resources, protection of the environment, and education in the management of the energy resources.
- Regional center for research in the area of railway transportation, that was establishes as a result of the international project from the FP6 group that is financed by European Union funds with Faculty of Mechanical Engineering, Kraljevo involvement and in cooperation with the Bulgarian, Romanian, an Austrian universities.
- The Business Technology Incubator is in formation at the Faculty of Mechanical Engineering, Kraljevo using as example The Business Technology Incubator of Technical Faculties Belgrade that has to support the development of the young enterprises and employment of young people with the university degree in the region's innovation businesses (Fig. 7).

These regional centers increase the social significance of the Faculty of Mechanical Engineering, Kraljevo, at the moment when there is ongoing European integrations, transition, and privatizations of the big industrial systems, that are potential users of the results from the scientific research projects. Privatized industrial systems will be the carriers of the development of the scientific institutes and application of the research results in the modern industrial enterprises.

Fig.7. Ongoing Project - The Business Technology Incubator Kraljevo

8. CONCLUSION

The ongoing technical cooperation with big industrial systems and small and medium enterprises in the region, Elektroprivredom Srbije, Railway Transportation enterprise, Surface coal exploitation, the city heating stations, the city public and utility enterprises, made the Faculty of Mechanical Engineering, Kraljevo one of the major business partner in applying modern technologies in industrial practice of regional enterprises.

The Faculty educational system is directed toward creating contemporary educated engineers following the educational practices of European Union countries. Educational program enables that our engineers fulfill all conditions for the European certifications to practice on the most complex development projects.

The spread of the international scientific and research cooperation and creating connections with other research institutions and universities in the country and abroad, enabled the Faculty of Mechanical Engineering, Kraljevo to be the main leader of the regional scientific, research, and industrial advancement both for the region and the Republic of Serbia.

REFERENCES

[1] Lj. Lukić, M. Gašić, R. Rakanović, N. Nedić, V.Karamarković, Lj. Djordjević: Application of Up-to-date Information Technologies in Revitalizing of Production Systems, Plenary paper, Proc. 5th International Conference "Heavy Machinery HM2005", Kraljevo-Mataruška banja, 20.06.-03.07.2005. pp.P1-P6.

[2] N.N.Nedić, D.H.Pršić, Lj.M.Dubonjić: Pressure Equipments safety Units Testing According to European Directive (PED) 97/23 EC, Proc. 5th International Conference "Heavy Machinery HM2005", Kraljevo-Mataruška banja, 20.06.-03.07.2005. pp.I B.49-I B.52.

[3] R.Rakanović: Present State of Railway Vehicles Center Kraljevo, Proc. 5th International Conference "Heavy Machinery HM2005", Kraljevo - Mataruška banja, 20.06.-03.07.2005. pp.I D.1-I D.4.

[4] Lj. Lukić, S. Ivanović: Studija izvodljivosti za osnivanje naučno-tehnoloških parkova u Srbiji - potprojekat "Razvoj tehnološkog inkubatora Kraljevo" Projekat TR-7026A, Mašinski fakultet Kraljevo - Ministarstvo nauke i zaštite životne sredine, 2005-2006.

[5] M.Gašić, M.Vesković, Z.Petrović: The Faculty of Mechanical Engineering in Kraljevo in function of Strategy of Economic and Scientific Development of Environment, Proc. 4th International Conference Heavy Machinery-HM'02, Kraljevo (2002), pp.P.7-P.11.

[6] R.Rakanović: Roll of the Centre for Railway vehicles at the Faculty of Mechanical Engineering in the time to come, Proc. 4th International Conference Heavy Machinery-HM'02, Kraljevo (2002), pp.C.1-C.4.

A SESSION:

AUTOMATIC CONTROL AND FLUID TECHNIQUE

ENERGY SAVING WITH VARIABLE SPEED DRIVES

V. Filipović, N. Nedić, D. Pršić, Lj. Dubonjić

Abstract: *The paper considers problem of energy savings in industry based on variable speed drives. The control valve dissipates hydraulic energy in controlled manner. Recent development in the power electronics, have resulted in an increased applications of electronic variable frequency regulator is to vary motor speed and to avoid hydraulic energy dissipation. In such system the central problem is extremely relevant. The practically important controller has: (i) fixed order (ii) capabilities to deal with amplitude and rate saturation of control signal (iii) possibilities for stochastic time delay compensation.*

Key words: *Energy saving, variable speed drives, fixed order controllers*

1. INTRODUCTION

In current industrial practice the control valves are used extensimely as final control elements to manipulate the process by varying a restriction in a flaming fluid. In essence a control valve is device that dissipates hydraulic energy in controlled manner. The control valve is important final controlling elements and is expected to maintain its position for many years to come. But, main drawback of control valve is energy dissipation [1].

During the last a few decades the alternative final control element is introduced. Normally, recent technical development and cost reduction, primarily in the field of semiconductor technology, have resulted in increased applications of electronic variable frequency drive technology [2]. Variable frequency drive technology employs solid - stable electronic techniques to vary motor speed, thereby varying the operating speed of a piece of equipment (for example centrifugal pumps). The main feature of such solution is energy saving owing the avoidance hydraulic energy dissipation. The main areas of application are: power stations, water distribution systems, HVAC systems, compressors systems etc.

Important part of the problem are, also, control algorithms. On the field of theory the significant progress is established. Kalman work on the linear quadratic regulator problem introduced state space based optimal control for multivariable feedback control systems [3]. In the meantime, also, are developed H^{∞} and $l^{\wedge}$ theory [4] and [5]. Unification H^2 and H^{∞} theory is presented in [6]. Nevertheless, more then 90% controllers in the industry are PID controllers. The main reasons are

(i) optimization methods (H^2, H^{∞}, $l^{\wedge}$) are numerical methods and engineering intuition is absent
(ii) the order of optimal controllers is high (for $l^{\wedge}$ in continuous domain the dimension of optimal controller is infinite)
(iii) the coefficient values of controllers is much different
(iv) small change controller parameters induces back of optimality and, even, instability.

Owing the above fact the controller of fixed structure (low order controllers) such as PID controller is extremely important. But synthesis of fixed structure controllers is very difficult task about which we will discus on the end of the paper.

In the paper we will first describe the control valves with flow characteristic and hydraulic energy dissipation. After that we will consider problem how one can replace control valve with combination: centrifugal pump-AC motor variable speed drive. Here is explained the concept of energy saving. Finally, the problem of fixed order controller synthesis and possible directions of solution is considered.

2. TYPICAL CONTROL LOOP IN INDYSTRY

Port of the controlled process is presented on the next figure.

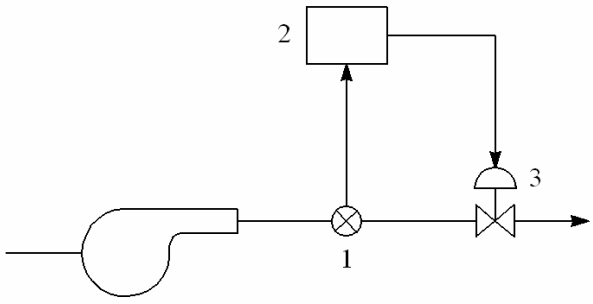

Fig. 1. Typical control loop
1-sensor; 2-PID controller; 3-control valve

Prof. dr Vojislav Filipović, Faculty of Mech.Engineering Kraljevo, filipovic.v@mfkv.kg.ac.yu
Prof. dr Novak Nedić, Faculty of Mech.Engineering Kraljevo, nedic.n@mfkv.kg.ac.yu
Prof. dr Dragan Pršić, Faculty of Mech.Engineering Kraljevo, prsic.d@mfkv.kg.ac.yu
Mr Ljubiša Dubonjić, Faculty of Mech.Engineering Kraljevo, dubonjic.lj@mfkv.kg.ac.yu

We will shortly consider control valve. Flow through the valve is given by [1]

$$F = Kf(x)\sqrt{\frac{\Delta p}{\rho}} \quad (1)$$

where

Δp - pressure drop across the valve

ρ - specific gravity of the flowing liquid (relative to water)

$f(x)$ - valve flow characteristic curve

K -constant

The valve flow characteristic curve depends on the geometrical shape of the plugs surface.
Figure 2 shows the flow capacity characteristics for the various valves.

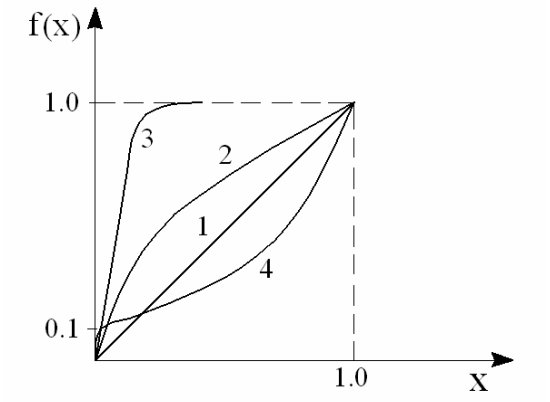

Fig. 2. Flow capacity characteristics for valves
x-valve stem position
1-linear; 2-square root; 3-quic opening; 4-equal percentage

The energy dissipated by the control valve can be calculated as [1]

$$\frac{F_{kg/\min}\Delta p_{bar}}{598{,}9}\ [\text{kW}] \quad (2)$$

The main task of investigation is to eliminate energy losses given by (2). In that sense the main role has variable speed drive.

3. NEW APPROACH

Solution from Fig. 1. can be replaced with the next one which is presented in Fig.3.

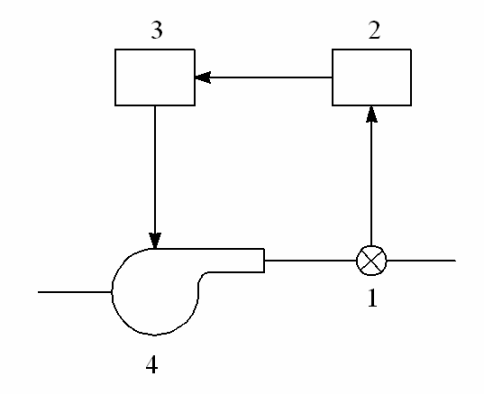

Fig. 3. Solution with frequency regulator
1-sensor; 2-PID controller; 3-frequency regulator; 4-centrifugal pump

New final control elements has a form as in the next figure

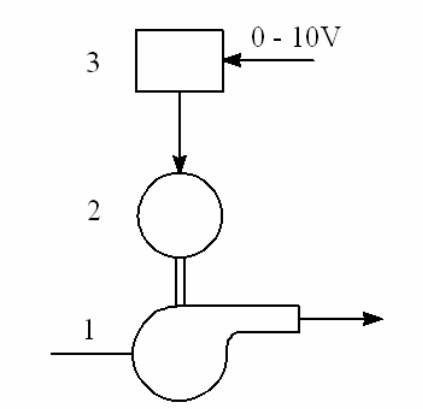

Fig.4. Final control element based on variable speed drift
1-centrifugal pump; 2-AC motor; 3-freqency regulator

The flow regulation now is performed by variation of AC motor speed. The philosophical difference exists between the control valve is a device that dissipates hydraulic energy while a variable speed drive is a device that can regulate the amount of hydraulic energy generated. As we can to see the final control element is more complex then standard control valve.

The centrifugal pump characteristic is given in next figure.

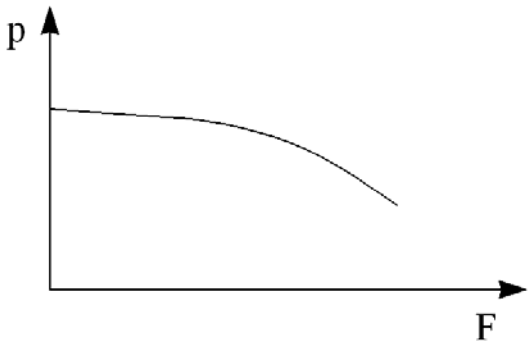

Fig.5. Centrifugal pump characteristic
F-flow; p-pressure

The mathematical model of the centrifugal pump is [8]

$$T_P = h_N \omega(t) - h_V \dot{V}_{(t)}^2 - h_S \frac{\dot{V}_{(t)}^3}{\omega(t)} \quad (3)$$

T_P required torque for the pump

$\dot{V}(t)$ valve flow

$\omega(t)$ angular speed

h_N , h_V , h_S constants

Frequently, the last term can be neglected. The mathematical model of induction is described by forth order coupled nonlinear differential equation [9]. Motor torque is

$$T_{ee} = k_T \psi_{Rd} I_{sq} \quad (4)$$

where ψ_{Rd} motor flux and I_{sq} is transformed stator current.

Finally, the mathematical model of power electrics (variable speed drive) is given as a first order system [9]. On the end of this part of paper we shortly will explain the concept of energy saving by frequency regulators. Torque for centrifugal pump is

$$T_{CP} = k_1 \omega^2(t) \quad (5)$$

and power required by the pump from the motor is

$$P_{CP} = k_2 \omega^3(t) \quad (6)$$

Example: If we reduce speed of motor from 100 to 90 percent to power will reduce

$1-(0,9)^3$

or 27%.

We can conclude that implementation of variable speed drives results in large energy saving. Also, frequency drives provide superior control characteristics due to good resolution and negligible dead time. But, in one thing the control valve is superior. That is shut off capability of control valve.

4. CHALLENGES FOR CONTROL THEORY

From above considerations follows that final control element based on variable speed drive is nonlinear and has dimension of vector states equal to seven. In addition we have model of the process so that resulting model of the system (model of final control element + process model), generally, is high. On the other side, in the industry dominant type of controller is PID controller. The design of such kind controllers is possible for second order of system (for example pole placement strategy). In the last a few years to the problem a controller with fixed structure is devoted much attention. Generally, that is unsolved (open) problem [10]. Let us shortly describe the mathematical side of the problem. Control systems is given on the next figure.

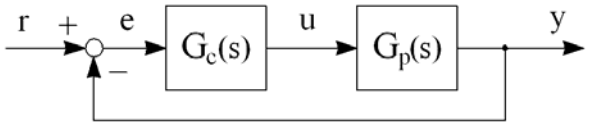

Fig.6. Feedback control systems

$G_c(s)$ - controller; $G_P(s)$ - process

The transfer function $G_P(s)$ and $G_c(s)$ are

$$G_P(s) = \frac{A(s)}{B(s)} \quad (7)$$

where

$$A(s) = a_0 + a_1 s + \ldots + a_m s^m$$

$$B(s) = b_0 + b_1 s + \ldots + b_n s^n$$

The question is: Can we stabilize the process $G_P(s)$ with the controller

$$G_c(s) = \frac{N(s)}{D(s)} \quad (8)$$

if the order of polynomials $N(s)$ and $D(s)$ with fixed orders so that polynomial

$$P(s) = A(s)N(s) + B(s)D(s) \quad (9)$$

is Hurwitz? If constraint on orders of polynomials $N(s)$ and $D(s)$ is absent the solution is well known. The problem with fixed order can be formulated in the next form. Let us suppose that polynomials $N(s)$ and $D(s)$ are

$$N(s) = q_1 + \ldots + q_k s^{k-1} \quad (10)$$

$$D(s) = 1 + q_k s + \ldots + b_l s^{l-k} \quad (11)$$

where k and l are fixed. Question is:
Is there in affine family of polynomials

$$G(s,Q) = \left\{ P(s,q) = P_0(s) + \sum_{i=1}^{l} q_i P_i(s), q \in R^l \right\} \quad (12)$$

stable polynomial. In relation (12)

$P(s) = B(s)$

$P_i(s) = s^{i-1} A(s)$, $i = 1, \ldots, k$

The problem is extremely difficult and solution exist for special cases: P and PI controller

A) P-controller

On Fig. 7. we take

$$G_c(s) = k \tag{13}$$

characteristic polynomial is

$$P(s) = B(s) + kA(s) \tag{14}$$

For next two cases the solution is simple.

(i) Stable process. Solution is based on Nyquist criterion. [11]

(ii) Minimum phase process. In this case $A(s)$ is stable polynomial and $a_m > 0$. The characteristic polynomial is

$$P(s) = B(s) + kA(s) = k(A(s) + \varepsilon B(s)), \tag{15}$$
$$\varepsilon = \frac{1}{k}$$

Follows that $P(s)$ is stable when

$$A(s) + \varepsilon B \tag{16}$$

is stable. The problem is solved in [12] and solution is based on result of Meerov from 1947 year.

B) PI controller

The solution is based on D-decomposition [13] and the main idea of the method is next. Let us suppose that characteristic polynomial for linear system is $p(s,k)$ where k is vector parameter. The boundary of a stability domain is given by the equation

$$p(j\omega,k) = 0,\ \omega \in (-\infty,\infty) \tag{17}$$

that is the imaginary axis (the boundary of instability in the the root plane) is mapped into the parameter space. If $k \in R^2$ then we have two equations (real and imaginary part of [17]) in two variables and can define the parametric curve $k(\omega)$, $\omega \in (-\infty,\infty)$ defining a boundary of the stability domain. Moreover, the curve $k(\omega)$ divides the plane into root invariant regions i.e. regions with a fixed number of stable and unstable roots of $p(s,k)$.
The further development of method is given in [14] and [15]. The extension to matrix case is done recently [16].

C) PID controller

The main condition for stability of linear invariant system is that characteristic polynomial is Hurwitz polynomial. There are several other equivalent conditions for ascertaining the Hurwitz stability of a given real polynomial. The classical Hermite-Biehler theorem is an alternative for studying the parametric robust stability problem, i.e. the problem of guaranteeing that the roots of a given Hurwitz polynomial continue to lie in the left – half plane under real coefficient perturbations. The generalization of Hermite–Biehler theorem is given in [17]. Such generalization gives a solution to the problem of feedback stabilization of a given linear bime invariant plant by a PID controller. The solution characterizes the entire family of stabilizing controllers in terms of a linear programming [18].

D) Input constraints

Classical control valve has nonlinearity in the form of saturation. The new final element with variable speed drive has, also, nonlinearity which is presented in the next figure.

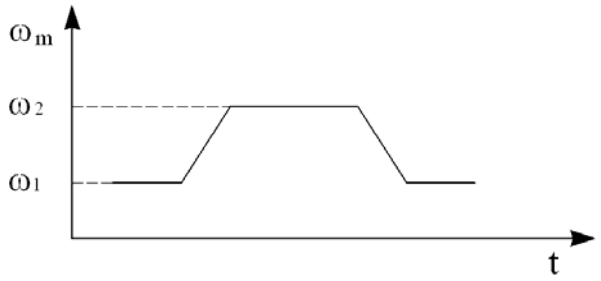

Fig. 7. Speed profile for AC motor ω_m - speed of motor

During the start-up phase, by the ramp limiter, the maximum acceleration/deceleration rates can be specified by the user. The main reason for such approach is keeping the motor current and the DC-bus voltage within the limits during the acceleration/deceleration phase. In described situation we have two nonlinearities: saturation nonlinearity which is defined by ω_1 and ω_2 speeds and rate saturation. Such constraints make the control problem very difficult. The amplitude saturation can be resolved by hybrid controllers [19] – [20]. The output regulation with actuators subject to amplitude and rate saturation is considered in [21].

E) Networked control systems

A networked control system is a feedback control system where information from the sensors and the controllers is sent over an electronic communication network [22]. The system is presented on the next figure

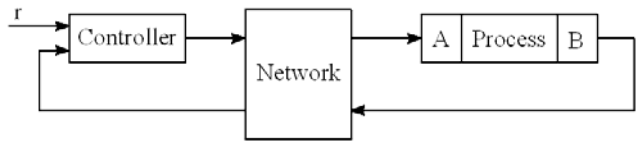

Fig. 8. A black diagram of the networked control system
r - reference signal; A-actuator; S-sensor

Networked control systems offer reduced cost and relatively simple implementation, as well as greatly increased flexibility. But such approach is not without drawbacks. At last, communication networks can introduce nontrivial delays in the form of stochastic process. In that case the system can be described with jump linear Markovican system [23] and analysis and design of controllers become difficult task.

Finally, the practically relevant controller for the energy saving system has

1. fixed order
2. capabilities to deal with amplitude and rate saturation of control signal
3. possibilities for stochastic time delay compensation

5. CONCLUSION

In this paper we are considered the important problem of energy saving in industry. The approach is based on replacing, where that possible, classical final element (control valve) which has drawback that dissipates hydraulic energy, with new type of final element (centrifugal pump + AC motor + frequency regulator) which eliminates the drawback. It is emphasized that control problem in new situation is nontrivial (that ss, of course, valid for general control problem). The controller must to be of fixed order and overcome problems with nonlinearities (amplitude and rate saturation). Also, in networked control systems the compensation of stochastic problem is relevant.

REFERENCES

[1] G. Bordon and P.G. Friedmann, “Control Valves”, Research Triangle Park, ISA, 1998

[2] B.K. Bose, “Modern Power Electronics and AC Drives”, New Jersey, Prentice – Hall, 2002

[3] R.E. Kalman, “When is a control system optimal?”, Journal of Basic Engineering, Transactions of the ASME, Series D, pp.456 – 470, 1964

[4] K. Zmov, J.C. Doyle and K. Glover, “Robust and Optimal Control”, New Jersey, Prentice – Hall, 1996

[5] A.E. Barabanov, “Design of Min – Max Controllers”, Sankt Peterburg, University Sankt Peterburg, 1996

[6] B. Hassibi, A.H. Sayed and T. Kailath, “Indefinite Quadratic Estimation and Control”, Philadelphia, SIAM, 1999

[7] L. Keel and S.P. Bhattacharyya, “Robust, fragile or optimal?”, IEEF Trans. Automatic Control, vol. 42, pp. 1098 – 1105, 1997

[8] S. L. Dixon, “Fluid Mechanics, Thermodynamic of Turbomachinery”, Oxford, Pergamon Press, 1966

[9] R. Krishnan, “Electric Motor Drives. Modeling Analysis and Control”, New Jersey Prentice – Hall, 2001

[10] V. Blondel, E. Sontag, M. Vidyasagar and J. Willems, “Open Problems in Mathematical Systems and Control Theory”, London, Springer – Verlag, 1999

[11] G. F. Franklin, J. D. Powell and A. Emami – Naeini, “Feedback Control of Dynamic Systems”, Reading, Addison – Wesley, 1986

[12] M.V. Meerov, “Design of Dynamic Control Systems with High Accuracy”, Moskva, Fizmattiz, 1959

[13] Yu. I. Nejmark, “Stability of linearized Systems”, Sankt Peterburg, LKVVIA, 1949

[14] D. Mitrovic, “Graphical analysis and synthesis of feedback control systems. I – Theory and analysis; II – Synthesis, III – Sampled – data feedback control systems”, AIEE Transactions (Application and Industry), vol. 77, pp. 476-496, 1959

[15] D. Siljak, “Nonlinear systems: the parameter analysis and design”, New Jork, Wiley, 1969

[16] E.N. Gryazina and B.T. Polyak, “Stability regions in the parameter space: D – decomposition revisited”, Automatica, vol. 42, pp. 13 – 26, 2006

[17] M.T. Ho, A. Datta and S.P. Bhattacharyya, “Generalization of the Hermite – Biehler theorem”, Linear Algebra and its Applications, vol. 302 - 303, pp. 135 – 153, 1999

[18] M.T. Ho, A. Datta and S.P. Bhattacharyya, “Robust and non – fragile PID controller design”, International Journal of Robust and Nonlinear Control, vol. 11, pp. 681 – 708, 2001

[19] V. Z. Filipovic, “Robust switching controllers in the presence of model uncertainty and saturation”, International Journal of Information and System Sciences, vol. 4, pp. 233 – 240, 2008

[20] V. Z. Filipovic, "Switching control in the presence of constraints and unmodeled dynamics", Chapter in: H. Aschermann (Ed.). New Approaches in Automation and Robotics, Vienna, I – Tech, 2008

[21] Z. Lin, "Semi – global stabilization of linear systems with position and rate limited actuators", Systems and Control Letters, vol. 30, pp. 1 – 11, 1997

[22] X. Jiang, Q.L. Han, S. Liu and A. Xue, "A new H^{∞} stabilization criterion for networked control systems", IEEE Trans. Automatic Control, vol. 53, pp. 1025 – 1032, 2008

[23] V.Z. Filipovic, "Exponential stability of stochastic switched systems", Transactions of the Institute of Measurement and Control, accepted for publications, 2008

LOADING COMPUTATION OF SLIDING CONTACTS BETWEEN VANE AND HOUSING OF THE VANE PUMP

N. Nedić, R. Petrović, S. Prodanović

Abstract: *In this paper, the vane pump with constant capacity is considered, because vast usage in industry. This is double-flow vane pump. The paper is focused on contact place between vane pick and housing, so called "sliding contact", as most stressed point. For that purpose, loading computation and analysis of sliding contacts are carried out using mathematics models of geometric dimensions and forces.*

Key words: *Pump geometric, forces on vane, sliding contact.*

1. INTRODUCTION

Vane pump has vast usage in industry. This is volumetric pump and it can be made with changeable and constant capacity. It will be explained later, that it is composed of stator, rotor and vanes, which are put into grooves made in rotor.

When we talk about pumps with changeable capacity it has stator with circular inner surface, while at types with constant capacity, we have elliptic shape. During rotor rotating, chambers are creating in pump, and they are filling on absorbing side, and empting on pressing side. Chambers are bounded with surfaces of rotor, stator and lateral surfaces of two adjacently vanes, which are overlapping on surface of stator with their picks and sliding over it.

Goal of this work is expressing resultant radial force on vane in function of time, in the contact point between vane and stator (sliding contact), as most stressed point.

In order to introduce sliding contact of pump we used earlier mathematics models of its geometry and forces on vane in function of mentioned geometry [1].

In this research we considered vane pump with constant capacity, i.e. double-flow vane pump.

2. DESIGN AND FUNCTIONING OF DOUBLE-FLOW VANE PUMP

At first, it is very important to emphasize difference between single-flow and double-flow vane pump. Single-flow pump has one period of absorbing and pressing of fluid, and double-flow pump has two periods.

Design of double-flow pump is based on elliptic shape of stator's inner surface, which enables two absorbing and two pressing intervals, as we can see in figure 1.

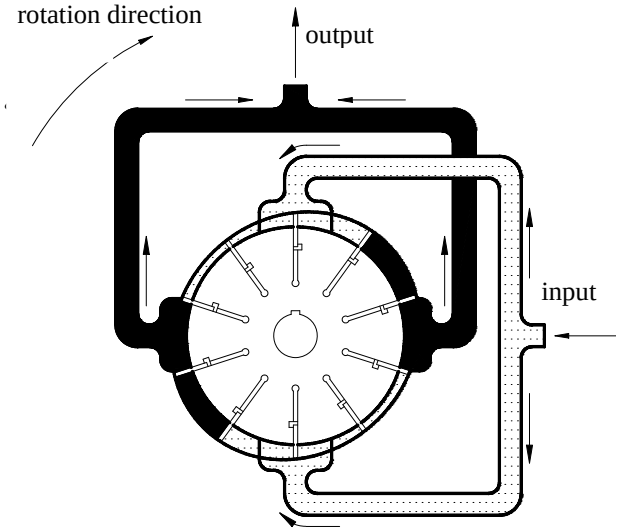

Figure 1. Double-flow vane pump

On input sides, fluid is filling space between rotor and stator in following way: with volumen increasing of that chamber, vacuum is being made in it and chamber is being filled with fluid.

With further rotating, chamber i.e. fluid is reaching minimal volume, and that is influencing rise of hydrostatical pressure, and it is flowing out under the pressure at output side.

Although, we can see that vanes are put into grooves and radially movable. Front edge of vane is in contact with housing (stator).

Pressure in front p_1 and pressure behind vane p_2 are reacting on each vane. Motion pressure p_B is pushing vane and inner vane through hole, so stator is pressed on whole interval of rotation angle φ. Design of this pumps provides relieving of bearings, because all radial loading are distributed symmetrically [1].

Novak Nedić, Faculty of Mechanical Engineering Kraljevo, nedic.n@mfkv.kg.ac.yu
Radovan Petrović, Faculty of Mechanical Engineering Kraljevo, petrovic.r@mfkv.kg.ac.yu
Saša Prodanović, Faculty of Mechanical Engineering East Sarajevo, University of East Sarajevo, elsing123@yahoo.com

3. LOADING COMPUTATION OF SLIDING CONTACTS BETWEEN VANE AND HOUSING

3.1 Pump geometry

Stator is eliptic, so its radius R_H is changing with change of rotation angle φ (figure 2.).

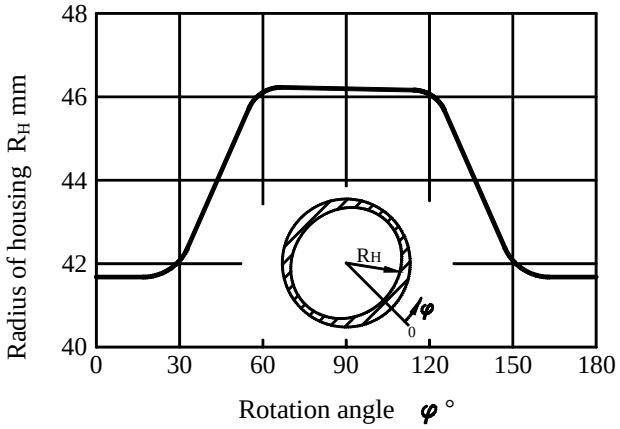

Figure 2. Change of radius of housing in function of rotation angle

Stator's symmetry of inner surface, as we said, is causing symmetric radial loading, radius change R_H and load depending on φ we are observing half of interval, i.e. from $0^o - 180^o$. That interval we share on zone for absorbing, splitting and pressing. In figure 2. we can see that R_H is constant when angle is $0^o - 20^o$ (splitting zone), then it is increasing in absorbing zone to maximum ($\varphi = 65^o$). In zone between absorbing and pressing zone it is little decreasing. (i.e. to $\varphi = 115^\circ$) and there is pri-compression. On the end of compression R_H achieves minimum and then $\varphi = 160^o$, after that it is constant again up to 180^o.

Examined pump has 12 vanes, so the circle is shared in equal parts, and between adjacent vanes we have angle $\varphi = 30^o$. There is difference in pressures in front and behind of the vane. In order to avoid sudden changes of pressure, there are grooves on input (absorbing) and output (pressing) openings of the pump referring to the rotation direction. They are used for relieving of pump and providing its stabile work. In the zone of minimal decreasing R_H, i.e. from $105^o - 115^o$ pressure behind vane p_2 is increasing gradually to its maximum [1].

3.2 Mathematics modeling

3.2.1 Geometric measures in the sliding contact

Computing of these values is necessary in order to allow us to compute forces between vane and houses. It is important to determinate radius of housing in contact point R_H, because it is changing with change φ. Following that we are using geometric model of housing contour in contact point (figure 3.).

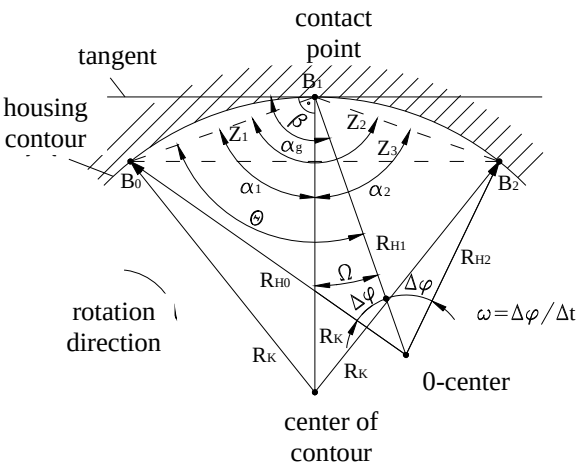

Figure 3. Housing contour in contact point

Radiuses of stator in this figure are signed in referring to middle point "0". R_{H1} is radius of housing in current vane position, R_{H0} and R_{H2} are radiuses in time, i.e. rotation φ, in front and behind R_{H1}. However, we determinate radius of curve (housing contour) in contact point R_K and opening angle β. This angle β is angle between tangent on stator and vane axis in contact point, as it is shown in figure 3. In order to determinate R_K and β we use auxiliary distances Z_1, Z_2 and Z_3 and auxiliary angles α_1, α_2, α_g, θ and Ω.
From figure 3. we have angles:

$$\beta = 90^o + \Omega \qquad \text{and} \qquad \Theta = \alpha_1 + \Omega$$

(3.1.)

Ω is angle between vane axes in contact point and radius of curve in that point. We determinate opening angle β using ratios between angles:

$$\beta = 90^o + \Theta - \alpha_1$$

(3.2.)

Auxiliary distances can be expressed using cosines theorem in following way:

$$Z_1^2 = R_{H0}^2 + R_{H1}^2 - 2 \cdot R_{H0} \cdot R_{H1} \cdot \cos\Delta\varphi$$

(3.3.)

$$Z_2^2 = R_{H1}^2 + R_{H2}^2 - 2 \cdot R_{H1} \cdot R_{H2} \cdot \cos\Delta\varphi$$

(3.4.)

$$Z_3^2 = R_{H0}^2 + R_{H2}^2 - 2 \cdot R_{H0} \cdot R_{H2} \cdot \cos 2\Delta\varphi$$

(3.5.)

$$Z_3^2 = Z_1^2 + Z_2^2 - 2 \cdot Z_1 \cdot Z_2 \cdot \cos\alpha_g$$

(3.6.)

Based on equation (3.6.) we obtain angle α_g

$$\alpha_g = \arccos\frac{Z_1^2 + Z_2^2 - Z_3^2}{2 \cdot Z_1 \cdot Z_2}$$

(3.7.)

Also we have:

$$R_{H0}^2 = Z_1^2 + R_{H1}^2 - 2 \cdot Z_1 \cdot R_{H1} \cdot \cos\Theta$$

(3.8.)

$$\Theta = \arccos\frac{Z_1^2 + R_{H1}^2 - R_{H0}^2}{2 \cdot Z_1 \cdot R_{H1}}$$

(3.9.)

We use angle α_1 to express R_K

$$R_K^2 = Z_1^2 + R_K^2 - 2 \cdot Z_1 \cdot R_K \cdot \cos\alpha_1$$

(3.10.)

$$R_K^2 = Z_2^2 + R_K^2 - 2 \cdot Z_2 \cdot R_K \cdot \cos\alpha_2$$

(3.11.)

Because $\alpha_g = \alpha_1 + \alpha_2$, we computing angle α_1 on following way:

$$\frac{Z_2}{Z_1} = \frac{\cos\alpha_2}{\cos\alpha_1} = \frac{\cos\alpha_g \cdot \cos\alpha_1 + \sin\alpha_g \cdot \sin\alpha_1}{\cos\alpha_1} =$$

$$= \cos\alpha_g + \sin\alpha_g \cdot tg\alpha_1$$

(3.12.)

$$tg\alpha_1 = \left(\frac{Z_2}{Z_1} - \cos\alpha_g\right)\frac{1}{\sin\alpha_g} \quad \Rightarrow$$

$$\alpha_1 = arctg\left[\left(\frac{Z_2}{Z_1} - \cos\alpha_g\right)\frac{1}{\sin\alpha_g}\right]$$

(3.13.)

Based on equation (3.10) we express R_K.

$$Z_1^2 - 2 \cdot Z_1 \cdot R_K \cdot \cos\alpha_1 = 0$$
$$Z_1\left(Z_1 - 2 \cdot R_K \cdot \cos\alpha_1\right) = 0 \quad \Rightarrow$$
$$Z_1 - 2 \cdot R_K \cdot \cos\alpha_1 = 0$$

$$R_K = \frac{Z_1}{2 \cdot \cos\alpha_1}$$

(3.14.)

On that way we obtained requested radius of curve R_K step by step using measurable values R_{H0}, R_{H1}, R_{H2} and $\Delta\varphi$ [1].

3.2.2 Forces

More forces have an effect on vane. There are forces of pressure which exert above and under vane, cenrtifugal forces which issued as effect of vane rotation, acceleration force and friction force. Resultant radial force is consisted of all of these forces and they appeares during rotation of rotor. However, because of necessary simplification, which we have to apply in order to perform simulation of resultant force, in this paper we will consider forces of pressure which exert on vane from above and under, because they have the bigest part in mentioned force. Geometric position in contact point is shown in figure 4.

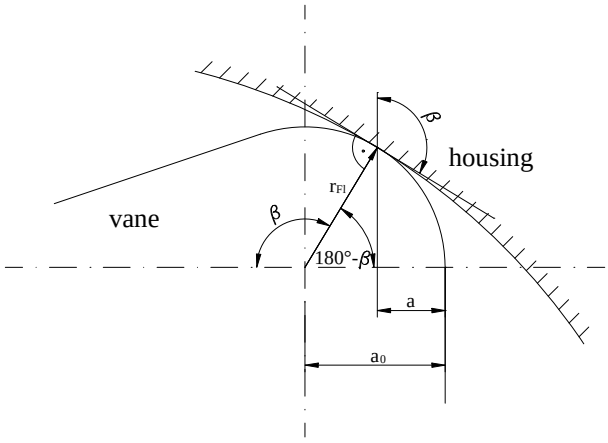

Figure 4. Geometric position in contact point

Distance „a“ is reach between contact point and front edge of the vane and it has influence on values of forces components on the top of the vane, so we determinate them depending on this distance. Equation for „a“ is obvious from figure 4.:

$$a = a_0 - r_{fl} \cdot \cos\left(180^o - \beta\right)$$

(3.15.)

In order to express all of these components we project them to normal direction in contact point [1]. Resultant radial force F_R between vane and housing is addition of all of the components forces.

3.2.2.1 Forces of pressure from above

During effect of these forces on vane there is pressure in front and behind contact point i.e. from fluid from two near chambers which are separated by that vane. Geometric position of the forces on upper side of vane is shown in figure 5.

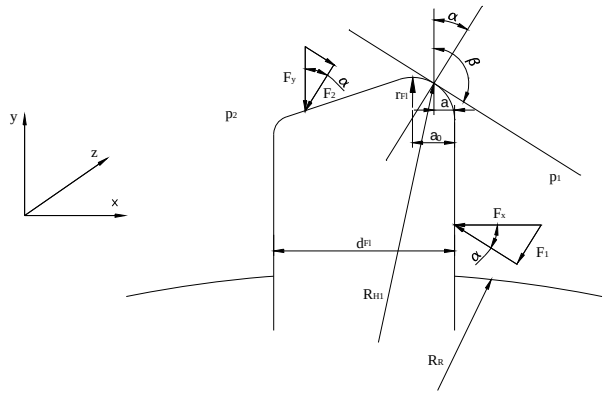

Figure 5. Forces on the upper side of the vane

We can see that vertical and horizontal force have effect on lenght of vane L_{Fl}. Considering pressures on vane p_1 and p_2, than radiuses of housing R_{H1} and rotor R_R, and determined distance „a“ vertical and horizontal force of pressure can be expressed using next equations:

- Vertical: $F_y = L_{Fl}\left[\mathrm{a}\cdot p_1 + (d_{Fl} - \mathrm{a})p_2\right]$

(3.16.)

- Horizontal: $F_x = L_{Fl}(p_1 - p_2)(R_{H1} - R_R)$

(3.17.)

After their projection on normal direction in contact point we have folowing equations:

$$F_1 = F_x \cdot \sin\alpha = L_{Fl}(R_{H1} - R_R)(p_1 - p_2)\sin\alpha$$

(3.18.)

$$F_2 = F_y \cdot \cos\alpha = L_{Fl}\left[p_2 \cdot d_{Fl} + \mathrm{a}(p_1 - p_2)\right]\cos\alpha$$

(3.19.)

After addition these forces we obtain resultant force on upper side of the vane [1]:

$$F_{Do} = F_1 + F_2$$

(3.20.)

3.2.2.2 Forces of pressure from below

Inner vane is put into vane and drive pressure p_B has effect in vane's hole. That providing force of pressure F_A between vane and housing. Force F_B on the remainder vane depends on pressure state behind vane p_2. These forces have effect on the vane thickness d_{Fl} and appropriate lenghts. They are expressed on folowing way:

$$F_A = p_B \cdot L_A \cdot d_{Fl}\ ,$$
$$F_B = p_2(L_{Fl} - L_A)d_{Fl}$$

(3.21.)

After their projection on normal direction and addition we have resultant force on vane from below [1]:

$$F_{Du} = (F_A + F_B)\cos\alpha$$

(3.22.)

3.3 Simulation of forces on the vane

Resultant force on the vane depends on rotation angle φ, because all vanes is in different position in regard rotor during the time. In order to perform simulation of forces on vane, we will express angle β in function rotation angle φ in equation (3.15.), which depends on time t. Like in early considerations, we observe change of loading in function of φ on the half of interval i.e. from $0^o - 180^o$.

Change of angle β during rotation is analysed using software CATIA V5R14, as we san see in figures 6. and 7.

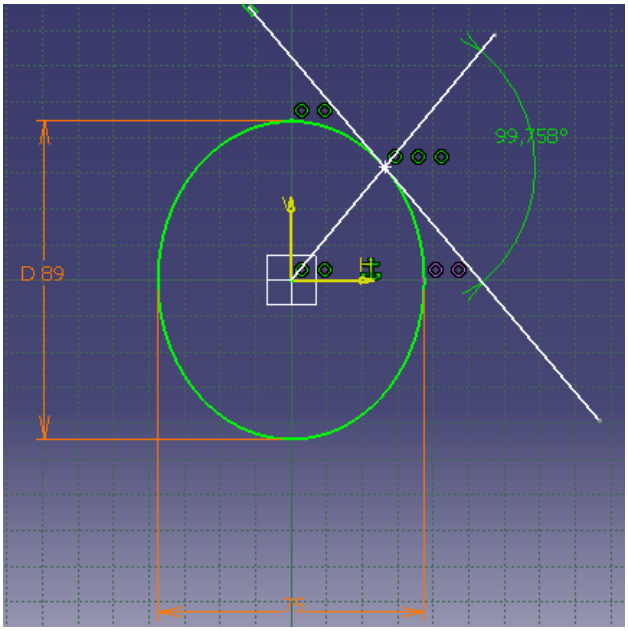

Figure 6. Display of maximum value of angle β (β_{max})

In figure 6. angle β_{max} = 99,758° is shown, and in figure 7. β_{min} = 80,242°.

Analysis was performed on model of pump LVP 41087, from manufacturer „VIKING PUMP“ from Cedar Falls, Iowa. In this paper we used pump caracteristics, which was available [3]. However, some inner dimensions of rotor and vanes wasn't available because manufacturers didn't give it, so we will simulate forces on vane using adoptid dimensions (which wasn't available).

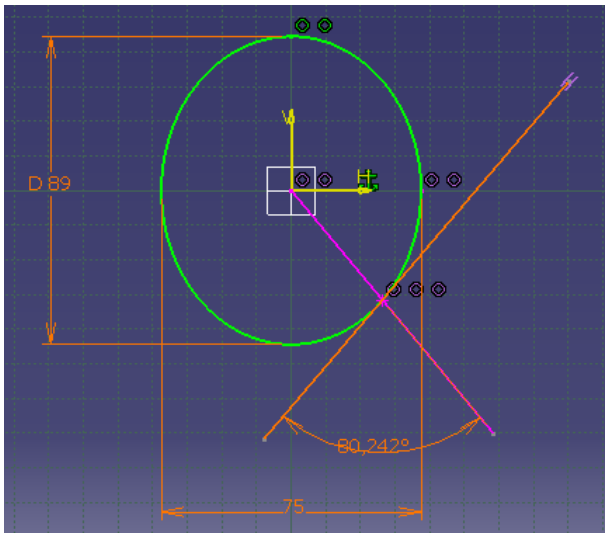

Figure 7. Display of minimum value of angle β (β_{min})

Adopted values are given below:
R_{H1} = 40 mm, R_R = 30 mm, d_{Fl} = 5 mm, r_{Fl} = 2 mm,
a_o = 1,5 mm, L_{Fl} = 110 mm, L_A = 30 mm, p_1 = 14 bar,
p_2 = 10 bar, p_B = 10 bar.
It is important to say that named pressures are changing their values during one revolution so we take in this case their maximum values (adopted for p_2 and p_B).

Basic characteristics of this pump model are:

- Capacity: Q = 0 – 36 m^3/h,
- Pressure: p = 0 – 14 bar,
- Temperature: t = -51 – 260 °C,
- Rated number of revolutions: n = 950 obr/min.

Therefore, angle $\beta \in [\beta_{\min}, \beta_{\max}]$ and respecting obtain values $\beta \in \left[80{,}242 \;,\; 99{,}758\right]$ during period T. This period represents a half of the one revolution time t_1:

$$T = \frac{t_1}{2}$$
(3.23.)

Using rated number of revolutions
n = 950 obr/min = 15,83 obr/s we have follow expressions:

$$t_1 = \frac{1}{15{,}83} \cong 0{,}06s$$
(3.24.)

$$T = \frac{0{,}06}{2} = 0{,}03s$$
(3.25.)

We made very small approximation and take that angle β has sinusoidal character, as we can see in figure 8. Based on that and figures 6. и 7. we obtained follow equation:

$$\beta(\varphi) = 90^\circ + \left(\beta_{\max} - 90^\circ\right)\sin 2\varphi$$
(3.26.)

and respecting value β_{max} we have next equation:

$$\beta(\varphi) = 90^\circ + 9{,}758^\circ \sin 2\varphi$$
(3.27.)

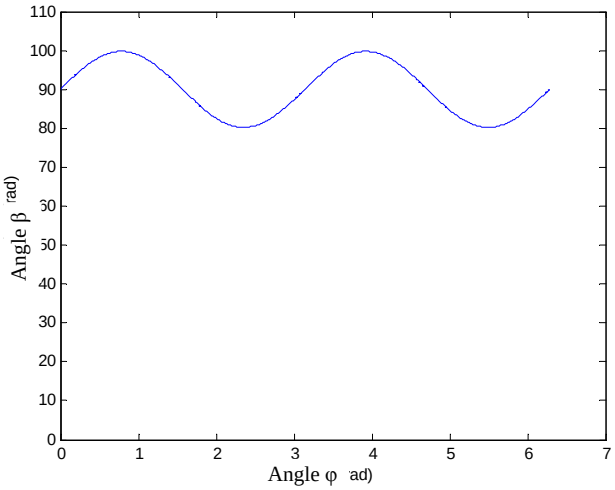

Figure 8. Angle β in function of rotation angle φ

Change of angle φ in time is obtained based on rated number of revolutions:

$$\varphi(t) = 6000t$$
(3.28.)

because period T = 0,03 s is time of a half of the one revolution, i.e. 180°.

Therefore, change angle β in time is:

$$\beta(t) = 90^\circ + 9{,}758^\circ \sin(12000t)$$
(3.29.)

Now, we have equation (3.15.) in follow form:

$$a(t) = a_0 - r_{fl} \cdot \cos\left\{180^\circ - \left[90^\circ + 9{,}758^\circ \sin(12000t)\right]\right\}$$

(3.30.)

Based on equation (3.30.) and well-known and adopted values and dimensions of pump, we can express change of resultant radial force on vane F_R.

$$F_R = F_{Du} - F_{Do}$$
(3.31.)

$$F_R(t) = \left[p_B L_A d_{Fl} + p_2 (L_{Fl} - L_A) d_{Fl}\right] \cdot \cos\left(9{,}758^\circ \sin(12000t)\right) - L_{Fl}\left\{(R_{H1} - R_R)(p_1 - p_2) \cdot \sin\left(9{,}758^\circ \sin(12000t)\right) + \left[p_2 d_{Fl} + \left(a_0 - r_{fl} \cos\left(90^\circ - 9{,}758^\circ \sin(12000t)\right)\right)(p_1 - p_2)\right] \cdot \cos\left(9{,}758^\circ \sin(12000t)\right)\right\}$$
(3.32.)

Next equation shows dependence of resultant radial force of time for concrete example of named pump model for one group of pump characteristics. As we said, some of those characteristics are well-known but some characteristics are evaluated and adopted in order to show concept of this mathematical model.

$$F_R(t) = 550 \cdot \cos\left(9{,}758^\circ \sin(12000t)\right) -$$
$$-110\left\{4\sin\left(9{,}758^\circ \sin(12000t)\right) +\right.$$
$$+\left(5+\left(1{,}5-2\cos\left(90^\circ - 9{,}758^\circ \sin(12000t)\right)\right)0{,}4\right)\cdot$$
$$\left.\cdot\cos\left(9{,}758^\circ \sin(12000t)\right)\right\}$$
(3.33.)

Based on equation (3.33.) and using software MATLAB 7 we obtain graph from which we san see change of force F_R in time t (figure 9.).

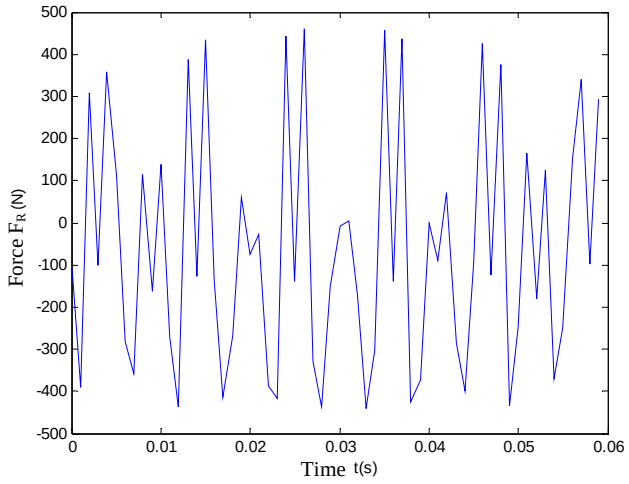

Figure 9. Resultant radial force on vane in function of time

From graph in the figure 9. we note that force F_R has negative values during one revolution too, which can mean that there wouldn`t be a contact between vane and stator (housing) on those intervals. Naturally that is inadmissible, so we assemble spring under the vane which compensates a lack of operating pressure p_B in those intervals. That negative value of force F_R can be used in selection of mentioned spring. Symmetry of this graph in regard time momentary t = 0,03 s, i.e., $\varphi = 180^o$ bears out consideration of loading change on half of the one revolution.

4. CONCLUSIONS

Although these pumps are substantially accomplished and prooved in exploatation, results of this simulation can be used for developing of better forms and selection more suitable materials of parts in sliding contact and all in the aim of improving quality of their operation and extending their lifetime.

Approximations in computation are applied by omiting less sygnificant factors, than we have results which have minor deviation from real values and they can be guessed as valid. That was done based on previously established (measured) values. Because of proportional assimilation of some dimensions and pressures, this simulation represent a model (principle) how we can show resultant force on vane using software MATLAB 7.

It is very important to mention flexibility of this simulation method in appliance in any tip of double-flow vane pump, and with small corrections on single-flow vane pump too.

REFERENCES

[1] Harald Ortwig : Analytische und experimentelle Untersuchung hochbelasteter Linienförmiger Gleitkontakte in einer Flügelzellenpumpe, Ahen

[2] Georgije Hajdin : Fluid Mechanics, University of Belgrade, 1992

[3] Catalogue:Viking Pump, Cedar Falls, Iowa

DYNAMIC MODELING OF THE MECHANISM WITH BARS BELONGING TO THE CONSTRUCTION UNIVERSAL MOBILE ROBOT WITH 7 DEGREES OF FREEDOM

A. Bruja, M. Dima, C. Frâncu

Abstract: *In this paper is presented a dynamical study of positioning and orientation mechanism of the Construction Universal Mobile Robot with 7 degrees of freedom. In this study were determined the reactions in kinematical joints of the mechanism for every working position. The kinetostatic is the method of choice and the results are obtained by using the computer.*

Keywords: *modeling, mehanism, mobile robot*

1. INTRODUCTION

The mobile robot for construction was designed to complete different technological tasks in construction works like: masonry and finishing, making it the central component of a robotized flexible cell for construction of residential buildings of 1...3 floors.

The mobile robot for construction is represented in figure 1 and is composed of an orientation mechanism with 2 DOF's RR (axes I and II), a positioning mechanism with 3DOF's TTR (axes III, IV and V) and chassis with mechanisms for moving, steering and wedging.

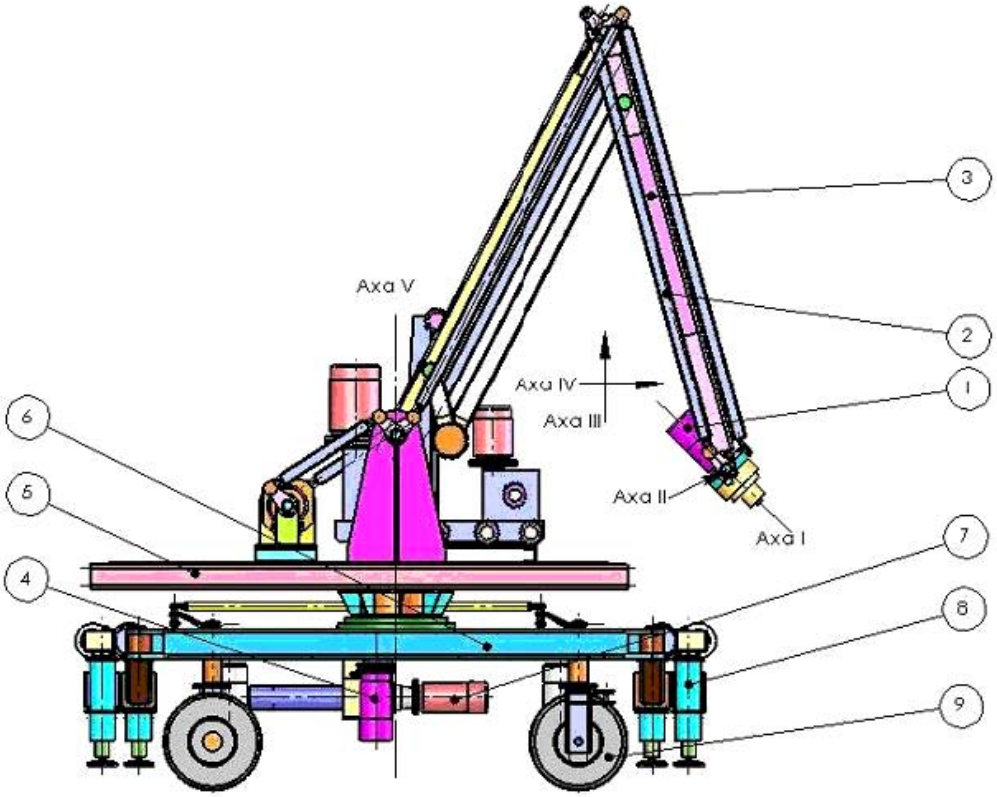

Fig. 1 Mobile robot for construction

The positioning and orientation mechanisms forms the robotic arm with 5 degrees of freedom and the steering, moving, horizontal and wedging mechanisms forms the mobile platform. Out of the 5 axes of the robotic arm 3 of them, are designed under the shape of bar mechanisms, figure 2. In this figure are represented 2 axes of the

Prof. Adrian Bruja, Universitatea tehnică de construcți București, bruja@utcb.ro
Ph.D. Marian Dima, Universitatea tehnică de construcți București, dima@utcb.ro
Lic. Eng. Cătălin Frâncu, Universitatea tehnică de construcți București, francu@utcb.ro

positioning mechanism shaped as a pantograph mechanism ACDEFG which allows the movement of the end-effector on the horizontal and vertical direction and 1 axis of the orientation mechanism in the shape of a succession of parallelogram mechanisms AKLE and EMNG which allows the end-effector to rotate around G point for a correct orientation of it. The connecting-rods KL and MN have the same length and are parallel with the bars AE and EG of the positioning mechanism. Other parallelism relations are between the bars AK and LE and respectively between EM and GN. The other 2 parallelogram mechanisms were placed in the arm composition, in order to avoid dead point and to avoid self-locking of the orientation mechanism.

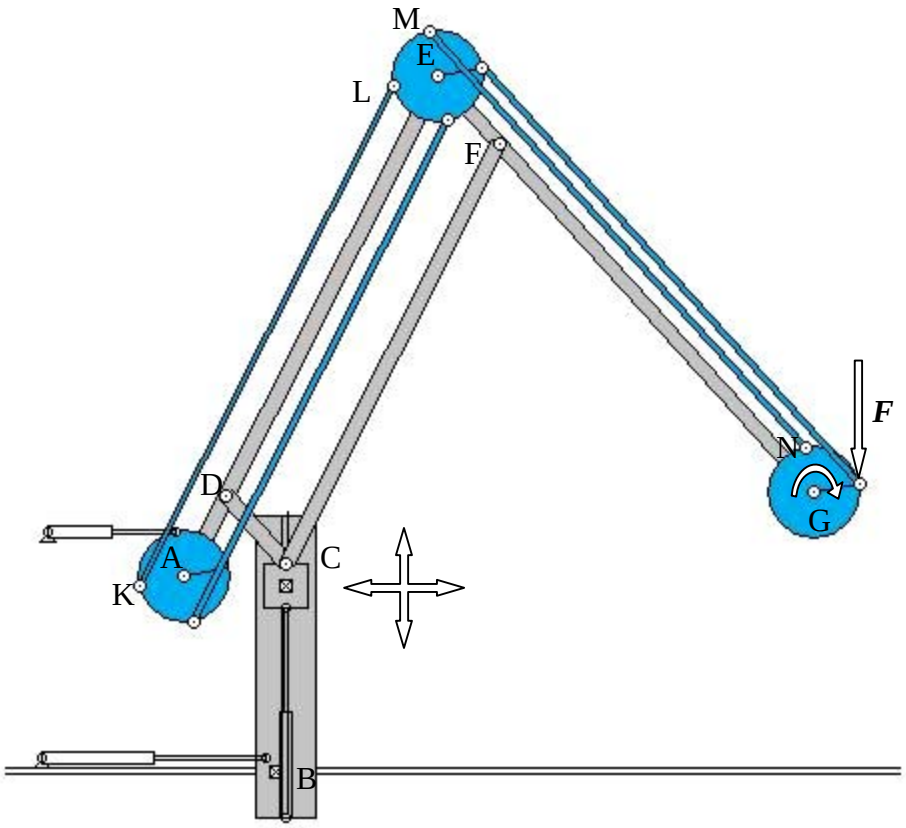

Fig. 2 Robot's bar mechanism

From structural point of view the bar mechanism in figure 2 can be decomposed only in dyads and their succession in the kinematic chain is: ADC, EFC, KLE and MNG.

2. METHOD OF CHOICE PRESENTATION

The kinetostatic is done by structural groups starting with the last dyad of the mechanism and going to the driving group, which is in opposite way as in the kinematic study.

Considering an RRR dyad, referenced to a reference coordinate system, figure 3, for which are known:

- Dyad position given by the coordinates (x_1,y_1), (x_2,y_2) and (x_3,y_3);
- Bars center of masses positions (xc_1,yc_1), (xc_2, yc_2);
- External forces torsor which acts on every element related to the center of mass of the element, (Fx1, Fy1, M1), (Fx2, Fy2, M2), 6 equilibrium equations can be written

$$
\begin{aligned}
&R_{x1} + F_{x1} - R_{x3} = 0;\\
&R_{y1} + F_{y1} - R_{y3} = 0;\\
&R_{x2} + F_{x2} + R_{x3} = 0; \qquad (1)\\
&R_{y2} + F_{y2} + R_{y3} = 0;\\
&R_{y1}(x_1 - x_3) - R_{x1}(y_1 - y_3) + F_{y1}(x_{C1} - x_3) - \\
&- F_{x1}(y_{C1} - y_3) + M_1 = 0 \qquad ;\\
&R_{y2}(x_2 - x_3) - R_{x2}(y_2 - y_3) + F_{y2}(x_{C2} - x_3) - \\
&- F_{x2}(y_{C2} - y_3) + M_2 = 0
\end{aligned}
$$

Solving this 6 equations system allows to determine reactions in the joints of the RRR dyads by its projections on the reference coordinate system that is R_{x1}, R_{y1}, R_{x2}, R_{y2}, R_{x3}, R_{y3}.

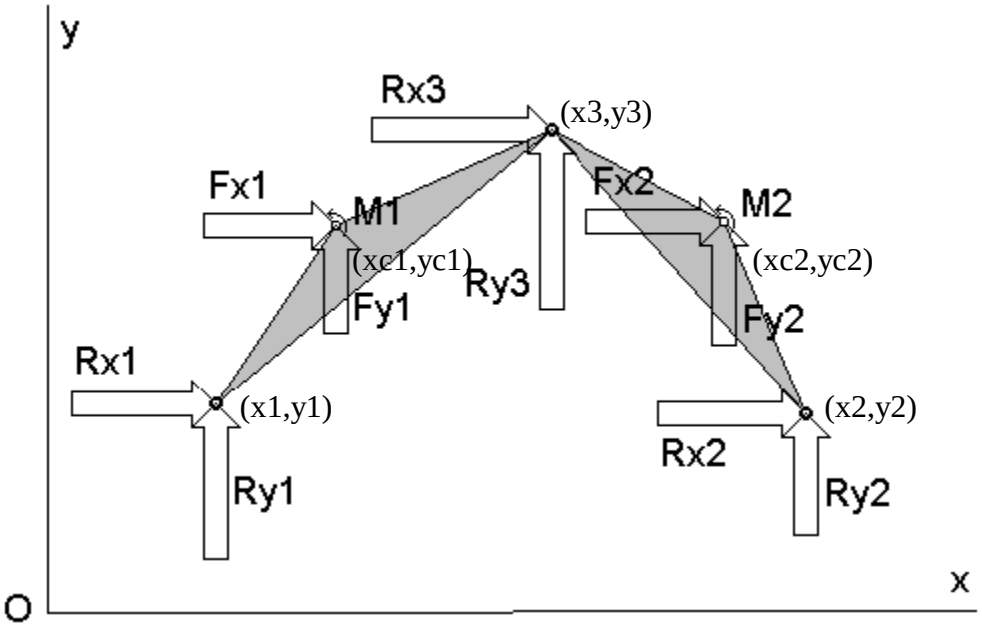

Fig. 3 Reactions determination on RRR dyad

To verify the solutions the equilibrium equations are written for the entire dyad

$$R_{x1} + F_{x1} + F_{x2} + R_{x2} = 0;$$
$$R_{y1} + F_{y1} + F_{y2} + R_{y2} = 0; \qquad (2)$$

3. USING THE METHOD

The algorithm for using the method for the robots mechanism follows:

a) Dyad MNG
External forces: force F;
Results: R_{Gx}, R_{Gy}, R_{Nx}, R_{Ny}, R_{Mx}, R_{My};

b) Dyad KLE
External forces: $-R_{Mx}$, $-R_{My}$;
Results: R_{Kx}, R_{Ky}, R_{Lx}, R_{Ly}, R_{Ex}, R_{Ey};

c) Dyad EFC_1
External forces: bars masses EG and CF, Forces, inertia moments and reactions $-R_{Gx}$, $-R_{Gy,}$ $-R_{Ex}$, $-R_{Ey}$;
Results: $R_{Ex}^{(1)}$, $R_{Ey}^{(1)}$,R_{Fx}, R_{Fy}, $R_{Cx}^{(1)}$, $R_{Cy}^{(1)}$;

d) Dyad ADC_2
- External forces: bars masses, AD and DC_2 Forces, inertia moments and reactions, $-R_{Ex}^{(1)}$, $-R_{Ey}^{(1)}$; $-R_{Kx}$, $-R_{Ky}$
- Results: R_{Ax}, R_{Ay}, R_{Dx}, R_{Dy}, $R_{Cx}^{(2)}$, $R_{Cy}^{(2)}$;

In the multiple joint C the reactions from the 2 dyads of the positioning mechanism are composed as it follows:

$$R_{Cx}^{(1)} + R_{Cx}^{(2)} = R_{Cx};$$
$$R_{Cy}^{(1)} + R_{Cy}^{(2)} = R_{Cy}.$$

The results R_{Cx} şi R_{Cy} represents the forces that are needed to be available at the motors for the movement on the vertical and horizontal of the end effector.

4. OBTAINED RESULTS

According to the algorithm previously presented, a computer program was written which allows to determine the reactions form the joints of the bar mechanism of the robot. For example in figures 4, 5, 6 are presented the variation graphs of the multiple joint C for the entire workspace of the robot.

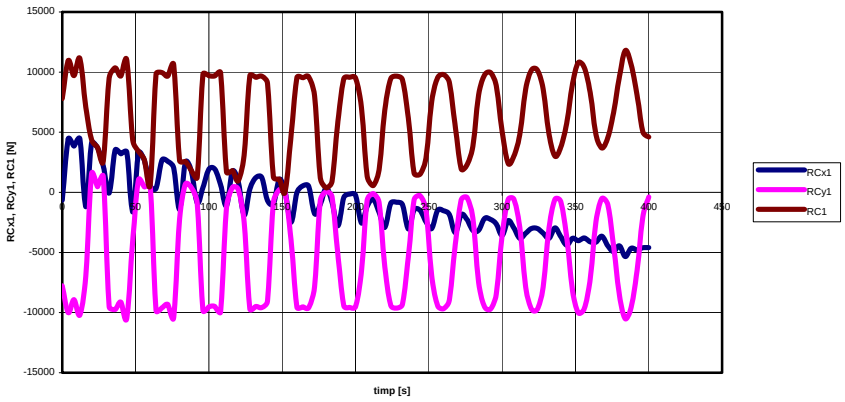

Fig. 4 Reactions variation in joint C on dyad EFC

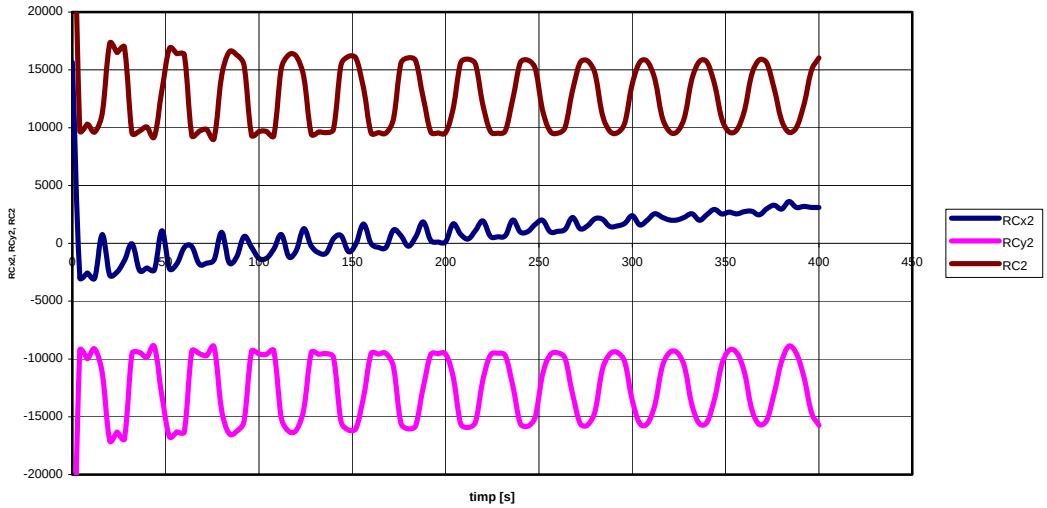

Fig. 5 Reactions variation in joint C on dyad ADC

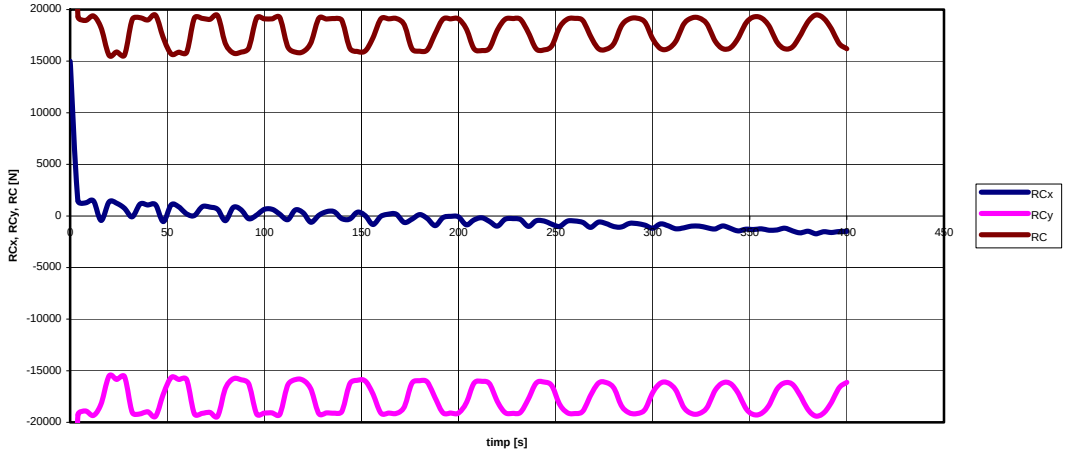

Fig. 5 Variation of the reaction in multiple joint C

REFERENCES

[1] *Bruja, A., ş.a.- Robot mobil universal pentru constructii cu 7 grade de libertate,* Contract nr.11CEEXI03/06.10.2005.

[2] *Adrian Bruja, Marian Dima, Cătălin Frâncu, Theodor Borangiu* - Designing and working simulation of the mechanisms of the mobile robot for construction. *16th Int. Workshop on Robotics in Alpe-Adria-Danube Region Ljubljana, June 7-9, 2007*

[3] *Adrian Bruja, Marian Dima, Cătălin Frâncu* - Constructions Mobile Robot and Working Technology. 24th International Symposium on Automation & Robotics in Construction 19 – 21 Sep 2007. Kochi, Kerala, India

MODELING AND SIMULATION OF A PUMP CONTROLLED MOTOR WITH LONG TRANSMISSION LINES

N. Nedić, Lj. Dubonjić

Abstract: *In this paper are given different mathematical models of the pump controlled hydro-motor with long transmission flow lines and the flow lines effects analysis on it's stability and response. The simulation results are obtained by using the Matlab-Simulink.*

Keywords: *hydrostatic power transmission systems, dynamic behavior, long transmission line*

1. INTRODUCTION

The pump is connected to the motor via line (pipe, tube) that could in some applications, such as mining, construction machines, heavy machines and remote control systems, be very long. In accordance with their strong behavior demands, for example, a motor is commanded to change to a different speed (from very low speed to very high speed and vice-versa) for short time. In such case the dynamics of the system must be considered, that is, the dynamics of the all elements coupled in the system (pump, line, motor etc.) must to be considered. Moreover, having servo control of that system, the dynamics of the coupled system becomes more important. Authors of this paper assumed usual type of a servo hydrostatic power transmission system with a variable- displacement pump and a fixed-displacement motor as shown in Fig.1. The coupled subsystem pump-line-motor is shown in Fig.2.

The modeling of fluid transmission line has received a great deal of attention over the past few decades (from about 1950) [1-3] and there are several hundreds publication that could be quoted relating to different theories and applications for air, water and oil hydraulic systems [4-6]. The effect of transmission line dynamics on the dynamic behavior of fluid power systems was studied by J. Watton [7]. Simulation and experimental analysis of dynamics and control of pump controlled motor are presented in [8-10] . Some results in regard to dynamics of pump controlled motor with long transmission line were presented in [11-13]. This paper presents analysis on dynamic behavior of pump controlled motor with long transmission line based on different mathematical line models in frequency and time domain.

Previous analyses did not include the analysis of stability and response of the automatic regulation system of a pump controlled motor from the aspect of the length change of a transmission line. Therefore the results of such analysis are presented in this paper.

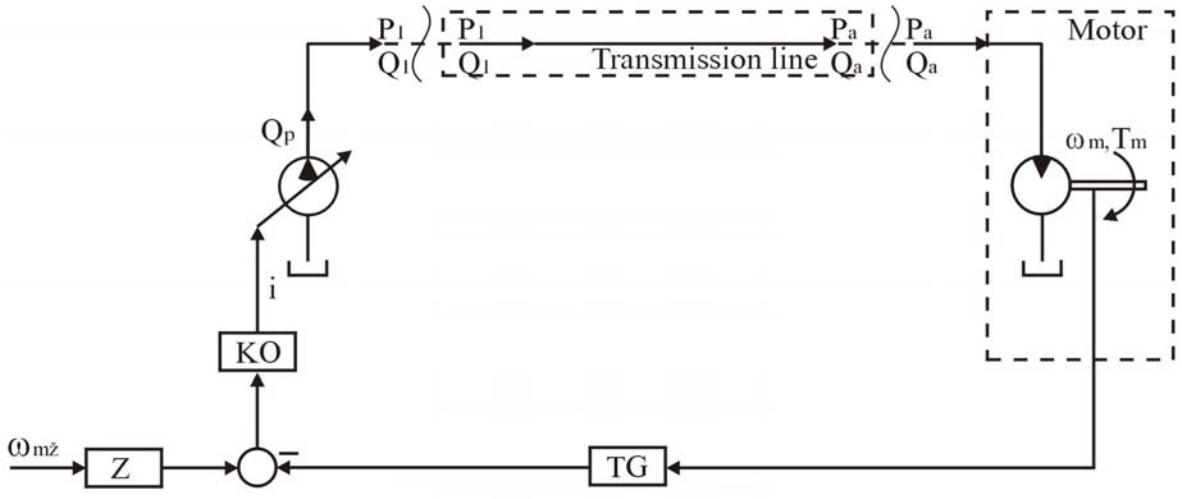

Fig.1. Symbolic diagram of the servo pump controlled motor

Prof. Dr Novak N. Nedić, Faculty of Mechanical Engineering Kraljevo, nedic.n@mfkv.kg.ac.yu,
M. Sc. LJubiša Dubonjić, Faculty of Mechanical Engineering Kraljevo, dubonjic.lj@mfkv.kg.ac.yu

2. DYNAMIC MATHEMATICAL MODEL OF A PUMP CONTROLLED MOTOR WITH LONGTRANSMISSION LINE

The mathematical model of the system was determined by describing each automatic regulation system element with fundamental equations, with appropriate assumptions. The structure of the system part on the basis of which modeling is done is presented in Figure 2.

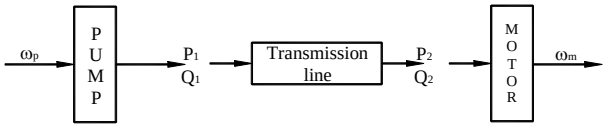

Fig.2. *The structure diagram of the coupled subsystem*

Pump

The pump has a variable working volume with the constant number of revolutions. Oil leakage and compressibility in the pump were taken into consideration through the coefficient of leakage resistance R_p and the compressibility module B. The flow at the exit port of the pump, $Q_p = Q_1$, is equal to the flow at the beginning of the long transmission line and it is described with the equation:

$$Q_1(t) = D_p(t)\omega_p - \frac{1}{R_p}p_1(t) - C_p\frac{dp_1(t)}{dt} \qquad (1)$$

By applying the Laplace Transform, the equation (1) obtains the following form:

$$Q_1(s) = D_p(s)\omega_p - \frac{1}{R_p}p_1(s) - C_p s p_1(s) + C_p p_1(0) \qquad (2)$$

$$Q_1(s) = D_p(s)\omega_p - Z_p p_1(s) + C_p p_1(0) \qquad (3)$$

where: $Z_p(s) = C_p s + \frac{1}{R_p}$; $C_p = \frac{V_p}{B}$

Hydro-motor

The hydro-motor has a constant working volume with the variable number of revolutions. Oil leakage and compressibility in the motor are covered through the characteristic coefficients R_m and C_m, respectively. The flow at the end of the long transmission line is equal to the flow at the hydromotor $Q_2 = Q_m$ and it is described with the equation:

$$Q_2(t) = D_m\omega_m(t) + \frac{1}{R_m}p_2(t) + C_m\frac{dp_2(t)}{dt} \qquad (4)$$

By applying the Laplace Transform, the equation (4) obtains the following form:

$$Q_2(s) = D_m\omega_m(s) + \frac{1}{R_m}p_2(s) + C_m s p_2(s) - C_m p_2(0) \qquad (5)$$

$$Q_2(s) = D_m\omega_m(s) + Z_m p_2(s) - C_m p_2(0) \qquad (6)$$

where: $Z_m(s) = C_m s + \frac{1}{R_m}$; $C_m = \frac{V_m}{B}$

The loads that should be overcome by the hydromotor are as follows: inertial, viscose and external. The moment equation of hydro-motor load is given in the following form:

$$D_m p_2(t) = J_m\frac{d\omega_m(t)}{dt} + B_v\omega_m(t) + T_L(t) \qquad (7)$$

By applying the Laplace Transform, the equation (7) obtains the following form:

$$D_m p_2(s) = J_m s\omega_m(s) - J_m\omega_m(0) + B_v\omega_m(s) + T_L(s) \qquad (8)$$

Transformation of the equation (8) results in the expression for pressure at the end of the long transmission line:

$$p_2(s) = Z_T D_m\omega_m(s) - \frac{J_m}{D_m}\omega_m(0) + \frac{T_L(s)}{D_m} \qquad (9)$$

where: $Z_T = \frac{J_m}{D_m^2}s + \frac{B_v}{D_m^2}$, the characteristic impedance of internal load on the hydro-motor.

Long transmission line

The long transmission line represents a connection between the pump and the hydro-motor. As the lengths of the hydraulic line ranges from several meters to several dozen meters, it is clear that the pressures and flows at the beginning and at the end of the line are not equal, so that its influence in such systems must not be neglected. The equation describing the connections between the flow and the pressure at the end and the beginning of the hydraulic line is given in the form of a transmission matrix. [12-15].

$$\begin{bmatrix} p_2(s) \\ Q_2(s) \end{bmatrix} = \begin{bmatrix} A_L & -B_L \\ -C_L & D_L \end{bmatrix} \cdot \begin{bmatrix} p_1(s) \\ Q_1(s) \end{bmatrix} \qquad (10)$$

The equation (10) represents the general form of transmission matrix of the long transmission line independent of whether the line is described with a model having distributed or lumped parameters. The values of parameters A_L, B_L, C_L and D_L, depending on the shape of model of long transmission line, are given in Table 1.

By connecting the equation (10) with the equations (3), (6) and (9) and on the basis of characteristics of coefficients of the long transmission line that: $A_L = D_L$ i $A_L D_L - B_L C_L = 1$, the transfer function of a part of the automatic regulation system is obtained in the form equation (11):

Coefficients / Shape of model	A_L	B_L	C_L	D_L	Z (Z^1)	Y (Y^1)	Z_c Γ
Model with distributed parameters	$ch(\Gamma l)$	$Z_c sh(\Gamma l)$	$\frac{sh(\Gamma l)}{Z_c}$	$ch(\Gamma l)$	$R + Ls$	Cs	$\sqrt{Z/Y}$ $\sqrt{ZY}$
Model with lumped parameters	$1+\frac{Z^1Y^1}{2}$	Z^1	$Y^1(1+\frac{Z^1Y^1}{4})$	$1+\frac{Z^1Y^1}{2}$	$R^1 + L^1 s$	$C^1 s$	

Table 1. The values of parameters A_L, B_L, C_L and D_L

$$D_m\omega_m(s) = \frac{D_p(s)\omega_p - \left[\left(Z_m + Z_p\right)A_L + Z_m Z_p B_L + C_L\right]\cdot\left[\frac{T_L(s) - J_m\omega_m(0)}{D_m}\right] + C_p p_1(0) + \left(A_L + Z_p B_L\right)\cdot C_m p_2(0)}{\left(1 + Z_m Z_T + Z_p Z_T\right)\cdot A_L + \left(Z_p + Z_p Z_m Z_T\right)\cdot B_L + Z_T C_L} \qquad (11)$$

3. THE SIMULATION ANALYSIS IN FREQUENCY AND TIME DOMEN

The simulation of dynamic behavior in frequency domain is done on the basis of the transfer function of open-loop which is described in the equation (12):

$$W_{ok}(s) = \frac{K_a K_{TG}\frac{\omega_p}{D_m}}{\left(1 + Z_m Z_T + Z_p Z_T\right)\cdot A_L + \left(Z_p + Z_p Z_m Z_T\right)\cdot B_L + Z_T C_L}$$

The program language for various models of a transmission line is written in Matlab, by means of which the results of amplitude and frequency characteristics of the open-loop of the automatic regulation system are obtained.
The results of these simulations are shown in the Fig.3 and Fig.4.
The values of the parameters for which the simulations are done are:

$E = 1{,}43\cdot 10^9\,N/m^2;\ \rho = 860kg/m^3;\ \mu = 0{,}033Ns/m^2;$

$B = 1{,}4\cdot 10^9\,N/m^2;\ R_p = R_m = 1\cdot 10^{11}Nm^{-2}/m^3s^{-1};\ d = 8\cdot 10^{-3}m;$

$l = 0,\ 2,\ 4,\ \ldots,20m;\ \omega_p = 130rad/s;\ c = 1290m/s;$

$D_m = 2.5\cdot 10^{-6}m^3/rad;\ B_v = 0.2Nms;\ I_m = 0{,}02kgm^2;$

Fig.3 presents amplitude and frequency characteristics of the open-loop when dynamics of the transmission line is included through the model with distributed parameters for 1=2m, Fig.3 (a); for 1=8m, Fig3 (b) and for 1=10m, Fig.3 (c).

Fig.4 presents amplitude and frequency characteristics of the open-loop when dynamics of the transmission line is included through the model with lumped parameters for 1=2m, Fig.4(a); for 1=8m, Fig.4(b) and for l=10m, Fig.4(c).

Based on these simulation results, the stability limits of the automatic regulation system of the pump controlled motor with long transmission line are determined. Gain limits of the open-loop K, depending on the change of transmission line length from ranging from 0 to 20 meters, are determined by means of non-general Bode criterion and are shown in the Fig.5. for the models of long transmission line with lumped and distributed parameters.

Fig.8 shows the change of the natural frequency f, in the function of the length change of the transmission line.
After the stability limits in frequency domain are determined, they are tested in time domain.

Fig.6 shows the system response for the gain value K=12,875, which presents stability limit for the model with distributed parameters for the transmission line length of 10m.

This limit for the model of the transmission line with lumped parameters and length of 10m is K=21,62. The system response for this gain value is shown in the Fig.7. from which it can be detected that the system is not stable.

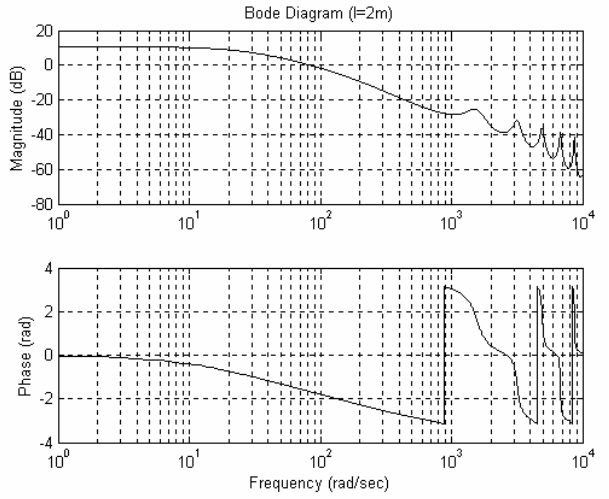

(a)

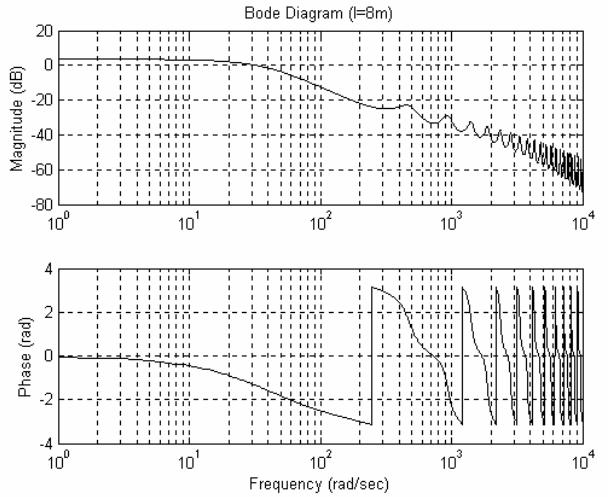

(b)

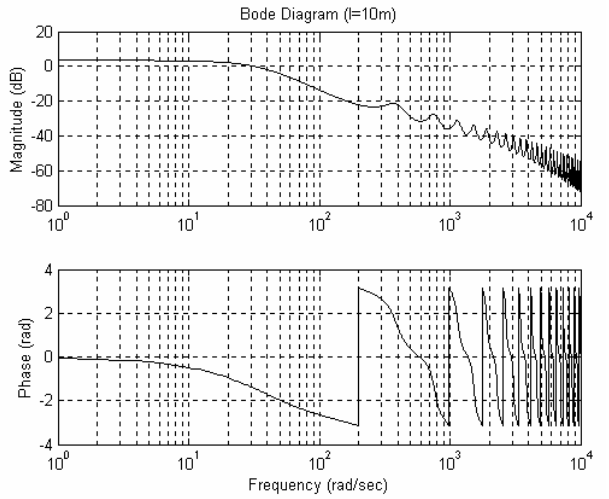

(c)

Fig.3. *Amplitude and frequency characteristics of the coupled system with distributed parameters*

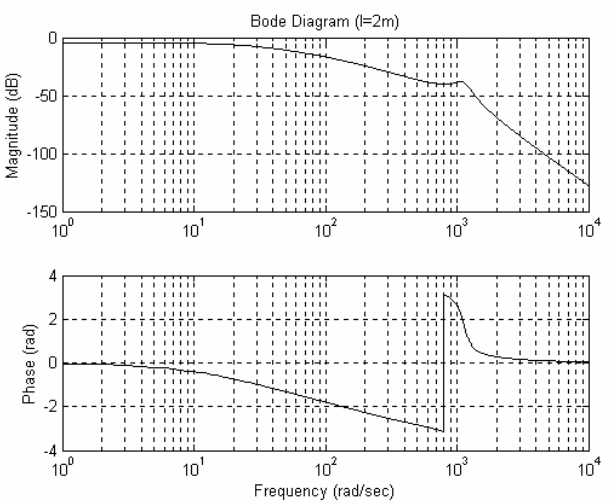

(a)

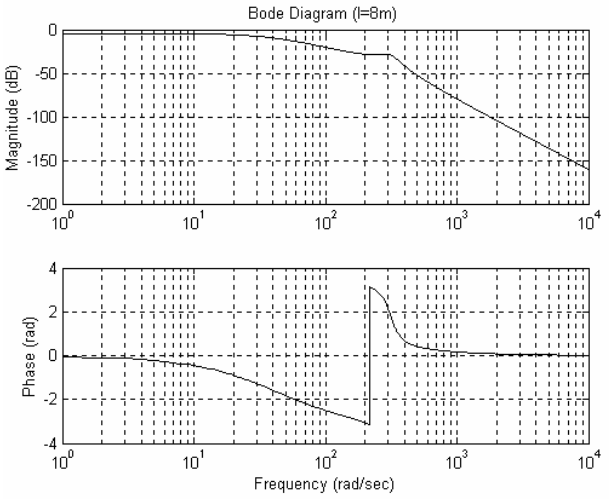

(b)

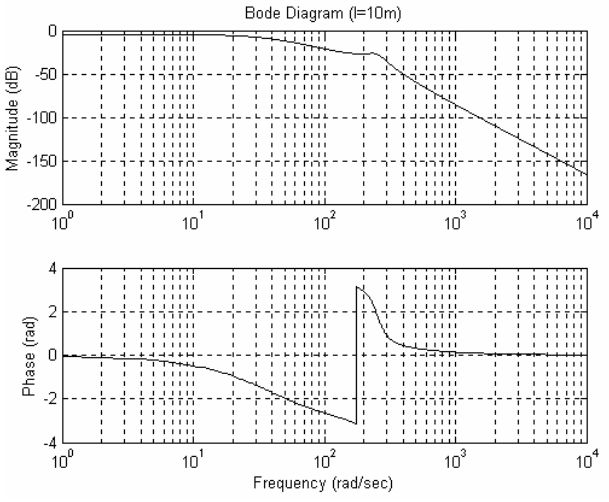

(c)

Fig.4. *Amplitude and frequency characteristics of the coupled system with fixed parameters*

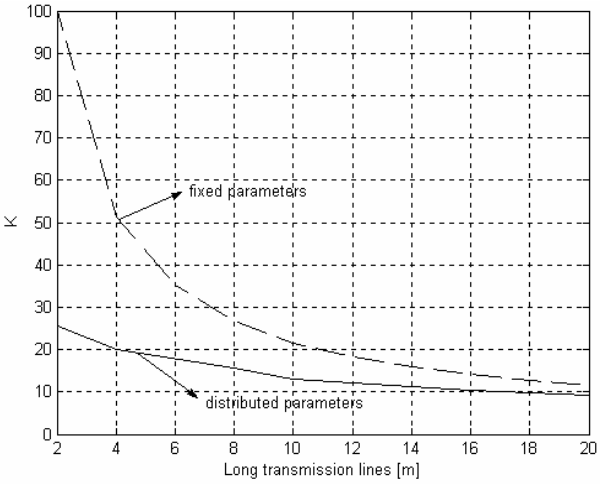

Fig.5. The gain dependence by the flow line length

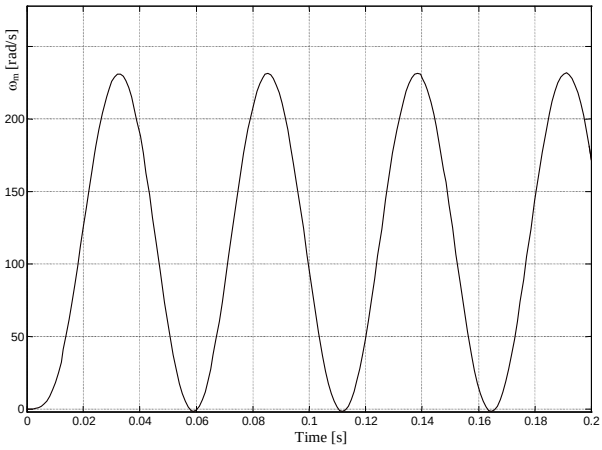

Fig.6. Transient relative motor speed, variation with time for K=12.875

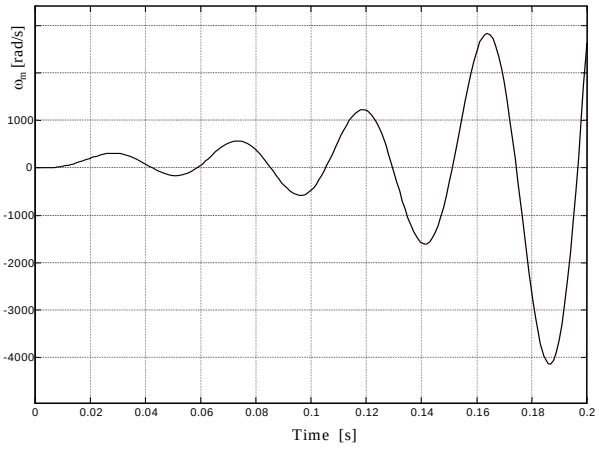

Fig.7. Transient relative motor speed, variation with time for K=21.62

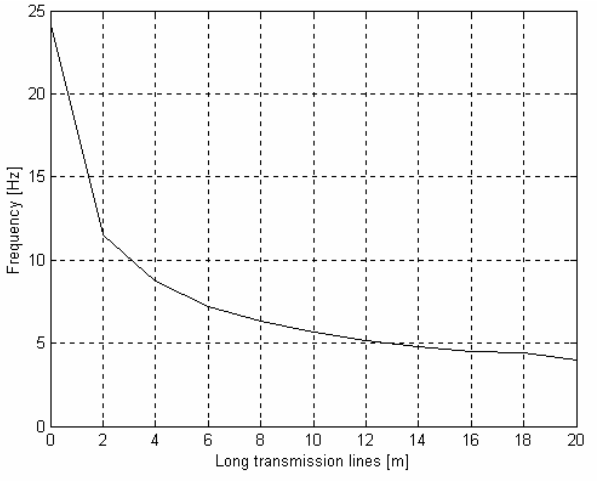

Fig.8. Natural frequency dependence, variation with flow line length

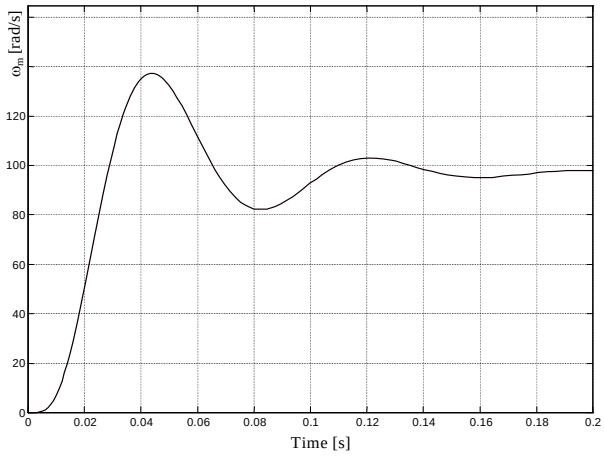

Fig.9. Transient relative motor speed, variation with time for K=5

4. CONCLUSIONS

Based on the analysis in frequency and time domain, the gain limit of the automatic regulation system of pump controlled hydro-motor is determined for various models of transmission line and coupled in the system of pump lines and motor.

With the increase of transmission line length, the value of the gain factor K which guarantees stability of the system, decreases from K=25,525 for the length of the transmission line of 2m to K=9,1 for the transmission line length of 20m, for the model of transmission line with distributed parameters.

The value of the gain factor K=5 for the transmission line length l=10m, described by the model with distributed parameters, is determined on the basis of the criterion for evaluation of the quality of a dynamic behavior of the system in frequency and time domain (Fig.9).

All this points out to the problem with designing of these systems, where the dynamics of transmission line, if not taken into consideration, may lead to the wrong conclusions in regard to their dynamic behavior.

NOTATION

A – rod cross-sectional-area
B_v – friction viscosity
C –line capacitance
C_m –motor capacitance
C_m –pump capacitance
d- line diameter
D_m – displacement motor
D_p – displacement pump
D_n–dissipation number
E – modulus of elasticity
K_a- coefficient current-voltage
K_{TG}-coefficient of tacho generator
I_m – momentum inertia
l – line length
L_T-hydro-motor inductance
P_1, P_2 –line pressure at inlet and outlet
P_{ref} – simulation reference pressure
Q_{ref} - reference flow rate
R - fluid resistance
R_{ref} – simulation reference resistance
R_p - leakage pump resistance
R_m – leakage motor resistance
s- Laplace operator
Q_1, Q_2 – line flow rates at inlet and outlet
Z – series impedance
Zc – characteristic impedance
Z_T – motor impedance
Y – shunt admittance
Γ - Propagation operator
ρ - Fluid density
μ - Fluid viscosity

REFERENCES:

[1] Tarko L.M., “Volnovie procesi v truboprovodah gidromehanizmov” Gosudarstvenoe naučno-tehničeskoe izdateljstvo mašinostroiteljnoj literaturi, Moskva, 1963.

[2] Korobočkin B.L., Komitovski M.D., “O peredatočnih funkcijah truboprovodov gidrosistem v sosredatočnih i raspredeljenih parametrah”, Mašinovedenie, No4, 1968.

[3] Hsue C.Y., Huulender, D.A., “Modal approximations for the fluid dynamics of hydraulic and pneumatic transmission lines”, Fluid Transmission line dynamics, published by ASME, 51-77.pp., 1983.

[4] Merritt N.E., “Hydraulic Control systems”, John Wiley & Sons, 1967.

[5] Blackburn J.F., Reethof G., Shearer, J.L., “Fluid Power Control”, M.I.T. Press.

[6] McCloy D., Martin H.R., “Control of fluid power”, Ellis Horwood Ltd.

[7] J.Watton, “Fluid Power Systems”, Prentice Hall,1989.

[8] N.N.Nedić, Z. Bučevac, D. Prsic "Experimental analysis and identification of piston- axial pump BVP 100, International Conference Heavy Machinery HM '96, Kraljevo 28-30 June,1996, 531-536 pp. (in Serbian)

[9] N.N.Nedić, D.H.Pršić, "Time Variable Speed Control of a Pump Controlled Motor Using Natural Tracking Control", Conference on Control of Industrial Systems, IFAC-IFIP IMACS, 20-22 May, Belfort, France, 1997, 197-202 pp.

[10] R.S.Petrović, N.N. Nedić, "Mathematical Modeling and Experimental Research of Characteristic Parameters Hydrodynamic Processes of a Piston Axial Pump", VII International SAUM Conference, V.Banja, September 26-28, 2001.

[11] N.N.Nedić, Lj.M.Dubonjić, “Ways of modelling and simulation of a pump controlled motor coupled by long transmission line”, VII International SAUM Conference, V.Banja, September 26-28, 2001.

[12] Lj.M.Dubonjić, ″Dynamical analysis of electrohydraulic control systems with long transmission line″, Master thesis, Faculty of Mechanical Engineering,Kraljevo, Dec. 2002. (in Serbian).

[13] Nedić N.N., Dubonjić LJ.M., ″Dynamical Model of Variable Displacement Piston Axial Pump with Shwashplate″ HIPNEF 2000, Beograd 2000, 28-33 pp. (in Serbian)

[14] N. N. Nedić, R. Petrović, LJ. M. Dubonjić, ″Dynamic Behavior of Servo Controlled Hydrostatic Power Transmission System with Long Transmission Line″, International Conference Mechanization, Electrification and Automation in Mines, Sofia 2003, 267-271 pp.

[15] N. N. Nedić, LJ. M. Dubonjić, M.Palić, ″The Stability and Response of the Electrohydraulic Valve Controlled Hydro-motor with Long Transmission Flow Line″ VIII Triennial International SAUM Conference on Systems, Automatic Control and Measurements Belgrade,Serbia,November 5-6,2004, 186-193 pp.

EXPERIMENTAL VERIFICATION OF MATHEMATICAL MODELING OF PARAMETERS OF VANE PUMP WITH DOUBLE EFFECT[1)]

R. Petrović, M. Savković, P. Ivanović, Z. Glavčić

Abstract: *In developing the vane pumps the fundamental basis is experimental research and mathematical modeling of nonstationary hydraulic processes inside the pump, in thrust space and suction and thrust pipeline. By means of experimental research and results of mathematical modeling and software package KRILP, it is possible to determine the parameters of operating processes of vane pumps precisely enough.*

Key words: *vane pump, mathematical modeling, hydrodynamic processes*

1. INTRODUCTION

Modern methods of designing and constructing the hydraulic pumps can not be done without using the appropriate mathematical models of effects and processes happening in real pump structures. The mathematical model of a process is analytical interpretation of the process with certain assumptions. In order to reach the mathematical model it is necessary to make detailed theoretical research based on the laws of fundamental sciences and explanation of processes, which is the basis for adopting the assumptions and defining the model equations.

2. MATHEMATICAL MODEL OF PRESSURE CHANGE IN THE OPERATING CHAMBER

The level of noise made by vane pump with double effect is crucially influenced by pressure rise and fall in the pump chambers in the areas of change of operating cycles. Constant conversion of thrust pressure into operating pressure in the installation and vice cersa is an important assumption for lowering the noise level. There are a number of researches done in order to define the optimal geometry of working volume when one operating cycle converts into another one. The processes occuring at the area of pressure change and their relation can be researched by experiments and by mathematical modeling by means of adequate software packages. For these researches the software KRILP has been developed and it has been written in program language Digital Visual Fortran 5.0.

The increase of rotation number provides better tightness of working chamber at the area of pressure change which can be explained by the increase of centrifugal force acting on the vanes and pressing them against the inner surface of the stator.

When the vanes are separated from the operating stator profile, pressure pulsation and amplitude changes are registered. These changes often occur with low number of revolutions and they lead to oil coming back from thrust area towards suction area.

When chambers are not sealed tight, i.e. when clearances are big, the pressure does not rise enough in the area of pressure change, which leads to unexpected relation between the chamber and thrust port and also leads to pressure balance. Thus the leakage between the suction and thrust zone is being increased as well as the amplitude of pressure pulsation.

Due to the influence of the clearance on the tightness in the chamber, the pressure change in the chamber should be presented by mathematical model depending on volumetric losses and it is necessary to make certain simulations on the computer. On the basis of data obtained by experiments and simulations we should determine geometries of suction and thrust ports as well as partitions between them at valve plate. The following phases can be distinguished in simulating the pressure change in the chamber while passing over the partition separating suction and thrust zones:

- the chamber is closed, i.e. there is no connection between the chamber and suction and thrust zone
- the chamber is connected to thrust port through the slot
- the chamber is connected to thrust port

1) This work is part investigation in project " Research of metodologis and softweres for design, simulation and optimization of vane pumps"

Prof. Dr.-Ing. Radovan Petrović, Faculty of Mechanical Engineering Kraljevo, petrovic.r@mfkv.kg.ac.yu
Dr.-Ing. Petar Ivanović,
Ass. Ing. Zoran Glavčić, Faculty of Mechanical Engineering Kraljevo, glavcic.z@mfkv.kg.ac.yu
Ass.Dr.- Ing. Mile Savković, Faculty of Mechanical Engineering Kraljevo, savkovic.m@mfkv.kg.ac.yu

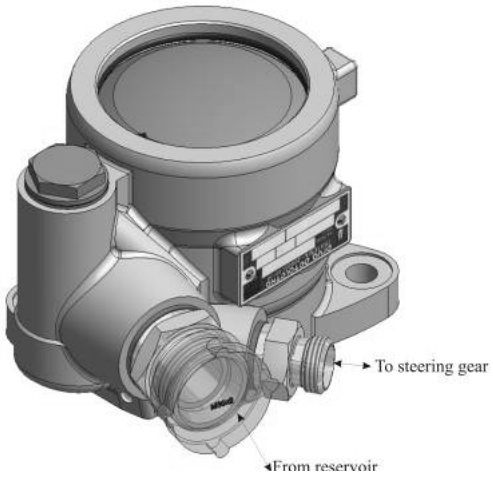

Figure 1a. -Vane pump with double effect
- made by Prva Petoletka Trstenik

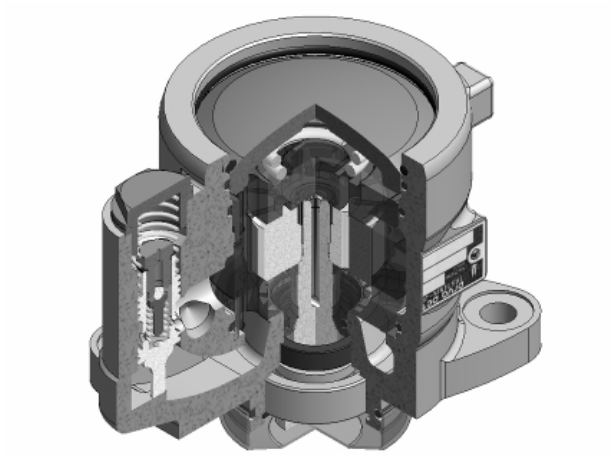

Figure 1b - Section

2.1.Volumetric losses affecting the speed of pressure change in the operating chamber at the zone of pressure change

In order to operate properly the pump must have appropriate clearances between vane rotor and valve plates. There is a certain flow through these clearances. Volumetric losses in the chamber can be classified as follows:

- losses at vane side made by axial clearances Q_{an} *(n=1,2)*
- losses over vane top made by radial clearances Q_{rn}*(n=1,2)*
- losses made by flow withdrawal Q_{pr}
- losses through the slot at valve plate Q_{pz}
- losses through the gap made by the vane in rotor groove Q_{pc}

2.1.1. Losses made by axial clearances

If we assume that the flow is streamline the losses through the axial clearances are:
a) volumetric losses for the chamber in front of the vane can be presented by following formula:

$$Q_{a1} = \frac{(\rho - r)\cdot z_{a1}^{\,3}}{12\cdot\eta\cdot s}\left|p_r - p_k\right| sign(p_r - p_k), \qquad (1)$$

b) volumetric losses for the chamber behind the vane can be presented by following formula:

$$Q_{a2} = \frac{(\rho - r)\cdot z_{a2}^{\,3}}{12\eta s}(p_k - p_u), \qquad (2)$$

where:
ρ- variable radius of the stator;
r- smaller radius of the stator
z_{a1}, z_{a2}- values of axial clearance;
s- vane thickness
η- dynamic viscosity of working fluid;
p_u- suction pressure
p_k- pressure in the chamber
p_r- operating pressure

2.1.2. Losses made by radial clearances

Between the inside surface of the stator and vane top working flow leaks which can be presented as follows:
a) volumetric losses for the chamber in front of the vane can be presented by following formula:

$$Q_{r1} = \frac{b\cdot z_{r1}^{\,3}}{12\cdot\eta\cdot s}\left|p_r - p_k\right| sign(p_r - p_k), \qquad (3)$$

b) volumetric losses for the chamber behind the vane can be presented by following formula:

$$Q_{r2} = \frac{b\cdot z_{r2}^{\,3}}{12\cdot\eta\cdot s}(p_k - p_u), \qquad (4)$$

z_{r1}, z_{r2} - values of radial clearances.

2.1.3. Losses made by flow withdrawal

The mean value of lossess made by flow withdrawal at the vane is presented by the expression:

$$Q_{pr} = \frac{z_{a1/2}\cdot\omega\cdot(R+r)(R-r)}{4}, \qquad (5)$$

where:
ω - angular speed of rotor;
φ - angle of rotor rotation
R,r - bigger and smaller radius of stator

2.1.4. Losses through the slot at valve plates

Losses through the slot in thrust port at valve plate are determined in the following manner:

$$Q_{pz} = \mu \cdot A \sqrt{\frac{2}{\rho}(p_r - p_k) \cdot sign(p_r - p_k)}, \qquad (6)$$

where:

μ - outflow coefficient;
A - cross-sectional area
ρ - density of working fluid

2.1.5. Losses made by the vane in rotor groove

If the pressure in the chamber is higher than working pressure of the pump there is a gap in rotor groove made by front vane tilting because of tangential load and there is oil leakage which can be presented by:

$$Q_{pc} = \frac{b \cdot z_{pc}^{\ 3}}{12 \cdot \eta \cdot l_r}(p_k - p_r), \qquad (7)$$

where:

z_{pc} - clearance in the gap;

$l_r = l - (r - r_r)$ - length of the front vane when rotor is in transmission area.

2.2. Speed of pressure change in the chamber when suction and thrust zones are being separated

If initial volume V is lowered for $dV = V_1 - V = -(V - V_1)$, due to pressure rise $dp = p_1 - p$ the relative volume -*dV/V*, calculated per pressure unit:

$$S = -\frac{1}{dp} \cdot \frac{dV}{V}, \qquad (8)$$

is compressibility coefficient.

The reciprocating value of compressibility coefficient is called the compressibility modulus (ε_S),

$$\varepsilon_s = \frac{1}{S} = -\frac{dp}{dV / V}, \qquad (9)$$

which has the same dimension as the pressure.

In previous expressions the minus sign shows that pressure rise corresponds to volume decrease and vice versa. The previous expression can be also presented in the following form, in case of final changes of pressure and volume

$$-\frac{\Delta V}{V} = \frac{\Delta p}{\varepsilon_S}, \qquad (10)$$

which represents so called Hooke's law. The marks in previous expression are:

$\Delta p = p_1 - p$ - pressure increment

$\Delta V = V_1 - V$ - change of volume

V_1- fluid volume at the pressure p_1

The pressure increment in the working chamber of vane pump with double effect can be reached from the following expression [10]:

$$\Delta p_k = \frac{\varepsilon_s}{V_{k(R)}}(\Delta V)_{k(R)}, \qquad (11)$$

where :

Δp_k - pressure increment in the chamber between the vanes $p_u < p_k < p_p$

ε_S- compressibility modulus of working fluid

p_u- suction pressure of working fluid

p_p- thrust pressure of working fluid

$V_{k(R)}$- volume of the chamber (when the chamber is in the zone of pressure change constrained by angle ε and bigger stator radius R)

Volume $V_{k(R)}$ is calculated like this:

$$\boldsymbol{V_{k(R)}} = \frac{b}{2}\left(R^2 - r_r^2\right) \cdot (\beta - \sigma), \qquad (12)$$

where:

(β-σ) [rad] - angle between two adjacent vanes

b - vane width

The speed of pressure change in the chamber is obtained by differentiating the expression [11] with respect to time t:

$$\frac{\Delta p_k}{\Delta t} = \frac{\varepsilon_s}{V_{k(R)}} \frac{\Delta V_{k(R)}}{\Delta t}, \qquad (13)$$

in case when $\Delta t \to 0$; $\Delta V_{k(R)} \to dV_{k(R)} \to 0$ and $\Delta p_k \to dp_k \to 0$, previous equation has differential form:

$$\frac{\Delta p_k}{\Delta t} = \frac{\varepsilon_s}{V_{k(R)}} \frac{d}{dt} (\Delta V)_{k(R)}, \qquad (14)$$

If we put the expressions for volumetric losses [1 ÷7] into the expression for speed of pressure change in the chamber [14] we reach the following expression:

$$\frac{dp_k}{dt} = \frac{\varepsilon_S}{V_{k(R)}}\Big(\frac{dV_{k(R)}}{dt} + 2Q_{a1} - 2Q_{a2} + Q_{r1} - Q_{r2} - Q_{pr} + Q_{pz} + Q_{pc} \Big). \qquad (15)$$

After replacing the values for volumetric losses we get required expression for speed of pressure change in relation to the clearance in the chamber of vane pump with double effect:

$$\frac{dp_k}{dt}=\frac{\varepsilon_s}{V_{k(R)}}\left[\frac{dV_{k(R)}}{dt}+2\frac{(\rho-r)\cdot z_{a1}^{\ 3}}{12\eta s}|p_r-p_k|\cdot sign(p_r-p_k)-\right.$$
$$-2\frac{(\rho-r)\cdot z_{a2}^{\ 3}}{12\eta s}(p_k-p_u)+\frac{b\cdot z_{r1}^{\ 3}}{12\eta s}|p_r-p_k|\cdot sign(p_r-p_k)-$$
$$-\frac{b\cdot z_{r2}^{\ 3}}{12\cdot\eta\cdot s}(p_k-p_u)-\frac{z_{a1/2}\cdot\omega\cdot(R+r)\cdot(R-r)}{4}+$$
$$\left.+\mu\cdot A\cdot\sqrt{\frac{2}{\rho}\cdot(p_r-p_k)\cdot sign(p_r-p_k)}+\frac{b\cdot z_{pc}^{\ 3}}{12\cdot\eta\cdot l_r}\cdot(p_k-p_r)\right] \quad (16)$$

Next section shows diagrams of speed of pressure change depending on the clearance in the operating chamber of vane pump with double effect. They are obtained by simulation of expression [16] by means of software package KRILP.

3. RESULTS OF SIMULATING THE PRESSURE CHANGE IN THE CHAMBER OF VANE PUMP WITH DOUBLE EFFECT

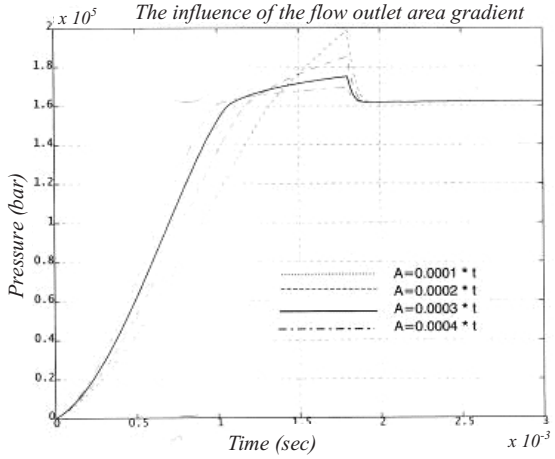

Figure 2. Results of simulating the expression for speed of pressure change in the chamber for various values of slot cross section

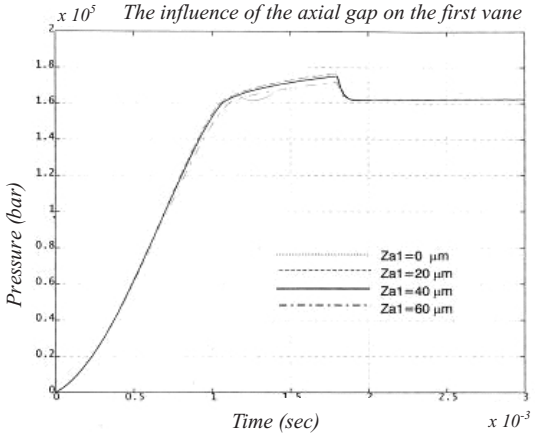

Figure 3. Results of simulating the expression for speed of pressure change in the chamber for various values of axial clearance at the first vane

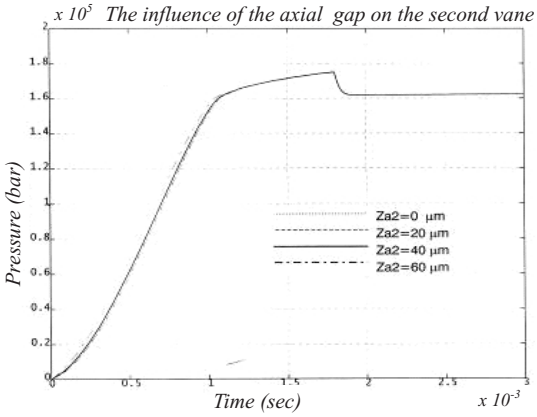

Figure 4. Results of simulating the expression for speed of pressure change in the chamber for various values of axial clearance at the second vane

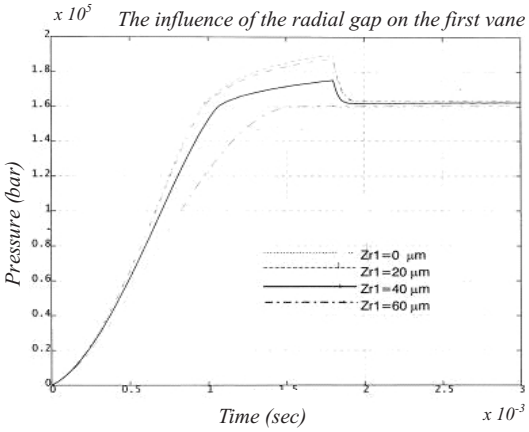

Figure 5. Results of simulating the expression for speed of pressure change in the chamber for various values of radial clearance at the first vane

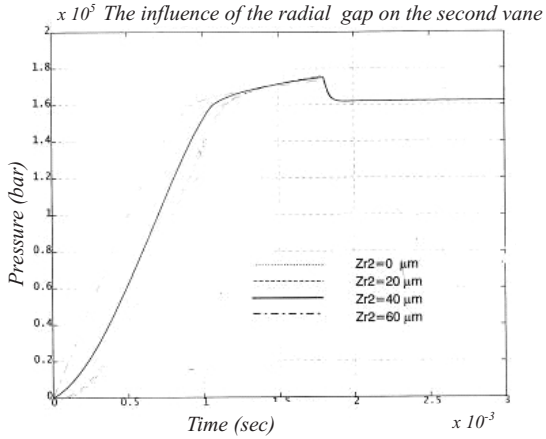

Figure 6. Results of simulating the expression for speed of pressure change in the chamber for various values of radial clearance at the second vane

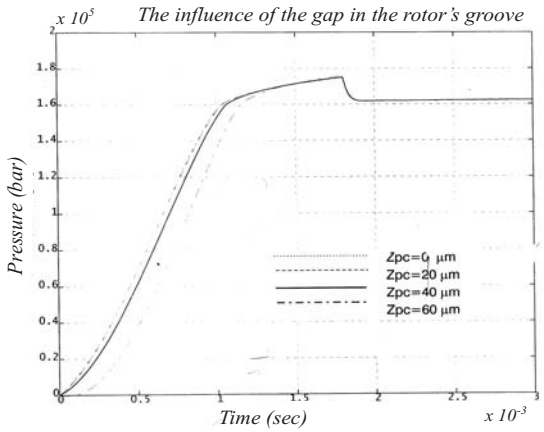

Figure 7. Results of simulating the expression for speed of pressure change in the chamber for various values of the gap in rotor groove

4. EXPERIMENTAL VERIFICATION OF OPERATING PARAMETERS

Experimental verification of operating parameters of vane pump with double effect has been done at the Laboratory of PTT-Namenska along with simulation of real conditions of pump exploitation. The following tests and diagrams have been made:

- -dependance between the pump pressure and flow at constant number of rotation of pump shaft,
- -dependance between the pump pressure and flow with oils of various kinematic viscosity at constant number of rotation of pump shaft.

The testing has been done at universal test stand AMS ZI 108-94262 FRESNES(FRANCE) TIP BAH 1622/B38-5.

The figure [8] shows the diagram of dependance between the outlet pressure and the flow of the pump (sample no.051) when tested at the test stand AMS. The pump flow is 70 l/min, the pressure is up to 5bar and by even pressure rise at thrust line and by closing the cock with keeping the constant rotation number the flow value is decreased for the value of losses made by the clearances at operating parts of the pump. The testing has been done with the oil of small kinematic viscosity ($10mm^2/s$ at 50^0C).

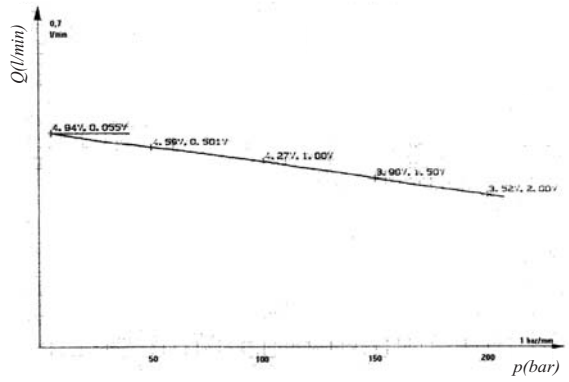

Figure 8. Diagram

The diagram at fig.[9] shows that the flow value at the pressure of 200bar has fallen for 20 l/min. This results from high temperature of the oil in the installation. The oil is warmed up at 90^0C, i.e. beyond the upper limit of working temperature.

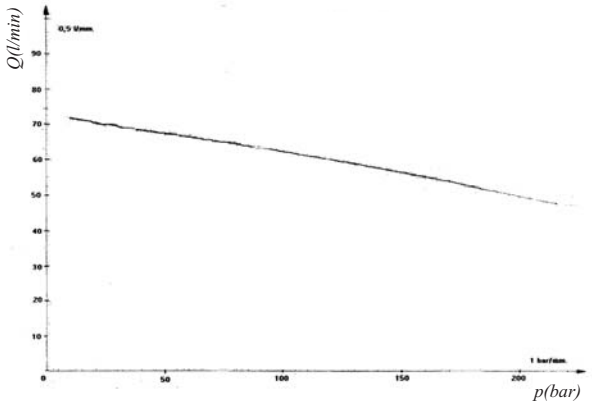

Figure 9. Diagram

The diagram at fig.[10] shows the jamming of operating parts of the pump because the oil temperature reached the value of 100^0C.

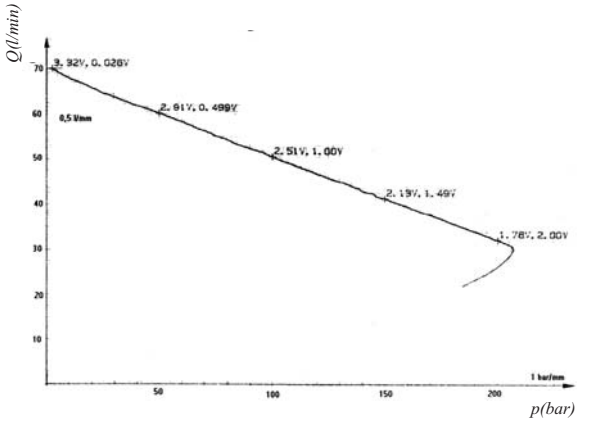

Figure 10. Diagram

The diagram at fig.[11] shows dependence between the outlet pressure and volumetric losses when oil of kinematic viscosity of $10mm^2/s$ has been used at the temperature of 50^0C and when oil of kinematic viscosity of $24mm^2/s$ has been used.

We can notice the decrease of volumetric losses when testing the pump with the oil of bigger kinematic viscosity.

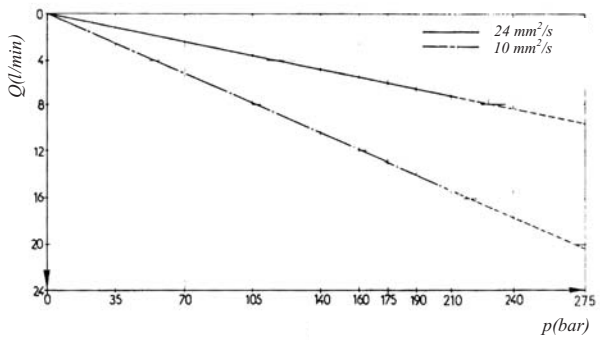

Figure 11. Diagram

5. CONCLUSION

It is not possible to determine precisely enough the parameters of hydrodynamic process of the vane pump with double effect neither by experiments nor by mathematical modeling only. Accurate working parameters can be reached by combined application of experimental measuring, mathematical modeling of hydrodynamic process and nonlinear optimization but at the same time the system errors of measuring and unknown parameters can be determined.
The program KRILP developed for mathematical modeling, identification and optimization of vane pumps provides developing of a whole family of vane pumps in further research of hydrodynamic processes along with the analysis of advantages and disadvantages of vane pumps with double effect.

REFERENCES

[1] *PETROVIC R..:* Mathematical modeling and identification of multicylindrical axial piston pump parameters, *PhD Thesis, Faculty of Mechanical Engineering, Belgrade, 1999. (in Serbian).*

[2] *JANKOV R..:* Development of new generation of ultra fast acquisition and control system ADS 2000, *Science and vehicle, Belgrade, (in Serbian).*

[3] *ČANTRAK S., GLAVČIĆ Z., PETROVIĆ R..:* Modelling of transition process behind the local resistance depending on flow rate circumference component, , *Third International Conference Heavy Machinery – HM '02, Kraljevo, 2002, E17-E20.*

[4] *PETROVIĆ R.., JANKOV R..:* Computer program for mathematical modelling and identification of hydrodinamic processes of a piston radial pump, *Third International Conference Heavy Machinery – HM '02, Kraljevo, 2002, E25-E28.*

[5] *GLAVČIĆ Z., ČANTRAK S., PETROVIĆ R..:* Analysis of flow energy losses in transition regimes of flow energetic parameter, *Third International Conference Heavy Machinery – HM '02, Kraljevo, 2002, E17-E20.*

[6] *PETROVIC R.,GLAVCIC Z.:* Systematic research of characteristic parameters of the piston axial pump, *III International Workshop on Computer Software for Design, Analysis and Control of Fluid Power Systems, Ostrava-Malenovice,Czech-Republic, 2003.*

[7] *PETROVIĆ R..:* Systematic research of characteristic parameters of the piston axial pump, *poster presentation, III International Fluid Power Conference 2002, Aachen, Germany, 2002*

[8] *BERGEMANN M:* Systematische Untersuchung des Geräuschverhaltens von Kolbenpumpen mit ungerader Kolbenanzahl, *Verlag Mainz, Wissenschaftsverlag, Aachen, 1994.*

[9] *HOFFMANN W.:* Dynamisches Verhalten hydraulischer systeme Automatischer Modellaufbau und digitale Simulation - *Dissertation TH Aachen, 1981, .*

[10] *PETTERSON M., WEDDFELT K., PELMBERG J.-O.:* Reduction of Flow Ripple from Fluid Power Piston - *Machines by Means of a Precompresion Filter, Volume 10., Aahener Fluidtechnisches Kolloquium, Bd. 2, 1992.*

[11] *PETTERSON M., WEDDFELT K., PELMBERG J.-O.:* Reduction of Flow Ripple from Fluid Power Piston - *Machines by Means of a Precompresion Filter, Volume 10., Aahener Fluidtechnisches Kolloquium, Bd. 2, 1992.*

[12] *GRAHL T.,* Geräuschminderung an Axialkolbenpumpen durch varia-ble Umsteuersysteme, *Ölhydraulik und Pneumatik 33 (1989), Nr.5*

[13] *HAARHAUS M., HAAS H.J.,* Untersuchung neuer Wege zur Geräuschminderung bei Axialkolbenpumpen, *Ölhydraulik und Pneumatik 29 (1985), Nr.2 und 3*

[14] *HOFFMANN D.,* Die Dämpfung von Flüssigkeitsschwingungen in Ölhydraulikleitungen, *Dissertation TU Braunschweig, 1975.*

[15] *FOMIN Y.:* Theory and Computing Fuel Injection Systems in Diesel Engines an a Digital high-speed Computer, *The Int. Comb. Eng. Conference, paper V. e., Bucharest, 1970.*

[16] *FOMIN Y. J.,* Gidrodinamičeskii rasčet toplivnih sistem dizelei s ispolzovaniem ECVM, *Mašinostroenie, Moskva, 1973 .*

EXPERIMENTAL RESEARCH OF CHARACTERISTIC PARAMETERS OF HYDRODINAMIC PROCESSES IN A PISTON AXIAL PUMP[1)]

R. Petrović, P. Ivanović, Z. Glavčić, M. Savković

Abstract: *Fundamental basis in developing the piston axial pumps are experimental research and mathematical modeling of non stationary high dynamic hydraulic processes in the pump cylinder, delivery chamber and intake and delivery pipe line.Based on the experimental research results,on the results of the mathematical modeling and, on developing and application of the identification method of unknown parameters of a mathematical model, the computer program AKSIP has been developed in order to enable the determination of some parameters of service processes in piston axial pumps.*

Key words: *piston axial pump, mathematical modeling, hydrodinamic processes*

1. INTRODUCTION

Modern design of a piston axial pump requires description of all processes and parameters in the pump. Complexity of hydrodynamic and dynamic processes in a piston-axial pump (pump cylinder, intake and delivery chamber,delivery valve and pipeline of high pressure) demands very studious physical and mathematical analysis of the same processes.

This approach is only possible having the special computer program. Such program (AKSIP) has been developed and presented in this paper [1-3].

2. MATHEMATICAL MODEL

For mathematical modeling of hydrodynamic and dynamic processes in a piston axial pump, fig.1, (pump cylinder, intake and delivery chamber, delivery valve and a high pressure pipeline), the following assumptions have been adopted [1]:

- Changes of the fluid state are pseudo stationary, except in the delivery pipeline;
- Kinetic energy of fluid in each control space, except in the delivery pipeline, is neglected;
- Fluid flow through clearances (crevices between the piston and cylinder, the flow through a jack panel and delivery valve) is pseudo stationary;
- The processes in the control spaces are isothermal or isentropic.

Simultaneous integration of the given non linear differential equations for boundary conditions and partial differential equations for flow in a delivery pipeline requires the application of computer and a corresponding computer program.

The program connecting and solving simultaneously all listed differential equations, the equations for change of characteristic flow sections and changes of physical characteristics of fluid, required a corresponding structure and organization. The program was written in the program language Digital Visual Fortran 5.0. and realized on the measuring and controlling system ADS 2000 [2].The principles of structural and modular programming were used. The programming consists of the main program and modules.

The more important programs were written as complete modules mutually connected or with the main program, but they can be used individually as well.

On the basis of the given equations a computer program named AKSIP was developed for mathematical modeling of flow and hydrodynamic processes for the complete time cycle of a piston axial pump with combined distribution of working fluid. AKSIP program is modular outlined and consists of the main AKSIP program and its modules.

2.1. Mathematical model of a pump process

Mathematical model is given for each element, considering the complexity of the processes and their mutual influence as well as the need for further mathematical modeling.

This makes program modules and their further improvement and monitoring much easier [1].

1) This work is part investigation in project " Research of metodologis and softweres for design, simulation and optimization of piston axial pumps"

Prof. Dr.-Ing. Radovan Petrović, Faculty of Mechanical Engineering Kraljevo, petrovic.r@mfkv.kg.ac.yu
Dr.-Ing. Petar Ivanović,
Ass. Ing. Zoran Glavčić, Faculty of Mechanical Engineering Kraljevo, glavcic.z@mfkv.kg.ac.yu
Ass.Dr.- Ing. Mile Savković, Faculty of Mechanical Engineering Kraljevo, savkovic.m@mfkv.kg.ac.yu

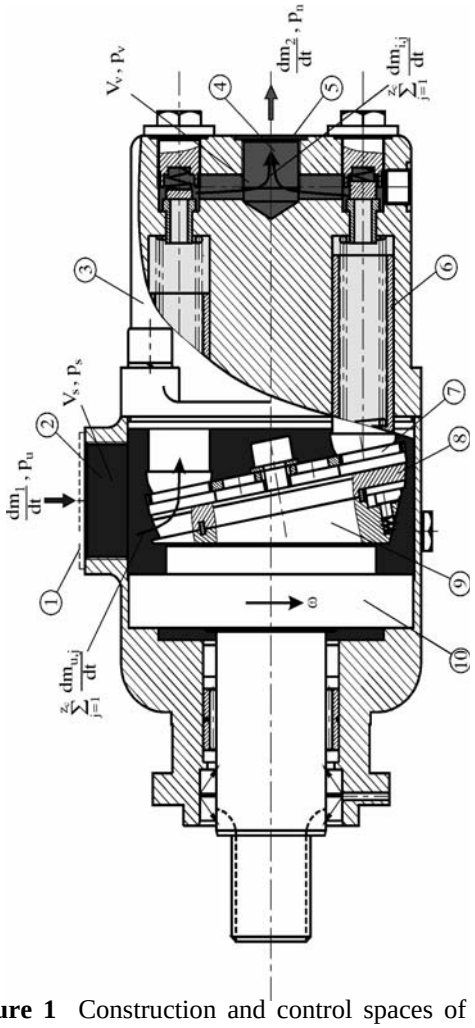

Figure 1 Construction and control spaces of a piston axial pump: (1)intake pipe line connection, (2)intake space of the pump, (3)cylinder block, (4)delivery chamber of the pump, (5)delivery pipeline connection, (6)piston, (7)jack panel, (8)inclined panel, (9)driving pump shaft, driving pump shaft bedding

- mass flow through the opening 1, on the entrance place into the intake space of the pump of fluid, fig. 1:

$$\frac{dm_1}{dt} = \sigma_1 \cdot \mu_1 \cdot A_1 \cdot \sqrt{2 \cdot \rho_s \left| p_u - p_s \right|}, \qquad (1)$$

where :
σ_1=*1* for $p_u \geq p_s$, σ_1=*-1* for $p_u \leq p_s$
A_1 - geometrical flow section of the intake pipe
μ_1 - flow coefficient of the intake pipe

- mass flow of fluid through the split pump organ during filling one of the pump cylinders:

$$\frac{dm_u}{dt} = \sigma_u \cdot \mu_u \cdot A_u \sqrt{2 \cdot \rho_s \cdot \left| p_s - p_c \right|}, \qquad (2)$$

where :
σ_u=*1* for $p_s \geq p_c$, σ_u = *-1* for $p_s \leq p_c$
A_u- geometrical flow section of the intake split organ
μ_u - flow coefficient of the intake split organ

- mass balance of the intake space is:

$$\frac{dm_s}{dt} = \frac{dm_1}{dt} - \sum_{j=1}^{z} \frac{dm_{u,j}}{dt}, \qquad (3)$$

where :
j=*1,2,...,*z_c, z_c - the numbers of cylinders

- differential equation for pressure in the intake pump space:

$$\frac{dp_s}{d\varphi} = \frac{E}{V_s \cdot \rho_s} \cdot \left(\frac{dm_1}{d\varphi} - \sum_{j=1}^{z_c} \frac{dm_{u,j}}{d\varphi} \right), \qquad (4)$$

E - modulus of elasticity;
φ - the driving shaft angle,

- differential equation for pressure in the pump cylinder:

$$\frac{dp_c}{d\varphi} = \frac{E}{V_c} \cdot \left[\frac{A_c \cdot v_k}{\omega} + \frac{1}{\rho_c} \cdot \left(\frac{dm_u}{d\varphi} - \frac{dm_i}{d\varphi} \right) \right], \qquad (5)$$

where:

$V_c = V_{c\min} + V_{cx}$; $V_{cx} = A_c \cdot x_k$ - current volume of the cylinder; the change of the pump cylinder volume caused by piston moving: $\frac{dV_c}{dt} = -A_c \cdot v_k$, x_k - current displacement of the piston.

- mass balance of the delivery chamber is:

$$\frac{dm_v}{dt} = \sum_{j=1}^{z_c} \frac{dm_{i,j}}{dt} - \frac{dm_2}{dt}, \qquad (6)$$

where : j=*1,2,...,* z_c - the numbers of cylinders

- mass flow out of the delivery chamber into the delivery pipe is:

$$\frac{dm_2}{dt} = \sigma_2 \cdot \mu_2 \cdot A_2 \cdot \sqrt{2 \cdot \rho_t \cdot \left| p_v - p_n \right|}, \qquad (7)$$

where: σ_2=*1* for $p_v \geq p_n$, σ_2 = *-1* for $p_v \leq p_n$
A_2- geometrical flow section of the delivery pipe line

- differential equation for pressure in the delivery pump chamber:

$$\frac{dp_v}{d\varphi} = \frac{E}{V_v \cdot \rho_v} \cdot \left(\sum_{j=1}^{z_c} \frac{dm_{i,j}}{d\varphi} - \frac{dm_2}{d\varphi} \right), \qquad (8)$$

- mass flow through a concentric clearance between the cylinder and the piston:

$$\frac{dm_z}{dt} = \frac{\pi \cdot D_c \cdot \Delta r^3}{12 \cdot \eta \cdot x_k(\varphi)} \cdot (p_c - p_s) \cdot \rho_c, \qquad (9)$$

where: D_c - diameter of cylinder, Δr - radial clearance between the piston and the cylinder, η- dynamic viscosity, $x_k(\varphi)$ - current displacement of the piston, p_c

- the pressure in the cylinder, p_s - the pressure in the intake space, ρ_c - the density of the fluid in the cylinder.

2.2 Modeling the flow in the intake and delivery pipe line of the pump

For mathematical modeling of a process in a pump, it is also necessary to include and consider a series of assumptions for a process occurring in the intake and delivery pipe line of the pump.

The following assumptions regarding the flow of the working fluid in the intake and delivery pipe line are taken and considered:

– The fluid flow is one-dimensional. The pipe cross section is constant. Temperature and flow fields across the pipe are homogeneous. Velocity vector follows the direction of the axis of the pipe at any moment and in any section.
– Viscosity friction between the layers of the fluid inside the pipe is neglected. The friction forces appear on the inside walls of the pipe.
– The processes in the pipes are isentropic. The change of entropy caused by friction, heat and mixing of fluid parts are neglected.
– Forces of gravitational, magnetic, etc. are neglected.

Continuity Equations

The equation of continuity of pressed fluid with functions p, v, ρ during the isentropic change of the state is:

$$\frac{\partial p}{\partial t} + v \cdot \frac{\partial p}{\partial x} + a^2 \cdot \rho \cdot \frac{\partial v}{\partial x} = 0 , \qquad (10)$$

where : ρ and v – values of density and velocity of fluid per cross section of the pipe, $a = \sqrt{\left(\frac{\partial p}{\partial \rho}\right)_s}$, the velocity of sound in the fluid,
where: $p = p(t,x)$ and $\rho = \rho(t,x)$ are functions of time t and coordinate x.

Momentum Equations

$$v \cdot \frac{\partial \rho}{\partial t} + \rho \cdot \frac{\partial v}{\partial t} + v \frac{\partial}{\partial x}(\rho \cdot v) + \rho \cdot v \cdot \frac{\partial v}{\partial x} + \frac{\partial p}{\partial x} = -f_r \cdot \rho , \quad (11)$$

where: f_r – friction force per mass unit.

In the scope of fluid dynamics of one-dimensional flow, such flows are considered as “non stationary flows in a flow fiber”.

3. MEASURING RESULTS OF WORKING PROCESS IN THE PISTON AXIAL PUMP

In the scope of performed experimental researches, the measuring of the pressure history in the cylinder, delivery chamber was done . The vibration of the pump housing was also measured dependening on the pump driving shaft angle. All pressures and vibrations were measured simultaneously on each cca 0.09^o step of the driving pump shaft (exactly 4.096 times per shaft rotation). As incremental angle encoder an optical encoder with 1.024 pulses per rotation was used. Pulses of the angle encoder were quadrupled by the interface for the angle encoder on the ADS 2000 system so that 4.096 pulses per shaft rotation were obtained. In order to see the repetition of the consecutive cycles with the unchanged working regime 10 consecutive cycles were measured. At the same time, a time interval from angle to angle was also measured in order to determine the variation of shaft speed and control of the incremental angle encoder. All the analogue signals (pressure, vibrations) were parallel converted into digital form by means of four (4) ultra speed A/D converters working simultaneously (parallel). The total number of measured data was (4+1) x 4.096 = 20.480 per rotation (cycle), that is, 204.800 for ten consecutive cycles. The number 4.096 was not chosen by chance, but in order to use the fast Furie's Transformation (FFT) of measured signals. Measurements were done for seven working regimes. Fig. 2 (a÷f) shows the measured pressure history for individual, i.e. ten consecutive cycles of the piston axial pump. The results are related to the experiment at the work regime p=200 bars and n=875.6 min^{-1}.

There is a great similarity of measured pressures for the first of ten consecutive cycles (MERF) in relation to the average one of ten consecutive cycles (MERM).

Figures 2a and 2b show the measured pressure history in the cylinder (p_c) for one, i.e. the average one of ten consecutive cycles as the driving shaft angle. The diagram shows the visual pressure gradients at the compression and expansion stage as well as the appearance of peaks during intake. Figures 2a and 2b also show the pressure intake in the discharge space (p_v) for one, i.e. for the average of the ten consecutive cycles as the function of the driving shaft angle. The pressure pulses in the delivery chamber depend on the number of the cylinders which is obvious in this case, because the pump has 8 cylinders.

Figures 2c and 2d show the appearance of peaks at the intake stage for one, that is, for the average one of ten consecutive cycles at the 120^o-270^o angle interval of the driving shaft.

Figures 2e and 2f show the measured pressure history in the cylinder (p_c) for one, that is for average of ten consecutive cycles at the angle interval of the shaft of 278^o-307^o angle interval of the shaft in order to analyze in detail the gradient increase of pressure at the compression stage. The same diagrams, at the same

interval, show the pressure pulses in the delivery chamber.

a) The pressure history in the cylinder (p_c) and delivery chamber (p_v) for one cycle
b) The pressure history in the cylinder (p_c) and delivery chamber (p_v) for the average cycle
c) The presure history in the cylinder (p_c) in the 120^o-270^o interval for one cycle
d) The pressure history in the cylinder (p_c) in the interval of 120^o-270^o for the average cycle
e) The pressure history in the cylinder (p_c) and delivery chamber (p_v) in the 278^o-307^o interval for one cycle.
f) The pressure history in the cylinder (p_c) and delivery chamber (p_v) in the 278^o-307^o interval for the average cycle.

The figures 2a) ÷ 2f) stand for diagrams of measured pressure at the work regime n=875.6 min^{-1} and p_n=200 bars.

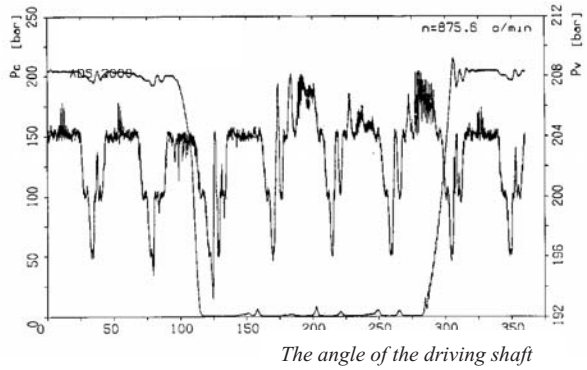

Figure 2a) The pressure history in the cylinder (p_c) and delivery chamber (p_v) for one cycle

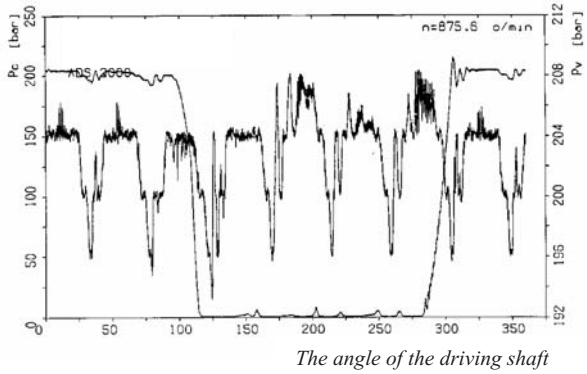

Figure 2b) The pressure history in the cylinder (p_c) and delivery chamber (p_v) for the average cycle

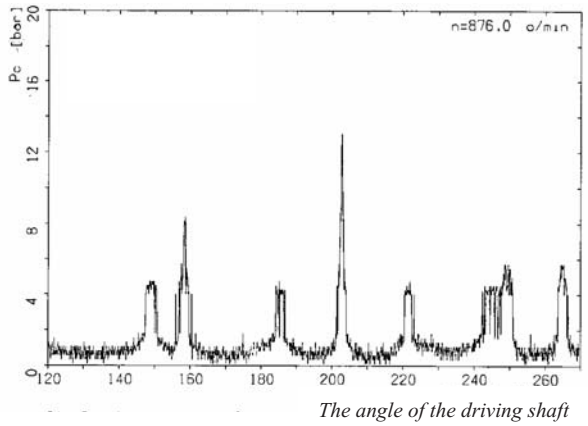

Figure 2c) The pressure history in the cylinder (p_c) in the$120^o \div 270^O$ interval for one cycle

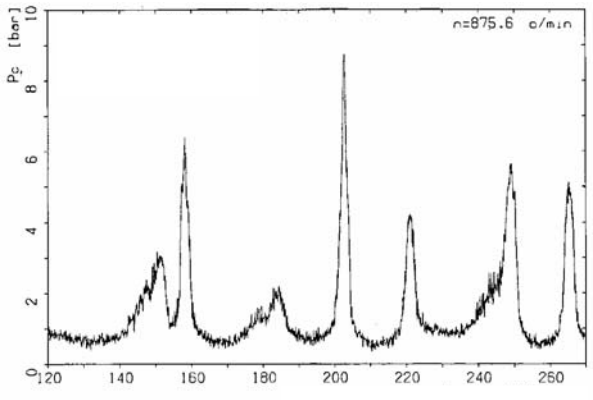

Figure 2d) The pressure history in the cylinder (p_c) in the$120^o \div 270^O$ interval for the average cycle

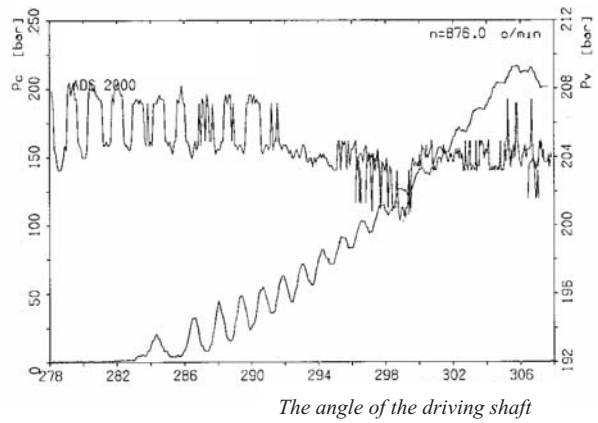

Figure 2e) The pressure history in the cylinder (p_c) and delivery chamber (p_v) in $278^o \div 307^O$ interval for one cycle

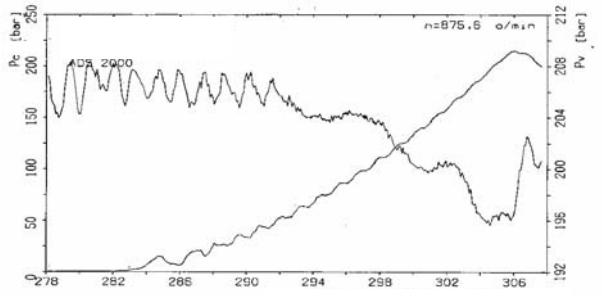

Figure 2f) The pressure history in the cylinder (p_c) and delivery chamber (p_v) in $278^o \div 307^O$ interval for the average cycle

4. CONCLUSION

The parameters of hydrodynamic processes in a piston axial pump cannot be precisely determined, neither by experiment nor by mathematical modeling. Precise parameters can be obtained by combining the experimental testing (measuring the pressure history in the cylinder), mathematical modeling of a real hydrodynamic process and the method of nonlinear optimisation which at the same time enable the determination of systematic measuring errors and unknown parameters.

The computer program AKSIP gives possibilities to combine 56 influential pump parameters in order to achieve optimal solution, in regard to flow losses, flow inlet etc.

Further research is possible regarding the construction of the piston axial pumps with a bent cylinder block and distribution of working fluid by means of a jack panel. In that case mathematical model should be expanded by a cylinder block dynamics and hydrodynamic processes in clearances between the cylinder block and the jack panel.

REFERENCES

[1] PETROVIC R.: Mathematical modeling and identification of multicylindrical axial piston pump parameters, *PhD Thesis, Faculty of Mechanical Engineering, Belgrade, 1999. (in Serbian).*

[2] JANKOV R.: Development of new generation of ultra fast acquisition and control system ADS 2000, *Science and vehicle, Belgrade, (in Serbian).*

[3] ČANTRAK S., GLAVČIĆ Z., PETROVIĆ R.: Modelling of transition process behind the local resistance depending on flow rate circumference component, *Third International Conference Heavy Machinery – HM '02, Kraljevo, 2002, E17-E20.*

[4] PETROVIĆ R.,JANKOV R.:Computer program for mathematical modelling and identification of hydrodinamic processes of a piston radial pump, *Third International Conference Heavy Machinery – HM '02, Kraljevo 2002, E25-E28* .

[5] GLAVČIĆ Z., ČANTRAK S., PETROVIĆ R.: Analysis of flow energy losses in transition regimes of flow energetic parameter, *Third International Conference Heavy Machinery – HM '02, Kraljevo, 2002, E17-E20.*

[6] PETROVIC R.,GLAVCIC Z.:Systematic research of characteristic parameters of the piston axial pump, *III International Workshop on Computer Software for Design, Analysis and Control of Fluid Power Systems, Ostrava-Malenovice, Czech-Republic, 2003.*

[7] PETROVIĆ R.:Systematic research of characteristic parameters of the piston axial pump, *III International Fluid Power Conference, Aachen, Germany, 2002.*

[8] BERGEMANN M.: *Systematische Untersuchung des Geräuschverhaltens von Kolbenpumpen mit ungerader Kolbenanzahl,* Verlag Mainz, Wissenschaftsverlag, Aachen, 1994.

[9] HOFFMANN, W.: *Dynamisches Verhalten hydraulischer systeme Automatischer Modellaufbau und digitale Simulation*- Dissertation TH Aachen, 1981

[10] PETTERSON M., WEDDFELT K., PELMBERG J.-O.: *Reduction of Flow Ripple from Fluid Power Piston*- Machines by Means of a Precompresion Filter, Volume 10., Aahener Fluidtechnisches Kolloquium, Bd. 2, 1992.

[11] PETTERSON M., WEDDFELT K., PELMBERG J.-O.: *Reduction of Flow Ripple from Fluid Power Piston*- Machines by Means of a Precompresion Filter, Volume 10., Aahener Fluidtechnisches Kolloquium, Bd. 2, 1992.

[12] GRAHL T.:*Geräuschminderung an Axialko-lbenpumpen durch varia-ble Umsteuersysteme,* Ölhydraulik und Pneumatik 33 (1989), Nr.5

[13] HAARHAUS M., HAAS H.J.: *Untersuchung neuer Wege zur Geräuschminderung bei Axialkolbe-npumpen,* Ölhydraulik und Pneumatik 29 (1985), Nr.2 und 3

[14] HOFFMANN D.: *Die Dämpfung von Flüssi-gkeitsschwingungen in Ölhydraulikleitungen,* Dissertation TU Braunschweig, 1975.

[15] FOMIN Y.: *Theory and Computing Fuel Injection Systems in Diesel Engines an a Digital high-speed Computer,* The Int. Comb. Eng. Conference, paper V. e., Bucharest, 1970.

[16] FOMIN Y. J.: *Gidrodinamičeskii rasčet toplivnih sistem dizelei s ispolzovaniem ECVM,* Mašinostroenie, Moskva, 1973 .

[17] FOMIN Y. J.: *Toplivnaja apparatura dizelei*, Mašinostroenije, Moskva, 1982.

XML SPECIFICATION OF HYDRAULICS COMPONENTS

D.Pršić, N.Nedić, A. Babić

Abstract: *Technical documentation in the field of hydraulics and pneumatics as well as in other fields of engineering today is mostly seen in electrronic form. Basic advantage is in the fact that such documents can be easily distributed using computer networks and the Internet. This influences the formation of a mutual, easily available distributed base of knowledge which further on speeds the development of these fields. However, the use of electronic documents causes a huge problem – incompatibility of different formats. Very often a document written on one platform (MS Windows, Linux, Mac OS X) is not readable on another platform, or by a different program on the same platform, or even by a different version of the same program. To solve this problem, many software companies distribute free file viewers for their proprietary file formats. The other solution is the development of standardized non-proprietary file formats (HTML, OD, XML). This paper presents the use of Extensible Markup Language (XML) for the description of information structures and semantics about hydraulic components.*

Key words: *XML, data exchange, axial-piston pump, parser, DOM, SAX*

1. INTRODUCTION

Generally speaking, communication between two computers program can be viewed as data and metadata interchange. Data carry out raw (basic) information while metadata are information about data. They are used to facilitate the understanding, characteristics, and management usage of data. For example, numerical value 170.52 may have infinite different meaning. To make sense of and use this data, context is important, and can be provided by metadata. If we write down "P170.52" metadata "P" suggests that it's the pressure, or if we write down "Q170.52" we know that it is volumetric flow rate. In many cases we have to specify which unit we mean so we introduce metadata [bar] or [N/m^2]. Even if we don't take into consideration different formats for numerical data (e.g. 170.52, 1.7052E2, 0.175052E3) the problem with different forms for metadata remains. For example, the same information can be marked up with "P170.52 bar", "P#170.52bar", "P170.52E5N/m^2". Basically, a computer doesn't have the possibility to conclude that this is the same information. From its point of view, these are all different data.

Different forms of metadata are the basic cause of software applications incompatibility. For two applications to communicate it is necessary to adopt universal rules for data marking. XML is the program that makes it possible for us to define those rules. It allows us to define our own tags which must be organized according to certain general principles, but they are flexible in their meaning [1,2].

For example, for preassure we can introduce text mark up <*pressure*>. In that case the very name tells about the information. Despite that, tag <*pressure*> doesn't tell anything about information format, data and metadata are included as strings of text, they only tell us that there is a piece of data called <*pressure*> and it's up to us to give the specific piece information specific meaning.

It is important to realize that XML is not markup language, but meta-markup language. In other words, XML describes the syntax that we use to create our own languages. Each specific XML-based markup language is called an XML application. Those are, e.g. Chemical Markup Language (CML), Mathematical Markup Language (MathML) or Bond Graph Markup Language (BGML).

2. DESCRIBING AXIAL-PITON PUMP WITH XML DOCUMENT

When we work with complex information it is necessary to arrange them in a specific way. While being modelled, the data are usually hierarchically grouped depending on the level of abstraction. There is a system on the highest level, then there are sub-systems on the next level, elements are found on the level beneath, etc. For example, a book consists of chapters, a chapter is broken down into sub-topics, and further broken down into paragraphs.

In figure Fig. 1 axial, fixed-displacement piston pump is shown. There are many information about it and it is usually better to group them into related subtopics, rather than to have all of them presented on the same level. This makes information easier to comprehend and more accessible.

The first step in forming XML data that describe the pump or any other component, is defining:

Dragan Pršić, Faculty of Mechanical Engineering Kraljevo, prsic.d@mfkv.kg.ac.yu
Novak Nedić, Faculty of Mechanical Engineering Kraljevo, nedic.n@mfkv.kg.ac.yu
Arandjel Babić, Faculty of Mechanical Engineering Kraljevo, babic.a@mfkv.kg.ac.yu

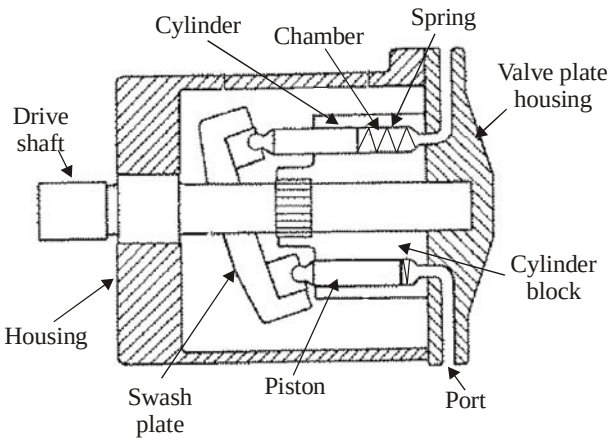

Fig.1. *Axial-piston pump*

- the set of relevant data
- relations between them

The pump can be described using the set of constructive (length, height, mass, diameter, etc.) and operating parameters (pressure, temperature, volumetric flow rate, etc.). Every parameter presents one of the pump metadata. The set of parameter-value pairs forms the content of the pump information. In order to complete the description of the pump it is necessary to define relations between these pairs. The only type of relation available is containment relation. This enables us to make connection (parent-child) between data on different level of abstraction. There is no direct relation between the data on the same level of abstraction (sibling-sibling).

Following the physical structure of the pump we come to the hierarchical structure of the data shown in Fig. 2

Graphically, pump information is shown using the so-called tree structure, which is very common in programming. Data and metadata are the basic components of information, whereas containment relations are shown using the lines. When reading information we move along the branches starting from the root of the tree. In that way the lines show the structure and the context of data.

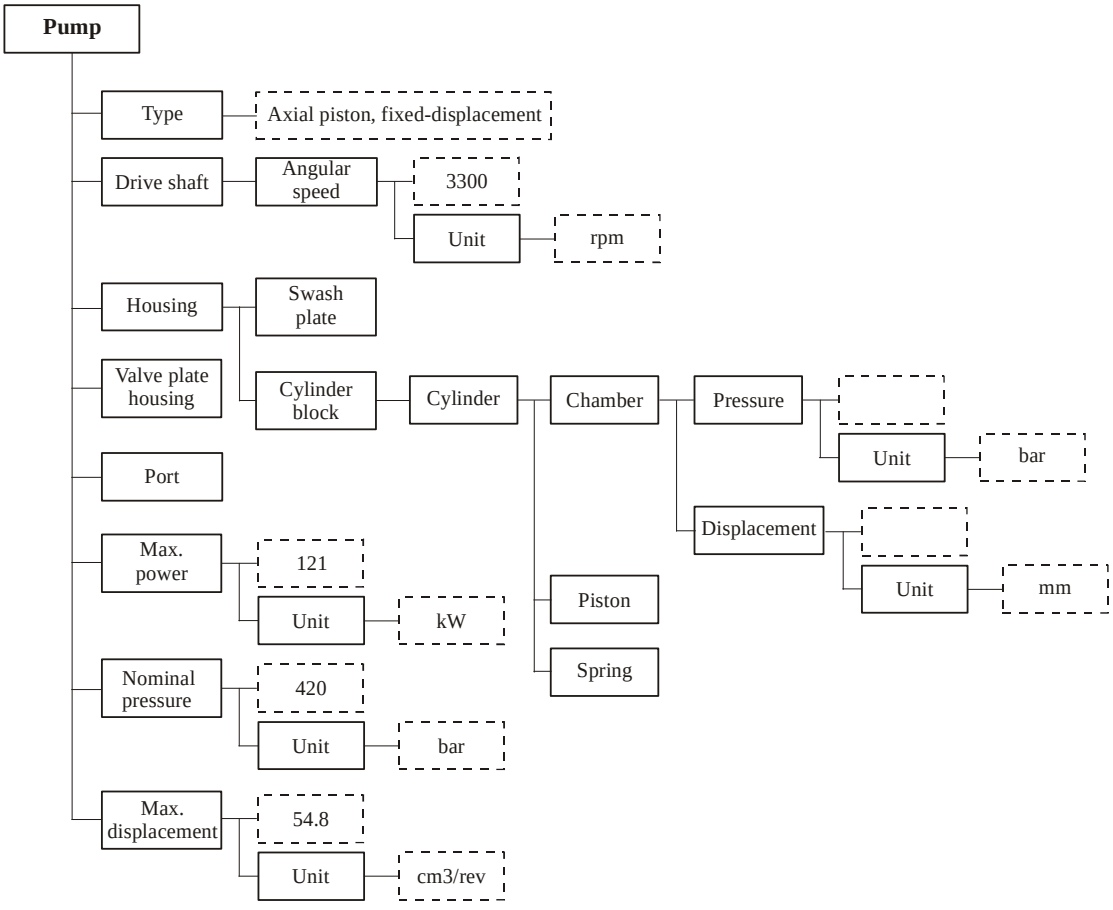

Fig.2. *Hierarchical data structure of axial-piston pump*

For example, meta information *Pump* consists of meta information *Nominal pressure*, which again contains information 420. In that way we find out that the nominal pressure of the pump is 420. Another branch Pump -> *Nominal pressure* -> *Unit->bar* is about bars. Between the items on two different levels of abstraction (*Pump* and *Nominal pressure*) there is parent - child relationship, and between the items on the same level of abstraction (*Unit* and *420*) there is sibling - sibling relationship. Although there can be elements with the

same name in the structure (*Unit*) every one of them is unambiguously specified using the parents elements on higher level. E.g. *Pump -> Nominal pressure -> Unit* is different from *Pump -> Max. power-> Unit*.

With the help of XML we textually describe the very thing that is graphically presented using the tree structure. Included data and markup that describes the data are strings of text. An XML that describes the pump model in Fig.2 is shown in Fig.3.

The document in Fig. 3 is composed of a single element named *pump*, which includes other child elements. Specifically, since it contains the entire document, this element is called the root element or document element. Every XML document has one element that does not have a parent. This is the first element in the document and the element that contains all other elements. Every well-formed XML document has exactly one root element. Elements may not overlap, and all elements except the root have exactly one parent. The *pump* element is called parent of *driveShaft*, *housing*, *valvePlateHousing*, *port*, *maxPower*, *nominalPressure* and *maxDisplacement*. The same relations (parent/child, sibling) hold for other elements: *housing* is parent for *swashPlate* and *cylinderBlock*, which are on the other hand siblings.

The text starting with a "<" character, and ending with a ">" character is called XML tag. Between them there is the name of element. XML tags look superficially like HTML tags. However, unlike HTML tags, we are allowed to make up new XML tags as we go along. The data of an information are contained within the various tags that constitite the markup of the document. This makes it easy to distinguish data in the information from the metadata. The tags are always paired together, any opening tag has a closing tag. These pair of tags are called start-tags and end-tags. The end-tags are the same as the start-tags except that they have a character "/" right after the opening "<" character. Everything between the start-tag and the end-tag of the element is called the element's content. All of the information from the start of a start-tag to the end of the end-tag, including everything in between, is called an element. For example, <*unit*> is a start tag, </*unit*> is an end-tag, *mm* is a content, and <*unit*>mm</*unit*> is an element. The element content can be other element or just data. In later case, the element content is reffered to as Parsed Character DATA - PCDATA.

Some of the elements as *unit* only contain character data. Others such as *housing* contain only child elements. For elements like as *maxPower*, that have both character data and child elements, are said to contain mixed content.

A mixed content is less common in computer-generated and processed XML documents. One of the strengths of XML is the ease with which it can be adapted to the very different requirements of human-authored and computer-generated documents. Dichotomy between elements that contain only character data and elements that contain only child elements is common in documents that are data oriented.

```
<pump>
    <type>axiapl-piston, fixed-displacement</type>
  - <driveShaft>
    - <angularSpeed>
        3300
        <unit>rpm</unit>
      </angularSpeed>
    </driveShaft>
  - <housing>
      <swashPlate />
    - <cylinderBlock>
      - <cylinder>
        - <chamber>
          - <pressure>
              <unit>bar</unit>
            </pressure>
          - <displacement>
              <unit>mm</unit>
            </displacement>
          </chamber>
          <piston />
          <spring />
        </cylinder>
      </cylinderBlock>
    </housing>
    <valvePlateHousing />
    <port />
  - <maxPower>
      121
      <unit>kW</unit>
    </maxPower>
  - <nominalPressure>
      420
      <unit>bar</unit>
    </nominalPressure>
  - <maxDisplacement>
      54.8
      <unit>cm3/rev</unit>
    </maxDisplacement>
</pump>
```

Fig.3. *XML document of axial piston pump*

Although XML doesn't allow us the freedom in the choice of elements that make the document it provides grammar for XML documents that says where tags may be placed, what they must look like, which element names are legal, how attributes are attached to elements, and so forth.

The document satisfying all rules of the XML grammar is said to be well-formed. Every XML document must be well-formed. Some of rules of XML grammar are [3]:

- Every start-tag must have a matching end-tag.
- Elements may nest, but may not overlap.
- There must be exactly one root element.
- Attribute values must be quoted.
- An element may not have two attributes with the same name.
- Comments and processing instructions may not appear inside tags.
- No unescaped < or & signs may occur in the character data of an element or attribute.

3. PARSING XML DOCUMENTS

Thanks to the precisely written specification, numerous programs, the so-called parsers (XML processor) have been written. They can analyze an XML document and give us information about its content and structure.We can use these parsers within our own programs, meaning our application never have to even look at the XML directly. The relationship between application, parser and XML document is shown in Fig.4.

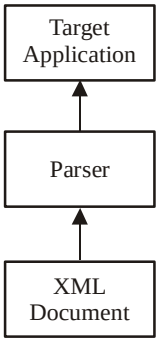

Fig.4. *Extracting information from XML document*

Two application programming interfaces (API) are mainly used for developing application specific XML processors: Document Object Model (DOM) as well as Simple API for XML (SAX). Both interfaces facilitate communication between the target application and the XML document, but they use completely different approaches.

The structure of processing an XML document by means of DOM interface is shown in Fig. 5. [4,5].

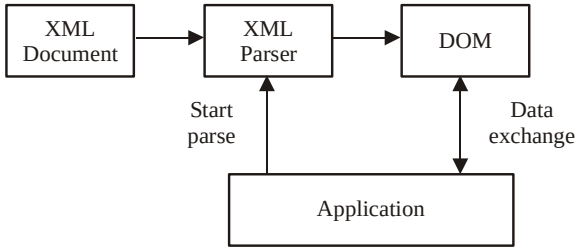

Fig.5. *DOM model of processing an XML document*

After the application sends the Start parse signal, the parser forms a tree-shaped document object model. The application then just navigates the tree to find the desired pieces of the document. The whole document that can be easily browsed and modified is always available. Working with a tree model of a document is conceptually similar to working with a document as a text. DOM is suitable when we should create a complete memory map of an XML document. However, this can be very exacting in terms of memory and time.

SAX is event-driven API. It is a form of agreement between the application and the parser which must be fulfilled by the application. While reading a document, the XML analyzer moves from its beginning to its end. Any change in the structure and content of the document (e.g. the start of an element, read the content of an element, end of element) is registered by the parser as an event, and the information about it is sent to the client application. The client application, through its module implementing the SAX interface, should decide how to process each of those events. The structure of processing an XML document by means of the SAX interface is shown in Fig. 6.

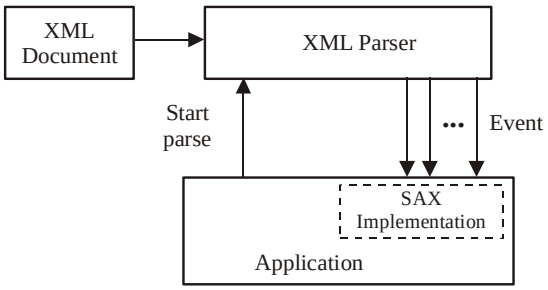

Fig.6. *SAX model of processing an XML document*

4. CONCLUSION

XML is extensible, non-proprietary, self-describing format especially suitable for data exchange over the Internet. In the beginning of this year Open XML file formats has received the necessary number of votes for approval as an ISO/IEC International Standard. Serbian Institute for Standardization also voted for the approval of this standard.

In order to develop XML application in the field of hydraulics it is necessary to do two things. First of all, it's necessary to reach an agreement on tag sets and on the way in which information in this field is structured. The bigger the number of users who will accept the agreement the easier information exchange. Secondly, it's necessary to develop modules for reading and writing of XML documents. XML parsers are of great help in that.

The benefits gained by accepting this format are big. For example, a module for listing the producers' catalogues and choosing the right component on its own could be installed into the design software.

REFERENCES

[1] W3C. Extensible markup language. http://www.w3.org/XML

[2] The Apache XML Project, XML. http://xml.apache.org

[3] E.R. Harold, W.Scott Means, *XML in a Nutshell*, Third Edition, O'Reilly Media, Inc 2004

[4] K. Cagle, et. al., *Beginning XML*, Wrox Press Ltd., Birmingham, B27 6BH, UK, 2000.

[5] D.Pršić, N.Nedić, A.Babić, "Transformation of XML Model into a Block Diagram", IX Triennial International SAUM Conference, Niš, Serbia, 2007, pp.

SOME EXPERIMENTAL DETERMINATIONS WITH SAND-BLASTING MOBILE UNIT

I. Bărdescu, C.G. Popescu-Ungureanu, A. Legendi

Abstract: *This theme deals with the testing last part done for a PhD thesis[1]. A* ***dry sand-blasting unit with free diphase jet****, classical type, was used for sand-blasting, using* ***sand+air-compressed mixture without material recovery****. Focusing a* ***sand-blasting modern technology****,* ***metallic granules*** *were used and the experiments to be done were realized in a view to accomplishing* ***minimal costs*** *and* ***real working conditions****. So, the sand-blasting unit was* ***essentially modified*** *regarding the constructive design, in a personal conception, using* ***metallic sand-blasting granules*** *instead of sand, and the* ***sand-blasting technology with discontinuous sand-blasting granules recovery,*** *with a minimal quantity of metallic sand-blasting granules.*

Key words: *sand-blasting-equipments, sand-blasting experiments, sand-blasting-technological parameters, sand-blasting measurements.*

1. INTRODUCTION

There have been done some experimental determinations regarding sand-blasting in a private company SUTCAS s.r.l.-Bucharest, producing very light (fewer than 100 kg/m^3) macro air-entrained polymeric concrete elements. The mechanical plant along with the manufacture hall is situated in Ciorogarla, Ilfov County, near Bucharest. Tests were done using a **sand-blasting mobile unit** essentially modified regarding the **constructive components**, designed and manufactured in a personal conception, so that could be attached to the existing sand-blasting mobile unit and then removed after tests, the initial construction and destination of that equipment remaining unchangeable.

Seven additional components for experiments were realized through personal means, being mentioned the following: **the cannular chamber** (cylindrical), low capacity, for controlled charges, that allows the use of small and measurable quantities of steel granules; **the spherical chamber** of mixing-dosing granules+air compressed (fig.1); t**he sand-blasting-recovery tight chamber** of metallic granules.

In the testing first part, the following were primarily analyzed using the correlation and comparison:

- the geometry of non-metallic material samples (concrete, natural river stone);
- the designed sand-blasting nozzles: long, short and cylindrical Venturi;
- the geometry of sand-blasting metallic, cylindrical and spherical granules (small shots).

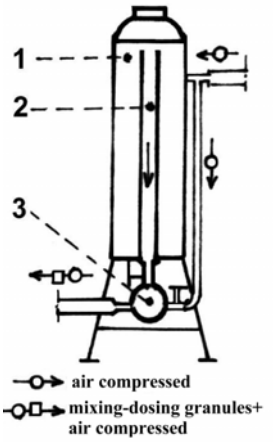

Fig. 1 a. Pressure tank assembly (1); cannular feeding chamber (2); spherical mixing-dosing chamber (3)

The technological parameters were measured for **the nozzle long Venturi type** having the outlet diameter d_{vl} **= 15 mm**, and **the length** l_{vl} **= 170 mm**, using **cylindrical metallic granules** having the diameter d_{gc} **= =2 mm**, the length l_{gc} **= 3 mm** şi and the apparent specific mass ρ_{gl} **= 4,92 kg/dm^3**.

2. COMPONENTS MECHANICAL ASSEMBLIES

Three **mechanical assemblies of components** were conceived and realized for measurements and calculus:

(1) **the cannular feeding chamber with granules**, put in the sand-blasting tank (fig.1 b), assembled to the spherical granules+air-compressed mixing-dosing chamber.

Prof. univ. dr. mech.eng. Ioan Bărdescu, Technical University of Civil Engineering Bucharest-Romania, bardescu.liz30@yahoo.com
Dr. eng. prof. Cristiana-Gabriela Popescu-Ungureanu, Scolar Group Industrial Construction Railway, Bucharest-Romania, cristianapug@yahoo.com
Associated prof. PhD eng. Amelitta Legendi, Technical University of Civil Engineering Bucharest-Romania, amelitta.legendi@gmail.com

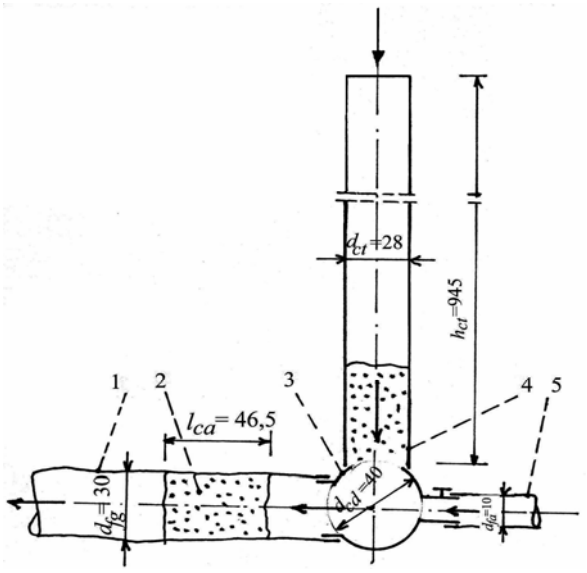

Fig. 1 b. Cannular chamber -spherical chamber − granules+air compressed mixture hose assembly.

(2) **Mixing-dosing spherical chamber** assembled with some pressure transducer (fig.2).
(3) **Pressure transducer** assembled with the nozzle long Venturi type (fig.3).

Using **the cannular chamber+mixing-dosing spherical chamber assembly**, several parameters were measured and calculated, such as:

- **Time in which the cylindrical charge**, granules+ air, passed within the nozzle joint hose

$$t_{ca} = 0,4 \text{ s} \quad (1)$$

- **The granules+air-compressed mixture outlet speed** from the nozzle

$$V_{1p} = 25 \text{ s} \quad (2)$$

- **The granules+air-compressed diphase jet length** (L_{jb}),depending on the interior diameter at the nozzle's outlet (d_{vl})

$$L_{jb} = 240 \text{ mm} = 16\, d_{vl} \quad (3)$$

- **The quasi-annular diameter** of the print remained on the sample after the sand-blasting

$$D_{as} = 60 \text{ mm} \quad (4)$$

- **The dispersion angle** (2β)

$$2\beta \cong 11° = f\left(V_{jb}\right) \quad (5)$$

The errors measured and calculated during tests, and compared to those mentioned in the specialized literature, were precise enough, max ± 5%.

For practical and fast applications, a **simplified calculus relationship** for the granules+air-compressed dry mixture **speed** (V_{1p}) **at the nozzle's outlet**, depending on the sand-blasting granule's greater diameter in mm (d_g), is proposed:

$$V_{1p} = 20 \cdot d_g^{0,4} \text{ [m/s]} \quad (6)$$

3. SAND-BLASTING TECHNOLOGICAL PARAMETERS MEASURED AND CALCULATED IN EXPERIMENTS' LAST PART

Components mechanical assemblies in figures 2 and 3 were used in this stage.

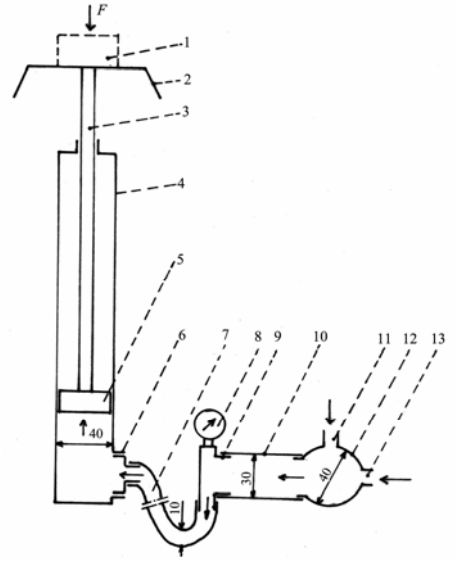

Fig. 2. The measurement of granules+air-compressed mixture pressure **at the mixing-dosing spherical chamber's outlet**.

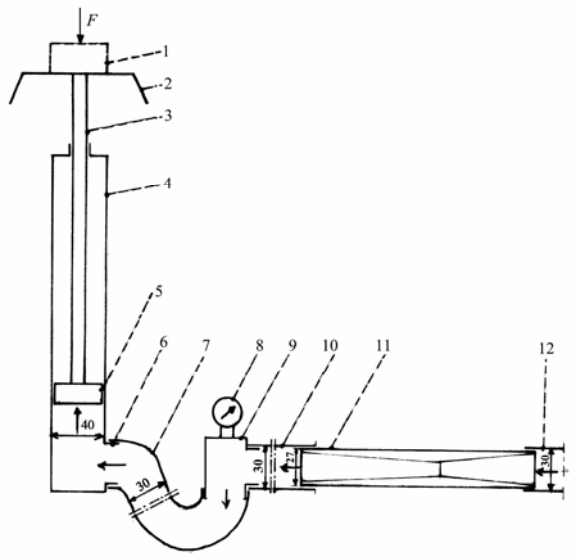

Fig. 3. The measurement of granules+air-compressed mixture pressure **at the sand-blasting nozzle's outlet**

As a result of measured or estimated data, and based on discussions with equipments and sand-blasting materials producers, a calculus algorithm was developed for granules masses, pressures, speeds, energies and impulses, whose values are reached during dry diphase sand-blasting process.

3.1. Masses of sand-blasting metallic granules used during tests

- Equivalent mass of granules **thrown from the nozzle** (m_{eg}) is equal to the charge mass corresponding to the mixing-dosing chamber's volume (m_{gd})

$$\boxed{m_{eg} = 160 \text{ g}} \quad (7)$$

- Granules charge mass that **hits the sample surface** and realizes the sand-blasting print

$$\boxed{m'_{eg} = 145 \text{ g}} \quad (8)$$

Differences between m_{eg} and m'_{eg} consists in the lost particles that comes outside the truncated cone of the diphase jet formed between nozzles surfaces, at the throw, and prints, at the hit.

3.2. The pressure of granules+air-compressed mixture at the mixing-dosing spherical chamber's outlet

In order to measure the pressure of granules+air-compressed mixture at the mixing-dosing spherical chamber's outlet (p_{ac}), the mixing-dosing spherical chamber **was connected to the transducer with a rubber hose, having the inner diameter 30 mm** and the length 1 m (fig. 2).

The pressure of the mixture at the mixing chamber's outlet (p_{ac}) is determined using the balance force (F_{ec})

$$p_{ac} = 59,7 \text{ N/cm}^2 \left(\cong 6 \text{bar}\right) \quad (9)$$

3.3. The pressure of granules+air-compressed mixture at the sand-blasting nozzle's outlet

The hose nozzle for granules+air-compressed mixture transport was connected to the pressure transducer through another ϕ30 mm hose (fig. 3).

The pressure of granules+air-compressed mixture at the nozzle's outlet is (p_{ad}) este

$$p_{ad} = 49,36 \text{ N/cm}^2 \left(\cong 5 \text{ bar}\right) \quad (10)$$

Speeds and energies determination

The previous measured data led to speeds and kinetic energy calculus at the granules+air mixture equivalent mass exit from the nozzle, and also the **displacement kinetic energy of material from the concrete and stone samples**.

3.4. The kinetic energy at the granules equivalent mass exit from the nozzle

$$\boxed{E_{v_1} = 50 \text{ Nm}} \quad (11)$$

$$u_{2d} - u_1 = v_1 \cdot e = 25 \cdot 0,56 = 14 \text{ m/s} \quad (12)$$

3.5. The displacement kinetic energy of particles in the sample

The displacement kinetic energy of particles in the sample ($E_{u_{2d}}$) is equal to energy due to speed lost of granules equivalent masses at impact.

$$E_{u_{2d}} = \frac{m'_{eg}\left(u_2 - u_1\right)^2}{2} = 14,21 \text{ Nm}$$

$$\boxed{E_{u_{2d}} = 14,21 \text{ J}} \quad (13)$$

3.6. The kinetic energy due to granules ricochet speed, u_1

The kinetic energy due to granules ricochet speed is estimated by the difference between the exit kinetic energy of granules equivalent mass from the nozzle (E_{v_1})and the displacement and ricochet kinetic energy of particles in the sample ($E_{u_{2d}}$):

$$\boxed{E_{u_1} = 35,79 \text{ J}} \quad (14)$$

$$\boxed{u_1 = 22,22 \text{ m/s}} \quad (15)$$

3.7. Speed of particles detached from the sample and ricocheted from the sample's surface at the impact's end u_{2d}

$$\boxed{u_{2d} = 36,22 \text{ m/s}} \quad (16)$$

3.8. The kinetic energy due to displacement and ricochet speed u_{2d} of particles from the sample

The particles detached and ricocheted mass:

$$\boxed{m_{pd} = 22 \text{ g}} \quad (17)$$

To be noticed that in the metallic granules impact with a non-metallic fix wall case (concrete, stone, bricks), when $v_2 = 0$, but $u_{2d} \neq 0$, the restitution **coefficient calculus relationship** is:

$$\boxed{e = \frac{u_{2d} - u_1}{v_1}} \quad (18)$$

3.9. The mass of detached particles

The mass of detached and ricocheted particles from the wall due to u_{2d}, in the done experiment's case represents about 15% from the sand-blasting granules (22 g/145 g).

3.10. The kinetic energy due to speed v_1

The kinetic energy due to speed v_1 (E_{v_1}) is the sum of energies due to u_1 (E_{u_1}) and u_{2d} $\left(E_{u_{2d}}\right)$:

$$E_{v_1} = E_{u_1} + E_{u_{2d}} = 50 \text{ J} \quad (19)$$

3.11. Impulses calculus

- The impulse due to granules charge **at the nozzle's outlet** having the speed v_1:

$$H_{v_1} = m_{eg} \cdot v_1 = 4 \text{ Ns} \quad (20)$$

- The impulse of **ricocheted granules** at impact with the sample's surface, due to u_1 speed:

$$H_{u_1} = m'_{eg} \cdot u_1 = 0,145 \cdot 22,22 = 3,22 \text{ Ns} \quad (21)$$

- The impulse due to u_{2d} speed for **material particles detached from the sample to ricochet**:

$$H_{u_{2d}} = m_{pd} \cdot u_{2d} = 0,022 \cdot 36,22 \cong 0,78 \text{ Ns} \quad (22)$$

The H_{u_1} impuls reprezents about 80% H_{v_1}, and $H_{u_{2d}}$ impulse, 20%:

$$H_{v_1} = H_{u_1} + H_{u_{2d}} = 3,22 \text{ Ns} + 0,78 \text{ Ns} = 4 \text{ Ns} \quad (23)$$

Comparative graphs plotting, representing masses, speeds, energies and impulses having the determined values during experiments done, are presented in figure 4.

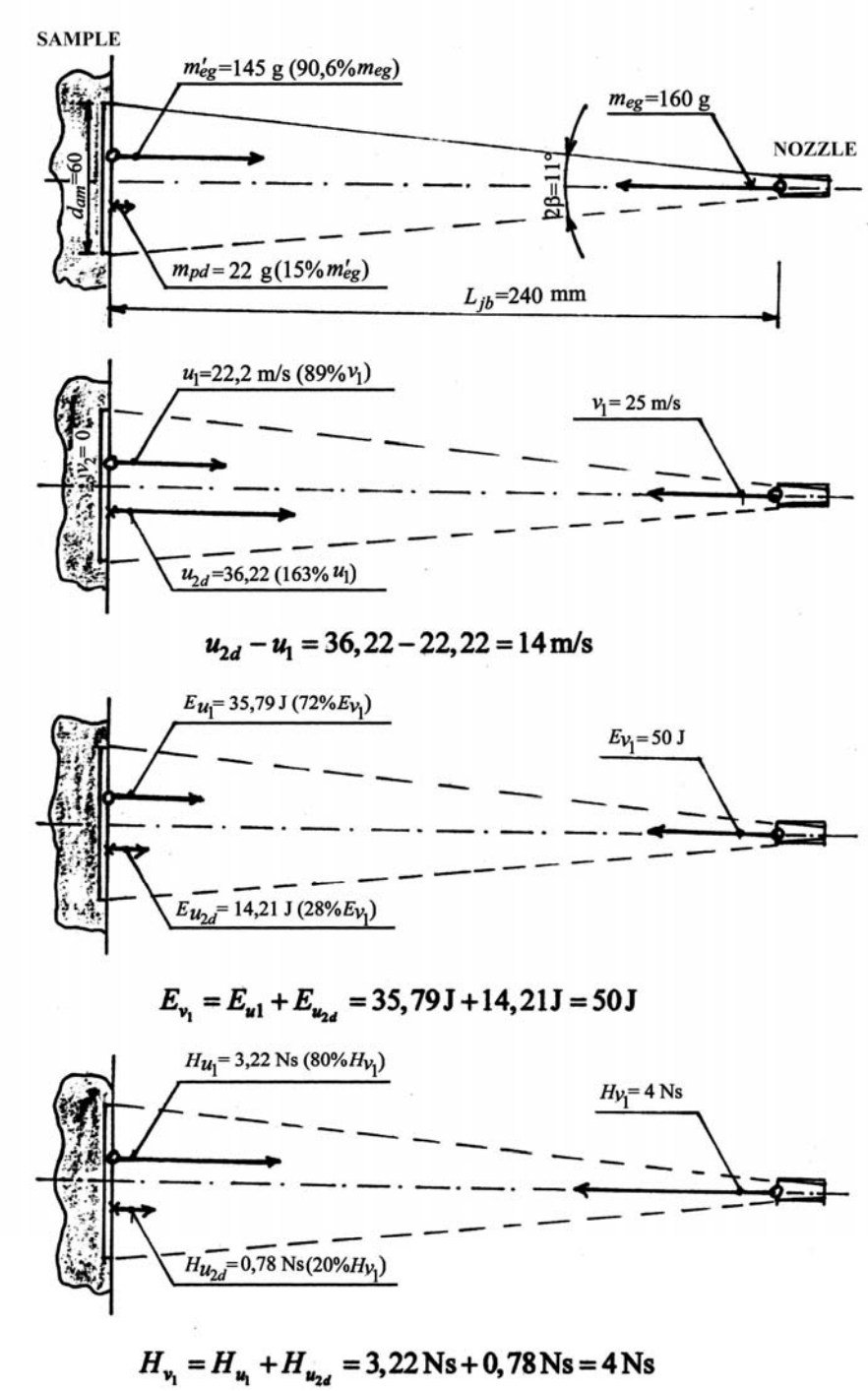

Fig. 4. Comparative graphs plotting, representing masses, speeds, energies and impulses.

4. CONCLUSIONS

During experiments done, measurements and calculus were carried out, which concluded to over 30 free diphase jet sand-blasting parameters.
The technological parameters values measured during tests and compared to those mentioned in the specialized literature were enough precise, the errors being up to max ± 5%.
The technological parameters values measured and/or calculated were transpositioned in „*Comparative graphs plotting, representing masses, speeds, energies and impulses for metallic sand-blasting granules and for material particles detached from the element to be sand-blasted*". The practical finality of this research paper is that the algorithm used in measurements and calculus can be transpositioned in some „*Dry sand-blasting procedure having free diphase jet*", useful both in works before sand-blasting experiments and in sand-blasting adjustment given the real conditions.

REFERENCES

[1] Popescu-Ungureanu Cristiana- Gabriela, (2005), *Contribuţii privind tehnologiile şi sistemele mobile de sablare în construcţii*. Teză de doctorat sub conducerea Ştiinşifică a prof. dr. ing. Ioan Bărdescu, UTCB.

[2] Voicu Vasile , (1988), *Tehnica desprăfuirii aerului*, Carte, Editura Tehnică, Bucureşti.

HYDROSTATIC TRANSSMISIONS FOR MOVEMENT OF MOBILE MACHINES ON WHEELS

D. Janosević, B. Anđelković, G. Petrović

Abstract: *Solution concept of hydrostatic transmision for movement of mobile machines on wheels. Integral hydrostatic drive of wheels. Parameters and characterristics of hydrostatic transmisions. Electric systems of movement regulations and controls on mobile machines. Defining and calculation procedure of hydraulic transmissions for movement of mobile machines on wheels.*

Keywords: *hydrostatic transsmisions*

1. INTRODUCTION

During developing time of mobile machines on wheels the hydrostatic systems were used first only for power supply of working attachments-manipulator. However in latest decade, on same types of machines more and more hydrostatic transmissions are used for movement system.
Leading manufactures of hydraulic components have already developed hydrostatic transmissions for movement of mobile machines on wheels in range of weight from *3000* to *30000 kg*, that corresponds the power *30* to *300 kW*. Solutions of hydraulic transmitssions are mostly with modular design and contain integrated within, following elements:

- elementary components for energy transformation and energy transmission (hydraulic pumps and hydraulic motors,
- hydrostatic systems for movement control,
- hydrostatic system for braking,
- hydrostatic systems for regulation, control and stabile maintaing of moving characteristics of mobile machines.

2. ENGINEERING SOLUTIONS

As a rule, hydrostatic transmissions on the mobile machines on wheels are in form of closed hydraulic circuit system, most frequently with axial piston hydraulic motors with constant or variable specific flow. Operating pressure in systems is in range of *35* to *45 MPa*. Depending of way of energy transmission from hydraulic motors to wheels there are following solution variants of transmission executive parts [1][2]:

- shaft of hydraulic motor (4) (Fig.1a) is connected directly to the wheel hub,
- hydraulic motor (4) (Fig.1b) is indirectly connected to the wheel hub, through reducing gearbox (5),
- hydraulic motor (4) (Fig.1,c), is connection to the wheels through gearbox (5), universal shafts (6) and driving axles (7).

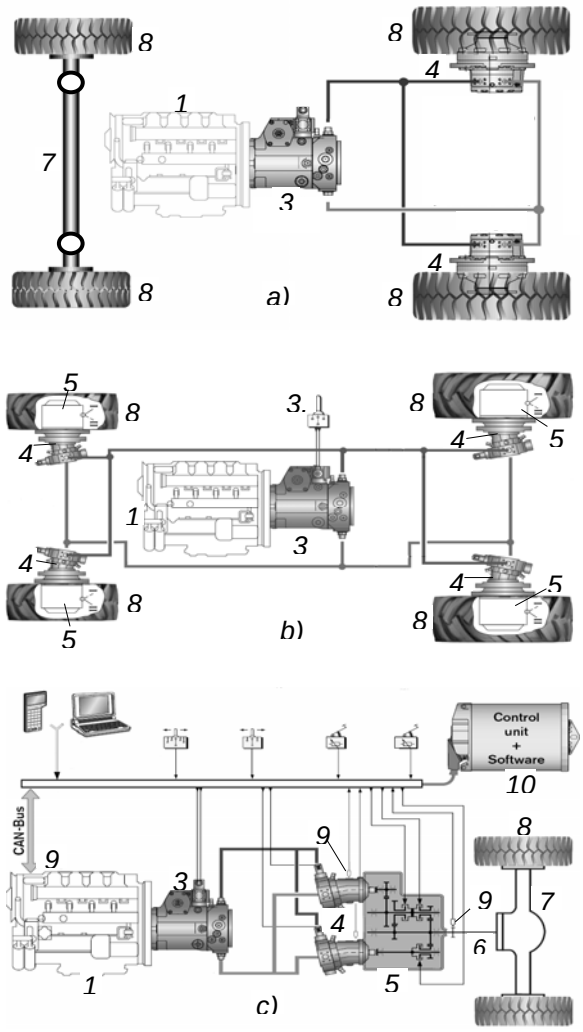

Fig.1. Mobile machines on wheels with hydrostatic transmission for movement.

prof. dr Dragoslav Janosević, Faculty of Mechanical Engineering of Nis
doc. Dr Boban Anđelković, Faculty of Mechanical Engineering of Nis
mr Goran Petrović, Faculty of Mechanical Engineering of Nis

As power producing members of transmissions are used most frequently diesel engines whose mechanical parameters of power N_h hydraulic pumps transform into hydraulic form of power, defined by appropriate pressure p and by flow Q.

Hidraulic motors with executive part of transmission the parameters of hydraulic form of power transform into appropriate drawing force F and movement velocity v of mobile machine.

General and elementary criterion for regulation of drawing characteristics of mobile machine can be expressed by equation:

$$N_h = p \cdot Q = F \cdot v = const \quad (1)$$

In contemporary solutions of hydraulic transmission for movement of mobile construction machines assumed criteria of requlation (equation 1) are realized by means of digital electronic system.

By appropriate sensors (9) (Fig.1c) [1][2] measured are parameters of driving, transforming and transmitting, transmissin components.

In microcontroller (10) monitored parameters are processed according to appropriate software that in fact represents previously assigned regulating criteria.

Deviations of real (measured) and previously assigned parameters are transformed inside microcontroller into the signals that act on the characteristics of transmission components.

By this way of regulation are achieved the following capabilities of hydrostatic transmissions:

- automatic regulation of drawing characteristics by changing of specific flow of hydraulic pumps and hydraulic motors beside great fuel savings and noise decreasing, even in higher movement velocities.
- continual decreasing of movement velocity (by inch pedal), for reason of directing more power for needs of working attachments - manipulators on machine.
- regulation of Limiting Load of driving engine.
- prevention of drive wheels skidding.

3. CALCULATION

General conceptual solution of transmission for movement on construction mobile machines for which is calculation is preformed consist of following: diesel engine (1) [3] (Fig.2), cunpling (2), hydraulic pump (3) with variable specific flow, hydraulic motor (4) with variable specific flow, transmission gearbox (5), cardan shaft (6), driving axle (7) and wheel (8).

Starting parameters that are assigned when the transmission calculation is preformed belong to the following set of valutes:

$$P_h = \{N_h, n_{en}, F_{max}, v_{r\,max}, v_{t\,max}, r_d\} \quad (2)$$

where is: N_h- maximal power that diesel engine transfers to the hydraulic pump; n_{en} - number of revolutions of diesel engine power; F_{max}- needed maximal drawing force of machine; v_{rmax} - maximal operating velocity of machine; v_{tmax} - maximal transporting velocity of machine; r_d - dynamic radius of wheel.

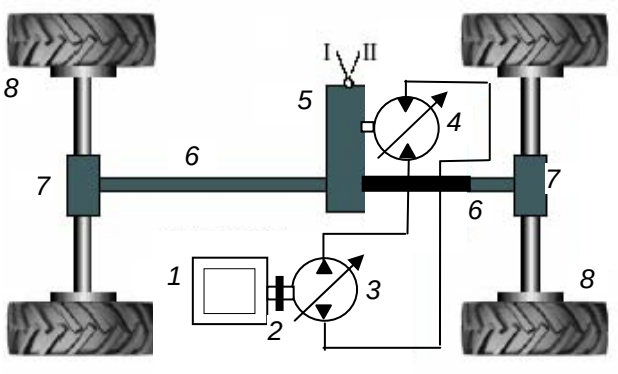

Fig. 2. General model of hydrostatic transmission for movement of construction mobile machines

Upon the basis of assigned parameters E_n needed is to define the sizes of transmission components expressed by the following set of values:

$$E_n = \{p_{max}, q_{p\,max}, q_{m\,max}, q_{m\,min}, i_{m1}, i_{m2}, i_o\} \quad (3)$$

where is: p_{max} - maximal pressure of the hydrostatic system; $q_{p\ max}$- maximal specific flow of hydraulic pump; $q_{m\,max}$- maximal specific flow of hydraulic motor; $q_{m\ min}$- minimal specific flow of hydraulic motor; i_{m1} - gearbox transmission ratio in operating velocity of machine; i_{m2} - gearbox transmission ratio in transporting velocities of machine; i_o- transmission ratio of driving axles.

Maximal pressure p_{max} is the main parameter of hydrostatic system. Value of this pressure prescribes the choice of transmission concept in other terms, the choice of types of hydraulic pump and hydraulic motor.

Size of hydraulic pump is defined according to input hydraulic power N_h. For the hyperbolic form of regulation of pump parameters (pressure and flow) (Fig.3) can be written equation:

$$N_h = \frac{p_{max}Q_{min}}{60\eta_{pv}\eta_{pm}} = \frac{p_{min}Q_{max}}{60\eta_{pv}\eta_{pm}} = \frac{pQ}{60\eta_{pv}\eta_{pm}} \quad (4)$$

where is: p_{min},Q_{max}- pressure and flow of start of pump regulation; p_{max},Q_{min}- pressure and flow of end of pump regulation; p,Q- pressure and flow inside the range of pump regulation; $\eta_{pv,}$ η_{pm} - volumetric and mechanical pump efficiency ratio.

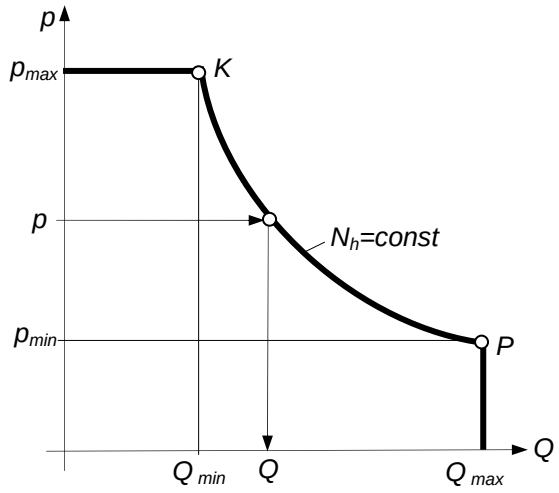

Fig. 3. Regulating diagram of pump

By introducing the range of regulation as ratio:

$$e = \frac{p_{max}}{p_{min}} \tag{5}$$

can be calculated maximal pump flow:

$$Q_{max} = \frac{60 \cdot N_h \cdot e}{p_{max}} \eta_{pv} \eta_{pm} \tag{6}$$

according which is calculated pump maximal specific flow:

$$q_{p\,max} = \frac{1000 \cdot Q_{max}}{\eta_{pv} \eta_{pm}} \tag{7}$$

where is: Q_{max} *[l/min]*,q_{pmax} *[cm^3]*, n_p- pump number of revolutions for the first step of calculation can be taken $n_p=n_{en}$.

On the basis of calculated value selected is from the manufacturers cataloque the size of hydraulic pump.
Size of hydraulic motor is defined from defined from condition that maximal drawing force F_{max} of machine is achieved at:

- maximal pressure p_{max} of pump,
- maximal specific flow $q_{m\,max}$ of hydraulic motor,
- transmission ratio of gearbox i_{m1}, that is used in operating velocities.

Needed maximal torque M_{max} on wheels at maximal drawing force:

$$M_{max} = r_d F_{max} \tag{8}$$

On the basis of maximal torque of hydraulic motor:

$$M_{m\,max} = \frac{(p_{max} - p_o) q_{m\,max}}{2\pi} \eta_{mm} = \frac{M_{max}}{i_{m1}\, i_o \eta_m \eta_o} \tag{9}$$

Calculated is needed maximal specific flow of hydraulic motor:

$$q_{m\,max} = \frac{2\pi\, M_{max}}{(p_{max} - p_o)\, i_{m1}\, i_o \eta_{mm} \eta_m \eta_o} \tag{10}$$

where is: $q_{m\,max}$ *[cm^3]*, M_{max}*Nm]*, p_o*[MPa]* - pressure value in return line of hydraulic motor; η_{mm}- mechanical efficiency ratio of hydraulic motor; η_m,η_o- efficiency ratio of gearbox and driving axles.

On the basis of calculated value $q_{m\,max}$, selected is from the manufacturers cataloque the size of hydraulic motor.
Needed minimal specific flow $q_{m\,min}$ of hydraulic motor is calculated from the condition that mobile machine achieves wanted transport velocity v_{tmax} at:

- maximal flow of pump Q_{max} ,
- minimal specific flow $q_{m\,min}$ of hydraulic motor,
- transmission ratio of gearbox i_{m2}, that is used at transport velocities of mobile machine.

For maximal flow of pump and maximal velocity of the machine:

$$Q_{p\,max} = \frac{q_{m\,min} n_{m\,max}}{1000 \eta_{mv}} \tag{11}$$

Hydraulic motor will have maximal specific flow:

$$q_{m\,max} = \frac{1000 \cdot Q_{p\,max}}{n_{mmax}} \eta_{mv} \tag{12}$$

where is: n_{mmax}- maximal revolution number of hydraulic motor.

Maximal revolution number of hydraulic motor nmmax appears when mobile machine reaches maximal transporting velocity:

$$n_{m\,max} = \frac{v_{t\,max}}{r_d} \frac{30}{\pi} i_{m2}\, i_o \le n_{md} \tag{13}$$

where is: $n_{m\,max}$ *[min^{-1}]*,$v_{t\,max}$ *[m/s]*, r_r*[m]*, n_{md} - maximal permitted revolutions number of hydraulic motor that is given in motor manufacturer cataloque.

Transmission gearbox and driving axles are produced by the specialized manufacturers. These components are selected according to maximal input torque. However, for driving axles selection must be precribed also maximal static and dynamic load on each axle. For all components manufacturers offers available transmission ratios.
When transmission ratio of gearbox and driving axles are selected must be satisfied the following ratio:

$$\frac{i_{m1}}{i_{m2}} = \frac{v_{t\,max}}{v_{r\,max}} \tag{14}$$

4. DRAWING FORCE DIAGRAM

Drawing force diagram presents mutual dependence of drawing force machine movement velocity (Fig.4)
Movement velocity v_i and drawing force F_i for any working conditions in the pump regulation range and for any transmission ratio of gearbox can be calculated with equation:

$$v_i = r_d \frac{n_m}{i_{mi} i_o} \frac{\pi}{30} \quad (15)$$

$$F_i = \frac{1}{r_d} M_m i_{mi} i_o \eta_{mm} \eta_m \eta_o \quad (16)$$

In that case revolutions number of hydraulic motor n_m for any value of the specific flow of hydraulic motor $q_m=[q_{max},q_{min}]$ has value:

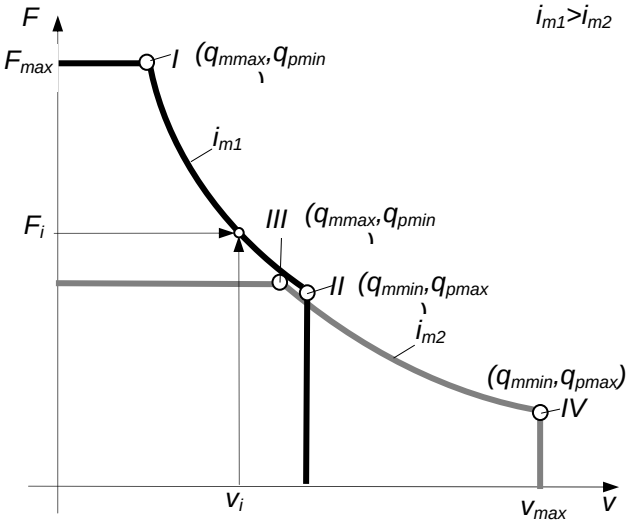

Fig. 4. Drawing force diagram

$$n_m = \frac{1000\,Q}{q_m} \eta_{mv} \quad (17)$$

and torque M_m of hydraulic motor for any of the specific flow of hydraulic motor $q_m=[q_{max},q_{min}]$ has value:

$$M_m = \frac{(p - p_o) q_m}{2\pi} \eta_{mm} \quad (18)$$

By pressure changing in the interval $p=[p_{min},p_{max}]$, along the calculation of appropriate pump flow (equation 4):

$$Q = \frac{60 \cdot N_h}{p} \eta_{pv} \eta_{pm} \quad (19)$$

can be completely defined the drawing force diagram (Fig.4) of construction mobile machine.

5. CONCLUSION

Last decade is time of very dynamic development of hydrostatic components and hydrostatic system used for movement transmission on the mobile machines on wheels. In paper is presented procedure for the calculation of the elementary transmission parameters, on the basis of assigned parameters for the needed values prescribed for machines movements.

REFERENCE

[1] *Mobile 2003*, International Mobile Hydraulic Conference, Rexroth Bosch Group, Ulm, 2003.

[2] *Mobile 2006*, International Mobile Hydraulic Conference, Rexroth Bosch Group, Ulm, 2006.

[3] D. Janošević: *Projektovanje mobilnih mašina*, Mašinski fakultet Univerziteta u Nišu, 2006.

HEALTH MONITORING AND PROGNOSTIC SENSORS APPLIED IN MECHANICAL AND ELECTRONIC SYSTEMS

D. Vujić

Abstract: *This paper deals with application of health monitoring and prognostics sensors in mechanical and electronic systems. It is shown that health monitoring and prognostics of mechanical systems and structure has a much longer history than electronic systems. Some sensors for electronic systems are still in a development stage.*

Key words: *sensors, health monitoring and prognostics, maintenance, reliability*

1. INTRODUCTION

Many systems and structures, such as avionic systems, civil infrastructures, nuclear facilities, and mining machinery, are designed for long-term operations and these operations need periodic maintenance or replacement for safety and reliability. Reliability is essential in these applications because failure of these systems and structures can be lead to serious loss of lives or properties.

Health monitoring and prognostics is a proactive system to identify fault and determine health conditions or likely failure occurrence. It provides information for maintenance and replacement so that a failure can be prevented in advance. In addition, prognostics in health monitoring and prognostics systems also provides prediction of life consumption and remaining life, which combined with other information on health conditions offers the possibility of maintenance and replacement on a complete per-need basis, and hence, the possibility of significant cost savings.

The health monitoring and maintenance of many systems and structures has so far been depending upon visual inspection and testing that are time consuming, labor intensive, and costly. Using sensors in health monitoring and prognostics enables continuous monitoring of a systems or structures with minimal human involvement and with no interruption of operation. It eliminates the need of disassembly or prior knowledge of likely damage locations in the health monitoring and maintenance operation.

Utilizing smart sensors developed with the latest technologies in microelectronics, micro-electro-mechanical systems, and nano-technology has become a clear trend in health monitoring and prognostics. These sensors provide extended sensing capability and performance, improved design flexibility for monitoring applications, and reduced cost. Combined with communication and networking technologies, particular the wireless networking technologies, the latest health monitoring and prognostics sensors offer possibility for developing a fully autonomous, condition-based maintenance management system.

At the beginning of the 80 s of the last century significant changes occurred in maintenance of turbojet engines, as in fighter aircraft so in engines for civil aircraft at commercial flights. Instead of maintenance to precisely defined number of flight hours appeared a new on-condition maintenance concept.

Owing to sensors integrated into aircraft structure, in recently time in aviation construction, it follows a propagation of the crack. The constructions build from so-called smart materials, especially composite materials, find in the last time a more and more usage. In this way it is expanded a design life of the construction and significantly reducing the costs. It is very important at military fighters exposed more loads than airplanes during commercial flights. One of the main problem in this case, it is a processing of the signal from sensors. The sensors need a central device or distributed networks for processing. Based to incoming results, this device decides about the preventive actions necessary to attempt. Many researches are performed in domain of the artificial intelligence, expert systems, fuzzy logic and pattern recognition. The artificial neural networks promise the best results in the domain of effective pattern recognition for damage detection. The significant progress is achieved in the past years in domain of determing of the optimal number and sensor position for damage location. The different optimization technique are developed. A new development in this area includes an application of genetic algorithm.

2. HEALTH MONITORING AND PROGNOSTICS SENSORS IN TRADITIONAL APPLICATIONS

Health monitoring and prognostics has traditionally been employed on safety-critical mechanical systems and structures, such as propulsion engines, aircraft structures, and railroad suspension systems. Even in today, the applications of health monitoring and prognostics systems on mechanical machineries and structures remain dominant compared with other applications, such as electronic systems. The

Prof.dr Dragoljub Vujić, Vojnotehnički institut, Beograd, vujicd@eunet.yu

reasons for this can be summarized from the following perspectives:

First, if operations are carried out under designated conditions, majority of failures now seen on properly tested and qualified mechanical systems are of wear-out failure mechanisms of fatigue, creep and corrosion. People have gained sufficient knowledge and developed technologies to avoid unexpected sudden failures. Unlike over-stress failures, wear-out failures are a result of damages accumulated in one or multiple processes. These failures can be prevented using periodic maintenance and replacement provided that the damage can be detected in advance. Fortunately, people have obtained enough knowledge and have mature technologies of damage detection and fault diagnostics on mechanical systems. These knowledge and technologies provide a fundamental basis for developing a feasible and an effective health monitoring and diagnose system for mechanical machineries and structures. As a result, people have been able to ensure a reliable operation of a mechanical system in each mission and use maintenance to achieve the reliable operation of the system for its entire cycle of life.

It is well known in the reliability engineering community that redundancy is an effective approach to improve the overall operational reliability of the system without improving technology itself. Although redundancy can be integrated into mechanical systems in some cases, such as the use of multiple instead of one engine on an aircraft, designing redundant mechanical systems is feasible in engineering only for very limited cases. Therefore, the health monitoring and prognostic approach, combined with periodic maintenance, needs to play a major role in high-reliability operation of mechanical systems and structures.

In addition, health monitoring and prognostics of mechanical systems and structure has a much longer history than electronic systems. An enhanced health monitoring and prognostics system utilizing the latest sensing technologies sees a broader need and electronic benefit on the mechanical systems and structures than for electronic systems. People have had a much more ready and mature sensing, fault diagnostics, and reliability prognostic technologies for mechanical systems than for electronic systems. Table 1 provides examples of health monitoring and prognostics applications on mechanical systems and structures.

2.1 Life monitoring of components that fail due to creep

Aerodynamic component failure in a gas turbine engine is often affected by creep. The mechanism of the creep is influenced by temperature and stress. The high temperatures of the gas path produce the first of the two requirements, and centrifugal stress from shaft rotation produces the second. If parts susceptible to this mode of failure go unmentioned, this will eventually result in catastrophic failure.

Table 1. *Examples of health monitoring and prognostics sensor applications on mechanical systems and structures*

Systems and structures	Application	Sensing mechanism
Jet engine and other turbo-machinery	• Crack propagation in rotating disks and blades	*Crack wire*
	• Rotor blade vibration, blade tip clearance • Fatigue accumulation, • Foreign object damage detection	*Capacitive sensing, eddy current, infrared, optical/laser, micro/millimeter wave*
	• Static and dynamic structural deformation in high-temperature environment	*Ceramic strain gage*
Aircraft structures	• Crack propagation and remaining life prediction	*Acoustic emission and fatigue cycle management*
	• Rotor head fault detection and fatigue life prediction	*Acoustic emission and fatigue cycle management*
	• Corrosion monitoring	*Electromechanical sensing, optical fiber*
	• Structural damage	*Fiber-optic accelerometer and displacement, ultrasonic, acoustic emission*
	• Composite structure damage, fatigue	*Piezoelectric/piezoceramic sensing*
Large infrastructure	• Deformation monitoring	*Inertia sensing*

2.2 Life monitoring of components that fail due to fatigue

Due to the nature of the operating environment of a gas turbine engine, aerodynamic components are constantly subjected to repeated loads, also called cyclic loads. Despite stresses below the material's ultimate strength, dynamic structural deformation over time leads to development of cracks that ultimately cause the failure of the material. This type of damage due to cyclic loading is termed fatigue. The state of stress created in a turbine blade comes from two principle factors. The torque created by the turning (deflection) of the gas as it passes through the turbine blade passages, in combination with the centrifugal stresses produced by the rotation of the shaft, creates a very complex asynchronous, two dimensional stress field.

2.3 Vibration sensors

There are three major types of sensors, which may be used to measure machine vibrations and they may be classified by what they measure: displacement, velocity or acceleration.

Piezoelectric accelerometers are for measuring the vibrations to get an indication of the machine's condition. Typical accelerometers have high natural frequencies of about 25000 Hz which is a lot higher than the natural frequencies of gas turbine engines. This creates a wide frequency band for measurements. The advantage of using accelerometers is that they are: convenient, small in size, rugged, good frequency response and can endure relatively high temperatures. For these reasons, the accelerometer is the transducer of choice for the health monitoring system.

The best choice is a tri-axial accelerometers mounted on the bearing housings to measure the movement of the shaft. The accelerometers used should have the following specifications to ensure valuable data: sensitivity of at least 100mV/g, amplitude range ±30g, temperature range 0-350 ºC

It is important to measure the vibrations at start-up and shutdown, since the forces that are affecting the engine are transient, and malfunctions may be exhibited which might not be apparent at cruise conditions.

3. HEALTH MONITORING AND PROGNOSTICS APPLICATION IN MICROELECTRONIC DEVICES AND SYSTEMS

Compared to mechanical systems, using sensors in electronic devices for health monitoring and prognostics purpose is an emerging application. Some IC sensors and cells that are designed for the reliable operation of safety-critical ICs have been developed and introduced. However, in contrast to a long application history of health monitoring and prognostics sensing for mechanical systems, these sensors and cells for electronic system remain in a development stage. Many issues need to be addressed before any actual applications become possible. So far, no reports have yet shown services of these health monitoring and prognostics sensors and in any actual applications.

Unlike mechanical systems and structures, electronic devices lack technologies in general for fault detection and diagnose. Fault of electronic devices are not limited to physical damages or defects. They also vary significantly in nature. Even for the physical damages, many of them are in a micron, submicron or even nano-scale and do not necessarily link to failures or a loss of designated electrical performance or function. Therefore, health monitoring and prognostics of electronic systems lacks straightforward approaches to proceed, compared to that of mechanical systems and structures. It can help to improve the mission reliability of an electronic system by integrated health monitoring and prognostics system. However, considering the complexity of an electronic system, it can also be difficult to quantify the improvement on a solid theoretical or experimental basis.

The proper functioning of most electronic systems depends on both the hardware and the software reliability of the system. Hence, an electronic system failure can be a result of hardware problems, software problems, or both problems. However, sensors and health monitoring and prognostics systems are effective primarily on hardware failures. Therefore, using the health monitoring and prognostics systems alone is not able to ensure highly reliable operation of complex electronic systems.

In contrast to mechanical systems an structures, which encounter inherent difficulty in implementing redundancies, design of redundancy is almost always feasible to an electronic system from the engineering standpoint. A simple theory on how to qualify the reliability improvement with redundancy is also available. To be able to evaluate reliability in a qualitative manner is essential to many safety-critical applications, such as avionics and nuclear operations, due to specified limits in reliability that the federal government requires on the operation of certain electronic devices in these applications.

Because of these issues, health monitoring and prognostics is unlikely to replace the role of redundancy in the high-reliability operations of electronic systems. The potential application of health monitoring and prognostics sensors in electronic devices will be likely used more for the purpose of cost reduction in maintenance and replacement than for the purpose of reliability improvement.

For health monitoring and prognostics system to be implemented in actual electronic system, other issues that need to be addressed include:

- Dependability of data interpretation and end of life prediction
- Additional design, manufacturing and operating cost for integrating an health monitoring and prognostics system vs. the cost saving for using the system in maintenance and replacement
- Operating reliability of the sensing and data processing system itself.

4. PHYSICS OF FAILURE BASED LIFE CONSUMPTION MONITORING

The parameters that are monitored in health monitoring and prognostics system can generally categorized as those that can be used to define the failures of the systems to be monitored and that cannot. The length of crack in aircraft structures in the health monitoring of ICs and oil consumption are examples of the first category of parameters. The measurement results of the parameters of this category in monitoring environment provide a direct indicator of health condition and reliability. The parameters of the second category are primarily those parameters that are measures of environmental and stress conditions, such as temperature, humidity, vibration and radiation. In general, the technologies that are required to monitor the parameters of the first category are application-specific, while those technologies required for monitoring the second categories are usually standardized and may have multiple options in selection of monitoring devices.

Based on parameters that need to be monitored, health monitoring and prognostics regime can also be in two categories: a test-based system and a physics of failure based system. A test-based system health monitoring and prognostics system requires direct measurement or monitoring of the parameters that can be used to define failures. With this approach, the health condition of an electronic system to be monitored can be determined by benchmarking the test results against the failure criteria defined in the remaining life prediction can be achieved by extrapolating the test data to the defined failure point with or without a degradation model available on the parameters.

However, in actual application of complex electronic systems, defining and monitoring failure including parameters can be difficult and sometimes it may not be feasible from the perspective of engineering and business. Another danger with this health monitoring and prognostics system is that it does not require a thorough understanding of failure mechanisms that govern the failure process. As a result, the parameters that are monitored in the process may not be sensitive enough for effective monitoring in the process may not be sensitive enough for effective monitoring until the ultimate failure occurs. The alternative approach is to adopt a physics of failure-based health monitoring and prognostics system. This system considers actual environmental and loading conditions, and requires the understanding of the dependence of failure on those external environmental and loading conditions. In return, the health monitoring and prognostics of an electronic system can be completed basically by monitoring the system's life cycle environment.

5. SUMMARY

With potential application in the health monitoring and prognostics of electronic systems, two types of cells and sensors have been developed. However, for these emerging technologies to be used in actual applications of electronic systems, many issues need to be addressed. Considering the engineering feasibility in sensor implementation health monitoring and prognostics sensor are unlikely to play a major role in applications, such as avionics, that require stringent reliability operation with specified quantitative limits imposed by the federal government. They will be likely used more for the purpose of cost reduction in condition based maintenance and replacement than for the purpose of reliability and safety.

REFERENCES

[1] **Vujić D.,** Turbojet engine maintenance systems, *Scientific Technical Review*, Vol.LIII, No.2, 2003.

[2] **Vujić D**., Sophisticated diagnostic systems in aircraft engines, *Scientific Technical Review*, Vol.LIII, No.4, 2003.

[3] **Bergaglio L., Tortarolo F**., RB199 Maintenance Recorder: an application of „on condition maintenance methods" to jet engines, Condition-based maintenance for highly engineered systems, Universita' degli Studi di Pisa, Pisa, Italy, September 25-27, 2000.

[4] **Boller C., Staszewski W., Worden K., Manson G., Tomlinson G**., Structure Integrated Sensing and Related Signal Processing For Condition-Based Maintenance, Condition-based maintenance for highly engineered systems, Universita' degli Studi di Pisa, Pisa, Italy, September 25-27, 2000.

[5] **Jingsong X., Michael P**., Applications of in-situ health-monitoring and prognostic sensors, University of Maryland, College Park, MD 20742, USA

EXPONENTIAL STABILITY OF NONLINEAR HYBRID SYSTEMS

V. Filipovic

Abstract: *This paper proposes a method for analysis of exponential stability of anayisis of deterministic nonlinear switched systems.The system models belong to a finite set of models. It is assumed that there is no jump in the state at switching instants and there is no Zeno behaviour, i.e. there is finite number of switches on every bounded interval. The hybrid system have wide applications; modelong of communication network, system with quantization, networked control systems and process control. For stability analysis the multiple Lyapunov function is used. It is considered autonomous nonlinear switched systems. The exponential stability is practically important Because such systems are robust to perturbation. The globally exponentially stability is proved.*

Key words: *Switching systems, multiple Lyapunov function,exponential stability.*

1. INTRODUCTION

Hybrid systems are digital real-time systems which are embedded in analog environments. Analog part of the hybrid systems is described with differential equations and discrete part of the hybrid systems is a event driven dynamics which can be described using concept from discrete event systems [1] – [2].

In this paper we will consider the switched systems which can be viewed as higher-level abstractions of hybrid systems [3]. The subsystems of the switched system are modeled as nonlinear deterministic differential equations.

In this paper we consider the exponential stability of switched deterministic systems. There are two ways to analyze stability of switched deterministic systems. The first one is construction of common Lyapunov function. Find the common Lyapunov function is a difficult task [4]. The second one utilizes multiple Lyapunov function [5]. Here we will use the second approach. We assume that

A) there is no jump in the state x at the switching instants

B) there is no Zeno behavior, i.e. there is a finite number of switches on every bounded interval of time.

The situation with jump in the state of x at the switching instants is considered in [6] and [7]. The hybrid control is an important tool for large class of real problems. That type of control systems cover the system with quantization [8], control of wireless network [10] and networked control systems [9]. Switching control strategy in [11] is used for control of time-delay system. Namely, here the concept of multiple models and concept of switching controllers is used.

The analog part of system is describe by finite set of continuous-time models with input delays and unmodeled dynamics in the form of affline family. As a result, the LQ switching controllers are given. In the [12] specific form of hybrid LQ controllers is derived using linear matrix inequalities.

The mathematical model for real process generally has the Hammerstein-Wiener form. It means that on the input and output of the process present nonlinear elements (actuator and sensor). In reference [13] the Hammerstein model (has only input nonlinearity) is considered. The controller for such case is combination of picewise lineae control (PLC) with low-and-high gain feedback law (LHG). The PLC control has associated switching surfaces in form of positively invariant set. The key features of PLC/LHG controllers is that the saturation level of control signal avoided.

In reference [14] the stochastic nonlinear hybrid sistem is considered. The exponential m-stability is proved. The main results of the paper are:

(i) the exponential m_1-stability os stochastic switched system whereby $m_1 \in (0, m)$;

(ii) the stability in probability

The presence of analog uncertainty is considered in [15] and [16].

The syrvey of recent results from theory of hybrid system is presented in [17]. A necessary and sufficient condition for asymptotic stabilizability of switched linear system is described.

In this paper we find a set of conditions under which the deterministic switching systems is exponentially stable. We use the multiple Lyapunov functions approach. The finite set of models is nonlinear. It is important to mention that exponentially stable equilibria is relevant for practice. Namely, such systems are robust to perturbation.

Prof. dr Vojislav Filipović, Faculty of Mech.Engineering Kraljevo, filipovic.v@mfkv.kg.ac.yu

2. PROBLEM FORMULATION

Let us suppose that E_1 and E_2 are subset of Euclidean space, let $C[E_1,E_2]$ denote the space of all continuous function $f:E_1\to E_2$ and $C^1[E_1,E_2]$ denote the space of all functions $f:E_1\to E_2$ that are once continuously differentiable. The functions $\alpha\in C[R_{\geq 0}, R_{\geq 0}]$ is of class K if α is increasing and $\alpha(0) = 0$.

We define a family of systems

$$\dot{x}(t) = f_p(x(t)) \quad , \quad t \geq 0 \quad , \quad \forall p \in \mathsf{P} \tag{1}$$

where $x\in R^n$ and $f_p:R^n\to R^n$, $f(0)=0$ for every $p\in\mathsf{P}$. The P is an index set.

For definition of switched system generated by the family (1) we will introduce a switching signal. This is a piecewise constant function

$$\sigma:[0,\infty] \to \tag{2}$$

Such a function has a finite number of discontinuities on every bounded time interval and takes a constant values on every interval between two consecutive switching times. The σ is continuous from the right everywhere

$$\sigma(t) = \lim_{\tau \to t^+} \sigma(\tau) \quad , \ \forall\, \tau \geq 0 \tag{3}$$

The switched system for the family (1) generated by σ is

$$\dot{x}(t) = f_{\sigma(t)}(x(t)) \tag{4}$$

Now we will define notion of exponential stability.

Definition 1. The equilibrium (1)is exponentially stable if there exists constants r, k_1, $k_2 > 0$ such that

$$\|x(t)\| \leq k_1 \|x(t_o)\| \exp\{-k_2 (t - t_o)\}$$

for $\forall t, t_o \geq 0$ and $\forall x(t_o) \in B_r$ where

$$B_r = \{x \in R^n : \|x\| < r\}$$

and $\|\cdot\|$ is Euclidean norm.

For our main result we need the following lemma which is adopted from [12].

Lemma 1. Consider the system having index p in the family (1). Suppose there exists constants a, b, c, r >0, m≥1 and a $C^1[R^n, R_{\geq 0}]$ function $V_p:R^n\to R^n$ such that

1^o $\quad a\|x\|^m \leq V_p(x) \leq b\|x\|^m, \ \ \forall t > 0, \ \forall x \in B_r$

2^o $\quad \dot{V}_p(x) \leq -c\|x\|^m, \ \ \forall t \geq 0, \ \ \forall x \in B_r$

Then the equilibrium of (1) is exponentially stable.

Clearly, exponential stability is a stronger property then uniform asymptotic stability. Also, from exponential stability follows asymptotic stability.

3. EXPONENTIAL STABILITY OF SWITCHED SYSTEMS

Now we will formulate the main result of this paper.

Theorem 1. Consider the switched system (4). Let us suppose that next assumptions are valid

1^o index set P is finite, i.e. $\mathsf{P}=\{1,2,...,N\}$

2^o function $V_p(\cdot) \in C^1[R^n, R_{\geq 0}]$ for $\forall p\in\mathsf{P}$

3^o function $U(\cdot) \in K$

4^o for $\forall x\in R^n$, $m\geq 1$, $\forall p\in\mathsf{P}$ and a, b>0, a<b

$$a\|x\|^m \leq V_p(x) \leq b\|x\|^m$$

5^o for $\forall x\in R^n$, $m\geq 1$, $\forall p\in\mathsf{P}$ and c>0

$$\dot{V}_p(x) \leq -c\|x\|^m$$

6^o for every $p\in\mathsf{P}$ and every pair of switching instants

$$\sigma(t_i) = \sigma(t_j) = p \quad , \quad \forall (t_i, t_j) \ , \ i < j$$

and

$$\sigma(t_k) \neq p \quad \text{for} \quad i < k < j$$

the inequality

$$V_p(x(t_j)) - V_p(x(t_i)) \leq U(\|x(t_i)\|)$$

is satisfied

Then the system (4) is globally exponentially stable

Proof: Let us consider subsystem (1) for fixed p. From 4^o and 5^o conditions of theorem follows

$$\frac{dV_p(x(t))}{dt} \leq -c\|x(t)\|^m \leq -\frac{c}{b} V_p(x(t)) \tag{5}$$

By integration of inequality (5) on interval $[t_o, t]$ one can get

$$V_p(x(t)) \leq V_p(x(t_o)) \exp\left\{-\frac{c}{b}(t - t_0)\right\} \tag{6}$$

Using condition 4^o of theorem we have

$$V_p(x(t)) \leq b\|x(t_o)\|^m \exp\left\{-\frac{c}{b}(t - t_0)\right\} \tag{7}$$

Let us, now, consider interval $[t_o, t_1[$. From relation (7) and 4^o and 5^o assumptions of theorem we have

$$\begin{aligned} &V_{\sigma(t_0)}(x(t_1)) \leq V_{\sigma(t_0)}(x(t_0)) \exp\left\{-\frac{c}{b}(t_1 - t_0)\right\} \leq \\ &\leq b\|x(t_o)\|^m \exp\left\{-\frac{c}{b}(t_1 - t_0)\right\} \end{aligned} \tag{8}$$

But, over the same interval, for $p\neq\sigma(t_0)$, using assumption 4^o of the theorem, the estimate

$$V_p(x(t_1)) \leq b\|x(t_1)\|^m = \frac{b}{a}\left(a\|x(t_1)\|^m\right) \leq \frac{b}{a} V_{\sigma(t_o)}(x(t_1)) \tag{9}$$

holds true.

From last two relations follows

$$V_p(x(t_1)) \leq \frac{b^2}{a}\|x(t_0)\|^m \exp\left\{-\frac{c}{b}(t_1 - t_0)\right\} \tag{10}$$

Now, consider the interval $[t_1, t_2[$. From (6) and (10) we have

$$V_{\sigma(t_1)}(x(t_2)) \le V_{\sigma(t_1)}(x(t_1)) \cdot$$

$$\cdot \exp\left\{-\frac{c}{b}(t_2 - t_1)\right\} \le \frac{b^2}{a}\|x(t_0)\|^m \exp\left\{-\frac{c}{b}(t_2 - t_0)\right\} \quad (11)$$

Over the same interval for $p \neq \sigma(t_1)$ we have

$$V_p(x(t_2)) \le b\|x(t_2)\|^m = \frac{b}{a}\left(a\|x(t_2)\|^m\right) \le$$
$$\le \frac{b}{a}V_{\sigma(t_1)}(x(t_2)) \quad (12)$$

Using relation (11) and (12) we have

$$V_p(x(t_2)) \le b\left(\frac{b}{a}\right)^2 \|x(t_0)\|^m \exp\left\{-\frac{c}{b}(t_2 - t_0)\right\} \quad (13)$$

The maximum possible value of the function V_σ occurs when the switching signal σ takes the every element from the finite set P. Let us suppose that t_j^* is the first switching instant after all subsystems have became active at least once since initialization at t_0.

From the above analysis follows

$$V_p(x(t_j^*)) \le b\left(\frac{b}{a}\right)^{N-1} \|x(t_0)\|^m \exp\left\{-\frac{c}{b}(t_j^* - t_o)\right\} \quad (14)$$

Let us define the

$$\gamma = \max\left(b, b\left(\frac{b}{a}\right)\exp\left\{-\frac{c}{b}(t_1 - t_0)\right\}, \ldots b\left(\frac{b}{a}\right)^{N-1} \cdot \right.$$
$$\left. \cdot \exp\left\{-\frac{c}{b}(t_j^* - t_0)\right\}\right) \quad (15)$$

From 6° condition of theorem we can conclude

$$V_{\sigma(t)}(x(t)) \le \gamma\|x(t_0)\|^m \exp\left\{-\frac{c}{b}(t - t_0)\right\} \quad (16)$$

If a σ becomes constant at some index (the case of switching stops in finite times) the switched system, according with condition 4° and 5° of theorem and Lemma 1, is stable.

The second situation is that exists at least one index $p \in \mathsf{P}$ such that positive subsequence

$$V_{\sigma(t_i)}(x(t_i)) \quad , \; i \ge 0 \; , \quad \sigma(t_i) = p \quad (17)$$

is infinite in length and decreasing according with hypothesis 6° of theorem.

From (16) and (17) follows that for $\exists p \in \mathsf{P}$

$$V_p(x(t)) \le \gamma\|x(t_0)\|^m \exp\left\{-\frac{c}{b}(t - t_0)\right\} \quad (18)$$

Using condition 4° of theorem

$$\|x(t)\|^m \le \frac{\gamma}{a}\|x(t_0)\|^m \exp\left\{-\frac{c}{b}(t - t_0)\right\} \quad (19)$$

From last relation we have

$$\|x(t)\| \le \left(\frac{\gamma}{a}\right)^{\frac{1}{m}} \|x(t_0)\| \exp\left\{-\frac{c}{bm}(t - t_0)\right\} \quad (20)$$

Theorem is proved.

The results of Theorem 1 can be extended to analysis of the switched systems with the feedback. Such possibilities now is under investigations.

Remark 1. In the reference [13] the method for stability analysis of switched systems perturbed by a Wiener process is considered. It is proved that stochastic switched systems is globally asymptotically stable in probability.

4. CONCLUSION

In this paper the analysis of exponential stability of switched systems is considered. The multiple models is given in the form of autonomous nonlinear differential equations. The analyses is based on multiple Lyapunov functions. The exponentially stable systems are robust with respect to unmodeled dynamics.

The results will be extended to the stochastic systems (stability of m-moment of state vector). Also, it is interesting to extend the results to input – to – state stability concept .

REFERENCES

[1] C.G. Cassandras, and S.Lafortune, *Introduction to discrete event systems*, Berlin, Springer-Verlag, 2008

[2] J.E. Hopcroft, R. Montwani and J. D. Ullman, *Introduction to Automata Theory, Lenguage and Computation*, New York, Addison-Wesley, 2006

[3] D. Liberzon, *Switching in Systems and Control*. Basel, Birkhauser, 2003.

[4] K.S. Narendra, and J. Balakrisnan, "A common Lyapunov function for stable LTI systems with commuting A-matrices", *IEEE Trans. Automatic Control*, vol. 39, pp. 2469-2471, 1944

[5] M.S. Branicky, "Multiple Lyapunov functions and other analysis tools for switched and hybrid systems", *IEEE Trans. Automatic Control*, vol. 43, pp. 475-482, 1998

[6] Z. Guan, J. D. Hill and X Shen, "On hybrid impulsive and switching systems and application to nonlinear control". *IEEE Trans. Automatic Control*, vol. 509, pp. 1058-1062, 2005

[7] Z. Li, Y. Soh and C Wen, *Switched and impulsive systems*. Berlin, Springer-Verlag, 2005.

[8] M. Huang, G.N. Nair and R.J. Evans, "Finite horizon LQ optimal control and computation with data rate constraints". In: *Proceedings of the CDC and ECC Conference*, Sevilja, Spain, pp. 179-184, 2005

[9] W. Zhang, M.S.. Branicky and S.M. Phillips, "Stability of networked control systems". *IEEE*

Control Systems Magazine, vol. 21, pp. 84-89, 2001

[10] T. Alpcan and T. Basar, "A hybrid system model for power control in multicell wireless networks.' *Int. J. of Performance Evaluation*, vol 57, pp. 477-495, 2004

[11] J. Lee, S. Bohacek, J.P. Hespanaha and K. Obraczka, "Modeling communication networks with hybrid systems", *IEE/ACM Trans. on Networking*, vol.15. pp. 663-672, 2007

[12] V.Z. Filipovic, "Hybrid control of systems with input delay". In: *CD IFAC World Congress*, Praha, Czech Republic, 2005

[13] V.Z. Filipovic, "Upper bounds of performances guided robust hybrid controller". *Facta Universitats, Seies: Electronic and Energetcs*, accepted for publicaton, 2008

[14] V.Z. Filipovic, "Switching control in the presence of constraints and unmodeled dynamics". Chapter in: H. Aschemann (Ed.): *New Approach in Automation and Robotics*, Vienna, I-TECH, 2008

[15] V.Z. Filipovic, "Exponential stability of stochastic switched systems". *Tansaction, of the Institute of Measurement and Control*, Accepted for publications, 2008

[16] V.Z. Filipovic and N. Nedic, "Robust hybrid control in the presence of matching conditions". *ETRAN*, Palic , 2008

[17] V.Z. Filipovic, "Robust hybrid systems with supervisor based on performance index". *INFOTEH*, Jahorina, 2008

[18] H.Lin and P.J. Antsaklis, "Stability and stabilizability of switched linear systems: A survey of recent results" *IEEE Trans. Automatic Control*, vol. 53, to appear, 2008

[19] M. Vidyasagar, *Nonlinear systems analysis*, Philadelphia, SIAM, 2002

[20] D. Chatterjee and D. Liberzon, "On stability of stochastic switched systems". *Proceedings of the CDC*, USA, pp.4125-4127, 2004

[21] H.K. Khalil, *Nonlinear systems*. New Jersey, Prentice-Hall, 1996

CONTROL ALGORITHMS OF EXPONENTIAL PRACTICAL TRACKING OF HYBRID SYSTEMS

M. J. Stojčić

Abstract: *In this paper we consider practical tracking of nonlinear time-invariant hybrid systems, that is formed from continuous-time object (plant) and digital computer (controller). The definition of practical exponential tracking of hybrid systems is given. Based on this definition are given and proven criteria and control algorithms that ensure practical exponential tracking. The simulation results worked out in an example, verify the proposed theory.*

Keywords: *practical tracking, exponential tracking, hybrid system, criteria and control algorithms*

1. INTRODUCTION

Generally, the task of a control process is to ensure a required closeness between real and desired dynamic behavior of a controlled process, of a controlled plant (object). Briefly, the control has to ensure a kind of tracking. In other words, the real dynamic behavior should track (follow) the desired dynamic behavior, even in circumstances, when disturbances act on the object.

We differentiate two concepts of tracking: Lyapunov tracking concept (introduced by Grujić in references [5] through [10] of the paper [1]) and practical tracking concept (defined also by Grujić, [1,2]). Later, the practical tracking concept was developed in the papers [3,4], done by the same author. A further contribution to the theory of practical tracking was given in [5] for continuous time, in [6,7] for digital and in [8,9] for hybrid systems. The practical exponential tracking (PET) firstly is given in [5] for continuous time and later, in [6,7] for digital and in [8] for hybrid systems.

Tracking in the sense of Lyapunov, requires the existence of a Δ neighborhood of an initial desired output $\boldsymbol{y}_{d0}$ such that for each $\boldsymbol{y}_0$ from that neighborhood, the object output converges to the desired output, as time increases infinitely. This is the classical, widely known and used tracking property called *asymptotic tracking*, or simply, *tracking.*

Different from Lyapunov tracking concept, the practical tracking (PT) concept takes into account all technical and construction constraints, as well as the object behavior is observed over prespecified or determined time interval, which can be finite or infinite. This concept starts with three groups of sets: 1. time sets $\mathcal{R}_\tau = [0, \tau[,\ \tau \in \Re^+$, $\mathcal{R}_s$ and $\mathcal{R}_r$, $\mathcal{R}_{(\circ)} \subset \mathcal{R}_\tau$, $_{(\circ)} =_{s,r}$; tracking, settling and reachability time sets respectively. 2. sets of permitted output errors : the set of initial error E_I, the set of actual error E_A and the set of final error E_F, $E_F \subset E_I \subseteq E_A$ (based on these sets we define a desired quality of tracking), and 3. group of sets: the set of desired outputs $\mathcal{S}_{yd}$, the set of admitted disturbances $\mathcal{S}_z$ and the set of realizable controls $\mathcal{S}_u$ (based on these sets we take into account technical and construction constraints of a real object). Sets of the output errors are defined as time invariant sets and they are closed connected neighborhood of zero output error $\boldsymbol{0}_e$.

Based on the time sets and the set of desired outputs, we transform the sets of the output errors to the adequate sets of admitted real output (initial $\mathcal{Y}_I, t = 0$,actual $\mathcal{Y}_A(t),\ t \in \mathcal{R}_\tau$ and final $\mathcal{Y}_F(t)$, $t \in \mathcal{R}_{(\circ),(\circ)=_{s,r}}$). Now the PT is achieved if there exist the control $\boldsymbol{u}(t) \in \mathcal{S}_u$, that the system real output $\boldsymbol{y}(t)$ transfer from a set of initial output $\mathcal{Y}_I$ to a set of final output $\mathcal{Y}_F(t)$ during time $\tau \in \mathcal{R}_\tau$, so that the system real output must not leave the set of the instantaneous output $\mathcal{Y}_A(t)$. At the same time disturbances should belong to the set $\mathcal{S}_z$. Depending on desired quality of tracking we differentiate several kinds of PT as follow: *tracking*, *tracking with the settling time*, *tracking with the reachability time* and the *exponential* kind of PT.

The tracking properties are dynamic properties which are related to the output space, or equivalently, to the output error space. In the latter case we express that the output error is the key signal for control synthesis. Therefore, related to tracking, we use the fundamental control principle, the principle of the negative output feedback. A controlled object is a real physical system, the dynamical behavior of which is mathematically described by differential equations. However, its controller might be continuous-time or discrete - digital. If a digital computer is used as the controller, then it connected to the object and the object form the hybrid con-

Mihajlo J. Stojčić, Faculty of Mechanical Engineering, Banja Luka, Republic of Serbs, Bosnia and Herzegovina, stojcicmihajlo@gmail.com

trol system. There is an interaction between two different dynamical systems: continuous-time object (plant) and digital computer (controller). From the viewpoint of hybrid control, the overall system is hybrid control system (Fig. 1.).

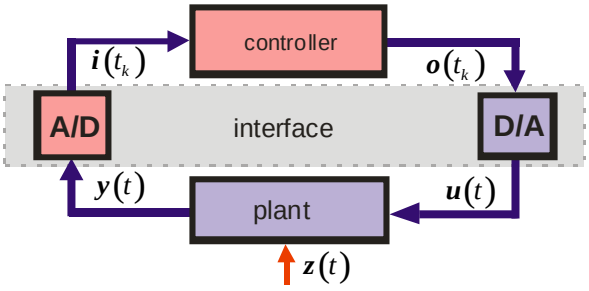

Fig 1. Hybrid Control System

And finally, we give some notation that used throughout: $\boldsymbol{e}(t_k)=\boldsymbol{y}_d(t_k)-\boldsymbol{y}(t_k)=\boldsymbol{e}_k$ - the vector of the output error; $t\in\mathcal{R}_\tau$ - the continuous time; $k\in\mathcal{Z}_n$ - the discrete time, $t_k=kT$, $T=t_{k+1}-t_k$ - the sampling period; $\Re,\Im^+,\Im$ - the real, nonnegative integer and integer sets; $n_p=]0,\infty]$, $n_p\in\Im^+$ - the discrete time up to which tracking is realized; $\tau=n_pT$, $\mathcal{Z}_n$ - discrete time sets of tracking defined as: $\mathcal{Z}_n=[0,n_p[$,; $\alpha,\beta\in\Re^+,\alpha>1$, $\gamma\in[\beta,\infty[$ -the real numbers; diagonal matrices $i\in[1,r]$; $\Lambda=diag\{\alpha_i\}$, $\Gamma=diag\{\frac{\gamma_i-1}{\gamma_i}\}$; $\boldsymbol{u}_m,\boldsymbol{u}_M$ - the vector minimum and maximum of the admitted control; $B\in\Re^{n\times m}$ - the matrix describing transmission of the control action; $\mathbf{1}$ -the unity vector of appropriate dimension .

In the criterion and algorithm, which follow below, we will use the vector functions $\boldsymbol{v}:\Re^r\to\Re^r$ from the class $\mathcal{V}$, often called "aggregate functions" (see [8] and its references). These functions can, but need not, be in general Lyapunov functions. Herein, they are not Lyapunov function because they belong to the Lurie class of functions $\mathcal{N}(\mathcal{L})$, $\mathcal{L}\in[L_1,\Lambda L_1]$. Next notation and definitions we will use below: $v_{im(\circ)}=min\{v_i(e_i):\ e_i\in E_{(\circ)}\}$, $v_{iM(\circ)}=max\{v_i(e_i):e_i\in E_{(\circ)}\}$, $_{(\circ)}=_{I,A}$ - the minimum and maximum of a function $\boldsymbol{v}\in\mathcal{V}$ for each component; $\boldsymbol{v}_{E(\circ)}(\boldsymbol{e}_0)$ - the vector of the minimum or of the maximum of a function $\boldsymbol{v}$, taken in the following sense: $v_{iE(\circ)}(e_{i0})=\{(v_{im(\circ)},e_{i0}<0)\vee(0,e_{i0}=0)\vee(e_{iM(\circ)},\ e_{i0}>0)$, $_{(\circ)}=_{A,F}\}$.

2. PROBLEM STATMENT

We consider a nonlinear stationary system which mathematical model of the plant, together with all actuators and sensors, is described by the vector ordinary differential equations as:

$$\boldsymbol{f}\left(\boldsymbol{x}(t),\dot{\boldsymbol{x}}(t),\cdots,\boldsymbol{x}^{(\eta)}(t),\boldsymbol{z}(t)\right)=B\boldsymbol{b}(\boldsymbol{u}(t))$$
$$\boldsymbol{y}(t)=\boldsymbol{g}\left(\boldsymbol{x}(t),\boldsymbol{z}(t)\right),\qquad(1)$$

where $\boldsymbol{x}\in\Re^n$, $\boldsymbol{z}\in\Re^p$, $\boldsymbol{u}\in\Re^m$ and $\boldsymbol{y}\in\Re^r$ are the state, disturbance, input and output vectors, respectively. The vector functions: $\boldsymbol{f}:\Re^{n\times(\alpha+1)}\times\Re^p\to\Re^n$, $\boldsymbol{g}:\Re^n\times\Re^p\to\Re^r$, $\boldsymbol{b}:\Re^m\to\Re^m$ describe the system internal dynamics, output and control function, respectively ($n,m,r,p,\eta\in\Re$). These functions satisfy the usual smoothness properties. For real physical system must be valid $n\ge m\ge r$.

Based on definition of perfect tracking [2] and equation (1), we calculate the nominal control $\boldsymbol{u}_N$ [8]. However, the tracking does not perfect, so that we have to perform some corrections to the mentioned nominal control. After these corrections, the function of control $\boldsymbol{b}(\boldsymbol{u})$ is obtained

$$\boldsymbol{b}(\boldsymbol{u}(t))=F^T\left(FF^T\right)^{-1}\left[F(CB)^{-1}C\boldsymbol{f}_t(\circ)+\boldsymbol{p}(\boldsymbol{e}(t))\right],\qquad(2)$$

where $\boldsymbol{f}_t(\circ)$ denotes $\boldsymbol{f}\left(\boldsymbol{x}(t),\dot{\boldsymbol{x}}(t),\cdots,\boldsymbol{x}^{(\eta)}(t),\boldsymbol{z}(t)\right)$. In this equation $C\in\Re^{m\times n}$ and $F\in\Re^{p\times m}$ are real matrices that satisfy relations: $\det(CB)\ne0$ and $\det\left(FF^T\right)\ne0$. The correction between nominal and real control, that mentioned above, is the function $\boldsymbol{p}(\circ):\Re^p\to\Re^p$, which depends from the output error and from its integrals and/or derivatives.

The interaction between the controller (computer) and the plant (object) is via the interface (that consist of A/D and D/A converters), and it occurs only at discrete k th instant. At each k th instants the first equation of the system (1) becomes

$$\boldsymbol{f}\left(\boldsymbol{x}(t_k),\dot{\boldsymbol{x}}(t_k),\cdots,\boldsymbol{x}^{(\eta)}(t_k),\boldsymbol{z}(t_k)\right)=B\boldsymbol{b}\left(\boldsymbol{u}(t_k)\right).\qquad(3)$$

Sets of the desired outputs, of the permitted output errors, of the admitted disturbances, the time sets as well as the desired algorithm of practical tracking are stored in the controller. In each k th instants of time (we assume that these instants are synchronous) controller “reads” data from the plant about its k th outputs, states and disturbances. Based on those and stored data, the controller calculate the new k th value of the control, and acts on the plant (see Fig. 1).

From analysis of the equation (2), easy to see that the control consists of two components: the first component, that depends of the function $\boldsymbol{f}_t(\circ)$ and of the

second component, that depends of implemented algorithm – exactly function $\boldsymbol{p}(\circ)$. If controller is computer, the function $\boldsymbol{p}(\circ)$ is discrete, but the function $\boldsymbol{f}_t(\circ)$ can be continuous or discrete, see [8]. In this paper we adopt, that this function is continuous. Also, we choose discrete function $\boldsymbol{p}(\circ)$, so that using this function we achieve practical exponential tracking (PET).

In order for the plant (1) to accomplish PET, next assumption, for every instant $k \in \mathcal{Z}_n$, must be satisfy:

A 1. All components of the output vector $\boldsymbol{y}(t_k)$ and of the disturbance vector $\boldsymbol{z}(t_k)$ are measurable,

A 2. Each component of the state vector $\boldsymbol{x}(t_k)$ is measurable or could be calculated as $\boldsymbol{x}(t_k) = \boldsymbol{g}^I(\boldsymbol{y}(t_k), \boldsymbol{z}(t_k))$. All components of the vectors $\boldsymbol{x}^{(i)}(t_k),\ i = 1, \cdots, \alpha$ are known,

A 3. The vector functions: of the internal dynamics $\boldsymbol{f}(\circ)$, of the output $\boldsymbol{g}(\circ)$ and of the control $\boldsymbol{b}(\circ)$ as well defined. There exist inverse function $\boldsymbol{b}^I(\circ)$ of the function $\boldsymbol{b}(\circ)$ related to $\boldsymbol{u}(t_k)$ and it is unique $\boldsymbol{u}(t_k) \equiv \boldsymbol{b}^I[\boldsymbol{b}(\boldsymbol{u}(t_k))]$.

3. DEFINITION AND CONTROL ALGORITHM

Definition 1: *The plant (1) controlled by* $\boldsymbol{u}(t) \in \mathcal{S}_u$ *exhibits practical exponential tracking with respect to* $\{n_p, \Lambda, \beta, \mathcal{Y}_I, \mathcal{Y}_A(\circ), \mathcal{S}_{yd}, \mathcal{S}_z\}$, *if and only if for every* $[\boldsymbol{y}_d(\circ), \boldsymbol{z}(\circ)] \in \mathcal{S}_{yd} \times \mathcal{S}_z$ *there exists a control* $\boldsymbol{u}(\circ) \in \mathcal{S}_u$ *such that* $\boldsymbol{y}_0 \in \mathcal{Y}_I(\boldsymbol{y}_{d0}, \mathcal{E}_I)$ *implies*

$$\boldsymbol{y}[k; \boldsymbol{y}_0; \boldsymbol{y}_d, \boldsymbol{u}(\circ), \boldsymbol{z}(\circ)] \in \mathcal{Y}_A(k),\ \forall k \in \mathcal{Z}_n \tag{4}$$

and that for every $[i,k] \in \{1,2,\cdots,r\} \times \mathcal{Z}_n$ *the following:*

$$y_i(k) \geq y_{di}(k) - \alpha_i (y_{di0} - y_{i0}) \beta^{-k}, y_{di0} \geq y_{i0} \tag{5}$$

$$y_i(k) \leq y_{di}(k) - \alpha_i (y_{di0} - y_{i0}) \beta^{-k}, y_{di0} \leq y_{i0} \tag{6}$$

hold, see Fig. 2.

□

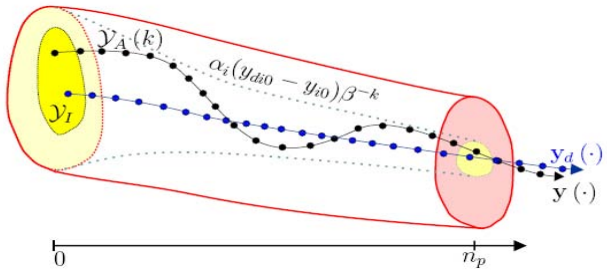

Fig. 2 Practical exponential tracking

Definition of PET for hybrid systems firstly is given in [8] and it is done to the output space.

Theorem 1. (***Criterion of PET***) *In order for the plant (1) controlled by* $\boldsymbol{u}(\circ) \in \mathcal{S}_u$ *to exhibit PET with respect to* $\{n_p, \Lambda, \beta, \mathcal{Y}_I, \mathcal{Y}_A(\circ), \mathcal{S}_{yd}, \mathcal{S}_z\}$ *it is sufficient that for the function* $\boldsymbol{v}(\circ),\ \boldsymbol{v}(\circ) \in \mathcal{N}(\mathcal{L}), \mathcal{L} \in [L_1, \Lambda L_1]$, *the control* $\boldsymbol{u}(\circ)$ *ensures:*

$$\Delta \boldsymbol{v}[\boldsymbol{e}(k; \boldsymbol{e}_0; \boldsymbol{y}_d(\circ), \boldsymbol{u}(\circ), \boldsymbol{z}(\circ))] = -\Gamma \boldsymbol{v}[\boldsymbol{e}(k)],$$
$$\forall [k, \boldsymbol{e}_0, \boldsymbol{y}_d(\circ), \boldsymbol{z}(\circ)] \in \mathcal{Z}_n \times E_I \times \mathcal{S}_{yd} \times \mathcal{S}_z, \tag{7}$$

where is $\gamma_i \in [\beta, \infty[,\ \beta \in]1, \infty[$ *and for every* $i \in \{1, \cdots, r\}$

$$\frac{e_{imA}}{e_{imI}} \leq \alpha_i \leq \frac{e_{iMA}}{e_{iMI}} \tag{8}$$

holds.

Theorem 2. (***Algorithm of PET***) *Let the assumptions* ***A1-A3*** *hold, and let the set* $\mathcal{S}_u = \{\boldsymbol{u}(\circ), \boldsymbol{u}_m \leq \boldsymbol{u}(k) \leq \boldsymbol{u}_M\}$ *with the control function*

$$\boldsymbol{b}(\boldsymbol{u}(t)) = F^T (FF^T)^{-1} [F(CB)]^{-1} C \boldsymbol{f}_k(\circ) + \Delta \boldsymbol{v}(\boldsymbol{e}_{k-1}) +$$
$$\Gamma \boldsymbol{v}(\boldsymbol{e}_{k-1})], \forall [k, \boldsymbol{e}_o, \boldsymbol{y}_d(\circ), \boldsymbol{z}(\circ)] \in \mathcal{Z}_n \times E_I \times \mathcal{S}_{yd} \times \mathcal{S}_z \tag{9}$$

where are $\gamma_i \in [\beta, \infty[,\ \beta \in]1, \infty[$ *and* $\boldsymbol{v}(\circ) \in \mathcal{N}(\mathcal{L})$. *The plant (1) controlled by* $\boldsymbol{u}(t) \in \mathcal{S}_u$ *exhibits PET with respect to* $\{n_p, \Lambda, \beta, \mathcal{Y}_I, \mathcal{Y}_A(\circ), \mathcal{S}_{yd}, \mathcal{S}_z\}$ *if for every* $i \in \{1, \cdots, r\}$ *equation (8) holds.*

In the equation (9) with $\boldsymbol{f}_k(\circ)$ we denoted value of function $\boldsymbol{f}(\boldsymbol{x}(t_k), \dot{\boldsymbol{x}}(t_k), \cdots, \boldsymbol{x}^{(\eta)}(t_k), \boldsymbol{z}(t_k))$ at the *k* instant.

PROOF: Proofs of the Theorem 1 and of the Theorem 2 are omitted because of a little space. The likewise proofs are given in [8].

From the viewpoint of hybrid control systems, equations (7) and (9) are the state and the output equations of hybrid controller respectively. The vectors of the state $\boldsymbol{q}_k$ and the output $\boldsymbol{o}_k$ of this controller are defined as: $\boldsymbol{q}_k = \boldsymbol{v}(\boldsymbol{e}_k)$, $\boldsymbol{o}_k = \boldsymbol{u}(t_k)$ respectively. The vector of continuous time control is given by $\boldsymbol{u}(t) = \boldsymbol{u}(t_k) = \boldsymbol{o}_k,\ kT \leq t < (k+1)T$.

4. SIMULATION RESULTS

For simulation of control algorithm that is proposed in Theorem 2, we use the manipulator with three rotating joints. Based on the technical feature and the desired output behavior we adopt next values:

- the time of tracking $\tau = 2s$; the sample period $T = 10^{-3}s$ (it is adopted by using Shennon's Theorem and linear model). Based on these times we define

the discrete time of tracking n_p and the time set $\mathcal{Z}_n$: $n_p = 2000$, $\mathcal{Z}_n = [0, 2000[$.

- the desired dynamical behaviour of the output , determined by the set

$$\mathcal{S}_{yd} = \left\{ \boldsymbol{y}_d : \boldsymbol{y}_d(t) = \begin{cases} \text{a } \cos(\pi/4\ \text{t})\text{e}^{-0.1\text{t}} \\ \text{b } \sin(\pi/4\ \text{t})\text{e}^{-0.1\text{t}} \\ \text{c } -0.3\ +0.2\ \text{t} \end{cases}, \begin{matrix} a = (l_2 + l_3)/2 \\ b = (l_2 + l_3)/1.5 \\ c = l_1 + a \end{matrix} \right\}$$

where are l_1, l_2 and l_3 length of the rods.

- the desired quality of tracking over above adopted time set is determined by the next output error sets, with given the initial vector error $\boldsymbol{e}_0$ and the initial E_I and the actual E_A error sets:

$$E_I = E_A = \left\{ \begin{pmatrix} -0.20 \\ -0.16 \\ -0.10 \end{pmatrix} \le \boldsymbol{e} \le \begin{pmatrix} 0.20 \\ 0.16 \\ 0.10 \end{pmatrix} \right\} \quad \text{e}_0 = \begin{pmatrix} -0.16 \\ 0.10 \\ 0.06 \end{pmatrix} [m]$$

- the sets of admitted disturbances and realizable controls are given:

$$\mathcal{S}_z = \left\{ \boldsymbol{z} : z(t) = \begin{cases} (0, t \le 0.5) \vee (-20, 0.5 \le t \le 1) \vee (-5, t > 1) \\ -50e^{-3t} \cos(3t)\, sign(\sin 10t) \\ -10 + 20 \sin(\pi/2\ \text{t}) \end{cases} \right\}$$

$$\boldsymbol{u}_m = -160, \quad \boldsymbol{u}_M = 160, \quad \mathcal{S}_u = \{\boldsymbol{u} : -160 \le \boldsymbol{u} \le 160\}[Nm]$$

- In this example, the function v_i is $v_i(\circ) = \sqrt[3]{(\circ)}$. Also, we adopt manner of the error change using next data: $\alpha_1 = \alpha_2 = \alpha_3 = 1$, $\beta = 1.002$, $\gamma_1 = \beta, \gamma_2 = 1.02\beta, \ \gamma_3 = 1.01\beta$. Based on these data we calculate matrices $\Gamma = diag\{0.002 \quad 0.0216 \quad 0.0119\}$ and $\Lambda = I$, I – unity matrix.

The matrices: B=diag (40,40,20) and $F = J(q_k)A(q_k)^{-1}B$ (see [6] and its references), where are $A(q_k)$ - matrix of inertia, $J(q_k)$ - Jacobian. The results of simulation of proposed algorithm by using selected data is given at Fig. 3.

5. CONCLUSION

In the paper we consider practical tracking of nonlinear time-invariant hybrid system. We give and prove the criterion and the exponential control algorithm that ensure EPT. The tracking properties are realized with respect to the prespecified sets of the times, of the permitted outputs and the errors, of the admitted disturbances and of the realizable controls. The controls are synthesized using digital computer which play a role of a controller, and using negative output feedback principle, also.

From result of simulation, we see that the control that is based on the proposed algorithm force the plant to exhibit exponential practical tracking and verify above proposed theory.

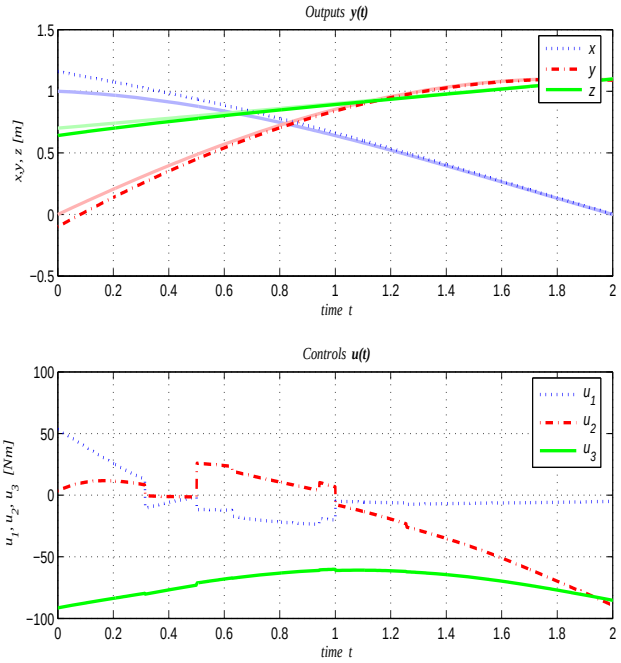

Fig. 3 Results of simulation

REFERENCIS

[1] Ljubomir T. Grujić: "*Stability Versus Tracking in Automatic Control Systems*", (in Serbian), *Preceedings JUREMA 29*, Zagreb, 1984, part I, pp 1-4

[2] Ljubomir T. Grujić: "*Phenomena, Concepts and Problems of Automatic Tracking: Discrete Time Non-Linear Stationary Systems with Variable Inputs*", (In Serbian), Proceedings of first International Seminar "Automation and Robot", Belgrade, 28-30. may 1985. page 402-421

[3] Ljubomir T. Grujić: "*Tracking Versus Stability: Theory*", (Tutorial Paper), Computing and Computers for control systems, P.Borne et all (editors), J.C. Baltzer AG, Scientific Publishing Co., IMACS 1989, 165-173

[4] Ljubomir T. Grujić: "*Tracking Control Obeying Prespecified Performance Index*", Computing and Computers for control systems, P.Borne et al. (editors), J.C. Baltzer AG, Scientific Publishing Co., IMACS 1989, Dragan V. Lazić: "*Analysis and Synthesis of Automatic Practical Tracking Control*", (In Serbian) Ph. D. Thesis, Belgrade 1995

[5] Mihajlo J. Stojčić: "*Practical Tracking of Nonlinear Digital Systems*", (In Serbian) Ph. D. Thesis, Banja Luka, March 2005

[6] Mihajlo J. Stojčić:*"Exponential Practical Tracking of Digital Systems"*, (In Serbian), Proceedings of IRMES '06, Banja Luka, September 21-22, 2006. ,pp 337-348

[7] Mihaylo Y. Stoychitch (in Serb language: *Михајло Ј. Стојчић) "On Practical Tracking of Hybrid Systems*", Nonlinear Analysis: Hybrid Systems 1 (2007), pp 280-295

[8] Mihaylo Y. Stoychitch (in Serb language: *Михајло Ј. Стојчић) "Summary Control Algorithms of Practical Tracking of Hybrid Systems"*, IX International Conference on Systems, Automatic Control and Measurements, Niš, Serbia, November 22-23, 2007, page 170 - 175

IONIZED GAS BOUNDARY LAYER ON THE POROSITY WALL OF THE BODY WHOSE ELECTROCONDUCTIVITY IS A FUNCTION OF THE LONGITUDINAL VELOCITY GRADIENT

S. Savić, B. Obrović, M.Despotović

Abstract: *Planar flow of the ionized gas in the boundary layer in the conditions of the so-called equilibrium ionization is studied. The contour of the body within the fluid is porous. The ionized gas is under the influence of the outer magnetic field which is normal to the contour of the body. The electroconductivity of the ionized gas is assumed to be a function of the longitudinal velocity gradient. In the paper, the governing equation system is with suitable transformations brought to a generalized form and numerically solved in the four-parametric approximation. Based on the obtained numerical solutions diagrams of important physical values and characteristics of the boundary layer are drawn. Adequate conclusions are also made.*

Key words: *boundary layer, ionized gas, ionized gas electroconductivity, porous contour, general similarity method, porosity parameter.*

1. INTRODUCTION

This paper presents a detailed study of a complex ionized gas flow in the boundary layer along a porous contour. As known, at supersonic flow velocities the gas dissociation is followed by ionization. Hence, the gas becomes electroconductive. When the ionized gas is exposed to a magnetic field, an electric flow is formed in the gas. Due to this flow, the so-called Lorentz force and Joule heat generate. As a result, additional terms, which contain the gas electroconductivity, appear in the governing equations.

The most significant results in investigation of the dissociated gas flow are given in the book by Dorrance [1]. Loitsianskii and the members of his school [2, 3, 4, 5] performed a detailed investigation of the dissociated gas flow in the boundary layer. Investigators of the so-called Belgrade School of the Boundary Layer led by Saljnikov [6, 7, 8] accomplished significant results in the field of dissociated gas flow in the boundary layer. In the works of Boricic et al [9, 10, 11] and Ivanovic [12], MHD boundary layer on a porous and nonporous contour of a body within the fluid is studied. In the paper [2], the ionized gas flow in the boundary layer along a flat plate in the presence of a magnetic field is studied. The paper [13] studies the ionized gas flow in the boundary layer along a nonporous body and papers [14, 15] study the ionized gas flow along a porous body of an arbitrary shape. In these papers, different electroconductivity variation laws are used.

The presented paper gives the results of investigation of the ionized gas flow in the boundary layer along a porous wall in the case when the electroconductivity is a function of the longitudinal velocity gradient. The ionized gas of the same physical characteristics as in the main flow is injected, i.e. ejected with the velocity $v_w(x)$. The outer magnetic field is normal to the wall of the body within the fluid. According to [2], it is considered that the power of this field is $B_m = B_m(x)$ and that the magnetic Reynold's number is very small. Therefore, in the case of the ionized gas flow in the magnetic field, the governing equation system of steady planar laminar boundary layer with the corresponding boundary conditions, according to [2], takes the following form:

$$\begin{aligned}
&\frac{\partial}{\partial x}(\rho u)+\frac{\partial}{\partial y}(\rho v)=0,\\
&\rho u\,\frac{\partial u}{\partial x}+\rho v\,\frac{\partial u}{\partial y}=-\frac{dp}{dx}+\frac{\partial}{\partial y}\left(\mu\,\frac{\partial u}{\partial y}\right)-\sigma B_m^2\,u,\\
&\rho u\,\frac{\partial h}{\partial x}+\rho v\,\frac{\partial h}{\partial y}=u\,\frac{dp}{dx}+\mu\left(\frac{\partial u}{\partial y}\right)^2+\frac{\partial}{\partial y}\left(\frac{\mu}{\mathrm{Pr}}\,\frac{\partial h}{\partial y}\right)+\\
&+\sigma B_m^2\,u^2,\\
&u=0,\quad v=v_w(x),\quad h=h_w \qquad \text{for}\quad y=0,\\
&u\to u_e(x),\qquad\qquad h\to h_e(x) \qquad \text{for}\quad y\to\infty.
\end{aligned} \tag{1}$$

By analogy with MHD boundary layer [9], the ionized gas electroconductivity σ is assumed to be a function of the longitudinal velocity gradient

$$\sigma=\sigma_0\frac{\nu_0}{u_e^2}\frac{\partial u}{\partial y},\qquad (\sigma_0,\,\nu_0=\text{const.}). \tag{2}$$

If the pressure is eliminated from the system (1), based on the conditions for the outer edge of the boundary layer, the following equation system is obtained:

Dr. Slobodan Savić, Assistant Professor, Faculty of Mechanical Engineering, Kragujevac, ssavic@kg.ac.yu
Dr. Branko Obrović, Full Professor, Faculty of Mechanical Engineering, Kragujevac, bobrovic@kg.ac.yu
Dr. Milan Despotović, Associate Professor, Faculty of Mechanical Engineering, Kragujevac, mdespotovic@kg.ac.yu

$$\frac{\partial}{\partial x}(\rho u)+\frac{\partial}{\partial y}(\rho v)=0,$$

$$\rho u\frac{\partial u}{\partial x}+\rho v\frac{\partial u}{\partial y}=\rho_e u_e\frac{du_e}{dx}+\frac{\partial}{\partial y}\left(\mu\frac{\partial u}{\partial y}\right)-\sigma B_m^2 u,$$

$$\rho u\frac{\partial h}{\partial x}+\rho v\frac{\partial h}{\partial y}=-u\,\rho_e u_e\frac{du_e}{dx}+\mu\left(\frac{\partial u}{\partial y}\right)^2+ \tag{3}$$

$$+\frac{\partial}{\partial y}\left(\frac{\mu}{\mathrm{Pr}}\frac{\partial h}{\partial y}\right)+\sigma B_m^2 u^2.$$

The boundary conditions remain unchanged.

2. TRANSFORMATION OF THE EQUATIONS

Modern methods of solution of boundary layer equations involve usage of a momentum equation. In the case of the ionized gas flow in the boundary layer along a porous wall, this equation will have the simplest form if instead of physical coordinates x and y we introduce new variables [3] in the form:

$$s(x)=\frac{1}{\rho_0\mu_0}\int_0^x \rho_w\mu_w\,dx,\qquad z(x,y)=\frac{1}{\rho_0}\int_0^y \rho\,dy \tag{4}$$

and a stream function $\psi(s,z)$ by means of the relations:

$$u=\frac{\partial\psi}{\partial z},\qquad \tilde{v}=\frac{\rho_0\mu_0}{\rho_w\mu_w}\left(u\frac{\partial z}{\partial x}+v\frac{\rho}{\rho_0}\right)=-\frac{\partial\psi}{\partial s}. \tag{5}$$

Quantities ρ_0 and μ_0 denote the known values of the density and the dynamic viscosity of the ionized gas (air) at a concrete point.

Using transformations (4) and (5) the governing equation system, together with the boundary conditions, is transformed and brought to the following form:

$$\frac{\partial\psi}{\partial z}\frac{\partial^2\psi}{\partial s\partial z}-\frac{\partial\psi}{\partial s}\frac{\partial^2\psi}{\partial z^2}=\frac{\rho_e}{\rho}u_e\frac{du_e}{ds}+\nu_0\frac{\partial}{\partial z}\left(Q\frac{\partial^2\psi}{\partial z^2}\right)-$$

$$-\frac{\rho_0\mu_0}{\rho_w\mu_w}\frac{\sigma_0 B_m^2}{\rho_0}\frac{\nu_0}{u_e^2}\frac{\partial^2\psi}{\partial z^2}\frac{\partial\psi}{\partial z},$$

$$\frac{\partial\psi}{\partial z}\frac{\partial h}{\partial s}-\frac{\partial\psi}{\partial s}\frac{\partial h}{\partial z}=-\frac{\rho_e}{\rho}u_e\frac{du_e}{ds}\frac{\partial\psi}{\partial z}+\nu_0\,Q\left(\frac{\partial^2\psi}{\partial z^2}\right)^2+$$

$$+\nu_0\frac{\partial}{\partial z}\left(\frac{Q}{\mathrm{Pr}}\frac{\partial h}{\partial z}\right)+\frac{\rho_0\mu_0}{\rho_w\mu_w}\frac{\sigma_0 B_m^2}{\rho_0}\frac{\nu_0}{u_e^2}\frac{\partial^2\psi}{\partial z^2}\left(\frac{\partial\psi}{\partial z}\right)^2; \tag{6}$$

$$\frac{\partial\psi}{\partial z}=0,\quad \frac{\partial\psi}{\partial s}=-\frac{\mu_0}{\mu_w}v_w=-\tilde{v}_w,\quad h=h_w\quad\text{for}\quad z=0,$$

$$\frac{\partial\psi}{\partial z}\to u_e(s),\qquad h\to h_e(s)\quad\text{for}\quad z\to\infty.$$

In the transformed equations (7), the nondimensional function Q and Prandtl number Pr are determined with the expressions:

$$Q=\frac{\rho\mu}{\rho_w\mu_w},\qquad \mathrm{Pr}=\frac{\mu c_p}{\lambda}, \tag{7}$$

where λ is the thermal conductivity coefficient c_p - the specific heat of the ionized gas at a constant pressure.

In order to solve the equation system (4), it is necessary to derive the momentum equation of the ionized gas on a body with a porous contour

$$\frac{dZ^{**}}{ds}=\frac{F_{mp}}{u_e}. \tag{8}$$

While deriving the momentum equation, the usual quantities are introduced: a parameter of the form $f(s)$, magnetic parameter $g(s)$, a conditional displacement thickness Δ^*, a conditional momentum loss thickness Δ^{**}, a shear stress at the wall of the body within the fluid τ_w, a nondimensional friction function $\zeta(s)$, a nondimensional value H and a characteristic boundary layer function on the porous wall F_{mp}. With the ionized gas flow, these quantities are defined with the relations:

$$Z^{**}=\frac{\Delta^{**2}}{\nu_0},\qquad f(s)=f_1(s)=\frac{u_e'\Delta^{**2}}{\nu_0}=u_e' Z^{**},$$

$$g(s)=g_1(s)=u_e^{-1}N_\sigma\nu_0^{1/2}Z^{**1/2},\quad N_\sigma=\frac{\rho_0\mu_0}{\rho_w\mu_w}N,$$

$$N=\frac{\sigma_0 B_m^2}{\rho_0},\qquad \Delta^*(s)=\int_0^\infty\left(\frac{\rho_e}{\rho}-\frac{u}{u_e}\right)dz, \tag{9}$$

$$\Delta^{**}(s)=\int_0^\infty\frac{u}{u_e}\left(1-\frac{u}{u_e}\right)dz,\quad \tau_w(s)=\left(\mu\frac{\partial u}{\partial y}\right)_{y=0}=$$

$$=\frac{\rho_w\mu_w}{\rho_0}\frac{u_e}{\Delta^{**}}\zeta;\quad \zeta(s)=\left[\frac{\partial(u/u_e)}{\partial(z/\Delta^{**})}\right]_{z=0},$$

$$H=\frac{\Delta^*}{\Delta^{**}};\quad F_{mp}=2\left[\zeta-(2+H)f\right]+g-2\Lambda.$$

Due to the porous wall of the body within the fluid, an addend appears in the momentum equation. Therefore, it is necessary to introduce a new parameter, the so-called porosity parameter $\Lambda(s)$:

$$\Lambda=-\frac{\mu_0}{\mu_w}\frac{v_w\Delta^{**}}{\nu_0}=-\frac{V_w\Delta^{**}}{\nu_0}=\Lambda(s) \tag{10}$$

where

$$V_w(s)=\frac{\mu_0}{\mu_w}v_w=\tilde{v}_w.$$

In order to apply the general similarity method, it is very important that the boundary conditions and the stream function on the wall of the body within the fluid remain the same as with the nonporous wall. For that reason, a new stream function $\psi^*(s,z)$ is introduced with the relation

$$\psi(s,z) = \psi_w(s) + \psi^*(s,z), \qquad \psi^*(s,0) = 0 \tag{11}$$

where $\psi(s,0) = \psi_w(s)$ denotes the stream function of the flow along the wall of the body within the fluid.

Applying the relation (11), the system (6) is transformed into the following equation system:

$$\frac{\partial\psi^*}{\partial z}\frac{\partial^2\psi^*}{\partial s\partial z} - \frac{\partial\psi^*}{\partial s}\frac{\partial^2\psi^*}{\partial z^2} - \frac{d\psi_w}{ds}\frac{\partial^2\psi^*}{\partial z^2} = \frac{\rho_e}{\rho}u_e u_e' +$$
$$+\nu_0\frac{\partial}{\partial z}\left(Q\frac{\partial^2\psi^*}{\partial z^2}\right) - \frac{\sigma_0 B_m^2}{\rho_0}\frac{\nu_0}{u_e^2}\frac{\rho_0\mu_0}{\rho_w\mu_w}\frac{\partial^2\psi^*}{\partial z^2}\frac{\partial\psi^*}{\partial z},$$
$$\frac{\partial\psi^*}{\partial z}\frac{\partial h}{\partial s} - \frac{\partial\psi^*}{\partial s}\frac{\partial h}{\partial z} - \frac{d\psi_w}{ds}\frac{\partial h}{\partial z} = -\frac{\rho_e}{\rho}u_e u_e'\frac{\partial\psi^*}{\partial z} +$$
$$+\nu_0 Q\left(\frac{\partial^2\psi^*}{\partial z^2}\right)^2 + \nu_0\frac{\partial}{\partial z}\left(\frac{Q}{\mathrm{Pr}}\frac{\partial h}{\partial z}\right) + \tag{12}$$
$$+\frac{\sigma_0 B_m^2}{\rho_0}\frac{\nu_0}{u_e^2}\frac{\rho_0\mu_0}{\rho_w\mu_w}\frac{\partial^2\psi^*}{\partial z^2}\left(\frac{\partial\psi^*}{\partial z}\right)^2;$$
$$\psi^* = 0, \quad \frac{\partial\psi^*}{\partial z} = 0, \quad h = h_w \quad \text{for} \quad z = 0,$$
$$\frac{\partial\psi^*}{\partial z} \to u_e(s), \qquad h \to h_e(s) \quad \text{for} \quad z \to \infty.$$

3. MATHEMATICAL MODEL

In order to derive the generalized boundary layer equations it is necessary to introduce new transformations from the very beginning:

$$s = s, \qquad \eta(s,z) = \frac{u_e^{b/2}}{K(s)}z,$$
$$\psi^*(s,z) = u_e^{1-b/2}K(s)\,\Phi\left[\eta,\ \kappa,\ (f_k),\ (g_k),\ (\Lambda_k)\right],$$
$$h(s,z) = h_1\cdot\bar{h}\left[\eta,\ \kappa,\ (f_k),\ (g_k),\ (\Lambda_k)\right]; \tag{13}$$
$$h_e + \frac{u_e^2}{2} = h_1 = const., \quad K(s) = \left(a\nu_0\int_0^s u_e^{b-1}ds\right)^{1/2};$$
$$a,\ b = const.$$

where $\eta(s,z)$ is the newly introduced transversal variable, Φ - the newly introduced stream function and $\bar{h}$ - the nondimensional enthalpy. Some important quantities and characteristics of the boundary layer (10) can be written in the form of more suitable relations:

$$u = u_e\frac{\partial\Phi}{\partial\eta}, \qquad \Delta^{**}(s) = \frac{K(s)}{u_e^{b/2}}B(s),$$
$$B(s) = \int_0^\infty\frac{\partial\Phi}{\partial\eta}\left(1 - \frac{\partial\Phi}{\partial\eta}\right)d\eta, \tag{14}$$
$$\frac{\Delta^*(s)}{\Delta^{**}(s)} = H = \frac{A(s)}{B(s)}, \quad A(s) = \int_0^\infty\left(\frac{\rho_e}{\rho} - \frac{\partial\Phi}{\partial\eta}\right)d\eta,$$
$$\zeta = B\left(\frac{\partial^2\Phi}{\partial\eta^2}\right)_{\eta=0}, \quad \frac{f}{B^2} = \frac{a\,u_e'}{u_e^b}\int_0^s u_e^{b-1}\,ds.$$

In the general similarity transformations (13), with the nondimensional functions Φ and $\bar{h}$, we introduced a local parameter of the ionized gas compressibility $\kappa = f_0$, a set of parameters of the form f_k of Loitsianskii's type [3], a set of magnetic parameters g_k and a set of porosity parameters Λ_k [16] by means of the following expressions:

$$\kappa = f_0(s) = \frac{u_e^2}{2h_1}, \qquad f_k(s) = u_e^{k-1}u_e^{(k)}Z^{**k},$$
$$g_k(s) = u_e^{k-2}N_\sigma^{(k-1)}\nu_0^{1/2}Z^{**k-1/2}, \tag{15}$$
$$\Lambda_k(s) = -u_e^{k-1}\left(\frac{V_w}{\sqrt{\nu_0}}\right)^{(k-1)}Z^{**k-1/2}\ (k = 1,\ 2,\ 3,\ ...).$$

They present new independent variables that are used instead of the longitudinal variable s.

The local compressibility parameter $\kappa = f_0$ and the sets of parameters satisfy the corresponding simple recurrent differential equations of the form:

$$\frac{u_e}{u_e'}f_1\frac{d\kappa}{ds} = 2\kappa f_1 = \theta_0,$$
$$\frac{u_e}{u_e'}f_1\frac{df_k}{ds} = \left[(k-1)f_1 + kF_{mp}\right]f_k + f_{k+1} = \theta_k, \tag{16}$$
$$\frac{u_e}{u_e'}f_1\frac{dg_k}{ds} = \left[(k-2)f_1 + \left(k - \frac{1}{2}\right)F_{mp}\right]g_k + g_{k+1} = \gamma_k,$$
$$\frac{u_e}{u_e'}f_1\frac{d\Lambda_k}{ds} = \left\{(k-1)f_1 + \left[(2k-1)/2\right]F_{mp}\right\}\Lambda_k +$$
$$+\Lambda_{k+1} = \chi_k. \qquad (k = 1, 2, 3, ...)$$

Applying the similarity transformations (13) and (15) to the equation system (12), we obtain the following boundary layer equation system:

$$\frac{\partial}{\partial\eta}\left(Q\frac{\partial^2\Phi}{\partial\eta^2}\right) + \frac{aB^2 + (2-b)f_1}{2B^2}\Phi\frac{\partial^2\Phi}{\partial\eta^2} +$$
$$+\frac{f_1}{B^2}\left[\frac{\rho_e}{\rho} - \left(\frac{\partial\Phi}{\partial\eta}\right)^2\right] - \frac{g_1}{B^2}\frac{\partial^2\Phi}{\partial\eta^2}\frac{\partial\Phi}{\partial\eta} + \frac{\Lambda_1}{B}\frac{\partial^2\Phi}{\partial\eta^2} =$$
$$= \frac{1}{B^2}\left[\sum_{k=0}^\infty\theta_k\left(\frac{\partial\Phi}{\partial\eta}\frac{\partial^2\Phi}{\partial\eta\partial f_k} - \frac{\partial\Phi}{\partial f_k}\frac{\partial^2\Phi}{\partial\eta^2}\right) + \right. \tag{17}$$
$$\left. +\sum_{k=1}^\infty\gamma_k\left(\frac{\partial\Phi}{\partial\eta}\frac{\partial^2\Phi}{\partial\eta\partial g_k} - \frac{\partial\Phi}{\partial g_k}\frac{\partial^2\Phi}{\partial\eta^2}\right) + \right.$$

$$+\sum_{k=1}^{\infty}\chi_k\left(\frac{\partial\Phi}{\partial\eta}\frac{\partial^2\Phi}{\partial\eta\partial\Lambda_k}-\frac{\partial\Phi}{\partial\Lambda_k}\frac{\partial^2\Phi}{\partial\eta^2}\right)\Bigg],$$

$$\frac{\partial}{\partial\eta}\left(\frac{Q}{\mathrm{Pr}}\frac{\partial\bar h}{\partial\eta}\right)+\frac{aB^2+(2-b)f_1}{2B^2}\Phi\frac{\partial\bar h}{\partial\eta}-\frac{2\kappa f_1}{B^2}\frac{\rho_e}{\rho}\frac{\partial\Phi}{\partial\eta}+$$

$$+2\kappa Q\left(\frac{\partial^2\Phi}{\partial\eta^2}\right)^2+\frac{2\kappa g_1}{B}\frac{\partial^2\Phi}{\partial\eta^2}\left(\frac{\partial\Phi}{\partial\eta}\right)^2+\frac{\Lambda_1}{B}\frac{\partial\bar h}{\partial\eta}=$$

$$=\frac{1}{B^2}\Bigg[\sum_{k=0}^{\infty}\theta_k\left(\frac{\partial\Phi}{\partial\eta}\frac{\partial\bar h}{\partial f_k}-\frac{\partial\Phi}{\partial f_k}\frac{\partial\bar h}{\partial\eta}\right)+$$

$$+\sum_{k=1}^{\infty}\gamma_k\left(\frac{\partial\Phi}{\partial\eta}\frac{\partial\bar h}{\partial g_k}-\frac{\partial\Phi}{\partial g_k}\frac{\partial\bar h}{\partial\eta}\right)+$$

$$+\sum_{k=1}^{\infty}\chi_k\left(\frac{\partial\Phi}{\partial\eta}\frac{\partial\bar h}{\partial\Lambda_k}-\frac{\partial\Phi}{\partial\Lambda_k}\frac{\partial\bar h}{\partial\eta}\right)\Bigg].$$

The transformed boundary conditions are:

$$\begin{aligned}&\Phi=\frac{\partial\Phi}{\partial\eta}=0,\quad \bar h=\bar h_w=const. \quad \text{for}\quad \eta=0,\\ &\frac{\partial\Phi}{\partial\eta}\to 1,\quad \bar h\to\bar h_e=1-\kappa \quad \text{for}\quad \eta\to\infty.\end{aligned}\tag{18}$$

The generalized equation system (17) represents a general mathematical model of the ionized gas flow along a porous wall of the body within the fluid for the assumed form of the electroconductivity variation law.

4. NUMERICAL SOLUTION

When the generalized equation system (17) with the boundary conditions (18) is numerically solved, a finite number of parameters should be adopted so that the solution is obtained in n- parametric approximation. The equation system can be solved only with a relatively small number of parameters. If we assume that all the similarity parameters from the second one onward equal zero:

$$\begin{aligned}&\kappa=f_0\neq 0,\quad f_1=f\neq 0,\quad g_1=g\neq 0,\\ &\Lambda_1=\Lambda\neq 0;\quad f_2=f_3=...=0,\quad g_2=g_3=...=0,\\ &\Lambda_2=\Lambda_3=...=0,\end{aligned}\tag{19}$$

the obtained equation system is significantly simplified. Furthermore, when the general similarity method is applied, the so-called localization is also performed. If we neglect derivatives per the compressibility, magnetic and porosity parameters, the equation system (17) is significantly simplified, and in a four-parametric three times localized approximation it has the following form:

$$\frac{\partial}{\partial\eta}\left(Q\frac{\partial^2\Phi}{\partial\eta^2}\right)+\frac{aB^2+(2-b)f}{2B^2}\Phi\frac{\partial^2\Phi}{\partial\eta^2}+$$

$$+\frac{f}{B^2}\left[\frac{\rho_e}{\rho}-\left(\frac{\partial\Phi}{\partial\eta}\right)^2\right]-\frac{g}{B^2}\frac{\partial^2\Phi}{\partial\eta^2}\frac{\partial\Phi}{\partial\eta}+\frac{\Lambda}{B}\frac{\partial^2\Phi}{\partial\eta^2}=$$

$$=\frac{F_{mp}f}{B^2}\left(\frac{\partial\Phi}{\partial\eta}\frac{\partial^2\Phi}{\partial\eta\partial f}-\frac{\partial\Phi}{\partial f}\frac{\partial^2\Phi}{\partial\eta^2}\right),$$

$$\frac{\partial}{\partial\eta}\left(\frac{Q}{\mathrm{Pr}}\frac{\partial\bar h}{\partial\eta}\right)+\frac{aB^2+(2-b)f}{2B^2}\Phi\frac{\partial\bar h}{\partial\eta}-$$

$$-\frac{2\kappa f}{B^2}\frac{\rho_e}{\rho}\frac{\partial\Phi}{\partial\eta}+2\kappa Q\left(\frac{\partial^2\Phi}{\partial\eta^2}\right)^2+\frac{2\kappa g}{B}\frac{\partial^2\Phi}{\partial\eta^2}\left(\frac{\partial\Phi}{\partial\eta}\right)^2+\tag{20}$$

$$+\frac{\Lambda}{B}\frac{\partial\bar h}{\partial\eta}=\frac{F_{mp}f}{B^2}\left(\frac{\partial\Phi}{\partial\eta}\frac{\partial\bar h}{\partial f}-\frac{\partial\Phi}{\partial f}\frac{\partial\bar h}{\partial\eta}\right).$$

The boundary conditions (18) remain unchanged.

In the equations of the system (20) the subscript 1 in some (first) parameters is left out.

For the numerical integration of the obtained system of differential partial equations of the third order, it is necessary to decrease the order of the differential equations. Using [7]

$$\frac{u}{u_e}=\frac{\partial\Phi}{\partial\eta}=\varphi=\varphi\,(\eta,\,\kappa,\,f,\,g,\,\Lambda),\tag{21}$$

we decrease the order of the differential equations of the system (20), so the system together with the boundary conditions comes to:

$$\frac{\partial}{\partial\eta}\left(Q\frac{\partial\varphi}{\partial\eta}\right)+\frac{aB^2+(2-b)f}{2B^2}\Phi\frac{\partial\varphi}{\partial\eta}+\frac{f}{B^2}\left[\frac{\rho_e}{\rho}-\varphi^2\right]-$$

$$-\frac{g}{B}\frac{\partial\varphi}{\partial\eta}\varphi+\frac{\Lambda}{B}\frac{\partial\varphi}{\partial\eta}=\frac{F_{mp}f}{B^2}\left(\varphi\frac{\partial\varphi}{\partial f}-\frac{\partial\Phi}{\partial f}\frac{\partial\varphi}{\partial\eta}\right),$$

$$\frac{\partial}{\partial\eta}\left(\frac{Q}{\mathrm{Pr}}\frac{\partial\bar h}{\partial\eta}\right)+\frac{aB^2+(2-b)f}{2B^2}\Phi\frac{\partial\bar h}{\partial\eta}-\frac{2\kappa f}{B^2}\frac{\rho_e}{\rho}\varphi+$$

$$+2\kappa Q\left(\frac{\partial\varphi}{\partial\eta}\right)^2+\frac{2\kappa g}{B}\frac{\partial\varphi}{\partial\eta}\varphi^2+\tag{22}$$

$$+\frac{\Lambda}{B}\frac{\partial\bar h}{\partial\eta}=\frac{F_{mp}f}{B^2}\left(\varphi\frac{\partial\bar h}{\partial f}-\frac{\partial\Phi}{\partial f}\frac{\partial\bar h}{\partial\eta}\right);$$

$$\begin{aligned}&\Phi=\varphi=0,\quad \bar h=\bar h_w=const. \quad \text{for}\quad \eta=0,\\ &\varphi\to 1,\quad \bar h\to\bar h_e=1-\kappa \quad \text{for}\quad \eta\to\infty.\end{aligned}$$

For the nondimensional function Q [15] and the density ratio ρ_e/ρ [4] that appear in the system (22), the following approximate formulae are used:

$$Q=Q(\bar h)=\left(\frac{\bar h_w}{\bar h}\right)^{1/3},\qquad \frac{\rho_e}{\rho}\approx\frac{\bar h}{1-\kappa}.\tag{23}$$

A concrete numerical solution of the obtained system of nonlinear and conjugated differential partial equations (22) is performed using finite differences method, i.e., ″passage method″. Based on the scheme of the plane integration grid [7], derivatives of the functions φ, Φ and $\bar h$ are substituted by finite differences ratios, and the equation system (22) is brought to the following system of algebraic equations:

$$(I)\quad a^i_{M,K+1}\varphi^i_{M-1,K+1} - 2b^i_{M,K+1}\varphi^i_{M,K+1} + $$
$$+ c^i_{M,K+1}\varphi^i_{M+1,K+1} = g^i_{M,K+1},$$
$$(II)\quad a^j_{M,K+1}\bar{h}^j_{M-1,K+1} - 2b^j_{M,K+1}\bar{h}^j_{M,K+1} +$$
$$+ c^j_{M,K+1}\bar{h}^j_{M+1,K+1} = g^j_{M,K+1}; \qquad (24)$$

$$M = 2,3,\ldots,N-1; \quad K = 0,1,2,\ldots; \quad i, j = 0,1,2,\ldots$$
$$\Phi^i_{1,K+1} = \varphi^i_{1,K+1} = 0, \quad \bar{h}^j_{1,K+1} = \bar{h}_w = const. \quad \text{for} \quad M = 1,$$
$$\varphi^i_{N,K+1} = 1, \qquad \bar{h}^j_{N,K+1} = 1-\kappa \qquad \text{for} \quad M = N.$$

The equation system (24) consists of two subsystems - dynamic (I) and thermodynamic (II).

For the concrete numerical solution of the equation system (22), i.e., the corresponding algebraic system, a program in FORTRAN program language has been written. It is based on the program used in the investigations [7]. Since Prandtl number depends little on the temperature, for air, it is assumed to be: $\Pr = 0.712$. The constants a and b, according to [7], have optimal values: $a = 0.4408; b = 5.7140$.

As the equation system (22) is localized per the compressibility, porosity and magnetic parameters, these parameters have become simple parameters. Therefore, the equation system (22) is solved by the usual procedure starting from the value $f = 0.00$ (flat plate), for values of the parameters κ, g and Λ given in advance.

5. CONCLUSION

Only some of the results are presented in this paper in the form of diagrams based on which important conclusions are drawn:

- Regardless of the fact whether the ionized gas is injected into the main flow or ejected from it, at different cross-sections of the boundary layer, the nondimensional velocity u/u_e very quickly converges towards unity (Fig. 1).
- The magnetic field has a great influence upon the boundary layer characteristic F_{mp} (Fig. 2).
- The influence of the magnetic field on the nondimensional friction function ζ, and therefore on the boundary layer separation point, is especially pointed out (Fig. 3). By increasing the values of the magnetic parameter, the separation of the boundary layer is postponed.
- The porosity parameter Λ has a great influence on the nondimensional friction function ζ (Fig. 4). Consequently, this parameter has also a significant influence on the boundary layer separation point. It is noted that the injection of air, in accordance with the relation (10), postpones the separation of the ionized gas boundary layer because the separation point moves down the flow.

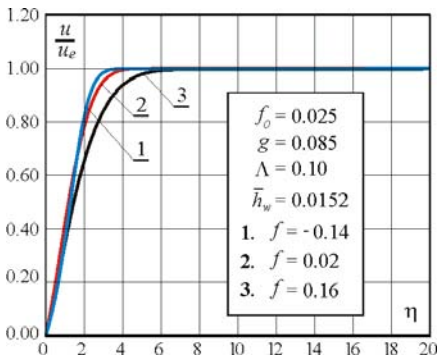

Fig. 1. Diagram of the nondimensional velocity u/u_e

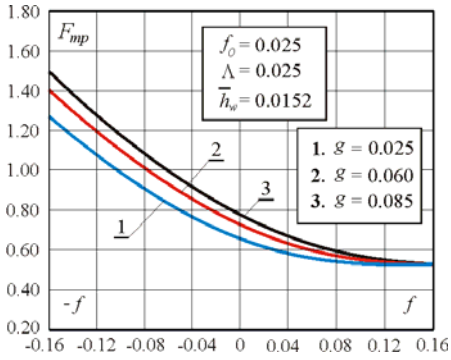

Fig. 2. Distribution of the characteristic function F_{mp}

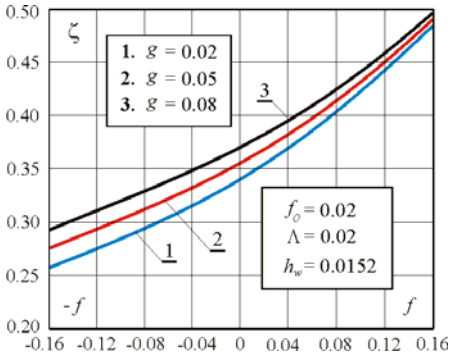

Fig. 3. Distribution of the nondimensional friction function $\zeta(g)$

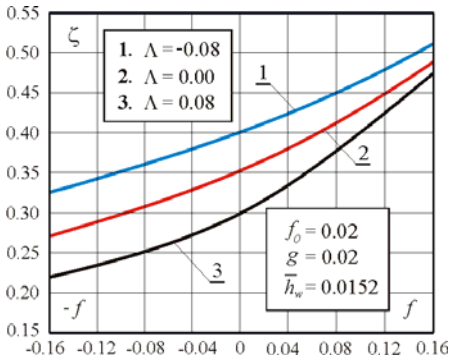

Fig. 4. Distribution of the nondimensional friction function $\zeta(\Lambda)$

REFERENCES

[1] Dorrance, W. H., Viscous hypersonic flow, Theory of reacting and hypersonic boundary layers (in Russian), Mir, Moscow, 1966.

[2] Loitsianskii, L. G., Laminar boundary layer (in Russian), FML, Moscow, 1962.

[3] Loitsianskii, L. G., Liquid and gas mechanics (in Russian), Nauka, Moscow, 1973, 1978.

[4] Krivtsova, N. V., Laminar boundary layer with the equilibrium dissociated gas (in Russian), Gidrogazodinamika, Trudi LPI, No. 265, pp. 35-45, 1966.

[5] Krivtsova, N. V., Parameter method of solving of the laminar boundary layer equations with axial pressure gradient in the conditions of equilibrium dissociation of the gas (in Russian), Engineering-Physical Journal, X, pp. 143-153, 1966.

[6] Saljnikov, V., A contribution to universal solutions of the boundary layer theory, Theoret. Appl. Mech. 4, pp. 139-163, 1978.

[7] Saljnikov V. and Dallmann, U., Verallgemeinerte Ähnlichkeitslösungen für dreidimensionale, laminare, stationäre, kompressible Grenz-schichtströmungen an schiebenden profilierten Zylindern, Institut für Theoretische Strömungs-mechanik, DLR-FB 89-34, Göttingen, 1989.

[8] Obrović, B., Boundary layer of dissociated gas (in Serbian), Monograph, University of Kragujevac, Faculty of Mechanical Engineering, Kragujevac, 1994.

[9] Boričić, Z., Nikodijević D. and Obrović B., Unsteady flow of the liquid, whose electro-conductivity is a function of the longitudinal velocity gradient, in MHD boundary layer on a body (in Serbian), XX Yugoslav Congress of Theoretical and Applied Mechanics, Kragujevac, pp. 136-139, 1993.

[10] Boričić, Z., Nikodijević D. and Milenković, D., Unsteady MHD boundary layer on a porous surface, Facta Universitatis, Series: Mechanics, Automatic Control and Robotics, Vol. 1, No. 5, pp. 631-643, 1995.

[11] Saljnikov, V., Boričić Z. and Nikodijević, D., Parametric method in unsteady MHD boundary layer theory of fluid with variable electroconductivity, Facta Universitatis, Series: Mechanics, Automatic Control and Robotics, Vol. 2, No 7/2, pp. 331-340, 1997.

[12] Ivanović, D., Unsteady incompressible MHD boundary layer on porous aerofoil in high accelerating fluid flow, Theoret. Appl. Mech., Vol. 27, pp. 87-102, 2002.

[13] Saljnikov, V., Obrović B. and Savić, S., Ionized gas flow in the boundary layer for different forms of the electroconductivity variation flow, Theoret. Appl. Mech., Vol. 26, pp. 15-31, 2001.

[14] Obrović B. and Savić, S., Ionized gas boundary layer on a porous wall of the body within the electroconductive fluid, Theoret. Appl. Mech., Vol. 31, No. 1, pp. 47-71, 2004.

[15] Savić, S., Solution of the problem of the ionized gas flow in the boundary layer in case of a nonporous and a porous contour of the body within the fluid (in Serbian), Ph.D. Thesis, Faculty of Mechanical Engineering in Kragujevac, Kragujevac, 2006.

[16] Obrović B. and Savić, S., About porosity parameters with the application of general similarity method to the case of a dissociated gas flow in the boundary layer, Kragujevac J. Math. 24, pp. 207-214, 2002.

Acknowledgement: *The research was supported by the Ministry of Science and Environmental Protection of the Republic of Serbia Grant ON144022*.

B SESSION:

EARTH-MOVING AND TRANSPORTATION SYSTEMS

РЕЗУЛЬТАТЫ ЭКСПЕРИМЕНТАЛЬНЫХ ИССЛЕДОВАНИЙ ТЯГОВЫХ И ТОПЛИВНЫХ ПОКАЗАТЕЛЕЙ ОДНООСНОГО КОЛЕСНОГО ДВИЖИТЕЛЯ

И.С. Суровцев, П.И. Никулин, Р.С. Солодов, В.Л. Тюнин

Аннотация: *В статье представлены результаты экспериментальных исследований по влиянию условий движения на тяговые и топливные показатели дифференциального моста снабжённого крупногабаритными пневматическими шинами при криволинейном движении.*

Ключевые слова: *Одноосный колёсный движитель, дифференциальный мост, стенд, тяговые и топливные показатели.*

Теоретические исследования процесса взаимодействия колёсного движителя (КД) снабжённого крупногабаритными пневматическими шинами (КГШ) с опорной поверхностью при криволинейном движении, выполненные в предыдущих работах, требуют проведения тщательных экспериментальных исследований, что возможно только при наличии специальных стендов, аппаратуры, датчиков и другого научного оборудования, необходимого для исследований.

В связи с этим, в Воронежском государственном архитектурно-строительном университете была разработана /1/, а затем усовершенствована конструкция стенда, позволяющая проводить экспериментальные исследования работы одноосного (рис. 1) колёсного движителя снабжённого КГШ при криволинейном движении.

Рис. 1 – Стенд для исследования работы одноосного колёсного движителя при криволинейном движении

Тяговые испытания ОКД с крупногабаритными шинами проводились на различных радиусах поворота, которые изменялись в пределах от 7,65 до 2,65 м, причем, внутреннее колесо двигалось по минимальному радиусу 1,25 м. В результате были подучены зависимости тяговой характеристики ОКД с крупногабаритными шинами размером 21,00-33 модели ВФ-166А и 21,00-28 мод. ДФ-27 при движении по цементобетонной поверхности (рис. 2) и плотному грунту (рис. 3) с внутренним давлением воздуха в шинах p_w = 0,6 ... 0,2 МПа для шин 21,00-33 и p_w = 0,4 ... 0,2 МПа для шин 21,00-28. Полученные тяговые характеристики дают возможность сделать анализ влияния радиуса поворота на тяговые и топливно-экономические показатели ОКД при криволинейном движении. Уменьшение радиуса поворота в исследуемых пределах приводит к существенному возрастанию коэффициента проскальзывания центральной опорной точки обеих шин моста θ_{o1}, θ_{o2} в результате чего при постоянной величине силы тяги снижается действительная скорость движения центра обоих колес, так и моста в целом, уменьшаются тяговая мощность и тяговый к.п.д.

Изменение радиуса поворота от 7,65 до 2,65 м при движении одноосного колесного движителя с диагональной и радиальной комбинированной шинами размером 21,00-33 модели ВФ-166А при p_w = 0,6 МПа по цементобетонной поверхности вызывает уменьшение максимальной тяговой мощности моста соответственно на 10,2 и 14,5 %, а так же максимального тягового к.п.д. моста на 15,3 и 17,8 %.

Игорь Степанович Суровцев, ректор ВГАСУ, доктор технических наук, профессор, Воронежский государственный архитектурно-строительный университет, Воронеж , Россия
Павел Иванович Никулин, доктор технических наук, профессор, Воронежский государственный архитектурно-строительный университет, Воронеж , Россия
Роман Сергеевич Солодов, кандидат технических наук, ассистент, Воронежский государственный архитектурно-строительный университет, Воронеж , Россия
Виталий Леонидович Тюнин, ассистент, Воронежский государственный архитектурно-строительный университет, Воронеж , Россия, sdm-vgasu@rambler.ru

На плотном грунте при R_0 = 2,65 м и p_w = 0,6 МПа величины $N_{тmax}$ и $\eta_{тmax}$ одноосного колесного движителя с диагональной шиной ниже, чем при R_0 = 7,65 м на 10,8 и 17 %, с радиальной комбинированной шиной при тех же условиях на 9,3 и 22,9 %. Следует отметить, что при движении ОКД с комбинированной шиной по цементобетонной поверхности значения максимальной тяговой мощности и максимального к.п.д. при R_0 = 6,15 м и p_w = 0,6 МПа выше, чем на плотном грунте в 1,5 и 1,1 раза. При движении ОКД с шинами размером 21,00-28 мод. ДФ-27 и p_w = 0,3 МПа по цементобетонной поверхности изменение радиуса поворота от 7,65 до 2,65 м приводит к уменьшению максимальной тяговой мощности моста на 12 %, а максимального тягового к.п.д. моста на 15 %. На плотном грунте при R_0 = 2,65 м и p_w = 0,3 МПа величины $N_{тmax}$ и $\eta_{тmax}$ одноосного колесного движителя ниже, чем при R_0 = 7,65 м на 11,8 и 18 %.

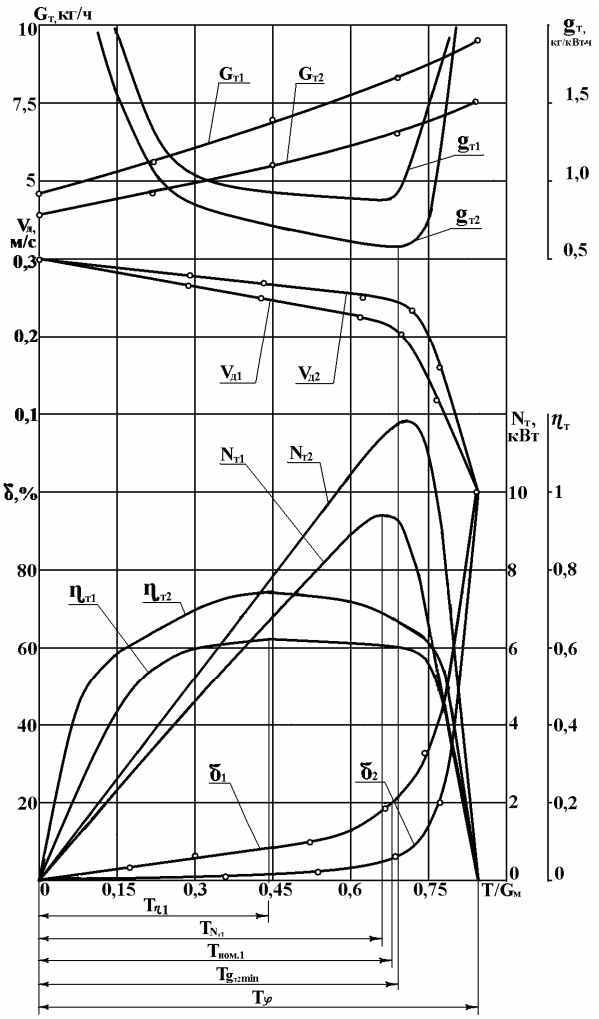

кривые: δ_1, N_{T1}, η_{T1}, G_{T1}, g_{T1}, $V_{Д1}$ – R_0 = 2,65м; δ_2, N_{T2}, η_{T2}, G_{T2}, g_{T2}, $V_{Д2}$ – R_0 = 7,65м

Рис. 2 – Тяговые характеристики одноосного колёсного движителя с шинами размером 21,00-28 мод. ДФ-27на цементобетоне при $G_м$ = 69,7 кН, $p_ω$ = 0,3 МПа и различных радиусах поворота

При исследовании влияния конструкции каркаса шин на тяговые качества одноосного колесного движителя использовали два варианта шин размером 21,00-33 модели ВФ-166А: диагональная, радиальная комбинированная, которые были изготовлены в одной пресс-форме и отличались, главным образом, только конструкцией каркаса.

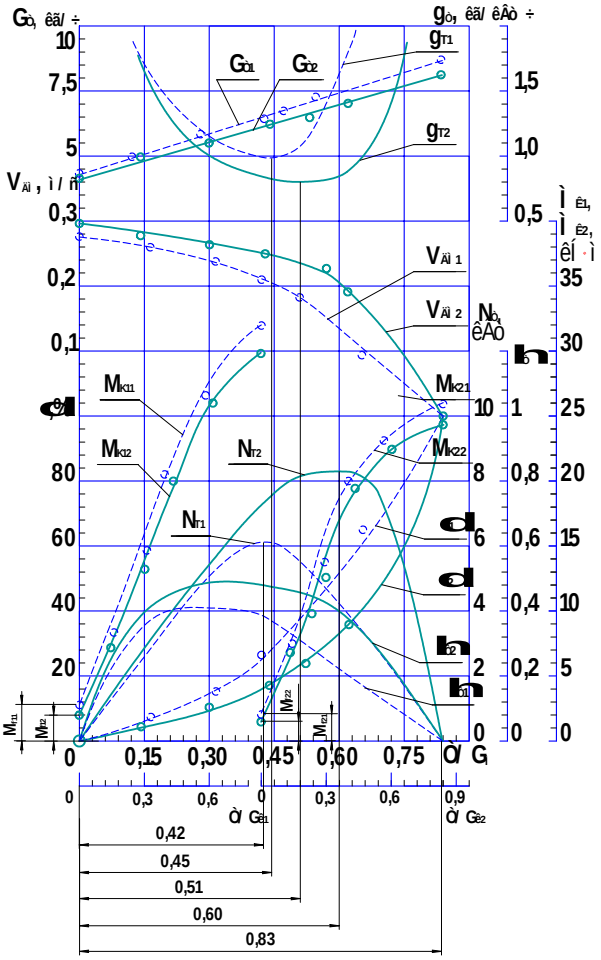

кривые: δ_1, N_{T1}, η_{T1}, G_{T1}, g_{T1}, $M_{к11}$, $M_{к21}$,$V_{ДМ1}$ – R_0 = 2,65м; δ_2, N_{T2}, η_{T2}, G_{T2}, g_{T2}, $M_{к21}$, $M_{к22}$,$V_{ДМ2}$ – R_0 = 7,65м

Рис. 3 – Тяговые характеристики одноосного колёсного движителя с шинами размером 21,00-28 мод. ДФ-27 на плотном грунте при $G_м$ = 69,7 кН, $p_ω$ = 0,2 МПа и различных радиусах поворота

Анализ полученных тяговых характеристик (рис. 4) показывает, что на плотном суглинистом грунте при R_o = 6,15 м и $p_ω$ = 0,6 МПа максимальная тяговая мощность ОКД с радиальными комбинированными шинами модели ВФ-166А выше, чем у движителя с диагональными шинами на 22,5 %, его к.п.д. на 9,5 %, сила тяги по сцеплению – на 19 %.

Аналогичные данные, подтверждающие преимущества по $N_{тmax}$, $\eta_{тmax}$ и $T_{φmax}$ ОКД с радиальными шинами по сравнению с диагональными, получены и на других опорных поверхностях: рыхлый грунт, цементобетон.

На рисунках 4.25, 4.26 представлены тяговые характеристики ОКД с шинами размером 21,00-28 мод. ДФ-27 соответственно на цементобетоне и плотном грунте при $G_м$ = 69,7 кН, R_0 = 7,65 м и различном давлении воздуха в шинах p_w.

Снижение внутреннего давления воздуха в шинах от 0,4 до 0,2 МПа благоприятно сказалось на тяговых и сцепных качествах ОКД при движении по цементобетону. Как показано на рисунке 5, зависимость коэффициента буксования δ = f(T/G$_М$),

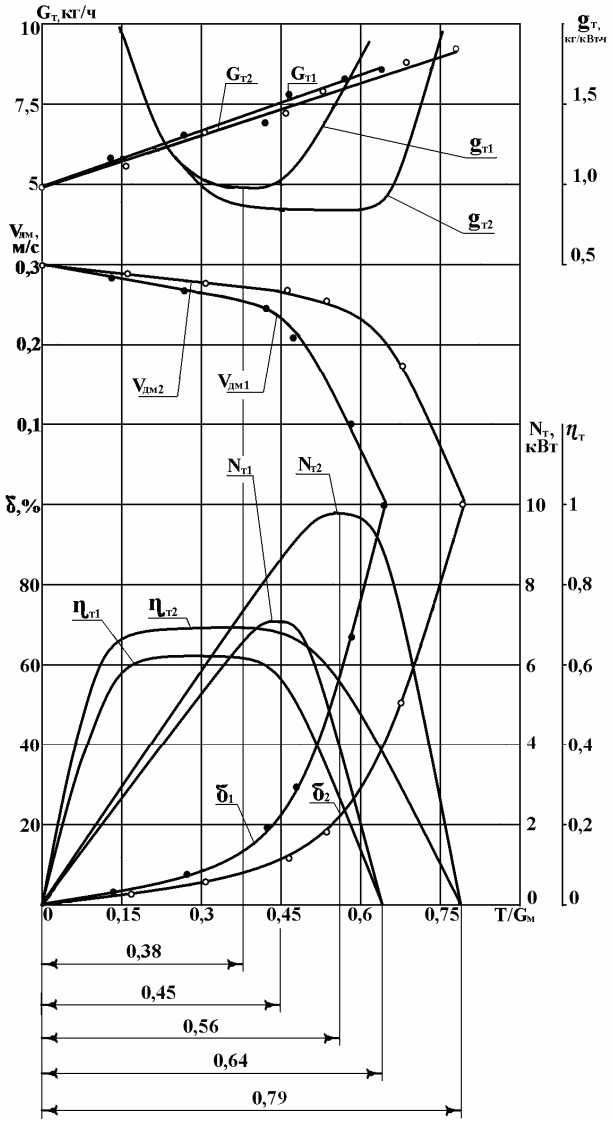

кривые с индексом: *1* – диагональная шина, *2* – радиальная комбинированная шина

Рис. 4 – Тяговые характеристики одноосного колёсного движителя с шинами 21,00-33 модели ВФ-166А различных конструкций на плотном связном грунте при $p_ω$ = 0,6 МПа, $G_{к1}$ = $G_{к2}$ = 65,7 кН, R_0 = 6,15 м

сместилась, при этом, в область меньших его значений по сравнению с зависимостью, полученной при p_w = 0,4 МПа. Это привело к увеличению коэффициента сцепления φ на 10,8 %, повысило величину N_{Tmax} на 8,5 %, $\eta_{тmax}$ на 6 % и снизило величину минимального значения удельного расхода топлива g_T на 13 %.

Аналогичные тенденции наблюдаются и при движении ОКД по плотному грунту. Зависимость коэффициента буксования δ = f(T/G$_М$), также сместилась, при этом, в область меньших его значений по сравнению с зависимостью, полученной при p_w = 0,4 МПа. Это привело к увеличению коэффициента сцепления φ на 18,8 %, повысило величину N_{Tmax} на 9,5 %, $\eta_{тmax}$ на 5 % и снизило величину минимального значения удельного расхода топлива g_T на 15 %.

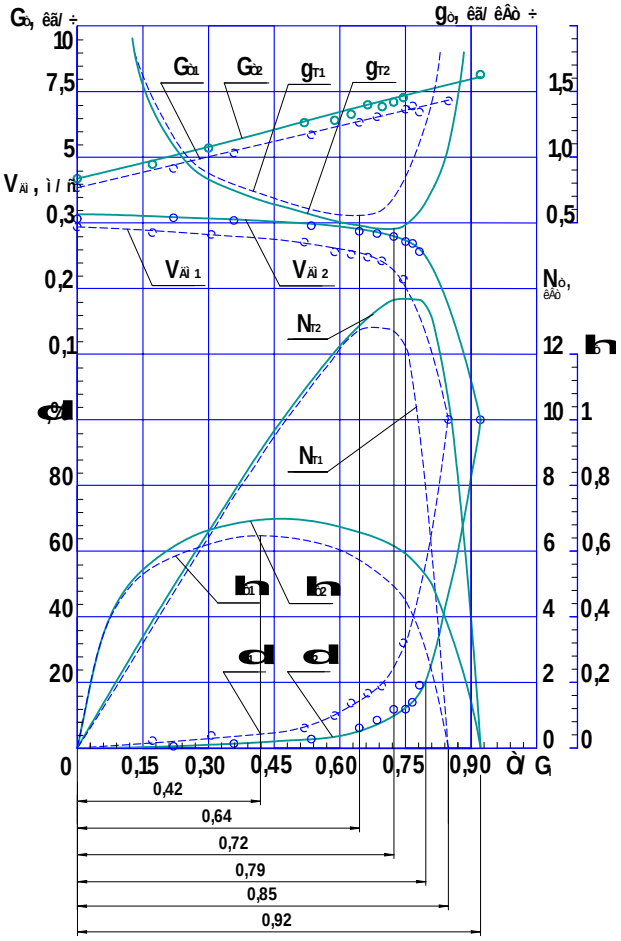

кривые: δ_1, N_{T1}, η_{T1}, G_{T1}, g_{T1}, $V_{дм1}$ – $p_ω$ = 0,4 МПа; δ_2, N_{T2}, η_{T2}, G_{T2}, g_{T2}, $V_{дм2}$ – $p_ω$ = 0,2 МПа

Рис. 5 – Тяговые характеристики одноосного колёсного движителя с шинами размером 21,00-28 мод. ДФ-27 на цементобетоне при $G_м$ = 69,7 кН, R_0 = 7,65 м и различном давлении воздуха в шинах

Уменьшение радиуса поворота вызывает снижение тяговой мощности, действительной скорости и тягового к.п.д. одноосного колесного движителя на исследуемых опорных поверхностях. При уменьшении радиуса поворота от 7,65 до 2,65 м на плотном суглинистом грунте для моста с крупногабаритными шинами размером 21,00-33 и $p_ω$ = 0,6 МПа снижаются N_{Tmax} и η_{Tmax} ОКД с диагональной шиной на 10,8 и 17 %, с радиальной

комбинированной шиной при тех же условиях на 9,3 и 22,9 %. При движении одноосного колесного движителя с шинами размером 21,00-28 мод. ДФ-27 и p_ω = 0,3 МПа по цементобетонной поверхности изменение радиуса поворота от 7,65 до 2,65 м приводит к уменьшению максимальной тяговой мощности моста на 12 %, а максимального тягового к.п.д. моста на 15 %.

Снижение внутреннего давления воздуха в шинах от 0,4 до 0,2 МПа благоприятно сказалось на тяговых и сцепных качествах одноосного колесного движителя при движении как по цементобетону, так и по плотному грунту. Это привело к увеличению коэффициента сцепления φ *н*а 10,8 ... 18,8 %, повысило величину N_{Tmax} на 8,5 ... 9,5 %, η_{Tmax} на 5 ... 6 % и снизило величину минимального значения удельного расхода топлива g_T на 15 ... 25 %.

Анализ результатов исследований показывает, что одноосный колесный движитель с радиальными крупногабаритными шинами имеет лучшие тяговые и сцепные качества. На плотном грунте при R_o = 6,15 м и p_ω = 0,6 МПа максимальная тяговая мощность одноосного колесного движителя с радиальными комбинированными шинами модели ВФ-166А выше, чем у движителя с диагональными шинами на 22,5 %, его к.п.д. на 9,5 %, максимальная сила тяги по сцеплению – на 19 %.

Для оценки топливных показателей ОКД используют тяговую характеристику, основной зависимостью которой является величина часового расхода топлива $G_T = G_T(T)$ и производная зависимость – кривая удельного расхода топлива $g_T = g_T(T)$.

В результате экспериментальных исследований были получены зависимости $G_T = G_T(T)$ при различных радиусах поворота моста, с шинами как радиальной, так и диагональной конструкции, с изменением внутреннего давления воздуха в шинах, вертикальной нагрузки, а также опорной поверхности качения колёс одноосного движителя. ОКД работал при этом в двух режимах нагружения: свободном и ведущем.

При движении одноосного колесного движителя с шинами размером 21,00-28 мод. ДФ-27 и p_w = 0,3 МПа по цементобетонной поверхности изменение радиуса поворота от 7,65 до 2,65 м приводит к повышению часового расхода топлива, на всём диапазоне изменения силы тяги, от 17 до 22,8 %. Минимальная величина удельного расхода топлива g_{Tmin} при R_0 = 2,65 м на 30,5 % выше, чем при R_0 = 7,65м. Характерно, что чем в более нагруженном режиме работает одноосный колёсный движитель, тем интенсивнее возрастает часовой расход топлива при уменьшении радиуса поворота ведущего моста.

Так, при изменении радиуса поворота ОКД от 7,65 до 2,65 м: в свободном режиме (T=0) часовой расход топлива увеличивается на 17 %; в режиме максимального тягового КПД ($T = T_{\eta max} = 0{,}45T/G_м$) – на 21,4 %; в режиме максимальной тяговой мощности ($T = T_{NTmax} = 0{,}7T/G_м$) – на 22 %; в режиме максимальной силы тяги по сцеплению ($T = T_{\varphi max}$) – на 22,8 %.

На плотном грунте при R_0 = 2,65 м и p_w = 0,3 МПа величина G_T, на всём диапазоне изменения силы тяги, выше в среднем на 20 %, а минимальная величина удельного расхода топлива g_{Tmin} на 33,5 % выше, чем при R_0 = 7,65м.

При качении колес моста по цементобетону с шинами размером 21,00-33 различных конструкций установлено, что на всем диапазоне изменения радиуса поворота G_T у шин радиальной конструкции несколько выше, чем у диагональной, однако g_{Tmin} у шин радиальной конструкции ниже, чем у диагональной, за счёт более высокого значения тяговой мощности N_T. Так, при R_0 = 2,65 м, p_ω = 0,6 МПа, $G_м$ = 130,4 кН величина G_T одноосного движителя с шинами 21,00-33 Рт мод. ВФ-166А на 16,5 % выше, при этом g_{Tmin} на 45 % ниже, чем у диагональных, а при R_0 = 7,65 м и прочих равных условиях G_T выше соответственно на 6,8 %, а g_{Tmin} ниже на 20,8 % у моста с радиальными шинами. Однако, при движении ОКД по плотному грунту величины и часового G_T, и минимального удельного расхода топлива g_{Tmin} для радиальных шин меньше, чем для диагональных на всем диапазоне изменения радиуса поворота, что обусловлено, в первую очередь, меньшим сопротивлением качению колес моста по причине более низкой деформации грунта вследствие снижения нормальных контактных напряжений в области контакта у шин типа "Р". Например, значение G_T при R_0 = 6,15 м, p_ω = 0,6 МПа, $G_м$ = 131,4 кН для диагональной шины размером 21,00-33 на 5,2 %, а g_{Tmin} на 19,3 % больше, чем для радиальной комбинированной шины того же размера (рис. 4).

Причём, чем меньше радиус поворота, тем существеннее разница в значениях G_T и g_{Tmin} между радиальной и диагональной шинами. Так, при R_0 = 2,65 м и прочих равных условиях G_T и g_{Tmin} для радиальных шин соответственно на 22 % и 39,5 % меньше, чем для диагональных.

Результаты экспериментальных исследований топливно-экономических показателей одноосного колесного движителя позволяют сделать следующее заключение. Уменьшение радиуса поворота вызывает существенное возрастание как часового расхода топлива G_T, так и минимального удельного расхода топлива g_{Tmin} одноосного колесного движителя на исследуемых опорных поверхностях, причём наиболее резкое увеличение G_T и g_{Tmin} происходит при радиусах поворота моста менее 4 м.

ЛИТЕРАТУРА

[1] Никулин П.И. Теория криволинейного движения колёсного движителя / П.И. Никулин. – Воронеж: Изд-во ВГУ, 1992. – 212 с.

[2] Ульянов Н.А. Самоходные колёсные землеройно-транспортные машины / Н.А. Ульянов, Э.Г. Ронинсон, В.Г. Соловьёв. – М.: Машиностроение, 1976. – 366 с.

ПРЕОБРАЗОВАНИЕ ПРИЦЕПНОГО СКРЕПЕРНОГО АГРЕГАТА В ПОЛУПРИЦЕПНОЙ

П.И. Никулин, В.А. Нилов, А.С. Кирьяк

Аннотация: *Разработано устройство блокировки переднего моста прицепного скрепера при его полном вывешивании на тяговом режиме. Вывешивание переднего моста прицепного скрепера дает возможность распределить часть веса скрепера на тягач, увеличивая его тяговые качества, что позволяет осуществлять набор грунта в ковш скрепера с шапкой без применения толкача тем самым, повышая производительность скреперного агрегата.*

Ключевые слова: *Прицепной скреперный агрегат, устройство блокировки шарнира арки-хобота, параметры устойчивости.*

Анализ различных способов агрегатирования скреперных агрегатов в составе скрепера и тягача дает возможность говорить о повышении эффективности работы скреперного агрегата за счет использования преимуществ различных способов агрегатирования скрепера и тягача на одном агрегате. Использование подобного рода модернизаций позволяет повысить эффективность использования скреперного агрегата без значительного изменения режимов работы и тем самым не повышать требования к квалификации оператора. Преимущества прицепной компоновки скреперного агрегата над полуприцепной на транспортном режиме и полуприцепной над прицепной на тяговом режиме реализована на существующем скреперном агрегате на полигоне Воронежского государственного архитектурно-строительного университета.

В качестве прототипа для создания экспериментального скреперного агрегата было принято тягово-сцепного устройство [1], так как оно уже было исследовано в работе [2] и не требовало существенных изменений в конструкции серийного тягача и скрепера (рис. 1). Такая компоновка универсального сцепного и догружающего устройства для серийного трактора Т-150К в агрегате с прицепным скрепером ДЗ-111А включает гидроцилиндр догрузки 1, который установлен между аркой-хоботом 2 и дышлом 3 на двух шаровых опорах.

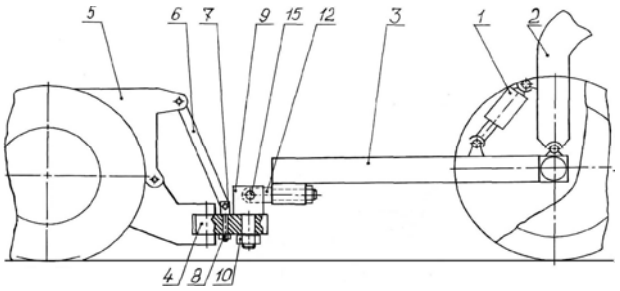

Рис. 1 - Конструкция тягово-сцепного догружающего устройства

Повышение давления в гидроцилиндре догрузки дает возможность переносить часть веса прицепного скрепера с грунтом на тягач, тем самым увеличивая его тяговые качества. Однако для максимального увеличения при копании сцепного веса тягача за счет веса поступающего в ковш грунта необходимо полное вывешивание переднего моста прицепного скрепера и поддержание его в данном положении при копании. Испытания проведенные на полигоне ВГАСУ показали, что при данной компоновке тягово-сцепного устройства полное вывешивание переднего моста скрепера невозможно. В процессе вывешивания моста (рис. 2) происходило потеря равновесия моста в шарнире арки-хобота и скреперный агрегат принимал положение показанное на рис. 3.

Павел Иванович Никулин, доктор технических наук, профессор, Воронежский государственный архитектурно-строительный университет, sdm-vgasu@rambler.ru
Владимир Александрович Нилов, доктор технических наук, профессор, Воронежский государственный архитектурно-строительный университет
Александр Сергеевич Кирьяк, аспирант, Воронежский государственный архитектурно-строительный университет

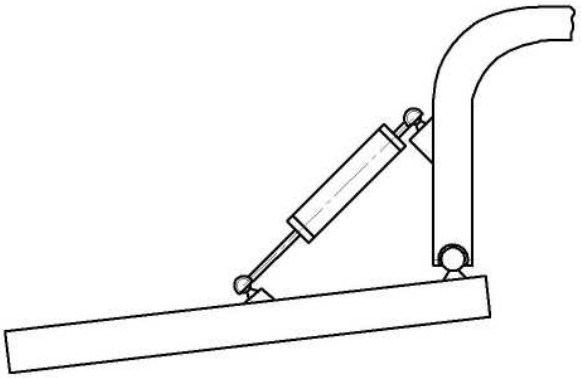

Рис. 2 – *Положение дышла, гидроцилиндра вывешивания и арки-хобота при вывешивании переднего моста скрепера*

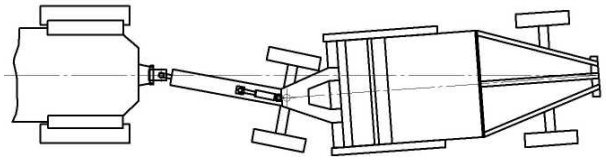

Рис. 3 – *План положения скреперного агрегата после попытки полного вывешивания переднего моста скрепера*

Предотвращение опускания переднего моста скрепера при попытке его полного вывешивания из-за неустойчивости трехшарнирного треугольника можно осуществлять двумя способами:

1) блокировать во время подъема один из шарниров (предпочтительнее верхний) гидроцилиндра догрузки во всех плоскостях, кроме вертикальной, проходящей через ось гидроцилиндра;
2)полностью блокировать во время подъема шарнир арки-хобота.

Оба эти способа в момент запирания полостей гидроцилиндра делают трехшарнирный треугольник жестким. Однако, первый способ отличается достаточной сложностью по кинематике исполнения, особенно принимая во внимание, что гидроцилиндр является исполнительным элементом и дополнительная нагрузка на его шарниры нежелательна. Поэтому задачу фиксирования переднего моста скрепера в вывешенном состоянии была решена вторым способом.

Было разработано устройство для блокировки шарнира арки – хобота в момент вывешивания переднего моста прицепного скрепера (рис. 4). Тягово-сцепное устройство *3* включает передний мост *6*, тяговый брус *7* и гидроцилиндр вывешивания *8*, установленный на шаровых опорах *9* между прицепным брусом *7* и аркой-хоботом *5* (рис. 4). С противоположной стороны к переднему мосту *6* жестко прикреплен нижний кронштейн *10* с направляющей *11*, а к арке-хоботу 5 – верхний кронштейн 12. Жесткость верхнего кронштейна 12 меньше жесткости нижнего кронштейна 10.

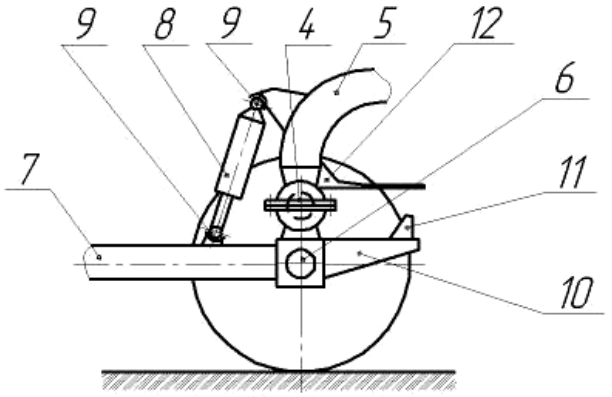

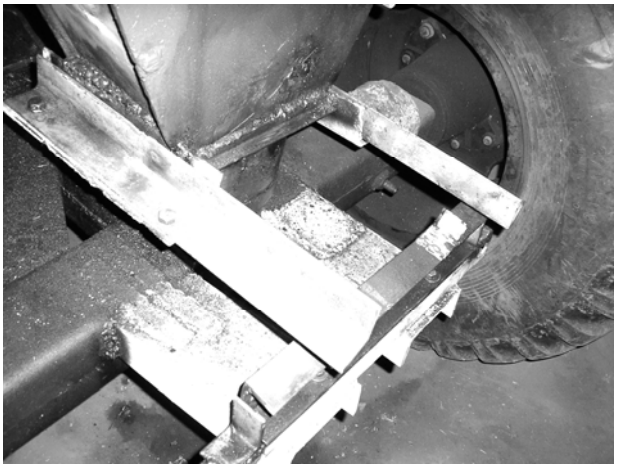

Рис. 4 – *Тягово-сцепное устройство в нерабочем положении*

Тягово-сцепное устройство работает следующим образом. В начале копания грунта при прямолинейном движении скреперного агрегата оператор тягача *1* подает гидрораспределителем масло в рабочую полость гидроцилиндра вывешивания *8*. Шток гидроцилиндра вывешивания *8* выдвигается, что приводит к отрыву колес переднего моста *6* прицепного скрепера *2* от грунта. При этом происходит перераспределение вертикальных нагрузок на мосты скреперного агрегата, приводящее к увеличению сцепного веса тягача *1*. Подъем переднего моста *6* будет происходить до тех пор, пока изменение угла между прицепным брусом *7* и аркой-хоботом *5* не приведет к соприкосновению направляющей *11* нижнего кронштейна *10* с верхним кронштейном *12* (рис. 5). При этом происходит выравнивание высоты *h* колес переднего моста *6* над грунтом (рис. 6) и постепенное деформирование верхнего кронштейна *12*. Необходимо отметить, что для исключения вращения шарнира 4 во всех плоскостях (в том числе и горизонтальной, как при повороте) в зоне

соприкосновения кронштейнов *10* и *12* должны возникать значительные силы трения, которые предотвратят поворот скрепера и опускание вывешиваемого моста. При этом длина гидроцилиндра вывешивания *8* должна фиксироваться гидросистемой на все время копания.

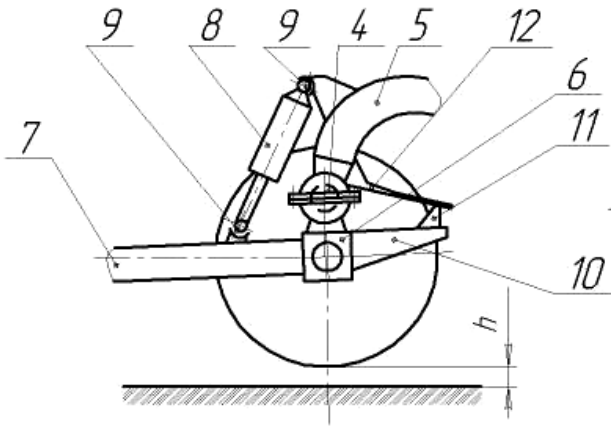

Рис. 5 - Рабочее положение тягово-сцепного устройства

Фиксированная длина гидроцилиндра вывешивания 8 блокирует шаровую опору *4* и превращает прицепной брус *7* и арку-хобот *5* в жесткую конструкцию, одной из опор которой является соединение прицепного бруса *7* с тягачом *1*. В результате скреперный агрегат из прицепного становится полуприцепным (рис. 5), для которого сцепной вес тягача *1* напрямую зависит от степени заполнения ковша грунтом. Скреперный агрегат начинает копание с увеличенным сцепным весом (за счет полного вывешивания переднего моста *6* прицепного скрепера *2*) и продолжает его с автоматически увеличивающимся сцепным весом тягача *1* за счет части веса поступающего в ковш грунта без дополнительных энергетических затрат на поддержание процесса вывешивания переднего моста *6* прицепного скрепера *2*.

После завершения заполнения ковша грунтом в момент его выглубления оператор тягача *1* подает гидрораспределителем масло в нерабочую (штоковую) полость гидроцилиндра вывешивания *8*. Гидроцилиндр вывешивания *8* сокращает свою длину, колеса переднего моста *6* опускаются на грунт, верхний кронштейн *12* и нижний кронштейн *11* перестают контактировать (рис. 5). Шаровая опора *4* разблокируется и скреперного агрегата снова становится прицепным.

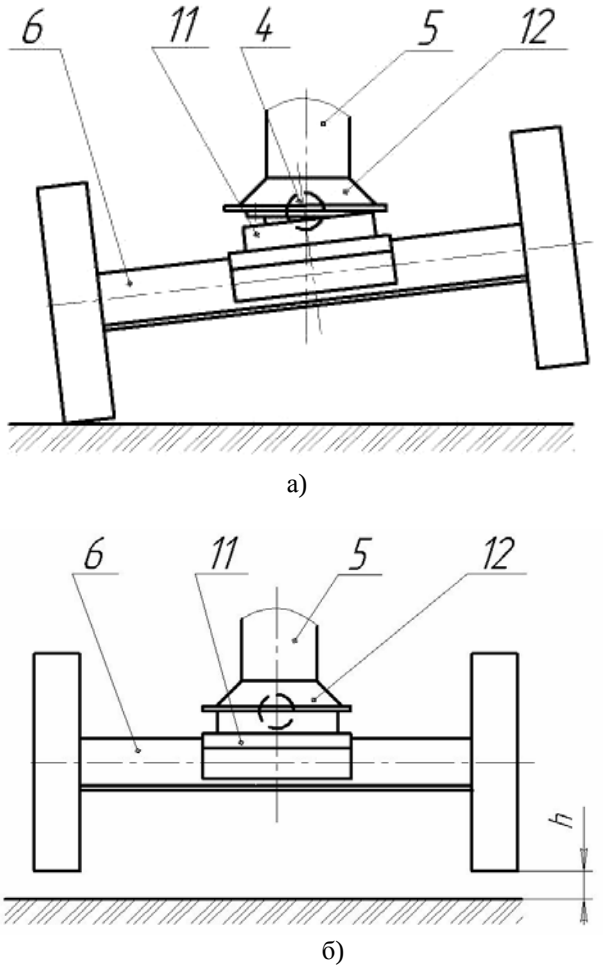

Рис. 6 – Выравнивание высоты колес переднего моста при его вывешивании: а) начало выравнивания; б) конец выравнивания

Данное тягово-сцепное устройство позволяет с минимальными энергетическими затратами преобразовать прицепной скрепер в полуприцепной и обеспечить непрерывное увеличение его сцепного веса при копании за счет части веса грунта, поступившего в ковш.

Первые испытания проводились в два этапа. На первом этапом была проведена проверка работоспособности данного устройства на транспортном режиме. После нескольких опытов экспериментально были подобраны оптимальные параметры устройства блокировки шарнира арки-хобота, при которых обеспечивалась не только устойчивость переднего моста скрепера в вывешенном состоянии, но и необходимые степени свободы шарнира арки-хобота при движении скреперного агрегата с опущенным передним мостом скрепера.

На втором этапе были проведены эксперименты на тяговом режиме. Набор грунта осуществлялся до полного буксования тягача с изменением глубины резания. По окончании набора грунта производился подсчет объема набранного грунта по сетке нанесенной на внутренних стенках ковша скрепера и высоте «шапки» грунта.

Результаты первых испытаний показали, что использование преобразования прицепного скреперного агрегата в полуприцепной на период копания повышает максимальный объем набираемого грунта и положительно влияет на эффективность работы скреперного агрегата без применения толкача.

ЛИТЕРАТУРА

[1] ПАТЕНТ № Россия, кл. E 02 F 3/64. . Авт изобр. Нилов В.А., Косенко А.А., Великанов А.В., Гаврилов А.В. (РОССИЯ) , - №/03; Заявлено 19.07.2000; Опубл. 27.05.2002, Бюл. №15.

[2] Косенко А.А. Повышение эффективности работы прицепного скрепера с колесным тягачом: Дис. ... канд. техн. наук. - Воронеж, 2003.- 182 с.

[3] Демиденко А.И. Повышение эффективности скреперных агрегатов. – Омск, 2005. – 282 с.

ИССЛЕДОВАНИЯ ИЗМЕНЕНИЯ СЦЕПНОГО ВЕСА ТЯГАЧЕЙ СКРЕПЕРНЫХ АГРЕГАТОВ

В.А. Нилов, П.И. Никулин

Аннотация: *В статье рассматривается вопрос изменения сцепного веса скреперных тягачей при заполнении ковша, приводятся результаты исследований, позволяющих обосновать постоянство сцепного веса тягача скрепера при заполнении ковша. Приводятся рекомендации по стабилизации и увеличению сцепного веса тягачей скреперов.*

Ключевые слова: *Тягач, сцепной вес, грунт, догрузка, нормальные реакции грунта*

Скреперы являются уникальными землеройно-транспортными машинами, которые в течение технологического цикла выполняют разработку грунта I…III категорий, его транспортировку в тело инженерного сооружения на расстояние до 3…5 км, послойную укладку, разравнивание и предварительное уплотнение грунта. Они отличаются высокой производительностью, низкой стоимостью выполняемых работ и с успехом применяются в дорожном, мелиоративном строительстве [1] и на открытых горных разработках [2].

В большинстве конструкций скреперных агрегатов (СА) разрушение грунта и заполнение ковша осуществляется за счет тягового усилия базового тягача. Поэтому увеличение эффективности их эксплуатации возможно за счет увеличения тягово-сцепных качеств базового тягача, величина тягового усилия которого зависит от параметров двигателя, трансмиссии и сцепного веса скреперного агрегата при копании грунта. При заполнении ковша скрепера грунтом должен изменяться сцепной вес тягача, причем, на этот процесс определенное влияние оказывает способ сочленения тягача и скреперного оборудования.

Экспериментальными исследованиями ряда авторов [3…6] установлено, что, несмотря на значительный объем грунта, поступившего в ковш (даже в конечной стадии заполнения ковша), сцепной вес тягача мало изменяется относительно его статического значения при порожнем ковше.

Сцепной вес самоходного скрепера на базе одноосного тягача при копании увеличивается всего на 12…15 % [3…5] (рис. 1), для прицепного скрепера сцепной вес тягача уменьшается на 14…18 % вне зависимости от типа движителя (колесный или гусеничный) тягача [6]. Столь небольшие изменения сцепного веса тягача объясняются значительным силовым взаимодействием грунтовой стружки, поступающей в ковш, с находящимся в нем грунтом.

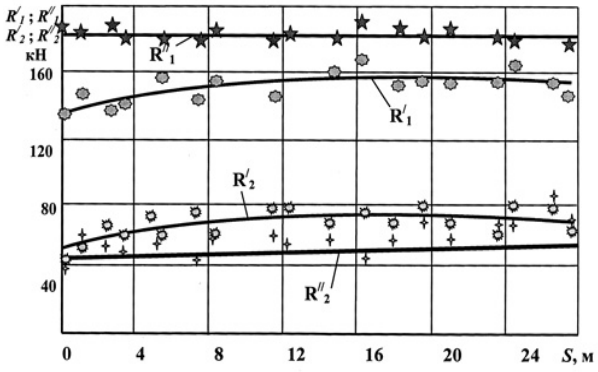

Рис. 1. Нормальные реакции грунта на колеса ковша скрепера при копании

В работе [3] предложно включить в схему сил, действующих в зоне ножа скрепера, сопротивление проталкиванию грунта в ковш $W_{ковш}$, которое не учитывалось ранее при изучении вертикальных реакций грунта на колеса ковша скрепера при копании. Физический смысл действия этой силы в зоне ножа заключается в том, что она стремится вывесить ковш на пласте, входящего в ковш грунта за счет сил трения в пограничных слоях уже набранного в ковш грунта.

Усилие $W_{ковш}$ изменяется в значительных пределах, увеличиваясь к концу заполнения ковша до 60…70 % от всего тягового усилия:

$$W_{ковш} = \left[BhH + (B+h)H^2 tg\,\theta_2/2 \right] \cdot \gamma_p e^{\mu\rho}, \qquad (1)$$

где B – ширина резания грунта;

h – глубина резания грунта;

H – высота заполнения ковша;

γ_p – объемный вес грунта;

Θ_2 – угол внутреннего трения грунта;

$e^{\mu\rho}$ – коэффициент, учитывающий сопротивление, возникающее при изменении направления движения стружки грунта на угол ρ.

Владимир Александрович Нилов , доктор техн. наук, профессор, Воронежский государственный архитектурно-строительный университет, Россия
Павел Иванович Никулин, доктор техн. наук, профессор, Воронежский государственный архитектурно-строительный университет, Россия, rector@vgasa.voronezh.su

Учет силы $W_{ковш}$, определяемой по зависимости (1), позволил количественно объяснить незначительное увеличение сцепного веса самоходного скрепера при копании грунта, однако зависимость (1) аналогична зависимости для определения сопротивления заполнению ковша, которое действует не в вертикальной, а в горизонтальной плоскости. Это обстоятельство указывает на необходимость проведения дополнительных исследований по изучению вертикальных нагрузок на мосты скрепера при копании.

Нами было предложено для расчета вертикальных нагрузок на мосты скрепера при копании [7] *исключить* вес призмы $G_{ПР}$ (столба) грунта (рис. 2), находящегося в активном движении в ковше, из баланса вертикальных сил, как опирающийся на массив ещё не разработанного грунта.

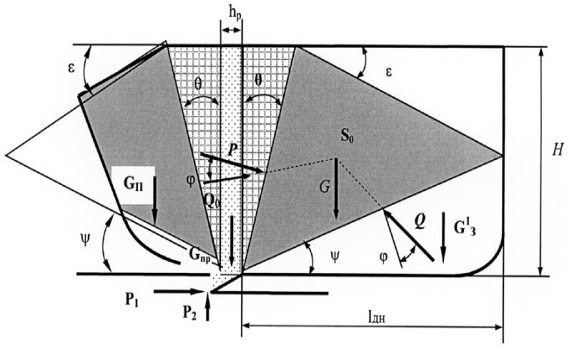

Рис. 2. Схема заполнения ковша скрепера при копании грунта

При определении вертикальных нагрузок на скрепер следует учитывать *вес не всего грунта*, набранного в ковш, а только *вес неподвижного грунта* в передней $G_П$ и задней $G^1_З$ частях ковша, т.е. грунт, находящийся со стороны передней заслонки и задней стенки. Вес столба (симметричной призмы) грунта $G_{ПР}$ не передается на ковш и не участвует в балансе вертикальных сил.

Такой подход позволяет объективнее воспроизвести физическую картину заполнения ковша скрепера и точнее рассчитывать нормальные реакции грунта на колеса скрепера в зависимости от степени заполнения ковша скрепера грунтом по простым аналитическим зависимостям:

для самоходного скрепера (рис. 3):

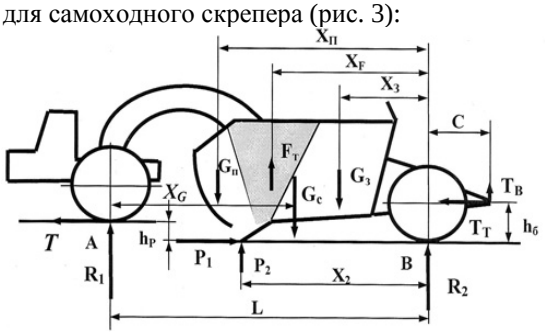

Рис. 3. Схема сил, действующих на самоходный скрепер при копании грунта

$$R_1 = 1/L\ [G_c(L\text{-}X_G) + G_П X_П + G_З X_З - P_2 X_2 - F_{тр} X_F + T_T h_б + T_B C], \quad (2)$$

$$R_2 = 1/L\ [G_C X_G + G_П(L\text{-}X_П) + G_З(L\text{-}X_З) - F_{тр}(L\text{-}X_F) - P_1 h_р - P_2(L\text{-}X_2) - T_B(L+C) - T_T(h_б - h_р)], \quad (3)$$

где L – продольная база скрепера, м;

$G_П$ и $G_З$ – вес грунта в передней и задней частях ковша, Н;

G_C – вес металлоконструкций скрепера, Н;

P_1 и P_2 – составляющие усилия копания, Н;

T_B и T_T – составляющие усилия толкача, Н.

для прицепного скрепера (рис. 4):

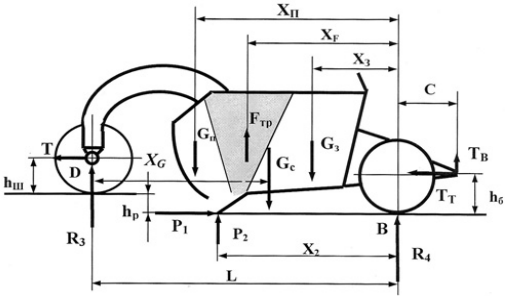

Рис. 4. Схема сил, действующих на прицепной скрепер при копании грунта

$$R_3 = 1/L\ [G_c(L\text{-}X_G) + G_П X_П + G_З X_З - P_2 X_2 - F_{тр} X_F + T_T h_б + T_B C + T(h_ш + h_р)], \quad (4)$$

$$R_4 = 1/L\ [G_C X_G + G_П(L\text{-}X_П) + G_З(L\text{-}X_З) - F_{тр}(L\text{-}X_F) + - P_1(h_ш + h_р) - P_2(L\text{-}X_2) - T_B(L+C) - T_T(h_б - h_ш)], \quad (5)$$

где $h_ш$ – высота шарнира шарового опорного устройства.

Расчеты, выполненные по приведенным зависимостям (2, 3), показывают увеличение нормальных реакций грунта на колеса самоходного скрепера при копании грунта с толкачом на 8…12 % при степени заполнения ковша грунтом соответственно 60 и 100 %, что хорошо согласуется с экспериментальными данными, полученными нами и другими авторами.

Расчеты по зависимостям (4, 5) показывают увеличение нормальных реакций грунта на мосты прицепного скрепера при копании без толкача на 20…30 %. Экспериментальные исследования, проведенные с прицепными скреперами, буксируемыми гусеничным [6] и колесным [8] тягачами дали обратную картину. Инструментальные исследования [8] прицепного скрепера ДЗ-111 с тягачом Т150К показали уменьшение вертикального нагружения переднего моста прицепного скрепера в зависимости от реализуемой им силы тяги на 4,5…10

кН (при вертикальной нагрузке на передний мост 35 кН).

Установленный факт имеет крайне отрицательное влияние как на тягово-сцепные качества самого тягача, так и на технико-экономические показатели скреперного агрегата в целом. Анализ конструкции серийного прицепного устройства скрепера ДЗ-111 (рис. 5) позволил установить причину этого явления.

Из схемы сил, представленной на рис. 5, можно определить вертикальное усилие K на прицепном устройстве скрепера:

$$K = \frac{1}{L_{бр}}\left[T\left(h_1 + h\right) - R_{Ш}\, b - G_{бр}\, a\right]; \qquad (6)$$

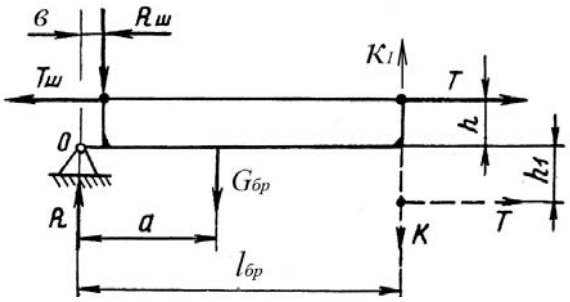

Рис. 5. Схема сил, действующих на прицепное устройство

где T – сила тяги колесного тягача;

$R_ш$ – вертикальная нагрузка на шаровую опору;

$G_{бр}$ – вес прицепного бруса;

$L_{бр}$ – длина прицепного бруса;

K – вертикальная уравновешивающая сила;

$в$, a, h, h_1 – плечи действия соответствующих сил.

Анализ выражения (6) показывает, что на *серийное прицепное устройство* при передаче тягового усилия T (пунктирные линии) с тягача на шаровое устройство арки-хобота скрепера *действует вертикальная сила К*, приложенная к прицепному брусу вниз (рис. 5). На тягач действует соответствующая сила K_1, направленная вверх и, следовательно, снижающая его сцепной вес. Такое силовое взаимодействие серийного прицепного устройства скрепера и тягача является следствием недостатка конструкции, а не результатом процесса копания.

В приведенном выражении (6) для практических расчетов двумя правыми слагаемыми можно пренебречь, т.к. плечо $в \approx 0{,}01L_{бр}$, а $G_{бр} \approx 0{,}15T$. В этом случае для исключения уменьшения сцепного веса тягача за счет силы тяги T при копании грунта необходимо соблюдение условия:

$$h = - h_1. \qquad (7)$$

В этом случае сила тяги, развиваемая колесным тягачом, не будет вызывать уменьшение сцепного веса тягача скреперного агрегата. Недостатком такой модернизации будет нагружение металлоконструкций прицепного бруса изгибающим моментом, что имеет место и в стандартной конструкции прицепного устройства.

На рис. 6 приведены результаты инструментальных исследований изменения грунта вертикальных нагрузок при копании на все мосты прицепного скреперного агрегата: тягач Т-150К, скрепер ДЗ-111 с догрузкой [9]. Догрузка тягача осуществляется за счет вывешивания переднего моста прицепного скрепера.

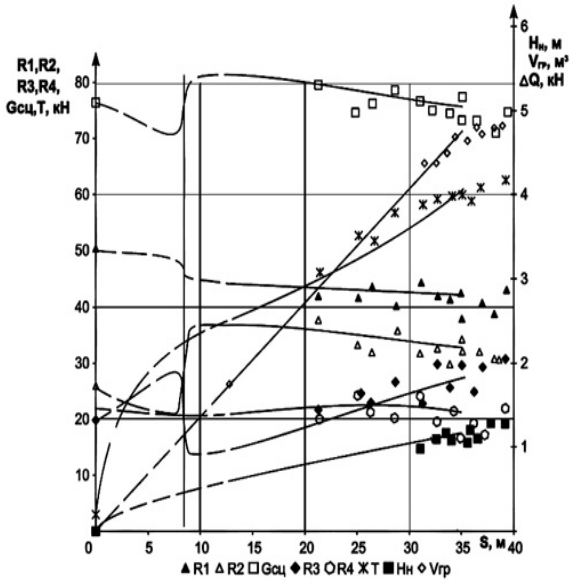

Рис. 6. Изменение вертикальных нагрузок на мосты ковша прицепного скрепера при копании грунта с увеличенным сцепным весом тягача (с догрузкой при постоянной глубине резания 80 мм [7])

На начальном участке копания (путь 6..9 м) хорошо видно (рис. 6), что копание начиналось без увеличения сцепного веса тягача. При этом сцепной вес тягача $G_{сц}$ и составляющие его вертикальные нагрузки на передний R_1 и задний R_2 мосты тягача уменьшаются. При включении гидроцилиндра догрузки (давления догрузки p = 10 МПа) происходит изменение вертикальных нагрузок на мосты скрепера и тягача. Все вертикальные нагрузки в этот момент изменяются ступенчато.

Вертикальная нагрузка R_2 на задний мост трактора резко возрастает на 80 %, а на передний мост R_1 – уменьшается на 7 %. Уменьшение вертикальной нагрузки на передний мост скрепера R_3 составляет 60 %, а на задний мост скрепера R_4 нагрузка возрастает на 35 %. Увеличение сцепного веса трактора $G_{сц}$ в этот переходный момент составляет 20 %. Далее в процессе копания (при постоянной глубине резания)

величина вертикальных нагрузок на мосты тягача *снижается*.

Из данных, приведенных на рис. 6, отчётливо видно, что с увеличением количества грунта в ковше и крюковой нагрузки на тягач происходит почти линейное *снижение сцепного веса тягача*. В конце копания сцепной вес тягача, несмотря на работу догружающего устройства [9], падает практически до его статического значения. Оказывается, что догружающее устройство при копании просто частично компенсирует отрицательное воздействие конструкции серийного прицепного устройства на сцепной вес тягача.

Инструментально зафиксировано увеличение вертикальной нагрузки R_3 на передний мост скрепера в процессе копания без догрузки к концу наполнения до 35 %. При наличии силы тяги на прицепной скобе тягового бруса опрокидывающее усилие K (рис. 5) *разгружает тягач и догружает передний мост скрепера*, то есть оно перераспределяет вертикальную нагрузку с тягача на передний мост скрепера. Именно этим обстоятельством можно объяснить такое высокое процентное увеличение нагрузки на передний мост прицепного скрепера ДЗ-111 (по сравнению с самоходными скреперами).

ВЫВОДЫ

1. Вертикальные нагрузки на мосты самоходного и прицепного скреперов при копании изменяются незначительно относительно их статического значения при порожнем ковше.

2. Для определения вертикальных нагрузок на мосты скрепера при копании необходимо исключать из баланса вертикальных сил вес активно движущегося в ковше столба грунта.

3. Необходимо изменить конструкцию серийного прицепного устройства прицепного скрепера таким образом, чтобы создаваемая тягачом сила тяги не уменьшала его сцепной вес, а, наоборот, увеличивала.

ЛИТЕРАТУРА

[1] Войнич Л.К., Прикащиков Р.Г. Справочник молодого машиниста бульдозера, скрепера, грейдера. 2-е изд. перераб. – М.: Высш. школа, 1979. – 119 с.

[2] Майминд В.Я., Арсентьев А.И. Скреперные комплексы на открытых горных разработках. – М.: Недра, 1976. – 204 с.

[3] Ронинсон Э.Г. Вертикальная реакция на нож самоходного скрепера // Строительные и дорожные машины. – 1969. – № 10.

[4] Ульянов Н.А. Основы теории колесного движителя землеройных машин. М., Машиностроение, 1963.

[5] Нилов В.А. Исследование скреперного поезда.: Дис…. канд. техн. наук. – Воронеж, - 1975.

[6] Зинченко Н.С. Исследование рабочего процесса прицепного скрепера, увеличивающего сцепной вес гусеничного тягача при копании грунта.: Автореф. дисс….канд. техн. наук. – Омск, - 1980.

[7] Нилов В.А., Косенко А.А., Летуновский К.П. Исследование вертикальных нагрузок на оси скрепера при копании // Строительные и дорожные машины. – 2005. – № 5. – С. 26-29.

[8] Никулин П.И., Нилов В.А., Косенко А.А. Испытания скреперного агрегата с изменяемым сцепным весом // Механизация строительства. – 2005. – № 8. – С. 9-12.

[9] Никулин П.И., Нилов В.А., Косенко А.А. Испытания скреперного агрегата с изменяемым сцепным весом // Механизация строительства. – 2005. – № 8. – С. 9-12.

ОСНОВЫ СОЗДАНИЯ КРАНОВ–МАНИПУЛЯТОРОВ ДЛЯ СТРОИТЕЛЬНО-МОНТАЖНЫХ РАБОТ

М. А. Степанов

Аннотация: *Для повышения производительности и качества строительно-монтажных работ необходимо внедрение современных роботизированных технологий. Первым шагом для решения этой проблемы является создания кранов-манипуляторов для строительства. Рассматриваются необходимые требования к кранам-манипуляторам , грузозахватам и системам управления кранами-манипуляторами. Проведены результаты анализа применения различных вариантов кранов для базовой модели крана-манипулятора. Наиболее полно требованиям к манипуляторам отвечают башенные краны. Приведены примеры технологии применения кранов-манипуляторов для строительства и основные конструктивные параметры кранов-манипуляторов и систем управления.*

Ключевые слова: *кран, манипулятор*

В последнее время в экономически развитых странах мира робототизированные технологии все с большей активностью вторгаются во все сферы человеческой деятельностью. Такие отрасли, как автомобиле- и машиностроение, самолетостроение, космическая не обходится без роботов и дистанционно-управляемых манипуляторов. Строительная отрасль в этом смысле отстает. Внедрение робототизированных технологий обеспечивает сокращение использования ручного труда, повышение производительности и качества строительства и перехода к малолюдной (в перспективе и безлюдной) технологиям строительно-монтажных процессов. Достижение высоких технико-экономических показателей в строительстве невозможно без глубоких преобразований, основную роль в которой призвана сыграть техническая реконструкция, комплексная механизация, автоматизация и робототизация. Однако применение механизированных технологических процессов с использованием оборудования серийно выпускаемого промышленностью не позволяет достичь указанной цели.

В настоящее время наиболее распространенные средства у монтажников: монтажный лом, подкос, отвес. Такие средства применяют потому, что современные башенные и стреловые краны технически не приспособлены к возведению зданий с ограниченным участием рабочих. Вручную рабочие осуществляют ориентирование конструкции в пространстве, гашение амплитуды раскачивания, рихтовку и выверку положений, временное крепление подкосами или кондукторами, устройство горизонтальных и вертикальных соединений потому, что краны оснащены неуправляемыми грузозахватами, а не поворотными крюковыми обоймами, закрепленными на стальных тросах. Кроме того, взаимодействие крана со строительным элементом осуществляется посредством промежуточного звена- стропа и траверсы с крюками на тросах, длина которых меняется. В результате чего кран подает строительный элемент на монтажный горизонт не сориентированный трем линейным и трем угловым координатам, как того требует расположение конструкции в здании. Применение же крановых лебедок и механизмов с различными скоростями линейных и вращательных движений, а также удаленность крановщика от места установки конструкции вызывает необходимость повторных включений приводов. Это приводит к раскачиванию монтажных элементов и требует окончательного гашения амплитуды колебаний при установки их в проектное положение вручную. При этом конструкция занимает положение с отклонением, часто превышающим предельное, и может привести к несчастным случаем среди монтажников.

Отмеченные выше факторы оказывают значительное влияние на процесс формирования ручных трудозатрат на монтажные процессы, в результате чего ручные затраты превышают механизированные в 4-5 раз. Эти факторы характеризуются как как факторы технологичности и обусловлены несовершенством объемно-планирочных и конструктивных решений зданий, недостаточным уровнем взаимной приспособленности монтажных машин и конструктивных элементов к процессам возведения зданий.

Одним из основных направлений, определяющим повышение производительности и качества монтажа конструкций является снижение соотношения ручной и машинной доли времени цикла работы крана. Факторами, формирующие продолжительность машинной доли времени цикла можно условно разделить на две основные группы.

Михаил Алексеевич Степанов, канд. техн. наук. проф., Московский государственный строительный университет, Россия

К первой группе относятся факторы, характеризующие технические возможности краны : скорости рабочих движений Ко второй – факторы, определяющие затраты машинного времени на дополнительные операции, обусловленные конструктивным решением строительного элемента и условием его установки в проектное положение. Учет факторов первой группы направлен на решение вопросов автоматизации и робототизации процессов монтажа. Для обеспечения требуемой точности позиционирования и обслуживания большой подстреловой зоны может двумя вариантами. Первый вариант- двухстадийное позиционирование элементов. На первой стадии строительный элемент перемещают из зоны захвата на монтажный горизонт крановыми механизмами с достаточной точностью ориентирования. На второй стадии при помощи нового механизма ориентирования конструкцию устанавливают в проектное положение с точностью, регламентируемой СНиПом. Второй вариант – установка монтируемой строительной конструкции непосредственно с крана – манипулятора. Функциональное назначение таких кранов состоит в исполнении собственными механизмами (без использования ручного труда) с дистанционным управлением следующих операций монтажного цикла: жесткий монтаж монтируемого элемента, транспортировка к месту монтажа, принудительное ориентирование элемента в пространстве, посадка закоординированного элемента с требуемой точностью, отцеп установленного элемента и обратный ход крана-манипулятора за очередным элементом. Сравнение двух вариантов, на наш взгляд, дает преимущество второму варианту, так как требуется дополнительного устройства ориентирования, если доставка на монтажный горизонт осуществляется обычным краном, то требуется время для установки конструкции в это устройство, а если доставляется элемент с достаточной точностью, тогда эта конструкция ориентирования представляется излишней.

Учет факторов второй группы обеспечивает существенное снижение непроизводительных затрат времени, связанных с временным удержанием неустойчивых конструкций в процессе монтажа. Одним из решений может быть использования метода пространственной самофиксации элементов на ранее установленные элементы. Оно кажется перспективным, но требует существенной доработки метода самофиксации с целью обеспечения надежности монтажа крупнопанельных зданий. Более простым решением является разработка закладных устройств, выполняющих функции не только самофиксирования, но и их самоустановки при посадки на место. Это позволит снизить требование к точности позиционирования и может быть осуществлено при расширении входных размеров самофиксирующих устройств.

Создание строительных кранов-манипуляторов должно учитывать разнообразные факторы: технологию производства работ, конструктивные особенности строительного объекта и его габариты, номенклатуру строительных конструкций (массу, габариты и форму), квалификацию обслуживающего персонала, обеспечение выполнения полного цикла работ (от нулевого цикла до возведения крыши).

Наиболее полно этим требованием удовлетворяют краны-манипуляторы, выполненные на база башенных кранов с существенными изменениями конструкции. Вместо стрелы подъемной или балочной на башни устанавливается крановo-манипулирующая установка, представляющая подвижную обойму с шарнирно-сочлененной стрелой. Для более точного позиционирования обойма перемещается по зубчатой рейки, укрепленной вдоль башни. Геометрические параметры башни, колен шарнирно-сочлененной стрелы подбирают в соответствии с технологией и габаритами возводимого строительного объекта.

Для широкого использования кранов-манипуляторов в строительстве можно создать базовую модель и модифицировать ее для работы на типовых строительных объектах. Например, для объектов до 20 метров можно определить такие размеры колен, которыен позволят выполнить полный комплекс работ без перемещения обоймы по башне. При возведении более высоких зданий кран-манипулятор должен быть оборудован системой видеонаблюдением.

Основным элементом, который обеспечивает преимущество кранов-манипуляторов, является грузозахватный орган. Он должен отвечать следующим требованием:

- иметь грузоподъемность соответствующая максимальной массе строительной конструкции;
- иметь 4-6 степеней свободы для удобства монтажа;
- иметь возможность подъема различных по форме конструкций одним грузозахватом или быстрого переоборудования для грузозахватов для типовых элементов;
- быть удобным в управлении;
- обеспечивать безопасность при перемещении груза.

Анализ грузозахватных приспособлений и устройств, применяемых в строительстве и других областях (например, в машиностроении), показал, что этим требованиям в большей степени отвечают гидравлические захваты.

Уравнение движения груза можно представить в виде:

$$m\ddot{g} = F_{ic} + F_{iy}$$
$$I_i\ddot{\varphi} = M_{ic} + M_{iy} \qquad (1),$$

где, m- масса груза, g_l-обобщенная линейная координата, F_{ic} – естественная сила, F_{iy} – сила управления, I_i- момент инерции, φ - угловая координата, M_{ic} –естественный момент, M_{iy} – момент управления.

Под естественными силами (моментами) мы будем понимать силы (моменты), определяющие

естественное движение груза. Под силами (моментами) мы будем понимать силы (моменты), обусловленные управлением груза.

Уравнение (1) представляет собой динамическую модель рабочей операции.
Оно определяет взаимосвязь между управляющими усилиями и усилиями, определяющими движение груза.

Из уравнения (1) видно, важную роль в точности позиционирования играет система управления грузозахвата. Применение гидравлического объемного гидрооборудования в строительных кранах-манипуляторов не отвечает сформированным требованиям. Для привода шарнирно-сочлененной стрелы и грузозахвата необходимо применить гидропривод с пропорциональным управлением, которое представляет собой следящую систему, оснащенную бортовым компьютером, куда необходимо задать все параметры работы крана при перемещении груза (допустимые геометрические перемещения, масса, скорости и ускорения). Датчики контролируют работу гидропривода и вносят коррективы в работу его элементов. Обеспечение точности позицио-нирования и уменьшения динамических нагрузок при перемещении груза динамической системой управления. При динамическом управлении контролируется ускорения движения грузозахвата и его геометрическое положение. Эти сигналы поступают на блок сравнения, после чего вносятся коррективы в силы (моменты) управления. Техническое приемущество пропорциональной системы заключается в плавном управлении заданными параметрами и в сокращении гидравлических элементов для обеспечения требуемой точностью позиционирования. Посредством пропорционального управления можно точно и быстро выполнить технологические процессы перемещения и монтажа строительных конструкций, снизить динамические нагрузки и, как следствие повысить производительность, качество и возможность автоматизации производства.

На рис.1 приведена блок-схема пропорционального гидроуправления предлагаемого крана-манипулятора. Рабочие процессы нового технологического решения робототизированного средства монтажа конструкций и кран-манипулятор, разработанный в МГСУ, представлен на рис. 2. Кран работает следующим образом: захватив на приобъектном складе конструкцию, он производит поворот башни в сторону возводимого здания. Монтаж конструкций ведется методом наращивания, поэтажно, для чего рабочие оборудование перемещается вдоль башни на необходимый горизонт.

Кран-ианипулятор представляет собой подъемно-транспортное средство с дистанционным управлением. Устройство передвижения крана состоит из ходовой платформы 2 кранового типа, установленного на ходовых тележках 1, которые перемещаются по подкрановому рельсовому пути. На ходовой платформе установлен опорно-поворотный круг с поворотной платформой 3. На платформе расположен противовес 4, обеспечивающий устойчивость крана, и жестко закреплена вертикальная башня 5. Она играет роль несущей и направляющей конструкции для для обеспечения вертикального хода обоймы 7 с опорами качения. Передвижение обоймы осуществляется реечным механизмом. На обойме установлена шарнирно-сочлененная стрела с гидроцилиндрами, которая состоит из корневой секции 8 и шарнирно соединенную с ней рукоять 12, движения стрелы задается гидроцилиндрами 10 и 11. Гидроцилиндр 13 отслеживает горизонтальность положения рабочего органа 14 и захваченного им элемента при угловых перемещениях стрелы. Гидропривод стрелы и грузозахвата установлен на обойме.

В состав звена монтажников входят три человека: оператор-монтажник, имеющий джойстик, контролирует надежность захвата конструкции, отправляет ее на необходимый монтажный горизонт. Второй оператор-монтажник продолжает монтаж конструкции на горизонте. После достижения конструкции заданного положения третий оператор-электросварщик надежно закрепляет ее электросваркой и затем отправляет кран за очередной конструкцией. Пока кран в пути, второй оператор монтажник заполняет стык раствором. Эффект очевиден: вместо 5 монтажников и одного сварщика занято всего три человека. Отпадает необходимость в кабине крана, ускоряется процесс и повышается качество монтажа.

Рис. 1 Блок-схема пропорционального гидроуправления

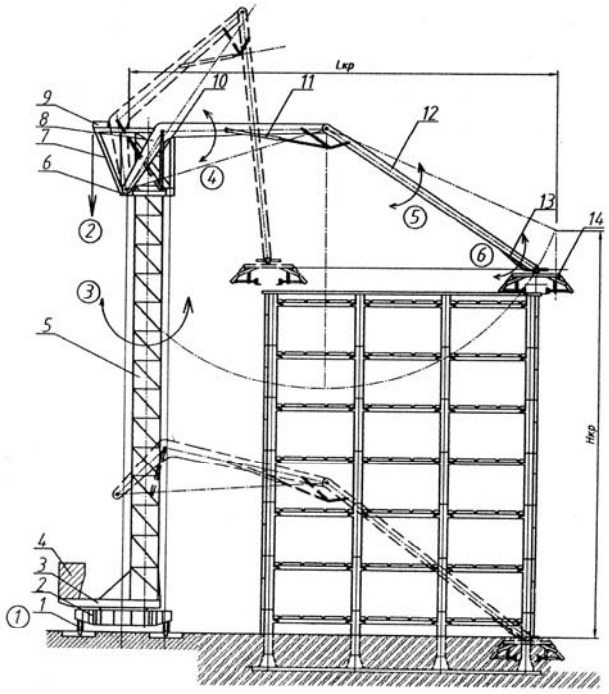

Рис. 2 Строительный кран-манипулятор

ЛИТЕРАТУРА

[1] **Дистанционно управляемые роботы и манипуляторы.** Кулешов В.С., Лакота Н.А., Андронин В.В. и др.; Под. общ. ред. Е.П.Попова, - М.:Машиностроение, 1986, - 328 с.

[2] **Вильман Ю.А., Степанов М.А.** Дистанционно-управляемые манипуляторы.. Механизация строительства- 2006-№1 – с 3-8.

МЕТАСИСТЕМНЫЙ ПОДХОД К ПРОЕКТИРОВАНИЮ СРЕДСТВ МЕХАНИЗАЦИИ СТРОИТЕЛЬСТВА

Ф.К. Клашанов

Аннотация: *В статье рассматривается системный метод проектирования средств механизации, применяемых в строительстве. Комплексное применение функционально-физического и функционально-стоимостного анализов на базе морфологических карт образуют метасистемный метод, который позволяет проектировать средства механизации с учетом современных научно-технических достижений. Метасистемный метод опирается на использование компьютерных технологий и позволяет разработать оптимальную конструкцию строительной техники.*

Ключевые слова: *метасистем, проектирование*

Накопленные результаты научно-исследовательских разработок, как отечественных исследователей, так и зарубежных в области создания новых средств механизации строительства, а также достигнутый уровень компьютеризации исследовательских процессов позволяет применить системный подход в проектировании. Создание нового (либо технологического процесса, либо средств труда и т.п.) всегда базируются на парадигме оптимального соответствия проектируемого объекта функциональному назначению, т. е привести в соответствие потребительскую стоимость с издержками на данный момент времени с учетом достижений научно-технического прогресса. Новый виток развития информационно-компьютерных техно-логий позволяет по-новому подойти и в части строительства, объекты которого отвечали бы всем требованиям потребителя. Разработка алгоритма поиска оптимального варианта конструкторского решения с применения ЭВМ наиболее полна на основе сочетания этих двух анализов и базируется на научно-технических достижениях на данный момент времени. Суть метасистемного анализа можно выразить в виде следующих процедур.

1. Формулируется цель (назначение) проектируемого объекта.
2. На базе функционально-физического анализа (ФФА) формулируются ранжированные функции проектируемого объекта. На этом этапе выделяются главные физические функции и сопровождающие их – вспомогательные, нейтральные и вредные. Выявляется физическая природа их реализации.
3. Каждая физическая функция проектируемого объекта экономически оценивается функционально-стоимостным методом с учетом всех экономических составляющих для ее реализации.
4. По результатам функционально-стоимостного анализа (ФСА) строится оптимизирующий алгоритм, позволяющий определить оптимальную конструкцию на данный момент исследований.

Метасистемный метод является открытым и позволяет на базе данных полученных функционально-стоимостным методом определяется оптимальное значение, предварительно построив функцию цели и критерии оптимальности.

При проектировании прежде всего необходимо учитывать, что согласно техническим регламентам, все вновь создаваемое должно быть безопасным для окружающей среды и персонала – это необходимое условие проектирования (создания) нового, т.е. при проектировании должна быть учтена система безопасности с введенным для этой цели соответствующих параметров $S= \{s_1, s_2, \ldots s_n\}$, т.е. множество S, обеспечивающее безопасность. Так, например, только при условии, что средства механизации строительства удовлетворяют этим параметрам, то средства механизации имеют право на жизнь. Это же относится и к любым технологическим процессам. Следующее условие - это надежное выполнение требуемых потребительских функций U, множество параметров которых $U = \{u_1, u_2, \ldots u_k\}$ и идентифицируют данный вид (класс) объекта проектирования.

Множество потреби-тельских функций следует из цели производства средства механизации и формулируется, как правило, в техническом задании. Каждая строительная машина может быть представлена описаниями, имеющими иерархическую соподчиненность. Описания характеризуются двумя свойствами: каждое последующее описание является более детальным и более полно характеризует машину по сравнению с предыдущим и каждое последующее описание включает в себя предыдущее. Ниже приведена блок-схема метасистемного метода.

Ф.К. Клашанов, канд. техн. наук. проф., Московский Государственный Строительный Университет, Россия

В.18

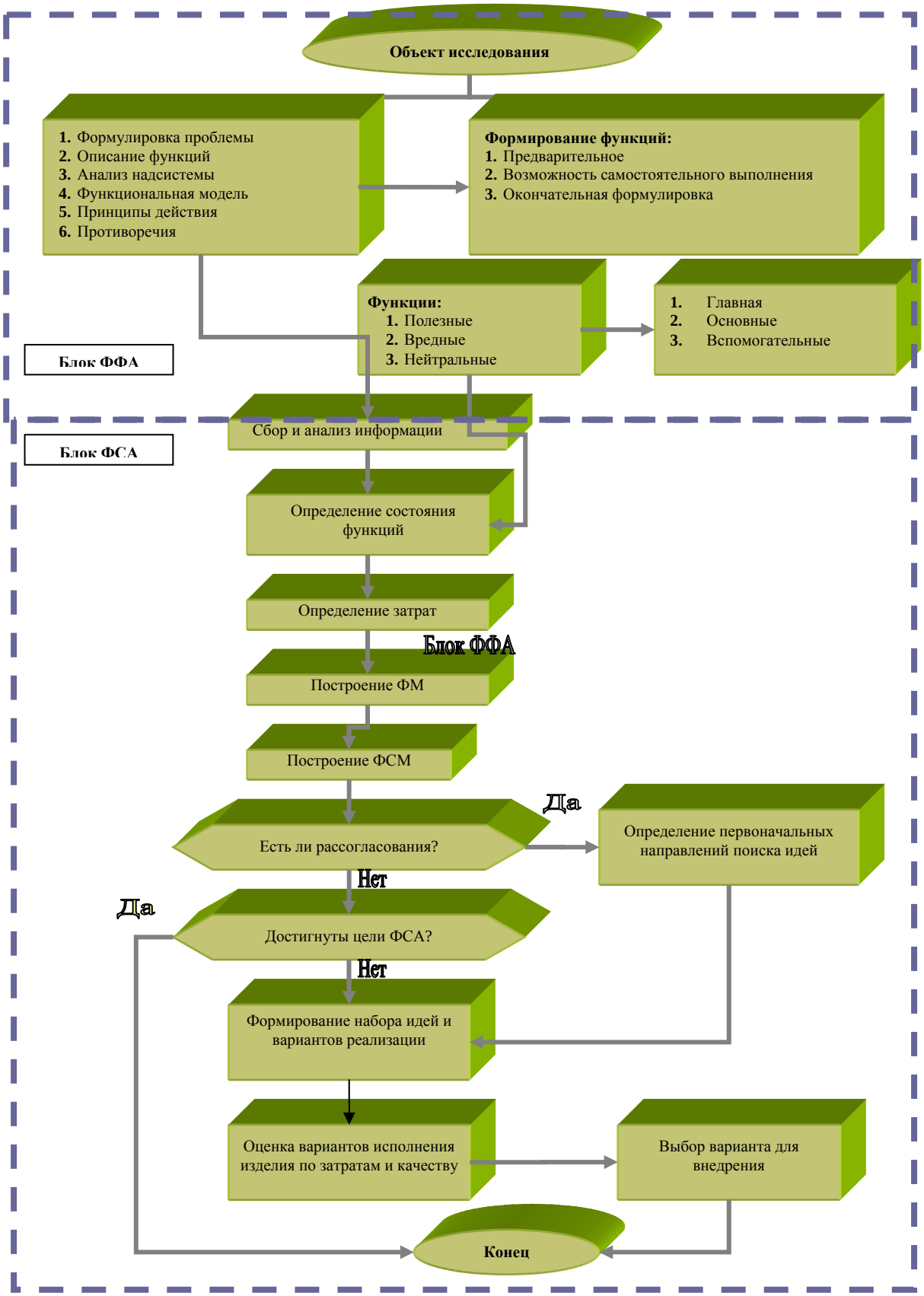
Объект исследования
1. Формулировка проблемы
2. Описание функций
3. Анализ надсистемы
4. Функциональная модель
5. Принципы действия
6. Противоречия
Формирование функций:
1. Предварительное
2. Возможность самостоятельного выполнения
3. Окончательная формулировка
Функции:
1. Полезные
2. Вредные
3. Нейтральные
1. Главная
2. Основные
3. Вспомогательные
Блок ФФА
Блок ФСА
Сбор и анализ информации
Определение состояния функций
Определение затрат
Блок ФФА
Построение ФМ
Построение ФСМ
Есть ли рассогласования?
Да
Определение первоначальных направлений поиска идей
Нет
Да
Достигнуты цели ФСА?
Нет
Формирование набора идей и вариантов реализации
Оценка вариантов исполнения изделия по затратам и качеству
Выбор варианта для внедрения
Конец

За основу структурно-логической схемы принята разработанная советскими исследователями /1, 2/ методология иерархического выбора проектных решений, которая представляется наиболее простой, достаточно строгой и последовательной. В этой методологии выделяются 5 уровней. На первом уровне выбирается удовлетворяемая потребность - функция машины, на втором - потребительские качества, на третьем - функциональная структура, на четвертом - принцип действия, на пятом - техническое решение.

Таким образом, 1-й и 2-й уровни (являющиеся, по сути, техническим заданием (ТЗ)), а также 3-й, 4-й, 5-й уровни составляют концептуальное проектирование, при котором формируются качественные параметры (свойства) техники, ее потребительские функции $\boldsymbol{U}$ с учетом требований безопасности $\boldsymbol{S}$.

Известным методом систематизированного поиска новых идей является морфологический анализ, предложенный швейцарским астрофизиком Цвикки. Морфологический анализ основан на построении таблицы, в которой перечисляются все основные элементы, составляющие объект и указывается, возможно, большее число известных вариантов реализации этих элементов. Комбинируя варианты реализации элементов объекта, можно получить самые неожиданные новые решения. Последовательность действий при этом следующая:

1) Точно сформулировать проблему, 2) Определить важнейшие элементы объекта, 3) Определить варианты исполнения эле-ментов, 4) Занести их в таблицу, 5) Оценить все имеющиеся в таблице варианты, 6) Выбрать оптимальный вариант.

Основной идеей морфологического анализа /3/ является упорядочение процесса выдвижения и рассмотрения различных вариантов решения задачи. Расчет строится на том, что в поле зрения могут попасть варианты, которые ранее не рассматривались. Принцип морфологического анализа легко реализуется с помощью компьютерных средств.

Однако для сложных объектов, имеющих большое число элементов, таблица становится слишком громоздкой. Появляется необходимость рассмотрения огромного числа вариантов, большая часть которых оказывается лишенной практического смысла, что делает использование метода слишком трудоемким. Таким образом, главными недостатками метода является упрощенность подхода к анализу объекта и возможность получения слишком большого для рассмотрения числа вариантов. Морфологический анализ имеет много как простейших, так и усложненных модификаций. Однако его применение рационально для простых объектов и там, где возможно найти новую идею за счет комбинации известных решений (реклама, дизайн и т. п.).

Сущность морфологического анализа состоит в выделении всех независимых переменных проектируемой системы, перечислении возможных значений (способов реализации) этих переменных и генерировании альтернатив перебором всех возможных сочетаний этих значений.

Целью морфологического поиска является составление морфологических карт, которые позволят расширить область поиска решений проектной проблемы. Морфологическая карта – это объектно-ориентированный элемент, являющийся банком данных для каждого проектируемого узла, для которого относительно не сложно составляется СУБД с целью автоматизированного поиска с помощью ЭВМ оптимального элемента строительной техники.

Преимущество морфологических карт состоит в том, что для заполнения матрицы требуется очень мало времени. Основная трудность заключается в определении набора функций, которые были бы: существенными для любого решения; независимыми друг от друга; охватывающими все аспекты проблемы; достаточно немногочи-сленными, чтобы можно было составить матрицу, допускающую быстрое изучение.

Формировать технические решения следует, используя по одному способу реализации из каждой независимой переменной. То или иное сочетание способов реализации всех независимых переменных и составляет вариант технического решения. Форма, удобная для разработки вариантов проектируемого объекта, представляется в виде таблицы. В ней указываются код технического решения, независимые переменные - $\boldsymbol{Y_i}$, а также способы реализации каждой независимой переменной - $\boldsymbol{X_{ij}}$.

Единицы в ячейках на пересечении строк и столбцов таблицы означают использование того или иного способа реализации каждой независимой переменной в данном варианте технического решения. Полученному техническому решению присваивается код в соответствии с обозначениями способов реализации, принятых в данном варианте для выполнения каждой независимой переменной.

Всего число технических решений будет равно произведению сумм числа способов реализации каждой независимой переменной. В условиях таблицы можно получить требуемое количество вариантов технических решений. Функциональные структуры технологических объектов практически решают выделение указанных независимых переменных. Таким образом, первая задача морфологического анализа может решаться с использованием функциональных структур

Для решения второй задачи, т.е. выявления возможных способов реализации этих переменных

можно использовать существующие классификации выделенных элементов объектов проектирования, а также патентные источники. Описания независимых переменных и способов их реализации оформляются в виде таблицы. Полученная морфологическая таблица является основой для синтеза технических решений.

После разработки морфологических карт проводится функционально-физический анализ. Главной целью ФФА является выявление по определенным правилам различных видов продуктивных знаний, позволяющих определять требования к объекту проектирования и давать соответствующие конструктивно-технологические решения. Овладение методикой проведения ФФА, как инструментария оперирования продуктивными знаниями, специалистами позволяет значительно повысить эффективность проектирования. Наиболее эффективной методикой является методология, разработанная В.В. Поповым. Принципиальным отличием его подхода является изначальная ориентация на компьютерную реализацию. Информационный и методический инструментарий инновационной деятельности представляется в виде так называемых продуктивных знаний (знаний, способствующих порождению новых знаний). Применяемая при этом формализация позволяет использовать базы продуктивных знаний в компьютерных средствах поддержки инновационной деятельности.

Формирование информационного обеспечения процесса проектирования, построенного в соответствии с системной методологией проектной деятельности, происходит при проведении функционально-физического анализа технического средства (ТС), методика которого предполагает следующую последовательность действий.

1. Дать алгоритм описания ТС (с указанием источников информации), схему ТС.
2. Выявить главную, основные, вспомогательные, вредные и нейтральные функции.
3. Сформировать функционально-логическую структуру ТС.
4. Выявить и описать реализуемые критерии эффективности (потребительские свойства) ТС, характеризующие меру ее полезности.

Применение ФФА позволяет повысить качество проектных решений, создавать в короткие сроки высокоэффективные образцы техники и технологий и таким образом обеспечивать конкурентное преимущество предприятия.

Практическое применение научных теоретических и экспериментальных исследований к строительной технике сводится к созданию новых поколений строительной техники или совершенствованию существующей применительно как к новым, так и функционирующим строительным технологическим процессам.

Разработанная системная методология проектной деятельности, базируется на законах развития строительной техники, соответствия между функциями и структурой строительных машин и законе прогрессивной эволюции технической системы**.**

Все функции проектируемого объекта делятся на следующие группы: основные, для осуществления которых предназначен данный объект; вспомогательные, способствующие осуществлению основных функций, и нейтральные, которые, как правило, сопровождают основные функции, но не несут полной нагрузки, и могут быть без ущерба ликвидированы вместе с их материальными носителями (узлами, деталями, видами работ, формами документации и т.п.).

Алгоритмические основы проектной деятельности являются базой для их практического использования при синтезе новых проектных решений с новыми конкурентоспособными качественными параметрами. Результативность ФФА заключается в сравнении последней (лучшей) реализации строительной техники с ее аналогом (прототипом).

Порядок проведения ФФА строительной техники включает в себя следующие этапы:

1. *Формулируется проблема.* Описание проблемы должно включать назначение проектируемого объекта, учитывать условия функционирования и предъявляемые технические требования. Формулировка проблемы должна способствовать раскрытию творческих возможностей и развитию фантазии для поиска возможных решений в широкой области.

2. *Составляется описание функций* назначения объекта. Описание базируется на анализе запросов потребителя и должно содержать четкую и краткую характеристику, с помощью которой можно удовлетворить возникшую потребность. Для понимания функций назначения проектируемого объекта необходимо дать краткое описание надсистемы, т.е. системы, в которую входит проектируемый объект. Описание функций включает: действия, выполняемые проектируемым объектом, объект, на который направлено действие, и условия работы для всех стадий жизненного цикла машины.

3. *Производится анализ надсистемы*. Анализ надсистемы производится с помощью структурной и потоковой модели объекта. При этом целесообразно воспользоваться эвристическими приемами, например, рассмотреть: можно ли выполнить функцию рассматриваемого объекта путем внесения изменений в смежные объекты надсистемы, нельзя

ли какому-либо смежному объекту надсистемы частично или полностью передать выполнение некоторых функций рассматриваемой системы, что мешает внесению необходимых изменений и нельзя ли устранить мешающие факторы.

4. *Строится функциональная модель* проектируемого объекта обычно в виде функционально-логической схемы.

5. *Анализируются физические принципы действия* для функций проектируемого объекта.

6. *Определяются технические и физические противоречия* для функций проектируемого объекта. Такие противоречия возникают между техническими параметрами при попытке одновременно удовлетворить нескольким требованиям потребителя.

Определяются приемы разрешения противоречий и направления совершенствования машины. Для того чтобы реализовать совокупность потребительских свойств объекта, отраженных в его функциональной модели, с помощью минимального числа элементов, модель преобразуется в функционально-идеальную. Поиск вариантов технических решений часто производят с помощью морфологических таблиц, которые отражают строение анализируемого объекта.

Рассмотрим более подробно каждый уровень структурно-логической схемы.

Потребность (функция). Реализация возникшей потребности является целью создания объекта. Описание потребности должно содержать следующую информацию: необходимое действие; объект (предмет обработки), на который направлено это действие; особые условия и ограничения.

Описание потребности формализовано можно представить в виде трех компонент:

$$P=(D,G,H),\ldots$$

где D – указание действия, производимого рассматриваемой техникой и приводящего к удовлетворению интересующей потребности;

G – указание объекта, на который направленно действие;

H – указание особых условий и ограничений, при которых выполняется действие.

Техническая функция (ТФ). Описание ТФ содержит следующую информацию:

– потребность, которую может удовлетворить проектируемый объект;

– физическая операция, с помощью которой реализуются потребности.

Таким образом, описание ТФ состоит из двух частей: $F=(P,Q), \ldots$

где P – удовлетворяемая потребность;

Q – физическая операция.

Описание физической операции (ФО) формализовано можно представить состоящим из трех компонент: $Q=(A_T,E,C_T)$,

где A_T , C_T – соответственно входной и выходной поток вещества, энергии или сигналов;

E – наименование операции Коллера по превращению A_T в C_T.

Функциональная структура (ФС). Подавляющее большинство строительных машин состоит из нескольких элементов (агрегатов, блоков, узлов) и могут быть естественным образом разделены на части. Каждый элемент как самостоятельный механизм выполняет определенную функцию и реализует определенную ФО, т.е. между элементами имеют место два вида связей и соответственно два вида их структурной организации.

Во-первых, элементы имеют определенные функциональные связи друг с другом, которые образуют конструктивную функциональную структуру.

Кроме функциональных связей, между элементами имеются еще потоковые связи, т.е. элементы, реализуя определенные физические операции, образуют поток преобразуемых или превращаемых веществ, энергии, сигналов или других факторов.

Физический принцип действия (ФДП). Описание ФДП, как правило, содержит изображение принципиальной схемы машины, в которой в упрощенно-идеализированной форме показаны основные конструктивные элементы, обеспечивающие реализацию ФДП, и указанны направления потоков и основные физические величины, характеризующие используемые физико-технические эффекты.

Техническое решение (ТР). Представляет собой конструктивное оформление ФДП и ФС. ТР конкретной машины, как правило, описывается в виде двухуровневой структуры через характерные признаки машины в целом и ее элементов. При этом используют следующие группы признаков: перечень основных элементов; взаимное расположение элементов в пространстве; способы и средства соединения и связи элементов между собой; последовательность взаимодействия элементов во времени; особенности конструктивного исполнения элементов; принципиально важные соотношения параметров для машины в целом или отдельных элементов.

ВЫВОД

Метасистемный метод дает возможность благодаря применению компьютерных технологий и современного программного обеспечения с учетом научно-технических достижений на данный момент разрабатывать системы автоматизированного проектирования оптимальных средств механизации строительства.

ЛИТЕРАТУРА

[1] Половинкин А.И. Основы инженерного творчества. М.: Машиностроение, 1988-360с.
[2] Дабагян А.В. Проектирование технических систем .- М.: Машиностроение, 1986. – 256 с.
[3] Джонс Дж. К. Методы проектирования. - М.: Мир. 1986. – 326 с.
[4] Справочник по функционально-стоимостному анализу. / Под ред. М.Г. Карпунина, Б.И. Майданчика. – М.: Финансы и статистика, 1988. – 431 с.

ИСПОЛЬЗОВАНИЕ ТРЕХВАЛЬНОГО БЕТОНОСМЕСИТЕЛЯ ДЛЯ ПРИГОТОВЛЕНИЯ МАЛОПОДВИЖНЫХ БЕТОННЫХ СМЕСЕЙ

И. А. Емельянова, В. В. Блажко, О. В. Доброходова

Аннотация: *Для приготовления малоподвижных и жестких бетонных смесей используют бетоносмесители принудительного действия, в частности, с горизонтальными лопастными валами. Существенным недостатком этих машин является низкая усреднительная способность исходных компонентов бетонной смеси и сравнительно низкий коэффициент заполнения рабочего пространства смесью.*
К числу новых эффективных машин, которые позволяют избавиться от вышеуказанных недостатков, следует отнести трехвальный смеситель, в котором каждый из валов участвует в трехконтурном движении материала с разрушением мелких агломератов из частиц растворной составляющей.
Трехконтурное движение частиц смеси в машине существенно увеличивает её рабочее пространство и способствует получению однородной смеси как по высоте этого пространства, так и по длине.
Кроме того, для использования сил гравитации и интенсификации движения частиц бетонной смеси в каскадном режиме валы установлены под углом β в горизонтальной плоскости и относительно друг друга в вертикальной плоскости располагаются на различных уровнях.
Процесс перемешивания компонентов смеси в новой машине рассматривается с позиций законов гидродинамики: определена минимальная длина лопатки, согласно закону Стокса получена зависимость для нахождения коэффициента сопротивления бетонной смеси движению лопаток с учетом конкретных условий процесса перемешивания.
Получена зависимость для определения угла установки валов в корпусе смесителя.
Найдена зависимость для определения технической производительности машины с учетом коэффициента возврата смеси.
Экспериментальным путем установлены диапазоны рационального использования трехвального бетоносмесителя для получения бетонных смесей высокой однородности.
Доказана эффективность использования нового трехвального бетоносмесителя.

Ключевые слова: *трехвальный бетоносмеситель, каскадный режим, трехконтурное движение частиц смеси, производительность.*

В настоящее время в Украине наблюдается резкий подъем строительства, который требует использования современных машин для приготовления строительных смесей.

Для приготовления малоподвижных и жестких бетонных смесей используются бетоносмесители принудительного действия, в частности, с горизонтальными лопастными валами как цикличного, так и непрерывного действия.

При этом, процесс смешивания компонентов смеси должен обеспечивать:

- равномерное распределение по всему объему исходных компонентов;

пространства, т. е. интенсивному перемешиванию подвергается незначительная часть рабочего объема смеси. Кроме того, не обеспечивается равномерность перемешивания по всей длине машины.

Кроме того, к минусам таких машин следует отнести:

- недопустимость образования в смеси комков и пустот;
- стабильное состояние зёрен крупного заполнителя;
- возможность сочетания процесса перемешивания с процессом активации, заключающегося в сдирании с зерен вяжущего и заполнителя неактивных поверхностных пленок.

Существенным недостатком бетоносмесителей с двумя горизонтальными валами является их низкая усреднительная способность исходных компонентов как на макро, так и на микроуровне.

У таких машин перемешивание происходит, в основном, в поперечном сечении рабочего

- невысокий коэффициент заполнения бетонной смесью рабочего пространства смесителя;
- повышенный расход мощности;
- трудности в равномерном распределении по объему добавок.

К числу новых эффективны машин, которые позволяют избавиться от вышеуказанных недостатков, следует отнести трёхвальный

Инга Анатольевна Емельянова, профессор, доктор технических наук, действительный член Академии строительства Украины, Харьковский государственный технический университет строительства и архитектуры, Украине, office@kstuca.kharkov.ua, helga_dov@rambler.ru
Владимир Владимирович Блажко, ассистент, кандидат технических наук, Харьковский государственный технический университет строительства и архитектуры, Украине
Ольга Валериевна Доброходова, аспирант, Харьковский государственный технический университет строительства и архитектуры, Украине

бетоносмеситель, который разработан в Харьковском государственном техническом университете строительства и архитектуры и испытан в производственных условиях. На бетоносмеситель получен патент Украины [1].

Машина содержит три вала (Рис. 1):

- два вала, верхний и нижний, служат для перемешивания загруженных компонентов смеси и участвуют в трехконтурном движении материала в смесителе с разрушением мелких агломератов из частиц растворной составляющей;
- средний вал имеет комбинированное конструктивное решение, левая часть которого выполнена в виде шнека, а правая часть оснащена лопатками, что позволяет ему, с одной стороны, участвовать в транспортировании смеси к разгрузочной части смесителя, а с другой стороны, участвовать в организации трехконтурного движения частиц смеси.

Трехконтурное движение частиц смеси в машине существенно увеличивает рабочее пространство, где осуществляется процесс перемешивания и способствует получению однородной смеси как по высоте этого пространства, так и по длине.

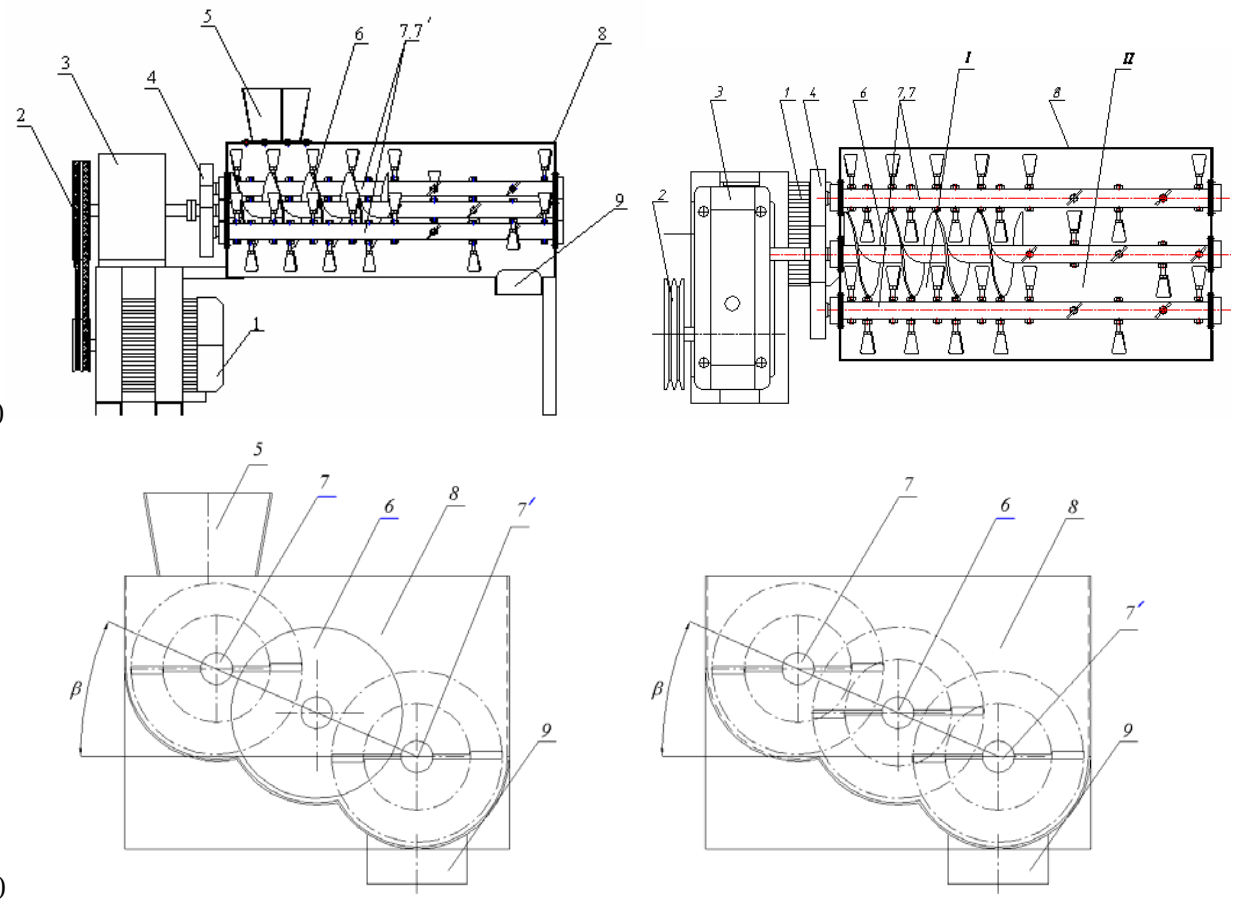

Рис. 1 Конструктивная схема трехвального бетоносмесителя
а) трехвальный бетоносмеситель; б) размещение валов в корпусе смесителя

1. двигатель; 2. клиноременная передача; 3. редуктор; 4. открытая зубчатая передача; 5. загрузочный бункер; 6. шнековый вал; 7,7′. верхний и нижний лопастные валы; 8. корпус бетоносмесителя; 9. разгрузочный патрубок;
I – зона перемешивания сухих компонентов бетонной смеси;
II – зона приготовления бетонной смеси с заданным водоцементным отношением.

Кроме того, для использования сил гравитации и интенсификации движения частиц бетонной смеси в каскадном режиме валы установлены под углом β в горизонтальной плоскости и относительно друг друга в вертикальной плоскости располагаются на различных уровнях [2].

Машина конструктивно решена таким образом, что справа, в I-ой зоне, происходит перемешивание сухих компонентов и наблюдается их активация. Во II-ой зоне, сухие компоненты смешиваются с водой, после чего завершается процесс приготовления бетонной смеси. Разгрузка готовой смеси осуществляется лопатками среднего вала.

Такой смеситель может работать самостоятельно, а также использоваться в технологическом комплекте оборудования для выполнения торкрет-работ мокрым способом.

Техническая характеристика бетоносмесителя

Производительность, м³/ ч…….....4,0….4,5
Максимальный размер заполнителя, мм……8 – 10
Частота вращения валов, $с^{-1}$……...1,03
Мощность двигателя, кВт…….5,5
Габаритные размеры, мм:
длина…….……..1000
ширина……...…576
высота……..……...…565
Масса смесителя, кг…….....…….250

При необходимости машина может быть спроектирована под большую производительность и работать на крупнозернистых бетонных смесях.

В сравнении с действующими смесителями новая машина позволяет:

- готовить однородные строительные смеси разной подвижности, включая малоподвижные, жесткие и особожесткие;
- совмещать процесс приготовления смеси с активацией ее составляющих;
- уменьшить габаритные размеры;
- на малоподвижных смесях на 7…10% повысить производительность машины.

Построение математических моделей для описания процесса смешения и показателей работы трехвального бетоносмесителя является новой ступенью в создании высокоэффективного оборудования, способного готовить качественные бетонные смеси малой подвижности [3].

Процесс перемешивания компонентов бетонной смеси в новой машине рассматривается с позиций законов гидродинамики.

Так рассматриваются условия обтекания лопатки смесителя потоком бетонной смеси при использовании уравнений Навье-Стокса, что позволяет определить толщину пограничного слоя, обеспечивающую процесс разрушения агломератов растворной составляющей при известной длине лопатки и наоборот, зная размеры мелких агломератов, можно определить минимальную длину лопатки

$$\frac{\delta}{l} \approx \sqrt{\frac{\mu}{\rho_0 v_0 l}} \qquad \text{или} \qquad \frac{\delta}{l} \approx \sqrt{\frac{l}{Re}} \qquad (1)$$

где δ - толщина пограничного слоя;

l - длина лопатки;

v_0 - скорость потока смеси вне пограничного слоя;

μ - динамическая вязкость смеси;

Re - критерии Рейнольдса

Для рабочей среды трехвального бетоносмесителя коэффициент сопротивления бетонной смеси движению лопаток может быть определен согласно закону Стокса:

$$C = \frac{12\mu}{\rho_0 r W_0} \qquad (2)$$

где r – радиус частицы бетонной смеси. Эта зависимость позволяет значение коэффициента С определить для конкретных условий смешения.

Известны численные значения этого коэффициента для общих случаев смесей различной подвижности, что дает большие погрешности при определении показателей трехвального бетоносмесителя. Зависимость (2) решает эту проблему и позволяет довольно точно учесть конкретные условия процесса смешения трехвальным бетоносмесителем.

Угол установки валов в корпусе бетоносмесителя можно найти, определив центры установки каждого из трех валов:

$$\theta = \arccos\left\{\frac{R_{ці} \cdot \cos\theta_{ці} + r_i \cos\theta_i}{r}\right\} \qquad (3)$$

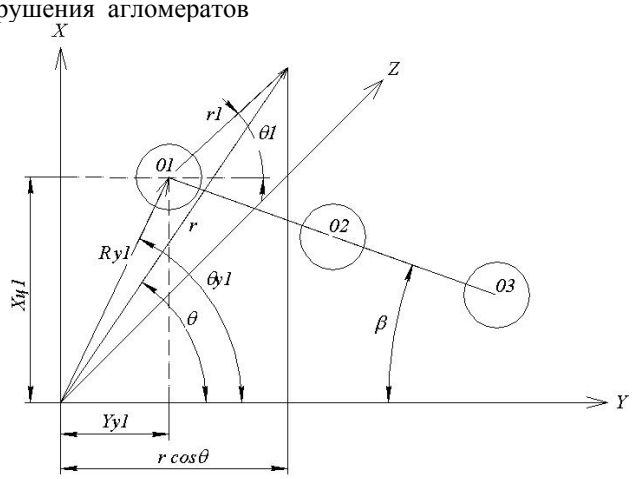

Рис.2 К определению угла установки валов в корпусе смесителя

Производительность трехвального бетоносмесителя определяется объемом бетонной смеси , который за единицу времени перемещается к выгрузочному отверстию корпуса смесителя.

Техническая производительность определяется с учетом коэффициента возврата:

$$П_{техн.} = 3600\frac{\pi}{4}(D^2 - d^2)bnZ_л \sin\alpha K_з^{ср} \cdot K_b^{II}, \quad м^3/ч \quad (4)$$

где D – диаметр по торцу вращения лопаток среднего вала, м;
d - диаметр среднего вала, м;
n – частота вращения среднего вала, м;
$Z_л$ – количество лопаток среднего вала;
α – угол атаки лопаток, град;
$K_З$ – коэффициент заполнения рабочего пространства смесителя бетонной смесью;
K_b^{II} - коэффициент возврата бетонной смеси во II-ой зоне смесителя.

$$K_b^{II} = \frac{m_b^{II} + m_н^{II}}{m_b^{II} + m_н^{II} + m_c^{II}} \quad (5)$$

где m_b^{II} - масса компонентов, находящихся в зоне верхнего вала;
$m_н^{II}$ - масса компонентов, находящихся в зоне нижнего вала;
m_c^{II} - масса компонентов, находящихся в зоне среднего вала.

Для второй зоны трехвального бетоносмесителя

$$K_b^{II} = 0,6...0,7; \quad K_з^{ср} = 0,65...0,75$$

Экспериментальные исследования [4,5] трехвального смесителя позволили выявить его основные параметры и определить их рациональные области для получения смесей высокой однородности: частота вращения рабочего органа n=47…65 мин$^{-1}$; угол атаки лопаток первой зоны α=42…45°; угол атаки второй зоны $α_2$=39…42°; площадь поверхности лопаток F=30…32 см^2; количество лопаток $Z_Л$=32…35; угол расположения рабочего органа относительно горизонтали β=5…10°.
Время приготовления малоподвижных смесей (П=2…4 см) составляет 40…45 с, тогда как у двухвального смесителя время на приготовление смесей той же подвижности составляет 60…65 с. Коэффициент заполнения рабочего пространства бетонной смесью может быть доведен до 0,8.
Главной качественной характеристикой приготовленной бетонной смеси является степень однородности, которая определена может быть согласно зависимости [6]:

$$f = \frac{1}{h}\int_0^h \left(\frac{W - W_1}{W_1}\right) dZ \quad (6)$$

где h – толщина сечения слоя смеси;
W – оптимальная концентрация компонентов смеси;
Z – текущая координата отбора пробы.
Дисперсия однородности при выходе из смесителя f=5,2…7,3% при производительности бетоносмесителя $П_{техн.} = 4,2...4,8$ м^3/ч; затраты мощности на приготовление малоподвижной бетонной смеси составляют $N = 4,9...6,1$ кВт.
Таким образом, можно констатировать, что трехвальный бетоносмеситель является эффективной машиной для приготовления, прежде всего, малоподвижных, жестких и особожестких смесей.

ВЫВОДЫ

1. Описана конструкция нового трехвального бетоносмесителя.
2. Указаны преимущества трехвального бетоносмесителя.
3. Приведен ряд зависимостей для определения основных параметров машины.
4. Найден ряд рациональных параметров смесителя для приготовления смесей высокой однородности.

ЛИТЕРАТУРА

[1] Ємельянова І. А., Баранов А. М., Блажко В. В., Тугай В. В. Змішувач для приготування будівельної суміші. Патент на винахід №74444. Бюл. № 12.2005.

[2] Емельянова И. А., Баранов А. Н., Емельянов В. П., Блажко В. В. Бетоносмеситель принудительного действия – составная часть технологического комплекта малогабаритного оборудования для стройплощадки //Вестник ХНАДУ – Харьков, 2005 – Вып. 29. – С 43-45.

[3] Демуцький В. П. Моделі некласичних середовищ: Нац. акад. наук України, Харківський державний університет, Технолог. Центр – Х: НФТЦ, 1994–72 с.

[4] Блажко В. В. Определение величины коэффициента заполнения и его влияние на качественные показатели работы трехвального бетоносмесителя // Науковий вісник будівництва – Харків, 2007 – Вип.. 40 – С. 128 – 132.

[5] Ємельянова И. А., Блажко В. В. Влияние рабочих параметров трехвального бетоносмесителя на однородность бетонной смеси // Науковий вісник будівництва – Харків; 2007 – Вип.. 42. – С. 124-128

[6] Ю. А. Веригин, С. В. Толстенев. Синергетические основы процессов и технологий. Барнаул: Изд-во АлтГТУ. 2007, 160 с.

EVALUATING THE LOADS ON BULLDOZER UNDERCARRIAGE UNDER LONGITUDINAL TRIM

I. Kirichenko

Abstract: *Based on the mathematic simulation of articulated air-wheel type machines, a bulldozer mathematic model for all its operating modes has been worked out. Evaluation of loads on the bulldozer undercarriage under longitudinal trim has been considered as an example of possible implementing the potential of the mathematical model proposed.*

Key words: *Modular approach, differential equations, D'Alambert's principle, undercarriage, loads.*

1. INTRODUCTION

Loads that develop on the undercarriage of articulated air-wheel type machines influence the performance and reliability of all machine elements. Formalized scheme for evaluating the loads on the undercarriage is in combination of differential equations that describe machine motion with D'Alambert's principle.

2. EVALUATING THE LOADS

Bulldozer articulation is a bigrade joint (Fig.1) ensuring independent angular travels of the power and production modules correspondingly under roll (axle Ox) and lateral movement (axle Oy) as well as cooperative travels of these modules under longitudinal trim (axle Oz).
Let us assume that:

- the mass of each articulated bulldozer module is centered in the vertical fore-and-aft plane;
- under the conveying mode and when the working attachment interacts with the ground, the relative movement of both the working attachment and the power module equals zero.

The mathematic simulation of the bulldozer longitudinal trim phenomenon lies in the fact that the main vector of external forces must be in the fore-and-aft plane, i.e. $\sum F^e_{k_Z} = 0$ (Fig.1); and the resultant moment of the external forces must be parallel to axle Oz, i.e. $\sum M^e_x = 0,\ \sum M^e_y = 0$.

When $t_O = 0$, then $\omega_O(0) = \omega_y(0) = 0,\ V_Z(0) = 0$ takes place.

The above mentioned conditions mean that under longitudinal trim the bulldozer makes a plane-parallel motion relative to plane $A\xi_1\eta_1$ (Fig.1). The system of coordinates $O\xi\eta\zeta$ is a progressively moving reference system, whose axes are parallel to $A\xi_1\eta_1\zeta_1$ fixed reference axes. The system of coordinates $O\xi\eta\zeta$ is rigidly connected with the carrier.

In order to evaluate loads R_{em} and R_{pm} on the bulldozer undercarriage we shall refer to D'Alambert's principle [1]; in compliance with it, the main vector and the resultant moment of inertial forces are represented in the figure, with point *O* being taken as the pole of inertial forces reduction. From equilibrium equations made by D'Alambert's principle, the roadway reacting forces are of the form:

$$R_{ЭМ} = \left[-F_1\left(l_1+l_2\right)\cos\theta + P_1\left(l_2+a_1\right)\cos\theta + P_2\left(l_2-a_2\right)\cos\theta - \Phi_\xi\left(b_0+h_0-\eta_0\right) - \Phi_\eta l_2\cos\theta - M_0^\Phi + P_3\left(L_1+l_2+\left(l_c+s\right)\cos\left(\theta+\theta_3\right)\right) + W_{KB}\left(L_1+l_2+\left(L_3-s\right)\cos\left(\theta-\theta_3\right)\right) - W_{KT}\cdot\delta_k + M_{(OP)_B}\right] \Big/ \left(l_1+l_2\right)\cos\theta \quad (1)$$

$$R_{TM} = \left[-F_1\left(l_1+l_2\right)\cos\theta + P_1\left(l_2+a_1\right)\cos\theta + P_2\left(l_2-a_2\right)\cos\theta - \Phi_\xi\left(b_0+h_0-\eta_0\right) - \Phi_\eta l_2\cos\theta - M_0^\Phi + P_3\left(L_1+l_2+\left(l_c+s\right)\cos\left(\theta+\theta_3\right)\right) + W_{KB}\left(L_1+l_2+\left(L_3-s\right)\cos\left(\theta-\theta_3\right)\right) - W_{KT}\cdot\delta_k + M_{(OP)_B}\right] \Big/ \left(l_1+l_2\right)\cos\theta \quad (2)$$

In equations (1) and (2) :

R_{em} and R_{pm} - reacting forces on the power and production modules;

F_1 and F_2 - elastic flexible up and down pull on the part of pneumatic tire, with $F_1 = c\left(\eta_0 + l_1\theta\right)$,;

$F_2 = c\left(\eta_0 - l_2\theta\right)$, c - vertical rigidness of pneumatic tire, η_0 – camber of pole *O* under longitudinal trim;

projections of the main vector of inertial forces onto inertial axes equal

$$F_\xi = ma_{c\xi} = m\left(\ddot{\xi}_0 - \left(x_c\cos\theta - y_c\sin\theta\right)\cdot\dot{\theta}^2 - \left(x_c\sin\theta + y_c\cos\theta\right)\cdot\ddot{\theta}\right)$$
$$F_\eta = ma_{c\eta} = m\left(\ddot{\eta}_0 - \left(x_c\sin\theta + y_c\cos\theta\right)\cdot\dot{\theta}^2 + \left(x_c\cos\theta - y_c\sin\theta\right)\cdot\ddot{\theta}\right)$$

$\ddot{\xi}_o$ and $\ddot{\eta}_0$ – pole *O* acceleration components; x_c and y_c - coordinates of bulldozer masses centre in the sys-

Igor Georgievich Kirichenko, Kharkov National Automobile and Highway University, Kharkov, Ukraine

tem of coordinates *Oxyz* rigidly connected with the carrier:

$x_c = (m_1 a_1 + m_2 a_2) / m; y_c = (m_1 b_1 + m_2 b_2) / m$.

These coordinates will be written in the inertial system as

$$x_{\xi'} = x_c \cos\theta - y_c \sin\theta$$

$$y_{\eta'} = x_c \sin\theta + y_c \cos\theta$$

The resultant moment of inertial forces equals $M_0^F = J_0 \ddot{\theta}$, where J_c is bulldozer inertia moment relative to the axis passing through pole *O* at right angle to the fore-and-aft plane of the machine;

m_1, m_2, m_3, - masses of correspondingly power and production modules, and working attachment, total mass $m = m_1 + m_2 + m_3$.

Parameters $\ddot{\xi}_0, \ddot{\eta}_0, \dot{\theta} and \ddot{\theta}$ that occur in (1) and (2), can be determined from the get from longitudinal trim differential equation system composed on the basis of the generalized mathematical model of articulated machines [2] using Lagrange's equations of the second genre.

The kinetic energy was determined similar to the method described in [3]. The bulldozer potential energy under longitudinal trim is equal to

$$\begin{aligned} \Pi = {} & 2c\eta_0^2 + c\left(l_1^2 + l_2^2\right)\theta^2 + 2c\left(l_1 - l_2\right)\eta_0\theta + \\ & + \frac{1}{2} c_{po} \left(\xi_0 \cos\theta + \eta_0 \sin\theta - s\right)^2 \end{aligned} . \qquad (3)$$

Traction forces T_1 and T_2, resistance forces W_{f_1} and W_{f_2} on each wheel were taken as in [4]:

$$T_{bi} = T_{0i}\left(1 - \frac{0,065}{V_n} \cdot \dot{x}_i - \frac{0,935}{V_n^5} \cdot \dot{x}_i^{\,5}\right) \qquad (4)$$

$i = 1, 2$

$$W_{f_i} = R_i \cdot f, \qquad (5)$$

where T_0 – the maximum value of tractive power on coupling; V_n – the bulldozer initial speed at the moment when the blade penetrates the ground.

Digging strength as in [4]:

$$W_k = A_x x + C_x x^2 + D_x x^3, \qquad (6)$$

where

$$A_x = 25.28 \cdot \left(\frac{\rho_X}{\rho_1}\right) \cdot \left(\frac{\delta_{1X}}{\delta_1}\right) \cdot \left(\frac{B_x}{B_1}\right),$$

$\mathrm{C_X} = 0.664 \cdot \mathrm{A_X}$, $\mathrm{D_X} = 0.81 \cdot \mathrm{A_X}$;

parameters that describe the developed ground, - they are ρ_1, B_1 and ρ_x, B_x - ground consistency and widths of scoops of the reference blade and the tested one, δ_{1x} - the thickness of the cut out ground.

The differential equations made on the basis of the generalized mathematical model of articulated machines and describing the bulldozer motion under longitudinal trim are in the following form:

$$\begin{aligned} & m\ddot{\xi}_0 - \left(B\cos\theta + A\sin\theta\right)\ddot{\theta} + \left(B\sin\theta - A\cos\theta\right)\dot{\theta}^2 = \\ & T_1 + T_2 - W_{f1} - W_{f2} - W_{кг}, \end{aligned}$$

$$\begin{aligned} & m\ddot{\eta}_0 - \left(B\sin\theta - A\cos\theta\right)\ddot{\theta} - \left(B\cos\theta + A\sin\theta\right)\dot{\theta}^2 = \\ & -4c\eta_0 + 2c\left(l_2 - l_1\right) - W_{кв}, \end{aligned}$$

$$\begin{aligned} & -\left(B\cos\theta + A\sin\theta\right)\ddot{\xi}_0 - \left(B\sin\theta - A\cos\theta\right)\ddot{\eta}_0 + J_0\ddot{\theta} = \\ & = 2c\left(l_2 - l_1\right)\eta_0 - 2c\left(l_2^2 + l_1^2\right)\theta + W_{кв} l_3 + W_{кг} l_3 + \\ & \left(W_{кг} - T_1 - T_2 + W_{f1} + W_{f2}\right)\left(H - \eta_0\right), \end{aligned} \qquad (7)$$

where A and B – coefficients that present the total of the static moments of bulldozer modules.

Equations (1) and (2) together with the differential equation system (7) evaluate loads on the bulldozer undercarriage under its longitudinal trim.

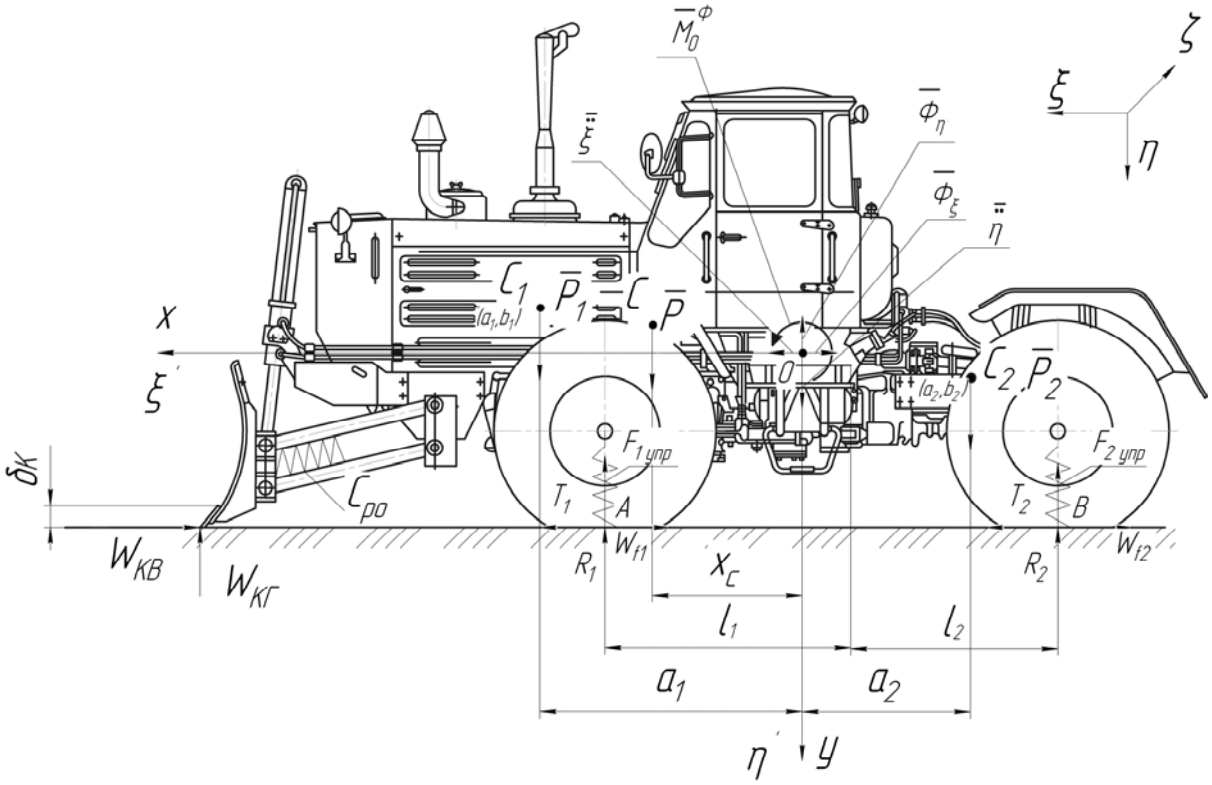

Fig. 1. Schematic view of forces affecting the bulldozer in the operating mode

Fig. 2 shows the graphs of the load variation range on the power and production modules.

a)

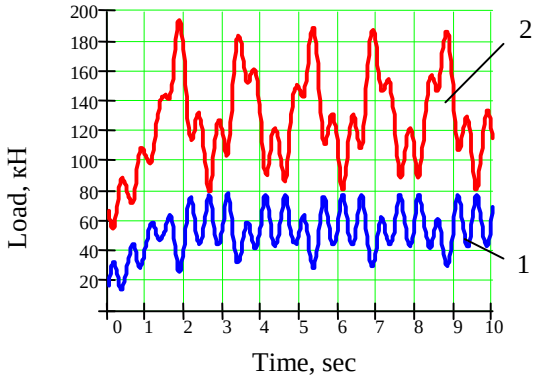

b)

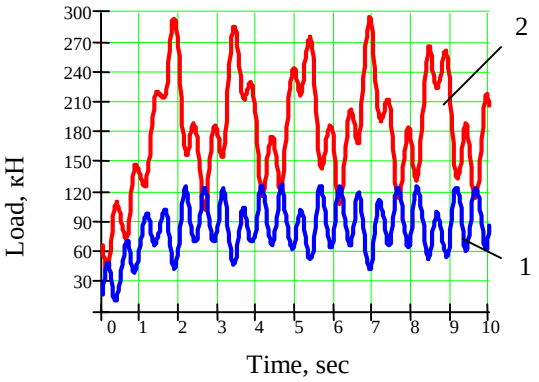

c)

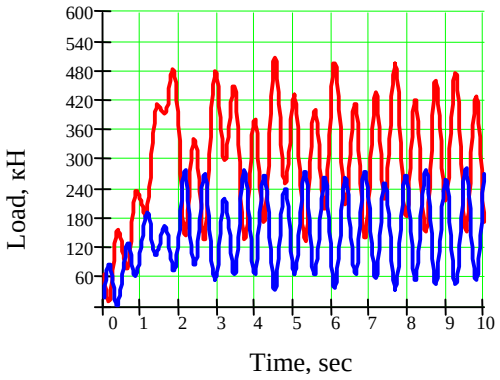

Fig. 2. Dynamics of the load variation range on the bulldozer undercarriage (2-EM; 1-PM) at various correlations of horizontal and vertical forces of resistance to digging:

а) $W_K = 0.6 \cdot W_{KG}$ б) $W_{KB} = 1.2 \cdot Wkg$ в) $W_{KB} = 2.6 \cdot W_{KГ}$

3. THE ANALYSIS OF RESULTS

As it follows from comparison of graphs a) and b), at the moment of speeding-up, which lasts for about 2 sec., loads reach their extreme values. They increase with the growth of the vertical component value; the load variation range increases at:

$W_{KB} = 0.6 \cdot W_{KГ}$-: 80 < R_{PM} < 190, and 30 < R_{EM} < 80; at

$W_{KB} = 1.2 \cdot W_{KГ}$: 120 < R_{PM} < 290, and 50 < R_{EM} < 120;

at $W_{KB} = 2.6 \cdot W_{KT}$: 140 < R_{PM} < 500, and 60 < R_{EM} < 270.
The variation range of loads on the power module makes up 30 < R_{EM} < 270, and on production one - 80 < R_{PM} < 500;

vibration frequency of loads on the power module is nearly four times as high as vibration frequency of loads on the production module;

the way curves R_{pm}, R_{em} change proves the overlapping of several vibrations of various frequencies; power and technological modules vibrate in antiphase.

4. CONCLUSIONS

1. The mathematical model of bulldozer that allows evaluating loads on its undercarriage under longitudinal trim has been formed.

2. The influence of a vertical component of the digging resisting force on the growth of loads on the power and production modules has been proved.

3. Loads on the power module are twofold, two and a half times as high as those on the production module.

4. The scheme of evaluating loads on the undercarriage: the generalized model, differential equations, D'Alambert's principle – can be used while evaluating loads on the undercarriage of various technological machines not only under longitudinal trim, but also during their rolling and lateral movement.

REFERENCES

1. Бутенин Н.В., Лунц Я.Л., Меркин Д.Р. Курс теоретической механики, том II.: Динамика.- М.:Наука, 1985.-496 с.

2. Кириченко И.Г. Модульная концепция проектирования технологических машин для строительного производства.- Харьков: Изд-во ХНАДУ,2002.-119 с.

3. Кириченко И.Г., Кулешова М.Ф., Щербак О.В. К вопросу составления кинетической энергии колесного шарнирно-сочлененного трактора// Весник ХГПУ.-1999. Вып.66., Харьков:ХГПУ.- С. 99-101.

4. Назаров Л.В. Динамические нагрузки на трактор Т-150К, агрегатируемый с бульдозерным оборудованием.-1978. // Тракторы и сельхозмашины. Москва, Россия. – № 3.-С. 17-21

MODELING THE BEHAVIOR OF TOWER CRANES UNDER SEISMIC STRAIN

M. Alamoreanu

Abstract: *Many countries are located in seismic activity zones. Seismic activities should be categorized, within the classification of actions affecting lifting equipment, under the group of "exceptional actions". However, all European norms ignore these actions. As a consequence, cranes are currently not verified under this additional type of strain. The earthquake of historic proportions that hit Romania on March 4th, 1977 is proof that this omission can be fatal: a tower crane from the building site for the Municipal Hospital then under construction tipped under the seismic strain and fell over, bringing down with it a part of the new building. In this paper we present a load model that includes seismic activity. We establish the differential equation of the oscillations of cranes under the additional seismic strain. We also present a solution to this problem if representing seismic movements as superimposed sinusoidal harmonics. The seismic action affects the crane both directly, at the base of the crane, and indirectly, through the body of the building that braces it, which allows the vibrations to be transmitted to the bracing anchors.*

Key words: *tower cranes, seismic action, behavior under seismic-equivalent load*

1. INTRODUCTION

Numerous countries are located on seismic activity rich ground. However, both the International Sstandard ISO 8686-1:1989 [1], and the European Standard EN 13001-2:2004 [2] ignore seismic actions upon cranes. These actions would normally fall under the category of "exceptional actions". Therefore, this omission must be supplanted by the national norms of the countries in question.

Romania is situated in a region characterized by intense seismic activity. During the period 1901-2008 there were over 30 seismic movements in Romania of magnitudes ranging from 5.5 M_L on the Richter scale to 7.4 M_L. Among these, the most powerful earthquakes were recorded in 1908 (6.75 M_L), 1940 (7.4 M_L) and 1977 (7.2 M_L). The 1977 earthquake caused the fall of a tower crane from a building site in Bucharest, near the Municipal Hospital under construction at that time. Because it was the only crane anchored at the site and in the nearby surroundings, and the quake occurred after 9p.m. (thus the site was deserted, and the crane not in service), the fall fortunately produced no casualties. However, it damaged part of the new building.

2. PROBLEM STATEMENT

The official technical regulations of the Romanian national body which oversees the exploitation of lifting machinery and governs the enforcement of the normal operation safety standards [3], include the obligation of supplementary safety inspections being conducted on cranes operating under seismic conditions, but there is no separate standard for these specific conditions.

Technical literature either fails to mention this issue altogether or, at best, treats it only superficially by referring to the norms of calculus applicable to buildings, as in [4], [5]; but there are cases when the application of these norms is not transferrable to cranes. One of these cases is that of tower cranes anchored at the foot of the building, for which seismic activity is present both directly, at the base of the crane itself, and indirectly, through the building and anchorages. As previously mentioned, it is exactly for these types of cranes that potential seismic activity can have the most disastrous effect, because it may topple the whole crane-building ensemble. On the other hand, while the buildings themselves behave as free structures (the binding effect onto structures by anchored cranes is negligible), anchored cranes cannot be considered as free, and as a result, the theory gets more complex in their case.

In essence, the question is finding the best model for the dynamic behavior of cranes under typical seismic actions considered as an additional type of load, with the purpose of elaborating a calculus recipe applicable to the engineering design phase. For this reason, the dynamic model utilized should be simple to implement in design calculations, and the equivalence model-to-real crane structure must be satisfactory. Our paper proposes such a method.

3. HYPOTHESES AND DYNAMIC MODEL

We depart from the following hypotheses:
The tower of the crane behaves as an elastic bar encased at the base, and free at the top;

Mr. Mircea Alamoreanu, Technical University for Constructions of Bucharest, alamor@utcb.ro

The tower is anchored at the building through *n* rigid pendulum anchors;
The mass of the crane's revolving part, as well as the equivalent mass of the tower are concentrated at the level of the fulcrum;
The seismic action is present directly at the base of the crane and indirectly through the anchors;
The effect of the crane on the building is negligible;
The second order effect of the behavior of the crane is negligible;
The inertia of the side oscillations of the revolving part of the crane is negligible.
The model thus described is presented in Figure 10-1.

According to these hypotheses, the dynamic system has two degrees of freedom (the displacements x_m and x_q of the equivalent mass *M* of the crane, and of the load *Q*, respectively), and is perturbed by displacements imposed onto the base and the anchors. Displacement x_q measures the load's deviation from the vertical (the load is suspended by a flexible element).

4. DIFFERENTIAL EQUATIONS OF THE MOVEMENT

Under the notation conventions from [6], the differential equations of the movement are:

$$\begin{cases} v_q = Q\ddot{x}_q\delta_{qq} \\ v_m = M\ddot{x}_m\delta_{mm} + Q\ddot{x}_q\delta_{mq} + \sum_{i=1}^{n} R_i\delta_{mi} \\ v_1 = \sum_{i=1}^{n} R_i\delta_{1i} \\ v_2 = \sum_{i=1}^{n} R_i\delta_{2i} \\ \dots \\ v_n = \sum_{i=1}^{n} R_i\delta_{ni} \end{cases}$$

Equation 4-1

where δ_{ij} are the influence coefficients (i.e. the horizontal elastic displacement of the crane's tower in point *i* under a horizontal unit force applied in point *j*).

Note: The last *n* equations do not contain the terms corresponding to the forces of inertia of masses *Q* and *M* because, according to hypothesis 5, the displacements v_i are completely determined by the construction itself and are assumed to be known.

To this system we associate the following relations between the relative and the absolute displacements, *v* versus *x* (see Equation 4-2, next):

$$\begin{cases} x_q = u - v_q - v_m \\ x_m = u - v_m \end{cases}$$

Equation 4-2

where u=u(t) is the function defining the seismic movement. For the time being, we also assume that the seismic movement is sinusoidal, of angular frequency Ω:

$$u(t) = U\sin\Omega t$$

Equation 4-3

This assumption will be justified (and generalized) below.

5. DISPLACEMENTS IMPOSED BY THE CONSTRUCTION

The effect of the displacements imposed by the building is assessed by computing the equivalent forces at the anchors R_i. These forces result from the last n equations of the system in Equation 4-1:

$$R_i = \frac{\Delta_{R_i}}{\Delta},$$

Equation 5-1

where

$$\Delta = \begin{vmatrix} \delta_{11} & \delta_{12} & \dots & \delta_{1n} \\ \delta_{21} & \delta_{22} & \dots & \delta_{2n} \\ \dots & \dots & \ddots & \dots \\ \delta_{n1} & \delta_{n2} & \dots & \delta_{nn} \end{vmatrix}$$

Equation 5-2

and

$$\Delta_{R_i} = \begin{vmatrix} \delta_{11} & \delta_{12} & \dots & v_1 & \dots & \delta_{1n} \\ \delta_{21} & \delta_{22} & \dots & v_2 & \dots & \delta_{2n} \\ \vdots & \vdots & \ddots & \vdots & \dots & \vdots \\ \delta_{n1} & \delta_{12} & \dots & v_n & \dots & \delta_{nn} \end{vmatrix}$$

Equation 5-3

Structures have an elastic rigidity which is sizably larger than that of cranes; hence the focus is usually limited to their elastic oscillations with the fundamental (lowest) angular frequencies. As a result, the construction can be modeled as a dynamic system of one single mass, as in Figure 10-1. The displacement of the building at the level of its equivalent mass, M_C, assuming a sinusoidal seismic action, is of the form:

$$v_C = \frac{\Omega U}{\Omega^2 - \omega_C^2}(\omega_C \sin\omega_C t + \Omega\sin\Omega t),$$

Equation 5-4

while the displacements at the level of the anchors can be expressed as a function of the building displacement through the influence coefficients of the building structure:

$$v_i = \frac{\delta_{hi}}{\delta_{hh}} \cdot v_C, \text{ with } h = \overline{1,n}$$

Equation 5-5

By substituting the expressions from Equation 5-5 into the determinant from Equation 5-3, and then substituting this determinant in Equation 5-1 of the reaction forces from the anchors, displacement v_C appears as a common factor, and we obtain:

$$R_i = \frac{\Delta_i}{\Delta} \cdot \frac{1}{\delta_{hh}} \cdot v_C,$$

Equation 5-6

where the new Δ_i replaces column i of the system determinant Δ with the h^{th} vector of the coefficients:

$$\Delta_i = \begin{vmatrix} \delta_{11} & \delta_{12} & \dots & \delta_{1h} & \dots & \delta_{1n} \\ \delta_{21} & \delta_{22} & \dots & \delta_{2h} & \dots & \delta_{2n} \\ \dots & \dots & \ddots & \vdots & \dots & \vdots \\ \delta_{n1} & \delta_{n2} & \dots & \delta_{nh} & \dots & \delta_{nn} \end{vmatrix}$$

Equation 5-7

6. REDUCING SYSTEM/EQUATION 4-1 TO THE CANONICAL FORM

By substituting Equation 5-6 in the expression of v_m from Equation 4-1 we obtain the new system:

$$\begin{cases} v_q = Q\ddot{x}_q \delta_{qq} \\ v_m = M\ddot{x}_m \delta_{mm} + Q\ddot{x}_q \delta_{mq} + \dfrac{1}{\Delta \delta_{hh}} v_c \sum_{i=1}^{n} \Delta_i \delta_{mi} \end{cases}$$

Equation 6-1

If we introduce in this system the expressions from Equation 4-2 of the absolute displacements and noting that the quantities:

$$\frac{1}{M\delta_{mm}} = \omega_m^2 \text{ and } \frac{1}{\mathrm{Q}\delta_{\mathrm{qq}}} = \omega_q^2$$

Equation 6-2

are the crane's and load's own angular frequencies, respectively; if we also note that — since the load is suspended as a pendulum through a flexible element — the displacement of the load is equal to the displacement in the barycenter of the crane:

$$\delta_{mq} = \delta_{mm}$$

Equation 6-3

then, after some transformations, we obtain:

$$\begin{cases} \ddot{v}_m + \omega_m^2 v_m - \dfrac{1}{M\delta_{qq}} v_q = \ddot{u} + (k\omega_m)^2 v_C \\ \ddot{v}_m + \ddot{v}_q + \omega^2 v_q = \ddot{u} \end{cases}$$

Equation 6-4

where *k* is by notation:

$$k = \frac{1}{\Delta \delta_{hh}} \sum_{i=1}^{n} \Delta_i \delta_{mi}$$

Equation 6-5

The system in Equation 6-4 represents the canonical form of an oscillating system with two degrees of freedom. The mutual influence of the two masses is reflected through the displacement coefficient v_q from the first equation, ü is the direct acceleration, and $(k \cdot \omega_m)^2 v_C$ is the indirect acceleration, through the construction which braces the crane. The non-dimensional factor *k* takes into consideration the elastic behaviors of both the crane and that of the construction.

Solving the system from Equation 6-4 is now trivial.

7. INITIAL CONDITIONS

Assuming that the seismic event finds the crane at rest, at the initial moment the displacements and the absolute velocities are null:

$$\begin{cases} x_m(0) = 0 \\ x_q(0) = 0 \end{cases} \text{and} \begin{cases} \dot{x}_m(0) = 0 \\ \dot{x}_q(0) = 0 \end{cases}$$

Equation 7-1

Using Equation 4-2 which describes the relation between the relative and the absolute displacements, one can easily obtain the following initial conditions, formulated in terms of relative displacements and velocities:

$$\begin{cases} v_m(0) = u(0) \\ v_q(0) = 0 \end{cases} \text{and} \begin{cases} \dot{v}_m(0) = \dot{u}(0) \\ \dot{v}_q(0) = 0 \end{cases}$$

Equation 7-2

8. PARTICULAR CASES

Unanchored crane. Term $(k \cdot \omega_m)^2 \cdot v_C$ from the right side of the first equation of the system from Equation 6-4 vanishes. The initial conditions from Equation 7-2 remain the same.

Anchored crane, not currently in service. In this case the load has no mass *Q = 0*, such that system of Equation will reduce to a single equation, which reflects the fact that the dynamic system reduces to a single-mass, one-degree of freedom system:

$$\ddot{v}_m + \omega_m^2 v_m = \ddot{u} + (k\omega_m^2)^2 v_C$$

Equation 8-1

The associated initial conditions are:

$$\begin{cases} v_m(0) = u(0) \\ \dot{v}_m(0) = \dot{u}(0) \end{cases}$$

Equation 8-2

Unanchored crane, not currently in service. The movement is described by the same differential equation as in the previous particular case, from which the second term of the right side disappears:

$$\ddot{v}_m + \omega_m^2 v_m = \ddot{u}$$

Equation 8-3

The initial conditions remain unchanged.

9. GENERALIZATION

If the seismic movement can be described by overlapping harmonics with different angular frequencies, which is to say

$$u(t) = \sum_j u_j(t) = \sum_j U_j \sin \Omega_j t$$

Equation 9-1

the core of the problem remains unchanged, and the insignificant differences that this representation of seismic movement entails will appear only in the description of the particular solutions of the system from Equation 6-4.

10. LOAD EQUIVALENT TO THE SEISMIC ACTION

This is the horizontal static force acting upon the equivalent mass of the crane, which determines an elastic displacement equal to the effective maximum elongation. As such:

$$F_{equiv} = \frac{v_m^{\max}}{\delta_{mm}}$$

Equation 10-1

Knowing the expression of the solution $v_m(t)$, the maximum value that F_{equiv} can attain during the earthquake can be obtained using a matrix library such as in MATLAB, which can also be used for the graphical representation of the time dependency of the elongations v_m and v_q.

REFERENCES

[1] ISO 8686-1: 1989 — *Cranes — Design Principles for Loads and Load Combinations*, Part I: General

[2] EN 13001-2: 2004 — *Crane Safety. General Design*, Part 2: Load Effects

[3] PT R1-2003

[4] Shapiro, I. Howard — *Cranes and Derricks*, McGraw-Hill, Third Edition, 1999

[5] Gohberg, M. — *Spravocinik po kranam*, Masinostrenie, Leningrad, 1998

[6] Ifrim, M. — Dynamics of Structures and Earthquake Engineering, E.D.P., Bucharest, 1984

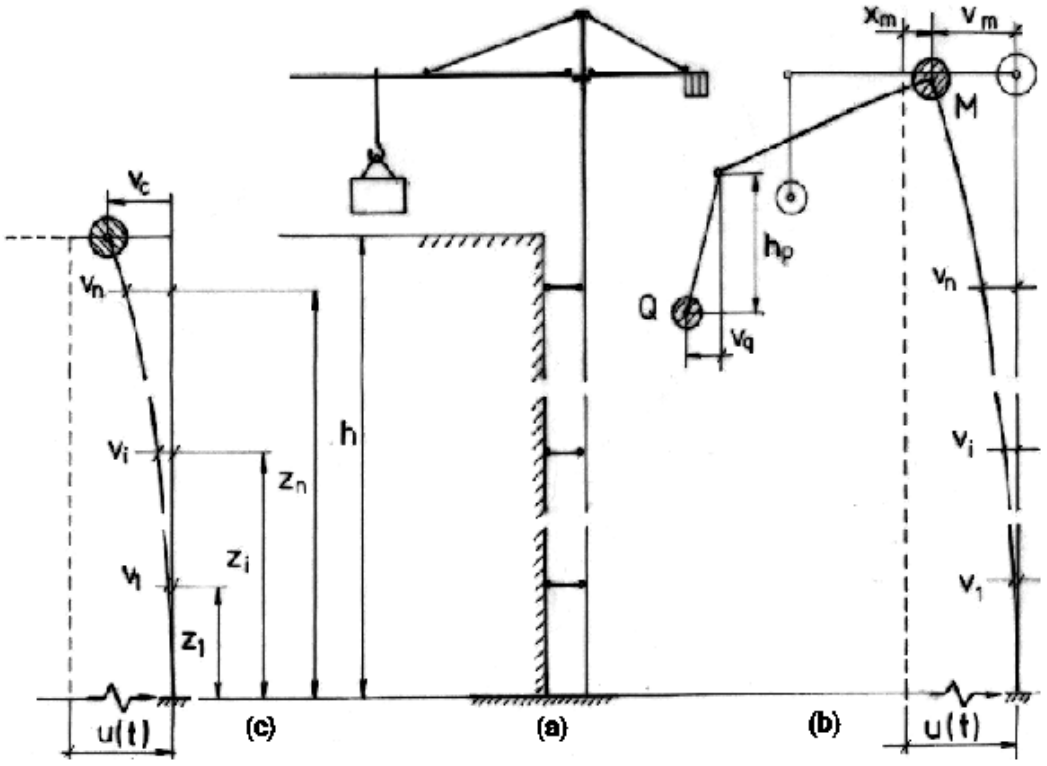

Figure **Error! No text of specified style in document.**-1 Dynamic model: displacement (c), crane (a), and building under construction (b)

THE ANALYSIS OF THE DYNAMIC LOADS DUE TO THE VIBRATIONS GENERATED BY THE DISPLACEMENT OF FRONT LOADERS

P. Bratu

Abstract: *The evaluation of dynamic performances in case of self-propelled construction machinery is based on the influence of kinematical excitations analysis transmitted to the metallic structure on the resistance limit.*
This article presents the influence of the dynamic excitations due to the bucket movement or displacement on dislevelmented roads. Basing on the adopted dynamic model and numerical and experimental tests for the MMT45 loader, the values of loading dynamic coefficients for the metallic structure have been determined.

Key words: *front loader, dynamic coefficient, rotational speed, vibrating mode, eigen pulsation*

1. INTRODUCTION

The determination of machinery dynamic response is realized by means of a calculus model that takes into consideration the mechanical and geometrical factors of the machinery.

The calculus model is based on the following hypotheses:

- characterization of exciter actions;
- evaluation of the dynamic response using one system of motion differential equations.

In order to model and analyse the most important stage of the technological process, namely the bucket loading, three physico-mathematical models having various complexity degree putting into evidence the profound dynamic character of the digging-loading process, have been conceived.

2. THE DYNAMIC MODEL

The complexity of the actual system led to a dynamic system based on simplifying hypotheses:

- the effect of the damping is neglected;
- the inertial forces are neglected;
- the axial and transversal rigidity of the arm are neglected;
- the clearances of kinematical joints (valid hypothesis in case of new machinery) and the oil compressibility from the hydraulic installation are not considered;
- the rigidity of tyres on the horizontal direction is neglected (valid hypothesis in case that the machinery is stopped which is similar with the loading process);
- there is mass symmetry with respect to median longitudinal plane.

In order to determine the performances of the bucket front loader operating in the actual regime, a dynamic model realized as a system having two masses m_1 (the mass of the base machinery and equipment) and m_2 (the mass of loaded bucket) and elastic supported, has been conceived.

The model has three degrees of freedom (y, φ_1, φ_2) that put into evidence vertical and angular oscillations of the base machinery and bucket.

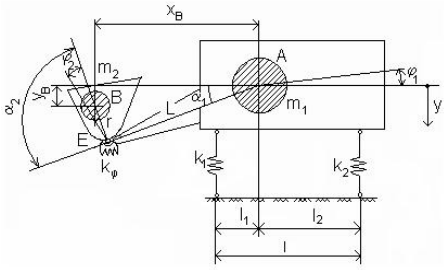

Fig. 1 – The dynamic model of the bucket front loader

The geometrical co-ordinates of the bucket centre of gravity with respect to machine centre of gravity are determined as follows:

$$\begin{aligned} x_B &= L\cos(\alpha_1+\varphi_1)+r\cos(\alpha_2-\varphi_2-\alpha_1-\varphi_1), \\ y_B &= -L\sin(\alpha_1+\varphi_1)+r\sin(\alpha_2-\varphi_2-\alpha_1-\varphi_1)+y \end{aligned} \quad (1)$$

In order to write the system of dynamic equilibrium equations of the two masses, the second order Lagrange equations are used:

By differentiation of relation (1) we can calculate the movement velocity of mass m_2:

$$v_B^2 = x_B^2 + y_B^2$$

$$\begin{aligned} v_B^2 = {} & \varphi_1^2\left(L^2+r^2+2Lr\cos\alpha_2\right)+\varphi_2^2r^2+ \\ & +2\varphi_1\varphi_2 r\left(r+L\cos\alpha_2\right)- \\ & -2\varphi_1 z\left[L\cos\alpha_1+r\cos(\alpha_2-\alpha_1)\right]- \\ & -2\varphi_2 zr\cos(\alpha_2-\alpha_1). \end{aligned} \quad (2)$$

In order to obtain the point B velocity the values of generalized co-ordinates have been considered low by comparison with the generalized velocities allowing the expression linearization. The following notations are introduced:

Prof. Polidor Bratu PhD, Research Institute for Construction Equipment and Technology - ICECON SA, Bucharest, icecon@icecon.ro

$R^2 = L^2 + r^2 + 2Lr\cos\alpha_2;$

$b_1 = r + L\cos\alpha_2;$

$b_2 = L\cos\alpha_1 + r\cos(\alpha_2 - \alpha_1),$

Then the kinetic energy of the system is written under the form:

$$E_c = \frac{1}{2}m_1\dot{y}^2 + \frac{1}{2}J_1\dot{\varphi}_1^2 + \frac{1}{2}m_2v_B^2 + \frac{1}{2}J_2(\dot{\varphi}_1 + \dot{\varphi}_2)^2$$

and becomes after replacements and simplifications:

$$\begin{aligned} E_c = {} & \frac{1}{2}m_1\dot{y}^2 + \frac{1}{2}J_1\dot{\varphi}_1^2 + \frac{1}{2}J_{2E}\dot{\varphi}_2^2 + \\ & + \dot{\varphi}_1\dot{\varphi}_2(J_2 + m_2rb_1) - \dot{\varphi}_1\dot{y}m_2b_2 - \\ & - \dot{\varphi}_2\dot{y}m_2r\cos(\alpha_2 - \alpha_1) \end{aligned} \tag{3}$$

we have

$m = m_1 + m_2$; m – the total mass of the system;

$J = J_1 + J_2 + m_2R^2$; J – the inertia moment of the bucket with respect to joint A;

$J_{2E} = J_2 + m_2r^2$; J_{2E} - the inertia moment of the bucket with respect to elastic joint E.

The potential energy of deformation stored within the elastic elements, illustrated in Figure 1 as the joint E where the bucket is clamping on the arm, the rigidity elements k_φ and the rigidity tyres k_1 and k_2, has the following expression:

$$V = \frac{1}{2}k_1(y + l_1\varphi_1)^2 + \frac{1}{2}k_2(y - l_2\varphi_1)^2 + \frac{1}{2}k_\varphi\varphi_2^2 \tag{4}$$

In case of conservative systems the second order Lagrange equations have the form:

$$\frac{d}{dt}\left(\frac{\partial E}{\partial \dot{q}_i}\right) + \frac{\partial E}{\partial q_i} = -\frac{\partial V}{\partial q_i}; \qquad i = 1, 2, 3, \ldots \tag{5}$$

where q_i represents the generalized co-ordinates of the system. The **q** vector has the form $q = [y, \varphi_1, \varphi_2]^T$.

Thus, the following system of linear differential equations is obtained:

$$\begin{cases} \ddot{y}m - \ddot{\varphi}_1m_2b_2 - \ddot{\varphi}_2m_2r\cos(\alpha_2 - \alpha_1) + (k_1 + k_2)y + \\ \quad + (k_2l_2 - k_1l_1)\varphi_1 = 0 \\ -\ddot{y}m_2b_2 + \ddot{\varphi}_1J + \ddot{\varphi}_2(J_2 + m_2rb_1) + y(k_2l_2 - k_1l_1) + \\ \quad + \varphi_1(k_1l_1^2 + k_2l_2^2) = 0 \\ -\ddot{y}m_2r\cos(\alpha_2 - \alpha_1) + \ddot{\varphi}_1(J_2 + m_2rb_1) + \ddot{\varphi}_2J_{2E} + \\ \quad + k_\varphi\varphi_2 = 0 \end{cases} \tag{6}$$

The second order Lagrange equation written under the matrix form can be rewritten as follows:

$$\mathbf{M}\ddot{\mathbf{q}} + \mathbf{K}\mathbf{q} = \mathbf{0} \tag{7}$$

where **q** is the vector of displacements according to the degrees of freedom;

M – is the matrix of inertia;

K – the matrix of rigidity;

The structures of the matrix of inertia and the matrix of rigidity are:

$$\mathbf{M} = \begin{bmatrix} m & -m_2b_2 & -m_2r\cos(\alpha_2 - \alpha_1) \\ -m_2b_2 & J & J_2 + m_2rb_1 \\ -m_2r\cos(\alpha_2 - \alpha_1) & J_2 + m_2rb_1 & J_{2E} \end{bmatrix} \tag{8}$$

$$\mathbf{K} = \begin{bmatrix} k_1 + k_2 & k_2l_2 - k_1l_1 & 0 \\ k_2l_2 - k_1l_1 & k_1l_1^2 + k_2l_2^2 & 0 \\ 0 & 0 & k_\varphi \end{bmatrix} \tag{9}$$

In order to solve the equation (7) particular solutions are chosen:

$$\begin{cases} y = A_1\sin(pt + \theta) \\ \varphi_1 = A_2\sin(pt + \theta) \\ \varphi_2 = A_3\sin(pt + \theta) \end{cases} \tag{10}$$

and by differentiation and replacement in (7) one could obtain the algebra system under the form:

$$\begin{cases} (k_1 + k_2 - mp^2)y + (k_2l_2 - k_1l_1 + m_2b_2p^2)\varphi_1 - \\ \quad - m_2rp^2\varphi_2\cos(\alpha_2 - \alpha_1) = 0 \\ (k_2l_2 - k_1l_1 + m_2b_2p^2)y + (k_1l_1^2 + k_2l_2^2 - Jp^2)\varphi_1 - \\ \quad - p^2(J_2 + m_2rb_1)\varphi_2 = 0 \\ -m_2rp^2y\cos(\alpha_2 - \alpha_1) - p^2(J_2 + m_2rb_1)\varphi_1 + \\ \quad + (k_\varphi - J_{2E}p^2)\varphi_2 = 0 \end{cases} \tag{11}$$

The eigen pulsations of the systems put into evidence the model behaviour when subjected to various perturbing factors, fact that leads to the necessity of knowing these factors.

From the vanishing condition for the determinant of the system (11) we have:

$$\begin{vmatrix} k_1 + k_2 - mp^2 & k_2l_2 - k_1l_1 + m_2b_2p^2 & -m_2rp^2\cos(\alpha_2 - \alpha_1) \\ k_2l_2 - k_1l_1 + m_2b_2p^2 & k_1l_1^2 + k_2l_2^2 - Jp^2 & -p^2(J_2 + m_2rb_1) \\ -m_2rp^2\cos(\alpha_2 - \alpha_1) & -p^2(J_2 + m_2rb_1) & k_\varphi - J_{2E}p^2 \end{vmatrix} = 0 \tag{12}$$

where we have the equation of pulsations under the form:

$$p^6 + C_1p^4 + C_2p^2 + C_3 = 0 \tag{13}$$

where C_1, C_2 and C_3 are constants depending on the geometrical and constructive parameters of the physical model.

Solving of the third degree equation in p^2 can be realized using the substitution:

$$p^2 = w - \frac{1}{3}C_1 \tag{14}$$

and we have

$$\left(w - \frac{1}{3}C_1\right)^3 + C_1\left(w - \frac{1}{3}C_1\right)^2 + C_2\left(w - \frac{1}{3}C_1\right) + C_3 = 0$$

or

$$w^3 - 3s_1w + 2n_1 = 0 \tag{15}$$

where

$$s_1 = \frac{C_1^2}{9} - \frac{C_2}{3}$$

$$n_1 = \frac{1}{2}\left(-\frac{C_1}{3}\right)^3 + \frac{1}{2}\left(-\frac{C_1}{3}\right)\cdot C_2 + \frac{1}{2}C_3$$

The roots of the cubic equation are determined as follows:

$$\begin{aligned} w_1 &= \pm 2\sqrt{s_1}\cos\left(\frac{\gamma_1}{3}\right) \\ w_2 &= \pm 2\sqrt{s_1}\cos\left(60^0 - \frac{\gamma_1}{3}\right) \end{aligned} \tag{16}$$

$$w_3 = \pm 2\sqrt{s_1}\cos\left(60^0 + \frac{\gamma_1}{3}\right)$$

where the "+" sign is for $n_1 > 0$, and the "-" sign is for $n_1 < 0$. The γ_1 angle is determined with the expression:

$$\cos\gamma_1 = \frac{|n_1|}{s_1\sqrt{s_1}} \tag{17}$$

Finally, the pulsations can be expressed as follows:

$$p_1^2 = w_1 - \frac{C_1}{3};\ p_2^2 = w_2 - \frac{C_1}{3};\ p_3^2 = w_3 - \frac{C_1}{3}; \tag{18}$$

In order to determine the eigen vectors the equation of matrix is developed as follows:

$$\begin{bmatrix} k_1+k_2-mp^2 & k_2l_2-k_1l_1+m_2b_2p^2 & -m_2rp^2\cos(\alpha_2-\alpha_1) \\ k_2l_2-k_1l_1+m_2b_2p^2 & k_1l_1^2+k_2l_2^2-Jp^2 & -p^2(J_2+m_2rb_1) \\ -m_2rp^2\cos(\alpha_2-\alpha_1) & -p^2(J_2+m_2rb_1) & k_\varphi-J_{2E}p^2 \end{bmatrix}\begin{Bmatrix} 1 \\ \mu_2 \\ \mu_3 \end{Bmatrix} = \begin{Bmatrix} 0 \\ 0 \\ 0 \end{Bmatrix} \tag{19}$$

and results in

$$\begin{cases} (k_1+k_2-mp^2)+(k_2l_2-k_1l_1+m_2b_2p^2)\mu_2-m_2rp^2\mu_3\cos(\alpha_2-\alpha_1)=0 \\ (k_2l_2-k_1l_1+m_2b_2p^2)+(k_1l_1^2+k_2l_2^2-Jp^2)\mu_2-p^2(J_2+m_2rb_1)\mu_3=0 \\ -m_2rp^2\cos(\alpha_2-\alpha_1)-p^2(J_2+m_2rb_1)\mu_2+(k_\varphi-J_{2E}p^2)\mu_3=0 \end{cases} \tag{20}$$

having the notations:

$$\mu_1 = 1;\ \mu_2 = \frac{p^2a_1+a_2}{p^2a_3+a_4};\ \mu_3 = \frac{p^4a_5+p^2a_6+a_7}{p^4a_8+p^2a_9} \tag{21}$$

where the coefficients of inertia a_j, j = 1 … 9 are under the form:

$$a_1 = J_2m + mm_2rb_1 + m_2^2b^2r\cos(\alpha_2-\alpha_1);$$
$$a_2 = -(J_2+m_2rb_1)(k_1+k_2) - (k_1l_1-k_2l_2)m_2r\cos(\alpha_2-\alpha_1);$$
$$a_3 = m_2b_2(J_2+m_2rb_1) + Jm^2r\cos(\alpha_2-\alpha_1);$$
$$a_4 = m_2r(k_1l_1^2-k_2l_2^2)\cos(\alpha_2-\alpha_1) + (J_2+m_2rb_1)(k_2l_2-k_1l_1).$$
$$a_5 = -mJ + m_2^2b_2^2;$$
$$a_6 = (k_1+k_2)J + m(k_1l_1^2+k_2l_2^2) + 2m_2b_2(k_2l_2-k_1l_1);$$
$$a_7 = -k_1k_2(l_2^2+l_1^2)^2;$$
$$a_8 = J_2m_2b_2 + m_2^2rb_1b_2 + Jm_2r\cos(\alpha_2-\alpha_1);$$
$$a_9 = (J_2+m_2rb_1)(k_2l_2-k_1l_1) - m_2r(k_1l_1^2+k_2l_2^2)\cos(\alpha_2-\alpha_1).$$

For the three eigen pulsations p_1^2, p_2^2 and p_3^2 the values of distributing coefficients are determined:

$$\mu_2^{(1)} = \frac{p_1^2a_1+a_2}{p_1^2a_3+a_4};\qquad \mu_2^{(2)} = \frac{p_2^2a_1+a_2}{p_2^2a_3+a_4};\qquad \mu_2^{(3)} = \frac{p_3^2a_1+a_2}{p_3^2a_3+a_4}; \tag{22}$$

$$\mu_3^{(1)} = \frac{p_1^4a_5+p_1^2a_6+a_7}{p_1^4a_8+p_1^2a_9};$$

$$\mu_3^{(2)} = \frac{p_2^4a_5+p_2^2a_6+a_7}{p_2^4a_8+p_2^2a_9}; \tag{23}$$

$$\mu_3^{(3)} = \frac{p_3^4a_5+p_3^2a_6+a_7}{p_3^4a_8+p_3^2a_9};$$

For the three vibrating modes we have:

$$\mu_2^{(1)} = \frac{A_2^{(1)}}{A_1^{(1)}} \to A_2^{(1)} = A_1^{(1)}\mu_2^{(1)};$$

$$\mu_2^{(2)} = \frac{A_2^{(2)}}{A_1^{(2)}} \to A_2^{(2)} = A_1^{(2)}\mu_2^{(2)};$$

$$\mu_2^{(3)} = \frac{A_2^{(3)}}{A_1^{(3)}} \to A_2^{(3)} = A_1^{(3)}\mu_2^{(3)};$$

$$\mu_3^{(1)} = \frac{A_3^{(1)}}{A_1^{(1)}} \to A_3^{(1)} = A_1^{(1)}\mu_3^{(1)};$$

$$\mu_3^{(2)} = \frac{A_3^{(2)}}{A_1^{(2)}} \to A_3^{(2)} = A_1^{(2)}\mu_3^{(2)};$$

$$\mu_3^{(3)} = \frac{A_3^{(3)}}{A_1^{(3)}} \to A_3^{(3)} = A_1^{(3)}\mu_3^{(3)}$$

Thus, the eigen vectors are under the form:

$$A^{(1)} = A_1^{(1)}\mu^{(1)} = A_1^{(1)}\begin{Bmatrix} 1 \\ \mu_2^{(1)} \\ \mu_3^{(1)} \end{Bmatrix};$$

$$A^{(2)} = A_1^{(2)}\mu^{(2)} = A_1^{(2)}\begin{Bmatrix} 1 \\ \mu_2^{(2)} \\ \mu_3^{(2)} \end{Bmatrix}; \tag{24}$$

$$A^{(3)} = A_1^{(3)}\mu^{(3)} = A_1^{(3)}\begin{Bmatrix} 1 \\ \mu_2^{(3)} \\ \mu_3^{(3)} \end{Bmatrix}.$$

The eigen pulsation p_1^2, together with the modal vector $A^{(1)}$ are defining the first eigen vibrating mode, characterized by the following co-ordinates:

$$\begin{cases} y_1^{(1)} = A_1^{(1)}\sin(p_1t+\theta_1); \\ \varphi_1^{(1)} = A_2^{(1)}\sin(p_1t+\theta_1) = \mu_2^{(1)}A_1^{(1)}\sin(p_1t+\theta_1); \\ \varphi_2^{(1)} = A_3^{(1)}\sin(p_1t+\theta_1) = \mu_3^{(1)}A_1^{(1)}\sin(p_1t+\theta_1), \end{cases} \tag{25}$$

where $A_1^{(1)}$ and θ_1 are determined from the initial conditions corresponding to the first vibrating mode.

Analogous, for the second and third eigen vibrating modes we have

$$\begin{cases} y_1^{(2)} = A_1^{(2)}\sin(p_2t+\theta_2); \\ \varphi_1^{(2)} = A_2^{(2)}\sin(p_2t+\theta_2) = \mu_2^{(2)}A_1^{(2)}\sin(p_2t+\theta_2); \\ \varphi_2^{(2)} = A_3^{(2)}\sin(p_2t+\theta_2) = \mu_3^{(2)}A_1^{(2)}\sin(p_2t+\theta_2), \end{cases} \tag{26}$$

$$\begin{cases} y_1^{(3)} = A_1^{(3)}\sin(p_3t+\theta_3); \\ \varphi_1^{(3)} = A_2^{(3)}\sin(p_3t+\theta_3) = \mu_2^{(3)}A_1^{(3)}\sin(p_3t+\theta_3); \\ \varphi_2^{(3)} = A_3^{(3)}\sin(p_3t+\theta_3) = \mu_3^{(3)}A_1^{(3)}\sin(p_3t+\theta_3). \end{cases} \tag{27}$$

By imposing these initial conditions when t = 0:

$$\begin{cases} z_0 = 0 \\ \varphi_{10} = 0 \\ \varphi_{20} = 0 \end{cases} \quad \text{and} \quad \begin{cases} \dot z_0 = v_0 \\ \dot\varphi_{10} = \omega_{01} \\ \dot\varphi_{20} = \omega_{02} \end{cases} \tag{28}$$

the following system is obtained:

$$\begin{cases} A_1^{(1)}\sin\theta_1 + A_1^{(2)}\mu_2^{(1)}\sin\theta_2 + \\ \qquad + A_1^{(3)}\mu_3^{(1)}\sin\theta_3 = 0 \\ A_1^{(1)}\sin\theta_1 + A_1^{(2)}\mu_2^{(2)}\sin\theta_2 + \\ \qquad + A_1^{(3)}\mu_3^{(2)}\sin\theta_3 = 0 \\ A_1^{(1)}\sin\theta_1 + A_1^{(2)}\mu_2^{(3)}\sin\theta_2 + \\ \qquad + A_1^{(3)}\mu_3^{(3)}\sin\theta_3 = 0 \\ p_1A_1^{(1)}\cos\theta_1 + p_2A_1^{(2)}\mu_2^{(1)}\cos\theta_2 + \\ \qquad + p_3A_1^{(3)}\mu_3^{(1)}\cos\theta_3 = v_0 \\ p_1A_1^{(1)}\cos\theta_1 + p_2A_1^{(2)}\mu_2^{(2)}\cos\theta_2 + \\ \qquad + p_3A_1^{(3)}\mu_3^{(2)}\cos\theta_3 = \omega_{01} \\ p_1A_1^{(1)}\cos\theta_1 + p_2A_1^{(2)}\mu_2^{(3)}\cos\theta_2 + \\ \qquad + p_3A_1^{(3)}\mu_3^{(3)}\cos\theta_3 = \omega_{02} \end{cases} \quad (29)$$

and we have $A_1^{(1)}$, $A_1^{(2)}, A_1^{(3)}$ and $\theta_1, \theta_2, \theta_3$.

The general solution for the system of linear differential equations (7) results in an overlap of the three movements:

$$\begin{aligned} y &= y_1^{(1)} + y_1^{(2)} + y_1^{(3)} = A_1^{(1)}\sin(p_1t+\theta_1) + \\ &\quad + A_1^{(2)}\sin(p_2t+\theta_2) + A_1^{(3)}\sin(p_3t+\theta_3) \\ \varphi_1 &= \varphi_1^{(1)} + \varphi_1^{(2)} + \varphi_1^{(3)} = \mu_2^{(1)}A_1^{(1)}\sin(p_1t+\theta_1) + \\ &\quad + \mu_2^{(2)}A_1^{(2)}\sin(p_2t+\theta_2) + \mu_2^{(3)}A_1^{(3)}\sin(p_3t+\theta_3) \\ \varphi_2 &= \varphi_2^{(1)} + \varphi_2^{(2)} + \varphi_2^{(3)} = \mu_3^{(1)}A_1^{(1)}\sin(p_1t+\theta_1) + \\ &\quad + \mu_3^{(2)}A_1^{(2)}\sin(p_2t+\theta_2) + \mu_3^{(3)}A_1^{(3)}\sin(p_3t+\theta_3) \end{aligned} \quad (30)$$

The velocities of the free vibrations, corresponding to the chosen co-ordinates will be:

$$\begin{aligned} \dot{y} &= p_1A_1^{(1)}\cos(p_1t+\theta_1) + \\ &\quad + p_2A_1^{(2)}\cos(p_2t+\theta_2) + p_3A_1^{(3)}\cos(p_3t+\theta_3) \\ \dot{\varphi}_1 &= p_1\mu_2^{(1)}A_1^{(1)}\cos(p_1t+\theta_1) + \\ &\quad + p_2\mu_2^{(2)}A_1^{(2)}\cos(p_2t+\theta_2) + p_3\mu_2^{(3)}A_1^{(3)}\cos(p_3t+\theta_3) \\ \dot{\varphi}_2 &= p_1\mu_3^{(1)}A_1^{(1)}\cos(p_1t+\theta_1) + \\ &\quad + p_2\mu_3^{(2)}A_1^{(2)}\cos(p_2t+\theta_2) + p_3\mu_3^{(3)}A_1^{(3)}\cos(p_3t+\theta_3) \end{aligned} \quad (31)$$

The accelerations of the free vibrations, corresponding to the three degrees of freedom, are:

$$\begin{aligned} \ddot{y} &= -A_1^{(1)}p_1^2\sin(p_1t+\theta_1) - \\ &\quad - A_1^{(2)}p_2^2\sin(p_2t+\theta_2) - A_1^{(3)}p_3^2\sin(p_3t+\theta_3) \\ \ddot{\varphi}_1 &= -\mu_2^{(1)}A_1^{(1)}p_1^2\sin(p_1t+\theta_1) - \\ &\quad - \mu_2^{(2)}A_1^{(2)}p_2^2\sin(p_2t+\theta_2) - \mu_2^{(3)}A_1^{(3)}p_3^2\sin(p_3t+\theta_3) \\ \ddot{\varphi}_2 &= -\mu_3^{(1)}A_1^{(1)}p_1^2\sin(p_1t+\theta_1) - \\ &\quad - \mu_3^{(2)}A_1^{(2)}p_2^2\sin(p_2t+\theta_2) - \mu_3^{(3)}A_1^{(3)}p_3^2\sin(p_3t+\theta_3) \end{aligned} \quad (32)$$

The dynamic behaviour due to the perturbing factors which are introducing vertical vibrations into the system and causing dynamic effects quantized by means of the dynamic coefficients is being studied by taking into consideration the initial conditions.

Having the identification data for the MMT45 loader manufactured by PROMEX S.A. Braila the eigen pulsations have been calculated, the final expressions of the machinery movement for the three degrees of freedom have been written and the frequency spectrum of those movements have been illustrated in Figure 2.

$p_1 = 2.97$ rad/s; $p_2 = 6.64$ rad/s; $p_3 = 30.9$ rad/s;

$$\begin{aligned} y(t) &= 0.87\sin(2.97t) - 0.41\sin(6.64t) - 0.002\sin(30.9t) \\ \varphi_1(t) &= 0.36\sin(2.97t) + 0.70\sin(6.64t) - 0.175\sin(30.9t) \\ \varphi_2(t) &= 0.03\sin(2.97t) + 0.03\sin(6.64t) + 1.282\sin(30.9t) \end{aligned} \quad (33)$$

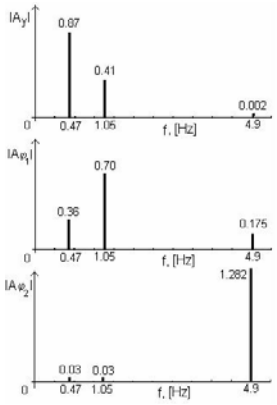

Fig. 2 Frequency spectrum for y(t), φ_1(t) and φ_2(t) functions

3. THE DYNAMIC RESPONSE DUE TO THE EXCITATION OF THE BUCKET DUMPING

In order to carry out the bucket closing action, the rotational speed $\Delta\omega$ is variable and this situation leads to major implications upon the loading of metallic structure and hydraulic drive system of the machinery as well.

For this situation to be analysed we consider for the initial point t = 0 that the machinery is in the position of stable static balance and the closing of the loaded bucket is performed suddenly. These conditions can be expressed under the following form:

$$\text{for } t = 0 \begin{cases} y_0 = 0; \dot{y}_0 = 0 \\ \varphi_{10} = 0; \dot{\varphi}_{10} = 0 \\ \varphi_{20} = 0; \dot{\varphi}_{20} = \Delta\omega \end{cases} \quad (34)$$

The system of differential equations has been resolved using the MAPLE software and the time history of the system output values has been illustrated in Figure 3.

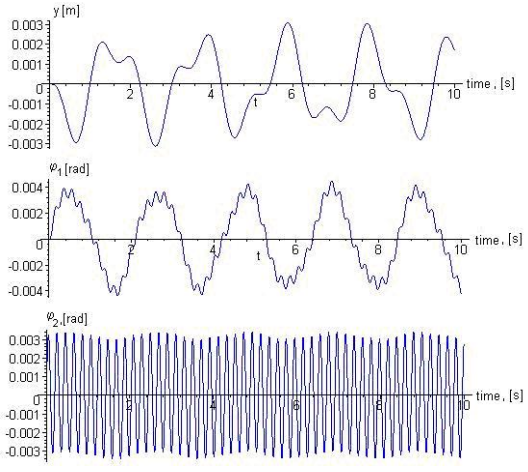

Fig. 3 The model response due to the sudden rotation of the bucket

The analysis of Figure 3 puts into evidence the fact that the sudden rotation of the bucket is being accompanied by vibrations transmitted within the machinery structure, the machinery performing oscillating movements according to the degrees of freedom.

The over loadings transmitted to the dumping system of the bucket having as a result the sudden closing of the bucket are quantized by a dynamic coefficient defined as the ratio between the total moment due to the static and dynamic forces, M_{d+st}, and the (minimum) total moment with respect to bucket-arm joint, M_{st}, in the static regime of forces operating upon the bucket.

$$\psi = \frac{M_{din+st}}{M_{st}} = 1 + \frac{k_\varphi}{m_2 g x_G}\varphi_2^{\max} \qquad (35)$$

The maximum value of the dynamic coefficient ψ depends in this case on the maximum value of the bucket angle of shearing-deformation φ_2^{max}. For the MMT45 loader we have $\psi = 1{,}22$.

It is important to know the influence that various structural elements of the model have upon the dynamic behaviour of the bucket dumping system.

The construction of the bucket dumping system, by its rigidity and rotational speed of bucket unloading, influences the dynamic effects transmitted within the hydraulic drive system and the structure of the machine, as we can see in Figure 4.

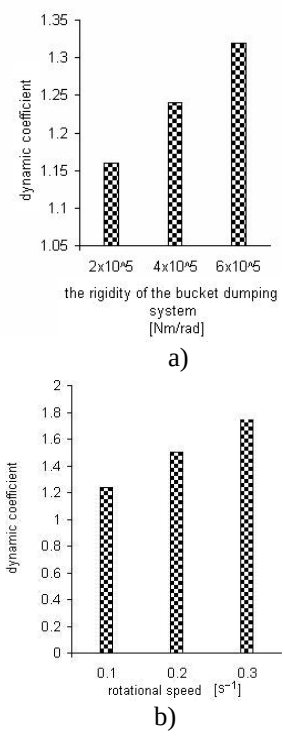

Fig. 4 The variation of the dynamic effect within the bucket dumping system
a) the influence of the bucket dumping rigidity;
b) the influence of the bucket rotational speed

In Figure 4 one can note that by increasing the rotational speed of bucket closing and opening the dynamic effect within the bucket dumping system increases.

Modifying the construction of dumping mechanism by increasing its torsion rigidity, the bucket angle of shearing-deformation decreases while the frequency of the bucket movement increases, phenomenon observed in Figure 5.

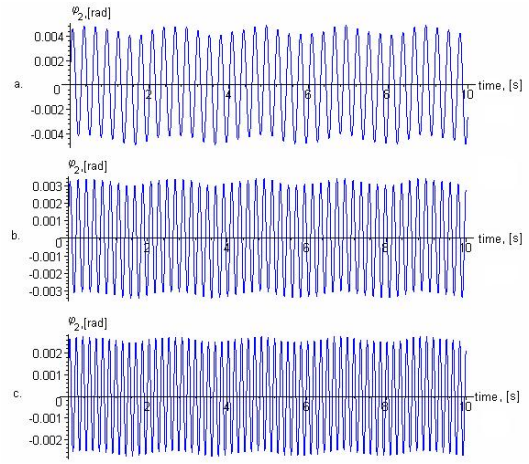

Fig. 5 The variation of the bucket rotational speed as a function of the dumping mechanism rigidity
a) k_φ=200 000 Nm/rad; b) k_φ = 400 000 Nm/rad;
c) k_φ =600 000 Nm/rad

4. THE RESPONSE OF THE LOADER WHEN SUBJECTED TO SUDDEN BRAKE DURING THE DISPLACEMENT IN ACCELERATED REGIME HAVING THE BUCKET LOADED

Taking into account the energetic considerations, the initial conditions imposed for t = 0 in order to simulate this situation have the following form:

$$\text{for } t = 0 \begin{cases} y_0 = 0; \dot{y}_0 = 0 \\ \varphi_{10} = 0; \dot{\varphi}_{10} = v\sqrt{\frac{m}{J}} \\ \varphi_{20} = 0; \dot{\varphi}_{20} = v\sqrt{\frac{m_c}{J_c}} \end{cases} \qquad (36)$$

where

m is the total mass of the machinery having the bucket in load;

m_c – the mass of the bucket having rated load;

J – the inertia moment of the machine;

J_c – the inertia moment of the bucket having rated load;

v – the displacement speed from which the sudden brake of the machine is realized.

The response of the system in case of the MMT45 loader having J = 14415,65 kgm^2, J_c = 683,75 kgm^2, m = 6180 kg, m_c = 1500 kg is illustrated in Figure 6. The initial conditions are $\dot{\varphi}_{10} = 1$ rad/s; $\dot{\varphi}_{20} = 2{,}35$ rad/s.

In order to put into evidence the dynamic effects as a function of the speed from which the machine is being braked, two cases will be simulated: braking from speed v = 1,59 m/s and from v = 1,2 m/s. In this situation the dynamic coefficient when braking from v = 1,59 m/s reaches the value $\psi = 6$.

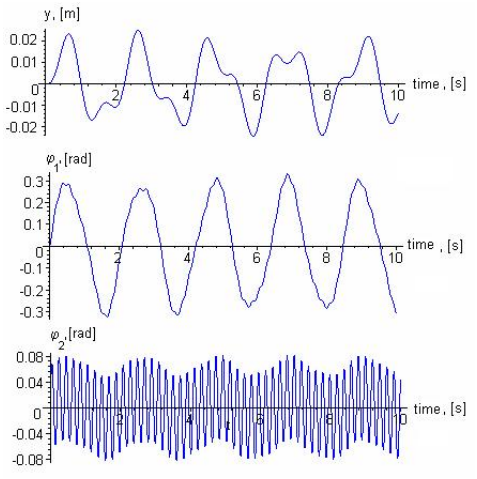

Fig. 6 The response of the system when braking the loader from speed v = 1,59 m/s.

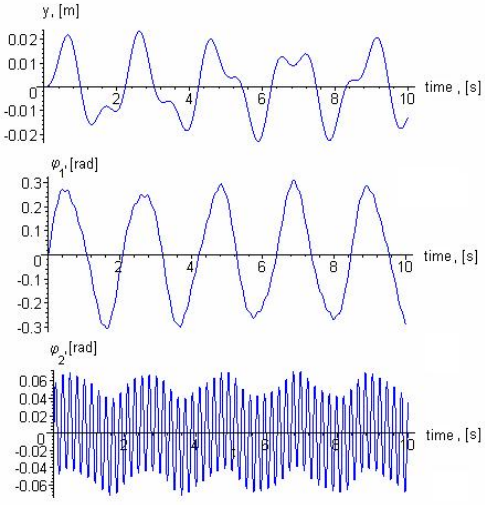

Fig. 7 The response of the system when braking the loader from speed v = 1,2 m/s.

5. THE RESPONSE OF THE LOADER WHEN SUBJECTED TO SUDDEN BRAKE DURING THE DESCENDING OF THE ARM HAVING THE BUCKET LOADED

The initial conditions for t = 0 are:

$$\text{for t} = 0 \begin{cases} y_0 = 0; \dot{y}_0 = 0 \\ \varphi_{10} = 0; \dot{\varphi}_{10} = \omega \dfrac{d_2}{d_3} \\ \varphi_{20} = 0; \dot{\varphi}_{20} = \omega \dfrac{d_1}{d_2} \end{cases} \quad (37)$$

where ω is the rotational speed of the arm when descending, previously to the braking of arm actuating cylinder; d_1 – the distance from the mass centre of the loaded bucket to the joint where the bucket clamps on the arm; d_2 - the distance from the mass centre of the loaded bucket to the joint where the arm clamps the base machine chassis; d_3 - the distance from the mass centre of the machine to the mass centre of the loaded bucket.
The response of the system is illustrated in Figure 8, the oscillating movement of the bucket in the joint where the bucket clamps on the arm has a peculiar interest.

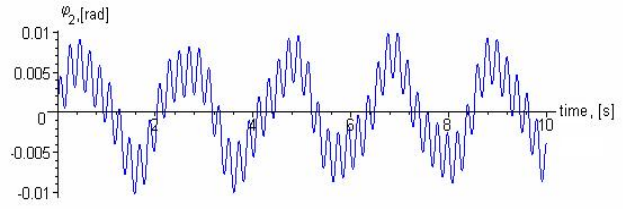

Fig. 8

In this case the dynamic coefficient reaches the value $\psi = 1,76$ for the MMT45 loader.

6. CONCLUSIONS

The adopted dynamic model approximates with sufficient precision the behaviour of the machinery in the three stages of excitations mentioned in the paper.
The dynamic coefficients can be determined basing on the mass and geometrical characteristics of the equipment and machinery and the working regime as well.

REFERENCES

[1] Bratu, P. – *The evaluation of dynamic effects due to transversal oscillations in case of front loaders*, Construction Mechanization Magazine, no. 1, 1985.

[2] Bratu, P. – *Machinery dynamics*, "Dunarea de Jos" University of Galati, 2000.

[3] Bratu, P. – *Elastic system vibrations*, Technical Publishing House, Bucharest, 2000.

[4] Debeleac, C. – *Theoretical considerations about maximum vibration limits for wheel loader affected by the ground conditions*, The Annals of "Dunarea de Jos" University of Galati, Fasc. XIV, Mechanical Engineering, 2003.

[5] Debeleac, C. – *The analysis of the dynamic regime in case of fast front loaders in order to establish the quality performances*, PhD Thesis, "Dunarea de Jos" University of Galati, 2006.

[6] Mihailescu, St., Bratu, P., Goran, V. – *Construction machinery*, vol. II, Technical Publishing House, Bucharest, 1984.

LIFETIME ESTIMATION OF THE LIFT TRANSMISSION POWER SYSTEM ELEMENTS

R. Durković, M. Damjanović

Abstract: *Load and lifetime of the lift transmission system elements powered by electromotive drive are considered. Element lifetime estimation, up to fracture – due to fatigue, is based on applying linear hypotheses on material damage calculation. Elements lifetime is expressed as the time of their work and cabin route.*

Key words: *ligt, lifetime, fatique, transmission power system, element.*

1. INTRODUCTION

Electromotive lift transmission power system is presented as a complex elasto – inertial dynamic system subjected in its operation to the drive moment and corresponding load. The very intensity demand for lift transport is continually changed within 24 hours with an accidental change character submitted to Poisson's distribution law [8].

In general case, with Poisson's distribution, a probability that, out of total λ independent events, within certain period of time, n-events may happen, is determined (n=0, 1, 2...), [3]:

$$P(n) = \lambda^n \cdot \frac{e^{-\lambda}}{n!} \qquad (1)$$

In this case it means that λ lift users at some time interval will need, namely use lift.

The intensity of lift use and load as well as the period of top intensity during a day depend on the purposes and characteristics of the object within which a lift is built. Static load is characterized by a number of persons being carried by a lift simltaneously. As a rule, the larger the number of the floors the greater a number being in the lift at the same time, the cabine route and lift use during a day or year are.

The gratest intensity demand for vertical transport is competent for technical solution choice, namely lift capacity.

However, such a demand is not responsible for lift element calculation, neither due to static hardness nor due to fatigue hardness.

Element calculation to static hardness is done according to maximum dynamic load at, for example, lifting of the cabin into seizure device or butter, namely at overload in the process of lift control.

To estimate elements lifetime according to fatigue hardness, it is necessary to know the total load for a corresponding element, in the course of its lifetime. It should be pointed out that, apart from static loads, determined by the cabine and people's weight (or load) and balancing elements in the working lift cycle, there appear dynamic loads. The dynamic load of oscillatory character may predominantly influence the lift elements lifetime according to wear and fatigue hardness criteria, especially for the reason the lift is a machine of cyclic operation with a great number of switching on during its lifetime.

According to [1] in literature is missing the methodology of estimating concrete lift element lifetime by virtue of fatigue hardness to give sufficiently reliable results.

This increasing the accuracy of estimating lift elements lifetime remains to be a further task to solve. In this paper, dynamic loads of the lift elements and their lifetime are considered.

2. DYNAMIC ELEMENT LOADS

Within the lift power transmission elements, dynamic loads are particularly expressed in periods of drive release and brake.

The forced oscillations that appear in the period of drive release and brake may be considered on simplified schemes of systems with one, two, and three masses.

The general lift scheme is shown in Fig. 1a), and its simplified scheme with two reduced masses are given in Fig. 1(b).

Ph.D. Radan Durković, Faculty of Mechanical Engineering Podgorica, Montenegro
Mr Milanko Damjanović , Faculty of Mechanical Engineering Podgorica, Montenegro

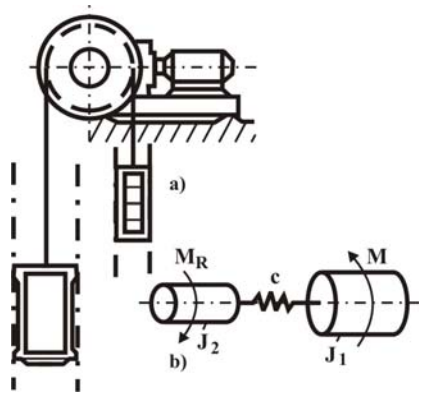

Fig. 1. Lift scheme; a) general scheme, b) simplified scheme with two reduced masses.

The signs in Fig. 1b) have the following meaming:
J_1 – reduced inertia moment of drive mass and counter – weight,
J_2 – cabin reduced moment of inertia,
M – drive moment,
M_R – operational moment,
c – reduced stiffness of serially connected ropes and hangers of cabin (depending on the rope length).

Dynamic load values of ropes and other power transmission elements depend on the growth speed of operational moment and system oscillatory characteristics [9], [12].

Operational moment velocity growth is shown by time t_o, Fig. 2, whereas system oscilatory characteristics are shown by a period of own oscillations T. Both influences are expressed by load parametres $\lambda=t_0/T$.

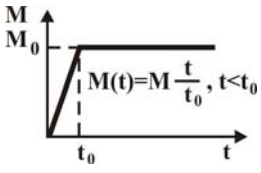

Fig. 2. Outer moment growth diagram (operational or braking).

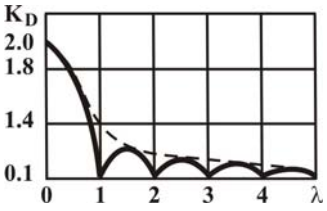

Fig. 3. Dynamic change coefficients diagram in dependence on load parameters.

The moment growth in Fig. 2 may be described in the following way:

$$M(t)=\begin{cases} M_0\dfrac{t}{t_0}, t<t_0 \\ M_0, \quad t\geq t_0 \end{cases} \tag{2}$$

The dynamic load grawth in ropes and power transmission elements is expressed by dynamic coefficients. For the lift scheme with two masses, Fig 1b), the dynamic coefficient in elastic connection (rope) is given by the expression, [9]:

$$K_D=1+\frac{\sin\pi\lambda}{\pi\lambda} \tag{3}$$

Dotted lines in Fig. 3 connect maximum dynamic coefficient values K_D obtained for $\lambda=\frac{3}{2},\frac{5}{2},\frac{7}{2}$ etc.

The moment in elastic bond of a two-mass system, Fig. 1b), at zero initial conditions:

$$t=0,\frac{dM}{dt}=0,M=0, \tag{4}$$

is expressed by, [9]:

$$M_c=M_{co}(1-\cos pt) \tag{5}$$

where:

$M_{co}=\dfrac{J_2\cdot M+J_1\cdot M_R}{J_1+J_2}$ - constant moment component,

$p=\sqrt{\dfrac{c\cdot(J_1+J_2)}{J_1+J_2}}$ - circular frequency of own oscillations of two – mass system.

Own oscillation period is:

$$T=\frac{2\pi}{p} \tag{6}$$

The result of equation (5) is that maximum dynamic moment value in elastic bond can reach double value of static and inertial loads.

At gaps existing in power transmission elements of elastic bond, when starting operation, a moment acts, [9]:

$$M_c=M_{co}(1-\cos pt)+\frac{\omega_0\cdot c}{p}\sin pt \tag{7}$$

In expression (7), the second member results from gap impact.

Angular velocity of masses colliding is:

$$\omega_0=\sqrt{\frac{2\cdot M_1\cdot\theta}{J_1}} \tag{8}$$

where θ – reduced gap in radians.

In case of gap existence, dynamic coefficient is given by an expression:

$$K_D=1+\sqrt{1+\left(\frac{\omega_0}{M_{co}\cdot p}\right)^2} \tag{9}$$

The expression (9) shows that $K_D>2$ for a value resulting from gap impact.
In this case dynamic loads can reach high values overcoming static element loads for several times.

3. LIFETIME OF ELEMENT

Mechanical characteristic variations of applied construction materials of lift power transmission system elements on one side, and accidentaly changeable load level on the other side make an accurate determination of element lifetime difficult. Thus their lifetime estimation is done.

Elements lifetime estimation is done by virtue of wear – e.g. at rope, and by means of fatigue hardness at driving gear elements.

In this paper, power transmission element lifetime estimation is considered in terms of fatigue hardness.

Lifetime estimation is based on applying linear hypotheses on material damage accumulation.

According to these hypotheses element damages accumulated in single strain levels, i=1÷k, are mutually independent, thus summed up, and the measure of total damages is interaction function:

$$a_r = \frac{n_1}{N_1} + \frac{n_2}{N_2} + ... + \frac{n_i}{N_i} + ... = \sum_{i=1}^{k} \frac{n_i}{N_i} \qquad (10)$$

where:
n_i – is the number of stress cycle of i-level (σ_i) for the total early element lifetime,
N_i – is the cycle number that the element can stand according to Wöhler′s curve at a continual σ_i stress action.

Interaction function a_r expresses the influence of working stresses spectre form deviations from stresses at basic durability.

The most significant linear hypotheses on material damage accumulation hypotheses on material damage accumulation are these ones: Palmogrin – Mainer's, Serensen – Kogaev's, Corten-Dlan's and Haibach's.

An explanation to the above hypotheses is given by using Fig. 4, [4], [5].

According to Palmgrin – Mainer's hypothesis, interaction function is a_r=1, whereas material damages are caused only by the stresses higher than permanent dynamic hardness, $\sigma_i > \sigma_D$. Sersen-Kogaev's hypothesis also takes into consideration only stress $\sigma_i > \sigma_D$ action, wheresas interaction function has the value a_r=0.1÷1 and is calculated for a concrete stress distribution. The influence on dynamic stress durability below permanent dynamic hardnes σ_D is taken by interaction coefficient a_r. Cortan – Dolan's and Haibah's hypotheses take into consideration all the stresses $\sigma_i > 0$. For the stresses $\sigma_i < \sigma_1$, these hypotheses modify (correct) Wöhler's curve, Fig. 4. the stress σ_1 in point W is the biogest stress within the spectre.

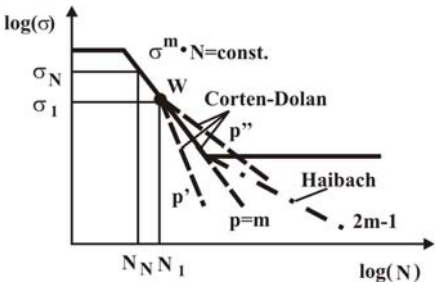

$$p = k_c \cdot m \begin{cases} k_c = 1 \Rightarrow p = m \\ k_c < 1 \Rightarrow p = p' \\ k_c > 1 \Rightarrow p = p'' \end{cases}$$

Fig.4. Wöhler's curve and stress distribution at operational load – an explanation to a linear hypothesis.

Lifetime of elements expressed by a total number of stress change cycles of al the levels an element can endure (for non-corrected Wöhler's curve) is:

$$N_R = \frac{N_D \cdot \sigma_D^m}{\sigma_{ekv.}^m} \qquad (11)$$

where:
σ_D – is a dynamic durability representing critical stress,
$\sigma_{ekv.}$- is an equivalent operational stress replacing operational stresses of all levels.

If n_T is the number of stress change cycles per element operational hour, and T is the number of its working hours, then $N_R = n_T \cdot T$, thus by replacing expression (11) we get:

$$T = \frac{R}{R_1} = \frac{N_D \cdot \sigma_D^m}{n_T \cdot \sigma_{ekv.}^m} \qquad (12)$$

In the previous expression R is the total element operational capacity (resource) disposable:

$$R = N_D \cdot \sigma_D^m \qquad (13)$$

and R_1 – is a needed operational capacity of elements per 1 working hour (unit working capacity or unit resource):

$$R_1 = n_T \cdot \sigma_{ekv.}^m \qquad (14)$$

3.1 Total Operational Capacity Disposable

A total operational capacity of R element available, expressed by N_D, σ_D and m depends on kind and way of load change, applied construction material, construction element form and technological process of its production (forming).

Types of loads, ways of their change, exponents of fatigue curves – m and asymmetry coefficients r, [2], [6], [7] are given in the Table 1 for the basic power transmission elements: gears, shafts and bearings.

Table 1. Types and characteristics of power transmission element load.

Element	Type of load	Load change	Exponent m	Asymmetry coefficinet
gear	tooth surface pressure	initial repeated cyclic	3	0
	tooth bending	initial repeated cyclic	9	0
shaft	bending	symmetric reversed cyclic	9	-1
	torsion	asymmetric reversed cyclic	2.5÷6	0 < r < 1
bearing	pressure	initial repeated cyclic	3-for ball-bering. 3.33-for roll-bearing.	0

Rope extension at transitional processes due to acceleration and cabin braking is alternatively asymmetrical one.

Stress asymmetry coefficient is defined by relation:

$$r = \frac{\sigma_{min.}}{\sigma_{max.}} \tag{15}$$

Stress asymmetry coefficient r influence, namely medial stress σ_m, on dynamic durability is illustrated by Wöhler's curve in Fig. 5. and Smith's diagram in Fig. 6.

Dynamic durability of single elements σ_D is determined by the dynamic durability of the tube σ_{DE}, taking into consideration the differences of element characteristics in relation to the tube by means of corresponding coefficients, [13].

For permanent area, durability is:

$$\sigma_D = \sigma_{DE} \frac{\zeta_1 \cdot \zeta_2 \cdot \zeta_3 \cdot \zeta_4 \cdot \zeta_5}{\beta_K} \tag{16}$$

Factors β_K and ζ_i (i=1÷5) express the following influences: β_K – stress concentration, ζ_1 - element and tube dimension differences, ζ_2 - surface roughness, ζ_3 – surface quality, ζ_4 – corrosion, and ζ_5 temperatur.

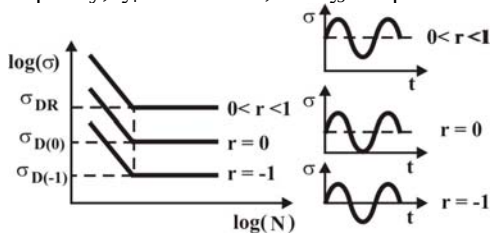

Fig. 5. Wöhler's curve, [10].

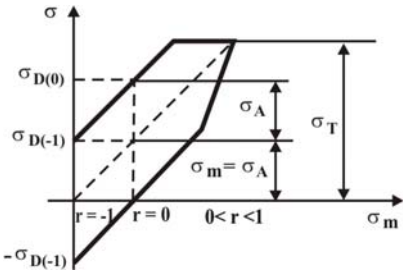

Fig. 6 Smith's diagram, σ_T-drawing limit, σ_A amplitude, *[13]*.

3.2 Needed Unit Operational Capacity

A unit operational ability of R_1 element needed depends, through parameters a_r, $\sigma_{ekv.}$, n_T, on the level and character of its operational level.

To determine σ_{ekv}, it is necessary to know relative frequencies of single stress levels for a given element, competent for the whote period of its work. These frequencies can be determined by a competent block of stress changes within an element. A relative participation of stress level σ_i in the competent block corresponds to their relative participation in element lifetime.

Stress distribution within the block can be shown in Fig. 7.

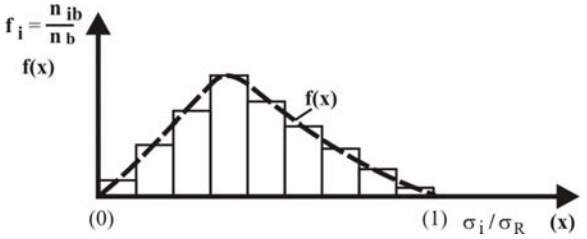

Fig. 7. Stress distribution; 1 - histogram of relative stress frequency; 2 - stress distribution density function.

On the histogram, Fig. 7, relative stresses σ_i/σ_R are on coordinate, whereas relative frequencies f_i are on ordinate axis.

An equivalent stress can be expressed in the form of:

$$\sigma_{ekv.} = \sigma_R \sqrt[m]{\frac{1}{a_r} \cdot \sum_{i=1}^{j} \frac{n_{ib}}{n_b} \cdot \left(\frac{\sigma_i}{\sigma_R}\right)^m} = \sigma_R \cdot K \tag{17}$$

where:

σ_R – calculating stress,

n_{ib} – number of stress changes of i–level in the block,

n_b – total number of stress changes in the block,

K – coefficient of reducing changeable cyclic strain/tension to a cyclic tension of a calculated regime, expressed by:

$$K = \frac{1}{\sigma_R} \cdot \sqrt[m]{\frac{1}{a_r} \cdot \sum_{i=1}^{j} \frac{n_{ib}}{n_b} \cdot \left(\frac{\sigma_i}{\sigma_R}\right)^m} = \frac{1}{\sigma_R} \cdot \sqrt[m]{\frac{1}{a_r} \cdot \sum_{i=1}^{j} f_i \cdot \left(\frac{\sigma_i}{\sigma_R}\right)^m} \quad (18)$$

A maximum stress in the considered competent block, or the stress at static cabin load with nominal load are taken for calculating stress.

If based on the histogram, a curve of the relative stress distribution thickness f(x) is formed, the following coefficient is:

$$K = \frac{1}{\sigma_R} \cdot \sqrt[m]{\frac{1}{a_r} \cdot \int_0^1 x^m \cdot f(x) \cdot dx} \quad (19)$$

where $x=\sigma/\sigma_R$.

3.3 Comparison of Operational and Critical Sfresses

Both operational and critical stresses at concrete calculations must, if compared, have the same change character, namely asymmetry degree.

Thus, it is necessary to bring either operational or critical stresses to a corresponding asymmetry degree.

In some cases, the following things can be done.

If the change of operational stress is alternatively symmetrical one, then σ_i stress as well as σ_R i $\sigma_{ekv.}$ stresses represent stress amplitudes, and $\sigma_{D(-1)}$ is taken for critical stress.

If the change of operational stress is direct one (one way), initial stress σ_i (σ_R and $\sigma_{ekv.}$) represent a sum of medial/mean stress and amplitude, namely a double amplitude, and critical stress is $\sigma_{D(0)}$.

If the change of operational stress is asymmetrical with asymmetry degree r=const. and amplitude σ_i, critical stress with the same asymmetry degree can be determined, [5]:

$$\sigma_{rD} = \frac{2 \cdot \sigma_{D(-1)}}{(1-r) + \psi \cdot (1+r)} \quad (20)$$

where ψ is coefficient of material sensitivity to asymmetry cycle.

In general case, if operational stress change is asymmetrical to changeable amplitude medial recording stress processing is made by applying the method of two – parameters systematization. Applying the two – parameters systematization, a correlation table with $\sigma_{max.i}$ and $\sigma_{min.i}$ are formed, then stress amplitudes are determined to be brought to a symmetrical cycle, [11]:

$$\sigma_i = \frac{\sigma_{max.i} - \sigma_{min.i}}{2} + \psi_\sigma \frac{\sigma_{max.i} + \sigma_{min.i}}{2} = \sigma_i(r_i) + \psi \cdot \sigma_{mi}(r_i) \quad (21)$$

where: $\sigma_i(r_i)$ and $\sigma_{mi}(r_i)$ – is amplitude and medial stress at r_i asymmetry coefficient.

3.4 Number of Cycles n_T

A number of cycles per working hour for gearing teeth as well as for shalts and other elements, a dominant load to bending is:

$$n_T = 60 \cdot n \left[\frac{\text{cycles}}{\text{h}}\right] \quad (22)$$

where n [min^{-1}] is the number of revolutions per minute.

A number of n_T cycles for shafts and other elements of gear wheels, a dominant load to twist is determined by the lowest own frequency of a given element n_H [Hz], thus:

$$n_T = 3600 \cdot n_H \left[\frac{\text{ciklusa}}{\text{h}}\right] \quad (23)$$

A number of cycles n_T can be defermined by applying the theory of accident functions, if stress oscillogram is available, [2]:

$$n_T = \frac{1}{T_e} = \frac{1}{2\pi} \sqrt{\frac{D_{v\sigma}}{D_\sigma}} \left[\frac{\text{ciklusa}}{\text{h}}\right] \quad (24)$$

where:
T_e – effective period of stress change,
D_x and D_{vx} – dispersion of operational stresses and velocity of its change.

3.5 Other Possibilities of Estimating Element Operational Lifetime

Lift power transmission element operational lifetime may also be expressed by the cabin route covered in kilometres (km).
If n_L is the number of stress change cycles in an elemet per km cabin route, and L a number of kilometres covered, then $N_R=n_L \cdot L$, thus by replacing within the expression (11), we obtain:

$$L = \frac{N_D \cdot \sigma_D^m}{n_L \cdot \sigma_{ekv.}^m} \quad (25)$$

In previous considerations we illustrated a deterministic method of estimating element operational lifetime. Apart from deterministic one, to determine element operational lifetime, we may also apply a probability method. The probability method takes into consideration the variation of mechanical characteristics of applied construction element materials, as well as the variation of their load. By this method, the following can be estimated:
- probability of element operation without failure for the planned lifetime $P(T_0)$,
- element lifetime for any probability with non operational failure, so – called gama percentage resource or gama percentual lifetime $T_{\gamma\%}$.

4. CONCLUSIONS

By virtue of the contents given in this paper, the following conclusions can be made:
- dynamic loads particularly present at releasing and breaking are of significant influence on the total operational loads of the lift power transmission elements;
- dynamic loads within power transmission elements, when there is a gap, can highly overcome statical ones;
- by construction material characteristics and systematic element loads, it is possible to determine their lifetime and express it per operating hours or covered kilometres;
- lift power transmission element system lifetime estimation is important at projecting, exploitation and lift maintenance.

LITERATURE

[1] Arhangeljskij G.G., Volkov D.P., Gorbunov E.A., Ionov A.A., Tkačenko V.J., Čutčikov P.I.: Lift, Izdateljstvo asociacija stroiteljnih vuzov, Moskva, 1999.

[2] Buharin N.A., Prozorov V.S., Šćukin M.M.: Avtomobili, ″Mašinostroenie″, Leningrad, 1973.

[3] Citovič I.S., Mitin V.E., Dzjun V.A.: Nadežnost transmisi avtomobilej i traktorov, ″Nauka i tehnika″, Minsk, 1985.

[4] Durković R., Damjanović M.: Radni vijek prenosnika snage motornih vozila – sistematske metode proračuna elemenata, Monografija povodom 30 godina časopisa International Jurnal for Mechanics, Engines and Transportation Systems Mobility & Vehicles mechanics, Kragujevac, 2005.

[5] Durković R.: Mobile working machines and their elements: calculation of liftime, Proceedings of Fifth International Conference Heavy Machinery – HM 2005, Kraljevo, 2005.

[6] Durković R.: Uticaj konstrukcionih i eksploatacionih parametara na radni vijek elemenata transmisija mobilnih mašina, Traktori i pogonske mašine, ISSN 0345-9496, Vol 10, No 3, Novi Sad, 2005.

[7] Grinevič G.P. i dr.: Nadežnost stroiteljnih mašin, ″Strojizdat″, Moskva, 1983.

[8] Gojnić G.: Vertikalni transport, Saobraćajni fakultet Univerziteta u Beogradu, Beograd, 1990.

[9] Kolesnik N.P.: Rasčeti stroiteljnih kranov, ″Višća škola″, Kiev, 1985.

[10] Lukin P.P., Gasparjanac G.A., Rodinov V.F.: Automobile chassis, Design and calculations, Mir publisches Moskov, 1989.

[11] Rjahin V.A., Moškarev G.H.: Dolgovečnost i ustrojčivost svarnih konstrukci stroiteljnih i dorožnih mašin, ″Mašinostroenie″, Moskva, 1984.

[12] Scheffler M., Dresig H., Kurth F.: Fördertechnik, Unstetigfördever 2, VEB Verlig Technik, Berlin, 1977.

[13] Vitas D.: Osnovi mašinskih konstrukcija II, ″Naučna knjiga″, Beograd, 1969.

ANALYSIS OF CALCULATION METHODS APPLIED TO THE RINGS OF PORTAL CRANE

M. Gašić, M. Savković, G. Marković, N. Zdravković

Abstract: *The paper deals with calculation methods which have been applied to circular rings of portal cranes having revolving columns. The first part of the paper includes theoretical analysis of the loads of circular rings and calculation methods, too. In the second part of the paper the theoretical results of the calculation have been checked by finite element method (FEM) and by calculation software. It has been proved that calculation results have a high level of conformity, which provides the possibility for theoretical analysis of influence of different parameters on the intensity of ring stress and ring deformation.*

Key words: *circular ring, portal, loads, calculation methods*

1. INTRODUCTION

The supports of revolving column of portal cranes transmit the external loads to carrying structure of the crane. Lower support, as a rule, takes the horizontal force from the moment and it also takes the vertical force from the resulting vertical loads (fig.1a). Circular ring connecting portal tops takes the second horizontal force from the moment. The ring carries not only the big gear which is a constituent part of the mechanism used for column revolution but also the circular track which supports column wheels used for transmission of horizontal force.

Depending on the geometric characteristics of the ring and portal, the following combinations are possible:

a) circular ring, and upper and lower part of the portal are elastic,
b) circular ring, and upper and lower part of the portal are rigid,
c) circular ring, and upper part of the portal are elastic, whereas the lower part of the portal is rigid, and
d) circular ring is rigid, whereas upper and lower parts of the portal are elastic.

The forces at connections between the circular ring and upper part of the portal are variables. They depend on the position which loaded boom takes with respect to direction of portal moving, on optional solution of the connection of the circular ring and portal as well as on the number of portal legs.

Four-legged portal supports can not be in contact with the track without additional elastic deformation of the portal or with the ring. In order to eliminate the influence, the analysis of calculation methods of circular ring is applied to three-legged portal.

2. CALCULATION MODEL OF CIRCULAR RING

Research results [1] show that three-legged portal having a rigid ring and elastic upper and lower part is an optimal solution in view of the intensity of forces at connections. Besides, that kind of solution provides forming the model of connection between circular ring and the portal by means of joints without bigger deviations.
If calculation theory of circular rings with constant cross sections [2] is applied, it is possible to analyse the loads of the rings. These loads are:

- horizontal force of revolving column,
- radial force of driving gear,
- peripheric force of driving gear,
- weights of the ring, circular track, and big gear.

Horizontal force of revolving column, radial force of driving gear and peripheric force of driving gear act in the plane of circular ring (fig. 1b).

Prof. Dr.-Ing. Milomir Gašić, Faculty of Mechanical Engineering Kraljevo, gasic.m@mfkv.kg.ac.yu
Ass.Dr.- Ing. Mile Savković, Faculty of Mechanical Engineering Kraljevo, savkovic.m@mfkv.kg.ac.yu
Ass.Mr.- Ing. Goran Marković, Faculty of Mechanical Engineering Kraljevo, markovic.g@mfkv.kg.ac.yu
Ing. Nebojša Zdravković, Faculty of Mechanical Engineering Kraljevo, zdravkovic.n@mfkv.kg.ac.yu

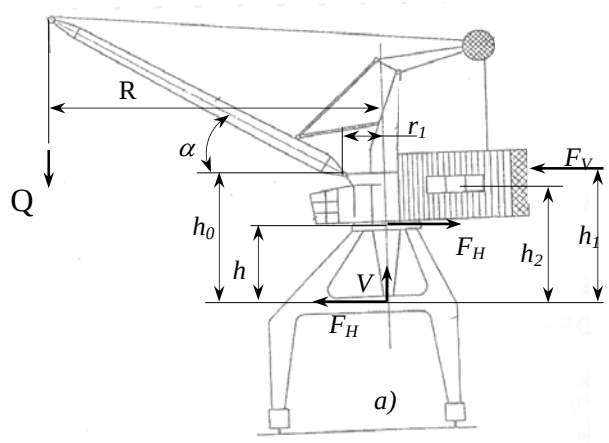

Fig. 1.

Weights of circular ring, circular track, and big gear act perpendicular to the plane of circular ring.
External loads of circular rings cause the following:

- bending moment X_1
- axial force X_2
- radial force X_3 (fig. 2)

Their values are defined by equation system (1) and expressions (2) [2]:

$$X_1 = \sum_{i=1}^{n} P_i \cdot r \cdot \chi_{1P}(\varphi_i) + \sum_{j=1}^{m} T_j \cdot r \cdot \chi_{1T}(\varphi_j) + \sum_{k=1}^{i} M_k \cdot \chi_{1M}(\varphi_k)$$

$$X_2 = \sum_{i=1}^{n} P_i \cdot r \cdot \chi_{2P}(\varphi_i) + \sum_{j=1}^{m} T_j \cdot r \cdot \chi_{2T}(\varphi_j) + \sum_{k=1}^{i} M_k \cdot \chi_{2M}(\varphi_k)$$

$$X_3 = \sum_{i=1}^{n} P_i \cdot r \cdot \chi_{3P}(\varphi_i) + \sum_{j=1}^{m} T_j \cdot r \cdot \chi_{3T}(\varphi_j) + \sum_{k=1}^{i} M_k \cdot \chi_{3M}(\varphi_k) \quad (1)$$

where:

$$\chi_{1P}(\varphi_i) = \frac{1}{2\cdot\pi}\cdot(1+\varphi\cdot\sin\varphi)$$

$$\chi_{1T}(\varphi_i) = \frac{1}{2\cdot\pi}\cdot(\varphi\cdot\cos\varphi-\sin\varphi-\varphi)$$

$$\chi_{1M}(\varphi_i) = \frac{1}{2\cdot\pi}\cdot(-\varphi-2\cdot\sin\varphi)$$

$$\chi_{2P}(\varphi_i) = \frac{-\varphi\cdot\sin\varphi}{2\cdot\pi}$$

$$\chi_{2T}(\varphi_i) = \frac{1}{2\cdot\pi}\cdot(-\varphi\cdot\cos\varphi+\sin\varphi)$$

$$\chi_{2M}(\varphi_i) = \frac{\sin\varphi}{\pi}$$

$$\chi_{3P}(\varphi_i) = \frac{-\varphi\cdot\cos\varphi}{2\cdot\pi}$$

$$\chi_{3T}(\varphi_i) = \frac{1}{2\cdot\pi}\cdot(\varphi\cdot\sin\varphi+\cos\varphi)$$

$$\chi_{3M}(\varphi_i) = \frac{\cos\varphi}{\pi} \quad (2)$$

P_i - radial force in the ring plane,
T_j - tangent force in the ring plane,
M_k - moment in the ring plane.

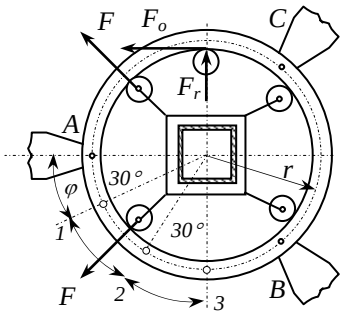

b)

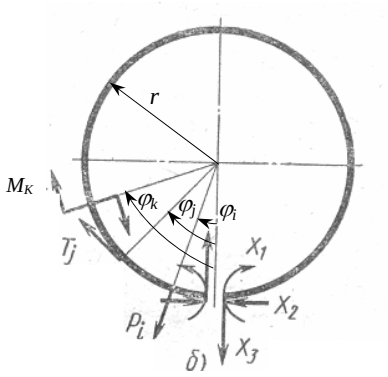

Fig. 2.

The loads caused by weights of circular ring, circular track, and big gear act in the plane perpendicular to the plane containing the ring. The moments X_1 and X_2 and forces X_3 (fig. 3) are defined by equation system (3) and expressions (4):

$$X_1 = \sum_{i=1}^{n} P_i \cdot r \cdot \mathfrak{M}_{1P}(\varphi_i) + \sum_{j=1}^{m} M_j \cdot \mathfrak{M}_{1M}(\varphi_j) + \sum_{k=1}^{i} M_k \cdot \mathfrak{M}_{1K}(\varphi_k)$$

$$X_2 = \sum_{i=1}^{n} P_i \cdot r \cdot \mathfrak{M}_{2P}(\varphi_i) + \sum_{j=1}^{m} M_j \cdot \mathfrak{M}_{2M}(\varphi_j) + \sum_{k=1}^{i} M_k \cdot \mathfrak{M}_{2K}(\varphi_k)$$

$$X_3 = \sum_{i=1}^{n} (-P_i)\cdot\varphi_i \cdot \frac{1}{2\cdot\pi} + \sum_{k=1}^{i} \frac{M_j}{2\cdot\pi\cdot r} \quad (3)$$

where:

$$\mathfrak{M}_{1P}(\varphi_i) = \frac{\varphi\cdot\sin\varphi}{2\cdot\pi}$$

$$\mathfrak{M}_{1M}(\varphi_i) = \frac{\varphi\cdot\cos\varphi+\sin\varphi}{2\cdot\pi}$$

$$\mathfrak{M}_{1K}(\varphi_i) = \frac{-\varphi-\sin\varphi}{2\cdot\pi} + \frac{\cos\varphi}{\pi\cdot\left(1+\frac{G\cdot I_0}{E\cdot I_x}\right)}$$

$$\mathfrak{M}_{2P}(\varphi_i) = \frac{-\varphi+\varphi\cdot\cos\varphi}{2\cdot\pi}$$

$$\mathfrak{M}_{2M}(\varphi_i) = \frac{-1-\varphi\cdot\sin\varphi+\cos\varphi}{2\cdot\pi}$$

$$\mathfrak{M}_{2K}(\varphi_i) = \frac{-\varphi \cos\varphi}{2\cdot\pi} - + \frac{\sin\varphi}{\pi\cdot\left(1+\frac{G\cdot I_0}{E\cdot I_x}\right)} \qquad (4)$$

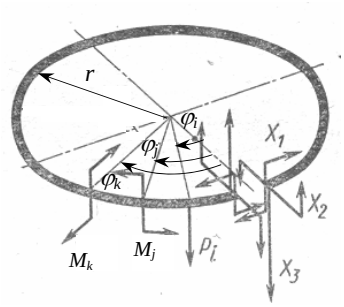

Fig. 3.

According to the expressions (4) relating to $\mathfrak{M}_{1K}(\varphi_i)$ and $\mathfrak{M}_{2K}(\varphi_i)$, there are relations GI_0/EI_x, too (5).

$$\frac{G\cdot I_0}{E\cdot I_x} \qquad (5)$$

where
E - modulus of elasticity,
G - modulus of sliding,
I_x - rectangular moment of inertia,
I_0 - torsional moment of inertia.

If the ring has the shape of a box-like carrier made of steel sheets having constant thickness, the dependence (5) can be transformed into less complicated form by means of relation [3].

$$\frac{I_x}{I_0} = \frac{2\cdot k}{3} \qquad (6)$$

where

$k = \frac{h}{b}$ - relation between the height and width of the cross section of box-like carrier (fig.4).

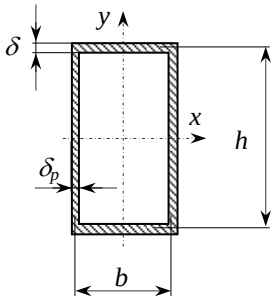

Fig. 4

A new relation is obtained by transformations (5):

$$\frac{G\cdot I_0}{E\cdot I_x} = \frac{\sqrt{3}}{3\cdot k} \qquad (5.1)$$

Radial and tangent forces act in the plane of circular ring, while forces act in the plane perpendicular to the ring plane, so the addends containing the moments M_k can be taken out from equation system (1). Only the first addends (perpendicular forces P_i, fig.3) remain in equation system (3).

Equations (1) and (3) as well as above mentioned conclusion have been applied in order to calculate the circular ring of a three-legged portal crane (fig. 1a) having the following characteristics:

Q = 3,2t - load weight
R = 22m - maximum boom reach
n = 1,6°/min - number of column revolutions
α = 25° - minimal angle of boom
h = 3,75m - distance between upper and lower support
r_1 = 1,2m - distance between boom joint and axis of revolving column
h_0 = 8,5m - distance between boom joint and lower support
h_1 = 8,5m - distance between wind force acting on the column and counterweight
h_2 = 6,5m - distance between counterweight centre and lower support
r = 1,5m - radius of circular ring

Pressure forces of supporting wheels acting on the ring, and peripheric and radial force of gear are presented although the calculation has not been shown here:

F= 270kN - force acting on a supporting wheel,
F_o = 96kN - peripheric force acting on the gear,
F_r = 35 kN - radial force acting on the gear.

The analysis of the ring loads is done at the part of the ring between two joints (A and B).

The values of moment X_1 at any cross section of the ring are determined if the first equation from equation system (1) is used. Diagram (fig.5) shows the calculation results of moment X_1 at ring cross sections A, 1, 2, 3 and B. Maximum value is at point 2:

$$X_{1,max} = \left(\frac{X_1}{r}\right)\cdot r = 110.51\cdot 150 = 16576.5\ kNcm$$

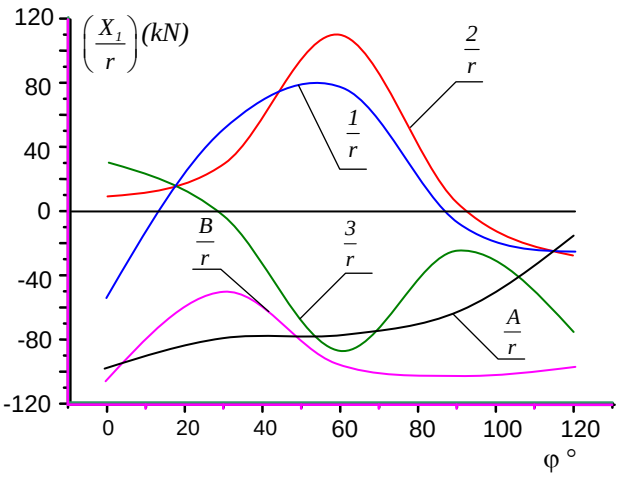

Fig. 5

The values of axial forces X_2 at any cross section of the ring are determined if the second equation from equation system (1) is used. Diagram (fig.6) shows the values for ring cross sections A, 1, 2, 3 and B.

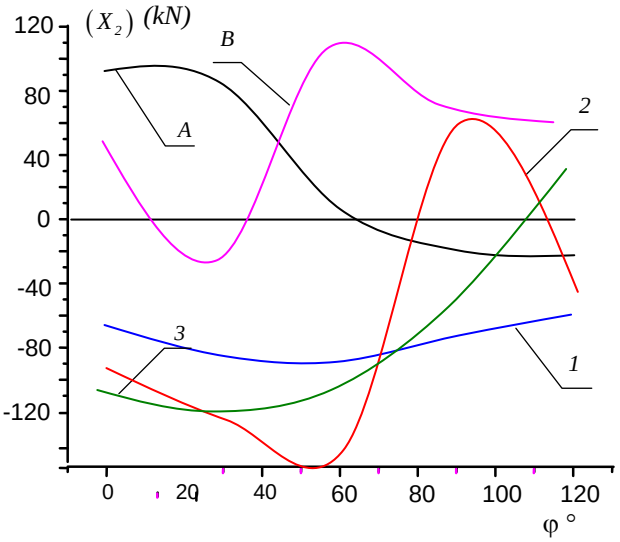

Fig. 6

The values of transversal forces X_3 at any cross section of the ring are determined if the third equation from equation system (1) is used. Fig.7 shows the calculation results of points A, 1, 2, 3 and B.

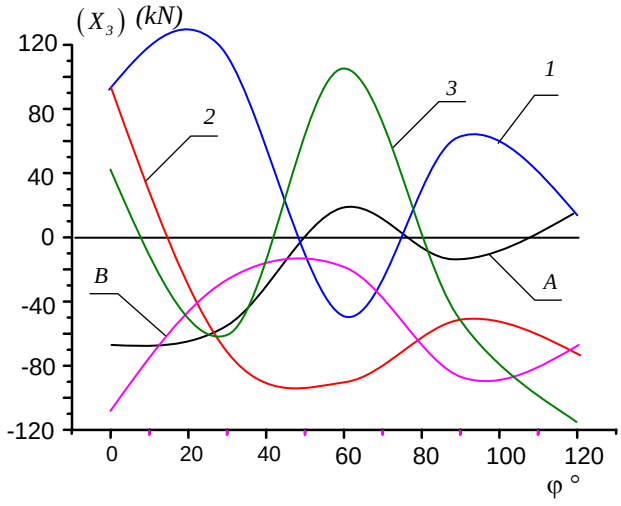

Fig. 7

The loads of ring, circular track and big gear are small in comparison to the loads at horizontal plane, so these influences are neglected, i.e. the moments X_1 and X_2 and force X_3 are not presented in the paper.

If loads are presented for that position of supporting wheel by means of FME, we get the following results (Table 1). These results are also maximum values of X_1, X_2 and X_3.

	Point	Axial force, kN	Transversal force, kN	Moment, kNm
FME	2	- 148,623	- 91,088	16634,260
Theoretical calculation	2	- 148,10	- 91,28	16576,50

Table 1

It should be mentioned that the values of X_1, X_2 and X_3 for points (A, 1, 3 and 4) are approximately equal to the values obtained by FME (deviations less than 10%).

4. CONCLUSION

If the calculation results of circular ring at portal cranes having a column are analysed by theoretical expressions for ring calculation, they fully correspond with the calculation results obtained by FME. This conclusion is very important because theoretical analysis of ring loads can be done with the influence of various parameters being significant for decreasing the ring stress.

REFERENCE

[1] KURTH, F., SCHULZE, W., UND WARKENTHIN. *Hinweise zur statischen berecnung von portalkranstruktionen fur Blocksaulen Drehkrane*, Wissenschaftiche Zeitschrift TH Magdeburg, 8 Jg 1984 N.1

[2] БОЯРШИНОВ С. В. *Основы строительной механики машин* , Машиностреоение, Москва, 1973.

[3] DEDIJER, S., GAŠIĆ, M. *Određivanje zavisnosti između krutosti na savijanje i uvijanje kod sandučastih nosača*, IX naučno stručni skup o transportnim procesima u industriji, Beograd, 1986.

LOADING CAPACITIES CURVES FOR HE-A/B-SECTION RUNWAY BEAMS ACCORDING TO BOTTOM FLANGE BENDING

Z. Petković, V. Gašić, S. Bošnjak, N. Zrnić

Abstract: *Designers of hoisting machines have to solve problems related to determination of structural elements in runway lines or single-girder cranes. Particularly, fast technical solutions are required in initial stages of design process, interactive with possibilities of structural elements suppliers and appropriate with demands of national regulative for designing those systems. This paper presents loading capacity curves of HEA/B beam runway beams according to capacities due to strength of bottom flange. Given curves are suitable for most industrial HEA/B runway beams and can be used for selection of HEA/B beam structural elements for different type of trolleys. Also, they can be used for fast capacity check of beams in runways, along with comparation with capacities of I-beams.*

Key words: *HE-A, HE-B beam, runway, bottom flange bending, single-girder crane.*

1. INTRODUCTION

Every runway beam need to have static calculus corresponding to national regulative. Design problems of HE-A/B section runway beams, as in single-girder overhead and underhung (suspension) cranes, are related with bending moments about its strong axis which lead to bending stresses at points in the middle of the structure. Furthermore, there is design check for local bending of steel beam bottom flange. Moreover, lateral buckling is important limit state that must be considered and there is check of structural deflections. All of these facts are necessary to be considered in design of runway beam. Design examples are given in [1], [5].

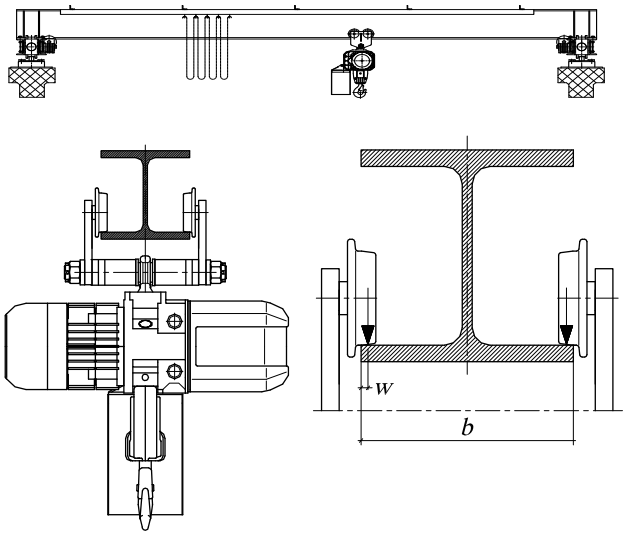

Fig. 1. *HEA section runway beam (single girder crane)*

As known, influence of trolley/crane wheels on HEA/B or I runway beams results in local loadings producing biaxial stresses. This area of research is presented in [4].

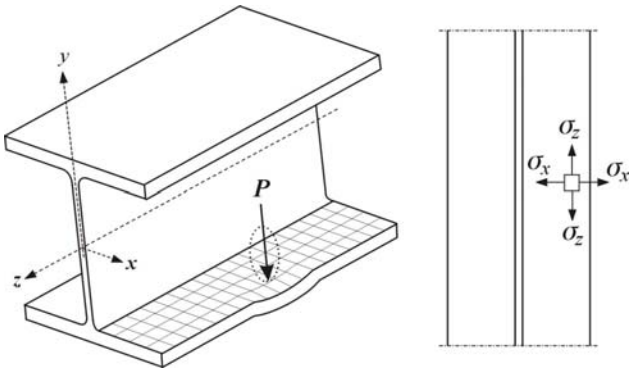

Fig. 2. *Biaxial stresses on flange under wheel loading*

Hence, overall stress field of runway beams and lateral buckling stability have to be checked by designers. Nowadays, designers face requests for fast problem solving and adoption of structural elements. HEA/B beams according to EURONORM 53-62 are widely used for crane systems. Generally, we can say that those beams have great lateral buckling stability but lower bottom flange capacity (this can differ from technical prerequisitions like span, trolley width...) than I-beams according to JUS.C.B3.131 with similar capacities [7].
In this paper are given useful charts for capacities of HEA/B section runway beams, due to bending and bottom flange bending as key critical state, for capacities up to 12 t, and spans up to 10 m. Lateral buckling capacity and structural deflection state are not considered here.

Prof. Dr.-Ing. Zoran Petković, Faculty of Mech.Engineering, Belgrade, zpetkovic@mas.bg.ac.yu
Ass.Mag.-Ing. Vlada Gašić, Faculty of Mech.Engineering, Belgrade, vgasic@mas.bg.ac.yu
Ao. Prof. Dr.-Ing. Srđan Bošnjak, Faculty of Mech.Engineering, Belgrade, sbosnjak@mas.bg.ac.yu
Ass.Dr.-Ing. Nenad Zrnić, Faculty of Mech.Engineering, Belgrade, E-mail: nzrnic@mas.bg.ac.yu

2. THEORETICAL PREREQUISITIONS

2.1 Corresponding expressions for bottom flange bending

Bottom flange bending depends of 3 parameters: bottom flange thickness, i.e. HEA/B section, the location of the wheels with respect to the beam end and load per wheel (***P***). There are several expressions for describing such influences. In Serbian design procedures for HEA/B runway beams, it is common to use Mendel recommendations for bottom flange bending [5], [2]. Design check is performed for bottom flange points A,C, fig.3.

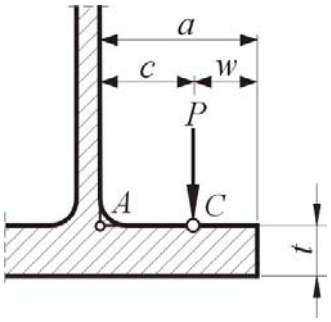

Fig. 3. *Review of bottom flange characteristic points*

Bottom flange bending stresses are presented as:

$$\sigma_{Ax} = \pm K_{Ax} \cdot \frac{P}{t^2}, \qquad \sigma_{Az} = \pm K_{Az} \cdot \frac{P}{t^2}$$

$$\sigma_{Cx} = \pm K_{Cx} \cdot \frac{P}{t^2}, \qquad \sigma_{Cz} = \pm K_{Cz} \cdot \frac{P}{t^2}$$

Coefficients (by Mendel) for bottom flange bending, in respect to ratio ***c/a*** and denotation on fig.3, are presented on following diagram, fig. 4.

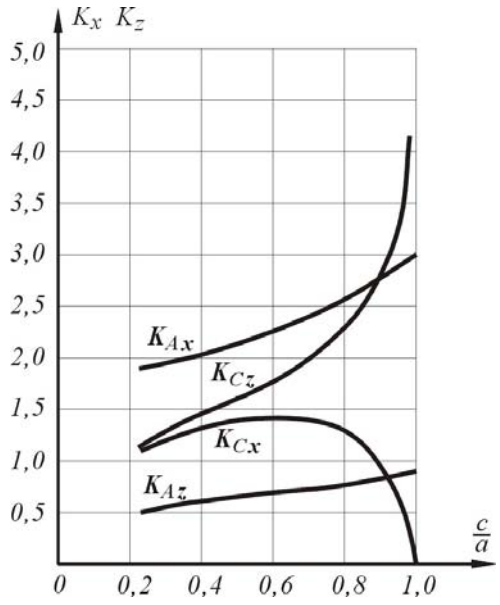

Fig. 4. *Bottom flange bending coeff. by Mendel*

Polynomial fits of these functions with errors up to 5 %, which satisfies engineering calculations, can be presented as follows:

$$K_{Ax} = 1.85414 - 0.06529 \cdot \xi + 1.20813 \cdot \xi^2$$

$$K_{Az} = 0.40677 + 0.47403 \cdot \xi - 0.00991 \cdot \xi^2$$

$$K_{Cx} = -0.53296 + 12.90617 \cdot \xi - 35.27425 \cdot \xi^2 + 45.32993 \cdot \xi^3 - 22.25349 \cdot \xi^4$$

$$K_{Cz} = -2.88333 + 43.90676 \cdot \xi - 179.1317 \cdot \xi^2 + 358.79953 \cdot \xi^3 - 344.40559 \cdot \xi^4 + 128.20513 \cdot \xi^5$$

where

$$\xi = \frac{c}{a}$$

Generally, design of HEA/B runway beam starts with stresses from global bending and finishes with design check for bottom flange, with above mentioned procedures. With higher level of global bending stresses design check of bottom flange can turn calculus to the beginning. Also, different manufacturers of trolleys have different wheels and their mounting instruction on HEA/B beams that can influence bottom flange bending. In this paper it is presented diagrams for loading capacity for commonly used HEA/B runway beams for fast determination of steel beams. Loading capacity is determined due to beam span (***L***) and wheel position on beam (***w***), fig. 3. FE analysis of runway beams is related to the finite element contact problems or shells [2], [3], and, with this complicacy and no possibility to generalize solution, can only be used for verification of analytical models, fig.5.

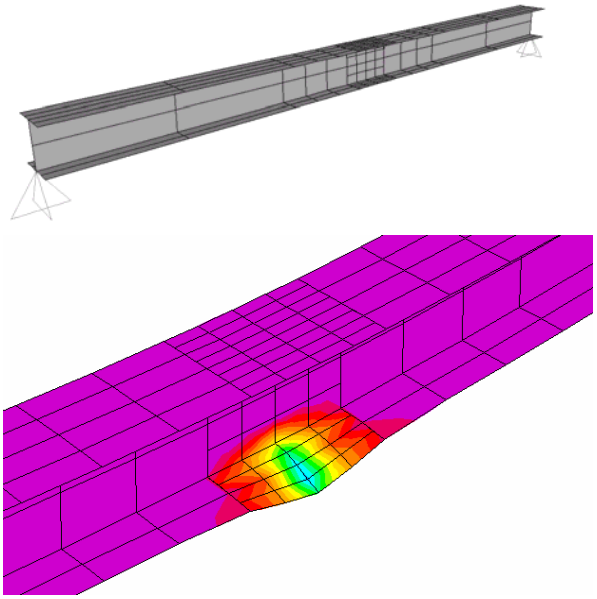

Fig. 5. *SAP 2000 presentation of bottom flange bending*

2.2 Stresses combination

Design criterion for this case, according to 2.1 of this paper, is that stress field in bottom flange of HEA/B section runway beam reach values of allowable stresses.
As known, global bending in runway beams are estimated as follows:

$$\sigma_z(z) = \frac{M_x(z)}{W_x},$$

where $M_x(z)$ is bending moment round x axis, and W_x is section modulus of runway beam about x axis.

Combined stresses on bottom flange are calculated as:

$$\sigma_A = \sqrt{\left(\sigma_z^A + \sigma_{Az}\right)^2 + \sigma_{Ax} - \left(\sigma_z^A + \sigma_{Az}\right)\sigma_{Ax}}$$

$$\sigma_C = \sqrt{\left(\sigma_z^C + \sigma_{Cz}\right)^2 + \sigma_{Cx} - \left(\sigma_z^C + \sigma_{Cz}\right)\sigma_{Cx}}$$

Stress design check for section bottom flange is

$$\sigma_A < \sigma_{dopI},\ \sigma_C < \sigma_{dopII}$$

where $\sigma_{dopI}, \sigma_{dopII}$ presents allowable stresses that depend on HEA/B beam material and load cases.

2.3 Algorithm formulation

According to above mentioned expression it can be concluded that strength of specific HEA/B beam depends of beam span ***(L)*** and wheel position on beam (***w***). It is known for runway beams that maximum bending stresses occurs in the middle of the span for hoist positioned there, fig. 6. Bottom flange bending stresses occurs on section where hoist is positioned.
Thus, loading capacity of runway beams comes from strength of its middle section.

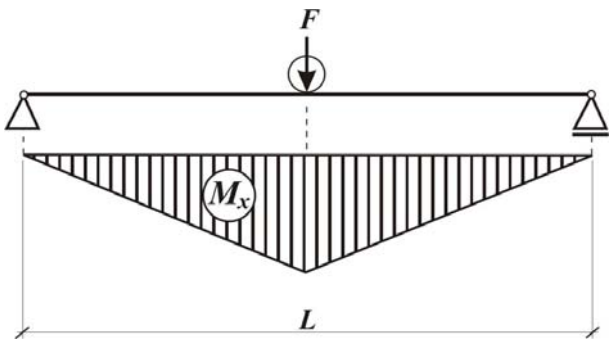

Fig. 6. *Maximum bending moment of runway beam*

Following algorithm aproximate and assumes maximum bending moment

$$M_{x\max} = 1.1\frac{F \cdot L}{4},$$

where multiplication coefficient 1.1 includes bending moment of beam self weight.
Also, following charts are gained for HEA/B runway beams for 4-wheel trolleys (which are mostly used). That gives load per trolley wheel

$$P = \frac{F}{4}$$

Developed algorithm in software MathCAD, include Mendel coefficients in terms of position of wheels respect to beam end, fig.3 , with obvious relation

$$w = a - c,$$

which is more suitable for trolley selection.

Presuming critical states when values of stresses reach values for allowable stresses

$$\sigma_A(F, L, w) = \sigma_{dopI}$$

$$\sigma_C(F, L, w) = \sigma_{dopII},$$

it can be found capacities due to strength criterion for characteristic points of bottom flange.
If we note loading capacity of bottom flange as minimum capacity of points A, C we have capacity as function of 2 variables

$$F(L, w) = \min(F_A, F_C)$$

and can be presented as contour plot. Generally, it can be presented as 3D plot, fig.7, but it would be more difficult for data collection. Presentation in contour plot has advantage because contours present loading capacities in terms of nominal hoists capacities, which is necessary for runway beams.

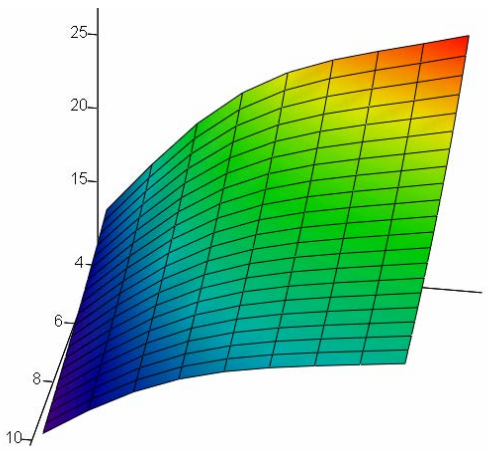

Fig. 7. *3D presentation of capacity F(L,w)*

3. INTERNATIONAL REGULATIVES

Paragraph 2. shows notation and bottom flange bending coefficients according to Mendel. Here is presented review of German recommendations for bottom flange bending of crane systems, which is detailed in [6]. Notation of characteristic sections, 0,1,2 for HEA/HEB beam and box-section beam is presented at fig. 8.

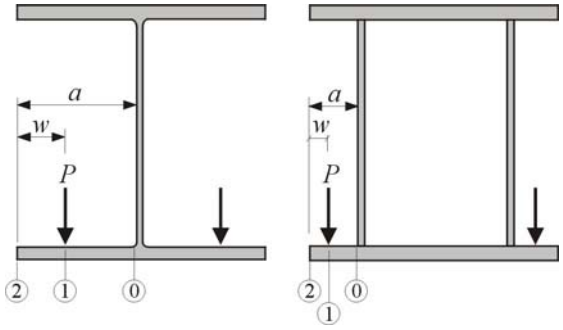

Fig. 8. *Bottom flange calculus,* [6]

Procedure for bottom flange calculus, according to this, is also given in terms of coefficients of local bending, depending on $\lambda = \frac{w}{a}$, and will be presented in tabular form, table 2.2.1.

Tab. 2.2.1 Coefficient of local bending, [6]

λ	Cz,0	Cz,1	Cz,2	Cx,0	Cx,1
0.10	0.192	2.303	2.169	-1.898	0.548
0.15	0.196	2.095	1.676	-1.793	0.759
0.20	0.204	1.968	1.290	-1.687	0.932
0.25	0.219	1.872	0.984	-1.577	1.069
0.30	0.242	1.789	0.737	-1.463	1.172
0.35	0.272	1.711	0.533	-1.343	1.244
0.40	0.312	1.635	0.362	-1.216	1.287
0.45	0.364	1.560	0.215	-1.077	1.303
0.50	0.428	1.485	0.085	-0.923	1.293
0.55	0.508	1.411	-0.032	-0.747	1.260
0.60	0.605	1.336	-0.138	-0.542	1.204
0.65	0.723	1.262	-0.238	-0.295	1.128

4. RESULTS

Previous algorithm can be used for any HEA or HEB section runway beam. Chart 1. presents results of capacities due to strenght of bottom flange for commonly used HEA beams (EURONORM 53-62) and chart 2. presents results of capacities due to strenght of bottom flange for HEB beams. Also, allowable stresses $\sigma_{dopI}, \sigma_{dopII}$ are taken for material S235JRG2 (C.0361).

However, since loading capacity is proportional to allowable stresses, following charts can give runway beam capacity for other materials as well. For runway beams built up from S355JR (C.0561), loading capacities can be calculated as

$$\boldsymbol{F(C.0561)} = 1{,}5 \cdot \boldsymbol{F(C.0361)}$$

According to the data of world known producers of hoists and single-girder cranes, charts are given with practical limits of variables, i.e. with beam spans (L) up to 10 m and wheel position dimension (w) up to 37 mm. For bigger spans, due to other influences on runway, it is common to use horizontal truss to prevent occurrence of lateral instability.

5. CONCLUSION

Previous algorithms give useful curves for application in design process of HEA/B runway beams. It is presented charts for loading capacity due to bottom flange bending. According to these values it can be easily found suitable structural element for runway beams, concerning demands of strength. Also, it can be used for design check of built up runway beams. Especially, it is useful in situation with unknown producers of trolleys where position of wheel load can't be easily determined. Thus, it provides analysis of loading capacity changes due to different wheel load positions according to width of trolley wheel. Also, it can be used for comparation of capacities with I-section beams. Finally, it can be used for design process of monorail tracks with chain or electric hoists.

REFERENCES

[1] BUĐEVAC, D., MARKOVIĆ, Z., BOGAVAC, D., TOŠIĆ, D, *Metalne konstrukcije*, Građevinski fakultet u Beogradu, Beograd, 1999.

[2] PETKOVIĆ, Z., BOŠNJAK, S., MATEJIĆ, P., *Analiza naponskih stanja usled lokalnog savijanja pojasa I nosača*, Transport u industriji, str. 337-342, Mašinski fakultet u Beogradu, Beograd, 1994.

[3] PETKOVIĆ, Z., BOŠNJAK, S., MARJANOVIĆ, B., *Comparative presentation of analytical and numerical method for determination of stresses due to local effects of the rail placed in the middle of the double-beam bridg crane band*, Proc. of the 16th International Conference on Material Handling and Warehousing, pp. 1208-1216, Faculty of Mechanical Engineering, Belgrade, 2000.

[4] MENDEL, G., *Berechnung der Tragerflansch-beansprung mit Hilfe der Plattentheorie*, Fordern und Heben, 14/1972.

[5] PETKOVIĆ, Z., OSTIĆ, D., *Metalne konstrukcije u mašinogradnji 1*, Mašinski fakultet u Beogradu, Beograd, 1996.

[6] SEEBELBERG, C., *Kranbahnen, Bemessung und konstruktive Gestaltung*, Bauwerk Verlag Gmbh, Berlin, 2005

[7] ZRNIĆ, N., BOŠNJAK, S.,GAŠIĆ, V., *Loading capacities curves for I-section runway beams according to bottom flange bending and lateral buckling*, MACHINE DESIGN monograph, pp. 181-186, Adeko, Novi Sad, 2008.

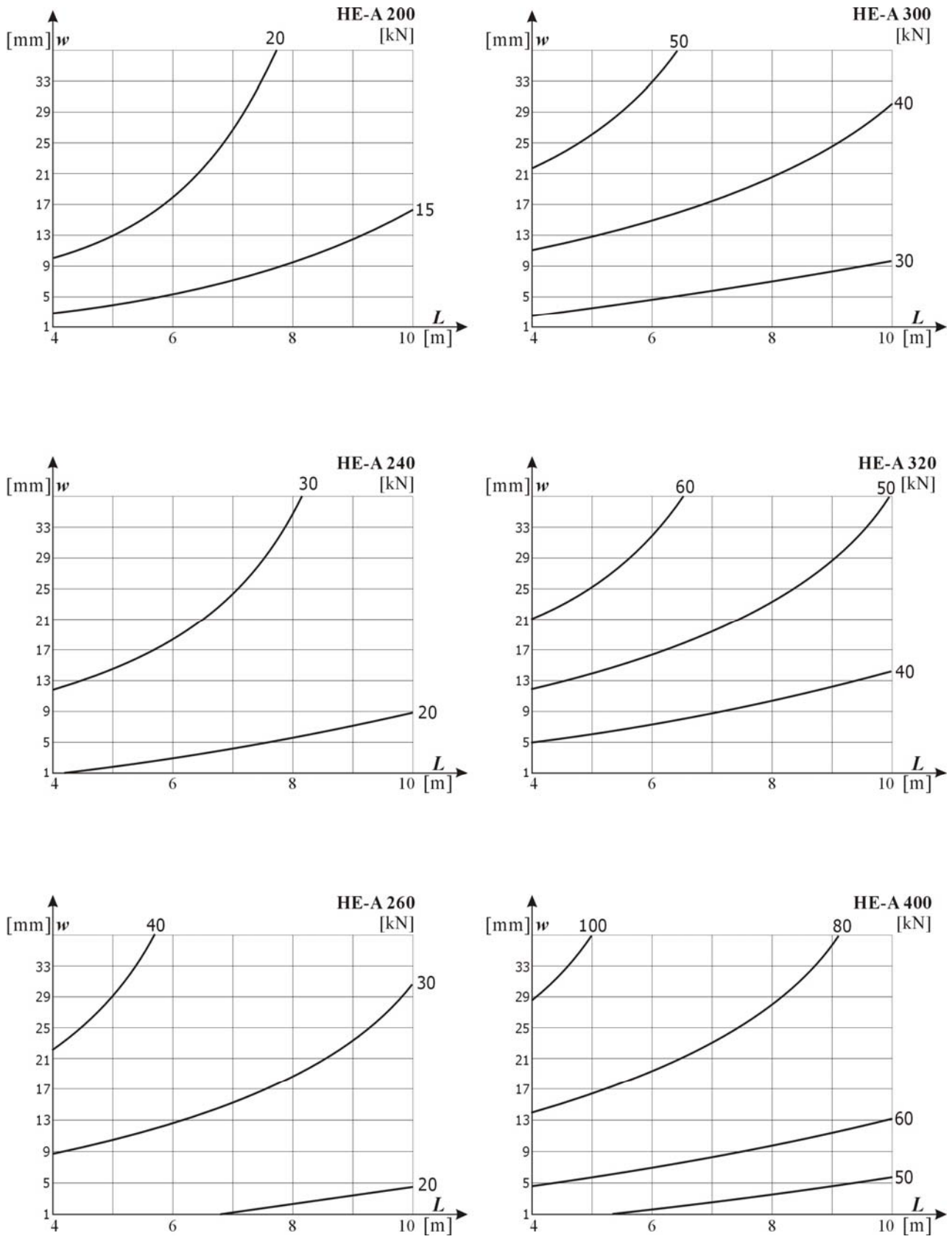

Chart 1. *Loading capacities of* ***HE-A*** *section runway beams due to bottom flange bending (EURONORM 53-62, S235JRG2 (C.0361)*

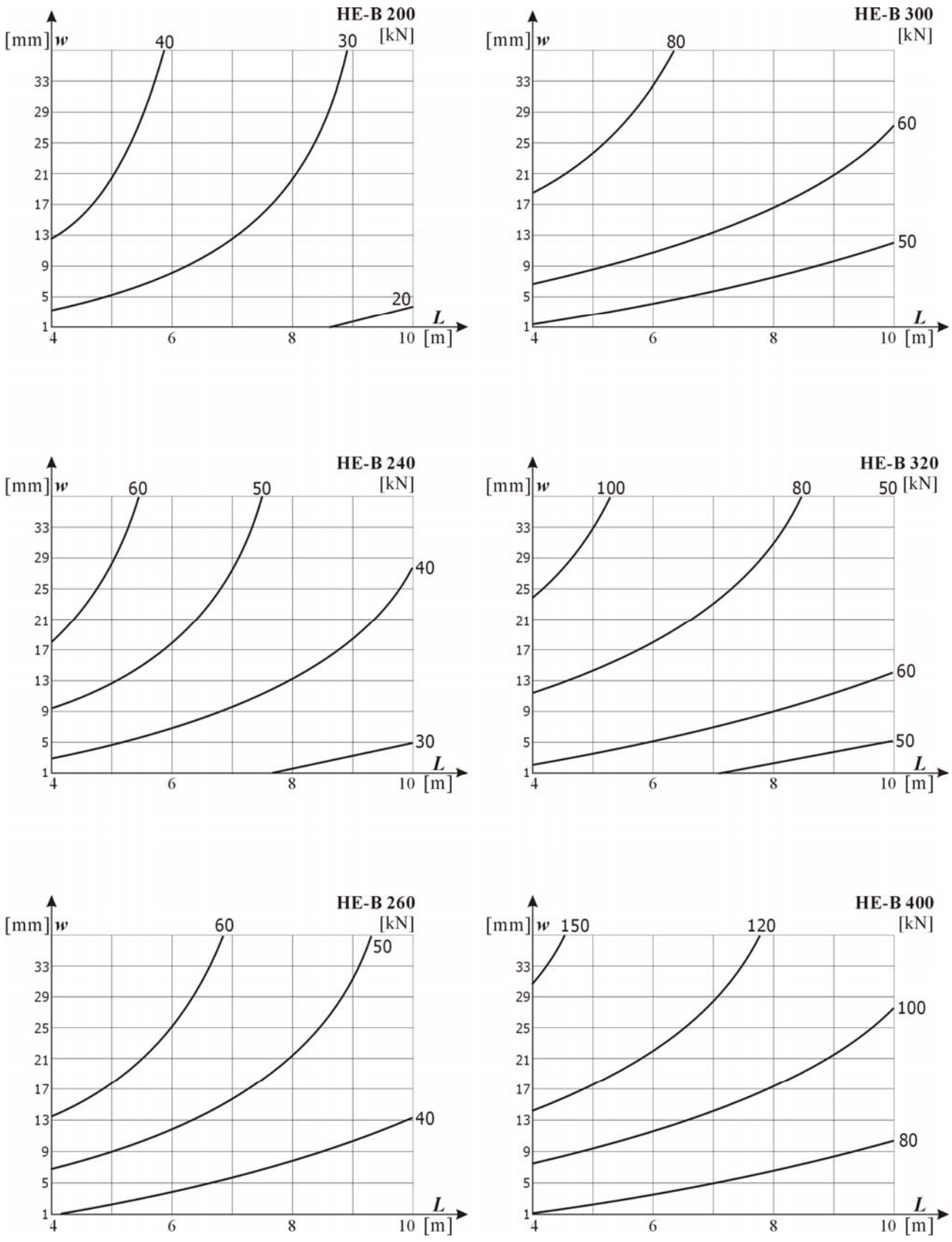

Chart 2. *Loading capacities of* ***HE-B*** *section runway beams due to bottom flange bending (EURONORM 53-62, S235JRG2 (C.0361)*

APPLICATION OF MOVING LOAD PROBLEM IN DYNAMIC ANALYSIS OF UNLOADING MACHINES WITH HIGH PERFORMANCES

N. Zrnić, S. Bošnjak, V. Gašić

Abstract: *The paper gives an analysis of dynamic behavior of cranes caused by action of moving loads. The paper gives an introductory survey of general papers treating moving load problem that can be useful in analysis of dynamic behavior of structures of unloading machines with high performances. Some recent results concerning application of moving load problem in analysis of structural dynamic behavior of boom of mega quayside container cranes are given.*

Keywords: *moving load, unloading machines, dynamics, modeling, structures.*

1. INTRODUCTION ON THE MOVING LOAD PROBLEM

The moving load problem is a fundamental problem in structural dynamics. In contrast to other dynamic loads these loads vary not only in magnitude but also in position. The importance of this problem is manifested in numerous applications in the field of transportation. Bridges, guideways, cranes, cableways, rails, roadways, runways and pipelines are examples of structural elements to be designed to support moving masses. Interest in analysis of moving load problems originated in civil engineering (from observation that when an elastic structure is subjected to moving loads, its dynamic displacements and stresses can be significantly higher than those due to equivalent static loads) for the design of rail-road bridges and highway structures. The detailed review of previous researches, including comprehensive references list, can be found in a dedicated excellent monograph written by Fryba [1] on the subject of moving load problems, where most of the analytical methods previously used are described.

Beam structures are commonly considered as three-dimensional bodies with one dimension significantly larger than the other two. In general a length to width (height) ratio of 5-10 of the structural members is sufficient. This means that the structures subjected to moving loads, such as bridges, guideways and large span cranes are often well qualified for being modeled as beam structures. It is generally applied fundamental beam theory according to Euler-Bernoulli and Saint Venant, which is not including warping (Vlasov) torsion, because cross sections of e.g. cranes relevant for moving load analysis have closed thin-walled profiles, such as for bridge cranes, gantry cranes, container cranes, etc. Some of structural assumptions in analysis of moving load problem are: initially straight beam, undeformable beam cross-section, linear elastic material and constant material properties over the beam cross section, small structural deformations, shear strains according to Saint Venant and negligible damping effects [2]. Bernoulli-Euler beam theory is valid for lower modes analysis of small vibration of slender beams at relatively low velocities that is the case for supporting structures of cranes, where merely the lower modes are of practical relevance for analysis of dynamic behavior and where the maximum currently existing velocities for e.g. mega container cranes are not exceeding 6 m/s that is small comparing with velocities of trains. For low velocities the bending effect is dominant factor on vibration of structures.

The basic approaches in vehicle modeling are: moving force model; moving mass model; vehicle suspension model. The simplest dynamic vehicle models are the moving force models. The consequences of neglecting the structure-vehicle interaction in these models may sometimes be minor. In most moving force models the magnitudes of the contact forces are constant in time. A constant force magnitude implies that the inertia forces of vehicle are much smaller than the dead weight of the vehicle. Thus the structure is affected dynamically through the moving character of the vehicle only. All common features of all moving force models are that the forces are known in advance. Thus structure-vehicle interaction cannot be considered. On the other hand the moving force models are very simple to use and yield reasonable structural results in some cases. Moving mass as suspension model is an interactive model. Moving mass model, as well as moving force model, is the simplification of suspension model, but it includes transverse inertia effects between the beam and the mass. Interaction force between the moving mass and the structure during the time the mass travels along the structure considers contribution from the inertia of the mass, the centrifugal force, the Coriolis force and the time-varying velocity-dependent forces. These inertia effects are mainly caused by structural deformations (structure-vehicle interaction) and structural irregularities. Factors that contribute in creating vehicle inertia effects include: high vehicle speed, flexible structure, large vehicle mass, small structural mass, stiff vehicle suspension system and large structural irregularities. Finally, the vehicle speed is assumed to be

Doc. Dr.-Ing. Nenad Zrnić, Faculty of Mechanical Engineering Belgrade, nzrnic@mas.bg.ac.yu
Prof. Dr.-Ing. Srđan Bošnjak, Faculty of Mechanical Engineering Belgrade
Ass. MSc.-Ing.. Vlada Gašić, Faculty of Mechanical Engineering Belgrade

known in advance and thus not depend on structural deformations. For moving mass models the entire vehicle mass is in direct contact with the structure. In general, the dynamic structure-vehicle interaction predicted by such models is very strong. Since most of the mass of most vehicles is suspended on rather weak secondary suspension springs the interaction is in general overestimated. The vehicle suspension models are representing physical reality of the system more closely, because, often, the vehicle mass is suspended by means of springs and dampers in such models – moving oscillator problem. Any analysis of moving load problems must address fully the effects of the mass ratio between the moving mass and the support structure (M/mL) and speed of moving load.

Vibration analysis of structures elastically constrained at discrete points and carrying concentrated masses can be useful for practical analysis of structures having cable stays or tie bars, e.g. tower cranes, quayside container cranes and ship unloaders. The tie bars of the crane are representing intermediate elastic supports modeled as linear springs with constant stiffness and in many cases for long span booms their mass could not be neglected and should be discretized in corresponding points. Research done by [3] is analyzing dynamic response of bridge girders with elastic bearings to moving train loads using an analytical approach can be applicable in analyzing dynamic behavior of gantry cranes traversed by a trolley if one would to consider the influence of axial stiffness of crane legs.

Since the mid 1980s many authors has investigated the application of FEM for solving moving load problem as an alternative to analytical approaches, e.g. [4]. However, even nowadays the role of FEM in dynamic analysis of structures subjected to moving loads has not been as dominant as may be expected. The main reasons for this are: 1) for design studies quasi static approach is applied and dynamic magnification factors are used; thus FEM is used for static analysis only in such studies, 2) modern FEM packages are not suited for the moving load problem, especially when the structure-vehicle interaction is to be considered and 3) much of the theoretical efforts up to now have been concentrated on the determination of dynamic magnification factor as functions of a limited set of parameters; thus studies have to be made of simple structural models, which often favors the method of generalized displacements.

For all approaches in analysis of dynamic behavior of structures under moving loads, it is desirable at first to obtain an estimate of natural modes and frequencies of the structure that can be done by employing traditional finite element models [5]. In some books can be found collection of final expressions for eigenfrequencies of beams, mostly for beams with classical boundary conditions for one or multi-span beams or having combination of classical and non-classical boundary conditions in some simpler cases, [6]. However, for more complicated cases of boundary conditions the existing expressions are not applicable and each problem should be separately solved. For majority of the continual systems it is impossible to solve eigenfrequency problem and obtain result in closed-form solution that leads to the employment of some of the approximate methods involving discretization of the continual system.

2. LITERATURE REVIEW ON THE APPLICATION OF MOVING LOAD PROBLEM IN CRANES DYNAMICS

In the last 30 years the application of moving load problem is present in mechanical engineering studies. A typical structure under moving mass in mechanical engineering is an overhead crane, gantry crane, unloading bridge, tower crane, and shipunloader or quayside container crane. The application of moving load problem in cranes dynamics has obtained special attention on the engineering researchers in the last years, but unfortunately little literature on the subject is available. The following two features distinguish the moving load problem in crane industry from that in civil engineering. The first is that the structure on which the moving mass moves always has traveling or rotating motion. The second is that the payload of a crane is attached via cables to a carriage moving along the structure. Thus the dynamics of a crane includes both the vibration of the structure and the dynamics of the payload pendulum.

The paper [7] is according to the authors' best knowledge the first attempt to increase the understanding of the dynamics of cranes due to the moving load. The overhead crane trolley, modeled as a simply supported beam according to Euler-Bernoulli beam theory, traverses the beam at a known prescribed uniform speed and that the pendulum may be adequately modeled as a rigid massless bar. The motion of the pendulum is assumed to be planar with small angular displacements and displacement rates from the vertical. A set of coupled, non-linear equations of motion is derived via Hamilton's principle. The effects of varying the various parameters are investigated. The results obtained from the numerical calculations that employed the non-dimensional formulation of the problem indicate that the deflection of the beam is dependent on both the trolley speed and the mass of the combined speed and payload mass. In particular, the magnitude of the deflection increases with increasing crane mass at all trolley speeds. Also, the value of the maximum beam deflection for a given set of trolley and payload masses is dependent upon the trolley speed. For higher carriage speeds, the maximum beam deflection occurs close to the end of the beam where the carriage stops because the deflections are dominated by inertial effects of the carriage. At very slow speeds the beam behaves in a quasi-static manner and the maximum beam deflections occurs close to the middle of the beam. Those "very slow speeds" are, in the fact, the real trolley speeds, having in mind that the trolley cross travel speed, for standard industrial overhead traveling cranes with spans up to 35 m and lifting capacities up to 80 t, is up to 0,5 m/s. The dynamics of the pendulum is dependent on the

trolley mass, the payload mass, the length of the pendulum, and the trolley speed.

The next paper on the subject [8] extends the previous investigation by including in-plane and out-of-plane motion. The flexibility of the beam in both directions is accounted for and the trolley can accelerate along the length of the beam and the beam can accelerate in a direction perpendicular to its axis. The Rayleigh-Ritz solution technique is used to obtain the equations of motion of the system which are solved with a modified Newmark method. The effects of the beam travel and carriage traverse profiles, the length of the pendulum, and the payload mass on the swing of the pendulum are investigated. The examples indicate that the swing angles and frequencies are dependent on the length of the pendulum and the payload mass or the combined payload and carriage mass. The pendulum length results show that the dominant frequencies in the swing responses decreased with increasing pendulum length. The amplitude of swing angle increased with increasing payload mass, because of the increasing contributions of the forcing terms. Minimal changes were observed in the swing angle frequencies for corresponding changes in payload mass. This analysis reveals the complexity of the three-dimensional overhead crane dynamics. Regardless the fact that simultaneous operation of more than two mechanisms is forbidden for industrial cranes, the obtained results may be worthwhile and can be applied in the future for control issues of fully automated cranes and design of effective controllers.

The work in [9] is devoted to the problem of the vibration of tower crane slewing flexible jib structure simultaneously traversed by a moving mass – carriage. The authors didn't specify more precisely the type and geometry features of analyzed tower crane, but they have adopted the solution with two tie bars and tower head (cat head). The jib structure is modeled as clamped-free Euler-Bernoulli beam attached to a rotating rigid tower. The payload is modeled as a sphere pendulum of point mass attached to via massless inextensible cable the carriage moving on the rotating beam. Non-linear coupled equations of motion of the in- and out-of-plane of the beam and the payload pendulum are derived by means of the Hamilton principle. Some remarks are made on the equations of motion. The main goal of the paper was to present the mathematical model for the prediction of the jib dynamics of operating tower crane and its payload, in order to make foundation of the dynamical design and computing dynamical stress of the jib structure of a tower crane. Authors in [9] are making a mistake by a priori neglecting flexibility of tower crane mast. That can be done only after analyzing the dynamic behavior of the whole structure of tower crane, i.e. after defining natural modes of tower crane structure either by experimental methods or by FEM. It is conclusive that the uncritical a priori neglecting of tower stiffness leads to the mistake in modeling. Authors in [9] have modeled each tie bar by linear springs in "in – plane" and "out – of – plane" model that is incorrect. Tie bars and their connections with tower and jib are structurally realized to support loads dominantly in one plane, in this case vertical plane. Yang et al. (2007) have adopted boundary condition for beam slope $w'(0,t)=0$, implying that the jib is considered as cantilever in vertical plane. Having in mind that connection between jib and mast is usually realized with the structural hinge in order to enable jib pivoting around horizontal axis, it is conclusive that adopted boundary condition is not in accordance with prevailing structural solutions.

The paper [10] presents a technique developed for using standard finite element packages for analyzing the dynamic response of structures to time-variant moving loads. Computer program has been written which calculates the time-variant external nodal forces on a whole structure, which provide the equivalent load to point forces that move around the structure. The calculation of the equivalent nodal forces to represent the moving loads has been performed by three approximate methods. To illustrate the method and for validation purposes, the technique is first applied to a simply supported beam subject to a single load moving along the beam and, finally, it is applied to the problem of calculation of the effects of two-dimensional motion of the trolley with four moving forces on the response of the base structure of a mobile gantry crane model.

Dynamic response of structures to moving loads using combined finite element and analytical methods is given in [11]. The authors have developed a technique that includes inertia effects in the analysis. Natural frequencies and mode shapes are first calculated using a standard FEM package. Forced response of the structure is calculated using separate code developed in the paper. Rotary inertia of moving bodies is ignored as unimportant for particular mobile crane problem. The technique is first applied to a clamped-clamped beam subjected to a single mass moving along the beam, and it is then applied to the problem of predicting the dynamic response of an experimental mobile gantry crane structure due to two-dimensional motion of trolley.

In the paper [] the three-dimensional responses of a crane structure due to moving loads is analyzed. The axial, vertical and horizontal dynamic responses of the three-dimensional framework of a tyred overhead crane under the action of a moving trolley hoisting a swinging object were calculated using the finite element method and the direct integration method. Instead of the conventional moving force problem where only the vertical inertia effect of the moving trolley was considered, the three-dimensional inertial effects due to the masses of both the moving trolley and the swinging object have been considered in this paper. An equivalent moving mass matrix has been presented and which is dependent on both the instantaneous swinging angle of the hoisted object and the instantaneous position of the moving trolley, so that the contribution of the moving mass on the overall mass matrix of the entire structure itself is easily tackled. The problem was solved by calculating the forced vibration responses of the three-dimensional framework with time-dependent overall mass and damping matrices and subjected to an

equivalent moving force. Some factors relevant to the problem, such as the magnitude, velocity and acceleration of the moving trolley and the swinging angles of the hoisted object were studied. Numerical results reveal that, in addition to the conventional dynamic responses in the vertical direction, the other two components in the axial and horizontal directions for a three-dimensional structure are also significant.

3. SOME PRACTICAL ASPECTS IN MODELING AND COMMENTS ON RECENT RESULTS

It must be mentioned that the results of previous investigations on the application of moving load problem in dynamics of cranes previously described are valuable for understanding behavior of cranes traversed by a moving trolley, but some of them are only of restricted practical relevance. This is the consequence of the fact that standard industrial cranes with slow velocities of trolley are behaving in a quasi-static manner. The real future challenge in this field is to investigate dynamic behavior of cranes with high performances (heavy payloads and heavy trolleys) and long spans. Some examples of such cranes suitable for investigation of moving load impact are mega container cranes with flexible structures of booms (Malacca-max cranes require outreach of ca. 70 m [13]), large unloading bridges (FEM model of unloading bridge with span between legs of 76,2 m is shown in Fig. 1 [Zrnić et al., 2005]) and shipunloaders.

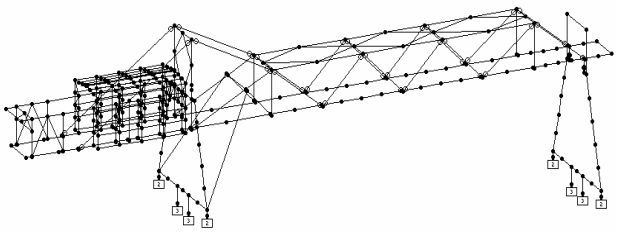

Figure 1. Large unloading bridge

Having in mind that the steel frame of the crane trolley is normally a stiff construction except some particular solutions of trolleys for unloading bridges for bulk materials, moving mass and moving load approach are most appropriate for analyzing influence of moving load on dynamic behavior of cranes. However, for heavy pay loads and trolleys, as for mega quayside container cranes where the weight of total moving load can exceed 170 t [13], the inertia of moving load could not be neglected so the moving mass approach will be appropriate for adequate analysis.

A recent application of moving load problem on analysis of dynamic behavior of mega container cranes is done in [13, 14]. Those works discuss influence of trolley motion to dynamic behavior of quayside large (mega) container cranes with flexible structure of monogirder boom with trapezoidal cross section for servicing container ships with 24 containers across beam (Malacca-max container ship). Some basic features of adopted crane are: boom length (outreach) is 69,2 m, span between rails (gage) is 30,48 m, backreach is 15,24 m and total moving load for machinery trolley system including weights of trolley, spreader, head block and two containers (twin twenties) is 175 t. Finite element model of this crane is shown in Fig. 2 [13].

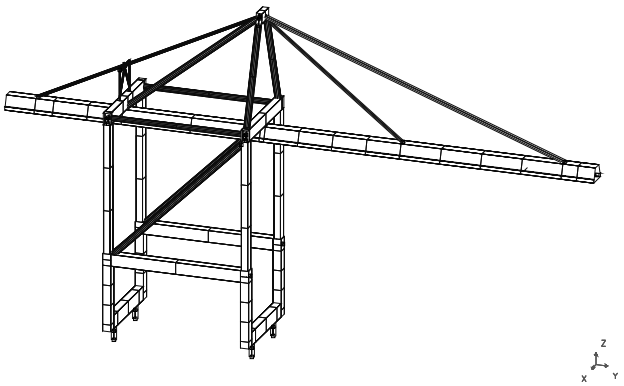

Figure 2. FEM model of mega container crane

By using FEM natural frequencies of crane structure are obtained. The first three modes that are relevant for dynamic analysis: vibrations of boom in horizontal plane; vibrations of structure in vertical plane in direction of trolley motion; vibrations of boom in vertical plane and in vertical direction perpendicular to direction of trolley motion. Excitation of structure in service due to the motion of load is most important from the aspect of dynamic analysis and it is ascertained that the boom on the water side (outreach), due to its large dimension and mass, is the most representative structural part identified for analysis of dynamic behavior. This fact confirms the cantilever nature of quayside container cranes, and imposes requirement for dynamic analysis of interaction problem between boom on water side leg of the crane and trolley as a moving load, i.e. trolley impact on the change of maximum values of deflections. Problem of dynamic behavior of quayside container cranes, i.e. vibrations of boom in vertical plane and vertical direction perpendicular to the direction of trolley motion, has not been analyzed in details since [13] because the concept of design of mega container cranes is still in progress and all dynamic problems could not be considered to the full. Application of flexible supporting structure for container crane which is adopted in [13], instead of the stiff structure, was pioneered in the last decade of 20th century, so that the cranes designed in such a way have higher values of dynamic deflections. Dynamic behavior of such mega quayside container cranes is quite different comparing with the elder types of cranes having fewer dimensions and worse performances of drives. It is observed that vibration of the boom on water side leg in vertical direction perpendicular to trolley direction are practically independent from other structural parts, and this vibration is recognized as one between first three

vibrations with lowest frequencies most important for dynamic analysis, figure 3 [13].

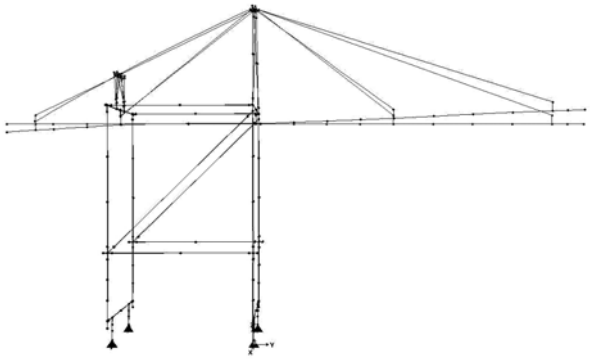

Figure 3. Vibrations of crane in vertical direction, f = 1,568 Hz

In the next stage of modeling process, consisting of several intermediate stages, the idealized equivalent reduced model is obtained. Relative deviation of natural lowest frequency of vibrations in vertical direction for idealized dynamic model is 1,36% in comparison with FEM model. FEM model is shown to be quite acceptable for validation of reduced idealized dynamic model, and the obtained deviation is very small from the view-point of an engineer. Equivalent mathematical model relevant for setting up differential equations of system motion is shown in Fig. 4. Equivalent stiffness c_1 and c_2 are representing, respectively stiffness of inner stay and forestay including stiffness of upper structure with mast, while lumped masses M_1 and M_2 comprise masses from stays weight. Length $L_r = L = 65{,}8$ m is presenting the real trolley path between the point A and forestay connection with boom in point C. The boundary conditions in point A have to be modeled as for a hinge, having in mind the real structural solution for the boom connection with other parts of the upper structure

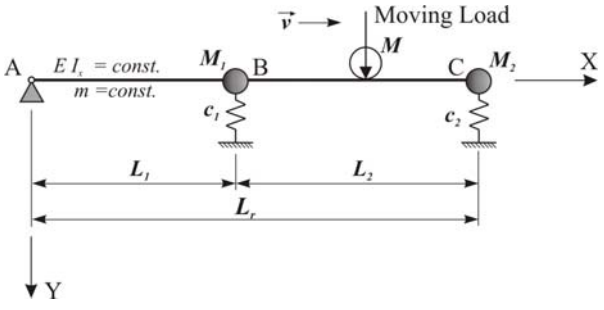

Figure 4. Mathematical model of container crane boom

The authors in [13,14] are using moving mass problem. In order to set up differential equations of mathematical model for the case of moving mass action, it was necessary to make model discretization, i.e. discretization of deflection shape of boom structure by predefined finite number of shape functions which belong to the class of admissible functions. Differential equations of motion for Euler-Bernoulli beam acted on by a mass with prescribed varying speed are formulated using a Lagrangian approach by using Assumed Modes Method to approximate the structural response in terms of finite number of admissible functions that satisfy the geometric boundary conditions of mathematical model. Differential equations are expressed to simulate shipment of container from dock to ship. It is assumed that the boom structure is not deformed at the beginning of trolley motion and that trolley travels with its maximum speed. The cycle of trolley motion is consisting of trolley uniform motion and trolley braking. Mathematical model formulated in such a way is also important from the aspect of analyzing problems occurring during positioning load in the shipment process due to the high values of flexible boom deflection. Selection and estimation of admissible functions is done by using variational approach of Rayleigh-Ritz. Admissible functions are employed because eigenfunctions of the system shown in Fig. 5 cannot be determined in practice due to the non-standard boundary conditions and added lumped masses. After several iterations the following admissible functions are assumed as:

$$\phi_1(x) = \frac{x}{L}, \phi_2(x) = \sin\frac{\pi x}{L}, \phi_3(x) = \sin\frac{2\pi x}{L},$$

$$\phi_4(x) = \sin\frac{3\pi x}{L}, \phi_5(x) = \sin\frac{4\pi x}{L}$$

The assumed admissible functions are satisfying all geometric boundary conditions in support A, and some of them are also satisfying natural boundary conditions as is the case for comparison functions. Deflection shape of the boom according to assumed mode method can be expressed in the term of admissible functions as the sum:

$$y(x,t) = \sum_{i=1}^{n} \phi_i(x) \cdot q_i(t)$$

The kinetic energy of the moving mass is given by

$$T_M = \frac{1}{2} M \left[v^2 + \left(\frac{dy(s,t)}{dt} \right)^2 \right]$$

The kinetic energy of the beam is

$$T_m = \frac{1}{2} \sum_{i=1}^{5} \sum_{j=1}^{5} m_{ij} \dot{q}_i(t) \dot{q}_j(t)$$

The potential energy of the moving mass is given by

$$V_M = -M \cdot g \cdot y(s,t) = -M \cdot g \sum_{1}^{5} \phi_i(s) \cdot q_i$$

The elastic strain energy of the beam is

$$V_m = \frac{1}{2} \sum_{i=1}^{n} \sum_{j=1}^{n} c_{ij} q_i(t) q_j(t)$$

The virtual work on the gravitational force of the system is

$$\delta W = M \cdot g \cdot \delta y_{(x=s)}$$

The quantity δy , the virtual displacement of y, is to be evaluated at $x = s$. Having in mind that total kinetic energy is $T = T_m + T_M$ and total potential energy is $V = V_m + V_M$ and by applying Lagrange's equations the system of differential equations was finally obtained:

$$\sum_{j=1}^{5}\left[m_{ij} + M\phi_i(s)\phi_j(s)\right]\ddot{q}_j(t) +$$
$$+\sum_{j=1}^{5}\left[2Mv\phi_i(s)\phi_j'(s)\right]\dot{q}_j(t) +$$
$$+\sum_{j=1}^{5}\left[c_{ij} + Mv^2\phi_i(s)\phi_j''(s) + Ma\phi_i(s)\phi_j'(s)\right]q_j(t) =$$
$$= Mg\phi_i(s), i = 1,2,3,4,5.$$

The system of differential equations is solved numerically by using Runge-Kutta method of V order (Method Runge-Kutta-Fehlberg – RKF5) [13]. The values of deflections under moving mass depending on the number of admissible functions (n = 2,3,4,5) are shown in figure 5. Fast and good convergence of solution for adopted 5 admissible functions is fulfilled.

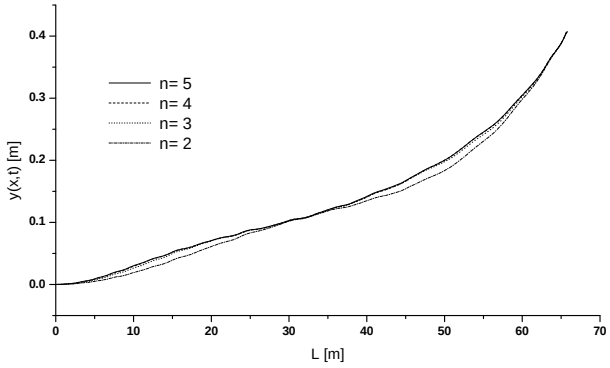

Figure 5. Deflection of boom under moving mass

4. CONCLUSION

The application of moving load problem in analyzing dynamic behavior of cranes can be found for various types of their constructions, but it is of practical relevance only for large structures with heavy trolleys and pay loads causing large deflections and with high performances of drive units, especially for modern flexible structures still in design process where exist the intention to avoid possible dynamic problems during exploitation and when the designer needs a real structural response in order to formulate control task for adopting appropriate control strategy. For such constructions with rigid steel frame of trolley application of moving mass problem is quite acceptable. The choice of an adequate model of a crane should be determined by the particular problem under consideration and must take into account the eigenfrequencies of the crane structure. However, numerical examination of a model that is not a prototype of some real system is of little interest unless some general conclusions, which can be applied to other, related configurations.

REFERENCES

[1] Fryba, L., Vibration of Solids and Structures under Moving Loads, Noordhoff International Publishing, Groningen, Netherlands, 1972.

[2] Olsson, M., On the Fundamental Moving Load Problem, JSV, 145(2), pp. 299-307, 1991.

[3] Yau, J. D., Wu, Y. S., Yang, Y. B., Impact Response of Bridges with Elastic Bearings to Moving Loads, JSV, 248(1), pp. 9-30, 2001.

[4] Rieker, J. R., Trethewey, M. W., Finite Element Analysis of an Elastic Beam Structure Subjected to a Moving Distributed Mass Train, Mech. Sciences and Signal Processing, 13(1), pp. 31-51, 1999.

[5] Henchi, K., Fafard, M., Dhatt, G., Talbot, M., Dynamic Behaviour of Multi-Span Beams under Moving Load, JSV, 199(1), pp. 33-50, 1997.

[6] Karnovsky, I. A., Lebed, O. I., Formulas for Structural Dynamics: Tables, Graphs and Solutions, McGraw-Hill Inc., Toronto, Canada, 2001.

[7] Oguamanam, D. C. D., Hansen, J. S., Dynamic response of an overhead crane system, JSV, 213(5), pp. 889-906, 1998.

[8] Oguamanam, D. C. D., Hansen, J. S., Dynamics of a three-dimensional overhead crane system, JSV, 242(3), pp. 411-426, 2001.

[9] Yang, W., Zhang, Z., Shen, R., 2007, Modeling of system dynamics of a slewing flexible beam with moving payload pendulum, Mechanics Research Communications 34, 260-266.

[10] Wu, J. J., Cartmell, M. P., Whittaker, A. R., The Use of Finite Element Techniques for Calculating the Dynamic Response of Structures to Moving Loads, Comp. & Structures, 78, pp. 789-799, 2000.

[11] Wu, J. J., Cartmell, M. P., Whittaker, A. R., Dynamic Response of Structures to Moving Bodies Using Combined Finite Element and Analytical Methods, Int. J. of Mechanical sciences, 43, pp. 2555-2579, 2001.

[12] Wu, J. J., Dynamic response of a three-dimensional framework due to a moving carriage hoisting a swinging object, Int. J. for Numerical Methods in Engineering, 59, pp. 1679-1702, 2004.

[13] Zrnić, N., 2005: Influence of Trolley Motion to Dynamic behaviour of Ship-To-Shore Container Cranes, Dr. Tech. Sc. dissertation in Serbian, Faculty of Mechanical Engineering Belgrade.

[14] Zrnić, N, Oguamanam, D., Bošnjak, S.: Dynamics and Modelling of Mega Quayside Container Cranes, FME Transactions, Vol. 34, No. 4, pp. 193 – 198, 2006.

CHOICE OF OPTIMAL TRANSPORTATION MECHANISATION AT OPEN PIT

J. Vladić, A. Gajić, R. Đokić, D. Živanić

Abstract: *Optimal transportation mechanisation selection is very important, from productivity standpoint as well as from an economic aspect. In this particular example, for open pit "Bogutovo selo" - Ugljevik, discontinued and combined transportation variations were discussed. Shown procedure has been based upon analysis of functional and work characteristics along with initial and operational expenses of equipment selected for use under the existing conditions in mentioned open pit.*

Keywords: *heavy truck, vehicle, transportation system*

1. INTRODUCTION

Solid matter/coal transportation is one of the most complex and expensive processes in a open pit operation. Transportation requires almost 2/3 of all investment expenditures during pit building as well as 40 – 70 % of operational expenses. Most of the highly skilled work force in open pit operations worldwide is tied to solid matter/overburden transportation.
Having in mind previously said, transportation largely affects open pit effectiveness and productivity.
Every excavation technique has its specifics., but common ground for all is that they all use different capacity machinery, which for themself require certain technical prerequisites limited by deposits' natural conditions. This means that for each site optimal techno-economic solution must be formulated.
Economic success of every open pit operation largely depends on transportation planning and expenses control. Adequate equipment selection accompanied with swift and appropriate decision making is very important from economic point of view.
Main directions in a solid matter/mineral substances transportation technological development are:

- Design and use of more complex, mobile and faster heavy vehicles for cyclic transportation and utilisation of loading excavators and heavy loaders with 8 to 30 m^3 capacity. In the near future bucket capacities of 40 to 60 m^3 will be available and that fact will influence building of transportation vehicles with increased capacity, mobility and power.
- Increased reliability and longer vehicle life. Larger truck capacity makes possible operation with fewer vehicles. This, on its part, requires better organisation and shorter equipment down time which can be obtained with improved design of heavy vehicles and powering units. Manner in which heavy equipment is maintained is also very significant (typisation, standardisation and unification).
- Due to worldwide energy crisis, rapid development of continuous transportation. Expensive oil is being replaced with somewhat cheaper electricity. Therefore, replacement of heavy mine vehicles.

Constant improvement of design characteristics and overall capacity, vehicle flexibility and small susceptibility to individual faults gives us number of advantages at the excavation process:
High flexibility in pit development dynamics, minimisation of initial overburden, high production plan fulfillment security, etc. which keeps this way of transportation still viable option comparable with alternatives.
Major shortcoming of belt conveyors is their lack of flexibility comparable to truck transportation, because breakdown of a single element brings complete system to a halt. Nowadays, every modern open pit operation utilizes truck as well as conveyor and railroad means of transportations.

2. TRANSPORTATION SYSTEMS – VARIATIONS

In order to secure constant supply of coal for the power plant it is necessary to make analysis of existing overburden transportation system. Coal transportation in combined as well as in discontinued technologies remains the same. Coal is being dug by hydraulic excavators and transported by dump trucks to the crushing site situated in the industrial plant. Therefore, establishing of more economical mean of overburden transportation will be performed through technical/economical analysis. It is necessary to make overview of excavation process for the following cases:
1. Discontinued transportation system (keeping the existing system)
2. Combined transportation system (truck transport to the crusher and conveyor system to the spreader)

PhD Jovan Vladić, grad. mech. eng., Faculty of Technical Sciences, Novi Sad, Serbia, vladic@uns.ns.ac.yu
MSc Anto Gajić, grad. mech. eng., Rudnik i termoelektrana Ugljevik, Ugljevik, Republika Srpska, antogajic@yahoo.com
grad. mech. eng.
Radomir Đokić, Faculty of Technical Sciences, Novi Sad, djokic@uns.ns.ac.yu
MSc Dragan Živanić, grad. mech. eng., Faculty of Technical Sciences, Novi Sad, zivanic@uns.ns.ac.yu

2.1 Discontinued transportation

Transportation with heavy dump trucks has been developed intensively by many open pit operations. Open pits situated in USA for 75% of transportation needs use heavy trucks.

Modern heavy trucks are being designed for operation in ascents of 10 – 40% with a specific power rating of 9 – 10 kW/t. Truck payload increase is the main development tendency with this mean of transportation and trucks with 250t capacity already operate worldwide. Limiting factors are tyre capacity and diesel engine power. Basic heavy truck selection rules are:

- Maximum equipment utilisation under all possible exploitation conditions
- Appropriate loading to transporting equipment ratio
- Heavy truck technological maneuverability limitations
- Transportation routes width
- Ascents which fully loaded trucks have to make

Some of the heavy truck transportation advantages are short acquisition period and quick incorporation in production process, significant maneuverability and manipulation abilities, possibility to purchase equipment of various capacities independently from existing fleet. "Bogutovo selo" pit production process, incorporating discontinued transportation system, consists of the following:

- Drilling and mining of harder soil layers
- Raw material excavation and loading with hydraulic and standard excavators
- Material transportation by heavy trucks from excavation site to external dump sites
- Raw material unloading and handling with bulldozers

Diesel-electric and mechanical dump trucks with various capacities are used for transportation.

Necessary number of dump trucks can be calculated according to this formula:

$$z = \frac{Q}{T} \cdot \frac{t}{q \cdot \eta} \qquad (1)$$

where: Q – quantity of materials being transported (8,321 x 106 m^3sm)
T – transportation time (3760 hrs)
q – average truck capacity (45 m^3)
t – work cycle duration (6 hrs)
η - efficiency factor (0,75 – 0,9, η = 0,79)

Necessary number of reserve transportation units, with heavy exploitation conditions present in open pit operations, is 25%.

Finally, the result is: $z = \frac{8{,}321 \cdot 10^6}{3760} \cdot \frac{0{,}6}{0{,}79 \cdot 45} = 46{,}69$

Adopting z = 47.

Loading cycle bucket excavator – dump truck is the most favorable when 3-5 bucket loads are needed to fill the truck body. Planned number of effective annual work hours is given by approved project documentation, based on 220 work days per year. Usable shift time factor is k = 0,71212. T=220x24x0,71212=3760 hours.

2.2 Combined transportation

When combine transportation method is used, production process comprises of:

- Raw material excavation and loading with hydraulic and standard excavators
- Dump truck transportation from digging site to crushing plant loading point
- Raw material crushing and loading onto conveyor
- Crushed material conveying to dump site
- Dumping raw material with the spreader

Before loading raw material on the conveyor it is necessary to pulverize material to the appropriate size. Open pit mines with harder raw materials can use one of the two transportation with crushing variations:

1. Raw material is transported to the central crushing site where trucks are unloaded into the reception bunker from which material is being dosed into the crusher. Crushed material is transported by conveyor out of the site. Disadvantage of this variation is that certain number of excavators and dump trucks has to be used. Although this number is very low, mine has to cope with supply of fuel, lubricants, tyres, etc., which makes it susceptible to inflation and price changes of this products). More flexibility in production is advantageous. This method implies use of semi-stationary crushing installations which have to be relocated periodically (every 12 to 24 months) and do not strictly follow field progress.
2. Immediately upon excavation raw material is being loaded into the crusher, processed and then transported by the conveyor outside mine. Advantage of this method is in a total elimination of trucks from transportation line, which effectively cancels any need for fuel, lubricants, tyres,... Work is less flexible, both in exploitation and development, and very susceptible to eventual stoppages and damages. This transportation system is already operational in some open pits and requires mobile crushers which strictly follow field development.

2.3 Etccs (excavator-truck-crusher-conveyor-spreader) structure in open pit "Bogutovo selo"

Combined system comprising of excavator-truck system, semi stationary crushers, conveyor system and spreader unit has been discussed as an alternative raw material transportation system in a open pit "Bogutovo selo".

Having in mind physical and mechanical properties of a raw material which has to be crushed, its dampness, abrasiveness, required capacity, mining operation concentration and explorations performed up-to-now flow-through double roller crusher. Dimensioning of a ETCCS system has been done according to projected raw material capacity of 8,321 x 10^6 m^3sm and work conditions prevailing in the mine.

Transporter capacity for the raw material needed for this operation can be calculated in the following manner:

A - dike section area [m^2]
v – belt speed [m/s]

According to fact that soil density (for this mine) is $\rho=2t/m^3$ and number of predicted working hours 3760, conveyer capacity per hour is:

$Q = 8{,}321x10^6x2/3760 = 4426.06$ t/h

Necessary active belt width $b=\sqrt{\frac{Q}{k_3 a \cdot v}}$

k_3 – conveyer slope reducing capacity factor. In case of worst possible T_1 slope of 8^0, $k_3 = 0{,}97$,
$a = 468+612\ tg\varphi$ – belt shape factor,
$\varphi=15^0$ – material free fall dynamic angle
$\beta=45^0$ – side cylinder angle (trough-shaped belt with 3 cylinders)

$$b=\sqrt{\frac{4426{,}06}{0{,}97\cdot(468+612tg\varphi)\cdot 3{,}35}} = 1{,}468 \text{ m}$$

Real belt width: $B=\frac{b+0{,}05}{0{,}95}=1{,}59m$

Adopted B = 1600 mm

Necessary drive power

Drive power for 3 conveyers is calculated according to formula: according to [3]

$$P_1 = U_1 \cdot v \text{ [kW]} \quad (2)$$

Perimeter force $U_1=\frac{1}{102}$ [CtL (q_t + q) ± qH] KN (3)

C – factor of drive force increasing considering conveyer drive secondary resistance
t – cylinder drums bearings friction factor,
L – conveyer length (between outer drums axis)

Movable coveyer parts mass:

$$q_t=2q_0+\frac{1}{g}\left(\frac{G_n}{t}+\frac{G_p}{t_p}\right) \text{ kg/m} \quad (4)$$

q_0[kg/m] – belt mass per length meter,
G_n[N] ; G_p[N] – carrying and back drums movable parts weight
t_n[m], t_p[m] – carrying and back drums step
g = 9,81[m/s] – gravity acceleration

Mass of transported material per length meter:

$$q=\frac{Q}{3{,}6v} \text{ kg/m} \quad (5)$$

v – belt speed [m/s]

Additional power for cleaner resistance:

$$P_2 = 1{,}6B\cdot v\cdot n, \text{ kW} \quad (6)$$

n – number of equipment which creates additional resistance

Additional power for guides friction resistance:

$$P_3 = 0{,}08xL_v, \text{ kW} \quad (7)$$

L_v – guide length [m]

Conveyer T_1

C=1,12, T=0,025, L=700 m, H= 89 m, B= 1,6 m,
Belt mass per meter is calculated according to following formula:

$$q_0 = 11B(1{,}25\cdot z+\delta_1+\delta_2), \text{ N/m} \quad (8)$$

z = 8 - number of belt layers,
δ_1 = 6 mm – workside lining thickness,
δ_2 =1,5 mm – lining thickness (nonwork side),
q_0=11x1,6(1,25x8+6+1,5)=308 N/m,

G_n=100B+70=230 N, G_p=100B+30=190 N,
t_n=1 m, t_p=3 m

Mass of conveyer movable parts according to formula (4): q_t=92,7 kg/m

Mass of transported material per meter, formula (5):

$$q=\frac{4426{,}06}{3{,}6\cdot 3{,}35}=367kg/m$$

Perimeter force, formula (3):

$$U_1=\frac{1}{102}\left[1{,}12\cdot 0{,}025\cdot 700(92{,}7+367)+367\cdot 89\right]=408{,}56KN$$

Necessary drive power, formula (2):

P_1= 408,56x3,35 = 1368,7 kW

Additionla power for cleaner resistance, formula (6):

P_2 = 1,6x1,6x3,35x1=8,576 kW

n = 1 – number of equipment which creates additional resistance

Additional power for guides friction resistance according to formula (7) :

P_3 = 0,08x12 = 0,96 kW, L_v = 4x3 = 12 m

Drive engine necessary power :

$$P_m\frac{P_1+P_2+P_3}{\eta}=1845{,}4KW$$

Adopted 2 (two) engines – power 950 kW

Conveyer T_2

C=1,12, t = 0,025, L= 700 m, H= 25 m, B= 1,6 m, z=8, δ_1= 6 mm, δ_2= 1,5 mm
According to calculated power, as in previous case, adopted engine power 950 kW

Conveyer T_0

C=1,2, t= 0,025, L= 1500 m, H= 15 m
According to calculated necessary power, adopted 2 (two) engines – 630 kW.

Table 1. Belt conveyers system – technical features

Description	T_1	T_2	T_0
Purpose	floor	major	postponing
Capacity, t/h	4430	4430	4430
Width, m	1,6	1,6	1,6
Speed, m/s	3,35	3,35	3,35
Length, m	700	700	1500
Conveyer hight, m	89	25	15
Installed power, kW	2x950	950	2x630
Total mass (without tracks and drives), t	140	140	300
Belt trough corner	45	45	45

3. DETERMINATION OF BASIC PARAMETERS FOR COMPARATIVE ANALYSIS

According to fact that coil production process is the same in the cases of discontinous or combined transport and it won't be subject of this analysis. Analysis of necessary dredges and trucks number for discontinous and combined transport is based on coil production of $8{,}321x10^6$ m^3 per year. Scale of norms as well as equipment price are based on information from equipment manufacturers, literature data and expirience data from PK " Bogutovo selo" and other mines with similar technology.

Its adopted that operation time of coil dig is about 20 (twenty) years (for purpose of this analysis). In this period should be replaced 3 complete equipment set (for discontinous transport), while continous transport requires replacement of 1 (one) set. Based on technical scale of norms we are calculated operational costs, with market price per unit of measurement.

Based on necessary workers number and their salaries in PK "Bogutovo selo" Ugljevik, we are calculated labour costs.

3.1 Discontinous transport system

Table 2 shows means of transportation necessary number, while table 3 shows machine prices for discontinous transport system. Table 2.10 shows scale of norms for materials for trucks and bulldozers.

Table 2. Number of necessary transport units for discontinous transport

Type of transport: Dredge/truck	RH-120/ FAUN K.100		RH-120/ KOMATSU 445E		H-241/ KOMATSU 510E	
	Dredges number	Trucks number	Dredges number	Trucks number	Dredges number	Trucks number
Discontinous transport system	5	15	5	17	5	15

Table 3. Value of equipment for discontinuity of transport system

gear	price(km)	amortization rate	quantity	total (km)
Truck capacity 91t	$1{,}5x10^6$	7	15	22 500 000
Truck capacity 109t	$1{,}9x10^6$	7	17	32 300 000
Truck capacity 136t	$2{,}4x10^6$	7	15	36 000 000
Bulldozer	$0{,}7x10^6$	7	4	2 800 000

Table 4. Material norms for dumpers and bulldozers

engine / expenses	TYPE OF DUMPER			BULLDOZER
	Faun K.100	KOM.445E	KOM.510E	
Annual consumption of fuel				
Total expenses KM per year	4,512.000	5,433.200	5,272.500	304.000
Annual consumption of tyres				
Total expenses KM per year	840.000	840.000	1,020.000	144.000
Current maintenance costs				
Norms	20% of fuel expenses	20% of fuel expenses	20% of fuel expenses	20% of fuel expenses
Total KM per year	902 100	1 320 900	1 054 500	608 800
Maintenance costs investment				
Norms,%	4	4	4	4
Total KM per year	900 000	1 292 000	1 440 000	112 000

3.2 Combined transport system (bkdto)

In table 6 are prices for equipment for combined transport system, while table 7 shows list of necessary labor. In table 8 are norms for dumpers, bulldozers. In table 9 are norms for striped transporters and delayers.

Table 5. Necessary number of transport units for combined transport

Transport type: Dredge/truck	RH-120/ FAUN K.100		RH-120/ KOMATSU 445E		H-241/ KOMATSU 510E	
	No. of Dredges	No. of Trucks	No. of Dredges	No. of Trucks	No. of Dredges	No. of Trucks
combined transport system	5	8	5	7	5	7

Necessary number of trucks in case of combined transport is determined by formula 1:

$$z=Q/T*(t_k/q*n)= 21{,}75$$

Time t_k (working cycle time) in this case we determine when from the cycle time in the case of discontinued transport, subtract time on 3 km transport route. When we know that average speed of empty and full truck is 18,5 km/h.

So we have $t_k=t-t_v$

t_v= 2*3km/18,5=0,32h
t_k=0,6-0,32=0,28
Accept 22 dumpers.

Table 6. Equipment prices for combined transport system

	price,km	amortisation rate,year	qua-ntity	total,km
Truck Faun K.100	$1,5x10^6$	7	8	12.000.000
Truck Komatsu 445E	$1,9x10^6$	7	7	13.300.000
Truck Komatsu 510E	$2,4x10^6$	7	7	16.800.000
Crusher Krupp	$6,85x10^6$	20	2	13.000.000
Transporters T1,T2,T0	3,7KM/kg	20	580t	2.134.080
AR_s1600x16,5	15,3KM/kg	20	490t	7.500.000
Bulldozer	$0,7x10^6$	7	2	1.400.000
	$0,75x10^6$	7	2	1.500.000
Equipment for vulcanization	$0,09x10^6$	7	2	180.000

Table 7. List of labor

qualific. / No.executors	QUALIFICATION					
	VSS	VKV	SSS	KV	PK	TOTAL
Total	16	70	137	112	31	366
DTO system						
Total	5	23	80	5	20	133
TOTAL	21	93	217	117	51	499
Expenses for labor, KM per year VSS 700x1,8=1260x21x12 317520 VKV,SSS,KV 500x1,8=900x427x12 4611600 PK 300x1,8=540x51x12 330480 LABOR TOTAL 5259600						

Table 8. Material norms for dumpers, bulldozers

ENGINE / expenses	TYPE OF DUMPER			BULLDOZER	
	Faun K.100	KOM.445E	KOM.510E		
Annual consumption of fuel					
Total expenses KM per year	2 406 400	2 237 200	2 500 400	152 000	76 000
Annual consumption of tyres					
Total expenses KM per year	448 000	392 000	420 000	72 000	36 000
Current maintenance costs					
Norms	20% of fuel expenses	20% of fuel expenses	20% of fuel expenses	20% of fuel expenses	20% of fuel expenses
Total KM per year	481 280	447 440	500 080	30 400	15 200
Maintenance costs investment					
Norms,%	4	4	4	4	4
Total KM per year	480 000	532 000	672 000	56 000	60 000

Table 9. Norms for striped transporters and retarder

NORM	UNIT PRICE	TRANSPORTERS		TOTAL KM per year
El.energy,kW/m^3hm	0,07KM/kWh	4160	1550	1502872
Oil l/year	10 KM/kg	2000	1000	30000
Grease kg/year	30 KM/kg	3000	2000	150000
Syllables of the roller load side,pcs/year	294 KM 62,5kgx4,7KM	480	48	155232
Syllables of the roller recurrent side,pcs/year	675 KM 71kgx9,5 KM	172	17	12757
Drum:6xφ1250,500kg 16xφ1000,2500kg	13,8KM/kg 9,0KM/kg	20%	20%	154800
Rubber strip B=1600	600KM/m	930m/year	220m/year	690000
Cleaning device	300KM/pcs	36pcs/year	12pcs/year	14400
Rubber wipers	200KM/pcs	18pcs/year	6pcs/year	4800
Bumper board on transfer place	450KM/pcs	9pcs/year	3pcs/year	5400
Rubber gasket on transfer place	250KM/pcs	36pcs/year	12pcs/year	18000
Installation	1KM/kg	580t	490t	1070000
Investment maintenance				
Norm		4	4	
Total, KM/year		612563	360000	972563

4. TECHNICAL-ECONOMIC ANALISYS FOR TRANSPORT EXPENSES

When you purchase new equipment first you calculate amount of investment. Choosing machine structure in transport system or transport system itself is compromise between technical-technological and economical factors. Operative expenses like expenses of current investment are not estimating correct enough, although it is more important than first investment during working time of machine. Methodology for estimating this expenses is very complex.
Principles for choosing economic most adequate system:
1. Reducing expenses through investments
2. Optimization of exploitation and replacing equipment
3. Minimization of operative expenses

The most important factor in economic analysis of trans.system is amount of investments and expenses of exploitation, also you have to rake care for technical indicators of system.
It is important to take care about technical-technological aspects and economical justify in the same time, so it is important to have functional connection between technological factors and expenses.

Table 10. Expenses dependence of type of transport

SYSTEM / EXPENSES(KM)	DISCONTINUITY OF TRANSPORT SYSTEM	COMBINED TRANSPORT SYSTEM
Equipment	280800000	158174080
Repromaterial	367314000	208457440
Current maintenance costs	77726000	50595780
Investment maintenance	74880000	56521340
Labor	123595200	105192000
Total	1501815200	561063200

On diagram are parallel expenses of discontinuity and combined transport system, figure 1.

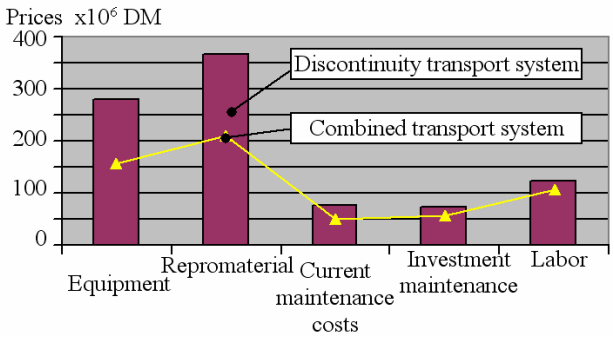

Fig. 1. Parallel expenses of discontinuity and combined transport system

Analysis show that material expenses and energy they are about 40% in total expenses. It is obvious that combined trans.system on 20 year period is more profitable because life for DTO system is around 20 year. Dumpers would be replaced every 7 years with amortization growth from 14,3% annual. Work expenses in case for combined transport system for that period are much lower.

5. CONCLUSION

Discontiuity way of transport is worked out in existing solution on PK "Bogutovo selo" where planned capacity of 1,750.000 tons of coal every year and $8{,}321 \times 10^6 m^3$ of solid barren soil.
In it's structure we have equipment characteristic which is used for digging up, transport and delaying for current discontinuity transport.
Like possible way of transport on this surface mine is discussed combined transport with complete structure BKDTO system.
There was carried out determination of transport equipment capacity provided for transport.
For realistic view both way of transport there was technical-economical transport expense analysis done which includes: equipment, repromaterial, current maintenance costs, investment maintenance, labor.
Needed transport capacity was based on 3760 hours of efective work. Analysis was made on 20 year period for using transport system.
No matter that lifetime of surface mine "Bogutovo Selo" is much shorter than this period, analysis showes that combined transport system is profitable and also used in expliotations for longer period and with different structure. In exploitation conditions on PK „Bogutovo Selo" it have to be selective used because in this mine was found 27% clay materials, and that is a problem in process of crushing and transport.
Based on mine projects about 40% of should be put inside of excavation site on small transport lenghts, what is also difficulty for using combined transport system on this excavation site.

REFERENCES

[1] Plavšić M. : "Civil Engineering Machines", Scientific book, Belgrade, 1990.

[2] Vladić J. "Reloading Mechanization II", FTN Novi Sad, 1991.

[3] Stojanović L.:" Simulation model for optimal transporting systems choice at open pit - Bogutovo Selo – Ugljevik", MSc thesis, Faculty of Mine and Geology, Belgrade, 2000.

[4] The main maining project of open pit "Bogutovo Selo" Ugljevik – Technical projetc projekat country rock for exploatacion period 1990-1995., RI Tuzla 1990.

ANALYSIS OF MATERIAL FLOWS AND LOGISTICS APPROACH IN DESIGN OF MATERIAL HANDLING SYSTEMS

J. Vladić, D. Živanić, R. Đokić, A. Gajić

Abstract: *In the material handling systems there is not a perfect solution, only partial answers to the solution. Whether designing a new system or modifying an existing one, decision-makers want to take the guesswork out of finding the best possible solution. Formation of optimum material handling systems demand, besides knowledge of material characteristics, material handling and information analysis in transporting process. Contemporary approach to solution of the material handling problem is directly related to industrial logistics which comprises series of activities like transport, stocking, reserve possession, manipulation, which are function of physical transfer products. Logistics approach to transporting systems design allude researches of the material flows through an operating system, with minimization of flows duration and quality utilization of productive capacities. In this paper is showed an overview of activities, with the accent on analysis of the material flows and logistics approach in design of material handling systems.*

Keywords: *material flows, logistic, design*

1. INTRODUCTION

The status of contemporary production and consumption and the forecasts that are implemented by experts, who work in the greatest companies in the world nowadays, indicate that market competition will demand participant's abilities in the supply chain, in the future, which enable the immediate response to the market demand. It requires an intensive development of the production, especially about organization and its complex mechanization and automatization. Also, it dictates an expressed requirement for adequate solutions in the domain of transport and storage problems.

Every technical system is different and has its own unique characteristics. To proceed from an initial concept to a finished design requires a detailed engagement between the client and supplier with particular focus on the processes that will be required in the new design.

The basic trends in modern good-distribution centers and warehouse systems are:

- improve capacity utilization (5-10%),
- minimize warehouse labor hours (10-30%),
- reduce direct transportation spend (5-25%),
- minimize total inventory (5%) and
- reduce shipping errors (80-100%).

Certain questions must first be answered before begin to conceptualize system. An overall objective must first be set, and a basic understanding of the type of system is important.

2. DESIGN OF MODERN MATERIAL HANDLING SYSTEMS

A few examples of the type of material handling systems are receiving, packaging, order picking, warehousing, shipping and production. For those who get the solution right for their business, the benefits can be substantial. Every industry, company, and applications have their unique characteristics, but these 9 steps outline must be accomplished during the design process to the material handling systems were selected from optimum viewpoint:

- acquaint with materials and material flows in systems,
- logistics study of problems,
- visit sites companies in similar industries,
- preliminary system design,
- executive summary and cost justification,
- modeling and simulation of systems,
- hardware and software supply,
- management team assignments,
- delivery, installation and implementation.

In the following text, every phases will be described, shortly.

It is also important to consider the size, shape, and age of the building, and possible future expansions. Environmental conditions must also be taken into account like temperature and humidity. Additional information should include, sales forecasts, combined with production capabilities, keeping in mind the need for flexibility since manufacturing is ever changing in this world economy.

Load characteristics are vital, and include the size, shape, weight, and material to be conveyed. The

PhD Jovan Vladić, grad. mech. eng., Faculty of Technical Sciences, Novi Sad, Serbia, vladic@uns.ns.ac.yu
MSc Dragan Živanić, grad. mech. eng., Faculty of Technical Sciences, Novi Sad, zivanic@uns.ns.ac.yu
grad. mech. eng. Radomir Đokić, Faculty of Technical Sciences, Novi Sad, djokic@uns.ns.ac.yu
MSc Anto Gajić, grad. mech. eng., Rudnik i termoelektrana Ugljevik, Ugljevik, Republika Srpska, antogajic@yahoo.com

footprint is important for it is what the conveyor will see, and will help determine the best type of equipment to use. Rate of flow is important for it will determine the speed that the conveyor needs to run, and product orientation if you are interfacing with automated equipment, and or need to incorporate accumulation of products. Now that you have a general layout, combined with the specific information of your system, you can begin to specify the type of equipment required. According to Brainstorm method we can solve the problems by simplifying material flow, control, speed, and process.

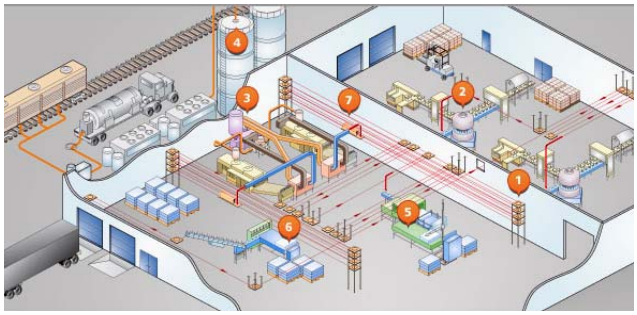

Figure 1.Material flows in systems

Logistics activities include transportation, order processing, storage layout, warehousing, inventory maintenance,… These activities provide functions for bridging between producers of goods and market consumers, which are separated by time and distance.
Forward-thinking manufacturers use logistics strategically to reduce safety stock levels and improve customer service – and hence profits – through better information.
We should interview the main material handling players, including operators to be identify key problems.

Figure 2. The logistics study process helping to identify and solve problem areas

Use a layout of facility to document the flow of material from receiving to shipping: chart and measure the actual material flow path through your facility. At every place material stops for whatever reason (e.g., inspection, storage, subassembly, final assembly, packaging, shipping) place a pin in the layout. When you have finished, connect the pins, in order, with string. Add up the length of all the strings; this will give you a good idea of how far material really travels and why it takes so long to get through your factory. In the end it is required to review applicable problem and solution scenarios and available material handling technology.
In the analysis of the possible solutions, we must see how companies in similar industries or with comparable operations have solved their material flow problems. Ask an equipment supplier/integrator to arrange site visits to see how the process works in a real-world setting and validate concepts.
Learn pitfalls, mistakes to avoid from users who have been through the process. For an expert opinion on this question, it is probably best to turn to a material handling consultant or a systems integrator.

Figure 3. Overhead monorail - fast, quiet, material transport system that saves considerable floor space

The following phase presents preliminary “feasibility study” or “concept study” as it is often referred to, where the business case is generally defined and one or more reasonable approaches are identified.
At the initial stages of planning, it is important to focus on techniques and not technologies. Deciding on the right techniques will guide you in determining the right technologies to use. A material handling engineer or specialist will analyze where product is stored, how it’s stored, and its loads, volumes and speeds.
Also, there are following: generate layout of material flow, create high-level description of function, operation of material control system and compare various equipment options.
This design engineering phase involves the refinement of one best-fit solution that has both technical and business merit. To design or re-design a material handling operation, one needs to develop a cost versus benefit analysis to include the systems to be considered.
Research of quantify cost savings, primary business advantages, and benefits include project return on investment (ROI). After that, we should generate

payback analysis, simple payback, net present value, and initial rate of return using a ROI calculation worksheet.
Automation can dramatically reduce labor costs by replacing repetitive tasks with intelligent systems, and redeploying human resources to points requiring true human decision-making.
Compare current system against alternative solutions and prepare a hard-hitting executive summary that makes your case quickly, concisely, and logically:

- how current system works,
- why it must be changed,
- alternatives considered,
- how new system will work,
- how much new system will cost,
- justification,
- design-build process and timetable.

Computer modeling and simulation are more and more becoming an integral part of the design and verification process for both small and large projects. It takes a unique combination of skills to do meaningful simulation modeling, especially when the systems are complex and involve new technologies.
Simulation has become a widely used tool in material handling. The primary purpose of simulation is to describe and analyze the behavior of a system, ask "what if" questions about a system, and aid in the design of real systems.

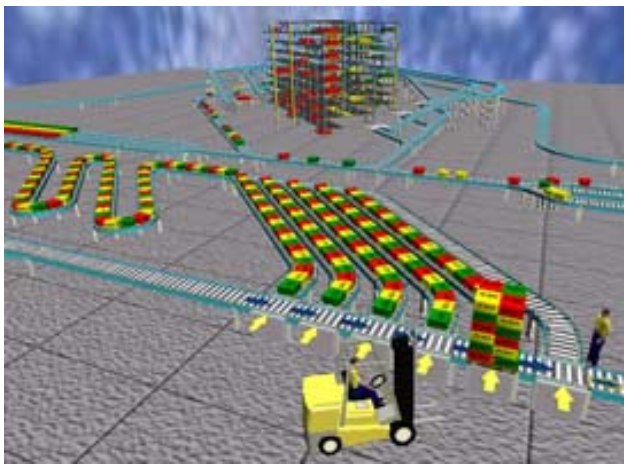

Figure 4. Simulation of material flows in warehouse-transporting systems

Simulations can be beneficial during all phases of a project. The cost of simulation is typically very small in relation to the total investment while the cost of change or modification after installation can be significant. Simulation can help prevent costly mistakes from happening. When designing new systems or modifying existing ones, consideration must be given to all factors impacting the functional areas involved. These include process flow, product flow, production cost, inventory cost, cost of facilities, new technologies, control systems, and equipment selection.

With simulation, a whole day of operation can be studied within a few minutes or two hours can be spent examining just one minute of operation. Simulation provides information on why something happens in a real system by recreating the system in a model and controlling the constraints to the system.
Once a valid simulation model has been developed, it is easy to explore new policies, operating procedures, or methods without the expense and disruption of experimenting with the real system. Simulation can be used to develop understanding about how a system operates. Simulation allows for identification and exploration of system constrains and interactions. Simulation can be used to test and specify the requirements of a system
Computer modeling and simulation has today become an affordable and invaluable tool to overcome design challenges and assure desired results, allowing our clients to:

- save time on system design and implementation,
- identify and resolve potential system bottlenecks,
- understanding how the operation really works,
- test and verify new operating procedures prior to making modification or committing resources,
- compare alternatives and make decisions with confidence,
- identify the variables having the greatest impact on performance,
- test and verify plans for future capacity increases
- identify and test the critical performance variables to be monitored after implementation,
- use the model to support marketing efforts or to "sell" projects internally.

These types of automation technologies require the installation of adequate software, which will support it, or only the software upgrade. We must be sure that chosen suppliers have proven experience on a system of similar size and scope. Write clear design specifications and document expectations for equipment performance and specify parameters for system acceptance tests. Develop a comprehensive transition plan, including installation and implementation schedule, workarounds to ensure system installation does not impede existing operations.
Clearly defined roles and responsibilities for both the suppliers and customer. Finalize system price, and negotiate terms for change orders. Ensure all terms and conditions are fair to both parties.

Figure 5. Mini load systems are closed off to employees to maximize safety and minimize loss

Today's material handling system managers face a number of challenges. Customers demand perfect order accuracy; smaller and more-frequent orders cover a greater number of SKUs; senior management calls for lower costs and increased productivity.
Because of this reason, it should be assembled a transition team including representatives from suppliers, an internal project manager, and key managers from all relevant departments. Logistics systems impact multiple departments and areas of your business; make sure you do not leave anybody out. Mission of this management team is:

- document internal procedures and process changes,
- implementation progress on a regular basis,
- determine process for dealing with problems and project roadblocks that may come up,
- educate internal audiences about the process change,
- workarounds to ensure system installation does not impede existing operations,…

After the phase of systems delivery, installation, test and launch, operators and maintenance personnel should be trained during installation and integration. Implement written procedures for operators using the new process. Document system design, operating manual, troubleshooting procedures, and recommend spare parts. Notify key internal/external customers of new process; possibility of short-term service disruptions. Schedule spare parts delivery before final integration testing. Negotiate long-term support agreement before final acceptance test and sign-off.

Perform regular preventive maintenance as recommended by the hardware supplier(s) including ongoing training of internal staff as needed. Define roles and responsibilities for internal and supplier service staff. Periodically system performance to identify possible maintenance issues and needs for repair or upgrades. Document operational performance to ensure system is meeting objectives. Bring the system suppliers in to conduct a periodic audit on processes and performance, recommend continuous improvements.

3. CONCLUSION

The basic problem is the fact of the noticeable investments limitation for new equipment. Nowadays, there are challenging and complex transporting operations, so we expect that the logistical approach to the solving these problems contribute incremental decrease of costs and increase in the production efficiency. In the paper the review of activity and the consideration of the logistical approach to modern transporting systems design were dealt. These transporting systems can respond to all requirements and challenges.
In summary then, the latest generation of automated solutions for material handling operations in distribution centers and warehouse now allows modular tried and trusted components to be combined in a large number of different permutations. Analysis of material flows and logistics approach, as the phase in design flow, which are described in this paper, are enabling to get effective, economy and reliable modern material handling systems.

REFERENCES

[1] VLADIĆ, J., *Transporting - manipulation systems*, Faculty of technical sciences, Novi Sad, 2005.

[2] VLADIĆ, J., *Automated design*, Faculty of technical sciences, Novi Sad 2007.

[3] GATES, C., TITZER, B.,… *Managing & Implementing Successful Automated Material Handling Projects*, Perspectives on Material Handling Practice, 2001.

[4] RUEHRDANZ, K., *Ten Factors Driving Automation in the Food Distribution Center*, Dematic Corp, 2006.

[5] HILL, J., *WMS Planing, Design and Procurement*, Supply chain forum, 2003.

[6] LIU, C., *Optimal Storage Layout And Order Picking For Warehousing*, International Journal of Operations Research Vol. 1, No. 1, 37−46, 2004.

CAD-CAM-CAE TECHNOLOGIES USED IN THE DESIGN OF BUCKET WHEEL EXCAVATOR CUTTING TEETH

Z. Jugović, R. Slavković, M. Gašić, M. Popović

Abstract: *The design of bucket wheel excavator cutting teeth is a complex process involving a huge number of dependability factors. One of the main problems lies in the lack of a thorough explanation of both the load applied to these cutting elements and its distribution during excavator operation. The design process itself is based on related assumptions and approximations. The cutting tooth design technology, on the other hand, is a challenge in itself, demanding satisfaction of specific and occasionally diametrally different requirements (great strength, proper hardness, wear resistance, cost-effectiveness of construction; optimum geometry, etc.). The paper presents a CAD/CEM/CAE-supported approach somewhat facilitating decision-making at certain cutting tooth design stages. As the approach is based on models, modelling and simulations, the cutting tooth and its features are defined using models that are further analysed by process simulation during operation and design.*

Key words: *CAD, CAE, CAM, design, bucket wheel excavator*

1. INTRODUCTION

Bucket wheel excavators are basic machines used in continuous overburden removal and coal excavations in opencast mines in Serbia. The buckets of the excavator bogie-wheel are fitted with cutting teeth, as demanded by the characteristic composition of excavated material. The cutting teeth are subjected to both intensive abrasive wear and alternating dynamic loads during operation, resulting in progressive wear of the tooth material and, in more severe cases, deformations or breakage. Therefore, as the tooth cannot perform its basic function properly, the operating capacity, loading and energy consumption of the excavation process are directly and indirectly affected. This results in reduced economic effects of coal production and a simultaneous cost increase, due to the excavator time lag and cutting element (tooth) replacement. The costs of the material wear process are impossible to eliminate; however, they can be considerably reduced. A delay in the wear process can lead to direct prolongation of the service life of the cutting teeth and, indirectly, of other excavation subsystem elements in bucket wheel excavators.

2. THE POSSIBILITIES FOR TOOTH SERVICE LIFE PROLONGATION

Welding of hard material onto the tooth surface and incorporation of hard metal inserts as methods of prolongation of the service life of the excavator tooth have been studied in opencast mines in Serbia. The studies have yielded certain positive results, the larger-scale application thereof, however, being rather limited.

The current limitations include the type of the excavated material related to the type and shape of the tooth and the technology and welding equipment to be used. The effects achieved are inadequate, considering the costs, and therefore restricted. Prolonged tooth service life can undoubtedly be obtained, but the method is a costly and relatively complicated one at the moment, considering the number of units welded and the weld geometry, and hence economically unjustifiable. According to the authors, in order to prolong the tooth service life, investigations at this stage should be focused on the development of new design solutions through geometry optimisation and the use of new single-piece tooth materials, but also through the development and use of a new two-piece tooth design in bucket wheel excavators.Previous studies have shown ([4], [5], [6]) that the two-piece tooth design has multiple advantages on all established criteria over the single-piece tooth, being also, for the time being, more suitable for use in opencast coal mining in Serbia as compared to the welding and insert incorporation methods.

3. LOADS AND CONSTRAINTS

The most critical factors affecting the digging process can be classified into four groups including: 1. the physico-mechanical characteristics of the material being excavated; 2. the design and kinematics of the bogie-wheel and the excavator as a whole; 3. block technological parameters and 4. the contact between the cutting element and the material being excavated.

Prof. Zvonimir Jugović, Ph. D., B. Sc. Mech. Eng., Faculty of Engineering, Cacak, zvonko@tfc.kg.ac.yu
Prof. Radomir Slavković, Ph. D., B. Sc. Mech. Eng., Faculty of Engineering, Cacak, slavkovic@tfc.kg.ac.yu
Prof. Milomir Gašić, Ph. D., B. Sc. Mech. Eng., Faculty of Mechanical Engineering, Kraljevo , gasic.m@maskv.edu.yu
Marko Popović, M. Sc., B. Sc. Mech. Eng., Faculty of Engineering, Cacak, marko@tfc.kg.ac.yu

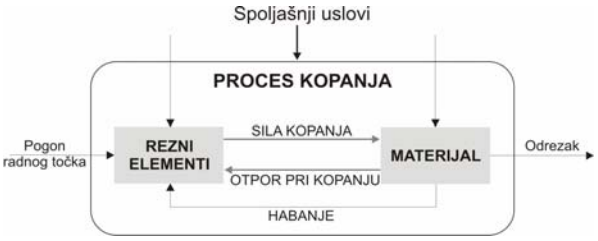

Figure 1. A schematic diagram of the bucket wheel excavator digging process

In designing both single- and two-piece bucket wheel excavator teeth, one should define the following: a) geometry; b) dimensions; c) material; d) assembly method; e) design technology etc. Proper design and optimum development of the two-piece tooth require definition of the load function of the tooth as well as of the size and shape of wear in operation as induced by the factors affecting the digging process.

During digging operations, the bucket scoops up the rock material using one portion of the cutter and a certain number of teeth. The cutter portion and the exact number of cutting teeth to be involved are dependent on the bucket type, tooth number and distribution, technological digging parameters adopted and the excavator arrow direction. Individual tooth loads are generally due to the cutting resistance of the rock material and the friction- and wear-induced resistance on the tooth cutting surfaces (Figure 2). The investigations have shown that theoretical definition of the digging resistance values is highly difficult and complicated, being dependent on a multitude of interrelated factors. Complex processes taking place during excavation are difficult to express through mathematical equations due to a large number of unknown values. Therefore, empirical forms obtained under laboratory or operating conditions are used in digging resistance determination ([8],[9]). The determination of these resistances as external loads of the bucket wheel excavator is essential in estimating characteristic cutting tooth dimensions. The data thus obtained can be used in generating approximate input data required for the estimation of characteristic dimensions and elements of the two-piece tooth.

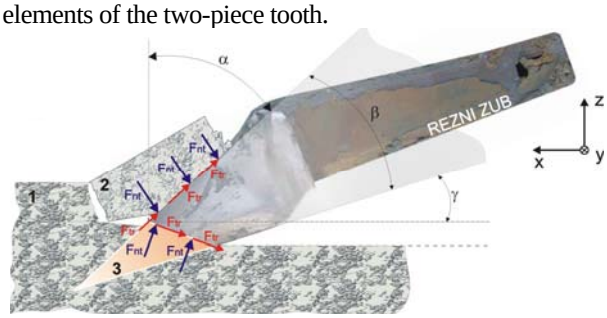

Figure 2. Tooth load during the digging operation

For proper geometric identification of the tooth dimensions, the external load of the characteristic parts of the bogie-wheel (buckets, cutter, teeth etc.) should be defined as a time function. Load distribution and exact direction should also be identified. Determination of an individual tooth load can be made by defining the total bucket load as divided by the cutting elements, considering their uneven engagement in the cutting operation. The analysis, the results thereof being given in [7], examines the distribution of the total bucket load over the cutting teeth and the cutter.

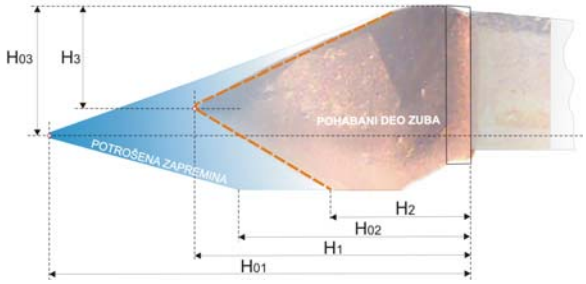

Figure 3. Geometric parameters used in wear measurements in single-piece teeth

In the two-piece tooth development process, maximum tooth wear values in previous operating conditions should also be determined. This is of utmost importance, as the wear of the tooth holder and the coupling elements should not be allowed during operation of the two-piece tooth, nor under extreme wear conditions, including tooth wear and shape and position of worn-out surfaces.

Any defects that may occur during casting, cooling and thermal treatment, as well as those related to the basic tooth material engineering have a huge effect on tooth performance and service life. The use of the most favourable tooth design technology is as important as the adoption of optimum tooth geometry, accurate estimation and proper determination of the dimensions of critical cross sections. This suggests that the two-piece tooth design is a complex process, primarily due to the unknown load character, demanding an integrated approach to achieve an optimum design.

4. AN INTEGRATED APPROACH TO THE TWO-PIECE TOOTH DEVELOPMENT

An integrated approach to the two-piece tooth development is aimed at the reduction of the development period and further improvement of the product at this stage [3]. The simultaneous virtual concept as a basis of the integrated approach increases the use of computer tools in providing three key activities, including communication, visualisation and simulation. The technologies providing the above approach include, among others, graphic 3D solid modelling and analyses and simulations based on the finite element method (FEM). This approach is based on models, modelling and simulation. Models are used to check the proposed solution under conditions similar to the operating ones thus enabling elimination of the defects observed. Product designing is also simulated until optimum design parameters are achieved. The effects produced by the said two-piece tooth development approach have yielded very significant results (figure 4).

The structural analysis of the two-piece tooth should be most efficiently started at the basic concept consideration stage. The starting point has been the checked and tested design solution for the GTZ-2 single-

piece tooth of the SRs2000 32/5.0 bucket wheel excavator used in overburden excavation. The tooth has yielded good performance, both in terms of geometry and material, the technology of its design being developed. The GTZ-2 tooth results have been used in adopting basic concepts and generating different design solutions of the two-piece tooth.

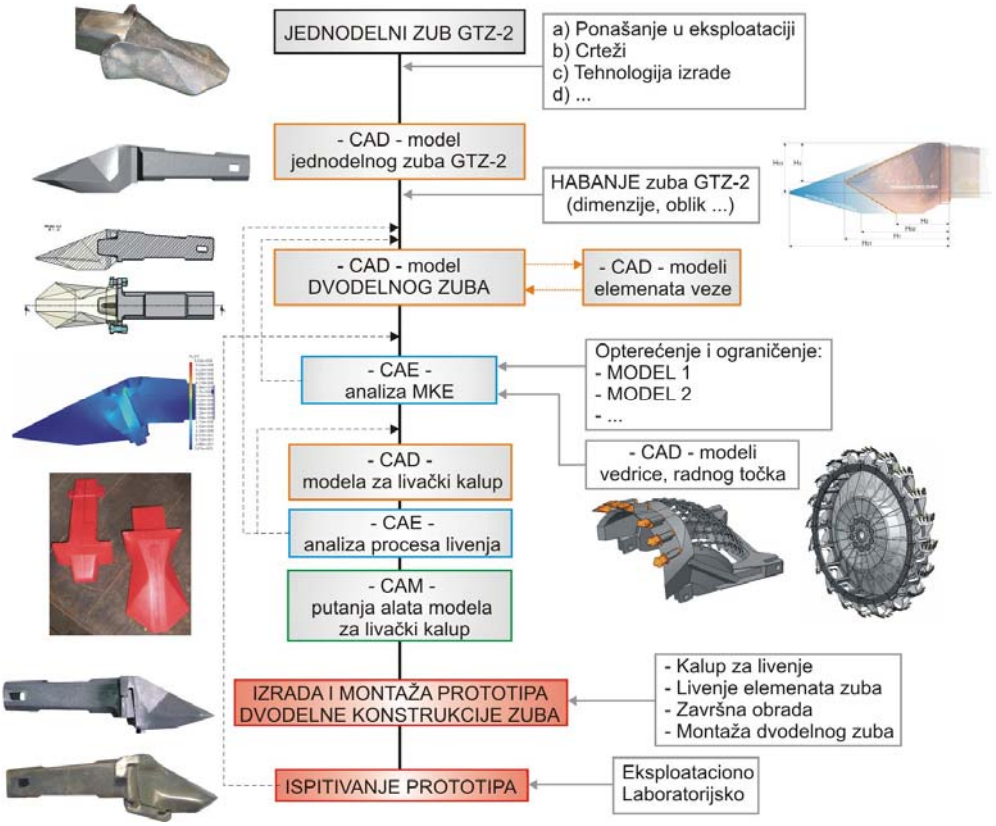

Figure 4. An integrated approach used in the two-piece tooth development

Each design solution has been simultaneously accompanied with the voltage state analysis using the final element method. A number of options have been considered regarding the use aimed at the two-piece tooth development. First, the highest voltage change trends in the construction for each load and constraint variants have been examined. Upon the adoption of an optimum design solution and prototype construction, qualification of the adopted constraint-and-load model has been performed in accordance with the operating test results. The objective has been to establish basic methodology for further development of the design.

A major issue occurring at the development stage has been to decide on the approximation to be used in problem resolution. The data in the FEM analysis are given according to current cutting tooth operating conditions; namely, careful examination should be performed of the boundary conditions, material properties, geometry, operating environment parameters, etc. It is often impossible to accurately describe the above requirements, as they are either unknown or beyond the designer control. In such cases, the trend analysis can be used as an efficient technique facilitating generation of specific useful data "managing" the design process. However, the trend analysis cannot provide data on real design performance, but it can show the effects of geometric changes and susceptibility to parameters such as material properties and applied load, thus highly contributing to the examination of the two-piece tooth design issue.

5. CONCLUSION

An inductive approach is of special importance in resolving engineering and other problems where general solutions cannot be obtained in closed forms. The solutions generated by models and simulations using the finite element method are approximate ones. In practical terms, approximations to the exact solution should be identified, i.e. it should be determined whether the results obtained are on the safety side.

The integrated approach used in the development of the two-piece tooth has a number of advantages being reflected in the cost reduction, the reason being the use of computer at one stage of the analysis, instead of testing under operating conditions. The process itself has been enhanced, due to the reduced number of the product development cycles, induced by the automatic elimination of unsatisfactory design conceptions. The advantages also include design improvements, brought about by the possibility of testing a great number of different conceptions by the finite element method, leading to better selection of the final design. The objective of the above analyses is to choose the optimum design out of many different ones to be subsequently tested under operating conditions. The subsequent testing provides, in

fact, feedback for input and output simulation data, enabling analysis correction and providing basis for future identical or similar design problems.

The importance of the simulation-based analyses lies in potentially higher cost-effectiveness at later product development stages. Therefore, not only can planned testing be performed more rapidly and be more cost-effective, but simulation can enable examination of load scenarios that would be too expensive to perform in real operating conditions. However, importantly, the real design performance can be comprehended only at the prototyping and testing stages. This is exactly the step taken in the design solutions adopted for the two-piece tooth.

REFERENCES

[1] Ivković, B., Rac, A., *Tribologija*, Jugoslovensko Društvo za Tribologiju, Kragujevac, 1995.

[2] Tanasijević, S., *Tribološki ispravno konstruisanje*, Mašinski fakultet, Kragujevac, 2004.

[3] Ognjanović, M., *Konstruisanje mašina*, Mašinski fakultet, Beograd, 2003.

[4] Jugović, Z., *Tribo-ekonomski efekti primene dvodelne konstrukcije zuba na rotornim bagerina*, Treća Jugoslovenska konferencija o tribologiji YUTRIB'93, Kragujevac, 1993.

[5] Jugović, Z., Trbojević, M., Stoisavljević, N., Stajčić, F., *Uticaj konstrukcije zuba za rotorne bagere na troškove proizvodnje*, Zbornik radova Prvog Jugoslovensko-čehoslovačkog simpozijuma „Tehnika, tehnologija i upravljanje procesima u površinskoj eksploataciji uglja“.

[6] Jugović, Z., *Konstrukcija reznih elemenata - zuba za rotorne bagere sa aspekta tribologije*, YUTRIB'89, Prva Jugoslovenska konferencija o tribologiji, Kragujevac, 1989.

[7] Ignjatović, D., *Izvod iz studije – optimizacija konstrukcije vedrice bagera u cilju povećanja kapaciteta*, Rudarsko geološki fakultet, Beograd, 2003.

[8] Hitzschke, K., Jacob, K., *Experimentelle Analyse der Belastung des Schaufelrades durch den Grabvorgang*, Teil 1,2, Hebezeuge und Fördermittel 24, Berlin, 1984.

[9] Raaz, V., *Assesment of the Digging Force and Optimum Selection of the Mechanical and Operational Parametars of Bucket Wheel Excavators for Mining of Overburden, Coal and Partings*, KRUPP Fördertechnik, Germany, 2005.

PLANNING, MODELING, SIMULATION AND ANALYSIS OF STORAGE PROCESSES

Z. Marinković, D. Marković, D. Marinković

Abstract: *In a modern logistics concept of industry, which comprises acquisition, production, distribution and sale of goods in order to achieve profit, a storage system has an important integrative role with the aim of forming reserves and providing synchronization of the aforementioned processes. A warehouse has to be an efficient, economic and safe system that accomplishes functions of receiving goods, their storage and handling and, finally, their shipping to the appropriate user.*

Design of storage system and the choice of storage technology are a complex task, which needs to be given special attention. One of the possible approaches consists in applying the methods of planning, modeling, simulation and analysis of the storage processes. The approach gets on its full significance once the developed software packages are used to perform a great number of computer simulations. In the paper, software package Flexsim is applied in order to deal with the problem. The approach provides means for inexpensive variant design of storage systems and relatively simple choice of optimal solution.

Keywords: *logistics, warehouse, planning, modeling, simulation, analysis*

1. INTRODUCTION

Logistics is a relatively new scientific discipline intensively used within the past 30 years in industrial, organizational and other activities. It determines complete and complex material (goods), information and money flows within single companies as well as between them on a regional or even global level. Offering good organization and reduced expenses, logistics is a basic presumption of successful functioning at all levels of industry [1, 2, 3].

The basic logistics concept of industry implies acquisition of primary raw materials, fuels and other materials necessary for production of goods or providing services and distribution of products to the market with the aim of achieving the maximal profit. In such an industrial concept, it is necessary to perform various activities, which increase the final price of the product. Those are packing, transshipment, storing, inner and outer transportation [4, 5].

Within this concept, the storage system has an integrative role in the processes of acquisition, production, distribution and selling goods. The aim of storage systems is to provide reserves and synchronization of processes preceding and succeeding storing. Storage has to be an efficient, economic and safe system. Therefore, the design of storage systems and choice of storage technology are given special attention. The modern approach to this issue implies usage of novel planning methods, modeling, simulation and analysis of storage systems, including the analysis of components and involved processes [6, 7, 8, 9].

2. DESCRIPTION AND PLANNING OF STORAGE SYSTEMS

The process of planning implies determination of system structure and in this specific case it is storage. Handling this issue requires [5]:

- knowledge of planning theory and methods,
- analysis of already existing examples,
- catalogues with necessary data for the choice of equipment and control systems, which are very important regarding the process of planning.

Successful planning and realization of optimal storage system requires detailed analysis, knowledge of purpose, organization, components and processes of the system. Storing can be described as a motionless state of material for a longer or shorter time period, which is organized and supervised in a specially developed storage system. Reasons for storing are various and the role of storage system in a logistic system is diverse and complex.

Storage system is organized in places where raw material is available (e.g. mines), where transshipment is performed (railway-road terminal), in the beginning and at the end of production line, in the process of good distribution to the market, collecting of waste, etc.

Storage is a complex logistic system consisting of several connecting components and elements, in which four basic processes are conducted [4]:

- receiving goods,
- storing goods,
- handling goods (sorting, separating, positioning, packing, commissioning, labeling, etc.),
- shipping goods.

Prof. dr Zoran Marinković, Mašinski fakultet Univerziteta u Nišu, zoranm@masfak.ni.ac.yu,
Danijel Marković, Mašinski fakultet Univerziteta u Nišu, daca17510@yahoo.com,
dr Dragan Marinković, Mašinski fakultet Univerziteta u Nišu, gagimarinkovic@yahoo.com

Elements and components of a storage system are: material goods (items), storage building with infrastructure and appropriate zones (receiving, storing, shipment), storage equipment necessary for the storage activities (transshipment, transport, control, positioning, etc.) and information system. Additionally, it is very important to define the organization of a warehouse, which can be divided into:

- structural organization, which describes the subsystems and elements of complex storage systems,
- organization of activities, which defines the tasks from the strategic (administrative), tactical (dispositive) and opertaive (executable) point of view and provides their realization,
- informational organization, which provides exchange of information between the storage system and its environment as well as within the storage system itself.

Material goods (items), as storage units, can be divided based on several criteria. One of the criteria yields unpacked and packed materials and products. We can also distinguish between piece, bulk, fluid and gas materials. However, with appropriate packing any good can be rendered piece good, which is relatively often the case. Another criterion is whether storing of material goods requires accessories, or not. Most frequently, those are standard pallets with predefined dimensions and shapes.

Storage objects are all open or closed areas with the purpose of storing goods. Their division can be done according to various criteria, such as: position with respect to the ground level, shape of the structure, construction and material it is made of, sort of stored goods, storage conditions, capacity, etc. [4]. With the aim of efficient realization of aforementioned four processes (receiving goods, storing, handling, shipment) storage objects are divided into zones. Typically, there are zones for receiving goods, their storage and shipment, while handling is done in one of those zones. A storage can also have a special zone for handling goods. Additionally, the storage zone can have subzones depending on the type of goods and necessary conditions for storing.

All the equipment used in the storage is denoted as storage equipment. It is used for various activities in handling goods, especially when work that is more efficient is required. Two basic groups of transport machines are used. The first group comprises machines of discontinuous transport, such as various types of cranes, forklifts, special purpose vehicles, etc. They perform transport cycles. The other group of machines comprises machines of continuous transport, such as various conveyors, elevators, etc. They transport material continuously. The capacity is a very important characteristic of all those machines. It is defined as a quantity of transported material per time unit. In the storage zone, there is equipment which is used to receive and to store the goods. Those are different types of racks, which provide manageable positioning of the goods in order to use efficiently the available storage surface and volume. However, warehousing can also be done by using only the ground surface and in this case the equipment is not needed. In a storage system, there is also accessory equipment, which is used for other activities when the goods are received, handled and shipped. Those are machines for packing, unpacking, palletizers, scales, control devices, etc.

The informational organization in storages consists of information and communication systems which operate by means of computers. There are work stations for receiving and providing data, and appliances for data transmission, which can be achieved by conductors, optically, inductively (infrared) and wireless (radio technique).

Since the storage system plays an important role in the logistic chain, there is a number of various storage technologies developed till date. The choice of technology is influenced by the type of goods, equipment for transshipment, transport and storing, equipment for storing goods, information system etc. In addition, the choice is influenced by the chosen strategies of manipulating the goods in storages. Some of them are: selectivity (direct approach), JIT (just-in- time), FIFO (first-in-first-out), LIFI (last-in-first-out,) random approach, the shortest time of realization of transport machine working cycles, strategy of double cycles, etc. A great number of typical storing technologies for piece, bulk, fluid and gas materials has been developed. The paper deals with strategies for piece and palletized goods. [4].

Some typical storing technologies are:

- ground storing (chaotic, linear and on a stack),
- storing in racks (selective, portable, transport racks).

High-rack storages are nowadays quite frequently used. The standardized pallet units are stored in high racks, the height of which is up to 40 m and the length of up to 100 m, by means of specialized high-rack cranes. Automatic high-rack storages are the state-of-the-art technology, with cranes operating as robots controlled by means of adequate computer programs [7, 8, 9].

The choice of adequate storage technology has the aim of providing efficient usage of warehouse surface and volume, lower expenses of handling goods during transshipment, transport, storing and other processes. Analysis of existing technologies by means of planning methods can result in their improvement and development of new atypical storing technologies, which can be later on accepted as typical ones.

The planning of logistic systems requires the following issued to be considered [6]:

- **type of planning:** a new system or reconstruction of old one,
- **object of planning:** storage system, transport system, etc,
- **planning step:** from idea to final realization,
- **type of storage:** transhippment, distributional, reserves, etc,.
- **goods:** type of goods (pieces, bulk...), palletized, etc.
- **sort of object:** openned, hall, high storage, metal structure,
- **owner of the storage:** state, company, etc.
- **storage technology:** ground or rack storage
- **positioning of goods:** manual, automatic
- **type of racks:** portable, transport, etc.
- **transportation means:** machines of continuous and discontinuous transport,
- **special conditions:** fire protection, assessment of economy, analysis of alternative solutions, etc.

The task of planning a storage system implies to apply adequate procedures in order to obtain the optimal

solution. The methods of modeling and simulation are successfully applied.

3. MODELING AND SIMULATION OF THE WORK OF STORAGE SYSTEM

Modeling implies description of real complex systems, in this case storages with equipment, by means of adequate relatively simple equivalent and analytical models. The simplified models are used to perform simulations.

Software package Flexsim is successfully used to perform the simulations of storage systems. It is well integrated with CAD and 3D modeling software packages. It also offers comprehendible precompiled C++ script (Flexscript), which makes it user friendly in praxis [8, 9].

Flexsim is an object oriented software. The Flexsim Tree provides a user friendly approach to handling the model. The basic unit of tree is node (Fig. 1).

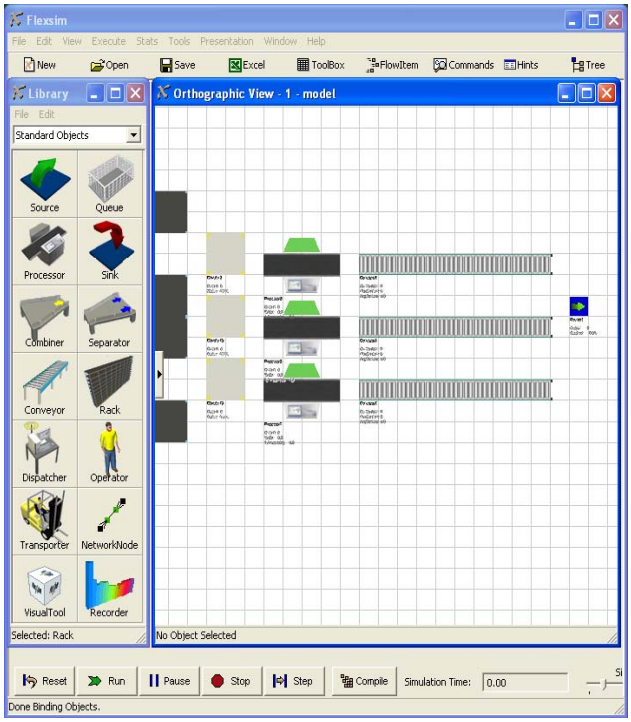

Fig. 1 *Node of the model tree - layout definition*

On the left hand side of Fig. 1 one may note the Library, which comprises ready-to-use elements. Those are standard elements (transport means, operators, pallets, racks…) necessary for simulation. The right hand side of the figure shows working area, where the layout is formed. For each element from the library the initial parameters are to be defined, when it is used.. Input parameters are defined in the Parameters Window. Every type of object has a corresponding Parameters Window.

The general procedure (algorithm) of modeling and simulation of storage system in Flexsim requires [8, 9]:

1. **Layout definition, i.e. positioning of the Library objects in the working area.** At first the Source is given, which defines the starting point of material flow. The elements that follow are: Conveyer, Queue, Transporter, Rack, as given in Fig. 1
2. **Defining the flow of storage units through the model, i.e. linking the objects by means of ports.** The term linking implies creation of output to input port connections between objects. The links are necessary to mark the product flow. Besides output to input connections, there are also central port to central port connections. They are used by Fixed Resources to call for transport or assistance during the work (Conveyer, Transporter). Hence, output to input connections create links between fixed objects (Sours, Queue, Processor), while central connections create links between fixed objects that require transport and mobile objects that perform the transport.
3. **Detailed definition of objects,** i.e. definition of their parameters (capacity, transport paths, velocities, accelerations, masses, coordinates, time…)
4. **Compiling and running the model** with the aim to perform the required simulations of storage operations.

The software provides following features:

- 3D pictures of all storage zones with storage equipment (transport machines, racks, etc),
- preliminary, and eventually final integration of aforementioned equipment in the storage,
- determination of storage capacity, i.e. the number of storage units, the efficiency of surface and volume usage,
- determination of transport equipment capacity,
- the choice of optimal characteristics for the involved equipment by varying relevant parameters in the model with the aim of obtaining the optimal technical solution of the storage,
- saving data in the form of excel files once the simulation is accomplished

This procedure of fast and comfortable modeling and simulation offers the possibility of investigating alternative variant solutions of storage systems by varying relevant quantities. In this manner the following tasks can be performed [6]:

- analysis of initial state,
- seeking the most suitable system by developing alternatives,
- assessment of alternatives,
- determination of optimal system alternative.

The approach will be demonstrated on an example dealing with planning a storage system, whereby several variant solutions are to be investigated. Modeling and simulation of storage in operation are performed in order to determine the optimal solution and deduce useful conclusions about designing storage systems.

4. EXAMPLE OF SIMULATION AND ANALYSIS

As an example of modeling and simulation of storage system, a small storage with palletized goods and selective racks is to be considered. Selective racks are put

together in pairs with a corridor between the pairs so that a path is provided for transport machines. The number of rack walls is double the number of corridors. In this way a direct approach is provided to each storage unit. However, the efficiency of surface usage is relatively small.

The storage zone surface (covered by racks and corridors) is $A_{sz} = 12 \times 20 = 240\ m^2$. The height of the storage can be varied depending on the transport machines used in the zone.

In the example the storage unit is a 800 × 1200 mm palette containing packed products. The maximal height of the unit is 1500 mm. The surface and volume of the unit are $A_{sj} = 0.8 \cdot 1.2 = 0.96\ m^2$ and $V_{sj} = 0.8 \cdot 1.2 \cdot 1.5 = 1.44\ m^3$.

The basic unit of volume usage in the storage is rack cell, the dimensions of which are defined by the vertical and horizontal dimensions of the rack's truss structure. In this example the dimensions of the rack cell are 2.0 × 1.6 m providing enough space for two palettes.

In this way the rack wall is divided into a number of columns and rows. The number of columns in this example reads 20.0/2.0 = 10, while the number o f rows depends on the height of the rack wall. If the height is up to 10 m, then various types of forklifts are used, and if the height is beyond 10 m (high-rack storages) special rack cranes are used. Also the width of the corridors depends on transport machines.

Two basic alternative solutions of this storage will be modeled and their functioning will be simulated. In the first solution the height of rack walls is under 10 m and the transport machines are forklifts. In the second solution a high-rack alternative with high-rack cranes is considered.

Figs. 2 and 3 are obtained by means of Flexsim and they show 3D models of the first solution with forklifts, the maximal lift height of which is 5 m. The necessary corridor width for their manipulating is 3.4 m. In this case, the surface of the storage zone is large enough for 4 racks with 4 rows and the height is 6.4 m. The volume of the storage zone is $V_{sz} = 12 \times 20 \times 6.4 = 1536\ m^3$. Since the rack has 10 columns, and in each cell 2 palettes can be put, each rack wall can contain 4 × 10 × 2 = 80 storage units, and for the whole storage the number reads 320. The degree of surface (η_A) and volume (η_V) usage for this solution are:

$$\eta_A = 320 \cdot 0.96 / 240 = 1.28 \approx 1.3,$$
$$\eta_V = 320 \cdot 1.44 / 1536 = 0.3.$$

Figs. 4 and 5 show the 3D model of the second solution with selective racks, but this time as a high-rack storage. Each corridor is foreseen to be served by one rack-crane. The width of the corridor is therefore only 1.4 m. The same surface now allows for 6 rack-walls and 3 corridors. The corridor width is determined by the larger dimension of palette, which reads 1.4 m. The racks have now 10 rows, so that the overall height of the rack is 16 m. The volume of the storage zone reads in this case $V_{sz} = 12 \times 20 \times 16 = 3840\ m^3$. Since the number of racks is 6, their height 16 m and the number of rows 10, the number of storage units is significantly increased to 1200. The capacity of this solution is 3.75 times larger compared to the first solution. The degree of surface (η_A) and volume (η_V) usage are now:

$$\eta_A = 1200 \cdot 0.96 / 240 = 4.8,$$
$$\eta_V = 1200 \cdot 1.44 / 3840 = 0.45.$$

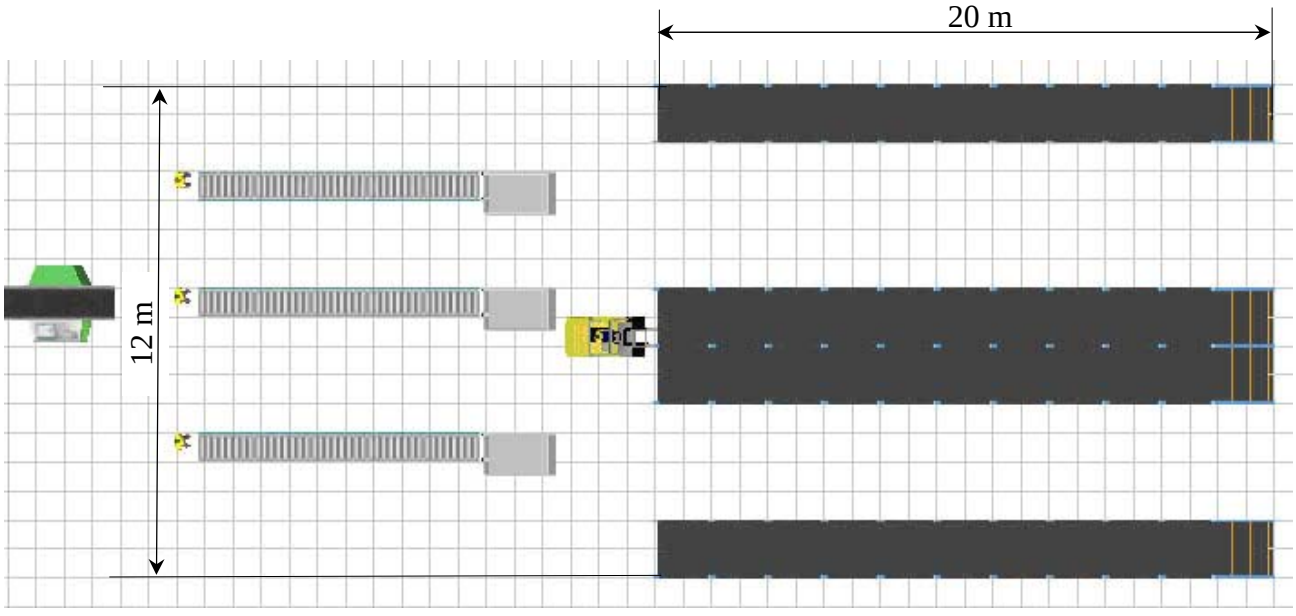

Fig. 2 *Top view – 3D model (layout) of the first solution*

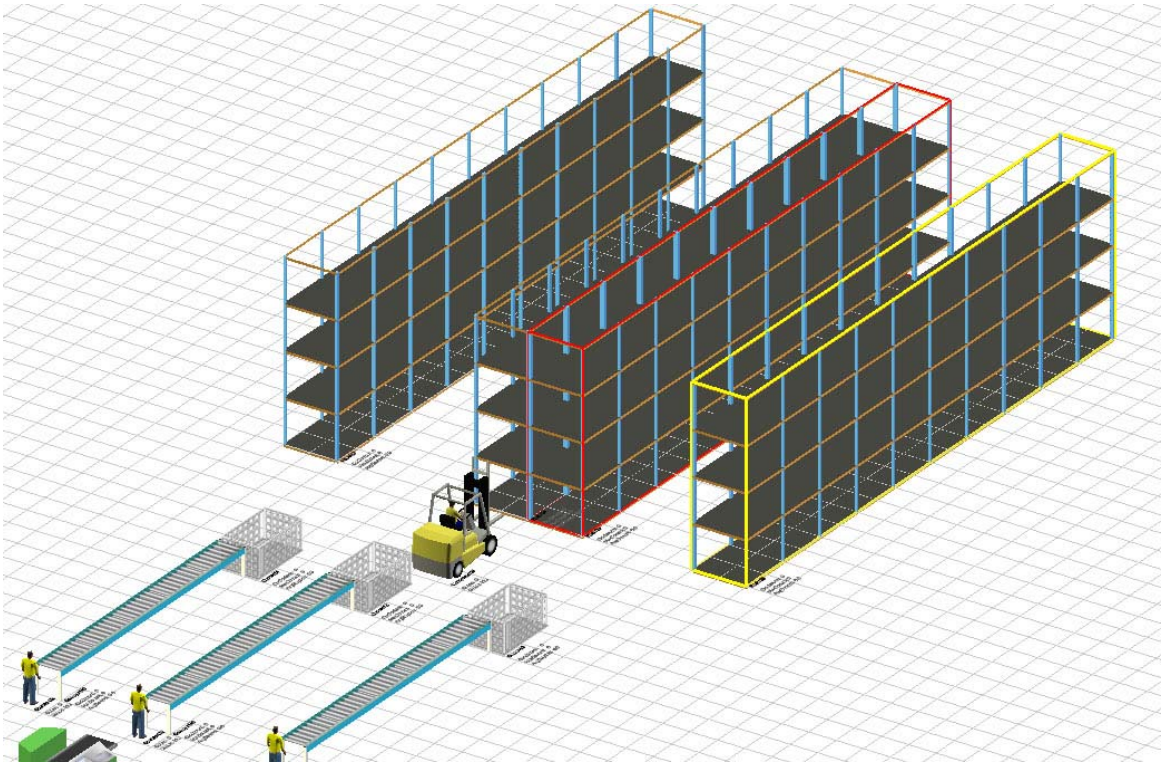

Fig. 3 *Axonometric view - 3D model of the first solution*

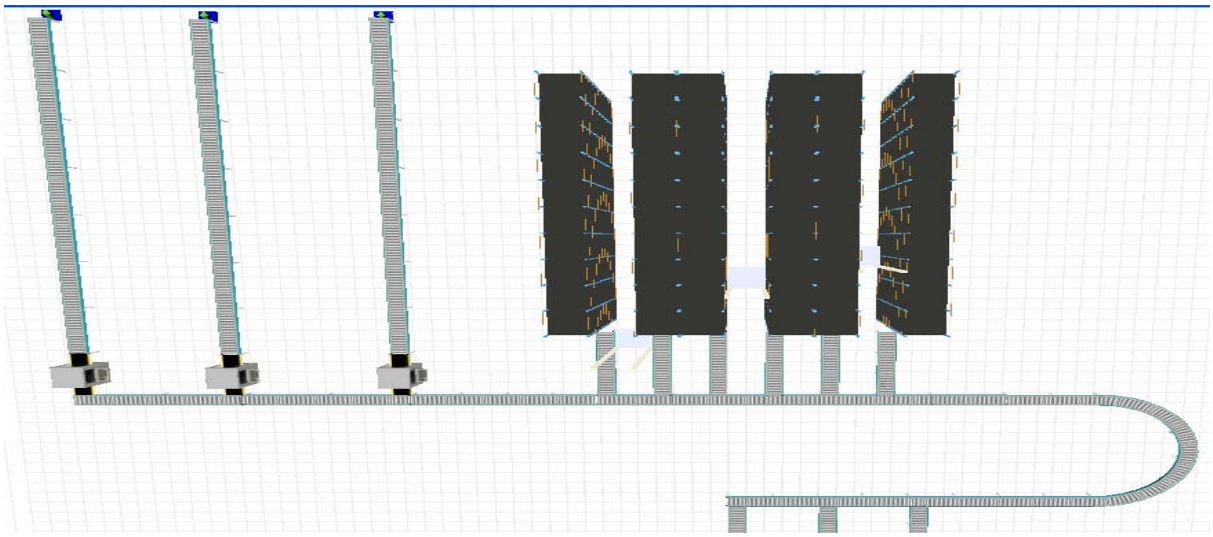

Fig. 4 *Top view – 3D model of the second solution*

Obviously, the surface usage degree is significantly increased in the second solution, approximately 3.7 times, while the volume usage degree is increased 1.5 times. The main reason for such different trends is the fact that the corridor width in the first solution is significantly greater compared to the second solution. This drawback of the first solution can be reduced by using special types of forklifts, such as hybrid telescopic forklifts or similar. In that case the corridor width can be reduced to 1.8 m and additionally the lift height can be increased up to 10 m [4].

As can be seen, Flexsim provides relatively easy and fast modeling of storage system's different variants and their 3D pictures, which is important for integration of storage equipment in the predefined location of storage zone and storage as a whole. The software also provides the possibility to simulate operation of equipment, i.e. processes that are performed in the storage, and to make a video file of the simulation. Varying the characteristics of transport equipment, such as velocities, accelerations, lengths of transport paths, it is possible to investigate and analyze the parameters that influence the capacity of equipment with the aim of choosing the optimal solution.

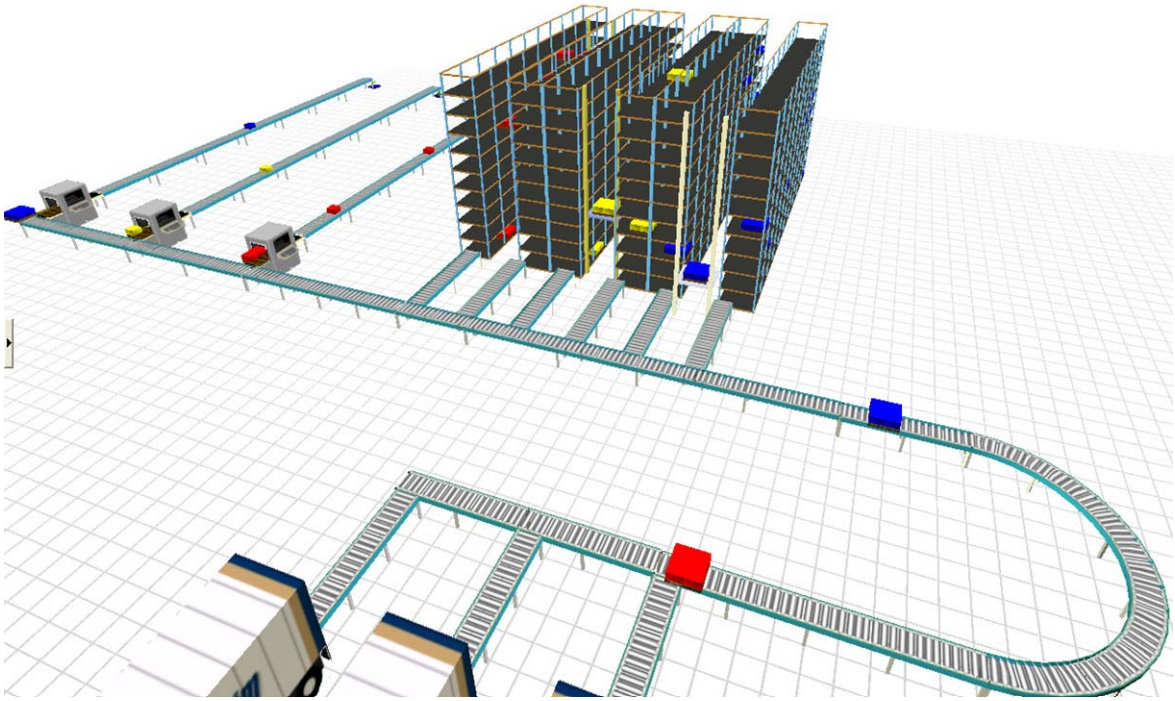

Fig. 5 *Axonometric view - 3D model of the second solution*

Once several solutions are obtained, the optimal one is determined by using the assessment methods. Each element of the analyzed solution is assessed based on weight factors defined by experts. The best graded solution is accepted for the final realization.

A rough comparison of the considered two solutions yields following remarks. The price per mass unit of rack is inconsiderable for both solutions. The second solution has a bit higher expenses due to assembly of high racks. A forklift is certainly less expensive than a high-rack crane, especially automatic one. Additionally, the second solution has a high-rack crane in each corridor. This solution is justified only for storages with high capacity and high material flow rate. Hence, the high-rack storages require higher investments, especially if they are automatically operated, but an intensive exploitation reduces final expenses. Finally, the first solution also requires a massive expensive building, which is not the case with the second solution.

5. CONCLUSIONS

The following conclusions can be drawn from the preceding analysis:

- storage is an important subsystem of the logistic concept of industry which provides a link between acquisition, production, distribution and sale of material and goods,
- a significant number of typical storage technologies has been developed and the appropriate choice is affected by a number of influencing factors, which need to be analyzed,
- an efficient way of selecting the adequate storage technology for a certain storage is to apply the methods of planning, modeling, simulation and analysis,
- a successful application of this approach is provided by software package Flexsim,
- software Flexsim gets on its full significance if a variant solutions are investigated, whereby the solution parameters are varied with the aim of obtaining the solution with optimal technical parameters.

LITERATURE

[1] Guenthner W.: ***Tokovi materijala i logistika***, prevod skripte, Mašinski fakultet Univerziteta u Nišu, Niš, 2006.

[2] Jevtić V.: ***Tehnička logistika***, skripta predavanja, Mašinski fakultet Univerziteta u Nišu, Niš, 2005.

[3] Arnold D.: ***Materialflusslehe***, 2. verbesserte Auflage, Viweg, 2000.

[4] Vukićević S.: ***Skladišta***, Preving, Beograd, 1994.

[5] Lippolt C.: ***Sistemi skladištenja i distribucije***, (prevod predavanja), Mašinski fakultet Univerziteta u Nišu, Niš, 2005.

[6] Martin H.: ***Planiranje logističkih sistema***, prevod knjige, Mašinski fakultet Univerziteta u Nišu, Niš, 2005.

[7] Zmić Đ., Savić D.: ***Simulacija procesa unutrašnjeg transporta***, Mašinski fakultet u Beogradu, Beograd, 1987.

[8] Marinković Z., Marković D., Marinković D., Milić P.: ***Modeliranje i simulacija rada visokoregalnih skladišta***, Treći srpski simpozijum sa međunarodnim učešćem TIL 2008, Niš 2008., CD, Mašinski fakultet Univerziteta u Nišu, Niš, 2008,

[9] Marković D.: **Automatizovana visokoregalna skladišta**, diplomski rad, Mašinski fakultet Univerziteta u Nišu, Niš, 2008

THE IMPORTANCE OF RESEARCH OF LOCAL-SCOPE PHENOMENA WITHIN SINGLE-ROPE CABLEWAYS

M. Čupović

Abstract: *Cableways are complex products, subjected to high security requirements and economic feasibility assessments. Some phenomena, which are not fully comprehended by calculations and testing, could significantly reduce a cableway service life and lead to sudden failures. Accordingly, positive economic effects of the cableway exploitation could be multiply reduced. One such phenomenon, with all its implications, will be presented in this dissertation.*

Keywords: *single-rope cableways, grip, hold-down sheave assembly, shock impulse, carrier acceleration, tension consequences, dynamic behaviour identification*

INTRODUCTION

The calculation of a cableway line is an itterative procedure, based on the flexible threads theory. The goal of the calculation is to determine the extreme stress values, in order to achieve optimal design of the cableway construction during the next development phase. By doing so, the necessary safety of the cableway is accomplished. Service life of individual cableway elements and the commodity of passangers are also affected by the so-called local scope phenomena. These phenomena are defined by having considerably less intensity than the so-called global scope phenomena and, as such, they are commonly overlooked by cableway designers.
The main purpose of this writing is to point out one of these phenomena and possible consequences of not evaluating it properly.

GLOBAL SCOPE PHENOMENA

Change of the resultant due to stress change on incoming and outgoing sides of the rope

The resultant force on the tower point, which has to be received by sheave assemblies and transmitted to the structure of the tower, is a vector sum of the forces inside the haul rope (on incoming and outgoing side) on that tower point. In the rulebook of technical standards for ski lifts /1, 2/, within articles 36, 37, and 38 (for ski lifts) and articles 58, 59, and 60, the legislator specified the following cases of tower stress:

1. Dead weight of the tower and its equipment;
2. Dead weight of the haul rope;
3. Weight of the haul rope with carriers;
4. Weight of the haul rope with carriers, with fully loaded (100%) uphill side and empty downhill side;
5. Weight of the haul rope with carriers, with empty uphill side and fully loaded downhill side;
6. Weight of the haul rope with carriers, with both uphill and downhill sides fully loaded;
7. The load induced by derailment of the haul rope on one side (the side without the load);
8. Dynamic stress caused by the passage of carriers over sheave assemblies:

Vertical load:

$$Fv = 2 * Gv$$

where Gv denotes *weight of the loaded carrier;*

Horizontal load:

$$Fh = Fk$$

where Fk denotes *static force on one sheave.*

In the bullwheel calculation, the resultant force is defined to be the function of:

- weight of the approved carrier
- geodetic position of the tower;
- approved tension force;
- the chosen type of line equipment (sheave and sheave bearing type);
- type of haul rope, through the weight of the rope on the related gauge;

The main disadvantage of such calculations is that they do not include local scope phenomena, which occur in brief

PhD Milomir Čupović, Faculty of Mechanical Engineering Kraljevo

intervals on the sheave assemblies and, depending on the cableway's basic features and the chosen type of equipment, may have significant impact on cableway's behaviour throughout its service life.

LOCAL SCOPE PHENOMENA

Change of refraction angles

During transition of the carrier from bullwheel to sheave assembly, the balanced configuration of the mechanism is disturbed. Consequently, there are movements in the mechanism's joints, after which the new position of equilibrium is established /3/.
Processes that occur within the sheave assembly mechanism's kinematics will be observed in aspect of the change in balanced configuration of the sheave assembly mechanism during the passage of a loaded carrier through it.

Passage of the grip over the sheave assembly

When the naked (bare) rope, between two adjacent carriers, pass over a support or hold-down sheave assembly, individual sheaves rotate as a result of a load difference between upcoming and outgoing side of the haul rope.
When a carrier approaches the sheave assembly, the grip becomes the source of various inputs. The grip is, actually, an element that bonds the chair with the haul rope. Figure 1 shows the position of the grip and a hold-down sheave assembly.

The angle of the resultant force is also variable and depends on the particular load case. The intensity and change of the angle of the resulting force, calculated in this way and adopted in their extreme minimum and maximum values, represent changes that depend on global conditions on the rope line.

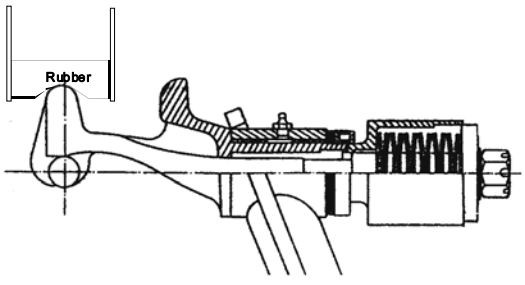

Figure 1

The passage of the grip over the sheave assembly is characterized by the process of transfer of energy. Part of the kinetic energy caused by the movement of the rope with the carrier, whether loaded or empty, will be transferred to the sheave assembly. It is this part of kinetic energy that causes relative movements of individual sheaves, as well as rotation and vertical movements of the assembly, while the remaining part transforms into the energy of deformation of sheave assembly and the tower, respectively.

Passage of grip over the hold-down assembly

What makes the hold-down (or negative) sheave assembly so specific, is the fact that grips pass below the sheaves. As a result, the upper surface of the grip, whose geometry is defined by strength calculation, comes *n*-times in and out of contact with the assembly (where *n* is the number of individual sheaves in the assembly).

The passage of the grip is usually followed by a series of tower tremblings. Sitting in the chair, passengers feel like they are riding on a road with many small holes. Figure 2 clearly depicts the elements that define the contact between the grip and the sheave as an impact of two solid bodies. However, the mass of the grip is many times greater than that of the sheave ($M >> m$), and there is also speed difference in the point of impact.

The differences in materials are also important. The sheaves are rubber-plated, while the grips are made of molded steel.
In the moment of impact, there is a strong shock impulse, whose intensity may easily be many times greater than the static force on each individual sheave. In the aspect of duration, this impulse is defined as instantaneous.

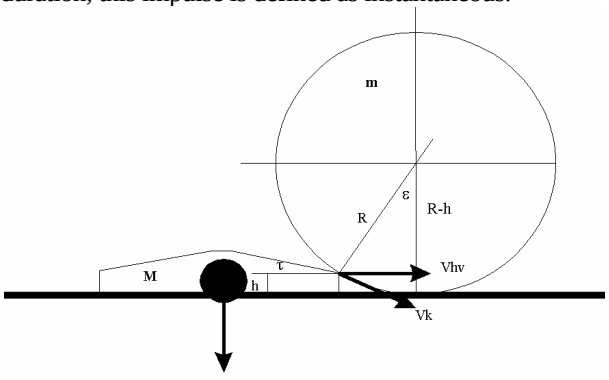

Figure 2

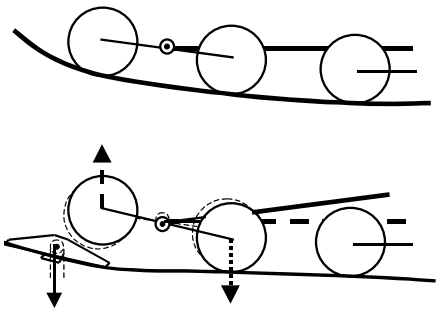

Figure 3

$$Vhv = v = (2.2 - 6)\,{}^{m}\!/_{s}$$

$$Vk = v$$

$$Vkh = v * \sin\varepsilon$$

$$\varepsilon = \arccos\frac{R-h}{R}$$

As a result of the shock impulse, redistribution of the load takes place. In the moment of impact, the shock impulse is being transferred to the haul rope by the opposite sheave, paired with the sheave being hit (see Figure 3).

Magnitude of the angle, around which the resultant changes its position, is the function of the force *Fi* (*Fi=Fr/n < 5Kn*) and depends on the defined refraction angle on the tower point and the structural characteristics of the sheave assembly. The frequency of this phenomenon can be calculated as:

$$f = \frac{1}{\frac{l}{v}}\ [Hz]$$

where: *l – distance between sheaves*
v – line speed of the cableway

For the most common dimensional relations in fixed grip cableways, the value of the force is somewhere around *f* = 4 -12 *[Hz].* The frequency of this phenomenon is relatively low and there's a risk of its superposition with the tower's own frequency. While the static implications of the phenomenon may be neglected, its dynamic implications must be taken into account.
After the impact between the grip and the sheave, the sheave assumes position shown in Figure 4. By leaning on the slanted surface of the grip, force *Fi* assumes direction that is perpendicular to the grip. The change of the angle results in the new redistribution of forces.
The same phenomenon, but with the change in direction of force *Fi sin τ,* occurs when the sheave is on the other side of the grip. The analysis is done for the initial position of the grip, when the slope angle of the haul rope is $\alpha = 0^{o}$. The change in the slope angle of the rope results in the change of the force magnitude *Fi'=Fi sin (τ+α).*
The possibilities of reducing the effects of this phenomenon should be searched within the structural characteristics of grips and sheave assemblies.

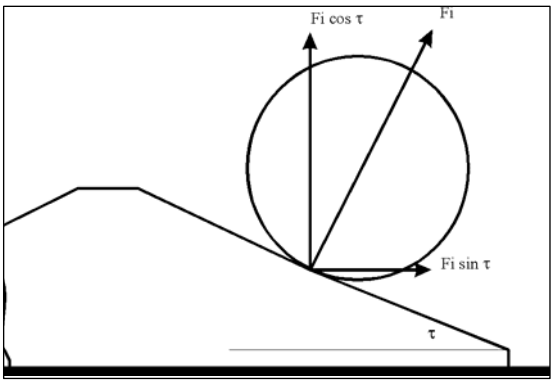

Figure 4

The load induced by carriers passing over the compression sheaves assembly

Figure 5 shows the diagram of a loaded carrier acceleration during its passage over a compression sheaves assembly.
The acceleration sensor, attached to the carrier structure, detected the acceleration signal, which is measured in vertical direction and shown in the figure. You can clearly see the moment when the carrier and the sheave assembly come into contact (650 s), and the moment when the grip leaves the assembly (1650 s).

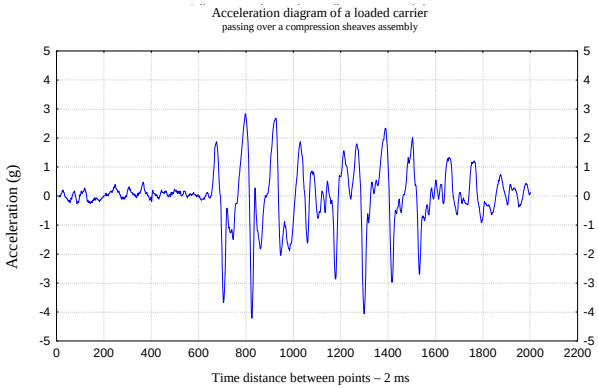

Figure 5

That very moment, as a clip in greater scale, is shown in Figure 6. The detected signal has relatively regular shape, with little noise.

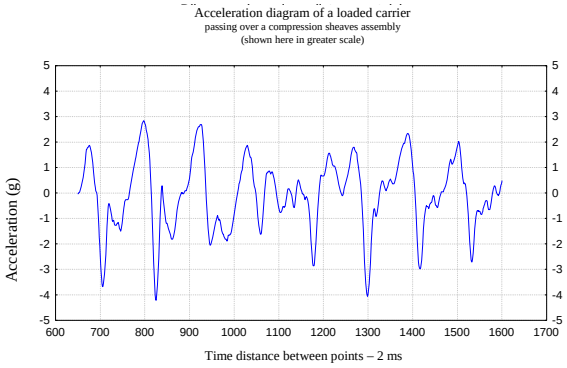

Figure 6

Passage of the carriers results in forced damped vibrations of the tower structure. The part of the tower that is most vulnerable to this input is the yoke, which is the firts that starts to oscillate. After a ceratin delay, these oscillations are transferred to the main part of the tower. It is important to see if there are any implications on the tension, that might be caused by these oscillatory movements of the structure.

Tension implications of the passage of carriers

Experimental testing of the established hypothesis has been done by measuring tension response on one of the chairlifts on Kopaonik mountain, during the winter season. The rosette-shaped measuring tape has been attached to the tower stem, right above the joint of the tower and anchor bolts, that is at the place where the highest carrying strength had been expected.
Such position of the measuring tape enables monitoring of normal tensions σ (in Y direction) and sliding tensions τ (in YZ direction).

The tension changes in all directions and components have been undoubtedly detected. What is actually the most logical conclusion, is the significant increase of normal tensions (pulling tensions, parallel to the vertical tower axis), as shown in Figure 7. The structure is made of steel Č. 0362, with $\sigma_{doz} \leq 18$ kN/cm^2. The observed increase of 13% in working tensions, comparing to calculated values of 12 kN/cm^2, might significantly shorten the service life of the construction.

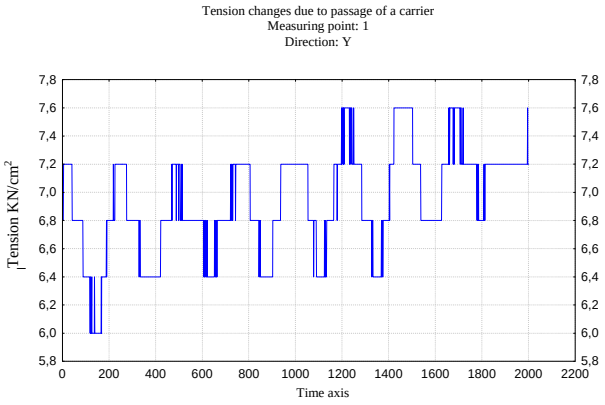

Figure 7

Tower structure that has been considered in this writing is one of the cableway elements that is the most resistant to the effects of the described phenomenon. As mentioned earlier, the input indirectly acts on the structure of the tower.

The element that is directly exposed to this kind of input is the carrying frame of the chair, whose mass is about 270 kg (with two passengers). As shown in Figure 7, this element suffers alternate accelerations of 4g, during time intervals in the order of milliseconds.

SUMMARY

The described phenomenon has distinctly dynamical properties, so it is necessary to dynamically identify the part of the structure that is mostly exposed to this kind of input. Frequency spectrum of the tower structure's tension response lies in the range of 3 – 6 *[Hz]*, with the mass frequency participation of 4 *[Hz]*.

It is also important to create a calculation model that would establish correlations between: resultant force per one sheave, the kind of sheave lining, geometry of the grip, and the distance between individual sheaves in the assembly.

REFERENCES:

[1] **Pravilnik o tehničkim normativima za osobne žičare,** Službeni list SFRJ, 2/85

[2] **Pravilnik o tehničkim normativima za ski-liftove,** Službeni list SFRJ, 5/84

[3] Dukelskij A.I.: **Podvesniye kanatnye dorogi i kabelnye krany**, Mašinostroenie, Moscow-Leningrad, 1966.

OPTIMISATION OF THE LIFE TIME OF THE CONTAINER CRANES

G. Bojanic, M. Georgijevic, V. Bojanic

Abstract: *In the calculation of life time of the cranes in the early phase of designing and constructing appears the problem especially in data collecting and analyzing. The standard which deals with fatigue issue JUS U.E7.150 for the welded support steel structure (Federal Institute for Standardization, Belgrade, 1987) is only partially changed translation of the DIN standard which itself is not sufficient for calculation which would more precisely define the fatigue that appears in the structure. Based on new standards which have been introduced in Serbia (SRPS EN 13001-2), it will be necessary to use the calculations which are defined in these standards which indicate that for designing and development of new products it is a must to have corresponding software packets for optimization. To make a calculation with reference to the fatigue in the field of the time dynamic strength it is needed to have many data. With development of software packet it has been enabled to copy a certain system with its dynamic process into the model appropriate for experimenting, aimed to get knowledge which are applicable in the reality (simulation models according to VDI).*

Keywords: *SRPS EN 13001-2, cranes, development, simulation, optimization*

1. INTRODUCTION

There are many papers about fatigue of various materials, with different frequencies of stress cycles, many experiments made in this field, but, however, no hypothesis is completely parallel to the real process which happens within the material, and result obtained by means of calculation to a certain extent deviate from data obtained by the experiment. Many papers about cranes have been written recently, but only few deal with the fatigue, and that is so in Serbia, as well, although to solve problems they must be noticed first and then started to be solved with presenting proposals and chosen the best solution. Even in the world there is no absolutely defined way which will bring an engineer to results which will be completely exact, but even there appears certain probability, proposals and hypotheses.

2. NEED FOR SIMULATION MODELS

There is wish and need to inform the machine industry in Serbia about this problem issue in order to make improvement in calculating of cranes and corresponding equipment so enabling the manufacturers of the components to give and to get data on the optimisation of their products with an aim to make products which will be concurrent in the world market. Over-sized structures can not be interesting because of the great consumption of material and the high price.
Simulation models advanced a lot in the last years, their understanding and application in the industry all over the world is greatly improved, also reflected in the lower price of the products, greater material saving, lighter structures and more mobile structures. Data obtained on the basis of research are saved and the manufacturers in order to stay concurrent give only data from the previous generations and not of the actual ones. Definitely Serbia is also even late in application of the simulation models and situation is even worse in optimization of the simulation models. Application of simulations requires knowing of phenomena that happen in the reality, and the calculation itself is a tool which is, sometimes, the only way to get results.

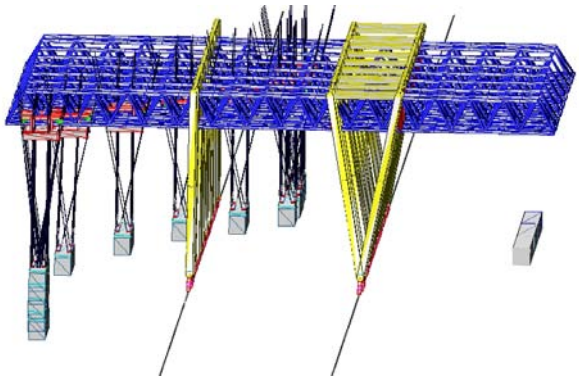

Figure 1: Simulation model (software ADAMS)

The engineer must know the nature of phenomena that appear and, also, advantages and shortages of the software used for performance of the calculation. So, the adequate use of simulation models requires an extreme knowledge but if we desire to reach and keep the step with the world we must constantly modify and permanently learn from our mistakes and those of the others. The software packets which will be presented in the paper are used now, but it will be so in a couple of years is to be shown by time. When new, more modern software packets appear it is needed to get acquainted

Goran Bojanic, Faculty of technical sciences, University of Novi Sad, g.bojanic@yahoo,
Milosav Georgijevic, Faculty of technical sciences, University of Novi Sad, georgije@uns.ns.ac.yu
Vladimir Bojanic, Faculty of technical sciences, University of Novi Sad, vlada.bojanic@yahoo.com

with their content what is not easy at all, but the rest of the philosophy is staying. The race has not been finished and this is to moment when we are deciding whether to continue to run and at what pace.

3. WORKING STRENGTH

To have the adopted solution meets its purpose it is needed that proves are carried out for: stress, elastic stability, deformation, joints safety, attenuation of structure's oscillation, dynamic stability, against tumble and durability to the fatigue. There are many various ways in which the named proves can be carried out, and the proving method left to the engineer.

Proof of fatigue durability is also called proof of fatigue strength and should present the approximation of the real fatigue damage in material. In order to perform the proof it is needed to acquire expected values of stress change in material, the hypothesis must be chosen and, as already said, the manner of application is left to the constructor. Approximation of fatigue that happens in material includes that the changeable stress of sufficiently high amplitude in material after certain number of working cycles causes material damage (phase of initial deformation, phase of micro-cracks, and phase of spreading of micro-cracks) which creates the technical cracks, its widening and finally the failure. All these phases can be viewed for different materials and it is concluded that they appear in all materials but they last differently. When the technical crack appears then the technical duration age is exhausted and then all further calculations are done with methods of the failure mechanics. In this paper will be viewed the calculations which are used in calculating of the technical life time.

Proof to fatigue durability can be viewed in multiple ways but, however, the one closest to the real process is when the proof is based on the working strength, i.e. when the analysis is being done for the case with variable loads which appear in the course of work. There are proves that are based upon approximations which the unevenness of the variable load and bearing capacity take over the certain coefficients.

In order to carry out the proof of fatigue strength it is necessary to have specific data serving as a base to do the calculation. That means that it is necessary to know working stresses which appear during operation, as well as knowing of a specific Wöhler curve for the given material. Of course, the constructor's idea itself imposes which of the fatigue hypotheses will be applied in order to get the concrete values about the age duration of the structure. That means that on the base of these data it is possible to reach as conclusion about durability age, with, of course, some probability because in collecting and application of these results an error appears which impact the final conclusion about how long the structure will work without danger that the failure due to fatigue of material will happen.

Special analysis of the stress states and their application in the calculation of duration age based on the driving strength tells that the nominal stresses should be corrected (coefficient of stress concentration, kind of stress, size of the part, surface quality...) or that it should be found how to directly reach the real stresses in the observed cross-section and using them to make corresponding calculation.

4. FREQUENCIES OF STRESS CYCLES

Based on the record of real process in the structure or on the basis of simulation models it is possible to attain the changes in stress in time. It should be stressed that thus obtained data must be revised by means of discrete method into the record which would be equivalent and applicable in life time calculation. So revised record is named as stress collective and represents a base for duration age calculation. In the course of the said transformation it is possible and usually happen some minor or greater errors, that primarily occur due to some of neglected influences like for example frequency or sequence of stress changes. Range of the greatest stress change can be divided into at least 8 classes, and decisions how many classes will be adopted depend on the concrete case, and the error also depends on the mentioned number of classes. In spite of the named shortcomings and errors and loss of some information it is necessary to present the variable stress in time. In spite of all listed shortcomings and errors and information loss it is obligatory to create stress collectives and apply some of hypotheses on fatigue damage that will be clarified later in the paper.

Because of simplification and errors that appear in case of some methods in this paper will be presented the method of range pairs (full cycles), i.e. „Rain flow"method is the most modern and the best from the aspect of information loss. Other methods analyzing only the extreme values, solely surpassing limits of classes, solely increasing or decreasing stress changes or solely instantaneous stress height make errors in forming the load collective and they will not be in this paper more analyzed.

Choice of the discrete method depends on available equipment (needed for making of the experiment or simulation programs), sole change of stress in time, as well as the purpose of the collective itself, and already named method „Rain flow" shows the best parallel with the experimental results.
Further analysis according EN 13001 and EN 13002 brings all amplitudes down to the constant stress ratio or the constant mean stress.

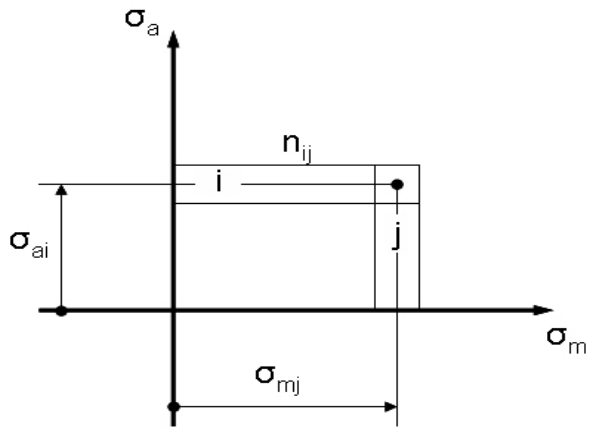

Figure 2: Two-parameter presentation of stress histories

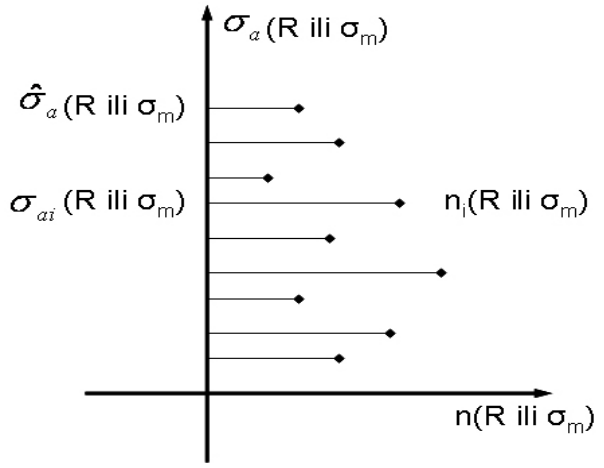

Figure 3: One-parameter presentation of stress histories (frequencies of stress amplitudes referred to constant stress ratio or constant mean stress)

σ_m - is the mean stress

σ_a - is the stress amplitude

n_{ij} – is the number of stress cycles of class ij

$$n_{ij} = \sum_r \alpha_r * C * n_{ij}^r$$

α_r - is the relative number of working cycles for each task

C – is the total number of working cycles

$$\hat{n} = \sum_i * \sum_j n_{ij}$$

$\hat{n}$ - is the total number of stress cycles

$\sigma_{a,i}(R) = (\sigma_{a,i} - \mu * \sigma_{m,i}) / (1 - \mu * (1 + R / 1-R))$

$\sigma_{a,i}(\sigma_m) = \sigma_{a,i} - \mu * (\sigma_m - \sigma_{m,j})$

$\sigma_{a,i}$ – is the stress amplitude of range i resulting from rainflow counting

$\sigma_{m,i}$ – is the mean stress of range j resulting from rainflow counting

$\sigma_{a,i}(R)$ – is the transformed stress amplitude of range i for constant stress ratio

$\sigma_{a,i}(\sigma_m)$ – is the transformed stress amplitude of range i for constant mean stress

R – is the constant stress ratio selected for one parameter classification of stress cycles

σ_m – is the constant mean stress selected for one parameter classification of stress cycles

μ – rises of lines of constant N in the σ_a- σ_m plane

When having only a part of the collective it is possible (based on probability which is permitted for certain parts of the crane) to stuff the collective with additional information need to calculate the life time. This is possible to be done if the representative part of the collective corresponds to the interval not shorter than the hundredth part of the overall collective and that that in the overall collective applies the lawfulness in appearing of the stress states as it is the case whole life time. Frequently, the collective is not unique but it is composed of more characteristic parts as it is in the example of the container quay crane as presented in the Figure 4.

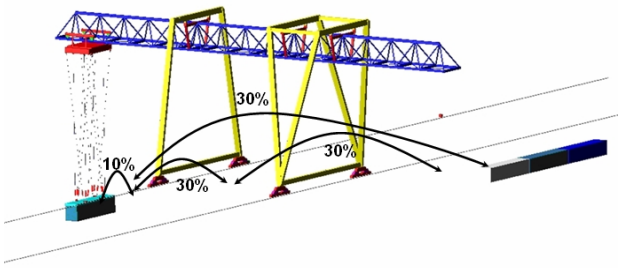

Figure 4: Load collective summarized from more various cycles

In experimental obtaining of data the cascade collectives are used because it is not possible to apply collectives with continuous distribution.

All this indicates to possible simplifications which can be done as well as preparations needed to be made in

order to get competent data on which base the further calculation is carried out.

5. IMPACT OF WORKING TASKS AND WORK CONDITIONS

Parameters which describe the work tasks include: mass and characteristics of load, velocity and acceleration of trolley moving, cranes, velocity and acceleration of hoisting and load turns, length of roads, inclination of paths, ways of load engagement, limitations for various operating tasks, degree of precision of positioning.

The work parameters include: atmospheric influences (temperature, wind, snow...), spatial or other limitations, control system...

Translation of simulations into routine procedure requires supplementing of the catalogue data of final products with parameters. This way will lead to more precise calculation in designing process.

6. DYNAMIC GOAL

To get the stress states which appear in the structure it is possible to the software KRASTA, but, however, to achieve the direct change in time for example of force in a specific cross-section of the beam some other software packet has to be used like ADAMS which is suitable for the dynamic analysis of the system.

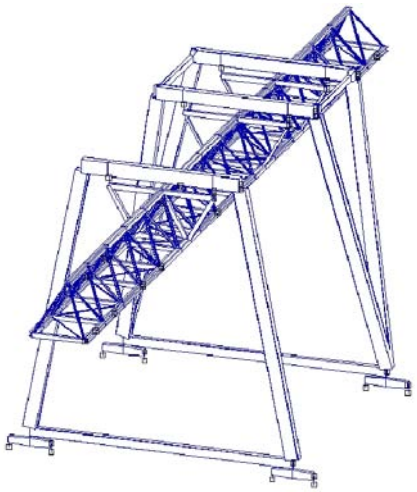

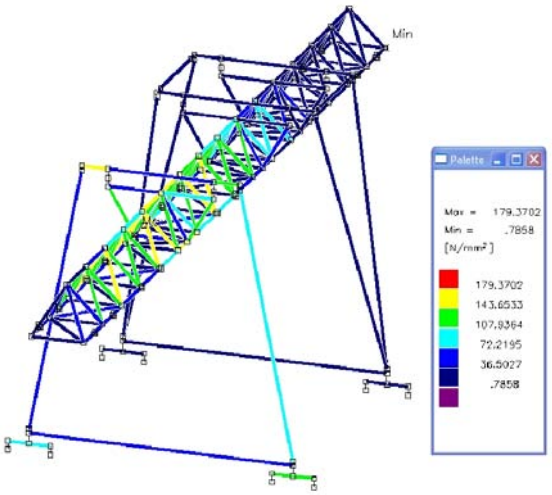

Figure 4: Simulation model (KRASTA)

By merging of data obtained in one or another way it is possible to get the parameters which are needed for calculation of life time. Sometimes the complexity of the process is so high that by means of the simple account it is not possible to get some data like swaying of container and control, monitoring and influencing upon oscillating period. The complexity of this period of oscillation (containers' mass, trolleys, cranes, impact of position of ropes, change of ropes' length...) imposes a conclusion that this is the only way for obtaining of these dynamic influences in the early designing phase.

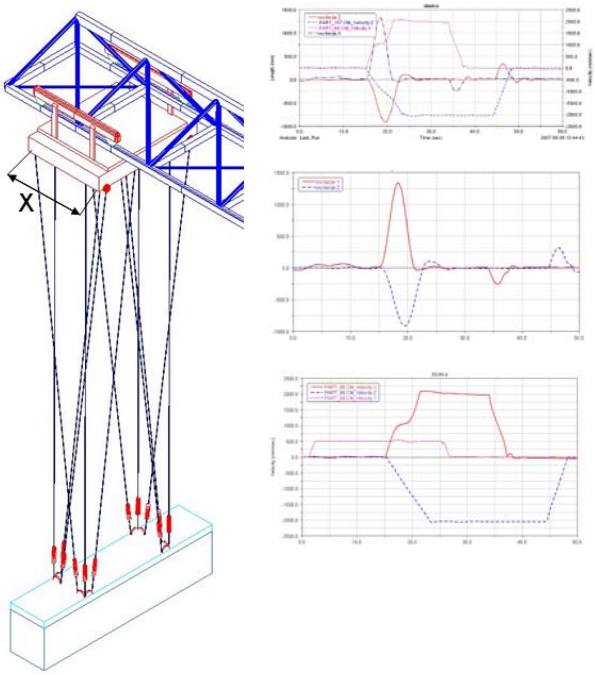

Figure 5: Dynamic analysis

7. CONCLUSION

Based on new standards which have been introduced in Serbia, it will be necessary to use the calculations which are defined in these standards which indicate that for designing of new products it is a must to have corresponding software packets.

Optimization of the duration age is something that in the future time will be one of more important parameters which directly impact the price of products.

In this paper is presented in which way it is possible to reach data which are needed for calculation of life time, as well as basic requirements for standards in Serbia and abroad.

The actual software packets KRASTA and ADAMS are presented, their application aimed to optimization of life time, their possibilities as a tool to satisfy some of the requirements imposed by the existing standards.

Dynamic influence which appears in the structure might be measured and used for calculation of similar structures but in designing of new products it is necessary to use the simulation models as a tool because, in the first place, of the complexity of the process.

When the crane is already made it is possible to monitor the spent life time.

REFERENCES

[1] Heibach E.: *Betriebsfestigkeit*, 2. Auflage, Spinger, 2002,

[2] Bathe K.J.: *Finite-Elemente-Methoden*, Springer, Berlin, 1996,

[3] Naubereit H, Weihert J.: *Einfuehrung in die Ermuedungsfestigkeit*, Hanser Verlag, Muenchen, 1999,

[4] Park J. B, Hong K. S, Huh C. D.: *Time-Efficient input Shaping Control of Container Crane Systems*, 2000 IEEE International Conference on Control Aplications, anchorage, Alaska, 2000,

[5] Huh C.D, Hong K.S.: *Input Shaping Control of Container Crane Systems: Limiting the Transient Sway Angle*, 15th Triennial World Congress, Barcelona, 2002,

[6] EN 13001-1 and 13001-2,

[7] EN 1990:2002, EUROCODE,

[8] 8. M. Georgijevic, R. Kostic, *Erhöhung der Lebensdauer von Fördermaschinen durch mechatronische Systeme,* 30. Tagung DVM – Arbeitskreis Betriebsfestigkeit *Mechatronik und Betriebsfestigkei*t - Stuttgart, 2003, (Predavanje po pozivu),

[9] Georgijervić M.: *Uticaj automatizacije rada i upravljanja na vek trajanja mašina*, Konstruisanje mašina- Jurnal of Mechanical Engineering Design, Novi Sad, No.1, 2004,

[10] Bojanić G, Georgijević M, Bojanić V.: *PRORAČUN KONSTRUKCIJA U ODNOSU NA ZAMOR PRIMER KONTEJNERSKE OBALSKE DIZALICE*, DEMI 2007,Banjaluka, 2007,

ОСНОВНЫЕ ПРИНЦИПЫ КОМПЛЕКСНОГО УПРАВЛЕНИЯ ПРОИЗВОДСТВОМ АСФАЛЬТОБЕТОНА

А. И. Доценко

В последние годы роль автомобильного транспорта в грузообороте страны возрастает. При этом бурно растет автомобильный парк – за последние десять лет число автомобилей в стране возросло в 2,5 раза и составило 24 млн. машин. Неизменно растущий автомобильный парк и объемы транспортных перевозок резко повышают требования к таким параметрам асфальтобетона (основного покрытия автодорог) как прочность и срок эксплуатации. Однако проведенный анализ показывает, что ни объемы ежегодно производимого материала, ни его качества не отвечают современным потребностям [[12]]. Автомобильные дороги Российской Федерации не обеспечивают в необходимой степени интересы государства, потребности экономики и населения, в частности:

- протяженность автомобильных дорог с твердым покрытием в Российской Федерации составляет 50 % от потребности. При этом около тридцати девяти тысяч населенных пунктов не имеют связи по автодорогам с твердым покрытием с транспортной системой страны. В результате, около десяти процентов населения страны в период весенней и осенней распутицы остается практически отрезанным от транспортных коммуникаций;

- до настоящего времени не завершено формирование опорной сети федеральных автомобильных дорог, связывающих все экономические регионы Российской Федерации;

- сформировавшаяся в 60-х – 80-х годах XX века древовидная конфигурация сети автомобильных дорог общего пользования не удовлетворяет потребностям товаропроизводителей;

- прочностные характеристики дорожных одежд не позволяют осуществлять повсеместное бесперебойное движение тяжеловесных транспортных средств.

Важнейшее значение для качества и долговечности покрытия дороги имеет качество асфальтобетонной смеси и асфальтобетона. Срок службы асфальтобетонных покрытий в нашей стране существенно ниже аналогичных показателей промышленно развитых стран. Данные анализа Бюро общественных автодорог США показывают, что средний срок службы асфальтобетонного покрытия составляет 16,8 лет [[7]].

Низкий срок службы асфальтобетонных покрытий связан с высокой вариацией качества асфальтобетона. Это происходит из-за нестабильности характеристик компонентов, неконтролируемых изменений свойств смеси при ее транспортировке, нестабильности параметров ее укладки и уплотнения. Особо остро эта проблема встает при использовании местных материалов. В условиях асфальтобетонного завода (АБЗ) реальным направлением решения данной проблемы является создание систем управления, компенсирующих нестабильность характеристик и стабилизирующих качество готовой асфальтобетонной смеси.

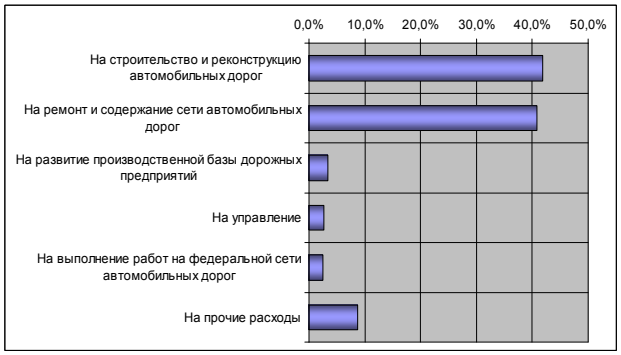

Рис. 1. Распределение средств в дорожной отрасли в 2002 году

Анализ распределения средств в дорожной отрасли (рис. 1) показывает, что основные средства расходуются на строительство новых дорог и на ремонт и содержание существующей дорожной сети [[12]]. Необходимо отметить, что при такой потребности в строительстве новых автодорог почти такие же средства тратятся и на ремонт существующей сети. Это подтверждает утверждение о крайне низкой долговечности имеющихся асфальтобетонных покрытий. При этом на развитие производственной базы дорожных предприятий расходуется только около 3,5% средств. Отсюда следует, что при строительстве новых

проф. др. Анатолий И. Доценко, Московский институт коммунального хозяйства и строительства, Россия, dotsenko_ant@mail.ru

автомобильных дорог в отрасли ориентируются главным образом на имеющуюся материально-техническую базу.

Процесс формирования свойств асфальтобетонной смеси и асфальтобетона представлен на рисунке (рис. 2). Как видно из анализа на свойства асфальтобетонного покрытия влияют:

- свойства компонентов смеси;
- технологические процессы;
  - производства асфальтобетона;
  - транспортировки асфальтобетонной смеси от асфальтобетонного завода до места ее укладки;
  - укладки и уплотнения асфальтобетонной смеси и формирования асфальтобетона;
  - технология содержания автомобильной дороги;
  - технологических процессов контроля параметров на всех этапах создания и эксплуатации покрытия;
- качество системы автоматического управления производством;
- качество проектов всех видов работ и проектирования состава асфальтобетона.

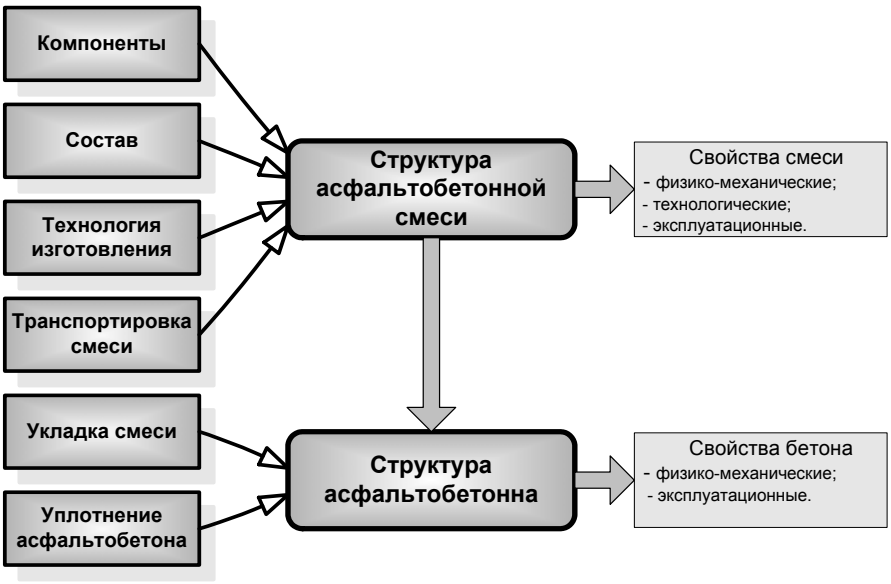

Рис. 2. Формирование свойств асфальтобетонной смеси и асфальтобетона

Структурно комплексная система управления производством асфальтобетона является многоуровневой иерархической системой (рис. 3). Рассмотрим отдельные уровни.

- Уровень 1. На нижнем уровне иерархии находится система локального управления (ЛСАУ) собственно технологическим оборудованием – агрегатами и механизмами. Источником информации на этом уровне являются сигналы от первичных преобразователей и органов ручного управления, а управление осуществляется различными исполнительными механизмами. Здесь решаются два основных типа задач:
  - Задачи логико-программного управления. Эти задачи связаны с управлением отдельными механизмами поточно-транспортных систем предприятия и другими аналогичными объектами. Для этого типа задач необходимо решать логические уравнения с различными наборами аргументов и функций.
  - Задачи цифрового управления. Эти задачи характерны для подсистем управления тепловыми процессами, дозированием компонентов. Здесь используются алгоритмы оптимального управления, фильтрации и прогнозирования, статистической обработки данных.
- Уровень 2. На этом уровне проводится согласование работы отдельных элементов технологического процесса. Так, например, ЛСАУ обеспечивает согласование производительности питателей дозаторов предварительного дозирования с уровнями компонентов в расходных бункерах дозировочного отделения.

• Уровень 3. На этом уровне обеспечивается решение задачи стабилизации качества асфальтобетонной смеси на выходе АБЗ. Этот уровень управления базируется на информации, поставляемой лабораторией завода.

- Информация о параметрах компонентов асфальтобетонной смеси (цепь 8 рис. 3). Например, гранулометрический состав минерального порошка.
- Информация о параметрах технологического процесса (цепь 9 рис. 3). Например, информация о рецептуре асфальтобетонной смеси.
- Информация о качестве готовой продукции (цепь 10 рис. 3). Например, информация о прочности асфальтобетона, полученная в ходе испытаний для аттестации партии готовой асфальтобетонной смеси.

• Уровень 4. На этом уровне управления анализируется информация о транспортировке асфальтобетонной смеси от АБЗ до места ее укладки. Эта информации может быть получена внешней, относительно АБЗ, лабораторией (цепь 11 рис. 3). Например, фактическая температура асфальтобетонной смеси в момент ее доставки к месту укладки, которая зависит как от температуры смеси при ее отгрузке на АБЗ, так и от времени транспортировки и температуры окружающей среды. Анализ этой информации позволит таким образом настроить технологический процесс АБЗ, чтобы минимизировать отклонение температуры смеси от заданного уровня в момент ее укладки. В результате реализации этой подсистемы формируется новое знание о среде (цепь 1 рис. 3).

• Уровень 5. На этом уровне анализируется информация о результатах укладки и уплотнения асфальтобетонной смеси (цепь 12 рис. 3). Также используется информация о результатах контроля качества асфальтобетонного покрытия в ходе эксплуатации (цепь 13 рис. 3). Эти данные должны поставляться на АБЗ внешней лабораторией. Анализ этих данных позволит уточнить модель формирования показателей качества асфальтобетона и повысить эффективность управления производством асфальтобетонной смеси. В результате реализации этой подсистемы так же формируется новое знание (цепь 2 рис. 3).

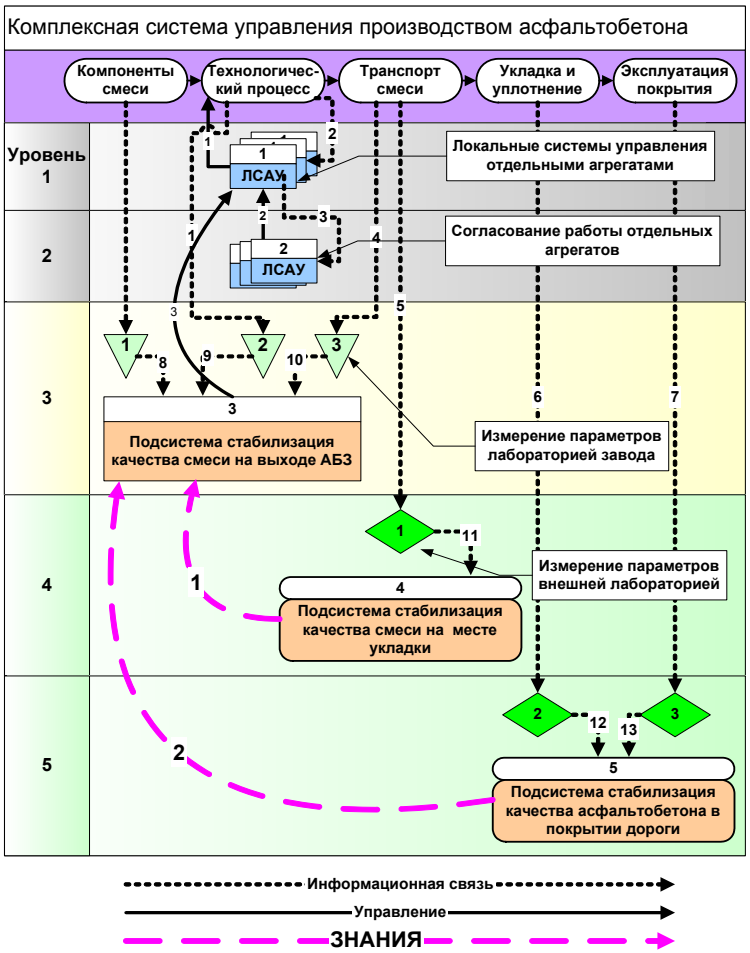

Рис. 3. Структура комплексной системы управления производством асфальтобетонной смеси

Системы управления нижнего уровня иерархии (уровни 1 и 2) реализованы практически на всех АБЗ с использованием различных технических средств и, следовательно, с различной эффективностью.

Система управления качеством асфальтобетонной смеси на выходе АБЗ (уровень 3) связана с исследованиями, проведенными в последние годы [[1], [2], [3], [5], [6], [8], [9]]. К сожалению данные системы до настоящего времени не получили широкого распространения. Однако подсистема управления данного уровня может быть легко внедрена на любом АБЗ, так как не требует для своей работы никаких технических средств кроме компьютера, на котором реализованы соответствующие алгоритмы.

Однако на качество готового асфальтобетонного покрытия влияет не только качество асфальтобетонной смеси на выходе АБЗ, но и технологический процесс транспортировки смеси до места ее укладки (рис. 2). При этом на свойства смеси в момент ее укладки влияют характеристики транспортного средства - *A*, условия внешней среды (температура - t^o, влажность - *W*, скорость - *V* и преимущественное направления ветра - *D* относительно перемещения транспортного средства) и время транспортировки - *t*. Исходя из этого, для каждого транспортного средства можно записать:

$$\Delta z_i^n(t) = \varphi[A_k, t_k^o(t), W_k(t), V_k(t), D_k(t), n], \quad (1)$$

где $\Delta z_i^n(t)$ - отклонение *i*-ого свойства асфальтобетонной смеси от его уровня на выходе АБЗ для момента времени *t* для *n*-ой площадки. Здесь в качестве показателя времени *t* используется дискретная величина – поставка порции асфальтобетонной смеси данным транспортным средством. Множество значений *t* упорядочено по моменту времени доставки к *n*-ому месту укладки;

A_k - набор характеристик k-ого транспортного средства;

$t_k^o(t), W_k(t), V_k(t), D_k(t)$ - средние температура, влажность, скорость и направление ветра в момент доставки асфальтобетонной смеси k-ым транспортным средством в t-ой поставке.

n - площадка, на которой производится укладка асфальтобетонной смеси.

Один АБЗ может обслуживать несколько площадок. Тогда можно получить оценку отклонения показателя качества асфальтобетонной смеси для n-ой площадки для интервала времени $t_2 - t_1$ вида:

$$\Delta Z_i^n = \frac{\sum_{t_1}^{t_2} \Delta z_i^n(t)}{t_2 - t_1}, \quad (2)$$

При усреднении характеристик смеси не только по времени, но и по площадкам получим:

$$\Delta Z_i = \frac{\sum_{n=1}^{N} \frac{\sum_{t_1}^{t_2} \Delta z_i^n(t)}{t_2 - t_1}}{N}. \quad (3)$$

Располагая значениями отклонений $\Delta z_i^n(t)$ и их оценками (2) и (3) можно ввести соответствующую коррекцию в алгоритмы управления для подсистемы стабилизации свойств асфальтобетонной смеси на выходе АБЗ (уровень 3).

Организация такого управления (уровень 4) осложняется рядом факторов:

1. Запаздывание в получении характеристик. То есть смесь, которая в текущий момент будет отгружена с завода, уже не может быть «исправлена». Потому необходимо прогнозировать оценки $\widehat{\Delta Z}$.

2. Стратегия управления существенно зависит от количества площадок и распределения между ними объемов поставок. При этом следует либо минимизировать суммарные отклонения с учетом объемов поставок, либо, возможно, учитывать приоритеты для различных объектов.

3. Ни сбор информации, ни ее обработка непосредственно на месте укладки асфальтобетонной смеси никак не организована, поэтому необходимо разработать как комплекс технических и программных средств для решения этой задачи, так и решить определенные организационные проблемы.

В процессе укладки и уплотнения асфальтобетонной смеси может быть получена информация о свойствах смеси по возникновению различных видов дефектов, например [[4]]:

1. Волнистая поверхность покрытия (короткие и длинные волны);

2. Разрывы покрытия по ширине, в середине и по краям;

3. Неравномерность структуры покрытия;

4. Неровность покрытия;

проф. др. Анатолий И. Доценко, Московский институт коммунального хозяйства и строительства, Россия, dotsenko_ant@mail.ru

5. Поверхностные тени;
6. Поперечные трещины;
7. Сдвиг покрытия при уплотнении катком;
8. Жирные пятна на поверхности покрытия;
9. Недостаточное уплотнение покрытия.

Возникновение этих дефектов связано, в том числе, и со свойствами асфальтобетонной смеси. Такими свойствами как состав и структура минеральной части смеси, доля битума в смеси, температура смеси и ее температурная неоднородность, ее сегрегация. Оперативное поступление информации о выявленных дефектах может существенно способствовать введению необходимой коррекции в управление технологическим процессом на 3-ем уровне иерархии систем управления.

Кроме того, непосредственно после укладки и уплотнения смеси, а так же в процессе эксплуатации покрытия проводится соответствующие испытания готового асфальтобетона с применением нормированных инструментальных методов [[4]]. Эта информация может быть эффективно использована для управления процессом производства.

Здесь может быть получен дополнительный эффект от получения новых знаний о процессе производства асфальтобетонной смеси. Так если v_i и v_j некие показатели компонентов асфальтобетонной смеси, а w_m и w_n показатели качества готовой продукции, то даже при наличии связей вида

$$w_m = \varphi(v_i) \text{ и } w_n = \varphi(v_j)$$

более сложные зависимости вида

$$w_m = \varphi(v_i, v_j), \quad w_n = \varphi(v_i, v_j)$$

и

$$\begin{cases} w_m = \varphi(v_i, v_j), \\ w_n = \varphi(v_i, v_j). \end{cases}$$

в технологии асфальтобетона не формализованы.

Имеющиеся результаты экспериментальных исследований в области технологии асфальтобетона, как правило, не позволяют синтезировать статистические достоверные технологические зависимости, так как в них исследуются зависимости вида $w_m = \varphi(v_i)$. При этом, как правило, не приводятся исчерпывающие данные о значениях других параметров $v_1, \ldots, v_p$, что не позволяет использовать результаты исследований в сходных ситуациях.

При помощи разработанной математической модели имеется возможность исследовать статистические технологические зависимости вида $w_m = \varphi(v_i, v_j)$ и получить модели технологического процесс производства асфальтобетонной смеси, которые могут быть использованы, в том числе и для повышения эффективности управления производством.

Данный подход реализуется на самом верхнем уровне предлагаемой системы управления (уровень 5). В настоящее время заканчивается разработка автоматизированной системы управления производством асфальтобетона, в которой реализуется изложенный в данной статье подход, основанный на расширении понятия объекта управления за пределы АБЗ и включение в контур управления транспорт, укладку и даже эксплуатацию готового асфальтобетонного покрытия.

ЛИТЕРАТУРА

[1] Александров А.Е. Автоматизация управления прочностью бетона. Автореферат канд. диссертации. М., МАДИ, - 1999.

[2] Бунькин И. Ф. Автоматизация управления производством асфальтобетонов: Автореферат докторской диссертации. М., МАДИ,, 2002.

[3] Гольнев Д.М. Структура и основные алгоритмы экспертной системы для автоматизации подбора состава асфальтобетона. «Прогрессивные технологические процессы в строительстве» труды секции «Строительство» российской инженерной академии, выпуск 4, Москва 2003

[4] Доценко А.И. Буренюк Я.Р. Прибор экспресс-контроля плотности строительных материалов и методика его применения. М.: «Строительные и дорожные машины», № 5, 1995

[5] Доценко А.И., Римкевич С.В. Общие принципы построения комплексной системы управления качеством асфальтобетона. // Академия проблем качества Российской Федерации, Московский Государственный Строительный Университет. Сборник научных трудов № 1 «Механизации и автоматизация строительства и строительной индустрии». –М.: 2004.

[6] Доценко А.И., Усачев Е.С. К вопросу о концепции управления качеством изделия. // Материалы конференции МИКХиС. -М.: МИКХиС, 2004

[7] МАРГАЙЛИК Е. Прогрессивные материалы и технологии дорожных работ в США «Строительство и недвижимость», http://www.nestor.minsk.by/sn/sn9806/sn82421.htm

[8] Марухин А.В. Автоматизация управления состава асфальтобетонной смеси. Автореферат канд. дис./М.: МАДИ, 1999 г.

[9] Милосердин О.Ю. Автоматизация лаборатории асфальтобетонного завода. Автореферат канд. дис./М.: МАДИ, 2004 г.

[10] Морозов Ю.Л. Автоматизация технологического процесса производства товарного бетона. Автореферат докторской диссертации./ Москва., МАДИ. – 2001.

[11] Римкевич С.В., Суворов Д.Н. Распределенные системы управления в производстве асфальтобетона. «Прогрессивные технологические процессы в строительстве» труды секции «Строительство» российской инженерной академии, выпуск 4, Москва 2003

[12] РОСАВТОДОР - Итоги исполнения федерального бюджета за 2002 год и задачи на 2003 год. http://exkavator.ru/main/information/inf_news

СЕМЕЙСТВО МАТЕМАТИЧЕСКИХ МОДЕЛЕЙ ШАРНИРНО-СОЧЛЕНЕННОГО ФРОНТАЛЬНОГО ПОГРУЗЧИКА

М. Ф. Кулешова

Аннотация: *Выстроено семейство математических моделей шарнирно-сочлененного фронтального погрузчика в его рабочем режиме, соответствующем рысканию. Семейство математических моделей образовано моделированием рабочего режима с различной степенью приближения. Выполнен анализ изменения основных кинематических характеристик по мере усложнения математической модели.*

Ключевые слова: *Фронтальный погрузчик, рабочий режим, математическое моделирование, степень приближения*.

1. ВВЕДЕНИЕ

Работы [1,2] явились началом аналитического исследования динамики шарнирно-сочлененных машин (ШСМ). Работа [3] относится к аналитическому исследованию строительно-дорожных колесных ШСМ, в которой введена обобщенная математическая модель, позволившая провести исследование динамики машин в общем случае.

Представляет интерес математическое моделирование рабочего процесса с различной степенью приближения к реальному движению. Задача рассмотрена на примере фронтального погрузчика (ФП), созданного на базе колесного шарнирно-сочлененного тягача Т-150К.

2. СЕМЕЙСТВО МАТЕМАТИЧЕСКИХ МОДЕЛЕЙ ФП В РАБОЧЕМ РЕЖИМЕ, СООТВЕТСТВУЮЩЕМ РЫСКАНИЮ

Введем следующие системы координат: условно неподвижную систему координат, жестко связанную с полотном дороги; инерциальную систему координат *Oxyz*, начало которой совпадает с полюсом *O* – точка пересечения вертикального и горизонтального шарниров тягача; системы координат $Ox_1y_1z_1$ и $Ox_2y_2z_2$ – также с началом в точке *O,* жестко связаны с полурамами 1 и 2 соответсвенно. Полагаем, что центр масс каждой из полурам расположен в вертикальной продольной плоскости. Для определенности считаем, что рабочее оборудование (РО) находится на первой полураме. Предполагаем, что связи голономные; во время выполнения рабочего процесса отсутствует буксование.

Степень приближения описания математической моделью рабочего режима любой ШСМ, и в частности ФП, определяется числом степеней свободы.

За первую степень приближения математического моделирования рабочего режима ФП примем случай, когда отсутствует относительное движение полурам и РО. Тогда это обычная жесткая одномассовая система с одной степенью свободы, описывающая прямолинейное движение. На базе этой модели исследована [4] динамика землеройно-транспортных машин (ЗТМ), где рассмотрены закономерности неустановившегося движения ЗТМ в процессе копания однородных грунтов и при взаимодействии рабочих органов с жесткими препятствиями большой массы, определены условия, способствующие буксованию ЗТМ. Описание движения приведено к линейному дифференциальному уравнению вида

$$m\ddot{x} = T - W_k \qquad (1)$$

в котором линейность обеспечена за счет введения линейной зависимости для изменения силы тяги Т и силы сопротивления копанию W_k.

В нашем исследовании характер изменение силы тяги Т и силы сопротивления копанию W_k приняты в соответствии с [5], в результате чего дифференциальное уравнение (1) становится нелинейным вида

$$m\ddot{x} = T_0(1 - 0,065 \cdot \dot{x}/V_n - 0,935\dot{x}^5/V_n^5) - \\ -(Ax + Cx^2 + Dx^3). \qquad (2)$$

Во втором приближении математического моделирования рабочего процесса ФП учтем наличие упругой связи между полурамой 1 и

М. Ф. Кулешова, Харьковский национальный автомобильно-дорожный университет, Украина

рабочего оборудования при прямолинейном движении ФП в целом. В этом случае система описывается двумя обобщенными координатами q_1= x и q_2=x_3, где x_3 смещение РО. Математическая модель представляет систему двух нелинейных дифференциальных уравнений

$$\begin{cases} m' \cdot \ddot{\xi}_0 = m_3 \cdot \ddot{s} - c_{po}(\xi_0 - s) + T_1 + T_2 - W_k \\ m_3 \cdot \ddot{s} = m_3 \cdot \ddot{\xi}_0 + c_{po}(\xi_0 - s) - W_k, \end{cases}$$

где изменение силы тяги T и силы сопротивления копанию W_k приняты в соответствии с [5].

Третье приближение будет соответствовать случаю, когда первая полурама вместе с РО разворачивается вокруг вертикальной оси, а вторая полурама продолжает прямолинейное движение. Система описывается тремя обобщенными координатами q_1= x, q_2=x_3 и q_3=ψ_1.

Система нелинейных дифференциальных уравнений записывается в этом случае как

$$\begin{cases} m' \cdot \ddot{x}_1 = (m_1 a_1 + m_3 l_1)\sin\psi_1 \ddot{\psi}_1 - m_3 x_3 \cdot \sin\psi_1 + \\ +m_3 \ddot{x}_3 \cdot \cos\psi_1 + (m_1 a_1 + m_3 l_1)\cos\psi_1 \dot{\psi}^2 - \\ -2m_3 \sin\psi_1 \cdot \dot{\psi}_1 \dot{x}_3 - m_3 \cos\psi_1 \dot{\psi}_1^{\,2} - \\ -c_{po}(x_1 - x_3) + T_1 \cos\psi_1 - P_{b1}\sin\psi_1 + T_2 \\ -W_k \cos\psi_1; \\ J_1' \cdot \ddot{\psi}_1 = (m_1 a_1 + m_3 l_1)\sin\psi_1 \ddot{x}_1 - m_3 \sin\psi_1 x_3 \ddot{x}_1 - \\ -c_{sum}\psi_1 + P_{b1} l_1 + W_k b; \\ m_3 \cdot \ddot{x}_3 = m_3 \cos\psi_1 \ddot{x}_1 + c_{po}(x_1 - x_3) - W_k. \end{cases} \quad (4)$$

Таким образом система нелинейных дифференциальных уравнений (2), (3) и (4) представляет семейство математических моделей, описывающих рабочий режим ФП с различным приближением:

- первое приближение соответствует внедрению рабочего оборудования в мягкий однородный грунт, когда жесткость металлоконструкций ФП значительно превышает жесткость со стороны грунта; равнодействующая W_k совпадает с продольной осью машины;

- второе приближение соответствует внедрению РО в однородный, но труднопреодолимый грунт, что вызывает деформацию упругой связи между полурамой 1 и РО, при этом результирующая сил сопротивления копанию продолжает совпадать с продольной осью машины;

- третья степень приближения, более реальная и чаще всего имеющая место, описывает ассиметричное приложение нагрузки на ковш, вызывающее разворот полурамы.

Первые два случая из рассматриваемого семейства математических моделей можно назвать идеальными рабочими режимами ФП, что для практики редкое явление. Эти случаи требуют незначительных усилий гидроцилиндров рулевого управления.

3. АНАЛИЗ РЕЗУЛЬТАТОВ

О величине динамических нагрузок, как известно, можно судить по величине ускорений элементов системы. На рис. 1-5 представлены графики ускорений. На рис.1-3 приняты обозначения: через 1 обозначены ускорения, возникающие в модели первого приближения; через 2 - ускорения второго приближения; через 3 - ускорения третьего приближения.

По рис. 1-3 видно, что с повышением степени моделирования выявляются колебания полурамы 1 и РО более высоких частот; можно сказать по другому: одномассовая математическая модель по первому приближению скрадывает имеющие место колебания более высокой частоты.

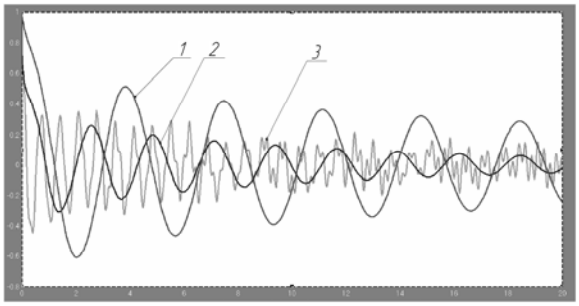

Рис. 1. Ускорения полюса О.
1- первое приближение; 2-второе приближение;
3- третье приближение

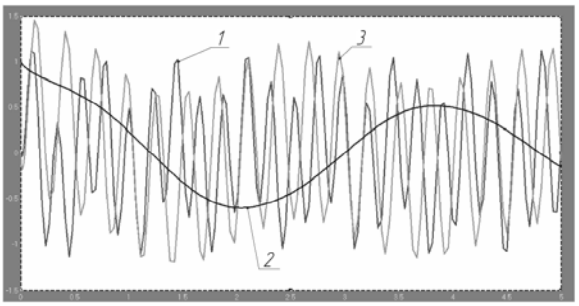

Рис. 2. Ускорения ковша.
1- первое приближение; 2-второе приближение;
3- третье приближение

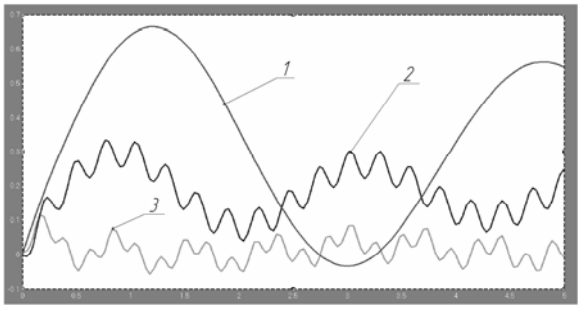

Рис. 3. Перемещение ковша.
1- первое приближение; 2-второе приближение;
3- третье приближение

Это существенно: так, в работе [4], относящейся к математическому моделированию в первом приближении, имеет место утверждение о том, что «…движение машины в каждом диапазоне скоростей продолжается ограниченное время, в течении которого не всегда ускорение может достигнуть своего максимума». Это заявление уже не справедливо для случая второго и тем более третьего приближений, когда в течение трех секунд копания ускорение ковша рабочего оборудования несколько раз меняет свой знак. Это же подтверждают графики на рис. 4-5, полученных в случае третьего моделирования, на которых для сравнения представлены перемещения и ускорения ковша и полюса *O*. Из графиков видно, что частота колебаний ковша примерно в 3 раза превышает частоту колебаний полюса *O*.

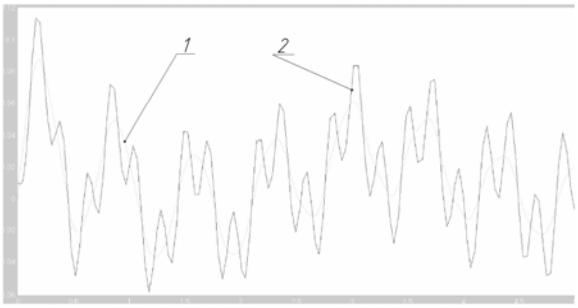

Рис. 4. Перемещение полюса *O* и ковша.
1- полюс; 2-ковшш

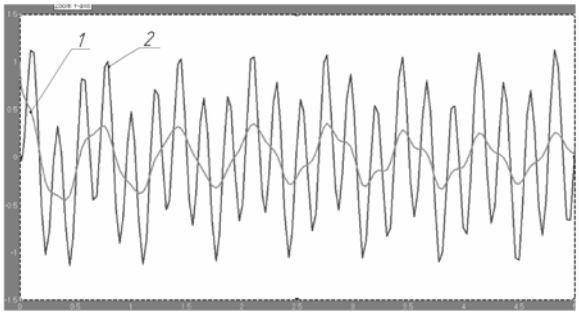

Рис. 5. Ускорение полюса *O* и ковша.
1- полюс; 2-ковшш

ВЫВОДЫ

1. Представлено семейство математических моделей для фронтального погрузчика с различной степенью моделирующих его рабочий процесс.

2. Степень приближения математического моделирования существенно меняет характер кинематических характеристик.

ЛИТЕРАТУРА

[1] Малиновский Г.Ю, Гайцгори М.М. Динамика самоходных машин с шарнирной рамой.-М.: Машиностроение, 1974.-175 с.

[2] Васильковская В.М., Гоберман В.А. Построение математических моделей в динамике дорожно-строительных машин/ Учебное пособие.-М.: Ин-т повышения квалификации Минстройдормаш СССР, 1981.-75 с.

[3] Кириченко И.Г. Модульная концепция проектирования технологических машин для строительного производства.- Харьков: Изд-во ХНАДУ, 2002.-119 с.

[4] Холодов А.М. Основы динамики землеройно-транспортных машин. –М.: Машиностроение 1968.-156

ИССЛЕДОВАНИЕ НАГРУЖЕННОСТИ СОЕДИНИТЕЛЬНОГО МОДУЛЯ ФРОНТАЛЬНОГО ПОГРУЗЧИКА И БУЛЬДОЗЕРА

О. В. Щербак

Аннотация: *Проведено исследование нагруженности соединительно-управляющего модуля шарнирно-сочлененных машин на примере фронтального погрузчика и бульдозера в рабочем режиме, соответствующее явлению рыскания, наиболее характерное для этих машин. Исследование выполнено на базе обобщенной математической модели*

Ключевые слова: *Шарнирно-сочлененная машина, фронтальный погрузчик, бульдозер, рыскание, соединительно-управляющий модуль, нагруженность.*

1. ВВЕДЕНИЕ

Создание современных комплексов модульных машин для строительного производства сталкивается с рядом трудностей, обусловленных недостатком их теоретического и экспериментального исследования. Как известно, в состав дорожной шарнирно-сочлененной машины входит три модуля. Первый – энергетический модуль (ЭМ) включает в себя двигатель, коробку передач, раздаточную коробку, ведущий мост и кабину с органами управления. Второй – технологический модуль (ТМ) включает в себя технологическое оборудование. ЭМ является единым для всего комплекса машин, а сменные ТМ обеспечивают специализацию конкретной технологической машины. Соединение ЭМ и ТМ осуществляется при помощи соединительно-управляющего модуля (СУМ), который имеет один вертикальный шарнир или два шарнира-вертикальный и горизонтальный и механизм рулевого управления. Необходимо отметить, что определение ЭМ и ТМ не носит абсолютного характера: некоторые элементы рабочего оборудования и оборудования в целом могут быть размещены на любом из ЭМ и ТМ. Так, для фронтального погрузчика характерно расположение рабочего оборудования (РО) на технологическом модуле, а для бульдозера- на энергетическом модуле.

Наличие СУМ позволяет более эффективно использовать модульную дорожно-строительную машину для выполнения различных технологических операций. Однако нагруженность соединительно-управляющего модуля исследована не достаточно. Первые работы по нагруженности СУМ изложены в [1, 2], в которых был исследован фронтальный погрузчик, созданный на базе колесного шарнирно-сочлененного трактора Т-150К. Данная статья отражает продолжение исследований нагруженности СУМ. Представляет интерес исследование нагруженности СУМ фронтального погрузчика и бульдозера, выполненных на базе тягача Т-150.

2. ДИФФЕРЕНЦИАЛЬНЫЕ УРАВНЕНИЯ ДВИЖЕНИЯ МАШИН В РАБОЧЕМ РЕЖИМЕ, СООТВЕТСТВУЮЩЕМ РЫСКАНИЮ

В основу составления дифференциальных уравнений положены принципы математического моделирования динамики модульных шарнирно-сочлененных технологических машин, изложенные в [2]. Получены следующие дифференциальные уравнения движения, как фронтального погрузчика, так и бульдозера в их рабочем режиме, соответствующем явлению рыскания:

$$\begin{cases} m' \cdot \ddot{x}_1 = (m_1 a_1 + m_3 l_1)\sin\psi_1 \ddot{\psi}_1 - m_3 x_3 \cdot \sin\psi_1 + \\ +m_3 \ddot{x}_3 \cdot \cos\psi_1 + (m_1 a_1 + m_3 l_1)\cos\psi_1 \dot{\psi}^2 - \\ -2m_3 \sin\psi_1 \cdot \dot{\psi}_1 \dot{x}_3 - m_3 \cos\psi_1 \dot{\psi}_1^{\,2} - \\ -c_{po}(x_1 - x_3) + T_1 \cos\psi_1 - P_{b1}\sin\psi_1 + T_2 \\ -W_k \cos\psi_1; \\ J_1' \cdot \ddot{\psi}_1 = (m_1 a_1 + m_3 l_1)\sin\psi_1 \ddot{x}_1 - m_3 \sin\psi_1 x_3 \ddot{x}_1 - \\ -c_{sum}\psi_1 + P_{b1} l_1 + W_k b; \\ m_3 \cdot \ddot{x}_3 = m_3 \cos\psi_1 \ddot{x}_1 + c_{po}(x_1 - x_3) - W_k, \end{cases} \quad (1)$$

где через x_1 обозначено прямолинейное движение машины; через x_3 – движение рабочего оборудования; через ψ_1 –разворот ЭМ или ТМ относительно вертикальной оси.

Ольга В. Щербак, Харьковский национальный автомобильно-дорожный университет, Украина, sherbako@mail.ru

В этих уравнениях для фронтального погрузчика масса m_1 –это масса энергетического модуля, а для бульдозера масса m_1 - это масса технологического модуля. Величина приведенного момента инерции J_1' является существенно различной для фронтального погрузчика и бульдозера.

3. АНАЛИЗ РЕЗУЛЬТАТОВ

Явление рыскания обуславливается ассиметричным приложением внешней нагрузки со стороны грунта на ковш (для погрузчика) или отвал (для бульдозера), вызывающем угловое смещение ТМ для погрузчика и ЭМ для бульдозера. За характеристику рыскания нами был принят круговой момент, возникающий в СУМ, линейно зависящий от круговой жесткости и угла рыскания.

При этом величина угла рыскания в первую очередь определяется круговой жесткостью c_{sum} соединительно-управляющего модуля и боковой жесткостью шин, которая входит в боковую силу P_{b1}.

Машинный эксперимент был проведен при постоянном значении круговой жесткости, равной 500 кНм, и различных значениях жесткостей шин, которые принимались равными 500, 750 и 1000 кН/м;

На рис.1-3 представлены графики изменения кругового момента бульдозера.

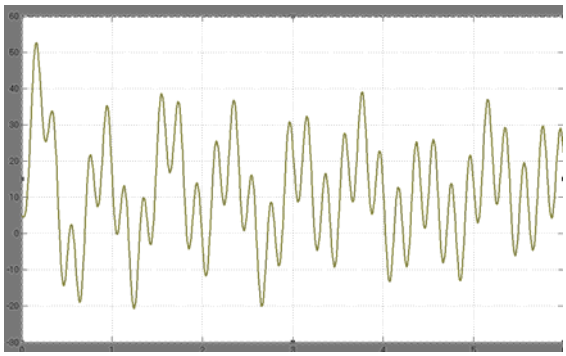

Рис. 1. Изменение кругового момента бульдозера при жесткости шины 500 кН/м

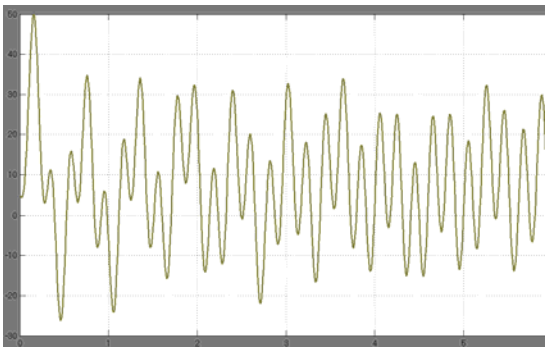

Рис. 2. Изменение кругового момента бульдозера при жесткости шины 750 кН/м

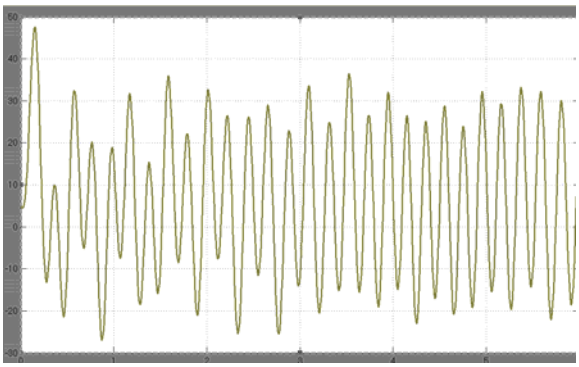

Рис. 3. Изменение кругового момента бульдозера при жесткости шины 1000 кН/м

На рис.4-6 представлены графики изменения кругового момента фронтального погрузчика.

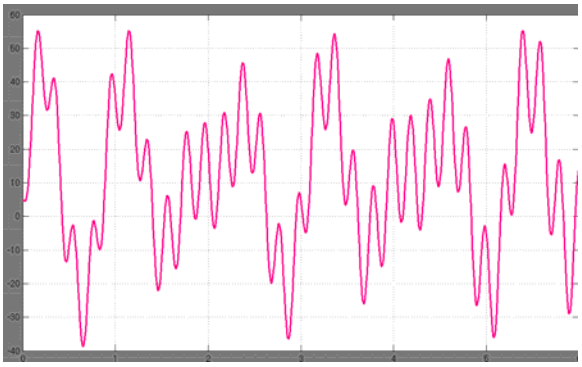

Рис. 4. Изменение кругового момента погрузчика при жесткости шины 500 кН/м

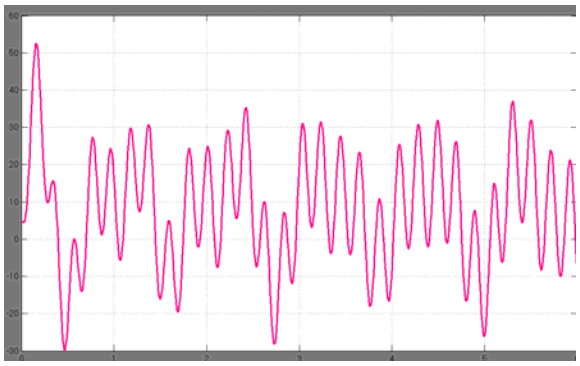

Рис. 5. Изменение кругового момента погрузчика при жесткости шины 750 кН/м

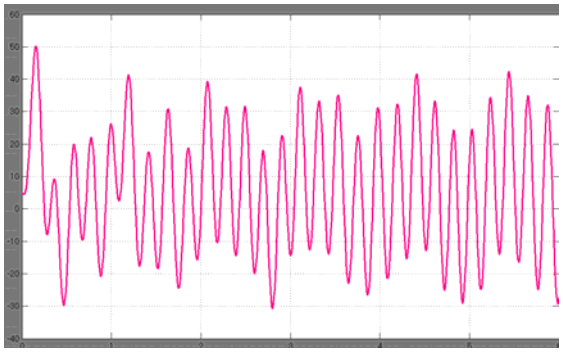

Рис. 6. Изменение кругового момента погрузчика при жесткости шины 1000 кН/м

Из сопоставления графиков 1-6 следует, что величина кругового момента фронтального погрузчика несколько превышает величину кругового момента бульдозера при прочих равных условиях. Это можно объяснить тем, что рабочее оборудование фронтального погрузчика расположено на технологическом модуле, масса которого в 2,5 раза меньше массы энергетического модуля, вследствие чего технологический модуль имеет большую подвижность.

Расположение рабочего оборудования бульдозера на массивном ЭМ несколько сдерживает явление рыскания.

Жесткость шины существенно влияет на величину кругового момента как погрузчика (рис. 4-6) так и бульдозера (рис.1-3). С увеличением жесткости шин возрастает частота кругового момента. Причем, для фронтального погрузчика разброс величины кругового момента выше, чем для бульдозера.

ВЫВОДЫ

1.Проведены исследования изменения кругового момента соединительно-управляющего модуля для фронтального погрузчика и бульдозера.

2. Установлено, что расположение рабочего оборудования на энергетическом или технологическом модуле влияет на изменение кругового момента.

3. Проведенные исследования свидетельствуют о необходимости дальнейших исследований с целью выработки практических рекомендаций.

ЛИТЕРАТУРА

[1] Щербак О.В. «Разработка и обоснование рациональных параметров соединительно-управляющего модуля фронтального погрузчика», Диссертация на соискание научной степени кандидата технических наук. Харьков – 2000.

[2] Кириченко И.Г. Модульная концепция проектирования технологических машин для строительного производства.- Харьков: Изд-во ХНАДУ, 2002.-119 с.

C SESSION:

RAILWAY ENGINEERING

IMPROVEMENT IN SUSPENSION SYSTEMS OF FREIGHT WAGONS

R. Rakanović, D. Petrović, Z. Šoškić, N. Bogojević

Abstraact: *This paper is a result of years-long researches of suspension systems of freight wagons. Basic results of the research are: technical solutions to cut down maintenance costs, preventing springs of "Fbd" wagons from cracking, and redesigned suspension system of "Ddam" wagon used for car transportation. All three technical solutions have been tested under laboratory and operation conditions. Number of spring cracks has been significantly decreased by these solutions, and "Ddam" wagon has been issued and international permit to run in S and SS regime.*

Key words: *suspension systems, springs, Laminated spring*

INTRODUCTION

When freight wagons run, the elements of suspension system crack. This is very noticeable at a "Fbd" wagon used for coal transportation (Fig.1), and at a three-axled "Ddam" wagon used for car transportation (Fig.2). Frequent cracks of suspension elements, not only at these wagons but at other wagons as well, considerably decrease the efficiency of regular transportation by rail. In some cases, they also cause derailments which lead to great expenses.

The causes of cracking of suspension elements have been analysed at the Centre for Railway Vehicles at the Faculty of Mechanical Engineering in Kraljevo. Some improvements have been recommended in order to repair the cracks, minimize the number of cracks, or to avoid them entirely. Optimal solutions have been reached by theoretical and experimental analysis. These solutions satisfy all conditions regarding their installation into current structures, all safety conditions which were defined by Serbian **(**ŽS**)** and international regulations (UIC), all conditions regarding spring repair, strength and service life.

RESEARCH GOALS

Main goal of the research work is minimizing the number of spring cracks, preventing suspension elements of freight wagons from failure, and preventing derailments. Safety and speed of rail transportation, therefore, would be improved. A "Ddam" wagon, which is used for car transportation, could be issued an international permit. This type of wagon got its permit suspended because of a large number of cracks of suspension elements. "Fbd" wagons are used for coal transportation in thermoenergetic systems, so entire production of electric power would be increased because coal would be regularly delivered. One more research goal is to develop the methodology for designing, calculating and testing suspension elements and their influence on dynamic behaviour of the whole wagon-track system under laboratory and operation conditions.

Figure 1. "Fbd" wagon which is used for coal transportation in TENT Obrenovac, Serbia

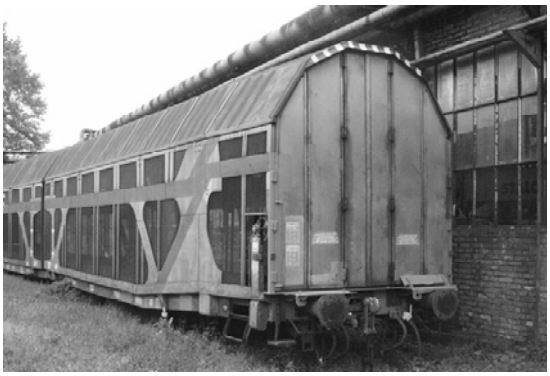

Figure 2. "Ddam" wagon used for car transportation (made in factory named "Bratstvo", Serbia)

Prof Dr Ranko Rakanović, Faculty of Mechanical Engineering Kraljevo, rakanovic.r@mfkv.kg.ac.yu
Prof Dr Dragan Petrović, Faculty of Mechanical Engineering Kraljevo, petrovic.d@mfkv.kg.ac.yu
Dr Zlatan Šoškić, Faculty of Mechanical Engineering Kraljevo, soskic.z@mfkv.kg.ac.yu
M. Sc. Nebojša Bogojević, Faculty of Mechanical Engineering Kraljevo,bogojevic.n@mfkv.kg.ac.yu

PROBLEM SOLVING

The problem of suspension system of freight wagons has been solved in following stages:

1. defining technical conditions of designing improved suspension systems,
2. developing preliminary solutions to improving suspension system,
3. developing methodologies and software in order to test solutions,
4. developing methodology of spring welding,
5. designing improved suspension systems,
6. testing improved solutions.

Researches have been done on current suspension systems of "Ddam" wagons used for car transportation (made in factory named "Bratstvo" in Subotica, Serbia), and of "Fbd" wagons which are a part of TENT Obrenovac, Serbia. Both suspension systems of these two types of wagons include laminated spring, so current elements should be repaired, unloaded and replaced with new ones. By way of illustration, the average number of spring cracks of "Fbd" wagons was 2,5-2,8 per wagon a year, which considerably decreases the transportation efficiency and increases maintenance costs.

The results of research done so far are:

- redesign and installation of parabolic springs into suspension system of "Ddam" wagons,
- installation of elastic rubber element into suspension system of a "Fbd" wagon,
- comparative tests being done on suspension system of "Fbd" wagons with or without elastic rubber element,
- developed technology of spring welding,
- tool used for tightening and positioning the spring being welded,
- designed measuring systems used for measuring the distance being run, and testing the working regime of spring under operating conditions,
- papers published at international conferences and national journals.

DECREASING SPRING CRACKS

"Fbd" wagons are adapted for loading and unloading coal at loading-unloading places at TENT Obrenovac. Because of their distinct structure shorter laminated springs have been installed into suspension system of "Fbd" wagon. Due to shorter length of the spring, heavy traffic at TENT railway, and uneven load on the axles, there are bigger stresses within the springs, which makes main leaf crack (Fig.3).

Figure 3. Laminated spring with cracked main leaf

Suspension systems have been theoretically and experimentally analysed and improvements have been designed in order to cut down maintenance costs. Technology of spring welding has been designed, whereas installation of elastic rubber element into suspension system of "Fbd" wagon has been recommended in order to decrease the spring stress under operation conditions.

TECHNOLOGY OF SPRING WELDING

Technology of spring welding has been designed in order to cut down maintenance costs and to decrease supply of new springs. This technology is successfully applied to the main leaf of laminated springs. Development of methodology for spring welding was preceded by following results:

- theoretical and service tests of "Fbd" wagons having laminated springs installed in order to gather all parameters relevant for improvement design,
- designing tools for tightening and positioning the main leaf (Fig.4).

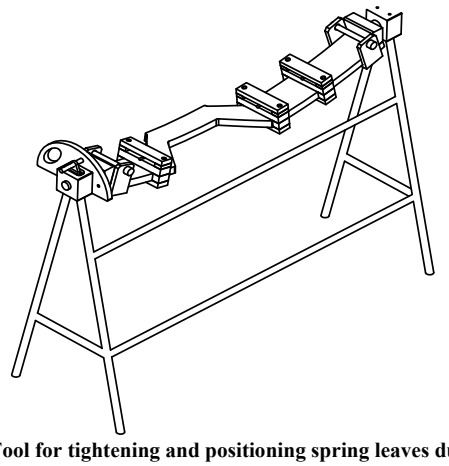

Figure 4. Tool for tightening and positioning spring leaves during welding

After welding the main leaf, the spring has been tested under laboratory and operation conditions.

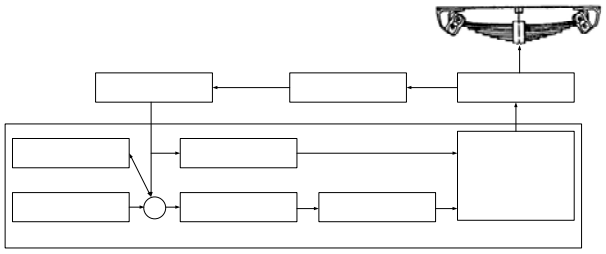

Figure 5. Schematic of testing fatigue of welded springs

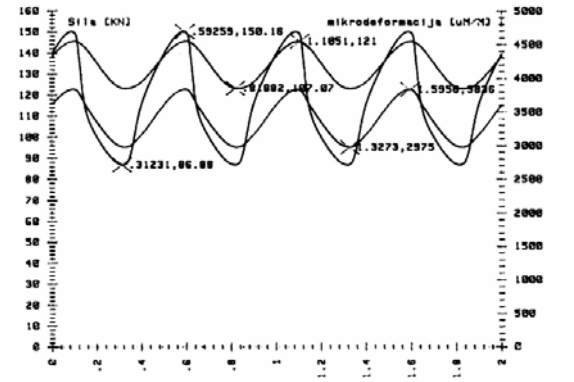

Figure 6. Change of stress and deflection of spring in relation to force during fatigue tests

During laboratory tests the spring has reached permanent dynamic strength.

Operation tests of "Fbd" wagons have been done at railway track in TENT Obrenovac, Serbia. Behaviour of welded spring has been observed but dynamic parameters have not been measured while the wagon has been running.

It can be concluded that the strength of springs with welded main leaf is equal to the strength of new leaves.

ELASTIC RUBBER ELEMENT

In order to solve the problem of frequent spring cracks of "Fbd" wagons, elastic rubber element has been designed on the basis of results obtained by testing suspension system.
The purpose of this element is to unload the spring under operating conditions and to take over a part of load. Figures 7 and 8 show elastic rubber element and elastic rubber element installed into suspension system of a "Fbd" wagon, respectively.

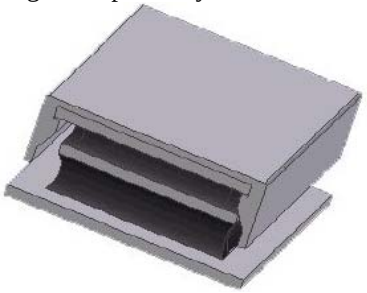

Figure 7. Elastic rubber element

Figure 8. Elastic rubber element installed into suspension system of a "Fbd" wagon

Amplifier KWS 50´ C
Force transducer
Oscillator
Cylinder
Regulator

During operating and laboratory tests (Fig.8), geometrical and elastic parameters of elastic rubber element (Fig.9) have been designed on the basis of structural details of a "Fbd" wagon.

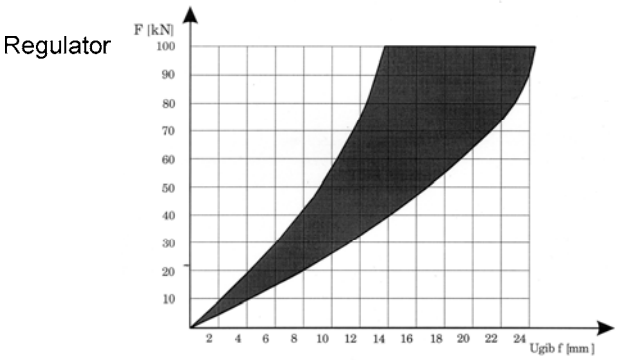

Figure 9. Recommended rigidity of elastic rubber elements

Figure 10. Operating tests of elastic rubber element in suspension system of "Fbd" wagon in TENT Obrenovac, Serbia

Number of spring cracks has been significantly lowered by installing elastic rubber element into suspension system of "Fbd" wagons (Table 1). Thus, laminated springs have reached permanent dynamic strength. The load, which is taken by elastic rubber element, is up to 30% of the load of spring without elastic rubber element. Maintenance and repair costs have been considerably cut down when elastic rubber element has been applied in TENT Obrenovac. Thus, productivity of railway transportation has been increased within TENT Obrenovac.

Year	Number of wagons with installed elastic rubber element	Number of replaced springs
2005	79	12
2006	150	20
2007	220	50

Table 1. Number of "Fbd" wagons with installed elastic rubber elements and number of replaced springs

REDESIGN OF SUSPENSION SYSTEM OF A "DDAM" WAGON

A "Ddam" wagon is a three-axled two-unit wagon used for car transportation. Due to its distinct structure, it is a very suitable wagon for operating in international traffic; namely, it has one axle less than standard wagons. On the other hand, that kind of structure caused many derailments. Designed suspension system of a "Ddam" wagon includes laminated springs installed above all three axles. Because of a large number of derailments this type of wagon got its international permit suspended. Testing the prototype of a "Ddam" wagon [1] has identified the causes of such a large number of derailments. Suspension system with parabolic springs has been designed on the basis of the testing results [2]. When parabolic springs have been installed, running behaviour of a "Ddam" wagon has been significantly improved, while according to reference [4], parabolic spring being installed is in light operating regime.

a) b)

Figure 11. Testing the operating regime of parabolic spring, a) determining amplitude, b) measuring the stress of spring leaf

CONCLUSION

Designed improvements in suspension system of "Fbd" and "Ddam" freight wagons had the following results:

- a "Ddam" wagon, which is used for car transportation, was reissued an international permit to run in S and SS regime,
- the number of spring cracks has decreased in the suspension system of "Fbd" freight wagons,
- maintenance costs have been cut down by technology of spring welding.

Savings on regular maintenance, repair and infrastructure maintenance are assessed at €400.000 a year. Damages caused by overloading "Fbd" wagons have been considerably decreased, as well as derailments of "DDam" wagons.

On the basis of obtained results, some improvements have been reached. These improvements can be applied to laminated springs of the wagons of Serbian Railways and UIC wagons, too.

REFERENCE

[1] Rakanović R., Petrović D., Elaborat br.:4/95 „Ispitivanje kola za prevoz automobila Ddam“, MFK 1995. god

[2] Rakanović R., Petrović D., Šoškić Z. Bogojević N. Elaborat br.: 11/04 „Ispitivanje kola za prevoz automobila Ddam“, MFK 2004. god

[3] Projekat ev. br.: TR 006313, “Poboljšanje vešajnih sistema teretnih vagona“, MNT Srbija

[4] Petrović D., Šoškić Z, Bogojević N. and Rakanović R.: „Work regime of DDam wagon parabolic springs“, FME Transaction, Faculty of Mechanical Engineering, Belgrade, 33, 129-133 (2005)

EQUIPMENT AND METHODS TO TAKE DOWN CHARACTERISTICS OF PRESSED-IN ELEMENTS OF RAILWAY WHEEL AXLES

N. Nenov, E. Dimitrov, P. Piskulev

Abstract: *The paper presents the development of electronic equipment and methods to register the processes mentioned above. The rolling stock wheel axles are an extremely responsible element of the vehicle wheeled unit. Their technical condition has a significant relation to the train traffic safety. The electronic measuring system (Fig.2) that registers pressing-in consists of a force sensor and a sensor of displacement, amplifiers, an analogue-to-digital transformer and a PC. The results obtained are saved as a file on the computer hard disk and are printed. The results are inseparable part of the passport of each wheel axle and are preserved as achieve. With the system operation the influence of the human factor is completely excluded.*

Key words: ***railway, railway wheel axles, characteristics of pressed-in***

1. INTRODUCTION

The rolling stock wheel axles are an extremely responsible element of the vehicle wheeled unit. Their technical condition has a significant relation to the train traffic safety. With a view to guaranteeing the traffic safety and operational resource of wheel axles, it is necessary to strictly keep [1]. According to them, the most important requirements to the process of pressing-in are expressed in the following:

- before pressing-in, the respective surfaces should be cleaned and lubricated with a thin layer of linseed oil;
- speed of pressing-in – 2÷5 mm/s;
- gradual decrease of the compression force with a stroke of 10 mm before the end of the process;
- maximal value of the pressing-in force 4÷6 kN/mm of the diameter of the under-boss part of the axle;
- registration of the compression (pressure) and displacement, i.e. the diagram of pressing-in the respective wheel-axle elements (Fig.1).

With forming and repairs of railway wheel axles, it is most often to implement cold-pressed fit between the axle and the wheel boss and between the axle and the boss (bearer) of the big gear of the wheel axle reducer. For some wheel axles it is also admissible to implement shrinkage fits (§44, art.2).

The paper presents the development of electronic equipment and methods to register the processes mentioned above.

2. THE ELECTRONIK MEASUREMENT EQUIPMENT

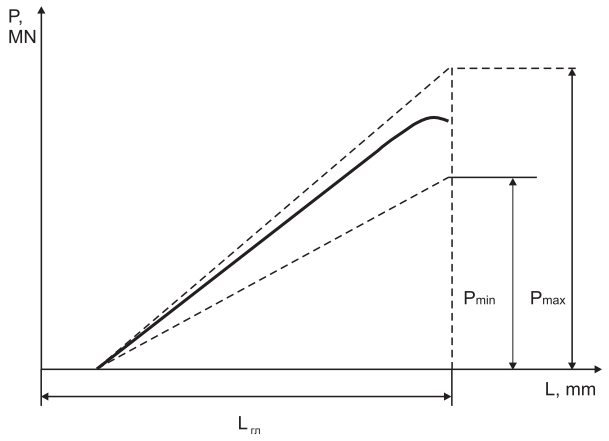

Fig.1

Pressing-in is performed by a hydraulic press of a maximal force value of 3000 kN and maximal stroke of 700 mm. The electronic measuring system (Fig.2) that registers pressing-in consists of a force sensor and a sensor of displacement, amplifiers, an analogue-to-digital transformer and a PC.

Nencho G. Nenov, Ph.D., Assoc Prof, Higher School of Transport, Sofia, Bulgaria, rector@vtu.bg
Emil N. Dimitrov, Ph.D., Assoc Prof, TU of Sofia, Bulgaria, edim@tu-sofia.bg
Petyo M. Piskulev, Senior Lecturer, Higher School of Transport, Sofia, Bulgaria, piskulev@vtu.bg

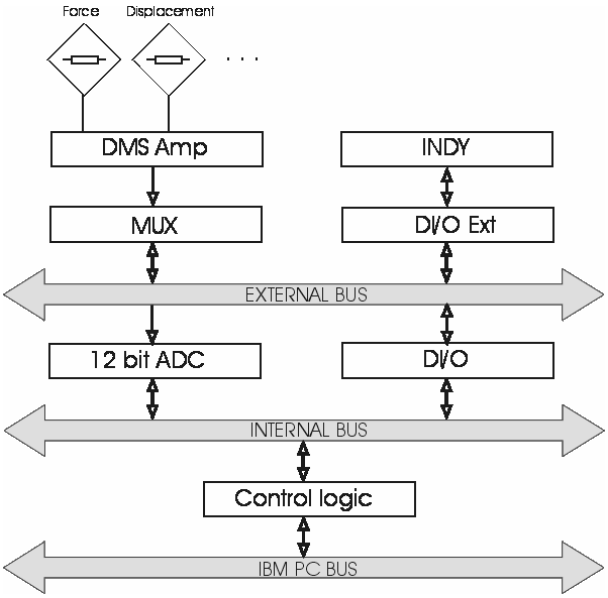

Fig. 2 Block diagram of electronic measuring unit of a pressing-in stand

The sensor of oil pressure (Fig. 3) measures the pressure of the oil in the press force cylinder with a view to determining the value of the piston force [2]. The sensor has a sensitive element **5** in a shape of cylinder. In the middle of the cylinder where it is hollow, two active strain gauges **3** are mounted positioned at 180° toward each other with axes perpendicular to the cylinder axis. In the upper massive part of the cylinder two compensating strain gauges **4** are mounted positioned at 180° toward each other. The strain gauges are connected in a full bridge. The sensitive element is mounted in a cylindrical body 1 appropriately shaped and connected to the atmosphere by an opening. This structure ensures a good mechanical protection of the strain gauges and gives indications with any possible destruction of the sensitive element. It also protects the operators of the press against the oil running under high pressure with a destructed sensitive element. Due to the considerable high values of the force, friction between the piston and cylinder can be neglected.

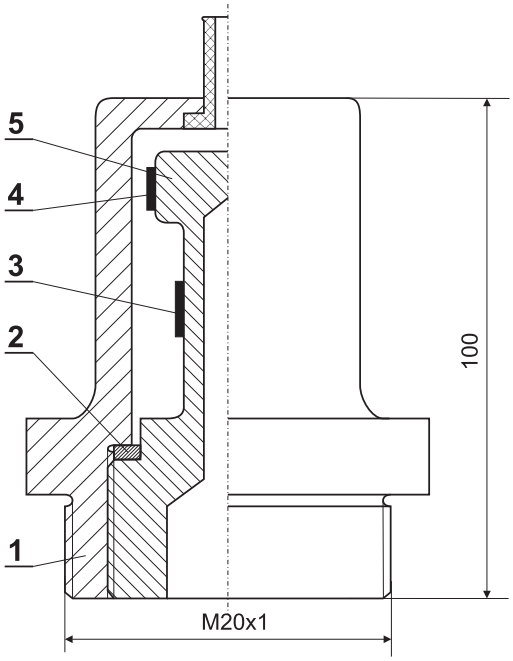

Fig.3 Sensor of force (pressure)

The press piston stroke is established by a sensor of displacement (Fig.4). It is implemented on the base of a multi-turn potentiometer **2**. The drive of the slider of the potentiometer **2** is performed by a roller **4**, pinched to a rod **5** stiffly connected with the press piston. The driving axle is on bearings 3 and is connected by an elastic link with the potentiometer. The sensor is put in a protected body **1**.

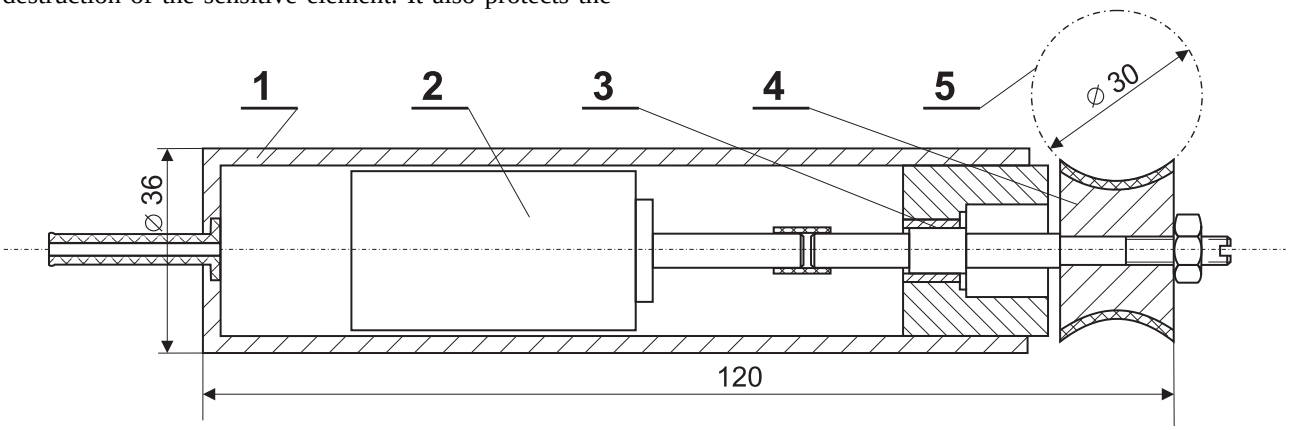

Fig.4 Sensor of displacement

The amplifiers are used to normalize the signal according to the operational range of the analogue-to-digital transformer that is from 0 to 10V. The block of the analogue-to-digital transformation is built on the base of the system KSI – 10. It presents a multi-channel 12-bit transformer with accuracy of measuring of 2,5mV. The control of the analogue-to-digital transformation is performed by a IBM PC/AT.

The measurement of the two values (force and displacement) is carried out with a frequency given by

the operator. The results obtained are saved as a file on the computer hard disk and are printed. The results are inseparable part of the passport of each wheel axle and are preserved as achieve.

3. RESULTS

The following figures show diagrams of pressing-in for different types of wheel axles of locomotives and trainsets in the BDZ fleet.

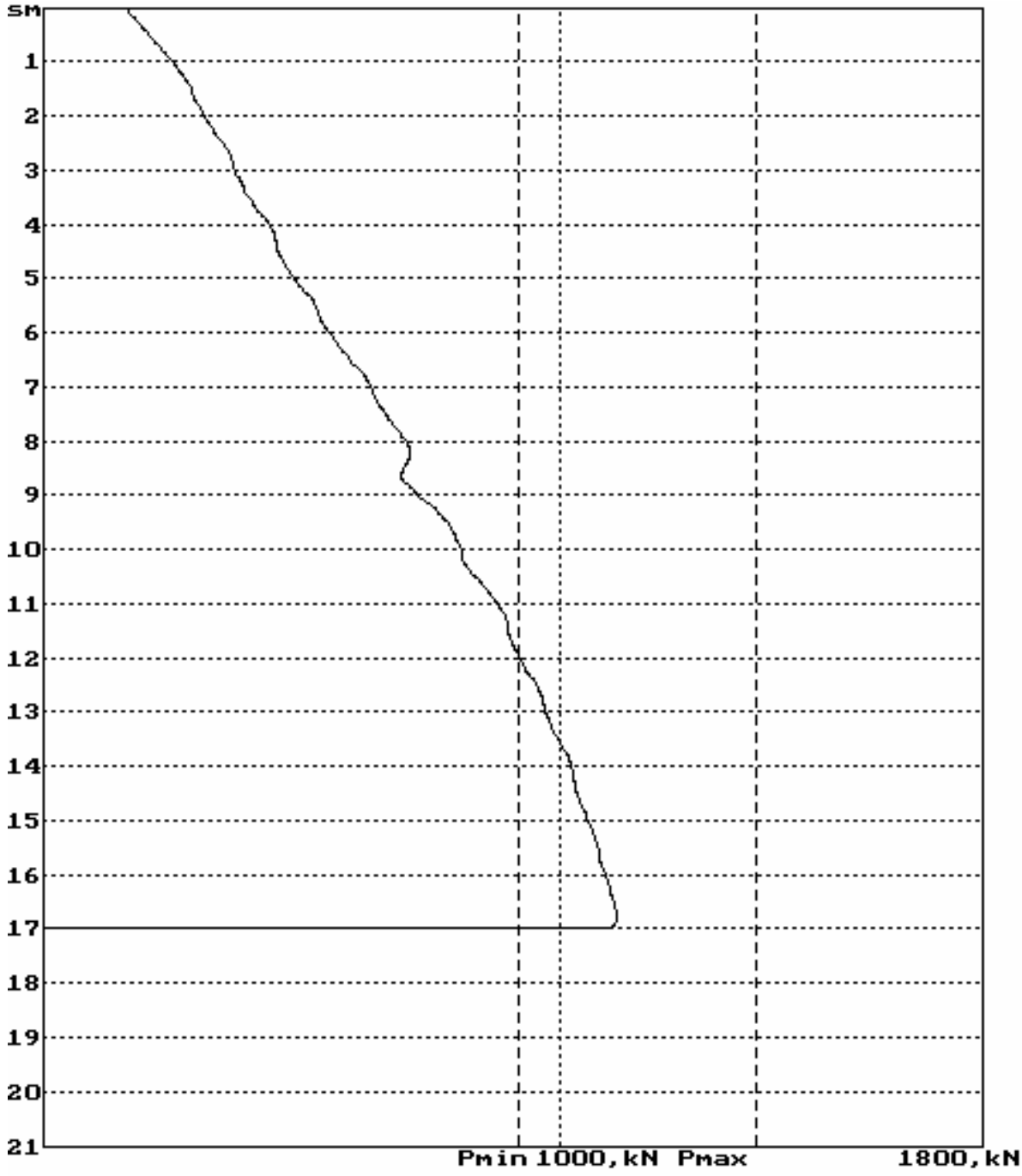

Fig.5 Diagram of pressing-in an axle of a locomotive series 46

The high precision with taking down the diagram of pressing-in has been established also by the fact that it takes into consideration the change of the force (reduction) with reaching and passing through the zone of the under-boss channel.

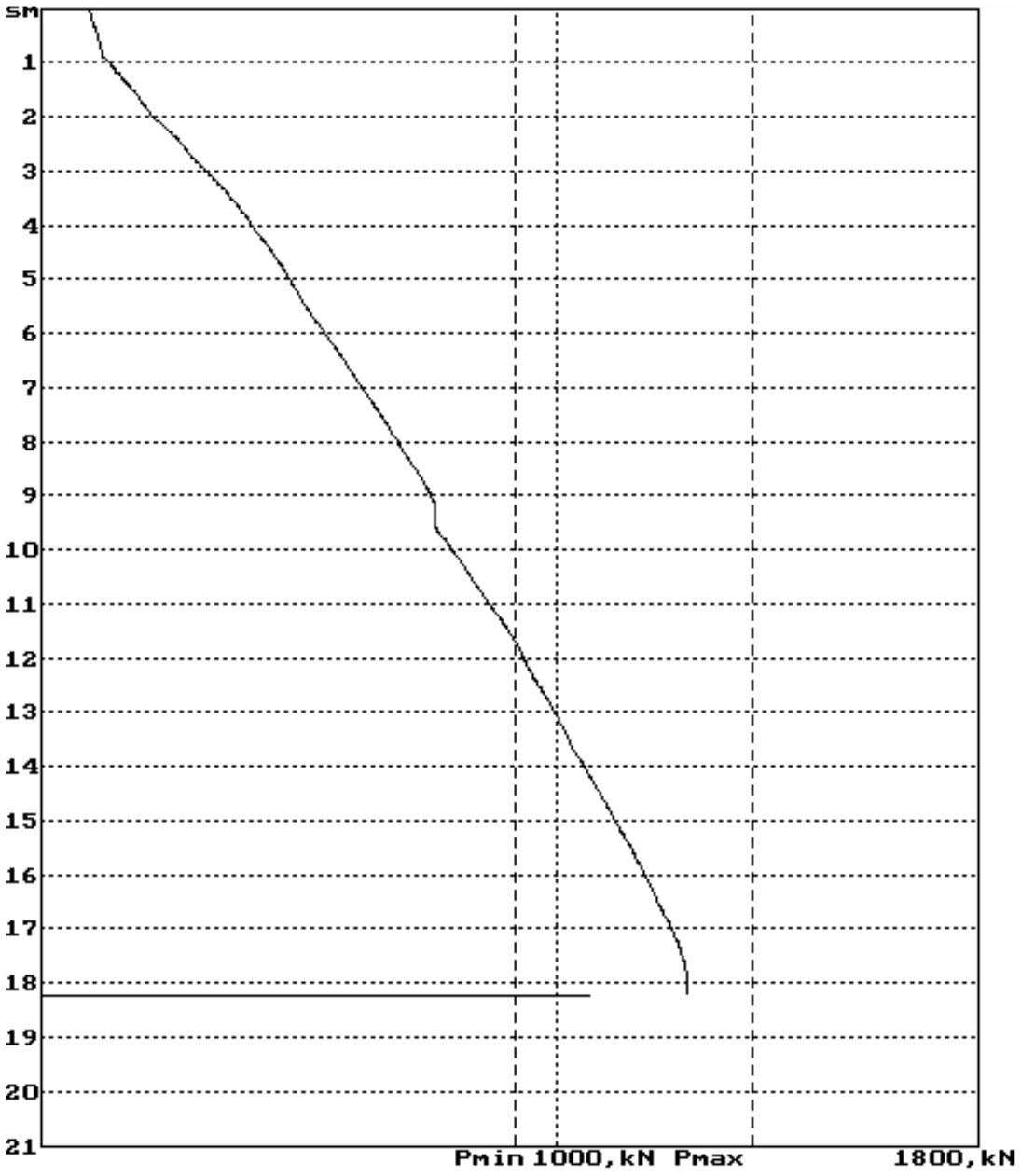

Fig.6 Diagram of pressing-in an axle of a locomotive series 44 (45)

4. CONCLUSION

The stand developed with the electronic measuring system to it has proved its serviceability for a long period of operation. After it has been set in operation, the number of defecting axles has been considerable reduced. With the system operation the influence of the human factor is completely excluded.

REFERENCES

[1] Regulations for Wheel Axles of Drive Rolling Stock of BDZ (PLS 410/85).

[2] Аш Ж. и др., Датчики измерителных систем, М., Мир, 1992.

[3] Max J., Methodes et techniques du signal et applications aus measures physiques, Paris, 1981

A METHOD OF EXPERIMENTAL DETERMINING STOCHASTIC PARAMETERS OF TRACK DISTURBANCE ON A LOCOMOTIVE WITH MOTION

E. N. Dimitrov, N. G. Nenov, G. D. Geshev, T. G. Ruzhekov

Abstract: *The disturbance transmitted to the locomotive mechanical system depends not only on the track geometric unevenness, but also on the changes of its parameters such as elasticity, dissipation and mass. All sources of disturbance are of random nature with a normal law of distribution. The above mentioned has shown that the method applied to affect on the locomotive mechanical system inputs by rail threads unevenness measured (dynamic unevenness) cannot reflect the dynamic process of the united system "track-locomotive" to a sufficient degree of adequacy. A way out of the situation can be looked for on the base of the results obtained from the physical modelling of the real process and its relevant transfer to other objects with known parameters of the locomotives. The result of the accomplished study is a data acquisition method for the disturbance on the locomotive with its running along a certain track section in a stochastic aspect (disturbance spectrum or correlation function). The method requires accurate data of the mechanical parameters of the locomotive used for the physical model of the track-locomotive interaction process: spring strength features, damper resistance forces, inertia and mass parameters. The scope of the method application is to optimize the mechanical parameters of the locomotive in the stage of its construction or to forecast the dynamic indices of existing locomotives with their running along a track with established disturbances. Another result of the method application is the obtained stochastic characteristics of the track parameters.*

Key words: *locomotive, dynamic, modelling*

1. INTRODUCTION

The parameters of the process of interaction of the track and locomotive with its motion are determined by the track disturbance and the mechanical parameters of the locomotive. The disturbance transmitted to the locomotive mechanical system depends not only on the track geometric unevenness, but also on the changes of its parameters such as elasticity, dissipation and mass. The disturbance nature gets more complex also due to the forces of pseudo slipping in the „wheel-rail" contact, which is an additional disturbance component. All sources of disturbance are of random nature with a normal law of distribution. The statement is grounded on the central boundary theorem of the probability theory [1]. It also has found operational confirmation [2]. The above mentioned has shown that, according to the authors, the method applied to affect on the locomotive mechanical system inputs by rail threads unevenness measured (dynamic unevenness) cannot reflect the dynamic process of the united system "track-locomotive" to a sufficient degree of adequacy. Its formal division into two subsystems, "track" and "locomotive", as the first one causes the reaction of the second subsystem, is not particularly correct. The creation of a mathematical model, which can present, from a practical viewpoint, substantial parameters of the united system dynamic process is a little possible, at least for now.

A way out of the situation can be looked for on the base of the results obtained from the physical modelling of the real process and its relevant transfer to other objects with known parameters of the locomotives. The purpose of this paper is to define, in general, the tools and the equipment necessary to implement the method mentioned.

2. IMITATION MODEL OF DISTURBANCE

The model of disturbance is formed by the following components

a. Frequency characteristics $W_{q_i}(i\omega)$ of the oscillations, defined by the locomotive summarized coordinates q_i.

It can be obtained from the transmitting function $W_{q_i}(s)$ after a transition from the Laplace functional transform to Fourier functional transform. The above mentioned is possible if it is admissible to assume that the mechanical system is linear. With both a linear and non-linear systems, it is expedient to use direct numerical integration of the system differential equations describing the oscillations of the locomotive and written in a vector-and-matrix form:

Emil N. Dimitrov, TU of Sofia, Bulgaria
Nencho G. Nenov, VTU T. Kableshkov, Sofia, Bulgaria, rector@vtu.bg
Georgi D. Geshev, TU of Sofia, Bulgaria
Toma G. Ruzhekov, VTU T. Kableshkov, Sofia, Bulgaria,

(1) $\ddot{\vec{q}}+[a].\dot{\vec{q}}^{m}+[b].\vec{q}=\vec{F}$, where

- [a], [b] - square matrices with nxn elements (n – number of the summarized coordinates);

- $\vec{q}$, $\dot{\vec{q}}$, $\ddot{\vec{q}}$ - vectors of the summarized coordinates and their first and second derivatives;

- $\vec{F}$ - matrix column determined by the external disturbance,

and on this basis, to obtain the frequency characteristics $W_{q_i}(i\omega)$.

b. Energy spectrum $S_{q_i}(\omega)$ of the oscillations for coordinate q_i.

The autocorrelation function $R_{q_i}(\tau)$ is determined after its Fourier functional transform:

(2) $$S_{q_i}(\omega)=2\int_0^{\infty}R_{q_i}(\tau)\cos(\omega\tau)d\tau,$$

where

(3) $R_{q_i}(\tau)=M\left[q_i(t).q_i(t+\tau)\right]$ - mathematical expectation for the product of two centralized values of summarized coordinate q_i shifted by time interval τ.

c. Energy spectrum of the disturbance causing oscillation

$q_i(t)$ - $\Phi_i(\omega)$.

The three components marked above are connected by the dependency:

$S_{q_i}(\omega)=\left|W_{q_i}(i\omega)\right|^2.\Phi_i(\omega)$, i.e. energy spectrum of the forced oscillations is determined by the product of absolute value square of the locomotive frequency characteristics $W_{q_i}(i\omega)$ for the summarized coordinate $q_i(t)$ and the energy spectrum of the disturbance that caused it $\Phi_i(\omega)$. From the frequency pointed-out for the energy spectrum of the forced oscillations $S_{q_i}(\omega)$, the energy spectrum of the disturbance $\Phi_i(\omega)$ can be defined:

(4) $$\Phi_i(\omega)=\frac{S_{q_i}(\omega)}{\left|W_{q_i}(i\omega)\right|^2}.$$

That is why it is necessary to know the locomotive structure and the values of its mechanical parameters (masses, inertia moments, coefficients of elasticity, etc.) to be known. On the base of them, through a mathematical model, the frequency characteristics $W_{q_i}(i\omega)$ can be determined. From the registered oscillations $q_i(t)$, the correlation function $R_{q_i}(\tau)$ and then the energy spectrum $S_{q_i}(\omega)$ are determined. It follows that the disturbance stochastic characteristics in the form of energy spectrum $\Phi_i(\omega)$ or the correlation function $R_{\eta_i}(\tau)$ are defined:

(5) $$R_{\eta_i}(\tau)=\frac{1}{\pi}\int_0^{\infty}\frac{S_{q_i}(\omega)}{\left|W_{q_i}(i\omega)\right|^2}\cos(\omega\tau)d\omega .$$

Thus the defined characteristics of disturbance $\Phi_i(\omega)$ and $R_{\eta_i}(\tau)$ relatively in the frequency and time areas, can be used to analyse the dynamic behaviour of the "track-locomotive" system at the stage of designing a certain locomotive or to give a dynamic characteristics of an existing locomotive along a track, which characteristics of disturbance $\Phi_i(\omega)$ or $R_{\eta_i}(\tau)$ have been defined.

3. THE ELECTRONIC MEASUREMENT EQUIPMENT.

The measuring equipment should be able to make measurements of the acceleration at different points of the locomotive structure and to receive results from a number of sensors. The signal sampling frequency is determined by the number of channels switched on. The block diagram of the equipment is shown in Fig.1.

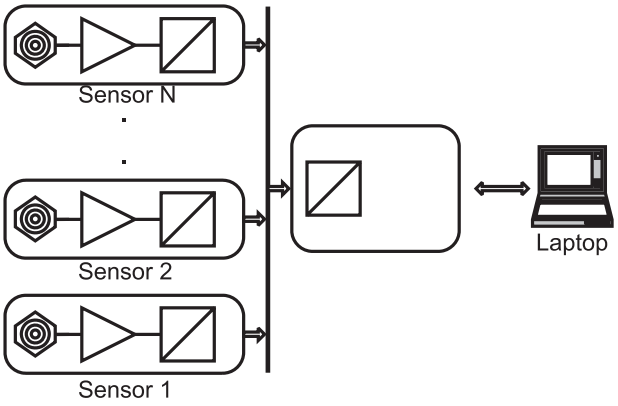

Fig.1. *Block diagram of electronic accelerometer equipment*

The used in the figure symbols are described below.

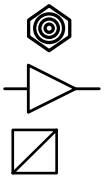

- Acceleration sensor
- Amplifier
- U/I or I/U converter

For the possibility to apply different algorithms, it is necessary to save the results and to process them later under laboratory conditions.

The sensors are integrated circuits make by Analog Devices Company using iMEMS® technology (integrated Micro Electro Mechanical System). The output signal is voltage proportional to the acceleration.

The accelerometers of ADXL3xx series can measure accelerations in one, two or three directions. They have a wide range of the amplitudes of registered accelerations with high sensitivity. It allows the amplifier to be with low coefficient of amplifying that reduces the noise level. Due to the distance of the sensor from the registering unit, a voltage-to-current U/I converter should be used. The receivers of the registering unit are current-to-voltage I/U convertors.

Thus the connection accomplished between the sensors and registering unit gives a possibility to find out a disrupted connection between them. The voltages obtained in the outputs of receivers are transferred to a data acquisition system (Data acquisition – DAQ). It is multi-channel with inbuilt frequency generator by which the sampling frequency of is specified. Data acquisition uses a combination of PC-based measurement hardware and software to provide a flexible, user-defined measurement system. A laptop and PCMCI DAQ KPCMCIA-12AIH of Keithley Company are used for data acquisition. The DAQ hardware possibilities are 8 differential or 16 unipolar analogue input channels.

4. SOFTWARE

The software for registering accelerations and saving on a hard disk through the module PCMCIA-12AIH on a laptop is implemented by MATLAB [3]. The processing of the information recorded will be done in MATLAB environment (gives a possibility of processing missives of big volume) in the following succession:

a. Determination of the locomotive frequency characteristics $W_{q_i}(i\omega)$ on the base of a set of non-linear differential equations (1) used in [3] for given values of frequency ω as a matrix.

b. Double integration of the signal for accelerations on the purpose of obtaining oscillations by particular summarized coordinates $q_i(t)$. The information is saved in a file on the purpose of its multiple processing.

c. Determination of the autocorrelation function (3) of oscillations $R_{q_i}(\tau)$ for the summarized coordinates $q_i(t)$.

d. Determination of the spectral density of oscillations $S_{q_i}(\omega)$ for the summarized coordinates $q_i(t)$ by formula (2).Determination of the spectral density $\Phi_i(\omega)$ of the disturbance causing oscillations $q_i(t)$ by formula (4).

e. Determination of the correlation function $R_{\eta_i}(\tau)$ of the disturbance causing oscillations $q_i(t)$ by formula (5).

5. CONCLUSION

The result of the accomplished study is a data acquisition method for the disturbance on the locomotive with its running along a certain track section in a stochastic aspect /disturbance spectrum $\Phi_i(\omega)$ or correlation function $R_{q_i}(\tau)$/. The method requires accurate data of the mechanical parameters of the locomotive used for the physical model of the track-locomotive interaction process: spring strength features, damper resistance forces, inertia and mass parameters.

To apply it more effectively, it is also necessary to examine the process of its natural oscillations exited by putting wedges under its wheels according to a certain scheme to cause desired oscillations. The study makes possible to determine the natural frequencies and attenuation of oscillations. The data is necessary to specify the values of the inertia parameters and dissipative forces.

The basis of the suggested method, frequency characteristics $W_{q_i}(i\omega)$ of the locomotive with non-linear elements in the spring system, is given in the paper prepared for publication by the authors [4].

The scope of the method application is to optimize the mechanical parameters of the locomotive in the stage of its construction or to forecast the dynamic indices of existing locomotives with their running along a track with established disturbances. Another result of the method application is the obtained stochastic characteristics of the track parameters.

The main advantage of the method using the physical modelling of the process of the track and locomotive interaction is in keeping the real unity of the mechanical system mentioned above.

REFERENCES

[1] Гутский, Е.И., Теория вероятностей с эматематической статистики, Высшая школа, М., 1971.

[2] Силаев, А.А., Спектральная теория подрессоривания транспортных мащин, Мащиностроение, М., 1972.

[3] Dimitrov E., N. Nenov and G. Geshev, Train Spring System Electronic Diagnostic Equipment Using Accelerometer Sensors, ISSE-2008, H002, Budapest, Hungary, 7-11 May, 2008

[4] Integrated assessment of the locomotive spring system dissipative forces.

A MODEL IN THE STUDIES ACTIVE STEERING ROTATION WHEELSETS

D. Atmadzhova

Abstract: *The active steering is to stabilize the wheelset and to provide a guidance control. The developed controller is able to maintain stability and good performance when parameter variations occur, in particular at the wheel-rail interface. This paper presents the development of control strategy for the active steering of railway vehicles with independently rotating wheelsets. The study has shown that a robust controller with practical sensors can be developed to stabilize the wheelset and to provide necessary guidance control. The control design has been formulated to tackle effectively parameter variations and unmodeled dynamics and the μ-synthesis technique has been used to examine and guarantee the robustness of the closed loop.*

Key words: *Railway vehicle, independently rotating wheelset, active steering.*

1. INTRODUCTION

In the railway industry, one of the significant developments is the use of active controls for railway vehicles. Tilting trains have been successfully used in Europe and the rest of the world, and it appears certain that active secondary suspensions will be widely used. A conventional railway wheelset comprises two coned or otherwise profiled wheels joined together by a solid axle. This arrangement has the advantages of natural centring and curving, but when it unconstrained also exhibits a sustained oscillation in the horizontal plane. This is overcome on conventional railway vehicles by means of springs connected from the wheelset to the bogie (truck) or the body of the vehicle. However, this added stiffness degrades the ability of the wheelset to curve and it may cause severe wear of the wheels and rails. Various active methods to steer the solid-axle wheelset have been proposed [1,4,5], where the main aim is to provide necessary stabilization control without interfering with the natural curving action. A major task has been to try and solve the difficult design conflict between the stability, curving performance, and passenger comfort requirements. However, studies have shown that the control demand from actuators can be excessively high [1]. Those design difficulties can be eased and the control demand greatly reduced by allowing the two wheels on the same axle to rotate independently from each other, hence the term independently rotating wheelset (IRW) [5]. Alternatively, directly steered wheel pairs have been proposed, where two wheels are mounted onto a frame and no axle is required [7]. However, new problems are created with these novel concepts. One of the main drawbacks is that the independently rotating wheelset (or wheel pair) does not have the natural curving ability of the conventional wheelset, and some form of guidance action becomes necessary.

One of the first issues for the control design is the measurement difficulty. Active steering for the independently rotating wheelset requires some essential feedback signals such as wheel-rail deflections for guiding the wheelset to follow the track, but a direct measurement of these signals is not feasible in practice. Although state estimation techniques such as Kalman filters can be used to estimate those signals, the studies so far have shown that it is extremely difficult to make observers work effectively in the presence of substantial parameter variations.

That must be addressed is how a control design tackles system uncertainty, which may result from several sources:

1) Railway vehicles are subject to parameter variations, especially those at the wheel-rail interface such as creep coefficients and wheelset conicity.
2) The dynamics of actuators also add to the uncertainty, as incorporation of the actuator dynamics would tend to make the design process overly complicated.
3) As a railway vehicle is a very complex and nonlinear dynamic system with very high order, a simplified model is normally used for the control design in practice and hence uncertainties due to unmodeled dynamics will have to be guarded against in the design.
4) The design conflict between the stability, curving performance and ride quality is eased by the use of the independently rotating wheelset, it is not completely eliminated. The wheelset instability still exists; the wheelsets must avoid flange contact on curved track; and the passenger ride comfort should be improved.

Dobrinka Borisova Atmadzhova, Associate Professor, Ph. D. VTU "T. Kableshkov", atmadzhova@abv.bg

2. SYSTEM DESCRIPTION AND MODELLING

The paper uses a two-axle vehicle for the study, the overall motivation being that the use of active control facilitates a simpler mechanical vehicle scheme than the conventional four-axle vehicle with two bogies (trucks).

The active steering action only affects the lateral and yaw motions of the vehicle, the plan view model of the vehicle is sufficient for developing active control schemes. Fig. 1 gives a simplified plan view diagram. The modeled scheme mainly consists of a body and two independently rotating wheelsets. The wheelsets are connected to the body via typical springs and dampers in the lateral direction with typical values for a secondary suspension.

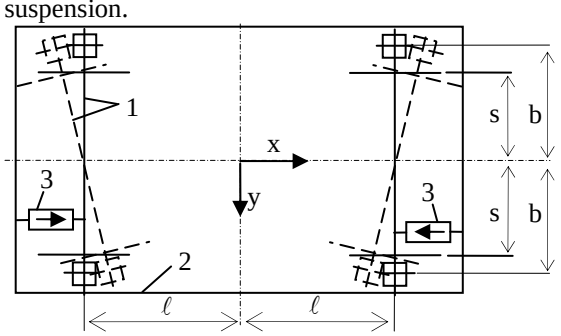

Fig. 1. Plan view of a two-axle vehicle.
1- Wheelset; 2 – Vehicle body (or bogie); 3 – Torque actuator.

The model of the vehicle can be represented by (1)–(8), where all variables are related to local track references.

The model can thus be described by the following equations:

Leading wheelset motions (lateral, yaw, and rotation):

$$(1)\ m_w\ddot{y}_{w1}+\left(\frac{2f_{22}}{V_s}+C_s\right)\dot{y}_{w1}+K_s y_{w1}-2f_{22}\psi_{w1}-$$
$$-C_s\dot{y}_v-K_s y_v-C_sL_v\dot{\psi}_v-K_sL_v\psi_v=m_w\left(\frac{v_s^{\,2}}{R_1}-g\theta_{c1}\right)$$

$$(2)\ I_w\ddot{\psi}_{w1}+\frac{2f_{22}L_g^{\,2}}{V_s}\dot{\psi}_{w1}+\frac{2f_{11}\lambda L_g}{r_0}y_{w1}+$$
$$+\frac{2r_0f_{11}L_g}{r_0}\dot{\phi}_{w1}=\frac{2f_{11}L_g^{\,2}}{R_1}+\frac{2f_{11}\lambda L_g}{r_0}y_{t1}+T_{w1}$$

$$(3)\ I_{w1}\ddot{\phi}_{w1}+\frac{r_0^{\,2}f_{11}}{V_s}\dot{\phi}_{w1}+f_{11}\lambda.y_{w1}+\frac{r_0f_{11}L_g}{V_s}\dot{\psi}_{w1}=$$
$$=\frac{r_0\,f_{11}L_g}{R_1}+f_{11}\lambda.y_{t1}$$

Trailing wheelset motions (lateral, yaw, and rotation):

$$(4)\ m_w\ddot{y}_{w2}+\left(\frac{2f_{22}}{V_s}+C_s\right)\dot{y}_{w2}+K_s y_{w2}-2f_{22}\psi_{w2}-$$
$$-C_s\dot{y}_v-K_s y_v-C_sL_v\dot{\psi}_v-K_sL_v\psi_v=m_w\left(\frac{v_s^{\,2}}{R_2}-g\theta_{c2}\right)$$

$$(5)\ I_w\ddot{\psi}_{w2}+\frac{2f_{22}L_g^{\,2}}{V_s}\dot{\psi}_{w2}+\frac{2f_{11}\lambda L_g}{r_0}y_{w2}+$$
$$+\frac{2r_0f_{11}L_g}{r_0}\dot{\phi}_{w2}=\frac{2f_{11}L_g^{\,2}}{R_2}+\frac{2f_{11}\lambda L_g}{r_0}y_{t2}+T_{w2}$$

$$(6)\ I_{w1}\ddot{\phi}_{w2}+\frac{r_0^{\,2}f_{11}}{V_s}\dot{\phi}_{w2}+f_{11}\lambda.y_{w2}+\frac{r_0f_{11}L_g}{V_s}\dot{\psi}_{w2}=$$
$$=\frac{r_0f_{11}L_g}{R_2}+f_{11}\lambda.y_{t2}$$

Body motions (lateral and yaw):

$$(7)\ m_v\ddot{y}_v+2C_s\dot{y}_v+2K_s y_v-C_s\dot{y}_{w1}-K_s y_{w1}-$$
$$-C_s\dot{y}_{w2}-K_s y_{w2}=\frac{m_vV_s^{\,2}}{2}\left(\frac{1}{R_1}+\frac{1}{R_2}\right)-\frac{m_vg}{2}\left(\theta_{c1}+\theta_{c2}\right)\ (8)$$
$$I_v\ddot{\psi}_v+2L_v^{\,2}C_s\dot{\psi}_v+2L_v^{\,2}K_s\psi_v-L_vC_s\dot{y}_{w1}+$$
$$+L_vC_s\dot{y}_{w2}-L_vK_s y_{w1}+L_vK_s y_{w2}=-\left(T_{w1}+T_{w2}\right)$$

where vehicle variables: C_s - lateral damping per wheelsets; f_{11}, f_{22} - longitudinal and lateral, creep coefficients; g – gravity; I_v, I_w - vehicle yaw inertia and wheelsets yaw inertia; I_{w1} - wheel inertia; K, or K(s) controller; K_s - lateral stiffness per wheelsets; Lg - half gauge of wheelset; m_v, m_w - vehicle mass and wheelset mass; P, or P(s) - vehicle model; r_0 - wheel radius; R_1, R_2 - radius of the curved track at leading and trailing wheelsets; T_{w1}, T_{w2} - control torque for leading and trailing wheelsets respectively; V_s - vehicle travel speed; y_{t1}, y_{t2} - track lateral irregularity at leading and trailing wheelsets; y_{w1}, y_{w2}, y_v - lateral displacement of leading, trailing wheelsets and body; θ_{c1}, θ_{c2} - cant angle of the curved track at the leading and trailing wheelsets; λ - wheel conicity; ϕ_{w1}, ϕ_{w2} - relative rotation angle of two wheels at leading and trailing wheelset; ψ_{w1}, ψ_{w2}, ψ_v - yaw angle of leading, trailing wheelsets and vehicle body.

The generalized formula of determining the attack angle α_{ijk} of attacking wheel № k (k = 1 for the right one; k = 2 for the left one) by j-wheel axle and **i**-bogie has been derived from the geometry dependencies of the "body – bogies – wheel axles – rails" system in a curve with radius R according to [3]:

$$(9)\quad \alpha_{ijk}=(-1)^{j+1}.\ell/R-(-1)^{i}.L/R+(-1)^{i}\psi_i-$$
$$-(-1)^{k}\gamma_{ij}-(-1)^{k}\xi_i-(-1)^{k}\beta_y$$

where: L and ℓ - the base of the vehicle, respectively of the bogie; ψ_i - angle of the bogie rotation towards the car body (it is always taken with its absolute value, i.e. with sign "+"); γ_{ij} - angle of the wheel axle rotation towards the bogie frame (sign "+" with clockwise rotation and sign "-" with counterclockwise rotation); ξ_i - angle of the bogie frame horizontal skew strain (sign "+" with clockwise rotation and sign "-" with counterclockwise rotation); β_y - angle of the body rotation towards its base position defined with the chord position of bogies and with an average position of the joined elements in "body – bogie" and "wheel axles – bogie frame" connections; it depends essentially on the difference of crosswise displacements in the system

reduced to the central bearing and is determined by the following formula:

$$(10)\ \beta_y = \left(Y_{\sum 1} - Y_{\sum 2}\right)/2L = $$
$$= (2L)^{-1}\left\{(-1)^k\, 0,5.\sigma_{12} + 0,5.(y_{b11} + y_{b12}) + y_{w1} - \right.$$
$$\left. -\left[(-1)^k\, 0,5.\sigma_{22} + 0,5.(y_{b21} + y_{b22}) + y_{w2}\right]\right\}$$

where: $Y_{\Sigma 1}$, $Y_{\Sigma 2}$ - total crosswise relations (displacement) of the body towards the outer rail reduced in the place of the central bearing of the first and second bogie; σ_{12}, σ_{22} - the distances "flange – outer rail" for the second (rear) wheel axle of the first and the second bogies; y_{b11}, y_{b12}, y_{b21}, and y_{b22} - crosswise relative displacement of the bogie frame towards the first and second wheel axles respectively of the first and the second bogie respectively; y_{w1}, y_{w2} - crosswise relative displacements (crosswise relations) of the body towards the first and second bogies in the point of the central bearing.

A state-space form can be readily derived from (1)–(9), as given in (11).

$$(11)\qquad \mathbf{x} = A.x + B.u + \Gamma.w$$

where we have the first equation for **x** and **u** shown:

$$\mathbf{x} = \left[\dot{y}_{w1} y_{w1} \dot{\psi}_{w1} \psi_{w1} \dot{\phi}_{w1} \dot{y}_{w2} y_{w2} \dot{\psi}_{w2} \psi_{w2} \dot{y}_v y_v \dot{\psi}_v \psi_v\right]^T;$$

$$\mathbf{u} = \left[T_{w1} T_{w2}\right]^T; \quad \mathbf{w} = \left[R_1^{-1}\theta_{c1} y_{t1} R_2^{-1}\theta_{c2} y_{t2}\right]^T$$

3. CONTROL DESIGN

The wheelsets must be controlled to follow the track with no flange contact allowed on both straight tracks with irregularities and curved tracks—in practice this means restricting the lateral wheel-rail displacement to less than around 8mm. Unlike a solid-axle wheelset, with IRWs the wheelsets are not required to follow a pure rolling line, but excellent curving performance is still an important requirement because this is difficult to achieve for a passive two-axle vehicle especially when high-speed stability is also required. In addition any control should improve, or at least not worsen, the ride quality of the vehicle.

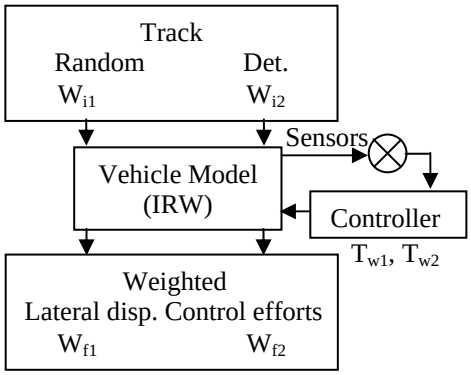

Fig. 2. Structure diagram of control design.

Fig. 2 shows the structure for the control design and (12) and (13) give the state and output equations that are derived from (11) and formulated for the control design purpose. Note that both input and output vectors are partitioned into two parts.

$$(12)\ \dot{x} = A.x + \left[B_1\ B_2\right]u_{in}$$

$$(13)\ \mathbf{y} = \begin{bmatrix} C_1 \\ C_2 \end{bmatrix}.\mathbf{x} + \begin{bmatrix} D_{11} & D_{12} \\ D_{21} & D_{22} \end{bmatrix}.\mathbf{u}_{in}$$

Selection of output measurements is not straightforward and some natural choices for active steering such as wheel-rail deflection and wheelset angle-of-attack are very difficult and expensive to implement in practice. Practical sensors [6] are used in the design, which are the last six variables defined in the output vector **y** measuring the lateral acceleration (accelerometers), yaw velocity (gyros) and relative rotation speed (spd) of the two wheels of each wheelset.

Designers of a railway vehicle are particularly interested in controlling the lateral wheel-rail displacement and the angle-of-attack (i.e., the yaw angle relative to the track) of the two wheelsets as far as wheelset steering is concerned. Lateral displacement is important because of avoiding contact between the wheel flanges and the rail, and the angle-of-attack affects the lateral creep forces. However, an optimization procedure concludes that it is only necessary to minimize the wheelset lateral displacements [4]. Therefore the lateral displacements of the two wheelsets ($y_{\omega 1}$ and $y_{\omega 2}$) are defined as the first two variables in the output vector y. The matrix W_{f1} shown in Fig. 2 and given in (14) is a dynamic weighting factor defined to shape the frequency response of the lateral displacement of each wheelset and to maintain stability in the presence of perturbations.

The next two variables in the output vector are the two control torques (T_{w1} and T_{w2}), because it is necessary to limit the control effort requirement for practical reasons. The matrix W_{f1} given in (14) is a dynamic weighting factor used as a constraint on the control torques, in particular to account for the actuator dynamics.

$$(14)\ W_{fi} = k_i \begin{bmatrix} w_i & 0 \\ 0 & w_i \end{bmatrix}\ (\text{i} = 1, 2)$$

and $$w_i = \frac{s^2 + 2\xi_{ia}\omega_{ia}s + {\omega_{ia}}^2}{s^2 + 2\xi_{ib}\omega_{ib}s + {\omega_{ib}}^2}\ (\text{i} = 1, 2)$$

where parameters of weighting matrices: k_1, k_2 - coefficients of weighting matrices on wheelset lateral displacements and control torques; w_i - input weighting matrix on random and deterministic track input; 2s - the distances "wheel – wheel" on wheelset; ω_{1a}, ω_{1b} - frequencies of the dynamic weighting on lateral displacements; ξ_{1a}, ξ_{1b} - damping ratios of the dynamic weighting on lateral displacements; ω_{2a}, ω_{2b} - frequencies of the dynamic weighting on control torques; ξ_{2a}, ξ_{2b} - damping ratios of the dynamic weighting on control torques.

The resulting controller is then examined using the μ–synthesis technique to also ensure its robustness against not only the parametric uncertainties, in particular the variation of two parameters which have

significant effect on the wheel-rail contact mechanics [8].

By tuning the parameters of all weighting functions, the vehicle performances with the active control can be optimized. The dynamic weighting W_{f1} has been selected to allow the wheelsets to follow the low-frequency (below 10 Hz) elements of the track, which is a compromise between the maximum wheel-rail deflection allowed, and the rejection of high-frequency components of the track and the high-frequency perturbations. The second dynamic weighting W_{f2} has been set to give a cut off frequency around 12 Hz mainly to reflect the fact that the bandwidth of the current actuator technology feasible for this type of application (hydraulic or electro-mechanical actuators) is normally 15–20 Hz. The coefficients of the two dynamic weightings (k_1 and k_2) are tuned for the overall tracking performance and control effort, where $k_1 = 1$ and $k_2 = 0{,}8 \times 10^{-7}$ are set in the simulation to meet both requirements. W_{i1} and W_{i2} are constant weighting matrices adjusted to balance the wheelset responses to the random and deterministic track inputs for the passenger comfort and curving performance. W_{i1} is set to unity and the coefficient of W_{i2} is tuned in the simulation to be 0.5—a value which gives the best compromise between the performance on curves and response on random track.

4. THE COMPUTER SIMULATION

The development of the robust control strategy has been carried out using a linearized model of the railway vehicle, which is justified on the basis that an active steering scheme will improve performance on curves in a manner which considerably reduces the effects of nonlinearities. The nonlinearities of a railway vehicle model are largely associated with nonlinear wheel-rail profiles and contact forces, which become particularly problematic when the wheel-rail contact point approaches the wheel flanges.

However, the use of active steering control largely overcomes this problem by steering the wheelset to operate at the linear region of the wheel tread and rail surface. As it will be shown later in the section, the difference between the linearized model and a full nonlinear model is very small for actively steered vehicles. On the other hand, a nonlinear model is essential for simulating passive vehicles on tight curves where flange contact is likely to occur. Although this justifies the use of the linearized vehicle model to assess the vehicle performance of the proposed active scheme, a full nonlinear model is also used in the simulation wherever the difference between the two models becomes significant. The nonlinear model is developed based on the well-known contact theory of Hertz and nonlinear creep theory of Kalker [2]. Also nonlinear wheel/rail profiles, which is a standard pair of profiles used by the railway industry.

In the simulation, both deterministic and random track inputs are used to study the responses of the actively controlled vehicles on different tracks.

5. CONCLUSION

This paper has presented the development of an robust control scheme for active steering of independently rotating railway wheelsets. The study has shown that a robust controller with practical sensors can be developed to stabilize the wheelset and to provide necessary guidance control. The control design has been formulated to tackle effectively parameter variations and unmodeled dynamics and the μ-synthesis technique has been used to examine and guarantee the robustness of the closed loop. The robustness achieved has been demonstrated in the computer simulation.

REFERENCES

[1] [1] Anon, “A powerful lightweight packed with innovative ideas—single-axle running gear,” *BahnTech*, vol. 3/97, 1997

[2] [2] Atmadzhova, D. “The theories Kalker for study of interaction of a wheel and rail”, XV SCIENTIFIC CONFERENCE "TRANSPORT 2005" University of Transport, Sofia, 2005

[3] [3] Atmadzhova, D. “Models of Examination on the Rolling Stock Wheeled Part With Running Along a Curvature” *Mechanics Transport Communications* number 2, 2007 http://www.mtc-aj.com

[4] [4] Mei, T. X. T. H. E. Foo, and R. M. Goodall, “Genetic Algorithms for Optimising Active Controls in Railway Vehicles,” in *Proc. Inst. Elect. Eng Colloq.*, London, U.K., 1998.

[5] [5] Mei, T. X. and R. M. Goodall, “Wheelset Control Strategies for a 2-Axle Railway Vehicle,” in *Proc. 16th IAVSD Symp.: Dyn. Vehicles Roads Tracks*, Pretoria, South Africa, 1999

[6] [6] Šoškić, Z., D. Petrović, N. Bogojević and R. Rakanović, **“**Suggestions for development of sensors for measurement of forces at wheel-rail contact”. XV SCIENTIFIC CONFERENCE "TRANSPORT 2005" University of Transport, Sofia, 2005

[7] [7] Wickens, A. H. “Dynamic stability of articulated and steered railway vehicles guided by lateral displacement feedback,” in *Proc. 13th IAVSD Symp.*, Chengdu, China, 1993

[8] [8] Wickens, A. H. “The dynamics of railway vehicles—from Stephenson to Carter,” *IMechE Proc. (Part F)*, vol. 212, 1998

SIMULATION AND ANALYSIS IN ACTIVE STEERING OF INDEPENDENTLY ROTATING WHEELSETS

D. Atmadzhova

Abstract: *This paper studies active steering of independently rotating wheelsets on a railway vehicle. The two-axle vehicle that is used in the study and modelling of the vehicle. Formulation and design details of the robust control, and the presents and analyzes simulation results.*

Key words: Railway vehicle, independently rotating wheelset, active steering, simulation.

1. INTRODUCTION

Although several schemes have been proposed for active control of independently rotating wheelsets, some fundamental problems still remain to be solved satisfactorily [4, 5]. One of the first issues for the control design is the measurement difficulty. Active steering for the independently rotating wheelset requires some essential feedback signals such as wheel-rail deflections for guiding the wheelset to follow the track, but a direct measurement of these signals is not feasible in practice. Although state estimation techniques such as Kalman filters can be used to estimate those signals [3], the studies so far have shown that it is extremely difficult to make observers work effectively in the presence of substantial parameter variations.

In addition, although the design conflict between the stability, curving performance and ride quality is eased by the use of the independently rotating wheelset, it is not completely eliminated. The wheelset instability still exists; the wheelsets must avoid flange contact on curved track; and the passenger ride comfort should be improved.

The primary objective of the active steering is to stabilize the wheelset and to provide a guidance control. Some fundamental problems for active steering are addressed in the study. The developed controller is able to maintain stability and good performance when parameter variations occur, in particular at the wheel-rail interface. The control is also robust against structured uncertainties that are not included in the model such as actuator dynamics. Further more the control design is formulated to use only practical sensors of inertial and speed measurements, as some basic measurements required for active steering such as wheel-rail lateral displacement cannot be easily and economically measured in practice.

2. SYSTEM DESCRIPTION AND MODELLING

The paper uses a two-axle vehicle for the study, the overall motivation being that the use of active control facilitates a simpler mechanical vehicle scheme than the conventional four-axle vehicle with two bogies (trucks). Because the active steering action only affects the lateral and yaw motions of the vehicle, the plan view model of the vehicle is sufficient for developing active control schemes.

The wheelsets must be controlled to follow the track with no flange contact allowed on both straight tracks with irregularities and curved tracks—in practice this means restricting the lateral wheel-rail displacement to less than around 8mm. Unlike a solid-axle wheelset, with IRWs the wheelsets are not required to follow a pure rolling line, but excellent curving performance is still an important requirement because this is difficult to achieve for a passive two-axle vehicle especially when high-speed stability is also required. In addition any control should improve, or at least not worsen, the ride quality of the vehicle.

A state-space form can be readily derived from [1], as given in (1).

(1) $\mathbf{x} = A.x + B.u + \Gamma.w$

The structure for the control design and (2) and (3) give the state and output equations that are derived from (1) and formulated for the control design purpose. Note that both input and output vectors are partitioned into two parts.

(2) $\dot{\mathbf{X}} = A.x + [B_1\ B_2]u_{in}$

(3) $\mathbf{y} = \begin{bmatrix} C_1 \\ C_2 \end{bmatrix}.\mathbf{x} + \begin{bmatrix} D_{11} & D_{12} \\ D_{21} & D_{22} \end{bmatrix}.\mathbf{u}_{\text{in}}$

where we have the second equation for y and u_{in}:

$\mathbf{y} = \left[y_{w1} y_{w2} T_{w1} T_{w2} \ddot{y}_{w1} \dot{\psi}_{w1} \ddot{y}_{w2} \dot{\psi}_{w2} \dot{\phi}_{w1} \dot{\phi}_{w2} \right]^T$; $\mathbf{u}_{\text{in}} =$

$$\left[v_{acc1} v_{gyro1} v_{acc2} v_{gyro2} v_{spd1} v_{spd2} \frac{1}{R_1} \theta_{c1} \frac{1}{R_2} \theta_{c2} y_{t1} y_{t2} T_{w1} T_{w2} \right]^T$$

Dobrinka Borisova Atmadzhova, Associate Professor, Ph. D. VTU "T. Kableshkov", Sofia, Bulgaria, atmadzhova@abv.bg

where vehicle variables: T_{w1}, T_{w2} - control torque for leading and trailing wheelsets respectively; y_{t1}, y_{t2} - track lateral irregularity at leading and trailing wheelsets; y_{w1}, y_{w2} - lateral displacement of leading, trailing wheelsets; θ_{c1}, θ_{c2} - cant angle of the curved track at the leading and trailing wheelsets; ϕ_{w1}, ϕ_{w2} - relative rotation angle of two wheels at leading and trailing wheelset; ψ_{w1}, ψ_{w2} - yaw angle of leading, trailing wheelsets; R_1, R_2 - radius of the curved track at leading and trailing wheelsets.

Selection of output measurements is not straightforward and some natural choices for active steering such as wheel-rail deflection and wheelset angle-of-attack are very difficult and expensive to implement in practice. Practical sensors [6] are used in the design, which are the last six variables defined in the output vector **y** measuring the lateral acceleration (accelerometers), yaw velocity (gyros) and relative rotation speed (spd) of the two wheels of each wheelset.

The total of 14 input variables defined in the input vector u_{in}. The first 12 variables of the input vector all represent disturbances, including sensor noises of the six measurements and track input features. There are two different types of track input. The curve radius (R_1, R_2) and cant angles (θ_{c1}, θ_{c2}) are the deterministic features, designed to satisfy passenger comfort requirements, whereas the random track inputs (y_{t1}, y_{t2}) are the unintended irregularities, i.e., the deviations from the intended alignment. Input weighting factors (T_{i1}, T_{i2}) are constant weighting matrices defined for the random and deterministic track inputs, respectively, which are used for fine-tuning of the curving performance and ride quality. The last two variables in the input vector are the control input signals $u_2 = [T_{w1}\ T_{w2}]^T$.

The next two variables in the output vector are the two control torques (T_{w1} and T_{w2}), because it is necessary to limit the control effort requirement for practical reasons. The matrix W_{f1} given in (4) is a dynamic weighting factor used as a constraint on the control torques, in particular to account for the actuator dynamics.

$$(4)\ W_{fi} = k_i \begin{bmatrix} w_i & 0 \\ 0 & w_i \end{bmatrix} \text{ (i = 1, 2)}$$

$$\text{and } w_i = \frac{s^2 + 2\xi_{ia}\omega_{ia}s + \omega_{ia}^2}{s^2 + 2\xi_{ib}\omega_{ib}s + \omega_{ib}^2} \text{ (i = 1, 2)}$$

where parameters of weighting matrices: k_1, k_2 - coefficients of weighting matrices on wheelset lateral displacements and control torques; w_i - input weighting matrix on random and deterministic track input; ω_{1a}, ω_{1b} - frequencies of the dynamic weighting on lateral displacements; ξ_{1a}, ξ_{1b} - damping ratios of the dynamic weighting on lateral displacements; ω_{2a}, ω_{2b} - frequencies of the dynamic weighting on control torques; ξ_{2a}, ξ_{2b} - damping ratios of the dynamic weighting on control torques; 2s - the distances "wheel – wheel" on wheelset.

The resulting controller is then examined using the μ–synthesis technique to also ensure its robustness against not only the parametric uncertainties, in particular the variation of two parameters which have significant effect on the wheel-rail contact mechanics [1]: the creep coefficient and the wheelset conicity. These two parameters may vary significantly in practice and typically the lateral and longitudinal creep coefficients can be considered to vary between 5MN and 10MN and the wheelset conicity between 0.05 and 0.4 (these are the typical ranges of values which are considered by passive suspension designers).

By tuning the parameters of all weighting functions, the vehicle performances with the active control can be optimized. The dynamic weighting W_{f1} has been selected to allow the wheelsets to follow the low-frequency (below 10 Hz) elements of the track, which is a compromise between the maximum wheel-rail deflection allowed, and the rejection of high-frequency components of the track and the high-frequency perturbations. The second dynamic weighting W_{f2} has been set to give a cut off frequency around 12 Hz mainly to reflect the fact that the bandwidth of the current actuator technology feasible for this type of application (hydraulic or electro-mechanical actuators) is normally 15–20 Hz. The coefficients of the two dynamic weightings (k_1 and k_2) are tuned for the overall tracking performance and control effort, where $k_1 = 1$ and $k_2 = 0{,}8 \times 10^{-7}$ are set in the simulation to meet both requirements. W_{i1} and W_{i2} are constant weighting matrices adjusted to balance the wheelset responses to the random and deterministic track inputs for the passenger comfort and curving performance. W_{i1} is set to unity and the coefficient of W_{i2} is tuned in the simulation to be 0.5—a value which gives the best compromise between the performance on curves and response on random track.

The values in parameters: coefficient of weighting matrices on wheelset lateral displacements $k_1 = 1$; coefficient of weighting matrices on control torques $k_2 = 0{,}8 \times 10^{-7}$; input weighting matrix on random track input $w_{i1} = 0{,}5*I_{4x4}$; input weighting matrix on deterministic track input $w_{i2} = 0{,}5*I_{4x4}$; frequencies of the dynamic weighting on lateral displacements $\omega_{1a} = \omega_{1b} = 15{,}15$ Hz; damping ratios of the dynamic weighting on lateral displacements $\xi_{1a} = \xi_{1b} = 1$; - frequencies of the dynamic weighting on control torques $\omega_{2a} = \omega_{2b} = 20{,}2$ Hz; damping ratios of the dynamic weighting on control torques $\xi_{2a} = \xi_{2b} = 1$.

3. SIMULATION AND ANALYSIS

Fig. 1 shows the diagram of the simulation model used in the study.

The development of the robust control strategy has been carried out using a linearized model of the railway vehicle, which is justified on the basis that an active steering scheme will improve performance on curves in

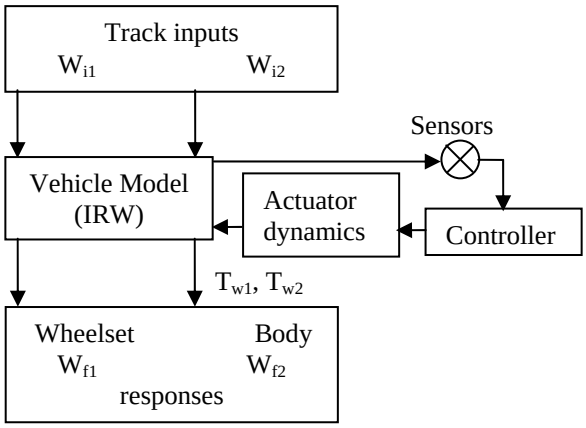

Fig. 1. Simulation model.

a manner which considerably reduces the effects of nonlinearities. The nonlinearities of a railway vehicle model are largely associated with nonlinear wheel-rail profiles and contact forces, which become particularly problematic when the wheel-rail contact point approaches the wheel flanges.

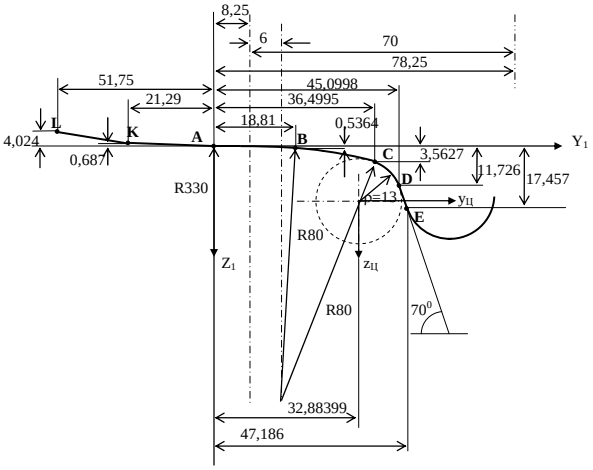

Fig. 2. Nonlinear wheel profiles.

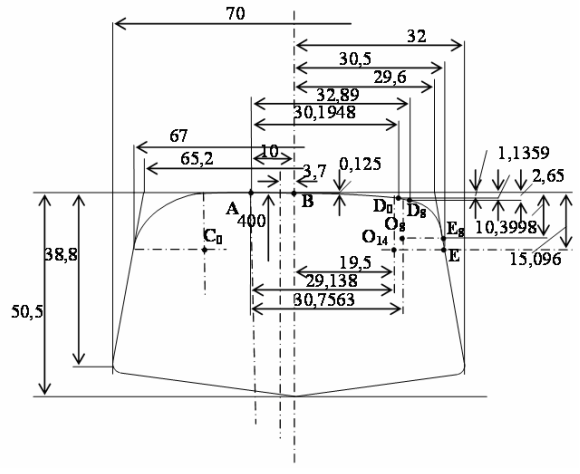

Fig. 3. Nonlinear rail profiles.

The difference between the linearized model and a full nonlinear model is very small for actively steered vehicles. A nonlinear model is essential for simulating passive vehicles on tight curves where flange contact is likely to occur. The nonlinear model is developed based on the well-known contact theory of Hertz and nonlinear creep theory of Kalker [2]. Also nonlinear wheel and rail profiles shown in Fig. 2 and Fig. 3 (wheel profiles – BDZ 2; rail profiles - operationexploitation) are used in the model, which is a standard pair of profiles used by the railway industry.

In the simulation, both deterministic track input is used for low-speed curves (vehicle speed 30 m/s), where the curvature radius is 300 m and having transition sections at both ends with a 1-s duration. The random track input represents the roughness of a typical high-speed main line. Nevertheless, real track data measured from a railway line between in NITIJT – Sofia, Bulgaria are also used in the simulation in addition to the generic track input.

Fig. 4 and Fig. 5 shows the diagrams of the simulation model used in the study for co-ordinates y_{aj}/y_{ij} (a – attacking wheel; j - number of wheelsets) in function of distance "wheelsets-rail" (σ) and radius r_{aj}/r_{ij} in function of co-ordinates y_{aj}/y_{ij}.

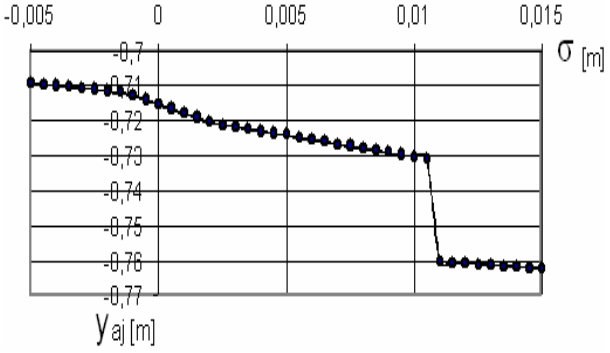

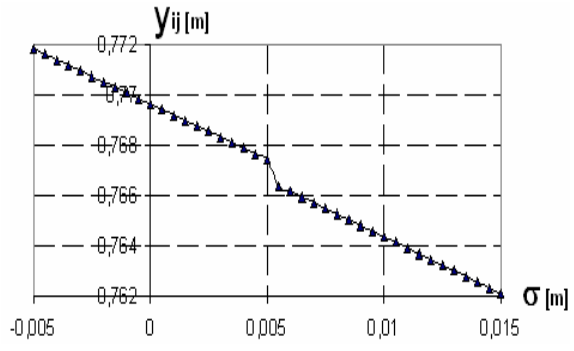

Fig. 4. The diagrams of the simulation model for co-ordinates yaj/yij in function of distance "wheelsets-rail".

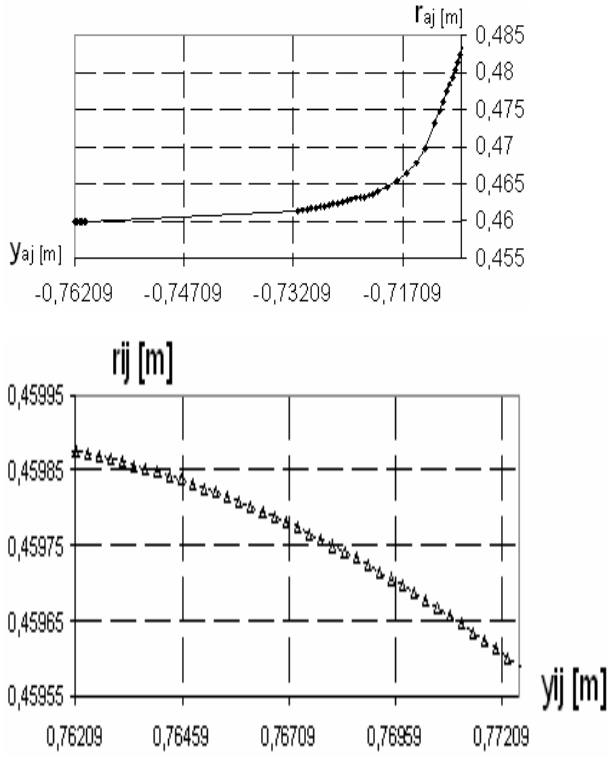

Fig. 5. The diagrams of the simulation model for radius r_{aj}/r_{ij} in function of co-ordinates y_{aj}/y_{ij}.

On the deterministic track, the active control scheme gives much improved curving performance when compared with the passive vehicle and shows a typical result. However a good guidance action is required such that the wheelsets follow the track and flange contact is avoided. At lower speed when railway vehicles negotiate tighter curves, the advantage of the active control is even more obvious as indicated in Fig. 6 where the vehicle speed is 30 m/s and the curve radius is 250 m.

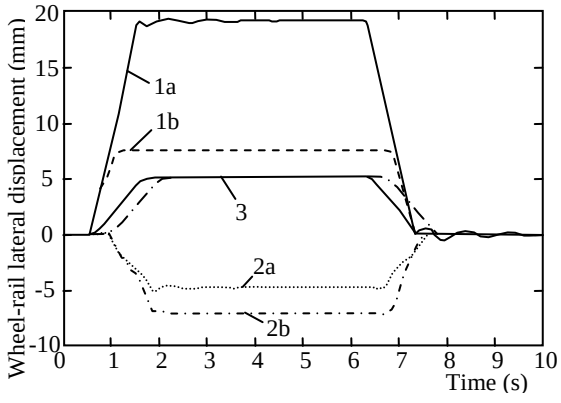

Fig. 6. Wheelset lateral displacement on a curved track (V_s = 30 m/s).
1a- Passive: front (linear); 1b – Passive: front (non-linear); 2a- Passive: rear (linear); 1b- Passive: rear (non-linear); 3- Active: both IRWs.

In this case the large wheel-rail displacement for the passive vehicle from the linearized model would in practice cause flange contact, which is best illustrated using the full nonlinear model as shown in the dotted lines. The hard flange contact for the two wheelsets of the passive vehicle would result in increased creep force and cause damage to both the wheels and the track.

Fig. 7 show the angles of attack for the two wheelsets for the two curves, and further illustrate the good curving performance achieved by the active control. The actively controlled wheelsets have the same angle of attack on the steady curve. By contrast, for the passive vehicle on the low speed curve (Fig. 7), the larger axle rotations mean that irregular angles of attack occur on the curve transitions, whereas they are much more orderly with active control.

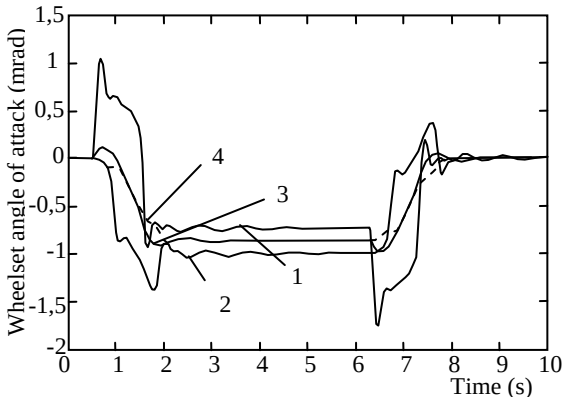

Fig. 7. Wheelset angle of attack on a curved track (V_s = 30 m/s).
1- Passive: front; 2 – Passive: rear; 3- Active: front; 4- Active: rear.

One of the critical design aims is that the controller must be robust against the structured uncertainties such as unmodeled actuator dynamics, parameter variations at the wheel-rail interface and nonlinearities of the vehicle dynamics. In this study, a nonlinear model of a hydraulic actuator is used in the computer simulation to assess the performance of the controller. For the parameter variations, a known worst case (the creep coefficient from 10MN to 5MN [7, 8]) is used. The full nonlinear model is also used to assess the control robustness. Fig. 8 shows the lateral displacements of the leading wheelset on a curved track at the vehicle speed of 30 m/s. When the actuator dynamics are considered in the simulation, the wheelset response is delayed and less damped. When the worst parameter variations are also included, the wheelset response shows a relatively large peak on the curve transitions and settles down to its quasistatic level on the constant curve. The delay and reduced damping is much less severe for lower vehicle speed. In addition, the robust controller is able to reduce significantly the effect of the nonlinearity of the vehicle dynamics.

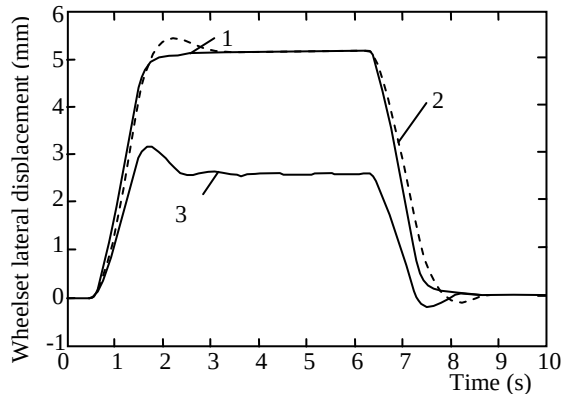

Fig. 8. Robustness analysis (V_s = 30 m/s).
1- No actuator dynamics; 2 – With actuator dynamics; 3- With actuator dynamics & parameter variations.

The combination of independently rotating wheelset and active control reduces significantly the longitudinal creep forces at the wheel/rail contact point(s). On pure curves there is no steady-state creepage for the independently rotating wheelset and the peak creep force on curve transitions is only in the order of tens of Newtons, whereas for the passive vehicle the steady-state creep force on constant curves can be as high as 125 kN. Even for the random track inputs, the creep force of the actively controlled IRW is several times smaller than the passively stabilized solid-axle wheelset.

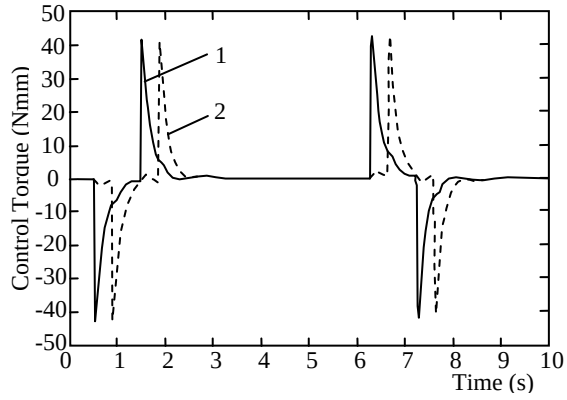

Fig. 9. Control effort on a curved track (V_s = 30 m/s).
1- On front wheelset; 2 – On rear wheelset.

The control torque required to steer the independently rotating wheelset on pure curved track is very small. Fig. 9 shows the actuator torques on a pure curved track at the vehicle speed of 30 m/s. Even for this tight curve where larger steering action is necessary, the maximum control torque on transition curves is 42 Nm and no steady-state torque is required on the constant curve. However much larger control effort is needed for the wheelsets to respond to the random track input effectively. This is particularly true for high-speed applications as the effect of the track roughness becomes worse when the vehicle travels faster. The r_{ms} value for each actuator is 1,35 kNm at top vehicle speed, which will decide the actuator size. It should be noted that the overall power requirement of the actuators is fairly low (in the order of tens of Watts per wheelset), because the actuator velocity is only 36mrad/s at the top speed.

One of the original objectives of the control design is that the active control scheme should also improve the ride quality on the vehicle body (at least it should not deteriorate the passenger comfort). The active control improves the ride quality significantly when compared with the passive vehicle, principally because the kinematics modes of the wheelsets are better controlled and body modes are less affected. The overall ride quality improvement on the vehicle body is 27,5%, with 31% at the front, 24% at the centre and 25% at the rear end of the vehicle.

However the study has shown that a significantly increased control torque will be required which can be disproportionate to the benefit gained on the ride quality.

4. CONCLUSION

This paper studies active steering of independently rotating wheelsets on a railway vehicle.

The control design has been formulated to tackle effectively parameter variations and unmodeled dynamics and the -synthesis technique has been used to examine and guarantee the robustness of the closed loop. The robustness achieved has been demonstrated in the computer simulation.

It has been demonstrated that with the active control scheme excellent curving and track following of the railway vehicle with independently rotating wheelsets are achieved. The wheel-rail lateral displacements are very small and well within the normal requirement for both curved track and random track inputs, even though these variables are not measured. The longitudinal creepage is significantly reduced due to the combination of the independently rotating wheelset and the effective active control. Simulation results have also indicated that the ride quality on the vehicle body is also improved by 25–30%, compared with the passive vehicle.

REFERENCES

[1] Atmadzhova, D. “A model in the studies active steering rotation wheelsets”, VI Triennial International Conference HEAVY MACHINERY HM 2008 MF Kraljevo, 2008

[2] Atmadzhova, D. “The theories Kalker for study of interaction of a wheel and rail”, XV SCIENTIFIC CONFERENCE "TRANSPORT 2005" University of Transport, Sofia, 2005

[3] Mei T. X., R. M. Goodall, and H. Li, “Kalman Filter for the State Estimation of a 2-Axle Railway Vehicle,” in *Proc. 5th Europ. Contr. Conf.*, Karlsruhe, Germany, 1999, CA-10-F812.

[4] Mei, T. X., T. H. Foo, and R. M. Goodall, “Genetic Algorithms for Optimising Active Controls in Railway

Vehicles," in *Proc. Inst. Elect. Eng Colloq.*, London, U.K., 1998.

[5] Mei, T. X. and R. M. Goodall, "Wheelset Control Strategies for a 2-Axle Railway Vehicle," in *Proc. 16th IAVSD Symp.: Dyn. Vehicles Roads Tracks*, Pretoria, South Africa, 1999

[6] Šoškić, Z., D. Petrović, N. Bogojević and R. Rakanović, **"**Suggestions for development of sensors for measurement of forces at wheel-rail contact". XV SCIENTIFIC CONFERENCE "TRANSPORT 2005" University of Transport, Sofia, 2005

[7] Wickens, A. H. "Dynamic stability of articulated and steered railway vehicles guided by lateral displacement feedback," in *Proc. 13th IAVSD Symp.*, Chengdu, China, 1993

[8] Wickens, A. H. "The dynamics of railway vehicles—from Stephenson to Carter," *IMechE Proc. (Part F)*, vol. 212, 1998

COMPUTER ALGORITHM FOR DETERMINING INFLUENCE OF TRACTION CURRENT ON COEFFICIENT OF FRICTION AND CREEP FORCE FOR THE ELECTROTRACTION VEHICLE OF "SERBIAN RAILWAY"

B. Gavrilovic, R. Vasiljevic, Z. Andjic

Abstract: *Measured creep force curves often decrease at high creepages. This phenomenon cannot be explained with common theories of rolling contact that are based on laws with a constant coefficient of friction. Due to sliding friction, one gets high contact temperatures. If the coefficient of friction is assumed to be decreasing at high temperatures, the calculated creep force curves agree well with measurements. In this paper, computer algorithm for determining temperature, coefficient of friction and creep force for wheel-rail contact evinced at the heating of the electrotraction vehicle of „Serbian Railway". The proposed computer algorithm will be able to be important for the calculating of the creep force after the start of traction vehicle because the high values of traction current and teperature at contact area.*

Keywords: *traction current, coefficient of friction, creep force.*

1. INTRODUCTION

The calculation of wheel-rail contact forces has always been important because of analysis of dinamic behaviour of rail vehicles, their running qualities and forces and stresses acting on the track. In a computer simulation, the computation of wheel- rail forces is repeated many times. Therefore a short calculation time is very important. The exact theory by Kalker (computer programme CONTACT (Kalker, 1990) is not possible to use in the simulations because of its very long calculation time. The simplified theory used in Kalker's programme FASTSIM (Kalker, 1982) is much faster than the exact theory, but the calculation time is also often too long for use in complicated multibody systems.

The analytical solution for the simplified model of line contact was found by Carter already in 1926 (Carter, 1926). Based on his work, Vermeulen and Johnson approximated the solution for point contacts with an elliptical area of contact (Vermeulen and Johnson, 1964). Shen, Hedrick and Elkins used the linear theory of Kalker to improve the accuracy of the solution of Vermeulen and Johnson. Their creep force law is fast and efficient while the results agree well with CONTACT and FASTIM computations (Kalker, 1990). Measured creep force curves often decrease at high creepages and the initial slope is much lower than in calculations (cf. Fig. Ia). For creep force calculations, the coefficient of friction is usually assumed to be constant and independent on operating conditions. With this assumption, the decrease of creep force curves cannot be explained. It is well-known that one gets high contact temperatures due to sliding friction (Ertz and Knothe, 2002). In this work, a temperature-dependent coefficient of friction at the electro-heating will be introduced into usual creep force models. With this extension, the calculated creep force curves agree well with measurements at high creepages.

In this paper we were insisted on the impact of traction current at temperature and creep force on wheel-rail contact after the start of trains because high amounts of traction current. However, the impact of traction current at temperature and creep force on wheel-rail contact is resident. Because we suggest the model and computer programme which can determinate impact of traction current at temperature and creep force on wheel-rail contact in each running regimes of the electrotraction vehicles.

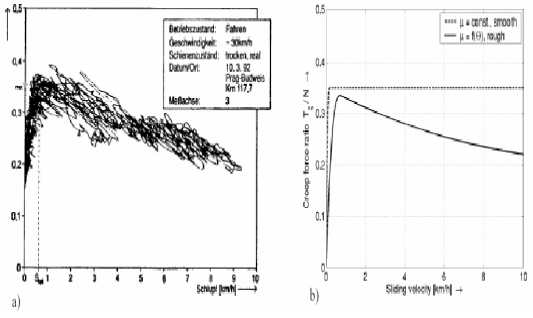

Fig. I. Measured creep force curve (a), calculation (b)

Branislav Gavrilovic, Railway College in Belgrade, brane23@sbb.co.yu,
Rade Vasiljevic, Scientific Researching Center, Uzice, nicue@verat.net,
Zoran Andjic, Scientific Researching Center, Uzice, nicue@verat.net,

2. ELECTRIC HEATING ON THE ABUTMENT OF THE MONOBLOCK WHEEL AND THE RAILWAY TRACK.

Each electric heating originates in the Joule's law. By this law, the generated thermal power in whichever segment of the monoblock wheel is equiavalent to the committed electric power (Gavrilovic and Popovic, 2006):

$$\frac{dQ}{dt} = \frac{dP}{dV} = \rho \cdot J^2 \qquad (1)$$

Where:

J - current density through the observed segment of the monoblock wheel $(\frac{A}{m^2})$;

ρ - specific resistance of steel for the monoblock wheel $(\Omega \cdot m)$.

Effectual value of current through observed segment of the monoblock wheel (I) is:

$$I = \int_{U_{Hertz}} J \cdot dS \qquad (2)$$

Where: U_{Hertz} – Hertz's contact area.

If effectual value of current through observed segment is constant:

$$\theta = \theta_0 + \frac{\left(\frac{I}{2 \cdot k_{ski} \cdot b \cdot \int_{-b}^{b} \sqrt{1 - \frac{x^2}{a^2}} \cdot dx}\right)^2}{c \cdot \rho_m \cdot} \cdot \eta_{th} \cdot \rho \cdot t \qquad (3)$$

Where:

θ -utter temperature heating of the monoblock wheel,

θ_0 - inchoate temperature heating of the monoblock,

k_{ski}- updated factor because decrement Hertz's contact area by skin effect,

a and b - the longitudinal and transversely semiaxis of Hertz's contact area,

η_{th} - coefficient of thermal operation,

t - heating period,

c - specific warmth of the monoblock wheel,

ρ_m - specific density of the monoblock wheel.

The average contact temperature from equvation (3) determinates the impact of traction current at temperature on the abutment of the wheel and the railway track in each running regimes of electrotraction vehicles. The highest values of traction current and average contact temperature has got after the start of the electrotraction vehicles and the trains (Gavrilovic and Popovic, 2006).

In made analysis we assume that the abutment of the wheel and the railway track is at ambient temperature before entering the area of contact. But after heating period (t) at constant operating conditions, the wheel temperature increases due to the continuous frictional heating.

3. TEMPERATURE - DEPENDENT COEFFICIENT OF FRICTION

The coefficient of friction is the most important parameter for the calculation of creep forces. We expect that the contact temperature should have a significant influence on the coefficient of friction According to Bowden and Tabor, friction is a process of continuous destruction and regeneration of microscopic contacts on the roughness peaks (asperities) (Bowden and Tabor, 1954). This process depends mainly on the strength of the material. We assume that the temperature-dependence of the coefficient of friction is similar to that of the yield strength of steel (cf. Fig. IIb). This assumption has been used first by Rick for the investigation of wheel/rail contact (Rick, 1998).

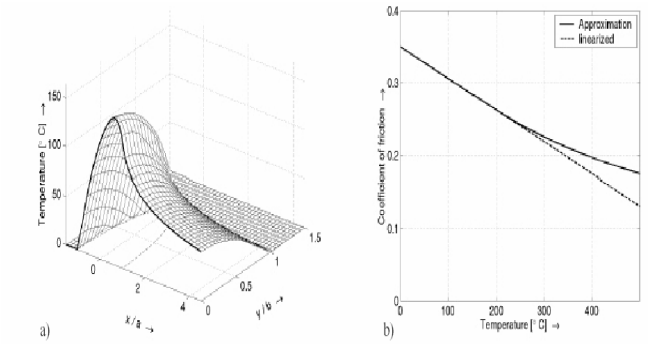

Fig. II Surface temperature for elliptical area of contact (a), temperature-dependent coefficient of friction (b)

4. CREEP FORCE LAW FOR FOR WHEEL - RAIL CONTACT

Models and computer programme which can serve for determinating of indirect impact of traction current at creep force are the algorithm FASTIM and ADAMS/Rail (N.N.,1998). The algorithm ADAMS/Rail has been used in the simulations in different programmes since 1990. This algorithm is used as an alternative parallel to programme FASTSIM. However, because of the short calculation time we shall employ the algorithm ADAMS/Rail instead Kalker's programme FASTSIM. Besides, algorithm ADAMS/Rail has been used in different simulation of dinamic behaviour of rail vehicles with very good experience.

In this model the coefficient of friction f is asusmed constant in the whole contact area. In view of the this surmise let us consider theoretical background of the algorithm ADAMS/Rail.

4.1 Theoretical background of the algorithm ADAMS/Rail

The proposed method assumes the ellipsoidal contac area with semiaxis **a**, **b** and normal stress ditribution according to Hertz. The maximum value of tangential stress τ at any arbitrary point is (Ertz and Knothe 2002):

$$\tau = f \cdot \sigma \qquad (4)$$

where: f – coefficient of friction, σ - normal stress.

The solution assumes a linear growth of the relative displacement between the bodies from the leading point (A) to the trailing point (C) on the edge of the contact area (Fig. III). At first the contact surfaces of the bodies stick firmly together and the displacement of the bodies is the result of the material creepage (area of adhesion). The tangential stress τ acts against the creep and its value grows linearly with the distance from the leading edge (the assumption is identical with Kalker's simplified theory). If τ in the adhesion area reaches its maximum value according to (4) a relative motion of the contact surfaces appears. This part of contact area is called the area of slip. The tangential stress acts against the slip according to (4).

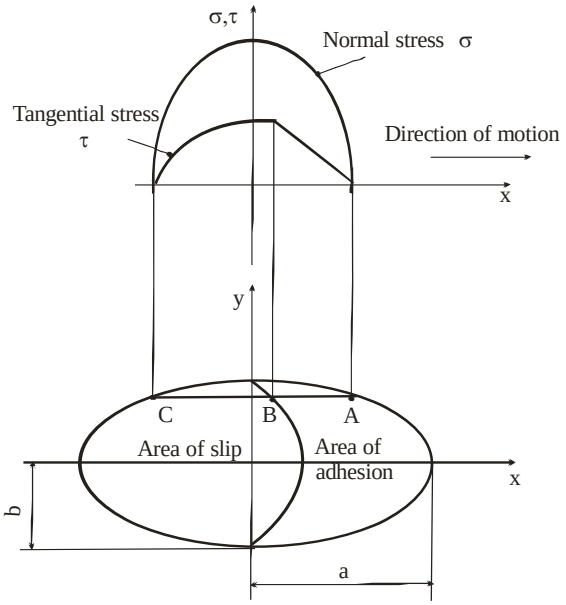

Fig. III Assumptiom of distribution of normal and tangential stresses in the wheel-rail contact area

The tangential force is determined as:

$$F = \iint_{U_{Hertz}} \tau \cdot dx \cdot dy \tag{5}$$

For vectors in x and y directions we get:

$$F_i = F \cdot \frac{s_i}{s} \qquad i = x, y \tag{6}$$

where:

$$s = \sqrt{s_x^2 + s_y^2} \tag{7}$$

s_x, s_y – slip in *x* and *y* directions.

Freibauer (Freibauer, 1983) has solved the creep-force law without spin using a transformation of the tangential stress distribution ellipsoid to a hemisphere with the formulae:

$$y^* = \frac{a}{b} \cdot y\,, \quad \tau^* = \frac{a}{\tau_0} \cdot \tau \tag{8}$$

where: y^* and τ^* - transformed variables: *y* and τ, τ_0 - the maximum stress in the centre of the contact area.

The tangential stress is proportional to slip s and the distance from the leading edge (Fig. III) with proportionality constant C, which is value characterising the contact elasticity of the bodies (tangential contact stiffness). The gradient of tagential stress in the area of adhesion is:

$$\varepsilon = \frac{2}{3} \cdot \frac{C \cdot \pi \cdot a^2 \cdot b}{Q \cdot f} \cdot s \tag{9}$$

where: Q – wheel load.

The tangential force is then:

$$F = \tau_0 \cdot \frac{b}{a^2} \cdot \iint_{U_{Hertz}} \tau^* \cdot dx \cdot dy^* = -\tau_0 \cdot \frac{b}{a^2} \cdot \frac{4}{3} \cdot a^3 \cdot \left(\frac{\varepsilon}{1+\varepsilon^2} + arctg(\varepsilon) \right)$$

According to the theory of Hertz:

$$\tau_0 = \sigma_0 \cdot f = \frac{3}{2} \cdot \frac{Q \cdot f}{\pi \cdot a \cdot b} \tag{10}$$

where: σ_0 – maximal normal stress in the contact area.

After substitution into last equation for the tangential forcewe obtain:

$$F = -\frac{2 \cdot Q \cdot f}{\pi} \cdot \left(\frac{\varepsilon}{1+\varepsilon^2} + arctg(\varepsilon) \right) \tag{11}$$

The vector forces F_x and F_y are calculated from (11) using formulae (6).

When solving the wheel-rail contact problem, the spin is of a considerable importance. Spin is a rotation about the vertical axis z.caused by wheel conicity. Further under the title spin we will understand the relative spin ψ which means the angular velocity about z-axis divided by speed v.

The spin is:

$$\psi = \frac{\omega \cdot \sin\gamma}{v} = \frac{\sin\gamma}{r} \tag{12}$$

where: ω– angular velocity of wheel rolling, γ – angle of contact surfaces and r – wheel radius.

In the following part a force effect of the spin wiil be mentioned. The moment effect of spin as well as the moment effect caused by lateral slip are neglected because they are too small in comparison with other moments acting on the traction vehicle.

At a pure spin the vector force F_x is zero. The centre of rotation is situated on the longitudinal axis of the contact area, but its position depends on the equilibrium of the forces and is unknown at the beginning of the solution. If the longitudinal semiaxis is too small ($a \to 0$), the centre of spin rotation is approaching the origin of the coordinate system.

Using the transformation of the tangential stress distribution ellipsoid to a hemisphere, the lateral tangential force caused by pure spin was found as:

$$F_y = -\frac{9}{16} \cdot Q \cdot f \cdot K_M \tag{13}$$

where K_M is :

$$K_M = |\varepsilon| \cdot \left(\frac{\delta^3}{3} - \frac{\delta^2}{2} + \frac{1}{6} \right) - \frac{1}{3} \cdot \sqrt{\left(1 - \delta^2\right)^3} \tag{14}$$

$$\delta = \frac{\varepsilon^2 - 1}{\varepsilon^2 + 1} \tag{15}$$

and creep **s** in equation (9) is given as $\psi \cdot a$. However this solution is valid only for $a \to 0$.

The detailed solution for different relations $\frac{a}{b}$ given by Kalker (Kalker, 1967) showed that with an increasing relation $\frac{a}{b}$ the force effect of the spin grows. Looking for a fast solution to be used in simulations, a correction of dependence (13) for $a >$ 1 was found. The forces caused by longitudinal and lateral creepages and the lateral force caused by spin are calculated seperately. In the equations (6), (7) and (9) instead of the slip **s** there is resulting slip s_c:

$$s_c = \sqrt{s_x^2 + s_{yc}^2} \tag{16}$$

where: $s_{yc} = s_y + \psi \cdot a$ for $\left| s_y + \psi \cdot a \right| > \left| s_y \right|$

$s_{yc} = s_y$ for $\left| s_y + \psi \cdot a \right| \le \left| s_y \right|$ (17)

The resulting force effect in lateral direction is given as the sum of both above described effects respecting the creep saturation as follows:

$$F_{yc} = F_y + F_{ys} \tag{18}$$

where: F_{ys} - increase of the tangential force caused by the spin.
Its value is:

$$F_{ys} = -\frac{9}{16} \cdot a \cdot Q \cdot f \cdot K_M \cdot \left[1 + 6{,}3 \cdot \left(1 - e^{-\frac{a}{b}} \right) \right] \cdot \frac{\psi}{s_c} \tag{19}$$

Where: K_M is obtained by (14) and ε is actually given as:

$$\varepsilon = \frac{2}{3} \cdot \frac{C \cdot \pi \cdot a^2 \cdot b}{Q \cdot f} \cdot \frac{s_{yc}}{1 + 6{,}3 \cdot \left(1 - e^{-\frac{a}{b}} \right)} \tag{20}$$

The contact stiffness C in (9) and (20) can be found by experiments or can by obtained from Kalker's constants (Kalker, 1967).

4.2 Use of the proposed method with the constants from Kalker

The value of the tangential contact stiffness C is derived by assuming an identical linear part of the creep force law according to Kalker theory and proposed method. According to the proposed theory, if the creep is close to 0 ($\varepsilon \to 0$), without spin

$$F = -\frac{8}{3} \cdot a^2 \cdot b \cdot C \cdot s \tag{21}$$

and according to Kalker:

$$F = -G \cdot a \cdot b \cdot c_{jj} \cdot s \tag{22}$$

where:: c_{jj} - Kalker's constants (c_{11} - for longitudinal direction, c_{22} - for lateral direction),

After the comparison of (21) with (22) we get:

$$C = \frac{3}{8} \cdot \frac{G}{a} \cdot c_{jj} \tag{23}$$

After the substitution of (23) in (9), the gradient **ε** of tangential stress is:

$$\varepsilon = \frac{1}{4} \cdot \frac{G \cdot \pi \cdot a \cdot b \cdot c_{jj}}{Q \cdot f} \cdot s \tag{24}$$

Because $c_{11} \neq c_{22}$, constant c_{jj} will be obtained as follows:

$$c_{jj} = \sqrt{\left(c_{11} \cdot \frac{s_x}{s} \right)^2 + \left(c_{22} \cdot \frac{s_y}{s} \right)^2} \tag{25}$$

The lateral force caused by the spin (13) is for $\varepsilon \to 0$ according to the proposed theory:

$$F_y = -\frac{1}{4} \pi \cdot a^3 \cdot b \cdot C_s \cdot \psi \tag{26}$$

and according to Kalker's theory:

$$F_y = -G \cdot c_{23} \cdot \psi \cdot \sqrt{(a \cdot b)^3} \tag{27}$$

With comperion (26) and (27) we get:

$$C_s = \frac{4}{\pi} \cdot \frac{G \cdot \sqrt{b}}{\sqrt{a^3}} \cdot c_{23} \tag{28}$$

After the substitution of (28) in (20) the gradient of tangential stress ε_s used for calculation of spin influence is:

$$\varepsilon_s = \frac{8}{3}\cdot\frac{G\cdot b\cdot\sqrt{a\cdot b}}{Q\cdot f}\cdot\frac{c_{23}\cdot s_{yc}}{1+6{,}3\cdot\left(1-e^{-\frac{a}{b}}\right)} \qquad (29)$$

4.3. Examples of results of the proposed method

Used variables for computer cod of the proposed method is:

F_x – longitudinal force in wheel-rail contact,
F_y – lateral force in wheel-rail contact,
s_x – longitudinal creep,
s_y – lateral creep,
ψ – spin,
Q – wheel load,
f – coefficient of friction ,
a – semiaxis of the contact ellipse (in longitudinal direction),
b – semiaxis of the contact ellipse (in lateral direction),
G – modulus of rigidity,
c_{11} – Kalker's constant,
c_{22} – Kalker's constant,
c_{23} – Kalker's constant c_{23}.

Based on the proposed computer code for constant coefficient of friction f= 0,3 modulus of rigidity $G = 8.4\cdot10^{10}\ \mathrm{Nm}^{-2}$ and wheel load $Q = 1\cdot10^{5}$ N ,we got Table 1, 2 and 3.

Table 1: $a = 6\cdot10^{-3}$ m , $b = 6\cdot10^{-3}$ m , c_{11}= *4.12*, c_{22}= *3.67*, c_{23}= *1.47:*

s_x= *0.004* s_y= *0* ψ= *0 m^{-1}* F_x= *- 26 732N* F_y= *0 N*	s_x= *0* s_y= *0.004* ψ= *0 m^{-1}* F_x= *0 N* F_y= *-25 872 N*	s_x= *0* s_y= *0* ψ= *0.004 m^{1}* F_x= *0 N* F_y= *-107 N*
s_x= *0.002* s_y= *0.002* ψ= *0.002 m^{-1}* F_x= *-16 362 N* F_y= *-16 398 N*	s_x= *0.004* s_y= *0.006* ψ= *0 m^{-1}* F_x= *-16 098 N* F_y= *- 24 147*	s_x= *0.00005* s_y= *0.004* ψ= *0.008 m^{-1}* F_x= *- 321 N* F_y= *- 25 834*
s_x= *- 0.00005* s_y= *0.004* ψ= *0.008 m^{-1}* F_x= *321 N* F_y= *- 25 834N*	s_x= *- 0.00005* s_y= *- 0.004* ψ= *0.8 m^{-1}* F_x= *323 N* F_y= *8 259 N*	s_x= *0.00005* s_y= *- 0.004* ψ= *- 0.008 m^{-1}* F_x= *- 321 N* F_y= *25 834 N*

Table 2: $a = 7.5\cdot10^{-3}$ m , $b = 1.5\cdot10^{-3}$ m , c_{11}= *7.78*, c_{22}= *8.14*, c_{23}= *6.63:*

s_x= *0.002* s_y= *0.002* ψ= *0 m^{-1}* F_x= *- 12 606N* F_y= *- 12 606N*	s_x= *0* s_y= *0.002* ψ= *0.002 m^{-1}* F_x= *0 N* F_y= *- 13 954N*	s_x= *0.002* s_y= *0* ψ= *0.002 m^{-1}* F_x= *- 13 421N* F_y= *- 0.3 N*

Table 3: $\mathbf{a} = 1.5\cdot10^{-3}$ m , $\mathbf{b} = 7.5\cdot10^{-3}$ m , $\mathbf{c_{11}}$=*3.37*, $\mathbf{c_{22}}$=*2.63*, $\mathbf{c_{23}}$ = *0.603:*

s_x= *0.002* s_y= *0.002* ψ= *0 m^{-1}* F_x= *- 5 549 N* F_y= *- 5 549 N*	s_x= *0* s_y= *0.002* ψ= *0.002 m^{-1}* F_x= *0 N* F_y= *- 4 419 N*	s_x= *0.002* s_y= *0* ψ= *0.002 m^{-1}* F_x= *- 6 254 N* F_y= *- 0 N*

4.4. Modeling influence of traction current on creep force

Alredy we accentuated ourselves that the average contact temperature from equvation (3) determinates the impact of traction current at temperature on the abutment of the wheel and the railway track in each running regimes of electrotraction vehicles. Besides, the highest values of average contact temperature has got after the start of the electrotraction vehicles because the highest values of the traction current (Gavrilovic and Popovic 2006). Based on research in »Serbien Railway«, the values of average contact temperature amount the few hundred ^{0}C after the start of the electrotraction vehicles (Gavrilovic and Popovic 2006).

According to Rick (Rick,1998) we may approximate the coefficient of friction to a polynomial of arbitrarily high order :

$$f(\theta) = f_0 + a_0\cdot\theta + a_1\cdot\theta^2 + \ldots + a_n\cdot\theta^n \qquad (30)$$

Based on this surmise and eguations (6), (11) and (19), influence of the traction current across the contact temperature on creep force described with the next equations:

$$F_X = -\frac{2\cdot Q}{\pi}\cdot\left(\frac{\varepsilon}{1+\varepsilon^2}+arctg(\varepsilon)\right)\frac{s_X}{s}\cdot f(\theta) \qquad (31)$$

$$F_y = F_y(\theta) = -\frac{9}{16}\cdot a\cdot Q\cdot K_M\cdot\left[1+6{,}3\cdot\left(1-e^{-\frac{a}{b}}\right)\right]\cdot\frac{\psi}{s_c}\cdot f(\theta)$$

According to equations (3) and (30) we calculated local temperature and local coefficient of friction for values of traction curren of about 50A and lesser time t= 10 ms. This solution is shown at Fig. IV.

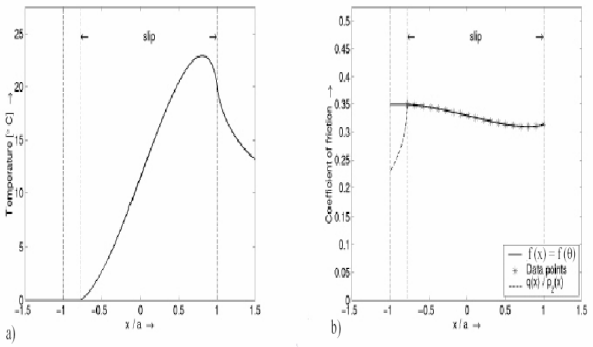

Fig. IV: Local temperature (a) and local coefficient of friction (b) (Traction current is about 50A)

If we use variables,

$$f_x = \frac{F_x}{Q \cdot f} \tag{32}$$

$$f_y = \frac{F_y}{Q \cdot f} \tag{33}$$

$$\upsilon_x = \frac{G \cdot a \cdot b \cdot c_{11} \cdot s_x}{Q \cdot f} \tag{34}$$

$$\upsilon_y = \frac{G \cdot a \cdot b \cdot c_{22} \cdot s_y}{Q \cdot f} \tag{35}$$

the tangential forces caused by longitudinal and lateral creepages for $f = 0{,}2$ and $v = 5m/s$ are sown at Fig. V. This solution is compared with adequancy solution of FASTIM (Kalker, 1990). and shown at Fig. V.

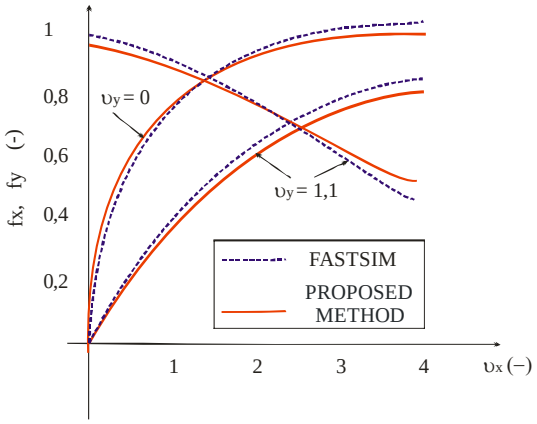

Fig V Tangential forces caused by longitudinal and lateral creepages for $f = 0{,}2$ and $v = 5m/s$

Based on the fig. V we shall be able to conclude that the results of presented model for tangential forces caused by longitudinal and lateral creepages for constant temperature-dependent coefficient of friction on wheel/rail contact $\boldsymbol{f}$ are nearly equal results of Kalker's programme FASTSIM (Kalker, 1982).

5. CONCLUSIONS

The article is shown modeling influence of traction current on coefficient of friction and creep force. According to Joul's law we were described influence of the traction current on the temperature of contact area and according to Rick we were described influence of the temperature on the coefficient of of friction. Based on this approach and by the algorithm ADAMS/Rail we may calculate very quickly and precisely the influence of traction current on the creep force in each running regimes of the electrotraction vehicles.

The proposed model will be able to be important primarily for the calculating of the creep force after the start of traction vehicle because the high values of traction current and teperature at contact area.

Future research in this area should concentrate on the investigation of the collective influence of traction current and creepages on the coefficient of friction and the creep force under realistic railway operating conditions, including high contact temperature.

REFERENCES

[1] Kalker, J.J. (1990).*Three-Dimensional Elastic Bodies in Rolling Contact.* Kluwer Academic Publishers Dordrecht, Netherlands.

[2] Kalker, J.J. (1982). *A fast algorithm for the simplified theory of rolling contact.* Vehicle System Dynamics 11, pp. 1-13.

[3] Carter, F.W. (1926): *On the action of a locomotive driving wheel.* Proceedings, Royal Society .A112,p.p.151-157.

[4] Vermeulen, P.J. - Johnson, K.L. (1964). *Contact of nonspherical elastic bodies transmitting tangential forces.* Journal of Applied Mechanics 31, p.338-340.

[5] Ertz, M. - Knothe, K. (2002). *A comparison of analytical and numerical methods for the calculation of temperatures in wheel/rail contact.* Wear 253, 3-4, p.498-508.

[6] Gavrilović S. Branislav, Popović Sreten (2006). *Električno zagrejavanje monoblok točkova železničkih vučnih vozila"*, 50. Konferencija ETRAN, Beograd.

[7] Bowden, F.P. - Tabor, D. (1954). *The Friction and Lubrication of Solids*, Clarendon Press, Oxford, 2nd Ed.,

[8] Rick, F. (1998). *Zur Erfassung der Geschwindigkeitsabhängigkeit des Kraftschlußbeiwertes eines hochbelasteten Rad-Schiene-Kontaktes.* Ph.D. Thesis, TU Clausthal,

[9] N.N. (1998). *Introducting ADAMS/Rail 9.0*, ADAMS/Rail News & Views, No 1, MDI Marburg, Germany.

INNOVATION AND INNOVATION POLICY IN THE TRANSPORT SYSTEM IN BULGARIA

M. Slavova-Nocheva

Abstract: *The paper presents some economic aspects o0f the innovations, its state and development in the process of Eurointegration. It is underlined on the priority of the European innovation policy and the necessity of effective long-term innovation strategy. On this bases some problems of the transport innovation policy are discussed.*

Key words: *innovation, innovation strategy, economic priorities, transport innovation policy.*

1. INTRODUCTION

Innovations are a key to the changes in the modern society and an engine to further economic and social progress. The creation of innovations is mostly connected with the entrepreneurship in economy. In the works of J. Schumpeter. the famous economist of Austro-American origin, innovations are examined also as a change aimed at implementing new consumer goods, new productions and transport means, markets and forms of the production organization.

2. INNOVATIONS AND INNOVATION ACTIVITIES IN THE REPUBLIC OF BULGARIA

Innovations are mainly presentation of new products and services at the market or new ways of their production. They are an important source of productivity which is assigned a definite substantial part in the theory of economic growth.

In this connection it is necessary to point out that the creation of new products, services and technologies is an extremely important side in the activity, management and strategy of company's undo-contemporary conditions.

The key dimensions of the company's strategy are markets, products and technology that the company applies in different activities: strategy planning, marketing, production, implementation, personnel motivation, funding, etc. The improvement of each one can influence on the competitive position of the company.

In a certain aspect the innovation strategy of a company, respectively of a transport company is directly connected with the general company strategy. It involves the management in a certain area of the company activity: the creation, introduction and implementation of innovations at the market. It is built according to the strategy in some other functional areas: production, marketing, finances, human resources management, etc.

The main aims of an innovation strategy can be systemized as stimulation of research in industry, fostering the cooperation of scientific units, universities and companies: improvement of innovations funding; fostering the implementation of new technologies and increasing the innovation activities of the companies; creation of mechanisms to implement and finance the intended measures of the innovation strategy.

The innovation strategy of the Republic of Bulgaria is implemented by measures to stimulate the innovations and technology development, create national Innovation Fund, optimize the system "science-technologies- innovations", training entrepreneurship, introducing the European indices for assessment of the innovation potential of enterprises, attracting foreign investments in the research activity, creating centers of entrepreneurship at universities, etc.

At present the share of the innovation companies in Bulgaria is only 11.4% of the total number of acting enterprises and is 4 times less than the share in the European Union.

The share of the enterprises accomplishing research and working in the field of information technologies, architecture and engineering sciences is 30.1% of the total number of innovative enterprises, which is 3,43% of the total number of enterprises. That proves the necessity of an active policy to stimulate the development of RTD units that should stimulate new products and technologies for industry.

The state policy in this area should be directed to stimulate the education of future entrepreneurs, increasing the quality of the company strategies and the

Maria Slavova-Nocheva, Assoc. Prof., Ph.D, Higher School of Transport, Sofia, Bulgaria, mslavovanocheva@abv.bg

potential of enterprises in using modern technologies and up-to-date information.

By the cost of innovation products at the market and those that are new for the enterprise. Bulgaria is lagging behind the European indices. At the same time the strategy of catching-up economic development of Bulgaria cannot be accomplished without achieving an innovation type of growth.

According to the *Global Completeness Report*, by national competitiveness Bulgaria occupies the 59lh place among 104 countries that have been surveyed on: by index of macroeconomic medium - 60lh : by technology index - 59lK; by index of public institutions - 56lh; by quality of national business environment - 72nd: by index of business competitiveness - 75,h. The country is still behind the other EU member states.

A number of empiric studies have also stated the low- innovation activity of the Bulgarian enterprises. By the value of the summary innovation index (SII) in 2006 Bulgaria again is among the countries lagging behind after it was included in the group of catching-up countries for the first time in 2004.

The reasons for the extremely low innovation activity of the Bulgarian economy are multi-aspect ones. In the transition period in the country there ware no purposeful innovation policy and innovation strategy. It was only in 2004 when the Innovation Strategy of the Republic of Bulgaria and the measures for its implementation were adopted. During the years of transition the national innovation potential was continuously decreasing. The state put aside less and less money for funding the RTD activities. In 1980s the RTD costs reached to 2.5% of the GDP and were comparable with those in the developed countries. However, for the recent years they have been sharply decreasing reaching only 0.5%.

The relative share of investments in the GDP reached nearly to 20% but it is still insufficient to implement the technology restructuring of economy that will provide sustainable economic growth. Despite that for the past few years the amount of the direct foreign investments has been increased, they are considerably smaller than in Czech Republic. Poland, Hungary. The reason is in the lack of favorable entrepreneurship environment: legislative base, tax system, public administration, economic infrastructure, developed capital market, entrepreneurship knowledge.

The macroeconomic environment in Bulgaria does not stimulate innovations: the tax. depreciation, financial and credit, custom policies do not help innovation activities. The domestic demand is not a stimulus for investments in Bulgarian enterprises as t.he share of the final consumption is near to the GDP. That hinders from increasing the real incomes and results in stagnation in the final consumption.

Innovations are a summarized notion for all activities connected with creating new knowledge and turning it into a value for users. They are basic elements in the economy based on knowledge. The EU lagging behind the USA and Japan in the innovation policy has imposed the necessity of better coordination of scientific and innovation policies of the community and member states.

The main factor to achieve that aim is to build up the European research area. In the field of research the aim set in that aspect is to spend 3% of GDP for research activities, as 2/3 of the funds should be ensured by private investments.

In the period after 2000 the EU innovation policy is connected, to a great extent, with the European research area. The integration in research activity and innovations will contribute to establishing knowledge economy and society formulated in the Lisbon strategic aim.

In that connection the European Commission has determined the following 5 priority in fostering innovations according to the innovation policies: coordination of the innovation policies; legal framework for innovations; fostering the creation and development of innovative enterprises, improving the main interfaces in the innovation system; society open to innovations.

3. ASPECTS OF THE INNOVATION POLICY IN TRANSPORT

The ideas of Lisbon strategy are embedded in FP7 of the European Commission, as a result of which Europe should become the most competitive and dynamic economy based on knowledge, capable to achieve sustainable economic growth, concerning different sectors and areas.

Innovations, innovation strategies and processes have a considerable significance for transport due to the fact that it connects all economic branches and spheres of social life. The main contents of an innovation policy are mainly determined by the implementation of the scientific and technology progress that unites equipment, technology and the production process organization. To accomplish its innovation role, the scientific and technology progress in transport should optimally combine the improvement of organizational forms of passenger and freight transport and the use of new methods for performing the activities in the railway sector.

Each transport mode in our country has oriented its innovation policy mainly to renewing the technical, technological and organizational aspects of the transport production process that ensure market advantages in comparison to other modes.

For instance, the railway transport has advantages in providing mass transport, savings from energy resources costs, production of a unit of transport production, higher ecological effectiveness and maintenance of the transport process in all seasons of the year, during the day and at night, regardless of the atmospheric conditions.

The innovation processes in transport are in connection with all activities and mostly with management. In many cases the management can be examined as an innovation function that is directly connected with the market principles in transport.

To successfully carry out a more active innovative policy under market conditions, it is required to increase the professional, economic and general training, the image and prestige of transport staff, to improve the qualification of specialists working in the transport system.

All that has imposed the necessity to expand our cooperation for more effective activities in future with colleagues from other universities, including from the Serbian universities in Belgrade, Nis, Kragujevac, Faculty of Mechanical Engineering in Kraljevo, etc.

It is also important for the governmental innovation policy in transport to create favorable innovation climate and stimulate the new inventions with the help of economic regulation in order to make passenger and freight transport more competitive.

The further development of research, education and innovation in this sector is a very important problem. The ecological innovations and environment technologies contribute a lot to increasing the quality of life, growth and employment mostly in the sectors of power engineering and transport. In connection with the integration of the transport system in Bulgaria with the European one. particular efforts are made to introduce and strengthen the European standards for modern, ecological and safety transport. On the base of established competitive relations, new conditions are created to increase the quality of transport services offered as «ell as measures to stimulate the innovation activity of transport enterprises. In modern transport, saving industrial and scientific-and-technological policies on the level of EU member states have been applied.

The challenges to the railway transport in this Held have lead to restructuring of the research activity. The development of innovative products is possible only on the base of international cooperation with uniting of many research organizations. In that connection the EURNEX project, which started in 2004. with participation of 66 institutes from 19 European countries, has created a network of excellence. Its task is to intensify the cooperation with the participation of the railway operating and infrastructure companies as well as with for network of excellence the railway industry. In connection with restructuring and consolidating of the research in transport, the EC supported also the idea of the FP6 project Regional Railway Transport Research and Training (RRTC). The project coordinator was the Higher School of Transport (VTU) in Sofia, Bulgaria and the Faculty of Mechanical Engineering in Kraljevo, Serbia was a partner. The centre established by the project is aimed to unite the efforts in research for implementing innovative technology products in the transport systems in the Balkan region.

The recommendation of the European Commission for the Regional Centre RRTC was to establish contacts with the ERIJRNEX project, thus being able to join the European Research Area (ERA).

***

The innovation policy implemented in Bulgaria both in industry and transport requires to be bound with the economic, research, social, regional policies, the policy of protecting .competition and other policies on national, regional and EU levels.

REFERENCES

[1] Schumpeter, J. Capitalism, socialism, and democracy, Harper & Row, New York, 1975.

[2] Angelov, I. & others. Economy of Bulgaria and the EU. strategy of catching-up economic development to 2020. Sofia. 2003 (in Bulgarian).

[3] The Global Competitiveness Report

[4] Annual Report on the State and Development of the Policy in the Field of Innovations. 2007, http:/./ wwvv.mi.government.bg

[5] Statistics Annual, National Institute of Statistics, Sofia. 2006.

[6] Statistics Annual. National Institute of Statistics, Sofia, 2007.

[7] Atmadzhova, D., A. Dzhaleva-Chonkova, M. Georgieva. B. Bentchev, N. Nenov: "RRTC FP6 project: opportunity of regional cooperation in rail research and education on the Balkans", Proceedings of the 14th International Symposium EURNEX - Zel 2006. University of Zilina, 2006.

WAGON MANUFACTURING AND MAINTENANCE IN THE BALKANS PART 1: BULGARIA AND SERBIA

A. Dzhaleva-Chonkova

Abstract: *The paper presents a brief outline of the wagon maintenance and manufacturing development as a sub-sector of the heavy engineering industry in the Balkan region. The first part of the historical examination is dedicated to the problems of the rolling stock in Serbia and Bulgaria, which after the WW I both established national factories for wagons and, in Serbia (Yugoslavia) also for locomotives. Instead of conclusions, it is marked that, under the new conditions of integration in Europe, both producers and researchers from the two countries have started activities to exchange knowledge and experience in wagon design and testing.*

Key words: *wagon maintenance and manufacturing, Serbia, Bulgaria, cooperation.*

1. INTRODUCTION

The railway development in the Balkan countries had a lot of common features especially in Bulgaria, Northern Greece and Macedonia as parts of the Ottoman Empire. Unlike them, Serbia had to plan its railway network independently using the help of French experts and companies. It explains why the first Serbian lines appeared only a few years earlier than the Bulgarian State Railways, BDZ (1888).

It is worth mentioning that the Bulgarian politicians adopted the management of railways as a state enterprise considering the problems Serbia had faced railway building and operation by private foreign companies (until 1889). However, the public property did not solve the main difficulty with the railway development in the Balkan countries: the lack of funding. It concerned both the infrastructure and rolling stock. While the infrastructure projects were funded mainly by foreign loans, the delivery of locomotives and wagons was on the expenses of the budget, which usually was insufficient to meet the real needs. Being agrarian economies, Serbia and Bulgaria did not have national engineering industry and they imported their rolling stock for long years. In many cases the financial insufficiency limited the choice of the latest models, so the railway fleets remained much behind the average technical level in Europe and North America.

2. ROLLING STOCK IN THE SERBIAN RAILWAYS AND BDZ UNTIL WW I

At the beginning of railway operation the Bulgarian administration used different types of passenger and freight wagons. Some of them were inherited with the purchase of Rousse – Varna railway line, the most luxurious one being the tree-axle saloon "Sultanie, which now can be seen at the National Transport Museum in Rousse. All freight wagons as well as the two saloon cars for official journeys were manufactured in Belgium in 1867.

Unlike the rolling stock along Rousse – Varna line, the wagons (of both types) for the railway line from Tsaribrod (today the town of Dimitrovgrad in Serbia) – Vakarel, the first one built in the restored Bulgarian state, were bought from the Wagon Factory in Görlitz (1888), Germany. It was also where the four-axle government carriage was produced (1898).

The second delivery of rolling stock was from the factory in Nürnberg, Germany (1891), followed by a bargain with the Czech factory Ringhofen. The new passenger carriages were four: two consisting of the first and second class compartments, constructed in a way to be used for sleeping as well, and two third-class carriages. That purchase was connected with the common decision of the Hungarian, Serbian, Bulgarian and Oriental railway administrations to provide traveling without changing the carriages at the boundary stations. Due to the relatively small number of locomotives and wagons, the first workshops were for mixed repairs both locomotives and wagons. The first one was in Rousse opened with the railway line construction. It is interesting to mention that next to the workshop there was a school for the children of foreign experts and masters who were the prevailing staff.

The construction of the railway line from Tsaribrod to Vakarel imposed the necessity of another workshop, which was built eastward from the main building of Sofia station (1887-1889). Ten years later its personnel included 8 managers and 62 workers headed by the French engineer Clinker due to the lack of Bulgarian specialists. The next workshop was built in Bourgas in 1890, after the construction of the railway line connecting the town with Yambol, the end station on the deviation of Tsarugrad – Belovo line beginning from

Anna Dzhaleva-Chonkova, Ph.D., Senior Lecturer, Higher School of Transport, Bulgaria, adzhaleva@abv.bg

Tirnovo-Seimen (now the town of Simeonovgrad), completed in 1875.

Comparing the Bulgarian situation of the rolling stock and workshops with that in Serbia, it can be noticed that there are a lot of similarities. The rolling stock in Serbia was also delivered from abroad and the first workshop was built in Nis, the end station of the railway line connecting it with the capital town of Belgrade. The service included repairs of all types of railway vehicles and the staff consisted mainly of French specialists while Serbian workers had to pass a period of training when they were considered to be students.

Another example of alikeness is the fact that the most comfortable passenger carriages were rhe ones used in the famous train called Simplon Orient. They were operated by the Wagons-Lits International Company (along Belgrade – Nis – Tsaribrod line).

What the Serbian railway administration managed to achieve unlike the BDZ, was the delivery of a motorcar with a small steam engine at its head part (1903). It was 13 years later than the appearance of such vehicles in Western Europe but yet it was a success because it could run at a speed of 60 kmph. That comfortable motorcar produced by the Ganz Company in Budapest served the line from Belgrade to Mladenovets.

3. WAGGON PRODUCTION AND MAINTENANCE IN SCS AND BULGARIA BETWEEN THE WARS

Although Serbia and Bulgaria participated on the opposite sides in the First World War, their railways suffered similarly of the severe post-war crises. The rolling stock condition had deteriorated considerably. A great number of passenger and freight wagons were either damaged (even totally destroyed) or more or less worn-out. In addition, many vehicles of the BDZ remained out of the country and were confiscated as a state property of a defeated country. So, the problem which the railway operators faced was not only to repair the wagons available but also to deliver new vehicles.

That was a great difficulty especially for Bulgaria, which owed a large amount of reparations and contributions. The only possible way to get out of the situation was to assign wagon repairs to some private enterprises as the capacity of the existing workshops turned to be insufficient. That was the reason for the owners of Zdravina AD in Drianovo to reorganize its activities taking the task to repair 700 freight wagons (1924). The second contract with the BDZ was for 400 wagons (1926) and another order of 400 vehicles was negotiated a year later. At the same time the repair s of passenger carriages began as well.

The Great Depression in early 1930s affected the joint-venture company, which finally went bankrupt and was sold to the BDZ, after being renamed as State Railway Workshop for repairing passenger carriages (by the Decree from 14 April 1935). Despite of its name, in 1942 the factory produced the first 50 open freight wagons of Bulgarian make.

Besides that enterprise, the BDZ continued to use the three workshops in Rousse, Sofia and Bourgas enlarging their capacities and improving the equipment. However, the new buildings were not considered with the further implementation of new technologies, the expansion was done according to the opinion of the local experts and the need at the moment.

In 1938 the workshop in Sofia was renamed as Main Railway Workshop, which according to the statistics was the biggest industrial enterprise in Bulgaria (by number of workers, area of working premises and technical level). It produced 1/3 of the spare parts that had been imported before for the needs of vehicle repairs. No locomotives and wagons were sent for repairs abroad or private factories any more. Due to the new method of the working organization, the wagons repaired increased to 11 a day. Another change was connected with the workshop in Bourgas, which specialized in maintenance only of passenger and freight cars.

The Main Railway Workshop was damaged very much by the bombs dropped over Sofia during the Second World War. At first it continued to work but later was evacuated (machines and people) to Drianovo, Rousse, Bourgas, the station of Yana and some other big locomotive sheds.

As for the railways across the western border of Bulgaria, the situation after the First World War was even worse but the process of their restoration went faster due to the fact that the newly-created state called Serbian-Croatian-Slovenian Kingdom (SCS) was considered as a winning country. The government had the possibility to use the reparation money received for the delivery of new locomotives and wagons. Most of them were produced in Germany and Hungary and covered the necessities both of the normal-gauge and narrow-gauge lines in the country. Furthermore, the railways in SCS gradually increased the quality of their rolling stock, especially in passenger transport by operating comfortable compartment carriages. The latter were not only of German make, but also manufactured by the first Yugoslav factory in Slavonski Brod (established in 1921). In 1937 it produced the carriages for 7 motor-car trains for narrow-gauge lines with engines delivered by the Ganz Company in Budapest. The advantages of those vehicles were proved by reducing the time of traveling from Belgrade to Dubrovnik (via Sarajevo) from 24 hours to 16.30 hours.
The home production of wagons was a big step forward to meet the demands of vehicles in SCS. Besides the factory in Brod, there orkshops in Krusevac, Sarajevo, Maribor, Smederevo started to manufacture passenger carriages as well. It was a great achievement for the

country that successfully began to develop its own manufacturing industry for the railway system.

4. MANUFACTURING EXPANSION AFTER THE WORLD WAR II

The postwar period brought considerable changes in the railway industry in Bulgaria. It became able to meet not only the domestic demands, but also the orders of exporting wagons to Poland, Hungary, Romania, Greece and even in some non-European countries.

That was achieved by transforming the former workshops into big factories, each specialized in maintenance and manufacturing of a certain type of wagons. Although that in wartime the factory in Drianovo produced freight wagons, its profile was directed to passenger carriages. In fact, the first wagon of Bulgarian make for passenger transportation was produced in 1949. In the period of transition to market economy (in 1990s), for a certain time the enterprise performed only refurbishing activities but now it has the ambition to return its fame as a manufacturer.

The other three workshops (in Sofia, Rousse and Bourgas) specialized in manufacturing different freight wagons. The rolling stock maintenance was assigned to smaller workshops, such as those in Septemvri, Karlovo, Samuil, etc.

After the reorganizations during the past decade, the Bulgarian railway industry has been trying to achieve economic and marketing sustainability. Now the biggest wagon manufacturer is TRANSWAGON EAD, which has inherited the traditions of the workshop in Bourgas. The other companies within the sector are the Wagon company in Karlovo, Trakcia Co. in Samuil (a successor of the repairing factory established in 1972), which has adopted the production of a new type of open wagon, the Wagon repairing plant 99 AD in Septemvri.

In comparison to Bulgaria, the former Yugoslavia possessed higher industrial potential in railway transport producing both locomotives and wagons. However, some of the companies were wholly located or had branches out of Serbia that made the situation after the separation quite complicated.

The development of manufacturing industry for the needs of the Yugoslavian and respectively Serbian railways was based both on expansion of the old workshops such as that in Nis, MIN (Masinska Industrija Nis) and Subotica (Bratstvo) and appearance of new modern enterprises.

Among the latter, it is the factory in Kraljevo, which in a short period of time became one of the most famous manufacturers of freight wagons in the country and Europe. Opened in 1872, it has used high research potential and innovative technologies keeping world-wide contacts in the field of heavy machinery.

What is also remarkable, are the traditions in integration with science and education. The Wagon factory was a powerful stimulus for the foundation of the Faculty of Mechanical Engineering (MFK), which for more than three decades of existence has proved to be a prestigious establishment of higher education in Serbia. At the same time, the successful research activities of the teaching staff have been highly evaluated both on national and international level by participation in projects within the EC programs.

5. INSTEAD OF CONCLUSION: OPTIMISTIC EXPECTATIONS

Having summarized the main historical facts, it should be said that under the conditions of the European integration the relations between Serbia and Bulgaria have been changing for good, including in the field of railway research and industry. The policy of cooperation is to further encourage joint activities in staff training, research and manufacturing, information and expertise exchange, knowledge transfer on rolling stock testing and design.

The past few years have been characterized with a number of positive signs in establishing intensive scientific communication in the Balkans. The project RRTC “Regional Railway Transport Research and Training Centre Foundation” developed by the Higher School of Transport (VTU) in Sofia and the Faculty of Mechanical Engineering (MFK) in Kraljevo under the FP6 of the EC (2005-2007) gave lots of possibilities for expanding the professional contacts between the partners and other organizations. The teachers from the VTU got acquainted with the process of wagon testing at the Centre of Railway Vehicles while the Serbian researchers showed interest to cooperation with TRANSWAGON EAD, Bourgas. The aim of the established four-institutional relations is to facilitate the interaction between the two educational institutions, on one side, and the representatives of the railway industry in Bulgaria and Serbia, on the other side. The first successful steps have much contributed to being hopeful and optimistic.

REFERENCES

[1] Central State Historical Archive of Bulgaria, fund 157.

[2] Atmadzhova, D. & A. Dzhaleva, Chonkova. State and Perspectives of Railway Transport in Republic of Bulgaria: Production, Scientific and Educational Potential, Proceedings of the 16th International Scientific Conference TRANSPORT 2006, Sofia, 2006, (in Bulgarian).

[3] Govedarovic, N. & Z. Bundalo, 120 years of the Railway in Nis, Nis, 2004 (in Serbian).

[4] Dzhaleva-Chonkova, A. & co-authors. History of the Railways in Bulgaria, S., 1997 (in Bulgarian).

[5] History of Railways. Serbia, Voivodina, Montenegro, Kosovo, Belgrade, 1980 (in Serbian).

[6] На скретници миленјума, т. 1, 2, Београд, 2000.

[7] Railway Collection, 1896-1900 (in Bulgarian).

[8] Railway Transport in Bulgaria 1866-1983, S.,1987 (in Bulgarian).

[9] http://www.railfaneurope.net/misc/mreil.htm. Accessed on 14 May 2008.

IMPLEMENTATION OF WIMAX TECHNOLOGY IN TRAIN COACH INTERNET SUPPLY

I. Topalov, M. Georgieva

Abstract: *In this paper we propose a special application of new wireless communication standards IEEE 802.16e in the railway vehicle. The WiMax possibilities for business coach implementation and some market and technological trends are described. The evolution of WiMax technology for mobile application and train internet supply in accordance with the new standards for wireless communications technologies and the most innovative projects in this area are enumerated.*

Keywords: WIMAX, train, mobility, IEEE 802.16 standards

1. INTRODUCTION

WiMAX is acronym that stands for Worldwide Interoperability for Microwave Access and certification mark for products that pass conformity and interoperability tests for the IEEE 802.16 standards. Although the 802.16 family of standards is officially called WirelessMAN, it has been dubbed "WiMAX" (from "Worldwide Interoperability for Microwave Access") by an industry group called the WiMAX Forum. The mission of the Forum is to promote and certify compatibility and interoperability of broadband wireless products.The working group number 16, is specialized in point-to-multipoint broadband wireless access [1], [9].
WiMAX Forum is an Industry Forum that promotes and certifies products based on 802.16 and ETSI HiperMAN Standards [3],[8]. The goal is to enable worldwide deployment of affordable, ubiquitous, always-on and interoperable multi-vendor mobile broadband wireless access networks that meet the needs of business and residential end user markets. So some of the functions are set in IEEE 802.16e.

2 BASIC FEATURES

2.1. WiMAX Standard Differences

Certified mobile/portable products are based on IEEE 802.16e which is an amendment to IEEE 802.16-2004, harmonized with ETSI HiperMAN.

The Study Group led the development of Project Authorization Request (PAR) 802.16e for Combined Fixed and Mobile Operation in Licensed Bands.

A comparison between the original Fixed WiMAX standard and the WiMAX standard that can be used for fixed, mobile and portable is done. The original 802.16 standard was released in 2004 and it was only capable of providing fixed wireless data services. It used OFDM modulation and could be deployed in both TDD and FDD formats. The 802.16e standard was released in 2005 (now merged into the original 802.16 standard) was designed for fixed, mobile and portable operation. It used OFDMA modulation with TDD and optionally FDD duplex capability. (Table 1)

2.2. Area covering

The WiMAX is developed for fixed locations initially and the portable version is issued later, but it ensures longer ranges with guaranteed QoS, increasing the throughput, having interoperability with optical transmission systems and lines of sites by lower cost. Mobile network deployments provide up to 15 Mbps of capacity within a typical cell radius deployment of up to three kilometers.

Assoc. prof. Ivaylo Topalov Ph.D. T. Kableshkov Higher School of Transport, Sofia, Bulgaria, ivo_topalov@yahoo.com.
Margarita Georgieva, M.Sc. chief assis. prof., T. Kableshkov Higher School of Transport, Sofia, Bulgaria, mgeorgieva@vtu.bg

Table 1

Characteristic	Fixed WiMax	Mobile WiMax
Industry Standard	802.16-2004	802.16e-2005
Access Type	Fixed	Fixed, Portable and Mobile
Modulation	OFDM	OFDMA
Duplexing	TDD, FDD	TDD, FDD Optional
Handoffs	No	Yes
Types of Service Providers	DSL, Cable Modems and Competitive Access Providers (CAPs)	Mobile Operators, DSL, Cable Modems, Wireless and Wired ISPs
Subscriber Units	High Performance Outdoor and Indoor CPE	Low Cost Consumer Electronics CPE and Embedded Modules
Preferred Frequency Bands	2.5 GHz, 3.4-3.6 GHz 5.8 GHz	2.3-2.4 GHz, 2.5-2.7 GHz, 3.3-3.4 GHz, 3.4-3.8 GHz

2.3.802.16e-2005 Technology

The 802.16e standard essentially standardizes 2 aspects of the air interface - the physical layer (PHY) and the Media Access Control layer (MAC). This section provides an overview of the technology employed in these 2 layers in the current version of the 802.16 specification (which is strictly 802.16-2004 as amended by 802.16e-2005, but which will be referred to as 802.16e for brevity).

A key feature of 802.16 is that it is a connection oriented technology. The subscriber station (SS) cannot transmit data until it has been allocated a channel by the Base Station (BS). This allows 802.16e to provide strong support for Quality of Service (QoS). The scheduling algorithm also allows the base station to control Quality of Service by balancing the assignments among the needs of the subscriber stations.

Each system profile is unique; certification is required for each profile even though equipment may support more than one.

Beyond the regulation constraints, WiMAX needs lower bands to economically deploy networks that will provide full mobility.

2.4. Physical layer

In physical layer WiMAX uses an OFDM to guarantee a spectral efficient and resistance to multipath effects– NLOS and fades (Fig.1).

It is suitable for mobility because OFDM splits the transmission up into many small bandwidth carriers. The original signal is spread over a wide bandwidth, so any nulls in the spectrum are unlikely to occur at all of the carrier frequencies. This will result in only some of the carriers being lost, rather than the entire signal [2],[4].

802.16e uses Scalable OFDMA to carry data, supporting channel bandwidths of between 1.25 MHz and 20 MHz, with up to 2048 sub-carriers. It supports adaptive modulation and coding, so that in conditions of good

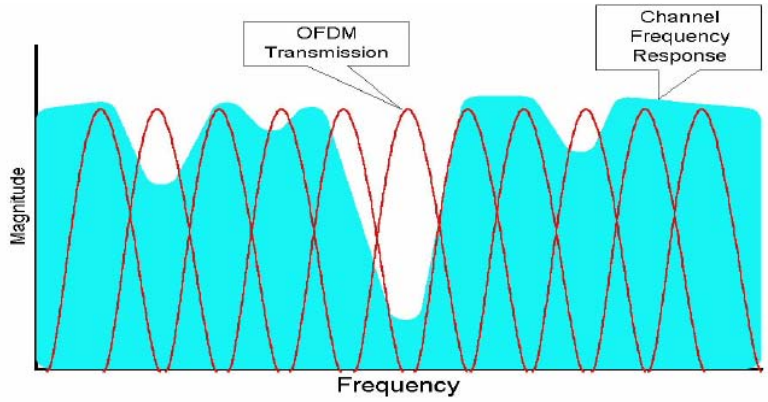

Fig.1. OFDM in Frequency Fade

signal, a highly efficient 64 QAM coding scheme is used, whereas where the signal is poorer, a more robust BPSK coding mechanism is used. In intermediate conditions, 16 QAM and QPSK can also be employed. Other PHY features include support for Multiple-in Multiple-out (MIMO) antennas in order to provide good NLOS (Non-line-of-sight) characteristics (or higher bandwidth) and Hybrid automatic repeat request (HARQ) for good error correction performance.

2.5. MAC layer and services comparison

An important aspect of the IEEE 802.16 is that it defines a MAC layer supports multiple physical layer (PHY) specifications. The MAC is significantly different from that of Wi-Fi and Ethernet from which Wi-Fi is derived. The 802.16 MAC is a scheduling MAC where the subscriber station only has to compete once (for initial entry into the network). After that it is allocated a time slot by the base station. The time slot can enlarge and constrict, but it remains assigned to the subscriber station meaning that other subscribers are not supposed to use it but take their turn. This scheduling algorithm is stable under overload and oversubscription (unlike 802.11). It is also much more bandwidth efficient.

The 802.16 MAC describes a number of Convergences Sublayers which describe how wire line technologies such as Ethernet, ATM and IP are encapsulated on the air interface and how data is classified, etc. It also describes how secure communications are delivered, by using secure key exchange during authentication, and encryption using AES or DES (as the encryption mechanism) during data transfer. Further features of the MAC layer include power saving mechanisms (using Sleep Mode and Idle Mode) and handover mechanisms

3. WIMAX TRAIN COACH CONNECTION.

On Fig.2 we propose a structure for train coach internet supply. According to Fig.2 the PAN give the connection between the train personal in one coach. Using IEEE 802.16 for business class the wireless LAN traffic is passed to the train server.

The train MAN equipment transfers the date stream to the near backbone base station. The last are placed into the railway station or stopping point according to the signal propagandation. If no optical cable is laid in the section, a backhauls for WIMAX line of sight transmission can be used. For safety data handling applications is recommendable to use routers for backbone path switching.

4. COMPATIBILITY WITH SIMILAR TECHNOLOGIES

Unlike earlier broadband wireless access (BWA) WiMAX interactions are highly standardized which cause a costs reduction. WiMAX's equivalent or competitor in Europe is HIPERMAN. WiMAX Forum, the consortium behind the standardization, is working on methods to make 802.16 and HIPERMAN interoperate seamlessly. Products developed by the WiMAX Forum members need to comply to pass the certification process.

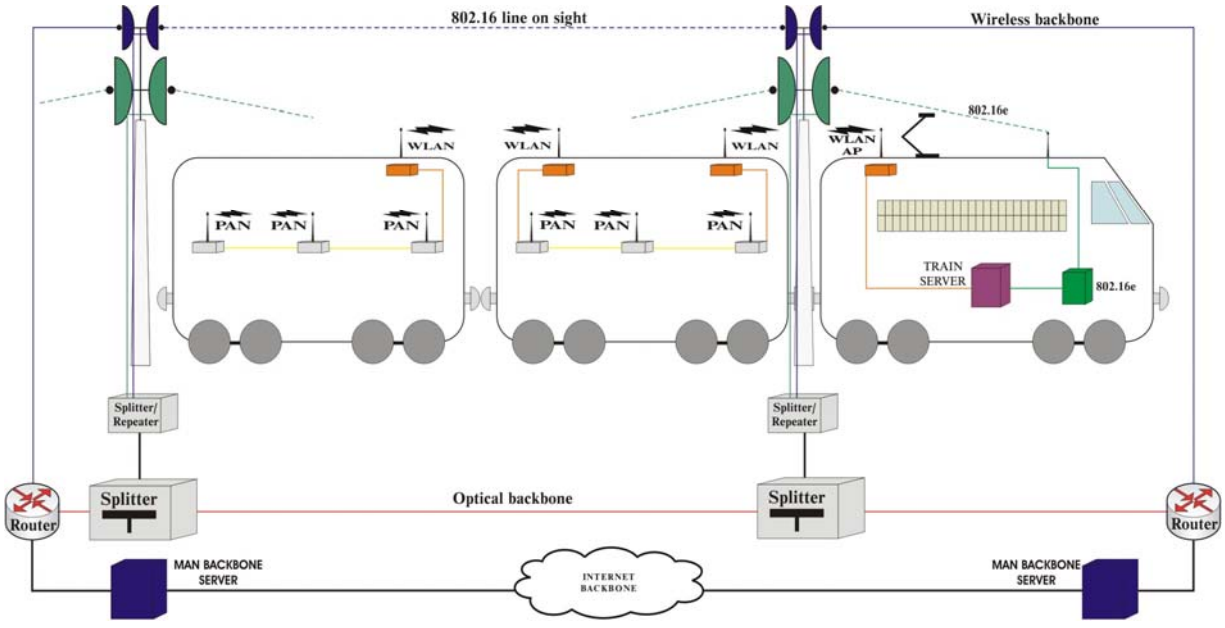

Fig.2. WiMAX train coach connection

5. CONCLUSIONS

In sum, the implementation of 802.16e mobility standard holds great promise for future developments in wireless broadband in transport systems, because it can be used for applications in both licensed and unlicensed spectrum, allows communications without the need for line-of-site connections, enables interoperability with different equipment using the same standard, and in the near future, will encompass both fixed and mobile wireless applications.

REFERENCES

[1]Sweeney D., WiMax Operator's Manual Building 802.16 Wireless Networks, Apress Berkeley, 2006, ISBN: 1-59059-574-2

[2]ETSI TR 102 079, Electromagnetic compatibility and Radio spectrum Matters (ERM); System Reference Document for HIPERMAN in the band 5,725 GHz to 5,875 GHz, 2002.

[3]LaBrecque M., Wimax Enabling Deployments through Standards & Interoperability, WiMAX Forum 2004.

[4]Considerations for deploying mobile WiMAX at various frequencies, Nortel Networks White Paper, 2006.

[5]Aguado M., E. Jacob, P. Sáiz, J. J. Unzilla, M. Higuero, J. Matías, Railway Signaling Systems and New Trends in Wireless Data Communication, Faculty of Engineering Bilbao, University of the Basque Country, VTC2005.

[6]WiMAX End-to-End Network system architecture: NWG network specification", WiMAX Forum, April 20, 2005

[7]Zou F., X. Jiang, Z. Lin, IEEE 802.20 Based Broadband Railroad Digital Network –The Infrastructure for M-Commerce on the Train, Fujian University of Technology, Fuzhou, 2004.

[8]Hoymann C., M.Puttner, I. Forkel, The HIPERMAN Standard – a Performance Analysis, Aachen University 2002.

[9]Marks R., The IEEE 802.16 WirelessMAN Standard for Broadband Wireless Metropolitan Area Networks, http:/wirelessMAN.org.

[10] Agrawal A., New Activities in WiMAX, WCA WiMAX Session, January 21, 2004

[11] A.W. Snyder, J. D. Love: Optical Waveguide Theory, Chapman and Hall, New York 1983

[12] Topalov I., M.Georgieva, Implementation of WIMAX Technology in Railway Telecommunications and Safety Systems, Zilina, Slovakia EURNEX -ZEL 2008, 4-5 June 2008

ЭКОНОМИЧЕСКИЕ ОСОБЕННОСТИ В АНАЛИЗАХ ПО РАСХОДАМ И ПОЛЬЗАМ ИНВЕСТИЦИОННЫХ ПРОЕКТОВ РАЗВИТИЯ ЖЕЛЕЗНОДОРОЖНОГО ТРАНСПОРТА

D. Todorova

Abstract: *The sources of investment projects are classified in a different way according to the different distinguishing features. The implementation of the investment policy in the railway transport is not provided with the necessary funds. The present report has as its main object to review the general presuppositions and peculiarities of the economic assessment of infrastructure investment projects in the field of railway transportation.*

Key words: *Railway Transport, Railway infrastructure,Coast Benefit Analysis, Transport Services, Assessment of investment projects.*

Транспорт является одним из основных факторов, влияющих на современную экономику. Переструктурирование железнодорожного транспорта и дальнейшее развитие его в качестве важной части системы транспорта Болгарии, развитие транспортных коридоров и приведение их в полное соответствие с нормами и требованиями Европейского союза создают более благоприятные условия для активизации инвестиционной деятельности.

Железнодорожный транспорт – это сектор экономики, связанный с интенсивными капиталовложениями больших размеров. Достижение более высоких скоростей движения, большей производительности и безопасности транспортной системы требует увеличения финансовых расходов со стороны транспортных фирм.

Инвестиции дают возможность реконструкции и модернизации железнодорожной инфраструктуры, обновления подвижного состава, внедрения новой техники и технологии в перевозочный процесс, что положительно повлияет на качество, эффективность и конкурентоспособность железнодорожных перевозок. Развитие железнодорожного транспорта зависит в значительной степени от проводимой инвестиционной политики. Разумное использование инвестиций, их оптимальное вложение в самые перспективные направления развития и реконструкции материально-технической базы являются гарантией достижения хороших результатов.

На европейском уровне существует ряд источников финансирования инвестиционных проектов. Такими являются Структурные фонды, Кохезионный фонд и кредиты со стороны Европейского инвестиционного банка. На период 2000-2006 гг. финансирование транспортных проектов из Европейского фонда регионального развития (ЕФРР) составляет около 35 млрд евро.

Кохезионные инструменты в настоящий период 2007-2013 гг. предоставляют более широкую и устойчивую основу для совместного финансирования железнодорожного транспорта на территории всей Европы. Регламенты ЕФРР и Кохезионного фонда ссылаются на интегрированные стратегии по обеспечению чистого транспорта.

Совместное финансирование со стороны ЕС при помощи кохезионных инструментов предусмотрено на инвестиции в инфраструктуру (напр. в области железнодорожного транспорта и терминалов). Предусмотрены также средства на восстановление и модернизацию или иные компоненты, являющиеся частью интегрированной и легко применимой системы городского общественного транспорта (дорожная информация, интегрированная система оплаты, управление передвижением и т.д.).

Анализ по расходам и пользам

Регламенты ЕС по Структурным фондам (СФ) и Кохезионному фонду (КФ) требуют анализа инвестиционных проектов по расходам и пользам (СВА) в целях определения их экономической и социальной целесообразности.

Подобный анализ требуется согласно регламентам ЕС по Структурным фондам, Кохезионному фонду и Доприсоединительному инструменту структурной политики (ИСПА), когда стоимость проекта превышает 50 млн, 10 млн и 5 млн евро.

Анализ расходов и польз является рамкой, введенной в целях систематической и количественной оценки публичных или частных проектов для определения того, до какой степени существует выгода с реализации проекта с социально-экономической точки зрения, с учетом

Daniela Todorova, MSc., Lecturer; Todor Kableshkov Higher School of Transport, Sofia, Bulgaria, daniela_dt@abv.bg

всех целей проекта, под формой польз и всех убытков и недостатков, в форме расходов, с точки зрения экономических интересов инвеститора, потребителей и общества в целом.

Для вычисления показателей, необходимых для принятия инвестиционных решений разработана единая методика анализа расходов и польз (Coast Benefit Analysis).

С точки зрения возможностей финансовой поддержки основные задачи анализа следующие:

- Доказать, что проект целесообразен с экономической точки зрения и будет способствовать достижению целей региональной политики ЕС;
- Доказать, что вклад Фондов необходим для обеспечения финансовой осуществимости проекта;
- Определить необходимый уровень оказания помощи.

Для выбора и определения приоритета инвеститорских проектов необходимо вычисление финансовых и хозяйственных показателей на основе альтернативных сценариев, включающих хотя бы три варианта:

- Не делать ничего;
- Реализовать минимальные изменения;
- Реализовать новые технические и технологические решения.

Основными показателями, определяемыми при помощи этого анализа, являются Внутренная норма окупаемости (IRR), Нетто настоящая стоимость (NPV) и коэффициент польз/расходов (C/B).

Цель и требования к модели

Стандартная методика включает основные требования к содержанию, форме и показателям анализа по расходам и пользам. Она, однако, не отражает транспорта и особенности социально-экономического развития по государствам, регионам и городам.

Предложенные в настоящей статье методика и модель дают возможность отразить эти особенности в анализах по расходам и пользам инвестиционных проектов развития железнодорожного транспорта на территории Болгарии.

Модель включает основные этапы и показатели унифицированной методики и в то же время учитывает следующие основные требования:

- соответствие с нормативами ЕС и национальными документами;
- учет специфики деятельности и структуры железнодорожного транспорта;
- учет особенностей социально-экономического развития страны;
- учет состояния железнодорожной инфраструктуры и необходимости в ее развитии в контексте Общей транспортной политики ЕС;
- учет финансовых, экономических расходов и польз для инвестора, операторов и общества;
- включение внешних влияний (externalities) в результате принятия инвестиционных решений – окружающей среды, социального воздействия, надежности и безопасности перевозок и т.д.

Методология

Для определения отдельных исходных параметров применяются техники, методы и подходы, адаптированные к специфике инвестиции и деятельности в области железнодорожного транспорта.

Для изготовлении прогнозы и анализ по расходам и пользам используются макроэкономические показателей Болгарии, стоймости, которые рассмотрены в табл. 1.

Таблица 1.

Наименование показателей	2007	Прогнозы 2008
ВВП, текущие цены,мил.лв.	49 021	53 274
ВВП, %	5,6	5,6
Валютный курс лв/щ.д.	1,55	1,55
Цен петроля щ.д./барель	67,0	65,0
Инфляция в год,%	6,5	6
Экспорт, млн.евро	13 548,6	15 133,8
Импорт, млн. евро	19 521,6	21 786,1
Инвестиции, мин.лв.	10 777,0	12 108,0
Равнище безработицы,%	9,0	8,7
Средная заработная плата, лв./год	4 872	5 273

Анализ предусматривает два основных этапа – финансовый и экономический анализ. Результаты экономического анализа включают социально-экономические аспекты реализации проектов (Фиг. 1).

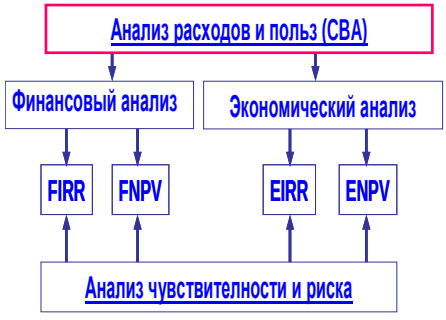

Фиг. 1.

Методики, которые необходимо разработаться следующие:

- Определение входных денежных потоков;
- Определение инвестиционных расходов;
- Определение експлоатационных разходов;
- Определение реалных экономических потоков.

Финансовый анализ проводится в целях определения финансовой внутренней нормы окупаемости инвестиции и собственного капитала (IRR), а также соответственной нетто настоящей стоимости (NPV) инвестиций, определенной на выбранный горизонт времени (Табл.2).

Времевой горизонт при оценки проектов, годы

Таблица 2.

	Средний времевой горизонт	Число проектов
Енергетика	24,7	9
Окружающея среда	29,1	47
Транспорт	**26,6**	**127**
Промишленость	8,8	96
Другие услуги	14,2	10
Средная общая	*20,1*	*289*

От данных в таблице наблюдается, что для транспортного сектора средний времевой горизонт в годы при оценки проектов один из самых высоких– 26,6г.

Полученные результаты применяются в качестве критерия оценки финансовой эффективности предложенных инвестиционных вариантов на микроекономическом уровне, т.е. с точки зрения частного интереса инвестора или бенефициента.

Его основные этапы предусматривают определение связанных с проектом:

- Входящих денежных потоков;
- Инвестиционных расходов;
- Оперативных расходов;
- Источников на финансирование;
- Финансовой внутренней нормы окупаемости (IRR) и финансовой нетто настоящей стоимости инвестиций (NPV).

Выбор времевого горизонта является особо важный для определении NPV. Кроме тога выбор стонтового фактора оказывает влияние на вычислении NPV (Фиг.2). Для определении NPV на инфраструктурных проектов в Болгарии принят сконтовы процент 6%.

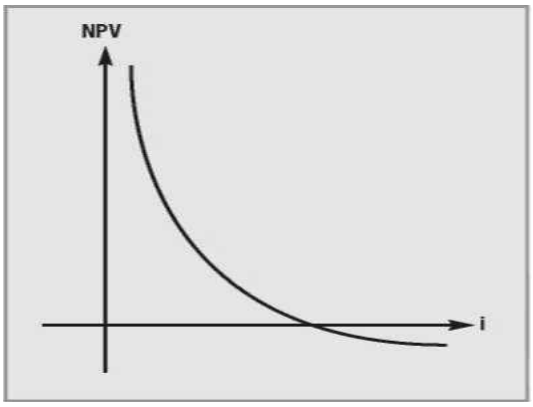

Фиг.2: NPV как функция на i.

Эта часть анализа не учитывает социальные расходы и пользы, связанные с проектом, и поэтому она не достаточна для принятия решения о финансировании из фондов ЕС.

Экономический анализ проводится в целях определения социальных расходов и польз с данного инвестиционного проекта. Он дает возможность оценки вклада проекта с точки зрения всего общества (региона или государства), что отличает его от финансового анализа.

Основным принципом экономического анализа является оценка вложенных в проект ресурсов по их альтернативной стоимости, а его результаты указывают на готовность потребителей платить за это.

Альтернативная стоимость, определенная в целях экономического анализа, отличается от установленных в финансовом анализе расходов, а готовность платить не во всех случаях находит адекватное отражение в рыночных ценах.

Переход с финансового к экономическому анализу и определение реальных экономических потоков требует преобразования рыночных цен (искаженные из-за недостатков рынка) в бухгалтерские, а также учета внешних эффектов. Это возможно путем определения одноразового индекса конверсии для каждой из входных или исходных позиций денежных потоков. Международная практика позволяет использовать стандартизированные индексы для некоторых групп входных/исходных ресурсов, а для других необходимо определение специфического индекса на каждый случай в отдельности.

Особенности транспорта, и в частности, железнодорожного транспорта требуют разработки специфических методик определения коррективов при переходе из финансовых к реальным экономическим потокам.

После установлении вероятностьных распределении критичных променливы возможно приступит к вычислении вероятностьного распределения NPV или IRR по проекту (Фиг.3)

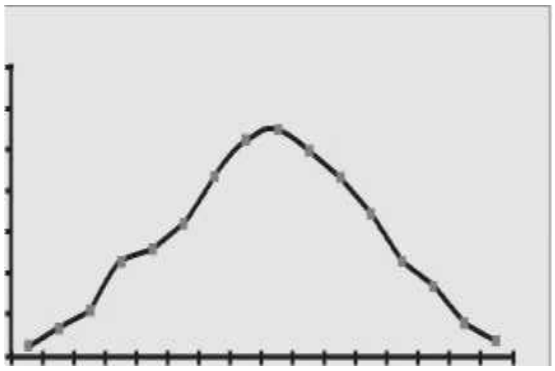

Фиг.3 Вероятностьное распределение IRR

Реальные экономические потоки

Реальные экономические потоки определяются при помощи корректировки финансовых входных и исходных потоков, учитывающих влияние:

- фискальных факторов;
- искажения цен (корректив с фактором превращения – калькулятивные цены – рыночные цены);
- искажения заработной платы (бухгалтерская поденная плата или поденная плата в тени);
- внешних воздействий (расходов и польз).

Фискальные коррективы

Рыночные цены включают в себя налоги и субсидии, а также некоторые переводные платежи, которые могут воздействовать на относительные цены. Вот почему, для корректировки этих искажений цен входных и исходных ресурсов необходимо определить конверсионные индексы.

Для определения „фискальной корректировки" и величины конверсионных индексов, применяемых в отношение рыночных цен, восприняты некоторые общие допущения:

- Цены исходных и входных ресурсов не включают налоговая добавленая стоимость (НДС) и налог на прибыль;
- Чистыми переводными платежами физическим лицам (социальным страхованием) необходимо пренебречь.

Коэффициенты корректировки, вычисленные по методике, и применимые для инфраструктурных инвестиционных проектов в Болгарии, представлены в таблице 3.

Таблица 3.

Элементы	Коэфф. корректировки
НДС на материалы, теплоснабжение и внешние услуги	0,83
Социальное страхование	0,55
Акциз на топливо(430лв./1000 л.)	0,77
Налог на прибыль	0,90

Целью инвестиционных проектов является обеспечение безопасности передвижения на железных дорогах, надежность процесса перевозок

В связи с присоединением Болгарии к Европейской системе транспорта требования направлены главным образом к: обеспечению конкурентности, более высокому качеству предлагаемых транспортных услуг. Осуществление инвестиционных проектов обеспечило бы развитие транспортной инфраструктуры вплоть до достижения европейского уровня, а также европейское качество транспортных услуг.

Предложенные здесь методика и модель дают возможность отразить особенности в анализах по расходам и пользам инвестиционных проектов развития железнодорожного транспорта на территории Болгарии.

ЛИТЕРАТУРА

[1] Ръководство за анализ на инвестиционни проекти по разходи и ползи: http://europa.eu.int/ commlregional policy/sources/docgener/guides/cost/ guide02 en.pdf;

[2] Методически указания за попълване на проектна документация,оценка и управление на инвестиционни проекти – изд. на Министерство на финансите.

[3] Директиви 2001/16/ЕО и 96/48/ЕО относно оперативната съвместимост на Транспортната железопътна система.

MATHEMATICAL MODEL FOR DETERMINATION OF TORSIONAL STIFFNESS OF THREE-AXLED WAGONS

N. Bogojević, Z. Šoškić, D. Petrović, R. Rakanović

Abstract: *The paper shows the analytical model for determination of torsional stiffness of three-axled wagons. Developed mathematical model for determination of torsional stiffness has been applied to the wagon "DDam" which is used for car transportation. The methodology of testing torsional stiffness of three-axled wagons can be suggested on the basis of obtained results.*

Key words: *torsional stiffness, derailment safety, wagons, three-axled wagon*

INTRODUCTION

Determination of torsional stiffness is an important step in evaluation of railway vehicles because it influences the wagons running over distorted track. Calculation and methodology of testing torsional stiffness of two-axled and four-axled wagons are determined by ERRI and UIC regulations [1], [2] and by EN standards [3].

There have lately been requirements for some non-standard wagon structures such as three-axled wagons. Because of their distinct structure, the methods used so far [1], [2], [3] can not be applied in order to determine torsional stiffness of three-axled wagons.

The problem of determining torsional stiffness of three-axled wagon "DDam" was approached at the Centre for Railway Vehicles of the Faculty of Mechanical Engineering in Kraljevo. "DDam" wagon is a three-axled two-unit wagon used for car transportation and it is manufactured in factory "Bratstvo" in Subotica, Serbia. Its tare weight is 27 t, and its maximum load is 20 t. The wagon runs in S and SS regime. Since regulations [1], [2] and standards [3] do not define the methodology for calculating torsional stiffness, an analytical model for calculating torsional stiffness of three-axled wagons is developed.

MODEL

The analysis of ORE's and Schadur's models has showed that aforesaid models can not be applied to three-axled wagons. A new model used for determining torsional stiffness [6] has been made on the basis of regulations [1], [2], [3] and research results [6], [8]. It can be applied to forming the model of three-axled wagons (Figs. 1, 2, and 3). The results obtained by new analytical model conform to the models used for calculating torsional stiffness according to current regulations [8].

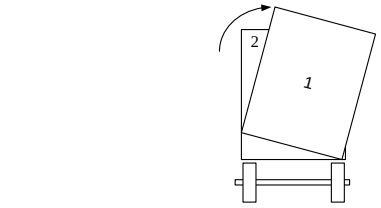

Figure 1.

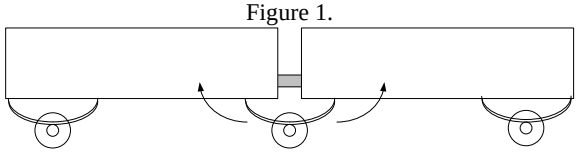

Figure 2.

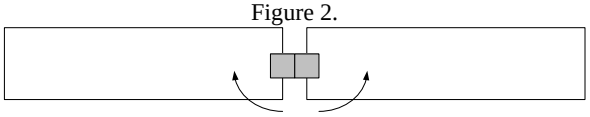

Figure 3.

Deformations of a wagon body

According to [8], the first step in determining torsional stiffness of the wagon is determining deformation of body δ when diagonally and symmetrically loaded. The expression for body deformation is:

$$\delta = \frac{z_1 - z_2 + z_3 - z_4}{4} \qquad (1)$$

where z_i (i=1,2,3,4) are vertical coordinates of body ends.

According to [1], [2] and [3], when a guiding wheel of the wagon runs over distorted track, diagonal and symmetrical load acts on wagon underframe [5]. Since a three-axled wagon has two units, each of them having its own body, deformation of the first body can be expressed as:

$$\delta = \frac{z_1 - z_2 + z_3 - z_4}{4} \qquad (2)$$

M.Sc. Nebojša Bogojević, Assistant, bogojevic.n@mfkv.kg.ac.yu
Dr Zlatan Šoškić, soskic.z@ mfkv.kg.ac.yu
Prof Dr Dragan Petrović, petrovic.d@ mfkv.kg.ac.yu
Prof Dr Ranko Rakanović, rakanovic.r@ mfkv.kg.ac.yu

whereas deformation of the second body is presented by following expression:

$$\delta' = \frac{z_5 - z_6 + z_7 - z_8}{4} \qquad (3)$$

where

- δ and δ' are deformations of wagon bodies,
- z_i are vertical coordinates of body ends of the first (i = 1, .., 4) and second wagon unit (i = 5, .., 8).

In order to determine coordinates of body ends, we observe the underframe and connection between underframe and axles. (Fig. 5).

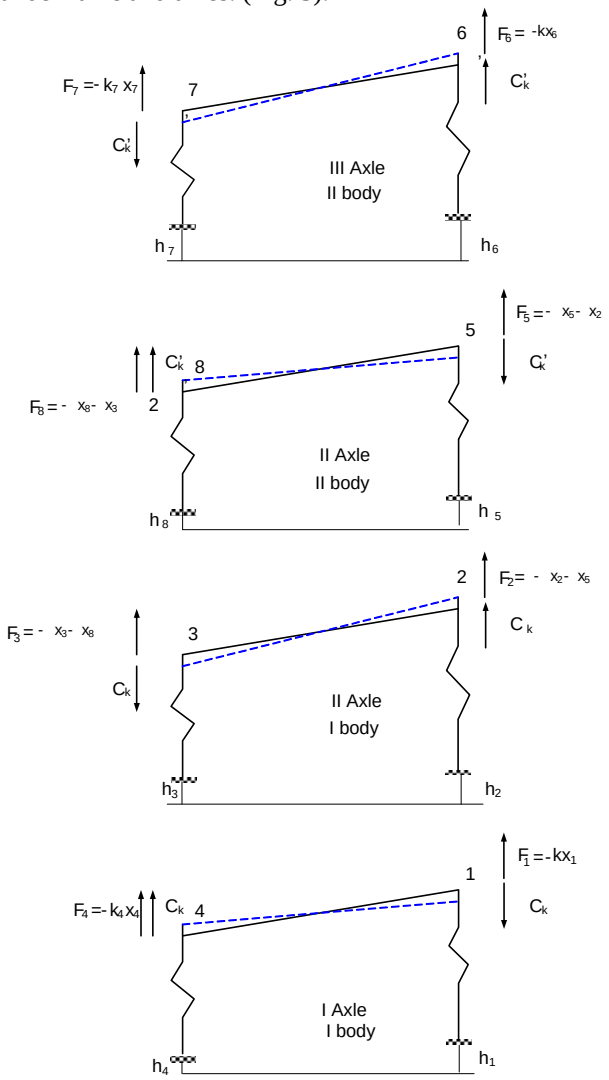

Figure 5. Forces acting on underframe of wagon body in relation to axles and suspension elements

Vertical coordinates of body ends z_i are determined in analogous manner as the method shown in papers [6] and [8], but we have taken into consideration deformations of all elastic elements of system consisting of springs and bodies.

Coordinates z_i in relation to the plane of water level can be presented as:

$$z_i = h_i + x_i, \quad i = 1,...,8, \qquad (4)$$

where

h_i - vertical distance from track to the plane of water level,

x_i - lengths of springs (i = 1,4 for wheels of the first axle, i=2,3 for wheels of the second axle when the first wagon unit is analyzed; i=5,8 for wheels of the second axle, and i=6,7 for wheels of the third axle when the second wagon unit is analyzed).

According to Figure 5, the spring lengths can be expressed as:

$$x_i = l_i + x_{iQ} + x_{ih}, \quad i = 1,...,8, \qquad (5)$$

where

l_i - length of undeformed springs,

x_{iQ} - spring deformations caused by weight of suspended mass,

x_{ih} - spring deformations caused by stiffness of wagon body.

If equations (4), (5), and (6) are placed into equations (2), and (3), deformations of wagon body are:

$$\delta = \frac{1}{4}\left(\left(h_1 - h_2 + h_3 - h_4\right) + \left(l_1 - l_2 + l_3 - l_4\right)\right) +$$

$$+\frac{1}{4}\left(\frac{Q}{4}\left(\frac{1}{k_1} - \frac{1}{k_2} + \frac{1}{k_3} - \frac{1}{k_4}\right) + \left(x_{1h} - x_{2h} + x_{3h} - x_{4h}\right)\right)$$

$$\delta' = \frac{1}{4}\left(\left(h_5 - h_6 + h_7 - h_8\right) + \left(l_5 - l_6 + l_7 - l_8\right)\right) +$$

$$+\frac{1}{4}\left(\frac{Q}{4}\left(\frac{1}{k_5} - \frac{1}{k_6} + \frac{1}{k_7} - \frac{1}{k_8}\right) + \left(x_{5h} - x_{6h} + x_{7h} - x_{8h}\right)\right)$$

Connection between wagon bodies

In order to determine torsional stiffness of wagon as whole, it is necessary to determine mutual influence of one wagon body on the other one by suspension system at central axle. If the influence is elastic, the forces acting on body ends above central axle have the following components:

- Due to motion of a body end, elastic force acting on that body end can be described by its own equivalent stiffness K,
- Due to motion of a body end, elastic force acting on the other body end can be described by mutual equivalent stiffness κ.

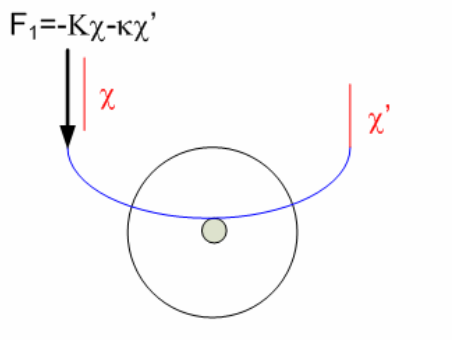

Figure 6. Definition of equivalent stiffnesses

Equations for forces acting on body ends above central axle can be described as (Fig. 6.):

$$F = K\chi + \kappa\chi' \quad (6)$$

$$F' = \kappa\chi + K\chi' \quad (7)$$

where χ and χ' are motions of body ends, F and F' are forces acting on adjacent body ends of the first and second wagon unit, respectively.

Determination of total torsional stiffness

Equations for forces acting on body ends above central axle of a three-axled wagon are (Fig. 5):

$$\begin{aligned} F_2 &= -Kx_{2h} - \kappa x_{5h} \\ F_5 &= -Kx_{5h} - \kappa x_{2h} \\ F_3 &= -Kx_{3h} - \kappa x_{8h} \\ F_8 &= -Kx_{8h} - \kappa x_{3h} \end{aligned} \quad (8)$$

Forces acting on wagon bodies above the first and third axles are:

$$\begin{aligned} F_1 &= -kx_{1h} \\ F_4 &= -kx_{4h} \\ F_6 &= -kx_{6h} \\ F_7 &= -kx_{7h} \end{aligned} \quad (9)$$

Following equations are based on force balance at contacting points of wagon bodies on one hand, and on springs at suspension system on the other hand:

$$\begin{aligned} F_i &= C_k\delta, \\ F_j &= C'_k\,\delta' \end{aligned} \quad (10)$$

where $i = 1,2,3,4$, $j = 5,6,7,8$, and C_k and C'_k are torsional stiffness of the first and second wagon bodies, respectively.

General equations which determine deformation of three-axled wagon bodies having elastic connection at the central axle can be summarized in the following table:

First body	Second body
$x_i = l_i + x_{iQ} + x_{ih}$	$x_j = l_j + x_{jQ} + x_{jh}$
$x_{iQ} = \frac{Q}{4k_i}$	$x_{jQ} = \frac{Q}{4k_j}$
$x_{1h} = -\frac{C_k}{k_1}\delta$	$-Kx_{5h} + \kappa x_{2h} + C'_k\,\delta' = 0$
$-Kx_{2h} + \kappa x_{5h} + C_k\delta = 0$	$x_{6h} = -\frac{C'_k}{k_4}\delta'$
$-Kx_{3h} + \kappa x_{8h} + C_k\delta = 0$	$x_{7h} = -\frac{C'_k}{k_7}\delta'$
$x_{4h} = -\frac{C_k}{k_4}\delta$	$-Kx_{8h} + \kappa x_{3h} + C'_k\,\delta' = 0$

Table 1. Equations describing general model used for determining torsional stiffness of a three-axled wagon

This model can be simplified by following assumptions:

- static load is equally apportioned at the body ends because of body weight,
- all springs at suspension system have the same stiffness characteristics,
- free lengths of unloaded springs are equal,
- torsional stiffness of both bodies are equal.

In that case, the equations describing deformations of both bodies are:

First body	Second body
$x_{1h} = -\frac{C_k}{k}\delta$	$-Kx_{5h} + \kappa x_{2h} + C_k\delta' = 0$
$-Kx_{2h} + \kappa x_{5h} + C_k\delta = 0$	$x_{6h} = -\frac{C_k}{k}\delta'$
$-Kx_{3h} + \kappa x_{8h} + C_k\delta = 0$	$x_{7h} = -\frac{C_k}{k}\delta'$
$x_{4h} = -\frac{C_k}{k}\delta$	$-Kx_{8h} + \kappa x_{3h} + C_k\delta' = 0$

Table 2. Equations describing a model used for determining torsional stiffness of a three-axled wagon in case of equal spring stiffness at suspension system

According to equations presented in Table 2, deformations of springs beneath the first and second bodies can be connected with deformations of bodies in the following manner:

$$
\begin{aligned}
x_{1h} &= -\frac{C_k}{\delta}, \\
x_{2h} &= \frac{K\delta + \kappa\delta'}{K^2 - \kappa^2} C_k, \\
x_{3h} &= -\frac{K\delta + \kappa\delta'}{K^2 - \kappa^2} C_k, \\
x_{4h} &= -\frac{C_k}{k}\delta, \\
x_{5h} &= -\frac{K\delta' + \kappa\delta}{K^2 - \kappa^2} C_k, \\
x_{6h} &= -\frac{C_k}{k}\delta', \\
x_{7h} &= -\frac{C_k}{k}\delta', \\
x_{8h} &= \frac{K\delta + \kappa\delta'}{K^2 - \kappa^2} C,
\end{aligned}
\qquad (11)
$$

According to system of equations (11), deformations of bodies and springs depend on torsional stiffness of bodies and on type of elastic connection between wagon units (parameters K and κ)

Determination of torsional stiffness of ''DDam'' wagon

Developed mathematical model has been applied to a three-axled "DDam" wagon used for car transportation. This wagon has a distinct type of connection at central axle. The ends of laminated spring are connected with the body ends, whereas axle-box case supports a spring buckle. This construction is unfavourable in view of load and working life of the spring. The spring at central axle, due to above described construction, is exposed to very unfavourable loads - in addition to bending, there spring torsion is also present.

In order to apply developed model, it is necessary to determine spring stiffness k at front and rear axles, equivalent stiffnesses K and κ, and torsional stiffness of body C_k. Spring stiffness k is a structure parameter provided by manufacturers while torsional stiffness of body C_k is numerically calculated or experimentally determined.

In order to determine equivalent stiffnesses K and κ the following have been taken into consideration: because of the type of spring connection above central axle, K and κ should meet the condition that force, in case of equal motion of both spring ends, should be equal to the force in case of equal motion of classic spring mounted into suspension system (Fig. 7).

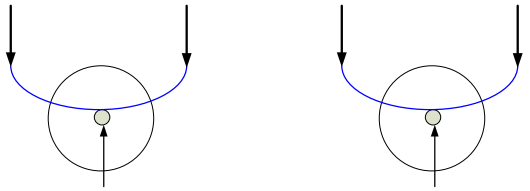

Figure 7. Forces acting on spring above central axle
a) during different motions of spring ends,
b) during equal motions of spring ends.

Thus, parameters K and κ must satisfy the following condition:

$$K + \kappa = \frac{k}{2} \qquad (12)$$

The analysis of experimental results shows that this type of connecting wagon units requires the following approximate equation:

$$K \approx \kappa \qquad (13)$$

This equation is used for evaluation of parameters *K* and *κ*.

The following equalities are obtained if equations (12) and (13) are placed into equation system (11):

$$\begin{aligned} x_{1h} &= -x_{4h} \\ x_{2h} &= -x_{3h} \\ x_{5h} &= -x_{8h} \\ x_{6h} &= -x_{7h} \end{aligned} \tag{14}$$

If only a guiding wheel runs over the unevenness of the track $h_1=h$, $h_2=h_3=h_4=0$, equation system (11) can be written like this:

$$\begin{aligned} & kx_{1h} = C_k\delta \\ & K\left(x_{2h}+x_{5h}\right)+C_k\delta = 0 \\ & kx_{6h} = C_k\delta' \\ & \delta = -\delta' \\ & \delta = \frac{h+x_{1h}-x_{2h}+x_{3h}-x_{4h}}{4} \\ & \delta' = \frac{x_{5h}-x_{6h}+x_{7h}-x_{8h}}{4} \\ & x_{1h} = -x_{4h} \\ & x_{2h} = -x_{3h} \\ & x_{5h} = -x_{8h} \\ & x_{6h} = -x_{7h} \end{aligned} \tag{15}$$

Body deformation of the first wagon unit is obtained by solving equation system (15):

$$\delta = \frac{h}{2\left(2+\frac{C_k}{k}\right)+2\frac{K\left(2+\frac{C_k}{k}\right)+C_k}{K}} \tag{16}$$

Total torsional stiffness of "DDam" wagon is determined on the basis of following:

- definition of torsional stiffness of wagon body, i.e. $\Delta F = C_k\delta$,
- definition of torsional stiffness of wagon as whole according to [1], [2], [3] which is defined as relation between force and track distortion caused by torsion, i.e. $C_u = \frac{\Delta F}{g^*}$, equation system (15).

Thus, total torsional stiffness of "DDam" wagon is:

$$\frac{1}{C_u} = \frac{8}{C_k}+\frac{4}{k}+\frac{2}{K} \tag{17}$$

According to equation (66) in reference [8], the expression for torsional stiffness of ""DDam" wagon is finally reached and it is in conformity with ORE [2]:

$$\frac{1}{C_{uORE\_3}} = 10^3\left[2\left[\left(2b_A\right)^2\frac{1}{C_t^*}\right]+\frac{1}{2a}\left(\frac{2b_A}{2b_Z}\right)^2\left[\frac{4}{k}+\frac{2}{K}\right]\right]$$

CONCLUSION

Mathematical model presented in Table 1 has a universal purpose and can be applied to calculating torsion of all types of three-axled railway vehicles consisting of two units which are connected by elastic connections but which are not included within regulations [1], [2], and standards [3]. When calculating wagon torsion by this method, a special attention should be directed to the model describing mutual connection between wagon units.

However, the model has a disadvantage. Namely, it does not consider horizontal guiding forces acting on axles, which is very important for calculating safety of wagons running over distorted track.

LITERATURE

[1] ERRI B12 / DT 135, “Allgemein verwendbare Berechnungsmethoden für die Entwicklung neuer Güterwagenbauarten oder neuer Güterwagenderhgestelle” European Rail Research Institute, Utrecht, 1995.

[2] ORE B 55, “Moyens propres á assurer la circulation normale sur des voies présentant des gauches”, ORE de UIC, Utrecht, 1983.

[3] EN 14363 Railway application-Testing for the acceptance of ruuning characteristic of railway-Testing of running behavior and stationary test, European committee for standardization, 2005 CEN.

[4] Л.А. Шадур „Вагоны конструкция, теория и расчет“, Москав „Транспорт“, 1980.

[5] Atmadžova D., Penčev C. „A geometrical model of determination load of biaxial (two bogie) rolling stock“, BG-2.11-BG-2.18 Mechanics transport communications, No.1, Sofia 2007.

[6] Bogojević N. Rakanović R. Petrović D. Šoškić Z. „A new approach in analytical determination of torsional stiffness in railway wagons“, VI-12-VI-15, Mechanics transport communications, No3/2007 part II, Per.No:0153, Sofia 2007

[7] R. Rakanović, A. Babić, D. Petrović i dr. Elaborat br. 4/95, “Ispitivanje uvojne krutosti, mirnoće hoda, stabilnosti kretanja i dinamičke čvrstoće elementa sistema ogibljenja DDam kola”, Mašinski Fakultet Kraljevo, Kraljevo, 1995.

[8] Nebojša Bogojević, Magistarska teza „Torziona krutost troosovinskih teretnih vagona“, Mašinski Fakultet Kraljevo, Novembar 2007.

TRANSPORTATION – POLICY, ECOLOGY, CULTURE

T. Simović, N. Bogojević

Abstract: *Conditions of our country transportation system are characterized by many shortcomings arisen as a result of objective circumstances such as low level of accomplished development of traffic infrastructure, transportation means and organization of transportation flows (before the disintegration of SFRY), complete suspension of development (during the sanctions) and significant extent of demolition of what Serbia had had (during the bombing). At the same time, as from 2000, not much has been done for the improvement of conditions. There have been no means and no clearly defined transportation policy, which has been accompanied by a low traffic culture and environmental problems.*
The present paper objective is to point out the indicated shortcomings and stress a need for specific measures aimed at the improvement of situation.

Key words: *transportation, transportation policy, culture, ecology,*

TRANSPORTATION AND ITS IMPORTANCE

Being a part of economic complex as a whole transportation is an important sector intended for the conveyance of passengers and transportation of goods. Without an intense development of all kinds of transportation and a widespread traffic network it is impossible to meet the needs of growing volume of social production, expansion of industrial use of natural resources, development of economic and cultural connections, country defense requirements.

Depending on the type of transportation means and traffic ways, we have the following kinds of transportation: **rail transport**, **motor transport**, **river transport**, **maritime transport** and **pipeline transport**. All kinds of transportation form a uniform transportation system in which they are tightly bound and exert influence on each other. The role and position of each kind of transportation in such a system is defined by its own peculiar qualities.

Transportation as a part of economy is, in essence, a number of transportation means and ways as well as accompanying systems, equipment and facilities required for an undisturbed advancement of economic activity.

Significance of transportation is illustrated by the fact that it engages more than 10 % of employees in one country. Furthermore, transportation sector uses more than 60 % of the world oil products, 20 % of steel, 80 % of lead, 70 % of plastic, 40- % of cast light metal, etc.

That is why one of the main indicators of one country development level is the level of development of transportation sector. As it can be observed, transportation sector is a strategically important complex that to a significant degree and according to different criteria depicts the strength of a country.

Our transportation system as well as the transportation systems of majority of transitional economies is incomplete, poorly developed, inefficient and expensive. It is characterized by insufficient social expediency, low technical level, technological lagging, economical exhaustion, lack of human resources and deficient market orientation.

Finally, it can be said that the present situation in the field of traffic and transportation system of Serbia is characterized by the following:

- poor transportation infrastructure
- obsolete transportation means
- large share of transportation charges in product price
- inadequate distribution of modes of transport
- unreasonable use of energy
- environment jeopardizing
- inexistence of proper transportation policy
- low traffic culture
- lack of qualitative human resources
- inefficient legislation, etc.

It should be said in this connection that the adopted strategies and proclaimed development policies, despite promoting basic guidelines of transportation system development, fail to identify those in charge of their development.

Prof Dr Tomislav Simović, Associate Professor at the Faculty of Mechanical Engineering in Kraljevo, General Manager of Montinvest a.d. Belgrade, simovic.t@mfkv.kg.ac.yu
M.Sc. Nebojša Bogojević, Assistant, bogojevic.n@mfkv.kg.ac.yu

TRANSPORTATION AND TRAFFIC POLICY

Adoption of country economic policy entails defining of traffic policy as a base of transportation, which implies defining of objectives and planning of necessary measures for their implementation. World political and economical trends impose conditions that our traffic policy has to satisfy, among which the first are conditions to be met by the traffic corridors through our country (land transport – corridor 10, water transport – corridor 7).

To be specific, traffic policy covers:

-investments in infrastructure and transportation means
-defining of priority traffic routes
-development and construction of terminals and cargo transport centers
-providing of financial resources
-effective fiscal policy
-schooling and education of human resources
-successful punishment policy
-environment protection
-rising of traffic culture, etc.

From the point of view of national interests, at the level of Government a more up-to-date approach is needed in perceiving the so far completed activities – from technical and technological to those from the field of domestic and foreign legislation, international treaties and conventions, harmonization with the plans and traffic development strategies defined in Europe.

TRANSPORTATION AND TRAFFIC CULTURE

Traffic, as an important civilization heritage has to be accompanied by proper culture of those that render services in this field as well as users.

It is the fact that “culture is a historical and dynamic category, i.e. development category of a specific time and space” that furthers economy, progress, improvement and sustaining of human development. This means that traffic culture represents the achieved level of consciousness in the attitude towards the traffic both on the side of those that offer services and those that use them.

A proper traffic culture ensures qualitative use of traffic system, which implies:

-selection of most profitable, safe and secure transportation means
-low energy consumption
-observance of prescribed operating conditions
-regular maintenance of means
-environment preservation
-civilized behavior of personnel and users
-insured means, goods and passengers.

To achieve a mass understanding, it is necessary to secure the following:

-general and traffic education of children and adults
-qualitative training and education of professionals and amateurs participants in traffic
-engagement of trained staff for solving of specialized issues
-extensive information on the existence, application and follow-up of standards in the field of production and operation of transportation means
-observance of regulations pertinent to occupational safety and transportation means cleanness
-respecting of environmental requirements.

It is of utmost importance, that school programmes cover the necessary measures that will encourage students to be more aware of traffic, and by that of transport itself, as a decisive factor for the standard of life and to behave, now as young and, later, as adults, in line with standards of high traffic culture.

TRANSPORTATION AND ECOLOGY

Transportation and Natural Resources Spending

In addition to the enormous role that transportation plays in the life of society, its development is followed by a series of negative consequences. Transportation today – it is a dense network of traffic routes that cover the globe. Transportation has a massive fleet of locomotives, self-propelled vessels, cars, aircrafts, stationary power plants. Their combined influence upon the environment leads to a detrimental environmental effects which involve dry land, atmosphere, water basin. These detrimental environmental effects introduce serious changes in the ecological systems and regulation in the biosphere as a whole.

Within the problem of interaction between transportation and environment, two mutually linked aspects are distinguishable: spending of natural resources and pollution of environment.

In the industrially developed countries, the share of transportation in the spending of energy resources amounts to 12 – 17 %, of which 50 – 60 % is motor transport. Energy consumption for different kinds of transport differs and it depends to a considerable degree on the vehicular fleet type (Table 4.1.).

Besides fuel and energy, transportation consumes other natural resources as well, especially metals (steel, copper, zinc, lead, etc.). Transportation also consumes an enormous quantity of water. Reduction of energy and material consumed for transportation for all the kinds of transport is an important task. Its solving

means the use of energy-conserving power sources, use of higher capacity and lower dead weight vehicular fleets, increase of technical maintenance levels and use efficiency of vehicular fleet.

As to maritime and river transports, the problem can be solved by the major use of lower quality and higher weight engine fuels, extended use of nuclear power plants, especially in the conditions of the Arctic, enhancement of hydrodynamic properties of vessels (use of jet streamline devices, bow thrusters, pushing instead of towing), etc.

Table 4.1. Energy consumption for the transportation using different kinds of transport

Vehicular Park Type	**Energy Consumption, MJ**	
	for 100 passengers/km	**for 100 t/km**
Air Transport		
Helicopter (Mi-4)	407	-
Aircraft		
- small (Jak-40)	550	-
- medium (Tu-134)	234	-
- large (Il-62)	270	-
Rail Transport		
Train		
- electric traction	5,5	2,8
- diesel traction	20,2	8,8
Water Transport		
Dry cargo		
- river (5 thousands t)	-	38,1
- maritime (13,5 thousands t)	-	16,0
Tanker ship	-	5,4
Pipeline Transport		
Oil pipeline (700 mm)	-	5,4
Gas pipeline (1420 mm)	-	230-360
Motor Transport		
Motor car	60 – 80	-
Bus		
- small gasoline-powered	40 – 50	-
- medium gasoline-powered	20 – 25	-
- large gasoline-powered	12 – 15	-
Freight transportation		
- medium gasoline-powered	-	300 – 400
- large gasoline-powered	-	140 – 160
Articulated truck, diesel	-	100 – 110

TRANSPORTATION AND ENVIRONMENT POLLUTION

Impact to atmosphere. Transport sends to the atmosphere an enormous quantity of dust and toxic matters contained in exhaust gases, generates high noise levels, pollutes ground and water basins on account of leakage of fuels and lubricants and produces many other matters harmful to the environment and human beings. Transport is a source of pollution with not only carbon dioxide, but also with other matters of which many are toxic and harmful for the environment.

More than 500 harmful matters that pollute the atmosphere are known today – in the Table 4.2. are given the main. As the Table 4.2. shows, transport is one of the main sources of atmosphere pollutants. The major share among the types of transport is that of the motor transport. Impact of other kinds of transport is not so big and it is evident in the places of concentration of its facilities. Constant growth of the value of air transport results in an increased air pollution caused by aircraft engine exhaust gases.

Air smoke content causes changes in atmosphere transparency and, as a consequence, reduction of visibility, illuminance, increased ultraviolet radiation and leads to a deterioration of microclimate in towns and cities and increase of number of foggy days.

Volatile matters of natural impurities that reach into the atmosphere and that are able to scatter and stay there for a very long time, get into the lungs and have a negative effect to human life, fall on leafs stopping photosynthesis process, slow down plant growing, prevent oxygen generation. Polluted air restricts the penetration of sun light radiation to the ground surface.

Atmosphere pollution causes considerable damage to economy. According to the Environment Protection Agency estimates, the losses of economy in connection to death rate and illness due to environment pollution in the USA every year amount to 6 billion Dollars. Damage caused by metal corrosion, crop yield reduction and plant destruction amounts to 4,9 billion Dollars.

Impact to hydrosphere. Traffic is a serious water pollutant. Together with the exhaust gases generated by transportation means driven by internal combustion engines, a large amount of detrimental matters gets into water – solid (soot, lead alloys) and gaseous (carbon oxides, nitrogen oxides, sulfur oxides, different hydrocarbons, aldehydes).

River transport exerts a detrimental effect upon water basins through chemical and biological pollution. Chemical pollution occurs as a consequence of oil spill in case of vessel accidents, spillout of oil products in the process of coal loading as well as in cases of aggressive chemical and other goods handling.

Table 4.2. Main atmosphere pollutants and their sources

Pollutants	Main Sources		Average Annual Concentration in Air mg/m3
	Natural	Anthropogenic	
Particulated matters (ashes, dust, etc.)	Volcanic eruptions, dust storms, forest fires	Fuel combustion in industrial and household installations	In cities and towns 0,04 – 0,4
Sulfur dioxide	Volcanic eruptions, oxidation of sulfur and sulfate scattered in the sea	Same	In cities and towns up to 1,0
Nitrogen oxides	Forest fires	Industry, transportation, thermal power plants	In areas with developed industry up to 0,2
Carbon oxides	Forest fires, ocean evaporations, terpenes oxidation	Transportation, industrial power plants, ferrous metallurgy	In cities and towns from 1 to 50
Evaporable hydrocarbons	Forest fires, natural methane, natural terpenes	Transportation, waste incineration, oil products evaporation	In areas with developed industry up to 3,0
Multiring aromatic hydrocarbons	-	Transportation, chemical factories and oil refineries	In areas with developed industry 0,01

Impact to dry land. Transport negative influence to dry land is the following:

1. Occupation of large territories by transport facilities (roads, ports, stations, etc.). For instance, between two main-line railway stations it is necessary to allot a 100-150 m wide belt. Much larger areas are required for motor roads, and the length of motor road network exceeds significantly the length of railway network. Large territories are occupied by sea and river ports. In the contemporary airport zone, up to 120 km2 becomes unfit for population for the flight safety reasons and because of excessive noise.

2. Destruction, in many cases, of upper fertile soil layer (when constructing motor roads, railways, laying of pipelines).

3. Soil pollution by poisonous components in transportation means exhaust gases – lead, sulfur compounds that with moisture make acids, ashes, soot.

4. Pollution by oil products, oils, different wastes, garbage, as well as by waste waters that get directly into soil and that contain matters detrimental to environment.

5. Covering of large areas by asphalt and concrete which alters soil conditions, disturbs its moisture supply, and in cases of abundant rains, soil is washed away by water currents.

Reduction of negative impact of transport to environment is a complex social, economical and technical task, the solution of which can be accomplished by applying complex environment protection measures. The most important of these measures are development and application in the vehicular fleet of new power generating units, as well as the use of less environmentally detrimental fuels.

In case of railway transport, further electrification of railway network will exclude atmosphere pollution generated by diesel engine exhaust gases.

River fleet is equipped with effective installations intended for cleaning and disinfection of household and waste waters as well as waters polluted by oil.

On fleet vessels are undertaken measures for the prevention of biological pollution of water basins.

Vessels are outfitted with containers for accumulation of pollutants, separation facilities, means for destruction and neutralization of pollution products, means of control of waste waters discharges.

Elimination of consequences of oil products spill and other polluting matters is carried out by means of special equipment for oil catching.

Important measures aimed at protecting water basins against pollutions are the measures of construction and reconstruction of water treatments plants, introduction of return water supply and enhanced means and methods of treatment of industrial and household waste waters, rationing of water consumption and reduction of untreated spills.

CONCLUSION

Influence of politics and culture upon the development and operation of traffic, i.e. transportation systems has as a consequence resultant effectiveness, safety, security and ease of use of the system and, especially, upon the environmental problems. This is the reasons why the warnings contained in this paper have special importance and urgency.

Modernization of infrastructure, transportation means and machinery is a big chance for our engineering industry and in that respect ability and readiness are to be shown.

At the same time, closer attention should be dedicated to the issue of transport in the engineering faculties programmes in our country.

LITERATURE

[1] Matejić, V., Prilozi istraživanju naučnog i tehnološkog razvoja – Federal Secretarial for Development and Science Savezni – Belgrade, 2002

[2] Group of authors, Strategija privrednog razvoja Srbije – Ministry for Science, Technology and Development – Belgrade, 2002

[3] Simović, T., OSNOVE INTEGRALNOG TRANSPORTA (textbook to be published)

D SESSION:

TERMOTECHNIQUE, ENVIRONMENT PROTECTION AND URBAN ENGINEERING

GAS COMPOSITION AND EXERGY EFFICIENCY DETERMINATION AT CARBON BOUNDARY POINT IN THE DOWNDRAFT BIOMASS GASIFICATION PROCESS

R. Karamarković, V. Karamarković, M. Marašević

Abstract: *Biomass as a renewable energy resource has a great energetic potential. There are a lot of incentives all over the world, such as for example CDM program, for implementation of waste biomass. This paper focuses on the wood chips gasification in an idealized downdraft equilibrium gasifier. The model for determination of carbon boundary temperature and other important parameters at carbon boundary temperature such as gas composition, exergy efficiency of the process was developed. The purpose of this paper is to determine upper limit for exergy efficiency that should be expected from the downdraft gasification process in dependace of moisture content in wood chips. In addition to this, to diagnoze if and what kind of measures should be taken with wood chips' moisture prior to the gasification process. In the model idealized gasifier is used in which chemical equilibrium is achieved, ashes are not taken into consideration and heat losses are ignored.The gasification efficiencies are calculated at carbon boundary temperature, where exactly enough air is added to achive complete gasification and avoid carbon in the solid residual. It is shown that the exergy efficiencies are lower than the energy efficiencies, and also, that exergy efficincies decrease with the increase of moisture content in the biomass. Also it is shown that overall exergy efficiency of the process decrase with slower rate than exergy efficiency based only on chemical exergy. For wood chips with high moisture content exergy efficiency could be improved by drying the biomass prior to gasification process.*

Keywords: *Biomass, wood chips, gasification, chemical equilibrium, carbon boundary point,exergy efficiency, energy efficiency.*

1. INTRODUCTION

According to [1] Serbia has relatively large biomass energy potential. The total excess biomass energy potential is estimated at 115 000 tera Joules per year (TJ/year) of which 50 000 TJ/year accounts for the local wood waste, while the remaining amount of 65 000 TJ/year accounts for agriculture waste. This work is focused to wood chips that are nowadays piled and wasted. Huge amounts of wood chips are deposited especially during summer period of year into rivers, and cause great environmental problems in the area of Kraljevo. Also, from huge piles of wood chips there are methane emissions that are caused from the anaerobic biomass decay. This methane emissions and wind dispersion are the main reason why wood chips are not allowed to pile just for the heating season.

Biomass gasification is an interesting energy conversion technology where this biomass could be used. Gasification is the process of gaseous fuel production by partial oxidation of a solid fuel. This means in common terms to burn with oxygen deficit. The gasification of coal is well known, and has a history back to year 1800. The oil-shortage of World War II imposed an introduction of almost a million gasifiers to fuel cars, trucks and busses especially in Scandinavian countries [2].

The main differences concern how reactants and products are moved around in the reactor, and the resulting reaction conditions. The reactors may be operated at atmospheric pressure or at higher pressures,

The Kyoto protocol emphasizing the need to combat carbon dioxide emission has also been an impetus for the interest in biomass gasification. Carbon dioxide emissions from using biomass as a fuel are perceived as neutral because this carbon dioxide is fixed by photosynthesis in a relatively short period.

Gasification belongs to thermochemical conversion processes together with combustion, pyrolysis, and liquefaction.

As a medium for gasification air, pure oxygen, water vapor, carbon dioxide and hydrogen can be used. In practice and in commercial applications air and water vapor are the most common, but also there are cases where pure oxygen is used as a gasifying medium.

The product of gasification is synthesis gas that consists mainly from carbon monoxide, carbon dioxide, methane, nitrogen, hydrogen and water vapor. The heating value depends on the gasification medium, solid fuel characteristics, gasification process and the temperature in the gasifier. The gas is used for electricity, heat and fuel production.

The types of gasifiers are various, but may be divided into three main groups [3]: entrained flow gasifiers, fluidized bed gasifiers (bubbling/circulating) and fixed bed gasifiers, where the last is subdivided into: counter-current (updraft), co-current (downdraft) and cross-current moving bed.

Ass.Msc. Rade Karamarković, Faculty of Mechanical Engineering Kraljevo, karamarkovic.r@mfkv.kg.ac.yu
Ph.d.-ing Vladan Karamarković, Faculty of Mechanical Engineering Kraljevo, karamarkovic.v@mfkv.kg.ac.yu
Ass.Msc. Miljan Marašević, Faculty of Mechanical Engineering Kraljevo, marasevic.m@mfkv.kg.ac.yu

but the latter is only available to bubbling or circulating fluidized bed reactors, but at considerable higher cost. The higher cost may be earned downstream due to smaller equipment size and higher reactivity.

2. GASIFIER MODEL

The gasification process considered in this paper is schematically presented in Fig.1. Biomass, in this case wood chips enter the gasifier from the top. Biomass, and air which is used as a gasification medium, are at the standard reference state (p = 0.1 MPa, t = 25 ^{0}C).

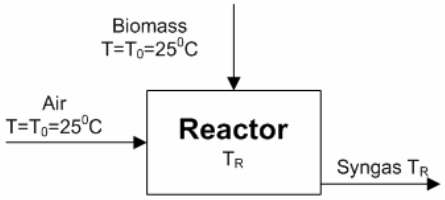

Fig. 1. Schematic diagram of the downdraft gasifier

A chemical equilibrium model is applied to predict carbon boundary temperature, product gas composition, gas amount and carbon conversion in the gasifier. There are a lot of equilibrium models in the literature [4] – [7]. In [7] there are a lot of references on gasification equilibrium models in literature, and on characteristics of these models.

Equilibrium models are valuable because they predict the thermodynamic limits of the gasification reaction system. However, equilibrium models are based on the following assumptions:

- The gasifier is regarded as a perfectly insulated device. It means that heat losses are neglected. In practice, gasifiers have heat losses to the environment, but this term can be incorporated in the enthalpy balance of the equilibrium model. In this model of the gasifier heat losses are included in energy balance equation as a parameter.
- Perfect mixing and uniform temperature are assumed for the gasifier. This can lead to large errors in some types of gasifier where residential time is to short and where uniform temperature could not be assumed. But, for downdraft gasifiers according to [7], the equilibrium model has good predictive potential. The reason is that in the downdraft gasification process devolatilization takes place in the upper part of the gasifier, and devolatilization products are forced to pass through a narrow cross-section, the so-called throat, in which the temperature is high. The syngas leaves the gasifer at the bottom with the temperature equal to the temperature in the reduction zone, which is placed under the hot oxidation zone.
- The model assumes that gasification reaction rates are fast enough and residence time is sufficiently long to reach equilibrium state.
- No information about reaction pathways/ formation of intermediates.
- Tar is not modeled.

Under gasification conditions (with temperature between 600 and 1500K) the only species present at concentrations greater than 10^{-4} mol% are H_2, CO, CO_2, CH_4, H_2, N_2 and solid C. Carbon monoxide, hydrogen and methane contribute to the heating value of the product gas, other gases are not desired in the synthesis gas. The following reactions are relevant for carbon conversion into gaseous components [7]:

$$C + 2H_2 = CH_4 \quad (1)$$
$$C + H_2O = CO + H_2 \quad (2)$$
$$C + CO_2 = 2CO \quad (3)$$

In steam and air gasification, all these reactions occur so that the endothermic water-gas (2) and Boudouard (3) reactions are coupled to the exothermic methane formation (1) reaction. Coupling of endothermic and exothermic reactions is very attractive in order to achieve a high thermodynamic efficiency.

Another very important characteristic of the gasification process that should be defined prior to the introduction of the model is the equivalence ratio ER. It is defined as the ratio of the oxygen (air) that is introduced into the gasifier to the amount of oxygen (air) which is needed for complete combustion of the given fuel, in this case wood chips.

The model calculates also the carbon boundary temperature. The temperature obtained when exactly enough oxygen is added to achieve complete gasification (no solid carbon present). It is important to say that the gasification process has its optimum at the carbon boundary temperature, because exactly enough oxygen is added to achieve complete gasification. If more oxygen is used the produced gas loses its heating value, until complete combustion is achieved.

The unknowns in the model are:

- gas amount,
- gasification temperature (carbon boundary temperature),
- molar fractions of H_2, CO, CO_2, CH_4, H_2, N_2,
- equivalence ratio ER.

In total there are nine unknowns, and two parameters:

- amount of ungasified carbon and
- gasification pressure.

In the model as gasifing medium combustion air is used with molar fractions of 21% and 79% for oxygen and nitrogen respectively.

The following reactions are used in the model:

- the sum of unknown molar fractions in the produced gas equals 1.

$$X_{CO} + X_{CO2} + X_{CH4} + X_{H2} + X_{N2} + X_{H2O} = 1 \quad (4)$$

- equilibrium equations for the three reactions (1)-(3)

for methane formation reaction (1)

$$K_e = \frac{X_{CH_4}}{X_{H_2}^2} \cdot \left(\frac{p_o}{p} \right), \quad (5)$$

for Boudouard reaction (3)

$$K_e = \frac{X_{CO}^2}{X_{CO_2}} \cdot \left(\frac{p_o}{p} \right), \quad (6)$$

for water gas reaction (2)

$$K_e = \frac{X_{CO} + X_{H_2}}{X_{H_2O}} \cdot \left(\frac{p_o}{p} \right). \quad (7)$$

For determination of the left hand sides of reactions (5)-(7) theoretical expressions are used. For determination of heat capacities for gases expressions were taken from [8], page 813. These heat capacities are used for determination of enthalpies, entropies and gibbs functions of all gases. In these calculations all gases are considered to be ideal, and expressions for ideal gases are used. For determination of solid carbon heat capacity that is used in energy balance equation the polynomial expression is taken from [9] (page 277).
The other reactions that are used in the model are:

- H_2/C balance,
- O_2/C balance,
- O_2/N_2 balance,
- Mass balance equation, and
- Energy balance equation.

Biomass composition that is used in the model was taken from [10] (page 210).
The model was made in Modelica language. It is object orientated language for modeling of large scale physical systems. As a tool that supports the language was used Dymola.

3. EXERGY EFFICIENCY

Exergy is defined in thermodynamics as a measure of the actual potential of a system to do work. In processes, such as combustion, gasification, hydrogenation and steam reforming, fossil and renewable fuels are converted into a different fuel and/or heat and/or electricity. For example, gasification of a fuel involves converting the chemical energy contained in the fuel into chemical energy contained in the gaseous products and sensible heat of the produced gas. According to the first law of thermodynamics, energy can never be lost. Therefore it is justified to state that energy conversion processes do not have energy losses, except for losses from the process system into the environment. However, the second law of thermodynamics should also be considered. Energy conversion processes are accompanied by an irreversible increase in entropy, which leads to a decrease in exergy (available energy). Thus, even though the energy is conserved, the quality of energy decreases because energy is converted into a different form of energy, from which less work can be obtained.

The exergy balance of the biomass conversion process is presented in the following form:

$$\sum_{in} E_J = \sum_{out} E_K + I \quad (8)$$

In this equation first and second term represents exergy flows of all entering and leaving stream, respectively.

In equation (8) the term *I* represents irreversibilities. It is the difference between all entering exergy streams and that of leaving streams. Exergy is not conserved but subjected to dissipation. It means that the exergy leaving any process step will always be less than the exergy in.
The exergy of stream of matter E depends on its composition (chemical exergy E_{ch}) and its temperature and pressure (physical exergy E_{ph})

$$E = E_{CH} + E_{PH} \quad (9)$$

In the above formula all terms are in kJ.
The standard chemical exergy of a pure chemical compound ε_{ch} is equal to the maximum amount of work obtainable when a compound is brought from the environmental state, characterized by the environmental temperature T_o and environmental pressure p_o, to the dead state, characterized by the same environmental conditions of temperature and pressure, but also by the concentration of reference substances in standard environment. The chemical exergy of the mixture $\varepsilon_{ch,M}$ is determined by the composition and concentration of components in the mixture:

$$\varepsilon_{ch} = \sum_i x_i \cdot \varepsilon_{0i} + R \cdot T_0 \sum_i x_i \cdot \ln x_i \quad (10)$$

In this formula X_i are molar fractions of gases in the mixture, R = 8.314 kJ/kgmole universal gas constant, and T_0=298 K environment temperature.
The physical exergy of a mixture can be calculated using enthalpies and entropies of all gases that are presented in the mixture:

$$\varepsilon_{ph} = (h - h_0) - T_0 \cdot (s - s_0) \quad (11)$$

where *h* (kJ/kgmole) and *s* (kJ/kgmoleK)are enthalpy and entropy of a system at given temperature and pressure, and *ho* (kJ/kgmole) and *so* (kJ/kgmoleK) are the values of these functions at the environmental temperature and pressure.
The exergy of the biomass is obtained by using the following forumula [11]:

$$\beta = \frac{\varepsilon_{ch}}{LHV_{biomass}} \quad (12)$$

Where ε_{ch} is the chemical exergy of biomass (kJ/kg), and LHV (kJ/kg) is the lower heating value of the biomass. The ratio β was statistically determined by Szargut and Styrylska (1964) and is taken from [11].

$$\beta = \frac{1.044 + 0.0160 \cdot \left(H/C\right) - 0.3493 \cdot \left(O/C\right) \cdot \left[1 + 0.0531 \cdot \left(H/C\right)\right] + 0.0493 \cdot \left(N/C\right)}{1 - 0.4124 \cdot \left(O/C\right)}$$

(13) – for solid biofuels.
Biomass' lower heating value is obtained by a formula taken from [10], page 214.

$$LHV = 340 \cdot C + 1190 \cdot \left(H - \frac{O}{8} \right) + 93 \cdot S - 25 \cdot W \quad (14)$$

Where in equations (13) and (14) C, H, O, S, W are mass fractions of carbon, hydrogen, oxygen, sulphur and water in the biomass.

Having defined all previous quantities all three efficiencies can be calculated. Chemical efficiency represents chemical energy that is conserved in the produced gas and is calculated by:

$$\eta_{ch} = \frac{LHV_{gas}}{LHV_{biomass}} \quad (15)$$

This efficiency is also known as the cold-gas efficiency.

The chemical exergy efficiency is defined as the ratio between chemical exergy of product gas and biomass:

$$\eta_{ex-ch} = \frac{\varepsilon_{ch,gas}}{\varepsilon_{ch,biomass}} \quad (16)$$

The definitions (15) and (16) have drawbacks [11] they ignore sensible heat contained in the synthesis gas. This gas at elevated temperature is preferred over environmental temperature and therefore the calculated efficiency should be higher. However, if the sensible heat were to be added to the energetic efficiency, this efficiency would always be 100% because the gasifier operates adiabatically. This problem can be overcome by using exergetic efficiency based on chemical as well as physical exergy:

$$\eta_{ex} = \frac{\varepsilon_{ch,gas} + \varepsilon_{ph,gas}}{\varepsilon_{ch,biomass}} \quad (17)$$

In all three equations (15)-(17) all terms are previously defined.

4. MODEL RESULTS

Table 1 shows the results of the model calculations. For large moisture content in the wood chips, larger than 25% (mass fraction), carbon boundary temperature is less than 600 ^{0}C. Since, under this temperature equilibrium is very difficult to be achieved and formation of high hydrocarbons take place, for moisture contents above 25 % (mass fraction) the amount of air that is introduced in the gasifier is larger than the amount needed to achieve carbon boundary temperature. And for wood chips with the moisture content larger than 25% in the gasifier are introduced larger amounts of air in order to achieve gasification temperature of 600^{0}C.

The efficiencies: chemical efficiency, chemical exergy efficiency and exergy efficiency of the gasification process are presented in Fig. 2.

W	0	5	7.5	10	12.5	15	17.5	20	22.5	25	27.5	30	32.5	35	37.5
C	50.57	48.04	46.78	45.51	44.25	42.99	41.72	40.46	39.19	37.93	36.66	35.40	34.14	32.87	31.61
H	6.00	5.70	5.55	5.40	5.25	5.10	4.95	4.80	4.65	4.50	4.35	4.20	4.05	3.90	3.75
O	41.86	39.76	38.72	37.67	36.63	35.58	34.53	33.49	32.44	31.39	30.35	29.30	28.25	27.21	26.16
N	0.57	0.54	0.53	0.51	0.50	0.49	0.47	0.46	0.44	0.43	0.41	0.40	0.39	0.37	0.36
A	1.00	0.95	0.93	0.90	0.88	0.85	0.83	0.80	0.78	0.75	0.73	0.70	0.68	0.65	0.63
Sum	100	100	100	100	100	100	100	100	100	100	100	100	100	100	100
LHVbiomass	19056	17981	17444	16905	16369	15831	15294	14756	14219	13681	13144	12606	12069	11531	10994
Exergy - biomass	21887	20652	20036	19417	18800	18183	17566	16948	16331	15714	15096	14479	13862	13244	12627
Equivalence ratio	0.3057	0.2579	0.281	0.3	0.3152	0.329	0.336	0.339	0.347	0.3536	0.422	0.432	0.442	0.453	0.466
Omin (m^3/kg)	0.987	0.938	0.913	0.888	0.864	0.839	0.814	0.790	0.765	0.740	0.716	0.691	0.666	0.642	0.617
Air flow (m^3/kg)	1.437	1.152	1.220	1.269	1.296	1.313	1.303	1.276	1.265	1.247	1.438	1.422	1.402	1.384	1.369
Carbon boundary T (K)	986	998	973	953	937	922	910	900	887	874	873	873	873	873	873
Carbon boundary T (0C)	713	725	700	680	664	649	637	627	614	601	600	600	600	600	600
CO	0.274	0.295	0.26	0.229	0.204	0.181	0.163	0.147	0.129	0.112	0.104	0.097	0.091	0.085	0.079
CO2	0.067	0.061	0.08	0.096	0.11	0.123	0.133	0.142	0.152	0.161	0.142	0.124	0.109	0.095	0.082
CH4	0.007	0.009	0.01	0.011	0.013	0.015	0.016	0.018	0.021	0.023	0.022	0.021	0.02	0.019	0.018
H2	0.202	0.235	0.225	0.217	0.211	0.206	0.204	0.203	0.199	0.194	0.189	0.184	0.18	0.175	0.17
N2	0.42	0.37	0.386	0.398	0.406	0.412	0.413	0.411	0.412	0.412	0.453	0.491	0.526	0.558	0.59
H2O	0.03	0.031	0.039	0.048	0.055	0.063	0.071	0.079	0.088	0.098	0.09	0.082	0.074	0.068	0.061
ngas(kgmole/kg)	0.1236	0.1062	0.111	0.114	0.1168	0.119	0.119	0.118	0.118	0.1173	0.117	0.1168	0.116	0.1151	0.1143
ngas(m^3/kg)	2.770	2.380	2.481	2.561	2.617	2.660	2.660	2.635	2.635	2.629	2.629	2.617	2.600	2.579	2.561
LHVsyngas	5897	6563	6063	5651	5321	5034	4843	4706	4513	4338	4143	3969	3803	3639	3467
Physical exergy	1341	1178	1186	1193	1193	1190	1173	1148	1130	1109	1088	1065	1041	1018	996
Chemical exergy	15921	15248	14647	14061	13499	12950	12440	11955	11449	10956	10461	9974	9491	9009	8524
Eff.(LHV)	0.857	0.868	0.862	0.856	0.851	0.846	0.842	0.84	0.837	0.833	0.829	0.824	0.819	0.814	0.808
Eff.(chem.exergy)	0.727	0.738	0.731	0.724	0.718	0.712	0.708	0.705	0.701	0.697	0.693	0.689	0.685	0.68	0.675
Eff.(exergy)	0.789	0.795	0.79	0.786	0.781	0.778	0.775	0.773	0.77	0.768	0.765	0.762	0.76	0.757	0.754

Table 1. Results of equilibrium model

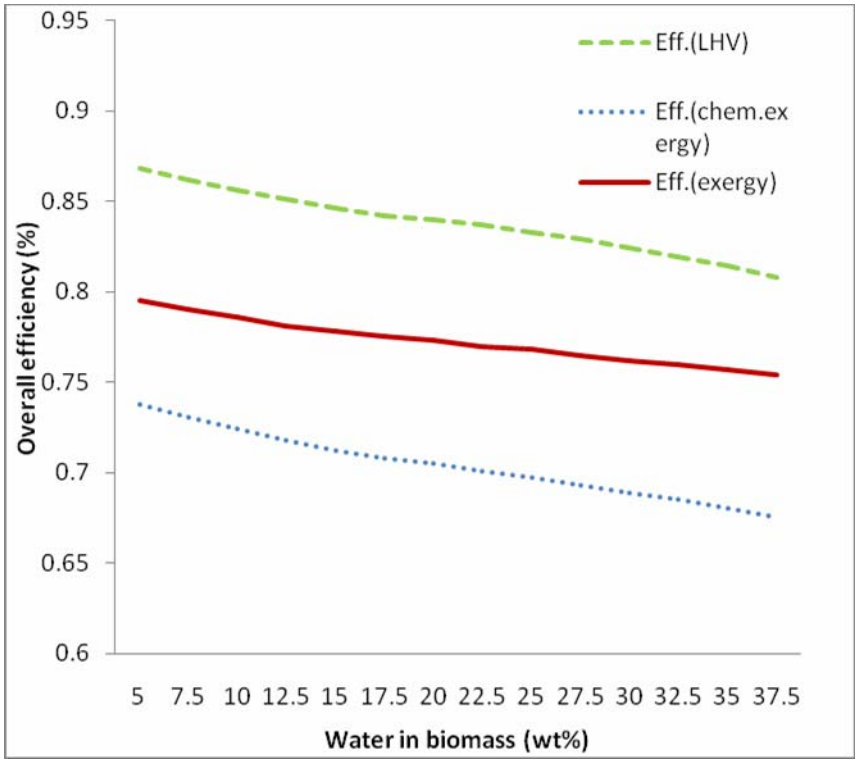

Fig. 2. Efficiencies of the gasification of wood chips with different moisture content at the carbon boundary temperature

5. CONCLUSION

Water content in wood chips can present huge problem for the gasification. Also, the product gas composition and the gasification temperature depend of the moisture content in the wood chips. The results of the model presented in the Table 1. give clear picture of the problem. Also, these data could be used to diagnose gasification of wood chips.

From Table 1. it is obvious, as it was expected, that with increase of moisture content in the wood chips the carbon boundary temperature decreases. Also, as it is known, the lower heating value and the biomass exergy decrease with an increase of the moisture content in the biomass. From Table 1. is obvious that the biomass exergy is larger than the biomass heating value. This is explained in [11] by the fact that polymers such as cellulose and hemi-cellulose are highly ordered structures, and work can be delivered if these are decomposed.

With change of the moisture content in wood chips product gas composition also changes. With the increase of moisture in wood chips the amounts of carbon dioxide, hydrogen, methane and water vapour increase and the amount of carbon monoxide decreases.

From Fig. 2 is apparent that energy efficiency is larger than both exergy efficiencies. In addition, chemical energy efficiency and chemical exergy efficiency decrease faster than overall exergy efficiency with the increase of moisture in the biomass.

From the data presented in Table 1. it is apparent that wood chips with the moisture content above 22.5 % must be dried prior to the gasification process.

6. REFERENCE

[1] Vladimir Janković: LIBER PERPETUUM The book on renewable energy in Serbia and Montenegro, Stojkov Novi Sad, 2004; 83

[2] Per Finden: Biofuels from lignocellulosic material - In the Norwegian context 2010 –Technology, Potential and Costs, NTNU, Norwegian University of Science and Technology, 2005; 22

[3] Bridgwater A.V., Renewable fuels and chemicals by thermal processing of biomass Chemical Engineering Journal 91/2003, 87-102

[4] Bošnjaković Fran: Heat science III dio, Naučna knjiga Zagreb, 1986; [in Serbo-Croatian]

[5] Vladan Karamarković: Biomass combustion and gasification, Faculty of Mechanical Engineering, Kraljevo 2003; [in Serbian]

[6] Anil Khadse, Prasad Parulekar, Preeti Aghalayam1 and Anuradda Ganesh: Equilibrium model for biomass gasification, National Conference On Advances In Energy Research, Bombay, 2006;

[7] Mark J. Prins, Krzysztof J. Ptasinski, Frans J.J.G. Janssen: From coal to biomass gasification: Comparison of thermodynamic efficiency; Energy Elsevier, Volume 32, Issue 7, July 2007; 1248-1259

[8] Balmer R.: Thermodynamics, West Publishing Company, 1990; 573-628, 813

[9] Abbott M., Van Ness H.,: Thermodynamics, Rensselaer Polytechnic Institute, 1972; 277

[10] Jankes G., Stanojević M., Karan M.: Industrial furnaces and boiler, Faculty of Mechanical Engineering Belgrade, 1996; 210 [in Serbian]

[11] Ptasinsky K. Prins M. Pierik A.: Exergetic evaluation of biomass gasification, Energy Elsevier 2007; 568-574

CONTRIBUTION TO THE NEW SOLUTION OF STEEL MULTI-STOREY DEMOUNTABLE CAR PARKS[1)]

R. Rakanovic, M. Gasic, M. Savkovic, N. Zdravkovic

Abstract: *Rapid growth and expansion suddenly brought about parking problems in larger cities in Serbia, so it became necessary to set up the demountable car parks. Accomplished researches and analyses show that there is a real demand for setting up the steel demountable multi-storey car parks in cities of Serbia whose number of citizens exceeds 20000. The number of needed demountable multi-storey car parks is greater in larger cities. The main goal of these researches considers the development of new solution adapted to our conditions, the advantages of which are: more storeys, easear assembling, lower price, engagement of domestic firms in production, assembling and accessory works.*

Keywords: *multi-storey car parks, module, steel construction.*

1. INTRODUCTION

Accomplished researches are related to the development of new solution accommodated to our conditions and should be distinguished with set of advantages such as: increased number of storeys, appreciably lighter construction, modular character of construction, lower price in comparison with imported ones, fast and easy assembling, disassembling and dislocating to new location without any extra work. By this research a new technical and technological solution of steel demountable multi-storey car park has been developed which meets the conditions and needs of our cities. The main activities which are to be performed are based on improving the single module variant solutions in order to obtain the original one. Designed modular solution should satisfy the wide rang of requirements of our market with capability of selling abroad, especially in contiguous countries. The development of this solution brings about the possibility of competitive domestic product by price and quality.

By now, the steel demountable multi-storey car parks have been imported from abroad exclusively, with many limitations with respect to conditions of usage in our cities, highly priced and with complex and non-efficient control and payment information system. By this project [1], a new solution has been obtained, suitable for our conditions with lighter construction and increased number of storeys.

Actually, the new multi-storey car park presents modular solution of multi-storey garage which can be easily accommodated to meet the wide range of requirements with respect to number of storeys and configuration of new car parks.

Also, the elements of construction are designed in such manner that they can be completely manufactured at domestic market, which is very important. The elements' shape and production technology are projected completely in accordance with capabilities of domestic middle rank companies, without extra investments in new high technology equipment.

It's very important to emphasize the advantage of this solution concerning the capability of easy demounting and dislocating to other locations, if required.

2. THE BASIC CHARACTERISTICS OF EXISTING SOLUTIONS

Italian company "Fast Park" is considered as the greatest manufacturer of demountable multi-storey car parks. The basic characteristic of that solution is that the carrying plate below the vehicle, made of reinforced concrete, is placed on steel tubular pillars by means of INP steel girders.

In some fields the braces are used as a stiffeners. This type of solution has satisfying carrying capacity and working stability. The main disadvantages of these solutions are: great mass of reinforced concrete plate (about 5 tons per field), difficult moving to new location, great number of engaged workers and machines in order to dislocate the car park to new location.

Just for these reasons, a new solution has been developed in the project [1], eliminating cited faults.

Examples of installed solutions of Italian company "Fast Park" are shown in figures 1-3.

1) The paper is a result of a research in the project "New solution of steel modular multi-storey car parks" financed by the Ministry of Science and Environmental Protection of Republic of Serbia

Prof. Dr.-Ing. Ranko Rakanovic, Faculty of Mech.Engineering Kraljevo,Dositejeva 19, 36000 Kraljevo,e-mail:rakanovic.r@mfkv.kg.ac.yu
Prof. Dr.-Ing. Milomir Gasic, Faculty of Mech.Engineering Kraljevo,Dositejeva 19, 36000 Kraljevo,e-mail:gasic.m@mfkv.kg.ac.yu
Ass. Dr.-Ing. Mile Savkovic, Faculty of Mech.Engineering Kraljevo,Dositejeva 19, 36000 Kraljevo,e-mail:savkovic.m@mfkv.kg.ac.yu
Ing. Nebojsa Zdravkovic, Faculty of Mech.Engineering Kraljevo,Dositejeva 19, 36000 Kraljevo,e-mail:zdravkovic.n@mfkv.kg.ac.yu

Fig. 1. *Storey car park - Bologna airport, capacity of 1500 parking places*

Fig. 2. *Storey car park -Empoli, capacity of 360 parking places*

Fig. 3. *Storey car park -Torino, capacity of 320 parking places*

It is often necessary to adapt the shape of storey car parks to the requirements, regarding the available location shape, the terrain configuration, the number of places, the outer look and shape, the existing buildings, etc. For these reasons, the shape of storey car parks could be irregular, which makes it much harder for the constructors and workers.
The examples of installed solutions, with special demands shown, are presented in figures 4-7.

Fig. 4. *Storey car park -Stockport, capacity of 232 parking places*

Fig. 5. *Storey car park -Charleroi, capacity of 204 parking places*

Fig. 6. *Storey car park -Via G. Borea, capacity of 320 parking places*

Fig. 7. *Storey car park -Ospedale di Circolo, capacity of 239 parking places*

3. THE BASIC CHARACTERISTICS OF NEW SOLUTION

In order to make an improved solution of constructing the metal demountable storey car park, it is necessary to consider the wide range of real demands at certain locations. We need to take the most important demands from the great number of them, by whose solving we get the solution that fulfils the greatest number of technical conditions for construction. Defined urban conditions in cities are the key element for forming the variety solution, because these conditions define the significant parameters in projecting, such as: drives, height and global shape of modular demountable storey car park.
Some of specific demands are shown in figure 8, regarding the location shape, and in figure 9 the terrain configuration.

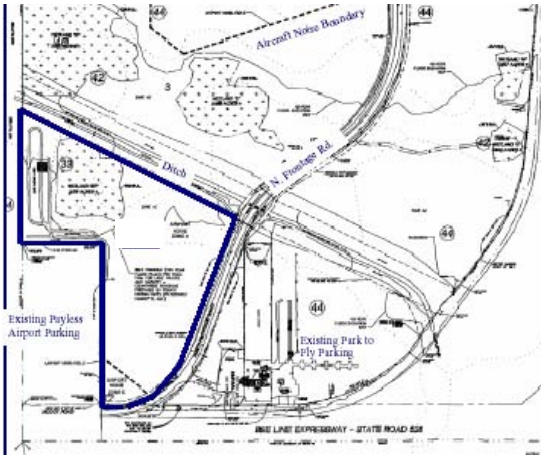

Fig. 8. *Complex shape of location for car park assembling*

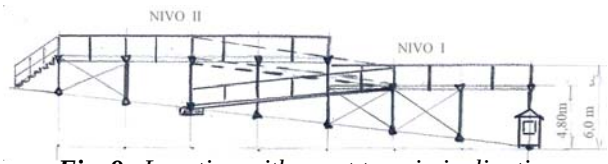

Fig. 9. *Location with great terrain inclination*

These parameters are determined beforehand by urban conditions and modular solution is planned in such way that it can be adjusted to all real regulated demands met in practise.
It is also necessary to take into consideration all the demands from the domain of traffic, which are defined by appropriate regulations regarding the determined inclination of paths for cars coming up and down, the size of drives, reciprocal position of approaching and leaving ramps, fire exit position, paths for people coming up and down - car park customers and working stuff.
The demounting storey car park module must be planned so that its combining with itself forms multi-storey car park in accordance with customers demands and regulations.
When the shape and large scale dimensions of module are achieved, it is necessary to develop its constituent elements.
In this activity it is especially important that the designed elements of module have the following characteristics emphasized:

- simple shape
- satisfactory carrying capacity
- simple fitting with other elements of module
- relatively simple production
- simple assembley
- smaller mass
- kind of material built in that can be obtained in domestic market.

After projecting the variety module solutions, it is needed to make the criteria for choice of the optimal one. The criteria for choice of optimal solution must contain elements of technical and technological conditions and limitations, as well as the economic indicators.
When criteria defining is finished, the analysis of proposed solutions and optimal variant choice are done. The look of plates carriers elements bond and two different storeys is shown in figure 10.

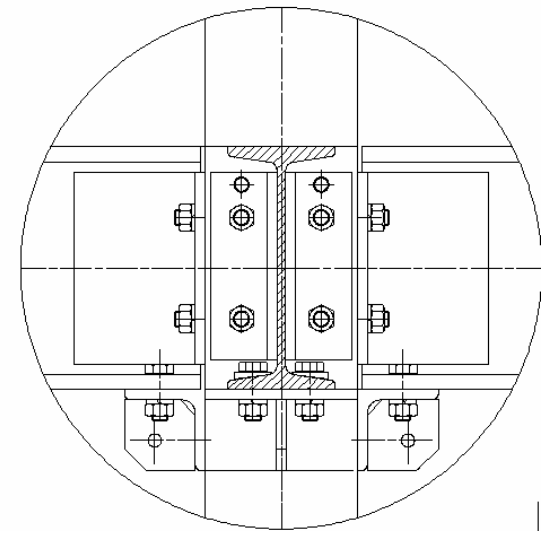

Fig. 10. *Bond of plates carriers and two storey elements*

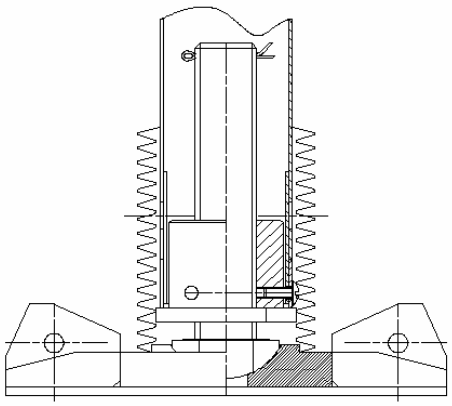

Fig. 11. *Pillar's support on concrete base*

The proposed solution enables easy levelling of storey car park on uneven terrains at which the construction stability is not endangered.

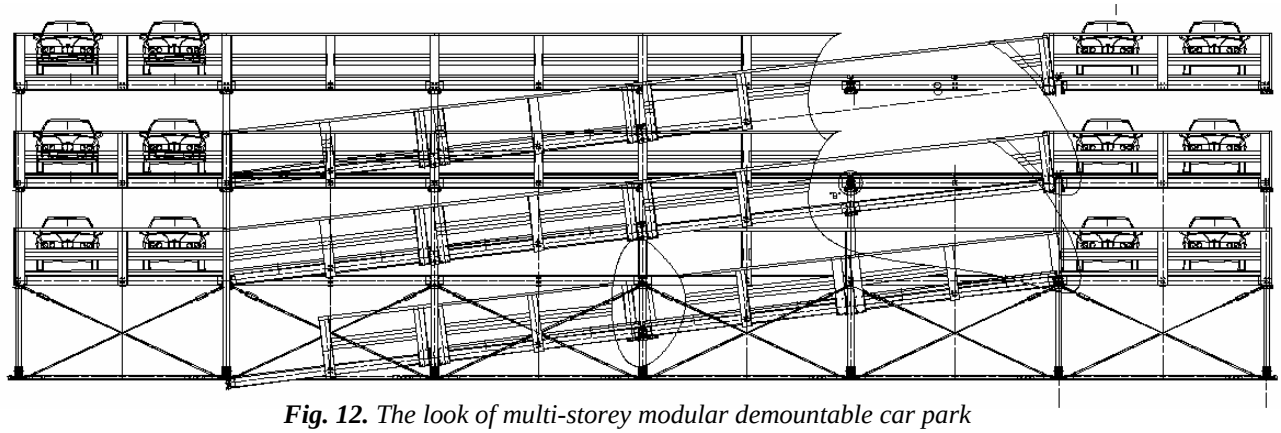

Fig. 12. *The look of multi-storey modular demountable car park*

Also, it is necessary to point out that carrying support plate of reinforced concrete is replaced by steel plate that in upper zone could be coated with thin layer of asphalt or perforated tin, depending on investor's demand. In this way we obtain significantly lighter construction of support plate itself, but also the skeleton of carrying steel construction.
New solution was successfully installed and researched on location in Jagodina (figure 13).

Fig. 13. *Storey car park - Jagodina, capacity of 139 parking places*

4. CONCLUSION

By making the new solution of modular demountable storey car park, we reached the basic demands which are represented in lighter construction, simple shape, satisfactory carrying capacity, simple fitting into surrounding with other module elements, relatively simple production and assembling. Analyses have shown that construction of one field is 30% lighter related to standard carryings out like "Fast park", that is 60% if the building in of complete metal support plate is done.
Also, analyses show that the price of making this solution, by the parking area unit, is about 25% lower compared to carryings out like "Fast park".

REFERENCE

[1] Rakanovic R., Gasic M., Savkovic M. and others.: New solution of steel multi-storey car park, Faculty of Mechanical Engineering Kraljevo, Innovation project, 2007.

[2] www.parkfast.com

INTEGRATION OF THE KINEMATIC CHARACTERISTICS OF SORTING WITH AUTOMATIC MANAGING OF SORTING WHILE COMMISIONING IN LOGISTIC CENTRES

M. Bukumirovic, A. Cupic, G. Markovic

Abstract: *While commissioning loads in great warehouses and distributive centres, or in post-office logistic centres, the most important thing is to foresee the appropriate system for sorting. For that it is necessary to know the kinematical parameters of sorting, that is, the possibilities of the executive machines for sorting. With an integration of kinematical parameters of sorting and managing possibilities of the processing and/or personal computer, we can successfully define sorting system, as well as the system for his automatic managing.*

Key words: *kinematics, sorting, sorting, logistic centres*

1. INTRODUCTION

In great warehouses and distributive centres, in the warehouses of mayor sale, and also in the larger supermarkets, there is constant need for unification of different articles for the request of the buyer (the user who delivered enquiry), from total quantity of the assortment, based on the demand. Analogue process is performed in great factory warehouses of montage parts and components. Then, for each final product, we need to locate and unify necessary made parts and/or components to provide the process of montage. This activity is known as process of commissioning [1,3].
Functionally the same process is being developed in post-office logistic centres, that is, their distributive warehouses. In that case, this process is even more complicated and noticeable because in postal centres there is also parcel sorting process.

2. MAIN TRANSPORT FLOW IN SORTING

Contemporary transport machines (of constant effect) are basic technical systems for accomplishing the transport flow. The separation itself – turning of the command load (material, parts, packed goods, parcels) from the main transport flow to the gathering place of a certain destination most frequently is realized by the turning machines – diverters [1,2,3]. In all the technical systems and processes this separation – turning of the elements of the flow from the main transport flow is called sorting or assorting [1,2,3,7].
Sorting itself can be performed in many ways, and most frequently:

- diverters with sliding arms (trips),
- turning the carrying platforms or carrying slats,
- moving the belt on horizontal cross-belt trays and
- moving the sliding shoes (plates) along the horizontal slats.

In transport flow, while sorting on belt transporters, with sliding diverter with arm (fig. 1.) independently of the fact if half-automatic sorting is applied, command load (parcel) is being identified in the beginning of the main transport flow in the translator spot of photocell (FĆ3) or scanner (in spot 0-0). Identification also shows the address of a load destination, about which a computer's informed with a signal (of position).
Between crossing of an identification of the position in the beginning of the transport flow in 0-0, and of the machine – of the chute of destination for users, on the road of transport (1, 2, 3,...,k,...) there are fixed (construction) distances: from 0-0 to 1 – L_1, from 0-0 to 2 – L_2, to Lk between 0-0 and k. Connected chutes like adding devices of destination have widths: L_1, L_2, L_3,..., Lk (fig. 1.). Next to the sorting transporter on one and/or the other side, belonging turners of the destination are embedded: S_1, S_2, S_3,..., Sk. Distance between the axis of the sliding arms, which are turning while sorting, related to the position of photocell (FĆ3) is also constant: L_{S1}, L_{S2}, L_{S3},..., Lsk,... (fig. 1.). What is important for the transport flow is that the command load, under the effect of the force of its own weight and the force of rubbing, stands still ("fixed") on the carrying element of the system: belt, tray, slats, beginning from crossing spot 0-0 position and the time of the start of transport (T_0=0) on the road of the destination distance Lk [1,3].

PhD. Milan Bukumirovic, retired professor emeritus, m.bukumirovic@sf.bg.ac.yu
Msc. Aleksandar Cupic, Faculty of Transport and Traffic Engineering, Belgrade, a.cupic@sf.bg.ac.yu
Msc. Goran Markovic, Faculty of Mechanical Engineering Kraljevo, g.markovic@mfkv.kg.ac.yu

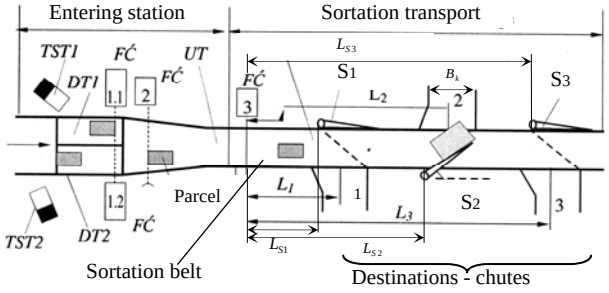

Figure 1. Transport system for sorting of command loads – parcels by sliding diverters with arms

Components of the entering station:

TST1, TST2 – keyboard 1 и 2; FĆ – photocells (1.1, 1.2, 2, 3); DT1, DT2 – dosing transporters; UT – introducing transporter;

Components of the sorter:

Sorting belt; S_1, S_2, S_3 – sliding diverters with arms.

3. KINEMATIC PARAMETRES OF SORTING AND WORK OF THE DIVERTERS

It is convenient to describe moving of the command wares while sorting with its kinematical parameters: transport road of sorting (L_{sort}), road of turning (S), speed of transport (transport flow) ν_t and speed of turning ν_s. Also it is necessary to know times: of transport (T_{tr}), turning (T_s) and sorting (T_{sort}).

From the figures 1 and 2, for the k-th diverter (S_k) transport road of sorting $L_{k.sort}$ is:

$$L_{k.sort} = L_{s.k.} + S \text{ (m)} \qquad (1)$$

The road of turning of the load – parcels along the sliding table – trip of the diverter (S) can be expressed in relation to the width of the belt of transporter (B) and the constructive angle of twisting of diverter (fender) α, while moving regularly is:

$$S = \frac{B}{\sin\alpha} \text{ (m)} \qquad (2)$$

Now, according to (1) and (2), the road of sorting is:

$$L_{k.sort} = L_{s.k.} + \frac{B}{\sin\alpha} \text{ (m)} \qquad (3)$$

At the stationary inclined diverter, slating turning plane (table trip) 1 twists around its axis 2 and directly affects the parcel (fig. 2.). Turning plane (straight or broken) can take two position parallel un-working position, or under the angle in relation to longitudinal axis for the belts of transporter, that is, working position.

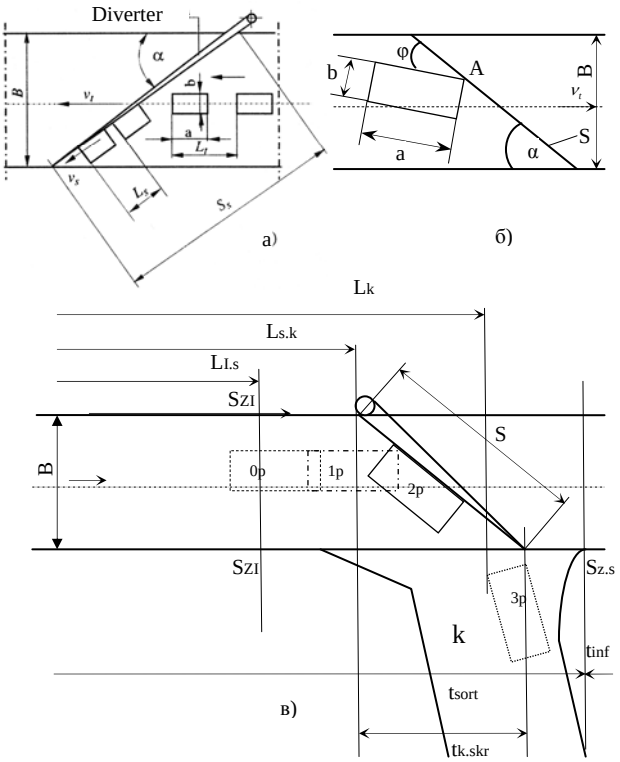

Figure 2. Schemes of the schedule of parcels on a vertical plane of the directing diverter and the belt of transporter while sorting

a) Schedule of parcels on the diverter and the belt of transporter; b) Contact (hit) of the load with the table trip and the beginning of twisting; c) Process of sorting (identification and diverting)

0p – 3p positions of parcel while sorting: 0p – place of identification; 1p – contact; 2p – twisting, sliding; 3p – parcel is sorted (on slider).

Each transporter has its own real (projected) speed of the belt ν_t. While diverting and sliding, relative speed of diverting ν_s (speed of sliding of the load along the table trip of the diverter, length S), with an angle of inclination α and angle of rubbing ρ, is calculated with a following formula [2,9]:

$$\nu_s = \nu_t \frac{\cos(\alpha + \rho)}{\cos\rho} \qquad (4)$$

Thanks to the obtained values (from the expressions 1 to 4), we can determine the times of diverting and sorting for k-th destination ($T_{k.sort}$) as a summary of the time of transport to the k-th diverter ($T_{k.tr}$) and times of diverting – sliding of load down the diverter (T_s):

$$T_{k.sort} = T_{k.tr.} + T_s \quad \text{за} \quad T_{k.tr.} = \frac{L_{sk}}{\nu_t} \quad \text{и} \quad T_s = \frac{S}{\nu_s} \qquad (5)$$

And so we obtain:

$$T_{k.sort} = \frac{L_{s.k.}}{v_t} + \frac{S}{v_s} = \frac{1}{v_t}(L_{s.k.} + \frac{B\cos\rho}{\sin\alpha\cos(\alpha+\rho)}) \quad (6)$$

For every kind of material, package, and similar, these values are being calculated and memorized (4-6).

3.1. Diverter working cycle time and minimal distance between materials

From what was pointed out earlier, it is clear that the time of the working cycle of diverter $T_{c.s}$ contains of:

- time of twisting (opening) and placing in working position, that is, ”triggering” of a table trip (T_o),
- time of working action and the position when the load is moving (that is, turning, sorting, separating) along the table trip (T_r) and
- time of recurrent turning/twisting - ”closing” of a table trip (T_p) in the starting position.

Positioning states of a table trip are being identified with the border (micro)switches (Sz) (fig. 2b).

For these values time of work of diverter is:

$$T_{c.s} = T_o + T_r + T_p \quad (7)$$

Times of the placing in a working position and recurrent twisting are the same: $T_z = T_o = T_p$, while the working time is equal to time of diverting $T_r = T_s$ so we gain (according to 4, 5, 6 and 7):

$$T_{c.s} = 2T_z + T_s = 2T_z + \frac{B}{v_t \sin\alpha\cos(\alpha+\rho)} \quad (8)$$

If the twisting of a table trip is realized (approximately) with a constant angle speed – ω_z., then the time of twisting (”triggering” and closing) of table trip:

$$T_z = \frac{\alpha}{\omega_z} \quad (9)$$

Now the time of a working cycle of diverter is:

$$T_{c.s} = 2\frac{\alpha}{\omega_z} + \frac{B}{v_t \sin\alpha\cos(\alpha+\rho)} \quad (10)$$

[4] Obtained equations characterize the regular movement of the load and the table trip of diverter while sorting. However, the process of sorting with a sliding diverter is much more complicated, and contains of the following phases: inclined hit of the load with the dimensions axb under the angle φ to the table trip in a spot A; twisting of the load around the hit spot A from the hitting moment till it touches the table trip of one of the lateral sides of the load; hit of the lateral side to the working surface of diverters table trip. Despite that, experimental data for time of sorting process confirm the justification of calculations with an approximate scheme of the regular moving [2].

3.2. Minimal distance between two parcels

Obtaining of a minimal interval of the time of diverter working cycle – $T_{c.s}$ (expressions 1 to 9) is important for two significant cases:

- for determination of a minimal step-distance between two adjacent parcels on a belt (Δl_p) in a transport flow which are being sorted to different destinations, with safe sorting provided and
- as parameter of automatic managing by work of diverter while sorting.

Obviously, for the non-stop transport flow on the sorter we need diverter to perform one working cycle with the parcel which is being sorted, that is, to return in a beginning – zero position in order for an upcoming load to bypass it. From this we conclude that the minimal distance between the adjacent parcels which are not diverted to same destination, and which are being transported without obstacles $\Delta l_{p\min}$ (fig. 1; fig. 2) must be:

$$\Delta l_p = T_{c.s} \cdot v_t = 2\frac{\alpha}{\omega_z} v_t + \frac{B\cos\rho}{\sin\alpha\cos(\alpha+\rho)} \quad (11)$$

This minimal distance in a transport flow should also provide the minimal distance of loads on Δl_s, so that the loads don’t touch or hit each other while being sorted. For that case, this condition has to be fulfilled:

$$\Delta l_s = \Delta l_p \frac{v_s}{v_t} \quad \text{и} \quad \Delta l_s \rangle 0 \quad (12)$$

4. TIMES OF TUNING FROM MOVING TRAYS AND SLATS AND TIMES OF SORTING

The process of diverting – sorting of load at the sorters with platforms is realized:

- with the force twisting (tilting) of trays or slats with command load,
- moving the motional belt diagonally from the transport flow at the platforms with a motional belt with width of B_p and
- moving along the horizontal slats of a group of shoe plates which determinately push the command load to its destinations.

4.1. Times of turning and sorting of tilting trays and/or slats

If we do the simplified analysis and forget about the starting sliding of the load down the tray even while still tilting, the process of diverting – sorting of the load has two phases:

- tilting of the tray by an angle α_p when the load is not moving in relation to the tray during the time of the tray tilting $T_{p.z}$ and

– sliding of the load down the tray, inclined by an angle α_p, during the time $T_{p.kl}$.

Load diverting time from the tray $T_{p.s}$ will have the following value:

$$T_{p.s} = T_{p.z} + T_{p.kl} \tag{13}$$

While the tray is being tilted with a constant angle speed $\omega_{p.z}$ and while the load slides down the tray with the width B, with the sliding coefficient while moving μ, just like down the inclined slider with the length B, without the initial speed, component times $T_{p.z}$ and $T_{p.kl}$ have value:

$$T_{p.z} = \frac{\alpha_p}{\omega_{p.z}} \tag{14}$$

and

$$T_{p.kl} = \frac{B}{\bar{v}_{p.kl}} = \sqrt{\frac{2B}{g(\sin\alpha_p - \mu\cos\alpha_p)}} \tag{15}$$

Where:

g – gravity acceleration force and

$\bar{v}_{p.kl}$ - medium value of load sliding speed in relation to the beginning speed ($v_0 = 0$) and the speed while descending from the tray $v_{p.kl}$:

$$\bar{v}_{p.kl} = \frac{v_{p.kl} + 0}{2} = \frac{\sqrt{2gB(\sin\alpha_p - \mu\cos\alpha_p)}}{2}$$

$$\bar{v}_{p.kl} = \sqrt{\frac{gB(\sin\alpha_p - \mu\cos\alpha_p)}{2}} \tag{16}$$

a) **For the known values of parameters** (from the equations 10, 14 and 15), time of diverting and descent of load from tray (according to 13 to 16) will be:

$$T_{p.s} = \frac{\alpha_p}{\omega_{p.z}} + \sqrt{\frac{2B}{g(\sin\alpha_p - \mu\cos\alpha_p)}} \tag{17}$$

б) **Sorting time of loads, wares, parcels.** On all destinations, on places defined with the conditions of sorting and computer managing with sorting, sensors of position are embedded – identifications of load while it is being sorted. Those distances are $L_{I1}, L_{I2}, ..., L_{Ik}, ..., L_{In}$. Sorting time of load with tilt-tray sorter for destination K will have value:

$$T_{k.s} = \frac{L_{s.k}}{v_k} + T_{p.s} = \frac{L_{s.k}}{v_k} + \left(\frac{\alpha_p}{\omega_{p.z}} + \sqrt{\frac{2B}{g(\sin\alpha_p - \mu\cos\alpha_p)}}\right) \tag{18}$$

4.2. Diverting and sorting times of crossed movable trays conveyors

As far as the tray conveyors with crossed movable belts and Linear Inductive Motor - LIM are concerned, it can be considered that the full speed of the cross-belt with piece load - v_p is established for a very short period of time. Therefore the time of descent – executive load sorting from the tray – $T_{p.s}$ is:

$$T_{p.s} = \frac{B_p}{v_p} \tag{19}$$

So, the time of sorting – $T_{k.s.tr.p}$, taking in account the beginning of sorting, has the value:

$$T_{k.s.tr.p} = \frac{L_{s.k}}{v_k} + \frac{B_p}{v_p} \tag{20}$$

5. AUTOMATIZATION OF SORTING PROCESS

Automatization of the sorting process supposes, as it was already stated above, existence of the firm relaying connection and orientation of the load on the carrying element of the transporters working organ and/or conveyor. Time of diverting is of order of longitude of one second if we speak about transporting – sorting machines which are moving at speeds to 1 m/s.

With development and embedding of the highly productive transporting – sorting systems with speeds from 2 to 3.5 m/s and capacities over 15 or 20 thousand pieces per hour ($15 \div 20 \cdot 10^3$ piece/h), embedding of faster diverters reduce in order to reduce the diverting time to the order of longitudes less than 0.5 seconds is necessary [2,5,6,7]. Therefore, at this systems, besides from the application of new types of diverters, when diverter with arm and sliding table trip is being embedded, table trip, when the load is diverting, aside from sliding over it, pushes the load on the exiting machines (inclined chute or roll-conveyor). That's how diverter becomes passively-active.

5.1. Description of load sorting – diverting management

Piece load on the sorter, when it comes into a sorting zone, is being identified in the spot which is on L_{Ik} distance from the beginning of the flow, with the position sensor. From the sensor, the information $I_{id.s}$ is being transmitted into the computer. The computer, after receiving this information, activates the subprogram of actuator managing of the belonging System of Automatic Managing (SAM) and terminates it after the receiving of information I_s that the load diverting has ended in time $t_{I.s}$ (fig. 2c, fig. 3.).

Actuators in SAM realize movements and conditions of the work cycle of diverting executive device (diverter, carrying tray and/or slat and others) (fig. 3.):

- they tilt the diverting device with their active work (for example, pulling the piston from its initial position to the state C^+ - to the ultimate position),
- they hold the executive device in a working position (for example, with the electromagnetic fluid distributor) until the load completely leaves the sorter and
- they return the device in starting position (for example, by pulling in the position from the ultimate to the starting position, to state C^-).

Sensors of positions "inform" us by the computer SAM about the positions of executive devices and loads.

5.2. Time of computer managing

For the user's analysis of the functional possibilities of computer managing [2,4,5,6,8,10], it is necessary to know the times of operations:

T_1 – time of choosing and detaining, transmission, and multiplexing of a signal,

T_2 – time of A/D conversion of the managing signal,

T_{prg} – time needed to perform the given program of managing,

T_3 – time of D/A conversion and transport – transmitting of the managing signal on the electromagnetic fluid distributor.

According to the mentioned states and of computer elaboration will have the following form:

$$T_{OR} = T_1 + T_2 + T_{prg} + T_3 \qquad (21)$$

The most unfavourable case of computer managing with sorting diverter or tray may occur when the computer forms the managing signal after receiving the information $I_{id.s}$ about the identification of an upcoming load in time $T_{id.s}$ and finding out that on that place (k-th) diverting of load needs to be realized. Then the operative time of divert managing ($T_{u.s}$) is longest and it has following value:

$$T_{u.s} = T_{id.s} + T_{OR} + T_{iA} + t_{I.s} \qquad (22)$$

Where T_{iA} – is the time needed to manage the actuator with fluid distributor [2,4].

If the time of managing with electromagnetic fluid distributor is included in time of start of the actuator $t_{st.A}$, along with the expressions for load diverting, and if the times of information transmission are the same: $T_{in.s} = t_{I.s} = t_I$, then the managing with diverting (22) (according to 7) has this shape:

$$T_{u.s} = 2t_I + T_{OR} + T_{c.s} \qquad (23)$$

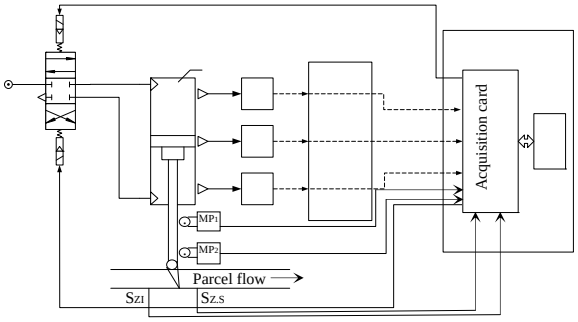

Figure 3. Structural scheme of managing with pneumatic (hydraulic) actuators by using the acquisition card
1(c) – cylinder; 2 – piston; 3(EMR) – electromagnetic fluid distributor; 4,5 – pressure sensors; 6 – speed sensors; RRK – distributional – regulative box; MP_1, MP_2 – micro-switchers of the position of the piston; SZI, SZS – load position sensors (respect to identification and turning); - - - information flows; ———— – managing flows.

Using the earlier obtained expressions for roads and times of load sorting, we can determine the time of managing for the particular kinds of sorters at any spot (k), that is, at any destination:

1. Time of managing while sorting with diverter with arm (according to 10):

$$T_{u.s.skr} = 2t_I + T_{OR} + 2\frac{\alpha}{\omega_z} + \frac{B}{v_t \sin\alpha\cos(\alpha+\rho)} \qquad (24)$$

2. Time of managing with tilting of the carrying tray or group of slat, under the load (according to 17):

$$T_{u.s.p} = 2t_I + T_{OR} + \frac{\alpha_p}{\omega_{p.z}} + \sqrt{\frac{2B}{g(\sin\alpha_p - \mu\cos\alpha_p)}} \qquad (25)$$

3. Time of managing while sorting by moving the horizontal cross-belted tray on the transporter, or by horizontal movement of a group of sliding shoes (according to19) is:

$$T_{u.s.tr.p} = 2t_I + T_{OR} + \frac{B_p}{v_p} \qquad (26)$$

When we observe the sorting from the entering station, that is, address scanner, managing the total process of sorting also includes the distance to the spot of identification (SZI) – LI.K, which is performed in periods of time (20).

On figure 4, we see the diagram road – time for the mechanical state of cylinder (including start + t_{st}) in the system of sorting (according to figure 3) and managing the diagram of its electromagnetic fluid distributor. The times of the computer managing are given in table 1.

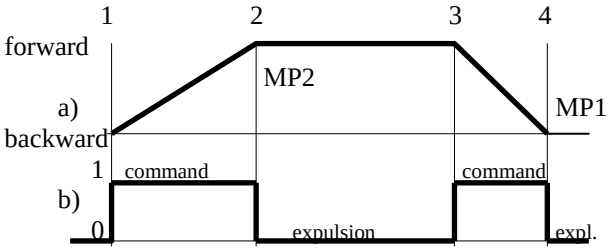

Figure 4. Functional diagram of piston movement of pneumatic cylinder in diverter (a) and managing diagram of electromagnetic pneumatic distributor (4/3) for managing the diverter cylinder (b)

Table 1. Times of the computer managing (in seconds)

Activation time of distributor when starting	Activation time of distributor when stopping	Time of signal transmitting from border sensors	Time of computer processing
0,020	**0,010**	**0,005**	**0,020**

6. CONCLUSION

When we use the times of computer managing (Tab. 1), given according to the characteristics of the computer and fluid distributor [2,6,8,11], then together with the calculated kinematical sizes we may obtain real times of diverting and total times of load sorting. These sizes are being used for the election of the executive device, that is, of the sorter, and for designing of its SAM [7].

REFERENCES

[1] Буланов А., „Подземно – транспортные устройства почтовой связи”, Радио и связь, Москва, 1985.

[2] Bukumirovic M., „Automatizacija procesa rada u postanskim sistemima”, Saobracajni fakultet, Beograd, 1999.

[3] Bukumirovic M., „Mehanizacija i automatizacija procesa prerade postanskih posiljki”, Saobrasajni fakultet, Beograd, 1997.

[4] Bukumirovic M., „Time parameters of microcomputer by the actuators in automation technical systems”, FACTA №4, Niš, 1997.

[5] Bukumirovic M., „Prilog razvoju i koriscenju algoritama i programa za automatsko razvrstavanje postanskih posiljaka do dostave”, POSTEL, Beograd, 2001.

[6] Bukumirovic M, Djogatovic M., „Automatsko upravljanje podsistemima u tehnickom sistemu za mehanizaciju i automatizaciju u glavnim postanskim centrima”, Savremena posta, №.1, Beograd, 2006.

[7] Cupic A., „Metodologija izbora tehnickog sistema za automatsku preradu paketa u glavnim postanskim centrima”, magistarski rad, Saobracajni fakultet, Beograd, 2007.

[8] Drndarevic V., „Personalni racunari u sistemima merenja i upravljanja”, Akademska misao, Beograd, 2003.

[9] Ивановский Е., „Теоретические основи перемещения штичних грузов”, Машиностроение, Москва, 1971.

[10] Nedic N., ”Praktikum za laboratorijske vezbe iz sistema automatskog upravljanja”, Masinski fakultet, Kraljevo, 1997.

[11] Katalozi proizvodjaca: „Prva petoletka (Serbia)”, FESTO, (Austria).

ANALYSIS AND DEFINITION OF CHARACTERISTICS OF WIND TURBINE POWER TRANSMISSION

M. Velimirović, V. Miltenović, M. Banić

Abstract: *This paper sums research in the field of wind turbines and power transmitters, which have been realized in long period of time at Mechanical Engineering Faculty in Nis. Basic problem regarding wind generators construction is in a fact that intensity and wind direction is constantly changing. The wind turbine impeller should always use maximum of the wind power potential, i.e. to operate in it's optimal regime which only depends on current speed of the wind. Generator work regime is in function of induced electric power. On the other hand, to connect wind turbine with power distribution network, it is necessary that deviation of voltage and frequency lies in narrow boundaries. Paper elaborates the transformation process of wind kinetic energy to mechanical energy in order to have optimal angular velocity of impeller at variable wind speeds. New concept of wind turbine power transmissions is elaborated, which instead of multiplicators with constant transmission ratio uses differential power transmission and power transmitters with variable transmission ratio (CVT).*

Key words: *wind turbine, multiplicator, CVT, differential transmitter*

1. INTRODUCTION

Solving actual energy crises demands rational use of present energy sources and research in the field of new energy sources. It is estimated that sun energy which arrives to the Earth is transferred in amount of 1-2% to wind kinetic energy.

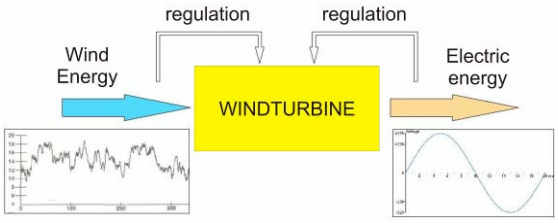

Fig. 1 Wind energy conversion in to electric power

Wind represents significant resource in electric power generation. Research in the field of electric energy generation using wind; represent one of the basic priorities in developed countries. Developed countries predict that participation of alternative energy sources in total energy production will be 40% (30% wind energy) until year 2020. From all installed equipment for electric power manufacturing in EU in last five years wind turbines represent 32%, which clearly indicates that research in this area is very interesting and important.

Major problem regarding wind turbines is that wind intensity and force are time variables. To obtain efficient connection of wind turbine and distributive network, variations in frequency and induced power must be in very narrow boundaries (*Fig. 1*).

Basic components of wind turbine (*Fig. 2*) beside pillar are: turbine, multiplication gearbox, generator and energy electronics.

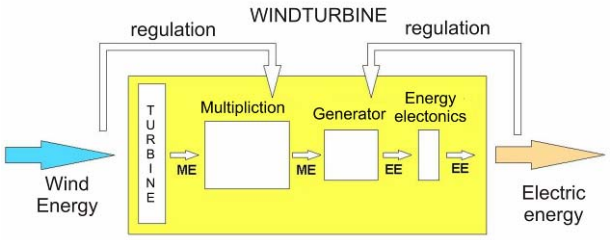

Fig. 2 Wind turbine basic components

Turbine converts wind energy into mechanical energy (ME) with relatively small number of rpm of rotor. Transmission multiplicities rpm and reduces torque and thus reduces stress and strain in a chain of power transmission. Generator transforms mechanical energy in to electric energy (EE). Electric energy frequency must be corrected if multiplicator with constant transmission ratio is used. Standard wind turbine solutions regulate induced electrical energy frequency using energy electronics. Frequency regulation through changing blades angle and by changing number of poles pairs does not yield satisfying results.

It is proposed that instead of multiplicator with constant transmission ratio differential transmission with variable transmission ratio is used (CVT). Main advantage of applying power transmission with variable transmission ratio is to disconnect rigid connection between turbine and generator. Turbine should be in optimal work regime depending on current wind velocity. The goal of regulation is too maximally utilize mechanical energy conversion to electric energy. Wind turbine work regime is just in function of induced electric energy parameters while generator works with maximum efficiency. CVT can achieve fast transmission ratio change and it can be directly applied for wind-generators. This approach is more economical then energy electronics.

Mr.-Ing. Miodrag Velimirović, Mechanical Engineering Faculty, University of Niš, m_velimirovic@yahoo.com
Prof. Dr.-Ing. Vojislav Miltenović, Mechanical Engineering Faculty, University of Niš, vojamiltenovic@yahoo.com
Dipl.-Ing. Milan Banić, Mechanical Engineering Faculty, University of Niš, banicmilan@hotmail.com

2. WIND ENEGY POTENTIAL

Wind is a renewable energy source. The main disadvantage of wind as energy source lies in its variable speed. The oscillations of wind speed can be very short and frequent, so wind intensity can never be considered as constant. If the wind speed is to low it can't be used for production of electric energy. In energetic sense wind turbines are used for replenishment of base load. If wind turbines are used as dominant source of energy for electric system, full reserve must be foreseen. Variances in wind speed require further increase of regulation system reserve. Analysis, calculation and determination of wind turbine location cannot successfully be performed without knowledge about basic characteristics of wind. For usage of wind as energy source it is necessary to have full aerological and energetic data (average month and annual speed, maximum wind speed, distribution of wind speed).

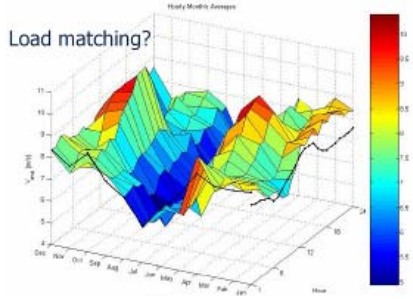

Fig. 3 Distribution of wind speed over the daily and monthly period

For estimation of wind energy potential it is very important to know distribution of wind speed over time and in space. Local wind characteristics must be determined by gathering of experimental data. All meteorological measurements must be extrapolated to height of blades rotation axis. Change of wind speed with increase of height can be presented by logarithmic or exponential function. The wind speed depends also from the ground shape. Logarithmic function of wind speed change is given by equitation:

$$V(z) = V(z_m) \ln(z / z_0) / \ln(z_m / z_0)$$

where: *V(h)*-wind speed on height z*; V(H)* – measured wind speed on height z_m*;* z_0 – parameter of ground shape (represent height over ground where wind speed is almost equal to zero).

Available wind energy in region is best to opserve on an annual level by using of annual avarage speed and wind distribution over the annual level. Avarage wind speed over a time interval is defined as:

$$V_m = \frac{1}{T}\int_0^T V(t)dt$$

where *V(t)* – current wind speed; *T* – time interval.

Distribution of wind speed correspond to Weibull distribution with shape parameter equal 2:

$$p(V) = \frac{2}{V_m} \cdot \frac{V}{V_m} \cdot \exp\left[-\left(\frac{V}{V_m}\right)^2\right]$$

Surface under the curve (Fig. 4) correspond to probability *P(v)* that wind will blow at certain speed (including 0 m/s) an it must be equal to 100%.

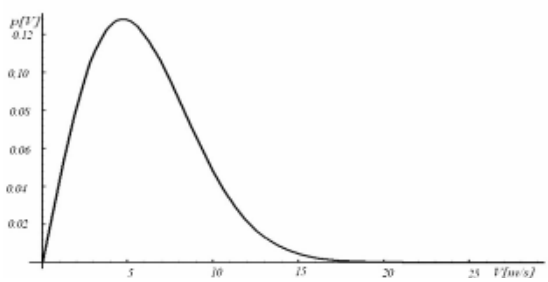

Fig. 4 Weibull distribution of wind speed which correspond to average annual speed of 6,7 m/s

Distribution of wind speed varies over the year as shown on Fig. 5.

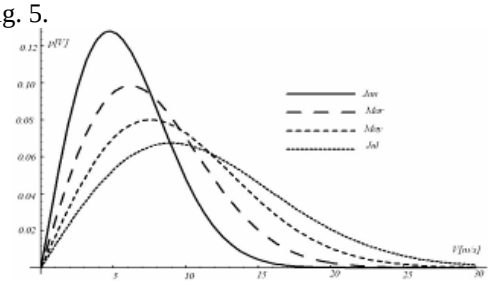

Fig. 5 Monthly distribution of wind speed

Energetic wind potential can be observed trough wind kinetic energy and power of the wind. Wind kinetic energy is:

$$E_W = 0{,}5m \cdot V^2$$

where: *m*- air mass; *V*- wind speed.

Wind power is given by equitation:

$$P_W = \frac{1}{2} \cdot \frac{\partial E_w}{\partial t} = \frac{1}{2}\frac{\partial m}{\partial t} \cdot V^2 = \frac{1}{2}(\rho \cdot A \cdot V) \cdot V^2 = \frac{1}{2}\rho \cdot A \cdot V^3$$

where: ρ - air density; A – surface of wind front.

Elemental power of the wind (Fig. 6) i.e. winds power to elemental surface normal to wind direction:

$$P_W^1 = 0{,}5\rho V^3 .$$

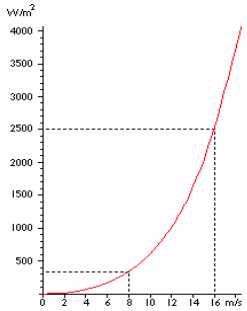

Fig. 6 Elemental power of the wind

Available energy potential of the wind on a certain location can be observed based on mathematical expectation, in other words multiplication of wind power at certain speed and probability of wind blowing at that exact speed (Fig. 6).

Based on above it can be concluded that it is unnecessary to design wind turbines for large wind speeds. If we limit the operation of wind turbine to wind maximum speeds of 20 m/s instead of 50 m/s we lose only 0,3% of power. The most efficient potential is located at wind speeds around 10 m/s. Available energy potential for certain location is much better anticipated if we use the integral of mathematical expectation (Fig. 7).

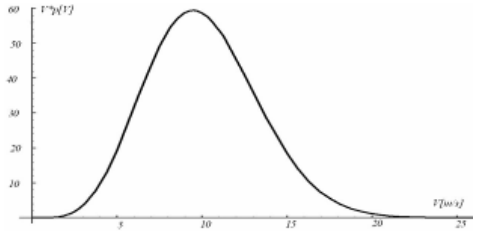

Fig. 6 Mathematical probability of elemental wind speed

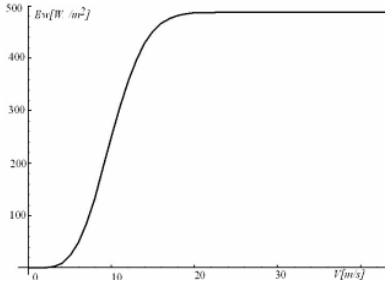

Fig. 7 Available potential of wind energy

3. WIND TURBINE POWER

Wind turbine cannot use the available power of the wind at full amount. Incoming wind current is gradually slowing while the pressure is increasing. One part of energy is converted to mechanical energy and the remaining part for fluid rotation behind the turbine and overcoming of friction forces on turbine blades. To determine the maximum power of wind turbine the following assumptions are made:

- Flow is uniform.
- Flow is friction free
- Flow through the flow pipe is in depended from the flow around it – continuity equitation is in place ρVA=const.
- Static pressures in section 0 and 2 are equal.

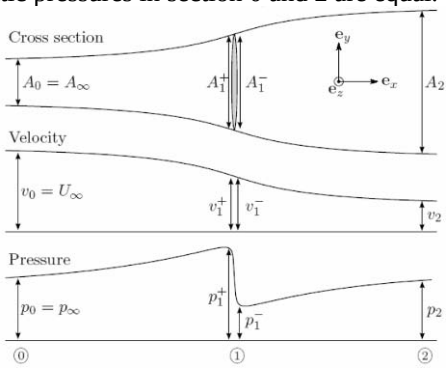

Fig. 8 Surfaces, velocities and pressure along direction of the wind

Power which rotor absorbs is equal to change of kinetic energy over time. It is also equal to difference of inlet and outlet power of the wind i.e. power in sections 0 and 2:

$$P_T = P_{W0} - P_{W2} = 0{,}5\rho \cdot A_0 \cdot V_0^3 - 0{,}5\rho \cdot A_2 \cdot V_2^3$$

i.e.:

$$P_T = 0{,}5\rho \cdot A_1 \cdot V_1 \cdot \left(V_0^2 - V_2^2\right)$$

For determination of wind turbine power surface of the rotor $A_T = A_1$ is used. In that section flow speed is:

$$V_1 = 0{,}5 \cdot \left(V_0 + V_2\right)$$

Decrease factor of flow speed a is defined as:

$$a = \left(V_0 - V_1\right)/V_0 = 0{,}5\left(V_0 - V_2\right)/V_0$$

By using the decrease factor of flow speed in wind turbine power equitation:

$$P_T = 0{,}5\rho \cdot A_T \cdot V_0^3 \cdot 4 \cdot a \cdot \left(1 - a\right)^2$$

Coefficient of wind turbine power is defined as rate of wind turbine power and inlet power of the wind:

$$C_{PT} = P_T / P_W = 4 \cdot a \cdot \left(1 - a\right)^2$$

Maximum absorbed power is case of a = 1/3 (Fig. 9).

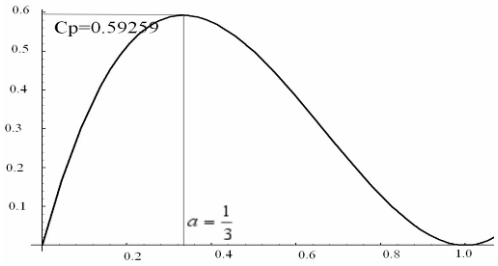

Fig. 9 Coefficient of wind turbine power

Maximum value of C_{PT} is known as *Betz* limit. According to *Betz* theoretical maximum of wind power which can be converted to mechanical energy is 59,25%. Maximum value of C_{PT} is achieved when outlet wind speed (section 2) is one third of inlet wind speed. Attempt to increase coefficient of wind turbine power by two (or more) axial impellers doesn't give satisfying results. According to [2] theoretical value of power coefficient of two stage turbine is C_{PT}=15/25 = 64%.

In previous consideration flow was treated as planar. But by flow of wind trough rotor it changes the direction and rotates of air mass around the turbine axis. Rotational path of air behind the turbine is consequence of reaction between air mass and turbine blades which use the wind energy. Rotation of the air is opposite to rotation of the turbine. Angular velocity ω, is small comparing the angular velocity of the turbine Ω.

Analysis of flow is focused to pipe in which ring cross-section fluid flows, with radius *r*, width *dr* and elemental surface $2\pi rdr$. H.Glauert gives the equitation of pressure drop in the rotor plane. Rotation causes decrease of pressure depended on the value *r* :

$$\Delta p = p_1^+ - p_1^- = \rho \cdot \left(\Omega + \omega/2\right) \cdot \omega \cdot r^2$$

On an intesimal surface with width *dr* inducted torque is:

$$dT = \rho \cdot V_1 \cdot \omega \cdot r^2 \cdot 2 \cdot \pi \cdot r \cdot dr$$

Based on Glauert-Schmitz research on rotation of the air mass inducted power on intesimal surface of rotational air front is:

$$dP = \Omega \cdot dT = \frac{1}{2}\rho \cdot V_1^3 \cdot \left[\frac{8}{\lambda^2} a' \cdot \left(1 - a\right) \cdot \lambda_r\right] \cdot d\lambda_r$$

where:

$\lambda = \Omega \cdot R / V_o$ - factor of rotor velocity factor (ratio of blade tip radius and wind speed,

$\lambda_r = \Omega \cdot r / V_o$ - factor of rotor velocity on radius *r* and

$a' = \omega / 2 \cdot \Omega$ - tangential induction factor.

Based on previous equitation coefficient of turbine power if we take into account rotation of air mass is:

$$C_{PS} = \int_0^1 4 \cdot \lambda \cdot \left(\frac{r}{R}\right)^2 \cdot \left[\sin^3\left(\frac{2}{3}\alpha_r\right) / \sin^2\alpha_r\right] \cdot d\left(\frac{r}{R}\right)$$

where: $\alpha_r = arctag(R / r \cdot \lambda)$

Further transformations of previous equitation:

$$C_{PS} = \frac{4}{\lambda^2}\int_0^{\lambda} \lambda_r^2 \cdot (\lambda_r^2 + 1) \cdot \sin^3\left(\frac{2}{3} arctag\left(\frac{1}{\lambda_r}\right)\right) \cdot d\lambda_r$$

This integral is possible to solve numerically. By solving of integral by range of λ values and by curve fitting the new approximation of the integral was obtained:

$$C_{PS} \approx \frac{16}{27}\left(1 - \frac{1.04359}{(1+\lambda)^{1.835}}\right)$$

Rotation of air mass behind the turbine inducts the aerodynamic losses which are the largest in the zone of low λ values. Boundary values of inducted power for low rpm turbines are considerably lower than Betz limit. Wind turbines should have significant aerodynamic efficiency so turbine should work with high values of λ. Absorbed power on turbine depends on achieved torque and angular speed of the turbine. To achieve the maximum absorbed energy it is necessary to have the maximum angular velocity and minimum torque of the blades, because with increase of the torque the energy of rotation of the fluid flow is increasing also. Efficiency ratio is best increasing by increasing of angular velocity and decreasing of flow. Because of that all modern wind turbines have low drag fast rotating turbines with two or three blades with optimal shape. How the turbine is absorbing energy from the air flow depends from the construction of the turbine. Different design of turbines causes they have very different performance. Turbines which use upward pressure absorb more of energy from the wind, while turbines which use the drag force have much higher staring torque (they can start to rotate at lower wind speeds).

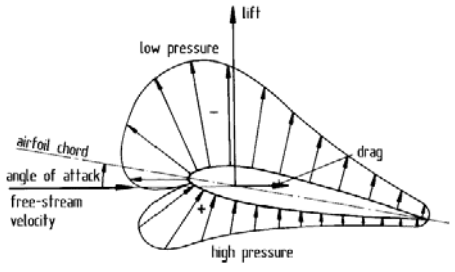

Fig. 10 Profile of wind turbine blades

On power coefficient of wind turbine, among previously noted, the friction forces have high influences. Power coefficient which takes this into account is given by equitation:

$$C_P = C_{PS}(\lambda) \cdot \eta_P(\lambda, \varepsilon) \cdot \eta_z(\lambda, z)$$

Blades shape influence factor $\eta_P(\lambda,\varepsilon)$ depends from shape and position of blades profile and it can be expressed as:

$$\eta_P(\lambda, \varepsilon) = 1 - \lambda / \varepsilon$$

where: ε – sliding coefficient $\varepsilon = C_L/C_D$ ratio of upward pressure force factor C_L and drag force factor C_D.

Factors C_L and C_D is dependent to change of blades profile position in relation to wind direction defined by angle β. It is possible to determine force factors experimentally.

Blades number factor $\eta_z(\lambda,z)$ is given by equitation:

$$\eta_z(\lambda, z) = 1 - 1/\lambda \cdot z$$

where *z* is number of blades.

Turbines with more than 3 blades cannot be theoretically explained. Glauert-Shmitz theory is only valid for up to three blades. In such circumstances, experimental results are used. Curves of power coefficient change C_P are formed for sliding coefficient $\varepsilon = C_L/C_D = 6$. Optimal range of wind turbine with one blade is defined by value $\lambda \approx 12$ and for four blades with value $\lambda \approx 6$.

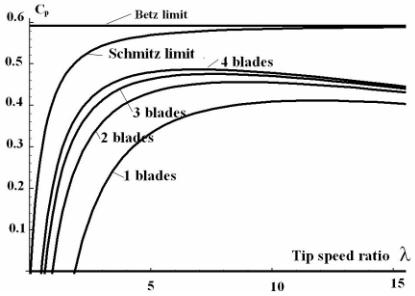

Fig. 11 Influence of blade number on power coefficient

Experimental results about wind turbine power coefficient are in accordance with theory for up to three blades. For horizontal wind turbine with 4 blades the difference between experimental and theory data is significant.

Efficiency in low speed range isn't a issue because of small energy, while in high speed range the excess energy must be discarded because the nominal power of the system is excided.

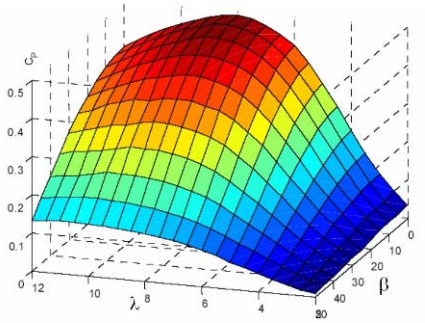

Fig. 12 Power function of wind tur. expressed by λ and β

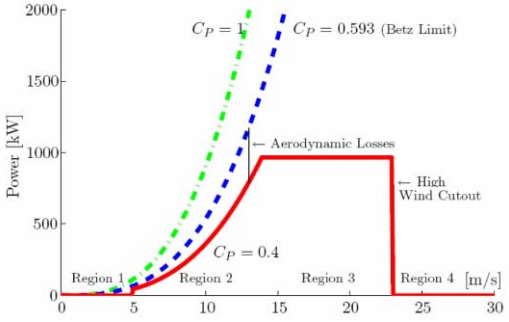

Fig. 13 Curves of wind turbine power

For wind turbines which mechanical characteristic is given on Fig. 13, for wind speed of 14 m/s maximum power which turbine can produce corresponds to nominal turbine power. For wind speeds larger than 14 m/s regulation is preformed in such way that by turning of blades profiles nominal power remains constant.

4. WIND TURBINES TYPES

Wind turbines differ by speed of the rotor (constant or variable), the type of electric network connection (direct or by converter) and by generator type (synchronous or asynchronous).

1. **Wind turbines with induction generator with cage rotor for constant speeds of the rotor** (Fig. 14) connects with the electric network directly. Most of smaller wind turbines share this concept. The rpm change (slip) is limited to 1-2%. The rigid connection between wind turbine and generator and substantial variance of wind speed, usually this wind turbines use generators which operate on two or more speeds. The speed change is achieved by change of pole pair's number of the stator coil. The second variant is to use two generators with different operating power outputs.

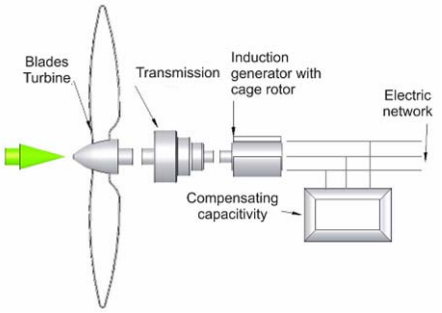

Fig. 14 Wind turbine with induction generator

If we add a variable resistive element to the rotor it is possible to change the rotor speed up to 10%. This system is known as semi-variable speed wind turbine. The main drawback of this wind turbine concept is, besides large inertia of the rotor and multiplication gearbox, that generator with cage rotor always uses reactive power for his work, which is especially unwanted in large wind turbines or in law capacity electric network. This energy can be compensated by usage of small permanencies. The advantage of this concept is in its simplicity. As the generator rpm determines the frequency of generated electric power, this concept of wind turbine isn't suitable for frequent change of wind speed as generated electric energy have low quality.

2. Wind turbine with synchronous generator and changeable pole pair number in which turbine shaft is directly connected to generator (Fig. 15).

Synchronous generator with changeable pole pair number has very good developed control so it is produced by many world companies. It is connected to electric network by relatively simple energy electronics. This is the main drawback of this concept; complete generated electricity goes to convertor which can be very complex and economically inefficient for larger wind turbines. Convertor also has a low efficiency ratio and usage of large capacitors is needed.

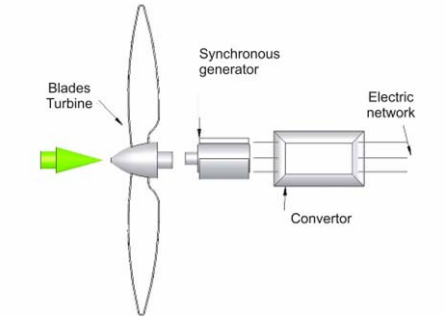

Fig.15 Wind turbine with synchronous generator

2. **Wind turbine with induction generator with cage rotor for full spectrum of speeds** is similar to previous but is used very rarely. The main difference with the previously described is in existence of multiplication gearbox between turbine shaft and generator shaft. Concept uses the full spectrum of wind speeds and connection to electric network is enabled by fully controlled inverter (Fig. 16).

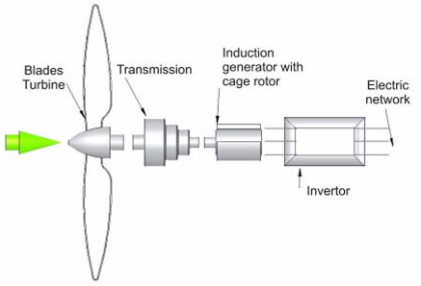

Fig. 16 Wind turbine with induction gen. and cage rotor

Advantage of this concept lies in its low production price and larger operating spectrum. It is important to emphasize that energy electronics can control the reactive power. The main drawback lies in usage of two inverters for full power in serial connection with generated power loss of approximately 3%. Usage of large capacitors for stable voltage insurance is also needed.

3. **Wind turbine with double powered induction generator** (coiled rotor) is used for powers over 1MW. Stator is directly connected to electric network, while rotor is connected to electric network by sliding contacts and back-to-back convertor. In that way mechanical and electrical frequencies of the rotor are separated and frequency of electrical energy doesn't depend on rotor rpm.

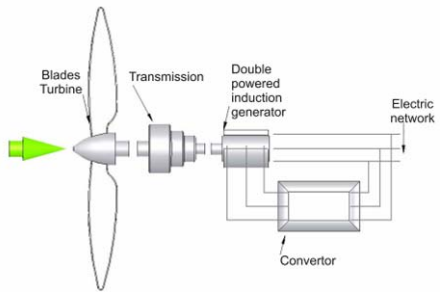

Fig. 17 Wind turbine with double powered induction generator

This concept uses smaller convertor because only around 25% of generated electric energy passes through it and power loss is smaller because of that.
The advantage of this concept lies in its efficiency, effective control and swift reaction to sudden wind strikes which lower the stresses on mechanical components. Maintenance of this wind turbine is very complicated and its reliability is law mainly because of sliding contacts. Induction generator with coiled rotor isn't standardized which lead to problems if malfunctions arise.

5. BASIC CHARACTERISTICS OF WIND TURBINE POWER TRANSMITTER

Design criterions for wind turbine power transmitter arise from criterions which are defined for system as a hole. In larger wind turbines regulation of turbine part is achieved trough change of angle of blades which can rotate around their central axis. The inducted power is monitored, and if that power surpasses the nominal value, blades are rotated in order to reduce power output. With CVT application transmission ratio is changed continuously, thus adjusting work of impellor and generator. This enables the optimal work regime of wind turbine. Transmission ratio and regulation spectrum are proportional to wind speed, diameter of turbine impellor, number of turbine blades, generator pole number and frequency of electric energy.
Based on number of blades and blades cross section the optimal value of rotor speed factor is determined λ_{op} at which power coefficient reaches its maximum. For wind turbine with three blades the λ_{op} is between 5,5 and 7,5.
Modern wind turbines are designed to withstand wind speeds up to 80 m/s, but the speed at they generating electricity is limited to range 4÷25) m/s. Power limiting usually starts at 16 m/s, so the important limiting speeds for transmitter are V_{min} = 4 m/s and V_{max} = 16 m/s. Accordingly the boundary values of angular velocities are:

$$\omega_{min} = \lambda_{op} V_{min}/R \text{ and } \omega_{max} = \lambda_{op} V_{max}/R$$

If the synchronous generator with changeable pole number is excluded, other types of wind turbines need the application of multiplying gearbox which increases the rotation speed from 20-60 rpm to 1500 rpm for four pole generators. Application of CVT ensures constant and swift change of transmission ratio and thus the generator rotor rpm. This vastly improves the efficiency of the system.
The basic functional criterions are: transmitter power, boundary values of transmission ratio, regulation spectrum, efficiency ratio, and the time for transmission ratio change trough whole regulation spectrum.
Besides these specific criterions CVT for wind turbines must satisfy some other demeans, as high reliability and high specific power transmission capability and low maintenance. The CVT must be very compact with low mass requirement.

6. CONCLUSION

Based on previous it can be concluded:

- Wind is a renewable energy source with main drawback in variability of its speed and large investments for installation;
- Wind as energy source is competitive to classic energy sources;
- Stochastic nature of the wind lead to relatively complicated concepts of wind turbines and their regulation;
- Effective range of wind speed for production of electric energy lies between 4 m/s and 25 m/s. Above 16 m/s power is limited by rotation of turbine blades;
- To effectively connect wind turbine to electric network variations of voltage and frequency must be in narrow boundaries;
- It is irrational to use constant ratio multiplication gearbox to connect the turbine with the generator;
- New concepts of wind turbines are based on CVT instead of multiplication;
- Regulation spectrum which enables the efficient usage of CVT at wind turbines is D_R=4.

LITERATURE

[1] Gasch, R.: *Windkraftanlangen*, B. G. Teubner Verlag, p. 157-158, Stuttgart, Germany, 1996.
[2] Schmitz: *Theorie und Entwurf von Windradem optimaler Leistung* - senschaftliche Zeitschrift der Universitat Rostock, Sonderheft, 5. Jahrgang. 1955/56
[3] Neman, B.G.: *Actuator-disc theory for vertical-axis wind turbine*, Journal of Wind Energy and Industrial Aerodynamics, Volume 15, Issue 1-3, 347-355, December 1983.
[4] Neman, B.G.: *Multiple actuator-disc theory for wind turbines*, Journal of Wind Energy And Industrial Aerodynamics, Volume 24, Issue 3, 347-355, October 1986.
[5] Milivojević, N.: *Najčešće korišćeni tipovi vetrogeneratora*, December 2003, B.E.S.T
[6] Engelen, T.G., van Hooft, E.L., van der Schaak, P.: *Wind Turbine Control for Industrial Us*e, EWEC 2001, Copenhagen, Denmark, 2001.
[7] Schaak, P., Engelen, T.G., van Hooft, E.L., van der Wiggelinkhuizen, E.J.: *Wind Turbine Control – Industrial Support*, Flyer, ECN Wind Energy, Netherlands, 2003.
[8] Grogg, K.: *Harvesting the Wind: The Physics of Wind Turbines*, Physics and Astronomy Comps Papers, Year 2005.

NATURAL GAS – ENERGY, ECOLOGY

T. Simović, B. Đorđević, M. Gojnić

Abstract: *The fundamental strivings towards the production of the most inexpensive energy, its mass accessibility and rational use, combined with a maximum environment protection have compelled the science, trade, politics and even people in general, to turn towards new energy production technologies.*
The shown example of power plant that as the primary energy source uses natural gas has to point out possible direction of development in Serbia, as this direction Europe has already taken.
For large public, health, industrial and business facilities, the value of required means for the connection to public utilities for the supply of electric and heating energies exceeds the value of investment in the erection of own power plants that provide full self-sufficiency in operation as well as high primary energy utilization level.
The forthcoming energy (especially gas) arrangement with the Russian Federation, arrival of foreign companies which, in addition to inexpensive workforce, are looking for a reliable and competitive energy supply, as well as technologically and economically obsolete power facilities that are due to be overhauled, open a space for the participation of engineering industry in the field of power production in Serbia.

Key words: *natural gas; energy; cogeneration; power generating unit; ecology; engineering industry*

INTRODUCTION

Low efficiency of electrical energy production in centralized large facilities (40%), transmission and distribution losses and high level of environmental pollution emphasized by the energy crisis of the 1970's gave rise to new tendencies in the development of power engineering. Bulky centralized sources are replaced with smaller production that is distributed on the place of consumption, which allows effective transformation of primary energy to electric, heating and cooling energy – distributed production.
As an example of state-of-the-art, effective and reliable power facility here is given the overview of the power generating unit of the Mostransgaz Business Centre that was erected in Moscow in 1996.

POWER PLANT DESCRIPTION

State-of-the-art heat-and-power engineering facilities and plants for large business complexes require tight technological binding in the production of heating, cooling and electric energies, which, in addition to a high utilization factor of energy sources, makes possible a complete self-sufficiency in the supply of all required kinds of energy during the whole year.

Cogeneration, a combined production of electric and heat energies, as an effective and economically justifiable way of reduction of high energy production costs in industry, public, health and business facilities represents a logical solution applied in the power plant for the supply of Mostransgaz Business Centre in Moscow. Choice of natural gas as the only fuel for both motor-generator sets and boilers was imposed not only because of its availability and price in Moscow, but also because it is superior to solid and liquid fuels in view of its environmental implications.
Self-sufficient power generating unit that burns natural gas and provides electric, heating and cooling energies over the whole year, hereinafter referred to as **BETR**, built and commissioned in 1996 was intended to meet the needs of the whole Mostransgaz Business Centre in Moscow erected in stages of a usable area of 105.000 m^2.
Based on the preliminary analyses of maximum electric load structure (*Enclosure 1.1*) and maximum daily heat and cold consumption of the future business complex (*Enclosure 1.2*) on the condition of providing safety reserve of ~30% in energy sources capacities, the following equipment was incorporated in the **BETR**:

	Capacity	Unit	Total
gas motor-generator unit (module)			
- electric power 10 kV	1,4 MW	4	5,6 MW
- thermal power 110/70°C	1,7 MW	4	6,8 MW
gas-fired boiler	9,0 MW	3	27,0 MW
absorption refrigerating machine	0,67 MW	3	2,0 MW

Dr Tomislav Simović,B. Sc., Associate Professor at the Faculty of Mechanical Engineering in Kraljevo, General Manager of Montinvest a.d. Belgrade, simovic.t@mfkv.kg.ac.yu
Branislav Đorđević, B.Sc.
Marko Gojnić, B.Sc.

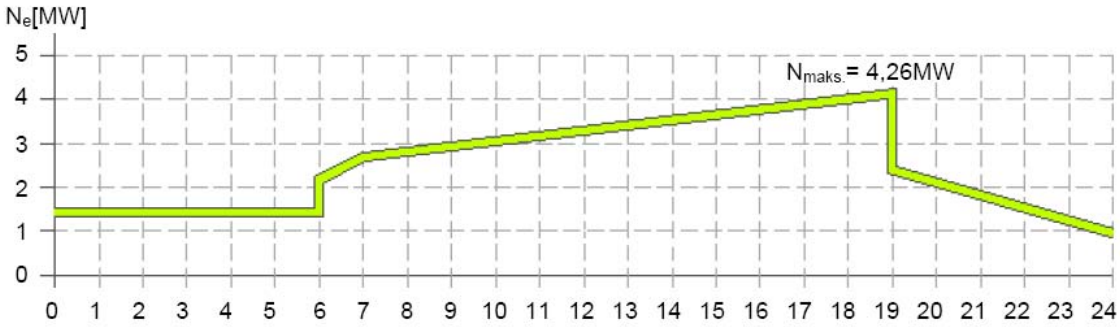

Design definition requirements for daily electrical load ***Enclosure 1.1***

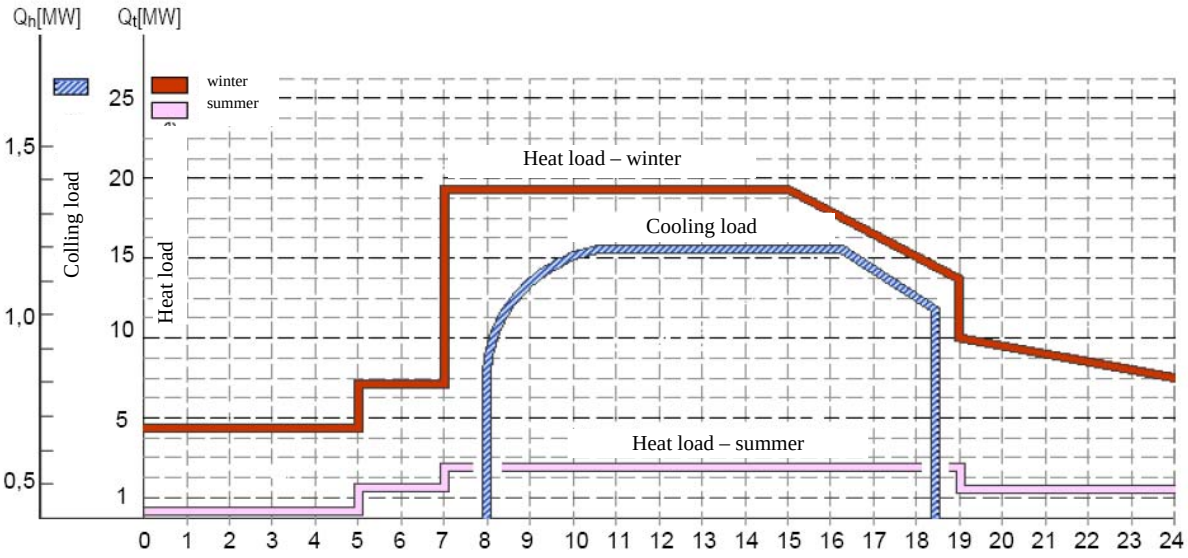

Design definition requirements for daily thermal and cooling load ***Enclosure 1.2***

Modules (gas motor-generator units) of a total electrical power of 5,6 MW are, by priority, in operation according to the needs of power consumers in the business complex. One module consists of the following:
- gas engine,
- alternating current generator
- heat exchanger for engine cooling water
- lubricating oil cooler
- heat exchanger at exhaust gases,
- distribution, control and power supply boards with equipment for synchronizing and parallel operation with the distribution power grid.

During the operation, heat exchangers cool the gas engine by water with temperature from 700C to 900C that circulates through the engine block. Engine exhaust gases come in with a temperature of 4500C and they can heat the water from 900C to 1100C through the utilizer or they can, uncooled, be thrown out to the atmosphere via the bypass line.
In this way, in the process of cogeneration the module, addition to the electrical, produces heat energy as well, as a result of which the total degree of utilization of gas input energy exceeds 86 % (*Enclosure 2*), i.e.:

$$\text{Gas } 1\text{Nm}^3 = 9{,}5 \text{ kWh} \Rightarrow 3{,}67 \text{ kWh}_{el.} + 4{,}49 \text{ kWh}_{term}$$

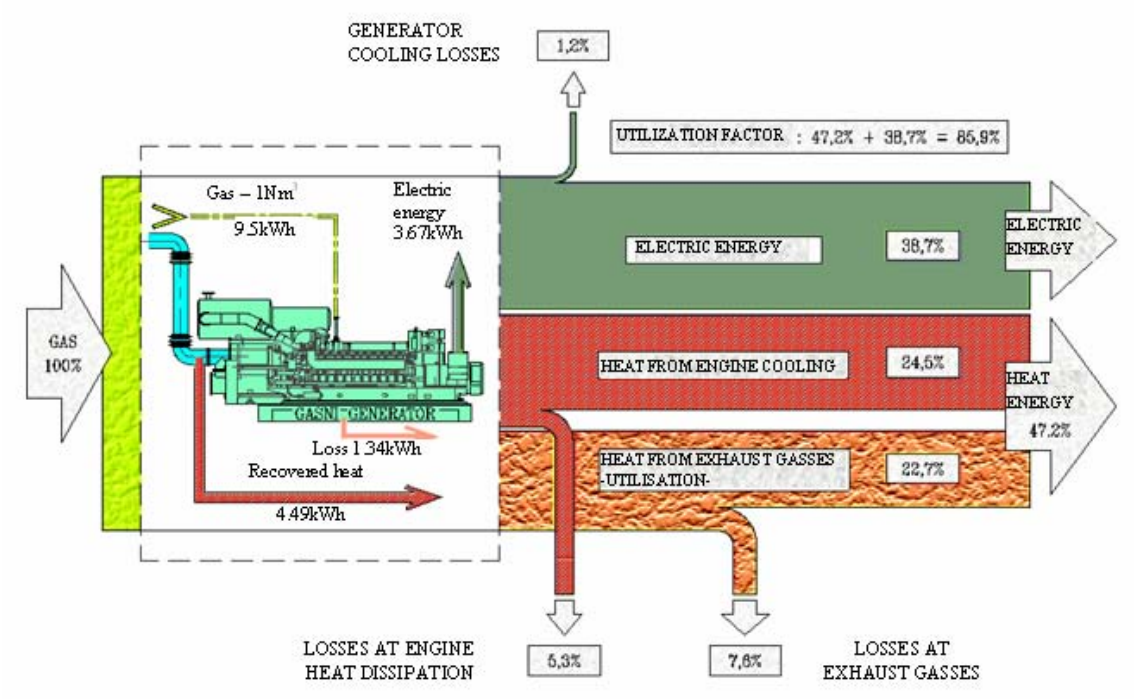

Balance of cogeneration – production of electric and heat energies ***Enclosure 2***

SYSTEM OPERATION

Multiple role of BETR – power generating unit for the production of electric, heating and cooling energies, shown on the energy flow block diagram (*Enclosure 3*), meets the following needs of the Mostransgaz Business Centre in Moscow:

- electric power,
- heat energy,
- cooling energy,
- preparation of hot sanitary water with circulation,
- potable water network transport and pressure maintenance,
- fire water network transport and pressure maintenance,
- process water chemical preparation.

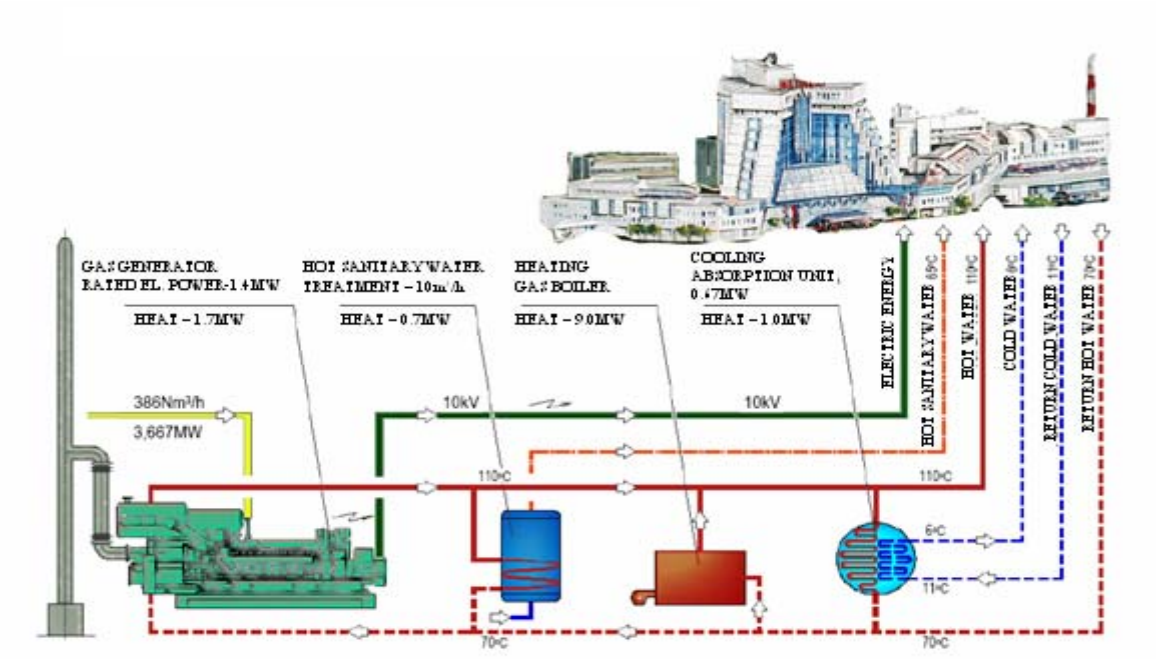

Power plant block diagram ***Enclosure 3***

Modules, gas motor-generators, are by priority in operation according to the needs of electric power consumption and can operate in three different running regimes:

- autonomous operation with no presence of city mains power supply – synchronization between generators
- autonomous operation with the city mains power supply present – generators synchronized with the power distribution
- parallel operation with the city mains power supply – minimum (preset) quantity of electrical power is taken from the power grid

As already emphasized, modules (gas motor-generators) operate depending on the power consumption and, at the same time, they provide proportionate recovered thermal capacity for the needs of heating, ventilation and hot sanitary water preparation over the cold period of year. In the hot period of year, the heat recovered from the cogeneration process is used for the preparation of hot sanitary water and for absorption refrigeration.

POWER BALANCE

The business complex of a total square area of 105.000 m2 has an annual consumption of 13.050 MWh for its own needs. Depending on the demand, gas motor-generators start the operation step-by-step at reaching full operating load producing as well an equivalent quantity of thermal energy (*Enclosure 4*).

From the *Enclosure 4*, which shows the annual heat consumption, it can be seen that 49 % of the required heat is produced by the boiler house and the second half is the energy from gas engines heat recovery. The Enclosure also shows high utilization factor of recuperation energy at the annual level with only 6 % of lost energy.

The analysis of annual gas consumption capacities (*Enclosure 5*) shows the correlation of the gas consumed in gas motor-generators (62,8%) as compared with boilers (37,2%).

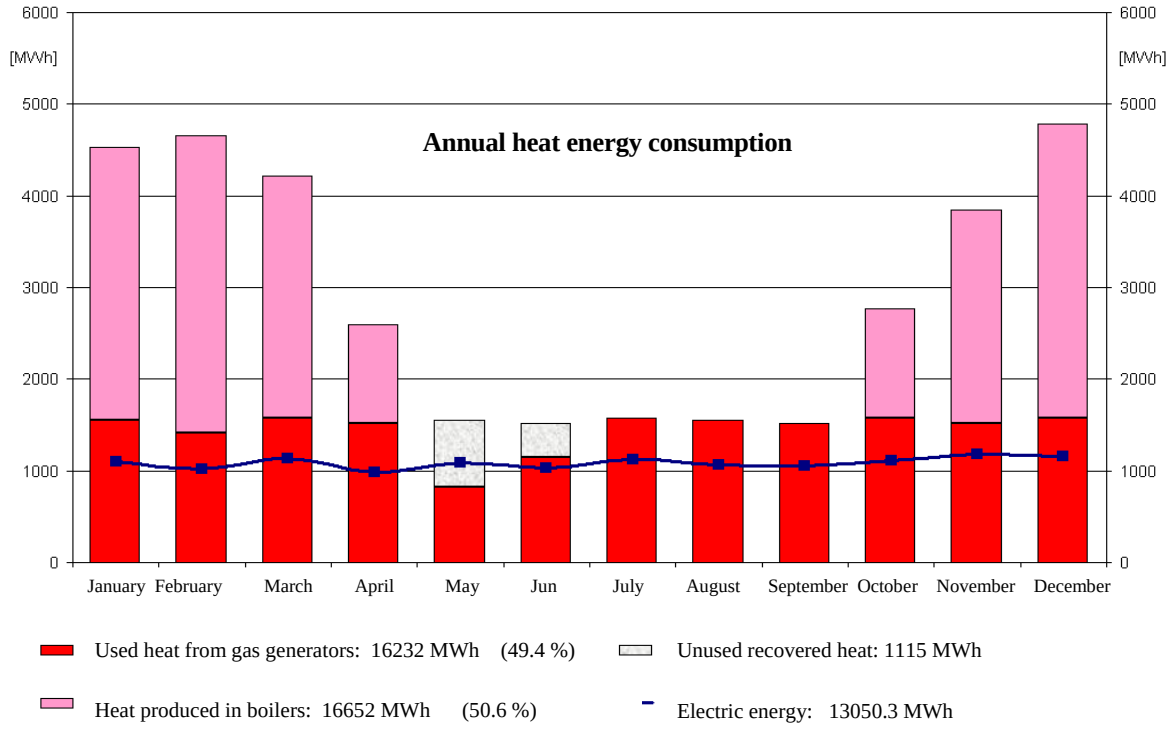

Annual heat and power consumption ***Enclosure 4***

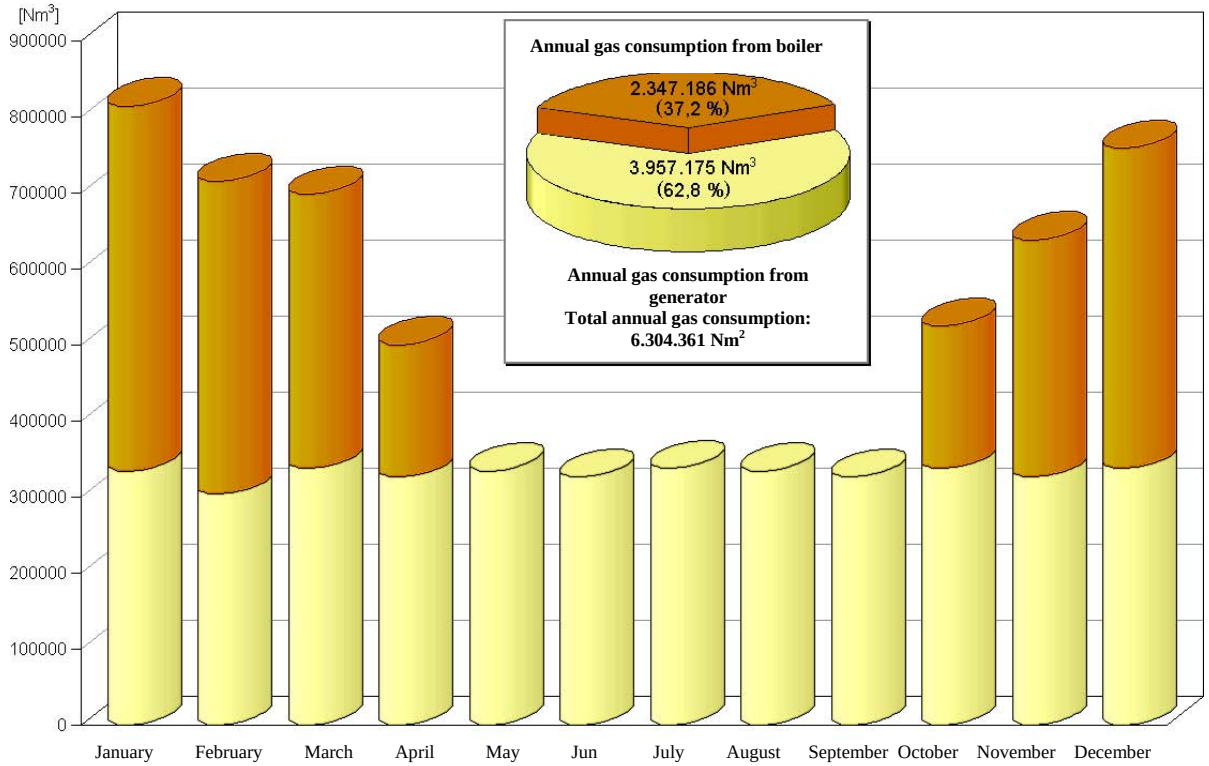

Monthly gas consumption ***Enclosure 5***

ECONOMIC ANALYSIS

Initial data for the assessment of module operation efficiency (gas motor-generator for the production of electric energy and heat energy recovery) are the natural gas input energy purchase price and price of electric power from the user's distribution network.

Financial effects of the reduction of operating costs by using cogeneration process are expressed based on the yearly power consumption of the business complex of 105 000 m^2 according to the following data:

annual electric power consumption	13 050 MWh
annual used recovered heat	16 232 MWh
annual gas engines gas consumption	3 957 175 Nm^3
equivalent quantity of gas proportional to used recovered heat	2 287 985 Nm^3
price of electric energy from power distribution grid	52,5 €/MWh
gas price	0,033 €/Nm^3

The financial result is a difference between the value of produced electricity as compared with the gas consumed by gas-motor minus the equivalent gas quantity proportional to the used recovered heat:

produced electric energy	13.050 MWh x 52,5 €/MWh	685.125 €
value of consumed gas	(3.957.175 – 2.287.985) Nm^3 x 0,033 €/Nm^3	55.083 €
total financial result is		**630.042 €**

Approximate investment value of the power generating unit part intended for the production of electric energy (BE) with the use of recovered heat is:

3 x 1 400 kW x 650 €/kW = 2 730 000 €

Comparison of the investment value of power generating unit part intended for the production of electric energy (**BE**) and the return resultant from the difference of costs of the complex power supply from the external distribution power grid and from its own electric energy production increased by the value of used recovered heat energy shows that the investment will be recovered in the fifth year of operation.

Longer period of investment recovery is due to the requirement of full self-sufficiency of the business complex in the supply of power consumption and coverage of possible extreme loads.

Depending on the gas and electricity prices, a cogeneration plant of the same operating characteristics will have different financial result:

Serbia	122.000 €	at the gas price of 0,31 €/m^3 and electricity price of 49 €/MWh
Germany	572.090 €	at the gas price of 0,40 €/m^3 and electricity price of 95 €/MWh

Feasibility of investments in the production of electric energy by gas modules stands in direct proportion to the difference of prices of electric energy from the distribution power grid and electric energy from gas modules (*Enclosure 6*).

The enclosed diagram shows the comparison of world countries depending on the absolute price difference of electric energy from distributive power grid and from gas motor-generator. Economic effects increase additionally due to the cogeneration process – combined production of electric and heat energy by gas motor-generator.

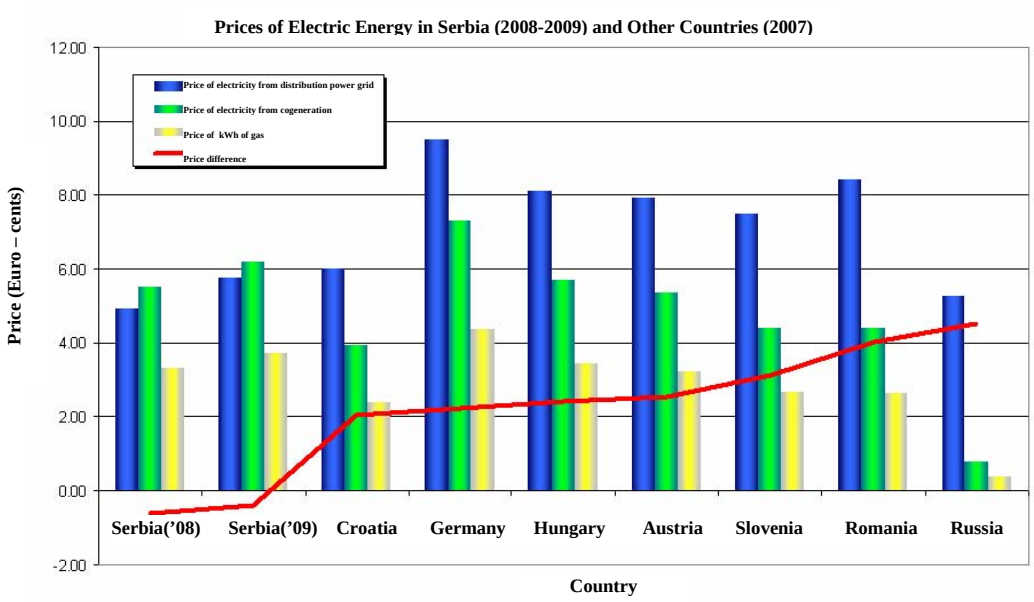

Enclosure 6

Price of participation of connection of a business complex of usable square area of 105 000 m^2 to distribution power grid should in particular be analyzed since it certainly exceeds many times an investment in a self-sufficient source for combined production of electric and heat energies by gas engines.

Feasibility of investment in the production of electric energy by gas motor-generators stands in direct proportion to the difference of prices of electric energy from the distribution power grid and electric energy from gas modules, quantity of used recuperated heat energy and achieved number of running hours during the year (*Enclosure 7*).

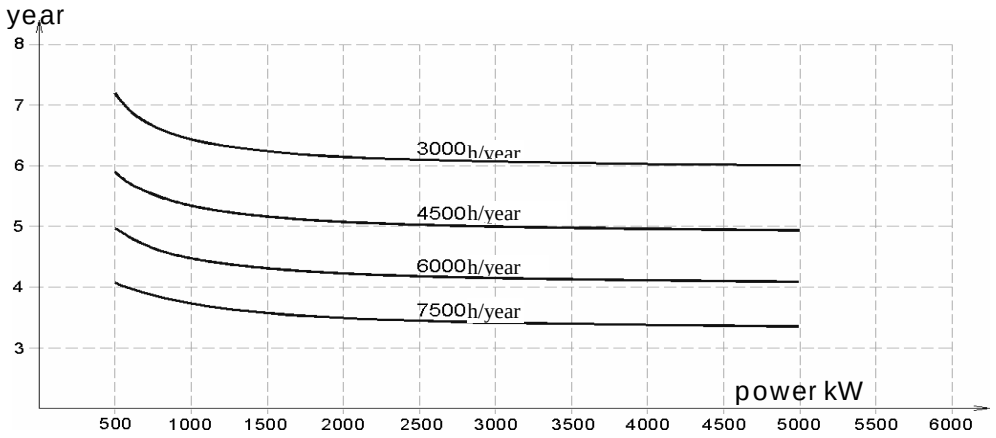

BE investment pay-off period ***Enclosure 7***

KYOTO PROTOCOL APPLICATION

After entering into force, the Kyoto Protocol has opened possibility for companies to obtain additional financial means for the realization of investments by acquisition of greenhouse gases emission reduction units.

Greenhouse gases (GHG), the emission of which is to be reduced, are carbon dioxide, methane, nitrous sub oxide, industrial gases (HFC and PFC) and sulfur hexafluoride.

In 1997 was signed the Kyoto Protocol according to which the countries that ratify it accept target values of reduction of quantified greenhouse gases emissions over a specific period of time. The countries specified in the Annex I (industrialized countries and economies in transition) accept the emission reduction target values and commit themselves to reduce GHG in the period from 2008 to 2012 by 5,2 % as compared to the level in 1990. The Kyoto Protocol entered into force on 16 February 2005 and until now 170 countries have joined it. The Assembly of the Republic of Serbia passed the Law on the confirmation of Kyoto program with the UN Framework Convention on Climate Changes.
The parties to the Annex I are allowed, in addition to the efforts put forth in the emission reduction within their own territories, to acquire greenhouse gases emission reduction units in the framework of Clean Development Mechanism projects by implementing projects in the countries that are not parties to the Annex I which is the case of Serbia. At the same time, participants in a project from Serbia may develop and register their own projects within the Cleans Development Mechanism and, in that way, take part in the process of greenhouse gases emission reduction on an international level. Emission reduction units achieved as a result of implementation of projects can be verified, issued and sold to a buyer – a country that is party to the Annex I (Certified Emissions Reduction, CER).
A Certified Emission Reduction unit is 1 CER and it is equal to the CO_2 emission reduction by 1 ton, the actual market price of which is 4 – 14 €.
In this way, participation in CDM opens, in fact, the possibility to the companies from Serbia to secure additional financing of their projects that meet the prescribed criteria.
Projects based on cogeneration can be registered as „climate project“ on the grounds of their effectiveness. Greenhouse gases emission reduction by producing electricity using cogeneration is based on the following data:

13.050,00	MWh	consumption of power supplied from power grid
1 CER	tCO_2/MWh	certified emission reduction unit for the Serbian national power grid
13.050,00	tCO_2	base emissions due to the use of power grid electricity
3.957.175,00	m^3	gas necessary for the production of 13.050 MWh of electric energy
2.287.985,00	m^3	reduced gas consumption in boiler room due to cogeneration heat utilization
1.669.190,00	m^3	consumption of gas with cogeneration effect
0,03348	GJ/m^3	natural gas heat capacity
55,88	TJ	energy required for the production of 13.050 MWh of electric energy reduced by the effect of used recuperation heat from the cogeneration process
56,1	tCO_2/TJ	natural gas emission factor
3.136	tCO_2	required emissions for the generation of 13.050 MWh of electric energy
9.914	tCO_2	emission reduction on account of electricity production in a cogeneration unit

Preliminary calculation indicated in the table which has to be certified by the competent institutions according to the UN procedure, shows the carbon dioxide reduction, i.e. the financial effect:

9.914 t CO_2/year = 9.914 CER/year x 10 €/CER = **99.140 €/year**

The total financial effect for the Kyoto period 2009-2012 is:

99.140 €/year x 4 years = **396.560 €**

Every company that wishes to take part in carbon trading can earn additional profit by registering its project as climate project before the commencement of its realization and find a purchaser for its emissions reductions.

CONCLUSION

Distributed combined production of energy directly on the place of consumption and firmly technologically connected in the production of electric, heating and cooling energies provides high utilization factor of primary energy source and represents optimum alternative to former erection of bulky centralized power systems. For the large public, health, educational, business and industrial facilities, the value of means needed for the connection to public utilities networks for the supply of electric and heating energy exceed the means required for the erection of own power supply unit, which provide full self-sufficiency in operation as well as high level primary energy utilization.

TYRES MAINTENANCE AT OPEN-PIT MINING AND THEIR LABELLING

A. Gajić, D. Živanić, R. Đokić

Abstract: *Serviceband life of tyres depends on many parameters which are complex and mutually influence each others, so that is necessary perform continuous logistic monitoring and analyzing of each parameter. This represents very complex task which cannot be realised in short period, but considering that working life of tyres can be increased up to 50 %, amount of saving realised by this justifies all undertaken measures and researches. Regular maintenance represents one of basic elements necessary for extension of working life of tyres, reducing losses of working hours as well as decreasing of entire costs related to tyres. In work, influential factors would be prominent which affect regular maintenance of tyres like tyre condition control, maintenance of road surface substrate, assembling and disassembling of tyres, handling, storing as well as keeping records and automatic data processing by computers, which does not have direct influence, but yet links and unites impact of other factors by which significantly quality, easier and simpler maintenance of tyres is achieved.*

Keywords: *tyre, maintenance, exploitation*

1. SERVICEBAND LIFE OF TYRES

1.1. Possibilities for extension of serviceband life

Having in mind that tyres take significant position in maintenance costs as well of machines used in mining (depending on conditions their participation goes up to 25 %), so that in process of exploitation in general (where they take third position, after explosives and fuel), it is very significant to find out solution for reducing costs for tyres. The only possibility for decreasing of these costs is extension of their serviceband life.

Defining of possible working life of tyres used on mining equipment for concrete operating conditions is very important and long-lasting procedure which requests logistic approach to the control and monitoring of numerous number of parameters which influences mutually interfere. For determination of influence level of each and single parameter, it is necessary to perform researches in detail, based on which a realistic situation picture is obtained that enables more precise determination of working life.

During tyre utilization/exploitation many abnormal wear and tear appear at certain positions and also increase participation of mechanical defects. There are different causes for this appearances : unadjusted front parts of the vehicles, failures in road cleaning against dispersed material, too sharp and incorrect curves, narrow part of a road when tyres are damaged by road slope during crossing/passing by of vehicles, brakes out of order causing over heating and even explosion of tyres, stone cleaners out of order with tyres in pair, mistakes in maintenance anticipated pressures in tyres and similar. By influence to the causes of actions, these unfavourable events may be reduced which can increase tyre serviceband life.

The researches have shown that for extension of tyre serviceband life and reducing costs they have in operation, there are three ways:

- extension of working life of normally worn tyres,
- reducing of participation of mechanical damages,
- renewal – of used tyres by a special method- so called protecting.

As normal worn-out tyres are considered those which were exploited to the final worn-out of surface layer-protector. There are several classification of parameters on which tyre working life depends on (given by various manufacturers), but all of them are similar and there are only minor differences in coefficients as they have origin in American mine researches. Based on these parameter classifications, as well as on the basis of researches carried out in our mines, we can form empiric formulae for calculating of possible tyre working life:

$$T = A \bullet B \bullet C \bullet D \bullet E \bullet F \bullet G \bullet H \bullet I \bullet Td \quad [h]$$

Where:

Td - expected serviceband life in an ideal conditions (based on research),

A, B,...,I - parameters of exploitation conditions.

In Table 1 values of condition parameters of exploitation are given according to literature, corrected on the basis of researches in our mines.

MSc Anto Gajić, grad. mech. eng., Mine and Thermal Power Plant Ugljevik, Republic of Srpska, antogajic@yahoo.com ,
MSc Dragan Živanić, grad. mech. eng., Faculty of Technical Sciences Novi Sad, zivanic@uns.ns.ac.yu,
grad. mech. eng. Radomir Đokić, Faculty of Technical Sciences Novi Sad, djokic@uns.ns.ac.yu

Table 1 – Condition parameters of exploitation

par.	name	conditions	value
A	maintenance	excellent	1.1
		good	1.0
		average	0.9
		bad	0.7
		very bad	0.4
B	outside temperature	cold weather	1.2
		moderate	1.0
		hot	0.8
		very hot	0.5
C	maximum speed	16 km/h	1.2
		32 km/h	1.0
		48 km/h	0.8
		64 km/h	0.5
D	curves	without curves	1.1
		moderate curves	1.0
		sharp (1 tyre)	0.8
		sharp (2 tyres)	0.7
E	load efficiency	50% of load	1.2
		80% of load	1.1
		110% of load	1.0
		120% of load	0.8
		140% of load	0.5
F	substrate condition	rolled snow	3.0
		frozen rolled substrate	1.2
		rolled substrate	1.0
		mud	0.8
		abrasive mud	0.5
		soft limes	0.7
		hard limes	0.6
G	wheel position	back left	1.0
		back right	0.9
		front bridge	0.7
H	rise for drive wheels	hard substrate	0.9
			0.8
			0.7
			0.4
		loose or sliding substrate	0.6
			0.5
			0.4
I	exploitation level	excellent	1.1
		good	1.0
		average	0.9
		bad	0.8
		very bad	0.7

While determining expected serviceband life in an ideal conditions, it has been established that the value is not for all dimensions of tyres, but it changes with diameter of tyre. This thesis comes out from the fact that by increasing of diameter while the speed stays the same certain parts of protector are more seldom in touch with substrate therefore intensity of wear and tear is less. Thus, with diameter increase, expected serviceband life also increases in ideal conditions of exploitation. So, for example, it was found by research that for tyres with dimensions 24.00 - 35 expected serviceband life is Td = 6500 h, and for tyres with dimensions 36.00 - 51 expected serviceband life is Td = 9600 h.

Parameter „A” represents the level of maintenance. To make appraisal of maintenance level and selection of coefficient more realistic, scope of maintenance should be defined. Maintenance of tyres consist of the following activities:

- assembling of tyre to felly/rim (cleaning of felly/rim, change of valves, change of sealed rubber rings etc.),
- assembling of wheel to the vehicle (adjustment of leaning cone surfaces, mantling of valves, tightening of a wheel etc.),
- monitoring of tyre condition during exploitation (subsequent control and tightening of screws of wheels, cleaning of material that penetrated to protector, control of regularity of stone cleaners at tyres in pair/double tyres, pressure control in the tyres etc.),
- control and adjustment of steering mechanism.

All mentioned activities , out of which some look simple, are very important but monitoring conditions during exploitation is basic parameter for defining maintenance level. Among mentioned activities, major influence to serviceband life has maintenance of prescribed pressures. Both higher and lower pressures of nominal one are bad. With higher pressures elasticity is less, resistance to mechanical damage is less and bigger wear and tear. Lower pressure causes increase in tyre temperature, unequal speed of attrition by width of protector as well as overload of second tyre (at double tyres).

Parameter „B” represents outside temperature. This is also important parameter, especially during selection of tyres. Yet, researches have shown that this parameter does not have priority influence to events of mechanical damages, although speed of worn-out is somewhat higher in summer period.

Parameter „C” represents maximum speed. This parameter is not of great importance considering that configuration of terrain does not allow high speeds. But, maximum speed may happen especially during move of unloaded/ less loaded vehicles.

Parameter „D” represents influence of curves. The curves in the most of mines are sharp and level of influence of this parameter increase with increase of the

width of tyres. This parameter is of special influence in case of double tyres, because during going through a curve bigger sliding occurs. This happens because double tyres drive different paths while going through a curve , so the larger wear and tear and damages appear, the sharper curves are.

Parameter „E” represents influence of load efficiency. With increase of load above prescribed value, greater increase in exertion of tyre happens and so more intensive wear and tear of protector.

Parameter „F” represents influence of substrate condition. This parameter is important also when selection of tyres is made. For determination influence of substrate condition it is necessary exact participation of each single type of substrate during year. Substrate has been classified into following six categories:

I	rolled snow
II	frozen rolled substrate
III	dry rolled substrate
IV	muddy substrate
V	wrinkled/rough muddy substrate
VI	road covered with gravel/macadam

From the point of influence to serviceband life of tyres, first three types of substrate as well as macadam belong to more favourable, but it has been found by research that increased damage and wear and tear of tyres is in action. Reason for this is that speed of moving is faster when substrate is more favourable, so that dispersion of material on the road is larger, whilst at the rough substrate speeds are smaller, and also operator's attention is better.

Parameter „G” represents influence of the wheel position. This parameter has significant influence to serviceband life of tyres because of differences of conditions in which tyres are toward road, load distribution, in curves and similar. It is noticeable lower value for the front bridge, what has been consequence of steering mechanism adjustment, higher sensitivity to pressure changes than at the back bridge, uneven material loading, sudden braking when tyres at the front bridge are overloaded, entering to sharp curves with high speed when appear high cross-sectional loads and sliding etc.

Parameter „H” represents influence of rise. While analyzing this parameter it has to be taken into account, besides influence of maximum rises also participation of rise in total road length. Within this parameter attention should be paid also to the transportation lengths. Shorter transportation lengths are more favourable because of cooling possibility during engine stopping. On the other hand, with shorter lengths loadings and unloading are more often when there are greater possibilities for mechanical damages and more intensified wear and tear.

Parameter „I” represents influence of exploitation level. This parameter is of special importance to serviceband life of tyres and it has been characterized by the following elements:

- obeying prescribe
- d loads,
- uniformity of loading to the box (basket) of truck (type 'dumper'),
- speed adjustment to road characteristics,
- obeying prescribed speeds,
- obeying braking regimes,
- moving through curves,
- road maintenance,
- access maintenance to loading and unloading sites.

Another mode of possibility for extension of tyre serviceband life represents reducing of participation of mechanical damages. Basic factors for reducing mechanical damages of tyres make tyre, maintenance level and exploitation level. Researches have shown that mechanical damages are more frequent during summer period, although roads are better in that period. The reason for this lies in fact that production is the most intensified in summer period so that load coefficient is higher, speeds are higher of moving so dispersion of material along road is bigger. Also, after rainy spring, the road are being repaired by covering with sand which is not rolled enough, so in that case tyres have role of rollers.

The third possibility for extension of tyre serviceband life represents renewal i.e. protecting of normally worn-out tyres. At the most of worn-out tyres come to permanent worn-out of protector, but karkas i.e. karkas structure, sides, steps/foot and similar stay in satisfactory working condition (if major defect did not occur) so that such a tyre can stand one more exploitation. For that reason, such a tyre can be renewed by addition of a new protector layer by vulcanisation process. Protecting of tyres can be done in two ways. First way is that a new layer of protector is put over the old, worn-out one, and the second way is removing of worn-out protector and then putting a new protector in vulcanisation process. Renewal i.e. tyre protecting is done in for that purpose specially equipped workshops or, what is more often, that procedure is done in the manufacturer's factory.

1.2. Measures for serviceband life extension

Based on the previous analyse and research of parameters influence tyre serviceband life, it can be concluded that by increase of exploitation and maintenance level extension of tyre serviceband life is to

be expected. In that meaning, the following measures are to be undertaken:

- the most attention should be paid to road design and construction; if possible make curves with as big diameters as possible and avoid extreme rises; during road construction use covering material that is less abrasive and compulsory roll the roads, during rainy days clean mud regularly, especially at rises, and also permanent presence of auxiliary mechanisation for cleaning of dispersed material;
- decrease maximum speeds to the lowest possible which will not essentially reduce vehicle performance and will not allow vehicle overload;
- pay greatest attention to maintenance of prescribed pressures in tyres;
- regularly analyze results and undertake measures as soon as declination is noticed compared to expected, and if necessary, change also characteristics of newly purchased tyres;
- participation of mechanical defects must be completely excluded, and if not possible reduce them to the lowest possible measure (as it is removing foreign bodies which stay in protector, maintenance of stone cleaners, cleaning fuel/or oil spots and similar).

Having in mind that parameters that affect tyre serviceband life are complex and that they mutually interfere, it is necessary to perform permanent monitoring and analyzing of each parameter itself, as well as continual correction of their coefficient values.

This has not been easy task at all and it is not feasible for short-term period, but considering that tyre serviceband life can be extended even up to 50 %, saving amount in that case justifies all undertaken measures and researches.

2. TYRE MAINTENANCE

2.1. Factors that influence regular maintenance of tyres

Maintenance of tyres that are being used in mining equipment of different purposes, represents very significant and influential factor on which depends both tyre exploitation i.e. serviceband life and exploitation of equipment itself on which tyres are positioned. Regular tyre maintenance represents basis for working life extension, reducing working hours losses because of machine stopping and also decreasing of entire costs related to tyres.

With regard that working conditions of mining machines and equipment are difficult and complex, one should have in mind that tyres on those machines are exposed to continuous both static and dynamic loads, which cause various defects on tyres. For that reason, depending of type of damage, tyres are temporary or continuously put out of use. The defects for which tyres become permanently or temporary useless are:

- various lacerations of surface or side part of tyre,
- blown down pieces of tyre,
- separation of protector from karkas,
- worn-out protector,
- blown down karkas and similar.

However, by regular maintenance many of these defects could be avoided or reduced to the minimum. Factors, which influence regular and timely tyre maintenance, make:

- tyre condition control,
- road maintenance,
- assembling and disassembling of tyres,
- handling and storing of tyres and
- keeping reports and automatic data processing.

Besides these factors i.e. maintenance jobs, to realize maximum maintenance effect permanent mutual co-operation between maintenance sector, machine and equipment operating staff is needed, as well as tyre manufacturer itself. Within sector for maintenance of machinery and equipment, there is a special workshop for tyre maintenance equipped with tools, instruments, compressor and other devices necessary for tyre maintenance. Also, There is professional staff exclusively in charge for tyre control and maintenance.

2.2. Tyre condition control

The objective of tyre condition control is to see and remove timely all before mentioned defects. By such examination and removal of defect causes serviceband life of tyres is extended. Examination is done every day when machine is used, both before and after use, and it consist of attentive visual observation of outside and inner surfaces of tyre elements, as well as of characteristics measurement and control (pressure, depth of groove on protector etc.).

At outside side of tyres, condition of protector is visually examined as well as sides and type of defect is found out. In case that in grooves of protector stones or other foreign bodies are spotted , they have to be removed, and spots of oil or fuel have to be cleaned and washed out. Minor defects, like lacerations or minor breakthroughs, by itself do not represent danger for further exploitation , but they contribute to further

destruction of tyre because they gradually increase. Some major defects , like fully worn-out of protector during intensive exploitation where karkas, foot and other parts in satisfactory condition, can be removed by putting new layer of protector i.e. by protecting. Yet, mainly, with major defects tyres are to be used up. Some typical tyre defects are shown in figure 1, and they can be represented as:

- slashes, stubs and breakthroughs on protector which happen as consequence of sharp and wedge-shaped stones and other foreign bodies at too high pressure in tyres, overload, speed above prescribed value, as well as because of bad road conditions;
- separation of protector's part from karkas can appear because of over speed, overload or over-pressure, as well as when moving on bad roads;
- slashes and wear and tear of central part of protector may occur because of over speed, over-pressure or overload, as well as due to sudden braking;
- slashes and cut through of tyre sides appear because of overload or too low pressure;
- tweaking protector's and karkas' parts may occur because of over speed, at overload or at too low filling pressure;
- damage of core and sides of tyre foot may occur at irregular value of filling pressure, at overload or sudden and too strong braking, as well as because inadequate or damaged felly/rim;
- explosion of tyre which may occur because over speed, overload or too high filling pressure while moving at bad road.

Visual examination must be done carefully, in order to notice and remove all foreign bodies of sharp edges which penetrate to tyres, and which are not visible at the first sight. Besides stains/spots from oil derivative it is necessary to clean all dirt, dust, water and other impurities because they stay in rifts and lacerations, and by their influence faster spreading of these minor defects occur.

Rims must be examined carefully to find out eventual distortions, bending, cracks or some other damages. Also, attention must be paid whether exists air exhaust. All screws which tie discus and wheel rim with shaft/axis of the vehicle must be checked and, if necessary make additional tightening or eventual change. Valves are examined to find out whether damages exist and if cap of a valve is lost a new one must be put to it. At double tyres, regularity of stone cleaners is checked and removal of stones is done to those spiked between tyres.

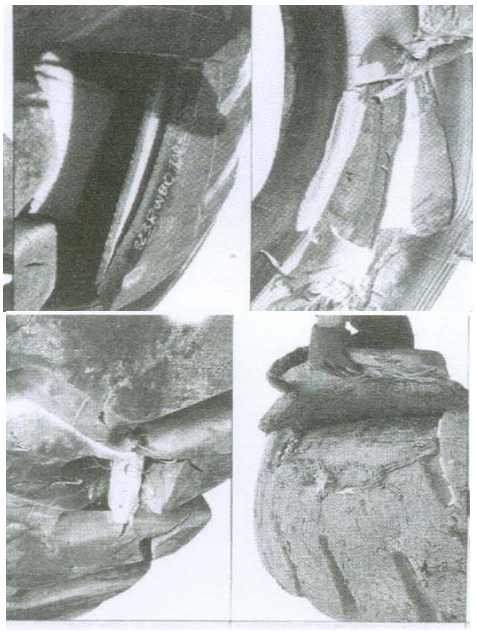

Fig. 1. Typical damages of tyres

Besides visual examination of tyre condition , control and measurement of tyre characteristics is performed, i.e. air pressure and depth of groove, as well as temperature control in work. Control and measurement of protector groove depth is used to determine amount of wear and tear of protector, which is obtained by comparison of groove depth of used and a new tyre. Measurement of groove depth is done in two points which are located about ¼ from the edge of both sides of protector, as it is shown in figure 2, and then an average value of both measurements is taken.

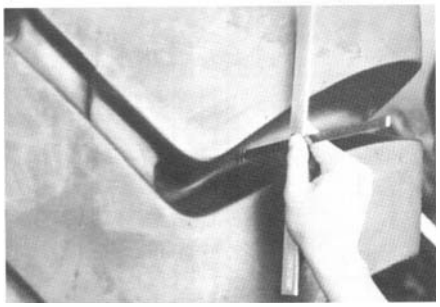

Fig. 2 – Groove depth measurement of protector

Obtained average value is compared with values for new tyres, which manufacturers usually attach in form of a table for each type and dimension of tyre. Tyre temperature control in work is important task , because very negative consequences may occur because of heat accumulated during heating of tyres. In Figure 3 dependency of temperature in tyres and hours of continual work is given. Maximum allowed temperature varies up to 107°C, considering that values of temperature, needed for conversion of raw rubber and additives to homogeny mixture during vulcanisation process are above 132°C. Measurement is performed at the thickest part of protector (which is also the hottest) in a several points along whole width of tyre.

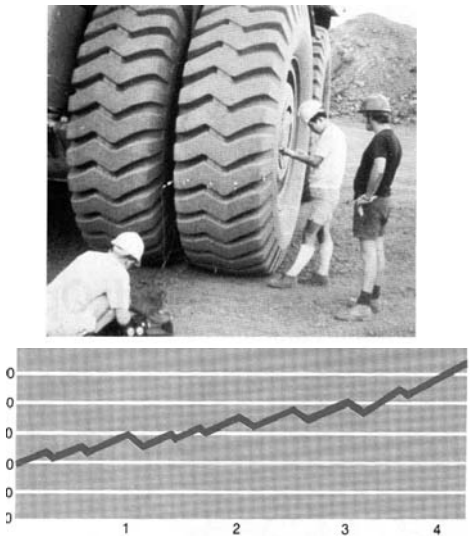

Fig. 3. Temperature control

2.3. Road maintenance

Permanent control and regular maintenance of loading-unloading sites and transportation roads represent one of important factors for exploitation and long working life of tyres especially for transportation machine tyres i.e. dumpers and scrapers. Having in mind that roads are considered as temporary, very often to their maintenance not much attention is paid, so they become negligent, as it is shown in figure 4.

Before beginning of work , it is necessary to check situation of loading-unloading sites and roads and remove all spotted obstacles (rocks, parts of equipment and similar) and roughness which may cause defects at tyres. Road surfaces must be always cleaned by dozers and graders. Also, anybody at the working site, in disregard with the job he is hired for, is obliged to remove spotted obstacles and foreign bodies without waiting for coming of professional machinery for road maintenance.

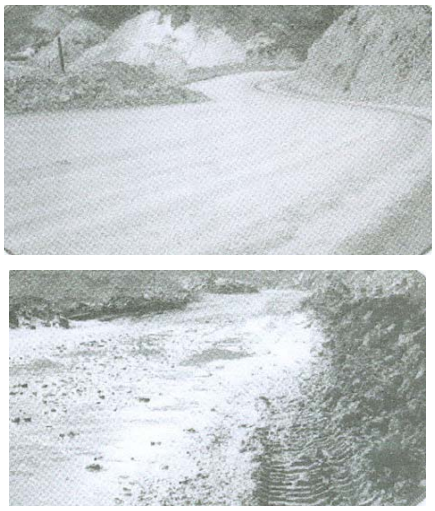

Fig. 4 – Good and bad road maintenance

Although constant maintenance of roads and loading-unloading sites takes time and efforts, standstills and costs which may appear because of bad condition of road substrate are several times bigger.

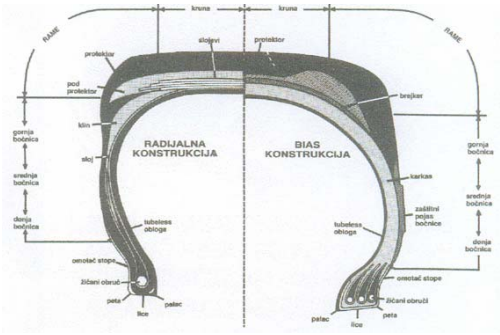

Fig. 5. Labelling of tyres

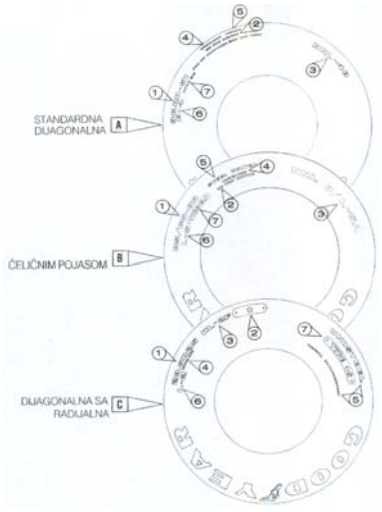

Fig .6. Labels at side wall of tyre and their meaning

3. CONCLUSION

Tyres that are used for mining equipment are of special manufacturing intended for work in difficult and complex conditions, which must meet special and specific requirements with which modern mining is facing with today. Considering that they have wide appliance for mining machines and equipment for different purposes, tyres have very important and significant influence as well to work of equipment itself so to entire process of exploitation of bed of mineral crude material where that equipment is applied. For that reason, tyres are manufactured in wide range of types, design and dimensions so that today there are tyres of radial and diagonal design, with or without inner tyre, with standard, wide or low profile dimensions, classified in a wide palette of different types.

Having in mind all requirements which they have to meet as well as conditions in which they have to apply, correct selection of tyres represents very complex and

responsible task which depends on series of parameters and factors, different by type, influence and scope that mutually supplement and interfere. Due to that reason, during selection of tyres it is very significant joint co-operation with manufacturers of tyres.

After tyre selection it is necessary to pay special attention during use i.e. tyre appliance so, to achieve maximum efficiency in work, by which costs are decreased, life increased and reduced losses of working hours to minimum. Having this in mind, during appliance of tyres it is necessary to obey prescribed speed values, not allow overload of tyres, maintain prescribed filling pressure value, pay attention to regular machine and equipment maintenance where tyres are applied, condition of road surface substrate should be correct and well maintained, not allow irresponsible, unprofessional and unaware handling of machines, obey prescribed advice and recommendations during use of double tyres and similar.

Extension of tyre serviceband life is of crucial importance in decrease of tyre costs, which are after costs for explosive and fuel, at the third place by amount. Many parameters, which are complex and mutually interfere each others, influence the extension of tyre serviceband life. So, it is necessary to perform permanent monitoring and analysing of each parameter. This represents very complex task that is not feasible for short period of time, but considering that working life of tyres can be extended up to 50 %, amount of saving realised in this way justifies all undertaken measures and researches.

Keeping reports and especially automatic data processing by computers represent very important and significant factor, which does not have direct impact to regular tyre maintenance, but, yet, it links and unites influence of other factors by which significantly quality, easier and simpler tyre maintenance is achieved.

Observing all aspects mentioned as well as trend of development and appliance of modern mining equipment, it can be concluded that correct selection, appliance and maintenance of tyres for mining equipment have tendency to become one of the most important and the most influential factors in economics of entire process of exploitation of crude material mineral beds.

REFERENCE

[1] RUŽANOVIĆ, S., FILARESKOVIĆ, R.: *Exploitations condition influence to age duaribility of pneuamatic tyres for heavy truck,* magazine „Bakar", Bor 1983,

[2] RUŽANOVIĆ, S.: *Depletion speed of pneuamatic tyres for heavy truck,* Magazine „Bakar", Bor 1982,

[3] 33 - 15 Service Manual, TEREX GM,

[4] *Practical Use of Toyo OTR Tires*, TOYO Tire & Rubber Co. LTD., Osaka, Japan,

[5] *Maintenance of Toyo OTR Tires,* TOYO Tire & Rubber Co. LTD., Osaka, Japan,

[6] *Caterpillar Performance Handbook*, Caterpillar Tractor Co., Peoria, Illinois, USA, 1985.,

[7] *Technical documentation*, Office for pneumatic tyres development, Factory of rubber products "REKORD", Rakovica

[8] RADULJČIĆ, S.: *Tyres for motor vehicles*, Technical administration SSNO, Belgrade 1968.,

[9] *Properly use of pneumatics*, Office for preferment of tyres, Belgrade 1965.,

[10] Yugoslav standard JUS.G.E3.005

[11] Standards E.T.R.T.O.

MATHEMATICAL MODELS INDUSTRIAL OBIJECT WHERE THERE IS AERATION, HEAT SOURCE AND BEGINNING HUMIDITY

Š. M.Bajmak

Abstract: *For studing the model methods, letis examine the next structure (building) specificly: exterior walls have openings for air flow, inside the building is a heat source, humidity and mechanical aeration system.The exterior of the building is exposed to wind.As a result of joined effect of heat, wind and mechanical aeration a detremined air change grows in the building, so a temparture regime is formed.The process of air change and temparture regime, we will analyse on the building model on working zone in air model. Obviesly , for this examanation iti is necessary to avail the condicionality, by which the model can be calculated, knowing the models dimensions, as well as air stream and power of heat source and humidity in model.*

Key words: *mathematical models, aeration , heat source, beginning humidity*

1. INTRODUCTION

For studing the model methods, letis examine the building shon in picture 1.On sides the building has openings, inside we have heat source and humidity is exposedto wind. As a result of joined effect of heat, wind and mechnical aeration, a defermined air change grows in the building, so a temparture regime is formed.

The process of air change and temperature regime we will analyse on the building model on working yone in air model. Obviesly, for this exemanation iti is necessary to avail the condicionality, by which the model can be calculated, knowing the models dimensions , as well as air stream and power of heat source, and humidity in model.It is necessary to know the formulas, by which escorts calculation in speed model, heat and humidity on becomingly natural siyes.

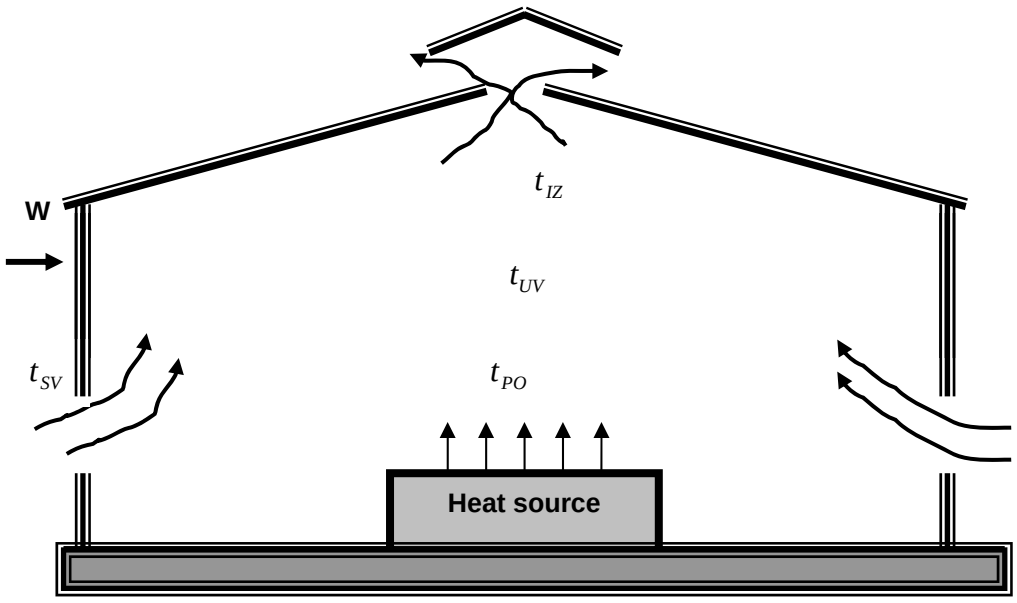

Picture 1. Bulding drowing in cross intersection

Prof. dr. Šefik M.Bajmak, Faculty of technical engineering University of Pristina

2. AIR CHANGE MODELING

We define speed as relation of air speed analagically in model and building:

$$C_v = \frac{v''}{v'} = \frac{\mu'' \sqrt{\frac{2\Delta p''}{\rho''}}}{\mu' \sqrt{\frac{2\Delta p'}{\rho'}}} = C_\mu \sqrt{C_{\Delta p}} \qquad (1)$$

Variables with pm (') mark are in reference for the building, and variables that have secund mark are in reference for the model (").

Pressure difference variable is sustained starting from air overinflate, analogically on the interior arear model and building barrier:

$$C_{\Delta p} = \frac{k_i'' \frac{\rho'' \left(W''\right)^2}{2}}{k_i' \frac{\rho' \left(W'\right)^2}{2}} = C_{ki} C_v^2 \qquad (2)$$

If we look at the building and modes as bad aerdynamic entity, and turbulent air flows are almost equals, than aerodynamic coefficients are equal $(k_i' = k_i'')$. Supstition in equation (1) variables for pressure difference and having in minid that $C_{ki} = 1$, we will get that:

$$C_\mu = 1 \qquad (3)$$

It is known that consumption coefficient depends on the number of Reynods . Whwn number Re increases, than on the building we have an increase, and than starting from some Re=2400 , consumption coefficient μ stays constant.For these kinds of buildings Raynolds number is allways bigger than the given $\left(R_e' > 2400\right)$, that is why for compleating the quideline in formula (2) , it is necessary to start, for the model as well that $R_e'' > 2400$. Pressure difference can be gotten starting from gravitacional pressure :

$$C_{\Delta p} = \frac{\Delta \rho'' g h''}{\Delta \rho'' g h'} = C_{\Delta p} C_l \qquad (4)$$

Vacissitudion of pressure difference variables in equation (1) and having in mind that $C_\mu = 1$, we will get the next formula for detemining the speed:

$$C_v = \sqrt{C_1 C_{\Delta p}} \qquad (5)$$

This formula can be shown differently. In that ain we use the known dependence for air density:

$$\rho = \frac{\rho_{sv}}{1 + \beta \cdot \Delta t} \qquad (6)$$

Than we have for air :

In the building:

$$\Delta \rho' = \rho_{sv}' - \rho' = \beta \rho' \Delta t' \qquad (7)$$

In the building model:

$$\Delta \rho'' = \rho_{sv}'' - \rho'' = \beta \rho'' \Delta t'' \qquad (8)$$

After clearing (solving) equation (4) we get:

$$C_{\Delta \rho} = \frac{\Delta \rho''}{\Delta \rho'} = C_{\Delta t} \qquad (9)$$

Vacissitudion of gotten formula (9) density difference in equation (5) , we will get that speed is:

$$C_v = \sqrt{C_1 C_{\Delta t}} \qquad (10)$$

Consumtion variable in that case would be:

$$G_G = \frac{G''}{G'} = \frac{\rho'' F'' v''}{\rho' F' v'} = C_l^2 C_v \qquad (11)$$

3. HEAT CHANGE MODELING

Heat amount can be presented like:

$$C_Q = \frac{Q''}{Q'} = \frac{c \cdot G'' \left(t_{IZ}'' - t_{SV}''\right)}{c \cdot G' \left(t_{IZ}' - t_{SV}'\right)} = C_G \cdot C_{\Delta t} \qquad (12)$$

Congruent with similarity theory, same amount can be shown in convective amount of heat :

$$C_Q = \frac{\alpha'' \cdot A'' \cdot \left(t_{PO}'' - t_{UV}''\right)}{\alpha' \cdot A' \cdot \left(t_{PO}' - t_{UV}'\right)} = C_\alpha C_l^2 C_{\Delta t} \qquad (13)$$

Let's define the heat transfer coefficient . this coefficient in correspondence with heat transfer theory is defined by formula:

$$\alpha = m \frac{\lambda}{l} \left(Gr\, Pr\right)^n \qquad (14)$$

Coefficient m and the degree shower (indicafor) n depend on the criteria $Gr\, Pr$, that is defined by formula:

$$Gr = \frac{gl^3}{\nu^3}\beta\Delta t; \qquad Pr = \frac{\nu}{a} \quad (15)$$

When the quality for λ, ν, a find for average temperature $t_{sr} = 0,5(t_s + t_u)$. For $Gr\,Pr = 5\cdot10^2 \div 2\cdot10^7$ we have amount for $m = 0,54$ and $n = 0,25$, and when $Gr\,Pr > 2\cdot10^7$, effluents that the heat transfer coefficient dimension would be without dimensions and for heat source, unequality $Gr^{"} Pr^{"} > 2\cdot10^7$ has to be complited in the model. In that case, we have:

$$C_\alpha = C_{\Delta t}^{1/3} \quad (16)$$

Vacissitudion C_α in formula (12) we have that:

$$C_Q = C_l^2 C_{\Delta t}^{4/3} \quad (17)$$

The solution for equations 10,11,12 and 17 permits us to establish a geometric dimension of the model by:

$$C_l = C_{\Delta t}^{1/3} \quad (18)$$

Heat radition coefficient

$$C_Q = \frac{4,96\varepsilon_1^{"}\varepsilon_2^{"}\phi^{"}A^{"}\theta^{"}\left(t_{PO}^{"} - t_{PRE}^{"}\right)}{4,96\varepsilon_1^{'}\varepsilon_2^{'}\phi^{'}A^{'}\theta^{'}\left(t_{PO}^{'} - t_{PRE}^{'}\right)} = C_\varepsilon^2 C_\phi C_l^2 C_\theta C_{\Delta t} \quad (19)$$

When temperature factor (θ) is equals to:

$$\theta = \frac{\left(\frac{T_{PO}}{100}\right)^4 - \left(\frac{T_{PRE}}{100}\right)^4}{t_{PO} - t_{PRE}} \quad (20)$$

It is seeable that $C_\phi = 1$ ofter geometric similarity, and $C_\theta = 1$, if the apsolute tempearture with aeration process in inconsiderably different one from the other.That is why equation (19) can be written as:

$$C_Q = C_\varepsilon^2 C_l^2 C_{\Delta t} \quad (21)$$

The joined solving of equations (12) and (21) we can get, the blackness degree of the area can be shown by:

$$C_\varepsilon = \sqrt{C_\nu} \quad (22)$$

The amount of heat through the barrier constructions can be shown by:

$$C_Q = \frac{k^{"}S^{"}\left(t_{PRE}^{"} - t_{SV}^{"}\right)}{k^{'}S^{'}\left(t_{PRE}^{'} - t_{SV}^{'}\right)} = C_k \cdot C_l^2 \cdot C_{\Delta t} \quad (23)$$

The uncompleted cofficient of heat flow in formula (23) can be shown like:

$$k = \frac{1}{\Sigma(\delta/\lambda) + 1/\alpha_0} \quad (24)$$

The joined solving of equations 11,12 and 23 , we will get that the amount of uncompleted coefficient heat flow can be shown like:

$$C_k = C_\nu \quad (25)$$

From equation (18) we get :

$$C_{\Delta t} = 1/C_l^3 \quad (24)$$

4. HUMIDITY MODELING

The amount of humidity can be shown as:

$$C_D = \frac{D^{"}}{D^{'}} = \frac{G^{"}\left(d_{IZ}^{"} - d_{SV}^{"}\right)}{G^{'}\left(d_{IZ}^{'} - d_{SV}^{'}\right)} = C_G C_{\Delta d} \quad (25)$$

If we put in equation (25) the amount of humidity difference, it can be detrmined , if the dimensions of angle siye are satisfied , which is used with graphical drawing of aeration process in $i - x$ diagram. In similar processes changes of heat and humidity in structure in its model, angle siyes have to be equal:

$$\Delta i^{'}/\Delta d^{'} = \Delta i^{"}/\Delta d^{"} \quad (26)$$

Or

$$\Delta t^{'}/\Delta d^{'} = \Delta t^{"}/\Delta d^{"} \quad (27)$$

It is caming out that:

$$C_{\Delta d} = C_{\Delta t} \quad (28)$$

Meaning:

$$C_D = C_Q \quad (29)$$

5. PRACTICAL USE OF MODELING

The calculation method and handling tests data is structred from:

1. Geometric sizes of model C_l are given, and difference of temparature $C_{\Delta t}$

2. The siyes are to be calculated : : $C_v = \sqrt{C_l C_{\Delta t}}$; $C_G = C_l^2 C_v$; $C_Q = C_G C_{\Delta t}$; $C_\varepsilon = \sqrt{C_v}$; $C_k = C_v$;

3. Calculations for wind speed and air speed model on the exit of aeration system the power of heat source, blackness degree and the uncompleted coefficient of heat flow by formulas;

   $w'' = C_v w'$; $v'' = C_v = v'$; $Q'' = C_Q Q'$; $\varepsilon'' = C_\varepsilon \varepsilon'$; $k = C_k k'$

4. model barrier thermal resistarce are determined; $\Sigma\left(\delta''/\lambda''\right) = 1/k'' - 1/\alpha_o''$

5. A defined barrier material is choosed , meaning –if we know the equality for λ'' than we find the thickness for δ''

6. After the model choosing we need to check the given conditions $R_e'' > 2400$ and $Gr\,Pr > 2 \cdot 10^7$

7. Than we measure the speed and the temparature

8. The measured speeds and tempartures on the model are to be calculated on natural by next formulas: $v' = v''/C_v$; $t' = t_s' + t'' + t_s''/C_{\Delta t}$

When there is a source of humidity , we need to additionaly detrmine the power of humidity source in the model , with equation (29) .The humidity , measured in the model, is naturally calculated by formula:

$$x' = x_s' + \left(x'' - x_s''\right)/C_{\Delta x}$$

Where is $C_{\Delta x} = C_{\Delta t}$.

6. EXAMPLE ANALASY

It is necessary to chek the air change on the projected machine room central power station. The barrier constructions for this room are to be calculated by the next uncompleted coefficients of heat flow: for walls $1,52\left(W/m^2C\right)$; for windowed (glassed) areas $17,4\left(W/m^2C\right)$; for roof construction $1,65\left(W/m^2C\right)$; for floor construction $0,35\left(W/m^2C\right)$.

In the room two turbines are to be , four big piplines, four heaters and two pump geneartors . The amount of heat that is produced in the model is: from turbines $1045(KW)$; from the pipelines $174(KW)$; from heaters $116(KW)$ and fromm one group of pumps $116(KW)$. The total amount of produced heat is $3482(KW)$; The amount of water steam , produced from the turbines is $460(kg/h)$. The total amount of the produced steam is $920(kg/h)$. With the aeration system we bring $80000(kg/h)$ to turbines working aeres, with the air speed of $0,25(m/s)$ and temparture of 35^0C . The exterior air temparture is 26^0C and the humidity is $9(g/kg)$. If we use this on the model made in ratio $C_l = 1:50$. If we working air average is of 25^0C and humidity of $7(g/kg)$. If we make that proporcion of the extra temparture is $C_{\Delta t} = 2$.

Than the expectet amounds are:

$$C_v = \sqrt{C_l C_{\Delta t}} = \sqrt{2/50} = 1/5 ;$$
$$C_G = C_l^2 C_v = (1/50)^2 \cdot 5 = 1/12500 ;$$
$$C_Q = C_G C_{\Delta t} = 1/6250$$
$$C_\varepsilon = \sqrt{C_v} = 1/2,24 ; C_k = C_v = 1/5 ;$$

7. CONCLUSION

If we reduce the model 10 times in comparance with natural objects, than the temparture difference in tha model has to be for example 1000 times bigger in comparance on temperature difference of the natural object and that is impossible. In the study of geometric dimension approximately. With the experimental checks of this approximately way of modeling it is known that the gotten mistake doesn't go over 5% , which is totally permited. It comes aut that the model room barriers have to have the next uncompleted coefficients of hat flow: for walls $0,302\left(W/m^2C\right)$; for windowed (glassed) areas $3,5\left(W/m^2C\right)$; for floor construction $0,07\left(W/m^2C\right)$.

These coefficients are possible , if the model barriers are mode from two linings $\left(\lambda'' = 0,15W/mK\right)$, thickness 4mm with a between living from heat isolation with different thickness, for example , the isolation with different, thickness, for example, the isolation materila whose heat flow coefficent is $\left(\lambda'' = 0,03W/mK\right)$, In this case unfulfilled coefficient

of heat flow (by formula 24) with $\alpha = 20\left(\mathrm{W/m^2K}\right)$ is equals to:

$$k'' = \frac{1}{2\frac{0,004}{0,15} + \frac{\delta''}{0,03} + 0,05}$$ from this we

$$\delta'' = 0,03\frac{1-0,103k''}{k''}$$

If we use the given formul a and know the coefficient of heat flow for same lings we can now calculate the thickness of the isolation material for: for walls $\delta_{zi} = 111\mathrm{mm}$; for windowed (glassed) areas $\delta_{op} = 7\mathrm{mm}$; for roof construction $\delta_{kr} = 104\mathrm{mm}$; for floor construction $\delta_{zi} = 500\mathrm{mm}$;

The amount of heta , produces from the model is :from turbines $167\left(\mathrm{KW}\right)$; pipelines $28\left(\mathrm{KW}\right)$; heters $18,5\left(\mathrm{KW}\right)$ and from one group of pomps $18,5\left(\mathrm{KW}\right)$. The total quantity of the produced heat is $557\left(\mathrm{KW}\right)$. The quantity of water steam produced in model of turbines is $74\left(\mathrm{kg/h}\right)$. In the model the blackness degree of the area and barrier construction , if we take that in nature is 0,91, than on the model it would be o,4. for taking the blackness degree of 0,4 letis take the next step. If a part of the area (for example, n) is covered with aluminum foil with a blackness degree of 0,195, and the blackness degree is known as 0,78. The the quanlity n is to be found from equation $0,4 = 0,196n + 0,78\left(1-n\right)$. By solving this equation we have that $n = 0,65$. If we put this amount on the model, we need to cover the model area with aluminum foil strip with the wiath of 13mm with footsteps of 7mm $\left[n = 13/\left(13+7\right) = 0,65\right]$. The quantity of brought air in the model is $6,4\left(\mathrm{kg/h}\right)$ with the speed of $0,05\left(\mathrm{m/s}\right)$ and tempearture of $25 + 2\left(35-26\right) = 43^0\mathrm{C}$. For calculations in natural dimensions, data-speed, temperatute and humidity, measured on the model, it is necessary to use the next formulas:

$v' = 5v''$; $t' = 26 + 0,5\left(t'' - 25\right) = 0,5t'' + 13,5$;

$d' = 9 + 0,5\left(d'' - 7\right) = 0,5d'' + 5,5$

8. OZNAKE

v	aerage speed flow on edge openings, m / s
μ	consumption coefficient
Δp	pressure difference in front of and behind the edge openings, Pa
ρ	air density, $\mathrm{kg/m^3}$
h	height of air stancion, m
Δρ	air density differences in stanchion and out of stanchion, $\mathrm{kg/m^3}$
C_1	geometric ratio proporation of the model
G	mass consunption , kg/s
F	opening area on edge wals, $\mathrm{m^2}$
α	surface coefficient of heat transfer, $\mathrm{W/m^2K}$
A	heat source of model area, $\mathrm{m^2}$
t_{PO}	surface tempearture on heat source or model, $^0\mathrm{C}$
t_{IZ}	tempearture of air that is comming out of a building or its model, $^0\mathrm{C}$
λ	coefficient of thermal conduction W/mK
Gr, Pr	Grasgofs and Prandelas criteria
a	conductance tempearture coefficient $\mathrm{m^2/s}$
4,96	radiance coefficient of apsolute black body $\mathrm{W/m^2K^4}$
$\varepsilon_1, \varepsilon_2$	surface blackness degree that is part of heat change
ϕ -	radiant angle coefficient
θ	tempearture factor
t_{PRE}	the inside temparture of the exterior building or model walls, $^0\mathrm{C}$
k	overall coefficient of heat transfer , $\mathrm{W/m^2K}$
S	jacket area of the building or model, $\mathrm{m^2}$
δ mm	lining thickness of the construction barrier ,
α_0	coefficient of heat exchange from construction barrier towards outside air or the working area, with the of easier modeling we will take that $\alpha_0' = \alpha_0''$, $\mathrm{W/m^2K}$
D	humidity consumption, g/kg
d_{IZ}	humidity in air that is coming out of the building or moder, g/kg
d_{SV}	humidity in exterior air, g/kg
c	specific heat KJ/kgK
k_i	aerodynamic coefficient
W	wind speed, m / s
h	height of air stanchion, m
Δρ	air density difference in stanchion, Pa
C_l	geometric ratio of the model
G	mass consumption, kg/s

LITERATURA

[1] Derek J.Croome., Brain M.Roberts: Air conditioning and Ventilation of Buildings. Pergamon press Oxford –New York-Toronto –Sydney, 1975

[2] V.M.Gusev: Teplosanbženii I ventiljacija, Leningrad, 1973.

[3] P.N.Kamenev: Otoplenie I ventilacija , Moskva 1964,

[4] Konstantin Voronjec, Nikola obradović: Mehanika fluida , Bograd 1973

THE DECISION METHODOLOGY OF OPTIMAL LOCATION OF REGIONAL LOGISTIC CENTRE

G. Marković, M. Bukumirović, A. Čupić, Z. Bogićević

Abstract: *Development of city logistics conception in the region is based on the concentration of goods, transport and information flows. In order to develop this concept adequate logistic centers must be formed and supply chains connecting incoming and outgoing goods flows must be provided. In sense of rationalization and acceleration flow of the goods in these logistic centers all activities on total flow and retaining of the goods in the region would be concentrated so that all activities related with logistic, transportation, production and trade. Transport requirements in supply chains, ecologic requirement and the need for living quality in stated towns in the regions particularly point out the significance of location selection of logistic centers as well as the manner and time for their supply. This paper gives the decision methodology and ranking different optimal location by multiple atribute decision.*

Key words: *multiple attributive decision methodology, location problem, logistic centres*

1. INTRODUCTION

Strategic up-to-date orientation of our economy forecasting development of small and medium enterprises points out the need for a new approach to improvement of regional prosperity. It must be started from basic requirements: decrease of both production and goods price and increase of the service quality level.

Very useful solution for improvement of business management in the regions is forming and development of regional logistic centers with a centralized industrial warehouse. In logistic centers all activities on total flow and retaining of the goods in the region would be concentrated.

Of course this claim goes in favour to researches on interim project, which refers to necessity of two levels of logistic centers in Serbia: EU level (Belgrade, Novi Sad, Subotica, Niš, Kragujevac i etc.) i national level centers (Kruševac, Kraljevo, Novi Pazar, Leskovac, Vršac i etc.). [1]

Today's world is globalize and dependent on safety and time of supply, enabled by quality logistic organization. The trend of moving production to regions with low cost production expenses gives the additional importance to logistic. Therefore, production expenses and inner supply chains expenses are cut down to minimum and the quality becomes crucial advantage in which logistic is the most important link**.**

The importance of logistic, as a base of safe and on time supply, has a great influence on overall development of a country. The development of logistic will increase the interest for investment in Serbia, logistic and related activities, as well as industry investments and high technology development. In order words if we want to accelerate European integrations we have to adjust legislative and technical regulations, which means that we have to clearly define and harmonize goods flows with EU and define important regional logistic centers [1].

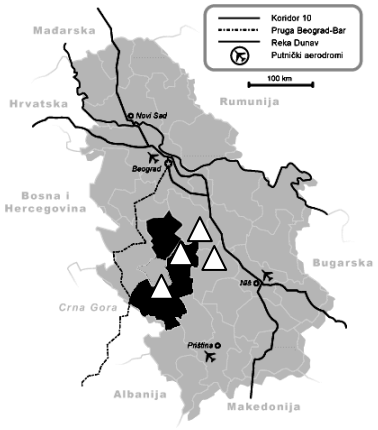

Figure 1 – Important regional logistic centers

Figures that influence the selection of logistic centre location are :

- Labour costs
- Accessibility and labour qualification
- Accessibility of raw materials and suppliers
- Market proximity
- Infrastructure and power costs
- Traffic connection
- Ecology and life standards

Ass.Msc. Goran Marković, Faculty of Mechanical Engineering Kraljevo, markovic.g@mfkv.kg.ac.yu
Ph.d.-Ing. Milan Bukumirović, Faculty of Transport and Traffic engineering, Belgrade, m.bukumirovic@sf.bg.ac.yu
Ass.Msc. Aleksandar Čupić, Faculty of Transport and Traffic engineering, Belgrade, a.cupic@sf.bg.ac.yu
Ass. Zoran Bogićević, Faculty of Mech.Engineering, Kraljevo, bogicevic.z@mfkv.kg.ac.yu

- Fiscal, monetary policy and political stability

The strategy development of logistic centers includes:

- Defining of prerequisites of logistic centers development
- Development of distribution logistic centers and their connection into integrated centre network
- Development of information support systems (information and transportation management and logistic)

By right choice of location of industrial warehouse and logistic centre the city logistics is basically improved as well as city and regional transport, which influences both the application and maintenance of traveling network.

2. MULTIPLE ATTRIBUTIVE DECISION METHODS

In order to solve practical problems of selection and ranking of different decision – alternatives, multiple decision methods are used. The suggested methodology can be seen by defining attribute systems for ranking alternative solutions in other words the selection of optimal location. Such defined attributes get certain weights,in other words relative importance of attribute are defined.In accordance to already defined attributes and appropriate selection methods and software application for ranking alternatives, we get some solutions which values confirm acceptability of suggested location of regional logistic centre.

The objective of this paper is to show some possibilities of decision maker to control the procedure of multiple attribute optimization as well as to paticipate in selection of final solution.

Selection and decision ranking in real problems today is unthinkable without computer usage. The computers are the most responsible for intensive development and usage of multiple attribute analyzing and optimization, because with any method there is suitable software application which usage does not require any knowledge of mathematical procedure and additional training of decision maker.

It is necessary that the selection of regional logistic centre optimal location should be more objective and mathematicaly modelled. By using fuzzy logics we overcome subjective decisions and enable more exact defining attribute weights. Naturally,we must know that in some cases that the value of alternative with respect to some attribute are not given quantitatively, but through corresponding linguistic terms [2]. This concept. The concept of linguistic variable is very useful in dealing with situations,which are too complex or too ill-defined to be reasonably described in conventional quantitative expressions.

This means, that during ranking of alternatives of regional logistic centre location, some attributes will be expressed through numerical values (investment costs,labour costs, etc.) while the others will be given linguistic variable (high, low, medium, very high ,etc).

According to evrything mentioned, it foolows that some values with respect to some attribute are “good transportation infrastructure of region ” or “low development posibilities of the region ” , etc.

In that case, some attributes could not be expressed quantitatively while the others are expressed by fuzzy numbers because of inability to provide the numerical data precision.

The solution would be the usage of fuzzy algorithms for the selection of optimal location or converting linguistic terms and fuzzy numbers to real (in case of linguistic terms we first convert them in to fuzzy numbers and then into real numbers) , which would enable the usage some classic methods of multiple attribute optimization (TOPSIS, PROMETHEE , etc.).

In references [3] the authors foresaw eight scales for conversion of linguistic terms. With conversion scales it is easy to convert linguistic terms to fuzzy number, for example, linguistic term “low“ for a scale of 6 linguistic terms correspond to triangle fuzzy number (0.1,0.2,0.3)(Table 1).

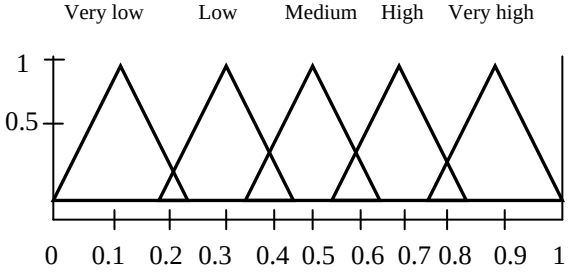

Figure 2. Five term linguistic scale for conversion linguistic terms to fuzzy number

Linguistic terms and their corresponding fuzzy numbers used in the proposed approach

	Linguistic terms	Scale 1	Scale 2	Scale 3	Scale 4	Scale 5	Scale 6	Scale 7	Scale 8
1	None								(0, 0, 0.1)
2	Very Low			(0, 0, 0.1, 0.2)		(0, 0, 0.2)	(0, 0, 0.1, 0.2)	(0, 0, 0.2)	(0, 0.1, 0.2)
3	Low–Very Low							(0, 0, 0.1, 0.3)	(0, 0, 0.1, 0.3)
4	Low		(0, 0, 0.2, 0.4)	(0.1, 0.25, 0.4)	(0, 0, 0.3)	(0, 0.2, 0.4)	(0.1, 0.2, 0.3)	(0, 0.2, 0.4)	(0.1, 0.2, 0.3)
5	Fairly Low				(0, 0.25, 0.5)	(0.2, 0.4, 0.6)		(0.2, 0.35, 0.5)	(0.1, 0.3, 0.5)
6	Mol. Low						(0.2, 0.3, 0.4, 0.5)		(0.3, 0.4, 0.5)
7	Medium (also Fair)	(0.4, 0.6, 0.8)	(0.2, 0.5, 0.8)	(0.3, 0.5, 0.7)	(0.3, 0.5, 0.7)		(0.4, 0.5, 0.6)	(0.3, 0.5, 0.7)	(0.4, 0.45, 0.5)
8	Mol. High (also Mol. Good)						(0.5, 0.6, 0.7, 0.8)		(0.3, 0.5, 0.7)
9	Fairly High (also Fairly Good)				(0.5, 0.75, 1)	(0.4, 0.6, 0.8)		(0.5, 0.65, 0.8)	(0.5, 0.6, 0.7)
10	High (also Good)	(0.6, 0.8, 1)	(0.6, 0.8, 1, 1)	(0.6, 0.75, 0.9)	(0.7, 1, 1)	(0.6, 0.8, 1)	(0.7, 0.8, 0.9)	(0.6, 0.8, 1)	(0.5, 0.7, 0.9)
11	High–Very High (also Good–Very Good)							(0.7, 0.9, 1, 1)	(0.7, 0.8, 0.9)
12	Very High (also Very Good)			(0.8, 0.9, 1, 1)		(0.8, 1, 1)	(0.8, 0.9, 1, 1)	(0.8, 1, 1)	(0.8, 0.9, 1)
13	Excellent								(0.9, 1, 1)

Mol.: More or less.

Table 1. Linguistic scales for conversion linguistic terms to fuzzy number [3]

Next step should be conversion of fuzzy numbers to real –defuzzification phase, so that the arithmetic process becomes easy, in other words the result of this phase is a decision matrix, which contains only crisp data. According to the fuzzy scoring method proposed by (Chen i Hwang (1992)), the fuzzy maximising set and minimising set should be first obtained,which are defined as:

$$\mu_{\max}(x) = \begin{Bmatrix} x, 0 \le x \le 1 \\ 0, \text{ otherwise} \end{Bmatrix} \quad (1)$$

$$\mu_{\min}(x) = \begin{Bmatrix} 1-x, 0 \le x \le 1 \\ 0, \text{ otherwise} \end{Bmatrix} \quad (2)$$

Then,the right score of fuzzy number B can be determined using

$$\mu_R(B) = \max_x \left[\min\left(\mu_B(x), \mu_{\max}(x) \right) \right] \quad (3)$$

The left score of B can be determined using

$$\mu_L(B) = \max_x \left[\min\left(\mu_B(x), \mu_{\min}(x) \right) \right] \quad (4)$$

The total score of B can be computed using

$$\mu_T(B) = \left[\mu_R(B) + 1 - \mu_L(B) \right] / 2 \quad (5)$$

After this phase, decision matrix contains only crisp data and we could use any multiple attribute decision methods.

3. CASE STUDY

Having in mind the problem of goods transport as well as the geographic location of this region (Kraljevo is about 50km far from Čačak and Kruševac but in opposite directions) and the increase of total goods exchange of the region, planned industrial development (after privatization, re-engineering of equipment and technologies) it can be stated that the conditions for starting then project of city logistics development in this region .

Each town, in this case the region as a whole, requires its own concept of city logistics which must be constantly followed and developed. In order to realize a project like this one must estimate and analyze a number of parameters related to this problem.

Development of city logistics conception in the region is based on the concentration of goods, transport and information flows. In order to develop this concept adequate logistic centers must be formed in accordance with EU regulations gives in introduction of this paper.

The selection methods of optimal location, in order words selection some alternative with respect to several attributes, is very complex problems, which would enable the usage some classic methods of multiple attribute optimization .

The set (of alternatives) is given by $X = \{X_1, X_2, X_3\}$:

X_1- Čačak; X_2 - Kraljevo; X_3-Novi Pazar

The selection decision is made on the basis of few figures that influence the selection of logistic centre (fig.3).

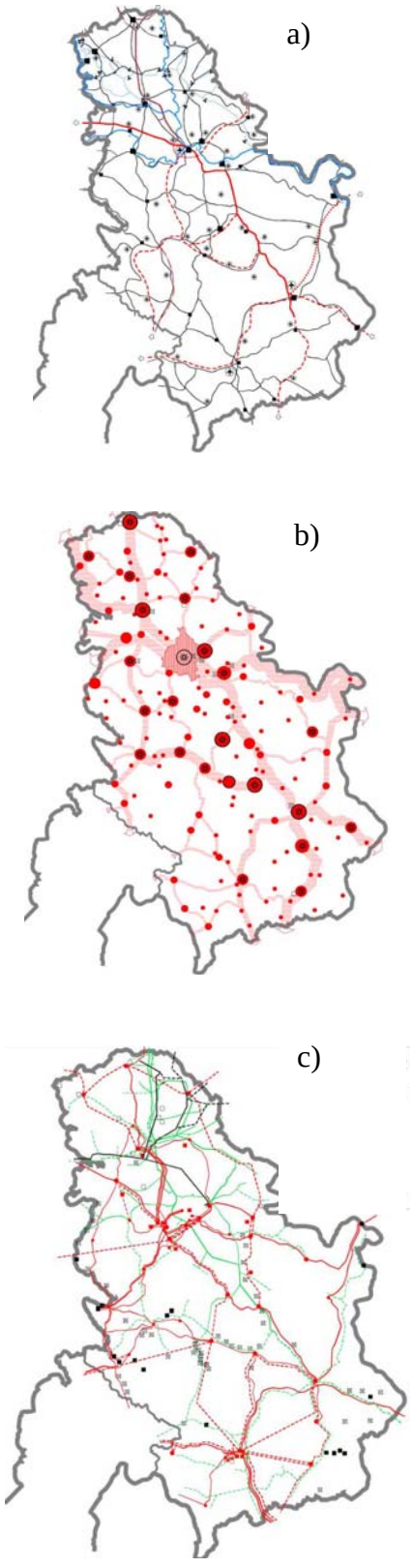

Figure 3. Figures that influence the selection of logistic centre
a)transportation network;b)industry;c) energetic infrastrucuture

The attributes,which are critical for the selection of optimal location,are the folowing:
A_1- Investment costs
A_2- Labour costs
A_3- Traffic infrastructure
A_4- Region development possibilities
A_5- Climatic condition of region
A_6- Accessibility of labour
Attributes properties of case study such as type of attributes and type of assessments are summarised in Table 2.

Attributes	Type of assessment	Typ of attribute
A_1	Crisp	Objective
A_2	Fuzzy (as approx. equal to)	Subjective
A_3	Linguistic terms	Subjective
A_4	Linguistic terms	Subjective
A_5	Linguistic terms	Subjective
A_6	Linguistic terms	Subjective

Table 2. Attributes properties of case study

Linguistic assessments for second attribute,for example “approximately equal to 6.6“ can be represented by fuzzy number (6.4,6.6,6.8). For the rest of the attributes linguistic assessments are transformed into fuzzy numbers by using appropriate scale.
In other words, each fazzy number $R_k = (a_k, b_k, c_k)$, given by decision maker *k*, we must translate into standardised fuzzy number
$R^*_k = (a_k / m, b_k / m, c_k / m) = (a^*_k, b^*_k, c^*_k)$
and $0 \le a^*_k \le b^*_k \le c^*_k \le 1$, where *m* is the maximum value of non-standardised fazzy numbers given by decision maker for the same attribute. (Table 3).

		X_1	X_2	X_3
		55	**54**	**75**
A_1				
max				
A_2	Expert opinions	**Approximately equal to 6.6**	**Approximately equal to 7.2**	**Approximately equal to 11.4**
max	Corresponding fuzzy numbers	(6.4,6.6,6.8)	(7.0,7.2,7.4)	(11.2,11.4,11.6)
	Standardised fuzzy numbers	(0.53,0.55,0.57)	(0.58,0.6,0.62)	(0.93,0.95,0.97)
A_3	Expert opinions	**Very high**	**Very high**	**Very high**
max	Corresponding fuzzy numbers	(0.8,0.9,1)	(0.8,0.9,1)	(0.8,0.9,1.1)
	Standardised fuzzy numbers	(0.8,0.9,1)	(0.8,0.9,1)	(0.8,0.9,1.1)
A_4	Expert opinions	**Low**	**medium**	**Very low**
max	Corresponding fuzzy numbers	(0.1,0.25,0.4)	(0.3,0.5,0.7)	(0,0,0.2)
	Standardised fuzzy numbers	(0.1,0.25,0.4)	(0.3,0.5,0.7)	(0,0,0.2)
A_5	Expert opinions	**High**	**High**	**High**
max	Corresponding fuzzy numbers	(0.6,0.75,0.9)	(0.6,0.75,0.9)	(0.6,0.75,0.9)
	Standardised fuzzy numbers	(0.6,0.75,0.9)	(0.6,0.75,0.9)	(0.6,0.75,0.9)
A_6	Expert opinions	**Very low**	**Very low**	**Very low**
max	Corresponding fuzzy numbers	(0,0,0.2)	(0,0,0.2)	(0,0,0.2)
	Standardised fuzzy numbers	(0,0,0.2)	(0,0,0.2)	(0,0,0.2)

Table 3. Decision matrix of 3 alternatives under 6 attributes and their corresponding (and standardised) fuzzy numbers

Hwang i Yoon (1981) developed the TOPSIS method based on the intuitive principle that the chosen alternative should have the shortest distance from the positive-ideal solution and the longest distance from the negative-ideal solution.

Because a different type of the attributes (for example cost, benefit, etc) we must calculate the normalised decision matrix, so that the existing matrix contains only crisp data. According to TOPSIS, we computing the elements of the normalised decision matrix $\left(r_{ji}\right)$

$$r_{ji} = \frac{x_{ji}}{\sqrt{\sum_{j=1}^{N} x_{ji}^2}}, j = 1,2,...,N; i = 1,2,...,k \quad (6)$$

where x_{ji} is value of alternative j with respect to attribute i.

The weighted normalized decision matrix can be calculated by multiplying each row of the normalised decision matrix with its associated attribute weight, because all attributes do not have same importance.

$$v_{ji} = w_i r_{ji}, j = 1,2,...,N; i = 1,2,...,k \quad (7)$$

where w_i is weight i –th attribute.

According to proposed method, for the specific case of evaulation of quality or quantity location caracteristics, there are many methods for assigning attribute weights.

Conventional and highly useful weighting technique is WET (Weight Evaluation Method). According to WET, decision maker assigned attribute relative importances (RI) on a zero to 100 scale. The most important attribute is assigned a weight of 100, and the other attribute relative importances are assigned relative to that (Table 4). The final step of the this procedure is to normalise the relative importances, $\{r_1, r_2, ..., r_k\}$ to obtain the weights $\{w_1, w_2, ..., w_k\}$, where:

$$w_i = \frac{r_i}{\sum_{i=1}^{k} r_i}, i = 1,2,...,k \quad (8)$$

and $0 \le w_i \le 1$ i $\sum_{i=1}^{k} w_i = 1$.

Attribute	*RI*	*w*
A_1	63	0.22
A_2	37	0.13
A_3	100	0.35
A_4	30	0.1
A_5	50	0.17
A_6	6	0.02

Table 4. Weight of attributes

For the solving of the real problem a preliminary definition weight approach can be used, combined with AHP based methods [3]. In this case aritmetical value of these calculated values present a finally weights vector. After calculations, some attributes could be more important, and the other could be less important.

After the weighting procedure step, positive-ideal solution A^* and negative-ideal solution A^- must be defined. Determination of the positive-ideal solution can be made by taking the largest elements for each benefit attribute,and the smallest element for each cost attribute. The negative-ideal solution is the opposite formation of the positive solution.

$$A^* = \{v_1^*, v_2^*, ..., v_i^*, ..., v_k^*\}$$

$$v_i^* = \left\{\max_j v_{ji}^*, i \in J_1; \min_j v_{ji}^*, i \in J_2\right\} \quad (9)$$

$$A^- = \{v_1^-, v_2^-, ..., v_i^-, ..., v_k^-\}$$

$$v_i^- = \left\{\max_j v_{ji}^-, i \in J_1; \min_j v_{ji}^-, i \in J_2\right\} \quad (10)$$

where J_1 is the set of benefit attribute and J_2 is the set of cost attributes.

Finally,distance between alternatives can be measured by the Euclidean distance.Separation of each alternative from the positive-ideal and negativ-ideal solution is given by:

$$S_j^* = \sqrt{\sum_{i=1}^{k} \left(v_{ji} - v_i^*\right)^2}, j = 1,2,...,N \quad (11)$$

$$S_j^- = \sqrt{\sum_{i=1}^{k} \left(v_{ji} - v_i^-\right)^2}, j = 1,2,...,N \quad (12)$$

Relative closeness of A_j with respect to A^* is defined as

$$C_j^* = \frac{S_j^-}{S_j^* + S_j^-}, 0 < C_j^* < 1; j = 1,2,...,N \quad (13)$$

where C_j^* is close to 1,the alternative is regarded as ideal,or when it is close to 0 the alternative is regarded as non-ideal.

Based on the above mathematical algorithm or PC-based computer program,after a phase of definition a set of attributes and alternatives, can be calculated a decision matrix and the rank of alternativies.

According to the descending order of C_j^* the preference order is $X_2 > X_1 > X_3$,where the second alternative is the leader and it is accordance with EU regulations gives in introduction of this paper. In other words that means, we could not chaoticly develop a potentional regional logistic centres .The regional centres must be support of centres EU level.

According to proposed methods of multiple attribute decision and alernativies of case study , the second alternative has to be ranked in the first position among others,or the optimal location for regional logistic centre is Kraljevo. Figure 4 shows the ranking of alternativies for this case.

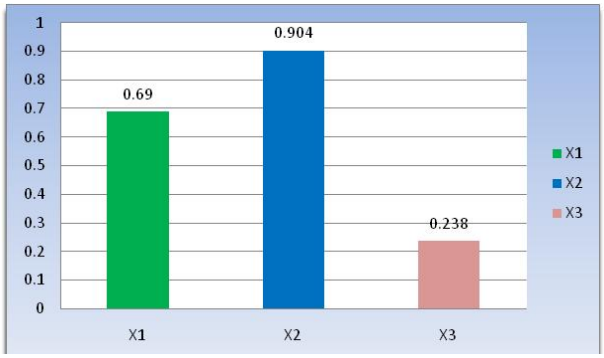

Figure 4. The ranking of alternativies by decision maker

Based on urban plans,and the fact that the conditions for starting the project of city logistics development in this region are achieved, for further analyzes we must propose a concrete regional centre location alternativies in Kraljevo town, also evaulate the alternativies and attributes by a group experts (decision maker).

Optimal location selected by proposed methodology should have the shortest distance from the positive-ideal alternative and it gives the additional importance to realization of logistic centre, which has appropriate traffic, technology and information-communication function on international, national and local level.

4. CONCLUSION

Increasing the objectivity of decision during a optimal location selection of regional logistic centre,will be able with using mathematics model of fuzzy logic or with combining many methods for assigning attribute weights. Naturally, presented methodology with small modification will be able to solve another real technical problems. Procces of selection of location could not be chaotic, but it must be in accordance with goods flows in EU. We have to harmonize goods flows with EU and that is best way for continuing development of country and European integration.

REFERENCES

[1] Georgijević M., Roknić S., Bojanić V. i dr..: *Logistika kao privredna grana*, III Srpski simpozijum sa međunarodnim učešćem- Transport i logistika, Niš, 2008.

[2] Bukumirović M., Čupić A.: *Primena višekriterijumske analize u izboru opreme za sortiranje paketa*, PosTel 2007, 25 simpozijum, Beograd, 2007

[3] Chen S.J.,Hwang C.L.: *Fuzzy Multiple Attribute Decision-Making: Methods and Applications*, Springer-Verlag,New ork,1992

[4] Olcer A.I.,Odabasi A.Y.:*A new fuzzy multiple attributive group decision making methodology and its application to propulsion/manoeuvring szstem selection problem*,Europian Journal of Operation Research 116,2005,pp.93-114

[5] Slavoljub M..: *Metodologija izbora glavnih poštanskih centara I lokacije poštanskih centara*, PosTel 2007, 25 simpozijum, Beograd, 2007

[6] Bukumirović M., Gašić M., Savković M., Marković G.:*Regional city logistics and supply chains in machinery*,V International conference HM2005,Mataruska Banja,2005

[7] Teodorović D.:*Fuzzy set theory applications in traffic and transportation*, Europian Journal of Operation Research 74/3,1994,pp.379-390

EXERGY EFFICIENCY OF A RADIATOR HEATING SYSTEM

V. Stojanović, R. Karamarković, M. Marašević

Abstract: *This paper wants to answer the following question– what is the change of exergy for a given radiator heating system? For this purpose a mathematical model in Matlab software was made and was simulated in Simulink.*
As a variable in the model is used environment temperature, as constants:
-Indoor temperature (in this paper is used t_u=20 ^{0}C)
-Geometrical and construction characteristics of the model (house)
-Radiator type(constant exponent for the radiator heating power for different temperature differences between the radiator's mean temperature and the room temperature)
The model allows the change of the next parameters between simulations:
-To change a type heating fluid (in this paper is used exclusively warm water)
-Difference of temperature between radiator's input and output
-A middle temperature of heating fluid

Key words: *Exergy efficiency, radiator heating system, heat requirement*

1. INTEGRATED ENERGY, ENTROPY, AND EXERGY ANALYSIS

Exergy is defined as the maximum useful work that could be obtained from a system at a given state with respect to a reference environment (dead state) [4]. In a process or a system, the total amount of exergy is not conserved but destroyed due to internal irreversibilities.
In a thermodynamic system, exergy can be transferred to or from a system in three forms:
heat, work and mass flow, which are recognized at the system boundaries.

The exergy transfer by heat is expressed as [4]:

$$\dot{X}_{heat} = \dot{Q}(1-\frac{T_0}{T}) \ \ (kW) \tag{1}$$

Where:
$\dot{Q}$ = rate of heat transfer crossing the system boundaries [kW];
T_o = environment temperature [K];
T = temperature of heat source [K].

In the case of mechanical work or electricity crossing the system boundaries, exergy transfer $\dot{X}_{work}$ [kW] equals the electricity or mechanical work itself $\dot{W}$ [kW].

In the case of mass flow crossing the system boundaries, exergy transfer by mass $\dot{X}_{mass}$ is:

$$\dot{X}_{mass} = \dot{m}x \ \text{[kW]} \tag{2}$$

Where:
$\dot{m}$ = mass flow rate crossing the system boundaries [kg/s];
x = exergy per unit mass [kJ/kg].

For a flow stream, the unit mass exergy can be expressed as:

$$x = (h-h_0) - T_0(s-s_0) \ \ [kJ/kg] \tag{3}$$

The exergy change of a flow stream is [5]:
$\Delta x = x_2 - x_1$, or in the developed form

$$\Delta x = (h_2 - h_1) - T_0(s_2 - s_1) \ [kJ/kg] \tag{4}$$

Where:

T =temperature, [K];
h =enthalpy, [kJ/kg];
s =entropy [kJ/kg·K].

The subscript "0" indicates the environmental dead state and subscripts "1" and "2" indicate different states of the flow stream.
For the steady-state flow process, there is no storage of energy, entropy as well as exergy within the system. The energy balance equation is:

$$E_{in} = E_{out} \ \text{[kW]} \tag{5}$$

The entropy balance equation is:

$$\dot{S}_{in} + \dot{S}_{generated} = \dot{S}_{out} \ \text{[kW/K]} \tag{6}$$

The exergy balance equation is:

$$\dot{X}_{in} = \dot{X}_{out} + \dot{X}_{destroyed} \ \text{[kW]} \tag{7}$$

Where the subscript "in" indicates the flow (energy flow, entropy flow or exergy flow) entering the system and the subscript "out" indicates the flow leaving the system.

Ph.D. student Vladimir Stojanović, Faculty of Mechanical Engineering Kraljevo, vlado_s@ptt.rs
Ass.Msc. Rade Karamarković, Faculty of Mechanical Engineering Kraljevo, karamarkovic.r@mfkv.kg.ac.yu
Ass.Msc. Miljan Marašević, Faculty of Mechanical Engineering Kraljevo, marasevic.m@mfkv.kg.ac.yu

Exergy destruction $\dot{X}_{destroyed}$ in a process is the product of entropy generation $\dot{S}_{generated}$ in the same process and the reference environment temperature T_0 :

$$\dot{X}_{destroyed} = T_0 \dot{S}_{generated} \text{ [kW]} \quad (8)$$

Wepfer et al. [6] stated that for a system, such as a heating system, the steady-flow exergy balance can also be expressed as:

$$\dot{X}_{\sup plied} = \dot{X}_{useful} + \dot{X}_{destroyed} + \dot{X}_{lost} \text{ [kW]} \quad (9)$$

The exergy supplied to the system is partially destroyed inside the system due to the irreversibilies, partially delivered to the outside with the effluents and partially used by the system.
The energy efficiency of a heating system is defined as:

$$\eta_1 = \frac{\dot{E}_{useful}}{\dot{E}_{\sup plied}} \quad (10)$$

The exergy efficiency, which provides the realistic measure of performance of engineering system [5], can be expressed in the following forms [6]:

$$\eta_2 = \frac{\dot{X}_{useful}}{\dot{X}_{\sup plied}} \quad (11)$$

$$\eta_2 = 1 - \frac{\dot{X}_{destroyed} + \dot{X}_{lost}}{\dot{X}_{\sup plied}} \quad (12)$$

In order to improve the exergy efficiency η_2, the amount of exergy destroyed inside a system plus the amount lost through the effluents should be reduced.

2. EXERGY EFFICIENCY OF THE RADIATOR WITH WARM WATER

In the radiator arrives, in the steady state, warm water with enthalpy H_1 and it gives off heat to a room (Figure 1).

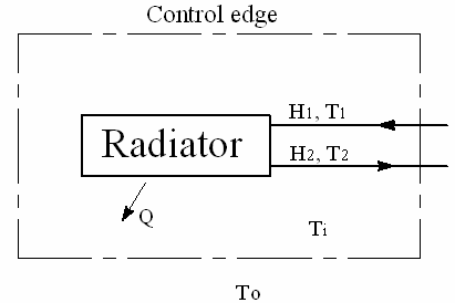

Fig.1. The scheme of the process

Where

T_i - room temperature [K];

T_o -environment temperature, [K];

T_1 -temperature of the water in the supply pipe [K];

T_2 -temperature of the water in the return pipe [K];

Q -heat which is liberated to the room [W];

The calculation is done on the following manner [1]: Warm water leaves the radiator with enthalpy H_2. According to the first low of thermodynamics, it will be

$$Q = H_1 - H_2 = \dot{m}(h_1 - h_2) \Rightarrow$$

$$Q = \dot{m}c(T_1 - T_2) \quad (13)$$

Exergy that enters the system in the supply pipe with the temperature T_1 will be:

$$E_{in} = \dot{m}\left|h_1 - h_2 - T_o(s - s_o)\right| \Rightarrow$$

$$E_{in} = \dot{m}c\left|T_1 - T_o - T_o \ln\frac{T_1}{T_o}\right| \quad (14)$$

Analogous to (14) output exergy in the return stream with the temperature T_2 will be:

$$E_{out} = \dot{m}c\left|T_2 - T_o - T_o \ln\frac{T_2}{T_o}\right| \quad (15)$$

Preserved exergy in the form of heat which is given to the room on the temperature T_i is:

$$E_{xg} = Q\frac{T_i - T_o}{T_i} = Q \cdot \left(1 - \frac{T_o}{T_i}\right) \quad (16)$$

When we include (13), previous equation will be:

$$E_{xg} = \dot{m}c(T_1 - T_2)\left(1 - \frac{T_o}{T_i}\right) \quad (17)$$

We mark Q_l as the heat which is lost passing through non–heating rooms. It was assumed that 1,75% of the heating need of the house was lost in for example unheating rooms and cellar which is a common case. For the house used in the model that is:

$$Q_l = 230 \text{ [W]} \quad (18)$$

Its corresponding exergy is:

$$E_l = Q_l\left(\frac{T_m - T_o}{T_m}\right) = Q_l\left(1 - \frac{T_o}{T_m}\right) \quad (19)$$

Where

$T_m = (T_1 + T_2)/2$ - middle water temperature in the radiator

Finally, after neglecting the work of pump, exergy efficiency of the radiator with warm water will:

$$\eta_{ex} = \frac{E_{in} + E_{xg}}{E_{out} + E_l} \quad (20)$$

The pump work is neglected for this system, because there are a lot of gravitational systems in the houses of this kind. In addition, the work required for circulation pumps could be neglected.

3. CASE STUDY

In this paper, a two-floor house was taken into consideration (Figure 2), and is shown as a box (without inside walls), or other words, as a single room.

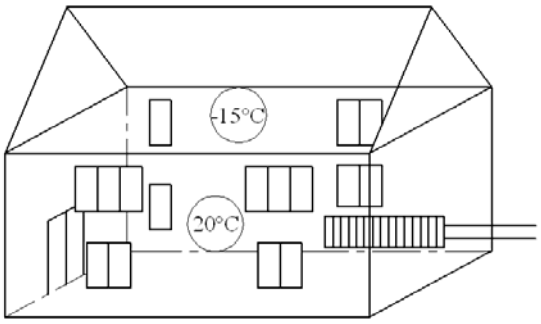

Fig. 2. The scheme of the house model

A radiator, with next characteristics, is used in the heating model [3]:

- $q_n = 146 \ \left[W / element\right]$, the power of a heating element at the nominal temperature
- $\Delta t_n = 50^\circ C$, is the nominal temperature difference between the radiator's middle temperature and the room.
- $m = 1{,}31199$, value of exponent

Outdoor temperature is shown as linear function of time, which is changed from $T_0 = -20^\circ C$ to $T_0 = 12^\circ C$, what is justified, because when environmental temperature exceeds $T_0 = 12^\circ C$, the heating stops. Inside temperature is kept constant at $T_i = 20^\circ C$, and the attic temperature is $T_a = -15^\circ C$.

A total necessary heat per unit time, Q, contains from transmission and ventilation heat losses:

$$Q = Q_T + Q_V \quad [W] \tag{21}$$

In calculation of heat losses we neglect the floor losses. The calculation of heat losses is lead at the following manner [2]:

1) A transmission losses are calculated as

$$Q_T = Ak(T_i - T_o) \tag{22}$$

where

- transmission heating coefficients:

$k = 0{,}8 \left[\frac{W}{m^2 K}\right]$ -through walls ;

$k = 3 \left[\frac{W}{m^2 K}\right]$ -through windows and the main door;

$k = 1{,}21 \left[\frac{W}{m^2 K}\right]$ -through ceiling;

- and house characteristics are:

The dimensions of the house are 12m×6m×5,44m.
The main door dimension (with two parts)- 1,5m×2,42m

The Windows dimensions:
single frame double glazed windows: 0,69m×0,9m
double winged windows: 1,45m×1,5m
triple winged windows -2,2m×1,5m

2) A ventilation losses is calculated as:

$$Q_V = 0{,}65 \sum (al)_S \cdot (T_i - T_o) \cdot R \cdot H \tag{23}$$

$R = 0{,}9$ - room feature,

$H = 3{,}09$ - building feature,

$\sum ls$ - lengths sum all of fissures,

with a is marked permeable coefficient, which is in our case 0,4 $\left[m^3 / mhPa^{2/3}\right]$;

Let us remark that 65% of the house's external surface is under influence of wind at a time instant.

Maximal heating demand per unit time is at the minimal outdoor temperature $T_o = -20^\circ C$, and is

$$Q_{\max}(-20^\circ C) = 13080 \ \left[W\right] \tag{24}$$

This is shown on Fig. 5.

Now, for different middle temperature of the heating fluid, in this case water, we can calculate number of elements from which our imaginary radiator consists.

- $T_m = 80^\circ C$

The temperature difference, is

$\Delta t = T_m - T_i \ \Rightarrow$

$$\Delta t = 80^\circ - 20^\circ = 60^\circ C \tag{25}$$

Calculating the heating power of the radiator at the projected conditions is [2]:

$$q = q_n \cdot \left(\frac{\Delta t}{\Delta t_n}\right)^m \tag{26}$$

or with our values

$$q = 185{,}45 \left[W / element\right] \tag{27}$$

Finally, the number of radiator elements is:

$$n = \frac{Q_{\max}}{q} = 70{,}54, \tag{28}$$

Well, under this condition, we adopt a radiator with 71 elements.

Similarly, for different mean radiator temperatures we obtain

- $T_m = 70^\circ C \Rightarrow 90$ elements
- $T_m = 60^\circ C \Rightarrow 121$ elements

If we multiple (26) with n, we give equation for the heating power which give our radiator gives off to the room:

$$Q = Q_n \cdot \left(\frac{\Delta t}{\Delta t_n} \right)^m \quad (29)$$

where Q_n marks the heat power which gives the radiator under nominal conditions,

$$Q_n = n \cdot q_n \quad [\text{W}] \quad (30)$$

From equation (29) we, also, can obtain T_1 in function of temperature difference, $\Delta T_r = T_1 - T_2$, environmental temperature, T_o, and middle radiator temperature, T_m.

In this paper, we considered $\Delta T_r = 20^\circ, 18^\circ, 15^\circ$ and 10°C to be the temperature difference between supply and return lines.

4. SIMLATION RESULTS

For the purpose of the paper, we made simulation in Matlab – Simulink, what is shown in Figure 3. In this program we can see next behaviours:

- ✓ Heating requirements of the house in function of the change of environment temperature;
- ✓ A mass flow in function of the change of environment temperature and difference between input and output fluid temperature;
- ✓ Exergy efficiency in function of the change of environment temperature, middle temperature in the radiator and difference between input and output fluid temperatures;
- ✓ Fluid temperature on input in function of the change of environment temperature, middle temperature in the radiator and difference between input and output fluid temperature;

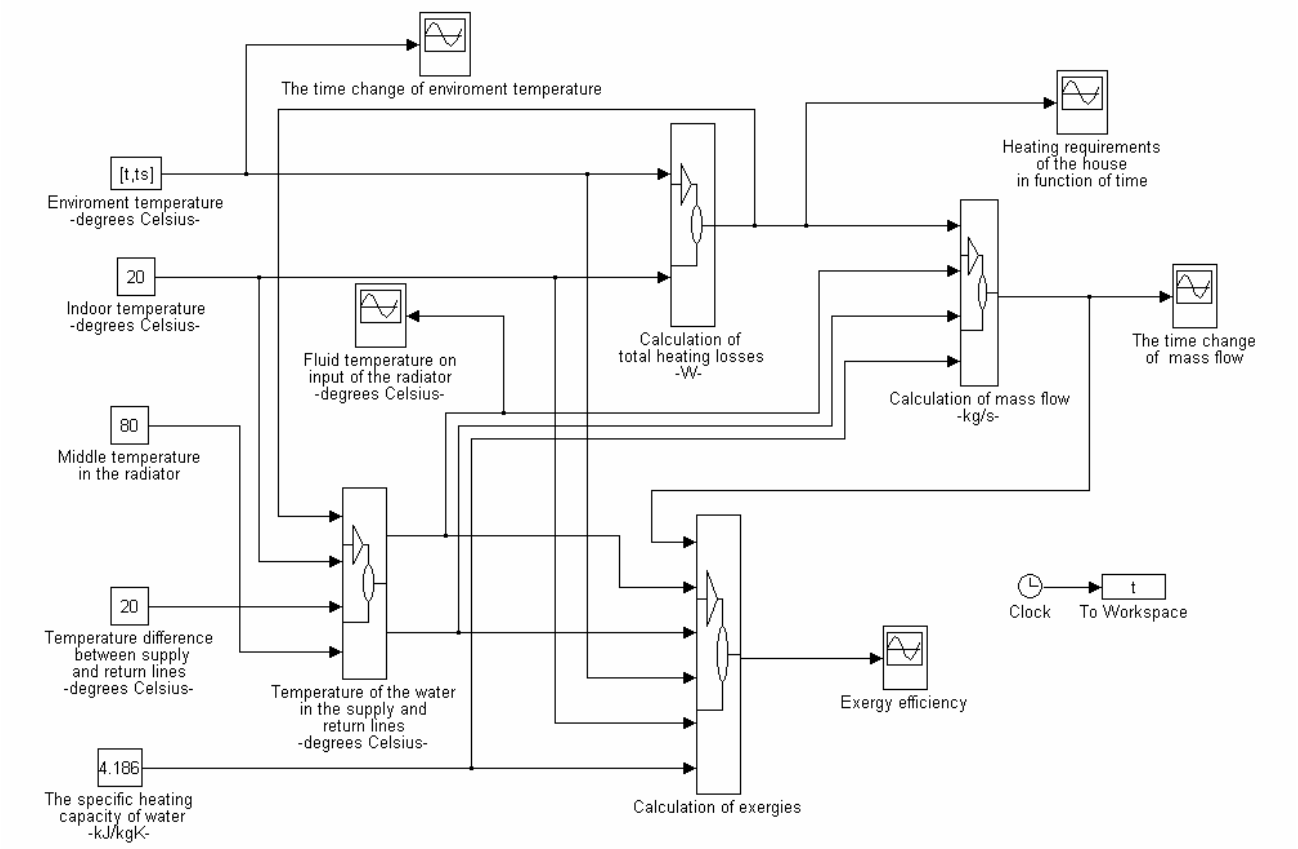

Fig. 3. The model scheme in Matlab - Simulink

Now, let's show the result of simulations.

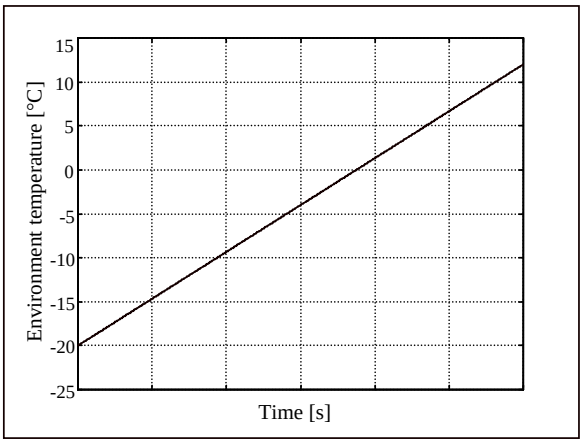

Fig. 4. Time change of environment temperature

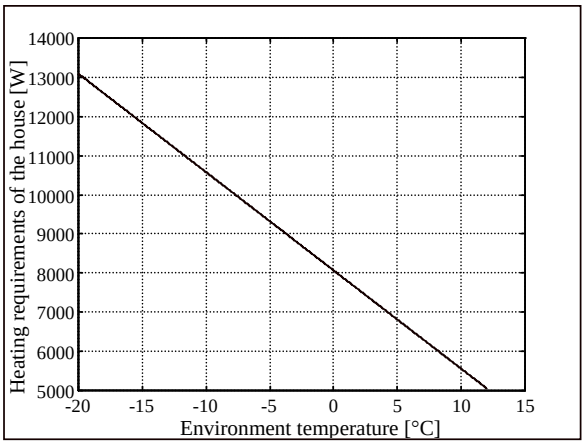

Fig. 5. Heating requirements of the house in function of the change of environment temperature

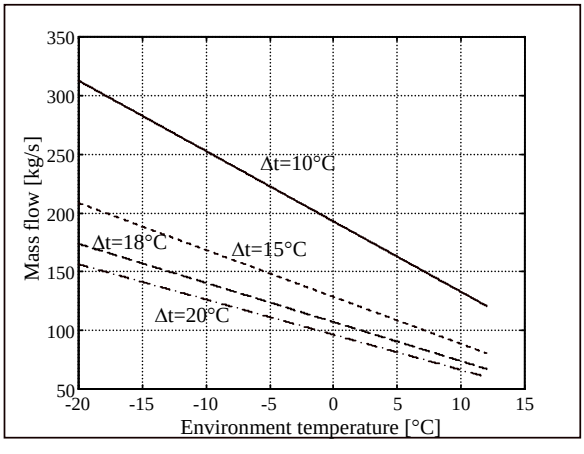

Fig. 6. Mass flow in function of the change of environment temperature, for different Δt

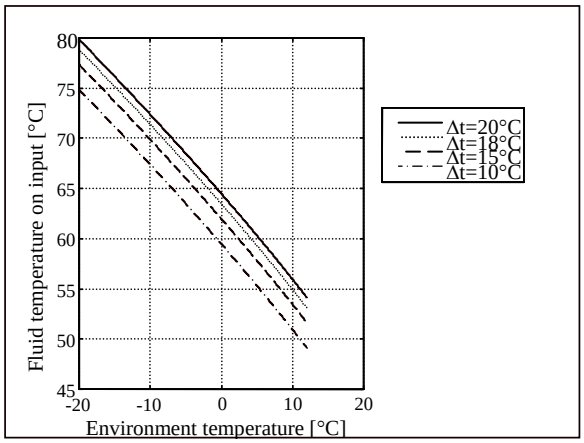

Fig. 8. Fluid temperature in function of the change of environment temperature, for different Δt; tm=70°C

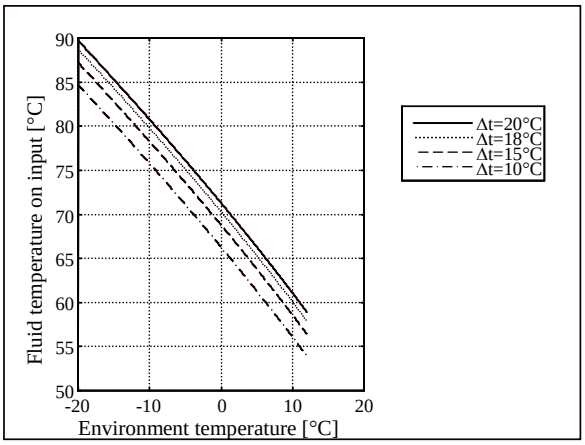

Fig. 7. Fluid temperature in function of the change of environment temperature, for different Δt; tm=80°C

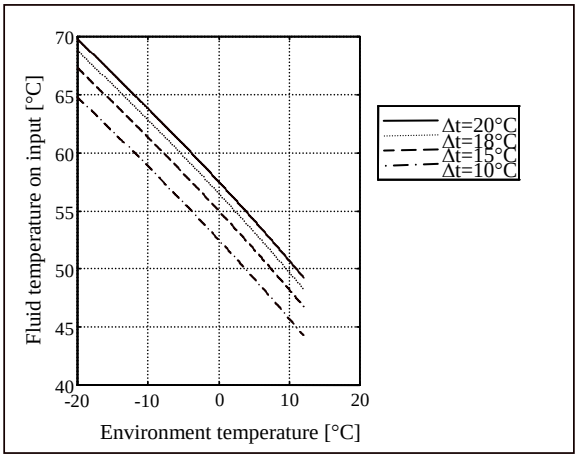

Fig. 9. Fluid temperature in function of the change of environment temperature, for different Δt; tm=60°C

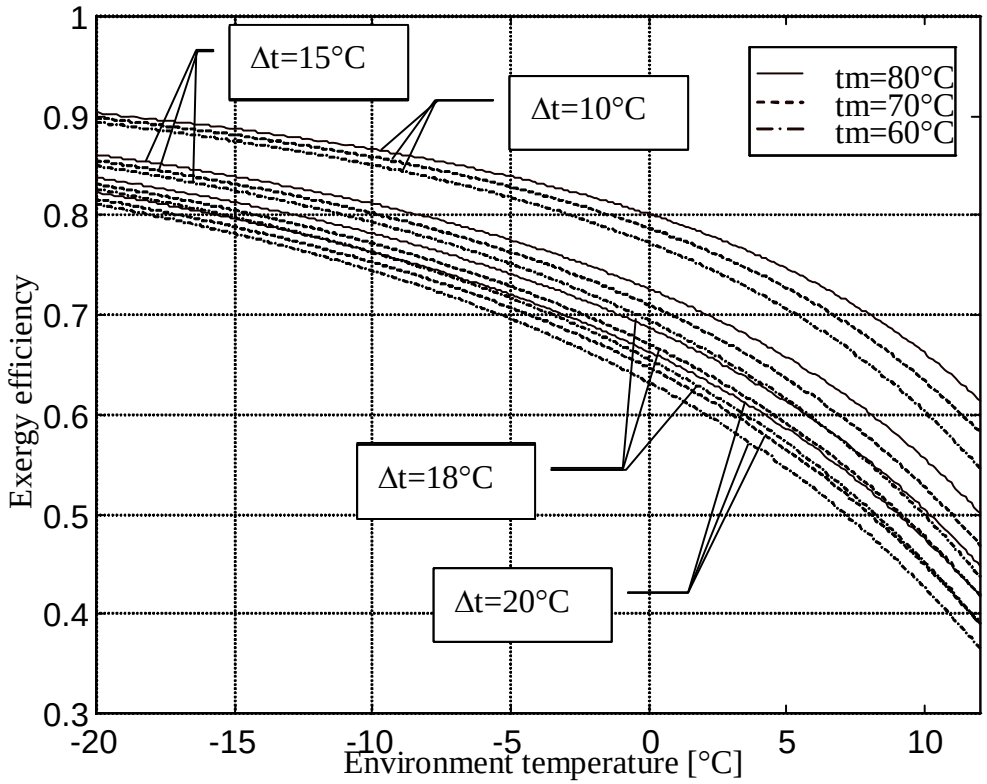

Fig. 10. Exergy efficiency in function of the change environment temperature, for different Δt and t

5. CONCLUSION

From the Figure 10. can be concluded that the temperature difference between supplying and returning lines has greater influence on the exergy efficiency of the radiator heating system than mean radiator temperature. The main reason lies in the fact that with the smaller temperature differences between supplying and returning temperatures preserved exergy in returning lines has larger value. The implementation of the smaller temperature differences between supplying and returning lines is favourable from the exergy efficiency point of view, however in practice it needs larger fluid flows, and because of those larger diameters of supplying lines or with the same piping system the price is paid in larger pressure losses.

6. REFERENCES

[1] D. Milincic, D. Voronjec, "*Thermodynamics*", Faculty of Mechanical Engineering,University of Belgrade, 2000, pp. 146-150.

[2] B. Todorovic, "*Projecting systems for central heating*", Belgrade, 2000.

[3] Catalog "Global", Vox radiators which made on Aluminium

[4] Cegel, Y. A. and Boles, M. A. (2002), "Thermodynamics: an engineering approach", 4th edition, McGraw-Hill.

[5] Rosen, M.A., Leong, W.H. and Le, M.N. (2001), "Modeling and analysis of building systems that integrate cogeneration and district heating and cooling", Proceedings of eSim 2001 Conference.

[6] Wepfer, W.J., Gaggioli, R.A. and Obert, E.F. (1979), "Proper evaluation of available energy for HVAC", ASHRAE Transactions, 85(1), 214-230.

DEVELOPMENT OF METHODOLOGY OF TESTING OF MULTI-STOREY PARKING GARAGES

M. Savković, Z. Šoškić, N. Zdravković, R. Rakanović

Abstract: *A proposal of methodology for experimental investigation of multi-storey parking garages is presented. Analysis has shown that only factors that are to be investigated are dead weight of structure and load weight. The paper describes analytical basis and results of calculations that lead to determination of critical points of structure where stresses are to be experimentally measured.*

Key words: *mechanical structures, testing, multi-storey parking garages*

INTRODUCTION

Rapid development of Serbian cities and towns caused by increase of population during last decade stressed problem with car parking space and urged need for building of multi-storey car garages, well-known to the rest of the world [1]. Increase of the demand made use of prefabricated components preferable choice in many cities (Belgrade, Novi Sad, etc). The components were imported from Italy and the fact motivated Serbian engineers to develop their own concept of multi-storey garages, which resulted in project "New solution of modular metallic multi-storey garage", financed by Ministry of Science and Technology of Republic of Serbia. The main idea of the concept is application of steel-made components instead of concrete, which makes garage structure lighter and enhances modularity of solution.

A new concept of structure requests also development of methodology for its testing, being that previous experiences in exploitation of the garages, or national legislation on the point do not exist.

This paper describes basis, concepts and proposed methodology for testing of multi-storey garages. The developed concept may also be utilized for other types of multi-storey garages made from prefabricated elements.

BASIS

The basis for development of methodology of investigation of multi-storey car parks is assumption that dead weight of structure and weight of load are factors which influences should be investigated by experiment in testing process. Seismic influence on structures of similar type is already known and may be calculated and estimated through developed procedures [2] and temperature influence may be neglected. One additional factor that was considered was the influence of the wind in case that outer side of garages is used for advertising panels. However, this cannot be considered as inherent influence to the structure being that its basic design does not include it, and this influence needs to be considered only in case that customer makes such request.

The basis for development of methodology for estimation of the influence of dead weight and load weight is calculation of stresses in garage structure. The calculation showed critical points that are exposed to highest levels of stress. Testing procedure comprises measurement of actual stresses at these points under selected loading conditions.

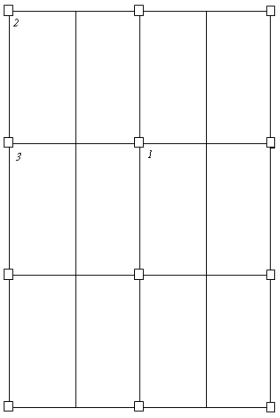

Fig 1. Schematic drawing of a floor of one garage level

All measurements that are to be performed are static, although exploitation conditions (loading and unloading during car parking processes) are essentially quasi-static. However, being that characteristic times of parking processes are much longer than relaxation processes of metallic structure, it is estimated that no dynamic measurements are needed.

Figure 1 presents schematic drawing of garage floor where large rectangles represent parking places and little

Dr Mile Savković, docent, Faculty of Mechanical Engineering Kraljevo, savkovic.m@mfkv.kg.ac.yu
Dr Zlatan Šoškić, docent, Faculty of Mechanical Engineering Kraljevo, soskic.z@ mfkv.kg.ac.yu
Nebojša Zdravković, mech.eng. Assistant, Faculty of Mechanical Engineering Kraljevo, zdravkovic.n@ mfkv.kg.ac.yu
Prof Dr Ranko Rakanović, full prof, Faculty of Mechanical Engineering Kraljevo, rakanovic.r@ mfkv.kg.ac.yu

squares (at corners of the rectangles) represent structure columns. Lines represent structure bearers. Three characteristic columns are marked by numbers: 1-column at inner intersection of bearers, 2-column at the corner of garage structure and 3-column at outer intersection of bearers, but still not at corner of structure.

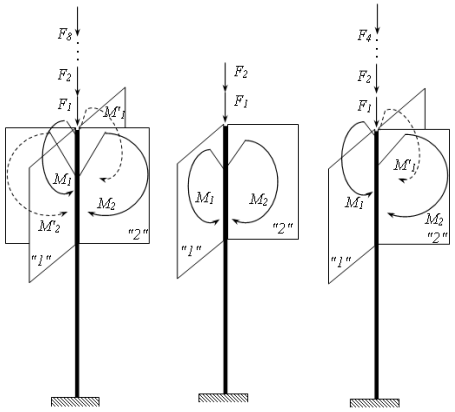

Fig.2. Basic static loads of selected columns
left-column 1, middle-column 2 and right-column 3

Basic static loads, resulting from static analysis, are shown at Figure 2. Column at position 1 has highest vertical loads, but bending moments acting on the column are of opposite signs and are being partially cancelled. Column at position 2 has the lowest vertical loads, but bending moments acting on it are the highest. Columns at position 3 have loads which are combination of two previous cases-vertical loads are lower compared to columns at position 1, but higher then at columns at position 2; bending moments acting on them are partially canceling each other in one plane, but in other plane there is no cancellation.

On basis of thus determined basic loads, calculation of stresses is performed by application of finite element method software. The calculation showed critical points at columns and bearers: at columns the highest stresses are expected at their top, and for bearers at joints.

PROPOSED METHOD

It is important to stress that, according to calculations, that dead weight of construction causes significant stresses (it holds especially for cases when structure includes some concrete parts). Therefore, stress measurements should reveal dead weight stresses as well.

Therefore, the proposed methodology for testing of multi-storage garages is the following:

1. Stresses are to be measured at points belonging to one parking cell which is at corner of parking; measuring points are at top of columns indicated by numbers 1, 2 and 3 and at joints of middle bearer of the cell.
2. As zero level of investigated stresses is considered level of stress that is existing in prefabricated elements before they are mounted in structure. All activities that are to be performed in order to determine zero-level of stresses (strain gauges sealing, measurements of initial voltage levels, etc) are to be performed before mounting;
3. Stresses caused by dead weight of structure at measurement points are to be measured while garage is empty.
4. Stresses caused by load are to be measured by parking cars at both parking places.
5. Stresses at all measurement points are to be lower than allowed level for material of structure.

CONCLUSION

Developed methodology takes into account dead weight induced stresses and load induced stresses, and comprises measurement of stresses at five critical points of structure. Although number of measuring points is low, serious measurement skills are needed in order to provide accurate and trustable results, considering the fact that standard measurement procedures for investigation of mechanical structures rely on measurement of zero-level stresses immediately before stress is applied, which in this case is not possible.

In process of development of testing methodology no assumptions were made except its geometric characteristics. Therefore, the developed testing procedure may be applied to any type of multi-storey parking garages with the same geometry.

LITERATURE

[1] Jane Holtz Kay, "A Brief History of Parking: The Life and After-life of Paving the Planet", Architecture Magazine, February 2001.
[2] Milićević M., Zdravković S, "*Dinamika konstrukcija"*, Izdavačka jedinica Univerziteta u Nišu , Niš 1991.

E SESSION:

MECHANICAL DESIGN AND MECHANICS

CALCULATION OF THE FREE END DEFLECTION AND SLOPE OF A CANTILEVER TRUSS IN DISTRIBUTED LOAD

M. Dedic, M. Todorovic

Abstract: *Truss beams are the most common type of load carrying structures for great loads in mechanical and civil engineering. Their main properties are easy and cheap manufacturing, and great carrying capacity to self weight, i.e. the great specific strength. In this paper one calculation method for the free end deflection and slope of the truss with constant cross-section and repeated cells under the distributed load is presented. The method is based on procedure that has been derived by the same authors. It is simple and effective, and uses elementary formulas. It is therefore suitable for quick calculating and influence assessment of particular structural parameters. The influence of the cell number – relative length to bending and shearing rigidity of this type of truss is analyzed.*

Keywords: *1) Continuum modeling, 2) Equivalent bending rigidity, 3) Equivalent shearing rigidity*

1. INTRODUCTION

The truss beams are the most widely used structures for carrying load in mechanical and civil engineering. Their advantages are simple and low cost manufacturing and above all their high load capacity – strength to self weight ratio. However, it is usually not easy to calculate deformations of trusses because of their complexity, and Finite Element Method (FME) is almost inevitable tool for that task. This problem made researchers try to replace a real truss with structural regularity, often called the trusses with repeated cells, by an equivalent continuum beam, so that the formulas for deformations simmilar to those in Strength of materials can be applied.

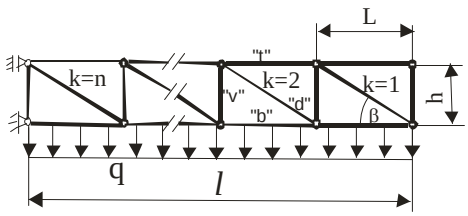

Fig.1 The planar truss with distributed load

The general theory of continuum beams can be found in [1]. In [2] to [6] different approaches to the problem of continuum modeling of trusses with repeated cells are presented. In this paper we elaborate a procedure for calculating displacements of a truss in uniformly distributed load. The procedure is simple and effective. It is based on the theory of the same authors published in more details in [7] to [8], and can be applied to the most common types of trusses with repeated cells in the engineering practise.

2. DISPLACEMENTS OF A PLANAR TRUSS

Within our introductory analysis we first consider a statically determinate planar truss in Fig.1 with pin jointed bars in n repeated cells or L, h, β = const. The overall length of the truss is $l = nL$. The properties and notation rule of the bars are: bottom longitudinal bars have index "b", length L and cross-section area A_b, top longitudinal bars with "t", L, A_t, vertical bars with "v", h, A_v and diagonal bars with "d", l_d and A_d. A *k-th* vertical bar is the left vertical bar of the *k-th* cell, so that the rightmost vertical bar is indexed zero!

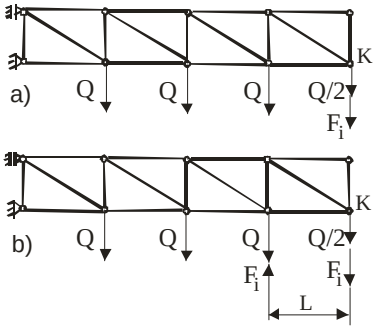

Fig.2 Dummy forces for the end deflection and slope

We assume that the truss is loaded in uniformly distributed load q[N/m]. The load is for the purpose of analysis devided in concentrated forces $Q = ql/n$ attached to the lower joints, Fig.2(a). In order that all the lower longitudinal or "b" bars are equally loaded with load $Q = qL$, the rightmost or K joint is loaded with $Q/2$. To apply the dummy force method the force $F_i = 0$ is also put in joint K. The internal bar forces $N(k)$ are calculated from equilibrium conditions:

$$N_b(k) = \frac{k(k+1)}{2}\frac{Q}{tg\beta} + k\frac{F_i}{tg\beta}$$

Prof. dr Milan Dedic, Professor, Faculty of Mechanical Engineering Kraljevo, dedic.m@mfkv.kg.ac.yu
Milica Todorovic, Lecturer, Higher Technical School, mtodorovic_vtms@yahoo.com

$$N_t(k) = \frac{(k-1)k}{2}\frac{Q}{tg\beta} + (k-1)\frac{F_i}{tg\beta}$$

$$N_v(k) = kQ + F_i$$

$$N_d(k) = \frac{kQ}{\sin\beta} + \frac{F_i}{\sin\beta} \qquad (1)$$

(The rightmost vertical and top bars are unstressed but they are kept for the reason of structural continuity.) The "*b*" and "*v*" bars are in compression, and "*t*" and "*d*" bars in tension. The bars are solely axially strained, so the strain energy of the truss has the form:

$$A_d = \frac{1}{2}\sum_{k=1}^{n}\frac{N_b^2(k)L}{EA_b} + \frac{1}{2}\sum_{k=1}^{n}\frac{N_t^2(k)L}{EA_t} + \frac{1}{2}\sum_{k=1}^{n}\frac{N_v^2(k)\,h}{EA_v} + \frac{1}{2}\sum_{k=1}^{n}\frac{N_d^2(k)\,l_d}{EA_d}. \qquad (2)$$

We apply the Castigliano's theorem to calculate the deflection of the point K:

$$f_K = \left.\frac{\partial A_d}{\partial F_i}\right|_{F_i=0} \qquad (3)$$

The result can be expressed as a sum of two components: f_B which contains all terms with cross-sectional areas of bottom and top bars, and the component f_S which contains of all terms with cross-section areas of vertical and diagonal bars:

$$f_B = \frac{Ql_1^3}{8E}\left[\frac{1}{h^2A_b}\left(1+\frac{1}{n}\right)^2 + \frac{1}{h^2A_t}\left(1-\frac{1}{n}\right)^2\right] \qquad (4)$$

$$f_S = \frac{Ql}{2E}\left[\frac{tg\beta}{A_v} + \frac{1}{\sin^2\beta\cos\beta\,A_d}\right] \qquad (5)$$

The expressions (4) and (5) have been got using summation formulas for series of integer powers k, k^2 and k^3 and by putting $h = L\,tg\beta$, $l_d = L/cos\beta$, $L = l/n$. In the course of that procedure the summation signs in (2) have vanished. In the papers [7] and [8] of the same authors it has been shown that the component f_B corresponds to the *structural bending* of the truss as a whole, and that the second component f_S corresponds to the *structural shearing* of the truss. However, no bar is either bent or sheared because they are pin jointed!

The last two expressions can be given a compact form. If we introduce new quantities:

$$I_{xe}^f(n) = \left[\frac{1}{h^2A_b}\left(1+\frac{1}{n}\right)^2 + \frac{1}{h^2A_t}\left(1-\frac{1}{n}\right)^2\right]^{-1} \qquad (6)$$

$$S_e = E\left[\frac{tg\beta}{A_v} + \frac{1}{\sin^2\beta\cos\beta\,A_d}\right]^{-1} \qquad (7)$$

we can write f_K via (4) and (5):

$$f_K = \frac{ql^4}{8EI_{xe}^f(n)} + \frac{ql^2}{2S_e} \qquad (8)$$

The corresponding deflection formula for a continuum cantilever beam, with cross-section area A and shearing modulus G, which includes shearing, reads:

$$f_K = \frac{ql^4}{8EI_x} + \kappa\frac{ql^2}{2GA} \qquad (9)$$

The products EI_x and GA/κ stand for bending and shearing rigidities. Parameter κ, called the *shearing number*, takes into account how the cross-section's shape influences the distribution of shearing stress.

Obviously $I_{xe}^f(n)$ is an *equivalent axial moment of inertia*, so that product $EI_{xe}^f(n)$ represents *equivalent bending rigidity*, and S_e is an *equivalent shearing rigidity*. We see that unlike usual moment of inertia I_x of the bulk cross-sections the $I_{xe}^f(n)$ depends on the cell number n! This link is going to be discussed later in this text in more details.

In a similar way we can calculate the end slope γ, i.e. the inclination of the right-most "b" bar to the horizontal. For that purpose we introduce the dummy moment $M_i = LF_i = 0$ through two forces F_i, Fig.2(b). We calculate then bar forces $N(k)$ as functions of q and M_i, change them into (2) and write:

$$\gamma_K = \left.\frac{\partial A_d}{\partial M_i}\right|_{M_i=0} \qquad (10)$$

We get again two components, one due to bending and the other due to shearing, so that we can write:

$$\gamma_K = \frac{ql^3}{6EI_{xe}^{\gamma}(n)} + \frac{ql}{S_e} \qquad (11)$$

The $I_{xe}^{\gamma}(n)$ reads:

$$I_{xe}^{\gamma}(n) = \left[\frac{1}{h^2A_b}\left(1+\frac{3}{2n}+\frac{1}{2n^2}\right)^2 + \frac{1}{h^2A_t}\left(1-\frac{3}{2n}+\frac{1}{2n^2}\right)^2\right]^{-1} \qquad (12)$$

and we see that $I_{xe}(n)$ is influenced by the type of the displacement as well! This is indicated by superscript "f" in (6) and "γ" in (12). The analogous formula for the end slope of a continuum cantilever beam reads:

$$\gamma_K = \frac{ql^3}{6EI_x} + \kappa\frac{ql}{GA}$$

The fact that the equivalent moments of inertia have similar form lead us to the conclusion that we can introduce a generalized form:

$$I_{xe}(n) = \left[\frac{K_b(n)}{h^2A_b} + \frac{K_t(n)}{h^2A_t}\right]^{-1} \qquad (13)$$

The coefficients $K_b(n)$ and $K_t(n)$ refere to the brackets in Eqs. (6) and (12). Their meaning and values are presented in broader details in Ref.[8].

3. THE DISPLACEMENTS OF SPATIAL TRUSSES.

The planar trusses considered in the previous chapter helped us introduce the theoretical concept of the procedure we have elaborated. We can now make an extension of that procedure to spatial trusses, refering to formulas (8) and (11), together with (6), (7) and (12).

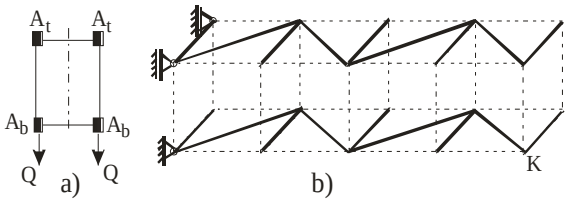

Fig.3 Spatial truss with rectangular cross-section

Of the two main types of spatial trusses with repeating cells, i.e. constant cross-section along their length, we start with rectangular cross-section, Fig.3(a). We assume that it is loaded with distributed load q along both grups of bottom longitudinal bars (which means that the truss is actualy in total load $2q$). This load is represented with $Q = qL$ forces in Fig.3(a). Calculation shows that the forces in the bottom and top horizontal filling bars, continuous lines in Fig.3(b), are negligible. (The dotted lines in Fig.3(b) serve only to indicate the geometric relations among joints.) Because of that formulas (8) for f_K and (11) for γ_K hold unchanged.

The second type has symmetric triangular cross-section with side angle α, Fig.4(a). We assume again that it is loaded with $2q$ total load represented by concentrated $Q = qL$ forces in lower joints on both sides. Additionally, to make ful use of symmetry, we assume that the cross-section area of the top bars is $2A_t$, and that forces $2N_t(k)$ act in them! If we caculate bar forces with these assumptions, we shall get formulas of the same form as (1), but instead Q and F_i we must put $Q' = Q/\cos\alpha$ and $F_i' = F_i/\cos\alpha$.

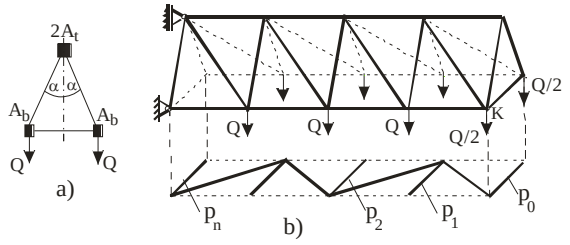

Fig.4 Spatial truss with triangular cross-section

Another difference is that we now have forces in transverse horizontal filling bars shown in continuous line in Fig.4(b). They are shown detached from the rest of the structure for the sake of clarity. If we denote them by index "p" and their cross-section by A_p, their values in the procedure of calculating f_K , Fig.2(a), will read:

$$N_p(k) = Q\,\mathrm{tg}\alpha + F_i\,\mathrm{tg}\alpha, \qquad k = 0$$
$$N_p(k) = Q\,\mathrm{tg}\alpha \qquad k = 1, 2 \ldots n\text{-}1 \qquad (13)$$

Formula for the end deflection will now read:

$$f_K = \frac{q l^4}{8EI_{xe}^{f}(n)} + \frac{q l^2}{2S_{etr}} + \frac{q l^2}{EA_p}\frac{\sin^3\alpha}{\cos^2\alpha}\frac{tg\beta}{n^2} \qquad (14)$$

and in the simmilar manner the formula for the end slope will read:

$$\gamma_K = \frac{q l^3}{6EI_{xe}^{\gamma}(n)} + \frac{q l}{2S_{etr}} + \frac{q l}{EA_p}\frac{\sin^3\alpha}{\cos^2\alpha}\frac{tg\beta}{n} \qquad (15)$$

The I_{xe}^{f} and I_{xe}^{γ} in (14) and (15) are the same as (6) and (12), or their generalized form (13), but length h is now the *vertical* distance, see Fig.4(a), not the length of "v" bar. The S_{etr} is now the equivalent shearing rigidity for triangular cross-section:

$$S_{etr} = E\left[\frac{tg\beta}{A_v}K_v + \frac{1}{\sin^2\beta\cos\beta\cdot A_d}\right]^{-1}\cos^2\alpha \qquad (16)$$

The third terms in (14) and (15) are due to the forces N_p in "p" bars. Its influence is low even for small n.

4. NUMERICAL RESULTS

The formulas derived enable us to analyse this type of structures in meny aspects. We shall restrict us here only to the influence of the equivalent moments of inertia and the fraction of shearing component in the total end deflection.

Let us first notice that both $I_{xe}^{f}(n)$ and $I_{xe}^{\gamma}(n)$ with increasing n tend to the value:

$$I_{xLB} = \left[\frac{1}{h^2A_b} + \frac{1}{h^2A_t}\right]^{-1} = \frac{h^2A_bA_t}{A_b + A_t} \qquad (17)$$

which is the axial moment of intertia calculated over the cross-section of only longitudinal bars (thereby the subscript "LB"). Table 1 shows convergence of I_{xe}, Eq.(6), to I_{xLB}, Eq.(17), for diagonal angle $\beta = 30^o$. In the same table the ratios of bending and shearing component to the total deflection are shown. We clearly see that shearing has high fraction for smaller n.

Table 1 Fractions of deflection components

n	4	6	8	10	12
$I_{xe}^{f}(n)/I_{xeLB}$	1,090	1,074	1,060	1,050	1,043
f_B / f	0,766	0,882	0,931	0,955	0,968
f_S / f	0,233	0,118	0,069	0,045	0,031

5. CONCLUSION

In this paper formulas for equivalent bending and shearing rigidities and for end deflection nad slope have been derived for a planar and spatial truss with unidirectional diagonal filling bars and constant cross-section. The truss is in uniformly distributed load. The formulas enable us to replace a real truss structure in calculating the end deflection and slope by an equivalent continuum beam. They are almost as simple as standard Strength of materials formulas for the corresponding continuum beams. They can replace the FME method in simmilar calculations. They enable easy analysis of influence of particular structural data. The numerical calcualtion shows high shearing component fraction in displacements for smaler cell numbers n.

REFERENCES

[1] Timoshenko S. P., Goodier J. N.*: Teorija elasticnosti*, Gradjevinska knjiga, Beograd, 1962.

[2] Kenner W. S.: *Lattice Truss Structural Response Using Energy Methods***,** North Carolina A&T State University, A Thesis Submitted to the Faculty of Old Dominion University in Partial Fulfillment of the Requirement for the Degree of Master of Sciences, 129 pages, NASA-TM-112361, 1987.

[3] Noor A. K., Mikulas M. M.: *Continuum Modeling of Large Lattice Structures, Status and Projections*, NASA Technical Paper 2767, pp.1-10, 1988.

[4] Burgardt B., Cartraud P.: *Continuum Modelling of Beamlike Lattice Trusses*, Advances in Computational Techniques for Structural Engineering, pp. 51-59, August 21-23, Budapest, Hungary, 1996.

[5] Savkovic M., Gasic M., Ostric D.: *Metoda uproscavanja izraza za savojnu krutost prostornih resetkastih konstrukcija*, 23th JUPITER Conference, pp. 373-379, Belgrade, 1997.

[6] Teughels A., De Roeck G.: *Continuum Models for Beam- and Platelike Lattice Structures*, IASS-IACM 2000 Fourth International Colloquium of Computations of Shell & Spatial Structures, pp.1-20, June 5-7, Channia Crete, Greece, 2000.

[7] Dedić M., Todorović M.: *An Analysis of The Equivalent Stiffness of Beam-like Trusses with Constant Cross-section*, Congress of Theoretical and Applied Mechanics, pp 347-352, April 10-13, Kopaonik, 2007.

[8] Todorović M., Dedić M.: *An Analysis of The Deformation of a Beam-like Truss Structure Using Method of Equivalent Continuum Beam*, 7th International Conference ″Research and Development in Mechanical Industry″ RaDMI 2007, 16 - 20. September 2007, Belgrade, Serbia, pp. 670-674, 2007.

RESTORABLE FREE VIBRATIONS COST BY GEAR TEETH IMPACTS

S. Ćirić-Kostić, M. Ognjanović

Abstract: *Teeth vibrations are, as a rule, treated as forced vibrations excited by variable stiffness of meshed gears. This approach provides good results in subcritical and critical ranges of teeth mesh frequency. In the supercritical range, according to the model of forced vibrations, vibrations should disappear. It is not the case with gears. In the supercritical range of teeth mesh frequencies, the level of vibrations still increases with the same gradient of increase as in the subcritical range. This paper gives the results of measurement and results of frequency analysis of measured vibrations which prove this statement. Further, the paper presents gear vibrations shown as restorable free vibrations that are renewed by teeth collision while entering a mesh. Teeth addendum collision was chosen for excitation after which there arises a response in the form of free damped vibrations. This approach allows explanation of the phenomenon of the high level of gear vibrations in the supercritical range of teeth mesh frequencies and development of an analytical model on the basis of which the balance of energy of teeth collision in gear mesh can be analyzed.*

Key words: gears, vibrations, collision, transmission

1. INTRODUCTION

Gear vibrations are the consequence of change of stiffness of meshed teeth. Due to the change of stiffness at constant load, the deformation manifested in the form of forced vibrations, and natural vibrations of the system are excited. The change of stiffness makes these vibrations nonlinear and complex for analytical procession. Nonlinearity of these vibrations has been considered in numerous papers, out of which paper [1] is cited. Research on influences of the meshing process, such as transmission errors caused by geometry deviations or wear damages, uses the model of forced vibrations, but only in subcritical and critical ranges of teeth mesh frequencies. This approach prevails in the field of gear dynamics reasearch (vibrations, dynamic forces, noise). One of such references where dynamic forces are determined is cited [2]. In the subcritical range of teeth mesh frequencies according to the model of forced vibrations, vibrations disappear. In gears, the level of measured vibrations further increases with the increase of rotational velocity. Due to significant differences in the level of measured and calculated vibrations, the supercritical range of frequencies is almost always excluded from consideration in the mentioned papers. The literature mentions, but much more rarely, another excitation of gear vibrations, i.e. teeth collision. Teeth collisions occur for various reasons and in different parts of gears, such as addendum collision, medium collision, collision due to interruption of contact, i.e. backlash, etc. Addendum collision arises at any entrance of a new pair of teeth in in mesh and it is which particularly intense in spur gears [3]. After each collision, the meshed masses respond with natural vibrations which are quickly damped, but which successively appear. A correlation between the parameters of teeth collision and measured gear vibrations is established for the purpose of defining the nature of gear vibrations in a new way. This approach enables definition of model for synthesizing measured gear vibrations and balance of collision energy emitted in the form of vibration energy propagates through the system structure.

2. ADDENDUM GEAR TEETH IMPACT

The process of gear teeth meshing is accompanied by several types of teeth impacts. In spur gears, teeth impact is most intense at addendum collision. This impact is, in the first place, the consequence of elastic deformations of gear teeth, and it can be intensified by deviation of dimensions and shapes of teeth profiles. Before a new pair of teeth enters the mesh, the previous pair of teeth is meshed. Under load, these teeth deform because the pitch of the next tooth in one gear increases, and it decreases in the other one. The next pair of teeth enters the mesh with a pitch difference. The first point of contact is replaced from the right position A, to the position A' which is behind the point A. The contact of the teeth pair starts with intensive addendum impact (Fig. 1a). The collision speed v_c is proportional to the teeth deformation, the speed of rotation n and the gear design parameters. By analysing the teeth geometry, deformations and speeds, the collision speed in the first point of teeth contact is defined as

MSc Snežana Ćirić-Kostić, Faculty of Mechanical Engineering Kraljevo, cirickostic.s@mfkv.kg.ac.yu
Prof. dr Milosav Ognjanović, Faculty of Mechanical Engineering Belgrade, mognjanovic@mas.bg.ac.yu

$$v_c = r_{b1}\omega_1\left(1+\frac{1}{u}\right)\left(1-\frac{\cos(\alpha'+\varphi)}{\cos\alpha_w}\right) \qquad (1)$$

The angular speed $\omega_1 = 2\pi n_1$, n-gear revolutions per minute (rpm), transmission ratio $u = z_2/z_1$, teeth number of connected gears z_1 and z_2, and other parameters are presented in Fig. 1a. The increase of load of teeth F_n/b results in the increase of teeth deformations, and thus in the increase of collision speed. In Fig. 1b, the relative collision speed v_c/n for the chosen parameters for the spur gear pair, is presented (z_1=z_2=25, module m=5mm, offset factors x_1=x_2=0). For other spur gear pairs, by using the ratio (v_c/n) from diagram in Fig. 1b, the collision speed is

$$v_c = \left(\frac{v_c}{n}\right)\left(1+\frac{1}{u}\right)\frac{r_b}{117.5}n \qquad (2)$$

The collision speed v_c is defined in the direction of the teeth contact line. For further application of this speed, it is necessary to reduce masses of machine parts in collision also in the direction of the same contact line.

These reduced masses are

$$m_{r1} = \frac{J_1}{r_{b1}};\quad m_e = \frac{m_{r1}m_{r2}}{m_{r1}+m_{r2}} \qquad (3)$$

where J_1 and J_2 are inertia moments of the corresponding gears and all connected rotating masses which rotate together with them. The radii of the basic circle of gears are $r_{b1} = (mz_1/2)\cos\alpha$ and $r_{b2} = (mz_2/2)\cos\alpha$, where α=20^0. The collision force of reduced masses is

$$F_c = v_c\sqrt{c'm_e};\quad m_e = \frac{m_{r1}m_{r2}}{m_{r1}+m_{r2}} \qquad (4)$$

where c' is the teeth stiffness at the moment of collision.

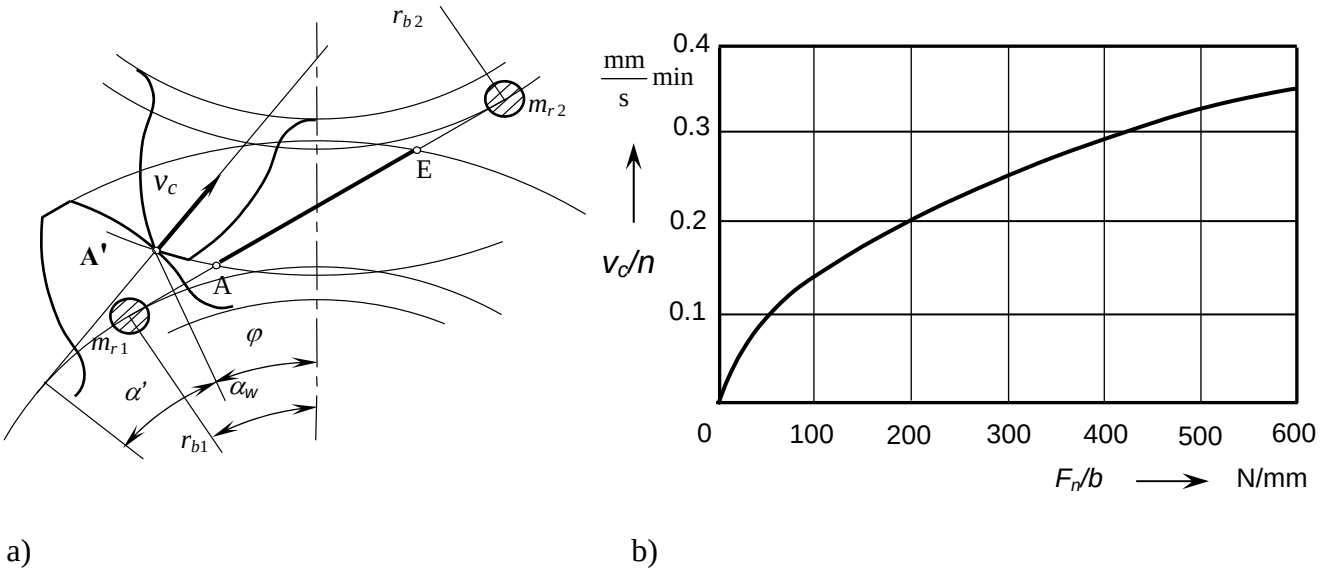

a) b)

Fig. 1 Teeth collision: a) addendum collision, b) relative speed of addendum collision for the chosen gear parameters

The collision speed may be increased if the pitch difference in meshed gears is increased due to the offset during manufacturing. The intensity of the collision force depends on the collision speed v_c and, to a great extent, on the size of rotating masses, i.e. the equivalent mass m_e and the teeth stiffness at the moment of first contact (impact). This momentary stiffness c' is smallest in comparison with the stiffness of meshed teeth and it does not change during an extremely short time of impact. In helicoid gears, the tooth starts meshing by one of its end, where the stiffness c' is very small as well as the intensity of the impact force.

After every collision of teeth, there arises natural oscillation of meshed gears, i.e. the equivalent mass m_e. The natural frequency is proportional to the average stiffness of meshed teeth c and this mass $f_{n1} = \sqrt{c_\gamma/m_e}/2\pi$. Figure 2 presents the time function of oscillation for a relatively slow gear rotation when the frequency of teeth collision f=nz/60 is considerably smaller than natural frequencies. These free vibrations are very quickly damped. A new collision renews them, and restorable free vibrations arise.

With the increase of the rotational speed, the frequency f increases, and the natural frequency f_{n1} remains the same. The difference in frequencies decreases to resonance when they become equal. In the supercritical range, the frequencies of teeth meshing are $f>f_{n1}$. Vibrations are realized by their natural frequency, but due to the increased intensity of teeth collision, the levels of these free vibrations with the frequency f_{n1} are higher.

3. EXPERIMENTAL RESEARCH WITH COMMENTS

The back to back system shown in Figure 3 was used for the needs of the research. The gear centre distance was 125 mm, with the continuous rotation speed change from zero to 6000 rpm. The angular gear vibrations were measured in the direction of the tangent onto the kinematic circle with the diameter of 125 mm. An accelerometer rotating with the disc was attached to the disc which was placed on top of an outlet shaft, in the direction of the tangent onto this circle.

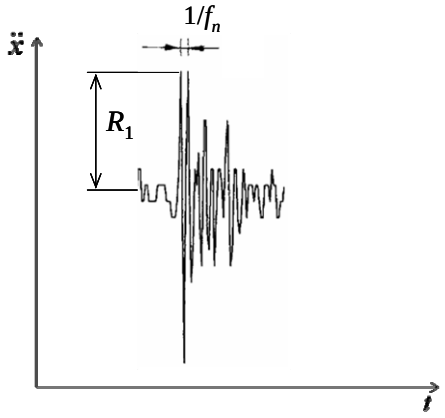

a)

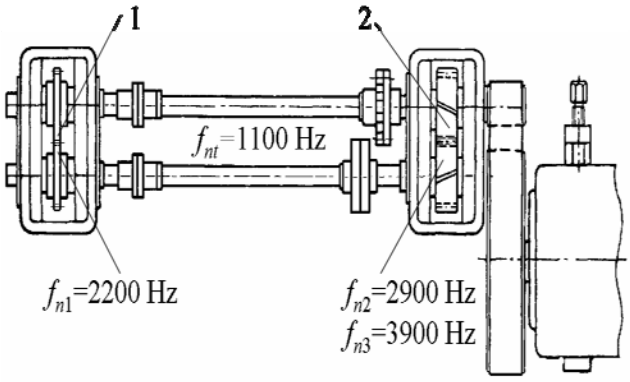

b)

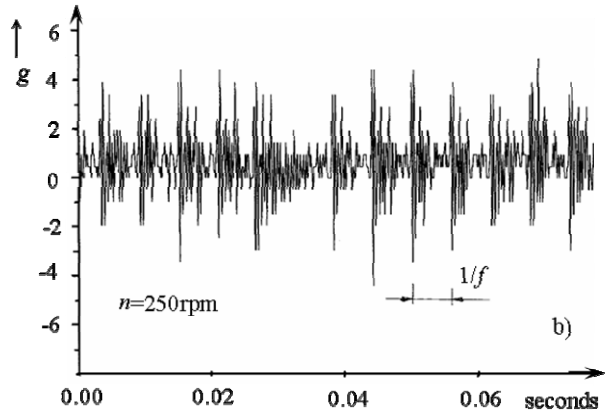

Fig. 2 Natural free restorable gear vibrations:
a) after one impact, b) successive impact repetition

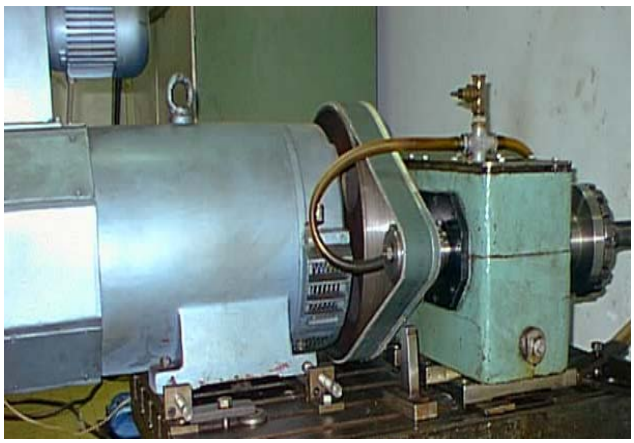

Fig. 3 Gear vibration measurement -test rig

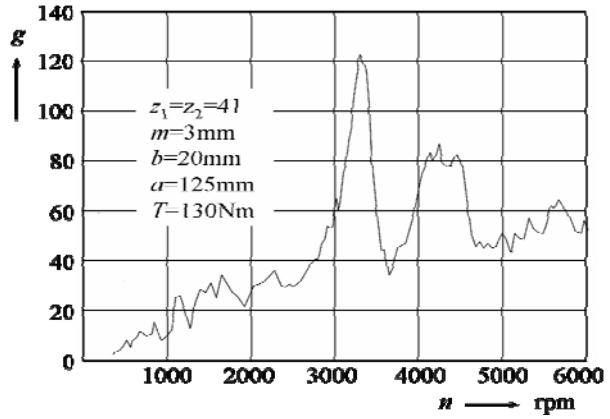

Fig. 4 Total level of angular gear vibration

The test was performed with spur gears with the transmission ratio u=1, teeth number z=41, module m_n=3 mm, thickness b=20 mm, by using the back to back system. The loading value of 130Nm was used, and the speed of rotation was within the range of 0-6000 rpm. Figure 4 presents the change of the general level of measured vibrations of this gear pair. The increase in the angular speed results in increasing the teeth mesh frequency, the intensity of teeth collision as well as the system response to excitation $R=\ddot{x}$.

In the subcritical range of angular velocity (up to 3000 rpm), this response after collision slowly increases. When the teeth mesh frequency f becomes close or equal to the natural frequency (for 3260rpm), there occurs resonance, and this response, i.e. acceleration considerably increases. In the supercritical range of teeth mesh frequency, the trend of slow vibration increase (response R) continues to that in the subcritical range. In the supercritical range of teeth mesh frequency, there occurred two additional resonances – supercritical resonances. They may be the result of influence of other natural frequencies in the system f_{n2}, f_{n3} or the result of instability of modal structure of the mechanical system in the state of high rotational speeds. For the purpose of establishing the nature of gear vibrations, a frequency analysis was performed for the chosen rotational speeds. The frequency analysis with the application of Fast Fourier Transformation – FFT analysis, was performed for a certain speed of rotation and in the short time period. The complex time function transformed into a set of elementary sine functions of different amplitudes, different frequencies and phase lags. The results of these analyses are presented in the form of frequency spectrums in Fig. 5. The amplitude values of the elementary sine functions expressed by the number of gravitation acceleration g are on the ordinates, whereas the frequencies of these functions in Hz are on the abscissas.

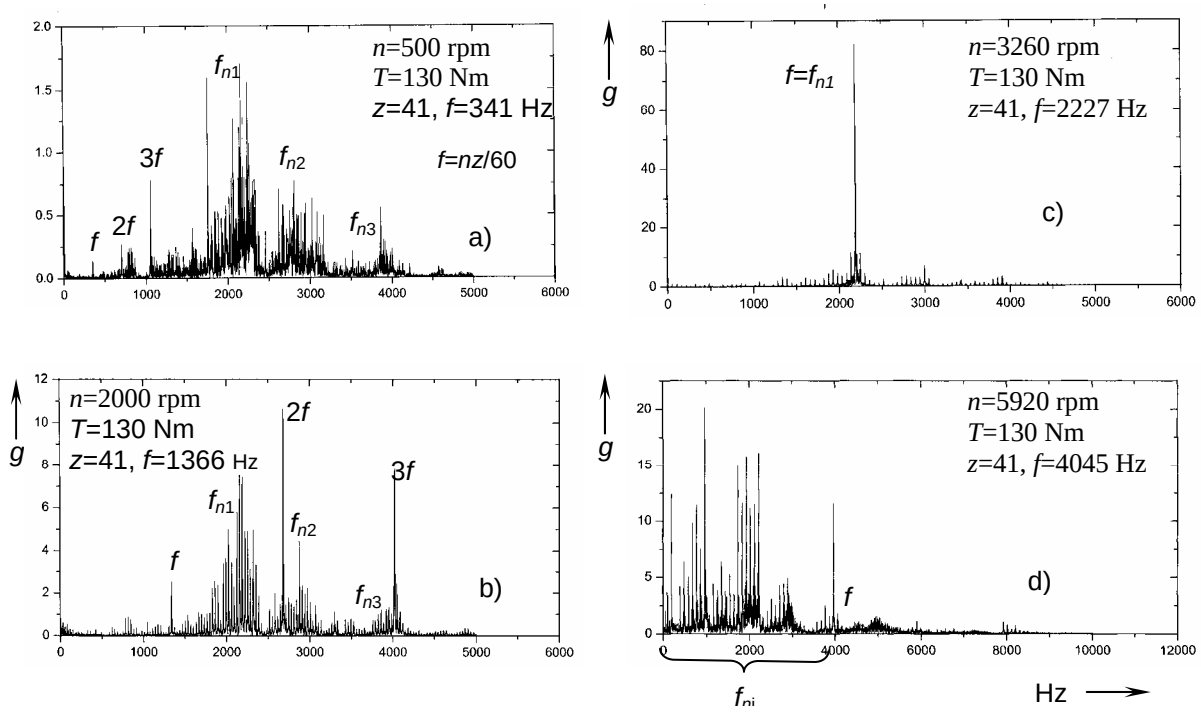

Fig. 5 Vibration spectrums of gears a) and b) in the subcritical, c) in the critical, and d) in supercritical frequency range

The diagrams of Figures 5a and b) show gear vibration frequency spectrums in the subcritical range of teeth mesh frequencies. At low speeds of rotation (500rpm), the intensity of teeth collision is low so that the level of vibrations for the frequencies f, 2f and 3f is lower than the level of vibrations for natural frequencies. At higher

speeds of rotation (2000rpm), these levels are higher and more uniform. In the resonance state (Fig. 5c), only natural vibrations of very high intensity are present. In the supercritical range of teeth mesh frequencies (5920rpm – Fig. 5d), the level of vibrations is reduced. The intensity of teeth collision is very high, but the level of vibrations for the teeth mesh frequency f and its higher harmonics $2f$ and $3f$ is almost equal to zero. It coincides with the fact that forced vibrations in supercritical frequency range disappear. Free undamped vibrations are restored in gears due to teeth collisions that repeat with the frequency f. They are realized by natural frequencies of the gears and the system as a whole. In this range, the frequency of modal structure of the system can even be changed, i.e. new natural frequencies frequencies f_{ni} can appear (Fig.5d).

4. CONCLUSION

The results of measurement and FFT analysis confirm the hypothesis that gear vibrations are restorable free (natural) vibrations that repeat after each teeth collision, i.e. teeth meshing.

It is of particular importance for the supercritical range of teeth mesh frequency because only in this manner can the high level of vibrations and dynamic forces for these frequencies be explained. The obtained experimental results can be modelled (synthesized) as restorable free vibrations. Such an analytical model allows defining distribution of energy at teeth collision in the system structure, its losses and damping.

REFERENCE

[1] Tamminana, V.K., Kahraman, A., Vijayakar, S.: A Study of the Relationship between the Dynamic Factors and the Dynamic Transmission Error of Spur Gear Pairs, ASME Journal of Mechanical Design, Vol. 129, 2007, pp 75-84

[2] Verdmar, L., Andersson, A.: A method to determine dynamic loads on spur gear teeth and on bearings, Journal of Sound and Vibration 267 (2003), pp 1065-1084.

[3] Ognjanovic, M.: Noise Generation in Mechanical Systems, Faculty of Mechan. Engin., Belgrade, 1995.

[4] Agemi, F. M., Ognjanovic, M.: Gear Vibration in Supercritical Mesh-Frequency Range, FME Transactions 32, 2004, pp 87-94.

[5] Rigaud, E., Perret-Liaudet, J., Mecibah, M. S.: Effect of an original gear mesh modelling on the modal behaviour of gear transmission, eprint arXiv:physics/0612226, 2006.

[6] Ciric-Kostic, S., Ognjanovic, M.: Gear Housing Modal Behaviour and Noise Emission, - Proceedings of the V International Conference ”Heavy Machinery-HM-05”, Kraljevo, 2005, pp I C 13-I C 16.

KINEMATICAL ANALYSIS OF A QUICK-RETURN MECHANISM BY USING MATLAB

R. Bulatović, M. Simović

Abstract: *The paper considers kinematical analysis of a quick-return mechanism. The analysis is done by using the method of complex numbers, forming equations for determination of positions, velocities and accelerations through the closed vector contours. The analytical expressions which enable complete computer analyisis of the given mechanism are obtained. For that purpose the programs are made in Matlab, by means of which are obtained the values of positions, angular velocities and angular accelerations of members, as well as the velocities and accelertions of the specific points of the mechanism referred.*

Key words: *quick-return mechanism, analysis, positions, velocities, accelerations, Matlab.*

1. INTRODUCTION

The function of a position of the mechanism presents a geometric characteristic of the mechanism, which does not depend on timing. In order to determine the values of that function it is necessary to give one or more generalized coordinates of the mechanism. The generalized coordinate is usually related to a driving member of the mechanism.

The analysis of the position of the quick-reeturn mechanism is done in the function of the given generalized coordinate, and that is the angle of rotation of the member 2, whereby the member 2 goes a full circle. The paths of specific points are the continuous curves.

During the determination of the angular velocities, angular accelerations of members, as well as velocities and accelerations of movable points, the expressions, obtained in the form of the complex numbers by using closed vector contours, are differentiated by timing. All these kinematics values are determined for 12 different positions of the driving member. Matlab programs which automatize the complete analysis of the given mechanisms are created.

2. THE ANALYSIS OF A POSITION AND DRAWING OF A PATH OF THE MOVABLE POINTS

The analysis of the given mechanism (Fig.1) will be done analitically, by using the method of complex numbers.

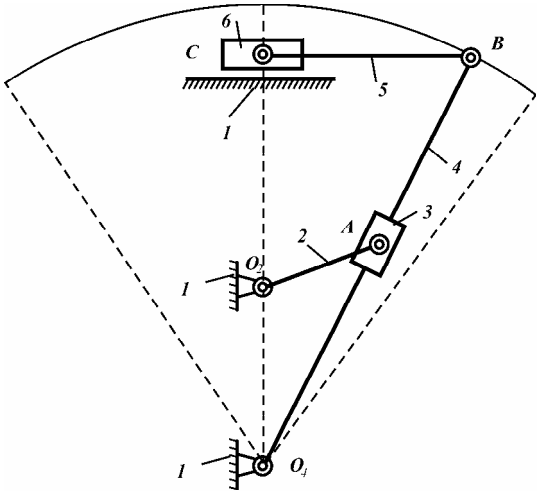

Fig. 1 Quick-return mechanism

When the specific points of the mechanism (A,B,C) are expressed in a complex plane which is determined by vectors $\overrightarrow{R_j}$ and angles θ_j for $(j=1,2...8)$, the figure of that mechanism will have the form presented in the Fig.2. After that are written the complex equations of the contour O_4AO_2 and contour O_4BC.

Radovan Bulatović, Faculty of Mechanical Engineering Kraljevo, ukib@tron-inter.net
Mladen Simović, Faculty of Mechanical Engineering Kraljevo, mladen.simovic@gmail.com

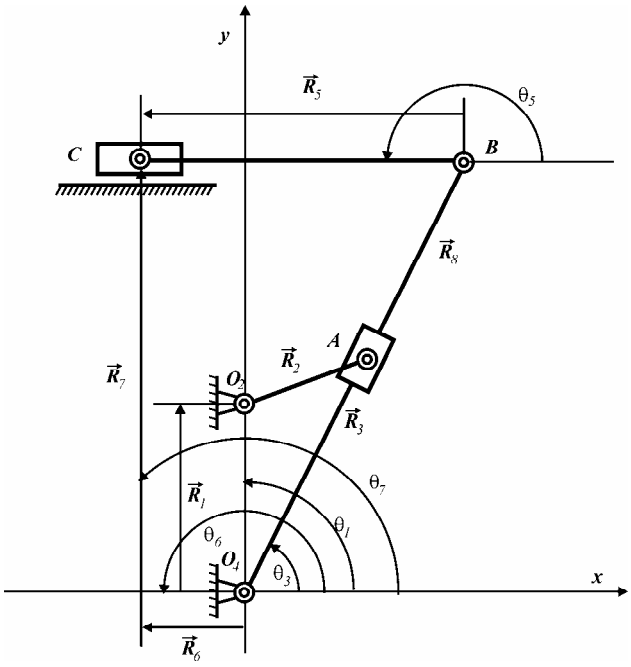

Fig. 2 Quick-return mechanism in a complex plane

$$\vec{R}_1 + \vec{R}_2 = \vec{R}_3, \tag{1}$$
$$\vec{R}_3 + \vec{R}_8 + \vec{R}_5 = \vec{R}_6 + \vec{R}_7, \tag{2}$$
$$\vec{R}_4 = \vec{R}_3 + \vec{R}_8, \tag{3}$$
$$\vec{R}_4 + \vec{R}_5 = \vec{R}_6 + \vec{R}_7, \tag{4}$$

where:

$$\vec{R}_1 = l_1\, e^{i\theta_1};\ \vec{R}_2 = l_2\, e^{i\theta_2};\ \vec{R}_3 = l_3\, e^{i\theta_4};\ \vec{R}_4 = l_4\, e^{i\theta_4},$$
$$\vec{R}_5 = l_5\, e^{i\theta_5};\ \vec{R}_6 = l_6\, e^{i\theta_6};\ \vec{R}_7 = l_7\, e^{i\theta_7} \text{ и } \vec{R}_8 = l_8\, e^{i\theta_4}.$$

Based on the equations (1) and (4) it is obtained:

$$l_1 e^{i\theta_1} + l_2 e^{i\theta_2} = l_3 e^{i\theta_4}, \tag{5}$$
$$l_4 e^{i\theta_4} + l_5 e^{i\theta_5} = l_6 e^{i\theta_6} + l_7 e^{i\theta_7}. \tag{6}$$

By using Euler transformations ($e^{i\theta_j} = \cos\theta_j + i\sin\theta_j$) the equations (5) and (6) obtain the following form:

$$l_1(\cos\theta_1 + i\sin\theta_1) + l_2(\cos\theta_2 + i\sin\theta_2) = l_3(\cos\theta_4 + i\sin\theta_4), \tag{7}$$
$$l_4(\cos\theta_4 + i\sin\theta_4) + l_5(\cos\theta_5 + i\sin\theta_5) = l_6(\cos\theta_6 + i\sin\theta_6) - l_7(\cos\theta_7 + i\sin\theta_7). \tag{8}$$

If we decompose given equations into a real and imaginary part, two systems of equations are obtained:

$$\begin{aligned} &(\text{Re})\ l_2\cos\theta_2 - l_3\cos\theta_4 = 0 \\ &(\text{Im})\ l_1 + l_2\sin\theta_2 - l_3\sin\theta_4 = 0 \end{aligned}, \tag{9}$$
$$\begin{aligned} &(\text{Re})\ l_4\cos\theta_4 + l_5\cos\theta_5 - l_6\cos\theta_6 = 0 \\ &(\text{Im})\ l_4\sin\theta_4 + l_5\sin\theta_5 - l_6\sin\theta_6 - l_7 = 0 \end{aligned}. \tag{10}$$

By solving the system of equations (9) and (10) the expressions for the change of angles are obtained:

$$\theta_4 = \arctan\left(\frac{l_1 + l_2\sin\theta_2}{l_2\cos\theta_2}\right), \tag{11}$$
$$\theta_5 = \arcsin\left(\frac{l_7 - l_4\sin\theta_4}{l_5}\right) \tag{12}$$
$$l_3 = l_2\frac{\cos\theta_2}{\cos\theta_4} \tag{13}$$

Based on the obtained equations, a Matlab code for drawing of the path of mechanism points (A, B, C) is written. The input values are:

l_1=47 (mm); % the length of member 1
l_2=30 (mm); % the length of member
l_4=100 (mm); % the length of member 4
l_5=57 (mm); % the length of member 5
l_7=82 (mm) % the distance between 0_4 and horizontal plane on which point C (1_7) moves along
theta_2=120^0; % slope of the angle of member 2
omega_2=2 (rad/s); % angular velocity of a driving member
epsilon_2=0 (rad/s^2); %angular acceleration of a driving member
n=12; % the number of the position for which the analysis is done.

By running the code for drawing of paths, the paths of specific points of the mechanism which is given in the Fig.3 are obtained.

3. THE ANALYSIS OF KINEMATICS VALUES

In order to obtain the laws of angular velocities and angular accelerations of memebers of the mechanism, as well as the velocities and accelerations of specific points, the equations (5) and (6) will be diferentiated and then their real and imaginary parts equalized.

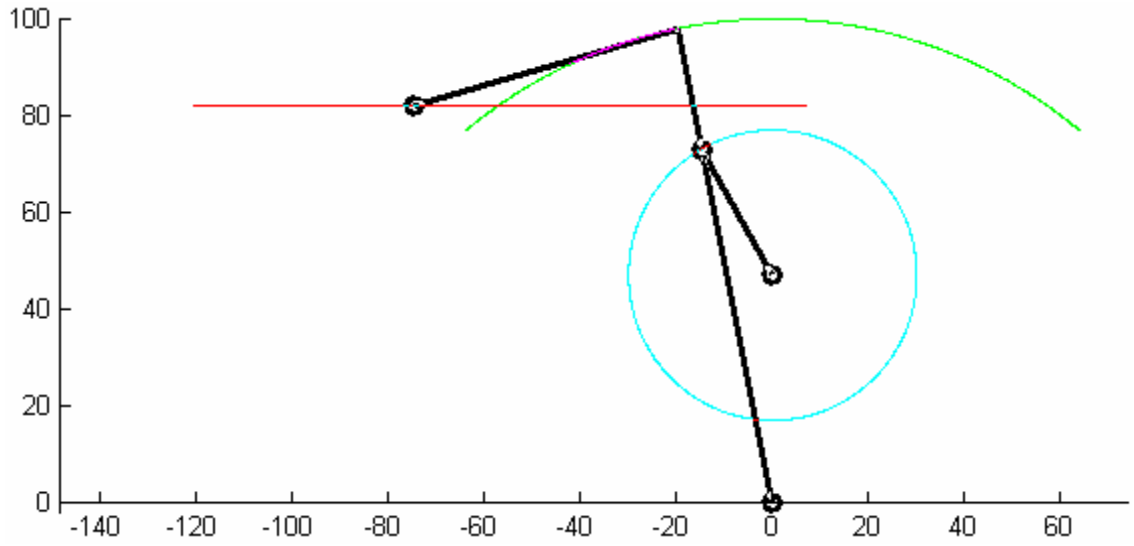

Fig. 3 The path of specific points of quick-returning mechanism

Angular velocities of the members

By differentiating the equations (5) and (6) the following systems of equations are obtained:

$$l_1 i\omega_1 e^{i\theta_1} + l_2\omega_2 e^{i\theta_2} = \left(\dot{l}_3 + l_3\omega_3 i\right)e^{i\theta_4}, \qquad (14)$$

$$l_4 i\omega_4 e^{i\theta_4} + l_5 i\omega_5 e^{i\theta_5} = \dot{l}_6 e^{i\theta_6}, \qquad (15)$$

if the given equations are decomposed into the real and imaginary part, the following systems of equations are obtained:

$$\begin{aligned} &(\text{Re}) \quad -l_2\omega_2 \sin\theta_2 - \dot{l}_3\cos\theta_4 + l_3\omega_4 \sin\theta_4 = 0 \\ &(\text{Im}) \quad l_2\omega_2 \cos\theta_2 - \dot{l}_3\sin\theta_4 - l_3\omega_4 \cos\theta_4 = 0 \end{aligned}, \qquad (16)$$

$$\begin{aligned} &(\text{Re}) \quad l_4\omega_4 \sin\theta_4 + l_5\omega_5 \sin\theta_5 + \dot{l}_6\cos\theta_6 = 0 \\ &(\text{Im}) \quad l_4\omega_4 \cos\theta_4 + l_5\omega_5 \cos\theta_5 = 0 \end{aligned}. \qquad (17)$$

By solving the system of equations (16) and (17) it is obtained:

$$\omega_4 = \frac{l_2\omega_2\cos\theta_2 - \dot{l}_3\sin\theta_4}{l_3\cos\theta_4}, \qquad (18)$$

$$\omega_5 = \frac{-l_4\omega_4\sin\theta_4}{l_5\cos\theta_5}, \qquad (19)$$

$$\dot{l}_3 = l_2\omega_2\sin\left(\theta_4 - \theta_2\right). \qquad (20)$$

Angular accelerations of members

When the equations (14) and (15) are diferentiated and the real and imaginery parts are equalized again, the following systems of equations are obtained:

$$\begin{aligned} &(\text{Re}) \quad l_2\left(-\omega_2^{\,2}\cos\theta_2 - \varepsilon_2\sin\theta_2\right) - \\ &-\left(\ddot{l}_3 - l_3\omega_4^{\,2}\right)\cos\theta_4 + \left(2\dot{l}_3\omega_4 + l_3\varepsilon_4\right)\sin\theta_4 = 0 \\ &(\text{Im}) \quad l_2\left(-\omega_2^{\,2}\sin\theta_2 + \varepsilon_2\cos\theta_2\right) - \\ &-\left(\ddot{l}_3 - l_3\omega_4^{\,2}\right)\sin\theta_4 - \left(2\dot{l}_3\omega_4 + l_3\varepsilon_4\right)\cos\theta_4 = 0 \end{aligned}, \qquad (21)$$

$$\begin{aligned} &(\text{Re}) \quad l_4\omega_4^{\,2}\cos\theta_4 + l_4\varepsilon_4\sin\theta_4 + \\ &+ l_5\omega_5^{\,2}\cos\theta_5 + l_5\varepsilon_5\sin\theta_5 + \ddot{l}_6\cos\theta_6 = 0 \\ &(\text{Im}) \quad -l_4\omega_4^{\,2}\sin\theta_4 + l_4\varepsilon_4\cos\theta_4 - \\ &-l_5\omega_5^{\,2}\sin\theta_5 + l_5\varepsilon_5\cos\theta_5 = 0 \end{aligned}. \qquad (22)$$

By solving the equations (21) and (22) it is obtained:

$$\varepsilon_5 = \frac{l_4\left(\omega_4^{\,2}\sin\theta_4 - \varepsilon_4\cos\theta_4\right) + l_5\omega_5^{\,2}\sin\theta_5}{l_5\cos\theta_5}, \qquad (23)$$

$$\varepsilon_4 = \frac{-l_2\left(\omega_2^{\,2}\sin(\theta_2+\theta_4) + \varepsilon_2\cos(\theta_2+\theta_4)\right)}{l_3} + \\ + \frac{\left(\ddot{l}_3 - l_3\omega_4^{\,2}\right)\sin(2\theta_4) - 2\dot{l}_3\omega_4}{l_3}, \qquad (24)$$

$$\ddot{l}_3 = l_2\left(-\omega_2^{\,2}\cos(\theta_2-\theta_4) - \varepsilon_2\sin(\theta_2+\theta_4)\right) + l_3\omega_4^{\,2}. \qquad (25)$$

Velocities and accelerations of specific points

The velocity of the point A is obtained from the expression (26):

$$\vec{V}_A = l_2 i\omega_2 e^{i\theta_2} = l_2 i\omega_2\left(\cos\theta_2 + i\sin\theta_2\right). \qquad (26)$$

From the expression (26), by equalizing the real and imaginary part the velocity of the point A is obtained:

$$\begin{aligned}\mathrm{Re}\left(\vec{V}_A\right) &= -l_2\omega_2\sin\theta_2 \\ \mathrm{Im}\left(\vec{V}_A\right) &= l_2\omega_2\cos\theta_2\end{aligned}, \tag{27}$$

$$V_A = \sqrt{\left(\mathrm{Re}\left(\vec{V}_A\right)\right)^2 + \left(\mathrm{Im}\left(\vec{V}_A\right)\right)^2}\ . \tag{28}$$

The acceleration of the point A is:

$$\begin{aligned}\vec{a}_A &= l_2\left(-\omega_2^{\,2} + i\varepsilon_2\right)e^{i\theta_2} = \\ &= l_2\left(-\omega_2^{\,2} + i\varepsilon_2\right)\left(\cos\theta_2 + i\sin\theta_2\right)\end{aligned}. \tag{29}$$

Like it is done for the velocity of the point A, the same way can be decompose the acceleration of the same point into real and imaginary part and calculated the magnitude:

$$\begin{aligned}\mathrm{Re}\left(\vec{a}_A\right) &= -l_2\left(\omega_2^{\,2}\cos\theta_2 + \varepsilon_2\sin\theta_2\right) \\ \mathrm{Im}\left(\vec{a}_A\right) &= l_2\left(-\omega_2^{\,2}\sin\theta_2 + \varepsilon_2\cos\theta_2\right)\end{aligned}, \tag{30}$$

$$a_A = \sqrt{\left(\mathrm{Re}\left(\vec{a}_A\right)\right)^2 + \left(\mathrm{Im}\left(\vec{a}_A\right)\right)^2}\ . \tag{31}$$

The velocity and acceleration of the point B are calculated in the similar way as in case of the point A:

$$\vec{V}_B = l_4 i\omega_4 e^{i\theta_4} = l_4 i\omega_4\left(\cos\theta_4 + i\sin\theta_4\right), \tag{32}$$

$$\begin{aligned}\mathrm{Re}\left(\vec{V}_B\right) &= -l_4\omega_4\sin\theta_4 \\ \mathrm{Im}\left(\vec{V}_B\right) &= l_4\omega_4\cos\theta_4\end{aligned}, \tag{33}$$

$$V_B = \sqrt{\left(\mathrm{Re}\left(\vec{V}_B\right)\right)^2 + \left(\mathrm{Im}\left(\vec{V}_B\right)\right)^2}\ , \tag{34}$$

$$\begin{aligned}\vec{a}_B &= l_4\left(-\omega_4^{\,2} + i\varepsilon_4\right)e^{i\theta_4} = \\ &= l_4\left(-\omega_4^{\,2} + i\varepsilon_4\right)\left(\cos\theta_4 + i\sin\theta_4\right)\end{aligned}, \tag{35}$$

$$\begin{aligned}\mathrm{Re}\left(\vec{a}_B\right) &= -l_4\left(\omega_4^{\,2}\cos\theta_4 + \varepsilon_4\sin\theta_4\right) \\ \mathrm{Im}\left(\vec{a}_B\right) &= l_4\left(-\omega_4^{\,2}\sin\theta_4 + \varepsilon_4\cos\theta_4\right)\end{aligned}, \tag{36}$$

$$a_B = \sqrt{\left(\mathrm{Re}\left(\vec{a}_B\right)\right)^2 + \left(\mathrm{Im}\left(\vec{a}_B\right)\right)^2}\ . \tag{37}$$

Calculation of the velocity and acceleration of the point C is obtained from the following expressions:

$$\vec{V}_C = \vec{V}_B + \vec{V}_C^{\,B}, \tag{38}$$

$$\vec{V}_C^{\,B} = l_5 i\omega_5 e^{i\theta_5} = l_5 i\omega_5\left(\cos\theta_5 + i\sin\theta_5\right), \tag{39}$$

$$\begin{aligned}\mathrm{Re}\left(\vec{V}_C^{\,B}\right) &= -l_5\omega_5\sin\theta_5 \\ \mathrm{Im}\left(\vec{V}_C^{\,B}\right) &= l_5\omega_5\cos\theta_5\end{aligned}, \tag{40}$$

$$\begin{aligned}\mathrm{Re}\left(\vec{V}_C\right) &= -\left(l_4\omega_4\sin\theta_4 + l_5\omega_5\sin\theta_5\right) \\ \mathrm{Im}\left(\vec{V}_C\right) &= l_4\omega_4\cos\theta_4 + l_5\omega_5\cos\theta_5\end{aligned}, \tag{41}$$

$$V_C = \sqrt{\left(\mathrm{Re}\left(\vec{V}_C\right)\right)^2 + \left(\mathrm{Im}\left(\vec{V}_C\right)\right)^2}\ , \tag{42}$$

$$\vec{a}_C = \vec{a}_B + \vec{a}_C^{\,B}, \tag{43}$$

$$\begin{aligned}\vec{a}_C^{\,B} &= l_5\left(-\omega_5^{\,2} + i\varepsilon_5\right)e^{i\theta_5} = \\ &= l_5\left(-\omega_5^{\,2} + i\varepsilon_5\right)\left(\cos\theta_5 + i\sin\theta_5\right)\end{aligned}, \tag{44}$$

$$\begin{aligned}\mathrm{Re}\left(\vec{a}_C^{\,B}\right) &= -l_5\left(\omega_5^{\,2}\cos\theta_5 + \varepsilon_5\sin\theta_5\right) \\ \mathrm{Im}\left(\vec{a}_C^{\,B}\right) &= l_5\left(-\omega_5^{\,2}\sin\theta_5 + \varepsilon_5\cos\theta_5\right)\end{aligned}, \tag{45}$$

$$\begin{aligned}\mathrm{Re}\left(\vec{a}_C\right) &= -[l_4\left(\omega_4^{\,2}\cos\theta_4 + \varepsilon_4\sin\theta_4\right) + \\ &+ l_5\left(\omega_5^{\,2}\cos\theta_5 + \varepsilon_5\sin\theta_5\right)] \\ \mathrm{Im}\left(\vec{a}_C\right) &= l_4\left(-\omega_4^{\,2}\sin\theta_4 + \varepsilon_4\cos\theta_4\right) + \\ &+ l_5\left(-\omega_5^{\,2}\sin\theta_5 + \varepsilon_5\cos\theta_5\right)\end{aligned}, \tag{46}$$

$$a_C = \sqrt{\left(\mathrm{Re}\left(\vec{a}_C\right)\right)^2 + \left(\mathrm{Im}\left(\vec{a}_C\right)\right)^2}\ . \tag{47}$$

Based on the given equations the code is written for calculation of angular velocities and accelerations of the mechanism memebers, as well as the velocities and accelerations of the specific points.

MATLAB code

```
V=importdata('import.m');

l_1=V(1);
l_2=V(2);
l_4=V(3);
l_5=V(4);
l_7=V(5);
theta_2=V(6)*pi/180;
omega_2=V(7);
epsilon_2=V(8);
n=V(9);

for i=1:n
   a1=l_1+l_2.*sin(theta_2)
   a2=l_2.*cos(theta_2)
   theta_4=atan(a1/a2);
   if theta_4<0
      theta_4=pi+theta_4
   end

   theta_5=asin((-l_7+l_4.*sin(theta_4))./l_5);
   l_3=l_2.*cos(theta_2)./cos(theta_4);
   dl_3=l_2.*omega_2.*sin(theta_4-theta_2);
    omega_4=(l_2.*omega_2.*cos(theta_2)-
   dl_3.*sin(theta_4))./(l_3.*cos(theta_4));
   omega_5=-.*cos(theta_4))./(l_5.*cos(theta_5));
   Dl_3=-l_2.*((omega_2^2).*cos(theta_2-
theta_4)+epsilon_2.*sin(theta_2-
theta_4))+l_3*omega_4^2;
epsilon_4=(l_2.*((omega_2.^2).*sin(theta_2+theta_4)+e
psilon_2.*cos(theta_2+theta_4))-
2.*dl_3.*omega_4.*cos(2.*theta_4)-(Dl_3-
```

```
l_3.*(omega_4.^2)).*sin(2.*theta_4))./(l_3*cos(2.*theta
_4));
   epsilon_5=(-l_4.*(epsilon_4.*cos(theta_4)-
omega_4.^2.*sin(theta_4))+l_5.*(omega_5.^2).*sin(thet
a_5))./(l_5.*cos(theta_5));
 dX_a=-l_2.*omega_2.*sin(theta_2);
 dY_a=l_2.*omega_2.*cos(theta_2);
 v_a=sqrt((dX_a).^2+(dY_a).^2);
 DX_a=-l_2.*(omega_2).^2.*cos(theta_2);
 DY_a=-l_2.*(omega_2).^2.*sin(theta_2);
 a_a=sqrt(DX_a.^2+DY_a.^2);

 dX_b=-l_4.*omega_4.*sin(theta_4);
 dY_b=l_4.*omega_4.*cos(theta_4);
 v_b=sqrt(dX_b.^2+dY_b.^2);
 DX_b=-l_4.*epsilon_4.*sin(theta_4)-
 l_4.*omega_4.^2.*cos(theta_4);
 DY_b=l_4.*epsilon_4.*cos(theta_4)-
 l_4.*omega_4.^2.*sin(theta_4);
 a_b=sqrt(DX_b.^2+DY_b.^2);
 dX_c=-l_4.*omega_4.*sin(theta_4)-
 l_5.*omega_5.*sin(theta_5);

dY_c=l_4.*omega_4.*cos(theta_4)+l_5.*omega_5.*cos(
theta_5);
   v_c=sqrt(dX_c.^2+dY_c.^2);

   DX_c=-l_4.*epsilon_4.*sin(theta_4)-
l_4.*omega_4.^2.*cos(theta_4)-
l_5.*epsilon_5.*sin(theta_5)-
l_5.*omega_5^2.*cos(theta_5);
   DY_c=l_4.*epsilon_4.*cos(theta_4)-
l_4.*omega_4.^2.*sin(theta_4)+l_5.*epsilon_5.*cos(the
ta_5)-l_5.*omega_5^2.*sin(theta_5);
   a_c=sqrt(DX_c.^2+DY_c.^2);

   Table(i,[1  2  3  4  5  6  7  8  9  10  11  12  13  14
15])=[theta_2*180/pi    theta_4*180/pi    theta_5*180/pi
omega_2  omega_4  omega_5  epsilon_2  epsilon_4
epsilon_5 v_a a_a v_b a_b v_c a_c];
   theta_2=theta_2+2.*pi/n;
   if (theta_2>2.*pi)
      theta_2=theta_2-2.*pi

      if (theta_2<pi./6)
         theta_2=0
      end
          else
      theta_2=theta_2
        end
end

fid1=fopen('aut.m','w')
fprintf(fid1,'i  teta_2  theta_4  theta_5  omega_2
omega_4  omega_5  epsilon_2  epsilon_4  epsilon
_5  V_ai  A_ai  V_bi  A_bi  V_ci
A_ci\n\n')
for i=1:n
   if(i<10)
      fprintf(fid1,'0%g  %g  %5.2f  %5.2f  %5.2f
%5.2f  %5.2f  %5.2f  %5.2f  %5.2f
%5.2f  %5.2f  %5.2f  %5.2f  %5.2f
%5.2f\n\n',i,Table(i,:));
   else
      fprintf(fid1,'%g  %g  %5.2f  %5.2f  %5.2f
%5.2f  %5.2f  %5.2f  %5.2f  %5.2f
%5.2f  %5.2f  %5.2f  %5.2f  %5.2f
%5.2f\n\n',i,Table(i,:));
   end
end
fclose(fid1)
```

By running the code for the mechanism analysis for the given n-positions, the output data file out.m has the following code:

Output data file

i	teta_2	theta_4	theta_5	omega_2	omega_4	omega_5	epsilon_2	epsilon_4	epsilon _5	V_ai	A_ai	V_bi	A_bi	V_ci	A_ci
01	120	101.61	16.25	2.00	0.76	0.28	0.00	-0.12	1.02	60.00	120.00	76.42	59.62	79.34	2.82
02	150	112.74	10.34	2.00	0.71	0.49	0.00	-0.31	0.66	60.00	120.00	71.03	59.38	70.52	28.21
03	180	122.55	2.30	2.00	0.58	0.55	0.00	-0.76	-0.21	60.00	120.00	57.90	83.41	50.06	65.87
04	210	129.07	-4.39	2.00	0.23	0.25	0.00	-2.21	-2.39	60.00	120.00	22.95	221.56	16.71	161.16
05	240	125.51	-0.60	2.00	-0.96	-0.98	0.00	-8.30	-7.15	60.00	120.00	96.31	835.37	77.80	670.45
06	270	90.00	18.41	2.00	0.67	0.00	0.00	-0.00	0.82	60.00	120.00	66.67	44.44	66.67	14.79
07	300	54.49	-0.60	2.00	-0.96	0.98	0.00	8.30	-7.15	60.00	120.00	96.31	835.37	78.98	788.86
08	330	50.93	-4.39	2.00	0.23	-0.25	0.00	2.21	-2.39	60.00	120.00	22.95	221.56	18.93	189.39
09	0	57.45	2.30	2.00	0.58	-0.55	0.00	0.76	-0.21	60.00	120.00	57.90	83.41	47.55	98.97
10	30	67.26	10.34	2.00	0.71	-0.49	0.00	0.31	0.66	60.00	120.00	71.03	59.38	60.51	68.55
11	60	78.39	16.25	2.00	0.76	-0.28	0.00	0.12	1.02	60.00	120.00	76.42	59.62	70.37	44.16
12	90	90.00	18.41	2.00	2.00	-0.00	0.00	0.00	7.40	60.00	120.00	200.00	400.00	200.00	133.13

4. CONCLUSION

In this paper complete kinematic analysis of quick-return mechanism is done by using programming language Matlab. Positions, angular velocities, angular accelerations of members, velocities and accelerations of specific points of the given mechanism are determined. The given methodology on kinematic analysis, with a slight modification can be applied to any type of planar mechanisms.

REFERENCES

[1] R.L.Norton, Design of machinery (An intriduction to the synthesis and analysis of mechanisms and machines), McGRAW-HILL, third edition, p.858, Worcester Polytechnic Institute Worcesete, Massachusetts, 2004.god

[2] R. R. Bulatović, S. R. Đorđević, On the optimum synthesis of a four-bar linkage using differential evolution and method of variable controlled deviations, *Mechanism and Machine Tehory*,

[3] *doi:10.1016/j.mechmachtheory.2008.02.01*.

[4] R. R. Bulatović, S. R. Đorđević, Optimal synthesis of a four-bar linkage by method of controlled deviation, *Theoretical and Applied Mechanics (TAM), Vol.31, No.3-4, pp.265-280, 2004, Belgrade.*

[5] R. R. Bulatović, Exploration of methods of synthesis of planary mechanisms by controling motion of the members, Doctoral dissertation, The Faculty of Mechanical Engineering, Belgrade, 2007. (in Serbian)

[6] T. L. Pantelić, The Analysis of Planar Mechanisms – a text-book with problems, The Faculty of Mechanical Engineering, Belgrade, 1985. (in Serbian)

KINEMATICAL ANALYSIS OF A SIX-BAR MECHANISM BY USING MATLAB

R. Bulatović, A. Nikolić

Abstract: *The paper considers kinematical analysis of a six-bar mechanism. The analysis is done by using the method of complex numbers, forming equations for determination of positions, velocities and accelerations through the closed vector contours. The analytical expressions which enable complete computer analyisis of the given mechanism are obtained. For that purpose the programs are made in Matlab, by means of which are obtained the values of positions, angular velocities and angular accelerations of members, as well as the velocities and accelertions of the specific points of the mechanism referred*.

Key words: *six-bar mechanism, analysis, positions, velocities, accelerations, Matlab.*

1. INTRODUCTION

The function of a position of the mechanism presents a geometric characteristic of the mechanism, which does not depend on timing. In order to determine the values of that function it is necessary to give one or more generalized coordinates of the mechanism. The generalized coordinate is usually related to a driving member of the mechanism.

The analysis of the position of the six-bar mechanism is done in the function of the given generalized coordinate, and that is the angle of rotation of the member 2, whereby the member 2 goes a full circle. The paths of specific points are the continuous curves.

During the determination of the angular velocities, angular accelerations of members, as well as velocities and accelerations of movable points, the expressions, obtained in the form of the complex numbers by using closed vector contours, are differentiated by timing. All these kinematics values are determined for 12 different positions of the driving member. Matlab programs which automatize the complete analysis of the given mechanisms are created.

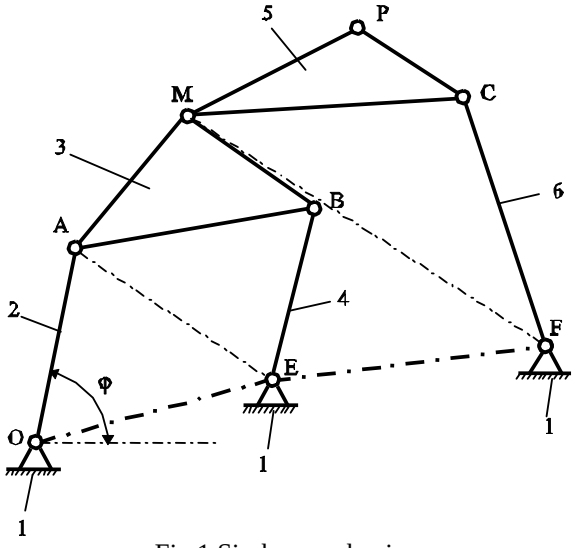

Fig.1 Six-bar mechanism

2. THE ANALYSIS OF A POSITION AND DRAWING OF A PATH OF THE MOVABLE POINTS

Vectors of the positions of points of mechanism can be presented in the following form:

$$\overrightarrow{R_i} = R_i \cdot e^{i \cdot \theta_i} \quad .$$

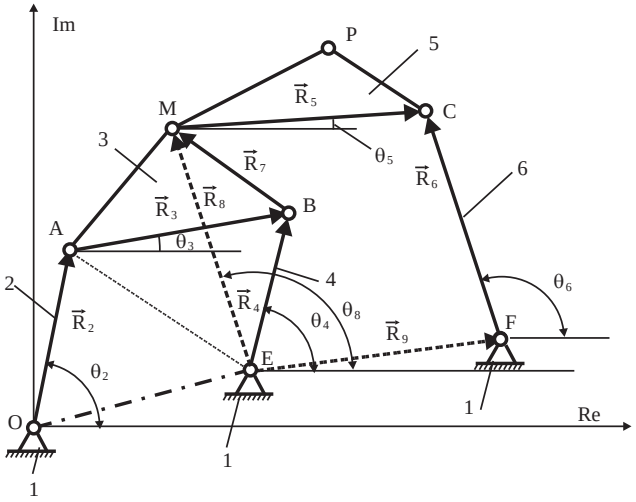

Fig.2 Six-bar mechanism in the complex plane

The analysis of the positions of this mechanism will be done in two steps. Basically, we will divide the

Radovan Bulatović, Faculty of Mechanical Engineering Kraljevo, ukib@tron-inter.net
Aleksandar Nikolić, Faculty of Mechanical Engineering Kraljevo, acon@krstarica.com

mechanism into two mechanisms OABE and EMCF and consider them that way. Observing the four-bar linkage OMBE we close the circle by using vectors $\overrightarrow{R_1}, \overrightarrow{R_2}, \overrightarrow{R_3}, \overrightarrow{R_4}$, so the following can be written:

$$\overrightarrow{R_2} + \overrightarrow{R_3} = \overrightarrow{R_1} + \overrightarrow{R_4}, \quad (1)$$

$$\overrightarrow{R_2} + \overrightarrow{R_3} - \overrightarrow{R_1} - \overrightarrow{R_4} = 0. \quad (2)$$

Presenting the vectors from the previous equation in the complex form, it is obtained:

$$R_2 \cdot e^{i\cdot\theta_2} + R_3 \cdot e^{i\cdot\theta_3} - R_1 \cdot e^{i\cdot\theta_1} - R_4 \cdot e^{i\cdot\theta_4} = 0. \quad (3)$$

The given equations can be transformed by using Euler's expressions, and by grouping the appropriate real and imaginary parts, it is obtained:

$$\left.\begin{aligned} R_2\cos\theta_2 + R_3\cos\theta_3 - R_1 - R_4\cos\theta_4 = 0 \\ R_2\sin\theta_2 + R_3\sin\theta_3 - R_4\sin\theta_4 = 0 \end{aligned}\right\}. \quad (4)$$

By solving the system of equations (4) through θ_4, it is obtained:

$$(\theta_4)_{1,2} = 2\cdot arctg\left(\frac{-B \pm \sqrt{B^2 - 4\cdot A\cdot C}}{2\cdot A}\right),$$

Where:

$$A = cos\,\theta_2 - k_1 - k_2\cdot cos\,\theta_2 + k_3,$$
$$B = -2\cdot sin\,\theta_2,$$
$$C = k_1 + k_3 - k_2\cdot cos\,\theta_2 - cos\,\theta_2 = k_1 + k_3 + (1 - k_2)\cdot cos\,\theta_2$$
$$k_1 = \frac{R_1}{R_2},$$
$$k_2 = \frac{R_1}{R_4},$$
$$k_3 = \frac{R_1^2 + R_4^2 + R_2^2 - R_3^2}{2\cdot R_2\cdot R_4}.$$

By solving the system of equations (4) through θ_3, it is obtained:

$$(\theta_3)_{1,2} = 2\cdot arctg\frac{-E \pm \sqrt{E^2 - 4\cdot D\cdot F}}{2\cdot D},$$

Where:

$$D = cos\,\theta_2 + k_4\cdot cos\,\theta_2 - k_1 + k_5,$$
$$E = -2\cdot sin\,\theta_2,$$
$$F = k_1 + k_5 + (k_4 - 1)\cdot cos\,\theta_2,$$
$$k_4 = \frac{R_1}{R_3},$$
$$k_5 = \frac{R_4^2 - R_2^2 - R_3^2 - R_1^2}{2\cdot R_2\cdot R_3}.$$

By observing the four-bar linkage EMCF we close the circle with the vectors $\overrightarrow{R_4}, \overrightarrow{R_5}, \overrightarrow{R_6}, \overrightarrow{R_7}, \overrightarrow{R_9}$, so it can be written:

$$\overrightarrow{R_4} + \overrightarrow{R_7} + \overrightarrow{R_5} = \overrightarrow{R_6} + \overrightarrow{R_9}. \quad (5)$$

The magnitude of the vector $\overrightarrow{R_7}$ is determined through according to the expression:

$$R_7 = \sqrt{r^2 + (b-d)^2},$$
$$\gamma = arctg\frac{r}{b-d},$$
$$\theta_7 = \pi - (\gamma - \theta_3).$$

A new vector $\overrightarrow{R_8}$ is introduced, so the following applies:

$$\overrightarrow{R_8} = \overrightarrow{R_4} + \overrightarrow{R_7},$$
$$R_8 \cdot e^{i\cdot\theta_8} = R_4 \cdot e^{i\cdot\theta_4} + R_7 \cdot e^{i\cdot\theta_7}. \quad (6)$$

By presenting the vectors from the previous equation in the complex plane, it is obtained:

$$R_8 \cdot e^{i\cdot\theta_8} + R_5 \cdot e^{i\cdot\theta_5} - R_6 \cdot e^{i\cdot\theta_6} - R_9 \cdot e^{i\cdot\theta_9} = 0. \quad (7)$$

By presenting the equation (7) in trigonometry form and by grouping the members into the real and imaginary part, the following system of equations is obtained:

$$\left.\begin{aligned} R_8\cos\theta_8 + R_5\cos\theta_5 - R_6\cos\theta_6 - R_9 = 0 \\ R_8\sin\theta_8 + R_5\sin\theta_5 - R_6\sin\theta_6 = 0 \end{aligned}\right\}. \quad (8)$$

By solving the system of equations (8) through θ_5 it is obtained:

$$\theta_5 = 2\cdot arctg\left(\frac{-K \pm \sqrt{K^2 - 4\cdot J\cdot L}}{2\cdot J}\right),$$

where:

$$J = -cos\,\theta_8 + k_7 - k_9\cdot cos\,\theta_8 + k_{10},$$
$$K = 2\cdot sin\,\theta_8,$$
$$L = cos\,\theta_8 - k_7 - k_9\cdot cos\,\theta_8 + k_{10},$$
$$k_7 = \frac{R_9}{R_8},$$
$$k_9 = \frac{R_9}{R_5},$$

$$k_{10} = \frac{R_8^2 + R_5^2 + R_9^2 - R_6^2}{2 \cdot R_5 \cdot R_8},$$

$$\theta_8 = arctg \frac{R_4 \sin\theta_4 + R_7 \sin\theta_7}{R_4 \cos\theta_4 + R_7 \cos\theta_7},$$

$$R_8 = \sqrt{R_4^2 + R_7^2 + 2R_4R_7 \cos(\theta_4 - \theta_7)}.$$

By solving the system of equations (8) through θ_6 it is obtained:

$$\theta_6 = 2 \cdot arctg \left(\frac{-H \pm \sqrt{H^2 - 4 \cdot G \cdot I}}{2 \cdot G} \right),$$

where:

$$G = k_6 \cdot \cos\theta_8 + k_7 + k_8 - \cos\theta_8,$$
$$H = 2 \cdot \sin\theta_8,$$
$$I = k_6 \cdot \cos\theta_8 - k_7 + k_8 + \cos\theta_8,$$
$$k_6 = \frac{R_9}{R_6},$$
$$k_7 = \frac{R_9}{R_8},$$
$$k_8 = \frac{R_5^2 - R_6^2 - R_8^2 - R_9^2}{2 \cdot R_6 \cdot R_8}.$$

After we have expressed the requested angles through the function of the given values, we can begin with the analysis of the position of the mechanism, and drawing of the path. For drawing of the path we will use the program language Matlab. It is necessary to follow the position of the specific points of the mechanism during time.

We create the input data file which contains data about lengths of every member of the mechanism, as well as the angle at the starting moment and angular velocity of the working member of the mechanism. When forming the input data file, we have to make sure that the Grashof conditions be satisfied. Output from the program can be seen on the Fig. 3 and it presents the printed positions of the specific points in every moment of the period (during that time).

The input data file has the following form:

```
a=100      % the length of the member 2
b=331      % the length AB
c=389      % the length  EB
d=165.5 % projection of the point M onto the line segment AB
f=431      %the length  MC
g=541      %the length  CF
h=215      % the projection of the point P onto the line segment MC
r=50 % the height of the triangle ABM from the point M
j=50   % the height of the triangle MCP from the point P
250      %coordinate  xf
0        %coordinate  yf
60       %theta_2
4        %omega_2
0        %epsilon_2
12       %the number of the positions
```

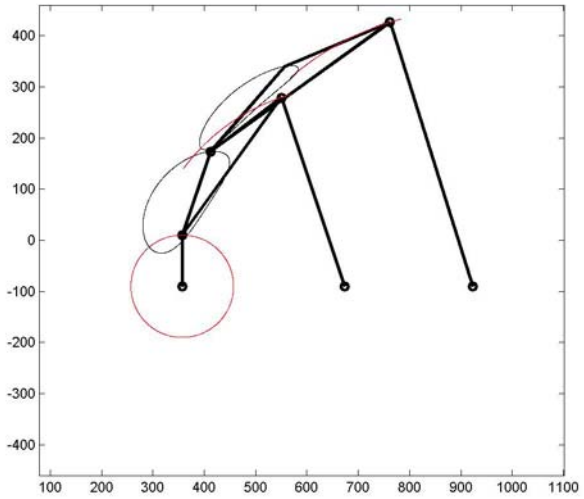

Fig.3 The paths of the specific points of a six-bar mechanism

3. THE ANALYSIS OF THE MECHANISM'S VELOCITIES

Angular velocities of the members

By differentiating the equation (3) by timing, the following expression is obtained:

$$R_2\omega_2 ie^{i\theta_2} + R_3\omega_3 ie^{i\theta_3} - R_1\omega_1 ie^{i\theta_1} - R_4\omega_4 ie^{i\theta_4} = 0, \qquad (9)$$

By presenting the previous equation in trigonometric form and by grouping the members into real and imaginary part, the system of equations is obtained:

$$\left.\begin{aligned} -R_2\omega_2 \sin\theta_2 - R_3\omega_3 \sin\theta_3 + R_4\omega_4 \sin\theta_4 = 0 \\ R_2\omega_2 \cos\theta_2 + R_3\omega_3 \cos\theta_3 - R_4\omega_4 \sin\theta_4 = 0 \end{aligned}\right\}. \qquad (10)$$

By solving the system of the equations, the expressions for angular velocities ω_3 and ω_4 are obtained:

$$\omega_3 = \frac{R_2}{R_3} \cdot \omega_2 \cdot \frac{sin(\theta_2 - \theta_4)}{sin(\theta_4 - \theta_3)},$$

$$\omega_4 = \frac{R_2}{R_4} \cdot \omega_2 \cdot \frac{sin(\theta_2 - \theta_3)}{sin(\theta_4 - \theta_3)}.$$

By differentiating the equation (5) by timing, the following expression is obtained:

$$R_4\omega_4 ie^{i\theta_4} + R_7\omega_7 ie^{i\theta_7} + R_5\omega_5 ie^{i\theta_5} - R_6\omega_6 ie^{i\theta_6} = 0\,, \quad (11)$$

that is:

$$\begin{aligned} &R_4\omega_4 \cos\theta_4 + R_7\omega_7 \cos\theta_7 + R_5\omega_5 \cos\theta_5 - \\ &-R_6\omega_6 \cos\theta_6 = 0 \\ &R_4\omega_4 \sin\theta_4 + R_7\omega_7 \sin\theta_7 + R_5\omega_5 \sin\theta_5 - \\ &-R_6\omega_6 \sin\theta_6 = 0 \end{aligned} \quad . \quad (12)$$

By solving the system of equations, the expressions for angular velocities ω_5 and ω_6 are obtained.

$$\omega_5 = \frac{R_4\omega_4 \cdot \sin(\theta_4 - \theta_6) + R_7\omega_7 \cdot \sin(\theta_7 - \theta_6)}{R_5 \sin(\theta_6 - \theta_5)},$$

$$\omega_6 = \frac{R_4\omega_4 \cdot \sin(\theta_4 - \theta_5) + R_7\omega_7 \cdot \sin(\theta_7 - \theta_5)}{R_6 \sin(\theta_6 - \theta_5)}.$$

Velocities of the specific points

$$\overrightarrow{V_A} = \frac{d}{dt}\left(\overrightarrow{R_2}\right) = \frac{d}{dt}\left(\overrightarrow{R_A}\right) = R_2\omega_2 \cdot i \cdot e^{i\cdot\theta_2} \quad . \quad (13)$$

By transforming the equation (11) into the trigonometric form, it is obtained:

$$\begin{aligned} &\overrightarrow{V_A} = -R_2\omega_2 \cdot \sin\theta_2 + (R_2\omega_2 \cdot \cos\theta_2)\cdot i\,, \\ &V_{AX} = -R_2\omega_2 \cdot \sin\theta_2\,, \\ &V_{AY} = R_2\omega_2 \cdot \cos\theta_2\,, \\ &V_A = \sqrt{V_{AX}^2 + V_{AY}^2}\,. \end{aligned}$$

In the same way the expressions for the velocities of the rest of the points are obtained as well.

$$\begin{aligned} &\overrightarrow{R_B} = \overrightarrow{R_2} + \overrightarrow{R_3}\,, \\ &V_{BX} = -R_2\omega_2 \cdot \sin\theta_2 - R_3\omega_3 \cdot \sin\theta_3\,, \\ &V_{BY} = R_2\omega_2 \cdot \cos\theta_2 - R_3\omega_3 \cdot \cos\theta_3\,, \\ &V_B = \sqrt{V_{BX}^2 + V_{BY}^2}\,, \\ &\overrightarrow{R_M} = \overrightarrow{R_2} + \overrightarrow{R_3} + \overrightarrow{R}, \\ &V_{MX} = -R_2\omega_2 \cdot \sin\theta_2 - d\omega_3 \cdot \sin\theta_3 - R\omega_3 \cdot \sin\left(\frac{\pi}{2} + \theta_3\right), \\ &V_{MY} = R_2\omega_2 \cdot \cos\theta_2 + d\omega_3 \cdot \cos\theta_3 + R\omega_3 \cdot \cos\left(\frac{\pi}{2} + \theta_3\right), \\ &V_M = \sqrt{V_{MX}^2 + V_{MY}^2}\,, \\ &\overrightarrow{R_C} = \overrightarrow{R_M} + \overrightarrow{R_5}\,, \\ &V_{CX} = V_{MX} - R_5\omega_5 \cdot \sin\theta_5\,, \\ &V_{CY} = V_{MY} + R_5\omega_5 \cdot \cos\theta_5\,, \\ &V_C = \sqrt{V_{CX}^2 + V_{CY}^2}\,, \\ &\overrightarrow{R_p} = \overrightarrow{R_M} + \overrightarrow{R_5'} + \overrightarrow{R'}, \\ &V_{PX} = V_{MX} - h\omega_5 \cdot \sin\theta_5 - j\omega_5 \cdot \sin\left(\frac{\pi}{2} + \theta_5\right), \\ &V_{PY} = V_{MY} + h\omega_5 \cdot \cos\theta_5 + j\omega_5 \cdot \cos\left(\frac{\pi}{2} + \theta_5\right), \\ &V_P = \sqrt{V_{PX}^2 + V_{PY}^2}\,. \end{aligned}$$

Angular accelerations of the members of a mechanism

By differentiating the equation (9) by the time, the following expression is obtained:

$$\begin{aligned} &R_2\varepsilon_2 ie^{i\theta_2} - R_2\omega_2^2 e^{i\theta_2} + R_3\varepsilon_3 ie^{i\theta_3} - R_3\omega_3^2 e^{i\theta_3} - \\ &R_4\varepsilon_4 ie^{i\theta_4} + R_4\omega_4^2 e^{i\theta_4} = 0. \end{aligned} \quad (14)$$

By transforming the equation (14) into the trigonometric form, it is obtained:

$$\begin{aligned} &-R_2\varepsilon_2 \sin\theta_2 - R_2\omega_2^2 \cos\theta_2 - R_3\varepsilon_3 \sin\theta_3 - \\ &-R_3\omega_3^2 \cos\theta_3 + R_4\varepsilon_4 \sin\theta_4 + R_4\omega_4^2 \cos\theta_4 = 0 \\ &R_2\varepsilon_2 \cos\theta_2 - R_2\omega_2^2 \sin\theta_2 + R_3\varepsilon_3 \cos\theta_3 - \\ &-R_3\omega_3^2 \sin\theta_3 - R_4\varepsilon_4 \cos\theta_4 + R_4\omega_4^2 \sin\theta_4 = 0 \end{aligned} \quad (15)$$

By solving the system of equations the expressions for the angular velocities ε_3 and ε_4 are obtained:

$$\varepsilon_3 = \frac{P}{Q},$$

where:

$$\begin{aligned} &P = -R_2\varepsilon_2 \sin(\theta_2 - \theta_4) - R_2\omega_2^2 \cos(\theta_2 - \theta_4) - \\ &\quad - R_3\omega_3^2 \cos(\theta_3 - \theta_4) + R_4\omega_4^2\,, \\ &Q = R_3 \sin(\theta_3 - \theta_4)\,, \\ &\varepsilon_4 = \frac{R}{S}, \\ &R = -R_2\varepsilon_2 \cdot \sin(\theta_2 - \theta_3) - R_2\omega_2^2 \cdot \cos(\theta_2 - \theta_3) + \\ &\quad + R_3\omega_3^2 - R_4\omega_4^2 \cdot \cos(\theta_4 - \theta_3)\,, \\ &S = R_4 \sin(\theta_4 - \theta_3). \end{aligned}$$

By differentiation of the equation (13) by time and grouping the members into the real and imaginary part, the following systems of the equations are obtained:

$$
\begin{aligned}
&-R_4\varepsilon_4 \sin\theta_4 - R_4\omega_4^2 \cos\theta_4 - R_7\varepsilon_7 \sin\theta_7 - \\
&-R_7\omega_7^2 \cos\theta_7 - R_5\varepsilon_5 \sin\theta_5 - R_5\omega_5^2 \cos\theta_5 + \\
&+R_6\varepsilon_6 \sin\theta_6 - R_6\omega_6^2 \cos\theta_6 = 0
\end{aligned}
\tag{16}
$$

$$
\begin{aligned}
&R_4\varepsilon_4 \cos\theta_4 - R_4\omega_4^2 \sin\theta_4 + R_7\varepsilon_7 \cos\theta_7 - \\
&-R_7\omega_7^2 \sin\theta_7 + R_5\varepsilon_5 \cos\theta_5 - R_5\omega_5^2 \sin\theta_5 - \\
&-R_6\varepsilon_6 \cos\theta_6 + R_6\omega_6^2 \sin\theta_6 = 0
\end{aligned}
$$

By solving the system of the equations the expressions for angular velocities ε_5 and ε_6 are obtained:

$$\varepsilon_5 = \frac{T}{U},$$

where:

$$
\begin{aligned}
&T = R_4\varepsilon_4 \sin(\theta_6 - \theta_4) - R_4\omega_4^2 \cos(\theta_6 - \theta_4) - \\
&-R_7\varepsilon_7 \sin(\theta_7 - \theta_6) - R_7\omega_7^2 \cos(\theta_7 - \theta_6) - \\
&-R_5\omega_5^2 \cos(\theta_5 - \theta_6) + R_6\omega_6^2, \\
&U = R_5 \cdot \sin(\theta_5 - \theta_6), \\
&\varepsilon_6 = \frac{X}{Y}, \\
&X = -R_4\varepsilon_4 \sin(\theta_5 - \theta_4) + R_4\omega_4^2 \cos(\theta_4 - \theta_5) + \\
&\quad + R_7\varepsilon_7 \sin(\theta_7 - \theta_5) + R_7\omega_7^2 \cos(\theta_7 - \theta_5) + \\
&\quad + R_5\omega_5^2 - R_6\omega_6^2 \cos(\theta_6 - \theta_5), \\
&Y = R_6 \cdot \sin(\theta_6 - \theta_5).
\end{aligned}
$$

Acceleration of the movable points

$$\overrightarrow{a_A} = \frac{d\overrightarrow{V_A}}{dt} = R_2\varepsilon_2 \cdot i \cdot e^{i\theta_2} - R_2\omega_2^2 \cdot e^{i\theta_2} \tag{17}$$

By transforming the equation (17) into trigonometric form, it is obtained:

$$
\begin{aligned}
&\overrightarrow{a_A} = \left(-R_2\varepsilon_2 \sin\theta_2 - R_2\omega_2^2 \cos\theta_2\right) + \\
&\quad + \left(R_2\varepsilon_2 \cos\theta_2 - R_2\omega_2^2 \sin\theta_2\right) i, \\
&a_{AX} = -R_2\varepsilon_2 \cdot \sin\theta_2 - R_2\omega_2^2 \cdot \cos\theta_2, \\
&a_{AY} = R_2\varepsilon_2 \cdot \cos\theta_2 - R_2\omega_2^2 \cdot \sin\theta_2, \\
&a_A = \sqrt{a_{AX}^2 + a_{AY}^2}.
\end{aligned}
$$

In the same way the expressions for the acceleration of the remaining points are obtained as well.

$$
\begin{aligned}
&\overrightarrow{a_B} = \overrightarrow{a_A} + R_3\varepsilon_3 \cdot i \cdot e^{i\theta_3} - R_3\omega_3^2 \cdot e^{i\theta_3}, \\
&a_{BX} = a_{AX} - R_3\varepsilon_3 \cdot \sin\theta_3 - R_3\omega_3^2 \cdot \cos\theta_3, \\
&a_{BY} = a_{AY} + R_3\varepsilon_3 \cdot \cos\theta_3 - R_3\omega_3^2 \cdot \sin\theta_3, \\
&a_B = \sqrt{a_{BX}^2 + a_{BY}^2},
\end{aligned}
$$

$$
\begin{aligned}
&\overrightarrow{a_M} = \overrightarrow{a_A} + d\varepsilon_3 \cdot i \cdot e^{i\theta_3} - d\omega_3^2 \cdot e^{i\theta_3} + \\
&\quad + R\varepsilon_3 \cdot i \cdot e^{i\left(\frac{\pi}{2} + \theta_3\right)} - R\omega_3^2 \cdot e^{i\left(\frac{\pi}{2} + \theta_3\right)}, \\
&a_{MX} = a_{AX} - d\varepsilon_3 \cdot \sin\theta_3 - d\omega_3^2 \cdot \cos\theta_3 - \\
&\quad - R\varepsilon_3 \cdot \sin\left(\frac{\pi}{2} + \theta_3\right) - R\omega_3^2 \cdot \cos\left(\frac{\pi}{2} + \theta_3\right), \\
&a_{MY} = a_{AY} + d\varepsilon_3 \cdot \cos\theta_3 - d\omega_3^2 \cdot \sin\theta_3 + \\
&\quad + R\varepsilon_3 \cdot \cos\left(\frac{\pi}{2} + \theta_3\right) - R\omega_3^2 \cdot \sin\left(\frac{\pi}{2} + \theta_3\right), \\
&a_M = \sqrt{a_{MX}^2 + a_{MY}^2},
\end{aligned}
$$

$$
\begin{aligned}
&\overrightarrow{a_C} = \overrightarrow{a_M} + R_5\varepsilon_5 \cdot i \cdot e^{i\theta_5} - R_5\omega_5^2 \cdot e^{i\theta_5}, \\
&a_{CX} = a_{MX} - R_5\varepsilon_5 \cdot \sin\theta_5 - R_5\omega_5^2 \cdot \cos\theta_5, \\
&a_{CY} = a_{MY} + R_5\varepsilon_5 \cdot \cos\theta_5 - R_5\omega_5^2 \cdot \sin\theta_5, \\
&a_C = \sqrt{a_{CX}^2 + a_{CY}^2},
\end{aligned}
$$

$$
\begin{aligned}
&\overrightarrow{a_P} = \overrightarrow{a_M} + h\varepsilon_5 \cdot i \cdot e^{i\theta_5} - h\omega_5^2 \cdot e^{i\theta_5} + \\
&\quad + R'\varepsilon_5 \cdot i \cdot e^{i\left(\frac{\pi}{2} + \theta_5\right)} - R'\omega_5^2 \cdot e^{i\left(\frac{\pi}{2} + \theta_5\right)}. \\
&a_{PX} = a_{MX} - h\varepsilon_5 \cdot \sin\theta_5 - h\omega_5^2 \cdot \cos\theta_5 - \\
&\quad - R'\varepsilon_5 \cdot \sin\left(\frac{\pi}{2} + \theta_5\right) - R'\omega_5^2 \cdot \cos\left(\frac{\pi}{2} + \theta_5\right), \\
&a_{PY} = a_{MY} + h\varepsilon_5 \cdot \cos\theta_5 - h\omega_5^2 \cdot \sin\theta_5 + \\
&\quad + R'\varepsilon_5 \cdot \cos\left(\frac{\pi}{2} + \theta_5\right) - R'\omega_5^2 \cdot \sin\left(\frac{\pi}{2} + \theta_5\right), \\
&a_P = \sqrt{a_{PX}^2 + a_{PY}^2}.
\end{aligned}
$$

Based on the given kinematical analysis the obtained equations are added to the program code in Matlab programming language. The analysis of the kinematical values is done for 12 positions of the mechanism, that is with the step of 30°.

The two output data files are created. The table 1 presents the output data file in which angular velocities and angular accelerations for all the 12 positions are shown. The Table 2 presents velocities and accelerations of movable final points.

Output data file

i	theta_2	omega_2	epsilon_2	omega_3	epsilon_3	omega_4	epsilon_4	omega_5	epsilon_5	omega_6	epsilon_6
01	60	4.00	0.00	-1.22	6.31	-0.02	7.63	-0.47	2.25	0.03	4.97
02	90	4.00	0.00	-0.47	5.03	0.74	3.96	-0.17	2.18	0.54	2.80
03	120	4.00	0.00	0.11	3.93	1.07	1.23	0.10	1.91	0.78	0.89
04	150	4.00	0.00	0.58	3.26	1.11	-0.52	0.32	1.55	0.80	-0.48
05	180	4.00	0.00	0.96	2.59	0.96	-1.58	0.50	1.06	0.67	-1.37
06	210	4.00	0.00	1.24	1.58	0.71	-2.20	0.59	0.36	0.45	-1.91
07	240	4.00	0.00	1.35	0.00	0.39	-2.70	0.58	-0.62	0.18	-2.27
08	270	4.00	0.00	1.20	-2.50	-0.01	-3.56	0.42	-1.90	-0.14	-2.65
09	300	4.00	0.00	0.63	-6.54	-0.58	-5.22	0.07	-3.32	-0.52	-3.16
10	330	4.00	0.00	-0.54	-10.96	-1.36	-6.19	-0.42	-3.83	-0.95	-3.04
11	360	4.00	0.00	-1.85	-6.70	-1.85	0.37	-0.78	-1.25	-1.15	0.81
12	390	4.00	0.00	-1.98	3.99	-1.16	8.76	-0.73	1.59	-0.69	5.42

i	theta_2	Va	Aa	Vb	Ab	Vc	Ac	Vm	Am	Vp	Ap
01	60	400.00	1600.00	5.94	2969.26	15.98	2688.17	208.36	2376.72	107.67	2596.82
02	90	400.00	1600.00	287.76	1556.99	292.06	1521.70	323.80	1592.53	298.26	1593.67
03	120	400.00	1600.00	415.34	653.72	419.71	583.31	412.24	1164.96	420.18	890.77
04	150	400.00	1600.00	430.08	516.76	431.50	429.67	432.67	1077.17	442.60	734.80
05	180	400.00	1600.00	374.04	713.65	363.56	781.88	400.94	1130.64	391.92	909.08
06	210	400.00	1600.00	276.44	877.02	245.51	1041.69	334.27	1227.51	291.76	1121.20
07	240	400.00	1600.00	152.26	1051.14	96.79	1229.09	253.74	1359.40	166.78	1318.99
08	270	400.00	1600.00	4.48	1386.41	76.71	1432.34	209.06	1559.40	118.81	1534.08
09	300	400.00	1600.00	224.70	2033.26	281.81	1714.79	292.35	1792.96	283.23	1767.76
10	330	400.00	1600.00	528.70	2512.32	512.01	1716.80	479.26	1572.02	508.15	1614.35
11	360	400.00	1600.00	720.37	1341.81	620.42	834.40	572.83	428.42	611.46	545.82
12	390	400.00	1600.00	451.73	3448.90	374.17	2941.73	372.03	2548.35	374.64	2798.46

4. CONCLUSION

In this paper complete kinematic analysis of six-bar mechanism is done by using programming language Matlab. Positions, angular velocities, angular accelerations of members, velocities and accelerations of specific points of the given mechanism are determined. The given methodology on kinematic analysis, with a slight modification can be applied to any type of planar mechanisms.

REFERENCES

[1] R.L.Norton, Design of machinery (An intriduction to the synthesis and analysis of mechanisms and machines), McGRAW-HILL, third edition, p.858, Worcester Polytechnic Institute Worcesete, Massachusetts, 2004.god

[2] R. R. Bulatović, S. R. Đorđević, On the optimum synthesis of a four-bar linkage using differential evolution and method of variable controlled deviations, *Mechanism and Machine Tehory,*

[3] *doi:10.1016/j.mechmachtheory.2008.02.01.*

[4] R. R. Bulatović, S. R. Đorđević, Optimal synthesis of a four-bar linkage by method of controlled deviation, *Theoretical and Applied Mechanics (TAM), Vol.31, No.3-4, pp.265-280, 2004, Belgrade.*

[5] R. R. Bulatović, Exploration of methods of synthesis of planary mechanisms by controling motion of the members, Doctoral dissertation, The Faculty of Mechanical Engineering, Belgrade, 2007. (in Serbian)

[6] T. L. Pantelić, The Analysis of Planar Mechanisms – a text-book with problems, The Faculty of Mechanical Engineering, Belgrade, 1985. (in Serbian)

HYPOTHESIS ABOUT AMPLITUDES OF MECHANICAL AND ELECTRICAL OSCILLATIONS OF THE SECOND AND THE HIGHER ORDERS

M. Rajović, D. Dimitrovski, V. Rajović

Abstract: *The significance of the amplitudes with engineering problems including oscillations is illustrated first in this paper. Two examples of collapses of bridges in two epochs are employed in order to emphasize insufficient mathematical consideration of the problem of amplitudes of oscillations. Several important, dramatic even, facts are stressed:*

1. *Amplitudes for all the linearly independent linear homogeneous differential equation* $L_n(y)=0$ *are rarely equal*
2. *The amplitudes are rarely constant too; they are dependent on* x*, but through frequencies* $g_i(x)$ *and periods* $T_i = T(g_i(x))$
3. *Amplitudes are the best indicator of effects of technical occurrences – not a single engineering calculation involving oscillations, either theoretical or practical, should and must not go without theoretical and practical control of the amplitudes.*
4. *The basic (mathematical) amplitude must be clearly told from integration constants* C_i*, especially with linear solutions in the form*

$$y = \sum_{i=1}^{n} C_i y_i(x)$$

where C_i *depend on initial conditions, while amplitudes* $A_i = A_i(x) = A(g_i(x))$ *do not depend on them, but on basic elements of the differential equation.*
Some of our results are given in the remainder of the paper

Keywords: *Collapses of two bridges in two epochs, oscillations, amplitudes, multi-amplitudal solutions.*

1. SOME HISTORICAL DATA – WHY DID TACOMA NARROWS BRIDGE COLLAPSE?

Moments in history when a big bridge collapses are the moments when mathematics gains a new momentum for research. Those events are thus very beneficial for mathematics; they also represent a turning point in engineering.

Tacoma Narrows Bridge collapsed on November the 7th 1941. It was a big suspension bridge across Tacoma Narrows, a strait in the state of Washington, USA, shortening traffic distance for more than 100km. It was collapsing for 24 hours, oscillating tremendously under gusts of wind, allowing for the traffic to stop on its eight lanes and the vehicles to withdraw. People having the opportunity to watch the video recording of the drama, likewise the authors of this paper, were astonished. The huge mass of the bridge danced rock and roll – it used to be said as a joke. There is no other engineering drama so big, witnessed and documented. Nevertheless, the solving of this engineering took almost 50 years – until 1990; mathematical clearing up took the additional years from 1991 to 1999.

Tacoma Narrows Bridge was a suspension bridge supported by hundreds of steel wire ropes. The initial calculations after the disaster were directed toward the idea that oceanic wind, blowing perpendicularly to the direction of the road and causing oscillations who in turn had been adding with the natural frequency of the mass of the bridge, and with the resonance originating from traffic, and the strength and the angle of the wind, had gradually been tearing the wire ropes off. However, after 50 years of analysis, it was shown that linear resonance is less likely to be the cause of the disaster. If a single wire rope of the suspension is considered, it is well known that its characteristics are different when stretching and squeezing. If the wire rope is stretched, there is a Hook's constant a; if the wire rope is squeezed back, there is another constant b. It comes from the experience that, within the same distance, it is always $0 < a < b$, that is squeezing is less than stretching. Furthermore, if the torsion within cylindrical steel wires is taken into account, a non-linear feature itself, it is obvious that an ordinary linear differential

Miloje Rajović, Faculty of Mechanical Engineering Kraljevo, rajovic.m@mfkv.kg.ac.yu
Dragan Dimitrovski
Vladimir Rajović

equation could not be used as a model. The problem is non-linear instead; according to the Newton's law, it writes

(1) $my'' + f(y) = g(t)$

where $f(y)$ is a non-linear force, written approximately as

(2) $$f(y) = \begin{cases} by, & y \geq 0 \\ ay, & y \leq 0 \end{cases}$$

while $g(t)$ is an external force, and m is the mass of the considered part of the bridge. Hence, the usual model of the bridge must have not been described by a simple differential equation

(3) $y'' + 4y = \sin 4t$

with initial conditions $y(0) = 0$, $y'(0) = \alpha$. As the period of total solution of this equation is $T = \frac{2\pi}{4} = \frac{\pi}{2}$, being moment when change of the sign of y takes place, the model consisting of (1) with (2) need be employed in time intervals

$\left[0, \frac{\pi}{2}\right], \left[\frac{\pi}{2}, \frac{3\pi}{2}\right], \left[\frac{3\pi}{2}, 2\pi\right], [2\pi, 3\pi]$ etc.

This way, we could use the general solution of the equation (3)

$y = C_1 \cos 2t + C_2 \sin 2t + Y_P$,

where the particular integral is

$Y_P = -\frac{1}{12}\sin 4t$.

Then, the actual solution of the problem (1) with (2) is quadruple:

For the initial conditions $y(0) = 0$, $y'(0) = \alpha$, there is $C_1 = 0$, $C_2 = \frac{\alpha + 1/3}{2}$. The oscillatory model is valid in this case, and the solution is

$$y(t) = \sin 2t \left[\frac{1}{2}\left(\alpha + \frac{1}{3}\right) - \frac{1}{6}\cos 2t\right]$$

The conditions for $t = \frac{\pi}{2}$ are $y\left(\frac{\pi}{2}\right) = 0$, $y'\left(\frac{\pi}{2}\right) = -\left(\alpha + \frac{2}{3}\right) (< 0)$

For $t > \frac{\pi}{2}$ the new problem is

$y'' + y = \sin 4t$, $y\left(\frac{\pi}{2}\right) = 0$, $y'\left(\frac{\pi}{2}\right) = -\left(\alpha + \frac{2}{3}\right)$,

with the solution

$$y(t) = \cos t \left[\left(\alpha + \frac{2}{5}\right) - \frac{4}{15}\sin t \cos 2t\right]$$

The conditions for $t = \frac{3\pi}{2}$ are $y\left(\frac{3\pi}{2}\right) = 0$, $y'\left(\frac{3\pi}{2}\right) = \alpha + \frac{2}{15}$.

This is regular, since elongations $y(t) > 0$ and $y'(t)$ is positive. This behavior repeats infinitely, with the period of $\frac{3\pi}{2}$.

However,

$$y(t) = \sin 2t \left[-\frac{1}{2}\left(\alpha + \frac{7}{15}\right) - \frac{1}{6}\cos 2t\right], \quad \text{for } t \in \left[\frac{3\pi}{2}, 2\pi\right]$$

$$y(t) = \sin t \left[-\left(\alpha + \frac{8}{15}\right) - \frac{4}{15}\cos t \cos 2t\right], \quad \text{for } t \in [2\pi, 3\pi]$$

After the second interval, the speed is $v_2 = \alpha + \frac{2}{15}$; after the fourth interval the speed is $v_3 = \alpha + \frac{4}{15}$. This means that the speed increases at the rate of $2/15$ per cycle. And it is known that the amplitude of oscillations $y(t)$ is directly proportional to the speed in the beginning of a cycle

$A \sim K \cdot v_i(0), i = 1, 2, 3, 4, ...$

As big amplitudes A correspond to big strains, it is obvious that this discord must be tragic both technically and mathematically. The presented formulae are nothing but a one-dimensional and linear approximation of the problem that had been solved for 50 years by means of partial equations and solutions for torsion. The drama happened due to undisturbed increase of amplitudes within a long period of intense traffic and strong wind, with the bridge already damaged for the same reasons. Some difficulties had been spotted, by the way, even at the beginning of the exploitation of the bridge, with no strong wind and small load (there is exhaustive literature on this [1], [2], [3], [4]).

This example shows the importance of calculation and estimation of amplitudes of oscillations.

2. COLLAPSE OF ANOTHER BRIDGE

One hundred year before, a bridge had fallen in England. There had been no indications of what would follow (as was the case with Tacoma Narrows bridge). Taking into consideration engineering capabilities of the time, it was still a big drama. The bridge collapsed during uniform movement of an ordinary train. The train was moving slowly, was not overloaded, and all the restrictions were obeyed. So, the bridge collapsed "out of the blue". A Cambridge professor, R. Willis, who was a member of the Royal Commission for Application of Iron to Railway Structures formed after the collapse, introduced the differential equation

(4) $$y'' + \frac{q^2}{\left(lx - x^2\right)^2} y = p$$

where constants l, q, and p all have specific and important mechanical meanings.

Back then differential equations were mostly solved by quadratures or only analytically – by means of series, since iterations and majority of modern approximation methods had not been developed yet. Consequently, the equation (4) became "the Willis' problem", who played an important role in the history of mathematics.

Due to the extent of this engineering drama, the problem has firstly been committed to famous mathematician and physicist, Stokes. He promptly presented a solution to the equation (4) in the form of a charted series.

Some times later, in the 1880's, the French mathematician and mechanic Boussinesq showed that, introducing the substitution

$$t = \frac{1}{2}\ln\frac{x}{l-x},\ y = \frac{pl^2}{8}\frac{1}{\cosh t}\cdot z$$

"the bridge equation" (4) transformed to non-homogeneous equation with constant coefficients

$$\ddot{z} + \left(\frac{2q}{l} - 1\right)z = \frac{z}{\cosh^3 t},$$

which could be solved exactly. This solution also showed a discord of amplitudes.

It is shown in the above two examples that amplitudes of oscillations are an important indicator for an oscillatory phenomenon, equal to period and frequency.

As a little miracle, there is still not much data on amplitudes in the literature on differential equations, especially out of the field of harmonic oscillations.

3. SINGLE-AMPLITUDAL OSCILLATIONS

For a given equations of oscillations

(5) $$y'' + a(x)y = 0,\ a(x) > 0$$

there are mostly single-amplitudal solutions of oscillations

(6) $$y_1 = A(x)\sin x, y_2 = A(x)\cos x$$

presented in the literature..

It is shown then that the equation

(7) $$y'' - \frac{2A'}{A}y' + \frac{A^2 + 2A'^2 - AA''}{A^2}y = 0$$

has got the same arrangement of zeros with harmonic oscillations $\{\sin x, \cos x\}$, but different and variable amplitudes. By means of known methods (reduction to the canonical form), it derives that the amplitude is dependent on $a(x)$

$$A = A(a(x)) = A(x)$$

and the issue is existence of more complex non-harmonic oscillations with equal amplitudes. We proved the theorem stating that more complex differential equations with two arbitrary functional parameters $g = g(x)$ and $F = F(x) = F(g(x))$

(8) $$y'' - \frac{g''F + 2F_g' g'^2}{g'F}y' + \frac{F^2 + 2F_g'^2 - F_g''}{F^2}g'^2 y = 0$$

have equally-amplitudal oscillatory solutions

(9) $$y_1 = F(g(x))\sin g(x)$$
$$y_2 = F(g(x))\cos g(x)$$

If the amplitude $A(x) = F(x) = \text{const} = A$, then there is the equation of equally-amplitudal oscillations, but with constant amplitude:

$$y'' - \frac{g''}{g'}y' + g'^2 y = 0$$

whose solutions are

$y_1 = \cos g(x), y_2 = \sin g(x)$

(but also $A\cos g(x)$ and $A\sin g(x)$).

It could also be shown that the amplitude in all the cases is

(10) $$A(x) = \frac{1}{\sqrt{g'(x)}}$$

depending only on the frequency $g(x)$ (Exhaustive information on single-amplitudal oscillations is given in [5]).

4. DOUBLE-AMPLITUDAL AND MULTIPLE-AMPLITUDAL OSCILLATIONS

Due to the notions, impressions, drawings and images from education and the courses in Euclidian Trigonometry, one is of the opinion that fundamental trigonometric functions $\sin x$ and $\cos x$ are equivalent, told only by a temporary phase of $\varphi = \pi/2$. This is the formally true only in the most common case. Actually, the difference is much bigger, and it will be shown below.

At the very beginning, let's first emphasize another mistake. Due to the linearity of the general solution of the linear homogeneous differential equation of the second order $y = C_1 y_1 + C_2 y_2$, the amplitudes of the solutions y_1 and y_2 are not considered much, especially with harmonic oscillations. Those amplitudes in a way merge with integration constants determined according to the initial conditions. The superficialness when expressly applying fundamental equations of oscillations adds up

$$y'' + 1\cdot y = 0, y = C_1\cos x + C_2\sin x, T = 2\pi, A = 1$$

$$y'' + \alpha^2 y = 0, y = C_1\cos\alpha x + C_2\sin\alpha x, T = \frac{2\pi}{\alpha}$$

and $A_1 = 1$, but $A_2 = \frac{1}{\alpha}$.

Nevertheless, the product $C_2\cdot\frac{1}{\alpha}$ is usually considered as a single constant $C_2^* = \frac{C_2}{\alpha}$; this way the big importance of α is hidden, even if it is a constant. It is even more obvious with derivative and integral

$(\sin\alpha x)' = \alpha\cos\alpha x, (\sin\alpha x)'' = -\alpha^2\sin\alpha x$

$(\sin\alpha x)''' = -\alpha^3\cos\alpha x, (\sin\alpha x)^{IV} = \alpha^4\sin\alpha x$

Obviously, the amplitude of the fourth derivative is α^4, quite naturally as it is a new function. The same is valid for integrals

$$\int\sin\alpha x dx = -\frac{1}{\alpha}\cos\alpha x, \iint\sin\alpha x dx^2 = -\frac{1}{\alpha^2}\sin\alpha x$$

$$\iiint\sin\alpha x dx^3 = \frac{1}{\alpha^3}\cos\alpha x, \iiiint\sin\alpha x dx^4 = -\frac{1}{\alpha^4}\sin\alpha x$$

This shows that the amplitude could vary significantly.

Let's show that an equation with a single coefficient could have multiple amplitudes with various solutions, as a consequence that an equation could have several frequencies.

The following theorems are easy to prove.

Theorem 1. The family of canonical oscillatory equations

(11) $y'' + B(x)y = 0$

where $B(x) > 0$ and $B(x)$ is a continuous function, has got the oscillatory general solution which is

(12) - single-periodical, with $T = 2k\pi$

- double-amplitudal, with $A_1 = f(x)$ and $A_2(x) = F(x)$,

reading

(13) $y = C_1 f(x)\cos x + C_2 F(x)\sin x$.

Theorem 2. For the equation (11) and the solution (13) it is valid that Wronskian is $W(y_1, y_2) = 1$, leading to the condition for the amplitudes

(14) $$2\frac{1+ fF}{f'F - fF'} = \sin 2x,$$

where $f > 0$, $F > 0$, $f' \neq kF(k = const)$, and the coefficient $B(x)$ depends on the amplitude

(15) $$B(x) = B(f, F) = -fF - 2f'F + f''F\cos^2 x + fF''\sin^2 x + \frac{1}{2}\sin 2x\left[f''F' - F''f' - Ff' + fF'\right]$$

The solutions (13) have two different and continuous amplitudes which are not constant, but dependant on x. There is $A_1 = f(x) \neq 0$ and $A_2 = F(x) \neq 0$, $W(y_1, y_2) \neq 0$, but their period is the same, $T = 2k\pi, k = 1, 2, 3, ...$

5. SERIES-ITERATION METHOD

In our paper [6] we introduced the series-iteration method for the oscillations equation $y'' + a(x)y = 0$, where $a(x)$ is a positive and continuous coefficient. This provides for symmetrical separation of generalized functions $\sin_{a(x)} x$ and $\cos_{a(x)} x$, defined by series of integrals

(16)

$$\cos_{a(x)} x = 1 - \int\int a(x)dx^2 + \int\int a(x)\int\int a(x)dx^2 dx^2 - ...$$

(17)

$$\sin_{a(x)} x = x - \int\int xa(x)dx^2 + \int\int a(x)\int\int xa(x)dx^2 dx^2 - ...$$

(if $a(x) = const > 0$, there are harmonic oscillations). If the theorem on mean value of integral is applied on the integrals:

$$\int_0^x a(x)dx = a(\xi_1)x, \int_0^x\int_0^x a(x)dx^2 = a(\xi_1)\frac{x^2}{2}$$

$$\int_0^x\int_0^x xa(x)dx^2 = a(\xi_1)\frac{x^3}{3!}$$

$$\int_0^x\int_0^x a(x)\int_0^x\int_0^x a(x)dx^2 dx^2 = a(\xi_1)a(\xi_2)\frac{x^4}{4!}, \text{ etc}$$

then geometric means are introduced, then means of means, then for the expressions (16) and (17) there is

$$\cos_{a(x)} x = 1 - \frac{\left(\sqrt{g_1}x\right)^2}{2!} + \frac{\left(\sqrt{g_2}x\right)^4}{4!} - \frac{\left(\sqrt{g_3}x\right)^6}{6!} + ...$$

$$\sin_{a(x)} x = x - \frac{\left(\sqrt{g_1^*}x\right)^3}{3!} + \frac{\left(\sqrt{g_2^*}x\right)^5}{5!} - \frac{\left(\sqrt{g_3^*}x\right)^7}{7!} + ...$$

It could be inferred from the above that the functions (16) and (17) could not have a same rate of increase, due to different values of $\sqrt{g_i}$ in different points ξ_i and ξ_i^*, and the difference between odd and even exponents. Thus, with $a(x) \neq 0$, the functions differ significantly in the sense of order of entire functions. If ordinary sine and cosine are used in order to approximate functions, there are the following simple results

(18) $$\cos_{a(x)} x \approx \cos\left(x\sqrt{a(x)}\right)$$

(19) $$\sin_{a(x)} x \approx \frac{1}{a(x)}\sin\left(x\sqrt{a(x)}\right)$$

wherefrom the amplitudes are deducted

$$A_1 = f \approx 1, A_2 = F \approx \frac{1}{\sqrt{a(x)}}.$$

Obviously, the amplitudes are different. This is the shortest derivation of the Prodi theorem, stating that the equation (11) has one oscillatory solution that is limited if $a(x)$ approaches infinity, and it has another solution which approaches zero. This disparity (Prodi theorem was proved 50 years ago) points out that amplitudes of the solutions of linear homogeneous differential equation of the second order are mostly unequal.

6. HYPOTETHICAL FORMULA FOR THE DEPENDENCE OF AMPLITUDE ON FREQUENCY OF $g(x)$

We showed that for the oscillations (7) (equation (6)) and (9) (equation (8)) there is the simple formula (10)

for the amplitude $A(x)$. The formula is physically understandable, as it states that the amplitude is reciprocal to frequency (the rate of oscillations). However, the proofs are valid only for solutions obtained by means of quadratures we partially presented above for now. The same is stated in [5]. For equations of oscillations which are not solved by quadratures $y''+a(x)y=0$, there is an intuition that there must be some similarity to harmonic oscillations. If $\cos\left(x\sqrt{a(x)}\right)$ (ordinary oscillations, but of complex function) is compared to $\cos_{a(x)}x$, there is for the frequency $g(x)$: $x\sqrt{a(x)}=xg(x)$, wherefrom $g=\sqrt{a(x)}$. Then $g'=a'/2\sqrt{a}$, and the amplitude is

$$A_1=\frac{1}{\sqrt{g'}}=\frac{1}{\sqrt{\frac{a'}{2\sqrt{a}}}}.$$

If $a(x)$ increases rapidly, then $a'/2\sqrt{a}>1$, and $A_1<1$, so the solution $y_1=\cos_{a(x)}x$ is limited. If the operation is repeated for $A_2<1$, there is

$$A_2=\frac{1}{\sqrt{a}}\frac{1}{\sqrt{g'}}=\frac{1}{\sqrt{a}}\frac{1}{\sqrt{\frac{a'}{2\sqrt{a}}}}=\frac{2}{\sqrt{a'}}.$$

As $a'(x)$ monotonically increases, that A_2 tends to zero when x approaches infinity; this is Prodi theorem. However, there does not exist more strict proof.

7. LINEAR EQUATIONS OF HIGHER ORDER

It is shown in the book [7], by means of series-iteration method, that the differential equation of the Hook's law $y^{IV}+a(x)y=0$

has four fundamental solutions for $a(x)>0$: two sines and two cosines

(20)

$$y_1=\cos^{IV,1}_{a(x)}x=1-\iiiint a(x)dx^4+$$
$$+\iiiint a(x)\iiiint a(x)dx^4dx^4-...$$
$$y_2=\sin^{IV,1}_{a(x)}x=x-\iiiint xa(x)dx^4+$$
$$+\iiiint a(x)\iiiint xa(x)dx^4dx^4-...$$
$$y_3=\cos^{IV,2}_{a(x)}x=x^2-\iiiint x^2a(x)dx^4+$$
$$+\iiiint a(x)\iiiint x^2a(x)dx^4dx^4-...$$
$$y_4=\sin^{IV,2}_{a(x)}x=x^3-\iiiint x^3a(x)dx^4+$$
$$+\iiiint a(x)\iiiint x^3a(x)dx^4dx^4-...$$

There are four different amplitudes. A formula of the type (10), most likely in the form $A=f(g)$, need be derived for them. The following is expected:

$$A_1=1, A_2=\frac{1}{\sqrt[4]{a(x)}}g(a), A_3=\frac{1}{\sqrt[4]{a^2(x)}}g(a),$$
$$A_4=\frac{1}{\sqrt[4]{a^3(x)}}g(a),$$

that is there are quadruple-amplitudal oscillations.
In a similar manner, for the equation of the third order,

$$y'''+a(x)y=0$$

there are three solutions. The first one is monotone and exponential

$$y_1=1-\iiint a(x)dx^3+\iiint a(x)\iiint a(x)dx^3dx^3-...$$

The other two solutions are oscillatory and analogue to (2)

$$y_2=x-\iiint xa(x)dx^3+\iiint a(x)\iiint xa(x)dx^3dx^3-...$$
$$y_3=x^2-\iiint x^2a(x)dx^4+\iiint a(x)\iiint x^2a(x)dx^3dx^3-...$$

Conclusions analogue to the ones for the fourth order will be applicable; but only for a sine and a cosine of the third order, definitely something to be particularly and seriously researched. Of course, for the sake of Hook's law, it is necessary to find as good as possible formulae for all the four amplitudes of oscillatory solutions of linear differential equation of the fourth order.

LITERATURE

[1] O. H. Amman, T. von Kármán, G. B. Woodruff. *The Failure of the Tacoma Narrows Bridge*. Washington, D.C.: Federal Works Agency, 1941

[2] A.C. Lazer, P.J. McKenna, *Large amplitude oscillations in suspension bridges: some new connections with nonlinear analysis*, SIAM Rev. 32 (1990), 537-578

[3] I. Peterson, *Rock and roll bridge*, Science News 137 (1990), 344.

[4] P. J. McKenna, *Large Torsional Oscillations in Suspension Bridges Revisited: Fixing an Old Approximation*, The American Mathematical Monthly, Vol. 106, No. 1 (1999), pp. 1-18

[5] L. M. Berkovich, *Transformations of ordinary linear differential equations*, Samara University, Samara, 2006 (in Russian).

[6] D. Dimitrovski, M. Rajović, R. Stojiljković, *On Types, Form and Supremum of The Solutions of the Linear Differential Equation of the Second Order with*

Entire Coefficients, Applicable Analysis and Discrete Mathematics, 1 (2007), 360–370.

[7] J.Mitevska, D.Dimitrovski, *Linear trigonometries of the fourth and the sixth order*, Annuaire de l'Institut des Mathematiques, special ed. Vol. II (23), Skopje, 1996 (in Macedonian)

RESEARCH OF PARAMETRIC VIBRATIONS OF DRIVE SHAFTS IN INDUCTION MACHINE

P. Hantel, M. Bogdevičius, B. Spruogis, V. Turla, A. Jakštas

Abstract: *A description of transient phenomena in an induction machine in connection with oscillation excitation in low-damped drive systems requires the solution of a system of non-linear differential equations. The coupling of variables from the electrical and mechanical system in the differential equations complicates the physical interpretability of the observed phenomena. The paper shows how non-stationary oscillations in the drive shafts, produced by transients in the induction machine, are explained in terms of parametric excitation. The knowledge of the excitation mechanism enables a simple excitation diagram to be constructed, indicating the critical speed ranges for the excitation of oscillations.*

Key words: *vibrations by parametric excitation, non-stationary oscillations, induction machine*

INTRODUCTION

Torsional vibrations in drive shafts are imperceptible by human senses. There is no noise, no vibrations on the machine bed human beeings can hear or feel. But measurements of the shaft torque show up to 25 times of the nominal machine torque [1] during the change over from one stable operation point to another like speed reversal or switch on situations. Especially in low–damped drive systems - as servo drives or direct driven machines - resonance excitation of torsional vibrations is critical to the mechanical strength of the shaft [2].

Resonance excitation of a vibrational system may be caused by different occurences:

1. impact,
2. excitation of the system with resonance frequency,
3. excitation by a sweep function.

An impact always happens at switch on, switch off operations. Excitation with resonance frequency is unusual but happens when the torsional resonance frequency is the net frequency or nearby. A sweep function excitation is the most problematically situation, because it runs continously through a wide range of frequencies. A sweep function is characterized by the following equation (1) and looks like figure (1).

$$f(t) = \sin(2\pi F(t)t), \quad \text{with } F(t) = k_1 t. \tag{1}$$

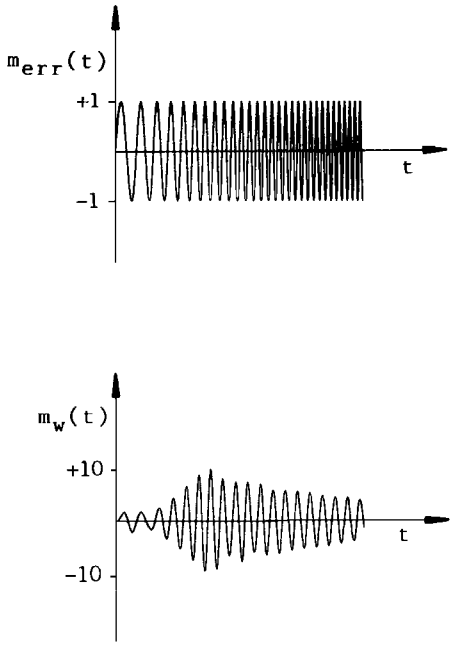

Fig. 1. Sweep function and excitation result

The research of torsional vibrations in various behaviors is also dedicated in papers [3, 4, 5, 6, 7]. This paper explains a sweep function excitation as the result of non linear parametric excitation.

Peter Hantel, Hantel Consulting, Aachen, Germany, peter.hantel@hantel-consulting.de
Marijonas Bogdevičius, Vilnius Gediminas Technical University, Lithuania, marius@ti.vgtu.lt
Bronislovas Spruogis, Vilnius Gediminas Technical University, Lithuania, bs@ti.vgtu.lt
Vytautas Turla, Vilnius Gediminas Technical University, Lithuania, vytautas.turla@me.vgtu.lt
Arūnas Jakštas, Vilnius Gediminas Technical University, Lithuania, arunas.jakstas@me.vgtu.lt

THE MATHEMATICAL DESCRIPTION OF THE INDUCTION MACHINE FOR TRANSIENT PHENOMENA

Transient phenomena in an induction machine are difficult to describe, because quasi–stationary approaches cannot be employed, as no stable operation point during transients exists. Linearization is likewise inappropriate, as the non–linear effects of interest in this instance are eliminated by definition. The Kovacs space vector theory [8] is suitable for describing induction machine transients. The space vector theory leads to a set of non–linear differential equations which cannot be solved in a general manner. Numerical methods are necessary to solve this set of non–linear differential equations. So it is possible to describe the transient behaviour of induction machines in the time scale.

The description of the induction machine by the space vector theory in complex numbers looks as follows:

$$\underline{u}_S(t) = r_S \cdot \underline{i}_S(t) + \frac{d}{dt}\underline{\Psi}_S(t) + j \cdot f_S \cdot \underline{\Psi}_S(t),$$

(2)

$$\underline{u}_R(t) = r_R \cdot \underline{i}_R(t) + \frac{d}{dt}\underline{\Psi}_R(t) + j \cdot f_R(t) \cdot \underline{\Psi}_R(t),$$

(3)

$$\underline{\Psi}_S(t) = x_S \cdot \underline{i}_S(t) + x_h \cdot \underline{i}_R(t),$$

(4)

$$\underline{\Psi}_R(t) = x_R \cdot \underline{i}_R(t) + x_h \cdot \underline{i}_S(t),$$

(5)

$\underline{u}$ – voltage space vector,
i – current space vector,
$\underline{\Psi}$ – flux space vector,
f – frequency,
r – resistor,
x – inductive reactance,
index S – stator,
index R – rotor.

Variables are all space vectors and additionally the rotor frequency $f_R(t)$.

The equation for the elektrical torque m_e is

$$m_e(t) = \frac{-Im\{\underline{\Psi}_R^*(t) \cdot \underline{i}_R(t)\}}{t_{m1}},$$

(6)

t_{m1} is a normative time constant, which represents the time the nominal torque of the induction machine needs to speed up the rotor mass to nominal rpm.

These equations show three things:

1. the system has a product of variables: $\frac{-Im\{\underline{\Psi}_R^*(t) \cdot \underline{i}_R(t)\}}{t_{m1}}$, which shows the non linearity of the set of equations,
2. the rotor frequency f_R is a time dependent parameter in equation 3 in combination with the rotor flux $f_R(t) \cdot \underline{\Psi}_R(t)$,
3. the system has only terms in the first derivation, what means, that the system is not able to swing.

Looking to the mechanical system, we have a free two–mass torsion oscillator. Θ_1 is representative for the rotor, where the eletrical torque M_e is the input to the torsional oscillator i.e. drive system. Via a shaft, a flywheel with the mass Θ_2 is coupled to the rotor mass Θ_1. The shaft can be considered as a spring with the stiffness c and a damper with the damping constant k (Fig. 2).

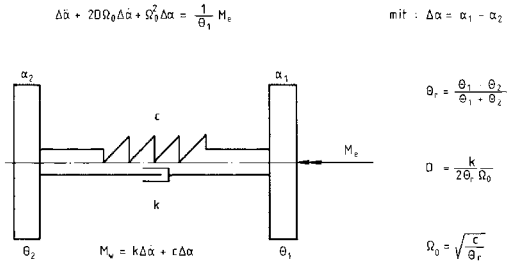

Fig. 2. Single degree–of–freedom torsional system

The differential equations for the torsional system are as follows [1]:

$$\Theta_1 \frac{d^2}{dt^2}\alpha_1(t) + k\frac{d}{dt}(\alpha_1(t) - \alpha_2(t)) + c(\alpha_1(t) - \alpha_2(t)) = M_e(t),$$

(7)

$$\Theta_2 \frac{d^2}{dt^2}\alpha_2(t) - k\frac{d}{dt}(\alpha_1(t) - \alpha_2(t)) - c(\alpha_1(t) - \alpha_2(t)) = 0. \quad (8)$$

According to the second derivation of the variables $\alpha_1(t)$ and $\alpha_2(t)$ the mechanical system is able to swing. The torsional oscillator with a low damping constant is a very good indicator for vibrations caused by the electrical torque $M_e(t)$.

The angular speed $\frac{d}{dt}\alpha_1(t)$ of Θ_1 is linked to the rotor freqency $f_R(t)$ as follows:

$$\frac{d}{dt}\alpha_1(t) = \frac{2\pi}{p} \cdot (f_S - f_R(t)). \quad (9)$$

The set of differential equations from eq. 2 to eq. 9 has to be solved.

NUMERICAL SIMULATION OF THE RUN UP PHASE FOR AN INDUCTION MACHINE

A test constellation as in Fig. 1 is assumed to simulate the transient phenomena. To solve the described set of differential equation, a special numerical differential equation solver is used. To start the simulation, the standardized voltage space vector $\underline{u}_S$ (eq. 2) jumps from 0 to 1.

This jump function is causing electromagnetic compensation phenomena in the electrical torque M_e during start up (Fig. 3a).

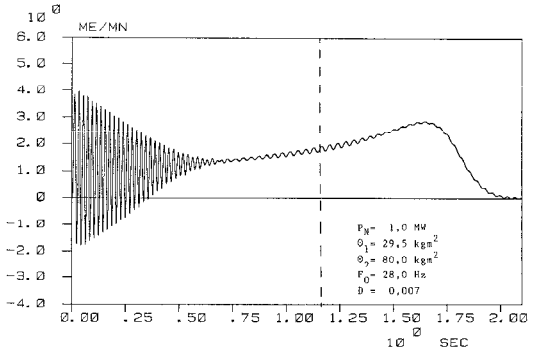

Fig. 3a. Simulation electrical torque (run up)

The frequency starts with line frequency (50 Hz) and goes down to 43 Hz as analysed in Fig. 3b.

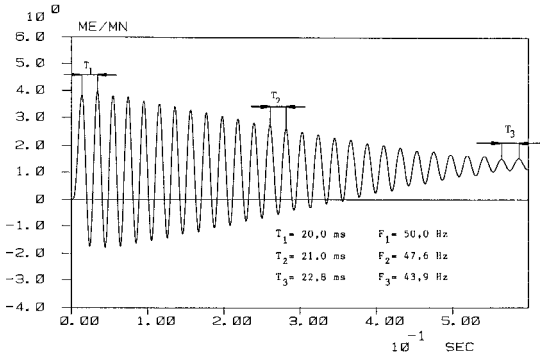

Fig. 3b. Analysis electrical torque after switch on

The electrical torque shows the behavior of a sweep function, as shown in Fig. 1. Responsible is the parametric excitation in eq. 3, where the rotor frequency $f_R(t)$ is multiplied with the flux space vector $\underline{\Psi}_R(t)$. According to eq. 6, $\underline{\Psi}_R(t)$ is one of the multiplier for the electrical torque M_e, which explains the sweep behavior.

The conclusion is, that the sweep frequency of the electrical torque runs from line frequency (50 Hz) at start up down to 0 Hz at nominal speed.

The shaft torque M_W shows in the first half second (Fig. 3c) an overlay from the forced electrical torque (50 Hz–43 Hz) and the resonance frequency of 28 Hz from the torsional oscillator.

Further on at about 1.2 seconds the amplitude of the shaft torque increases again with only the resonance frequency of 28 Hz of the torsional vibration system.

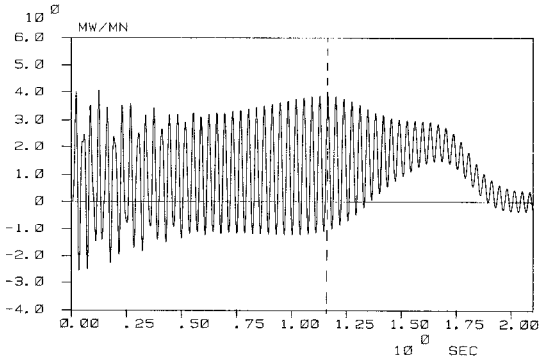

Fig. 3c. Parametric excitation of the shaft torque (run up)

Looking at the speed (fig. 3d) at that moment, the relative speed is n=0,44.

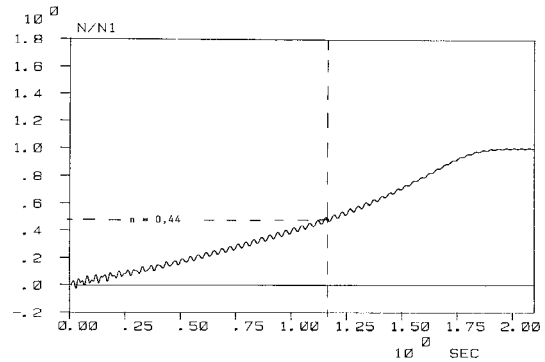

Fig. 3d. Simulated speed (run up)

Eq. 9 can also be written in a normative way as follows:

$$\frac{N}{N_1} = 1 - \frac{f_R}{f_S}, \qquad (10)$$

with $\frac{N}{N_1} = 0{,}44$ f_R is calculated to:

$$f_R = (1 - 0{,}44) \cdot 50\,Hz = 28\,Hz .$$

28 Hz is the resonance frequency of the mechanical system. Thus the parameter f_R leads to an excitation of a torsional vibration system, that can be explained by equation 3.

This is a typical parametric excitation phenomena.

Understanding the parametric excitation as a sweep function, the excitation condition can be determined very easily by Fig. 4:

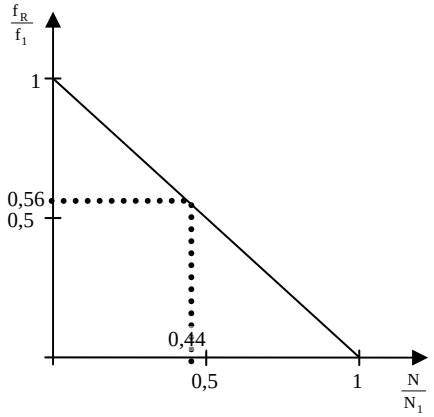

Fig. 4. Excitation condition diagram for run up

To proof this theory a simulation is made with a resonance frequency of the torsional vibration system of 75 Hz. The motor is a 55 kW induction machine with a squirrel cage rotor. As the maximum excitation frequency is 50 Hz, no resonance excitation should shown in the shaft torque.

Fig. 5a is the simulation of the shaft torque. It shows only the forced torque of the electrical torque comparable to fig. 3c.

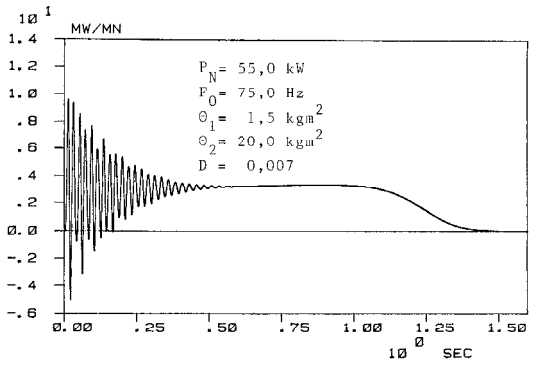

Fig. 5a. No parametric excitation of the shaft torque (run up)

Also the run of the curves of the electrical torque (fig. 5b) and the speed (fig. 5c) give no hints of a parametric excitation.

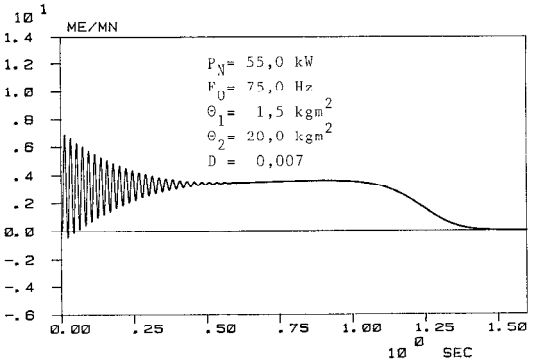

Fig. 5b. Simulation electrical torque (run up)

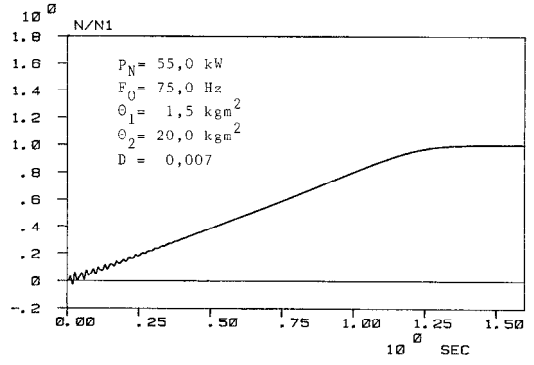

Fig. 5c. Simulation speed (run up)

As to the theory of the space vector modell it is to expect, that the resonance frequency should be excited during reversal, because the rotor frequency f_R runs from 100 Hz to 0 Hz during reversal. According to eq. 10 the torsional system with the resonance frequency of 75 Hz should be excited at a speed of

$$\frac{N}{N_1} = 1 - \frac{f_R}{f_S} = 1 - \frac{75Hz}{50Hz} = -0{,}5 \,. \qquad (11)$$

The simulation for reversal starts with the conditions at idle speed of 1500 rpm.

After the switch, the torsional oscillator is excited at its resonance frequency of 75 Hz (Fig. 6a) by the impact of the electrical torque. After the decline of the amplitude, the resonance frequency is again excited (Fig. 6a) by the parameter f_R.

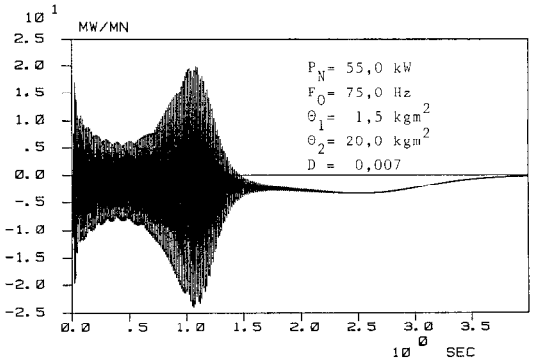

Fig. 6a. Parametric excitation of the shaft torque during reversal

The parametric excitation takes place as calculated according eq. 11 (Fig. 6b).

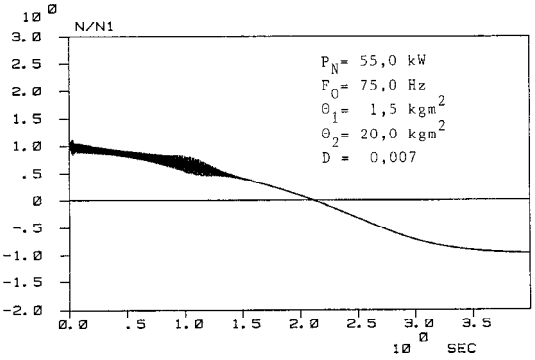

Fig. 6b. Simulation of the speed during reversal

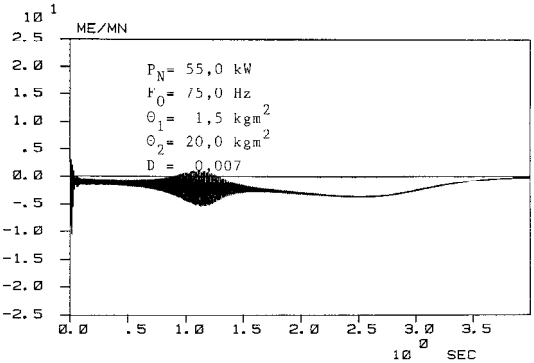

Fig. 6c. Simulation electrical torque (reversal)

The high amplitudes of the shaft torque, which are up to about 25 times of the nominal torque of the electrical machine, shows the feedback of the mechanical system to the electrical system during the parametric excitation.

Fig. 6c shows the impact of the electrical torque with about 20 times of the nominal torque. The shaft torque reacts with an amplitude of about 30 times of the nominal torque, due to the low damping of D=0,007.

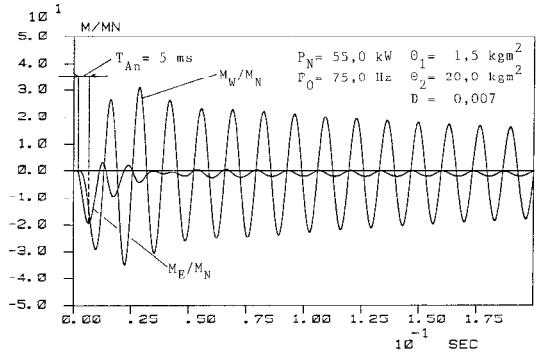

Fig. 7. Electrical impact and response of shaft torque at reversal switch

So the excitation diagram of fig. 4 can be expanded as follows:

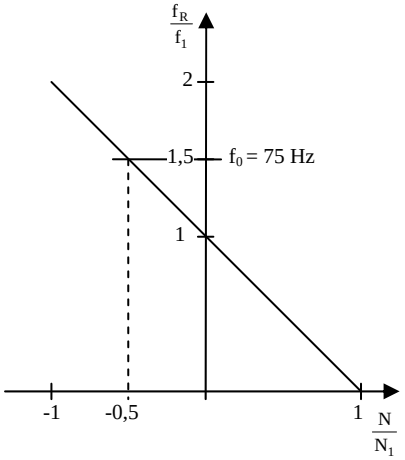

Fig. 8. Expanded excitation diagram

With the excitation diagram for an induction machine, it is very easy to predict parametric excitations of torsional vibrations during transients as speed up or reversal.

The alternating torques after switch-on are clearly recognizable, with values of roughly 6 times rated torque. Of special note is the fact, that the electrical torque frequently becomes negative, resulting for example in the much-feared “chattering teeth” effect on rigidly–coupled gears (geared motors) [9].

CONCLUSION

During transient phenomena the induction machine causes parametric excited torsional vibrations. The excitation mechanism is a sweep that runs through all frequencies from 100 Hz to 0 Hz. In low damped systems this might cause an overload of the torque in the mechanical system.

As the amplitudes of the torque become also negative, in geared drives the chattering of the teeth will reduce the lifetime of the gearbox.

REFERENCES

[1] Hantel, P. Theoretische und experimentelle Untersuchungen von transienten Vorgängen bei Asynchronmaschinen in schwach gedämpften Antriebssystemen. Dissertation 1986, RWTH Aachen.

[2] Spruogis B., Turla V. A Damper of Torsional Vibrations and Investigation on Its Efficiency. *Journal of Mechanical Engineering*, ISSN 0039–2480, Vol 52(4), 2006, Slovenia, p. 225–236.

[3] Bogdevičius M., Spruogis B., Turla V. A Dynamic Model of Rotor System with flexible Link in the presence of Shafts Missalignment. Journal of Mechanical Engineering, ISSN 0039-2480, Vol.50, 2004. Slovenia, p.598–612.

[4] Spruogis B., Turla V., Jakštas A. Universal coupling for the shafts of actuators in mechatronic systems. *Solid State Phenomena*, ISSN 1012–0394, Mechatronic systems and materials, ISBN: 3–908451–21–1, Vol 113, 2006, Trans Tech Publications Inc., p. 199–203.

[5] Beck, H.P.; Sourkounis, C.; Tulbure, A. Schwingungsdämpfung in Antriebssystemen mit Doppelkäfig-Asynchronmaschine, VDI-Berichte Band 1606 (2001) Seite 113-126, ISBN 3-18-091606-0.

[6] Böcker, Joachim; Amann, Notker; Schulz, Bernd Active suppression of torsional oscillations MECHATRONICS, IFAC Conference on Mechatronic Systems, 3 (2005) Seite 319-324, ISBN 0-08-044263-3.

[7] Gold, P., W.; Schelenz, R.; Bauermeister, R.; Mödder, R,. Design guideline for elastic torsion couplings, Kautschuk, Gummi, Kunststoffe Band 60 (2007) Heft 12, Seite 689-692, ISSN 0948-3276.

[8] Kovacs, P. Transient phenomena in electrical machines. Studies in electrical and electronic engineering 9, Elsevier, 1984.

[9] Park, S., S.; Qin, Y., M., Robust regenerative chatter stability in machine tools, International Journal of Advanced Manufacturing Technology Band 33 (2007) Heft 3-4, Seite 389-402, ISSN 0268-3768.

ВЫДЕЛЕНИЕ СПЕКТРАЛЬНЫХ ХАРАКТЕРИСТИК УЗКОПОЛОСНОГО ПРОЦЕССА ДЛЯ ДИАГНОСТИРОВАНИЯ ЗУБЧАТЫХ ПЕРЕДАЧ

В.А. Жулай, В.И. Енин

Аннотация: *Рассмотрены теоретические основы, используемого в задачах виброакустической диагностики технического состояния зубчатых передач, метода спектрального анализа виброакустического узкополосного сигнала, представляющего собой поток импульсов с высокочастотным заполнением имеющих одинаковую форму. Приведены аналитические зависимости для определения спектральных характеристик такого виброакустического сигнала зубчатой передачи. Представлен анализ полученных зависимостей. Обоснованы значения параметров режима работы зубчатой передачи при её виброакустическом диагностировании и показана необходимость поддержания их точного значения в процессе диагностирования.*

Ключевые слова: *зубчатые передачи, виброакустическая диагностика, спектральный анализ*

В задачах виброакустической диагностики машин и механизмов для анализа структуры виброакустического процесса широко используются спектрально-корреляционные методы обработки первичного информационного сигнала.

Ударные динамические нагрузки, возникающие при пересопряжении зубьев, возбуждают в динамической системе редуктора сложные затухающие колебания. При этом вынужденный переходный режим спустя некоторое время, равное длительности действия импульса возмущающей силы, прекращается, а система дальше совершает затухающие свободные колебания в диапазоне собственных частот.

Таким образом, виброакустический сигнал зубчатой передачи представляет собой поток импульсов с высокочастотным заполнением, вызванных последовательностью силовых импульсов следующих друг за другом с зубцовой частотой.

При одновременном воздействии возмущающих импульсов на систему со многими степенями свободы откликаются все собственные частоты этой системы. Однако наибольшая амплитуда отклика будет наблюдаться на одной из собственных частот элемента конструкции

$$x_u(t) = A_0 e^{-\alpha t} \sin \omega_0 t \,, \qquad (1)$$

где A_0 – амплитуда огибающей;

α – коэффициент затухания;

ω_0 – собственная частота механической системы.

В уравнении (1) выражение $A_0 e^{-\alpha t} = x_0(t)$ является огибающей колебательного процесса, редуктора, наиболее близко расположенного к месту приложения возмущающего воздействия.

По этому считают, что для виброакустического диагностирования дефектов зубчатых передач наиболее перспективным является анализ узкополосного процесса, полученного в результате полосовой фильтрации исходного сигнала в районе частоты наиболее значимых собственных колебаний конструкций редуктора [1].

Предлагаемый метод используется в тех случаях, когда наиболее информативными диагностическими признаками являются спектральные характеристики исходного виброакустического процесса.

Рассмотрим детерминированную задачу спектрального анализа отфильтрованного узкополосного виброакустического сигнала, вызванного соударениями зубьев одной пары шестерён, при отсутствии случайных шумовых и импульсных дополнительных воздействий (помех). Виброакустический сигнал в этом случае представляет собой поток импульсов с периодом следования T_u. В качестве модели импульса можно, в первом приближении, принять классический пример реакции гармонического осциллятора на дельта-импульс, описываемый следующим уравнением [1]

вызванного одиночным импульсом возмущающих сил.

Следовательно,

$$x_u(t) = x_0(t) \sin \omega_0 t. \qquad (2)$$

Для спектра огибающей одного импульса S_0 можно записать следующее выражение [2]

$$S_0(\omega) = \int_{-\infty}^{\infty} x_0(t) e^{-i\omega t} dt = \int_{-\infty}^{\infty} A_0 e^{-\alpha t} e^{-i\omega t} dt \,. \qquad (3)$$

Поскольку импульс начинается с нуля,

Владимир Алексеевич Жулай, доктор технических наук, профессор, Воронежский государственный архитектурно-строительный университет, Россия, zhulai@vgasu.vrn.ru
Владимир Иванович Енин, кандидат физико-математических наук, доцент, Воронежский государственный архитектурно-строительный университет, Россия

$$S_0(\omega)=\int_0^{\infty}A_0e^{-(\alpha+i\omega)t}dt=\frac{A_0}{\alpha+i\omega}. \qquad (4)$$

Спектр огибающей одиночного импульса является комплексной величиной. Здесь и далее будем рассматривать только модуль спектра, т. к. именно он характеризирует распределение интенсивности гармонических составляющих сигнала. Модуль огибающей одиночного импульса равен

$$|S_0|=\frac{A_0}{\sqrt{\alpha^2+\omega^2}}. \qquad (5)$$

Для спектра одиночного импульса можно получить

$$S_u(\omega)=\int_{-\infty}^{\infty}A_0e^{-\alpha t}\ \sin\omega_0 t\ \ e^{-i\omega t}dt=$$

$$=\int_0^{\infty}A_0\ \sin\omega_0 t\ \ e^{-(\alpha+i\omega t)}dt=$$

$$=\frac{A_0\omega_0}{\omega_0^2+(\alpha+i\omega)^2}=\frac{A_0\omega_0}{(\omega_0^2+\alpha^2-\omega^2)+2\alpha\omega i}. \qquad (6)$$

Спектр одиночного импульса также является комплексной величиной, модуль которой равен

$$|S_u(\omega)|=\frac{A_0\omega_0}{\sqrt{(\omega_0^2+\alpha^2-\omega^2)^2+4\alpha^2\omega^2}}. \qquad (7)$$

Неограниченный поток импульсов может быть представлен в виде

$$x(t)=\sum_{k=-\infty}^{\infty}x_u(t')\delta\left[t'-\left(t+kT_u\right)\right], \qquad (8)$$

где δ – дельта-функция;

k – целое число.

Записывая сигнал с учетом свойств дельта-функции, получим

$$x(t)=\sum_{k=-\infty}^{\infty}x_0\left(t+kT_u\right)\sin\left[\omega_0\left(t+kT_u\right)\right], \qquad (9)$$

Определим спектр потока как

$$S(\omega)=\int_{-\infty}^{\infty}x(t)e^{-i\omega t}dt. \qquad (10)$$

Подставляя значение $x(t)$ в уравнение (10), получим

$$S(\omega)=\sum_{k=-\infty}^{\infty}\int_{-\infty}^{\infty}x_0\left(t+kT_u\right)\sin\left[\omega_0\left(t+kT_u\right)\right]e^{-i\omega t}dt. \qquad (11)$$

Введём замену переменных $t+kT_u=t_0$ или $t=t_0-kT_u$. Тогда

$$S(\omega(=\sum_{k=-\infty}^{\infty}\int_{-\infty}^{\infty}x_0(t_0)\sin\left[\omega_0\left(t+kT_u\right)\right]\ e^{ik\omega T_H}dt_0e^{-i\omega t_0}=$$

$$=\sum_{k=-\infty}^{\infty}e^{ik\omega T_H}\int_{-\infty}^{\infty}x_u(t_0)e^{-i\omega t_0}dt_0. \qquad (12)$$

Заметим, что в уравнении (12) интеграл представляет собой спектр одиночного импульса

$$S(\omega)=\sum_{k=-\infty}^{\infty}e^{ik\omega T_u}S_u(\omega)=S_u(\omega)\sum_{k=-\infty}^{\infty}e^{ik\omega T_u}. \qquad (13)$$

В [3] показано, что

$$\sum_{k=-\infty}^{\infty}e^{ik\omega T_u}=\frac{2\pi}{T_u}\sum_{m=-\infty}^{\infty}\delta(\omega-m\Omega), \qquad (14)$$

где $\Omega=\frac{2\pi}{T_u}$.

Окончательно имеем

$$S(\omega)=S_u(\omega)\Omega\sum_{m=-\infty}^{\infty}\delta(\omega-m\Omega). \qquad (15)$$

Спектр потока является комплексным и имеет в качестве огибающей спектр одиночного импульса. Таким образом, спектр неограниченного потока импульсов (рис. 1) носит линейчатый характер с периодом $\Omega=\frac{2\pi}{T_u}$.

Как видно из представленного графика, на частоте модуляции спектральной линии может и не быть. Спектральная линия будет на частоте модуляции, только если $\omega_0=k\Omega$.

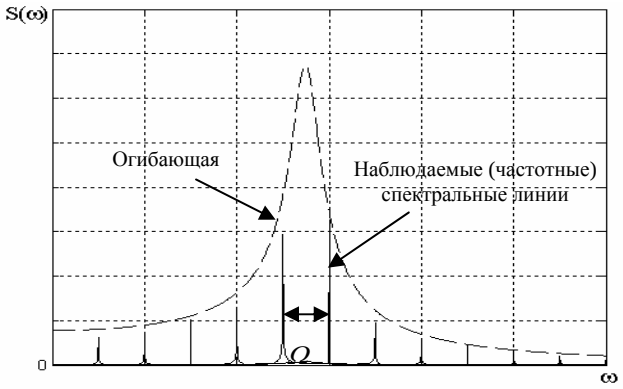

Рисунок 1 – Спектр импульсного потока

Рассмотрим в качестве примера поток слабоперекрывающихся импульсов с частотой заполнения f_0 = *550* Гц (собственной частотой механической системы редуктора ω_0 = *691* рад/с), следующих с периодом T_{u1} = *0,0091* с, что соответствует зубцовой частоте f_Ω = *110* Гц. Здесь и далее в разделе 6.2 образцы сигналов и их спектров получены методами математического моделирования в среде Matlab с помощью специально созданных программ.

В соответствии с формулой (15) спектральные линии будут на частотах (рис 2)

$f_{1[4]} = 440$ Гц (кратность $k = 4$), $f_{1[5]} = 550$ Гц (кратность $k = 5$), $f_{1[6]} = 660$ Гц (кратность $k = 6$). Центральная спектральная линия совпадает с собственной частотой системы $f_0 = 550$ Гц.

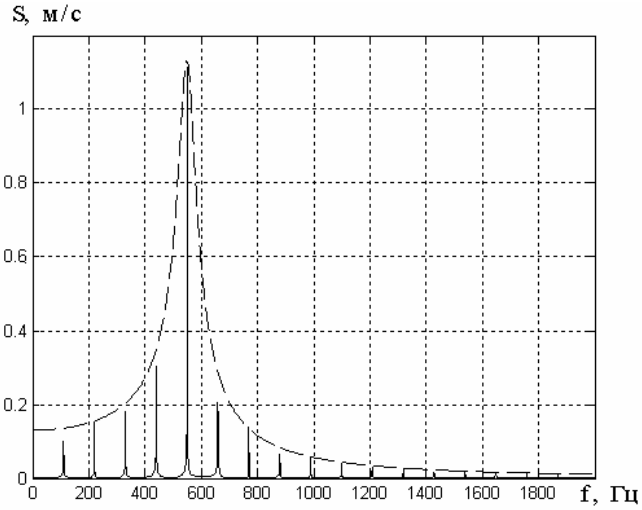

Рисунок 2 – Спектр импульсного потока с $f_\Omega = 110$ Гц

При изменении периода следования импульсов T_u спектральные линии смещаются по частоте с изменением амплитуды в соответствии с формой огибающей этих линий, представляющих собой спектр огибающей импульса. Так, для периода $T_{u2} = 0{,}0088$ с, что соответствует зубцовой частоте $f_\Omega = 114$ Гц (увеличение частоты вращения на 3,6 %), спектральные линии будут на частотах $f_{2[4]} = 456$ Гц, $f_{2[5]} = 570$ Гц, $f_{2[6]} = 684$ Гц со значительным уменьшением амплитуды центральной линии (рис 3).

Поскольку амплитуда спектральных линий зависит от частоты следования импульсов, то необходимо зубцовую частоту устанавливать кратной собственной частоте системы. Конечность времени анализа приведёт к увеличению ширины спектральных линий, т.к. в этом случае спектр конечного (ограниченного во времени) сигнала будет равен свёртке спектра неограниченного сигнала со спектром прямоугольного импульса с длительностью, равной времени анализа. Следовательно, при проведении диагностирования необходимо устанавливать значение зубцовой частоты, кратное частоте собственных колебаний, и увеличивать время анализа для повышения разрешающей способности по частоте, что справедливо и для неперекрывающихся импульсов.

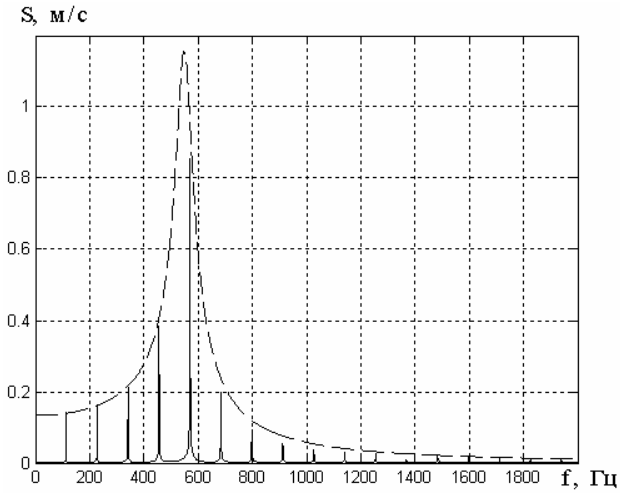

Рисунок 3 – Спектр импульсного потока с $f_\Omega = 114$ Гц

Заметим, что одновременно зубцовую частоту f_Ω желательно брать как можно большой, чтобы амплитуды остальных линий, отстоящих от центральной линии на $\pm f_\Omega$, были значительно меньше. Это особенно важно при анализе спектра импульсов, дополнительно промодулированных по амплитуде.

Определим для потока спектр огибающей импульсов. В этом случае необходимо рассмотреть два случая: поток неперекрывающихся импульсов и поток перекрывающихся импульсов. Эффективной длительностью импульса будем считать время его действия с амплитудой огибающей более 5 % от максимальной. Тогда в месте перекрытия импульсов по уровню 0,05 максимальная амплитуда не может быть более 0,1, что соответствует глубине модуляции $M_м = 1/0{,}1 = 10$.

В случае потока неперекрывающихся импульсов (рис. 4) считаем, что их составляющие не складываются, и тогда для огибающей можно записать

$$x_{on}(t) = \sum_{k=-\infty}^{\infty} x_0(t_0)\delta(t_0 - (t + kT_u)) = \sum_{K=-\infty}^{\infty} x_0(t + kT_u)\,. \quad (16)$$

Спектр огибающей будет

$$S_{on}(\omega) = \int_{-\infty}^{\infty} \sum_{k=-\infty}^{\infty} x_0(t + kT_u)e^{-i\omega\omega}dt\,. \quad (17)$$

Введя замену переменных $t_1 = t + kT_u$; $t = t_1 - kT_u$, получим

$$S_{on}(\omega) = \sum_{k=-\infty}^{\infty} \int x_0(t_1)e^{-i\omega\omega(t+kT_u)} = \quad (18)$$

$$= \int_{-\infty}^{\infty} x_0(t_1)e^{-i\omega t_1}dt \sum_{k=-\infty}^{\infty} e^{i\omega\omega T_u}\,.$$

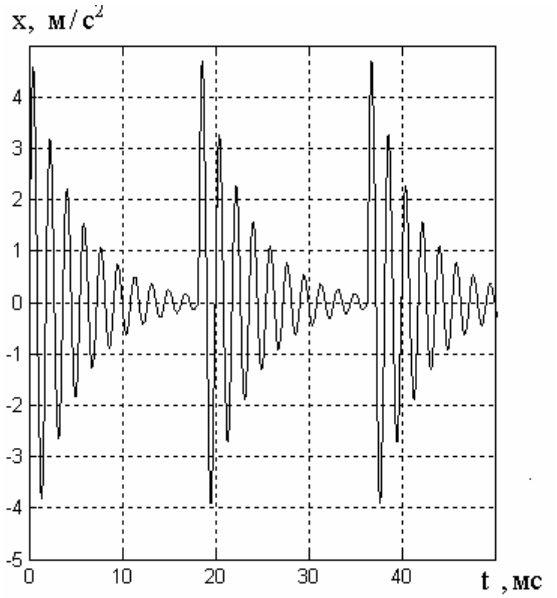

Рисунок 4 – Вид потока неперекрывающихся импульсов

Интеграл в квадратных скобках является Фурье-преобразованием огибающей одного импульса (в нашем примере $A_0 e^{-\alpha t}$).

Используя (6.19), получим

$$S_{on}(\omega) = S_0(\omega) \sum_{m=-\infty}^{\infty} \delta(\omega - m\Omega) \frac{2\pi}{T_u} = \tag{19}$$

$$\Omega S_0(\omega) \sum_{m=-\infty}^{\infty} \delta(\omega - m\Omega).$$

Таким образом, спектр огибающей неперекрывающихся импульсов представлен равноотстоящими на величину Ω спектральными составляющими – линиями с огибающей в виде спектра огибающей одиночного импульса.

На рисунке 5 приведен пример спектра огибающей потока неперекрывающихся импульсов с параметрами: $\alpha = 200$ с$^{-1}$; $f_0 = 550$ Гц ; $f_u = 25$ Гц.

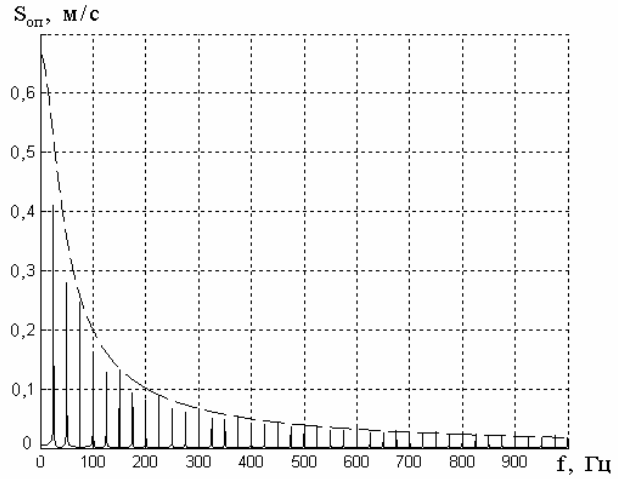

Рисунок 5 – Спектр огибающей потока неперекрывающихся импульсов

Вид спектра огибающей потока неперекрывающихся импульсов может служить основой для расчета коэффициента затухания α , а также необходимого соответствующего значения зубцовой частоты f_Ω .

Из представленного материала следует.

1 При виброакустической диагностике технического состояния зубчатых передач диагностическими признаками целесообразно выбирать характеристики огибающей. В частотной области диагностическими признаками могут служить различные параметры спектральных характеристик огибающей отфильтрованного узкополосного процесса.

2 При использовании в виброакустической диагностике спектрального анализа исходного сигнала необходимо выбирать значение зубцовой частоты, кратным собственной частоте механической системы, и поддерживать это значение с максимальной точностью.

3 При анализе огибающей отфильтрованного процесса период следования импульсов T_u должен быть минимально возможным, но не менее длительности этих импульсов.

ЛИТЕРАТУРА

[1] Коллакот, Р. А. Диагностирование механического оборудования / Р.А. Коллакот; пер. с англ. – Л. : Судостроение, 1980. – 295 с.

[2] Сергиенко, А. Б. Цифровая обработка сигналов / А.Б. Сергиенко. – СПб. : Питер, 2003. – 608 с.

[3] Сороко, Л. М. Основы голографии и когерентной оптики / Л.М. Сороко. – М. : Наука, 1971. – 616 с.

DYNAMIC STUDY OF SELF-ERECTING CRANES BAR MECHANISM

A. Bruja, M. Dima, C. Frâncu

Abstract: *In this paper is presented a dynamic study of the erection mechanism Following this study were obtained reactions in joints of the mechanism needed to size the bars and the power needed to power-up this mechanism. The results were obtained by using computer programs written especially for this type of problems*

Keywords: *Self erecting cranes, bar mechanisms, dynamic study*

The kinematic chain of the folding-unfolding mechanism of 7.5 tm Girueta tower crane is presented in unfolded state in figure 1 and in folded state in figure 2.
Unfolding mechanism is done by using a tackle placed between D and E joints and is done in 2 stages, figure 3. In the first stage (the backstay fixed between A and H is loosened), by shorting the length of the tackle, the lower tower BCE rotates counterclockwise around the B joint and the rocker bar 1, through 3 and 4 bars, are pushing up the superior tower EFG along with the HGK boom and are rotating clockwise around the E joint. In stage 2, when the AH distance becomes equal with the backstay length, the HGK boom is rotating around G joint until GK becomes horizontal.

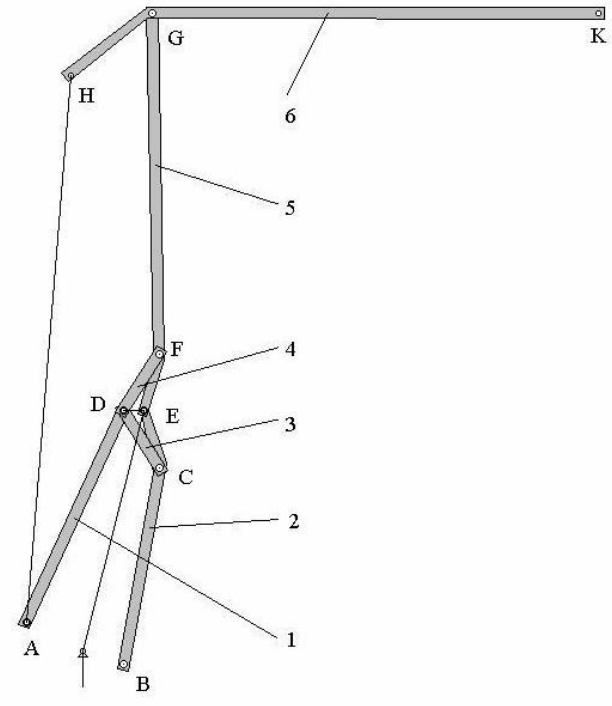

Fig. 1 Girueta tower crane in unfolded position

Prof. Adrian BRUJA, Universitatea tehnică de construcţi Bucureşti, bruja@utcb.ro
Ph.D. Marian DIMA, Universitatea tehnică de construcţi Bucureşti, dima@utcb.ro
Lic. Eng. Cătălin FRÂNCU, Universitatea tehnică de construcţi Bucureşti, francu@utcb.ro

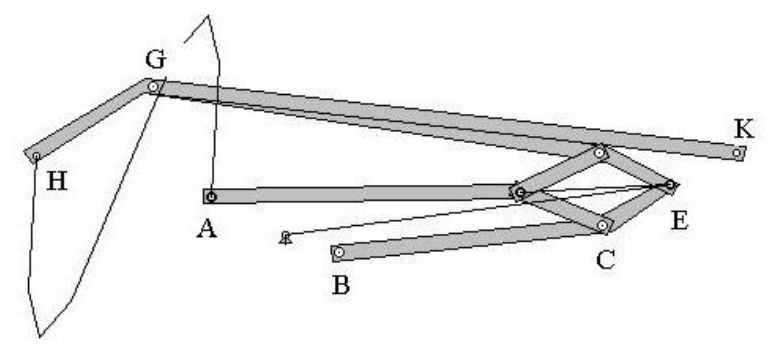

Fig. 2 Girueta tower crane in folded position

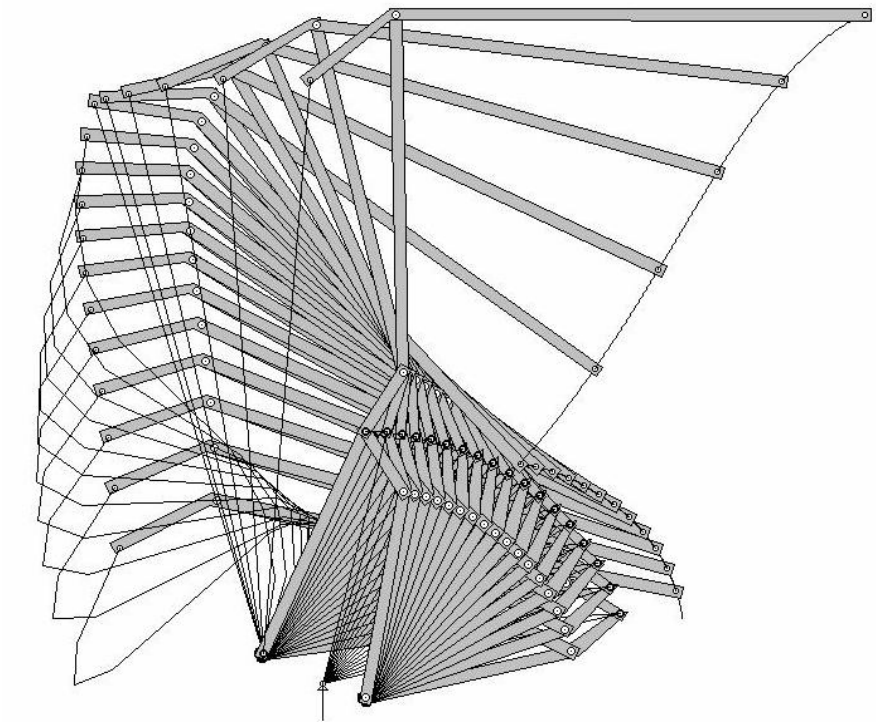

Fig. 3 Girueta tower crane workspace while self-erecting

Joints reactions study is done for every dyad at once. Two different computing stages are taken into account due to the stages that are met in mechanism working.

The study starts with GHK dyad, figure 4. Having in mind that the backstay works only when stretches, its action can be replaced by a force $\overline{F}_H$ that has all the time the AH direction. The problem is reduced to the equilibrium study of an articulated bar in G. The moment equation related to the G joint:

$$\left(\sum \overline{M}_G\right)_6 = 0\,, \qquad (1)$$

Knowing the force $\overline{F}_H$ the components of the $\overline{R}_G$ reaction can be determined by summing the forces on bar 6,

$$\left(\sum \overline{F}_{kx}\right)_6 = 0\,; \qquad \left(\sum \overline{F}_{ky}\right)_6 = 0 \qquad (2)$$

For DFE dyad, the diagram is presented in figure 5. The unknown forces $\overline{R}_E$ and $\overline{R}_D$ are determined as follows. The reactions are split in two components, $\overline{R}^t$ (perpendicular with the bar) and $\overline{R}^n$ (parallel with the bar). The components $\overline{R}^t_{E1}$ and $\overline{R}^t_D$ are determined with the equation moments on bar 5 and 4 respectively related to the F joint,

$$\left(\sum \overline{M}_{kF}\right)_5 = 0\,; \ \left(\sum \overline{M}_{kF}\right)_4 = 0 \qquad (3)$$

and normal components $\overline{R}^n_{E1}$ and $\overline{R}^n_D$ are determined from the equilibrium of forces which acts among all the dyads. The forces are added by components over the 2 axes,

$$\left(\sum \overline{F}_{kx}\right)_{4,5} = 0\,; \ \left(\sum \overline{F}_{ky}\right)_{4,5} = 0 \qquad (4)$$

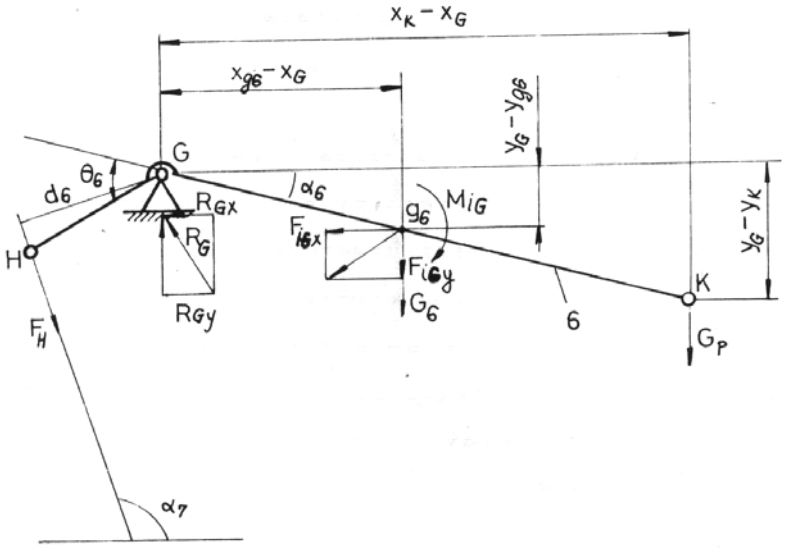

Fig. 4 GHK dyad diagram

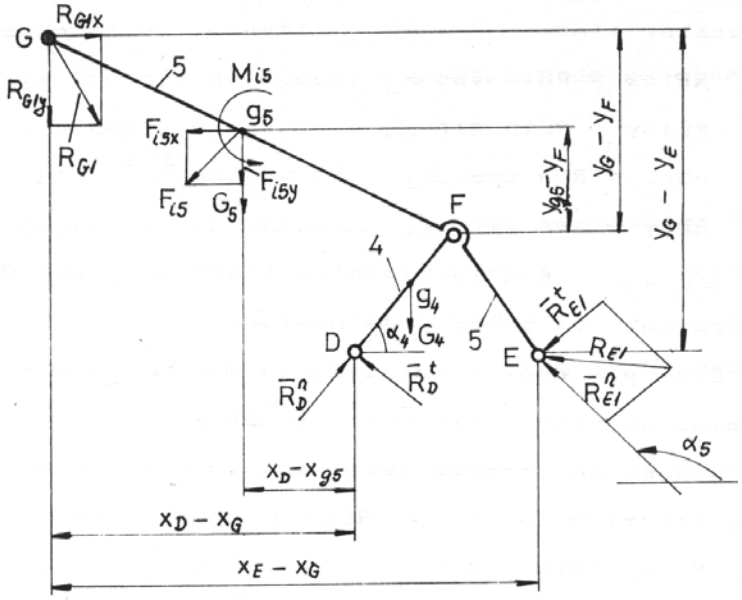

Fig. 5 DFE dyad diagram

In figure 6 is presented the BCE dyad, diagram. There are 7 unknown forces: $\overline{R}_n$, $\overline{R}_t$, $\overline{R}_{Cx}$, $\overline{R}_{Cy}$, $\overline{R}_B^n$, $\overline{R}_B^t$, $\overline{F}_p$. In order to determine these unknown forces, the following 7 equations can be written:

a) Moments equation on bar 3 related to joint C

$$\left(\sum \overline{M}_{kC}\right)_3 = 0; \qquad (5)$$

b) Moments equation on bar 2 related to joint C

$$\left(\sum \overline{M}_{kC}\right)_2 = 0; \qquad (6)$$

c) Projection equilibrium equation of forces on x axis for the whole dyad

$$\left(\sum \overline{F}_{kx}\right)_{2,3} = 0; \qquad (7)$$

d) Projection equilibrium equation of forces on y axis for the whole dyad

$$\left(\sum \overline{F}_{ky}\right)_{2,3} = 0. \qquad (8)$$

e) Projection equilibrium equation of forces on x axis for bar 3

$$\left(\sum \overline{F}_{kx}\right)_3 = 0; \qquad (9)$$

f) Projection equilibrium equation of forces on y axis for bar 3

$$\left(\sum \overline{F}_{ky}\right)_3 = 0; \qquad (10)$$

g) Moments equation on bar 2 related to joint B

$$\left(\sum \overline{M}_{k\,B}\right)_2 = 0\,; \qquad (11)$$

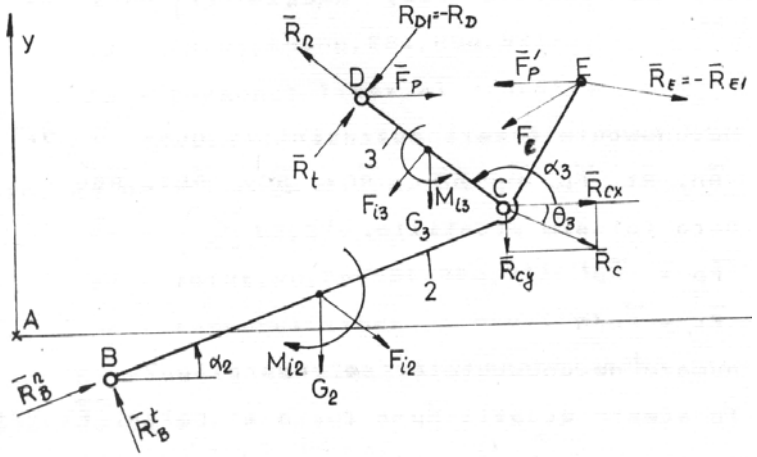

Fig. 6

The equations (5)...(11) are making a inhomogeneous, linear, system of 7 equations with 7 unknown variables. The system can be solved using the Kramer method.

Based on this method a computer program was written and with it, were determined the reactions in the joints for the entire kinematic cycle of the erection mechanism of the tower crane. From among the results, in figure 7 is presented as an example the variation in time of the force in the tackle for the unfolding of the mechanism, where the units are Newton for forces and seconds for time.

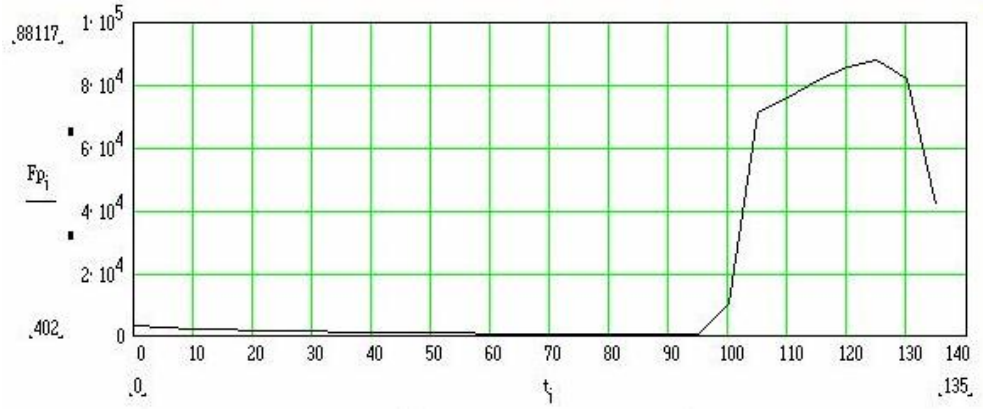

Fig. 7

From this graph it is noticeable that in the second stage of the unfolding when the backstay is fully stretched and the boom is rotating relative to the superior tower, the force needed in the tackle for continuing the unfolding it is very high than the force in the first stage of the unfolding. The reactions in the joints and the loads in the bars of the mechanism are very high due to this situation.

Having these in mind the authors of the present paper have proposed some solutions for lowering the force in the tackle and implicitly lowering the loads to which the elements of the mechanism are put.

REFERENCES

[1] **Bruja A., Dima M.** – *Optimizarea parametrilor cineto-statici ai mecanismului de pliere-depliere a macaralei turn de 7,5 tm*. Contract 59/1991, Beneficiar ICPAIUC Bucureşti.

[2] **Raicu A.** – *Mecanisme*. Editura ICB, 1980.

ORIENTATION MECHANISM OF THE 3D SCANNING OF BUILDING FACADES (OBJECT RETRIEVING) ROBOT

A. Bruja, M. Dima, C. Frâncu

Abstract: *In this paper is presented the orientation mechanism of the 3D scanning robot, which is composed of a vertical locus orientation mechanism having 2 DOFs, a linear moving mechanism having 1 DOF and a pan-tilt mechanism with 2 DOF's. These mechanisms ensures that both3D scanning of the surfaces is done strictly by vertical and horizontal and results scaling meaning that the acquired data is reported to a fixed referenced system*

Keywords: *3D scanning, decorative element, three-dimensional retrieval*

1. INTRODUCTION

The robot mechanism is a part of an equipment for 3D retrieving of the decorative elements of buildings facades and historical monuments.

The equipment, figure 1, is composed of a carrying module, pos 1 and robot mechanism for 3D retrieving, pos. 2.

The robot mechanism, figure 2, is composed of a laser robotic scanning module, pos.1, a robotic translation mechanism, pos. 2, and a mechanism for determining the horizontal locus, pos.3.In order to obtain a resolution good enough to scan the decorative elements of buildings facades it is necessary that the scanning module to be at a distance of 2...3 m from the elements to be scanned. Taking into account the relative small distance to the façade, the surface to be scanned (window), figure 1, will have comparable dimensions. The scanning module will have to be moved along the wall vertically and horizontally. This function is completed by the carrying module, which allows the movement of the trolley 4, figure 2, on which is fixed the robot mechanism, along the wall vertically and horizontally.

Only the robot mechanism is presented in this paper.

2. ROBOT MECHANISM

As shown above the robot mechanism, figure 2, is composed of a laser robotic scanning module, pos.1, a robotic translation mechanism, pos. 2 and a mechanism for determining the horizontal locus, pos.3.

2.1 Scanning module

The scanning module is composed of a mechanism wit 2 DOF's (RR) and laser for distance measuring. The module has for every axis a step-by-step motor harmonic reducer and allows rotation of ±159º horizontally +31º/-47º vertically with a precision of 0,0129º on every axis of rotation. The laser unit can measure in calibration mode distances up to 16m with a precision of 2.5 mm.
The 3D scanning building façades decorative elements is done by moving a laser beam on the scanning surface (window), simultaneously with distance measuring from the laser to the surface to be scanned. Productivity and constructive reasons of the scanning process, the motion of the beam on the surface to be scanned is done by placing the scanning device to a fixed distance off the wall and rotating the beam in two planes perpendicular on the surface (vertical and horizontal plane).
The two rotations in perpendicular planes are done by the RR mechanism.

In this way a number of pints in spherical coordinates reported to a reference frame fixed to the laser device is obtained. The coordinates of every point are:

- Radius *r* – measured by the laser;
- Longitude θ- measured by the RR mechanism in respect to vertical axis;
- Latitude α - measured by the RR mechanism in respect to horizontal axis;

After scanning the whole surface those spherical coordinates of the point on the surface are transformed in Cartesian coordinates in respect to a coordinate frame fixed to the building façade, using some markers fixed prior on the building before the scanning operation. For highlighting of hidden decorative elements (placed in the shadow of some other elements relative to the laser beam) every surface has to be scanned from several directions, the 3D model is an overlapping of all scans of the same surface.

In order to be scanned, eventually then small surfaces will be put together to obtain the model of the whole facade.

Prof. Adrian BRUJA, Universitatea tehnică de construcţi Bucureşti, bruja@utcb.ro
Ph.D. Marian DIMA, Universitatea tehnică de construcţi Bucureşti, dima@utcb.ro
Lic. Eng. Cătălin FRÂNCU, Universitatea tehnică de construcţi Bucureşti, francu@utcb.ro

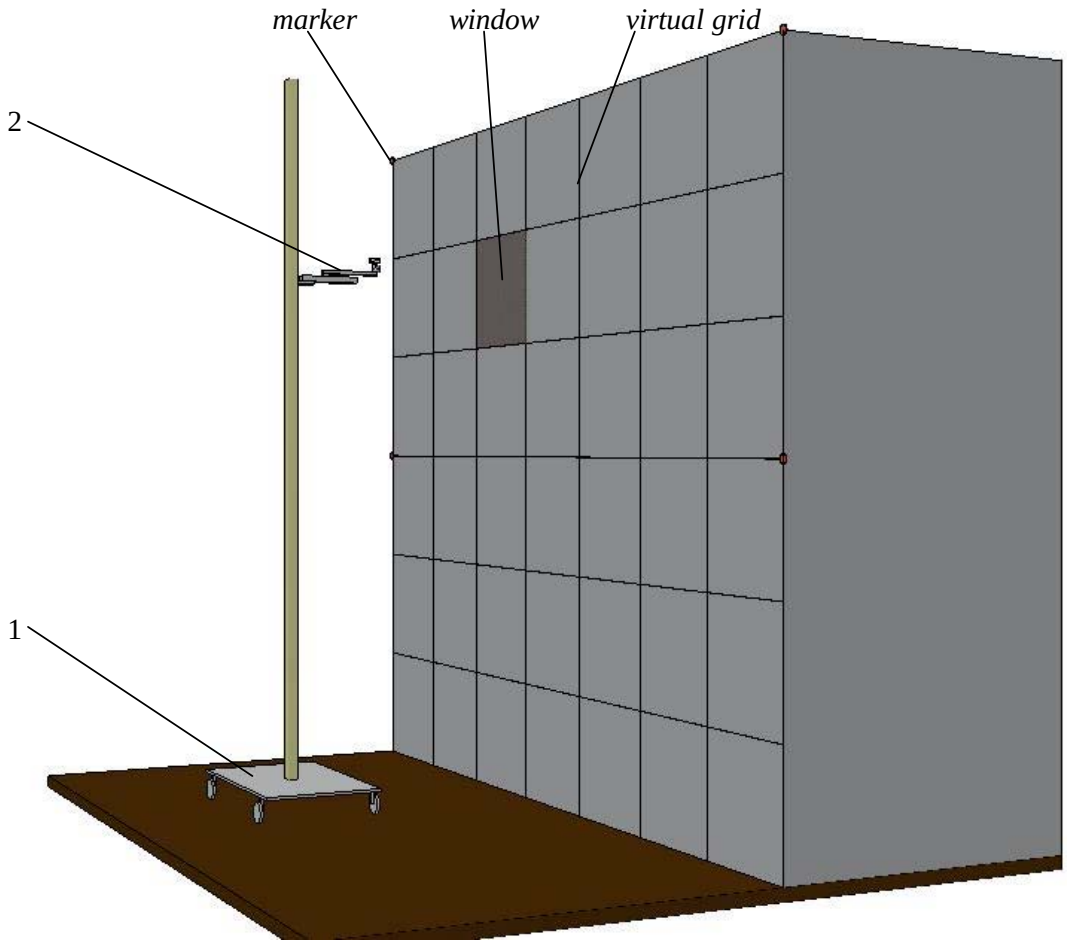

Fig. 1. Equipment for 3D retrieval

2.2 Translation mechanism

It is composed of translation module with toothed belt 2, on the table of which is fixed the bracket where the scanning module is fixed.

The role of the translation mechanism is to determine a reference direction in respect to which the windows scanning is done, direction that allows the reporting of coordinates of measured points from the laser coordinate frame to the reference frame fixed to the building. The bracket is used in order to place the laser in front of all elements of the equipment to increase the visibility of the scanning module.

2.3 Vertical locus mechanism

This mechanism serves the purpose to orient the scanning module before staring the scanning, after the vertical locus so that the scanning is done strictly on horizontal and vertical directions. This kind of orientation of scanning allows dividing a big surface into smaller ones in order to scan them from one by placing of the robot mechanism.

Vertical locus mechanism is in fact a spatial mechanism with 2 DOF's, being rotations in respect with two axes in horizontal plane.

The mechanism is composed of inferior bracket 5, which orients after the trolley 4, superior frame 6, which orients after the vertical locus and driving mechanisms in respect to the two axes. The superior frame is fixed to the bracket by using a spherical joint 7.

Driving mechanisms in respect to the two axes are identical and each one is composed of: gear motor, clutch, ball screw, ball nut and forks for fixing it to the bracket and frame. All the joints are done with the possibility of removing the backlashes.

The vertical locus is determined by using a biaxial inclinometer with 0,03º precision and which is mounted on the superior frame and linked in the command circuit of the motors.

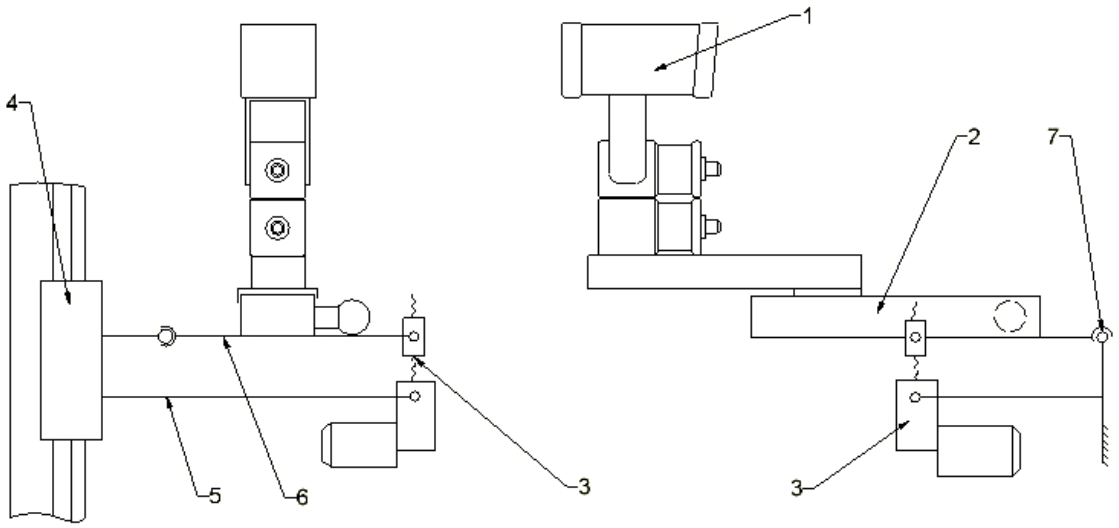

Fig. 2 Robot mechanism

3. WORKING ALGORITHM

a) On the building markers with known position and at known distances are placed for the markers are visible to the laser.

b) A virtual grid which defines the scanning windows is considered attached to the building facade.

c) The carrying module is moved along the wall in front of the window to be scanned.

d) Robot mechanism is moved vertically along the column of the carrying module until it reaches approximately the middle of the window to be scanned.

e) The vertical locus of the robot mechanism is determined.

f) From the retreat position of the translation mechanism the distances to the markers placed on the building are read.

g) With the translation mechanism extended, the measurements of the same markers using the scanning module are repeated. These two readings allow determining the exact origin and orientation of the reference system fixed to the laser in respect to the reference frame of the building.

h) The window is scanned and the point cloud is stored.

i) If in the scanned window the decorative elements are complicated and aren't visible from only one point of view the tasks from c) to h) are repeated from several angles (up, down, left, right).

j) The coordinates of the point cloud are transformed from the laser reference frame in the building reference frame.

k) If the scanning of the same window was done from several angles, the point clouds are overlapped obtaining the final cloud.

l) The final point cloud is transformed in a 3D model of the scanned window.

m) After scanning the whole facade, all the scanned windows are assembled making thus the 3D model.

REFERENCES

[1] Adrian BRUJA, Marian DIMA (2006) Algoritmul de lucru al robotului pentru relevarea tridimensională a elementelor decorative ale fațadelor clădirilor şi monumentelor istorice, *Al XII-lea Simpozion Național de Utilaje pentru Construcții, SINUC 2006*, Bucureşti 14-15 dec. 2006. ISSN 1842 − 6352.

[2] Adrian BRUJA, Marian DIMA (2006) Componența şi funcționarea robotului pentru relevarea tridimensională a elementelor decorative ale fațadelor clădirilor şi monumentelor istorice, *Simpozionul INFOSOC „Cercetări privind Societatea Informațională – rezultate şi perspective”*, Sibiu, 7 – 9 dec..

FREQUENCY RESPONS OF AUTOMOTIVE WHELL RIM UNDER IMPULS DYNAMIC LOAD

I. Savić, M. Jovanović

Abstract: *This paper shows overview for dynamic analysis of steel automotive wheel rim using the Finite Element Analysis. The two analysis were conducted in this paper: modal analysis and transient dynamic analysis under influences of radial impact load. Purpose of this paper is determining of dynamic properties and frequency respond (acceleration and amplitudes) under impulse road driving forces.*

Key words: *wheel rim, modal analysis, linear transient dynamic analysis.*

1. INTRODUCTION

The suspensions for modern vehicles are assembly with very important role in behaviour of vehicles in driving on paved roads and off-roads. Wheels are parts of this assembly and understanding behaviour of wheel rim under static and dynamic impact load is very important for aspect safety, reliability and durability of vehicles.

The Dynamic analysis provides mass reduction of rims, improves driving conformity of vehicles but bring possible risk for local damages and global deformation with effects for impact load.

The Quality constructions assume FEM (*Finit Element Analysis*) analysis engagement for discovery local sensibility of constructions on outer dynamic influences.

This paper shows numerical analysis of vehicle wheel rim under impact dynamic loads influence caused by irregularities and roughnesses of road surfaces. Therefore two dynamic analysis ware made for impact dynamic influence caused by one mode shape of road surface roughness.

In the analysises in this paper was used common material. – cold rolled steel sheet likes RSt37-2 (EU 20), S235 JR [x]. Thickness of this material is 3,0 to 6,5 mm for light duty vehicles and 8 to 10 mm for heavy on-road vehicles. The steel wheel rim for light duty vehicles was observed. Official mark of wheel rim according to ETRTO standard is 51/2JK16H**.**

2. DYNAMIC ANALYSIS

The basic concept of the Finite Element Method in engineering analysis of discrete systems allowes solving Steady-state problems, Propagation problems, and Eigen value problems. Analysis software for program formulation of Continuous Systems can be generated from Differential and Variation formulation, and Weighted residual methods and Ritz method [7].
Formulation of the displacement-based Finite Element Method in Linear Analysis of Solid and Structural Mechanics requires general derivation of finite element equilibrium equations, Imposition of boundary conditions, generalized coordinate models, lumping of structure properties, checking of results convergence and calculation of stresses.
Numerical integration in dynamical analysis can be realized using an Interpolation polynomial, the Newton-Cotes formulas (one-dimensional integration) the Gauss and other methods [7].
Solution of equilibrium equations in Static analysis, is obtained by using Direct Solutions Algorithms Based on Gauss Elimination, Direct solutions using Orthogonal Matrices, the Givens factorization, the Householder factorization or the Gauss-Seidel iterative solution and Solution of Nonlinear Equations can be derivated by using Newton-Raphson schemes, the BFGS method (quasi-Newton method).
Solution of Equilibrium Equations in Dynamic Analysis can be found by Direct **Integration Methods** (the central difference method, the *Houbolt* method, the *Wilson* θ method, the *Newmark* method) and **Mode Superposition.** Solution of Large Eigenproblems is conducted by using the **Subspace iteration method** [7]**.**

2.1 Direct integration methods

In direct integration the equations in (2.1) integrated a numerical step by-step procedure is used. The term "direct" means that prior to the numerical integration, no transformation of the equations into a different form is carried out.

In essence, direct numerical integration is based on two ideas: First, instead of trying to satisfy (2.1) at any time ***t***, it is aimed to satisfy (2.1) only at discrete time intervals Δt apart. This means that, basically, (static) equilibrium, which includes the effect of inertia and damping forces, is sought at discrete time points within the interval of solution. The second idea, on which a direct integration method is based, is that a variation of displacements, velocities, and accelerations within each time interval Δt is assumed. It is the form of the assumption on the variation of displacements, velocities, and accelerations

Ivan Savić, dipl.inž. TRAYAL Corporation – Kruševac, savicivan@yahoo.co.uk
Prof. dr Miomir Jovanović, Mašinski fakultet u Nišu, miomir@masfak.ni.ac.yu

within each time interval that determines the accuracy, stability, and cost of the solution procedure.
In the following, assuming that the displacement, velocity, and acceleration vectors at time 0, denoted by U, $\mathring{\mathbf{U}}$, and $\ddot{\mathbf{U}}$, respectively, are known, and let the solution to (2.1) be required from time 0 to time T.

The equations of equilibrium governing the linear dynamic response of a system of finite elements:

$$\mathbf{M}\cdot\ddot{\mathbf{U}} + \mathbf{C}\cdot\mathring{\mathbf{U}} + \mathbf{K}\cdot\mathbf{U} = \mathbf{R} \qquad (2.1)$$

Where M, C, and K are the mass, damping, and stiffness matrices; R is the external load vector and U, $\mathring{\mathbf{U}}$, and $\ddot{\mathbf{U}}$ are the displacement, velocity, and acceleration vectors of the finite element assemblage.

Mathematically, (2.1) represents a system of linear differential equations of second order and, in principle, the solution to the equations can be obtained by standard procedures for the solution of differential equations with constant coefficient. In practical finite element analysis, we are therefore mainly interested in a few effective methods of solution: direct integration and mode superposition.

The Central Difference Method
If the equilibrium relation in (2.1) is regarded as a system of ordinary differential equations with constant coefficients, it follows that any convenient finite difference expressions to approximate the accelerations and velocities in terms of displacements can be used. Therefore, theoretically a large number of different finite difference expressions could be employed. However, the solution scheme should be effective, and it follows that only a few schemes need to be considered. One procedure that can be very effective in the solution of some problems is the central difference method, in which it is assumed that:

$${}^{t}\ddot{U} = \frac{1}{\Delta t^2}\left[{}^{t-\Delta t}U - 2\cdot{}^{t}U + {}^{t+\Delta t}U\right] \qquad (2.2)$$

$${}^{t}\dot{U} = \frac{1}{2\cdot\Delta t}\left[-{}^{t-\Delta t}U + {}^{t+\Delta t}U\right] \qquad (2.3)$$

The displacement solution for time:

$$M\cdot{}^{t}\ddot{U} + C\cdot{}^{t}\dot{U} + K\cdot{}^{t}U = {}^{t}R \qquad (2.4)$$

Substituting the relations for $\mathring{\mathbf{U}}$, and $\ddot{\mathbf{U}}$ into (2.5), we obtain:

$$\left[\frac{M}{\Delta t^2} + \frac{C}{2\cdot\Delta t}\right]\cdot{}^{t+\Delta t}U = {}^{t}R - \left[K - \frac{2\cdot M}{\Delta t^2}\right]\cdot{}^{t}U - \left[\frac{M}{\Delta t^2} - \frac{C}{2\cdot\Delta t}\right]\cdot{}^{t-\Delta t}U \qquad (2.5)$$

The displacement solution for time t+Δt is obtained by relation (2.1) at time ***t***, from which we can solve for ${}^{t+\Delta t}$U. It should be noted that the solution of ${}^{t+\Delta t}$U is thus based on using the equilibrium conditions at time ***t***; The ${}^{t+\Delta t}$U is calculated by using (2.5). For this reason the integration procedure is called an **explicit** integration method, and it is noted that such integration schemes do not require a factorization of the (effective) stiffness matrix in the step-by-step solution.

On the other hand, the *Houbolt*, *Wilson*, and *Newmark* methods use the equilibrium conditions at time ***t+Δt*** and are called **implicit** integration methods.

The advantage of using the central difference method now becomes apparent. Since no stiffness and mass matrices the complete element assemblage need to be calculated, the solution can essentially be carried out, with relatively little high-speed of storage. The method becomes even more effective if element stiffness and mass matrices of subsequent elements are the same, because in that case it is **only** necessary to calculate or read from back-up storage the matrices corresponding to the first element in the series. Using the central difference scheme, systems of very large order have been solved effectively.

A second very important consideration in the use of the central difference scheme is that the integration method requires that the time step Δ***t*** is smaller than a critical value, $\Delta\mathbf{t}_{\mathbf{CR}}$ which can be calculated from the mass and stiffness properties of the complete element assemblage. T is the smallest period of the finite element assemblage with n degrees of freedom.

$$\Delta t \le \Delta t_{CR} = \frac{Tn}{\pi} \qquad (2.6)$$

(Recommended Δ***t***=Tn/10 in [1])

The Wilson θ Method is essentially an extension of the linear acceleration method, in which a linear variation of acceleration from time ***t*** to time ***t*** +Δ***t*** is assumed. The Wilson θ method the acceleration is assumed to be linear from time ***t*** to time ***t*** + ***θ·Δt***, where θ≥l.0. When θ= 1.0, the method reduces to the linear acceleration scheme, and usually we employ *θ = 1.40*. The ***Newmark*** integration scheme can also be understood to be an extension of the linear acceleration method.

2.2 Modelling problem

Modelling mechanical response for radial tyre mounting on wheel rim is very complex task. In regular exploitation of vehicles where are achieved, permanent all function for wheel and tyre, character of model was defined with non-linear character of tyre and linear character of wheel rim. The complexity of that model and important of strong dynamical presence have influence that representing analysis treat only wheel rim fixed on wheel hub.
While vehicle is moving, basic load of wheel is radial. Dynamic force for analysis was determined according to vehicle speed 33 m/sec^2 and recess on roud surface 0.33 m length with aproximation for state of static pressure on wheel and dynamic koeficient. The force obtain impuls character and aproximation of it is shown on graph, fig. 1.

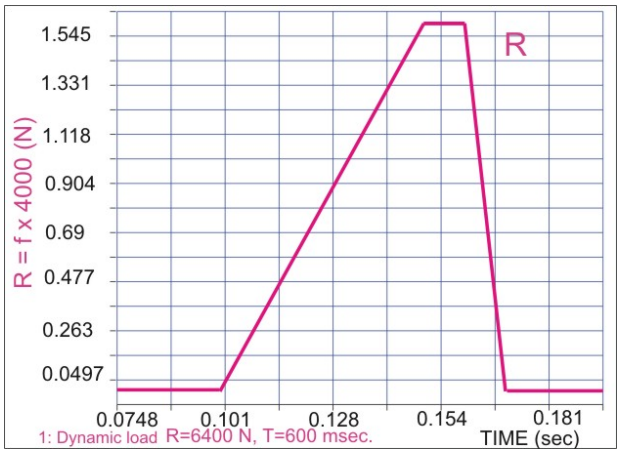

Sl. 1 Dijagram impulsne sile

On the model of rim in this case act impulse radial force $F_{MAX} = 6400\ N$. The model was fixed through surfaces on it and it is the place for the rest of screw nut for fixing wheel on vehicle. Original discrete model of wheel with 44777 nodes and 22356 tetrahedron finite elements (fig.2) was developed for this analysis. Linear character of material was used in dynamic analysis. In order to determine the risk for overload and beginning for plastic deformation of model, higher static load ($R_{MAX}=8000\ N$) and poor less material for rims was used. For these conditions, results for non-linear analysis of model fig.2, for stress and deformations of wheel rim are shown on the end of this paper.

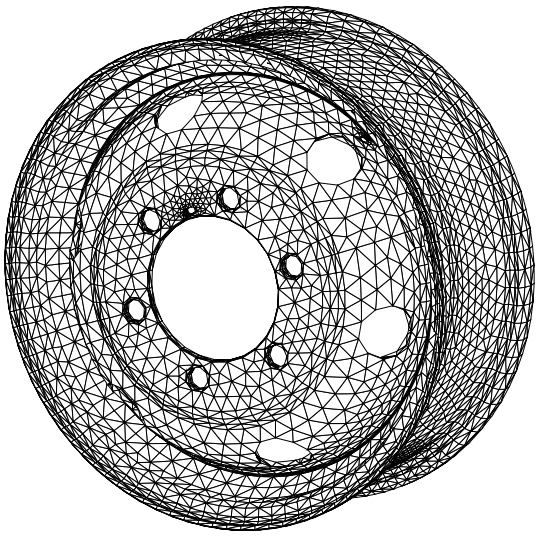

Sl. 2 Diskretni model čeličnog točka

The Dynamic load was put in small local zone on outer side where the bead of a tyre, theoretically rests on the rim. Being modelled in this way it has fairly high stiffness and gained results are corresponding with appropriate dynamic stiffness for rigidly suspension of wheel. The more realistic model would be obtained with the full vehicle model. These models, because of the number of degree of freedom, do not allow numerical researching of the construction details.

2.3 Modal analysis of wheel rim

First step in dynamic analysis is modal analysis, whereby shapes and frequency of the free oscillations for model (according to tab.1), and that, they were used for parameters improvements were found of direct transient analysis (proportional damping according to speed of oscillations).

Damping frequency of system is the lowest frequency ($\varpi_3 = 272{,}3Hz$). Analysis was conducted with 3000 steps in time interval of integration:

$$\Delta t = 0{,}0002\ \sec \le T_{CR} = \frac{1}{272.3 \cdot \pi} = 0{,}001169 \sec .$$

Entire time of integration (impact analysis) is 0.6 sec. In analysis nodes on the place where concentrated dynamic force is acting was observed. Fig. 3, 4, 5 are showing the values of acceleration for this points in three Cartesian axes x, y, z (tagged with T1, T2, T3).

Mode number:	Frequency [*Hz*]
1	272,359
2	273,1841
3	358,8863
4	363,6432
5	667,6583
6	668,2036
7	730,0074
8	1173,667
9	1178,204
10	1470,636

Tab. 1 Table of modal frequency

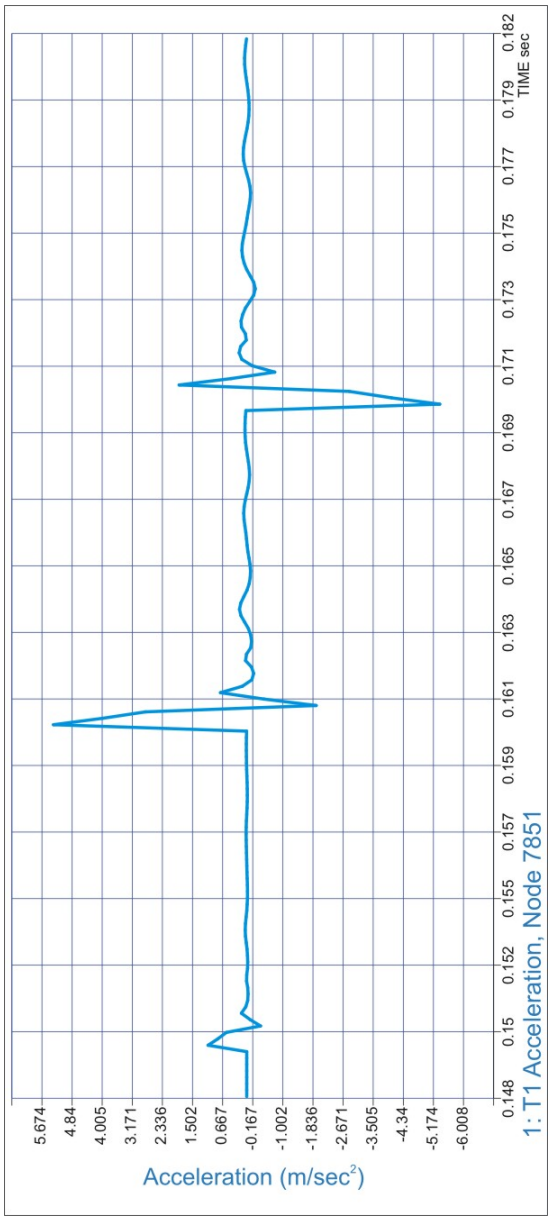

Fig.3 Oscillation component of acceleration for observed node No. 7851 for direction T1

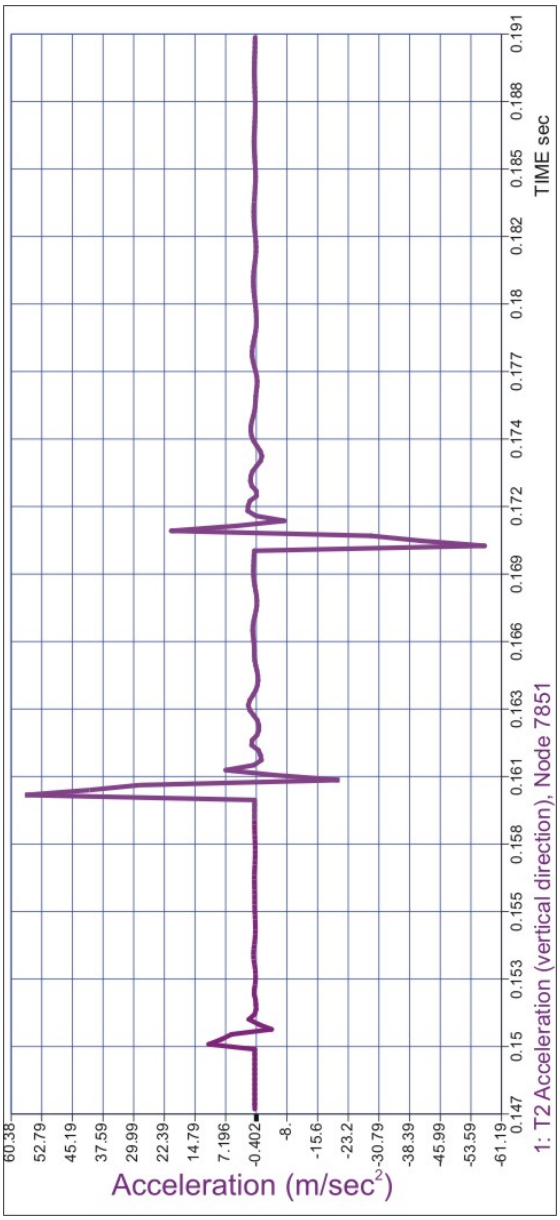

Fig.4 Oscillation component of acceleration for observed node No. 7851 for direction T2

Annotations: Very fast settling, high frequencies are in acoustic domain, less values longitudinal acceleration from vertical acceleration. The amplitude frequency is growing in points of changing outer impulse load. Comparative graphs show equality for disturbance time. Maximum acceleration is about 57 m/sec^2.

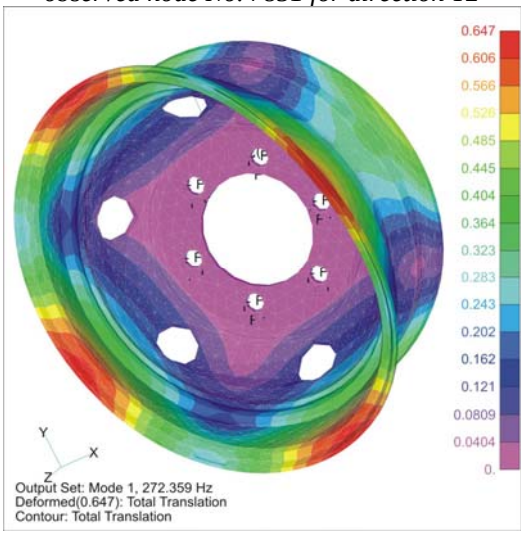

Fig. 6 First form of oscillation (mod) ω_1=272,359 Hz

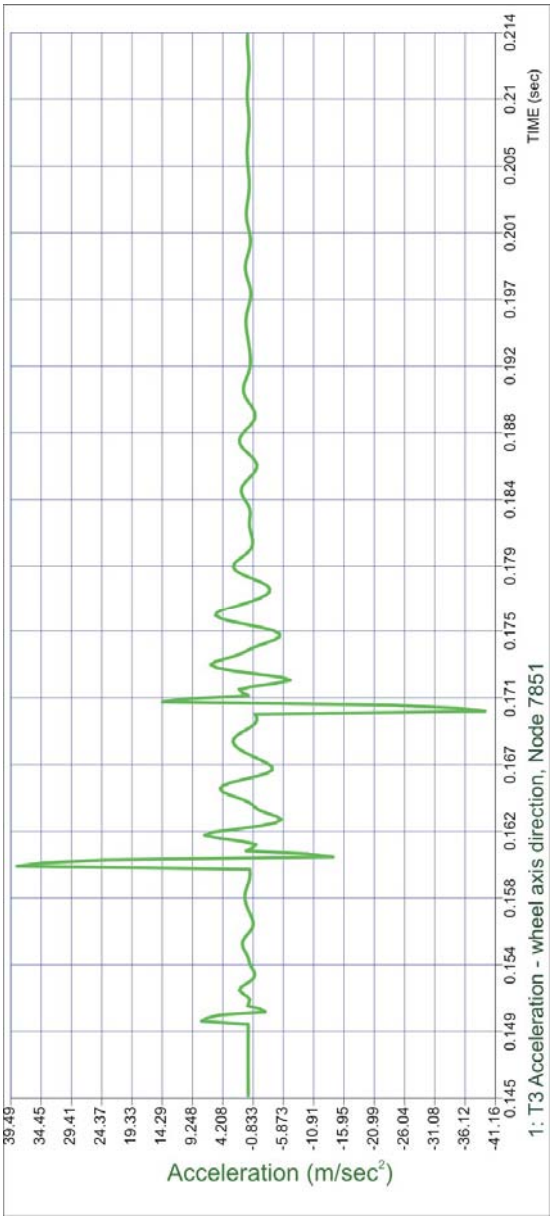

Fig.5 Oscillation component of acceleration for observed node No. 7851 for direction T3

2.4 Results of non-linear analysis

The results of non linear analysis for the model of steel wheel show that for high expressed load, the highest displacement amount is 0.0219 m and steel wheel is permanently plastic deformed. It means at the material of wheel exceeds from elastic to plastic range and wheel deflected in the place of load acting. Place of deflected part is on the inner side of the wheel fig. 7. This disposition of deformation corresponds to the expected state of deformation in reality. Von Misses stresses in combination with deformation shown in fig. 7. Image shows that the highest stress in plastic range is on the place with the highest deformation. The value of highest Von-Misses stress is σ_{VM}=36,878 kN/cm^2.

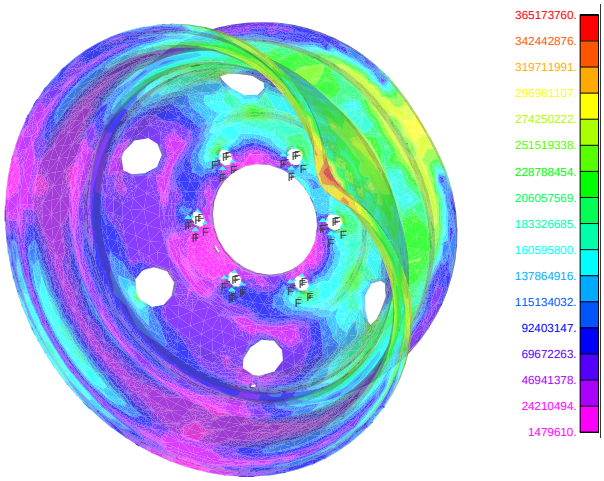

Fig. 7 Image of dispositions for Von Misses stress and deformations from non linear static analysis

Characteristics of the material for nonlinear plastic analysis in this case is shown in form of function which represents multiple linear approximation of function stress-elongation, according to fig. 9.

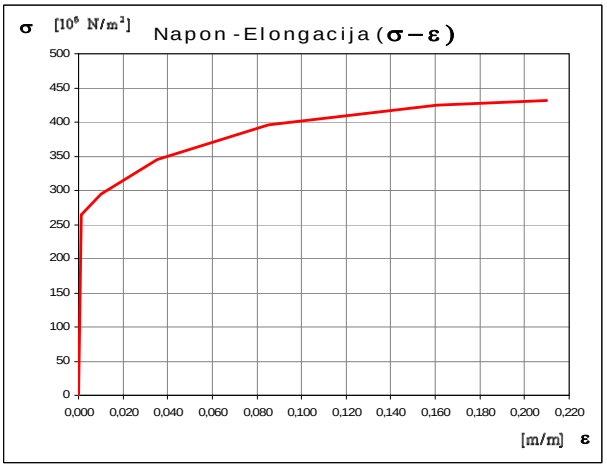

Fig. 8 Nonlinear characteristic of material

The model was made for complex influence of pneumatic radial tyre which is fitted on steel wheel rim with static radial load of 8000 N and inflation of pneumatic tyre of 2.5 bar and distribution of loads showed in paper [8].

3. CONCLUSION

On the basis of the analyses above, using method of finite element and influence of load on steel wheel rim for light duty vehicles, we can make the following conclusion:

1. Under influence of radial load, rim attends to deform and transform to oval shape in place of contact tyre bead with rim.

2. Deformation starts under the load in the place of contact of the tyre with the rim.

3. Deformations from the inner side of rim can cause loss of inflation in pneumatic tyre and dropping the tyre from rim.

4. The result of dynamic analysis for this model shows that with this load and adopted approximations, damping of oscillation occurs in observed time. Maximum of acceleration which assumes impact is great according to other amplitudes of oscillation. Damping start after appearance of those two to three extreme peaks. And these peaks are results of the stiffness of model and nature of constrains. This model with fixed constrains gives significant and unfavorable image of oscillation.

5. The frequency respond is similar to “bell effect”.

REFERENCES

[1] Bhattacharyya Sandip, Adhikary M., Das M.B., Sudipo Sarkar, Failure analysis of cracking in wheel rims – material and manufacturing aspects, Science Direct, Engineering Failure Analysis 15 (2008),

[2] Stearns J., Srivatsan T.S., Prakash A., Lam P.C., Modeling the mechanical response of an aluminum alloy automotive rim, Materials Science and Engineering A366 (2004), p.p. 262-268

[3] Muggleton J.M., Mace B.R., Brennan M.J., Vibration response prediction of pneumatic tyre using an orthotropic two-plate wave model, Jurnal of Sound and Vibration 264 (2003), p.p. 929-950

[4] Jornsen R., Stoll H., Betyier W. J., The Automotive Chassis Engineering Principles (second edition), 2002

[5] Pacejka B. H., Tyre and Vehicle Dynamics, 2003.

[6] Mizoguchi, H. Nishimura, K. Nakata, J. Kawakami, Research & Development (Kobe Steel Ltd.) 32 (2) (1982) 25-28.

[7] Klaus-Jurgen Bathe - Finite element procedures in engineering analysis, Prentice-hall. inc, Englewood Cliffs New Jersey, 1982.

[8] I. Savić, M. Jovanović, Dinamički odgovor automobilskog naplatka pri udarnom opterećenju, *til* 2008. MF Niš.

EXPERIMENTAL – NUMERIC ANALYSIS OF DYNAMIC PROCESS HYDRO – ENERGETIC BREECHES PIPE

P. Milić, G. Petrović, M. Jovanović, M. Burić, N. Petrović

Abstract: *Within the scope analysis stress – strain medium of toward – turbine pipelines, it was analyzed dinamic medium steel`s construction – breeches pipe, like responsible part of water hydro – energetic system. Development numerical models for FEM analyses were verificationed for experimental tensor – measure analyzing. Analysis are interesting because they show the size of numerical analysis which is enough for quality to bring two diferent models. Paper on research way shows dificult geometric and discrete modeling a breeches pipe for bigger energetic machines, flows 80.75 m^3/min. Analysis shows stress medium of the body breeches pipe, occurence of hydraulics oscillation within work toward – turbine flange. Paper was configured to show practical usefull modern information technologies, technology of experimental analysis, science concept of design multiplex geometric and FEA access. At that were evaluated boards of appliance modern personal desk – top computers.*

Key words: *Pipeline structure, experimental analysis, FEM analysis, breeches pipe*

1. INTRODUCTION

This paper were demonstrated interesting results of analysing breeches pipe A6 transmiting pipelines system of hydroelectric power station HE-P-2008 with Pelton work turbines. Analysis were derivative experimental (tensor – measure) and numerical. Template of experimental analysis is numerical FEM analysis of breeches pipe A6 within the scope pipelines C3. FEM (*Finite Element Method*) analysis are characteristics with great numerical size in relation to previous analysis [6]. Breeches pipe analysis are managed because of set up experiment and analysis maximum stress mediums. With this analysis was done defining stress medium of geometric dificult assembly, details like didn`t done in time when it`s project. This analysis are interesting because they discover real stress medium in richly shape from all so far derivate analysis. Also, today much perfect technologies of measuring are enabled view in work stresses of pipelines why initiate the basic for assessment of security substations.

2. CALCULATION MODELS OF BREECHES PIPE A6

For analysis was opserved a part of pipelines system, length 146,890 m and width 19,025 m. From pipeline system is for analysis development a geometric model which continue from entry pipeline block T9 to exit plumbing further turbines in mechanical hall. Geometric model is make like lines forms in most part of pipeline system, while is in a part of breeches pipe is make like solids (cubage are fulfilling of continuum).

Breeches pipe A6 is a analysis target, so it`s for much geometric details describe in solid shape geometry. Picture 1. shows geometric model pipeline system C3 and breeches pipe A6 who was specify separated. Pipeline system was modeling with lines geometry while across breeches pipe A6 and the rest of pipeline system existed transitive geometry. Geometric model of breeches pipe is development with geometric software SolidWorks 2005. In further text, at pictures 2.-5. are shows geometric model of breeches pipe A6.

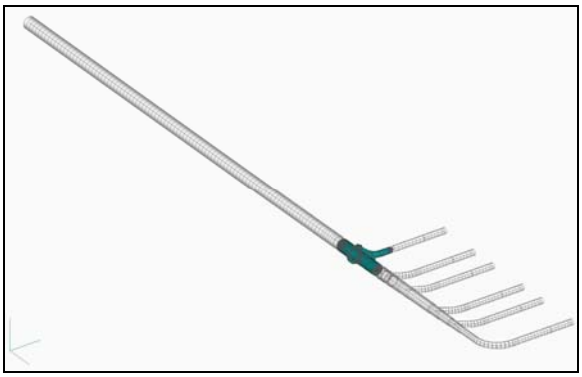

Picture 1. Geometric model of transmit pipeline C3 with breeches pipe A6

Mass of geometric model breeches pipe is 44333, [kg]. The main pipeline have a diametar 2.5 m, with variable wall thickness of structure elements 35-50 [mm]. Plumbing further turbines have a diametar 1.2 m, with wall thickness 15/18 mm. Pipelines and breeches pipe are made of alloy steel Nioval 47. Pipeline system is free based at sustentations and in horizontal plane are movable. In coming and outcoming points the pipeline system are fixed. Masive geometry of breeches pipe is a assembly of heavy engineering and it`s have special resposibility.

Predrag Milić, dipl.ing. assistant Mechanical faculty of Niš, pmilic@masfak.ni.ac.yu
Mr Goran Petrović, dipl.ing. assistant, Mechanical faculty of Niš, pgoran@masfak.ni.ac.yu
Prof. dr Miomir Jovanović, Mechanical faculty of Niš, miomir@masfak.ni.ac.yu
Prof. dr Milorad Burić, Mechanical faculty of Podgorica,
Petrović Nikola, dipl.ing. Ph.D student Mechanical fac. of Niš

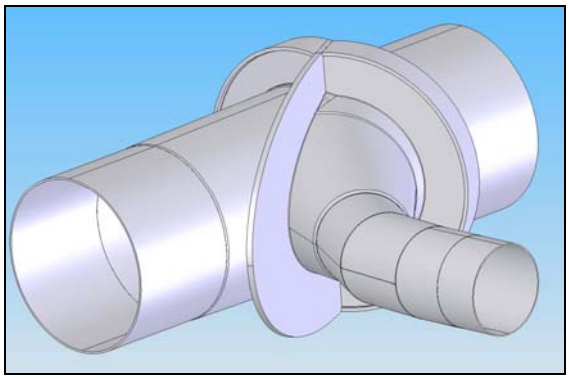

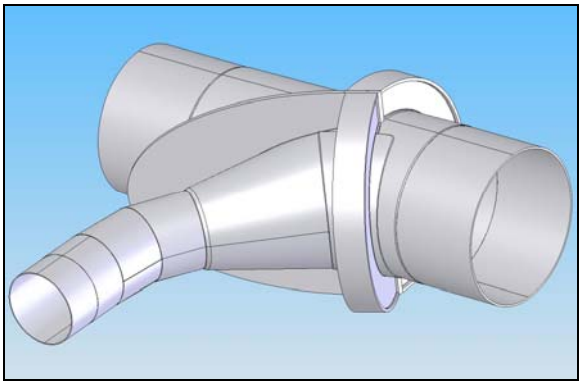

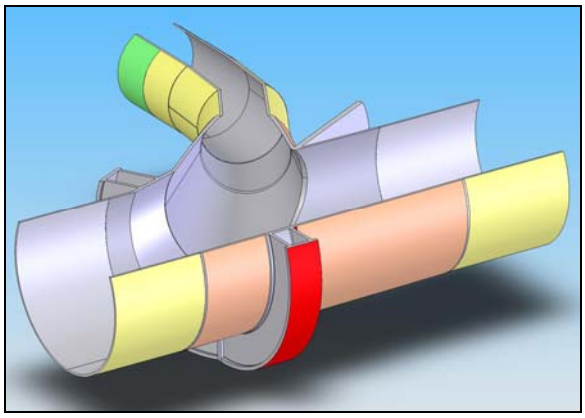

Picture 2-4. Geometrical model A6 (position of curve breeches pipe)

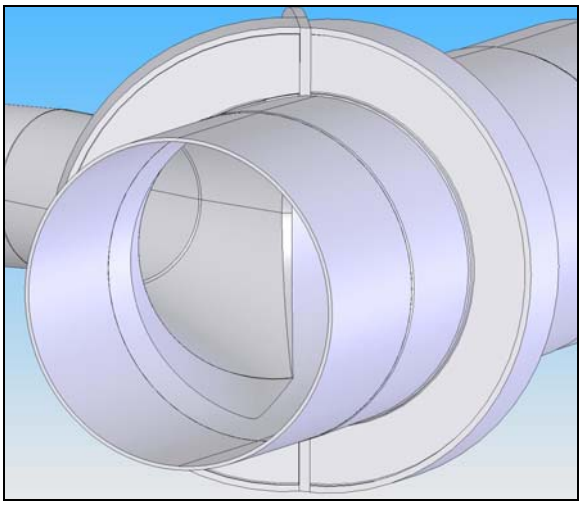

Picture 5. Geometric model A6 (view on cutting edge)

Discrete model is development with software MSC NASTRAN 2004 [1,2,3]. Finite elements are dimension from 22.8 x 20 mm to 64 x 52 mm. Model contains 399410 elements and 130871 nodes with 785226 degrees of movement freedom – equations. Average volume a one finite element is 8,07 [cm^3]. Page of one average finite element (tetrahedron) is 4,1 [cm]. Picture 6. shows a breeches pipe A6 detail model.

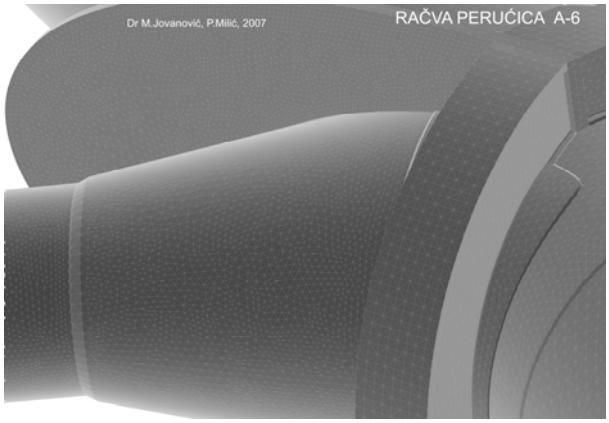

Picture 6. Discrete model A6 (solids - callar detail)

3. THE RESULTS OF FEM ANALYSIS

Numeric analysis was derivative in MSC NASTRAN 2004 software in elastic domain of continuum. Analysis involve a hydrostatics pressure, gravitation influence, friction in strengths, elastic of template, influences of fixed points in toward – turbine wall and strength T9. Geometry of pipeline system is import promptly without approximations. Analysis was derivative for measured hydrostatics pressure on day when was the experiment. Picture 7 and 8 shows overcome strain (displacements) and multiplex VonMises stress. Model is weighty length and because of that are overcoming visable displacements than 0.0151m. Max overcoming stress by *Hencky-Huber-Mises* hypothesis is 452267712, N/m^2 on picture 8. This stresses are below of limit expatiation Nioval 47 but they are sizeable. Maximum stress place is on the cutting edge of breeches pipe where the spout intersect and share on two sides. Because of that, outside around breeches pipe there is ellipsis excitation and circle boxes strenghtening around main pipeline (callar).

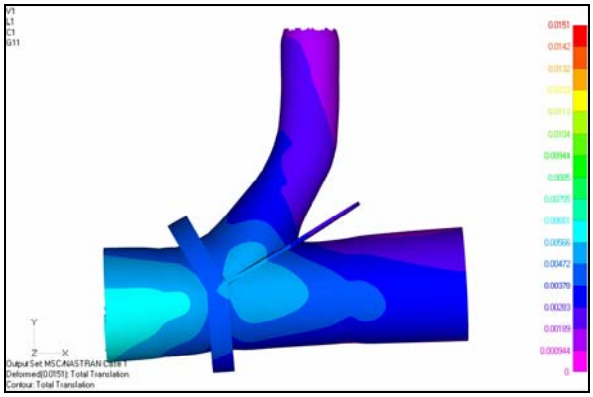

Picture 7. Contour Total translation A6

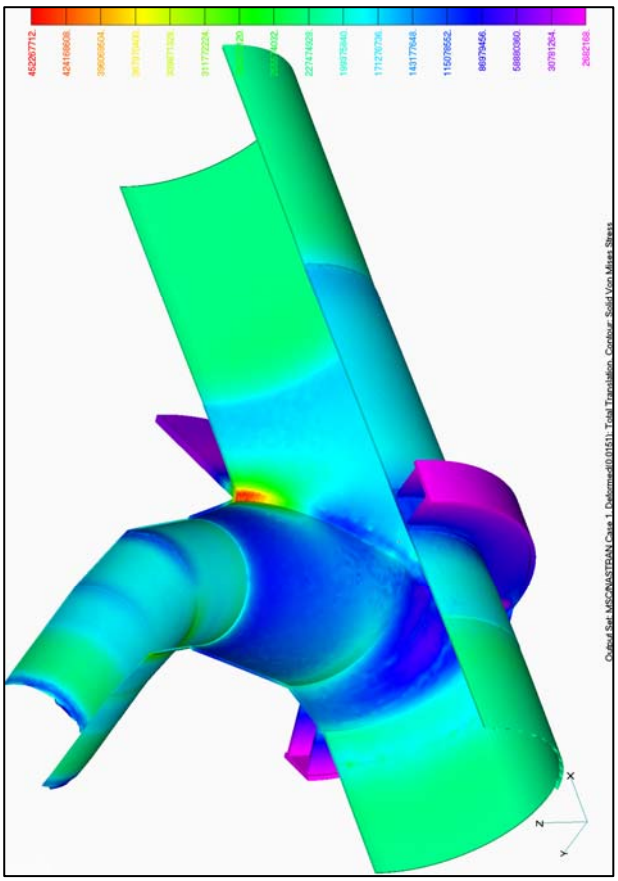

Picture 8. Contour Solid VonMises Stress A6

4. COMPARING ANALYSIS

Experiment was derivative in regime charging the pipelines system up to max measured hydrostatics pressure 52.69 bar. Measure of stress was derivative tensor – measure strake HBM RY 11-10/120 and measure system HBM MGC+. For measured and processing results it`s used Catman software.
Displacements breeches pipe were folowed by comparator in three ways.

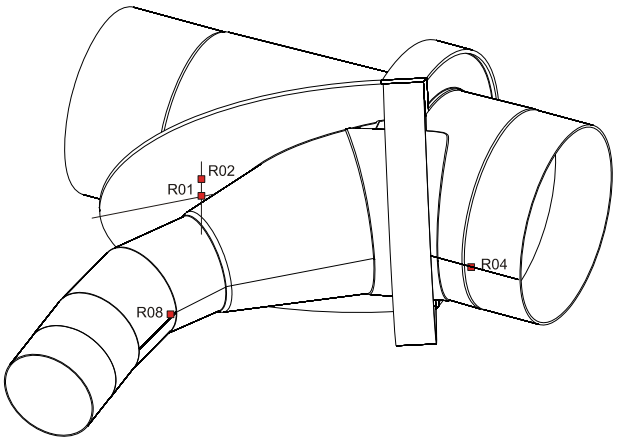

Picture 9. Schedule analysis measure points A6

Observing was a dinamic medium metal construction of breeches pipe issued charging the pipelines system what is run on cca 11 hours. Measured displacement strength of breeches pipe than 13 mm are consistent with calculate analysis. Picture 9 show schedule of couple measured places. Folow table give a comparing with results FEM analysis and experimental results. In table were given stress FEM analysis for membrane finite elements (on solid areas) on which is done experiment.

MM	Element No	**FEM** Von Mises stress N/m^2	**Experiment** N/m^2	Difference experiment FEM %
1	811	257500032	293116000	12.15
2	814	203426752	206669000	1.568
	815	205028592		0.794
8	757	235730400	233604000	-0.910
	758	235098768		-0.640

Maximum ripples from this table go up to 12.15 % at measure place 1. Overcome ripples are consequent a difference derivative geometric breeches pipe and development geometric model. This are not final calculations because it`s necessarily to development more quality geometrics and FEM models which will put down a difference of results. One of the problem is software rejection to generate a model with more smaler finite elements because they notice numerical problems with little contact geometrics areas. Backing up further correction of model refers to the more smaler distance mesh which success are stipulate from larger size further development of model. The larger number of elements have to upgrade the equability expansion energy of strain, enlarge a number of compatibility conditions and stipulate the attendance of stress concentration in transitional braze zones.

5. DYNAMIC ANALYSIS

Within the scope dynamic analysis they showed the biggest measured results at measure point 8 in two work regimes: The first regime is charging the pipeline system trought circuit line. The second regime is work with two aggregates, increase of power up to A6+A7=59+59 MW and quikly stopping (closing). Listing reference stress and presure in pipeline system give folow diagrams:

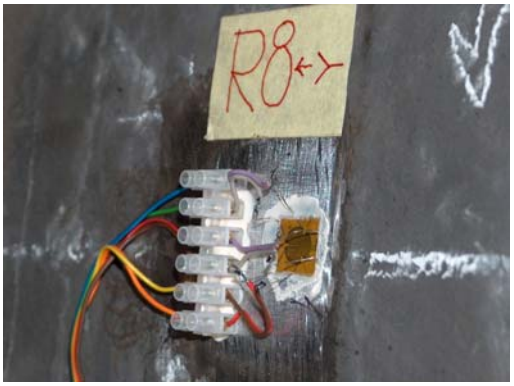

Picture 10. Photography of measure point 8

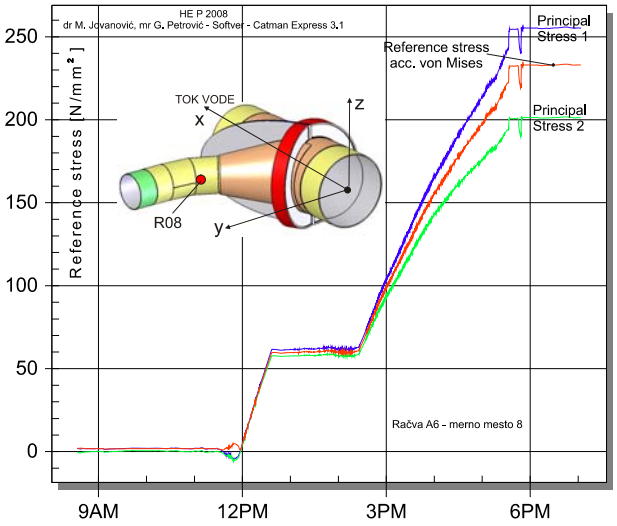

Picture 11. Measured results with water charging C3, stress and strain A6 – measure point 8

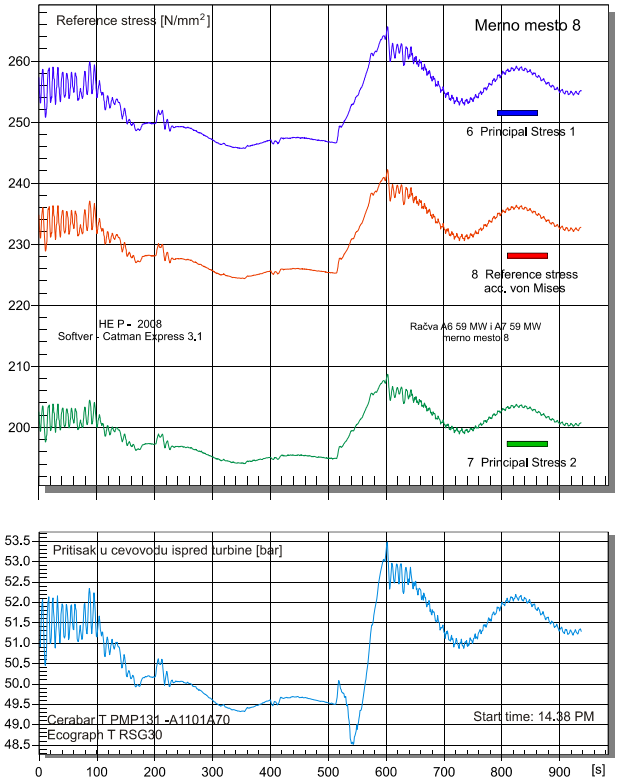

Picture 12. Measured results with quikly closing A6 + A7, presure and stress A6 – measure point 8

On presure diagram, picture 12, after 540 seconds begin a closing toward – turbine flange which run on cca 60 seconds and specify by program. Like consequent of that issued a hydraulic sling and attendance reversible wave motion with period of 190 seconds. Hydraulic sling was generate a build up presure with maximal dynamic coefficient Kd=53.55/48.5=1,105. Dynamic effects are analogously to be present and at main and multiplex stress, picture 12. Carrier wave is process of water waving in pipeline system, while is continuum oscillate around carrier wave oscillate of breeches pipe.

6. NOTINGS

In realization breeches pipe analysis it`s very important the responsibility next thesis category:

1. Complicity geometric model. It`s necessarily some of that kind project a breeches pipe which perfectly solve a assembling envelope (thick sheet metal),
2. It`s necessarily have assembling technic documentation no matter on system age,
3. Alignment mesh with point of view of little finite elements in transitive curve zones,
4. FEM analysis take up a procesor limit of hardware. Mass of teat model demand a model development with more number finite elements. Maximum development model for dual/quad procesor have a 1687877, finite elements and 1610301, (million and six hundred ten thousand) degrees of movement freedom. Topology of discrete model with more finite elements layers by mining size stipulate demand for much powerfull hardware. Researching a project is always longer and it`s stipulate hydro medium and knowledge of complicity this short describing work.

REFERENCE

[1] ANSYS - Release 7.0, Theory Reference, Nonlinear Structural Analysis, 2000.

[2] MSC/NASTRAN for Windows V 4.0, Theory Reference, FEMAP, 1998.

[3] Kojić M.: APPLIED THEORY PLASTICITY, University of Kragujevac, 1979.

[4] Timoshenko S., Strength of materials, Part II, Princeton, New Jersey, 1956.

[5] Klaus-Jurgen Bathe - finite element procedures in engineering analysis, prentice-hall. inc, Englewood Cliffs New Jersey 07632, 1982.

[6] Analiza stabilnosti cevovoda III HE Perućica, Energoprojekt Beograd, 2000.

THERMAL-ELASTIC BEHAVIOUR NUMERICAL ANALYSIS OF THE HIGH SPEED MAIN SPINDLE ASSEMBLY

M. Zeljkovic, A. Zivkovic, Lj.Borojev

Abstract: *In this paper is present mathematical model of main spindle assembly. There are, also, presented results obtained by computer modeling using software system of general purpose which is based on finite element method. Using of this system enabled thermal-elastic behavior analysis of for construction solution of main spindle assembly supported by bearing ball with angular contact.*

Key words: *main spindle, thermo and elastic behavior, finite elements method, conventional and hybrid bearings*

1. INTRODUCTION

It is very important, still in the main spindle assembly design process, to predict mutual connected influences of the mehanic and thermo characteristics for different machining conditions. Effects of the main spindle assembly thermo-elastic behavior have to be, with great probability, predicted still in the machine tool design phase.
To obtain machine tool satisfactory structure, based on the concept of the thermo-elastic behavior, appropriate model should be established. Mentioned model should take into consideration a large number of the parameters which influence on the appropriate main spindle assembly behavior.
On the model, it is necessary to inspect following parameters: friction torque, thermal displacement, clereance, pressure contact in the bearing.
It is the fact that today exist a great possibilities for thermo-elastic behavior analysis by finite elements method usage.
Up-to-date hardware and software give opportunities that design process can be significantly faster. In that way time for product development can be decreased and obtained solutions can be much better [7].¶
gyroscopic moments and unbalanced mass is investigated (bearings with ceramic balls).

2. MAIN SPINDLE ASSEMBLY THERMO-ELASTIC MODEL

Within main spindle assembly computer modelling an analysis of the thermo-elastic behavior by usage of the common purpose software package based on the FEM is performed.
Purpose of mentioned analysis is to examine appropriate design solution of the main spindle assembly with ball bearings with angle contact.
Two types of the bearings with angle contact are analyzed: with steel balls (conventional bearings) and with ceramic balls (hybrid bearings). Both bearing types are analyzed for the following bearing arangements: "O on distance" and "X on distance".
In order to make more efficacious and accurate calculation, thermo and elastic analysis are separated. Results of the thermal analysis has been used for analysis of the elastic assembly behavior

2.1 Main spindle assembly thermo model

Establishing of the mathematical model of the object is based on the previously defined volume model in the system for modeling.
Volume model (Fig. 1.) consist of main spindle (2), front bearings (2), distance rings (3), rear bearings (4) and hausing (5). Other assembly elements are leaved out because theirs influence on the thermal analysis is small in comparison with consider elements

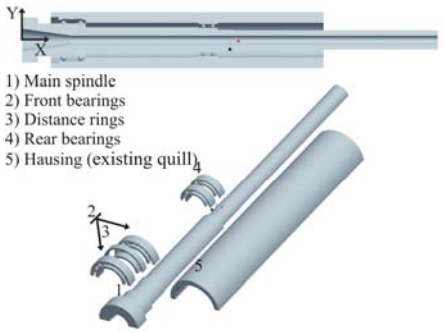

Fig. 1 Main spindle assembly model with basic elements

Based on the volume model a mesh of 271059 finite elements, 291072 nodes and 187 contact pairs is generated.

For discretization 3D finite element SOLID 87 (isoperimetric tetrahedron) is used. For contact pairs and contact surfaces definig a finite elements TARGET 170

Ph.D professor, Faculty of technical science, Novi Sad, milanz@uns.ns.ac.yu
M.sc assistent, Faculty of technical science, Novi Sad, acoz@uns.ns.ac.yu
Ph.D professor, Faculty of technical science, Novi Sad, borojevlj@uns.ns.ac.yu

are used. For establishing of the contacts between rolling balls and rolling paths and contacts between rings and spindle/hausing a finite elements CONTA 174 are used.
On the Figure 3. thermo model discretized by finite elements is shown. It should be emphasized that geometry of the front bearing is carried out by exact dimensions because of the influence of the contact conductivity on the analysis results. In the model, also, the clereances in the main spindle assembly have been taken into cosideration.

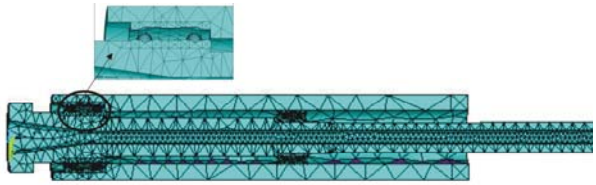

Fig. 3 Main spindle assembly thermo model

Defining of the thermo model is based on the following assumptions /1/:

- The model is axisymmetrical and assumes a uniform average clearance between the outer bearing ring and the housing around the entire perimeter. In the actual spindle, the bearing ring makes contact with the housing at one side and has twice the average clearance at the opposite side. The radial heat conduction through the air gap is modeled by linear averaging of the gap size.
- The heat flow resistance due to the grease film between balls and raceways is neglected here for grease lubrication, which results in a layer of grese film with minimum film thickness.
- The outer ring and the housing have an initial clearance fit. Heat conduction through a clearance fit requires more extensive calculation. For the inner ring and the shaft, a press fit is assumed at all operating conditions, so that the thermal resistance for conduction through the inner ring is modeled as a constant and does not require further analysis

2.2 Generated heat and heat transfer mechanisms

2.2.1 Generated heat

In analyzed model is assumed that the main heat sources in the assembly are bearings, because the power transmission is enabling by wheeled belt, which is setup on the spindle end, and its influence is discarded.
Generated heat in bearings is calculated based on the friction moment due to load and the friction moment due to lubrication.

$$M = M_0 + M_1 \quad (1)$$

The friction moment due to lubrication is caused, mostly, by hydrodinamic losses in the grease and it depends of the viscosity of the lubrication resource and of the speed bearing. It could be calculated based on the relation:

$$M_0 = 10^{-7} f_0 (\nu n)^{2/3} d_m^3 \text{ [Nmm]} \quad (2)$$

where:
f_0- coefficient depended of the bearing type and lubrication type (for bearings with contact angle and grease lubrication its value is between 2 -4)
ν- kinematic viscosity of the lubrication [mm^2/s] (for grease LGLT 2 and working temperature 40 [°C] its value is 18 [mm^2/s];
d_m- middle bearing diameter; $d_m=(D+d)/2$ [mm];
D-outer bearing diameter [mm] ; d- inner bearing diameter [mm];
Friction moment due to load could be calculated based on the relation:

$$M_1 = f_1 \text{ x } P_1^a \text{ x } d_m^b \quad (3)$$

where;
a,b-constants which depend of the bearing type (for ball bearings with contact angle theirs value is 1);
f_1-coeficient which depends of the bearing type;
P_1- bearing load
Generated heat in the bearings is calculated based on the friction moment due to load and friction moment due to lubrication, from relation 1. Total generated heat on the one bearing is obtained from the relation:

$$Q_{uku.} = M \omega \quad (4)$$

where:
Q_{uku}-generated heat amount [W], M – friction moment [Nm]; ω-angular speed [rad/s] .

2.2.2 Heat transfer mechanisms

The main inner mechanisms of the heat transfer in this model are : convection due to bearing rotation, convection due to spindle rotation, conduction between bearing balls and rings, conduction between rings and housing/spindle (Fig. 4.)

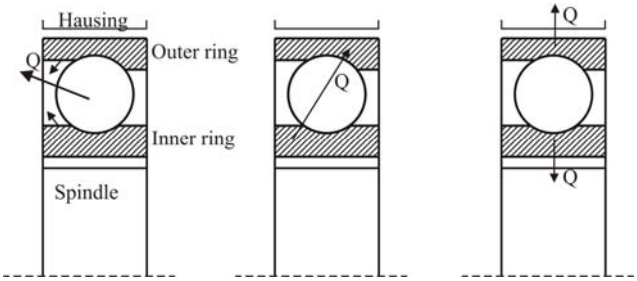

Fig. 4. Heat transfer through bearings:

Heat transfer through the bearing is realized only between bearings and surroudings air.
Absorbed heat from the greas, in this paper is not discussed. Because of the small difference in temperature radiation could be neglected, coeficient of the heat transfer is calculated according to [1], from the condition of the flow air through bearing which belogngs to the turbulent motion. At this transfer, total air flow velocity, caused by the bearing rotation, is calculated from the axial and tangential component.

Axial flow velocity could be calculated as a velocity between two cylinders, from the relation [1]

$$u_{ax.} = \frac{V}{A_{ax}} = \frac{4V}{\pi(D+d)} \ [m^2/s] \quad (5)$$

where V – volume air amount.
Tangential velocity component, on the midlle diameter, could be calculated from relation for air flow between movable and immobile cylinder:

$$u_{tan.} = \frac{\omega}{2}\frac{(D+d)}{2} \quad (6)$$

where: ω -angular velosity [rad/s]; D – outer ring diameter [m]; d- inner ring diametera [m].
Resultant air velocity at the bearing rotation is calculated :

$$U = \sqrt{u_{ax}^2 + u_{tan}^2} \ [m^2/s] \quad (7)$$

Coefficient a is calculate according to [1]:

$$\alpha = (c_0 + c_1 U^2)\left[\frac{W}{m^2 K}\right] \quad (8)$$

c_0 i c_1 are constants obtained in the paper [1] and could be used for approximate calculating. If, in the previous relation is put that U = 0, i.e. that rotation doesn't exist, in this case $\alpha=c_o$, i. e. according to /1/ c_o = 9,7-10 [W/m^{2}K]. Temperature increase, at the outer ring, depends of the conductance at the contact, i.e. on the heat resistance of the contact itself. Contact heat resistance depends of the contacts shape and size and it is connected to bearing geometry and inner contact pressures in the bearing (Fig. 4).

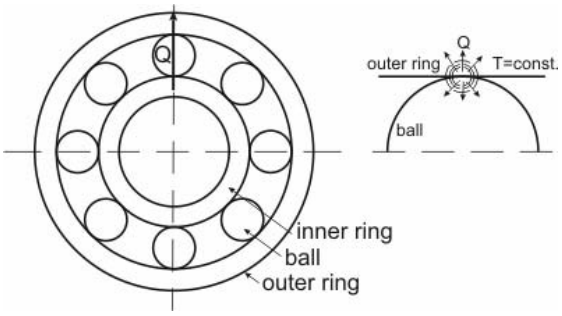

Fig 4. Conduction between balls and rings

Heat contact resistance at the contact of the rolling balls and rings is calculated from the mixed boundary condition [2]:

$$R = \frac{1}{4\pi\lambda}\int_0^\infty \frac{du}{\sqrt{(a^2+u)(b^2+u)u}} \quad (9)$$

where: λ-heat conductance, *a* i *b* halfaxises of the eliptic contact surface.
Using the complete elliptic integral of the first kind, Eq. (9) can be rewritten in the following form as

$$R = \frac{\psi}{4\lambda a} \quad (10)$$

where Ψ is a geometric factor depending on the size of the contact area; therefore, it is a function of $k = 1 - \frac{b^2}{a^2}$ and is defined as:

$$\psi = \frac{2}{\pi}\int_0^{\pi/2} \frac{d\alpha}{\sqrt{(1-k^2\sin^2\alpha)}} \quad (11)$$

For simpler calculating Eq.11 using Gaus hiperbolic function:

$$\psi = \left\{1 + \left(\frac{1}{2}\right)^2 k^2 + \left(\frac{1}{8}\right)^2 k^4 + ... + \left[\frac{(2n-1!!)}{2^n n!}\right] k^{2n}\right\} \quad (12)$$

For a bearing ball, its contact resistance to the outer ring becomes

$$R_{kt} = \frac{\psi}{4\lambda_1 a} + \frac{\psi}{4\lambda_2 a} \quad (13)$$

where λ_1 and λ_2 are the thermal conductivities for the outer ring and the ball respectively.
Coefficient of the heat conduction at the main spindle assembly depends of the clereance between outer ring and housing., i. e. inner ring and spindle (fig. 5).

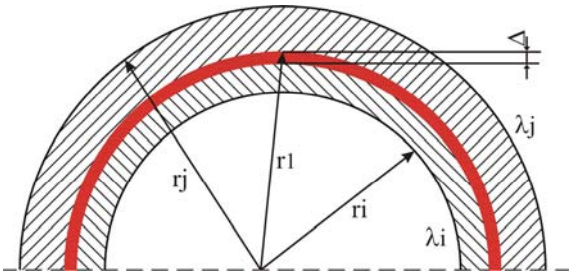

Fig.5 Conduction between outer ring and housing

Heat conductance between two elements could be calculated from the relation [5]:

$$\lambda_{ij} = \frac{\ln\left(\frac{r_j}{r_i}\right)}{\frac{\ln\left(\frac{r_j}{r_1}\right)}{\lambda_j} + \frac{R_w}{r_1} + \frac{\ln\left(\frac{r_1}{r_i}\right)}{\lambda_i}} \quad (14)$$

where λ_i i λ_j – heat conductances of the ring and housing; r_j- housing radius; r_i- inner ring radius; r_1- rolling path radius on the outer ring.
R_w is heat contact resistance at the contact of the ring and housing and, according to [5], is calculated from relation:

$$R_w = \frac{r_1}{\lambda_{ij}} \ln\left(\frac{r_1 + \Delta}{r_1}\right) \quad (15)$$

where Δ - clereance between outer ring and housing.
At the same way conductance at the contact between inner ring and spindle could be calculated

2.3 Analysis of the main spindle assembly heat behavior results

Computer analysis has been conducted for five number of the revolutions n = 2800, 3550, 4500, 5600 i 6300 [rpm] at the unloaded state.

Temperature distribution at the main spindle assembly and bearing elements, at the moment of the temperature steady-state reaching, with maximal number of revolution and bearing arrangement "O on distance", for conventional and hybrid bearings is shown on the Fig. 6, At the higher number of revolutions, bearing rings have the same temperature distribution, because due to bearing rotation heat is uniform distributed at the inner rings (Fig. 6).

From the computer analysis could be concluded that the temperatures, on the earing balls, rolling paths and inner ring are greater for 5 to 10 [°C] than temperatures at the outer bearing ring.

The greatest temperature increase is in the first spindle work period (after 10 min). It is form 21,7 [°C] (for n=2800 [rpm]) to 59,4 [°C] (for 5600 [rpm]) for conventional bearings. By the hybrid bearings it is from 12, 64 [°C] (for n= 2800 [rpm]) to 50 [°C] (for n= 5600 [rpm]). Period of the temperature steady-state reaching depends of the number of revolution. At the smaller number of revolution (n <3550 [rpm]) temperature steady-state is reched for 60-70 [min]. At the highest number of revolution (n > 3550 [rpm]) temperature steady-state is reached for 20-40 [min].

By the temperature in the steady-state comparison it could be concluded that bearing arrangement in the front bearing support, at the same number of revolution, has very small influence on the temperature increase, which is caused by the same amount of the generated heat.

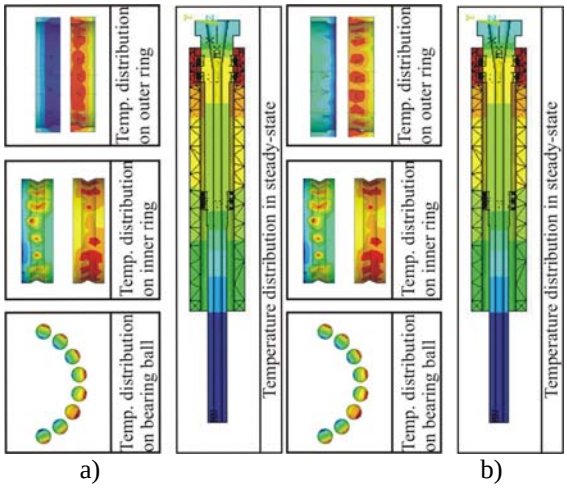

a) b)

Fig. 6 Temperature distributions on main spindle assembly elements: a) conventional; b) hybrids bearings

On the Figures 7 i 8 front bearing temperature increase for: 2800 [rpm] and 5600 [rpm] and bearing arrangement "O on distance" for conventional and hybrid bearings.

Based on the mentioned Figures, it could be concluded that first bearing in the front support (from the spindle nose) has greater temperature than second bearing for 4 to 6 [%] depending of the number of revolution.

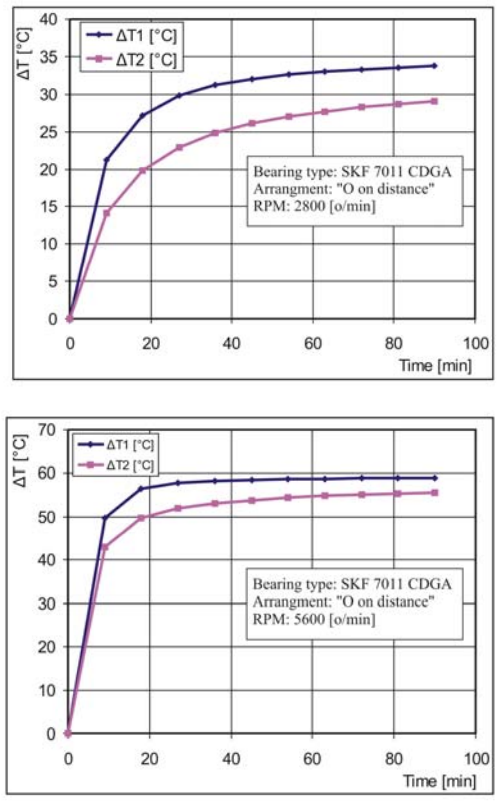

Fig. 7 Temperature rise for conventional bearings

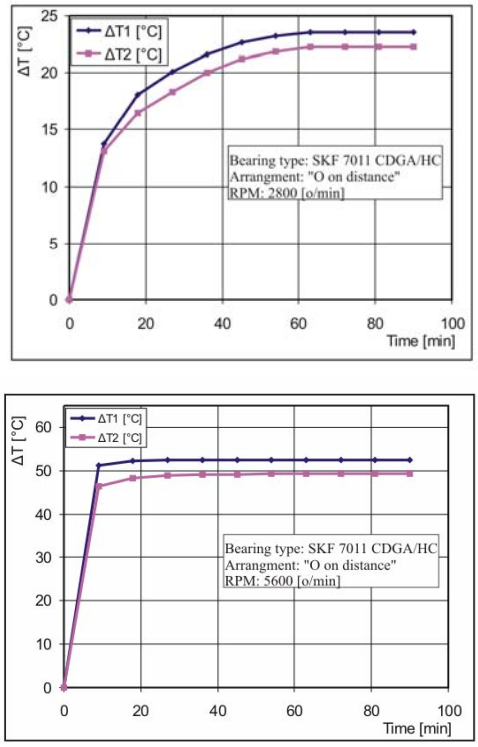

Fig. 8 Temperature rise for hybrid bearings

Number of revolution increase, caused increase of the temperature difference between conventional and hybrid bearings. By the higher number of revolution n > 3550 [rpm], temperature increase is faster by the conventional

bearings. One of the reasons for smaller temperature increase by the hybrid bearings is in the fact that hybrid bearings have smoller mass (for 40%) and smaller friction. It caused smaller amount of the generated heat. On the other hand they have greater heat conduction resistance, so smaller heat amount could be transfered on the outer bearing ring.

Based of the experimental investigations [9] a comparison of the temperatures at the front bearings has been conducted. It could be concluded that result deviation between computer modeling and experimental investigation is 10 [%] by conventional and 15 [%] by hybrid bearings. One of the reasons for greater. One of the reasons for greater results deviation by hybrid bearings is in the fact that there are not enough data about this bearings. Values of the particular thermo-physics characteristics are in wide limits (for example, conduction coefficient is between 25 and 40 W/mK, depended of the bearings producer)

At the end, it could be concluded that results of the thermo behavior obtained by computer modeling are satisfactory. Special attention should be paid to defining of the generated heat amount and heat transfer coefficient.

2.4 Main spindle assembly elastic model

At elastic behavior modeling only influence of the thermo load, without external forces, is discussed. Model for elastic behavior analysis is smplified because of the analysis complexity. For mentioned analysis main spindle assembly consists, only, of main spindle, while bearings are approximated by the linear finite element LINK 11. Linear springs are arranged on the main spindle circumference. Because of the number of the analyzed solutions an automation of the modeling and calculating by parametric programming is carried out. Mentioned automation based on the information about thermo load, bearing stiffness and coordinates of the characteristic point og the main spindle cross section (Fig. 9.).

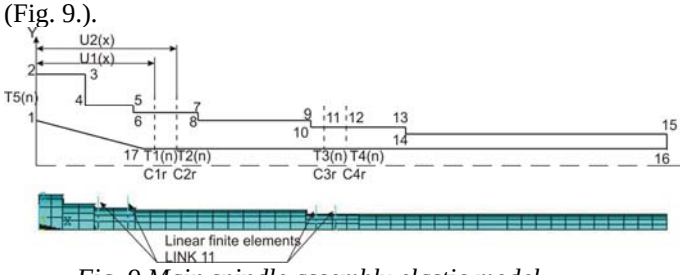

Fig. 9 Main spindle assembly elastic model

2.5 Analysis of the main spindle assembly elstic behavior results

On the Fig. 10. and 11. dependences of the displacement on the spindle nose of the number of revolution for different types and variants of the bearing support, obtained by computer modeling are shown.

By the displacements analysis at the front bearing, it could be concluded that, at conventional bearings, mentioned displacements are greater for 18 [%], when the bearings are in arrangement "X on distance". At hybrid bearings, also, displacements are greater for 25 [%], when the bearings are in arrangement "X on distance".

Comparison of the displacements on the front front bearing support shows that displacements are smoller for 29 [%] when the main spindle is supported by hybrid bearings with arrangement "X on distance" and for 34[%] in bearing arrangement "O on distance".

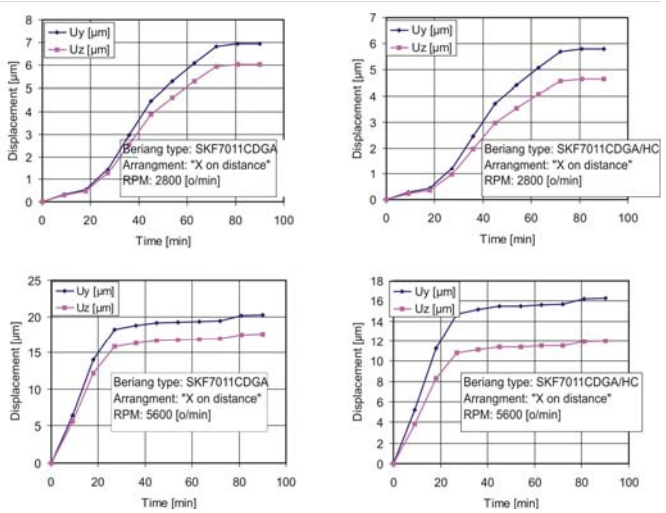

Fig. 10 Increase of displacements on spindle nose for arrangements "X on distance"

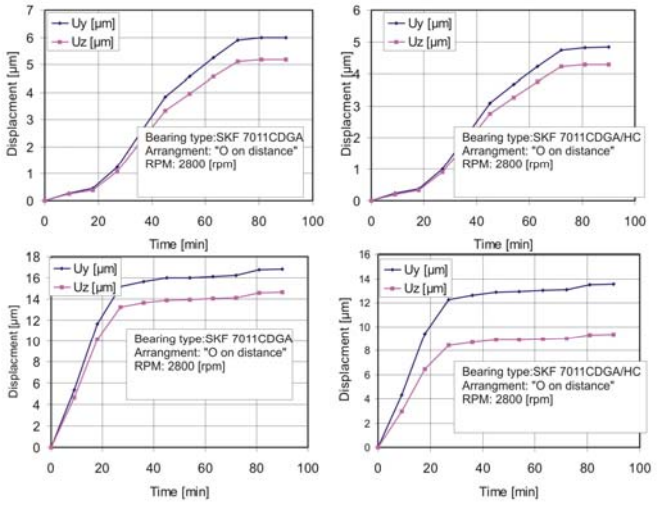

Fig. 11 Increase of displacements on spindle nose for arrangements "O on distance"

3. CONCLUSION

Investigation results, shown in this paper, present an attempt to compare conventional and hybrid bearings from the viewpoint of the high-speed main spindle

assembly thermo-elastic behavior. Developed mathematical model should enable, still in the design phase with great probability, prediction of the thermo-elastic behavior in the exploitation. In the paper a great significance of the main spindle in the machine tool structure is emphasized. It should satisfy a number of the requirements. Most important, of mentioned requirements, are limited temperature increase on the front bearing and displacement on the spindle nose decrease.

Also, possibility of the up-to-date numerical calculating methods application, at the identification of the main spindle assembly thermo behavior, is emphasized.

REFERENCE

[1] BOSSMANNS, B.: *Thermo-mechanical modeling of motorized spindle systems for high speed milling*, Ph.D. Dissertation, Purdue University, 1997.

[2] BOSSMANNS, B., TU, J.,F: *A thermal model for high speed motorized spindles*, International Journal of Machine Tools & Manufacture Vol. 39, Pages 1345–1366, 1999.

[3] CHI-WEI, L., TU, J., F., KAMMAN, J.: *An integrated thermo-mechanical-dynamic model to characterize motorized machine tool spindles during very high speed rotation*, International Journal of Machine Tools & Manufacture Vol. 43, Pages 1035–1050, 2003.

[4] JĘDRZEJEWSKI, J, KOWAL1, Z KWAŚNY, W, MODRZYCKI, W.: *Hybrid Model of High Speed Machining Center Headstock*, Annals of the CIRP, Vol. 54/1, 2004.

[5] JEDRZEJEWSKI, J.: *Effect of the thermal contact resistance on thermal behavior of the spindle radial bearings*, International Journal of Machine Tools & Manufacture, ISSN 0890-6955, 1988, Vol. 28, Pages 409-416.

[6] HONGQI, L., YUNG, C. S: *Analysis of bearing configuration effects on high speed spindles using an integrated dynamic thermo-mechanical spindle model*, International Journal of Machine Tools & Manufacture Vol. 44, Pages 347–364, 2004.

[7] ZELJKOVIĆ, M: *System for automated design and behavior prediction of machine tool main spindle assembly*, Ph.D thesis, Faculty of technical sciences, Novi Sad, 1996.

[8] ZELJKOVIĆ, M., GATALO, R.: *Experimental and computer aided analysis of high-speed spindle assembly behavior*, Annals of the CIRP Vol. 48/1 , 325–328, 1999.

[9] ŽIVKOVIĆ, A.: *Experimental and computer analysis thermal-elastic behavior high-speed main spindle assembly*, Master thesis, Faculty of technical sciences, Novi Sad, 2007

The paper is a result of investigation on the project "advancement of the system of technical preparation in the condition of the small batch production by using up to date software package of the universal application" no.tr6630a, supported by ministry of the science of the republic of serbia.

A STRUCTURAL OPTIMIZATION OF A CELLULAR PLATE MADE OF RECYCLED CORRUGATED CARDBOARD

M. Veljovic, M. Dedic

Abstract: *The main properties of corrugated cardboard are easy and cheap manufacturing, easy processing and good strength to self-weight ratio, which makes it the main material for general purpose packaging for decades. One of its very important characteristics is ability of recycling without environmental damage as well, due to which it has become ecologically highly valued material. In this paper an analysis of different structures of light load carrying cellular plates with filling made of recycled corrugated cardboard is presented. An analysis of the mechanical characteristics of the plate treated as an orthotropic material through comparison of specific bending, shearing and twisting capacities is given. The aim of the analysis is to indicate the optimum structure of the filling layer for various purposes.*

Key words: *1) Specific strength, 2) Recycling, 3) Corrugated cardboard*

1. INTRODUCTION

Corrugated cardboard is the most important material for commercial package boxes. Among its numerous good characteristics we shall mention the most important: it has good mechanical strength to carry and protect a package box content from damage, it is light and cheap material, and it can be easily shaped to a vast variety of boxes, stiffeners, frames and other packaging elements, [1], [5], [8]. An important characteristic of this material is that it can be easily either destroyed without any environmental consequence, or recycled, [4]. Because of all this it is considered ecologically highly valued material.

Ever increasing demand for recycling makes one tempted to consider the possibility of not recycling the wasted corrugated cardboard in the sence of reprocessing it, but rather remanufacturing it, whenever possible, for example, to make strengthening elements in the form of cellular composite plates that can be inserted in heavilly loaded cardboard boxes or other load carrying elements. The challenge of this idea would be to find the filling pattern of such plates that has the most efficient shape regarding strength-to-weight ratio.

In this paper we shall take into consideration three possible filling patterns for such plates that satisfy simple technology demand, Fig.1, in order to find which one has the best overall strength-to-weight ratio. In all cases both outer sheats and the filling sheat are made of the same corrugated cardboard sheats with waves in the same direction. To make drawings simpler, instead of full representation, the corrugated mid-layer cross-section is going to be only partially indicated as in Fig.1. The sheats are glued in contact faces. We assume that these cellular plates are typically used as box bottom stiffeners, and that the main modes of strain are bending and shearing.

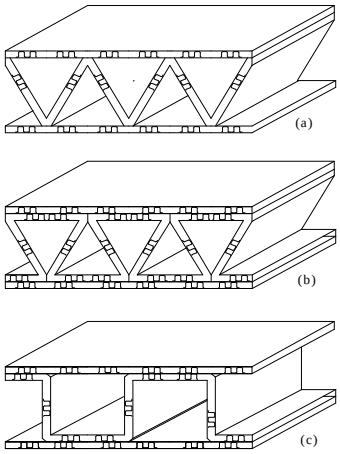

Fig.1 The cellular composite plate cases

The first mode is responsible to carrying load and the second primarily te resist damages during handling. To compare different filling patterns, we shall consider the specific strengths - ratios of the allowed load to the referent volume of material.

2. THE STRUCTURAL ELEMENTS OF THE CELLULAR PLATES

We treat one-layer corrugated cardboard as transversly orthotropic material with the main material axis (1), Fig.2, in the direction of mid-layer wave ridges. The corresponding theory can be found in [2], but we shall restrict our analysis to the effects that can be treated by Strength of materials formulas. We assume that the allowed compressive stresses in the main directions (1) and (2) are σ_{d1} and σ_{d2}, and that the allowed shearing stress in the main plane (1), (2) is τ_d .

MiljanVeljovic, Mechanical Engineer, Faculty of Mechanical Engineering Kraljevo, veljovic.m@mfkv.kg.ac.yu
Dr Milan Dedic, Professor, Faculty of Mechanical Engineering Kraljevo, dedic.m@mfkv.kg.ac.yu

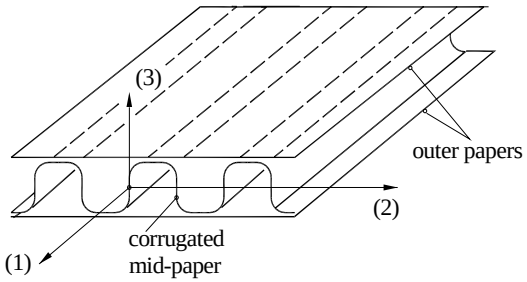

Figure 2 The corrugated cardboard principal material axes

The cellular plates we analyize in this paper are made of cardboard sheets of the equal thickness *t* glued in the contact faces. Refering to the cellular plates with the filling shown in Fig.1 we define the following analytical planes, see Fig.3: longitudinal plane in the direction of the filling readges, transverse plane, frontal cross-section plane, indexed "1" and the side cross-section plane, indexed "2". We point out that the directions of the longitudinal and transverse plane coincide with the main material directions of the cellular plates considered!

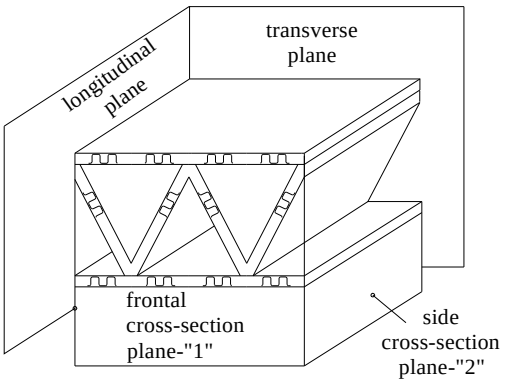

Fig.3 Characteristic planes of the cellular plate

We shall observe specific bending strength S_M and specific shearing strength S_T related to a "unit" volume $V = b \times h \times L$ of the cellular plate, Fig.4, where b is a step-distance between filling walls, h is distance between the mid-lines of outer walls and L is an arbitrary length. Our approach to the problem follow the theory of structures in [4] and similar examples of structural analysis of cellular plates in [6] and [7].

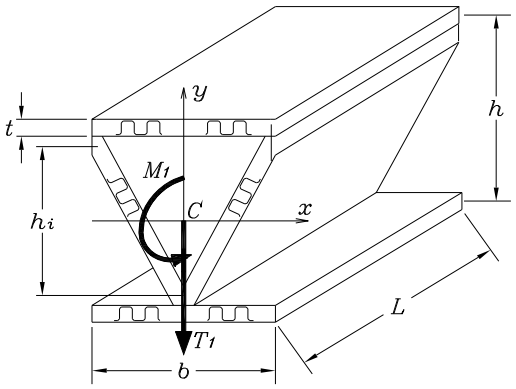

Fig.4 The unit volume *V* of the cellular plate and its dimensions

3. SPECIFIC STRENGTHS – PLANE "1"

We first observe the action of moment M_1 and shearing force T_1 that cause stresses in the first cross-section plane "1" - frontal plane in the Figs.3 and 4. To make calculation easier, while remaining within the practical inegineering accuracy, we shall calculate the properties of the cross-section using lengths of its wall's mid-lines and coordinates of their ends. For that purpose we define the internal height $h_i = h - t$. In that manner the length of the filling wall, Fig.4, i.e. the distance between its mid-line ends, will be:

$$l_3 = \sqrt{(b/2)^2 + h_i^2}$$

Using these quantities we obtain the axial moment of inertia I_x in the observed cross-section of the unit volume *V* (actually the moment of inertia per unit with *b*!) and maximum distance y_{max}:

$$I_x = 2\left[(\frac{h}{2})^2 bt + \frac{h_i^2 l_3 t}{12} \right] \quad (1)$$

$$y_{\max} = \frac{h+t}{2} \quad (2)$$

The maximum or allowed bending moment in the longitudinal plane per unit widh *b* is:

$$M_{1d} = \frac{I_x}{y_{maz}} \sigma_{d_1} \quad (3)$$

The area of the cross-section and the unit volume are:

$$A = 2(bt + l_3 t) \quad (4)$$

$$V = A \cdot L = 2(bt + l_3 t)L \quad (5)$$

We define the specific bending strength as ratio between the allowed moment (3) and the unit volume (5):

$$S_{M1(a)} = \frac{M_{1d}}{V} = S'_{M1(a)} \frac{b\sigma_d}{h} \quad (6)$$

The *(a)* in subscript denotes the case (a) in Fig.1. The $S'_{M1(a)}$ at the right side above is the *no dimensional specific bending strength* and it depends only on the ratio *h/b* of the unit volume. Values $S'_{M1(a)}$ are given in Table 1 (M) row "a", as function of *h/b*. We can apply the same procedure for cases (b) and (c) to obtain $S'_{M1(b)}$ and $S'_{M1(c)}$. However, it is more interesting to compare these quantities, so, instead of $S'_{M1(b)}$ and $S'_{M1(c)}$ the ratios $S'_{M1(b)} / S'_{M1(a)}$, row "b/c", and $S'_{M1(c)} / S'_{M1(a)}$, row "c/a", are given in the Table 1.

Table 1 (M)						
h/b	0,75	1,00	1,25	1,50	1,75	2,00
a	1,36	1,76	2,12	2,46	2,78	3,09
b/a	1,12	1,07	1,06	1,08	1,09	1,10
c/a	1,18	1,23	1,26	1,29	1,30	1,32
Table 1 (T)						
h/b	0,75	1,00	1,25	1,50	1,75	2,00
a	0,30	0,33	0,36	0,37	0,38	0,38
b/a	0,89	0,87	0,88	0,91	0,94	0,97
c/a	0,64	0,71	0,78	0,85	0,91	0,97

In the same manner we do about the *specific shearing strength*. First we calculate the static area moment $S_{x(1/2)}$ for the upper half (hence subscript (1/2)) of the cross-section:

$$S_{x\,(1/2)} = \frac{hb + h_i l_3}{2} t \qquad (7)$$

The maximum shearing stress, that is allowed to reach the value τ_d at most, appears along the centroidal axis *x*, Fig.4. Using (7) we can write:

$$\tau_{\max} = \frac{T_1 S_{x(1/2)}}{I_x(2t)} = \tau_d$$

where (2*t*) is the width of material in two filling walls that transfer the shearing stress at a distance *y* from the axis *x*. The allowed shearing force is:

$$T_{1d} = \frac{I_x(2t)}{S_{x(1/2)}} \tau_d \qquad (8)$$

Similarly to (6) we now have:

$$S_{T1(a)} = \frac{T_{1d}}{V} = S'_{T1(a)} \frac{\tau_d}{h} \qquad (9)$$

where $S'_{T1(a)}$ is the *nondimensional specific shearing strength*, a function of the ratio *h/b* only. Values of $S'_{T1(a)}$ are given in the lower half of Table 1, row "a", and ratios $S'_{T1(b)}/S'_{T1(a)}$ and $S'_{T1(c)}/S'_{T1(a)}$ in the rows "b/a" and "c/a" respectively.

4. SPECIFIC STRENGTHS – PLANE "2"

Let us now observe the action of moment M_2 and shearing force T_2 that cause stresses σ and τ in the cross-section plane "2" – side plane in the Fig.5. We can easily see that only the outer sheets transfer bending so that M_2 acts through the couple of forces F in the transverse plane. These forces act on the area Lt, and may produce the stress σ_{d2} at most. Thereby the value of the allowed force F is:

$$F_d = (Lt)\cdot\sigma_{d2}$$

and the allowed moment in transverse direction per length L of the volume element V is:

$$M_{2d} = F_d \cdot h = hLt\cdot\sigma_{d2} \qquad (10)$$

Repeating the formula (6) we write:

$$S_{M2(a)} = \frac{M_{2d}}{V} = S'_{M2(a)} \frac{h\sigma_{d2}}{L} \qquad (11)$$

Here the $S'_{M2(a)}$ is the nondimensional specific bending strength in the transverse direction. It is given in the Table 2, upper half, row "a". As in the previous chapter instead of $S'_{M2(b)}$ and $S'_{M2(c)}$ the ratios $S'_{M2(b)}/S'_{M2(a)}$ and $S'_{M2(c)}/S'_{M2(a)}$ have been given in rows "b/a" and "c/a".

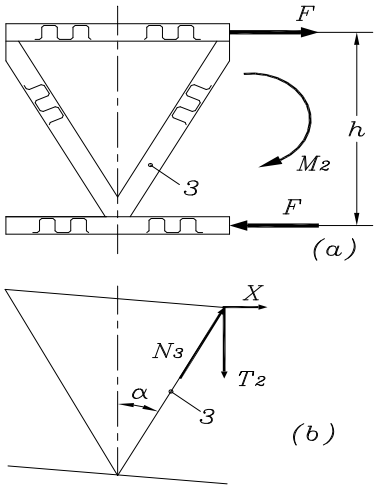

Fig.5 Action of forces in the transverse plane

Considering the action of the shearing force T_2 in the cross-section plane "2" we see that it is transferred not through shearing stresses in the walls but rather through tension or compression of the filling walls. From the equilibrium of the forces acting upon the end point of one filling wall, Fig.5, we come to:

$$\sum Y_i = N_3 \cos\alpha - T_2 = 0 \quad \Rightarrow$$

so that the allowed force T_2 is to be expressed by the allowed normal stress σ_{d2} in the manner:

$$T_{2d} = N_3 \cos\alpha = (Lt\sigma_{d2})\cdot\cos\alpha \qquad (12)$$

Similarly to (9) we can write:

$$S_{T2(a)} = \frac{T_{2d}}{V} = S'_{T2(a)} \frac{\sigma_{d2}}{b} \qquad (13)$$

The S'_{T2} is the nondimensional specific shearing strength in the cross-section plane "2", and it depends on the ratio *h/b* only. Values of $S'_{T2(a)}$ are given in the lower half of Table 2, row "a", and ratios $S'_{T2(b)}/S'_{T2(a)}$ and $S'_{T2(c)}/S'_{T2(a)}$ in the rows "b/a" and "c/a". The last ratio equals zero because the filling pattern in the case (c), Fig.1, forms an unstable structure incapable of carrying shearing, so that we have put $S'_{T2(c)} = 0$ for all *h/b*. Actually the third case has very low shearing capacity at the level of the outer cardboard sheats alone. Yet, this filling pattern has been included in the analysis because it has good specific bending strength.

Table 2 (M)

h/b	0,75	1,00	1,25	1,50	1,75	2,00
a	0,29	0,35	0,40	0,45	0,48	0,52
b/a	0,42	0,42	0,41	0,41	0,40	0,40
c/a	1,43	0,74	0,76	0,77	0,78	0,79

Table 2 (T)

h/b	0,75	1,00	1,25	1,50	1,75	2,00
a	0,049	0,050	0,049	0,046	0,044	0,041
b/a	0,42	0,42	0,42	0,41	0,40	0,40
c/a	0,00	0,00	0,00	0,00	0,00	0,00

5. NUMERICAL RESULTS

Numerical results presented in the Tables 1 and 2 give a possiblity of interesting comparison of different filling types introduced in Fig.1. As it was told in the introductori part of this paper, the aim of it was to find out what one of the cases (a), (b) or (c) would be the most suitable from the aspect of bending and shearing load carying capacity. In the practise, of cours, one must take into c++onsideration the other influencing factors like technological evaluation, etc. We will not consider these other aspects in this text but we will restrict us only to the structural strength.

What the three cases considered speak to us? First we see from the Table 1 (M), row „c/a", that the third or (c) case has a an advantage over the others in the sence of the specific bending strength. However the Table 1 (T), rows „b/a" and „c/a" speak that the first or (a) case has an advantage over the other cases in approximately the same proportion. This advantage however slowly diminishes with *h/b* tending to 2.

The Table 2 (M) shows however that the first or (a) case has an even greater advantage in the sence of the specific bending strength over the other cases in almost the whole range of *h/b* ratios considered. The same holds for the specific shearing strength, Table 2 (T).

What would be the best solution considering actions in both cross-section planes? If we assume that the cellular plate is not supported on point supports, and if its in-plane length to height *h* ratio is greater than, say, 6 to 8, than the bending strength S_M would have greater importance.

If the plate is extended in the direction of corrugated wave ridges (longitudinal direction), then the bending in that direction will be decisive, and the case (c) is the best solution. And if the in-plane length to in-plane width of the whole cellular plate are similar, than comparison of the Table 1 (M) and Tables 2 (M) speaks that the case (a) is the best solution. It is on the specific demand and on the designers sence to choose between these two types of filling in every particular situation.

6. CONCLUSION

This paper analyses three different filling types for simple cellular cardboard plates made with corrugated mid-layer. The aim of the analysis was to find out what filling case is the most suitable regarding strengthening in bending and shearing mode. The filling patterns were chosen so as to reusing of the recycled cardboard sheats is possible. The comparison was made on the basis of the specific capacities – allowed load-to-qunatity of material used. The numerical data obtained show that if the accent is put to bending mode in a general case of load carying capacity, then the last case has advantage in longer plates, and that the first case has an advantage for shorter plates. However, the third case has very low shearing capacity at the level of the outer cardboard sheats alone, and that is its significant disadvantage over the first two cases.

REFERENCES

[1] Rodin A., *Ambala`a od valovitog kartona*, "Progres", Zagreb, 1964.

[2] Jones R. M., *Mechanics of Composite Materials*, Mc-Graw-Hll Book Company, 1975.

[3] D. Ruzic, *Otpornost konstrukcija*, Masinski Fakultet u Beogradu, Beograd, 1995.

[4] Jovicic N., *Upravljanje cvrstim otpadom*, Masinski Fakultet Univerziteta u Kragujevcu, 2004.

[5] Krgovic M., Perviz O., *Graficki materijali*, Tehnolosko-metalurski fakultet, Beograd, 2005.

[6] Milovancevic M., Dedic M., *Critical Transverse Pressure of A Composite Plate with Mid-layer made of Longitudinal Strips*. Proceedings of the Fifth International Conference 'Heavy Machinery HM '05', Kraljevo, Yugoslavia, June 28th – 30th, 2005., pp. I C. 25-28.

[7] Dedic M., *An Analysis of Local Stability of Composite Plate with Stripped Mid-layer*, Proceedings of the Fifth International Conference 'Heavy Machinery HM '05', Kraljevo, Yugoslavia, June 28th – 30th, 2005., pp. I C. 33-36.

[8] Krgovic M., Osap D., Konstantinovic V., Perviz O., Uskokovic P., *Ispitivanje grafickih materijala*, Tehnolosko-metalurski fakultet, Beograd, 2006.

A DEFORMATION ANALYSIS OF A SPATIAL TRUSS BEAM WITH TRIANGULAR CROSS-SECTION BY MEANS OF CONTINUUM MODELING

M. Todorovic, M. Dedic

Abstract: *Deformation analysis of truss beams constant cross-section can be done by means of continuum beam with bulk cross-section, which enables us to use formulas from the Strength of materials. This paper presents a procedure for calculating the equivalent bending and equivalent shearing rigidity of a truss beam as a whole. The paper considers a cantilever beam truss with repeating cells and constant triangular cross-section loaded by force at its free end. The expressions obtained are analyzed for different numbers of cells. The bending and shearing rigidity are analyzed both separately and in their relation.*

Key words: *1) Spatial trusses, 2) Continuum modeling, 3) Equivalent bending rigidity, 4) Equivalent shearing rigidity*

1. INTRODUCTION

Truss beams with repeated cells are widely used in load carrying structures. Their main advantages over continuum beams are easy manufacturing, low costs and low weight-to-load capacity ratio. To calculate their deformations one needs a lot of work, so that the finite element method (FME) is an inevitable tool for that task. Because of that researchers have made a significant effort in the last two decades in trying to replace a real truss with repeated cells by an equivalent continuum beam, so that the simple formulas for deformations like those in Strength of materials can be applied.

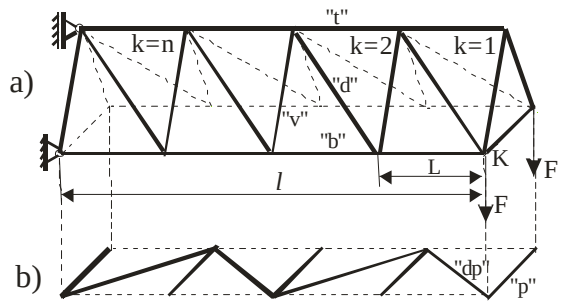

Fig. 1. The spatial truss with triangular cross-section

The theory of continuum beams was presented in [1]. Various approaches to continuum modeling of trusses with repeated cells have been presented in [2] to [6]. The procedure elaborated in this paper is based on the theory of the same authors in [7] and [8], and it enables analytical observing of particular structural parameters cell number, bar cross-section areas, diagonal angle, etc.

2. THE END DEFLECTION OF THE TRUSS

In this paper we consider a statically determinate cantilever truss beam, Fig.1(a), of n repeated cells. It is shown with the bottom set of filling bars detached in Fig.1(b) for the sake of clarity. It has unidirectional filling diagonals, and triangular cross-section with the side angle α, Fig.2(a). All the cells have the length L and height h, so that the diagonal bars angle β in side plane is constant. Thereby the overall length of the truss is $l = nL$. The truss is loaded by two forces F at the free end.

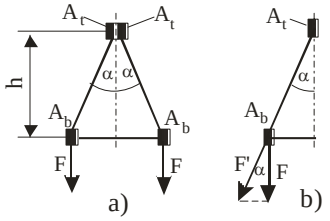

Fig. 2. The cross-section of the truss

We assume the following properties and notation rules for the side bars: bottom longitudinal bars have index "b", length L and cross-section area A_b, transverse side bars "v", l_v, A_v and diagonal bars "d", l_d and A_d, see Fig.1(a) and (b). In order to use symmetry of the truss cross-section, Fig.2(a), the top longitudinal bars, index "t", have the cross-section area $2A_t$. Due to that one A_t belongs to one symmetric half of the truss, Fig.2(b), and one A_t is strained by force N_t.

In the bottom side of the truss, Fig.1(a), the transverse bars are indexed "p", their length is l_p and cross-section area A_p. For the bottom diagonal bars we put "dp", l_{dp} and A_{dp}. These bars are shown in

Milica Todorovic, Lecturer, Higher Technical School, Trstenik, mtodorovic_vtms@yahoo.com
Milan Dedic, Professor, Faculty of Mechanical Engineering in Kraljevo, dedic.m@mfkv.kg.ac.yu

continuous lines in Fig.1(b). The rightmost "*v*" and "*p*" bars are indexed *k = 0*, so that *k*-th transverse bars belong to *k*-th cell.

We observe one symmetric half of the truss loaded by one force *F* at its free end, Fig.2(b). The bar forces are calculated from the equilibrium conditions. The side bar forces can be expressed in terms of force *F* or its component $F'=F/\cos\alpha$ as follows:

$$N_b(k)=\frac{k(F/\cos\alpha)}{tg\beta}=\frac{kF'}{tg\beta}$$

$$N_t(k)=\frac{(k-1)(F/\cos\alpha)}{tg\beta}=\frac{(k-1)F'}{tg\beta}$$

$$N_v(k)=\frac{F}{\cos\alpha}=F'$$

$$N_d(k)=\frac{(F/\cos\alpha)}{\sin\beta}=\frac{F'}{\sin\beta} \qquad (1)$$

The expressions for forces in the side bars as functions of *F'* have the same form as the corrseponidng forces in the planar truss as functions of *F*, Fig.3, which we are going to utilize in our argument to come.

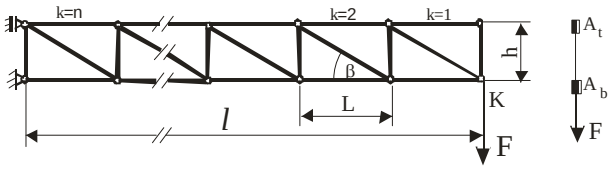

Fig. 3. The planar truss

The rightmost vertical and top bars are unstressed but they are kept for the reason of structural continuity. The "*b*" and "*v*" bars are in compression, and "*t*" and "*d*" bars in tension. All the filling bars in the bottom set are unstressed, except the free end transverse bar ("*p*" for *k* = 0) which is in compression:

$$N_p(0)=\frac{F}{\cos\alpha}\sin\alpha=Ftg\alpha \qquad (2)$$

The strain energy A_d of the one half of the truss is sum of the strain energies of all bars belonging to it:

$$A_d=\sum_{k=1}^{n}A_{db}+\sum_{k=1}^{n}A_{dt}+\sum_{k=1}^{n}A_{dv}+\sum_{k=1}^{n}A_{dd}+A_{dp(0)}$$

where the last term is actually taken in one half of the "*p*" bar. The Castigliano's theorem applied to A_d gives for the deflection of point K:

$$f_K=\frac{\partial A_d}{\partial F} \qquad (3)$$

The result can be expressed as sum of three components: 1) f_B which contains all the longitudinal bars properties A_b and A_t, 2) f_S containing all the side filling bars properties A_v and A_d, and 3) f_P caused by the end "*p*" bar with A_p:

$$f_B=\frac{Fl^3}{3E}\left[\frac{1}{h^2A_b}\left(1+\frac{3}{2n}+\frac{1}{2n^2}\right)+\frac{1}{h^2A_t}\left(1-\frac{3}{2n}+\frac{1}{2n^2}\right)\right] \qquad (4)$$

$$f_S=\frac{Fl}{E}\left[\frac{tg\beta}{A_v}+\frac{1}{\sin^2\beta\cos\beta\,A_d}\right]\frac{1}{\cos^2\alpha} \qquad (5)$$

$$f_P=\frac{Fl}{EA_p}\frac{\sin^3\alpha}{\cos^2\alpha}tg\beta\frac{1}{n} \qquad (6)$$

Eqs. (4) and (5) have appeared after using summation formulas for series of integer powers *k* and k^2, and by changing $h = L\,tg\beta$, $l_d = L/\cos\beta$, $L = l/n$, $h=l_v\cos\alpha$.

In the papers [7] and [8] of the same authors it has been shown that the component f_B corresponds to the *structural bending* of the truss as a whole, and the second component f_S corresponds to the *structural shearing* of the truss. However, no bar is either bent or sheared because they are all pin jointed!

To simplify the formulations of (4) and (5) we introduce new quantities:

$$I^f_{xe}(n)=\left[\frac{1}{h^2A_b}\left(1+\frac{3}{2n}+\frac{1}{2n^2}\right)+\frac{1}{h^2A_t}\left(1-\frac{3}{2n}+\frac{1}{2n^2}\right)\right]^{-1} \qquad (7)$$

$$S_{etr}=E\left[\frac{tg\beta}{A_v}+\frac{1}{\sin^2\beta\cos\beta\,A_d}\right]^{-1}\cos^2\alpha \qquad (8)$$

The final expression for the deflection f_K will read after summing up all the components:

$$f_K=\frac{Fl^3}{3EI^f_{xe}(n)}+\frac{Fl}{S_{etr}}+\frac{Fl}{EA_p}\frac{\sin^3\alpha}{\cos^2\alpha}tg\beta\frac{1}{n} \qquad (9)$$

The formula for the free end deflection of a continuum cantilever beam with cross-section area *A* and the shearing modulus *G*, derived in Strength of materials, reads:

$$f_K=\frac{Fl^3}{3EI_x}+\kappa\frac{Fl}{GA} \qquad (10)$$

The first term in (10), which is consequence of bending, contains the *bending rigidity* EI_x. The second term, which is consequence of shearing, contains the *shearing rigidity* GA/κ. Parameter κ, called the *shearing number*, takes into account how the cross-section's shape influences the distribution of shearing stress.

Obviously $I^f_{xe}(n)$ in (9) is an *equivalent axial moment of inertia*, and product $EI^f_{xe}(n)$ represents an *equivalent bending rigidity*. The S_{etr} is an *equivalent shearing rigidity*. We see that unlike usual moment of inertia I_x of continuous beams the $I^f_{xe}(n)$ depends on the cell number *n*!

The free end deflection of the planar truss in Fig.3, elaborated in details in [7] and [8], has the form:

$$f_K=\frac{Fl^3}{3EI^f_{xe}(n)}+\frac{Fl}{S_e} \qquad (11)$$

Components f_B and f_S have the same form in the expressions (9) and (11), and component f_P , of course, does not appear in the expression for the planar truss. One should only bear in mind that, unlike to the planar truss, the quantity h in $I^f_{xe}(n)$ represents the height of the truss cross-section and not the length of the "v" bars. The equivalent shearing rigidity S_{etr}, of the spatial truss differs from the one for planar truss in the term $cos^2\alpha$. One can conclude that formula (11) for f_K of planar truss may be used for spatial trusses with triangular cross-section, if the proper correction is applied.

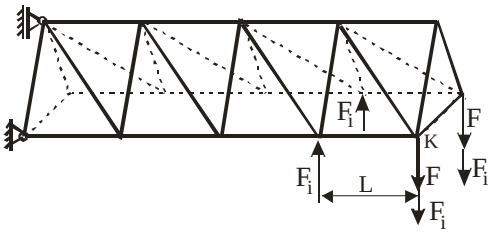

Fig. 4. The dummy forces for calculating slope

3. THE END SLOPE OF THE TRUSS

To calculate the slope γ relative to the horizontal of the end bottom bar, the bar ending in the point K, we introduce two pairs of dummy forces F_i that make dummy moments $M_i = LF_i$ shown in Fig.4. The bar forces are calculated as functions of these dummy forces, they are changed in the expression for A_d and the Castigliano's theorem is applied:

$$\gamma_K = \left.\frac{\partial A_d}{\partial M_i}\right|_{M_i=0} \tag{12}$$

The slope obtained again contains three terms:

$$\gamma_K = \frac{F\,l^2}{2EI^{\gamma}_{xe}(n)} + \frac{F}{S_{etr}} + \frac{F}{EA_p}\frac{sin^3\alpha}{cos^2\alpha}tg\beta \tag{13}$$

where the equivalent axial moment of inertia $I^{\gamma}_{xe}(n)$ is:

$$I^{\gamma}_{xe}(n) = \left[\frac{1}{h^2A_b}\left(1+\frac{1}{n}\right)+\frac{1}{h^2A_t}\left(1-\frac{1}{n}\right)\right]^{-1} \tag{14}$$

The corresponding formula for the continuum cantilever beam loaded by one force F at its free end would read:

$$\gamma_K = \frac{F\,l^2}{2EI_x} + k\frac{F}{GA} \tag{15}$$

so that we can see the full analogy between components in expressions (13) and (15).

4. THE GENERALIZED FORMS OF THE EQUIVALENT RIGIDITIES

Expressions (7) and (14) for equivalent moments of inertia have the similar form, and can be put in the form:

$$I_{xe}(n) = \left[\frac{K_b(n)}{h^2A_b} + \frac{K_t(n)}{h^2A_t}\right]^{-1} \tag{16}$$

The superscripts "f" in (7) and "γ" in (14) indicate they are linked to the type of deformation. This difference is contained in coefficients $K_b(n)$ and $K_t(n)$ so that we can write:

$$K^f_b(n) = 1+\frac{3}{2n}+\frac{1}{2n^2} \qquad K^f_t(n) = 1-\frac{3}{2n}+\frac{1}{2n^2} \tag{17}$$

$$K^{\gamma}_b(n) = 1+\frac{1}{n} \qquad K^{\gamma}_t(n) = 1-\frac{1}{n} \tag{18}$$

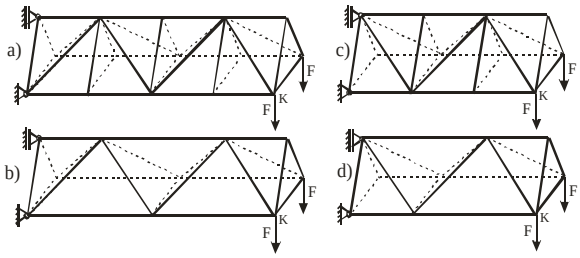

Fig. 5. Different types of the filling patterns

Coefficients $K_b(n)$ and $K_t(n)$ depend also on the filling pattern. In case of the filling pattern with even number n shown in Fig.5(a,b) they have the values:

$$K^f_b(n) = 1-\frac{1}{n^2} \qquad K^f_t(n) = 1+\frac{2}{n^2} \tag{19}$$

$$K^{\gamma}_b(n) = 1 \qquad K^{\gamma}_t(n) = 1 \tag{20}$$

and in case of truss with odd number n, Fig.5(c,d):

$$K^f_b(n) = 1+\frac{2}{n^2} \qquad K^f_t(n) = 1-\frac{1}{n^2} \tag{21}$$

$$K^{\gamma}_b(n) = 1+\frac{1}{n^2} \qquad K^{\gamma}_t(n) = 1-\frac{1}{n^2} \tag{22}$$

The S_{etr} is the equivalent shearing rigidity of a symmetric *triangular* cross-section:

$$S_{etr} = E\left[\frac{tg\beta}{A_v}K_v + \frac{1}{sin^2\beta\cos\beta\cdot A_d}\right]^{-1}cos^2\alpha \tag{23}$$

Coefficients $K_v(n)$ in that expression have the forms:

- for the filling type in Figs.1 and 4:

$$K^f_v(n) = K^{\gamma}_v(n) = 1$$

- for the filling type in Fig.5(a,b):

$$K^f_v(n) = K^{\gamma}_v(n) = 0$$

- for the filling type in Fig.5(c,d):

$$K_v^f(n) = K_v^\gamma(n) = \frac{1}{n}.$$

5. NUMERICAL RESULTS

Value of the equivalent axial moment of inertia $I_{xe}^f(n)$, formula (7), depends on the cross-section areas of the longitudinal bars, of the truss height h and the number of cells n. With increasing n it converges to the axial moment of inertia I_{xLB} of the truss cross-section calculated solely over the cross-section areas of longitudinal bars:

$$I_{xLB} = \left[\frac{1}{h^2 A_b} + \frac{1}{h^2 A_t}\right]^{-1}$$

Convergence of $I_{xe}^f(n)$ to I_{xLB} for the truss cantilever beam, triangular cross-section and data: A_b = 3,6cm^2, A_t = 1,98cm^2, h = 75cm, diagonal angle $\beta = 30^0$, is given in the Table.

The fractions of deflection components to the total deflection of the truss are also given in the Table. With increasing n the bending component is f_B ever more influential. However in short trusses the high fraction of the shearing component f_S is conspicuous, and it does not drop under 5% even for n = 8. The influence of the bottom (horizontal) filling bars is negligible (1,8% even for n = 2) so that it may be ommitted from the analysis.

Table 1.

n	2	4	6	8	10	12
$\frac{I_{xe}^f(n)}{I_{xeLB}}$	1,102	1,084	1,062	1,049	1,040	1,034
f_B / f	0,519	0,815	0,910	0,948	0,966	0,976
f_S / f	0,479	0,185	0,090	0,052	0,034	0,024
f_P / f	0,0018	0,0004	0,0001	0,000	0,000	0,000

6. CONCLUSION

This paper presents a simple and effective procedure for calculating deflection and slope of a spatial truss beam with repeated cells with triangular cross-section. The formulas for the equivalent bending and shearing rigidity of the truss have been derived, which enable easy and quick calculating its displacements. They are analogous to the well known Strength of materials formulas for continuum cantilever beam. The formulas are suitable for analyzing the influence of particular design data.

Numerical results obtained illustrate the influence level of particular deformation components of the total deformation as function on cell number n. The shearing component has high fraction for short trusses, while the fraction of the bottom filling bars is negligible in the most practical cases.

REFERENCES

[1] Timoshenko S. P., Goodier J. N.*: Teorija elasticnosti*, Gradjevinska knjiga, Beograd, 1962.

[2] Kenner W. S.: *Lattice Truss Structural Response Using Energy Methods***,** North Carolina A&T State University, A Thesis Submitted to the Faculty of Old Dominion University in Partial Fulfillment of the Requirement for the Degree of Master of Sciences, 129 pages, NASA-TM-112361, 1987.

[3] Noor A. K., Mikulas M. M.: *Continuum Modeling of Large Lattice Structures*, Status and Projections, NASA Technical Paper 2767, pp.1-10, 1988.

[4] Burgardt B., Cartraud P.: *Continuum Modelling of Beamlike Lattice Trusses*, Advances in Computational Techniques for Structural Engineering, pp. 51-59, August 21-23, Budapest, Hungary, 1996.

[5] Savkovic M., Gasic M., Ostric D.: *Metoda uproscavanja izraza za savojnu krutost prostornih resetkastih konstrukcija*, 23th JUPITER Conference, pp. 373-379, Belgrade, 1997.

[6] Teughels A., De Roeck G.: *Continuum Models for Beam- and Platelike Lattice Structures*, IASS-IACM 2000 Fourth International Colloquium of Computations of Shell & Spatial Structures, pp.1-20, June 5-7, Channia Crete, Greece, 2000.

[7] Dedić M., Todorović M.: *An Analysis of The Equivalent Stiffness of Beam-like Trusses with Constant Cross-section*, Congress of Theoretical and Applied Mechanics, pp 347-352, April 10-13, Kopaonik, 2007.

[8] Todorović M., Dedić M.: *An Analysis of The Deformation of a Beam-like Truss Structure Using Method of Equivalent Continuum Beam*, 7th International Conference ″Research and Development in Mechanical Industry″ RaDMI 2007, 16 - 20. September 2007, Belgrade, Serbia, pp. 670-674, 2007.

ANALYTICAL SOLUTION OF THE THREE-DIAGONAL, FIRST ORDER, LINEAR HOMOGENOUS DIFFERENTIAL EQUATIONS SYSTEM WITH CONSTANT COEFFICIENTS

U. Bugarić, D. Petrović, D. Glišić

Abstract: *The explicit analytical expression as a solution of three-diagonal, first order, linear homogenous differential equations system with constant coefficients is given. A corresponding system of n first order linear homogenous differential equations is solved (n - integer number, n ≥ 2). Detail analytical procedure of solving differential equations system is presented. Obtained analytical expression consists only of elementary mathematical functions.*

Keywords: *Chebyshev polynomial, analytical solution, queuing theory*

1. INTRODUCTION

Explicit analytical solution of differential equations systems with number of equations less then five always exists, but if the number of equations is greater then five analytical solution of differential equations systems rarely exists and if they exists their obtaining tend to be quite difficult and complicated. Particularly, general analytical solution of differential equation systems with arbitrary number of equations rarely exists. As it is well known all those difficulties are in most cases connected with problem of finding roots of characteristic polynomial.

Three-diagonal, first order, linear homogenous differential equations system with constant coefficients is used in queuing theory for defining system state probabilities of continuous-time Markov process of a birth-death type defined on finite state space. [4]

2. DEFINITION OF THE PROBLEM

Three-diagonal, first order, linear homogenous differential equations system with constant coefficients has the following form:

$$\begin{aligned} y_1'(x) &= \alpha \cdot y_1(x) + \beta \cdot y_2(x) \\ &\vdots \\ y_i'(x) &= \gamma \cdot y_{i-1}(x) + \alpha \cdot y_i(x) + \beta \cdot y_{i+1}(x); \\ i &= 2, ..., n-1 \\ &\vdots \\ y_n'(x) &= \gamma \cdot y_{n-1}(x) + \alpha \cdot y_n(x) \end{aligned} \qquad (1)$$

where α, β and γ are constant coefficients, y_i is function of x, $y_i'(x)$ is first derivation of $y_i(x)$ per x i.e. $y_i'(x) = dy_i(x)/dx$, i=0, 1, ..., n, while x is independent variable.

System (1) can be written in matrix form as:

$$\mathbf{Y'}(x) = \mathbf{Q} \times \mathbf{Y}(x)$$

where

$$\mathbf{Q} = \begin{bmatrix} \alpha & \beta & 0 & 0 & . & 0 & 0 & 0 \\ \gamma & \alpha & \beta & 0 & . & 0 & 0 & 0 \\ 0 & \gamma & \alpha & \beta & . & 0 & 0 & 0 \\ . & . & . & . & . & . & . & . \\ 0 & 0 & 0 & 0 & . & \gamma & \alpha & \beta \\ 0 & 0 & 0 & 0 & . & 0 & \gamma & \alpha \end{bmatrix}_{n \times n} \qquad (2)$$

and $\mathbf{Y'}(x) = [\, y_i'(x)]_{n\times 1}$, $\mathbf{Y}(x) = [\, y_i(x)]_{n\times 1}$ are column vectors.

It is important to notice that all terms of matrix **Q** are equal to zero except ones on the main, upper and lower diagonals (three-diagonal system).

3. GENERAL PROCEDURE FOR PROBLEM SOLVING

General solutions of the first order linear homogenous differential equations system, defined with (1), has the following form: [5]

$$\begin{aligned} y_1(x) &= C_1 \cdot B_1^{(r_1)} \cdot \exp(r_1 \cdot x) + C_2 \cdot B_1^{(r_2)} \cdot \exp(r_2 \cdot x) + ... \\ &... + C_n \cdot B_1^{(r_n)} \cdot \exp(r_n \cdot x) \\ y_2(x) &= C_1 \cdot B_2^{(r_1)} \cdot \exp(r_1 \cdot x) + C_2 \cdot B_2^{(r_2)} \cdot \exp(r_2 \cdot x) + \\ &... + C_n \cdot B_2^{(r_n)} \cdot \exp(r_n \cdot x) \\ &\vdots \end{aligned} \qquad (3)$$

Uglješa Bugarić, Faculty of Mechanical Engineering Belgrade
Dušan Petrović, Faculty of Mechanical Engineering Belgrade
Dušan Glišić, Spinnaker New Technologies, Belgrade

$$y_n(x) = C_1 \cdot B_n^{(r_1)} \cdot \exp(r_1 \cdot x) + C_2 \cdot B_n^{(r_2)} \cdot \exp(r_2 \cdot x) + ...$$
$$... + C_n \cdot B_n^{(r_n)} \cdot \exp(r_n \cdot x)$$

where
C_j (j=1, 2, ..., n) – are integration constants which should be determined upon initial values y_i (i=0, 1, ..., n); r_j (j=1, 2, ..., n) – are eigenvalues of matrix **Q**; while column matrices $\mathbf{B}^{(r_j)}$ are eigenvectors of matrix **Q** which corresponds to eigenvalue r_j. Eigenvector $\mathbf{B}^{(r_j)}$ has the following form:

$$\mathbf{B}^{(r_j)} = \left[B_i^{(r_j)} \right]_{n \times 1}; \text{ (i=1, 2, ..., n).}$$

Eigenvalues will be determined as roots of characteristic polynomial of matrix **Q**, while characteristic polynomial will be obtained by expanding of the characteristic determinant of matrix **Q** [2]. Characteristic determinant of matrix **Q** is defined as $\det(r \cdot \mathbf{E} - \mathbf{Q})$, where matrix $(r \cdot \mathbf{E} - \mathbf{Q})_{n \times n}$ is characteristic matrix of matrix **Q** and **E** is unit matrix.

Expanding of the characteristic determinant and obtaining of the characteristic polynomial of matrix **Q** will be done by using difference equations i.e. homogeneous linear difference equation with constant coefficients will be solved. [1]

Eigenvectors $\mathbf{B}^{(r_j)}$ are defined with matrix equation:

$$(r_j \cdot \mathbf{E} - \mathbf{Q}) \times \mathbf{B}^{(r_j)} = 0, \qquad (4)$$

for each eigenvalue r_j (j=1,2, ..., n). Matrix equation (4) is in fact system of homogeneous linear equations.

4. DERIVATION OF THE ANALYTICAL EXPRESSION

As it was said in previous chapter characteristic polynomial will be obtained by expanding of the characteristic determinant. Determinant D_n, which will be expanded into polynomial, can be written as:

$$D_n = \det(r \cdot \mathbf{E} - \mathbf{Q}) =$$

$$= \begin{vmatrix} r-\alpha & -\beta & 0 & 0 & . & 0 & 0 & 0 \\ -\gamma & r-\alpha & -\beta & 0 & . & 0 & 0 & 0 \\ 0 & -\gamma & r-\alpha & -\beta & . & 0 & 0 & 0 \\ . & . & . & . & . & . & . & . \\ 0 & 0 & 0 & 0 & . & -\gamma & r-\alpha & -\beta \\ 0 & 0 & 0 & 0 & . & 0 & -\gamma & r-\alpha \end{vmatrix}$$

where n is number of rows and columns i.e. dimension of the determinant.

Also determinant D_n can be written as:

$$D_n = (r-\alpha) \cdot D_{n-1} - \gamma \cdot \beta \cdot D_{n-2}, \qquad (5)$$

where determinants D_{n-1} and D_{n-2} have the same form as determinant D_n but their dimensions are (n–1) and (n–2).

Expression (5) presents second order homogeneous linear difference equation with constant coefficients. For its solution D_n should be substituted with u^n. [1]

Solution of difference equation (5) is:

$$D_n = a \cdot (u_1)^n + b \cdot (u_2)^n,$$

where u_1 and u_2 are solutions of equation $u^2 - (r-\alpha) \cdot u + \gamma \cdot \beta = 0$, and have following values:

$$u_1 = 0.5 \cdot \left[(r-\alpha) + \sqrt{t} \right], \quad u_2 = 0.5 \cdot \left[(r-\alpha) - \sqrt{t} \right],$$

while a and b are arbitrary constants which should be determined upon initial values and $t = (r-\alpha)^2 - 4 \cdot \gamma \cdot \beta$.

Initial values for determining arbitrary constants a and b are:

$$D_1 = r-\alpha; \; D_2 = \begin{vmatrix} r-\alpha & -\beta \\ -\gamma & r-\alpha \end{vmatrix} = (r-\alpha)^2 - \gamma \cdot \beta.$$

System of two linear equations from which arbitrary constants a and b should be determined is:

$$D_1 = a \cdot u_1 + b \cdot u_2; \; D_2 = a \cdot (u_1)^2 + b \cdot (u_2)^2.$$

Expressions for arbitrary constants a and b are:

$$a = \frac{1}{2} \cdot \frac{r-\alpha+\sqrt{t}}{\sqrt{t}}; \; b = -\frac{1}{2} \cdot \frac{r-\alpha-\sqrt{t}}{\sqrt{t}}.$$

Finally, determinant i.e. polynomial D_n has the following form:

$$D_n = \frac{1}{2^{n+1}} \cdot \frac{\left[r-\alpha+\sqrt{t} \right]^{n+1}}{\sqrt{t}} - \frac{1}{2^{n+1}} \cdot \frac{\left[r-\alpha-\sqrt{t} \right]^{n+1}}{\sqrt{t}} \qquad (6)$$

Reverting values substituted with t and using elementary algebra transformations expression for D_n can be written as:

$$D_n = \frac{1}{2}\cdot\left(\sqrt{\gamma\cdot\beta}\right)^n \cdot \frac{\left[X+\sqrt{X^2-1}\right]^{n+1} - \left[X-\sqrt{X^2-1}\right]^{n+1}}{\sqrt{X^2-1}}. \quad (7)$$

where X is substituting expression $\frac{r-\alpha}{2\cdot\sqrt{\gamma\cdot\beta}}$.

If expression (7) is multiplied and divided with (n+1) at the same time, it takes following form:

$$D_n = \frac{\left(\sqrt{\gamma\cdot\beta}\right)^n}{n+1}\cdot\frac{1}{2}\cdot(n+1)\cdot\frac{\left[X+\sqrt{X^2-1}\right]^{n+1} - \left[X-\sqrt{X^2-1}\right]^{n+1}}{\sqrt{X^2-1}} \quad (8)$$

Expression

$$\frac{1}{2}\cdot(n+1)\cdot\frac{\left[X+\sqrt{X^2-1}\right]^{n+1} - \left[X-\sqrt{X^2-1}\right]^{n+1}}{\sqrt{X^2-1}} \quad (9)$$

presents first derivation of the Chebyshev polynomial of the first kind of order (n+1) i.e. dT_{n+1}/dr: [3]

$$T_{n+1} = \frac{1}{2}\cdot\left\{\left[X+\sqrt{X^2-1}\right]^{n+1} - \left[X-\sqrt{X^2-1}\right]^{n+1}\right\},$$

which should be also written in trigonometric form as:

$$T_{n+1} = \cos\left[(n+1)\cdot\arccos X\right].$$

First derivation of previous expression (dT_{n+1}/dr) is:

$$\frac{dT_{n+1}}{dr} = \frac{1}{2}\cdot(n+1)\cdot\frac{1}{\sqrt{\gamma\cdot\beta}}\cdot\sin\left[(n+1)\cdot\arccos X\right]\cdot\frac{1}{\sqrt{1-X^2}}$$

By substituting previous expression instead of expression (9) into expression (8), reverting values substituted with X finally D_n can be written in form suitable for obtaining eigenvalues:

$$D_n = \left(\sqrt{\gamma\cdot\beta}\right)^{n-1}\cdot\frac{1}{2}\cdot\sin\left[(n+1)\cdot\arccos\left(\frac{r-\alpha}{2\cdot\sqrt{\gamma\cdot\beta}}\right)\right]\cdot\frac{1}{\sqrt{1-\left(\frac{r-\alpha}{2\cdot\sqrt{\gamma\cdot\beta}}\right)^2}} \quad (10)$$

Roots of polynomial (10) i.e. eigenvalues of matrix **Q** will be obtained from following equation:

$$\sin\left[(n+1)\cdot\arccos\left(\frac{r-\alpha}{2\cdot\sqrt{\gamma\cdot\beta}}\right)\right] = 0.$$

Eigenvalues of matrix **Q** are:

$$r_j = 2\cdot\sqrt{\gamma\cdot\beta}\cdot\cos\left(\frac{j\cdot\pi}{n+1}\right)+\alpha;\ j = 1, 2, ..., n. \quad (11)$$

Eigenvectors, defined with matrix equation (4), will be obtained for each eigenvalue in a following way: [5]

$$B_i^{(r_j)} = K_{1,i}^{(r_j)} / K_{1,1}^{(r_j)};\ i = 1, 2, ..., n;\ j = 1, 2, ..., n,$$

where $B_i^{(r_j)}$ is i-th element of eigenvector which corresponds to the j-th eigenvalue. $K_{1,1}^{(r_j)}$ is cofactor (signed minor) which corresponds to the element of matrix ($r_j\cdot\mathbf{E} - \mathbf{Q}$) in first row and first column for j-th eigenvalue and $K_{1,i}^{(r_j)}$ is cofactor which corresponds to the element of matrix ($r_j\cdot\mathbf{E} - \mathbf{Q}$) in first row and i-th column for j-th eigenvalue.

Cofactors $K_{1,1}^{(r_j)}$ are in fact determinants D_{n-1} for j-th eigenvalue, defined with expression (7). Therefore their values can be obtained by substituting $r = r_j$, (j=1, 2, ..., n) in expression (7).

Analyze of matrix ($r_j\cdot\mathbf{E} - \mathbf{Q}$) structure shows that cofactors $K_{1,i}^{(r_j)}$ are also determinants D_{n-i} (dimension of those determinants is n–i) for j-th eigenvalue. Their values can be obtained by substituting $r = r_j$, (j=1, 2, ..., n) in expression (7).

For eigenvalues $r_j = 2\cdot\sqrt{\gamma\cdot\beta}\cdot\cos\left(\frac{j\cdot\pi}{n+1}\right)+\alpha$, cofactors $K_{1,1}^{(r_j)}$, $K_{1,i}^{(r_j)}$ and elements of eigenvector $B_i^{(r_j)}$ after elementary trigonometric transformations, has following values:

$$K_{1,1}^{(r_j)} = \left(\sqrt{\gamma\cdot\beta}\right)^{n-1}\cdot\frac{\sin\left[n\cdot\left(\frac{j\cdot\pi}{n+1}\right)\right]}{\sin\left(\frac{j\cdot\pi}{n+1}\right)};$$

$$K_{1,i}^{(r_j)} = \gamma^{i-1}\cdot\left(\sqrt{\gamma\cdot\beta}\right)^{n-i}\cdot\frac{\sin\left[(n-i+1)\cdot\left(\frac{j\cdot\pi}{n+1}\right)\right]}{\sin\left(\frac{j\cdot\pi}{n+1}\right)};$$

$$B_i^{(r_j)} = \left(\sqrt{\frac{\gamma}{\beta}}\right)^{i-1}\cdot\frac{(-1)^{j+1}\cdot\sin\left[i\cdot\left(\frac{j\cdot\pi}{n+1}\right)\right]}{\sin\left[n\cdot\left(\frac{j\cdot\pi}{n+1}\right)\right]}, \quad (i = 1, 2, ..., n;\ j=1, 2, ..., n). \quad (12)$$

Finally, by substituting expressions (11) and (12) into expressions (3) and after elementary trigonometric transformations analytical expression as a solution of three-diagonal, first order, linear homogenous differential equations system with constant coefficients is obtained and has following form:

$$y_i(x) = \left(\sqrt{\frac{\gamma}{\beta}}\right)^{i-1} \cdot \sum_{j=1}^{n} C_j \cdot \frac{(-1)^{j+1} \cdot \sin\left[i \cdot \left(\frac{j \cdot \pi}{n+1}\right)\right]}{\sin\left[n \cdot \left(\frac{j \cdot \pi}{n+1}\right)\right]} \cdot e^{\left[2\sqrt{\gamma\beta} \cdot \cos\left(\frac{j\pi}{n+1}\right) + \alpha\right] \cdot x};$$

i=1, 2, ..., n

5. CONCLUSION

In this paper analytical expression as a solution of three-diagonal, first order, linear homogenous differential equations system with constant coefficients is derived. Obtained analytical expression is quite simple and consists only of elementary mathematical functions. Further work could be the determination of integration constants C_j (j=1, 2, ..., n) upon initial values.

REFERENCES

[1] C. M. Bender, S. A. Orszag, Advanced Mathematical Methods for Scientists and Engineers, McGraw-Hill, New York, 1978.

[2] B. P. Demidovich, I. A. Maron, Computational Mathematics, Mir Publishers, Moscow, 1987.

[3] E. Janke, F. Emde, F. Lösch, Tafeln Höherer Funktionen, B. G. Teubner Verlagsgesellschaft, Stuttgart, 1960.

[4] L. Kleinrock, Queueing Systems, Volume I: Theory. John Wiley & Sons, New York, 1975.

[5] C. R. Wylie, L. C. Barrett, Advanced Engineering Mathematics. McGraw-Hill, New York, 1982.

ANALYSIS OF PLATE SPRINGS TYPES AND PACKAGES TENSION FEATURES ACQUIRED BY WORK SIMULATION

J. Nešović

Abstract: *Basic features of plate springs, as well as the analysis of states of tension and fields of deformation acquired by the work simulation in an adequate software of plate springs types and packages are presented in this study. The work simulation of spring plate type and package is quite complex due to friction on connecting surfaces between the spring and the base, as well as the connecting surfaces between the springs themselves. However, the developed model with the use of final contact elements through which friction can be introduced into the construction gives results that almost coincide with the theoretical, i.e. the developed model can be used in practice.*

Key words: *plate spring, tension, work simulation, package, type*

1. PREFACE

The role of spring elements generally in constructions is that they elastically deform under the effect of external load, i.e. they receive the mechanical work and change into the potential deformation energy. Besides, these elements can change the absorbed energy back into mechanical work. Basic values that are important for plate springs are load and deformation. Dependence between the load and the deformation (bend) is called the feature of the spring element, and it can be linear, digressive and progressive. If a spring element load line in a deformational diagram coincides with the unload line then there is no turning of potential energy into heat. On the contrary, a part of mechanical energy can turn into heat, i.e. there is deadens and its influence is positive on the effect of stroke amortization and vibrations reduction.

Plate springs, as spring elements, are used in constructions that have significant length loads (forces), and small movements, that is length deformations (for example vibroisolator on the forge machine [3]) are needed. Besides that, the advantage of these springs reflects in the fact that the feature can be changed by simple addition or removal of spring elements. The major defect of plate springs is uneven distribution of tension on cross section. Depending on thickness, the plate springs can be shaped in three ways, and that: cold shaped ($t<1$ mm), cold shaped with edge cutting and rounding ($1<t<4$ mm) and hot shaped where the edges are processed on leaning areas ($t>4$ mm). Springs with thickness above 4 mm are analyzed in this study.

2. PLATE SPRING FEATURES

Plate springs cone-shaped and they belong to a group of complexly tensed springs. They are usually used as types or packages. The types are composed of a number of springs of same diameters and they can have same or different thicknesses with contact on the edges, while the packages are composed of a number of springs of same thicknesses with contact on surfaces.

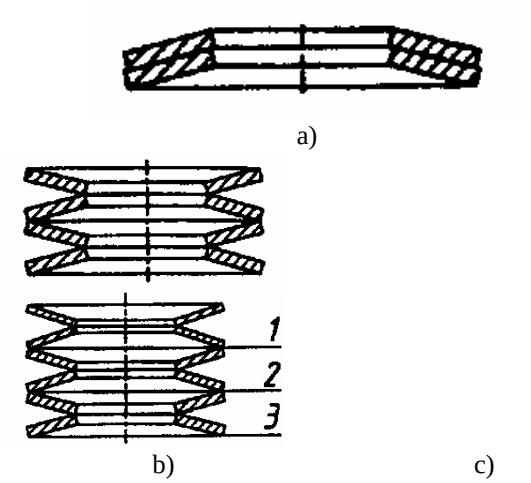

Picture 1. Plate springs package (a), plate springs types (b- spring type, c- different thickness spring type)

Plate springs types and packages are applied with the static load and with dynamic one-way load. The load brings about a complex tension state of a spring where normal tensions due to bending and tensions due to pressure are dominant. Tension distribution on cross section surface of a plate spring is shown in diagram 2.a.

Mr Jovan Nešović, Faculty of Mechanical Engineering Kraljevo

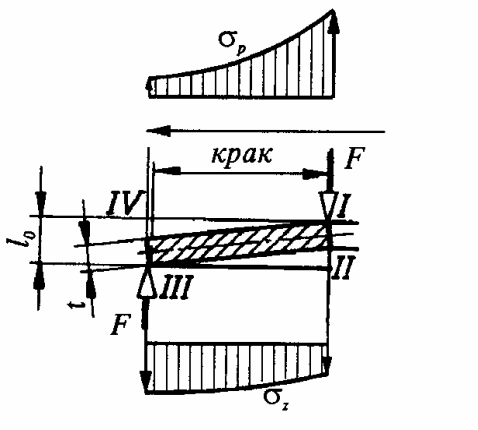

a)

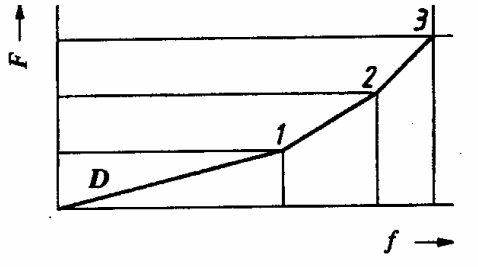

b)

Picture 2. Tension distribution on cross section surface of a plate spring (a) and one of the possible features (b)

Depending on constructional performance, the feature of these spring elements (dependence of force and deformation) can be linear and digressive, and with the use of springs of different thicknesses in types a progressive feature can also be achieved (2.b.).

Important is the fact that a plate spring deformation during exploitation can be up to $f=0{,}75h_o$, because above this value we enter into the field of plastic deformations on contacting surfaces, which is not allowed in constructions.

3. ANALYTICAL ESTIMATE

Based on picture 2.a. we can see that the biggest tensions appear in the points I, II and III, and the equations used for their calculation are the following [1]:

Normal tension in point I (pressure)

$$\sigma_I = k\frac{f}{K_1 \cdot D_e^2}\left[K_2\left(h_o - 0{,}5f\right) + K_3 t\right]$$

Normal tension in point II (tightening)

$$\sigma_{II} = k\frac{f}{K_1 \cdot D_e^2}\left[K_3 \cdot t - K_2\left(h_o - 0{,}5f\right)\right]$$

Normal tension in point III (tightening)

$$\sigma_I = k\frac{f}{K_1 \cdot D_e^2 \cdot \psi}\left[K_4\left(h_o - 0{,}5f\right) + K_3 t\right]$$

In the aforementioned equations, k is the elasticity coefficient and it depends on the kind of material of a plate spring, and the coefficients K_1, K_2, K_3, K_4 are coefficients which derive from tables, $\psi = D_e/D_i$.

Using our example of a spring: f=1 mm, D_i=46 mm, D_e=90 mm, h_o=2 mm, t=5 mm we come to a result that the maximum tension is in point I and it amounts to $\sigma_I = 1285{,}6$ N/mm^2. If a package of two springs of same features (t=10 mm) is used we come to a result that the biggest tension is also in point I and that it amounts to $\sigma_I' = 2234{,}6$ N/mm^2.

4. PLATE SPRING WORK SIMULATION

In order to perform a plate spring work simulation, it is required to perform the modeling in respective software. The volume models in this example are done in Solid Works and the estimate is done in Cosmos. Since the dimensions of plate springs are standardized, and the geometry itself is axis symmetrical, it was enough to define the cross section and to get the spring volume model by revolving afterwards. Spring type as well as spring package is gained by simple operations of addition of modeled single plate springs (picture 3.).

On the basis of the defined volume model we also determine the discretized model, however, the net of final elements which is used in the estimate is of medium density. Reference 1

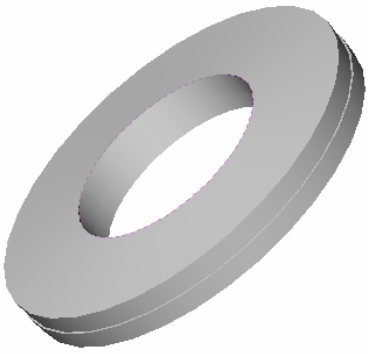

a)

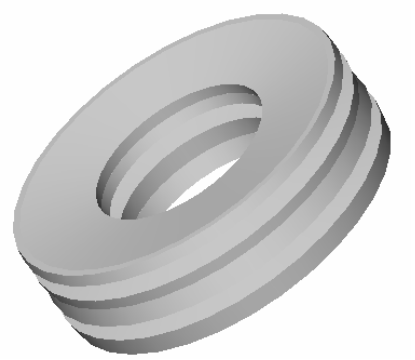

b)

Picture 3. Solid model of plate springs package (a) and of plate springs type (b)

For the estimate to be as accurate as possible, we have to take into consideration the elements that appear in the exploitation while modeling the work of plate spring package and type. In the estimate itself, the body of a spring is modeled with 3D final elements. Since there is friction on contact between the plate spring and the base it also has to be introduced in the model. This has been achieved through the gep final elements and the connection model between these elements is „touch to touch“. The friction coefficient on these contact surfaces is between 0.14 and 0.16, and the coefficient 0.15 has been used in the estimate.

Friction is very distinct when the plate springs are set in package (friction between contact surfaces of springs). When the plate springs are set in type the influence of friction is considerably reduced because the contact surface is significantly smaller, and for that reason it can be disregarded in the analysis.

Determining the assigned loads or desired deformations and supports of the construction itself, by the estimate of the developed models we come to the result that the biggest tensions on pressure are in point I.

As far as plate springs type of different thickness is concerned, the biggest tension is on the first spring (spring with smallest thickness), and it amounts to $\sigma_I' = 1374$ N/mm^2, for the deformation f=2 mm. The whole field of tension and deformation for the analyzed spring type is shown in pictures 4 and 5.

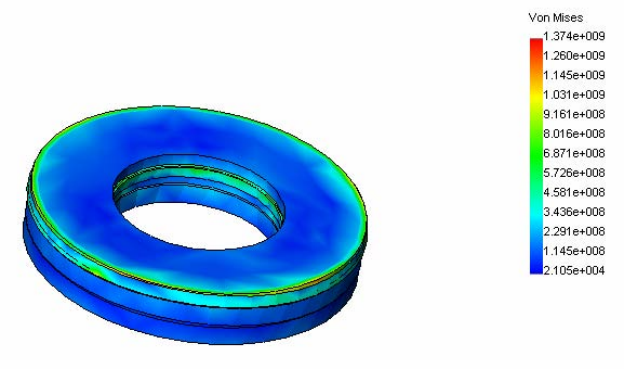

a)

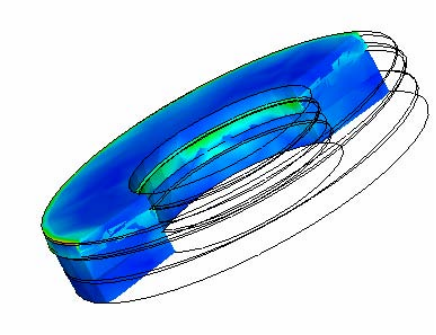

b)

Picture 4. Tension field a) on external surfaces, b) at cross section of plate springs type

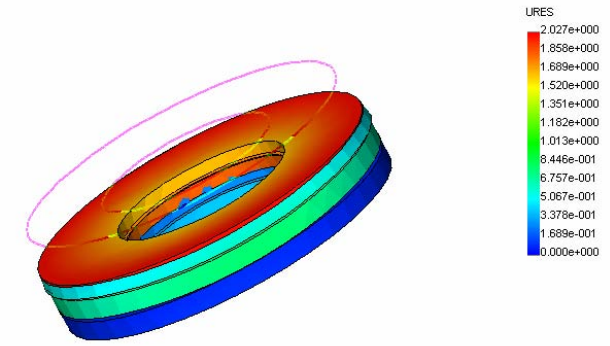

Picture 5. Deformation field of plate springs type of different thickness

With the plate spring packages there is intense friction and it is received for the deformation of f=1 mm, the biggest tension of $\sigma_I' = 2055$ N/mm^2, what is something less than the value received by theoretical analysis. However, that difference is below 10% what makes the developed model good. The tension field and the deformation field of the plate springs type is shown in pictures 6 and 7.

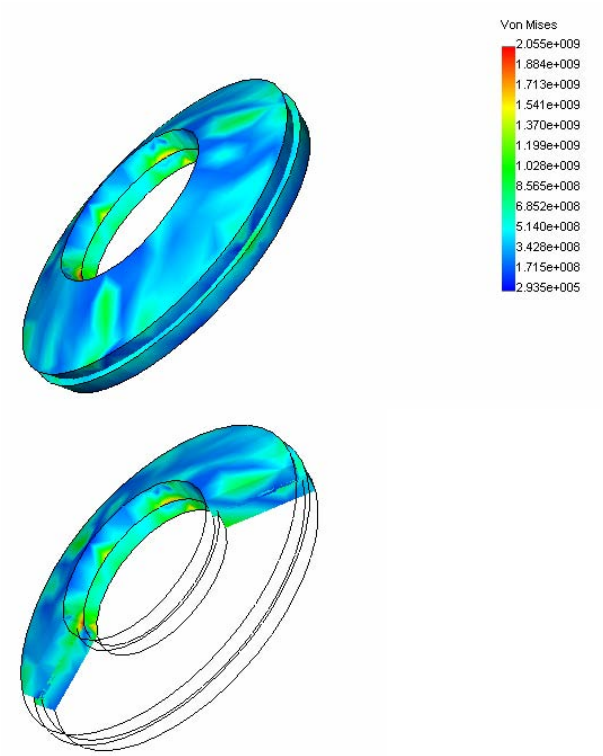

Picture 6. Tension field of plate springs package

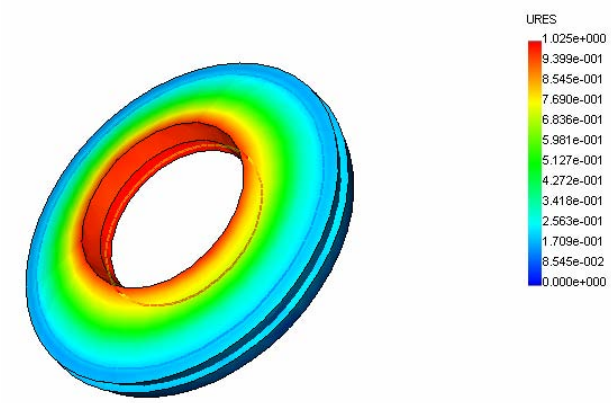

Picture 7. Deformation field of plate springs package

5. CONCLUSION

Based on the obtained results, we conclude that the developed estimation system of plate springs packages and types can be completely applied in practice by MKE. The results of the biggest tensions obtained on the basis of the theoretical analysis and the simulation in the respective software almost coincide; there is a difference of a couple of percent (up to 10%). This gives us the possibility to model different shapes of plate spring types and packages and by introducing different load constellations to relatively quickly obtain the tension states, i.e. different variant of a solution and on basis of everything look for the optimal. Further continuance of these researches can take the direction of plate springs packages work simulation where intense friction is apparent on contact surfaces and the analysis of friction influence on features and tensions.

LITERATURE

[1] Vojislav Miltenović, „Mašinski elementi - oblici, proračun, primena“, Mašinski fakultet Niš, 2002.godina.

[2] Milosav Ognjanović „Mašinski elementi“ , Mašinski fakultet Beograd, 2006. godina.

[3] Ljubodrag Đorđević „Tehnologija postavljanja mašina“ , Mašinski fakultet Kraljevo, 2006. godina.

[4] Jovan Nešović „Istraživanje radne sposobnosti prstenaste opruge odbojnika vagona“ Magistarski rad, Mašinski fakultet Kraljevo, 2000. godina.

[5] Milosav Ognjanović ,, Modeliranje mašinskih sistema, Mašinski fakultet Beograd, 1992. godina.

F SESSION:

PRODUCTION TECHNOLOGIES, MATERIAL APPLICATION AND ENTERPRENEURIAL ENGINEERING AND MANAGMENT

MODEL OF MULTICRITERIA OPTIMIZATION USING COMPLEX CRITERIA FUNCTIONS

M. Kolarevic, M. Vukicevic, M. Bjelic, B. Radicevic

Abstract: *Specific problem in multicriterial optimization is rating of large number of alternatives by using complex multicriteria functions which are composed of subcriteril functions. These papers suggest model which is based at use of average values of pure flow Φ subcriteria functions derived by PROMETHEE III method.*

Key words: *multicriteria optimization, complex multicriteria functions*

1. INTRODUCTION

Family of methods with the full name „Preference Ranking Organization Method for Enrichment Evaluations" which are better known by abbrevation PROMETHEE for multicriterial optimization problem solution has been developed in a variants I, II, III и IV by several authors leadnig with BRANS (BRANS/1982/, BRANS & MARECHAL/1984, 1992, 1994/, BRANS & VINCKE/1985/, MARECHAL/1986, 1988/).

The main features of these methods compared to the corresponding criteria of decision maker are six generelized criteria. Method PROMETHEE I ensures partial order, method PROMETHEE II gives full order, method PROMETHEE III gives interval order of compared alternatives and PROMETHEE IV considers a continuous series of alternatives .

The adoption of decisions on multicriterial optimization problem solving using PROMETHEE methods consists of sequence of delicate phases:

- definition of multicriteria base i.e. system of criteria for alternatives sorting,
- selection of generalized criteria for displaying of preference in relation to the adequate criteria,
- determination of criteria relative weight,
- sorting of alternatives by one of PROMETHEE I-IV, methods,
- decision making
- Specific problems that occurs in multicriterial optimization are criteria for alternatives sorting which consist of subcriterial functions where level of function decomposistion can raise up to (*r*-th) level [3].

Below was shown a model for resolving the aforementioned problems and which is based on transformation of intermediate values of pure stream F subcriterial functions (which are calculated in interval order of compared alternatives of PROMETHEE III method) at level of criterial function of higher order until creation of unique first order criteria.

2. MODEL SOLUTION OF ALTERNATIVES RANKING PROBLEM USING COMPLEX CRITERIAL FUNCTION

Formal writing of problem is given at Table 1, where are:

m – number of alternatives

n – number of *r*-th level criterial functions

s – number of *(r-1)*-th level criterial functions

l - number of *2-nd* level criterial functions

k - number of *1-st* level criterial functions

Criteria functions are characterized by K_j and proper index for observed ranking level. So are the basic criteria presented by criterial function of *1-st* level and characterized by K_j^1. Subcriterial functions i.e. 5-th level are characterized by K_j^5.

Each criteria has its own relative weight which expresses by weight coefficient characterized by W_j^s and by demand for function (criteria) minimization or maximization. It is not necessarily for subcriteria fiunctions of certain level to have the same demand for minimization or maximization.

The problem is solved by using average values of pure flow Φ on the following way:

PhD Milan Kolarevic, Faculty of Mechanical Engineering Kraljevo, *kolarevic.m@mfkv.kg.ac.yu*
PhD Miomir Vukicevic, Faculty of Mechanical Engineering Kraljevo, *vukicevic.m@mfkv.kg.ac.yu*
Miso Bjelic mech. eng., Faculty of Mechanical Engineering Kraljevo, *bjelic.m@mfkv.kg.ac.yu*
Branko Radicevic mech. eng., Faculty of Mechanical Engineering Kraljevo, *radicevic.b@mfkv.kg.ac.yu*

- real values of criteria functions are used only at last r-th level,
- at other ranking levels, as values of subcriteria functions are introduced transformed values of pure flow Φ from *k*-th level at *(k-1)*-th ranking level with the process repeating until *1*-st (basic) level,
- transformation of average values of pure flow are calculated using:

$$e_i = \frac{\overline{\Phi}(a_i) - min\,\overline{\Phi}}{R} \qquad (1.1)$$

where:

$$R = max\,\overline{\Phi} - min\,\overline{\Phi} \qquad (1.2)$$

and represents i.e. difference between maximum minimum value of pure flow.

Algorithm of proposed method for solving of multicriteria optimization with complex criteria functions which in themselves contain subcriteria functions is shown at figure 1.

3. EXAMPLE

For example is taken choice of products (alternatives **A_1 - A_8**) based on three criteria at first level [4]:

- time for product developement - t
- product development costs - T
- product quality – Q

Each of the above criteria is composed of multitude subcriteria functions. Decomposition is derived only to second level. Function t is composed of subcriteria functions marked as t1, t2, t3, t4 and t5, function T is composed of 10 subcriteria functions (T_1, T_2, ... ,T_{10}) and function Q is composed of 24 subcriteria functions (q_1, q_2, ... , q_{24}).

Basic data for algorithm execution are shown in table 2.

Table 2. Algorithm data

Number of alternatives	m=8
Number of *1-st* level criterial functions	n=3
Number of *2-nd* level criterial functions	K_t^2= 5 K_T^2= 10 K_Q^2= 24

Multicriteria analysis is executed in two phases based on experimental data shown in table 3.

I phase – multicriteria analysis with criteria functions of II level using PROMETHEE III method:

a) multicriteria analysis based on criteria t_1, t_2, t_3, t_4 и t_5;

b) multicriteria analysis based on criteria T_1, T_2, ... ,T_{10}

c) multicriteria analysis based on criteria q_1, q_2, ... ,q_{24}.

Values of pure flows that are calculated based on this analisys are transformed using formula (1.1) и (1.2) and they are shown in table 4.

Table 4. Transformed values of pure florws after phase I

	C_{ij}		
	Time	**Costs**	**Quality**
A_1	0,00000	0,00000	0,00000
A_2	0,49822	0,31443	0,21040
A_3	0,37571	0,40197	0,20665
A_4	0,71401	0,75213	0,56167
A_5	0,07791	0,51209	0,35125
A_6	0,77862	0,55234	0,76741
A_7	0,73510	0,64564	0,66410
A_8	1,00000	1,00000	1,00000

II phase – multicriteria analysis of I level criteria functions using PROMETHEE I, II и III methods. Entry data are transformed values of pure flows calculated at previous phase. Results of this phase are shown in table 5. The best alternative is A8.

For all calculations that are performed at I and II phase of proposed methodology is used software MODIPROM в.1.0 [4].

Table 1. Formalized inscription of multicriteria analisys problem

CRITERIA LEVEL					ALTERNATIVES						Relative weight coefficients						
1	2	...	r-1	r	A_1	A_2	...	A_i	...	A_m	r	max/ min	...	2	max / min	1	max / min
K_1^1	K_1^2	...	K_1^{r-1}	K_1^r	C_{11}	C_{21}	...	C_{i1}	...	C_{m1}	W_1^r	max/min	...	W_1^2	max/min	W_1^1	max/min
				K_2^r	C_{12}	C_{22}	...	C_{i2}	...	C_{m2}	W_2^r	max/min					
			K_2^{r-1}	K_3^r	C_{13}	C_{23}	...	C_{i3}	...	C_{m3}	W_3^r	max/min	...				
				K_4^r	C_{14}	C_{24}	...	C_{i4}	...	C_{m4}	W_4^r	max/min					
	K_2^2	...	K_3^{r-1}	K_5^r	.	.		.		.	W_5^r	max/min	...	W_2^2	max /min		
	K_3^2	...	K_4^{r-1}	K_6^r	.	.		.		.	W_6^r	max/min	...	W_3^2	max/min		
			K_5^{r-1}	K_7^r	.	.		.		.	W_7^r	max/min	...				
				K_8^r	.	.		.		.	W_8^r	max/min					
. .	. .	. .	. .	. .	.	.		.		.	. .	. .	. .	. .	. .	. .	. .
	. . .				.	.		.		.							
					.	.		.		.				. . .	. . .		
					.	.		.		.							
					.	.		.		.							
K_j^1			K_j^{r-1}	K_j^r	C_{1j}	C_{2j}	...	C_{ij}	...	C_{mj}	W_j^r	max/min				W_j^1	max/min
	. . .				.	.		.		.							
					.	.		.		.				W_j^2	max/min		
					.	.		.		.							
					.	.		.		.							
					.	.		.		.							
. .	. .	. .	. .	. .	.	.		.		.	. .	. .	. .	. .	. .	. .	. .
	. . .				.	.		.		.							
					.	.		.		.				. . .	. . .		
					.	.		.		.							
					.	.		.		.							
					.	.		.		.							
K_k^1					.	.		.		.						W_k^1	max/min
	. . .				.	.		.		.				. . .	. . .		
					.	.		.		.							
					.	.		.		.							
					.	.		.		.							
					.	.		.		.							
	K_l^2				.	.		.		.							
			K_s^{r-1}		.	.		.		.				. . .	. . .		
				K_n^r	C_{1n}	C_{2n}	...	C_{in}	...	C_{mn}	W_n^r	max/min					

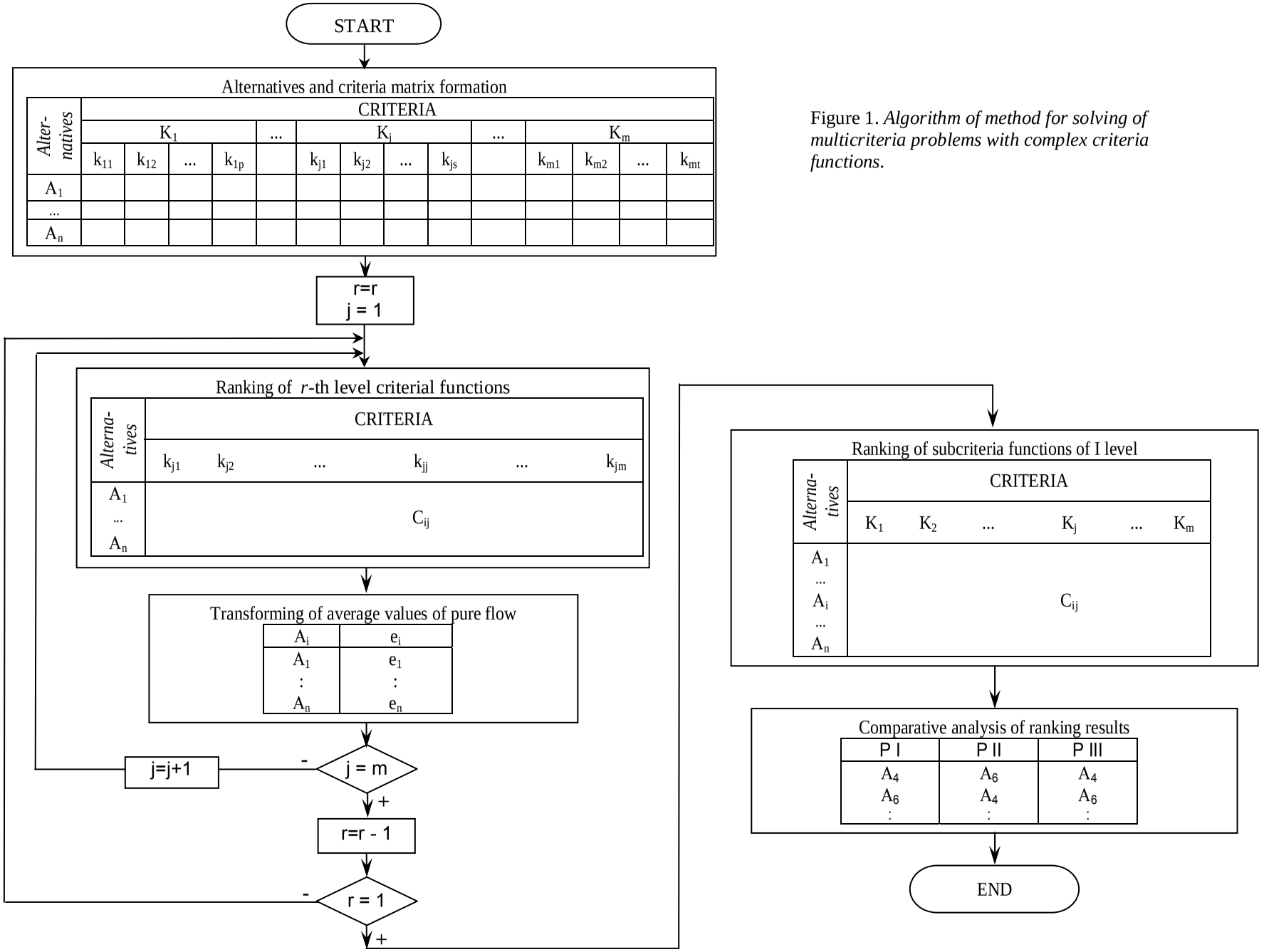

Figure 1. *Algorithm of method for solving of multicriteria problems with complex criteria functions.*

Table 3. Entry data for multicriteria analysis

Criteria		ALTERNATIVES								W_j	max/ min
		A_1	**A_2**	**A_3**	**A_4**	**A_5**	**A_6**	**A_7**	**A_8**		
t	t_1	4	4	4	4	4	4	4	4	1	min
	t_1	6	7	6	7	7	7	7	7	1	min
	t_1	43	28	27	18.5	39	28	27.5	18	1	min
	t_1	27	20	27	20	24	14	16	18	1	min
	t_1	16	14	15	14	32	21	21	13	1	min
T	T_1	520	520	520	520	520	520	520	520	1	min
	T_2	1200	1400	1200	2100	1400	2100	2100	2100	1	min
	T_3	7000	4200	4100	2600	5440	5110	5110	2470	1	min
	T_4	1600	1400	1300	1100	1400	1400	1300	1000	1	min
	T_5	2700	2000	2700	2000	2400	1400	1600	1800	1	min
	T_6	2560	2240	2400	2240	2240	2240	2240	2080	1	min
	T_7	1445	1859	852	680	767	529	625	359	1	min
	T_8	3375	2760	3059	1797	2119	1883	1323	636	1	min
	T_9	3175	3060	1920	1480	1600	2030	1710	575	1	min
	T_{10}	415	348	375	110	115	215	78	65	1	min
Q	q_1	0.82	0.86	0.84	0.90	0.87	0.95	0.92	0.98	0.20	max
	q_2	0.81	0.85	0.85	0.91	0.89	0.94	0.93	0.98	0.10	max
	q_3	0.80	0.83	0.95	0.96	0.90	0.92	0.96	0.97	0.05	max
	q_4	0.80	0.82	0.90	0.93	0.89	0.93	0.94	0.97	0.03	max
	q_5	0.92	0.92	0.92	0.92	0.92	0.92	0.92	0.92	0.04	max
	q_6	0.90	0.90	0.90	0.90	0.90	0.90	0.90	0.90	0.04	max
	q_7	0.93	0.93	0.93	0.93	0.93	0.93	0.93	0.93	0.04	max
	q_8	0.90	0.90	0.90	0.90	0.90	0.90	0.90	0.90	0.03	max
	q_9	0.93	0.93	0.93	0.93	0.93	0.93	0.93	0.93	0.03	max
	q_{10}	0.90	0.90	0.90	0.90	0.90	0.90	0.90	0.90	0.04	max
	q_{11}	0.80	0.84	0.82	0.89	0.87	0.93	0.90	0.98	0.04	max
	q_{12}	0.97	0.97	0.97	0.97	0.97	0.97	0.97	0.97	0.04	max
	q_{13}	0.83	0.87	0.85	0.92	0.89	0.96	0.93	0.99	0.05	max
	q_{14}	0.82	0.86	0.84	0.90	0.87	0.95	0.93	0.99	0.05	max
	q_{15}	0.97	0.97	0.97	0.97	0.97	0.97	0.97	0.99	0.04	max
	q_{16}	0.95	0.95	0.95	0.95	0.95	0.95	0.95	0.98	0.03	max
	q_{17}	0.83	0.87	0.85	0.90	0.87	0.95	0.93	0.99	0.01	max
	q_{18}	0.92	0.92	0.92	0.92	0.92	0.92	0.92	0.92	0.02	max
	q_{19}	0.90	0.90	0.90	0.90	0.90	0.90	0.90	0.90	0.01	max
	q_{20}	0.89	0.92	0.90	0.94	0.90	0.96	0.94	0.98	0.02	max
	q_{21}	0.94	0.94	0.94	0.94	0.94	0.94	0.94	0.94	0.02	max
	q_{22}	0.88	0.88	0.88	0.88	0.88	0.88	0.88	0.88	0.03	max
	q_{23}	0.82	0.86	0.84	0.90	0.87	0.95	0.92	0.98	0.03	max
	q_{24}	0.70	0.70	0.70	0.70	0.70	0.70	0.70	0.70	0.01	max

Table 5. Comparative analysis of ranking results

Rank	**PROMETHEE I**	**PROMETHEE II**	**PROMETHEE III**
1	A8	A8	A8
2	A6	A6	A4
3	A4	A7	A6
4	A7	A4	A7
5	A2	A2	A2
6	A3	A5	A3
7	A5	A3	A5
8	A1	A1	A1

4. CONCLUSION

Complex conditions for bussines that are present today, require multicriteria approach at process of solving bussines problems for objective comparation of alternatives which are given in different units, with different factor of importancy and with opposite extremization demands.

Thera are many methods for multicriteria analysis problem solving like: ELECTRE I-IV, PROMETHEE I-IV, AHP, VIKOR, etc. and softwer[5].

Implementation of these methods at bussines decision making is neccessary to defende chosen alternative with strong arguments.

Specific problem occurs when criteria functions on the basis of which alternatives ranking should be done consists of subcriteria functions. Problem becomes mor complex with increasing number of levels of subcriteria functions. Algorithm that was developed permits to resolve this problem using classical methods of multicriteria optimizationоптимизације on a relatively easy way so that through several phases of iteration get an unique solution.

The proposed procedure can have practical application at solving of different problems of multicriteria ranking of alternative solution particularly to choose an investment alternative where criteria can be given at quantitative and qualitative form.

LITERATURE

[1] Brans J.P., Mareschal B.: How to Decide with PROMETHEE, ULB and VUB Brussels Free Universities, http://smg.ulb.ac.be

[2] Radojicic M., Zizovic M.: Primena metoda višekriterijumske analize u poslovnom odlučivanju, Tehnički fakultet, Cacak, 1998.

[3] Djukic R.: Rangiranje alternativa metodom normalizacije kriterijuma funkcija na više nivoa, Naucno-tehnicki pregled, vol. XXXIX, 1989, br. 6.

[4] Kolarevic M.: Brzi razvoj proizvoda, Zaduzbina Andrejevic, Beograd 2004.

[5] Nikolic I., Borovic S.: Visekriterijumska optimizacija, metode, primena u logistici, softver, Centar vojnih skola Vojske Jugoslavije, Beograd, 1996.

THE ANALYSIS OF MODE, CONSEQUENCES AND CRITICALITY AT POTENTIAL FAILURES OF GEAR PUMP

B. Radicevic, Z. Petrovic, M. Kolarevic, M. Dinic,

Abstract: The analysis of mode and effects of failures (FMEA) is the procedure for the estimation of reliability of the device in all phases of its operating circle, which is based on observing all potential failures of items and their effects on the device. FMEA is a systematical technique and formal help in thinking which enables the weak places in technical system known from the experience, the potential failures, consequences and risks, to be seen on time, and to be brought into the process of decision making together with measures of corrective maintenance.
Here we present a short instruction to perform the procedure of FMEA and analyses of mode, effects and criticality at failures (FMECA), namely the procedures FMEA / FMECA, with the description of the steps to perform the procedure. The process of performing the procedure FMEA /ANEKO is illustrated on the example of hydraulic system, precisely on the example of its subsystem – gear pump.

Key words: gear pump, failure modes, effects and criticality analysis (FMECA)

1. INTRODUCTION

The method of FMECA has many advantages in comparison with the other methods of failure analysis, but some comparative disadvantages as well. The advantages of FMECA are:

- Possibility of systematic evaluation of relations between causes and consequences at certain failures
- Pointing to the forms of failures especially undesirable for the work of the system
- Pointing to the forms and systems not previously expected, actually not analyzed or neglected
- Clarification of previous failures which were not enough observed, namely more realistic evaluation of certain actions which might cause failure of the system
- Thus we especially stress that the analysis by the method of FMECA is very useful in the cases without enough experience or relevant information. This refers largely to the new systems, which are being designed, or in developing phase or installation.

The disadvantages of FMECA are the following:

- Huge tabular statements with much data, even for relatively simple systems
- Difficulties in embracing all important facts, e.g. the difference in operating time of certain items (compared with operating time of the system), working conditions, possibilities of restoration etc.
- Impossibility of direct performing of mathematical model describing the possibility of system failure, namely its reliability
- Difficulties in the analysis of system with complex structural correlations between the items (e.g. `specific correlations` which have the qualities of even and parallel, under the same conditions) etc.

Failure Modes and Effects Analysis (FMEA) represents one of methods in analysis of potential failures in components of the system and could come true in each phase of system operating circle. The aim of the analysis is to discover the causes of component failure in order to decrease the consequences of failure in performing the functional aim of the system [1]. FMEA is possible to be performed on any level of system division. The system is divided into subsystems, which are divided into structures, substructures and items. To maintain correct performing of FMEA all potential modes of system failures should be exactly identified. Different code systems are used and one of them can be performed like this:
A – technological system
A.B – substructure, which gets into A
A. B. C – structure which gets into B
A.B.C.D – substructure, which gets into C
A.B.C.D.E - item which gets into D

Code system can be solved with numbers as well using the same principle as the larger number on a certain level of division represents numbers in rising line.
For each item of the lowest level of division the data on reliability are provided. The most appropriate is to

Radičević Branko, Faculity of Mechanical Engineering Kraljevo, radicevic.b@mfkv.kg.ac.yu
Petrović Zoran, Faculity of Mechanical Engineering Kraljevo, petrovic.z@mfkv.kg.ac.yu
Kolarević Milan, Faculity of Mechanical Engineering Kraljevo, kolarevic.m@mfkv.kg.ac.yu
Dinić Miodrag, „Hidraulika" a.d., Prva petoletka Trstenik

use the average intensity of failure (for irreparable items) or average operating time between failures (for reparable items).

Based on structural and functional analyses and experiences in exploiting the system all consequences of system failure are formed, and all potential modes of item failures at the lowest level of division are listed, respecting the code system.

To perform the procedure of FMEA, all the consequences of failure are classified in four categories:

- I catastrophic consequences for the system and or the operator
- II final break of exploiting the system
- III jamming of the system or setback of output parameter system
- IV slight jamming of the system

Going from hierarchic higher to hierarchic lower levels, the items of the lowest levels are chosen causing severe consequences. This information gives the possibility (depending on the phase of operating system circle of decision making on eliminating and preventive modes of failures taking to severe consequences (according to accepted classification).
The analysis of criticality of failure can be added to the procedure of FMEA. The criticality of failure is the degree of quality performing the function within the limits of allowed variation. Each mode of failure is added corresponding criticality in accordance with serious consequences of failure. Mutual procedure FMEA and Criticality Analysis (CA) of failure is named Failure Modes and Effects and Criticality Analyses. The procedure of FMECA including Criticality Analysis of failure enables increasing of system safety by taking into consideration of potential failures consequences.

The procedure of Criticality Analysis is performed in three basic steps:

1. Defining the criticality mode of failure, which causes p category of failure consequences (P=I, II, III, IV). In other words, this is prognosis of number j mode i item.

$$C_{ij}^{(p)} = \alpha_{ij} \cdot \beta_{ij}^{(p)} \cdot \lambda_i \cdot t_i \qquad (1)$$

where:

$\lambda_i = \sum_i \lambda_{ij}$ - intensity of i item failure

λ_{ij} - intensity j mode failure i item

t_i - operating time of i item

λ_{ij} - `weigh` (heavy part, relative part, measure of frequency) j mode of item i failure

$$0 \le \alpha_{ij} \le 1, \sum_j \alpha_{ij} = 1$$

$\beta_{ij}^{(p)}$ - conditioned possibility that j mode of item i failure will cause p category of consequences according to the accepted classification under the condition for this mode of failure to appear.

Values $\beta_{ij}^{(p)}$ are given roughly, using the recommendation of table1.

Table 1. Rough values of conditioned probability $\beta_{ij}^{(p)}$

Degree of p category of failure consequences	$\beta_{ij}^{(p)}$
Certain	1
Probable	0.1 ÷ 1
Remote	0 ÷ 0.1
Very unlikely	0

Calculation $C_{ij}^{(p)}$ enables separating of the most important (from the safety aspect) modes of item failures, in order to eliminate their causes.

2. Defining criticality of failure i item, which causes p category of failure consequences:

$$C_i^{(p)} = \sum_j C_{ij}^{(p)} \qquad (2)$$

Calculation $C_i^{(p)}$ enables separating the most important items whose failure takes to undesirable consequences.

3. Defining criticality of n consequence of system failure:

$$C_{p(n)} = \sum_i \sum_j C_{ij(n)} \qquad (3)$$

where $C_{ij(n)}$ - criticality of failure j mode i item takes to n failure consequence.
Defining these potential failures on system components goes on in the procedure of exploiting on the basis of observation in regular technical checking, based on listed failures, expert analysis for maintenance and diagnostic tests.

The mode of failure detection provides mode for reliable parameters defining, thanks to which the type of failure is defined by the observation of operator. Sensor or donor also does this. Detection of failure can be normal, abnormal or wrong. At normal detection, parameters show normal values for the correct system work. Abnormal detection shows that the system

doesn't function properly. Improper sensors or donors or wrong conslusion of the operator causes wrong detection.
Through this procedure it is necessary to predict the activities for the failure elimination. It includes corresponding spare parts, security and safety measures used for the protection of the failure as well as corresponding alternative to continue the operation while some item failed. It is also important to identify the effects caused by improper system handling at the appearance of abnormal process or detection of the failure.

2. ANALYSIS OF MODE, CONSEQUENCES AND CRITICALITY OF ITEM FAILURE OF GEAR PUMP

The complex procedure FMEA is done at the hydraulic system in which gear pump represents its subsystem. Therefore structural functional division of gear pump was performed in hydraulic system. Corresponding code sign of belonging is added to each functional unity.
In the picture, there is a cutting of gear pump which consists of: operating cogwheel shaft 1, operated cog wheel shaft 2, casing 3, cover 4, packing 5 and bearing 6.

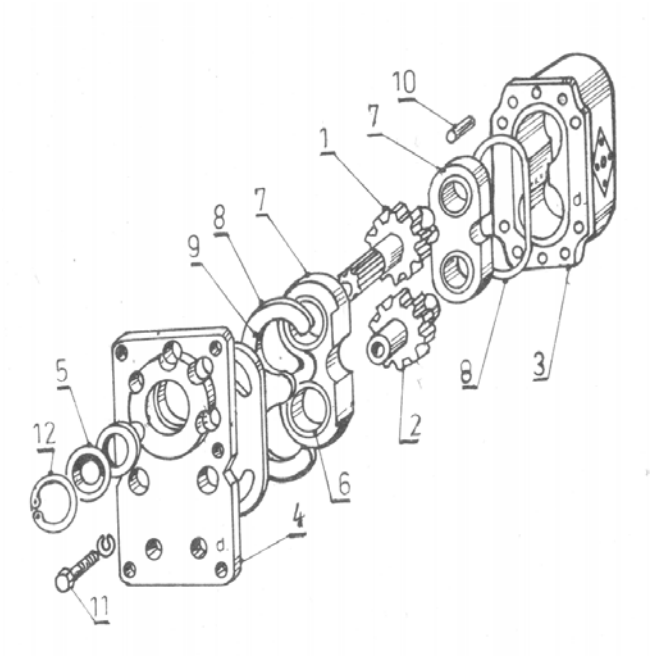

Picture 1. Component detail of the gear pump

2.1 Gear pump- the principle of the work

Operating cogwheel shaft rotates toothed pair, making sub pressure on the absorbed side, the oil gets to the cogwheel and is pressed through between teeth area, which is closed by inside surface of casing (3) in the pressing line. Precise construction of cogwheel doesn't let the oil go back. The mentioned constructive form with the preciseness of construction provides gear pump with huge capacity of efficiency (0.9 to 0.98)
Bearing flanges (7) stick to head surface of cogwheel (1 and 2). Surface A_2 (limited by static packing 8 and 9) is connected with the zone of high pressure (pressing line). The pressure between bearing flanges and head surface of cogwheel is adjusted not to cause jamming. By connecting the surface in front of the packing (5) with absorbing line, the leaking of the oil between packing (5) and operating cogwheel (1) is prevented.
On the pressing side of gear pump, the pressure is higher than on the absorbing side which takes to wearing out of split flange (6), therefore to wearing out of gear pump casing at the absorbing line.

2.2 Allocation of reliability

The procedure of allocation reliability searches for the adjustment of certain characteristics in separated items into the real probability of their manifestation. This procedure requires at least rough values of failures at all system items.
Distribution of necessary reliability on certain items is performed proportionally to `statistic weight` of corresponding accepted failure intensity values through the coefficient of allocation (ARINC method):

$$\omega_i = \lambda_i / \sum_{i=1} \lambda_i = \lambda_i / \lambda_s \quad (4)$$

where:

λ_i - is allocated subsystem failure intensity, namely items for the period t

λ_s - system failure intensity

Coefficients of allocation must meet the condition

$$\sum_{i=1}^{n} \omega_i = 1 \quad (5)$$

The permitted value of failure intensity considering terms (4) and (5) is:

$$\lambda_i^* = \omega_i \cdot \lambda_s \quad (6)$$

If the system reliability of gear pump is modeled as 11 connected items (Tab.2.) with the exponential law of distribution and if it is accepted with the value of failure intensity for certain items according to the literature [2], the coefficients allocation value of each item can be calculated. In the literature [2] there is a data for failure intensity of hydraulic pump
$\lambda = 1{,}68 \cdot 10^{-6}$ (čas^{-1}) The intensity of each item failure is calculated based on this data and calculated coefficients of allocation.
Comparing the data of intensity form with the reccomemded in the table (2) there is a huge difference. Therefore, the failure intensity is defined

according to the average operating time (judging by the data of Prva petoletka Trstenik), taking into consideration that on average the pump works 300 days in two shifts (16 hours) in the period of 10 years, which makes 48000 of operating time. Considering the supposition of exponential distribution of reliability of system items, the intensity of system failure represents reciprocal value of the average operating time. So $\lambda = 20{,}8 \cdot 10^{-6}$ ($čas^{-1}$).is an initial data for the definition of failure intensity at the items of gear pump.

Considering the values of allocation coefficients previously defined, the intensity of failure for all items is calculated.

These values largely match the recommendations in the literature. Therefore they are taken as initial for the calculation of failure criticality.

Based on the criticality analysis it is obvious there are catastrophic failures of gear pump connected with parameters of hydraulic system (pressure, flow, amortization), and then comes the items of the gear pump as shown in the table number 4.

As the final consequences 2, the complete break of exploitation of the gear pump, the biggest influence has packing and cogwheel shaft.

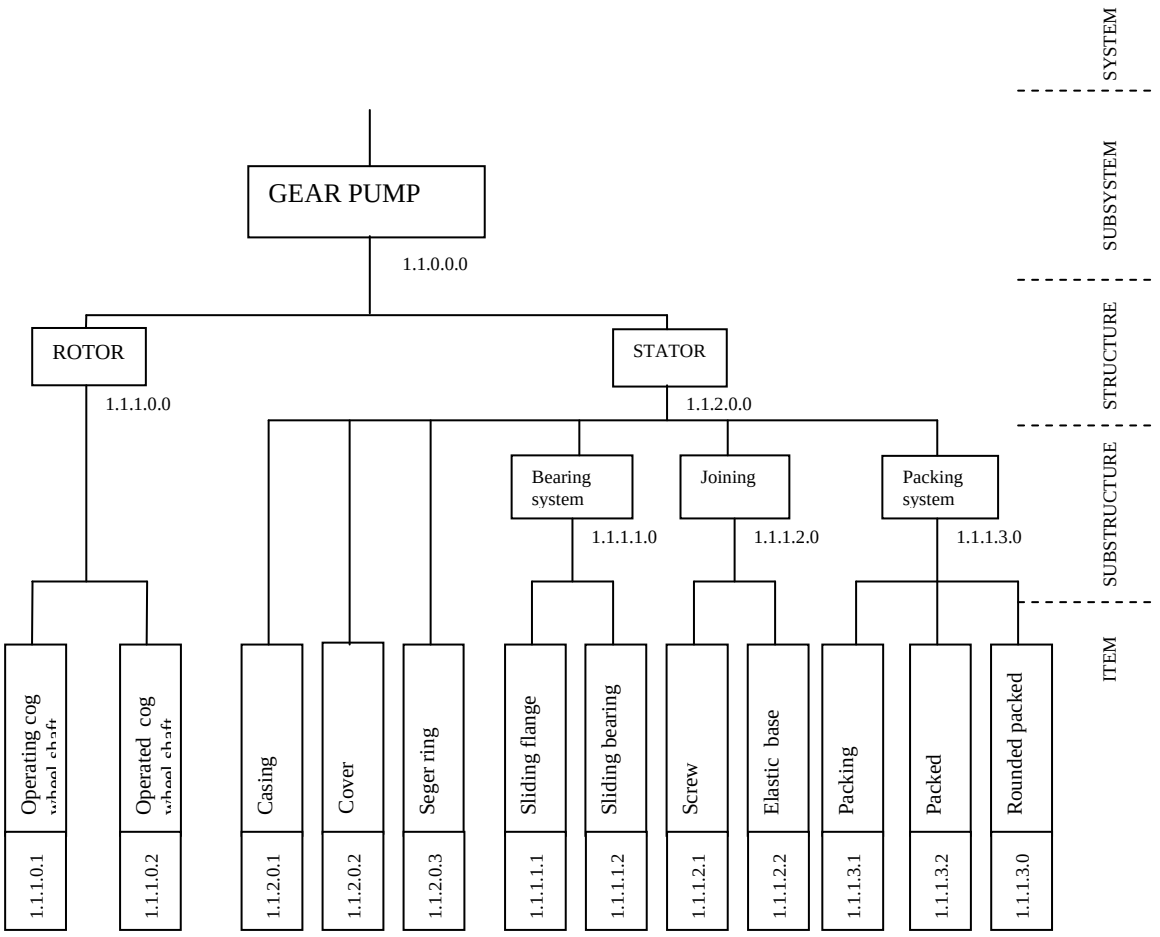

Picture 2. Scheme of subsystem division of gear pump

Table 2. Table form FMEA of substructure-gear pump

Code	Item	Type of failure	Code type of failure	Cause of failure	High effect	α_{ij}	$\beta_{ij}^{(p)}$	λ_{ij} $\cdot 10^{-6}$ (h^{-1})	λ_i $\cdot 10^{-6}$ (h^{-1})	$C_{ij}^{(p)}$ $\cdot 10^{-6}$ (h^{-1})
11101	Operating cog wheel shaft	Damage of teeth sides	N1	Surface pressure, cavitations, bad thermo processing	P.2	0.5	1	2.01	4.02	2.01
		Wearing out of head surfaces of toothed wheel	N2	Overloading	P.3	0.2	0.5	0.804		0.402
		Wearing out of journal of shaft	N3	Metal sawdust in fluid	P.2	0.2	0.5	0.804		0.402
		Error fabricate groove	N4	Non-axis shafts, badly shaped	P.2	0.1	0.1	0.402		0.040
11102	Operated cog wheel shaft	Damage of teeth sides	N5	Surface pressure, cavitations, bad thermo processing	P.2	0.5	1	2.01	4.02	2.01
		Wearing out of head surfaces of toothed wheel	N6	Overloading	P.3	0.2	0.5	0.804		0.402
		Wearing out of journal of shaft	N7	Metal sawdust in fluid	P.2	0.2	0.5	0.804		0.402
		Error fabricate groove	N8	Non-axis shafts, badly shaped	P.2	0.1	0.1	0.402		0.040
11201	Casing	Wearing out of casing	N9	Bad centering of toothed wheel in relation to journal	P.1	1	0.5	0.33	0.33	0.165
11202	Cover	Bad gasket	N10	Bad evenness, damage of packing	P.2	1	1	1.77	1.77	1.77
11131	Packing	Deformation of packing mouth	N11	Harshness, age, expansion, change of solidity	P.2	0.95	1	5.082	5.35	5.082
		Damage of spring	N12	Change of inflexibility, breaking	P.3	0.05	0.1	0.267		0.027
11112	Sliding bearing	Wearing out of sliding bearing	N13	Porosity, non-straighten teeth sides	P.2	0.4	1	0.708	1.77	0.708
		Annulment of the gap between journal and deposit of flange	N14	Non-axis shafts	P.1	0.4	0.1	0.708		0.071
		Uneven wearing out on intake and lifting sides	N15	Overloading	P.3	0.2	0.8	0.354		0.283
11111	Sliding flange	Bad gasket	N16	Bad evenness, damage of packing	P.2	1	1	1.77	1.77	1.77
11132	Packed	Improper installment	N17	Montage	P.3	0.05	0.1	0.066	1.33	0.007
		Aging of rubber	N18	Pressed filter carbon dust	P.3	0.95	1	1.263		1.263
11130	Rounded packed	Aging of rubber	N19	Pressed filter carbon dust	P.2	1	1	1.33	1.33	1.33
11121	Screw	Breaking of screw head	N20	Mode of galvanic protection	P.3	1	0.1	0.027	0.027	0.027
11203	Seger ring	Breaking	N21	Improper montage, bad thermo processing	P.2	1	0.1	0.27	0.27	0.027
10000	System	Jamming of toothed wheel	N22	Unfitted parameters of hydraulic system (Pressure, flow, amortization)	P.1	1	1	100	100	100

Table 3. Criticality type of failure at P.1

Code	Item	Type of failure	Code type of failure	High effect	α_{ij}	$\beta_{ij}^{(p)}$	λ_i	t_i	Criticality type of failure
10000	System	Jamming of toothed wheel	N22	1	1	1	100	1.00	100
11201	Casing	Wearing out of casing	N9	1	1	0.5	0.33	1.00	0.165
11112	Sliding bearing	Annulment of the gap between journal and deposit of flange	N14	1	0.4	0.1	1.77	1.00	0.071

Table 4. Item failure intensity

1	2	3	4	5	6
Pos.	Item	$\lambda \cdot 10^{-6}$ (h^{-1})	ω_i	$\lambda \cdot 10^{-6}$ (h^{-1})	$\lambda \cdot 10^{-6}$ (h^{-1})
1	Operating cog wheel shaft	3	0.193	0.324	4.02
2	Operated cog wheel shaft	3	0.193	0.324	4.02
3	Casing	0.25	0.016	0.026	0.33
4	Cover	0.05	0.016	0.026	0.33
5	Packing	4	0.257	0.431	5.35
6	Sliding bearing	1.32	0.085	0.142	1.77
7	Sliding flange	1.32	0.085	0.142	1.77
8	Packed	1	0.064	0.107	1.33
9	Rounded packed	1	0.064	0.107	1.33
10	Screw	0.2	0.013	0.021	0.27
11	Seger ring	0.2	0.013	0.021	0.27

3. THE CONCLUDING NOTES

One of the basic elements in gathering reliability data of technological system represents a subsystem of the analysis of mode, consequences and criticality of failure items (FMECA).

The procedures FMEA and FMECA are done on the example of hydraulic system, namely its subsystem, gear pump. The analysis ends in ranging the items of the observed subsystem according to the level of criticality of failure type and criticality of items.

There are certain difficulties due to lack of evidence on reliability of the items at the lowest level. In some cases these can be solved if instead of dotted values of failure intensity a certain value diapason is given.

LITERATURE

[1] Papic LJ., Holovac S., *Methods in the failure analysis* – book I -The analysis of mode, consequences and criticality of failure (AVPKO), theoretical and practical aspects, D&QM Cacak, 1994

[2] Ivanovic G., Stanivukovic D., *Reliability of technical systems* – The collection of the solved problems, Mechanical Engineering University Belgrade, 1987

[3] Zelenovic D., Todorovic J., *The efficiency of system in mechanical engineering*, Science book Belgrade, 1990

PARAMETRIC MODELLING OF MODULAR VAULT ROOMS

M. Kolarević, Lj. Cvetković, R. Bošković

Abstract: *These papers show parametric modelling of vault rooms of „Modulprim" types which are based on modular structure. Suggested approach enables quick response at customer's specific demands, better product quality and reduction of manufacturing expenses. This approach increases efficiency of whole manufacturing system and its competitivness at market.*

Key words: *parametric modelling, modular design, vault room*

1. INTRODUCTION

A vault room is a place where we deposit our valuables, which are nowhere else secure enough. Today when we speak about quality of life security plays a crucial role. Security that can be seen, felt and experienced - the most important feature of vault rooms.

Constructing a vault room we must give precise attention to assuring long term reliability. In existing buildings we must find the most adequate solution and optimum grade of security.

A reason for construction of vault room is a number of valuables that should be protected. From the technical aspect a construction of a vault room must meet demands of future generations and assure highest level of security in spite of future improvements of burglary equipment.

Each vault room is a new product which should be necessarily adapted to available dimensions. For that reason we must repeat all phases of designing process. Classic method design with 2D modelling is slow and with a low-quality designing documentation.

The goal of these papers is to indicate the basic advantages of 3D parametric modelling of vault rooms of "Modulprim" types which are based on modular structure. Software Autodesk Inventor is used for these needs.

2. MODULAR VAULT ROOM

The vault room is a very complex engineering object with the next requirements:

- hight level of security of burglary equipment
- fire resistance
- radiation resistance
- flood control etc.

The users of vault room are:

- The banks for deposit of valuables: money, precious metals, security documents, valuables of their account holders in the cash boxes,
- The post offices for deposit of money and security documents,
- The gouvernment, administration, army and police for deposit of security documents, drafts etc.
- the industrial firms for deposit of security documents (patents, innovation ...), drafts etc.

All modules of vault rooms are manufactured in the Security Equipment factory and are transported on a construction site where a modular construction is composed of standardized units that can be easily and flexibly arranged.

PhD Milan Kolarević, Faculty of Mechanical Engineering Kraljevo, *kolarevic.m@mfkv.kg.ac.yu*
Ljubinko Cvetković, B. Sc.E., Primat Oprema DOO, Baljevac, *po.cvetkovic@nadlanu.com*
Radiša Bošković, B. Sc.E., *kolarevic.m@mfkv.kg.ac.yu*

The final part of modular vault room is the vault door with different security grades, different types of locks and different types of day doors (optional day grill or glass door).

The furnishing of vault rooms is also customised:

- cash boxes (mechanical or electronic version)
- 24-Hours - system - always available cash boxes
- cabinets and racks.

The scheme of modular vault room with components is shown in figure 1.

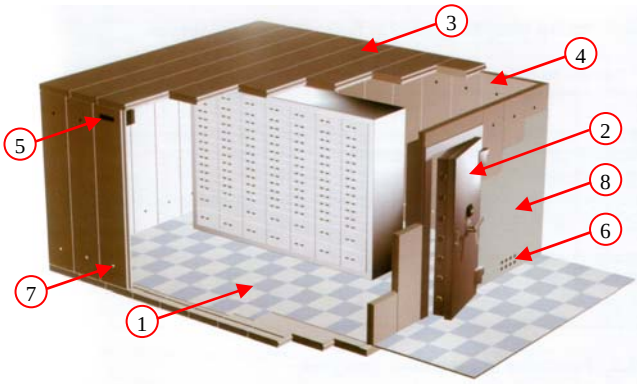

Figure 1: *Scheme of modular vault room*
1. Floor and ceiling components 2. Vault door 3. Construction components 4. Inner covering 5. Ventilation system 6. Airing 7. Cables 8. Outer coverings

The modular vault room is often rectangular because that configuration is simple for manufacturing and assembly. However rectangular configuration is not the only one.

The modular vault room with round sides and corners is undesirable and impractical but it is possible to realise configuration with more rectangulars.

All modules are assembled with welding. From statics view it is useful. The components of construction are estimated to carry their own weight and added load of 300 daN/m^2 to span 5,0 m between walls. This is significant when a vault room must be assembled in bank halls or office halls.

The height of a vault room i.e. the length of lamella is limited on 3,0 m because of standard machine tools.

The wall thickness of modular vault room is two or three times thinner than walls of massive vault room and the weight of modular vault room is smaller than massive vault room.

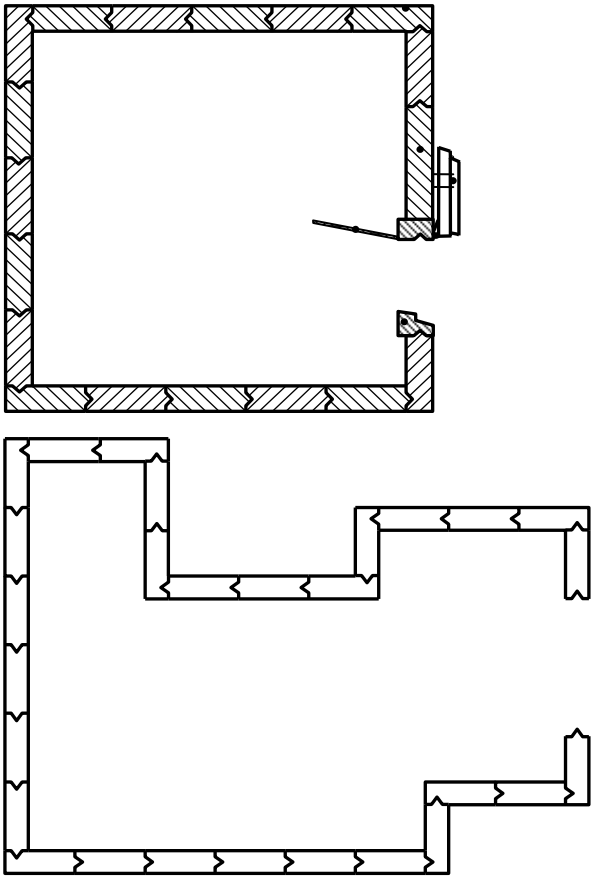

Figure 2: *Scheme of horizontal intersection of modular vault room*

Modular vault rooms have numerous advantages compared to massive construction of vault rooms. Basic advantages of a modular vault room are[1]:

- Thin walls enable high usability of space.
- Possibility of setting up vault room in upper floors of new buildings or rebuilding of existing rooms into vault rooms.
- Modulprim components are welded together and this makes the object compact. Theoretically, it is also possible to disassemble the object and transfer to another location.
- Short assembly time.

3. MODULAR STRUCTURE OF VAULT ROOM "MODULPRIM"

For representative of modular vault room "Modulprim" from company „Primat ad"- Maribor is selected the model "Modulprim 5" whose basic parameters are specificatied in the table 1.

Table 1. *Specification of vault room "Modulprim 5"*

Model		MODULPRIM 5
Security grade according to EN 1143 – 1		V / 270 RU
Wall thickness		100 [mm]
Weight / m^2		295 [kg]
Max. span (inner lights) at ceiling load	100 daN / m^2	6000 [mm]
	300 daN / m^2	5000 [mm]

The basic modules of vault room "Modulprim 5" are (Figure 3):

- Lamella type **A**,
- Lamella type **B**,
- Lamella type **C**,
- Lamella type **C***,
- Lamella type **D** and
- Lamella type **E.**

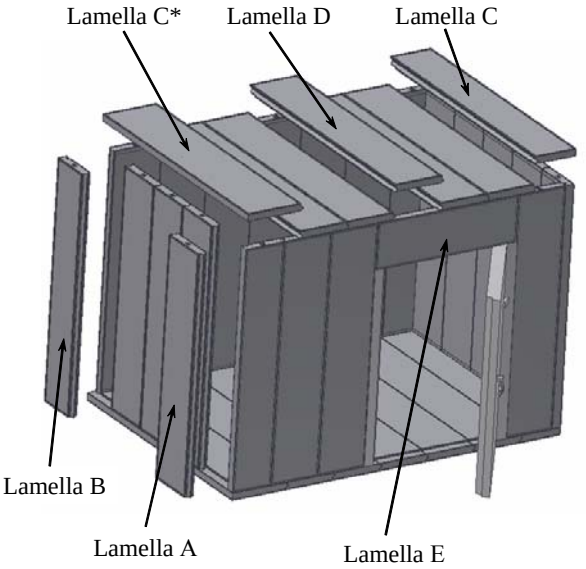

Figure 3: *Modular vault room "Modulprim 5" with construction components*

Structural scheme of "Module 1" i.e. "Lamella A" is presented in the figure 4. The other modules are with similar structural scheme. Number of components for forming the module is minimal. Hierarchial structure of modular vault room with components is illustrated in figure 5.

4. PARAMETRIC MODELLING OF BASIC MODULS OF VAULT ROOM "MODULPRIM"

The Parametric modelling is a method which uses CASE – *Computer Aided Softwer Engeneering* – tools for searching and making technical solutions and managing with dimensions for creating a geometric model of product. In the relation of traditional design this is a large progress because it is a possible to manage with "the design parametars" in every design phase. The values of paremeters are determined in the design process. However, the value of paremeters are possible to know on the start of the designing process.

For illustration of the parametric modelling a model of "lamella A" of a vault room "Modulprim 5", especially a cover plate, has been selected. The geometry of a cover plate of lamella A is defined across contours and constraints for all gamma of lamellas A. Process modelling of components of product is reduced only to defining the dimensions of geometric parametars of 3D model.

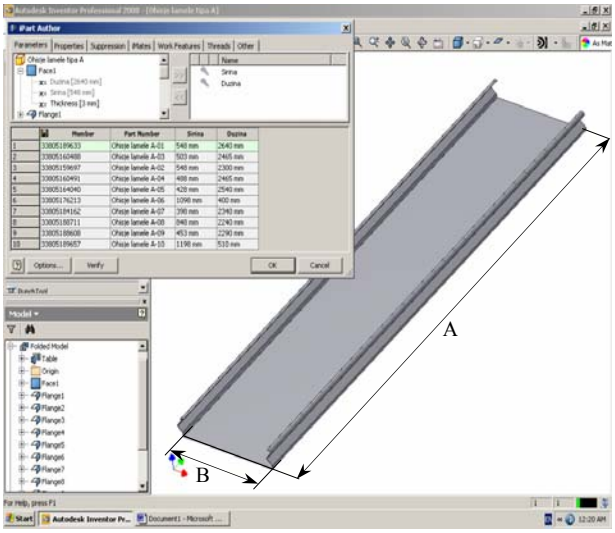

Figure 6: *Geometric model of steel cover plate of lamella type A with a table of parametars*

Drawings of modules and all components of a vault room are formed with a table of parametars (figure 7).

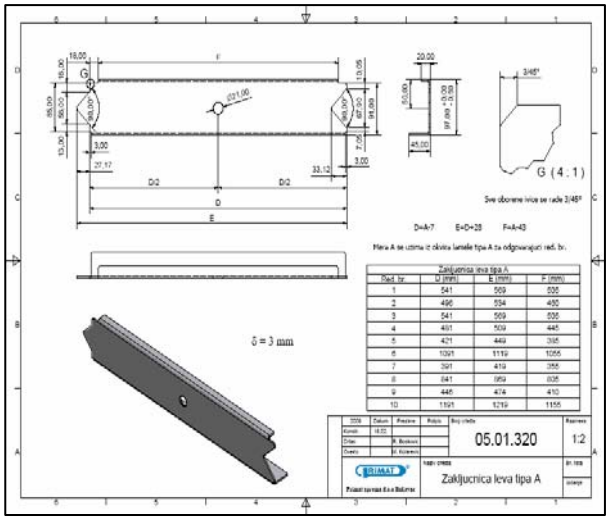

Figure 7: *Drawing of right cover with a table of parametars*

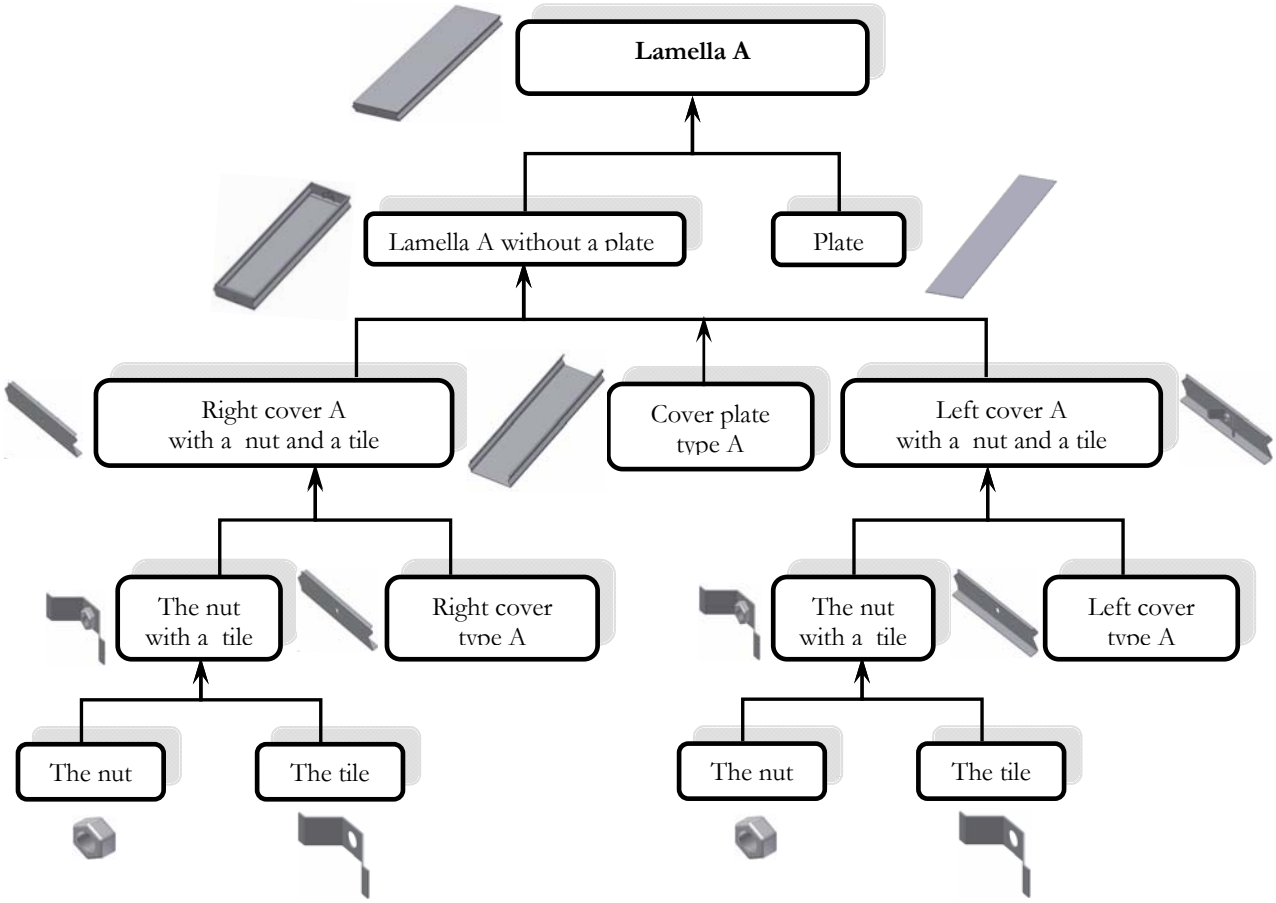

Figure 4: *Structural scheme of cover plate type A*

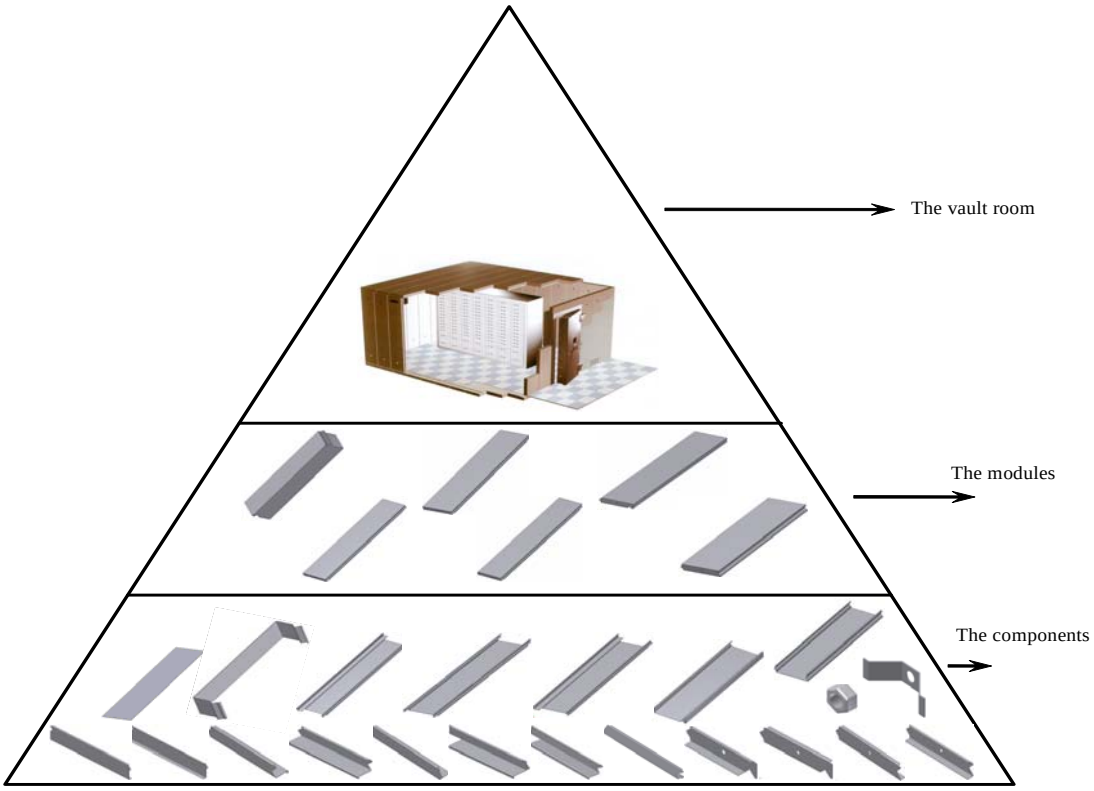

Figure 5: *Hierarchial structure of modular vault room with components*

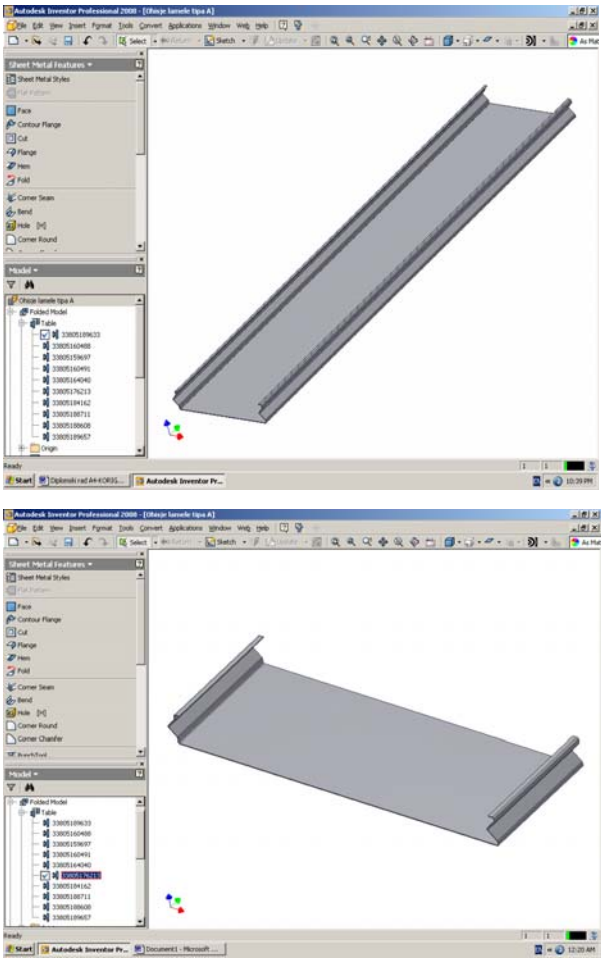

Figure 8: *Change of geometric model of cover plate typeA with a change of parametars of length and width*

After defining the customer's requirements and main dimensions of vault room, the designing process now consists of these phases:

- defining of number of basic modules and specification of dimension caracteristics of modules and components,
- designing of modules and components includes the value of dimensions entered in adequate tables of parametars,
- 3D design of vault room.

5. CONCLUSION

The products as a modular vault room "Modulprim" are manufactured according to customer's requirements. Customer selects a security grades and defines available dimensions of vault room. The concept which is based on modular structure assures preferences of a serial production and design of product which responses at customer's specific demands. However, every vault room is a new project without possibility to make a model or a prototype. 3D design which is available to modern CAD software provides a possibility to make virtual prototype of a vault room.

The geometry of modules of a vault room is the same for every new project and the difference is in the number of elements and dimensions. The preference of the use of modern CA (Computer Aided) tools and a concept of parametric modelling is reduction of time design for 90%. Now it is possible to make a hight-quality product because drawings are of high-quality without design errors.

Suggested approach to the designing of modular vault room with modern Computer Aided tools enables quick response at customer's specific demands, better product quality and reduction of manufacturing expenses. This approach increases efficiency of the whole manufacturing system and its competitivness at market.
It is planned in the future a software for automatic generate of parametars to be made after defining customer requirements and main dimensions of vault room.

6. REFERENCES

[1] Štefanec E.: Trezorski prostori, Narodna in univerzitetna Knjižnica Ljubljana, Maribor 2003.

[2] Kolarević M.: Brzi razvoj proizvoda, Zadužbina Andrejević, Beograd 2004 ,

[3] Babić A.: Projektovanje tehnoloških procesa, Mašinski fakultet Kraljevo, Kraljevo 2005 ,

[4] Standard EN 1143-1, 2005,

COMPLEXITY CHALLENGES IN CAPP SYSTEMS AND PROMISES OF MULTI-AGENT TECHNOLOGY

D. Polajnar, J. Polajnar, Lj. Lukić, M. Djapić

Abstract: *The rising global competition in manufacturing requires rapid development of cost-effective, high-quality production processes for newly designed products. This motivates research in advanced systems for computer-aided process planning (CAPP), including the use of multi-agent systems (MAS) technology, but many challenges remain due to the extraordinary complexity of the problem. In this paper we examine the specific complexity challenges arising in process planning, analyze how properties of multi-agent systems could be used to address those difficulties, and propose meta-model abstractions for the representation of process plans and for the structuring of multi-agent teams that construct them. In particular, we introduce inter-related models representing different aspects of parts, set-ups, and process plans, suitable for concurrent development by cooperating agents. We then discuss the profiles of agent roles involved in plan construction and optimization, and outline team composition for CAPP.*

Keywords: *Multi-agent technology, CAPP, Flexible manufacturing systems*

1. INTRODUCTION

Current trends in manufacturing industry strongly motivate the development of advanced computing systems that support *process planning* – the manufacturing activity that determines in detail the processing steps of machines in the production cell that transform each workpiece type from its initial to its final state [1]. The rising global competition requires rapid development of cost-effective, high-quality production processes for newly designed products. At the same time, relevant computing technologies have advanced significantly in recent years. In particular, there has been growing research on the use of multi-agent systems (MAS) technology [2] in computer aided process planning (CAPP) [3], [4]. Nevertheless, CAPP remains substantially less automated than other phases of the manufacturing cycle, such as computer-aided design (CAD), computer-aided manufacturing (CAM), or shop-floor control. A recent survey [5] notes that most existing systems are off-line, centralized, and not integrated with related activities such as scheduling. Practical advances have often added CAPP elements to either CAD or CAM systems, narrowing rather than methodically bridging the existing gap.

This paper addresses some aspects of the problem from the perspective of MAS technology. In our view, CAPP remains a weak link of the emerging integrated manufacturing because of its extraordinary inherent complexity. We first examine the nature of complexity in CAPP (in Section 2), and then discuss the strengths of MAS technology that could be used in overcoming the complexity challenges (in Section 3). Based on that analysis, Section 4 presents a collection of inter-related CAPP models for chip-removal metal-cutting processes, designed to support cooperative process planning by a multi-agent team. The models employ feature-based CAPP concepts [6]–[10] and refer to STEP AP224 standard [11] for a comprehensive taxonomy of process attributes. Section 5 derives multi-agent team concepts from the preceding CAPP modeling. Section 6 contains conclusions and remarks on future work.

2. CAPP COMPLEXITY CHALLENGES

In order to build efficient CAPP systems one must overcome the complexity of the problem by relying on properly chosen abstractions. As a first step we outline the in order to build efficient CAPP systems one must overcome the complexity of the problem by relying on properly chosen abstractions. As a first step we outline the leading global companies (Siemens, ABB, Schneider Electric, Arewa, etc.). elements of the process planning task, review the types of decisions involved in the construction of a process plan, and analyze the nature of domain-specific complexity challenges in CAPP.

A *process planning task* consists of: an assortment describing the part series to be machined; the manufacturing cell configuration describing the available machinery; and the requirements that the generated plan must satisfy.

An *assortment* is a set of *part series*, each specifying

Desanka Polajnar, MSc, Computer Science Department, University of Northern British Columbia, Prince George, B.C., Canada, desa@unbc.ca,
Prof. Jernej Polajnar, PhD, Computer Science Department, University of Northern British Columbia, Prince George, B.C., Canada, polajnar@unbc.ca,
Prof. Ljubomir Lukić, PhD, Faculty of Mechanical Engineering Kraljevo, lukic.lj@mfkv.kg.ac.yu,
Doc. Mirko Djapić, PhD, Faculty of Mechanical Engineering Kraljevo, djapic.m@mfkv.kg.ac.yu.

the number of instances of a particular part type. The *part type* is specified as a *part design model* generated by a computer-aided design (CAD) system. Each physical part to be produced is identified by its part type and its instance number.

The *cell configuration* specifies the set of ava- ilable machines that will carry out the machining operations during the processing of the assortment.

The *planning requirements* specify the conditions that the process plan is required to meet, apart from the technical specifications of the assortment. They may include constraints, goals, and a priority structure. A *constraint* is a crisp predicate (e.g., the total manufacturing cost must not exceed a given limit) that must be satisfied. A *goal* is a fuzzy predicate (e.g., the total machining time must be close to a given required value) that is targeted on a best-effort basis. The *priority structure* specifies the relative importance of the goals. As the plan is constructed, evaluated, and improved in iterative steps, the relative emphasis on specific goals may evolve.

In order to construct a plan, a modern CAPP system: decomposes every part type into individual process elements called machining features, each to be realized by one or more machining operations; determines the machine, cutting tool, and parameters for each operation; decides how workpieces will be combined into set-ups (to be clamped and processed together on the same pallet); derives the sequencing of machine actions (such as machining operations, tool changes, or pallet rotations) in the processing of each set-up; and identifies the sequencing constraints between set-ups that the shop floor scheduler must observe. The system evaluates each version of the plan and, if improvements are needed, selects an optimization strategy and constructs a new version, until a version is approved. Note that changes affecting the planning task may occur during planning (e.g., a machine becomes unavailable and is replaced by a different type). A robust CAPP system must dynamically deal with such changes.

We next examine the nature of CAPP complexity. We see the following seven components as fundamental.

Combinatorial complexity. The construction of process plans involves numerous steps with many choices in every step for each of the multitude of machining operations that a complex pro- duct may require (Fig. 1).

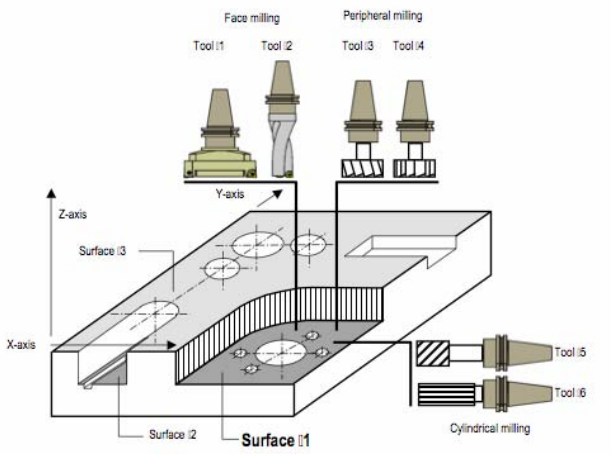

Fig. 1. Designer's choices of operation and tool types for a single machining feature illustrate the combinatorial complexity of process planning

The set-ups can be formed in many different ways. All this leads to a huge decision space.

Technological complexity. The construction, evaluation, and optimization of process plans involve diverse types of specialist expertise and software support. Feature recognition, selection of cutting tools and parameters, composition of set-ups, design of fixtures, and choice of optimization strategies all require different types of skills and experience.

Logical complexity. The planning decisions are highly interdependent. For instance, a choice of cutting parameters may result in cutting forces endangering set-up stability, forcing the planner to backtrack. Each decision influences performance and may affect balance of conflicting objectives.

Social complexity. In the emerging distributed manufacturing paradigm, parts of the production cycle, as well as its technological knowledge sources, are increasingly spread across organizations and countries with administrative, linguistic, cultural, and other systemic differences. A production environment with complex social interactions adds to CAPP communication and coordination requirements.

Empirical nature of knowledge. Cutting tech- nologies are largely based on empirical research, with the knowledge base rapidly expanding as new part and tool materials become available. This poses challenges to systematic formal representation, organization, and maintenance of knowledge.

Reasoning is hard to formalize. A human expert in one of CAPP technologies with an intuitive understanding of other areas can use such contextual knowledge to substantially reduce the decision space. However, such intuitive, qualitative, or app- roximate human reasoning is difficult to capture formally and to efficiently emulate by an automated system.

Surface 1 can be machined by any of three possible types of milling, each with two possible tool types (and many choices of other details). A complex product may require thousands of individual machining operations.

Decisions with local scope have global effects. Most decisions in the construction of a process plan (such as the choice of a machining operation method) have a narrow scope with respect to both sub-problem size and requisite expertise. Their effects are typically evaluated through performance metrics (such as total cost or total machining time) involving the plan as a whole. This discrepancy poses challenges in providing feedback on the effects of individual planning decisions and complicates optimization.

3. MAS ADVANTAGES FOR CAPP

We next consider how specific properties of MAS technology [2] can be used to address the complexity challenges of CAPP.

Concurrency and parallelism. The development of a process plan generates many alternative choices that can be explored concurrently. Examples include concurrent construction of machining operation methods for alternative operation types, concurrent evaluation of a plan version with respect to different metrics, and concurrent exploration of alternative improvement strategies. Agent technology provides a high level conceptual framework for the design of concurrent software, and the wide availability of inexpensive parallel computing platforms makes its efficient implementation feasible.

Decentralization and distribution. An essential tool in mastering system size and complexity is decentralized architecture. The reliability requirements of CAPP motivate a level of fault- tolerant design that entails a distributed computing platform. Furthermore, CAPP systems rely on distributed resources, such as tool manufacturer knowledge bases, and increasingly operate in the context of distributed manufacturing enterprice. MAS architectures fit naturally in this framework.

Autonomy. Technological complexity and knowledge organization issues in CAPP can be ef- fectively addressed if each type of expert knowledge is encapsulated along with relevant decision procedures into an autonomous entity responsible for a particular aspect of planning, i.e., a specialist agent. Decision autonomy is a distinctive characteristic of agent technology. Cooperation between specialists is naturally represented as MAS teamwork.

Reactive and proactive behavior. In a decentralized approach to plan development, the specialists monitor the joint planning activities, recognize and react to events according to their authority and expertise, and proactively initiate activities in their areas. This is naturally represented by situating the elements of the developing plan in a shared environment where agents can perceive events and contribute in reactive or proactive manner.

Intelligent problem solving. The logical complexity of CAPP requires flexible intelligent problem solving using suitable reasoning techniques. The traditional paradigm for cooperative problem solving involving specialized knowledge sources is the blackboard system, in which the problem is posted and the solution cooperatively constructed in a commonly accessible space called the blackboard. Recent advances in the modeling of shared environments for MAS [12] offer increased support for blackboard functionality.

Learning. Specialist expertise of human engineers is enhanced through learning and accumulation of experience. Corresponding learning and knowledge base development techniques should be inherent to software agents performing expert roles. The resulting distribution of capabilities and responsibilities should facilitate the management of the complex and evolving empirical knowledge base of the CAPP system as a whole.

Social ability and teamwork. The logical and social complexities of CAPP require sophisticated interactions. At the basic level, the ability of agents to interact with other agents and possibly with humans is viewed as an essential component of their intelligence [2]. In the CAPP context, the agents must act as a team to achieve common objectives. An often-cited example of teamwork in [13] is driving in a convoy, where a leader and a follower monitor each other's actions and adjust their own actions accordingly. Interdependence of decisions in process planning requires a similar attitude. CAPP requires flexible teamwork in the sense of [14] in order to deal with unexpected events such as changes in the planning task. Inter- action with humans is also required. Substantial progress in that area has been achieved in recent research on joint human-robot teamwork [15]. Teamwork theories and platforms in MAS provide a suitable basis for CAPP, but more domain-specific research is needed.

Virtual organizations. The social complexity of CAPP requires agents to cooperate smoothly across organizational boundaries. This ability has recently been receiving attention in MAS research on virtual organizations. Manufacturing agent teams of the future will likely depart from the traditional model in which individual interests and goals simply reflect the team objectives. We expect that the expert agents will be independently designed by different groups, and used in distri- buted manufacturing environments. Such agents will have a degree of self-interest in balancing consistent professional behavior with the specific priorities of organizations and teams with which they become affiliated.

While MAS technology holds strong promise for development of efficient CAPP systems, substantial multidisciplinary efforts will be needed in order to advance the most relevant aspects of MAS in general and find the most suitable solutions for CAPP based on domain-specific research.

4. CAPP MODELING FOR MAS

Having examined the nature of CAPP complexity and some relevant aspects of MAS technology, we now return to the question of finding suitable abstractions that make CAPP complexity manageable. In the rest of the paper we make two steps in that direction – one related to CAPP abstractions and the other to multi-

agent team abstractions. We take a meta- modeling approach and describe, in generic terms, the types of models underlying concrete CAPP activities. In this section we describe a collection of inter-related models that will be cooperatively constructed by the multi-agent team. The models represent elements and structures that constitute a process plan in the domain of metal-cutting chip-removal technologies. The models are to be developed concurrently by the team members or sub-teams, with coordinating interactions, and integrated into a model of process plan. The modeling is limited to elements that directly affect machining of workpieces.

The part machining model

The process planning begins with the construction of a machining model for each part type in the assortment. The machining model comprises four constituent models: design model (DM), machining feature model (MFM), machining operation type model (MOTM), and machining operation method model (MOMM). The major part of each model is derived from its predecessor in this sequence, except for the design model, which comes from the planning task. The construction of a model may also cause some modifications in its predecessors. We therefore adopt that in the construction of a part machining model the development of its four constituents proceeds concurrently, with mutual interactions. The constituent models do not replicate information in order to be self-contained, but reference each other instead.

Design model defines the stock from which the part is produced, including its geometry and part material, and the part, including its geometry, surface finish, dimensional accuracy, and geometric tolerances [1].

Machining feature model represents the part in terms of its constituent machining features and their relationships. A machining feature is a type of manufacturing feature[1)] that contains all information relevant to machining process planning as defined by the STEP standard AP224 [7], [11]. In particular, it includes the volumetric feature geometry (e.g., blind slot, step, through hole), representing the volume that can be removed by a certain type of machining process (e.g., drilling, peripheral milling, face milling); and surface features, representing the surfaces bordering the part and the volumetric feature, in terms of: surface geometry; dimensional accuracy; surface finish (as defined by ISO 4287-1); geometric tolerances (as defined by the ISO 1101 standard for tolerances of forms and positions).

The relationships between machining features are in part induced by geometric tolerances, in that one feature refers to another through a datum reference.

In particular, orientation (perpendicularity, angularity, parallelism), location (position, concentricity), and runout (circular, total) always use a datum reference; and profile (of a line, of a surface) may use a datum reference. Other (concurrently developed) machining models may require addition of new feature relationships.

The machining process that starts with stock and ends with part can now be viewed as a sequence of steps in which individual volumetric features are removed. We shall use the term 'workpiece' to denote the state after each step. More precisely, we can apply the term to a part type, and regard its evolution as a sequence of workpiece types, or apply it to an instance of part type, and view its evolution as a sequence of workpiece instances, representing the processing states of the same physical piece.

Machining operation type model represents the processing of the part in terms of machining operation types. In general, a machining feature is decomposed into several operations. For instance, the machining of a hole can be decomposed into center drilling, drilling, and reaming operations, to be performed in that order of precedence. For each machining feature, the model specifies the types of its constituent machining operations, their precedence, and the possible tool access directions (TAD). For each operation type it specifies the set of machines in the cell that can perform it.

Machining operation method model represents the processing of the part in terms of machining operation methods. For each instance of operation type in MOTM it determines the cutting tool, the cutting parameters (e.g., length of cut, depth of cut, cutting speed, feed rate, tool life, cutting forces), and the set of machines supporting the machining operation method.

The set-up model

In order to be machined, a workpiece must be clamped to a pallet in a set-up that may also involve other workpieces (made of the same material) of the same or different part type. Once all operations on the exposed sides of workpieces are completed, the set-up is dissolved and unfinished workpieces enter new set-ups. During its lifetime, a set-up behaves like a composite workpiece. Set-up model specifies a collection of set-up types. Every set-up type includes: a set of workpiece roles, each of a certain workpiece type, representing the placeholders for workpiece instances that will fill the roles when the set-up type is instantiated; the set-up geometry that determines the positioning of workpieces[2)] and their exposed sides; the precedence of machining operations; and datum surface features that serve as reference in the positioning of the cutting tools. The precedence of operations may reflect the fixture constraints, datum dependency, parent-child dependency (one operation must be performed first to allow tool

[1)] In general, a manufacturing feature is defined as a 'collection of related geometric elements which correspond to particular manufacturing method or process, or which can be used to reason about suitable manufacturing methods or processes for creating that geometry' [6].

[2)] Our set-up model includes the precise positioning of the workpieces, which in fact comes from the fixture model that was constructed from initial set-up information. We ignore the details of this interaction.

access for the other), or aim at avoiding cutter damage or achieving better machining efficiency [8]. They are represented by two partial orderings, corresponding to hard (mandatory) and soft (recommended) precedence constraints. A set-up type can be instantiated by filling each of its workpiece roles by a specific workpiece instance of the specified type.

The process plan model

A process plan specifies in detail the machining processes involved in the manufacturing of a given assortment using the available resources and satisfying the given requirements, as defined in the planning task. In order to define its structure we first introduce the concepts of set-up step, set-up plan, and set-up program.

A *set-up step* is a set-up type whose all operations can be performed on one machine. In general, the machining operations occurring in a given set-up type may require several machines in a certain order, which leads to decomposition of the set-up type into a partially ordered collection of set-up steps. The ordering must be observed by the shop-floor scheduling system, which allocates the manufacturing cell resources and schedules the machining of set-up instances. For simplicity, we make the decomposition transparent and assume that each set-up type consists of a single step.

A *set-up plan* for a given planning task is a partially ordered collection of all set-up instances needed in the processing of the entire assortment. In the ordering graph, every part instance has a unique path representing its individual process plan. The path starts with the set-up instance that includes the initial (stock) state of the corresponding workpiece, leads through set-up instances containing all the intermediate workpiece states in the correct order, and ends in the set-up instance containing the workpiece in its final (part) state. The scheduler must observe the ordering to ensure the correct sequencing of operations on every workpiece instance.

A *set-up program*, defined for each set-up type, is an alternating sequence of all machining operations and their connecting inter-operation steps (such as pallet rotation, tool change, or tool repositioning), consistent with the operation precedence in the set-up model.

A *process plan* consists of a set-up plan and the collection of set-up programs for all set-up types occurring in the set-up plan.

5. AGENT TEAM COMPOSITION

In this section we outline the generic structure of the multi-agent team that incrementally constructs the process plan through the sequence of models defined in Section 4, and iteratively optimizes it until it meets the requirements.

All agent roles in the team are derived from five abstract role classes for CAPP application domain, introduced in [16]. The planning is initiated by the team leader role in the *Manager* class. The agent roles that construct the models belong to the *Designer* class, and are further specialized, based on their expertise, into concrete classes such as *Machining Feature Designer, Machining Operation Designer, Tool Selection Designer, Set-up Designer,* or *Fixture Designer*. The concrete roles can be instantiated, and their instances assigned to specific software or human agents. When a version of the plan is constructed, agent roles in the abstract *Evaluator* class examine its performance; concrete classes can specialize for different metrics. Based on the results, *Strategist* roles propose possible improvement me- thods. The team leader selects a strategy that guides the designers in constructing a new version of the plan, and the cycle is repeated until a version is approved. The CAPP team interacts with other manufacturing teams, such as CAD and scheduling, and with external organizations such as tool manufacturers. These interactions are performed by specialized roles derived from the *Interagent* class. Interagents are active, intelligent interfaces between the CAPP team and external world.

The structure of a planning team is defined in terms of role instances and their interactions. It can be populated with agents in different ways to produce concrete team realizations. Instances of the same role can be replicated and distributed to enhance performance and fault tolerance. Multiple roles can be assigned to the same agent. Roles can be reassigned dynamically. A team can have sub-teams.

Fig. 2 illustrates a team organization in which role instances derived from the same basic abstract class form a sub-team. The environment is also segmented into four areas, each associated with a group.

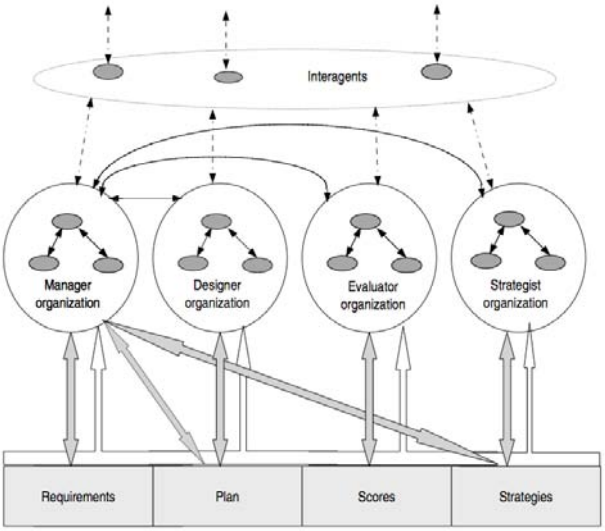

Fig. 2. Collaboration in a large CAPP team

Each group reads from the environment as a whole, but generates information in its own area. The manager group can write in *strategy* and *plan* areas, but only to select and approve already generated alternatives. Most messages are passed within groups. Agents associated

with the same abstract role thus follow a specific communication pattern that may be viewed as a social rule in the team. The patterns can also have a practical significance, as they suggest a natural partitioning across a distributed platform, with local writes and global read-only access.

A group of agents collaborating towards a common goal relies on a teamwork model that specifies the principles and policies underlying their cooperation. A realistic CAPP teamwork model must be sufficiently general and flexible to deal with uncertainties arising from equipment failures or changes in the environment [14]. It should also permit incorporation of domain-specific policies aligned with the human organization with which the system interacts, as in [15].

6. CONCLUSIONS

Exploring the prospects for overcoming the challenges in CAPP development through MAS technology, the paper examines the sources and nature of complexity in process planning, and analyzes how specific properties of MAS could be advantageous in addressing particular difficulties. The pur- pose of the analysis is to identify the domain-specific meta-model abstractions on which efficient multi-agent systems for CAPP could be built. In the CAPP domain, the paper proposes a collection of inter-related models that are concurrently constructed through cooperation of specialized designers in a multi-agent team.

In the MAS domain, the paper proposes team structures based on a domain-specific classification of agent roles. Plans for future work include a study of the mental states of specialized agents and their teamwork in joint pursuit of domain-specific CAPP objectives.

REFERENCES

[1] D. Polajnar, J. Polajnar, and Lj. Lukic, “Metamodel abstractions of agent roles in cooperative process planning,” in Proc. IEEE SMC Int. Conf. on Distributed Human-Machine Systems, 2008, pp. 77–82.

[2] W. Shen, L. Wang, and Q. Hao, “Agent-based distributed manufacturing, process planning, and scheduling: A state-of-the-art survey,” *IEEE Transactions on Systems, Man, and Cybernetics – Part C: Applications and Reviews*, vol. 36, no. 4, pp. 563–577, July 2006.

[3] W. J. Zhang and S. Q. Xie, “Agent technology for collaborative process planning: a review,” The *International Journal of Advanced Manufacturing*, vol. 32, no. 3/4, pp. 315–325, March 2007.

[4] L. Wang, W. Shen, and Q. Hao, “An overview of distributed process planning and its integration with scheduling,” *Int. J. Computer Applications in Technology*, vol. 26, no. 1/2, pp. 3–14, 2006.

[5] J. Shah, M. Mantyla, and D. Nau, “Introduction to feature based manufacturing,” in *Advances in Feature Based Manufacturing*, J. Shah, M. Mantyla, and D. Nau, Eds. Esevier , 1994, ch. 1.

[6] M. Mantyla, D. Nau, and J. Shah, “Challenges in feature-based manufacturing research,” *Comm. ACM*, vol. 39, no. 2, pp. 77–85, 1996.

[7] Y. F. Zhang and A. Y. C. Nee, “Application of genetic algorithm and simulated annealing in process planning optimizaton,” in *ComputationalIntelligence in Manufacturing Handbook*, J. Wang and A. Kusiak, Eds. CRC Press, 2001, ch. 9.

[8] S. Huang and N. Xu, “Automatic set-up planning for metal cutting: an integrated methodology,” *International Journal of Production Research*, vol. 41, no. 18, pp. 4339–4356, 2003.

[9] Z. Liu and L. Wang, “Sequencing of interacting prismatic machining features for process planning,” *Computers in Industry*, vol. 58, pp. 295–300, 2007.

[10] P. R. Cohen and H. J. Levesque, “Teamwork” *Nous*, vol. 25, no. 4, pp. 487–512, 1991.

[11] M. Tambe, “Toward flexible teamwork,” *Journal of Artificial Intelligence Research*, vol. 7, pp. 83–124, 1997.

[12] M. J. Johnson et al. “Coordinated operations in mixed teams of humans and robots,” in Proc. IEEE SMC Int. Conf. on Distributed Human- Machine Systems, 2008, pp. 63–68.

ПОВЫШЕНИЕ РАБОТОСПОСОБНОСТИ СВАРНЫХ КОНСТРУКЦИЙ ТРАНСПОРТНЫХ СРЕДСТВ

И.В. Дощечкина, Е.И. Давиденко

Аннотация: *Большое количество деталей, получаемых листовой штамповкой, соединяют между собой сваркой. Качество сварного соединения определяет работоспособность узла и машины в целом. В условиях усложнения конструкций и эксплуатации транспортных средств, требуют решения вопросы повышения надёжности сварочных узлов. Показаны пути увеличения конструкционной прочности и хладостойкости сварных соединений из строительных сталей путём микролегирования наплавленного металла редкоземельными элементами..*

Ключевые слова: *сварные соединения, структура, хладостойкость, металл шва, добавка иттрия, усталостная прочность*

ВВЕДЕНИЕ

Надёжная эксплуатация машин и оборудования определяется надёжностью отдельных узлов, механизмов, деталей.

В практике машиностроения широко используются сварные соединения из строительных сталей: рамы, лонжероны, балки, диски колёс и др. Качество сварного соединения определяет работоспособность машины в целом. Сварные конструкции зачастую выходят из строя по причине образования трещин как в процессе их производства , так и во время эксплуатации. Трещины возникают под влиянием ударных и циклических нагрузок, смены температур, агрессивной среды. В современных условия усложнения как машин, так и условий эксплуатации (увеличение скорости движения, удельных нагрузок, напряжений) вопрос повышения надёжности и долговечности ответственных сварочных соединений весьма актуален.

АНАЛИЗ ПУБЛИКАЦИЙ

Эксплуатационные свойства металла шва и околошовной зоны зависят от структуры, которая определяется химическим составом, размером зерен, скоростью охлаждения от температуры аустенизации, термической обработкой. Улучшить качество и повысить работоспособность сварных соединений можно за счет рационального легирования наплавленного металла, использования сварочных материалов с минимальным количеством вредных примесей, улучшения технологических параметров сварки [1]. Известно, что перспективным направлением повышения надежности сварных соединений является микролегирование наплавленного металла редкоземельными элементами (РМЗ). Благодаря своей высокой химической активности по отношению к вредным примесям, РМЗ очищают металл от кислорода, серы, фосфора, азота. В работе [2] отмечается, что уже через 2 минуты после ввода в жидкую ванну

РМЗ связывают 85-90% кислорода и 50-60% серы. РМЗ уменьшают склонность к перегреву и обеспечивают получение мелкого однородного зерна наплавленного металла, способствуют увеличению дисперсности и глобуляризации неметаллических включений, очищению границ зерен [3]. Отмеченные эффекты увеличивают устойчивость сварных соединений к хрупким разрушениям и делают их более надежными. РМЗ также существенно улучшают технологичность и производительность сварочных процессов, повышают плотность наплавленного металла. Из литературных данных следует [3] и наш опыт также свидетельствует [4], что среди РМЗ более эффективное влияние на структуру и свойства металла оказывает иттрий.

ЦЕЛЬ И ПОСТАНОВКА ЗАДАЧИ

Целью работы является повышение эксплуатационных свойств сварных конструкций из строительных низколегированных сталей, работающих в условиях динамических и вибрационных нагрузок, а также климатической смены температур. В соответствии с поставленной целью необходимо решить следующие задачи:
- изучить влияние иттрия на структуру и свойства наплавленного металла;
- разработать сварочный материал, обеспечивающий повышение хладостойкости, статической и усталостной прочности сварных соединений из сталей 09Г2С, 10ХСНД, широко используемых в машиностроении (рамы, лонжероны, диски колес).

Ирина Василивна Дощечкина– доц., к.т.н., Харьковский национальный автомобильно-дорожный университет, Харьков, Украина, ktm@khadi.kharkov.ua, diana@khadi.kharkov.ua
Елена Игоревна Давиденко– асс., Харьковский национальный автомобильно-дорожный университет, Харьков, Украина, ktm@khadi.kharkov.ua, diana@khadi.kharkov.ua

МЕТОДИКА И РЕЗУЛЬТАТЫ ИССЛЕДОВАНИЙ

При разработке сварочного материала (электрода, проволоки) необходимо учитывать тот факт, что иттрий обладает большим сродством к кислороду и при сварке окисляется в первую очередь. Следовательно материал, в который вносится иттрий, должен иметь невысокий окислительный потенциал и содержать элементы, обладающие большим сродством к кислороду при температуре сварочных процессов. Окисляясь, эти элементы в определенной степени защищают иттрий от выгорания, что способствует более полному его переходу в металл шва. Эти факторы обусловили выбор электрода для исследования - электрод марки УО-1 типа Э50. Электроды изготавливали по стандартной технологии с использованием проволоки Св08 диаметром 4 мм. Сварку и наплавку выполняли на постоянном токе обратной полярности с силой тока 200-210 А. Для химического анализа, исследований микроструктуры и механических свойств проводим многослойную наплавку на сталь 10. Сварные соединения изготовили из листовых сталей 09Г2С и 10ХСНД.

РЕЗУЛЬТАТЫ ИССЛЕДОВАНИЙ

Иттрий в покрытии электрода вносили в расчетных количествах 0,2-3,0%. Остаточное содержание иттрия в наплавленном металле в зависимости от процента добавки в покрытие составляло 0,005-0,015% соответственно. Несмотря на очень малую степень усвоения иттрия, химический анализ наплавленного металла показал заметное уменьшение содержания серы (от 0,019 до 0,01%) и понижение концентрации фосфора, хотя и менее значительное. Добавка иттрия наряду с уменьшением содержания серы способствовали её более равномерному распределению, очищению границ зерен. Под влиянием иттрия изменяется количество, характер и расположение всех неметаллических включений в наплавленном металле. После добавки 0,3% иттрия их общее количество снижается, они измельчаются, приобретают округлую форму и распределяются равномерно. При присадке более 1% иттрия наблюдается дальнейшее измельчение включений, но заметно увеличивается их количество. Таким образом, максимальный модифицирующий и рафинирующий эффект иттрия наблюдается при его добавке в количестве до 0,3%. Иттрий оказывает очень большое влияние на размер зерна. В наплавленном металле без иттрия наиболее вероятный размер зерен соответствует 50мкм (~60%). Добавка 0,3% иттрия резко измельчает зерно: более 70% занимают зерна размером 15мкм, а наиболее крупные зерна (35мкм) занимают только 6%. При добавке 0,6-1% иттрия тенденция к измельчению зерна сохраняется – в максимальном объеме фиксируются зерна размером от 6-10мкм.
Иттрий приводит к изменениям перлитной составляющей структуры: участки перлита дробятся, становятся менее плотными, их распределение имеет островковый характер.

При электронномикроскопическом исследовании обнаруживается дробление пластин цементита, закругление их и приближение к строению, близкому к зернистому перлиту. При добавке более 1% иттрия в покрытие электрода по границам зерен и в самом зерне феррита выделяется новая хрупкая фаза, обогащенная иттрием до 1,5%. Отмеченные изменения микроструктуры существенно повлияли на уровень механических свойств наплавленного металла. С увеличением концентрации иттрия в покрытии (0,2-0,6%) повышаются характеристики прочности (σ_{02} возрастает от 340 до 550 МПа), несколько увеличивается пластичность. Ударная вязкость от 18 Дж/см^2 повышается до 25-30 Дж/см^2, наиболее высокие значения фиксируются при концентрации иттрия 0,3%.

С повышением содержания иттрия (более 1%) упрочняющий эффект от структурных изменений нивелируется негативным влиянием хрупкой иттриевой фазы. Важным показателем работоспособности наплавленного металла является поведение его ударной вязкости при отрицательных температурах. Поскольку иттрий есть активный раскислитель, десульфуратор и модификатор, то, безусловно, должен эффективно повлиять на сопротивление динамическим нагрузкам при снижении температуры. Наибольший эффект оказывает добавка 0,3% иттрия – ударная вязкость при -60ºС в 2 раза выше, чем у металла, наплавленного серийным электродом, и сохраняется на уровне значений, полученных для серийного электрода при комнатной температуре. Увеличение содержания иттрия в покрытии до 0,6-1% приводит к снижению показателей ударной вязкости во всём температурном интервале, что связано с загрязнением структуры окислами иттрия и другими соединениями, образующимися при сварке. Однако значение ударной вязкости для всех исследованных составов остаются более высокими, чем для серийного электрода при одинаковых температурах. Сама по себе ударная вязкость еще не характеризует сопротивление металла к хрупкому разрушению. Для получения необходимой информации были определены составляющие работы разрушения $КС_з$ и $КС_р$. Наличие иттрия приводит к повышению работы зарождения трещины ($КС_з$) во всём интервале исследованных температур. Работа развития трещины ($КС_р$) заметно увеличивается при комнатных температурах, но по мере снижения температуры разница между значениями $КС_р$ для металла без иттрия и с добавкой иттрия уменьшается.

Иттрий заметно улучшает сварочно-технологические характеристики: повышается стабильность горения дуги, уменьшается разбрызгивание металла, образующаяся шлаковая корка хорошо защищает металл и легко отделяется при охлаждении. Поскольку электроды с 0,3-0,4% иттрия показали высокие свойства при пониженных температурах, рационально использовать их для сварки хладостойких сталей 09Г2С и 10ХСНД. Результаты механических испытаний сварных со-единений из этих сталей приведены в таблице 1. Из таблицы видно, что прочностные характеристики сварных

Таблица 1 Механические свойства сварных соединений сталей 09Г2С и 10ХСНД, выполненных серийным и опытным электродами

Сталь	Электрод	$\sigma_{в.}$ МПа	σ_{02}, МПа	δ, %	ψ, %	KCU, МДж/м^2					
						+20	0	-20	-40	-60	-70
09Г2С	Серийный	550	400	29	72	1,9	1,7	1,7	1,2	0,9	0,7
	Опытный	600	440	30	68	2,3	2,2	2,2	1,8	1,4	0,9
10ХСНД	Серийный	580	470	28	68	1,8	1,6	1,3	1,2	0,7	0,6
	Опытный	620	490	28	67	2,1	1,8	1,8	1,5	1,2	1,0

соединений, выполненных иттрий содержащим электродом, выше по сравнению с серийным. Пластичность при этом сохраняется практически на том же уровне, тогда как ударная вязкость, особенно при низких температурах возрастает. Улучшение свариваемости, запас пластичности, повышение ударной вязкости при комнатной и отрицательных температурах увеличивают сопротивление наплавленного металла хрупкому разрушению.

С целью повышения предела выносливости сварного соединения был использован метод упрочнения металла сварного шва холодной пластической деформацией. После упрочнения проводились испытания на растяжение при симметричном изгибе до полного разрушения образцов, которые вырезались из сварного шва. Результаты исследований показали, что предел выносливости сварных швов из стали 10ХСНД при плюсовой температуре в 1,5 раза выше, чем у основного металла, но на 10% ниже, чем у соединений из стали 09Г2С. При снижении температуры испытаний до -40ºС зафиксировано увеличение предела выносливости соединений из стали 10ХСНД до 105 МПа, что на 15% выше, чем у стали 09Г2С. Следует отметить, что повышение сопротивления усталости сварных соединений при отрицательных температурах имело место лишь в том случае, когда нагружение было выше 2,5 Н/мм^2. При таких условиях благоприятные сжимающие напряжения более стойкие.

ВЫВОДЫ

Увеличение хладостойкости сварных конструкций из сталей 09Г2С и 10ХСНД в сочетании с повышенной прочностью и запасом пластичности может быть достигнуто с использованием сварных материалов, содержащих иттрий. Определена оптимальная добавка иттрия, обеспечивающая улучшение технологических параметров процесса сварки и уменьшение вероятности хрупкого разрушения сварного соединения при одновременном повышении его прочности. Для повышения сопротивления усталости рекомендована холодная пластическая деформация сварного шва с удельным нагружением более 3 Н/мм^2.

ЛИТЕРАТУРА

[1] Ефіменко М.Г., Радзівілова Н.О. Металознавство і термічна обробка зварних з'єднань. – Харків, - 2003. – 488с.

[2] Фраге Н.Р., Гуревич Ю.Г., Филинков М.Д. Модифицирование чугуна малыми добавками лигатуры РМЗ.// Известия вузов. ЧМ, 1981,№2. - С. 93-97.

[3] Александров А.Г., Лазебнов П.П. Влияние иттрия на структуру и механические свойства шва при сварке чугуна, стали и сплавов. // Автоматическая сварка, 1982, №12. – С. 34-37.

[4] Дощечкина И.В., Кафтанов С.В., Костик В.О. Повышение конструкцилнной прочности и

хладостойкости литой низкоуглеродистой стали. // Вестник национального технического университета «ХПИ», 2002, т.10. – С. 36-39

EXPERIMENTAL INVESTIGATION AND MATHEMATICAL MODELING OF CUTTING SPEED BY ABRASIVE WATER JET

P. Janković, M. Radovanović

Abstract: *New, difficult-to-machine materials and increased part complexity have resulted in the creation of new manufacturing processes, known as nontraditional manufacturing processes. Water jet cutting is one of the newest technique in non-traditional machining processes. This paper presents concrete use and advantages of the multiple factor experiment by modeling of cutting speed in abrasive water jet machining.*

Key words: *nontraditional manufacturing processes, abrasive water jet cutting, experimental design*

1. INTRODUCTION

Abrasive water jet machining is unique process that is able to cut almost all materials cost effectively and is quickly becoming a new "standard tool" in machine shops around the world. The basic technology is both simple and extremely complex.

The use of the abrasive water jet for machining or finishing purposes is based on the principle of erosion of the material upon which the jet hits. Each of two components of the jet, i.e. the water and the abrasive material has both a separate purpose and a supportive purpose. It is the primary purpose of the abrasive material within the jet stream to provide the erosive forces. It is the primary purpose of the jet to deliver the abrasive material to the workpiece for the purpose of erosion. However the jet also accelerates the abrasive material to a speed such, that the impact and change in momentum of the abrasive material can perform its function. In addition it is an additional purpose of the water to carry both the abrasive material and the eroded material clear of the work area so that additional processing can be performed. In one way or another in any machining process the spent material must be gotten our of the way and the water jet provides that mechanism [1], [3].

2. ABRASIVE WATER JET CUTTING PROCESS

Abrasive water jet machining is appropriate and cost effect for a number of procedures and materials and are applied in nearly all areas of modern industry, such as automotive industry, aerospace industry, construction engineering, environmental technology, chemical process engineering, and industrial maintenance.

In the area of manufacturing, the water jet-technique is used for: material cutting, deburring by plain water jets, surface peening by plain water jets, conventional machining with water-jet assistance, cutting of difficult-to-machine materials by abrasive water jets, milling and 3-D-shaping by abrasive water jets, turning by abrasive water jets, piercing and drilling by abrasive water jets, polishing by abrasive water jets etc.

At its basic, water flows from a pump, through plumbing, and out of a cutting head. The energy required for cutting materials is obtained by pressurizing water to high pressures and then forming a high-intensity cutting stream by focusing this water through a small orifice.

There are essential two types of water jets - pure and abrasive. With either, the water must be pressurized if it is to erode materials - and water jet is essentially an erosion process.

The abrasive waterjet differs from the pure waterjet in just a few ways. In pure waterjet, the supersonic stream erodes the material. In the abrasive waterjet, the waterjet stream accelerates abrasive particles and those particles, not the water, erode the material. The abrasive waterjet is hundreds, if not thousands of times more powerful than a pure water jet. Both the water jet and the abrasive water jet have their place. Where the pure water jet cuts soft materials, the abrasive water jet cuts hard materials, such as metals, stone, composites and ceramics.

An abrasive water jet is a jet of water which contains abrasive material. Solid particles – the "abrasive" – join the water jet in mixing chamber (Fig. 1) and are focused by the abrasive nozzle. High pressure water enters the upper portion of the nozzle assembly and passes through a small-diameter orifice to form a narrow jet. The water jet then passes through a small chamber where a Venturi effect creates a slight vacuum that pulls abrasive material and air into this area through a feed tube. The abrasive particles are accelerated by the moving stream of water, and together they pass into a long, hollow cylindrical nozzle. The nozzle acts like a rifle barrel to accelerate the abrasive particles. The abrasive and water mixture exits the nozzle as a coherent stream and cuts the material. It's critical that the orifice and the nozzle be precisely aligned to ensure that the water jet passes directly down the center of the nozzle. Otherwise the quality of the abrasive water jet will be

Predrag Janković, Mašinski fakultet Niš
Miroslav Radovanović, Mašinski fakultet Niš

diffused, the quality of the cuts it produces will be poor, and the life of the nozzle will be short. In the past, most cutting head designs required the operator to adjust the alignment of the jewel and nozzle during operation. Modern cutting head designs rely on precisely machined components to align the orifice and nozzle during assembly, thereby eliminating the need for operator adjustments.

Nozzles are approximately 70 mm long, with inside diameters that can vary from about 0.8 mm to 1.2 mm. The normal standoff distance between the nozzle and the workpiece is usually between 0.25 mm and 2.5 mm.

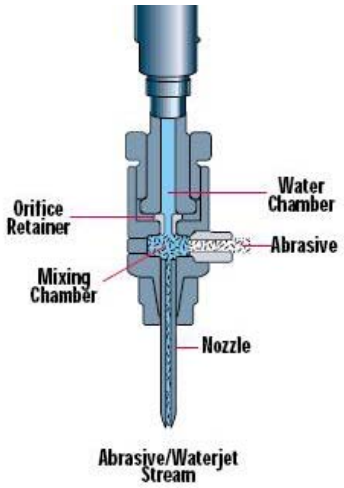

Figure 1. Abrasive water jet cutting head

3. INFLUENCING PARAMETERS OF ABRASIVE WATER JET CUTTING SPEED

Abrasive water jet cutting process depends on a large number of process parameters such as water pressure, orifice diameter, standoff distance, abrasive rate, cutting speed etc.

The key parameter that controls cutting speed is the water nozzle diameter. The other two parameters that greatly influence the cutting speed are the water pressure and the abrasive rate. Water pressure has a great influence on the cutting speed. Most in abrasive water jet cutting circles follow a simple rule: the higher the pressure, the higher the cutting speed, the lower the costs. Higher pressures result in faster cutting. To cut as fast as possible, the system should be operated using the maximum pump power available. The pump power is the determining factor in the water jet cutting. The most common pump size is the 37 kW pump powering one head. The order of popularity follows 75 kW, 18 kW, and 112 kW. Over 60% of all pumps produced today are of 37 kW or 75 kW.

The power in the abrasive jet at the exit of the nozzle is a function of pressure, flow and nozzle size. Power output is more sensitive to changes in nozzle diameter than pressure: doubling the nozzle diameter increases the jet power by a factor of 4, whereas doubling the pressure increases the power by a factor 2.8. In abrasive water jet cutting it is often thought that to reduce the abrasive rate saves money. There is a peak performance point that abrasive water jets operate. As abrasive rate is increased cut speed goes up and cost per meter goes down. Cut speed and cost per meter are both at their optimum. This fact is independent of the material of workpiece, or the power of the system. But, too much abrasive will clog in the mixing chamber. However, the optimum values of these parameters are not totally independent. The optimum abrasive rate can be related to the water rate. Orifice/nozzle size combination has an influence on cutting speed. The orifice size dictates the volume of water output by the cutting head. Larger orifices will typically produce a faster cut but will require more pump power. Generally a focusing tube which is about three times larger than the orifice provides optimal cutting efficiency, balancing cost and cutting speed. Typical orifice/nozzle combinations are: 6/21 (0.15/0.54 mm), 9/30 (0.23/0.76 mm), 13/43 (0.33/1.10 mm), 18/63 (0.45/1.60 mm) for water pressure of 400 MPa.

The abrasive used in abrasive water jet cutting is hard sand that is specially screened and sized. The most common abrasive is garnet. Different mesh sizes are used for different jobs: 120 mesh - produces smooth surface, 80 mesh - most common, general purpose, 50 mesh – cuts a little faster than 80, with slightly rougher surface. Cutting speed depends and on the material, the thickness, the quality of the edge finish and tolerance. Cutting speed varies and as a function of the geometry of the part ([2],[5], [6],[7]).

4. METHODOLOGY OF EXPERIMENT

In the present study, the influence of orifice size and abrasive nozzle, material thickness, water jet pressure and abrasive flow rate on the performance of abrasive water jet cutting. Experimental design approach is employed for conducting the experiments considering the water jet pressure, abrasive flow rate and material thickness at different levels. To identify the process parameters that are statistically significant in the process, analysis of variance is performed. By considering these significant parameters, the orthogonal polynomial models are developed in order to predict the cutting performance in terms of cutting speed. These empirical relations are used to develop the response surfaces, which are used to generate model available in MATLAB software package.

With today's ever-increasing complexity of models, design of experiment has become an essential part of the modeling process. Design of experiment (DOE) is the process of planning the experiments considering the process parameters at different levels so as to acqure necessary information for building statistical models, which can aid in predicting the process performance.

The design editor within the MBC Toolbox - a part of MATLAB software package is used as a help in

design of experiment. Central composite design provides a simple, efficient and systematic approach for optimal design of experiments to asses the performance, quality and cost. In order to detect curvature in the ralationshop between an input factor (independent) and an outcome (dependent) variable, we need at least 3 levels for the respecive factor (three design points). One of designs for three factors is faced (CCF) designs, that have the star points on the faces of the cube (Fig. 2).

For analytical model and analysis of experimental data it is used Model-based calibration toolbox, design of experiments and statistical modeling, version 1.1 of software package MATLAB, version 6.5, release 13.

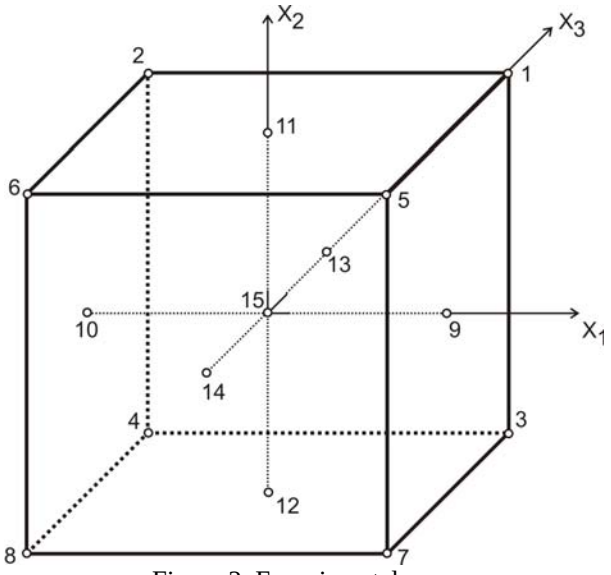

Figure 2. Experimental space

The experiment was planned by adopting full factorial experimentation procedure. In these experiments, the water jet pressure, abrasive flow rate and material thickness were varied at different levels and the orifice size and abrasive nozzle was kept constant.

In the experimental plan, the process parameters such as water jet pressure, abrasive flow rate and material thickness are varied at three levels. In Table 1, the range of different process parameters and factor levels used for this study are shown.

Table 1. Process parameters and their levels considered for experimentation

Symbol	Parameters	Units	Level 1	Level 2	Level 3
s	Material thickness	mm	3	5	7
p	Water pressure	MPa	360	380	400
q	Abrasive flow rate	g/min	300	350	400

Other influencing parameters, such: orifice size, abrasive nozzle diameter and abrasive size kept constant. All the cutting experiments are single pass experiments conducted by choosing standoff distance of 3 mm, jet impact angle of 90°, garnet abrasives of 80-mesh, orifice/focusing tube size of 0,33/1,10 mm.

Cutting data (Table 2) is given from manufacturer "KMT Waterjet Systems Inc." for material carbon stool and medium edge quality.

Table 2. Cutting data

Exp. num	Code			Input factors			Output factor
	X_1	X_2	X_3	q (g/min)	s (mm)	p (MPa)	v (mm/min)
1	+1	+1	+1	400	7	400	190
2	-1	+1	+1	300	7	400	170
3	+1	-1	+1	400	3	400	520
4	-1	-1	+1	300	3	400	465
5	+1	+1	-1	400	7	360	150
6	-1	+1	-1	300	7	360	135
7	+1	-1	-1	400	3	360	430
8	-1	-1	-1	300	3	360	380
9	+1	0	0	400	5	380	255
10	-1	0	0	300	5	380	230
11	0	+1	0	350	7	380	160
12	0	-1	0	350	3	380	450
13	0	0	+1	350	5	400	270
14	0	0	-1	350	5	360	220
15	0	0	0	350	5	380	240

5. MATHEMATICAL MODELING OF CUTTING SPEED

For mathematical modelling of cutting speed is chosen power function:

$$v = Cs^{p_1} p^{p_2} q^{p_3} \quad (1)$$

where v – cutting speed, s – material thickness, p – water pressure, q – abrasive flow rate, C, p_i – constants. This analytical model, in form of power function, can make linear by logarithm [8].

$$\ln v = \ln C + p_1 \ln s + p_2 \ln p + p_3 \ln q \quad (2)$$

Put in y=lnv, p_0=lnC, x_1=lns, x_2=lnp and x_3=lnq we have:

$$y = p_0 + p_1 x_1 + p_2 x_2 + p_3 x_3 \quad (3)$$

In setup it is given test plan of experimental model with three input variables (material thickness, water pressure and abrasive flow rate) and one output variable (cutting speed). Experimental data can be loaded in test plan from files, from the MATLAB workspace, and from tailor-made Excel sheets. Next step is creating of test plan, which compose of data inputs and a model. The type of the model is the shape of curve used to fit the test data, for example, quadratic, cubic, or polyspline curves.

After program run the response feature pane appears, showing the fit of the model to the input data. Response model with diagnostic statistics are shown in Figure 3.

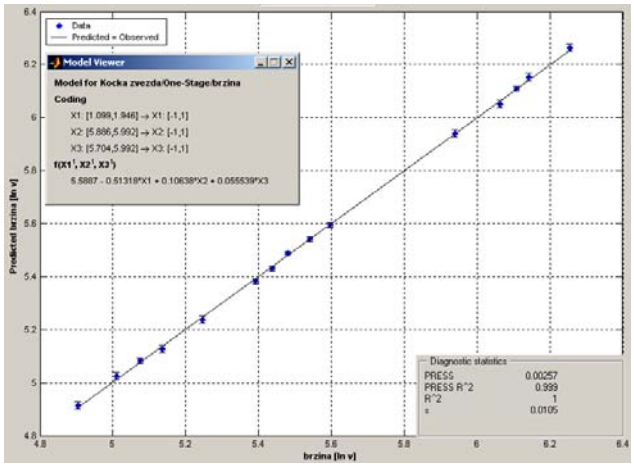

Figure 3. Response model

Model viewer (Fig. 3) gives correlation coefficients. Regression equation now is:

$$y = 5.5887 - 0.51318 \cdot x_1 + 0.10638 \cdot x_2 + 0.055539 \cdot x_3 \quad (4)$$

Coding values in equation (4) are:

$$x_1 = 1 + 2\frac{\ln q - \ln q_{max}}{\ln q_{max} - \ln q_{min}} = 1 + 2\frac{\ln q - \ln 400}{\ln 400 - \ln 300} = -40.651 + 6.952 \cdot \ln q$$

$$x_2 = 1 + 2\frac{\ln s - \ln s_{max}}{\ln s_{max} - \ln s_{min}} = 1 + 2\frac{\ln s - \ln 7}{\ln 7 - \ln 3} = -3.5932 + 2.3604 \cdot \ln s \quad (5)$$

$$x_3 = 1 + 2\frac{\ln p - \ln p_{max}}{\ln p_{max} - \ln p_{min}} = 1 + 2\frac{\ln p - \ln 400}{\ln 400 - \ln 360} = -112.6907 + 18.9753 \cdot \ln p$$

Substitute of coding values we obtain regression equation for cutting speed in form:

$$v = \frac{1}{910} \cdot \frac{p^{2.019} q^{0.386}}{s^{1.211}} \quad (6)$$

where v (mm/min) – cutting speed, p (MPa) – water pressure, q (g/min) – abrasive rate, s (mm) – material thickness.

6. CONCLUSION

Abrasive water jet is the fastest growing major machine tool process in the world. As complex process water jet cutting depends on a large number of process parameters, which determine machined part quality. Whereby "quality" describes the combination of surface finish, tolerance and other properties of the cut.

In this work, investigations were carried out to study the influence of some process influencing parameters (such as water pressure, abrasive flow rate) on the cutting performance, such as cutting speed using full factorial experimentation procedure.

The cutting speed is one of the most important parameter of this technology, because with the quality of the machined surface and the costs of the technology can be controlled.

LITERATURE

[1] Hoogstrate A.M., van Luttervelt A.M.;Opportunitirs in Abrasive Water-Jet Machining, Annals of the CIRP Vol. 46/2/1997

[2] Janković P., Radovanović M., Parameters of Abrasive Waterjet Cutting Process, 6th International Conference ″Research and Development in Mechanical Industry″-RaDMI 2006, Budva, Montenegro, 2006, pp.343-346

[3] Janković, P., Radovanović, M., Vicovac, N.: High-pressure pump - "Heart" of the machine for contour cutting by an abrasive water jet, 29. HIPNEF, 2004, Vrnjačka Banja

[4] Radovanović M., Characteristics of Abrasive Waterjet, 3th International Conference "Research and Development in Mechanical Industry"-RaDMI 2003, Herceg Novi, Serbia and Montenegro, 2003, pp. 469-473

[5] Radovanovic M., Dasic P., Stefanek M., Some Possibilities for Determining Abrasive Waterjet Cutting Parameters, 13. International Conference "Co-Mat-Tech 2005", Trnava, Slovakia, 2005, pp. 969-976

[6] Radovanovic M., Determining of Cutting Data by Abrasive Waterjet Cutting, XII International Conference ″Machine-building and Technosphere of the XXI Century″, Sevastopol, Ukraine, 2005, pp.221-225

[7] Radovanovic M., Estimate of Cutting Speed by Abrasive Waterjet Cutting, The 31st Internationally Attended Scientific Conference "Modern Technologies in the XXI Century", Bucharest, Romania. 2005, pp. 8.196-8.203

[8] Radovanović M., Mathematical modeling of cutting speed by abrasive waterjet, Nadiinist instrumentu ta optimizacia tehnologičnih sistem, No.21 2007, ISBN 966-379-149-4, UDK 621.9: 658.3: 519.8, Sbornik naučnih trudov, Ministerstvo osviti i nauki Ukraini, Donbaska deržavna mašinobudivna akademia, Kramatorsk, Ukraina, 2007, pp. 273-279

ВЛИЯНИЕ МАТЕРИАЛА ИНДЕНТОРА И НАГРУЗКИ НА ЗНАЧЕНИЯ ТВЁРДОСТИ КОНСТРУКЦИОННЫХ МАТЕРИАЛОВ.

В.И. Мощенок, Е.А. Нестеренко, А.А. Ляпин, Д.Б. Глушкова

Аннотация: *Исследовалась истинная и универсальная твёрдость железоуглеродистых сплавов и цветных металлов, используемых в тяжёлом машиностроении. При испытаниях использовали инденторы, изготовленные из различных материалов при разных нагрузках.*
Полученные результаты позволили определить влияние исследуемых параметров на значения твёрдости испытуемых металлов.

Ключевые слова: *индентор, твёрдость, металл, машиностроение*

В качестве материалов для деталей машин тяжелого машиностроения широко применяются железоуглеродистые сплавы и цветные металлы.

Для определения качества деталей после изготовления и в процессе эксплуатации широко используются неразрушающие методы контроля. Наиболее простой и широко распространенный метод-это метод определения твердости.

В связи с тем, что используемые в настоящее время в практике предприятий методы определения твердости носят чисто экспериментальный характер и лишены физического смысла [1], авторами определялась истинная и универсальная твердость исследуемого материала, а также влияние материала индентора и нагрузки на их значения.

Измерения производились на универсальном твердомере [1]

Рис.1 Твердомер универсальный

В качестве инденторов - использовались шарики диаметром 10 мм изготовленные из твердосплавного материала и из стали. Нагрузка индентирования изменялась в интервале от 0 до 1600Н, что соответствует реальным нагрузкам при эксплуатации. Схема индентирования представлена на рисунке 2.

На первом этапе работы определяли характер изменения универсальной твердости исследуемого материала.

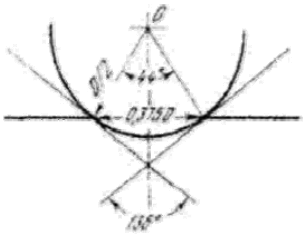

Рис.2 Схема индентирования

Универсальная твердость представляет собой сопротивление металлов упругому и пластическому деформированию индентором в диапазоне прилагаемых нагрузок [2].

$$HU = \frac{P}{A(h)}, N/mm^2 \qquad (1)$$

где P – нагрузка, Н, A (h)- площадь боковой поверхности внедренной части индентора, мм^2

Василий Иванович Мощенок – проф., к.т.н., Харьковский национальный автомобильно-дорожный университет, Харьков, Украина, ktm@khadi.kharkov.ua,
Елена Анатольевна Нестеренко – ассистент, Харьковский национальный автомобильно-дорожный университет, Харьков, Украина, ktm@khadi.kharkov.ua, diana@khadi.kharkov.ua
Александр Александрович Ляпин – ассистент, Харьковский национальный автомобильно-дорожный университет, Харьков, Украина, ktm@khadi.kharkov.ua, diana@khadi.kharkov.ua
Диана Борисовна Глушкова – доц., к.т.н., Харьковский национальный автомобильно-дорожный университет, Харьков, Украина, ktm@khadi.kharkov.ua, diana@khadi.kharkov.ua

Универсальная твердость $H_{10ун}$ для измерения шариком диаметром 10 мм рассчитывали по формуле:

$$H_{10ун} = \frac{P}{(31,41 \cdot h)}, N/mm^2 \qquad (2)$$

где h – глубина проникновения индентора, мм^2

Проведенные исследования представляют научный ипрактический интерес, так как в литературе отмечается, что зависимость универсальной твердости от прилагаемой нагрузки полностью не изучена [2,3].

Определялась универсальная твердость и истинная твёрдость стальной пластины.

Результаты измерений представлены на рис. 3-4

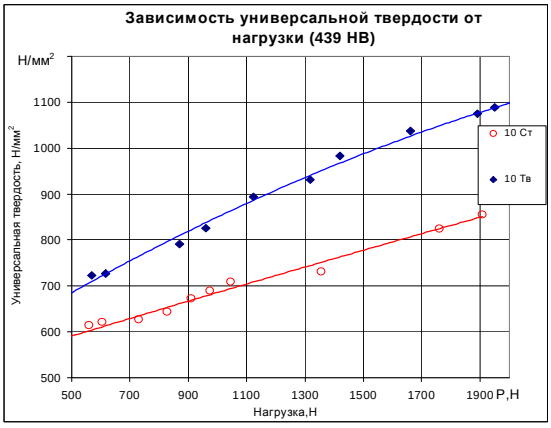

Рис.3

Различие универсальной твёрдости измеренной твёрдосплавным и стальным шариком колеблется от 15% при нагрузки 500 Н до 26% при нагрузки 900 Н.

Истинная твёрдость определялась пол формуле:

$$HB_u^{10} = \frac{P}{V} = \frac{P}{1,04719 \cdot h^2 \cdot (15 - h)}, \ N/мм^3 \qquad (3)$$

Где V – объем отпечатка, мм^3

Измерения проводили с помощью инденторов - шариков диаметром 10 мм изготовленных из твердосплавного материала и из стали.

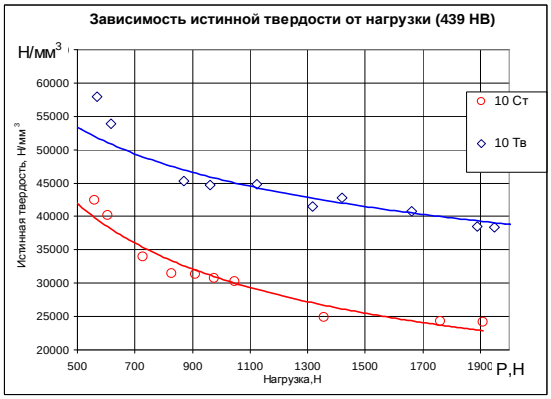

Рис.4

Полученные результаты нами позволили сделать следующий вывод.

ВЫВОДЫ:

1. Универсальная твердость исследуемого материала увеличивается с возрастанием нагрузки. Характер изменения одинаков при измерении индентором, выполненным как из стали, так и из твердосплавного материала.
2. Истинная твердость уменьшается с увеличением нагрузки.
3. Характер изменения истинной и универсальной твердости не зависит от материала индентора.
4. Величина твердости, измеренная стальным индентером ниже, чем твердосплавным. Вероятно это связано с разным накоплением упругой и пластической деформации, а также ее релаксацией после снятия нагрузки в зависимости от материала индентора, что требует дальнейших исследований.

ЛИТЕРАТУРА

[1] Мощенок В.И., Тарабанова В.П., Глушкова Д.Б. Спосіб оцінки твердості матеріалу. Пат. України UA 74654 C2, 601 N3/40. Опубл. 16.01.06. Бюл. №1. – 3 с.

[2] Мощенок В.И., Глушкова Д.Б., Ковтун Г.П., Стоєв П.І. Спосіб визначення фізико-механічних властивостей та пристрій для його здійснення. Пат. України UA 50486 A.60/N3/46. Заяв. 23.01.2002. Опубл. 15.10.2002. Бюл. №10. – 5 с.

[3] Мощенок В.И.Определение истинной твердости деталей дорожных машин инденторами различной формы. Вестник ХНАДУ. Сб. научн. трудов. – 2007. Вып. 38. – С. 285 – 289.

МОДЕЛЬ ВЗАИМОДЕЙСТВИЯ МИКРОНЕРОВНОСТЕЙ ПОВЕРХНОСТЕЙ ТРЕНИЯ С УЧЕТОМ АДСОРБЦИОННОЙ ПЛЕНКИ ПОВЕРХНОСТНО-АКТИВНЫХ ВЕЩЕСТВ

С. Е. Селиванов, В. Б. Косолапов, С. В. Литовка

Аннотация: *Рассмотрена модель взаимодействия микронеровностей поверхностей трения в присутствии адсорбционного слоя поверхностно-активных веществ (ПАВ) при условии упругого металлического контакта сопряженных пар. Установлены условия контактирования при которых роль адсорбционной пленки ПАВ становится незначимой в процессе износа трибосопряжения.*

Ключевые слова: *граничное трение, адсорбционная пленка, воспринимаемая нагрузка, площадь контакта.*

1. ВВЕДЕНИЕ

Основной причиной выхода из строя в процессе эксплуатации технических систем является изнашивание их поверхностей трения, при этом повышенная интенсивность износа трибосопряжений происходит в неустановившихся режимами нагружения. Это приводит к снижению показателей надежности машины, а точнее, снижение срока службы механизмов, в которых наблюдаются процессы трения.

2. АНАЛИЗ ПУБЛИКАЦИЙ

Наиболее интенсивно процесс износа трибосопряжений развивается в граничном режиме смазки [1].

В соответствии с международным стандартом ISO 4378-3-1999 под граничной смазкой понимается такой вид смазки, которому не могут быть приписаны объемные вязкостные свойства и который определяется свойствами граничных слоев, возникающих при взаимодействии смазочного материала и поверхности трения в результате физической или химической адсорбции. [2]

При контактировании граничные слои частично выдавливаются из зоны контакта и утончаются, при этом происходит сближение между поверхностями твердых тел [3].

Увеличение сближения вызывает возрастание площади фактического касания по адсорбционной пленке до тех пор, пока суммарная реакция по пленке не станет равной по величине и противоположной по направлению нормальной нагрузке. Если нагрузка превысит своё предельное значение, то происходит выдавливание адсорбционной пленки из зоны контактирования, что приводит к взаимодействию металлических поверхностей микронеровностей. При этом площадь фактического контакта, включающая площадь по адсорбционной пленке и площадь металлического контакта, будет увеличиваться до тех пор, пока возникающие в зонах фактического контакта силы отталкивания не уравновесят внешние сжимающие силы. Максимальная внешняя нагрузка, которую слой молекул ПАВ способен выдержать без разрушения есть его предельная несущая способность [2].

3. ЦЕЛЬ РАБОТЫ И ПОСТАНОВКА ЗАДАЧИ

Целью данной работы является определение роли адсорбционной пленки ПАВ при упругом металлическом контакте поверхностей трения.

Задачами исследования являлось определение площадей контакта и нагрузок, приходящихся на адсорбционный слой молекул ПАВ и микронеровности, при условии упругого металлическом контакта поверхностей трения.

4. МОДЕЛЬ ВЗАИМОДЕЙСТВИЯ МИКРОНЕРОВНОСТЕЙ

Рассматриваем взаимодействие микронеровностей при металлическом контакте (рис. 1, зона 2), когда в контакт вступают как адсорбционная пленка ПАВ, так и упругодеформирующаяся микронеровность.

Единичные микронеровности, в присутствии смазочного материала, моделируем сферическими

Станислав Евгеньевич Селиванов, д.т.н., профессор, Харьковский национальный автомобильно-дорожный университет, Украина
Виктор Борисович Косолапов, к.т.н., доцент, Харьковский национальный автомобильно-дорожный университет, Украина
Сергей Владимирович Литовка, аспирант, Харьковский национальный автомобильно-дорожный университет, Украина, litovka@khadi.kharkov.ua

сегментами. Схема их силового взаимодействия представлена на рисунке 2.

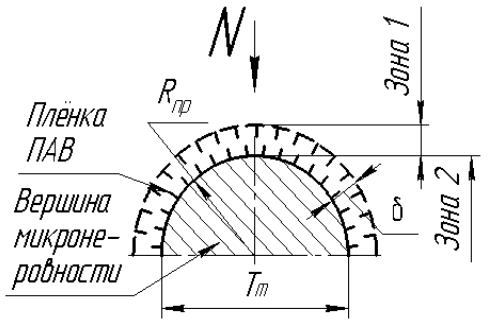

Рис. 1. Схема представления вершины микронеровности

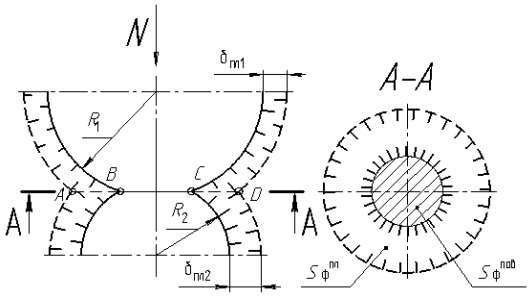

Рис. 2. Схема взаимодействия микронеровностей ($P^к$ – контактное давление, $S^{пл}$ – фактическая площадь контакта пленок, R_1, R_2 – радиус кривизны, соответственно первой и второй микронеровности, $\delta_1^{пл}, \delta_2^{пл}$ – толщина адсорбированной плёнки ПАВ на первой и второй микронеровности)

Расчётная модель контакта двух микронеровностей может быть приведена к контакту эквивалентной микронеровности с гладкой плоскостью. [4, 5]. В этом случае применяем приведенные значения параметров шероховатости.

Суммарная контактная нагрузка, приходящаяся на единичный микровыступ, с учетом адсорбционной плёнки ПАВ определяется выражением

$$N = N^{пл} + N^{пов}, \qquad (1)$$

где $N^{пл}$ – нагрузка, воспринимаемая адсорбционным слоем; $N^{пов}$ – нормальная нагрузка, воспринимаемая металлическим контактом микронеровностей.

Нормальную нагрузку $N^{пов}$, воспринимаемую металлическим контактом микронеровностей, можно определить на основании решения Герца [6]:

$$N^{пов} = \frac{4}{3} \cdot h^{3/2} \cdot R_{пр}^{1/2} \cdot E_{эф}^{пов} \qquad (2)$$

где h – сближение контактирующих микронеровностей во второй зоне; $R_{пр}$ – приведенный радиус кривизны микронеровностей определяется из соотношения

$$R_{пр} = \frac{R_1 \cdot R_2}{R_1 + R_2}, \qquad (3)$$

где R_1, R_2 – радиусы кривизны микронеровностей; $E_{эф}^{пов}$ – эффективный модуль упругости сжимаемых микронеровностей определяется выражением

$$E_{эф}^{пов} = \frac{E_1 \cdot E_2}{E_2\left(1-\mu_1^2\right) + E_1\left(1-\mu_2^2\right)}, \qquad (4)$$

где E_1, E_2 и μ_1, μ_2 – соответственно модули упругости и коэффициенты Пуассона материалов контактирующих выступов обоих тел.

Для определения нагрузки, воспринимаемой адсорбционным слоем $N^{пл}$, в первом приближении, воспользуемся представлением об однородности полимолекулярного адсорбированного слоя ПАВ, который может рассматриваться как квазитвердое многослойное кристаллическое образование, имеющий постоянные прочностные характеристики [11].

При этом для облегчения расчетов принимаем, что толщины адсорбированных слоёв ПАВ и радиусы кривизны на обеих микронеровностях имеют одинаковую величину $\delta_1^{пл} = \delta_2^{пл} = \delta^{пл}$ и $R_1 = R_2 = R_{пр}$. Величина сближения h изменяется в пределах $h \le \delta^{пл}$.

По данным работ [7, 8] упругая деформация смазочных слоёв происходит при давлении $p < 5-6\ МПа$. При давлении $p \ge 5-6\ МПа$ происходит потеря полимолекулярным слоем упругости, что приводит к выдавливанию молекул из зоны контакта.

Эксперименты, проведенные А.С. Ахматовым [7], позволили установить, что толщина адсорбированных слоёв, в зависимости от вещества, из которого образуются эти слои, изменяется в пределах 0,05 – 0,1 мкм, а в некоторых случаях может достигать 1 мкм. Эти слои имеют вид квазикристаллических образований и обладают определенной несущей способностью, увеличивающейся по мере уплотнения слоя.

Исследования Л.В. Пановой [8] механических свойств смазочных слоёв на поверхности металлов, проведенные методом "стопы", дали значения модуля сжатия $E_{сж} \cong 6 \cdot 10\ МПа$. Кроме того

известно, что мономолекулярный слой граничной пленки на поверхности твердого тела очень прочен и по модулю упругости близок к твердому телу ($E \cong (3-5)\cdot 10^5$ *МПа*) [11]. Так как адсорбционный слой ПАВ представляется квазикристаллическим телом, то можно предположить, что модуль упругости по толщине пленки изменяется равномерно, и для расчетов принять среднее значение из представленного диапазона, $E^{пл} \cong 2\cdot 10^5$ *МПа* .

Используя приведенные значения, определим нагрузку, воспринимаемую адсорбционным слоем, расположенным в зоне единичного контакта микронеровностей, при условии, когда прочностные свойства по глубине адсорбционного слоя одинаковы [9]:

$$N^{пл} = E^{пл} \cdot h \cdot S^{пл}, \qquad (5)$$

где $E^{пл}$ – модуль упругости адсорбированного слоя ПАВ; $S^{пл}$ – площадь контакта пленок во второй зоне контактирования, определяется выражением:

$$S^{пл} = \pi\left(2R_{пр}\cdot\delta^{пл} + \left(\delta^{пл}\right)^2\right) \qquad (6)$$

где $\delta^{пл}$ – толщина адсорбированной плёнки ПАВ.

Подставляя выражение (6) в (5), получим:

$$N^{пл} = \pi \cdot E^{пл}\cdot\delta^{пл}\cdot h\left(2R_{пр} + \delta^{пл}\right). \qquad (7)$$

Таким образом, суммарная нагрузка, приходящаяся на единичный упругий контакт микронеровностей в зоне взаимодействия выступов определяется выражением:

$$N = \frac{4}{3}\cdot h^{3/2}\cdot R_{пр}^{1/2}\cdot E_{эф}^{пов} + \\ +\pi\cdot E^{пл}\cdot\delta^{пл}\cdot h\left(2R_{пр}+\delta^{пл}\right) \qquad (8)$$

Для расчетов принимаем толщину адсорбционной пленки $\delta^{пл} = 0{,}1$ мкм. По характерным классам чистоты поверхности гидропривода выбираем радиус кривизны микронеровности R, так для аксиально-поршневого насоса 210.225 гильзы блока цилиндров обработана по 8 классу чистоты, сфера сопряжения с распределителем по 10 классу чистоты, сфера сопряжения с блоком цилиндров распределителя обработана по 12 классу чистоты. При этом предполагаем, что радиус кривизны микронеровности R равен высоте микронеровности R_z, тогда $R = 3{,}2$ мкм – ∇8, $R = 0{,}8$ мкм – ∇10, $R = 0{,}2$ мкм – ∇12.

Результаты расчетов представлены на рисунках 3, 4.

Оценку роли адсорбционной пленки проведем с помощью процентного сравнение между суммарной нагрузкой, приходящейся на единичный упругий контакт микронеровности и нагрузкой, воспринимаемой адсорбционным слоем ПАВ,

$$\xi = \frac{N^{пл}}{N}\cdot 100\,\%. \qquad (9)$$

Для расчетов принимаем следующие данные:

– толщина адсорбционной пленки, $\delta^{пл} = 0{,}1$ мкм;

– приведенный радиус кривизны микронеровности, $R_{пр} = 0{,}8$ мкм;

– сближение поверхностей, $h = 0{,}1$ мкм;

– модуль упругости, $E = 2{,}15\cdot 10^{11}$ Па;

– коэффициент Пуассона, $\mu = 0{,}275$.

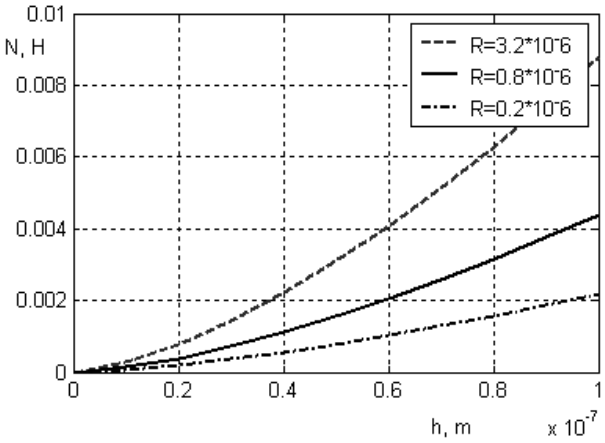

Рис. 3. График зависимости нагрузки при металлическом контакте от сближения для различных радиусов кривизны микронеровностей

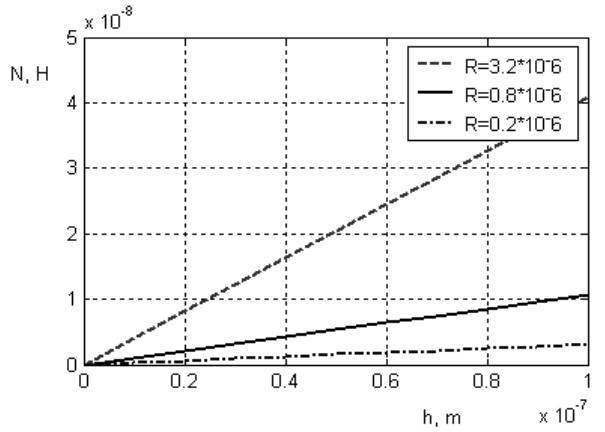

Рис. 4 График зависимости нагрузки, воспринимаемой адсорбционным слоем ПАВ от сближения для различных радиусов кривизны микронеровностей

Таким образом,

$$\xi = \frac{1{,}0681 \cdot 10^{-8}}{4{,}3858 \cdot 10^{-3}} \cdot 100\,\% = 2{,}46 \cdot 10^{-5}\,\%\,.$$

Из чего следует, что нагрузка, воспринимаемая адсорбционным слоем ПАВ при условии упругого металлического контакта не играет ведущей роли в процессе перераспределения контактного давления.

5. ВЫВОДЫ

Характер взаимодействия поверхности сопряженных пар гидропривода определяется радиусом кривизны микронеровностей в контакте.

Нагрузка, воспринимаемая адсорбционным слоем ПАВ, прямопропорционально зависит от радиуса кривизны микронеровности при условии упругого металлического контакта и постоянства прочностных характеристик пленки. Кроме того, следует отметить, что при моделируемом упругом металлическом контакт несущая способность адсорбционной пленки ПАВ не играет существенной роли в процессе перераспределения контактного давления по микронеровностям.

ЛИТЕРАТУРА

[1] Войтов В. А. Конструктивная износостойкость узлов трения гидромашин. Часть II. Методология моделирования граничной смазки в гидромашинах. – Харьков: Центр Леся Курбаса, 1997. – 152 с.

[2] Чичинадзе А.В., Хебда М. Справочник по смазочным материалам. Т.1. – Москва: Машиностроение, 1989. – 400 с.

[3] Литвинов В. Н., Михин Н. М., Мышкин Н. К. Физико-химическая механика избирательного переноса при трении. – М: Наука, 1979. – 187 с.

[4] Крагельский И. В., Добычин М. Н., Комбалов В. С. Основы расчета на трение и износ. – М: Машиностроение, 1977. – 525 с.

[5] Дёмкин Н. Б. Контактирование шероховатых поверхностей. – М: Наука,1970. – 266 с.

[6] Крагельский И. В. Трение и износ. – М.: Машиностроение, 1968. – 480 с.

[7] Ахматов А. С. Молекулярная физика граничного трения. – М: Физматгиз, 1963. – 472 с.

[8] Сердобинцев Ю. П., Шаравин С. И. Трение и износ гетерогенных покрытий в условиях граничной смазки. Часть 2. Граничное трение при скольжении деталей с упрочняющими покрытиями // Трение и износ. – 1992. – Т. 13. – № 6. – С. 985–991.

[9] Сопротивление материалов / Писаренко Г. С., Агарев В. А., Квитка А. Л., Попков В. Г., Уманский Э. С. – К.: Вища школа, 1986. – 775 с.

[10] Хусу А. П., Витенберг Ю. Р., Пальмов В. А. Шероховатость поверхностей (теоретико-вероятностный поход). – М: Наука, 1975. – 344 с.

[11] Розенберг Ю.А. Влияние смазочных масел на долговечность и надежность деталей машин. – М: Машиностроение, 1970. – 312 с.

ПЕРСПЕКТИВНЫЙ МЕТОД ИСПОЛЬЗОВАНИЯ ЭЛИНВАРНЫХ СПЛАВОВ В ПРИБОРАХ И ИЗДЕЛИЯХ ТЯЖЕЛОГО МАШИНОСТРОЕНИЯ

А.П. Любченко, Д.Б. Глушкова, В.П. Тарабанова, С.Н. Кучма

Аннотация: *В ряде приборов и изделий, которые можно отнести к области тяжелого машиностроения, используются элинварные сплавы. В частности, они применяются в качестве особо эффективного конструкционного материала для изготовления элементов систем автоматического управления автономными специализированными устройствами, в командно-измерительных системах движущихся аэрокосмических объектов, на специфичных производствах, когда в заданных условиях необходимо принципиально исключить присутствие человека, в качестве чувствительных элементов в нефтегазовой промышленности. Изделия из элинварных сплавов работают в чрезвычайно жестких условиях, обеспечивая высокий уровень разнообразных функциональных свойств.*

Для обеспечения новых разработок некоторых отраслей тяжелого машиностроения перспективным материалом является элинварный сплав 44НХМТ, который должен иметь близкий к нулю температурный коэффициент частоты в сочетании с высокой добротностью в температурном интервале от -60℃ до +85℃.

Перспективным методом получения высокодобротных прутков из элинварного сплава 44НХМТ является динамическое старение – один из видов термомеханической обработки.

Исследовано влияние процесса динамического старения на физико-механические и элинварные свойства сплава 44НХМТ. Термомеханическая обработка повышает не только прочностные и пластические свойства сплава, но и добротность сплава, снижает чувствительность ТКЧ к точности поддержания температуры последующего старения, обеспечивает большую размерную стабильность резонаторов ЭМФ. Такое изменение свойств связано со структурными превращениями, происходящими в сплаве при динамическом старении.

Определены режимы термомеханической обработки, обеспечивающие получение высокодобротных прутков из элинварного сплава 44НХМТ с необходимым комплексом свойств.

Ключевые слова: элинварные сплавы, температурный коэффициент частоты, динамическое старение, термомеханическая обработка, прочностные, пластические свойсвтва, структурные превращения, размерная стабильность.

ВВЕДЕНИЕ

Создание новых и совершенствование имеющихся устройств, приборов и изделий радиоэлектронной промышленности требует разработки, освоения производства и совершенствования качества прецизионных сплавов со специальными физическими и физико-механическими свойствами. Изделия и детали из таких прецизионных сплавов должны обеспечивать стабильность свойств в разнообразных условиях работы, сужение диапазона изменения свойств, гарантии уровня свойств в рабочих режимах. Несмотря на свой малый размер, указанные изделия играют основную роль – служат источником, усилителем или фильтром основного сигнала, приводящего в действие всю систему, определяя ее точность и надежность.

Так, основным элементом канального электромеханического фильтра (ЭМФ) является резонатор, который изготавливается из элинварного сплава 44НХМТ – прецизионного сплава с высокими свойствами упругости. Резонаторы работают в жестких условиях и должны обладать повышенным уровнем прочностных свойств, гарантированной высокой добротностью (более 25000 ед.) при температурном коэффициенте частоты (ТКЧ) в пределах $\pm 3\times10^{-6}°C^{-1}$ в интервале температур от –60°С до +85°С.

Анатолий Петрович Любченко – проф., д.т.н., Харьковский национальный автомобильно-дорожный университет, Харьков, Украина, ktm@khadi.kharkov.ua, diana@khadi.kharkov.ua
Диана Борисовна Глушкова – доц., к.т.н., Харьковский национальный автомобильно-дорожный университет, Харьков, Украина, ktm@khadi.kharkov.ua, diana@khadi.kharkov.ua
Валентина Павловна Тарабанова.– доц., к.т.н., Харьковский национальный автомобильно-дорожный университет, Харьков, Украина, ktm@khadi.kharkov.ua, diana@khadi.kharkov.ua
Светлана Николаевна Кучма.– ст. преподаватель, Донбасский государственный технический университет, Алчевск, Украина, ktm@khadi.kharkov.ua, diana@khadi.kharkov.ua

АНАЛИЗ ПУБЛИКАЦИЙ

Анализ публикаций показал, что в последние годы успешно разрабатываются и внедряются новые методы упрочнения различных металлов и сплавов, среди которых преимущественное значение занимает термомеханическая обработка во всех ее разнообразных вариантах. Одним из видов термомеханической обработки является динамическое старение – процесс распада пересыщенного твердого раствора в непрерывно изменяющемся поле упругих напряжений, созданном внешней нагрузкой, и соответственно непрерывно изменяющемся напряженном и структурном состоянии сплава.

Динамическое старение сплавов различного состава и структуры в результате происходящих при этой обработке структурных, субструктурных и релаксационных процессов приводит к существенному улучшению широкого комплекса механических свойств. Улучшение всего этого комплекса свойств в результате динамического старения определяет соответственно и рост надежности практически всех деталей и изделий.

Помимо воздействия на рост надежности и других качественных показателей службы деталей и изделий, динамическое старение позволяет повысить и их размерную стабильность. Это объясняется тем, что размерная стабильность определяется величиной сопротивления малым пластическим деформациям и релаксационной стойкостью, т.е. тех свойств, которые в наибольшей мере улучшаются в результате динамического старения [3].

Положения о связи размерной стабильности деталей с указанными свойствами справедливы только в том случае, когда материалы, из которых изготовлены эти детали в условиях эксплуатации характеризуются структурной стабильностью, т.е. они не претерпевают в указанных условиях структурных и фазовых превращений и в них не изменяется уровень микро- и остаточных напряжений. При этом значение имеет стабильность структурного и напряженного состояния не просто в свободном, т.е. ненагруженном состоянии, но главное – при нагружении до уровня, соответствующего условию эксплуатации деталей [2].

В этом отношении процесс динамического старения имеет несомненное преимущество перед традиционно осуществляемыми процессами отпуска или старения, поскольку он проводится под действием напряжений, возникающих от внешней нагрузки, вызывающих дополнительную стабилизацию структурного и напряженного состояния сплава в результате снижения уровня внутренних напряжений. Кроме того, сплавы с гетерогенной структурой в результате динамического старения, проводимого в нагруженном состоянии, обладают меньшей упругой энергией именно в том состоянии, в котором они эксплуатируются, чем при нагружении сплава после обычного старения. Это изменение состояния сплава в нагруженном состоянии после предварительного динамического старения обеспечивает и большую стабильность размеров деталей, меньшую степень развития в них неупругих эффектов, повышенный уровень свойств прочности, а также релаксационную стойкость и надежность. Совмещение в одном процессе действия напряжений и температуры приводит после обработки к существенному повышению сопротивления микропластическим деформациям [2]. Такое изменение свойств связывают с изменением морфологии и пространственного расположения выделяющейся при старении второй фазы, кинетике распада пересыщенного раствора и дислокационной структуре. Эффективность применения динамического старения применительно к аустенитным дисперсионно-твердеющим сплавам типа 36НХТЮ показана в работах [2,3].

ПОСТАНОВКА ЗАДАЧИ

Основным полуфабрикатом для изготовления резонаторов канальных ЭМФ являются прутки из сплава 44НХМТ диаметром 4,5 мм. В состоянии поставки элинварный сплав не отвечает требованиям, которые необходимы для создания резонаторов ЭМФ. Проведенные экспериментальные исследования на прутках диаметром 4,5 мм показали возможность получения комплекса физических и элинварных свойств, отвечающих мировому уровню.

Однако существующая технология получения малогабаритных прутков из проволоки диаметром 4,5 мм из сплава 44НХМТ, предусматривающая механическую рихтовку с последующим старением, хотя и обеспечивает необходимый комплекс свойств, но обуславливает большие потери дорогостоящего материала и высокую трудоемкость их изготовления. Кроме того, обработка проволоки рихтовкой на рихтовальном станке осложняется ограничениями по диаметральному размеру заготовки, что требует применения специального косовалкового устройства для качественной рихтовки проволоки.

Задачей данной работы является исследование возможности использования старения под напряжением (динамического старения) для замены механической рихтовки проволоки из элинварного сплава 44НХМТ этим процессом.

МЕТОДИКА ИССЛЕДОВАНИЙ

Динамическое старение проволоки диаметром 3,4 м проводилось на установке термоволочильного отделения. Величина прикладываемых растягивающих напряжений составляла приблизительно 4 кг/мм2. Температура динамического старения изменялась в интервале от 500 до 700 С. Время выдержки металла при заданной температуре составляло 25 минут. Учитывая, что оптимальное время старения для дисперсионно-твердеющего сплава 44НХМТ

составляет 2…3 часа, для окончательного формирования свойств использовалась комбинированная термическая обработка, состоящая из динамического старения и старения в течение 2-х часов [4].

Температурный коэффициент частоты и добротность при крутильных колебаниях определялись на цилиндрических образцах диаметром 3,4 мм, длиной 110±1 мм по известной методике [1]. Нагрев образцов осуществлялся в климатической камере с точностью поддержания температуры ±1 С. Измерение частоты крутильных колебаний проводилось с помощью прибора «Эластомат». Для повышения точности определения частоты измерения проводились на III-ей гармонике.

Добротность измерялась по логарифмическому декременту затухания на III-ей гармонике крутильных колебаний.

РЕЗУЛЬТАТЫ ЭКСПЕРИМЕНТА

В ходе экспериментальных исследований были определены значения ТКЧ, полученные на проволочных образцах после старения в интервале температур от 500 до 700 °С. Изменение значения ТКЧ от температуры старения представлено на рисунке 1. При температурах старения до 600°С ТКЧ имеет отрицательную величину. С повышением температуры старения ТКЧ растет и при температуре 650…700 °С пересекает нулевые значения. Так, после старения при 650°С в течение 2 часов ТКЧ при температуре –60°С равен 1×10^{-6} °С$^{-1}$, а при температуре +85°С ТКЧ равен -8×10^{-6} °С$^{-1}$. После старения при температуре 700°С в течение 2 часов ТКЧ при температуре -60°С равен $+4\times10^{-6}$ °С$^{-1}$, а при температуре +85°С ТКЧ равен $+1{,}6\times10^{-6}$ °С$^{-1}$. Получить варьированием температуры старения значения ТКЧ, равное $\pm3\times10^{-6}$ °С$^{-1}$ как при отрицательных, так и при положительных температурах на плавке данного химического состава не удалось. При всех температурах старения $ТКЧ_{-60\,°C}$ располагается на графике выше $ТКЧ_{+85\,°C}$.

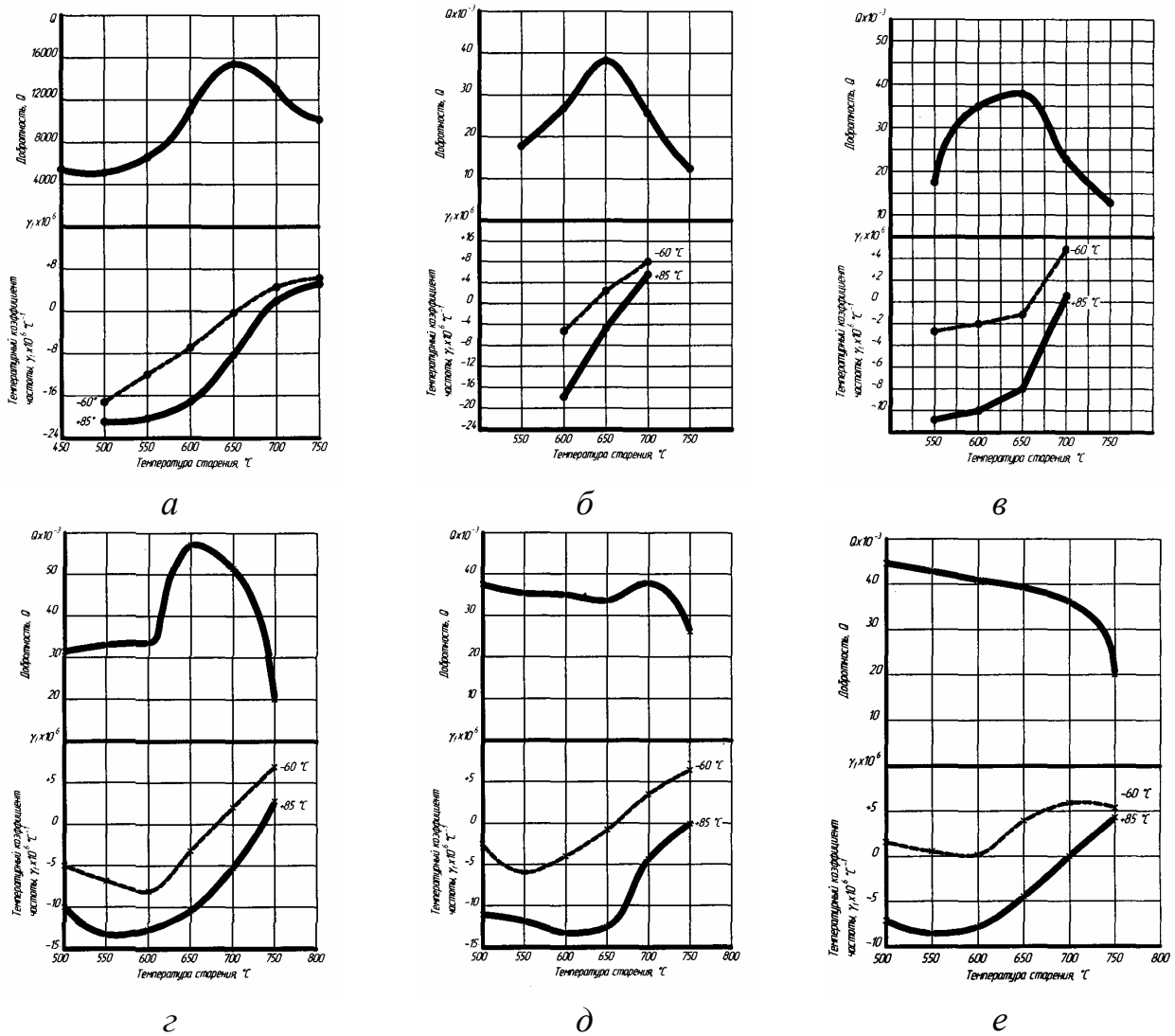

Рисунок 1 – Графики изменения ТКЧ и добротности

Динамическое старение проволоки проводилось в интервале температур от 500° до 700°. Изменения ТКЧ при различных режимах динамического старения и комбинированной обработке приведены на рисунках 1,*б*…1,*е*. Низкие температуры динамического старения (500…550°С) слабо изменяют величину и характер поведения ТКЧ от температуры старения. Минимальные значения ТКЧ наблюдаются при тех же температурах старения, что и у проволоки (650…700°). Разница между значениями $ТКЧ_{-60\ °C}$ и $ТКЧ_{+85\ °C}$ уменьшается, и при старении 675°С значения ТКЧ удовлетворяют требованиям, предъявляемым к резонаторам ЭМФ, и имеют величину $\pm 2\times10^{-6}$ °C^{-1} для динамического старения при температуре 500°С; для динамического старения при температуре 550°С – $\pm 2{,}5\times10^{-6}$ °C^{-1}.

Однако, после динамического старения при более высоких температурах (650°С + старение при 650°С, 2 часа) разница между $ТКЧ_{-60\ °C}$ и $ТКЧ_{+85\ °C}$ увеличивается и достигает 12 единиц. Сравнение данных по ТКЧ, полученных на проволоке и после динамического старения, позволяет сделать вывод, что динамическое старение снижает чувствительность ТКЧ к температуре старения. Наименьшее изменение ТКЧ при термообработке имеют образцы после динамического старения при температуре 700°С (величина ТКЧ изменяется от -8×10^{-6} °C^{-1} до $+5\times10^{-6}$ °C^{-1} при изменении температуры старения от 500° до 750°) (рисунок 1,*е*). С ростом температуры динамического старения происходит повышение значений ТКЧ. Динамическое старение повышает добротность при крутильных колебаниях. Наибольшее значение добротности, полученное на проволочных образцах после старения при 650°С, составляет 14000 (рисунок 1,*а*). Повышение или понижение температуры старения уменьшает добротность. Так после старения при температуре 700°С, когда обеспечивается минимальное для этой плавки значение ТКЧ, добротность снижается до 12000 [5].

Обобщенные результаты исследования образцов представлены в таблице 1.

ВЫВОДЫ

Динамическое старение при высоких температурах дает возможность получения малогабаритных прутков из сплава 44НХМТ, минуя процесс рихтовки.

В результате проведенных исследований влияния процесса динамического старения на физические и элинварные свойства сплава 44НХМТ установлено, что термомеханическая обработка повышает добротность сплава, снижает чувствительность ТКЧ к точности поддержания температуры последующего старения.

Определены режимы термомеханической обработки, обеспечивающие получение малогабаритных прутков с заданным комплексом свойств: минимальными, стремящимися к нулевому, значениями ТКЧ при высокой добротности, но при этом требуется корректировка химического состава сплава.

ЛИТЕРАТУРА

[1] *Кучма С.Н.* Исследование влияния режимов термической обработки на физико-механические и элинварные свойства сплава 44НХМТ/ Восточно-европейский журнал передовых технологий. - №6/1(18). – 2005. – С.27 – 29.

[2] *Ж.П. Пастухова*, А.Г. Рахштадт, Ю.А. Каплун Динамическое старение сплавов М.: Металлургия. – 1985.

[3] *Ж.П.Пастухова,* П.П.Дураев, Ю.А.Каплун. Новые конструкционные стали и сплавы и методы их упрочнения. М.: МД НТП, 1984 г., с.110 – 113

[4] Заявка С–/12-07 України, МПК[8] С21D8/06. Спосіб отримання малогабаритних прутків з дроту елінварного сплаву / Кучма С.М.; заявник ХНАДУ, Кучма С.М.; пат. повірений Кулагіна Л.І. – u200714161; заявл. 17.12.2007; опубл. 15.01.2008.

[5] Любченко А.П., Глушкова Д.Б., Кучма С.Н., Стародубов С.Ю.. Исследование влияния динамического старения на свойства прутков из элинварного сплава 44НХМТ / Восточно-европейский журнал передовых технологий. – №5/(30). – 2007.

УНИВЕРСАЛЬНАЯ И ИСТИННАЯ НАНОТВЁРДОСТЬ МАТЕРИАЛОВ

А.П. Любченко, В.И. Мощенок, Н.А. Лалазарова

Аннотация: *Представлен метод определения универсальной и истинной нанотвёрдости материалов путём кинетического индентирования. Разработаны методика и формулы для определения универсальной и истинной нанотвёрдости материалов. Расчёт площади и объёма внедрённой части индентора рекомендуется осуществлять по глубине внедрения трёхгранной пирамиды Берковича, которая определяется как перемещение индентора от поверхности образца. Выявлена зависимость универсальной твердости от нагрузки, так называемый размерный эффект. Данная методика позволяет определять нанотвердость практически любых материалов*

Ключевые слова: *универсальная и истинная нанотвёрдость, трёхгранная пирамида Берковича, кинетическое индентирование*

Основные эксплуатационные свойства деталей машин определяются в основном структурой и свойствами поверхностных слоёв. Наиболее распространённым способом определения свойств поверхностных слоёв, тонких плёнок является метод кинетического индентирования, который позволяет изучать процессы упругой и пластической деформации в очень малых объёмах, определять микро- и нанотвёрдость и ряд механических, трибологических и других свойств. Метод кинетического индентирования позволяет изучать свойства как пластичных, так и хрупких материалов из-за их квазихрупкого разрушения (керамик, стёкол, карбидов, нитридов, боридов тугоплавких элементов) [1, 2].

Измерение нанотвёрдости связано со значительными трудностями. Поэтому совершенствование методов определения нанотвёрдости позволит интенсифицировать процесс изучения свойств различных материалов в нанообъёмах.

Суть метода кинетического индентирования заключается в том, что на основании испытаний на нанотвёрдость регистрируется перемещение алмазного индентора (пирамиды Берковича) как при его нагружении, так и в период разгрузки и строятся диаграммы нагружения в координатах нагрузка – перемещение.

В 1992 году В. Оливер и Дж. Фарр разработали методику определения твёрдости по глубине контакта при максимальной нагрузке [3]. Сложность методики заключается в том, что прибор измеряет не глубину отпечатка, а перемещение индентора h, которое является суммой нескольких слагаемых:

- глубины контакта h_c,
- упругого прогиба на краю контакта h_s,
- прогиба силовой рамы h_f,
- теплового расширения стержня, в котором закреплён индентор h_{ui} (фиг.1):

$$h = h_c + h_s + h_f + h_{ui} \qquad (1)$$

Фиг. 1 Схематическое представление сечения отпечатка: 1 – исходная поверхность; – поверхность под нагрузкой; 3 – поверхность внедрённой части индентора; 4 – поверхность после снятия нагрузки

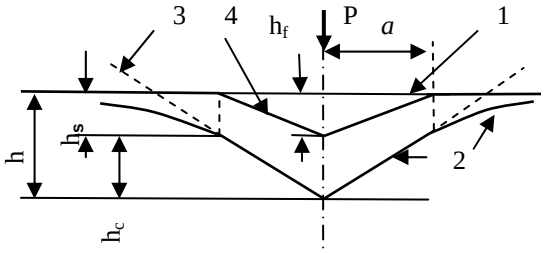

Твёрдость по методике Оливера и Фарра определяется по формуле:

$$H = \frac{P_{max}}{a} \qquad (2)$$

где P_{max} – максимальная нагрузка:

A – площадь проекции отпечатка для идеально острого индентора Берковича:

$$A = 24{,}56 \cdot h_c^2 \qquad (3)$$

Анатолий Петрович Любченко – проф., д.т.н., Харьковский национальный автомобильно-дорожный университет, Харьков, Украина, ktm@khadi.kharkov.ua, diana@khadi.kharkov.ua
Василий Иванович Мощенок – проф., к.т.н., ., Харьковский национальный автомобильно-дорожный университет, Харьков, Украина, ktm@khadi.kharkov.ua, diana@khadi.kharkov.ua
Наталия Алексеевна Лалазарова – доц., к.т.н., Харьковский национальный автомобильно-дорожный университет, Харьков, Украина, ktm@khadi.kharkov.ua, diana@khadi.kharkov.ua

Площадь проекции отпечатка определяется по глубине контакта h_c, которая для различных схем контакта будет определяться по разному.

При определении нанотвёрдости измеряют так называемую «невосстановленную» твёрдость в отличие от метода измерения микротвёрдости, когда измеряют «восстановленную» твёрдость, искажённую упругим восстановлением отпечатка. Наибольшая трудность методики Оливера и Фарра заключается в нахождении упругого прогиба на краю отпечатка. Данная методика позволяет найти нанотвёрдость только для одной точки диаграммы нагружения индентора Берковича [3].

Цель работы – определение нанотвёрдости материалов по глубине внедрения индентора при различных нагрузках индентирования..

Методика Оливера и Фарра даёт хорошие результаты для случая упруго-пластического контакта индентора с исследуемым материалом, который представлен на рис.1, с прогибом на краю отпечатка.

Работает ли методика Оливера и Фарра, если имеют место другие схемы контакта? Другой случай упруго-пластического контакта индентора с исследуемым материалом предполагает наличие вытесненного материала вокруг индентора – наличие навала (фиг. 2). Такая схема контакта имеет место при измерении твёрдости упруго-пластичных и пластичных материалов.

Фиг. 2 Схема контакта индентора с материалами, у которых присутствует навал

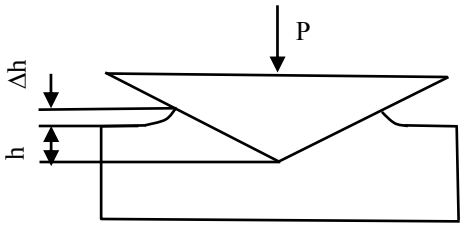

В этом случае глубина контакта индентора должна равняться $h_c = h + \Delta h$.

Рассмотрим другие случаи контакта. Например, для абсолютно упругого тела схема контакта приведена на рис. 3.

Фиг. 3 Схематическое представление контакта абсолютно упругого тела с индентором: h – упругое перемещение индентора

.

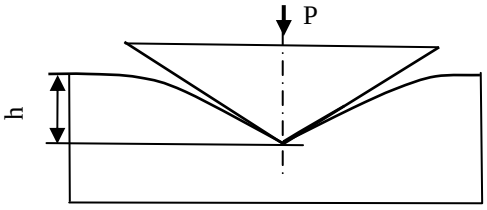

Если контакт индентора осуществляется с абсолютно упругим телом (например, резиной), то в этом случае глубина перемещения индентора равняется прогибу на краю отпечатка: $h = h_s$. Тогда: $h_c = h - h_s = 0$.

Для схем контактирования, представленных на фиг.2 и 3, методика Оливера и Фарра не позволяет определять нанотвёрдость.

На кафедре технологии металлов и материаловедения ХНАДУ разработана методика определения универсальной и истинной твёрдости любых материалов [4].

Универсальная твёрдость определяется как отношение силы сопротивления внедрению индентора к площади погружённой в материал части индентора – трёхгранной пирамиды Берковича:

$$НБ_у = \frac{F}{A} = \frac{F}{26,968 \cdot h^2} \quad (4)$$

(угол при вершине 65°)

$$НБ_у = \frac{F}{A} = \frac{F}{26,4342 \cdot h^2} \quad (5)$$

(угол при вершине 65°03′)

$$НБ_у = \frac{F}{A} = \frac{F}{26,3673 \cdot h^2} \quad (6)$$

(угол при вершине 65°27′)

где F – сила сопротивления внедрению пирамиды, Н;

h – глубина внедрения пирамиды Берковича, мм;

A – площадь поверхности внедрённой части пирамиды, мм^2.

Истинная твёрдость определяется как отношение силы сопротивления к объёму внедрённой части пирамиды:

$$НБ_у = \frac{F}{V} = \frac{F}{10,5398 \cdot h^3} \quad (7)$$

(угол при вершине 65°)

$$НБ_у = \frac{F}{V} = \frac{F}{10,31 \cdot h^3} \qquad (8)$$

(угол при вершине 65°03′)

$$НБ_у = \frac{F}{V} = \frac{F}{10,2825 \cdot h^3} \qquad (9)$$

(угол при вершине 65°27′)

где F – сила сопротивления внедрению пирамиды, Н;

h – глубина внедрения пирамиды Берковича, мм;

V – объём внедрённой части пирамиды, мм^3.

Глубина внедрения пирамиды h для любого контакта (фиг. 1. 2, 3) равна перемещению пирамиды. Для случая упруго-пластического контакта с навалом h также определяется как перемещение индентора и измеряется от поверхности образца без учёта высоты навала (фиг.2). Для случая абсолютно упругого контакта (фиг.3) глубина внедрения также равна величине перемещения индентора. Для этой схемы контакта нанотвёрдость можно определить только этим методом, так как при измерении универсальной и истинной твёрдости измеряется глубина внедрения индентора, а не параметры отпечатка, который в данном случае отсутствует.

Методика, разработанная на кафедре технологии металлов и материаловедения ХНАДУ, позволяет определять нанотвёрдость не только для максимальной нагрузки на индентор, но и для всех промежуточных значений величин нагрузок.

Рассмотрим процесс измерения универсальной и истинной нанотвёрдости на примере диборида титана [1]. На фиг.4 представлена диаграмма в координатах нагрузка-глубина внедрения индентора, где левая ветвь – это участок нагружения, правая – участок разгрузки индентора. Этот метод исключает необходимость в трудоёмком измерении параметров отпечатка, получаемого при малых нагрузках на индентор.

Фиг. 4 Диаграмма нагружения индентора Берковича для диборида титана [1]

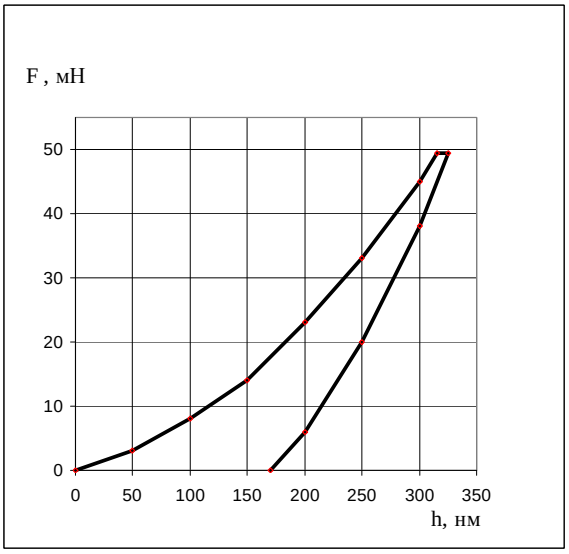

На основании диаграммы F-h непрерывного индентирования были построены графики зависимости универсальной (фиг. 5, а) и истинной (фиг. 5, б) нанотвёрдости.

С уменьшением нагрузки (и соответственно глубины внедрения индентора) наблюдается увеличение нанотвёрдости. Рост нанотвёрдости объясняется размерным фактором. С уменьшением объёма деформируемого материала изменяются механизмы пластической деформации, что и приводит к резкому возрастанию нанотвёрдости в нанообъёмах [5].

Фиг.5 Зависимость универсальной (а) и истинной (б) нанотвёрдости для диборида титана

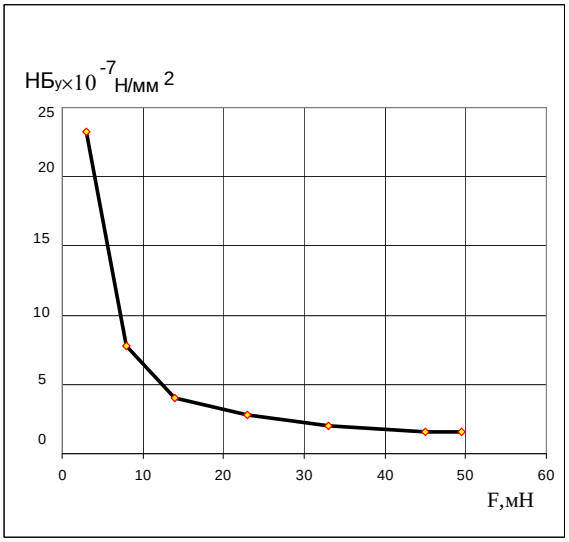

а

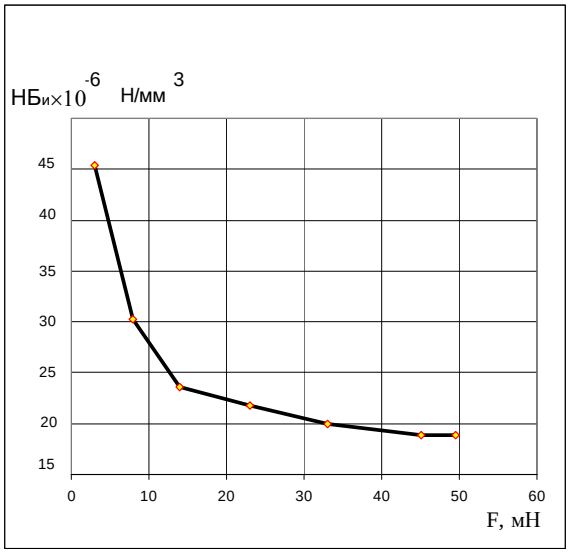

б

Полученные зависимости позволяют определять нанотвёрдость при малых нагрузках в поверхностных слоях наноразмерной толщины для любых материалов.

ВЫВОДЫ

1. Область использования методики Оливера и Фарра по определению нанотвёрдости ограничена упруго-пластической схемой контакта индентора без навала.
2. Основная трудность методики Оливера и Фарра заключается в определении прогиба на краю отпечатка и определении глубины контакта индентора.
3. При определении универсальной и истинной нанотвёрдости материалов расчёт площади и объёма внедрённой части индентора осуществляется по глубине внедрения трёхгранной пирамиды Берковича, которая определяется как перемещение индентора от поверхности образца.
4. Определение глубины внедрения не требует сложных расчётов и измеряется на нанотесторе.
5. Универсальная и истинная нанотвёрдость также имеют размерный эффект (с уменьшением нагрузки, а, значит, и глубины внедрения индентора, наблюдается значительный рост нанотвёрдости).
6. Зависимость универсальной и истинной нанотвёрдости от нагрузки (глубины внедрения индентора) позволяет определять твёрдость очень тонких поверхностных слоёв любых материалов.

ЛИТЕРАТУРА

[1] С.Н. Дуб, Н.В. Новиков. Испытания твёрдых тел на нанотвёрдость // Сверхтвёрдые материалы. - 2004. - №6. - С.16-33.

[2] А.В. Панин, А.Р. Шугуров, К.В. Оскомов. Исследование механических свойств тонких плёнок Ag на кремниевой подложке методом наноиндентировангия//Физика твёрдого тела. - 2005. - Т. 47. -Вып. 11. - С. 1973-1977.

[3] Oliver W.C., Pharr G.M. An improved technique for determining hardness and elastic moduley using load and displacement sensing indentation experiments//J. Mater. Res.-1992.-7. №6. -P. 1564-1583.

[4] Мощенок В.І., Тарабанова В.П., Глушкова Д.Б. Спосіб оцінки твердості матеріалу. Пат. України UA74654 C2, G01N3/40. Заявл. 30.12.2003. Опубл. 16.01.2006. Бюл. №1.-3 с.

[5] Ю.И. Головин, В.И. Иволгин, В.В. Коренков, Б.Я. Фарбер. Размерный и зависящий от времени эффекты в нанотвёрдости керамик на основе ZrO_2 // Физика твёрдого тела. – 2001. – Т.;3. – Вып.11. – С. 2021-2024.

INDENTOR GEOMETRY INFLUENCE ON THE SIZE EFFECT AT DETERMINATION OF HARDNESS

V. Moshchenok, I. Doshchechkina, S. Bondarenko, A. Lyapin

Abstract: *Hardness determination is widely used for express checking of product quality and forms also the basis for numerous scientific investigations .*
The possibility of evaluating physical and mechanical properties using hardness has very great importance. So hardness must be the most accurate and particular characteristic of studied material. At the same time the existing methods of determining static hardness give only its averaged values. In this work kinetic (continuous) indentation was performed and its results were used for calculating universal hardness. Formulae for universal hardness determination are offered. Dependence of universal hardness on indenter geometrical form and applied load values is shown. Fundamental different character of hardness curves for different indenter types is revealed. Conditions for realizations of size effect are defined.

Key words: *universal hardness, indentor, ball, cone, pyramid, size effect*

A great quantity of different metallic materials and methods of their treatment are used in manufacture and machinery repair to secure required complex of mechanical properties for reliable service. It demands of applying distinct methods of article quality inspection.

Hardness determination is widely used and sometimes the only possible method of article quality inspection. Each specific case demands of using one or another method of hardness measuring. On the opinion of many authors the most widespread static methods (Brinell, Rockwell, Vickers) give only conditional and very averaged hardness values that do not reflect the behaviour of material in the testing process and are not always correlated between themselves. Using hardness it is possible to determine many characteristics of material such as follows: elastic properties, resistance to plastic deformation and fracture, adhesion strength, tribological qualities and wear resistance. In this connection it is necessary to have the most precise and specific estimation of hardness for material under study.

At present it is finding increasing use method of kinetics hardness (continuous indenting), according to which calculated value of universal hardness (HU) is recommended to determine as a ratio of maximum applied load P, N to contacted impression area under load A, mm^2

$$HU = \frac{F}{A}, N/mm^2 \qquad 1)$$

During forming the impression in continuous indenting the wide spectrum of relative deformation rates and deformed metal size (indenter depths) in dependence on applied load and indenter form, is realized that should have effect on hardness values.

In works [3-6] it has been conformed that universal hardness is larges by dependent on the form and size of indenter and applied load. But the character of this dependence is complicated and up to now has not been completely studied.

Many authors pointed out sharp increasing hardness in use of small loads. Such phenomenon has been named the indentation size effect [7] and it should be taken into consideration when determining hardness.

The aim of this work is to study the influence of indenter geometry on value and character of universal hardness change in dependence on applied load for soft and hard steels.

The authors have suggested formulae for calculating universal hardness H_U of materials with different indenters.

When measuring hardness with balls of different diameters (2,5; 5; 10 mm) it is recommended to use the following formulae:

$$HB_U^{2,5} = \frac{F}{7,854 \cdot h}, \ N/mm^2 \qquad 2)$$

$$HB_U^{5} = \frac{F}{15,708 \cdot h}, \ N/mm^2 \qquad 3)$$

$$HB_U^{10} = \frac{F}{31,4159 \cdot h}, \ N/mm^2 \qquad 4)$$

Prof. Vasiliy Moshchenok, Kharkiv National Automobile and Highway University, Kharkiv, Ukraine, ktm@khadi.kharkov.ua
Assist. Irina Doshchechkina, Kharkiv National Automobile and Highway University, Kharkiv, Ukraine, diana@khadi.kharkov.ua
Assist. Stanislav Bondarenko, Kharkiv National Automobile and Highway University, Kharkiv, Ukraine, diana@khadi.kharkov.ua
Engin. Alexandr Lyapin , Kharkiv National Automobile and Highway University, Kharkiv, Ukraine, lyasu@narod.ru

where P – resistance strength to penetrating corresponding indenter (N) and h – penetration depth (mm).

In use as indenter of cone with an angle of 120 and vertex spherical part radius of 0,2 mm hardness may be calculated with the formulae (5, 6):

$$HR_U^{con} = \frac{F}{1,257 \cdot h}, \ N/mm^2, \qquad 5)$$

if penetration depth of cone $h \le 0,027$ mm.

$$HR_U^{con} = \frac{F}{10,88 \cdot h^2 + 0,66824 \cdot h + 0,00796}, \ N/mm^2, \qquad 6)$$

if penetration depth of cone $h > 0,027$ mm.

If Vickers pyramid serves as indenter hardness should be determined with the formulae (7):

$$HV_U = \frac{F}{26,428 \cdot h^2}, \ N/mm^2 \qquad 7)$$

Values of universal hardness for reference standards made of soft and hard steels were calculated with using distinct indenters (balls of dissimilar diameters, diamond cone, Vickers pyramid with an angle of 136).

Penetrating into surface was performed under continuously increasing load.

Universal hardness curves for both steels determined with different indenters are presented in Fig. 1.

"Teared" appearance of some curves is evidently due to surface roughness and testifies about great precision of hardness values.

When indentating with balls of distinct diameters the character of hardness change curves for both steels are basically the same but naturally there are difference in absolute values.

Hardness determined with ball of 2,5 mm in diameter intensively grows with increasing load up to 500 N. Then hardness growth is slowed down and with load more than 1700 N retains practically unchanged.

Analogous dependencies were obtained for balls of 5 and 10 mm in diameters. But less intensive hardness growth especially for hard steel (Fig. 1b) has engaged our attention.

As we might expect the lowest hardness for both steels was obtained with ball of 10 mm in diameter. It is due to the size of deformed metal area under indenter.

Hardness curves determined with Vickers pyramid have basically another character. Hardness intensively decreased with growing load to 500 N and when load exceeds 1000 N it retains unchanged. Size effect is observed for both steels. It is the most sharply defined with load less than 100 N for soft steel (Fig. 1a) and with load less than 50 N for hard steel (Fig. 1b). For hard steel with low loads (less than 50 N) hardness grows noticeably more intensively and its absolute values are substantially higher.

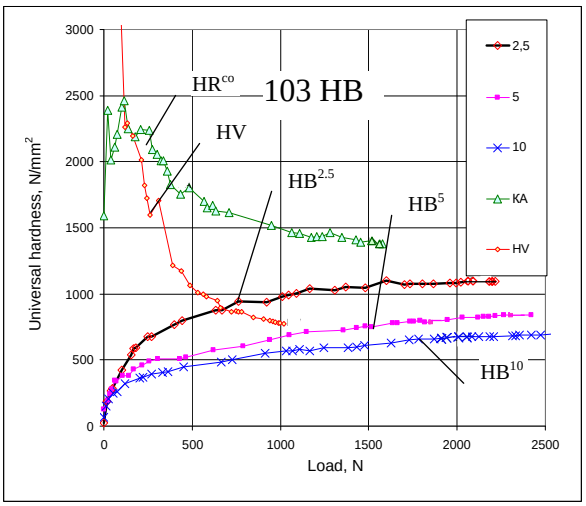

a)

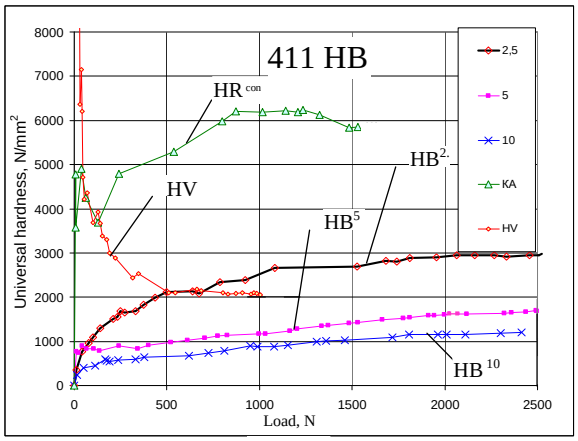

b)

Fig. 1 Dependence of universal hardness on indenter geometry and load for soft (a) and hard (b) steel

Using diamond cone as indenter hardness curve change with increasing load has complex character with two maximums in the range of low loads (to 100 N).

For soft steel hardness fairly reduces with increasing load (Fig. 1a) and for hard steel it grows.

Size effect for hard steel is absent. For hard steel increasing hardness (from 1500 to 2500 N) is substantially less then with the use of Vickers pyramid.

Such contradictory character of hardness curve change for steels with different plasticity is evidently due to peculiarities of diamond cone geometry namely to presence at its vertex of spherical part that has been reflected in formulae (5, 6).

In summary it may be said that hardness is dependent on the structure and properties of material

under study and to the great degree is also controlled by the test conditions. The hardness cannot be considered as “simple” property because a complicated picture of very high local stresses occurs during trials. This picture depends on load value and indenter type. In this case several mechanisms of stress relaxation are realized and they primarily depends on indenter geometry.

From this experiments it were made the following conclusions.

1. Universal hardness of materials regardless of their properties is dependent on indenter geometrical form and penetration depth under load.
2. In determining universal hardness with spherical indenters under continuous load indentation size effect doesn’t manifest itself.
3. For comparison of different materials on hardness it should be determined using Vickers pyramid.

LITERATURE

[1] Золотаревский В.С. Механические свойства материалов. – М.: Металлургия, 1983. – 352 с.

[2] Бронштейн М.А., Займовский В.С. Механические свойства материалов. – М.: Металлургия, 1979. – 495 с.

[3] Gao X.-L. Strain gradient plasticity solution for an internally pressurized thick-walled spherical shell of an elastic linearhardening material. // Mech. Adv. Mater. Struct. – 13. – 2006. – 43 p.

[4] Jonson K.L. The correlation of indentation experiments. // J. Mech. Phys. Solids. – 18. – 1970. – 115 p.

[5] Gao X.-L., Jing X.N., Subhash G. Two new expending cavitymodels for indentation deformations of elastic strainhardening materials. // Int. J. Solids Struct. – 2006. – 2193 p.

[6] Gerberich W.W., Tymiak N.I., Grunlan J.C., Horstemeyer M.F., Baskes M.I. Interpretations of indentation size effects. // ASME J. Appl. Mech. – 69. – 2002. – 433 p.

[7] Gubicza Y., Roziosnik N., Yuhauz A. Comment on Indentation Size Effect: reality or artifact. // Journal of materials science. – 16. – 1997. – 1904 p.

ОПРЕДЕЛЕНИЕ УНИВЕРСАЛЬНОЙ И ИСТИННОЙ НАНОТВЁРДОСТИ ДЛЯ РАЗЛИЧНЫХ МАТЕРИАЛОВ

В.И. Мощенок, Н.А. Лалазарова, О.Н. Тимченко

Аннотация: *Рассмотрены особенности определения универсальной и истинной нанотвёрдости для типичных представителей различных классов материалов. Проведен анализ P–h-диаграмм для всех исследуемых материалов. На основании P–h-диаграмм получены зависимости универсальной и истинной нанотвёрдости от нагрузки. Для всех индентируемых материалов наблюдается рост динамсической твёрдости с уменьшением глубины индентирования.*

Ключевые слова: *универсальная и истинная нанотвёрдость, кривые нагружения и разгрузки, глубина внедрения индентора, размерный эффект*

Метод кинетического индентирования (кинетической твёрдости) применяется для определения универсальной и истинной нанотвёрдости материалов. Однако только этим не исчерпываются возможности метода основанного на непрерывном вдавливании индентора в исследуемый материал. Этот метод позволяет определять целый ряд параметров, характеризующих физико-механические свойства материала. Особенно актуально применение метода кинетического индентирования для тех материалов, для которых нельзя использовать традиционные методы определения свойств.

В ряде работ рассмотрены особенности методики определения твёрдости, микротвёрдости и нанотвёрдости материалов на основе анализа кривой непрерывного индентирования [1-3].

Диаграммы, построенные в координатах «нагрузка на индентор P – глубина отпечатка h», показывают, что методом индентирования можно: измерять нанотвёрдость при максимальной нагрузке, измерять нанотвёрдость в процессе нагружения, при выдержке под нагрузкой и в процессе разгрузки; оценивать упругие свойства материала; исследовать свойства материалов у которых отпечаток очень сильно изменяет свои размеры после снятии нагрузки; регистрировать скорость внедрения индентора в материал и т.д.

Теоретические исследования этого метода позволяют определять: модуль упругости, ползучесть и релаксацию напряжений, гистерезисные потери при повторном нагружении-разгружении, вязкость разрушения, пористость материалов, толщину, степень адгезии и механические свойства тонких плёнок и т.д. [1-3].

Цель работы – определение универсальной и истинной нанотвёрдости по глубине внедрения пирамиды Берковича различных материалов, сравнительный анализ упругих свойств материалов на основании анализа кривых непрерывного индентирования, выявление размерного эффекта.

Для определения универсальной и истинной нанотвёрдости, сравнительного анализа упругих свойств были взяты твёрдые материалы различной природы: нанокристаллические плёнки TiSiN, монокристалл кремния (ковалентный кристалл), поликристаллическая медь (металл). Типичные кривые наноиндентирования этих материалов взяты в работе [2] (фиг. 1).

На кафедре технологии металлов и материаловедения ХНАДУ разработана методика определения универсальной и истинной твёрдости любых материалов [4].

Универсальную твёрдость определяли как отношение силы сопротивления внедрению индентора к площади погружённой в материал части индентора – трёхгранной пирамиды Берковича (фиг. 2), истинную – как отношение силы сопротивления внедрению индентора к объёму внедрённой части индентора (фиг. 3). Для максимальных значений нагрузки и глубины внедрения рассчитаны значения нанотвёрдости в ГПа (табл. 1).

Василий Иванович Мощенок – проф., к.т.н., Харьковский национальный автомобильно-дорожный университет, Харьков, Украина, ktm@khadi.kharkov.ua, diana@khadi.kharkov.ua
Наталия Алексеевна Лалазарова – доц., к.т.н., Харьковский национальный автомобильно-дорожный университет, Харьков, Украина, ktm@khadi.kharkov.ua, diana@khadi.kharkov.ua
Ольга Николаевна Тимченко – студентка, Харьковский национальный автомобильно-дорожный университет, Харьков, Украина, ktm@khadi.kharkov.ua, diana@khadi.kharkov.ua

Фиг. 1 Диаграмма нагружения индентора Берковича: а – TiSiN, б – Si, в – Cu [2]

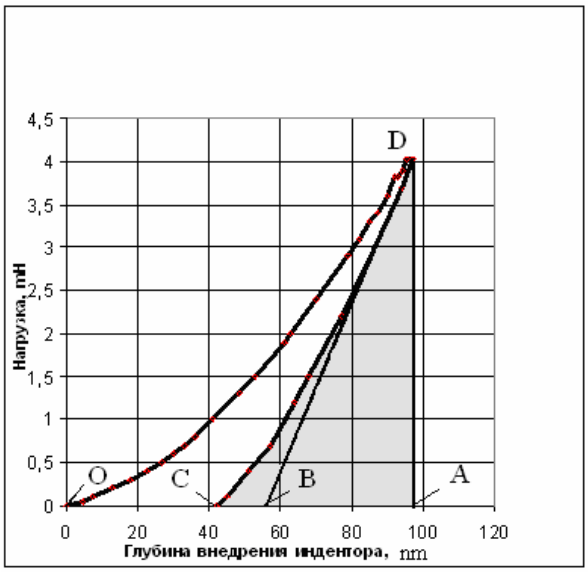

а

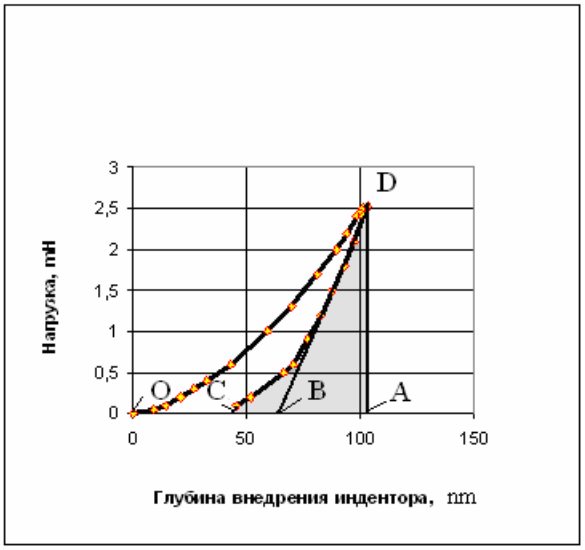

б

в

Исследуемые материалы имеют различную твёрдость: наиболее высокую нанотвёрдость имеют тонкие нанокристаллические плёнки из TiSiN, самую низкую – поликристаллическая медь.

Фиг. 2 Зависимость универсальной нанотвёрдости от нагрузки для TiSiN, Si, Cu

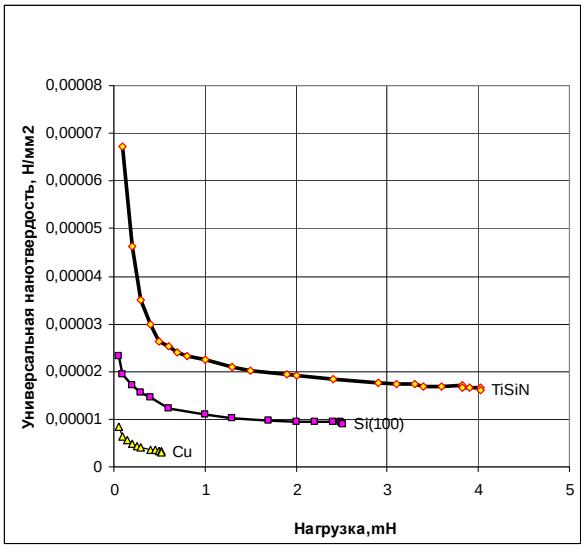

Для проведения анализа упругих свойств исследуемых материалов на диаграммах выполнены дополнительные построения (фиг. 1). Из вершины кривой наноиндентирования опущен перпендикуляр на ось x и проведена касательная к начальному участку кривой разгрузки. Начальный участок кривой разгрузки прямолинейный.

Фиг. 3 Зависимость истинной нанотвёрдости от нагрузки для TiSiN, Si, Cu

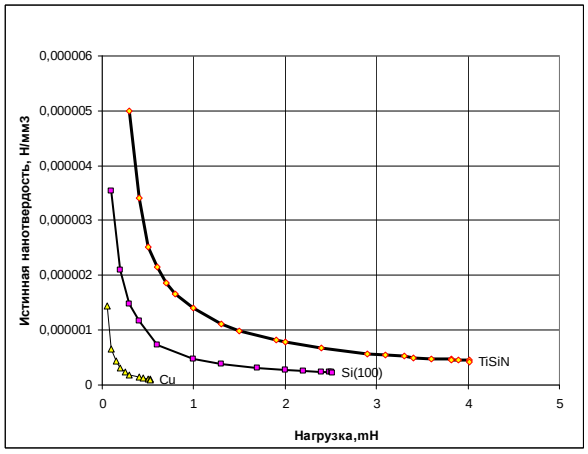

Участок OD – это кривая нагружения, которая отражает сопротивление материала внедрению индентора, участок DC – кривая разгрузки описывает возврат деформации после снятия внешней нагрузки и характеризует упругие свойства материала. Деформация материала при внедрении индентора имеет как упругую, так и пластическую составляющую. AC – упругая составляющая деформации материала. OC – глубина отпечатка, оставшегося (восстановленного) после снятия нагрузки (h_f). OA – глубина внедрения индентора (h) (глубина не восстановленного отпечатка). AB –

упругий прогиб поверхности на краю отпечатка. ВС – упругий прогиб поверхности в отпечатке. По диаграмме нагружения можно не только определить нанотвёрдость материала, но и оценить долю упругой деформации в общей деформации или упругое восстановление из соотношения (1):

$$R=\frac{(OA-OC)}{OA}=\frac{(h-h_f)}{h_f} \qquad (1)$$

Для тонкой плёнки TiSiN R=62 %; для кремния – 62 %; для меди – 14 %.

По диаграммам нагружения для всех исследуемых материалов были проведены расчёты соотношения упругой и пластической работ. Упругая составляющая работы индентирования (W_y) характеризуется площадью DAC (фиг. 1), пластическая составляющая – площадью DOC, полная работа индентирования (W_y) – площадью DOA. Соотношение упругой и пластической составляющих работы рассчитывали из соотношения площади DAC к площади DOC. Результаты расчётов приведены в табл. 1.

Таблица 1
Свойства материалов, определённые из диаграмм индентирования

Материал	$НБ_{y,}$ ГПа	Соотношение $(W_y/W)\cdot 100\%$
TiSiN	16	64
Si	9	58
Cu	3	10

Анализ кривых индентирования позволяет полностью идентифицировать материалы. Кремний, плёнки из TiSiN имеют высокую твёрдость, низкую пластичность, высокие упругие свойства. Для тонкой плёнки TiSiN и для кремния в связи с большой долей упругой составляющей работы (64% и 58% соответственно) и деформации определение твёрдости по восстановленному отпечатку приведёт к получению искажённых значений: твёрдость будет очень сильно завышена. Поэтому определение твёрдости по не восстановленному отпечатку для этих материалов даёт наиболее точные результаты.

Для всех исследуемых материалов наблюдается размерный эффект: с уменьшением нагрузки наблюдается увеличение твёрдости. Однако степень интенсивности роста твёрдости различна для различных материалов. Например, наиболее интенсивно возрастает с уменьшением нагрузки универсальная твёрдость тонкой плёнки TiSiN, менее интенсивно – кремния и ещё в меньшей степени – меди, что можно объяснить различиями в уровне удельных давлений в области деформирования.

ЛИТЕРАТУРА

[1] С.И. Булычёв, В.П. Алёхин. Испытание материалов непрерывным вдавливанием индентора. – М.: Машиностроение, 1990. – 224 с.

[2] М.И. Петржик, Д.В. Штанский, Е.А. Левашов. Современные методы оценки механических и трибологических свойств функциональных поверхностей. Материалы X Междунар. научно-техн. конф. «Высокие технологии в промышленности России», Москва, ОАО ЦНИТИ «Техномаш» 9-11 сентября 2004г. – С. 311-318.

[3] С.Н. Дуб, Н.В.Новиков. Испытания твёрдых тел на нанотвёрдость // Сверхтвёрдые материалы. - 2004. - №6. - С.16-33.

[4] Мощенок В.І., Тарабанова В.П., Глушкова Д.Б. Спосіб оцінки твердості матеріалу. Пат. України UA74654 C2, G01N3/40. Заявл. 30.12.2003. Опубл. 16.01.2006. Бюл. №1.-3 с.

ОПРЕДЕЛЕНИЕ ВЛИЯНИЯ СПОСОБА ПОЛУЧЕНИЯ И ОБРАБОТКИ ЧУГУНА НА ИЗМЕНЕНИЕ ЕГО ИСТИННОЙ И УНИВЕРСАЛЬНОЙ ТВЕРДОСТИ

Костина Л.Л.

Аннотация: *Высокопрочные чугуны, в частности, высокопрочный чугун с вермикулярным графитом, находят все более широкое применение для деталей машиностроения: коленчатых и распределительных валов автомобилей, деталей тормозных механизмов и пр. Для обеспечения достаточных свойств материала проводят термическую обработку по различным режимам. Важным вопросом контроля качества термической обработки и соответствия деталей из ЧШГ и ЧВГ предъявляемым требованиям является измерение твердости. Современные методики предполагают измерение истинной и универсальной твердости материала, позволяющее говорить о кинетике сопротивления нагружению и о реакции на нагрузку поверхностных и приповерхностных слоев материала.*
В статье рассмотрены вопросы определения истинной и универсальной твердости в применении к конкретным материалам – чугунам различных классов и способов получения. Приведены результаты измерения твердости чугунов с помощью универсального твердомера оригинальной конструкции, с применением в качестве индентора стального шарика. Показаны особенности влияния способа получения и исходного состояния чугунов (микроструктуры металлической матрицы, степени ее химической неоднородности, вида графитных включений) на характер изменения кинетической твердости, измеренной алмазным конусом. а также рассчитанных значений универсальной и истинной твердости. Установлено, что характер процессов деформации, происходящих при кинетическом измерении твердости, в значительной мере зависит от вида и исходного состояния чугуна.

Ключевые слова: *высокопрочный чугун, графитное включение, шаровидный, вермикулярный, компактный графит, универсальная и истинная твёрдость, кривые нагружения, глубина внедрения индентора, сопротивление нагружению*

Высокопрочные чугуны с вермикулярным графитом (ЧВГ) являются литейными материалами с достаточно высокими эксплуатационными характеристиками [1]. Причина этого кроется в особенностях формирования и строения графитных включений [2]. Вермикулярные, шаровидные и некоторые компактные включения могут формироваться из отдельных частей (блоков) в полностью замкнутой оторочке аустенита, а могут сохранять в процессе формирования одностороннюю связь с жидким расплавом. В первом случае в ВЧШГ формируется так называемая структура «бычьего глаза».

Шаровидные включения кружены равномерной ферритной оторочкой, за которой вплоть до границ эвтектического зерна располагается перлит. Структуры литых высокопрочных чугунов характеризуются значительной степенью химической неоднородности, возникающей в процессе затвердевания. Участки матрицы вокруг графитных включений (впоследствии ферритные) обогащены кремнием и содержат меньше марганца и углерода. Окружающие их перлитные участки обогащены марганцем и углеродом и содержат меньше кремния. Во втором случае чаще формируются вермикулярные или компактные включения, окруженные ферритными областями, а в участках связи с жидким расплавом формируется перлит или даже цементит (при достаточно быстром охлаждении).

Применяемое в настоящее время измерение универсальной и истинной твердости позволяет оценить влияние сопротивления металла кинетическому нагружению. В этом плане чугуны представляют особый вид материалов, т.к. они не чувствительны к концентраторам напряжений. Нечувствительность чугунов к концентраторам напряжений обусловлена прежде всего наличием огромного количества графитных включений, являющихся концентраторами в металлической матрице изначально. Однако существует еще такой фактор, как форма концентратора напряжений, т.е., в применении к чугунам, форма графитных включений. Более высокие свойства высокопрочных

Людмила Леонидовна Костина – доц., к.т.н., Харьковский национальный автомобильно-дорожный университет, Харьков, Украина, e-mail: ktm@khadi.kharkov.ua

чугунов объясняются не только меньшим суммарным объемом и меньшей площадью поверхности компактных включений графита. Немаловажный вклад вносит и острота кромок включения (радиус его кривизны). Поэтому для чугунов кривые изменения истинной и универсальной твердости могут иметь характер, отличный от кривых изменения твердости однородных сплавов. В то же время характер кривых истинной и универсальной твердости для чугунов может оказаться аналогичным, т.к. при определении сопротивления по поверхности или по объему влияние графитных включений должно быть аналогичным и достаточно усредненным вследствие большого их количества и различной ориентации в пространстве.

В работе измеряли твердость высокопрочного чугуна с шаровидным графитом с перлито-ферритной и феррито-перлитной структурой металлической матрицы. В чугуне 1 (Ч1) форма графита в основном ближе компактной, Гф12,13, больше Гф 12, среднего размера (Граз 45). Матрица перлито-ферритная, до 20% феррита (структура бычьего глаза). Чугун 2 (Ч2) имеет графит практически идеальной шаровидной формы, Гф12,13, преимущественно Гф 13; среднего размера (Граз 45). Матрица феррито-перлитная, порядка 60% феррита.

Измерена твердость чугуна при кинетическом нагружении стальным закаленным шариком, построены кривые зависимости нагрузки от глубины внедрения индентора, истинной твердости и универсальной твердости от величины нагрузки. Размер образцов составляет 30x50x10 мм на универсальном твердомере конструкции В.И. Мощенка [3] с параллельной съемкой на видеокамеру.

Зависимость нагрузки (P) от глубины проникновения индентора (h) (рис.1) имеет параболический характер:

$$P = a\,h^2,$$

где для Ч1 a ≈1, а для Ч2 a ≈0,7.

Построение кривых такого типа предполагает зависимость от глубины проникновения индентора не нагрузки на индентор, а равной ей силы реакции, с которой материал противодействует внедрению. Тогда сила сопротивления внедрению, т.е. кинетическая твердость, выше у чугуна с большим количеством перлита. Это соответствует и более высоким значениям общепринятой твердости по Бринеллю.

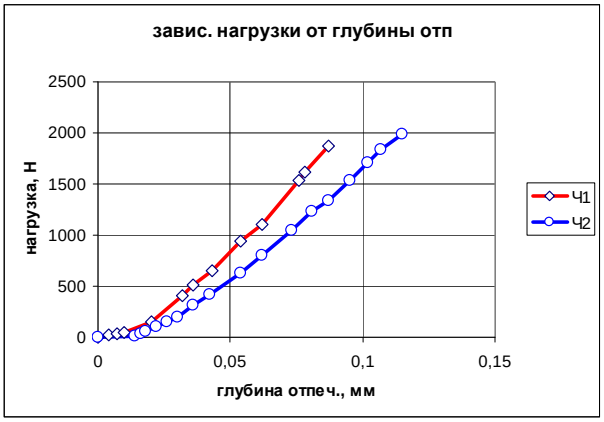

Рис. 1. Зависимость нагрузки от глубины отпечатка

Рис. 2. Зависимость Ну от нагрузки

Зависимости универсальной твердости (Ну) от величины нагрузки (Р) также носят параболический характер:

$$Ну = b\,P^2,$$

где b ≈0,088 для Ч1 и b ≈0,1 для Ч2.

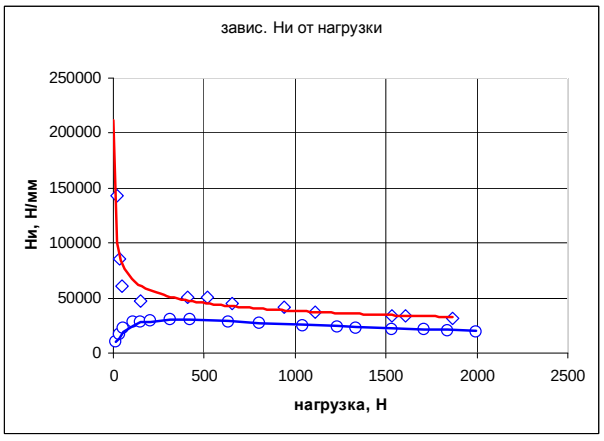

Рис. 3. Зависимость Ни от нагрузки

Однако из этих зависимостей следует, что при тех же значениях нагрузки универсальная твердость перлитного чугуна несколько ниже, чем ферритного.

Причиной этого может быть меньшая компактность графитных включений: суммарная поверхность металлической матрицы, которая собственно и сопротивляется внедрению индентора, меньше. Возможно также влияние феррита: большее его количество в матрице Ч2 увеличивает долю пластической составляющей работы сопротивления.

Характер изменения истинной твердости в зависимости от нагрузки для Ч1 и Ч2 различен принципиально. Для Ч1 кривая зависимости Ни от Р близка к гиперболе (рис.2):

$$Ни \approx 0{,}5+1/P.$$

Если рассматривать величину Р как нагрузку, действующую на металл, то увеличение нагрузки приводит к снижению истинной твердости. С этой точки зрения можно сказать, что увеличение нагрузки приводит к увеличению глубины проникновения индентора, сначала к преодолению сопротивления поверхностных слоев металла, а потом к увеличению объема, захваченного деформацией, и уменьшением удельного (отнесенного к объему) сопротивления. Если говорить о нагрузке как о силе реакции материала, то уменьшение удельного сопротивления нагружению при увеличении силы сопротивления также объясняется увеличением объема металла, вовлеченного в деформацию.

Для Ч2 кривая изменения истинной твердости носит довольно сложный характер, автоматическая аппроксимация ее в программе Exel дает неудовлетворительные результаты. Более всего график похож на график суммы двух или более функций, одна из которых является степенной

($y=\sqrt[n]{x}$), одна – гиперболической.

Трудность в отождествлении кривой состоит в постепенном плавном снижении значений твердости (у) на ветви параболы. Такой характер изменения истинной твердости может свидетельствовать о наличии нескольких механизмов реализации сопротивления кинетическому нагружению. Вначале доминирует механизм, дающий повышение твердости при увеличении нагрузки. Затем вступает в действие и становится преобладающим механизм снижения твердости, аналогичный механизму, действующему в Ч1. интересно, что Ч2 отличается большим количеством феррита, и повышение истинной твердости для него может быть аналогичным повышению универсальной твердости, т.е. обусловленным значительным содержанием пластичной фазы и увеличением доли пластической составляющей работы сопротивления.

Таким образом, характер изменения универсальной твердости высокопрочных чугунов определяется формой и количеством графитных включений; характер изменения истинной твердости в основном определяется объемом матрицы, вовлеченным в деформацию, и, возможно, содержанием пластичной фазы в матрице.

ЛИТЕРАТУРА

[1] Справочник по чугунному литью. Под ред. Гиршовича Н.Г., Л., Машиностроение, 1978 г., с.758.

[2] Солнцев Л.А., Костина Л.Л., Кропивный В.Н. Пути упрочнения нового конструкционного материала – чугуна с вермикулярным графитом. В сб.: Новые конструкционные стали и сплавы и методы их обработки для повышения надежности и долговечности изделий, Запорожье, 1983 г., с. 199.

[3] Мощенок В.І., Тарабанова В.П., Глушкова Д.Б.

[4] Спосіб оцінки твердості матеріалу. Пат. України

[5] UA74654 C2, G01N3/40. Заявл. 30.12.2003.

[6] Опубл. 16.01.2006. Бюл. №1.-3 с.

[7] С.И. Булычёв, В.П. Алёхин. Испытание

[8] материалов непрерывным вдавливанием

[9] индентора. – М.: Машиностроение, 1990. – 224 с.

TEHNOLOGICAL SUITABILITY OF SHAPING VITAL MACHINERY PARTS MANUFACTURED BY COMPRESSION PROCESSING

S. Lj. Marković, D. M. Erić

Abstract: *Technological suitability of shaping is achieved by adjusting construction details to the need of simplifying the manufacturing procedure, taking into consideration not to impair the function, toughness, appearance or some other characteristic of a machinery part. The shape of the part must provide conditions necessary for forging to be as simple as possible allowing the least possible expenditure of the die and the least damage. The inclination of the surfaces to the plane perpendicular to the separating plane must be such as to prevent the forging being stuck in the die. The radius of the die edge rounding over which the pressurized material is sliding (flowing) must be great enough. Ribs are not desirable at forged parts. Besides the above mentioned recommendations, this paper contains many other which the constructor must adhere to in order to shape technologically suitable product manufactured by compression processing.*

Key words*: technological suitability of shaping, vital machinery parts, forging, pressing.*

1. INTRODUCTION

Compression processing implies shaping of materials regarding their volume performed on the presses and hammers. Basically, compression can be free and in the dies. From the aspect of deformation speed we can differentiate between dynamic and static compression. Dynamic compression called forging is performed on the hammers. On the other side, static compression, often called pressing, is performed on the presses, where deformation speeds are small. Forging is more economical then pressing for individual production and production in small series, while at mass production and production in large series pressing is always more suitable. When it comes to the series of middle size, the choice is made upon the calculations regarding the price of the ready-made product obtained by either manufacturing procedure [5].

The main advantages of forging in comparison to other methods of manufacturing machinery parts are [1]:

- Very good mechanical characteristics of the manufactured parts, which can be useful with great load and in most important places,
- Relatively simple and rapid production of parts, even of those with complex geometry and greater dimensions,
- Very high level of utilization of materials (small percentage of scrap material during production),
- Lower price of production,
- Relatively smaller expenditure of energy per mass unit of the product.

Forging, of course, as all the other manufacturing procedures, has its disadvantages. They are in the following:

- The full economic justification and the most prominent results are most often achieved through serial production, production in large series and mass production,
- Evident troubles at processing the materials with very low original ductility (some steel-based alloys, for example),
- The occurrence of great forces and pressures during some processes, which complicates and raises the price of manufacturing the tools and demands machinery of great power.

Forging is the most often applied at manufacturing [3]:

- ✓ All types of vehicles, ships, airplanes and other flying objects, machines, tools and devices,
- ✓ Joining elements: bolts, nuts, nails, shafts...,
- ✓ Reservoirs, pots, cans and other packaging,
- ✓ Building elements (roof and wall construction...),
- ✓ Parts in electrical engineering and electronics,
- ✓ Hand tools and surgical instruments,
- ✓ Products for military industry.

The pressings can be obtained by various pressing methods, such as [1]:

- **Pressing by bending**, performed in one or several passes depending on the configuration of the pressing.
- **Pressing by rolling**, where there are two forging rolls rotating in opposite directions. Sector dies are fixed to these rolls. The work piece is placed between the rolls at the moment when the moulds are moving away one from another. The main operation on the forging rolls is drawing with shaping the work piece, both in longitudinal and cross-sections.
- **Specialized operations**, which comprise:

Dr. Eng. Svetislav Lj. MARKOVIĆ, professor, Technical College Čačak, svetom@nadlanu.com.
Mr Dragan M. ERIĆ, Company „Sloboda" Čačak, ericmdragan@yahoo.com

- **Forging on rotary forging machines**. It is a technological operation performed on rotary forging machines for drawing in forging dies
- **Thinning of the rings by rolling**. The basic materials for thinning of the rings by rolling are the rings obtained by forging on horizontal forging machines, or on hammers. Thinning by rolling allows manufacturing ring-shaped forgings with small addition and deviation.
- **Rolling the teeth of the gears**. It is performed on special machines for rolling the teeth which allow individual and group rolling.
- **Cross-sectional rolling**. It is highly productive operation in mass production of axially symmetrical pressings of simple shape.
- **Composite process**. It implies manufacturing different parts of the forging on separate machines.

- **Additional processing** operations which comprise:
  - **Trimming and removing the wreath**. The wreath, formed on the joined edge of the forging during pressing in open dies, is removed by the trimming die, placed on the shaft trimming presses. The wreath can be internal also, and occurs at rough punching of the forging during pressing. This wreath should be removed by the punching die in order to get a passable hole.
  - **Straightening pressed forgings**. The forgings are straightened in hot or cold condition. Hot straightening is performed after the wreath has been removed without pre-heating, or in the finishing process dies on the hammers (in production of small series), or in the special straightening dies (in production of large series) on separate hammers, or on the shaft presses (big and complex forgings) and on the trimming presses as well (forgings of the middle size). Cold straightening is performed in straightening dies, usually on friction hammers or presses, after heat treatment (forgings of small and middle size).
  - **Calibrating**. Calibrating enables achieving accurate dimensions, high quality surfaces and accurate weight of the forging. Calibrated surfaces should not be subjected to subsequent mechanical processing very often. There are several types of calibrating: *surface*, *volume* and *composite calibrating*.

2. SHAPING OF THE FORGINGS REGARDING THE MANUFACTURING TECHNOLOGY

There are certain limitations that are necessary to adhere to at shaping forgings. They primarily include the following [2]:

- The forging inclinations.

It is necessary to plan the inclinations in the following places:

- On the cylindrical parts of the forging, the length of which exceeds 30 percent of their diameter and which are set deeper in the pattern cavity: from $\alpha = 0{,}25^0$ (for $\frac{L}{D} = 0{,}3 \div 1{,}3$) to $\alpha = 1^0$ (for $\frac{L}{D} = 3{,}3 \div 4{,}3$) (figure 1, on the left);
- On the walls of the deeper cuts which are formed in the deep circular concavity of the mould: from $\alpha = 1^0$ (for $\Delta \le 10\ mm$) to $\alpha = 10^0$ (for $\Delta > 80\ mm$) (figure 1, in the middle);
- On the walls of the deep openings which are imprinted by the imprinter: from $\alpha = 0{,}25^0$ (for $\frac{L}{D} = 0{,}5 \div 1{,}5$) to $\alpha = 2^0$ (for $\frac{L}{D} = 7{,}5 \div 8{,}5$) (figure 1, on the right).

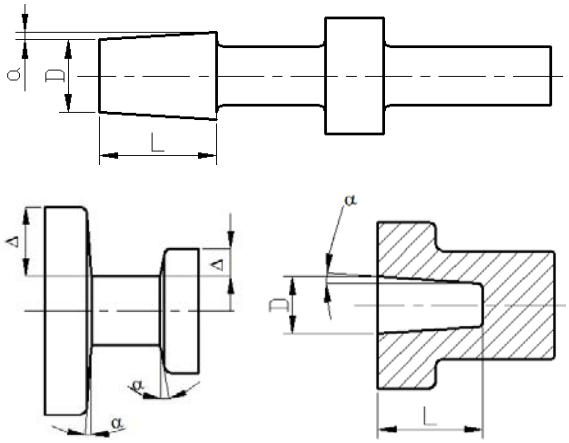

Figure 1. Forging inclinations

- The transits.

At forgings the transits should be made with the radius of the rounding ranging from 1,5 to 2 *mm* (figure 2).

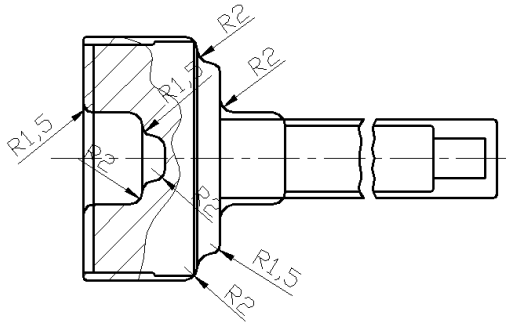

Figure 2. Forging transits

- The shaping of shafts and shafts, which have a rim (thickening) in the middle or at the end.

What should be taken in account is that the volume of the rim (V_1) does not exceed the volume of the shaft (V_2) of the given diameter and length $l = (10 \div 12)d$ (figure 3).

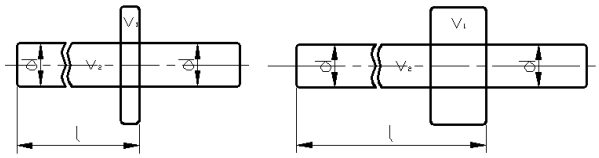

Figure 3. Shaping the shaft with a rim (thickening) correct (on the left) and incorrect (on the right)

- The narrowing in the longitudinal section of the forging, which limits the flow of the metal during forging in the direction opposite to that in which the puncher is moving.

The shape of the forging including a significant narrowing should be avoided (figure 4).

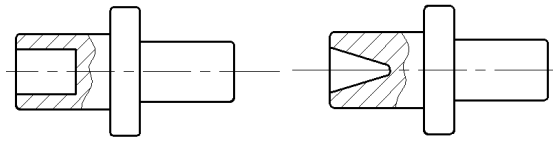

Figure 4. Shaping the forgings regarding the flow of the metal: correct (on the left) and incorrect (on the right)

- The concavities at the end of the rim, positioned laterally on the gripping part of the mould.

Suchlike concavities are necessary to avoid during shaping the forgings (figure 5).

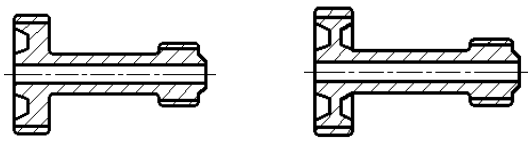

Figure 5. Shaping the forging regarding the concavities: desirable (on the left) and undesirable (on the right)

- The thickness of the walls.

It is desirable to construct the parts containing the holes at which the thickness of the walls exceeds 15 percent of the outer diameter of the part (figure 6).

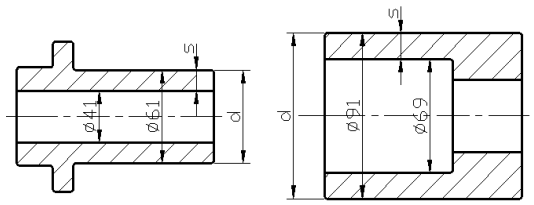

Figure 6. Shaping the forging regarding the thickness of the walls: desirable $s > 0{,}15d$ *(on the left) and undesirable* $s < 0{,}15d$ *(on the right)*

3. SHAPING THE PARTS MANUFACTURED BY FREE FORGING

During the shaping of the parts manufactured by free forging the following recommendations should be adhered to [1]:

- Conical (figure 7) and wedge-shaped (figure 8) forgings should be avoided, especially the ones with the small cones and inclination.

Figure 7. Shaping of the forging with conical surfaces: desirable (on the left) and undesirable (on the right)

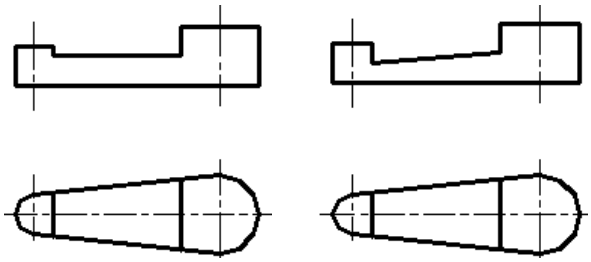

Figure 8. Shaping of the wedge-shaped forgings: correct (on the left) and incorrect (on the right)

- Mutual intersection of cylindrical surfaces should be avoided (figure 9).

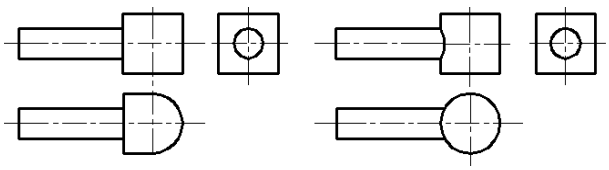

Figure 9. Shaping of the forging with intersection of cylindrical surfaces: correct (on the left) and incorrect (on the right)

- Cylindrical surfaces should not intersect prismatic elements of machinery parts (figure 10).

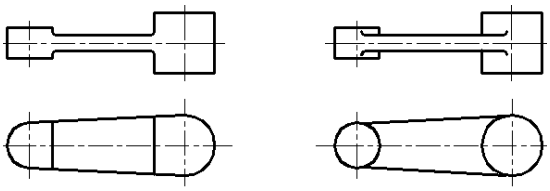

Figure 10. Shaping of the forging with intersection of cylindrical and prismatic surfaces: desirable (on the left) and undesirable (on the right)

- It is recommendable to construct protuberances only on one side of the part instead of on both sides (which especially applies to smaller parts) (figure 11).

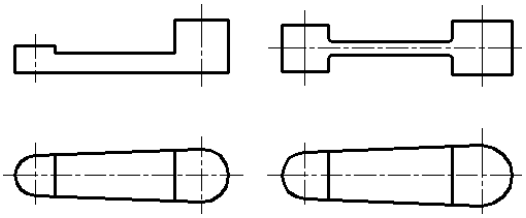

Figure 11. Shaping of the forging with protuberances: desirable (on the left) and undesirable (on the right)

- Ribbed cross-sections should be avoided since ribs, in most cases, cannot be manufactured by forging and outlets must be planned (figure 12). So-called stiffening ribs are not permitted in forgings.

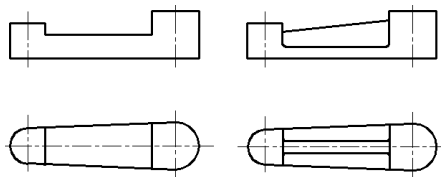

Figure 12. Shaping of the forging with the ribs: desirable (on the left) and undesirable (on the right)

- Outlets, support pads, thickenings and similar solutions should not be allowed on the main body of the forging (figure 13), and between the arms of the fork-shaped parts (figure 14).

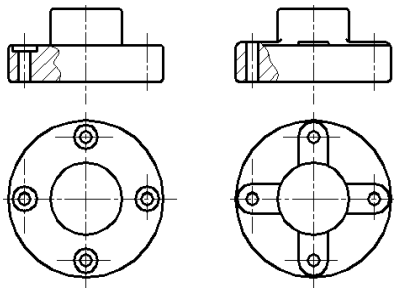

Figure 13. Shaping of the forging with the outlets: correct (on the left) and incorrect (on the right)

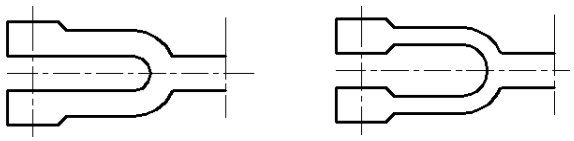

Figure 14. Shaping of the fork-shaped forging with thickenings: desirable (on the left) and undesirable (on the right)

- Machinery parts with prominent differences in dimensions of cross-sections (figure 15), or the parts the complex shape of which cannot be avoided (figure 16), should be substituted with several joined forged parts of simpler shapes, if it is possible.

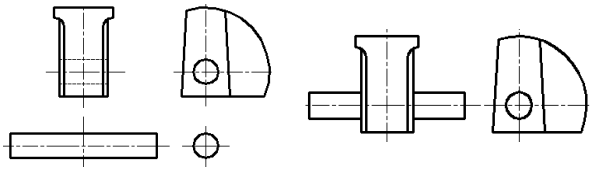

Figure 15. Shaping of the forging with a great difference between cross-sections: correct (on the left) and incorrect (on the right)

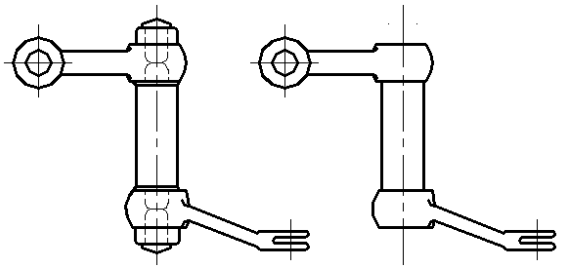

Figure 16. Shaping of the forging of a complex shape: desirable (on the left) and undesirable (on the right)

- It is most useful to manufacture complex parts by joining several forgings by welding, or by joining forged (1) and cast (2) elements by welding (figure 17).

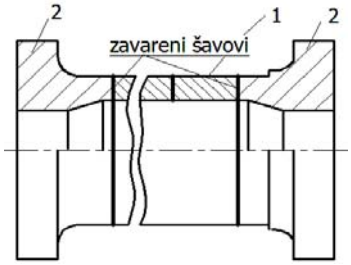

Figure 17. A complex part consisting of two forgings and one casting, joined by welding

4. CONCLUSION

The shaping of the forgings demands that some limitations be adhered to. They primarily refer to the following: forging inclinations, transits, shaping of the shafts and shafts which have a rim (thickening) at the end or in the middle, narrowing in the longitudinal section of the forging which impedes flowing of the metal during forging in the direction opposite to that in which the puncher is moving, concavities at the end of the rim which are positioned laterally on the gripping part of the die, the thickness of the walls [4].

When it comes to the shaping of the parts manufactured by free forging, it is recommendable to avoid: conical and wedge-shaped forgings, mutual intersections of cylindrical surfaces, intersection of cylindrical and prismatic elements of machinery parts ribbed cross-sections since the ribs cannot be made by forging in most cases, the so-called stiffening ribs in the forgings, outlets, support pads, thickenings and similar solutions on the main body of the forging and between the arms of the fork-shaped parts. It is recommendable: to construct protuberances on one side of the part instead of on both sides, to substitute the machinery parts with prominent differences in dimensions of cross-sections and the parts the complex shape of which cannot be avoided with the combination of several joined forged parts of simpler shapes and to manufacture the complex parts by joining several forgings by welding, or by joining forged and cast elements by welding.

REFERENCES

[1] *Inžinjersko tehnički priručnik*, knjiga 5, grupa autora, "Rad", Beograd, 1976.

[2] Kuzmanović S.: *Zbirka zadataka iz konstruisanja, oblikovanja i dizajna*, Fakultet tehničkih nauka, Novi Sad, 2003.

[3] Ognjanović M.: *Mašinski elementi*, Mašinski fakultet, Beograd, 2006.

[4] Charlotte & Peter Fiell: *Design 20th Century*, Taschen, Köln-London-Los Angeles-Madrid-Paris-Tokyo, 2006.

[5] www.cevip.kg.ac.yu, Centar za virtuelnu proizvodnju, Kragujevac.

G SESSION:

COMPUTER-INTEGRATED PROCESSES AND DESIGN OF MACHINING PROCESSES

INTEGRATED MANAGEMENT SYSTEMS - REQUIREMENT OF CONTEMPORARY BUSINESS PRACTICES

M. Djapic, Lj. Lukic, S. Arsovski

Abstract: *Many organizations encounter the problem of development and implementation of Integrated Management System (IMS), based on the quality requirements (ISO 9001), preservation of environment (ISO 14001) and occupational health and safety assessment standard (OH&SAS 18000). In order to help the organizations in this venture, the paper presents some of the key definitions which explain the concept. This work provides an approach to the integration of different standards requirements, based on the interrelation of mutually connected business processes.*

Keywords: *IMS, QMS, EMS, OH&SAS, Business processes*

1. INTRODUCTION

The aim of the International Organization for Standardization– ISO is to develop, based on the best global practices, ISO – standards in various domains of human activity which will provide comprehension, cooperation and expeditive communication on the global market.

Many organizations are trying to develop and implement the integrated management system (IMS) which will satisfy requirements of the ISO 9001, ISO 14001 OHSAS 18001, ISO/IEC 27001 standards etc. What they need now is a clear structure of the new system and time schedule of actions that will provide them certification without major problems.

Similarities in the framework and structure of standards ISO 9001, ISO 14001, OHSAS 18001 ISO/IEC 27001 etc. point out that this integration can be performed. The International Organization for Standardization ISO has undoubtedly assisted this goal, by defining, at the proposal of the Dutch Institute for Standardization as early as 1998., the preliminary specification ISO Guide 72 - Guide on Justification and Drafting of Management System Standards. This Guide has been endorced in 2002. ISO Guide 72 is intended to improve the interface between the standards developing committees and the market they serve, as well as to make optimal use of resources by only developing management system standards for which there are clear market requirements (De Grood, Hortensius, 2002).

Organizations beginning integration of different management systems usually have developed and implemented one or two systems. Most often it is the QMS according to requirements of ISO9001, or EMS according to requirements of ISO14001. These systems were developed in different time intervals, with different sets of documents. There has been confusion in the market place as to what constitutes an integrated management system. This was the basic reason why BSI developed and introduced new specification for management system integration (Wang 2008).

In order to assist organizations that are starting this venture, the paper presents and explains several key definitions that will surely facilitate this work. It also demonstrates how orientation toward business processes represents the key for integration, that is, how business processes represent the backbone of integration.

2. INTEGRATED MANAGEMENT SYSTEM (IMS-QEHS)

Integrated management system represents the reality facing top management in every organization and each process "owner". It can be argued that each organization has some form of integrated management system, the leadership and the executive officers (top-menagement) having the obligation to implement legal and other national regulations regarding the fulfillment of demands of "interested parties": society, owners, employees, customers, suppliers and others. Question should be asked – to what extent is such an IMS formalized (documented), efficient and effective, giving management the opportunity of insight into every part of the business system, enabling them to make timely business decisions based on facts? Having the certificate for quality management system, ISO 9001:2000, testifies only (usually) that the organization successfully controls processes significant for product quality. However, QMS certificate does not necessarily mean the fulfillment of requirements of interested parties.

Fast development and spreading of influence of the ISO 9000 series standards have induced the emergence of other standards in the domain of management, such as environment protection (ISO 14000), occupational safety and occupational health and safety assessment (OHSAS 18000), information safety (ISO/IEC 27001), information technologies (ISO 2000) etc. New standard series are being prepared for other management systems (in health care and occupational safety– ISO 18000, risk

Ass. prof Mirko Djapic, Ph D, Faculty of Mechanical Engineering Kraljevo, LOLA Institute Belgrade, mdjapic@yahoo.com
Prof. Ljubomir Lukic, Ph D, Faculty of Mechanical Engineering Kraljevo, lukic.lj@mfkv.kg.ac.yu
Prof. Slavko Arsovski, Ph D, Faculty of Mechanical Engineering Kragujevac, cqm@kg.ac.yu

– ISO 31000, finances– ISO/TR 10014 etc.), establishing partial requirements for specific management domains, which will be mutually complementary.

Emergence of ISO 14000 standards and the development of the management systems for environment protection according to this standard implied its integration with QMS. When this occurred (in the second half of the past decade), the researchers and practitioners were faced with the problem of integrating these systems. This problem gains in significance later on as an entire series of new management systems emerged, some of which have been listed above. The researchers and practitioners were faced with two key problems. They are:

1. What does "integration" of management systems mean, how should it be defined?
2. How to perform this integration, how to implement it, measure it and finally how to improve it?

Literature in English gives a variety of different answers to these questions. These topics have been a frequent subject of journals such as Quality World, Quality Progress and TQM Magazine.

2.1 Integration, Connection and Compatibility of Different Standards of Management Systems

Introduction of a new concept into business practice invariably imposes the need to define it. The basic reason for this is unimpaired and unambiguous communication between researchers and practitioners.

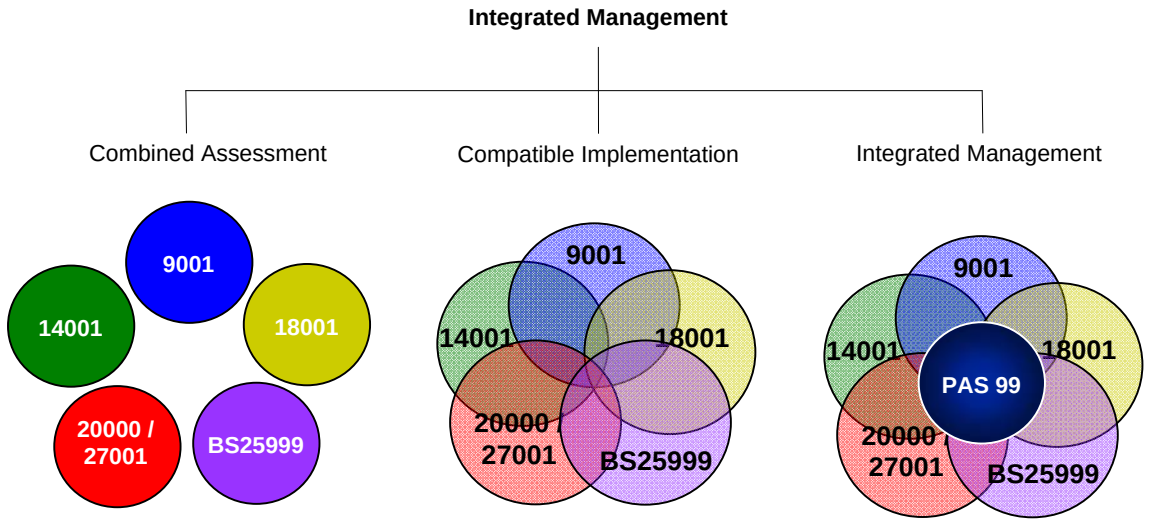

Figure 2.1. Integration and connection of different management system standards

When speaking of integrated management systems (IMS), the need arises to define the term "integrated", in the way that it is most frequently used in standardization and in the system approach to management. An excellent basis for this is the study of MacGregor Associates of 1996. This study points out the need to precisely define "integrations" and "connections" of standards. Integration is viewed as a unique essential standard of the highest management level with optional modules covering different (specific) requirements, such as PAS 99:2006.

Connection implies "parallel standards of management systems specified for a particular discipline, having high level of uniformness of structure and contents" (Figure 2.1)

In (Wilhelm 2008) a definition is given of integrated management system as:

"Integrated Management System is where an organization has a single management system that is a combination of two or more management systems standards (e.g. ISO 9001, 14001, 27001,...) and also complies with PAS 99:2006 - Specification of common management system requirements as a framework for integration" ((Figure 2.6).

If we want to imply management integration, then the kernel of the management system (Figure 2.2) must cover QMS, EMS, OHSMS, ISMS etc., as well as all future standards to be developed.

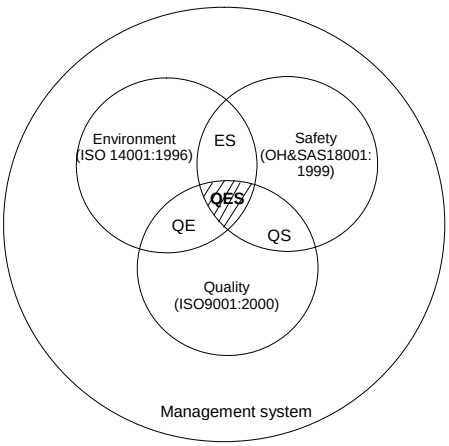

Figure 2.2. Integration and connection of quality, environment protection and safety

Backing the above statement, it is interesting to quote the ISO/TAG 12 recommendation of the technical group, requiring that ISO 9000 and ISO 14000 series should not be joined but made compatible. Under compatibility of standards, we consider "that common elements of standards can be implemented in such a way as to fulfill all standards in their entirety or in part, without unnecessary duplication or imposing requirements that are mutually exclusive".

2.2 Models of Integrated Management Systems

Quite a number of models can be found in literature. We point out models of Wilkinson and Dale (Figure 2.3) and Karapetrović model (Figure 2.4).

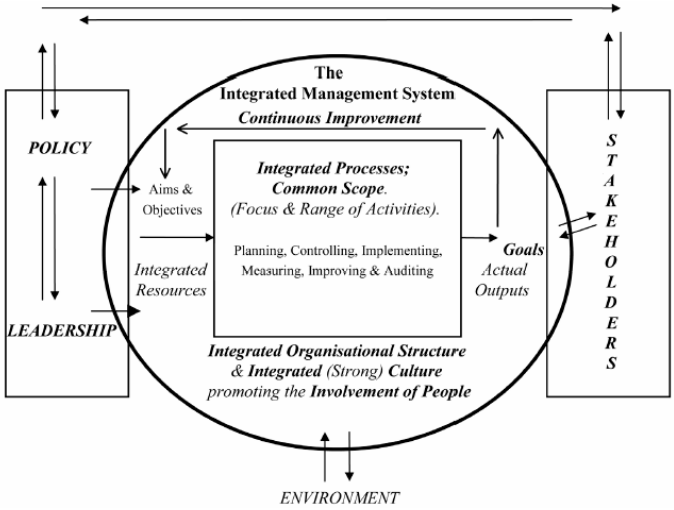

Figure 2.3. A model of an integrated quality, environment and health and safety management system (Willkinson&Dale 2001)

BSI has in 2006. established the standard for integrated management systems. BSI's intention was to simplify the implementation of multiple management system standards and any associated conformity assessment. Based on ISO Guide 72, BSI recommends integrated approach to (Wang, 2008):

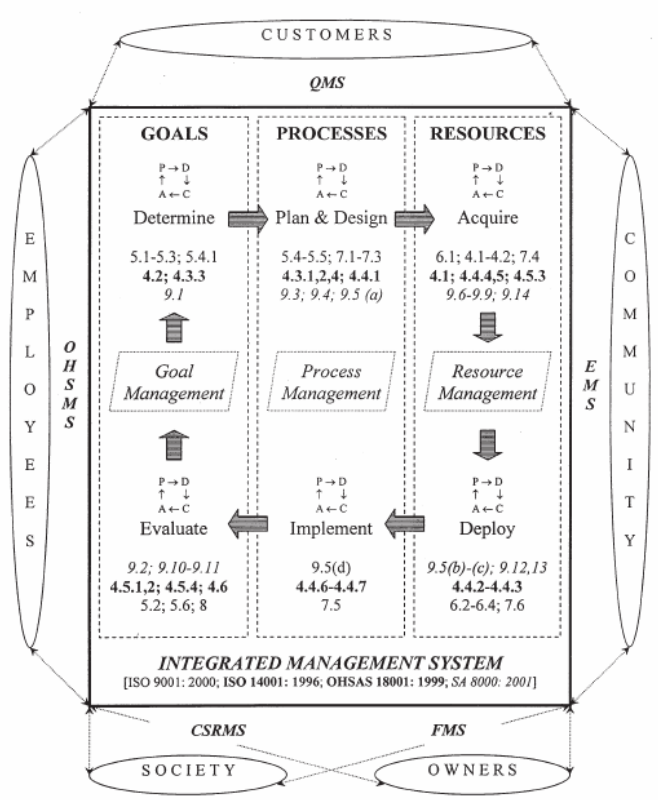

Figure 2.4. A model of IMS (Karapetrovic 2001)

- Management review that considers the overall business strategy and action plan;
- An integrated approach to internal audits upon the integrated system;
- An integrated approach to policy and objectives setting;
- An integrated approach to looking at the aspects, impacts, and risk to the business;
- An integrated approach to systems processes;
- An integrated documentation set including integrated desk instructions and work instructions;
- An integrated approach to improvement mechanisms (Corrective Action, Measurement and Continual Improvement);
- Unified management support and a coherent participation

PAS 99 is a Publicly Available Specification of common requirements for management systems that can be used as a framework for an integrated management system.

Organizations with more than one management system can view PAS 99 as an aid to achieving a single holistic management system.

PAS 99 takes account of the six common requirements for management systems standards outlined in ISO Guide 72 guidance document.

These six common requirements are:

- Policy
- Planning
- Implementation and Operation
- Performance Assessment
- Improvement
- Management Review

Integrated management model is providede on figure 2.5 and 2.6.

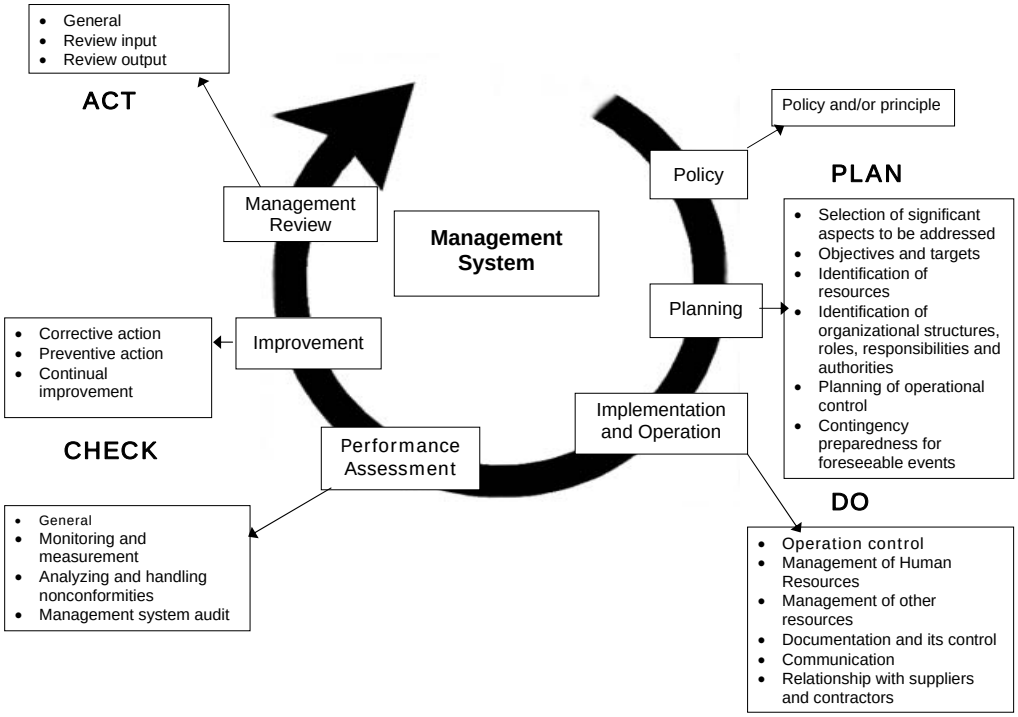

Figure 2.5. PAS 99 PDCA cycle

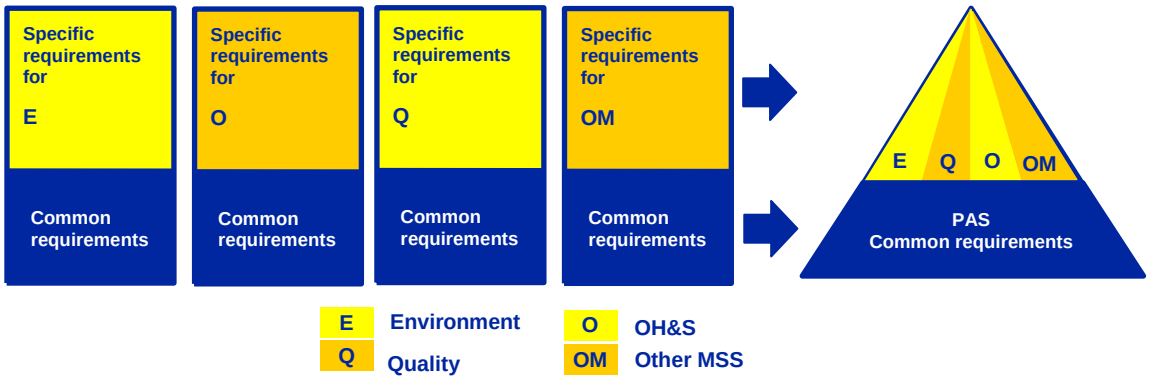

Figure 2.6. Integration of requirements of different management systems according to BS PAS 99:2006

BUSINESS PROCESSES – KEY TO THE INTEGRATION OF MANAGEMENT SYSTEMS

Many organizations starting the development of IMS have implemented at least one management system. The problem they are faced with is how, under such circumstances, to develop and implement an integrated system.

The first step that has to be performed is to analyze whether there exists a business justification for such a project. It is important to consider requirements of all interested parties, as well as the influence of the new system on them.

If the answer to the first question is affirmative, it is necessary to plan everything and to provide resources and the necessary budget for the implementation of IMS.

The next key task is to determine where does the organization stand with respect to the requirements of all standards constituting the scope of IMS. It is important to asses the efficiency of the existing management system.

Diagram of business processes (Figure 3.1) is a useful tool for this analysis. If it has not been made previously, it should be generated now. Based on this diagram, it can be determined how are the standard requirements making the scope of IMS implemented in all organization's processes, and especially in basic processes. In this way **business process becomes the backbone of the integration requirements of different standards** (Figure 3.2).

Within the structure of business processes, not every process has the same potential for integration of different standards' requirements. Processes having the greatest potential for integration of requirements of quality, environment protection and occupational health and safety are:

- Document control
- Record control
- Strategic planning and organization management (investigation by the leadership)
- Human resources management (education and training of employees)
- Research and development control
- Control of the operative product realization (Production management)
- Control of the measuring, testing and control equipment
- Equipment maintenance
- Control of supply of semifinished products, components and services
- Corrective measures
- Preventive measures
- Internal audits.

For each of these processes, it is possible to identify an integration strategy.

Figure 3.2 Business process as the backbone of integration of different standards' requirements

3.1 Strategy for Integrating Requirements diferent

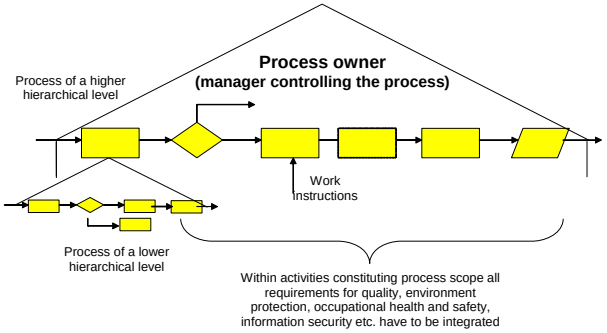

Management System Standards (MSS)

Existence of three or more separate approaches to operative production process management can lead to confusion among employees about which approach is best to be used. Many organizations generate different manuals referring for example to quality, environment protection and occupational health and safety. Such manuals are usually made without analyzing their

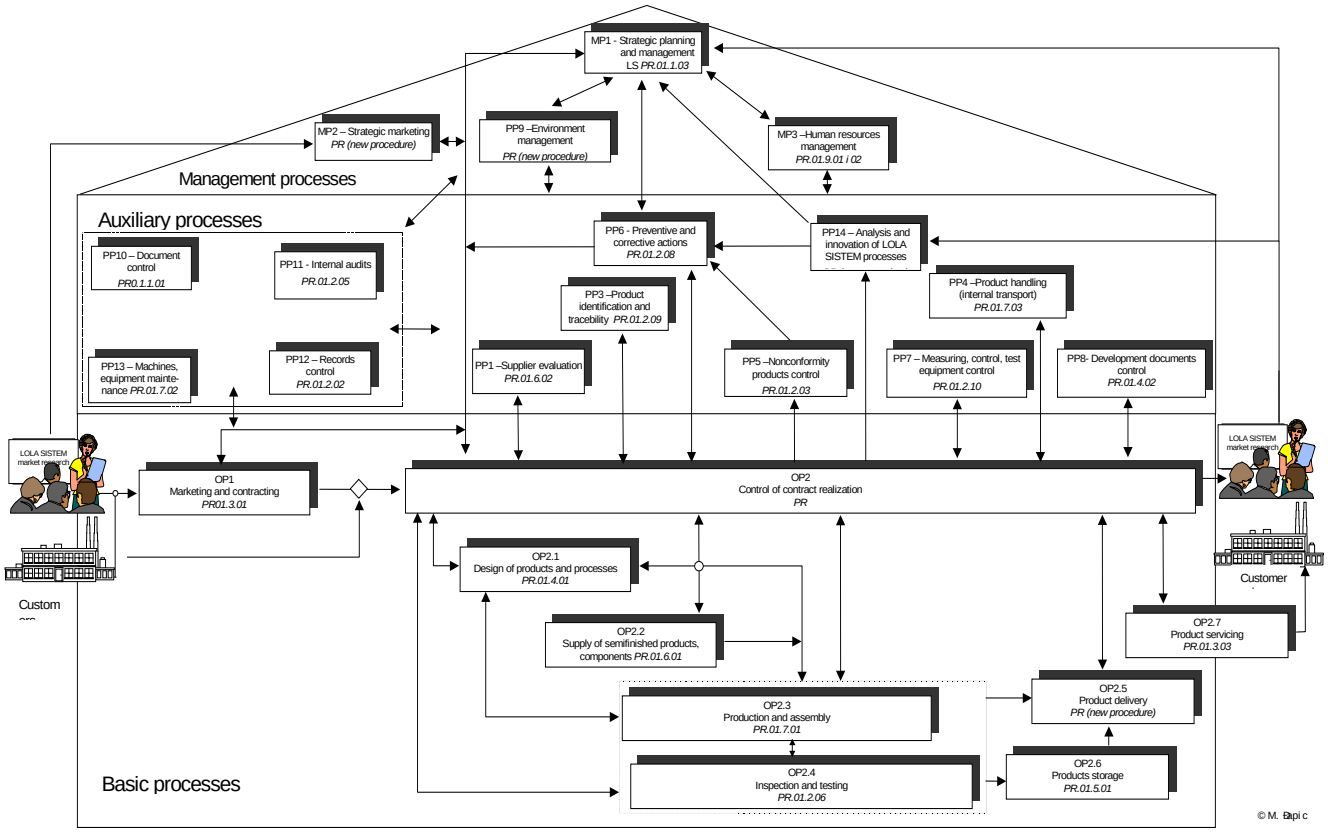

Figure 3.1 Bussines processes diagram

mutual influence, and most often they are mutually conflicting. In this way, they can lead to misunderstandings, especially when novice employees being introduced to particular activities in the process are introduced to them.

Therefore it is useful to identify **strategy for the integration of these requirements** (Phillips 2002)**:**

- Identify those activities in the production process that can influence quality, environment, and occupational health and safety.
- With the help of employees engaged in the production process, develop and document procedure(s) for operative management of the production process with operating manuals **that clearly define operative criteria for the production of high quality products observing occupational health and safety, which least affect the environment**.
- Develop and operatively manage processes in order to ensure that raw materials, parts in the production process, and final products are clearly identified.
- Develop and operatively manage processes for handling, storage, packing and delivery of products.

Benefits from integrating requirements are:

- Organizations that have integrated operative management of the production process have great support from the employees.
- Confusion and conflicts that can be generated by mutually contradictory documents are decreased.
- Employee training is less tedious.
- The greatest benefit is that in this way the developed management system displays how the tasks are performed and controlled within the organization.

When integrating operative management of the production process, organizations have to avoid usual catches. Some of them are:

- Employees are not involved in the design of the process and documentation demonstrating how the process is operatively managed.
- Generation of lengthy, discursive documents that are rarely used or read.
- Nonconformity to specified procedures of process realization, as defined in documents, especially by the management.

4. CONCLUSION

Many organizations wishing to satisfy requirements for quality, environment protection and occupational health and safety are faced with the problem how and in what way to integrate different management systems. Integration of several systems into one is more efficient and economical than developing and implementing separate systems.

In order to aid organizations that are starting this project, the paper presents and explains several key definitions that will surely facilitate this venture. Also, it is demonstrated how orientation toward business processes is the key to integration, that is, how business processes represent the backbone of integration.

REFERENCE

[1] Djapic, M., Uzunovic, R., Business process orientation - Key for management system integration, VII YSQ Conference with foreign participation "Development and realization Serbian national strategy for quality improvement, Niska Banja, 27. and 28 Mach 2003.

[2] Wang, Wilhelm, PAS 99:2006 - Integrated Management System, BSI Mangement systems presentation, Mexico City, May 2008.

[3] BS PAS 99:2006, Specification of common management system requirement as a framework for integration, British Standard Institution, 2006.

[4] MacGregor Associations, Study of Management Systems Standards, British Standards Institute, 1996.

[5] Phillips, A., Integrating Green into an Existing Management System: Most Commonly Integrated Process, ASQ's 56th Annual Quality Congress, Colorado, May 20.-22. 2002.

[6] Mors, A., T., Integrating Green into an Existing Management System: Return on Investment, ASQ's 56th Annual Quality Congress, Colorado, May 20.-22. 2002.

[7] Douglas, A., Glen, D., Integrated management systems in small and medium enterprises, Total Quality Management, Vol. 12., No. 4/5&7, 2001, (S686-S690).

[8] Wilkinson, G, Dale, B. G., Integrated management systems: an examination of the concept and theory, The TQM Magazine, Vol. 12., No. 1., 1999., pp. 95-104.

[9] Shaw, A., Question time, Quality World, February 2003, pp. 51.

[10] BSI, Question time, Quality World, February 2003, pp. 52.

[11] Hoyle, D., Quality systems – a new perspective, Quality World, October 1996, pp. 710-713.

[12] Tranmer, J., Overcoming the problems to integrated management systems, Quality World, October 1996., pp. 714-718.

[13] Massey, G., Tasman holds the combination to management systems, Quality World, October 1996, pp. 727-730.

[14] Karapetrovic, S., Willborn, W., Integration quality and environmental management systems, TQM Magazine, Vol. 11., No. 3., 1998., pp. 204-217.

[15] De Grood, R., Hortensius, D., ISO Guide 72 on justification and drafting of management system standards, ISO Bulletin, March 2002.

DATABASE DESIGN FROM TECHONOLOGICAL AND KINEMATIC PARAMETERS OF NC PROGRAM FOR PRODUCTION IN FLEXIBLE MANUFACTURING SYSTEM

Ivanović S., Lukić Lj.

Abstract: *Changes of input parameters in flexible manufacturing system are bringing to incompleting of technological demands during production process. In that circumstances it is necessary to change factors in NC programs which have to influence over changes of values that corresponding to technological demands. Changes of machining regimes and/or tools in NC programs are leading up to changes of machining times and production costs, therefore it is necessary to add some modules in information component of flexible manufacturing system. These modules have to lead values of machining regimes or tool parameters up to meeting of technological demands before NC program executing.*

Key words: *Database, Flexible manufacturing system (FMS), NC program*

1. INTRODUCTION

Fundamental input parameters for information component of flexible manufacturing system (FMS) are:

a) configuration of flexible manufacturing system (layout of FMS, data about machining centres, etc.),
b) assortment of working pieces,
c) technological database (database of materials, tools, machining regimes, etc.),
d) technological demands (number of pieces in series from assortment, production time for whole assortment of working pieces, production costs for whole assortment of working pieces, etc.).

According to assigned assortment of working pieces, pallet contents are setting up in CAD system. Considering basic characteristics of production process in FMS and accepted conventions, a number of different pallet contents is calculating, and pallet contents as new working pieces are presenting input in CAM system. In accordance with system configuration, technological database and technological demands, CAM system as output produces NC programs. Execution of NC programs produces a statistics that contains data as it is execution time of NC programs, number of tools, indexing number, etc. Using data from statistics of executed NC programs it is possibly to estimate shall be technological demands completed or not. Estimated positive result is enabling continuation of production process, whereas negative result is ordering changes of machining regimes and/or tools NC programs until meeting of technological demands.

Changes of input parameters are bringing to incompleting of technological demands during production process. Therefore, it is necessary to change some blocks in NC programs that influence to changes of values that corresponding to technological demands. Changes of machining regimes and/or tools in NC programs are leading up to changes of machining times and production costs. The special case is breakdown of some machining centre when the same number of pallet contents have to dispose on lower number of machining centres. The consequence of that case is growing of production time for whole assortment of working pieces. Therefore, machining regimes and/or tools are changing for the purpose to decrease of machining time for pallet content, and finally, to decrease of total production time and to increase of total production costs.

Described information component of FMS functioning is not enabling on time completing technological demands because of chaanges of input parameters. It is necessary to add modules that have to lead values of machining regimes and/or tool parameters up to meeting of technological demands before NC program executing, modul that have to inspect this changes and modul for reading and writing of changed NC programs. For this procedure it is necessary to create convenient database tables for changes of values of machining regimes and tool parameters called NC tables.

In accordance with data in NC tables it is executing calculation or simulation to obtain parameters that are needful for comparison with placed technological demands, total production time and production costs. If obtained parameters do not reach demands, there are executing variations of machining regimes and tools in NC tables according to limit tables. The procedure is repeating until meeting og technological demands.

The information component of FMS during production process can be defined so input and output for this component are NC programs (fig.1.).

mr Slobodan Ivanović, Faculty of Mechanical Engineering Kraljevo, ivanovic.s@mfkv.kg.ac.yu
dr Ljubomir Lukić, Faculty of Mechanical Engineering Kraljevo, lukic.lj@mfkv.kg.ac.yu

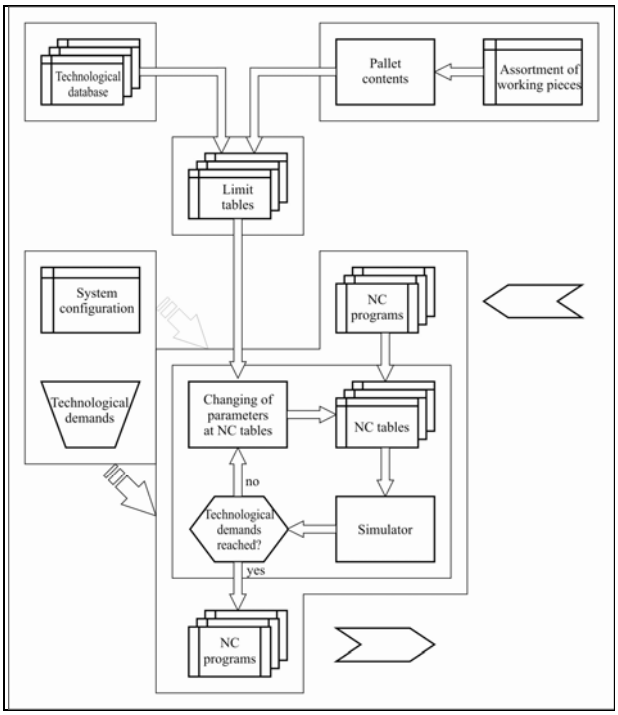

Fig.1. Information component operation of flexible manufacturing system required during production process

2. TECHNOLOGICAL DEMANDS

Technological demands are understanding to define criterions and strategies for parameters changing in NC tables for the purpose of meeting technological demands /01/.

General criterions are:
1. maximal exploitation of power characteristics of machining centres,
2. maximal exploitation of tool life,
3. simultaneous change of all tools in tool magazine of machining centre,
4. on single pallet pieces of same material and
5. one shrinkage one CNC program.

Criterions that can be changed are:
1. production time of complete assortment of working pieces, and
2. production costs of complete assortment of working pieces.

Strategy can be:
1. change of parameters of machining regimes, or
2. change of cutting edges (tools).

3. ANALYSIS OF DATA AT NC PROGRAMS

For the purpose to changing of machining regimes and/or tools in NC programs according to placed technological demands it is necessary to calculate time of NC program execution and create tables with data about tools and machining parameters in accordance with data contained in programs.

3.1. Execution time of NC program

Execution time of NC program is sum of tools changing time, indexing time, rapid traverse time and machining time.

$$t_{NC} = t_{iza} + t_{ind} + t_{brz} + t_{obr}$$

Tools changing time is sum of all of single tool changing time that is constant and it depends on type of the machining centre, in other words it is product of tools changing number widh time necessary for single tool changing:

$$t_{iza} = n_{iza} \cdot t_{iza1}$$

where:
n_{iza} - is number of tools changing and it is equal to number of calling M-function M06 in single NC program:

$$n_{iza} = \sum_{i=1}^{N} 1 \, , f(m) \ni NCb(i), f(m) = \{M06\}$$

where:
N - is number of program block
$NCb(i)$ - is i-th program block
t_{iza1} - is time of single tools changing

Indexing time is the time necessary for changing sides of palet contents (rotation of palet).

$$t_{ind} = n_{ind} \cdot t_{ind1}$$

where:
n_{ind} - is number of indexing
t_{ind1} - is time of single indexing

Rapid traverse time is obtaining as sum of quotients of rapid traverse path and rapid traverse speed of tool for each program block:

$$t_{brz} = \sum_{i=1}^{N} \frac{d_{brz}}{v_{brz}}$$

where:
N - is number of program blocks
d_{brz} - is rapid traverse path at i-th program block
v_{brz} - is rapid traverse speed of tool, it is constant and depends on machining centre

Path that tool passed during rapid traverse in one program block is calculating according to values of coordinates located in the same program block and in preceding program blocks or values of coordinates

located only in that program block depending on definition of absolute (G90) or incremental (G91) input of length values, and it is realized most frequently:

1. using function G00 (rapid traverse) by coordinates X, Y and Z:
for G90

$$d_{brz} = \sqrt{(x - x_o)^2 + (y - y_o)^2 + (z - z_o)^2}$$
$$x = \begin{cases} f('X'), 'X' \exists NCb(i) \\ x_o, \quad 'X' \nexists NCb(i) \end{cases}$$
$$y = \begin{cases} f('Y'), 'Y' \exists NCb(i) \\ y_o, \quad 'Y' \nexists NCb(i) \end{cases}$$
$$z = \begin{cases} f('Z'), 'Z' \exists NCb(i) \\ z_o, \quad 'Z' \nexists NCb(i) \end{cases}$$

for G91

$$d_{brz} = \sqrt{x^2 + y^2 + z^2}$$
$$x = \begin{cases} f('X'), 'X' \exists NCb(i) \\ 0, \quad 'X' \nexists NCb(i) \end{cases}$$
$$y = \begin{cases} f('Y'), 'Y' \exists NCb(i) \\ 0, \quad 'Y' \nexists NCb(i) \end{cases}$$
$$z = \begin{cases} f('Z'), 'Z' \exists NCb(i) \\ 0, \quad 'Z' \nexists NCb(i) \end{cases}$$

where: x, y, z - are values of coordinates defined at i-th program block
x_o, y_o, z_o - are values of coordinates defined before i-th program block
$f()$ - is evaluation of coordinates

2. using cycles G81, G82, ... G89 by coordinates X and Y and reference plane R (funcija G17 - plane selection XY):
for G90

$$d_{brz} = \sqrt{(x - x_o)^2 + (y - y_o)^2 + (r - r_o)^2}$$
$$x = \begin{cases} f('X'), 'X' \exists NCb(i) \\ x_o, \quad 'X' \nexists NCb(i) \end{cases}, f(g) \exists NCb(i)$$
$$y = \begin{cases} f('Y'), 'Y' \exists NCb(i) \\ y_o, \quad 'Y' \nexists NCb(i) \end{cases}, f(g) \exists NCb(i)$$
$$r = \begin{cases} f('R'), 'R' \exists NCb(i) \\ r_o, \quad 'R' \nexists NCb(i) \end{cases}, f(g) \exists NCb(i)$$

for G91

$$d_{brz} = \sqrt{x^2 + y^2 + r^2}$$
$$x = \begin{cases} f('X'), 'X' \exists NCb(i) \\ 0, \quad 'X' \nexists NCb(i) \end{cases}, f(g) \exists NCb(i)$$
$$y = \begin{cases} f('Y'), 'Y' \exists NCb(i) \\ 0, \quad 'Y' \nexists NCb(i) \end{cases}, f(g) \exists NCb(i)$$
$$r = \begin{cases} f('R'), 'R' \exists NCb(i) \\ 0, \quad 'R' \nexists NCb(i) \end{cases}, f(g) \exists NCb(i)$$

where: r - is coordinate of reference plane
r_o - is coordinate of reference plane defined before i-th program block
$f(g)$ = $\{G81, G82, \ldots G89\}$

3. using function G98 (return to initial level) in cycles G81, G82, ... G89:
for G90

$$d_{brz} = \sqrt{(x - x_o)^2 + (y - y_o)^2} + |z_i - z_o|$$
$$x = \begin{cases} f('X'), 'X' \exists NCb(i) \\ x_o, \quad 'X' \nexists NCb(i) \end{cases}$$
$$y = \begin{cases} f('Y'), 'Y' \exists NCb(i) \\ y_o, \quad 'Y' \nexists NCb(i) \end{cases}$$
$$z_i = \begin{cases} f('Z'), 'Z' \exists NCb(j), f(g) \exists NCb(j)|_{j=1}^{i-1} \\ 0, \quad f(g) \nexists NCb(j)|_{j=1}^{i-1} \end{cases}$$

for G91

$$d_{brz} = \sqrt{x^2 + y^2} + |z_i - z_o|$$
$$x = \begin{cases} f('X'), 'X' \exists NCb(i) \\ 0, \quad 'X' \nexists NCb(i) \end{cases}$$
$$y = \begin{cases} f('Y'), 'Y' \exists NCb(i) \\ 0, \quad 'Y' \nexists NCb(i) \end{cases}$$
$$z_i = \begin{cases} f('Z'), 'Z' \exists NCb(j), f(g) \exists NCb(j)|_{j=1}^{i-1} \\ 0, \quad f(g) \nexists NCb(j)|_{j=1}^{i-1} \end{cases}$$

where: z_i - is z coordinate of initial plane defined by funktions G50 or G92
$f(g)$ = $\{G50, G92\}$

Machining time is obtaining as sum of quotients of path that tool passed during machining and table feed for each program block:

$$t_{obr} = \sum_{i=1}^{N} \frac{d_{obr}}{v_{obr}}$$

where:
N - is number of program blocks
d_{obr} - is cutting feed path at i-th program block
v_{obr} - is table feed at i-th program block

Path that tool passed during machining in one program block is calculating according to values of coordinates located in the same program block and in preceding program blocks or values of coordinates located only in that program block depending on definition of absolute (G90) or incremental (G91) input of length values, and it is realized most frequently:

1. using function G01 (linear interpolation) by coordinates X, Y and Z:
for G90

$$d_{brz} = \sqrt{(x - x_o)^2 + (y - y_o)^2 + (z - z_o)^2}$$

for G91

$$d_{brz} = \sqrt{x^2 + y^2 + z^2}$$

2. using cycles G81, G82, ... G89 by coordinates X, Y and Z and reference plane R (function G17 - plane selection XY):
for G90

$$d_{obr} = |z - r|$$
$$z = \begin{cases} f('Z'), 'Z' \exists NCb(i) \\ z_o, \quad 'Z' \nexists NCb(i) \end{cases}$$
$$r = \begin{cases} f('R'), 'R' \exists NCb(i) \\ r_o, \quad 'R' \nexists NCb(i) \end{cases}$$

for G91

$$d_{obr} = |z|$$

$$z = \begin{cases} f('Z'), 'Z' \exists NCb(i) \\ z_o, \quad 'Z' \nexists NCb(i) \end{cases}$$

3. using functions G98 and G99 and reference plane R (function G17 - plane selection XY):
for G90

$$d_{obr} = |r - z|$$

$$z = \begin{cases} f('Z'), 'Z' \exists NCb(i) \\ z_o, \quad 'Z' \nexists NCb(i) \end{cases}$$

$$r = \begin{cases} f('R'), 'R' \exists NCb(i) \\ r_o, \quad 'R' \nexists NCb(i) \end{cases}$$

for G91

$$d_{obr} = |z|$$

$$z = \begin{cases} f('Z'), 'Z' \exists NCb(i) \\ z_o, \quad 'Z' \nexists NCb(i) \end{cases}$$

4. using funkctions G02 and G03 (circular interpolation) by coordinates X, Y, Z, I, J and K:
for G90

$$a = \sqrt{(x - x_o)^2 + (y - y_o)^2 + (z - z_o)^2}$$

$$b = \sqrt{(i - x_o)^2 + (j - y_o)^2 + (k - z_o)^2}$$

$$\alpha = \arccos\left(1 - \frac{a^2}{2 \cdot b^2}\right)$$

$$d_{obr} = \frac{\pi \cdot b \cdot \alpha}{180^o}$$

$$x = \begin{cases} f('X'), 'X' \exists NCb(i) \\ x_o, \quad 'X' \nexists NCb(i) \end{cases}, \quad i = \begin{cases} f('I'), 'I' \exists NCb(i) \\ 0, \quad 'I' \nexists NCb(i) \end{cases}$$

$$y = \begin{cases} f('Y'), 'Y' \exists NCb(i) \\ y_o, \quad 'Y' \nexists NCb(i) \end{cases}, \quad j = \begin{cases} f('J'), 'J' \exists NCb(i) \\ 0, \quad 'J' \nexists NCb(i) \end{cases}$$

$$z = \begin{cases} f('Z'), 'Z' \exists NCb(i) \\ z_o, \quad 'Z' \nexists NCb(i) \end{cases}, \quad k = \begin{cases} f('K'), 'K' \exists NCb(i) \\ 0, \quad 'K' \nexists NCb(i) \end{cases}$$

for G91

$$a = \sqrt{x^2 + y^2 + z^2}$$

$$b = \sqrt{i^2 + j^2 + k^2}$$

$$\alpha = \arccos\left(1 - \frac{a^2}{2 \cdot b^2}\right)$$

$$d_{obr} = \frac{\pi \cdot b \cdot \alpha}{180^o}$$

$$x = \begin{cases} f('X'), 'X' \exists NCb(i) \\ 0, \quad 'X' \nexists NCb(i) \end{cases}, \quad i = \begin{cases} f('I'), 'I' \exists NCb(i) \\ 0, \quad 'I' \nexists NCb(i) \end{cases}$$

$$y = \begin{cases} f('Y'), 'Y' \exists NCb(i) \\ 0, \quad 'Y' \nexists NCb(i) \end{cases}, \quad j = \begin{cases} f('J'), 'J' \exists NCb(i) \\ 0, \quad 'J' \nexists NCb(i) \end{cases}$$

$$z = \begin{cases} f('Z'), 'Z' \exists NCb(i) \\ 0, \quad 'Z' \nexists NCb(i) \end{cases}, \quad k = \begin{cases} f('K'), 'K' \exists NCb(i) \\ 0, \quad 'K' \nexists NCb(i) \end{cases}$$

where: i, j, k - are coordinates of interpolation circle center
a - is length of chord that matching to arc of a circle at circular interpolation
b - is radius of circular interpolation
α - is central angle that matching to arc of a circle at circular interpolation

Angle α obtained on this way has two different values: $\alpha_1 \leq 180°$ and $\alpha_2 > 180°$. To find right value of angle α it is necessary to examine relation between values x, y, z and i, j, k. For example, determining of right value of angle α for function G91 in plane XY is shown in fig.2.

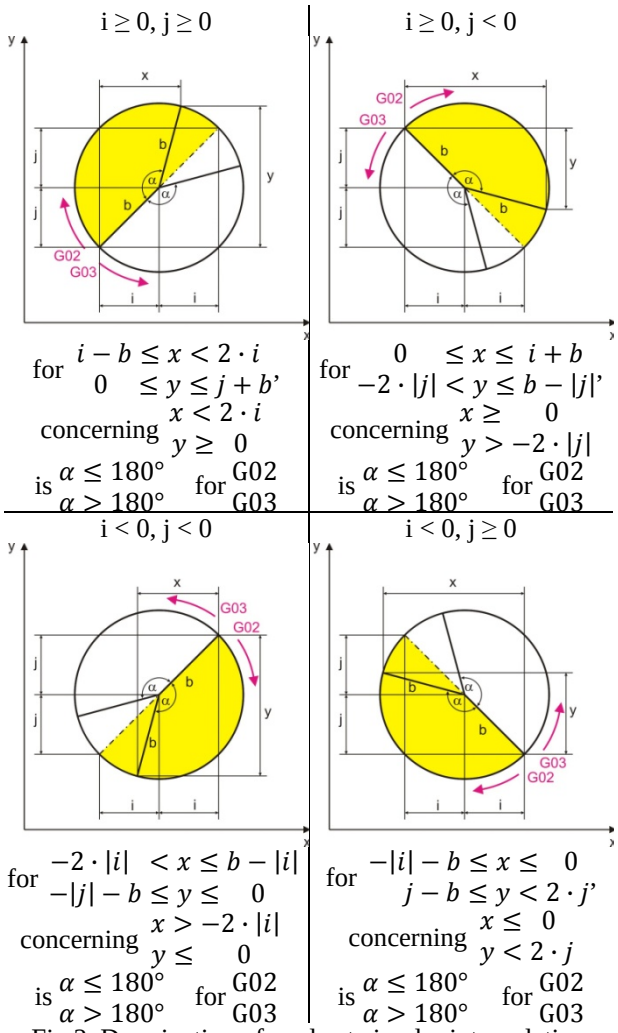

Fig.2. Dermination of angle at circular interpolation

Table feed during machining time in one program block is calculating in accordance with values of cutting feed and spindle speed or just value of cutting feed is located in same program block or in preceding program blocks depending on writing feed in milimeters per revolution (G95) or milimeters per minute (G94) for G21, or inches per revolution (G95) or inches per minute (G94) for G20:

$$v_{obr} = s$$

where:
s - is cutting feed in milimeters or inches per minute (G94)

or: $v_{obr} = s \cdot n$

where:
s - is cutting feed in milimeters or inches per revolution (G95)
n - is spindle speed in revolutions per minute

3.2. Tools and machining regimes

Tools data used in shrinkage are determining according to NC program blocks which contain program word beginning with T and contain functions M06 i M05.

Therefore, tool with number a_{obr} starts with using in program block $NCb(i_1)$ which contains function M06, and stops in program block $NCb(i_0)$ which contains function M05:

$$a_{obr} = f('T'), 'T' \exists\, NCb(i), f(m) \exists\, NCb(i), f(m) = \{M06\}$$
$$i_1 = i, f(m) \exists\, NCb(i), f(m) = \{M06\}$$
$$i_0 = i, f(m) \exists\, NCb(i), f(m) = \{M05\}$$

where:

$f('T')$ - is evaluation of tool no

Value of spindle speed n_{obr} or value of cutting feed s_{obr} is determinate according to NC program blocks which contain program word beginning with S or with F:

$$n_{obr} = f('S'), 'S' \exists\, NCb(i)$$
$$s_{obr} = f('F'), 'F \exists\, NCb(i)$$

where:

$f('S')$ - is evaluation of spindle speed

$f('F')$ - is evaluation of cutting feed

Spindle speed is changing value in program blocks which contain M-functions:

$$n = \begin{cases} n_{obr}, f(m) \exists\, NCb(i), f(m) = \{M03, M04\} \\ 0, \quad f(m) \exists\, NCb(i), f(m) = \{M00, M05, M30\} \end{cases}$$

Cutting feed is changing value in program blocks that contain G-functions:

$$s = \begin{cases} s_{obr}, f(g) \exists\, NCb(i), f(g) = \{G01, G02, G03, G81, \dots\} \\ 0, \quad f(g) \exists\, NCb(i), f(g) = \{G00, G80\} \end{cases}$$

4. USING OF DATA FROM NC PROGRAMS

Every single NC program block $NCb(i)$

N	G	X	Y	Z	I	J	K	R	F	S	T	M

can be transformed into one record of database table with structure shown as:

NCtabela1(N, G, X, Y, Z, ...)

N	G	...	tool no	rapid traverse path	cutting feed path	table feed	time	cutting feed	spindle speed
				mm	mm	mm/min	min	mm/o	o/min

In every record (row) of table NCtabela1(N, G, X, Y, Z,...) according to fields obtained by transformation of data from NC program block (G, X, Y, Z, ...) corresponding fields (path, speed, time, ...) are calculating. According to records of this table there are created records in database tables with structures shown as:

NCprogrami(nazivncprg, vrukuncprg, ...)

NC program name	total time	tools changing time	indexing time	rapid traverse time	cutting feed time
	sec	sec	sec	sec	sec

AlatiRezimi(nazivncprg, oznalncprg, ...)

NC program name	tool no	cutting feed	spindle speed	cutting feed time	cutting feed path
		mm/o	o/min	sec	mm

Every record of the table NCprogrami(nazivncprg, vrukuncprg, ...) corresponds to one NC program, but fields that relate to times are presenting added times for whole program. One record of the table AlatiRezimi (nazivncprg, oznalncprg, ...) corresponds with one tool, one cutting feed and one spindle speed in one NC program.

Therefore, NC programs placed in ASCII files are transforming into database tables. First, every NC program block converts into corresponding record of NC table, then in accordance with fields obtained by transformation of data from NC program block (G, X, Y, Z, ...) corresponding fields (path, speed, time, ...) are calculating. Afterwards, in accordance with records of this table, record of the table that corresponds single NC program is created, but fields that are relating to times are presenting added times for whole program. Records of the table that corresponding with one tool, one cutting feed and one spindle speed in one NC program are filled in simultaneously.

Example:

```
N0010 G21 G40 G80 G90
N0020 M08
N0030 M06 T01
N0040 S1000
N0050 G99 G81 X30 Y30 Z-206 R-200 F0.2 M03
N0060 X170
N0070 Y140
N0080 X30
N0090 G98 X100 Y85 M05
N0100 G80 M09
N0110 G28 Z0
N0120 M06 T02
N0130 S705 M03
N0140 G99 G81 X30 Y30 Z-177 R-150 F0.176 M08
N0150 X170
N0160 Y140
N0170 G98 X30 M05
N0180 G80 M09
N0190 G28 Z0
N0200 M06 T03
N0210 S217 M03
N0220 G99 G81 Z-183 R-175 F0.33 M08
N0230 X170
N0240 Y30
N0250 G98 X30 M05
N0260 G80 M09
N0270 G28 Z0
N0280 M06 T04
N0290 S199 M03
N0300 G99 G82 Z-184 R-160 F0.02 M08
N0310 X170
N0320 Y140
N0330 G98 X30 M05
N0340 G80 M09
⋮
```

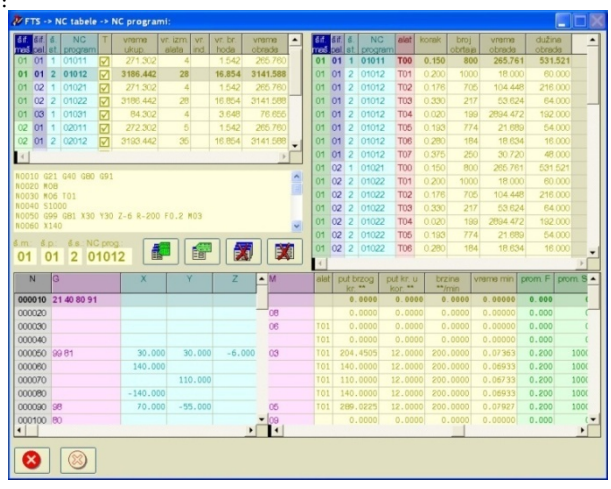

NCtabela1(N, G, X, Y, Z, ...)

N	G	X	Y	Z	I	J	K	R	F	S	T	M	tool no	rapid tra-verse path	cutting feed path	table feed	time	cutting feed	spindle speed
000010	21 40 80 90													0	0		0	0	0
000020												08		0	0		0	0	0
000030											01	06	T01	0	0		0	0	0
000040										1000			T01	0	0		0	0	0
000050	99 81	30	30	-206				-200	0.2			03	T01	204.4505	12	200	0.06341	0.2	1000
000060		170											T01	140	12	200	0.06233	0.2	1000
000070			140										T01	110	12	200	0.06183	0.2	1000
000080		30											T01	140	12	200	0.06233	0.2	1000
000090	98	100	85									05	T01	289.0225	12	200	0.06482	0.2	1000
000100	80											09		0	0		0	0	0
000110	28			0										0	0		0	0	0
000120											02	06	T02	0	0		0	0	0
000130										705		03	T02	0	0		0	0	705
000140	99 81	30	30	-177				-150	0.176			08	T02	174.4276	54	124.08	0.43811	0.176	705
000150		170											T02	140	54	124.08	0.43754	0.176	705
000160			140										T02	110	54	124.08	0.43704	0.176	705
000170	98	30										05	T02	290	54	124.08	0.44004	0.176	705
000180	80											09		0	0		0	0	0
000190	28			0										0	0		0	0	0
000200											03	06	T03	0	0		0	0	0
000210										217		03	T03	0	0		0	0	217
000220	99 81			-183				-175	0.33			08	T03	175	16	71.61	0.22635	0.33	217
000230		170											T03	140	16	71.61	0.22577	0.33	217
000240			30										T03	110	16	71.61	0.22527	0.33	217
000250	98	30										05	T03	315	16	71.61	0.22868	0.33	217
000260	80											09		0	0		0	0	0
000270	28			0										0	0		0	0	0
000280											04	06	T04	0	0		0	0	0
000290										199		03	T04	0	0		0	0	199
000300	99 82			-184				-160	0.02			08	T04	160	48	3.98	12.06297	0.02	199
000310		170											T04	140	48	3.98	12.06263	0.02	199
000320			140										T04	110	48	3.98	12.06213	0.02	199
000330	98	30										05	T04	300	48	3.98	12.0653	0.02	199
000340	80											09		0	0		0	0	0
⋮																			

NCprogrami(nazivncprg, vrukuncprg, ...)

NC program name	total time	tools changing time	indexing time	rapid traverse time	cutting feed time
⋮					
01012	3186.442	28	0	16.854	3141.588
⋮					

AlatiRezimi(nazivncprg, oznalncprg, ...)

NC program name	tool no	cutting feed	spindle speed	cutting feed time	cutting feed path
⋮					
01012	T01	0.2	1000	18	60
01012	T02	0.176	705	104.448	216
01012	T03	0.33	217	53.624	64
01012	T04	0.02	199	2894.472	192
01012	T05	0.193	774	21.689	54
01012	T06	0.28	184	18.634	16
01012	T07	0.375	250	30.72	48
⋮					

5. CONCLUSIONS

According to technological and kinematic parameters of NC program that are transformed into fields of database, calculations or simulation are executing to get parameters for comparison with placed technological demands. If that parameters (total time and/or production costs) are not reached demands, machining regimes and/or tools contained in the database are changing in accordance with placed limits. The procedure is repeating until placed technological demands are reached.

6. REFERENCES

[01] Lukić Lj. – Flexible manufacturing systems – 2007. - Faculty of mechanical engineering Kraljevo

[02] Pusztai J., Sava M. – Computer Numerical Control – 1983. - A Prentice-Hall Company

[03] Sandvik Coromant Catalog – 2008. - www.coromant.sandvik.com

MODEL FOR REVITALIZATION OF INDUSTRIAL MANUFACTURING OF POWER PLANT EQUIPMENT – ABS HOLDINGS CASE STUDY

Z. Radosavljević, Lj. Lukić

Abstract: *ABS Holdings is an international holdings company, which is composed of many factories working in the area of metal processing, electronics, electrical power systems, facilities and equipment. The factories within ABS Holdings develop, design and manufacture electrical power distributive equipment, parts of thermo and hydroelectric plants, realization of projects in the area of industrial automation and electrical power processes. The factories are located in Russia and Serbia, and the company also has offices in other countries within Europe, in countries that are part of the CIS, China and the Middle East. During the past three years ABS Holdings purchased Minel factories in Serbia working in the area of electrical power systems, and made program and organizational changes as well as reengineering of business processes, on the basis of past experiences obtained when privatizing Russian factories in the transitional process. Accomplished results and experiences are observable in the work of ABS Holdings, which had multiple increases in the volume of production, improvement of the quality of products and an achievement of 70 million USD revenue in the year of 2007, with 40% exports.*

Keywords: *Reengineering, business processes, re-vitalization of production systems*

1. INTRODUCTION

ABS Holdings purchased a group of factories with a 50 year tradition and experience in the area of electrical power systems and equipment and which were earlier under the name of Minel and were oriented towards the markets in the ex Yugoslav countries. From the year 2005 to the present ABS Holdings has the following factories and enterprises in its composition (Figure 1):

- ABS Minel Trafo - Mladenovac, a factory producing oil and dry-type distributive transformers,
- ABS Minel EOP - Ripanj, a factory producing a variety of different disconnectors, metal clad switchgear cubicles for substations of different voltage levels,
- ABS Minel Fepo - Zrenjanin, a factory producing line separation, low voltage facilities for substations, insulators, current and measurement transformers,
- ABS Minel Elektrogradnja i dalekovodi - Belgrade, enterprise for project development and construction of overhead lines and infrastructural electrical power facilities,
- ABS Minel Kontaktne mreže - Belgrade, enterprise for project development and construction of traction switchgear on rail and city traffic electrical routes,
- ABS Minel Projektinženjering - Belgrade, enterprise for project development for electro-distributive system facilities and investing into electric power system industrial facilities.

When privatizing these factories, it was necessary to reengineer business processes (BPR - Business Process Reengineering) individually in each of these factories, and at the same time integrate production processes into one single system. As a cause of the situation in our industrial sector before privatization, all of the enterprises in Minel were in bad shape in all the business processes. Which is why most of the business processes had to be "begun from the same beginning" and attempt to make the business activities unwind in a more efficient process then was done before.
Reengineering of business processes has taken a fundamental and radical redesign of business processes in order to achieve better results, reduction in costs, higher performance quality products, efficiency and productivity in production and services, as well as entering foreign markets and to be competitive with leading global companies (Siemens, ABB, Schneider Electric, Arewa, etc.).

Zoran Radosavljević, MBc.Mech.Eng., general manager ABS Holdings, Beograd, zradosavljevic@abs-beograd.co.yu,
Prof. Ljubomir Lukić, Ph.D.Mech.Eng., Faculty of Mechanical Engineering Kraljevo, lukic.lj@mfkv.kg.ac.yu.

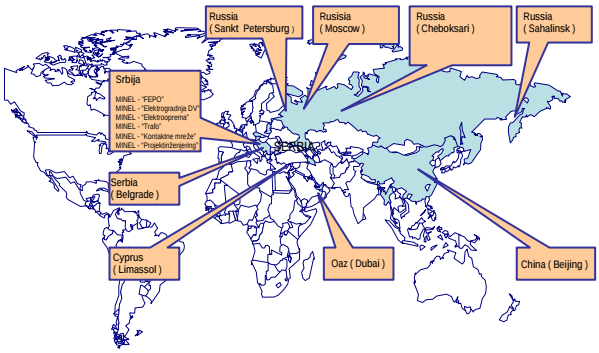

Figure 1. ABS Holdings – largest Serbian energetic global company

Reengineering is a process that is implemented in order to change the organizational culture, create new processes, form new structures and achieve general success of ABS Holdings, which has the goal to become the leading company in the region of its activity. The basic activities that are carried out, are related to the orientation towards the processes, of changing the approach and implementation of creativity and ingenuity in solving problems, drastic changes in the mode of realization of certain job activities, reorganization and redesign of business processes and a business concept on the centralization of business functions.

2. GENERAL CHARACTERISTICS OF INDUSTRIAL PRODUCTION OF ELECTRICAL POWER FACILITIES UNDER CONDITIONS OF PRE-PRIVATIZATION

Industrial production (Figure 2, Figure 3) of equipment and facilities relies on the developmental investment program of the electrical industry and electro-distributive systems as the paramount infrastructural industrial resource of every country. In the past two decades the price of electrical energy was a social category, industry under sanctions and the geopolitical relations affected not only the absence of investment projects of construction and modernization in the area of manufacturing and distributing electrical energy, but also the absence of minimal necessary funds for liquidity maintenance. Under such conditions the volume of production in Minel factories was reduced to a minimum, with a high amount of workers on a temporary vacation, reduction of work engagement and complete stagnation in the area of development of products and achievement of new production technologies compared to competing companies.
Industrial production of electrical power systems under our conditions in the last 20 years has certain general characteristics:

Figure 2. Distributive transformers with conservers

- All products after the year 2000 were at their expiration date, even though their working life (Figure 4), compared to other industrial products, is very long (from 30 to 50 years of exploitation).
- The commencement of manufacturing was five decades ago on the basis of initial partnership relations with then famous world manufacturers (Sprecher, Magrini, Schneider, Siemens itd.), but there was no organization of development that would one day be crucial to lead the company into further modernization and development of products with high quality characteristics.

Figure 3. High voltage demountable aparatus (Disconnectors)

- The organization of production and factory infrastructure was designed for a large amount of workers and high production capacity, which takes into account high fixed costs and which doesn't have flexibility in the conditions of a reduced production volume, reduced domestic market, and changed industrial economic conditions.

- Total inability of entering foreign markets as a cause of lack of competitiveness, inability to offer complete solutions and non existence of necessary certificates and attests for equipment with evidence for fulfillment of conditions required by standards and regulations of certain countries.
- General state of the personnel, which are barely adequate (a large amount at the end of their working life, lacking working condition and without necessary knowledge of contemporary methods of work and the use of contemporary information technology in business management, development of products and technologies).
- The work environment is in a very bad state, after years of no investments and adequate maintenance.

Figure 4. Overhead high voltage lines and aerial towers and aerial systems

The technological and financial state in the electrical power factories in the past years has been very bad. Large debts, debts to suppliers, unsettled legal duties, and lack of liquidity have made consolidation a difficult task for the future owner.

3. PHASES OF REENGINEERING OF BUSINESS PROCESSES IN ABS HOLDINGS

The reengineering of business processes in the last three years was present in all areas of business, but most of the reengineering was focused on a couple of most important business functions:

- The reform of the legal regulations, normative acts, creation of branches of management, top management and medium level managers,
- Optimization of personnel resources and creation of a new work environment, work atmosphere, work discipline, creation of new company logos, installment of a new internal and external work space, creation of an independent security service, and organizational changes,
- Reengineering and radical strengthening of the market function,
- Reengineering in the area of the development of products and technologies (Figure 5):,
- Reengineering of technological processes in the area of production of transformers, metal clad switchgear, disconnector systems, electrical power equipment, installment of overhead lines and traction switchgear.

Successful business today is based upon good organization of market onset, directing the company development to the demands of the customers, complementing the offer with systematic technical offers, monitoring the activity of the competition and constant initialization of development projects according to contemporary world trends, current scientific and technological advances (Figure 6, Figure 7). With that goal in mind ABS Holdings directed its activities in the following ways:

Figure 5. Construction of railway track

- Centralization of the market function in the shape of forming a sector for system sales, composed of experienced engineers who know the market needs, customer needs, functional characteristics of the products and system project solutions.

- Orientation of the system sales sector into three groups of engineers with the following functions: contact and doing business with customers, preparation of offers – tendering groups and a group of project managers which manages and organizes the realization of negotiated contracts.
- Development of cooperation with the most famous world manufactures of complementary equipment, such as Siemens, ABB, Schneider Electric and others.
- Entering the Russian market and market of CIS states in cooperation with the factories, institutes and business units of ABS Holdings in Russia.
- Entering with offers the markets of electrical power equipment in Europe, the Middle East, and African countries.
- Formation of a network of representative offices and authorized agents in countries and regions which might become a potential market for the placement of the products and services offered by ABS Holdings, accessing those markets through technical fair manifestations in those regions.

Figure 6. Energetic systems for transport

The Minel factories which are today within the composition of ABS Holdings had a total annual revenue of around 5 million USD in 2005, as well as the last working year before the privatization. With centralization, strengthening and contemporary organization of the market function the products and services offered by the factories in 2007 had more than 70 million USD in revenue. With a realistic plan, even with all the difficulties, the company plans to achieve in the next year 100 million USD in revenue (Figure 8).

Figure 7. Medium and high voltage measurement transformers and conducting insulators

With the liberalization, the placement of the electrical power equipment on the domestic market met fierce competition with famous world manufacturers, which is why it was necessary to restore the activity of development of the products and technologies according to the demands of the market and the company's technological capabilities. Reengineering in the area of development was composed of the following activities:

Figure 8. Production coils of transformers

- Formation of a list of strategic company products and the formation of a unique coordinating working body for strategy planning and development of products, which researches market needs for certain products, their characteristics and functional requirements, the state of competition, price, legal acts in the area of ecology, security and other important questions for orientation of certain products (Figure 9).
- Formation of design teams, for every strategic product, which have the function of development, creation of project construction documentation,

designing technologies, and their certification in accredited laboratories by European accrediting bodies.

Figure 9. Metal- arrmoured demountable plants

- ntroduction of unique CAD/CAM methods of integrated designing of products and technologies using software packages in the area of electric designing Eplan Pro8, in the area of mechanical designing Solid Works and other software packages in the area of building designing, designing of metal constructions and overhead lines.
- Creating procedures for testing the quality of products and their certification in accredited laboratories in Krajovi (Romania) for the fulfillment of all functional requirements according to the IEC, GOST and other standards.
- Development of new products which are competitive with world brands: transformers with lowered losses, transformers with coils cast in epoxy materials, disconnectors with contemporary construction with polymer insulators, cells with structural parts developed on the modular design basis, adapted for production using programmable laser systems or automated punch presses, innovative design of measurement and current transformers, insulators with passage for a conductor, line separation and other products.
- Capturing specialized modular components of metal clad gear, which today are now bought from competitive companies (Siemens, ABB) – breaker systems and protection of relays with microprocessor control systems, development solutions, which will allow for technological independence and possibility for own solutions and complete products.
- Organization of specialized sectors for designing and development of projects for realization of electrical power systems, facilities and equipment as well as complete investment into infrastructural facilities, for support to the system sales sector and project engineering function in factories in the composition of ABS Holdings.

High quality of equipment in ABS Holdings in large is achieved thanks to the formation and revitalization of the laboratories for high voltage and other testing, in order to verify prototype solutions and previous characteristics of the quality of products before systematic testing in accredited laboratories. (Figure 10).

Figure 10. Laboratory for high voltage testing

Three factories within ABS Holdings manufacture completely different products (transformers, disconnectors and metal clad switchgear), but almost all have identical machine tools in machining, for metal deformation and metal cutting processes. The factories do not have a complete level of employment with these capacities, so an optimization of the technological operations was performed, in order to make production more economical.

- Manufacturing is specialized in the domain of transformer sheets and is done in the factory Minel Trafo in Mladenovac, epoxy materials casting in the factory Minel Fepo in Zrenjanin (Figure 11), and sheet refinement in the factory Minel EOP in Ripanj.
- The system of intermediate goods acquisition is centralized for all factories, in order to join all the orders and order directly from the producers this way cutting costs of materials.
- Installment of a unique system of marking and classification of materials, components and products in all factories, in order to create conditions for optimal planning and production management.
- Application of a unique system of creating product documentation and normalization of technological

operations with the “full-cost” system of monitoring production costs.

Figure 11. Technological line for preparation of mass and preasure casting of epoxy resin

The company has completed projects for the modernization of the product technological system for the automated production of magnetic cores, coils and parts of the transformer casing, for the automated creation of metal clad equipment and breakers, as well as installing contemporary machine with microprocessors. With this investment project costs of production are significantly reduced, achievement of high product quality and the increase of the overall production capacity of the factory of transformers and electrical equipment.

4. CONCLUSION

Reengineering of business processes was necessary in the Minel privatized factories in the area of production of transformers and electrical power systems in order to meet the demands of the customers, also because of more and more existence of competition, both on the domestic and international market. Implementation of processual and team organizational ingenuity and flexible structure, with multifunctional teams (the same people are used on different projects).

Every member of ABS Holdings had to change, restructure, reorganize and redesign. With the reengineering of business processes, a more competitive company was achieved, with the chief orientation towards the demands of the customers.

Reengineering led to the creation of conditions for the enlargement of the company in the area of complementary products program, cooperation with colleges, scientific research organizations, and world famous companies in the area of energetics. Successful establishment of research and development projects in the area of micro-controllers and microprocessor relay protection for in house purposes. Increasing tendency to form a scientific research institute within ABS Holdings.

REFERENCES

[1] Z. Radosavljević: Reengineering of Business Processes of Privatized Factories of Electrical Power Substations - By Example ABS Holdings, 34th JUPITER Conference, Belgrade (2008), CD medium.

[2] Z. Radosavljević: Metodologija CAD projektovanja familije obrtnih stolova, Magistarski rad, Mašinski fakultet, Beograd, 1997. .

[3] Z. Radosavljević i grupa saradnika: Investicioni elaborat o modernizaciji tehnološke linije za proizvodnju transformatora u fabrici ABS Minel Trafo Mladenovac, ABS Holdings Beograd, 2008.

[4] Lj. Lukić, Z. Andjelković: CIM systems - Example of the developped solution implemented in industrial conditions, Preliminary paper, Proc. 8th International Conference on Flexible Technologies MMA 2003, Novi Sad (2003), pp.173-174 & CD ROM.

[5] Lj. Lukić, M. Gašić, R. Rakanović, N. Nedić, V.Karamarković, Lj. Djordjević: Application of Up-to-date Information Technologies in Revitalizing of Production Systems, Plenary paper, Proc. 5th International Conference "Heavy Machinery HM2005", Kraljevo-Mataruška banja, 20.06.-03.07.2005. pp.P1-P6.

[6] Lj. Lukić, S. Ivanović: Studija izvodljivosti za osnivanje naučno-tehnoloških parkova u Srbiji - potprojekat "Razvoj tehnološkog inkubatora Kraljevo" Projekat TR-7026A, Mašinski fakultet Kraljevo - Ministarstvo nauke i zaštite životne sredine, 2005-2006.

THE LASER ADJUSTMENT METHOD ALIGNMENT OF DRIVE SHAFTS IN OPEN PIT „KOLUBARA"

M. Dukanac, B. Nikolić, R. Spasojević, B. Sekularac

Abstract: *In this paper is described the maintenance function as an integral part of the production system. Perfect alignment of machinery shafts is crucial in preventing premature bearing failures, shafts fatigue, sealing problems and vibrations. It further reduces the risk of over-heating. The SKF Shaft Alignment Tool TMEA 1 offers an easy and accurate way for the adjustment of two units of rotating machinery.*

Key words: *Maintenance, reliability, alignment*

1. INTRODUCTION

Since the year 2003, the project of preventive maintenance of essential machine assemblies in open pit „Kolubara" has been conducted supported by the laboratory service for measurements and examinations in the company „Kolubara-Metal". Elementary method of this maintenance is vibrodiagnostic measurements of the parameters of machines condition with two elementary corrective methods:
1.Dynamic balancing in own bearings in one or two correcting planes without dismounting of the rotor, clutch etc.
2.Adjustment of alignment of shafts.
The second method has especially given important results concerning reliability of drive unit, which is the main issue of this work.
Operation and reliability of a machine mostly depends on how has the problem of alignment of shafts been solved.Misaligned shafts create moment which further leads to appearance of additional reactions in their supports(bearings)-in driving as well as in operating unit. Loud increase by 20 % reduces life-time of bearings for almost 50 % . If loud rises by 100 % , life-time will be equal to 15 % of the anticipated. Failure of bearings makes:

- potential failure of other parts of machine
- costs of replacement
- costs of new bearing
- costs of break-period in work.

Other serious consequence of misalignment is wearing and failure of gaskets, that increases possibility of additional failures of bearings because of dirt penetration into the bearing and/or leaking out of bearing lubricant.
Misaligned shafts can causes:

- load on bearing increase
- bearing life-time decrease
- gaskets wearing increase
- vibration and noise increase
- consumption of energy increase.

All of that can be avoided by the adjustment of alignment of shafts. Misaligned machines consume more energy. Thus alignment of shafts produces energy savings of 3 % to 8 % (by some sources even 15 %).

- drive of electric pump in thermal plant „Kolubara" (1MW, 380V), after aligning current intensity is reduced from 450A to 430A

$$\Delta P = U \cdot I \cdot \sqrt{3} \cdot \cos\varphi = 380V \cdot 20A \cdot \sqrt{3} \cdot 0{,}92 = 12kW$$

Annual saving = 12kW · 3 din/kWh · 24h · 350 days = 302400 din.
Economic aspect of regular adjustment of alignment is even more important because of material savings (bearings, ring seals, windings) and the decrease of duration of break-period in work.

2. ADJUSTMENT OF ALIGNMENT OF SHAFTS – MANNERS AND RECCOMENDATIONS

One should know that about 50 % failures on the rotary machines are appearing because of misalignment. That is why adjustment of alignment is very important. A good alignment means larger production scope and smaller maintenance costs. When misaligned shafts are connected (picture 1), they are exposed to additional load which is further transmited on the bearings, ring seals and clutch itself – additional radial and axial forces also appear.

mr Milun Dukanac, dipl.maš.inž., Kolubara Metal, Vreoci, milun.dukanac@gmail.com, labcrv@absolutok.net
mr Branko Nikolić, dipl.maš.inž., Kolubara Metal, Vreoci
Rajko Spasojević, dipl.el.inž., Kolubara Metal, Vreoci
Bojan Šekularac, dipl.maš.inž., Kolubara Metal, Vreoci

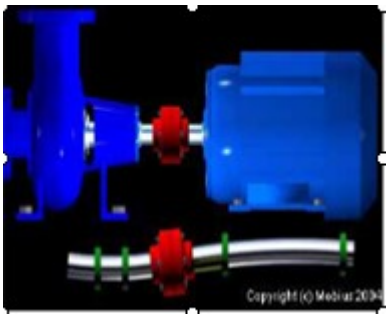

Picture 1 – Misaligned shafts connection

Before the beginning of aligning of shafts, one should:

- Establish tolerance in which the machine should be brought (on the basis of producer recommendations or number of revolutions of machine)
- Establish whether the temperature correction by height is necessary
- Establish how big axial clearance at clutch is needed.

Alignment is always done when a new drive installation is in process, a machine after repair is being returned and when misalignment is consolidated. Disregarding method used for alignment of shafts (comparators or lasers), what we want to measure is a parallel and angular misalignment in the middle of the clutch. On the basis of measured misalignment we want to get values which will inform us how to correct footstep (foundation) of movable machine. This complete calculation is based upon a unique mathematical principle- the similitude of triangles. Tolerances of alignment depend on:

- typ of clutch
- distance between machines
- number of revolution.

Tolerances for adjustment of alignment are the most frequently provided by producer or, if that result is unknown, on the basis of speed of rotation machine(Picture 2).

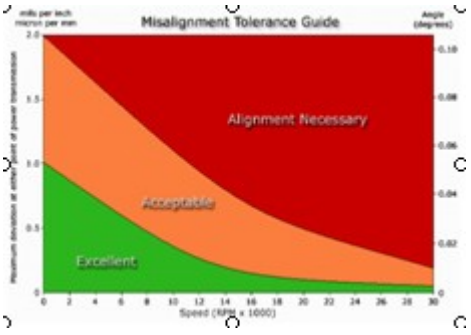

Picture 2 – Misalignment Tolerance Guide

3. LASER ALIGNMENT – PRINCIPLES OF WORK, RESULTS

Vibrations which are being generated because of rotary motion misaligned shafts produce failures on the machine but also on nearby machines. It is so called „Brinel“effect- a machine which is indirectly exposed to vibrations while it is not at work, after putting into operation fails. There are more types of misalignment:

- parallel misalignment (picture 3a)
  - horizontal
  - vertical
- angular misalignment (picture 3b)
  - horizontal
  - vertical
- combined misalignment (the most frequent in practice).

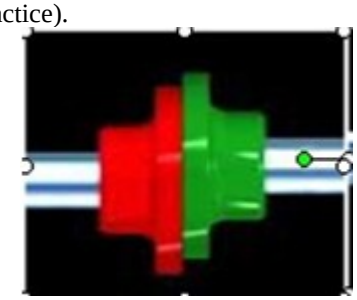

Picture 3a- Parallel misalignment

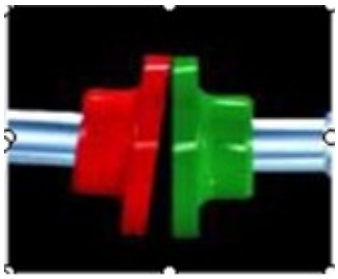

Picture 3b – Angular misalignment

The best manner for quantitative determination of misalignment is to establish values of parallel and angular misalignment on the place of power transmission (center of the clutch).
When aligning shafts, we use four values:

- vertical movement-Vδ
- vertical angle-Vα
- horizontal movement-Hδ
- horizontal angle-Hα

Precision adjustment of alignment in space requires application of complex techniques and tools. Modern method which gives the best results is laser method of alignment of shafts (picture 4). In the company „Kolubara-Metal“ it is used for alignment of machine assemblies of big power and dimensions (generating groups, belt drives on the bucket wheel excavators, pump stations in thermal plants and thermal power plants etc.) on whose regular function depend successful work of the whole installations. Laser device for adjustment of alignment consists of two basic elements:

1. A laser with reflexive prism
2. A pair of laser beam transmitters and receivers(photo-sensitive sensor-for one or two directions).

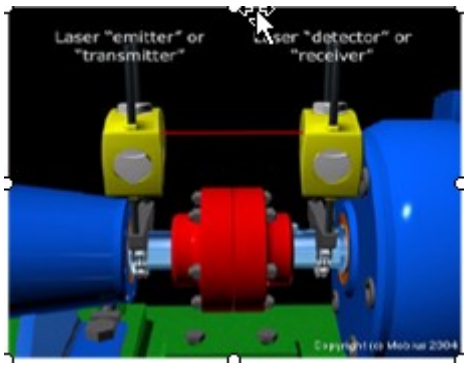

Picture 4 –Laser adjustment method alignment of shafts

In the company „Kolubara-Metal“ application of a good organized program for regular adjustment of alignment of shafts, especially at critical machines, means real costs decrease. Life-time of bearings and gaskets, on vibrodiagnostic monitoring the state over years, is considerably longer. The other effects are also present such as vibrations, noise and consumption of energy decrease. Measuring modules are being set on adjacent ends of shafts one opposite the other, on distance up-to one metre. Measuring modules have the possibility of laser beam simultaneous emission (power 1 mW) and reception through a surface sensor element. We can identify value of angular and parallel deviation of shafts from alignment by measuring in three positions (9, 3 and 12 hours). Necessary corrections of position of movable shaft are calculated automaticly in the processor unit, and the results are shown on its display with accuracy of 0, 01mm.

In the laboratory service for measurements and examinations in the company „Kolubara-Metal“ device TMEA 1 (producer SKF) (Picture 5) is used for adjustment of alignment, and it has given exceptionaly good results in practice, especially in adjustment of alignment of machines of big power.

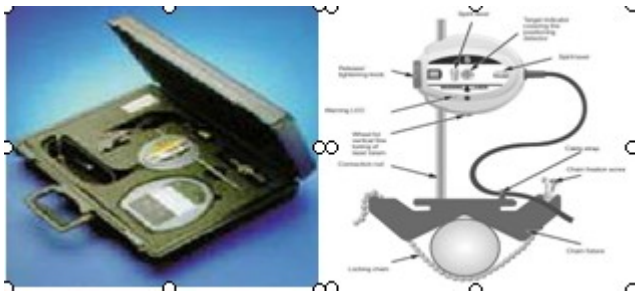

Considering the fact that this corrective method is of essential significance for work plant, a whole bunch of different type devices for laser alignment (more producers) has appeared lately. Method of laser adjustment of alignment is always used when investment repair of mining machines in open pit „Kolubara“ is being done (Picture 6), on all important assemblies, and also after establishing misalignment by monitoring machines condition by vibro-diagnostic methods and thermovision.

Picture 6 – Bucket wheel excavator

4. CONCLUSION

The main reasons for alignment of machine assemblies shafts are:

- productivity increase
- costs decrease
- quality increase.

Transmiting to preventive maintenance, which is applied by the Laboratory service in the company „Kolubara-Metal“ on all essential excavator assemblies (electric motor-gear box) in open pit „Kolubara“, and whose main corrective measure is the alignment of drive shafts, has given significant results which are mainly seen through break-period decrease and spare parts use decrease. According to the data received from machines condition monitoring device, the number of failures of bearings on regularly aligned drives has decreased by 30 % in the last two years. Also, in the year 2007, the number of break-period hours on machine assemblies of bucket wheel excavators has decreased by 15 %. Considering the fact that all coal excavation systems in „MB Kolubara“ work continually 24 hours a day, the savings are considerable with all the elements of preventive maintenance. That shows that the project of machine assemblies maintenance by corrective methods, the most important being the adjustment of alignment of shafts, gives very good results in practice. The Laboratory service for measurements and examinations in the company „Kolubara-Metal“ has performed over 80 adjustments of alignment on more than 30 mining machines during the year 2007, which has considerably upgraded the maintenance system and the driving reliability of machines.

LITERATURE

[1] Adamović Ž. „The Maintenance technology“ – The University of Novi Sad, Novi Sad, 1998

[2] Šiniković G. „ The Methods of technical diagnostics“, Postgraduatal thesis – The Faculty of Mechanical Engineering, Belgrade, 2006, 140 pages

[3] Pešić A. „ The Monitoring and diagnostics of the machine systems working ability“, Graduatal thesis- The Faculty of Mechanical Engineering, Niš, 2002

[4] Pešić A. „ The Monitoring and diagnostics of the machine systems working ability“, Graduatal thesis- The Faculty of Mechanical Engineering, Niš, 2002

[5] Papić Lj. „ The Mathematical processing of experimental results of measurements and examinations“, Čačak, 2004, 18 pages

AUTOMATIZATION OF CONTROLING FUNCTIONS THE DRIVE SYSTEM OF PRESS ECCENTRIC WITH CONVENTIONAL DIRECTION

R. Slavković, I. Milicević, M. Popović, N. Bošković

Abstract: *In current industry processing the metal of machine tools with conventional directions is necessary to fulfill adequate technical-technological changes in order to improve their productive features. Some of these changes require automatization of controlling features, so the maximum effects regarding the service features should be achieved. This paper described changes in controlling modulus of system the compress of eccentric press, made 35 years ago (image 1.1), using the PLC controller.*

Key words: *Control, Programmable Logic Controller, Eccentar Press, Compress*

1. INTRODUCTION

The great number of made parts are done on eccentric press from the fragment made parts, during the one working cycle. Press operator should put prepared parts into tool and activate single press work. In this situation process of activating is led out with two buttons, so the both operator hands are on the buttons, from the safety reasons, and probability that hand can be put in working zone during the working cycle is obstructed.

Figure 1.1: Press Eccenter Q=500 KN with conventional control

However operators idea to press one button with something and with one hand to put prepared elements , it is faster and easier option, is not safe and must be neutralized.
This problem is solved: press can not be activated if the both buttons are underground pressed, or between two pressing, the first and the second buttons doesn't pass more than 500 ms. Press is stopped when compress finish one cycle, apart the state of buttons.
To start new cycle, operator should dismisses both buttons and within new pressing in appropriate described manner activate it again.

2. DRIVE SYSTEM, ITS WORKING AND PLC APPLIANCE

Electromotor as machinery of flywheel of press inaugurated is with one switch that is during the work, always turned on. Within compress motion (pivoting the press shaft) we direct with electromagnet friction staple. Staple as executive element is activated with electromagnet, when he is under pressure can activate friction part of staple and so rotary motor momentum that's mean kinetic energy of flywheel is transferred to the shaft, and than to eccentric ring and bouillon and finally to press compress (Fig. 2.1).

Prof. Radomir Slavković, Ph. D., B. Sc. Mechanical Eng., Technical Faculty, Čačak
Ivan Milićević, M. Sc., B. Sc. Mechanical Eng., Technical Faculty, Čačak
Marko Popović, M. Sc., B. Sc. Mechanical Eng., Technical Faculty, Čacak
Nikola Bošković, B. Sc. Mechatronic Eng.

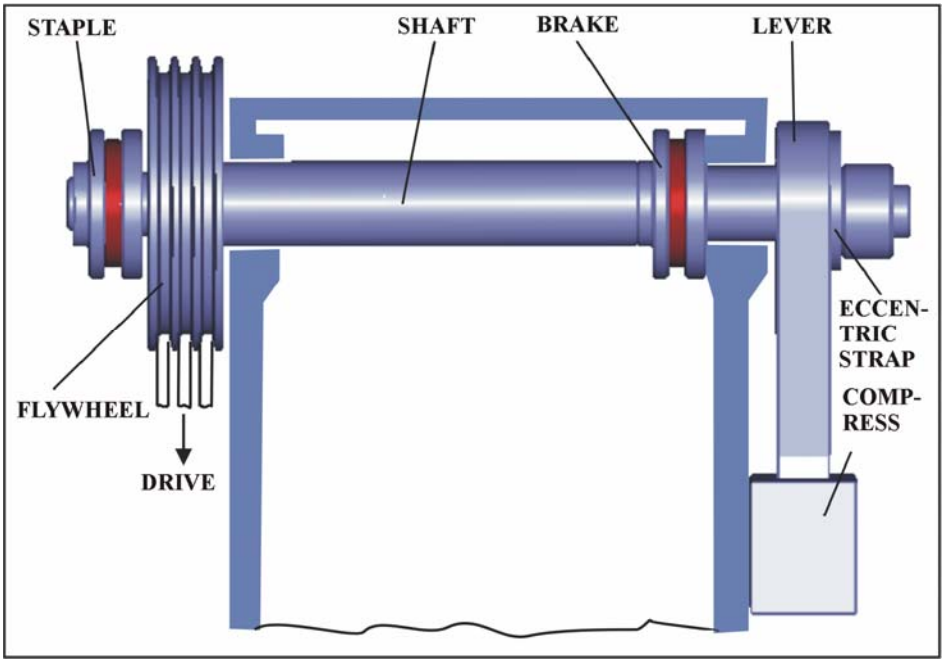

Figure 2.1: Executive component of the drive system the eccentric press compress

Considering the machine process of eccentric press, signal to direct the electromagnet staple is formed according to state of both buttons and to compress position. For identification upper limiter position of compress is used limiter switch, in normal position, he is opened. In terminal upper position of compress when the electromagnet staple is activated limiter switch is closed. In this example input signals to **PLC** are:

- Signal from the button of left hand (**Taster1**)
- Signal from the button of right hand (**Taster2**)
- Signal from the upper limiter switch (**Gp**)

Just one signal is output, and carries one-bit information for command the electromagnet staple, so signal must be connected within one-bit modulus. Issue line has also joined address and mnemonic marker (**Spojnica**). Scheme of the conjunction the input and output modulus with signals donors and executive element – Staple is given on Fig. 2.2.

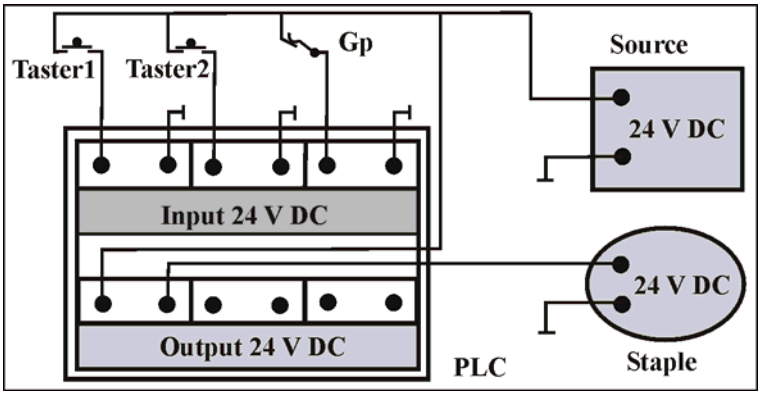

Figure 2.2: Schema of the conjunction the input, output modulus of PLC with signal donors and actuator of the drive system of the compress of press

3. PROGRAMMING THE PLC

In order to program **PLC** (image 3.1) the work of press should be analyzed over the input and output signals, [1]. For activating the press is necessary that both buttons are pressed in the same time and that upper limiter switch is closed. That's mean that on the input lines **Taster1**(0.00) , **Taster2**(0.02) and **Gp**(0.01) should be binary values 1.Moreover between two pressing the buttons mustn't past more than 500 ms. This condition is fulfilled by pressing the one of two buttons, than the time-counter is activated. Press is activated only if the time-counter didn't measure 500 ms, or if the on the appropriate address is only binary "0".If the resolution of timer is 50 ms, than **SV**=500/50=10.Mnemonic address of dates in which is put timer output is **Tim003**.When the press is activated, compress should do the working cycle, no matter what is the state of timer and buttons. That's mean that parallel with function for activating the press is also reached function of self-preserving.

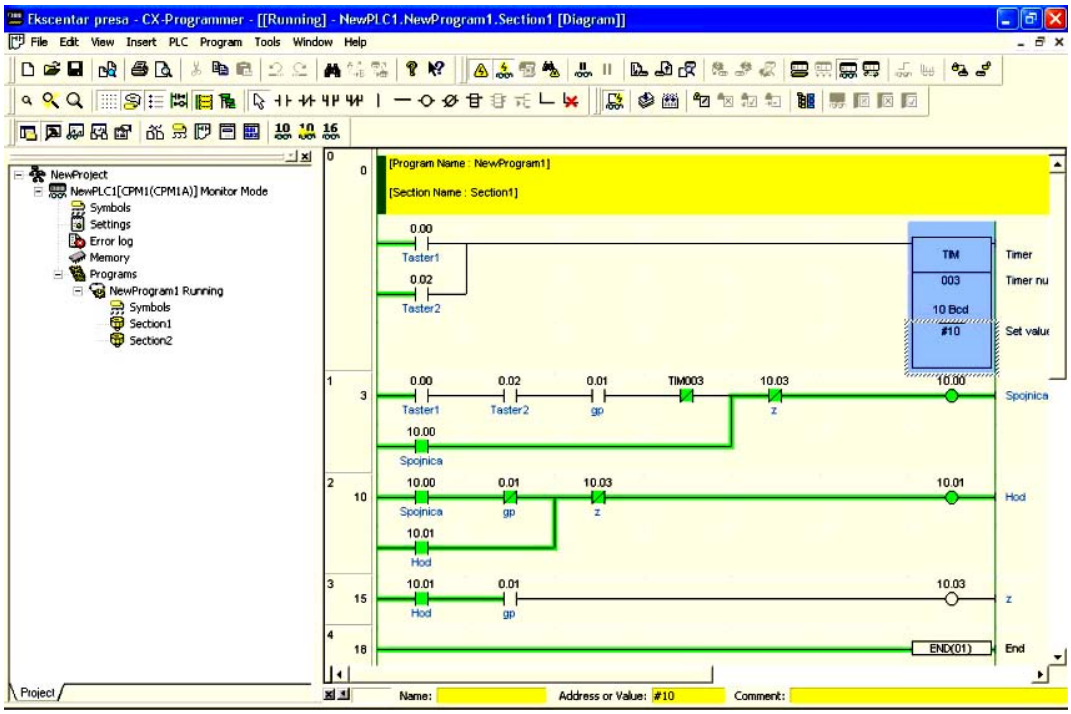

Figure 3.1: Leder diagram direction the moving compress of eccentric press: Software CX-Programmer

After the activating the press (**Gp**) is opened and compress is moving until (**Gp**) is not closed. The state in which is found compress of press is marked with internal variable **Hod** (10.01), which has value 1 during the moving the compress. Finally when compress finished his working cycle (**Gp**) is closed. Considering the (**Gp**) is closed in the moment when compress is starting the working cycle and also finishing it, new variable must be added for indication this condition, that is variable **Z**(10.03) and she takes value 1 in the moment of ending the press motion. Based on these two values deactivated are staple and moving of the compress is stopped, and variable (**Z**) takes value 0. Interface for simulation Leder diagram directing is given on image 3.2, [2], [3].

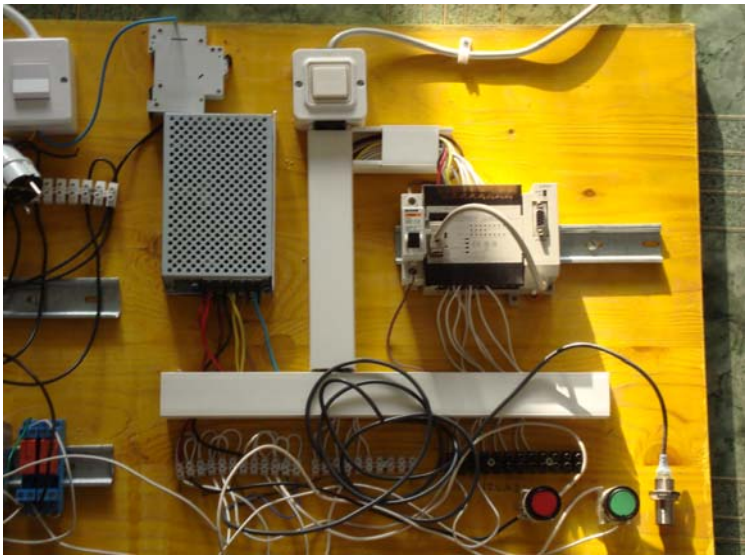

Figure 3.2: Interface for simulation Leder diagram directing, with Omron CPM1-A PLC, [4]

The first line of instructions: define logical condition for starting the timer. Timer is beginning with work when (**Taster1**) or (**Taster2**) gets value 1, before that, and for the time less than 500 ms **Tim003** has value binary 0. If the pressed button **Taster1** or **Taster2** is discharged, before the other button is pressed, timer is stopping his work and is resetting the measured time to zero. If between pressing the two buttons past more than 500 ms, timer is giving binary 1, and again is getting binary 0 when the both buttons are discharged.

The second line of instruction: define logical condition for activating the staple **Spojnica**(10.00). (**Spojnica)** is getting value 1 only if (**Taster1**) and (**Taster2**) have values 1 (the both buttons are pressed), **Tim003** has value 0 (timer has not measured 500 ms from the moment of closing the one button), (**Gp**) is getting value 1 (upper limiter switch is closed, that is mean that compress is in upper level) and (**Z**) is getting value 0 (finished one moving cycle).When the (**Spojnica**) is activated over the process of self- preserving , parallel branch stays active until the variable (**Z**) gets the value 1 (compress has finished his working cycle) When that variable (**Z**) gets value 1 condition is no longer satisfied.(**Spojnica**) is getting value 0, apropos staple is deactivated and compress is stopped.

The third line of instructions: define the state of moving the compress. Compress is moving, (**Hod)** has value 1 until the (**Spojnica**) has also value 1 (Staple is active).(**Gp**) has value 0 (limiter switch is opened) and (**Z)** has value 0 (is not finished current working cycle).The value of variable (**Hod**) should be put on 0 when the variable (**Z**) gets value 1, independent of other values (self-preserving).

The forth line of instructions : define logical condition for stopping the press.(**Z**) is getting value 1 when the press is in the state of moving (**Hod** has value 1) and when compress is again in upper limitier level, so the upper limiter switch is closed (**Gp** has value 1).When (**Z**) gets the value 1 in the next scening the program, variable (**Spojnica**) and (**Hod**) are getting the values 0, and than (**Z**) is getting the value 0.Eccenter press is ready for new cycle. In the last line of this program is direction for ending the program

4. CONCLUSION

Nowadays in metal-prefabricate industry a lot of machine tools with conventional direction did not improve their own service age , but because of functional outmoded their further use in manufacturing process is non-productive .In that cases with automatization their functions we can make better their technical-technological features, and it has influence on upgrading their manufacturing productivity. From this reason and reason of safety on work in this example is given retro fit-up of drive system the eccenter press **Q= 500 KN, IK ″Guca″, A.D. ″Farmakom″Sabac.**

REFERENCES

[1] Pilipovic, M., Automatization of production processes, Mechanical Faculty of Belgrade, 2006.
[2] Matic, N., Programmable Logical Controllers, MicroElectronic, Belgrade, 2001.
[3] Omron: CX-Programmer User Manual, Version 3.0, Omron, 2002.
[4] Matic, N., PIC Microcontrollers, MicroElectronic, Belgrade, 2003.

NEW DIRECTIVE 2006/42/EC ON MACHINARY - SCOPE

V. Zeljkovic, M. Đapic

Abstract: *This paper[1] points out to the process of introduction the New Machine Directive 2006/42/EC. The differences between the MD 98/37/EC and MD 2006/42/EC are shown in several areas: scope; safety requirements; categories of machinery; Notified Bodies. There are some administrative/technical issue following some supplements / changes introduce by new Machine Directive 2006/42/EC like: Entry into force and transition period; Harmonized Standards; Status of machines in operations. In this paper, the scope of new Directive comparing to existing machine Directive is emphasized.*

Key words: Directives on Machinery, Scope, Safety

1. INTRODUCTION

The occupational safety is varying important industrial and society aspect. The statistical data show the evidence of the injuries, including the fatal injuries, predominantly in the area with higher machinery risk, like: the sawing machines, presses, machinery for underground work, vehicle servicing lifts, machines for lifting the goods and persons, machines for the manufacture of pyrotechnics, and the others [3].

To reduce the potential occupational risks, the European Union have been introducing the technical regulations in the forms of the Directives and Harmonized Standards, imposing the obligation to all the machine manufacturers and users to apply the essential health and safety requirements and to protect the workers from the occupational injuries (Figure 1). In the area of machinery, until now the current Machinery Directive 98/37/EC [2] were applicable. In accordance to some technical achievements and necessary precision and correlation to the other Directives, the new Directive on machinery was adopted.

The new Directive 2006/42/EC on machinery was published on June 9th, 2006, and it came into force on 29th June 2006 [1]. It becomes applicable on 29th December 2009. During the transition period all the states has to take the necessary steps in the national regulations, adequate to the provisions of the new Directive. The new/revised Machinery Directive 2006/42/EC replace the current Machinery Directive 98/37/EC [2]. This replacement and introduction of the new Machinery Directive 2006/42/EC impose certain technical and administrative questions, winches has to be solved in this transient period.

This paper gives short review of the changes in the new Machinery Directive 2006/42/EC, and little wider approach to the extensions in the scope, comparing to the current Machinery Directive 98/37/EC.

2. COMPERING CURRENT AND NEW MACHINARY DIRECTIVES

The two subgroups of activities/adaptations come from the introduction of the new Machinery Directive 2006/42/EC and the replacement of the current Machinery Directive 98/37/EC. This is the technical subgroup and the administrative subgroup.

The administrative activities are mainly pointed to the following questions:

- The transition period and the date when the new Machinery Directive become applicable,
- Legal status of the machines manufactured in accordance to the current Machinery Directive 98/37/EC, after the new Machinery Directive 2006/42/EC become obligatory.
- legal frame for market surveillance proposed by the new Machinery Directive 2006/42/EC

[1] In this paper there are some parts of research framed in project MD 14010 "Development and improvement product conformity assessment infrastructure according to European directives" which is partly finance by Republic Serbia Ministry of science.

Dr Vladimir Zeljkovic, ITN SANU, Belgrade, vladazz@yahoo.com
Dr Mirko Đapic, LOLA Institute, Belgrade, mdjapic@yahoo.com

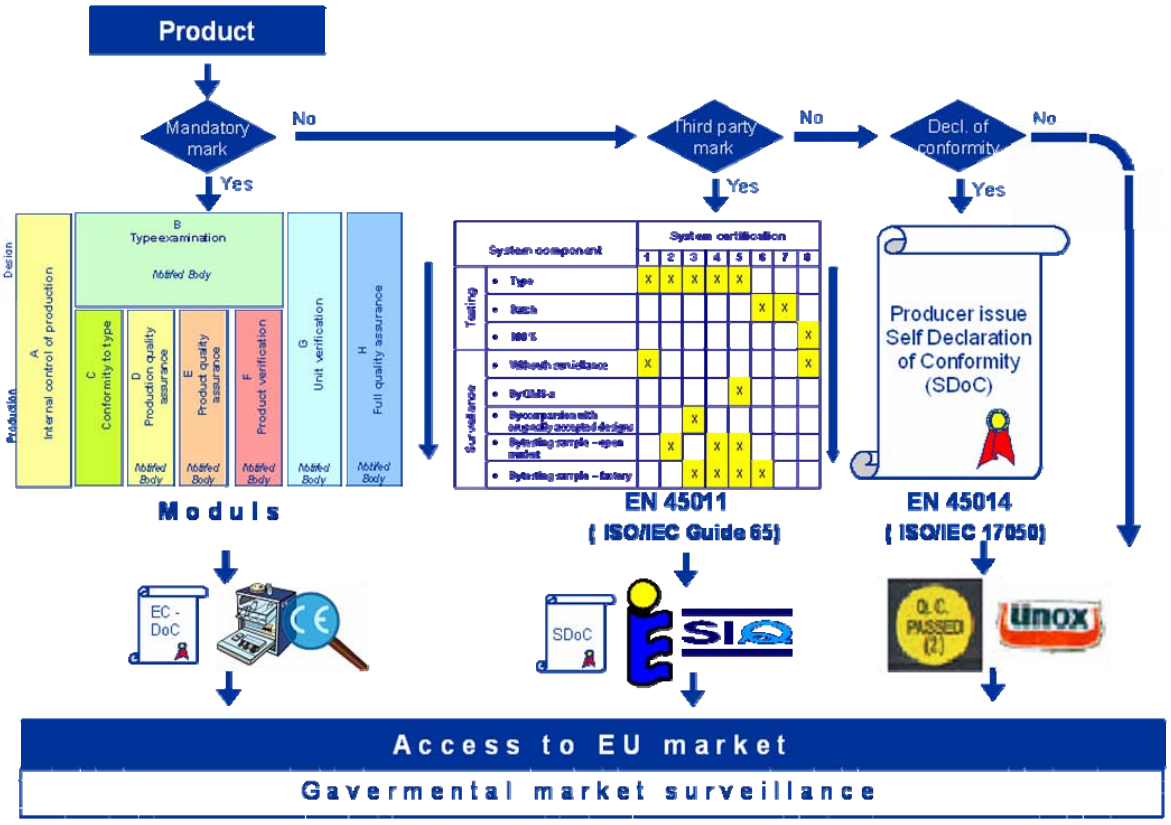

Figure 1. Eoropean approach to product conformity assessment

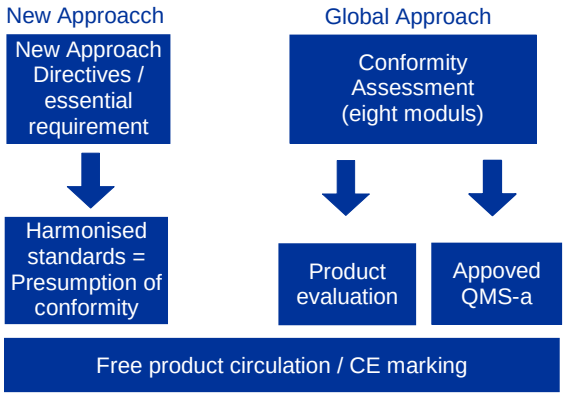

Figure 2. New and Global Approach

- legal frame for the current and the new Notified Bodies proposed by the new Machinery Directive 2006/42/EC

The technical subgroup is mainly pointed to the following segments:

- The scope extension introduces by the new Machinery Directive 2006/42/EC
- The changes/extension of the machines quoted in the Annex IV of the new Machinery Directive 2006/42/EC
- The changes/extension of the safety components quoted in the Annex V of the new Machinery Directive 2006/42/EC
- The essential health and safety requirements relating to the machinery are slightly added
- The conformity assessment procedures prescribed by the new Machinery Directive 2006/42/EC are modified, especially when Harmonized Standards cover the all relevant essential requirements.
- The validity of the current Harmonized Standards prepared in accordance with the current Machinery Directive 98/37/EC and changes to the Harmonized Standards introduced by the new Machinery Directive 2006/42/EC

These extensions/changes introduced by the new Machinery Directive 2006/42/EC in relation to the current Machinery Directive 98/37/EC impose certain number of questions and practical solutions. These solutions are very important to the machine manufacturers and users of the products to be able to adapt all the technical and administrative requirements, and to continue with the cooperation and exports of the machinery to the European market.

3. THE SCOPE DEFINED BY NEW MACHINARY DIRECTIVE 2006/42/EC

The article 1 in the booth Machinery Directives defines the scope. In the following, the summary of the article 1 of the new Machinery Directives MD 2006/42/EC will be quoted:

''1. This Directive applies to the following products:

(a) machinery;

(b) interchangeable equipment;

(c) safety components;

(d) lifting accessories;

(e) chains, ropes and webbing;

(f) removable mechanical transmission devices;

(g) partly completed machinery.

2. The following are excluded from the scope of this Directive:

(a) safety components intended to be used as spare parts ...

(b) specific equipment for use in fairgrounds and ...

(c) machinery ... for nuclear purposes ...

(d) weapons, including firearms;

(e) the following means of transport:

- agricultural and forestry tractors ...

- motor vehicles and trailers ...

- vehicles covered by Directive 2002/24/EC ...

- motor vehicles ... for competitions, and

- means of transport by air, on water and rail ...

(f) seagoing vessels and mobile offshore units and ...

(g) machinery ... for military or police purposes

(h) machinery ... for research purposes for temporary use in laboratories

(i) mine winding gear

(j) machinery ... artistic performances

(k) electric and electronic products ... for use within certain voltage limits:

- household appliances intended for domestic use,

- audio and video equipment,

- information technology equipment,

- ordinary office machinery,

- low-voltage switchgear and control gear,

- electric motors;

(l) the following types of high-voltage electrical equipment:

- switch gear and control gear,

- transformers.''

Comparing the scope of new MD 2006/42/EC and the current Machinery Directive 98/37/EC one can notices the differences. The differences can be grouped into several areas, as:

- The scope of the new Machinery Directive MD 2006/42/EC includes machinery like construction-site hoists, cartridge-operated fixing and other impact machinery. Those machinery where excluded by current Machinery Directive 98/37/EC.
- The overlapping area between the Machinery Directive and Low Voltage Directive is clarified, and the line dividing the scope of MD and LVD is pointed. As quoted in paragraph (k), the Low Voltage Directive covers the list of six categories of electrical machinery. For other electrical machinery, the new Machinery Directive MD 2006/42/EC state the procedure for conformity assessment and placing on the market, while the safety aspects of the electrical risks is under the Low Voltage Directive.
- Also, the line between the Machinery Directive and the Lifts Directive has been clarified. For example, the lifts with a travel speed no greater than 0.15 m/s are subject of the new Machinery Directive and are excluded from the Lifts Directive.
- The specific part of the new Machinery Directive refer to the rang of safety components. The full list of the safety components are given in the Annex V, and include 17 groups of safety components, as:
    1. Guards for removable mechanical transmission devices.
    2. Protective devices designed to detect the presence of persons.
    3. Power-operated interlocking movable guards ...
    4. Logic units to ensure safety functions.
    5. Valves with additional means for failure detection ...

    :

8. Monitoring devices...

:

10. Emergency stop devices

:

12. Energy limiters and...

:

16. Two-hand control devices.

17. Components for machinery designed for lifting ... (a) –(g).

As can be seen, the new Machinery Directives MD 2006/42/EC introduced the four (new) segments defined by scope, as: a) extended machinery list (by construction-site hoist, cartridge-operated fixing and other impact machinery); b) the line between the Machinery Directive and Low Voltage Directive is clarified; c) the borderline between the Machinery Directive and Lifts Directive; and d) the safety components.

4. CONCLUSION

The revised Machinery Directive 2006/42/EC was published on 9th June 2006. This Directive becomes applicable on 29th December 2009. The new/revised Machinery Directive 2006/42/EC replace the current Machinery Directive 98/37/EC. In this transition period, all the required activities has to be done, to provide the smug step from current to new Machinery Directive.

This paper point out certain segments, differences and extensions of the new Machinery Directive comparing to current Machinery Directive. Some technical and administrative aspects are underlined. The scope of the new Machinery Directive MD 2006/42/EC is analyzed in the details.

For ours entities (Institutes, Faculties, and coresponding Ministries), it is very important to follow the technical regulation of European Union. But, particular attention has to be given to the Industries (Machinery, Electro,) in regards to new Machinery Directive. In this way, the necessary condition are fulfilled for the placing our products (machinery) to the come European market.

REFERENCE

[1] Directive 98/37/EC of the European Parliament and of the Council of 22 June 1998 on the approximation of the laws of the Member States relating to machinery, *Official Journal L 207, 23/07/1998 P. 0001 – 0046*

[2] Directive 2006/42/EC of the European Parliament and of the Council of 17 May 2006 on machinery, and amending Directive 95/16/EC *Official Journal of the European Union L 154/24/2006*

[3] Donald Millar: Injuries and amputations resulting from work with mechanical power presses, Current 49, DHHS (NIOSH) Publication No. 87-107, May 22, 1987. P 14.

[4] Djapic, M., Zeljkovic, V., *European Approach to Product Conformity Assessment*, The Fifth International Conference ”Heavy Machinery - HM 2005”, Kraljevo, 28. June – 03 July, 2005., pp (IIC.13 – IIC.17).

[5] TD-7082B (Djapic, M., Zeljkovic, V., and others), *Research, Development and Applications of Methods, Procedures for Testing, Inspections and Certifications Machine Tools in according to Requirement of EU Directives*, LOLA Institute, Belgrade, 2004-2008.

[6] Presern, S. *Notification body obligation*, Project SCG-Quality, Course CA-1, Belgrade, 2005.

[7] Blue Guide, *Guide to Implementation of Directives Based on the New Approach and the Global Approach*, Luxembourg: Office for Official Publications of the European Communities, 2000.

[8] Gundlach, H.C.W., Marks of Conformity for products (discussion paper), EOTC-European Organization for Conformity Assessment, October 1999.

[9] ISO, Certification and related Activities, 1992.

IMPLEMENTING EXTERNAL PROGRAM IN MODULAR PLUGIN ARCHITECTURE FOR MONITORING NUMBER OF CURRENTLY LOGGED-IN USERS IN COMPUTER NETWORKS

G. Vujačić, Lj.Lukić

Abstract: *In this paper we have tried to present one, of many developed, plug-in programs, which monitors number of currently logged in users on a Linux system, using* ***Nagios™ open source*** *package and its interfaces and services, which is primarily used to monitor and control various types of computer networks and configurations. This program package is very flexible and versatile and its quality and usability is by no means lower than other commercial packages present on the market nowadays.*

Key words: *modular architecture, computer networks, Nagios*

1. PREAMBLE

Nowadays, network monitoring systems are primarily used to analyze characteristics and behavior of a physical system in real-time, and to notify subscribed users, (system operators or engineers) about any anomalies or events that have occurred. Those anomalies can be of different kind, importance and origin, and are mainly caused due to errors or system failures. Software solutions that have been used to monitor technically defined systems are on primary, architectural level defined by two key elements or entities:

- Group of sensors which gather all necessary information from systems' key places, and
- Group of work terminal or consoles, which notify operator about anomalies or other events using light or sound effects

Positive characteristics of those systems are manifested through just-in-time notifications about failures or errors. On the other side, main anomalies are reflected through the absence of detailed insight of systems' functioning till the moment of signaled anomaly, and a very small chance of identifying the cause that rendered the system in signaled, malfunctioning state or unusable. It is not possible to determine if the same behavioral pattern has not occurred before, in some discrete period of time, nor what were the exact actions taken to identify and remedy the problem of the signaled type. One of the ways to solve this kind of problem is to use software packages that can monitor and analyze wide scale of systems and network configurations in real time and as portable and resource friendly as possible.
By applying those software packages on real, live system, one can use standard mechanisms of acknowledged reliability which were also used for a long time, and have proven to be simple to maintain, develop and adapt to any kind of distributed system. Knowing that many business users, non-profit organizations, etc. have very limited IT budget, and that many open source solutions are of equal or similar quality as their commercial alternatives, many organizations implement them in order to manage and monitor their network infrastructure. In this paper, we will describe some of the most important characteristics of one open source package, Nagios™. In the second part of the paper, we will present one program solution, implemented as external plug-in for Nagios package.

2. NAGIOS™ FEATURES

As previously stated, Nagios™ is one open source software package of very high quality, which is used to monitor status and availability of network and other system services, resources and components. This package was primarily designed to work on Linux platform, but can be easily ported to other UNIX compatible platforms as well. Program is licensed under the GNU GPL license v2, as published by the Free Software Foundation.

a) Main features

Some most important features of Nagios are:

- monitoring the availability of network services and protocols (PING, DNS, HTTP, SSH, SMTP, POP3, IMAP, etc.),
- monitoring system resources of target hosts (CPU load, RAM memory usage, state of network interfaces, hard disk available space, status of vital processes, etc.),
- simple plug-in concept which enables the user to easily implement and develop its own programs which will be used to monitor specific entities of interest,
- parallel service monitoring,
- finding and leveling hosts which are

mr Goran Vujačić dipl.inž Visoka železnička škola strukovnih studija Beograd,
dr Ljubomir Lukić dipl.inž. Mašinski fakultet Kraljevo

unreachable and hosts which have failed, using embedded concept of parent hosts and device hierarchy,

- the same time as occurring event or service and to determine current status of the network , sent notifications, problem history, log files, etc.,
- simple authorization scheme implemented via the web interface, which can be used to easily manipulate user access rights

b) Modular plug-in architecture

Nagios is based on simple plug-in architecture which main concepts rely on the functional separation of the software package on the core and external programs, which are called plug-ins. The core of the Nagios itself is consisted of one central process, described in program documentation as Nagios Process or Core Logic, which has none of the internal mechanisms to check the status of the monitored objects. Insetad, Nagios core is relying on its plug-in programs to do the entire process of monitoring. This kind of design gives Nagios very high degree of flexibility, and the program itself can be easily integrated with other software packages and modules.
Nagios can also be imagined as the framework for controlling and monitoring the network. In short, the way that Nagios functions can be described in the following way:
Nagios executes plug-in whenever there is a need to check the status of certain service or host that is monitored. Plug-in is then doing its work (here one ought to notice the emphasized phrase) in order to perform a check of the desired entity, and after that sends the results back to Nagios. Received results are processed and needed actions are performed if needed, and defined in the configuration files (event handlers, sending notifications, etc.)

Figure1. shows the separation level between program core and plug-in programs. Nagios executes plug-in programs, which check local or remote resources or services of some kind.

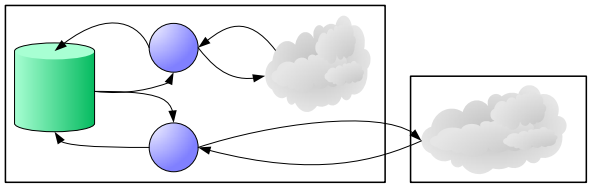

Figure 1. Nagios plug-in architecture

Finally, when plug-in checks are complete and the results of checks are handled to the core, Nagios starts processing them. One positive side of plug-in architecture is that it gives almost unlimited possibilities and ways of implementing monitoring logic. **If the process of monitoring some entity can be automated, it is then possible to monitor such process via Nagios.**

3. REALISATION OF THE PLUG-IN WHICH CHECKS NUMBER OR CURRENT LOGGEDIN USERS

Nagios package comes with certain set of standard plug-in programs, which perform checks of almost all of the usual network services and resources, such as: availability of TCP/UDP ports, CPU load, hard disk space usage, ping response time, state of the SNMP variables, etc. Our goal was to implement the plug-in that can be used to monitor number of users logged in on a Linux terminal server we use at our facility. Plug-in reads the records from utmp file (Linux maintains the data about currently logged in users as a utmp record archive) which is consisted of the array of data about username, name of the virtual terminal, host from which the user has accessed the server, time when session occurred, login shell and PID (process id) of the login process, etc.

Plug-in reads the needed stats, collects the data and handles results to Nagios, which then interprets them and indicates the current state of the entity.

Plug-in can handle 3 arguments from the command line or stdin:

-w, **–warning** <**num_users**>, number of currently logged in users for which the plug-in signals **WARNING** Nagios status
-c, **–critical** <**num_users**>, number of currently logged in users for which the plug-in signals **CRITICAL** Nagios status
-a, **–all**, instructs plug-in to count both network and local users, if this switch is omitted then only network users are counted

In order to use this plug-in we must have ***Python 2.3*** or greater and ***pythonutmp 0.73*** module or greater. The plug-in presened in this paper is simplified version of the plug-in we use on the real monitoring system. Computer system we used to test and implement the program was: Pentium IV 1.8GHz, RAM 512MB, 80 GB hard disk, with Open Suse 9.0 (32bit), with latest Nagios version and its core plugins installed. Python was the language of choice because of its great portability and somewhat object oriented characteristics, as well as its syntax which ensures easy understanding of program logic and features.

Listing 1.1. check_logged_on plugin

```
#!/usr/bin/env python
# This script is put into the public
domain
#
# Ovaj skript implementira Nagios
plugin za proveru
```

```
# korisnika trenutno logovanih na
sistem
# Skript moze da razlikuje mrezne
korisnike
# i lokalne korisnike
import os,sys
import utmp
from UTMPCONST import *
from optparse import OptionParser
#povratne vrednosti koje plugin vraca
u skladu sa statusima servisa
ERROR =
{'OK':0,'WARNING':1,'CRITICAL':2,'UNKN
OWN':3,'DEPENDENT':4}
#funkcija koja vraca proces id, nazive
i hostove logovanih korisnika
def   getLogins():
      urecs = utmp.UtmpRecord()
      logins = [ ]
      pids = [ ]
      for urow in urecs:
         if urow.ut_type ==
      USER_PROCESS:
              if urow.ut_host == "":
                   urow.ut_host =
      "lokal"

      logins.append(urow.ut_user+""+
      urow.ut_host)
              pids.append(urow.ut_pid)
      urecs.endutent()
      return pids,logins
if __name__ == "__main__":
   #opcije za parser predatih
   argumenata
   usage = """
   Ovaj plugin proverava broj trenutno
   logovanih korisnika.
   Plugin moze razlikovati da li su
   korisnici logovani lokalno
   ili preko mreze.\n
   """
   usage += "check_logged_on w
   <broj_korisnika> c <broj_korisnika>
   a"
   version = """%prog 0.95 -
   Copyright(c) 2006 by Goran Vujacic
          ::sungod bless me with your
   rays:::"""
            parser =
OptionParser(usage,version=version)
            parser.add_option("-
w","warning",dest="warnlevel",
              help="Postavlja WARNING
status ako je vise od WARNLEVEL \
                              korisnika
logovano",default=5,type="int")
     parser.add_option("c","-
critical",dest="critlevel",
              help="Postavlja CRITICAL
status ako je vise od CRITLEVEL \
                              korisnika
logovano",default=10,type="int")
     parser.add_option("a","-
all",dest="showall",action="store_true
",
              help="Da li da se
racunaju logovani mrezni ili lokalni i
\
                              mrezni
korisnici zajedno. Ako se ne navede
samo \
                              mrezni se
broje",

default=False)
     (opts,arg) = parser.parse_args()
     if len(sys.argv) == 1:
     print "Koristim podrazumevane
vrednosti w=5,c=10,a=false"
      #predate vrednosti za upozorenje
i kriticni nivo ne smeju biti <= 0
  if opts.warnlevel <= 0:
       parser.error("WARNLEVEL ne sme
biti manji ili jednak nuli")
  if opts.critlevel <= 0:
       parser.error("CRITLEVEL ne sme
biti manji ili jednak nuli")
     (p,l) = getLogins()
  #promenljiva sa brojem logovanih
  korisnika
            count = 0
  if opts.showall == True:
            count = len(l)
  else:
            for i in l:
                  if i.split("")[1]
  != "lokal":
                        count += 1
  # string koji se stampa a sadrzi
  izvestaj o statusu
  # deo iza ''|" znaka se koristi u
  performance data
  # izvestavanje u Nagiosu
  s = " %d korisnika trenutno
  logovano |users=%d;%d;%d;%d" \
                        %
  (count,count,opts.warnlevel,opts.cr
  itlevel,0)
  # u zavisnosti od statusa servisa
  stampamo izvestaj
  # i vracamo vrednost statusa
  provere
  if count >= opts.critlevel:
            s = " LOGOVANI KORISNICI
  CRITICAL " + s
            if opts.showall:
                  print "SVI" + s
            else:
                  print "MREZNI" + s

  sys.exit(ERROR['CRITICAL'])
  if count >= opts.warnlevel:
            s = " LOGOVANI KORISNICI
```

```
WARNING " + s
          if opts.showall:
               print "SVI" + s
     else:
               print "MREZNI" + s
     sys.exit(ERROR['WARNING'])
     s = " LOGOVANI KORISNICI OK " +
s
     if opts.showall:
               print "SVI" + s
     else:
               print "MREZNI" + s
     sys.exit(ERROR['OK'])
```

When Nagios executes plug-in, concerning passed arguments, plug-in output can be similar as one of the following:

```
MREZNI LOGOVANI KORISNICI OK 3
korisnika trenutno logovano
      |users=3;7;10;0
MREZNI LOGOVANI KORISNICI
WARNING 15 korisnika trenutno
logovano
      |users=15;10;30;0
MREZNI LOGOVANI KORISNICI
CRITICAL 30 korisnika trenutno
logovano
      |users=30;10;30;0
SVI LOGOVANI KORISNICI OK 1
korisnika trenutno logovano
      |users=1;3;5;0
SVI LOGOVANI KORISNICI WARNING -
25 korisnika trenutno logovano
      |users=25;20;50;0
SVI LOGOVANI KORISNICI CRITICAL
40 korisnika trenutno logovano
      |users=40;20;40;0
```

In order to use the plug-in, we must write Nagios configuration file (several of them to be more precise). First, we define commands used to check our desired state (in our case the number of users), and plug-in will use the exact format of the command given here to actually perform a check,

```
#komanda za proveru svih logovanih
korisnika
define command{
      command_name      check-all--
loggedon
      command_line
$USER1$/check_logged_on w $ARG1$ c
$ARG2$ a
      }
#komanda za proveru svih logovanih
mreznih korisnika
define command{
      command_name            check-
net-loggedon
      command_line
      $USER1$/check_logged_on w $ARG1$
c $ARG2$
      }
```

$USER1$, $ARG1$ and $ARG2$ variables are macros which Nagios fills with the following values: $USER1$ user macro1, gets the path of the directory in which the plug-in reside, $ARG1$ and $ARG2$ represent the positional arguments which Nagios passes to our plug-in for -w and -c switches respectively. Now we need to define services which will have upper defined commands as their *check_command* option:

```
define service{
      use genericservice
      host_name           localhost
#ime hosta servisa
      service_description
Provera svih logovanih korisnika
      max_check_attempts   5
      normal_check_interval  5
      retry_check_interval     1
      ... ostale opcije servisa ...
      check_command       checkall-
loggedon!5!7#nasa komanda
      }
define service{
      use generic service host_name
      localhost #ime hosta servisa
      service_description
      Provera mreznih logovanih
      korisnika
      max_check_attempts   5
      normal_check_interval  5
      ... ostale opcije servisa ...
      check_command        checknet-
      loggedon!2!4 # nasa komanda
      }
```

In the end, we need to add the name of our command in the definition of option ***check_command*** and the appropriate positional arguments. As we can see in the example, arguments which will Nagios hand over to our plug-in whill be separated by **"!"** character, wich will be omitted. For the first service, the command ***check-all--logged-on!5!7*** is equivalent to the following ***checkall-logged-on -w 5 -c 7 -a*** ("a" is transferred from the command itself), for the second service we should have following **check-net-logged-on - w 2 – c 4.** After we have changed the configuration files we need to send the **SIGHUP** signal, in order to reload Nagios forcing it to reread its configuration files and activate new services and commands we created.

4. CONCLUSION

One question arises. Should one buy commercial software package which is very expensive or use free software package like Nagios? Nagios has very complex configuration and it is very hard to set it up the right way for the first time, unlike commercial packets that almost automatically configure themselves. On the other side, Nagios' complex configuration is very flexible and

the program can be adapted to the large scale of usage case scenarios, it can be easily extended and dynamically reconfigured. Maintaining it is hard, but in the long terms, it becomes easier, especially because there are other programs used just to ease the configuration of Nagios. It is on the IT department to decide, low total cost of ownership and flexibility are a must these days.

REFERENCE

[1] http://www.openview.hp.com

[2] http://www.nagios.org

[3] http://nsclient.ready2nin.nl

[4] http://www.net-snmp.org

[5] http://people.ee.ethz.ch/~oetiker/webtools/mrtg

[6] http://www.gnokii.org

[7] http://www.linuxfromscratch.org

MODELLING OF THE ADDITIONAL AXIS OF THE MACHINE TOOL IN ORDER TO IMPROVE TECHNOLOGICAL PROCESS OF THE PRODUCTION OF THE PART

M. Pljakić, A. Babić, N. Ilić, A. Petrović

Abstract: *The approach of the integrated design represents the bridge that connects certain phases of the product and technologies design and plays a significant role in the reduction of total design time, as well as production costs. This means that the design of technological processes has to be connected with the production planning, that is the choice of tools, equipment, pressing device and machine tool.*

Key words: *Technological process, Tightening, Additional axes, Machine tools*

1. INTRODUCTION

This work shows the process of the design of the product from the production programme of the factory „Prva Petoletka" Trstenik on the example of the hydraulic motor housings. Within the process of forming a competative product, special attention is paid to the elements, that is the parameters of the technological process which significantly reduce production costs, e.g. choice of tools and the way of tightening and positioning of the part. By the technological analysis of the object it has been established that the tightening device of the working pieces presents a predominant factor in the production realization. For that reason special attention was paid to the modelling of the machine tool with the special tightening device which in this case represents an additional fourth control axis.

2. FUNCTIONAL ANALYSIS OF THE PART

Preliminary analysis of the part was done based on the following:

a. Geometrical shape,
b. Dimensions and their tolerances,
c. Tolerances of the shapes and positions,
d. Quality of the surfacing done (roughness), and
e. Material.

These general observations present the basis for the starting point of the production methods of handling the part evaluations.

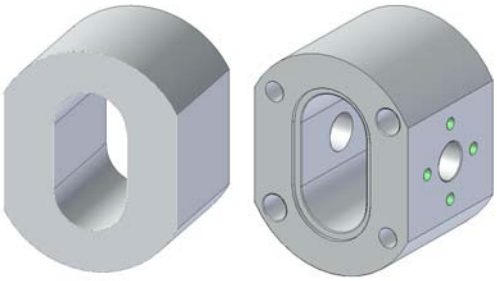

Picture 2.1. Prepared part and finished part

Based on the rule of priority using the dimensional, geometrical, technological and economic limitations, the matrix of dependence was acquired. By using thus established dependences, the matrix of succession is formed. As the way out of the matrix of succession a logical sequence of actions appears (theoretical actions).

3. THE CHOICE OF THE CUTTING TOOLS

When we talk about the choice of the cutting tool we need to fully define the needed tools so that all the requests defined by technology can be fulfilled in the process of production. When choosing the tools the rule for the tools to be standard should be followed if possible.
In this part the tools for specific operations are chosen. Taking into consideration the analysis done from the previous chapter, every operation is observed separately and standard tools are selected. One type of standard tools is selected here which doesn't mean that these are the only acceptable tools.

M.Sc. Marina Pljakić, Mech. Eng., marinap@gonet.co.yu,
Ph.D. Arandjel Babic, Profesor of the Faculty of Mechanical Engineering Kraljevo, babic.a@mfkv.kg.ac.yu,
M.Sc. Nemanja Ilic, Mech. Eng., ilic.n@mfkv.kg.ac.yu,
M.Sc. Aleksandra Petrović, Mech. Eng., petrovic.a@mfkv.kg.ac.yu

4. THE ANALYSIS OF THE POSITIONING AND TIGHTENING

In order to produce a mechanically properly functioning part (working object), it is necessary to perform its proper tightening and location definition (of the position and orientation) in space.

As an addition to the definition of the characteristic surface positioning, it's necessary to design the way of holding tight the part in the assigned position, under the influence of external forces like the gravitation force, cutting force, vibration force, centrifugal force, etc. This is the role of the devices known as 'vices' or 'holders of the working object'. It doesn't have to influence the earlier defined positioning function, but it has the function of enabling the stability of the part. Tightening devices have to have an appropriate tightening force so as not to damage the part in the points of contact by excessive pressure.

4.1. Types of tightening in case of cutting and drilling

The design of the tightening equipment and the tightening devices of the working piece on the machine is the same as in the case of any other designing. The position of tightening, previously described, has to follow the demands of the production precision and to take into consideration the relation between the segments of the parts. Also we have to make sure that the part doesn't move during the machine processing, that parts of the tightening equipment don't interrupt the movement of the tools or cause the growth in the operation of the of the tools and that easy removal of filings is enabled.

Some additional characteristics that have to be taken into consideration are as follows:

- vices should be set and tightly adjusted directly above the support surface of the tightening device;
- vices should always touch the part in its hardest points;
- cutting forces should be directed towards the positioner, not towards vices;
- the direction of the tightening forces should be towards the positioners of the geometrical object and in such cases as a way to keep the part in the tightening device;
- the surface of the holders should be flat and equally holding onto, without any deformations caused by the tightening forces in the tightening device
- positioners of the tightening device have to be separated as much as possible;
- positioners have to be set so as to avoid filings and other unfamiliar objects whenever possible;
- the part has to be able to be pressured in the tightening device in only one position;
- drilling in the guides is applied whenever possible.

5. MODELING OF THE MOUNTING STRUCTURE OF THE MACHINE TOOL AND ADDITIONAL AXIS

Continuing the analysis after product and technology defining ther is the need for the definition of the concept of the machine tools that would realize the technology In order to perform the needed actions when machine processing hydraulic motor housings, machine tools have to have suitable movements that are enabled by the independent wholes – modules. For every movement, whether main or accessory, there has to be an appropriate module that enables that movement. For the tightening of the working piece the tightening device has to be designed. Therefore, modular design of machine tools and tightening devices has been done. From the available modules those that enable the necessary movements of machine so that they could process the hydraulic moitor housings are selected.

5.1. Modules for modelling of the mounting structure of the machine tools and tightening devices

The first module is the module of the stand for horizontal or vertical machine tool. This module is stationary. Within this module there is the driving system and guides that enable translatory movement to another module that is mounted onto it.

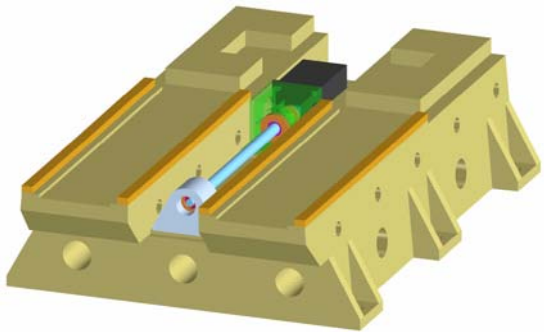

Picture 5.1. Unmovable part of the module for translatory movement with the horizontal machine (the stand)

The second module is the module for the main movement of the tool with the horizontal machine tool. There is an independent driving system for this movement. On this module there are the sliders over which you can mount onto another module thus acquiring vertical translatory movement, too.

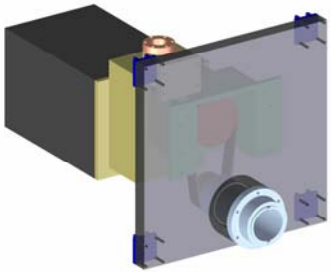

Picture 5.2. Module for the main movement with the horizontal machine tool

The third module is the module for the main movement of the tool with the vertical machine tool. There is an independent driving system for this movement. On this module there are the sliders over which you can mount onto another module thus acquiring vertical translatory movement, too.

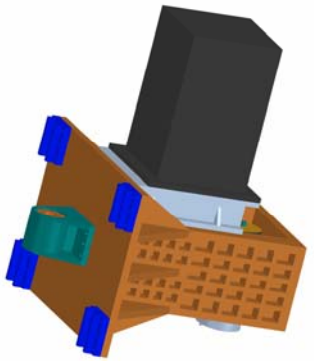

Picture 5.3. Module for the main movement of the tool with the vertical machine tool

The fourth module is the module of the ladders that enables tranlatory movement of the tools. It has a driving system with which vertical movement of the module of the tool girders with horizontal machine tool is enabled.

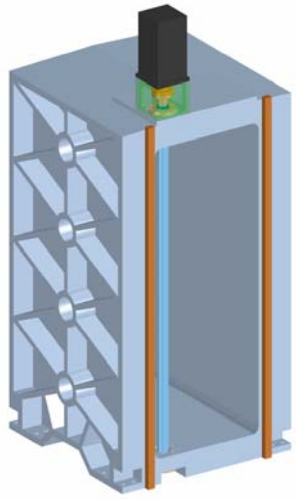

Picture 5.4. Module of the ladders with the horizontal machine tool

The fifth module is the module of the ladders that is needed to enbable the vertical movement of the module of the tool girders. It has a driving system that enables that movement. This module is called unmovable pillar.

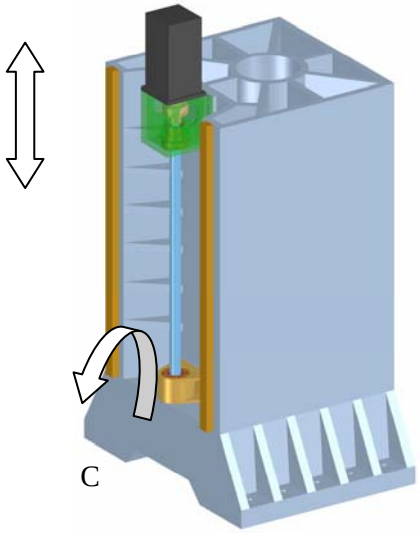

Picture 5.5. Module of the ladders with the vertical machine tool (unmovable pillar)

The sixth module enables two movements on the machine tool and these are two translatory movements. It has a pair of guides and a driving system that enable translatory movement of another module. Also it has two pairs of sliders that are used for translatory movement of this module over the stand with horizontal/vertical driller-cutter.

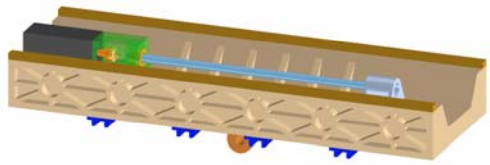

Picture 5.6. Transversal support

The seventh module – the module of the working table enables one translatory movement. It doesn't have a driving system but it has sliders and it accepts movements from the driving system of another module.

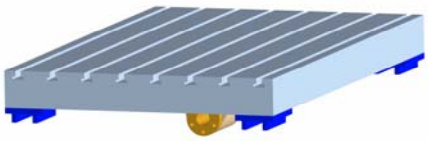

Picture 5.7. Module of the working table

The eighth module is the module of the rotary table. It has a special driving system that enables rotary movement of the rotator. Using this module, an additional control axis is introduced with the vertical and horizontal drillers-cutters.

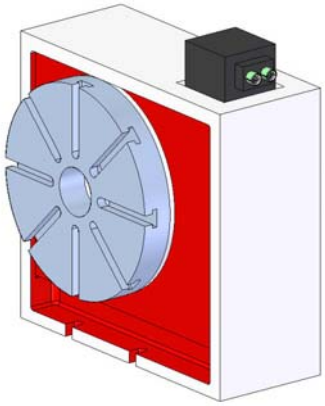

Picture 5.8. Module of the rotary table

The nineth module is the module of the tightening devices girders. It enables the positioning of 16 tightening devices, 4 on each side, at the same time. This module is connected with the rotary table on one and sinking on another side.

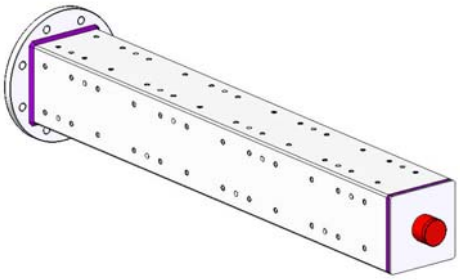

Picture 5.9. Module of the tightening devices girders

The tenth module is the module of sinking. It is used to connect the tightening device girders with the module of the machine tool table.

Picture 5.10. Module of sinking of the tightening device girders

The eleventh module is the module of the tightening device. It is used for tightening and positioning of the working object (hydraulic motor housings) while being processed.

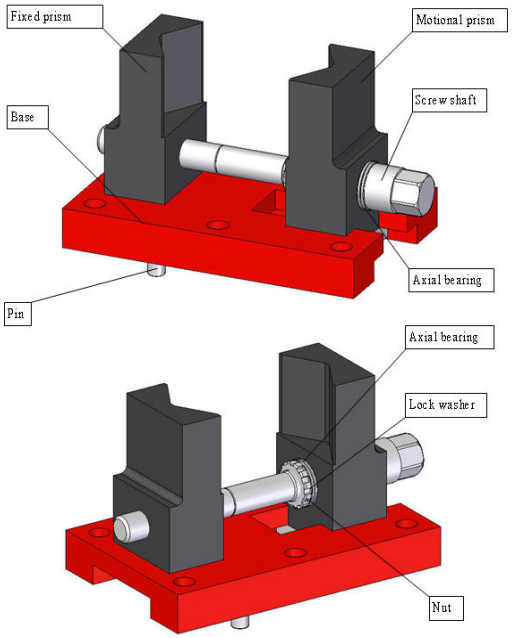

Picture 5.11. Module of the tightening device

Tightening device, together with the girder, sinking and rotary table presents an additional axis on machine tools. In this and the next variant triaxial horizontal driller/cutter, and the triaxial vertical driller/cutter are chosen, so that the structure of the tightening device presents the fourth additional axis. By this additional axis productivity is increased, within one tightening 16 hydraulic motor housings are processed. The number of the housings that are processed at the same time is conditioned by the maximum stability of the tools, so that tools can process all 16 housings, without having to change the tools in the meantime. The process having been done, the tools and working objects are changed. In the next picture 5.12. we can see what the tightening device looks like, this one is modelled parametrically and variantly so that it can be used for tightening of the hydraulic motor housings of different dimensions and for the right number of pieces that are acceptable.

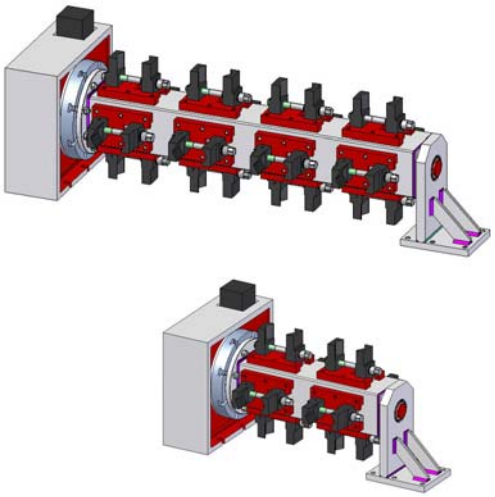

Picture 5.12. Tightening device with the sinking designed for 8 and 16 hydraulic motor housings

5.2. The realization of the adopted technological processes on variantly chosen machine tools

The prepared part for the production of the hydraulic motor housing is an extruded aluminium rod, and it's shown in the next picture.

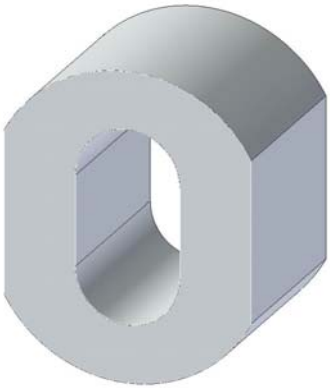

Picture 5.13. The prepared part

Based on the technology that is the way out of the matrix of succession, the process of the hydraulic motor housing production is done in two tightenings.

In the first tightening the prepared parts are put in the tightening, one by one, and what the prepared parts look like is seen in pictures 5.14 and 5.15.

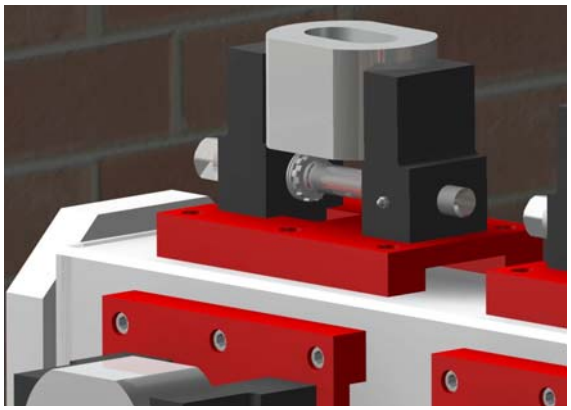

Picture 5.14. The prepared part in the tightening device

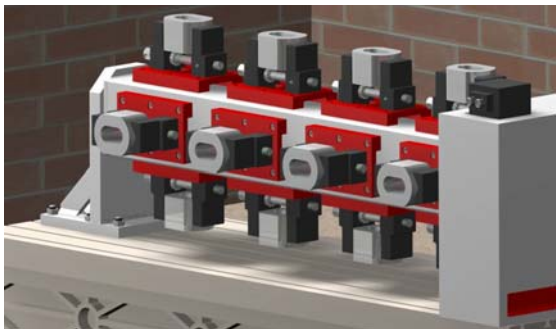

Picture 5.15. The prepared part in the tightening device – Tightening A

In the first variant machine tool used to process hydraulic motor housing is a vertical drilling/cutter picture 5.16. This machine tool has two translations and one rotation of the working object, one translatory and one rotary movement of the tools. On this machine 4 axis-X',Y',Z, and A' are numerically controlled.

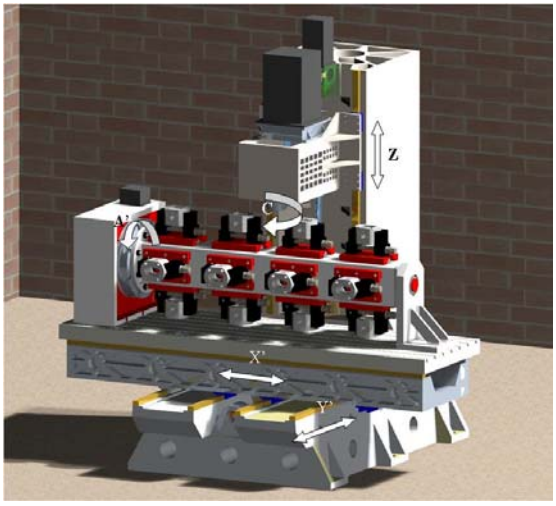

Picture 5.16. Vertical driller/cutter

Having done the operations in the first tightening the working object turns over and then the operations in the second tightening are done. The working object, having completed operations in tightening A is shown in picture 5.17.

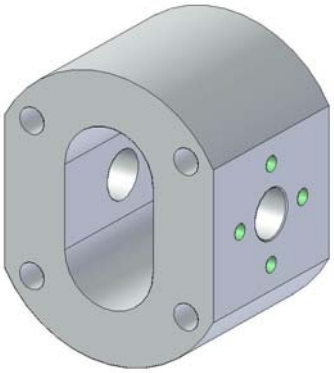

Picture 5.17. Hydraulic motor housing after tightening A
What the prepred parts look like in the tightening device - Tightening B is shown in picture 5.18.

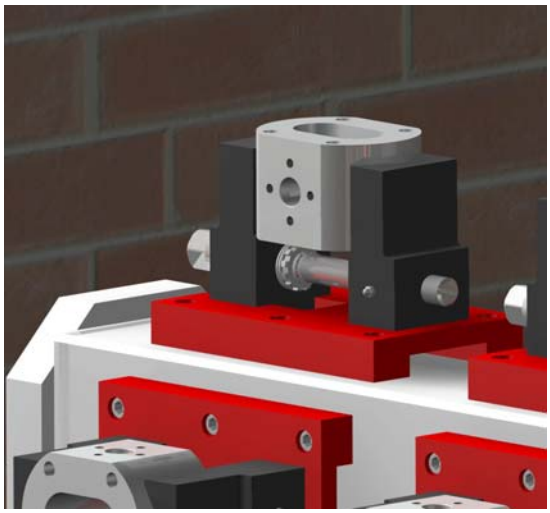

Picture 5.18. Prepared part in the tightening device – Tightening B

What the final product of the hydraulic motor housing looks like after the completed processing assigned by technology, after tightening B, is shown in picture 5.19

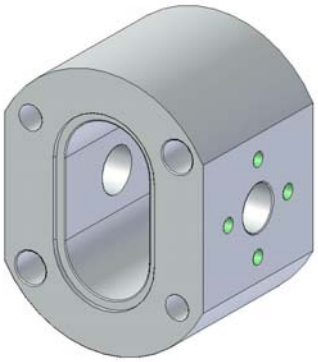

Picture 5.19. The final shape of the hydraulic motor housing

The second variant is different from the first only in the choice of the machine tool. In stead of the vertical, the horizontal driller/cutter was chosen, and the tightening equipment and the tightening tools are the same as those from the first variant.

Horizontal driller/cutter is shown on picture 5.20. This machine tool has two translations and one rotation of the working object, one translatory and one rotary movement of the tools. On this machine 4 axis-X',Y',Z, and A' are numerically controlled, too.

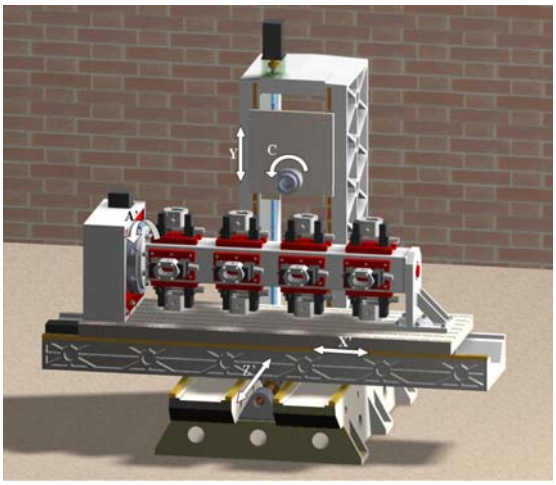

Picture 5.20. Horizontal driller/cutter

6. CONCLUSION

The achieved results in this work are the reflections of the research of the variant option of the technological production process of the hydraulical motor housings by using the already existing machine tools. There is the need for the introduction of the additional axis on the already existing triaxial processing centres.

The results of the research are derived from a very large theoretical analysis of the separate parametres that directly influence the generating of the technological process. The following parametres are mentioned here:

- the sequence of technological operations
- the choice of the tool
- the design of the specific tightening device,
- mou nting structures of the machine tool based on the number of the available modules.

LITERATURA

[1] Babić, A., Tehnologija montaže, Mašinski fakultet Kraljevo, 2005.

[2] Babić, A., Projektovanje tehnoloških procesa, Mašinski fakultet Kraljevo, 2005.

[3] Babić, B., Projektovanje tehnoloških procesa, Mašinski fakultet Beograd, 1999.

[4] Halevi, G., Weill, R., Principles of Process Planning.

[5] Milojević, M., Lukić, LJ., Modularno projektovanje, LOLA Institut Beograd, 1996.

[6] Milačić, V., R., Mašine alatke I, Sistem analiza, Mašinski fakultet Beograd, 1980.

[7] Pljakić Marina, Modelovanje montažne strukture mašine alatke na osnovu dela iz proizvodnog programa kompanije PPT Hidraulika AD Trstenik, diplomski rad, Kraljevo, jul 2007.

CIP – Каталогизација у публикацији
Народна библиотека Србије, Београд

621 (082)
621.86/ .87(082)
629.3/ .4(082)
622.6(082)

INTERNATIONAL Triennial Conference Heavy Machinery (6; 2008; Kraljevo)
Proceedings / The Sixth International Triennial Conference Heavy Machinery – HM 2008, Kraljevo, 24. - 29. June 2008.;
[organized by] University of Kragujevac, Faculty of Mechanical Engineering, Kraljevo; [editor Novak Nedić]. – Kraljevo: Faculty of Mechanical Engineering, 2008 (Kraljevo: Riža). – 1 knj. (razl. Pag.): ilstr. ; 29 cm

Radovi na engl. i na rus. jeziku.- Tekst štampano dvostubačno. -Tiraž 200.-Napomene i bibliografske reference uz radove.-Bibliografija uz svaki rad.

ISBN 978-86-82631-45-3
1. Faculty of Mechanical Engineering (Kraljevo)
a) Машиноградња – Зборници
b) Производно машинство – Зборници
c) Транспортна средства – Зборници
c) Шинска возила - Зборници
COBISS.SR-ID 149485324